

SOIL PHYSICAL CHARACTERISTICS RELATED TO FAILURE OF STORMWATER
BIOFILTRATION DEVICES

by

REDAHEGN SILESHI

ROBERT E. PITT, COMMITTEE CHAIR

S. ROCKY DURRANS
DEREK G. WILLIAMSON
KAREN M. BOYKIN
SHIRLEY E. CLARK

A DISSERTATION

Submitted in partial fulfillment of the requirements
for the degree of Doctor of Philosophy
in the Department of Civil, Construction, and Environmental Engineering
in the Graduate School of
The University of Alabama

TUSCALOOSA ALABAMA

2013

Copyright Redahegn Sileshi 2013
ALL RIGHTS RESERVED

ABSTRACT

The main theme of this dissertation research was to investigate and test solutions to overcome common failure mechanisms of bioinfiltration stormwater devices. Bioinfiltration can be an effective option for the management of stormwater runoff from urban areas, mainly through enhanced infiltration of the runoff to better balance the urban hydrologic cycle. There are increasing interests in the use of bioinfiltration practices for managing stormwater runoff, as infiltration practices promote groundwater recharge, reduce runoff peak flow rates and volumes, and can reduce pollutant discharges to surface water bodies. However, there are known problems causing failure of these devices (such as clogging, under-sizing, improper underdrain use, and inefficient treatment media). In addition, few quantitative guidelines are available for the design of biofilters and bioinfiltration devices for specific treatment goals while minimizing these operational problems.

Some types of stormwater control practices are intended to include standing water for varying lengths of time for enhanced sedimentation and scour protection. In areas having restrictive soils, underdrains are used to minimize long periods of standing water (less than 3 days) to minimize nuisance conditions such as breeding of mosquitoes.. Alternatives that result in greater flexibility and efficiency in the design of biofiltration and bioretention devices were tested and developed during this research.

The drainage rate in biofiltration devices (having an underdrain) is usually controlled using an underdrain that is restricted with a small orifice or other flow-moderating component. These orifices used for flow control frequently fail, because they are very small (<10 mm) and

are prone to clogging over time. The performance of a foundation underdrain material (SmartDrain™) that could be used in biofilter devices was evaluated. This material was found to have minimal clogging potential while also providing very low discharge rates. The flow capacity and clogging potential of the SmartDrain™ material was examined under severe service conditions.

Laboratory and field-scale studies were conducted to provide insight into the existing soil characteristics of a poorly operating biofilter facility. Surface double-ring infiltration tests (comprised of three separate setups each) and bore hole infiltration measurements were conducted in the field to determine the surface infiltration and the subsurface infiltration characteristics of bioinfiltration sites in Tuscaloosa. The effects of different compaction levels on the infiltration rates through the soil (obtained from the surface and subsurface of the bioinfiltration sites) were examined during laboratory column tests for comparison to the field observations.

A controlled laboratory column tests conducted using various media to identify changes in flow with changes in the mixture characteristics, focusing on media density associated with compaction, particle size distribution (and uniformity), and amount of organic material (due to added peat). The results of the predicted performance of these mixtures were also verified using column tests (for different compaction conditions) of surface and subsurface soil samples obtained from Tuscaloosa, AL, along with biofilter media obtained from Kansas City, North Carolina, and Wisconsin.

The results of this research indicated that soil compaction has dramatic effects on the infiltration rates; the effects of compaction therefore need to be considered during construction of stormwater treatment facilities. Data from the infiltrometers also need to be cautiously

evaluated as they show high rates that only occur during the initial portion of the event and are not representative of fully saturated conditions throughout the infiltration facility that would occur during actual storm conditions. It is important that stormwater practice designers determine the subsoil characteristics before designing stormwater treatment facilities and consider the use of added amendments (sand and peat) to the soils.

DEDICATION

To my loving mother, Ehite Gebre, who always supported and encouraged me.

To Dr. Robert Pitt, whose support and guidance has helped me reach this milestone.

LIST OF ABBREVIATION AND SYMBOLS

<i>μm</i>	Micrometer
<i>μS/cm</i>	Micro-Siemens per Centimeter
<i>in/hr</i>	Inch per Hour
<i>meq/100g</i>	millequivalents per 100 grams of Soil
<i>mm/hr</i>	Millimeter per Hour
<i>mg/L</i>	Milligram per Liter
<i>°C</i>	Degree Centigrade
<i>%</i>	Percentage
<i>ac</i>	Acre
<i>Al</i>	Aluminum
<i>AL</i>	Alabama
<i>ANOVA</i>	Analysis of Variance
<i>As</i>	Arsenic
<i>ASTM</i>	American Society for Testing and Materials
<i>B</i>	Boron
<i>Ba</i>	Barium
<i>C</i>	Carbon
<i>Ca</i>	Calcium
<i>Cc</i>	Coefficient of Curvature

<i>Cd</i>	Cadmium
CEC	Cation Exchange Capacity
<i>cm</i>	Centimeter
<i>COV</i>	Coefficient of Variation
<i>Cr</i>	Chromium
<i>Cu</i>	Copper
Cu	Uniformity Coefficient
D50	Grain Diameter at 50% Passing
de	Effective depth
DI water	Distilled water
<i>Fe</i>	Iron
<i>ft.</i>	Feet
<i>ft²</i>	Square feet
<i>GPM</i>	Gallons Per Minute
<i>hr.</i>	Hour
<i>in</i>	Inch
<i>K</i>	Potassium
<i>Kg</i>	Kilogram
<i>KW</i>	Kruskal-Wallis
<i>Ks</i>	Saturated Hydraulic Conductivity
<i>L</i>	Liter
<i>m</i>	Meter
<i>m²</i>	Square Meter

<i>mg</i>	Magnesium
<i>mL</i>	Milliliter
<i>mm</i>	Millimeter
<i>Mn</i>	Manganese
<i>Mo</i>	Molybdenum
<i>N</i>	Nitrogen
<i>Na</i>	Sodium
<i>n/a</i>	Not Available
<i>Ni</i>	Nickel
<i>NTU</i>	Nephelometric Turbidity Units
<i>OM</i>	Organic Matter
<i>P</i>	Phosphorous
<i>Pb</i>	Lead
<i>ppm</i>	Parts per Million
<i>PSD</i>	Particle Size Distribution
<i>PVC</i>	Polyvinyl Chloride
<i>QA</i>	Quality Assurance
<i>QC</i>	Quality Control
<i>S</i>	Spacing Between Drain
<i>S</i>	Sulfur
<i>SAR</i>	Sodium Adsorption Ratio
<i>SD</i>	SmartDrain
<i>SSC</i>	Suspended Solids Concentration

<i>TDS</i>	Total Dissolved Solids
<i>TN</i>	Total Nitrogen
<i>TP</i>	Total Phosphorus
<i>TS</i>	Total Solids
<i>US EPA</i>	United States Environmental Protection Agency
<i>Vs.</i>	Versus
<i>Zn</i>	Zinc

ACKNOWLEDGEMENTS

First and foremost, I would like to sincerely thank my advisor and committee chairman, Dr. Robert Pitt, for his continuous guidance, support throughout the course of my study. Special thanks to my dissertation committee, Dr. S. Rocky Durrans, Dr. Derek G. Williamson, Dr. Karen M. Boykin, and Dr. Shirley Clark for their technical guidance and helpful suggestions.

I would like to thank Dr. Kenneth Fridley, Head of Civil, Construction, and Environmental Engineering Department and the National Science Foundation EPSCoR program for their financial support of this research. I want to thank all my fellows of Dr. Pitt's research group, especially Ryan Bean who helped me with laboratory column construction and various field infiltration tests. I would like to thank the City of Tuscaloosa, especially Chad Christian for helping us in conducting the borehole tests.

I would like to thank my parents, without your love, encouragement and support none of this even be possible. I would like to specifically thank my mom, brothers Ermiyas Kassu, and Dr. Aschalew Kassu for being such a great role model. Dr. Aschalew Kassu thank you for all that you have done for me throughout my life thus far. I would like to express my deepest appreciation to my wife, Bethlehem Mamo, whose love and encouragement allowed me to finish this journey. I would like to extend my gratitude to my best friend Moges Kifle for his constant support and motivation. Thank you for being genuinely happy for my success.

I would like to express my gratitude to Ms. Darlene Burkhalter, Lensey Shaw, Shauna Westberry and Tim Ryan for their professional assistance provided during the course of my

study. Thank you again for the faculty and staff of the Department of Civil, Construction, and Environmental Engineering for your support in the completion of this degree.

CONTENTS

ABSTRACT.....	ii
DEDICATION.....	v
LIST OF ABBREVIATION AND SYMBOLS	vi
ACKNOWLEDGEMENTS.....	x
LIST OF TABLES.....	xxxii
LIST OF FIGURES	xxxvii
1. INTRODUCTION	1
1.1 Research Objectives	3
1.2 Dissertation Organization.....	5
2. LITERATURE REVIEW	9
2.1 Urban Stormwater Runoff Management	9
2.2 Stormwater Filtration Techniques.....	10
2.3 Sand Filters.....	11
2.3.1 Surface Sand Filter	12
2.3.2 Underground Sand Filters.....	13
2.3.3 Perimeter Sand Filters	14
2.3.4 Organic Media Filter	15

2.3.5 Multi-Chambered Treatment Train	15
2.4 Biofiltration Systems.....	16
2.4.1 Biofilter/Bioretenion Media	20
2.4.2 Underdrains	22
2.4.3 Underdrain Effects on the Water Balance	24
2.4.4 Biofilter/Bioretenion Pollutant Removal.....	27
2.5 Infiltration Mechanism.....	27
2.5.1 Factors Affecting the Infiltration Process.....	28
2.5.2 Horton Equation	31
2.5.3 Green-Ampt Infiltration Model	33
2.5.4 Measuring Infiltration Rates.....	35
2.6 Soil Compaction.....	37
2.7 Soil Amendments.....	39
2.8 Need for Research.....	40
2.9 Dissertation Research.....	41
3. HYPOTHESES AND EXPERIMENTAL DESIGN	43
3.1 Hypothesis	44
3.2 Experimental Design.....	51
3.3 Quality Control (QC) and Quality Assurance (QA) Procedures	53
3.4 Data Analyses.....	54
3.4.1 Probability and Scatter plots.....	54
3.4.2 Grouped Box and Whisker Plots	54
3.4.3 Regression Analyses.....	55

3.4.4 Analyses of Variance (ANOVA).....	58
3.4.5 Nonparametric Kurskal–Wallis ANOVA.....	59
3.4.6 Post-hoc Tests.....	60
3.4.7 Statistical Significance Measures.....	60
3.4.8 Factorial Experiment.....	61
3.4.9 Model.....	62
4. THE PERFORMANCE OF AN ALTERNATIVE UNDERDRAIN MATERIAL (SMARTDRAIN™) FOR URBAN STORMWATER BIOFILTRATION SYSTEMS	63
4.1 Introduction.....	63
4.2 SmartDrain™ Material Characteristics.....	67
4.3 Field Application of SmartDrain™.....	69
4.3.1 Biofilter Facility Using SmartDrain™ as Underdrain.....	69
4.3.2 SmartDrain™ Drainage System Performance Installed in Sports Turf Facility	72
4.3.3 Biofilter/Bioretenion Facility Hydraulics and Design of Dewatering Facilities.....	74
4.4 SmartDrain™ Material Performance Experiments under Controlled Pilot-Scale Biofilter Conditions.....	82
4.4.1 SmartDrain™ Material Drainage Characteristics Tests.....	82
4.4.2 Testing the SmartDrain™ Belt for Potential Particulate Clogging.....	85
4.4.3 Evaluating the Performance of SmartDrain™ Material under Biofouling Conditions	87
4.5 Results and Discussion.....	90
4.5.1 SmartDrain™ Drainage Characteristics Tests.....	90
4.5.2 SmartDrain™ Material Particulate Clogging Tests.....	94
4.5.3 Reynolds Number in a SmartDrain™ Belt.....	99
4.5.4 SmartDrain™ Material Biofouling Tests.....	103
4.6 Data Analyses.....	107

4.6.1 SmartDrain™ Drainage Characteristics Tests.....	107
4.6.2 Model Fitting for Drainage Characteristics Tests.....	113
4.6.3 SmartDrain™ Clogging Tests	119
4.6.4 Statistical Analyses for SmartDrain™ Clogging Tests	120
4.6.5 Model Fitting for Clogging Tests	124
4.6.6 SmartDrain™ Biofouling Tests.....	127
4.6.7 Statistical Analyses for Biofouling Tests	129
4.6.8 Model Fitting for Biofouling Tests.....	132
5. ASSESSING THE IMPACT OF SOIL MEDIA CHARACTERISTICS ON STORMWATER BIOFILTRATION DEVICE PERFORMANCE.....	139
5.1 Introduction	139
5.2 Description of Test Site and Methodology.....	142
5.2.1 Description of Test Site	142
5.2.2 Field Infiltration Study at Biofiltration Facility	145
5.2.3 Water Content and Density Measurements of the Soil Media	148
5.2.4 Plant Nutrients	149
5.2.5 Biofilter Surface Ponding.....	156
5.2.6 Laboratory Column Tests.....	158
5.3 Results	161
5.3.1 In-Situ Biofilter Infiltration Measurements Results	161
5.3.2 Laboratory Infiltration Results	166
5.4 Statistical Analyses.....	173
5.4.1 Model Fitting	177
5.4.2 Pooled Standard Error	179

5.5 Statistical Comparisons of Different Levels of Compaction	184
5.6 Chapter Summary	190
6. SOIL MEDIA CHARACTERISTICS OF PROPOSED STORMWATER BIOINFILTRATION CONSTRUCTION SITES	193
6.1 Introduction	193
6.2.1 Description of Test Sites.....	197
6.2.2 Field Surface Infiltration Study at Proposed Bioinfiltration Site	198
6.2.3 Water Content and Density Measurements of Surface Soil Media at Bioinfiltration Site	204
6.2.4 Borehole Infiltration Tests.....	207
6.3 Laboratory Column Tests	209
6.4 Results	211
6.4.1 Surface and Subsurface Soil Nutrient Reports from Bioinfiltration Study Sites	211
6.4.2 Field Surface and Subsurface Infiltration Test Results	216
6.4.3 Laboratory Column Infiltration Test Results Using Surface Soils.....	219
6.4.4 Laboratory Column Infiltration Test Results Using Subsurface Soils	223
6.4.5 Comparisons of Different Levels of Compaction and Sample Locations	227
6.5 Chapter Summary	234
7. LABORATORY COLUMN TESTS FOR PREDICTING CHANGES IN FLOWS AND PARTICULATE RETENTION WITH CHANGES IN BIOFILTER MEDIA CHARACTERISTICS	241
7.1 Introduction	241
7.2 Description of Various Media and Test Methodology	244
7.2.1 Laboratory Column Flow Tests.....	249
7.2.2 Laboratory Column Particle Trapping Tests	252
7.2.3 Particle Trapping Test Sample Analysis	256

7.2.4 Laboratory Solids Analysis (Figure 118 shows the solids analysis flow sheet).....	257
7.2.5 Suspended Sediment Concentration (ASTM, 1997)	259
7.2.6 Total Dissolved Solid (TDS) Analysis Procedure (Standard Method, 2005).....	260
7.3 Results and Discussions	261
7.3.1 Sand-Peat Mixture Nutrient and Other Constituents Report	261
7.3.2 Infiltration Results for Sand and Peat Mixture Tests	264
7.3.3 Biofilter Media Nutrient and Other Constituents Report	267
7.3.4 Infiltration Results using Biofilter Media.....	269
7.3.5 Comparisons of Different Levels of Compaction and Percentage of Peat in the Sand-Peat Mixture.	274
7.3.6 Statistical Analyses of Infiltration Rates Through Sand-Peat Mixture and Tuscaloosa Soil.....	278
7.3.7 Model Fitting	288
7.3.8 Statistical Analyses of Infiltration Rates through Sand-Peat Mixture Only.....	295
7.4 Particle Trapping Tests	300
7.4.1 Particle Trapping Tests for Sand and Peat Mixtures	300
7.4.2 Particle Trapping Test Results for Coarse Media.....	304
7.4.3 Statistical Analysis for the Particle Trapping Experiment	307
7.5 Chapter Summary	311
8 APPLICATIONS AND CONCLUSIONS	313
8.1 Typical Biofilter as Modeled using Research Results for a Commercial Area in Tuscaloosa	313
8.2 Typical Grass Swale as Modeled using Research Results for a Residential Area in Tuscaloosa.....	319
8.3 Factorial Statistical Analyses of Sand-Peat Mixture Column Experiments to Identify Significant Factors Affecting Particulate Removal Performance	323

8.4 SmartDrain™ Underdrain SSC and Particle Size Data and Analyses from Full-Scale Biofilter Monitoring in Kansas City.....	325
8.5 Dissertation Research Hypothesis	328
8.6 Summary of Dissertation Research Finding.....	331
REFERENCES	336
APPENDIX A: SMARTDRAIN™ PERFORMANCE CHARACTERISTICS TEST	349
Appendix A.1: Example Calculation Showing Biofilter Facility Hydraulics and Design of Dewatering Facilities	349
Appendix A.2: Stage-discharge Relation Plots Summary for Different SmartDrain™ Lengths and Slope	352
Appendix A.3: Regression Statistics on SmartDrain™ Length 9.4 ft and Slope 0%.....	352
Appendix A.4: Regression Statistics on SmartDrain™ Length 9.4 ft and Slope 3%.....	354
Appendix A.5: Regression Statistics on SmartDrain™ Length 9.4 ft and Slope 6%.....	356
Appendix A.6: Regression Statistics on SmartDrain™ Length 9.4 ft and Slope 9%.....	358
Appendix A.7: Regression Statistics on SmartDrain™ Length 9.4 ft, Slope 12% and Probability Analysis Detail.....	360
Appendix A.8: Regression Statistics on SmartDrain™ Length 7.1 ft and Slope 0%.....	362
Appendix A.9: Regression Statistics on SmartDrain™ Length 7.1 ft and Slope 3%.....	364
Appendix A.10: Regression Statistics on SmartDrain™ Length 7.1 ft and Slope 6%.....	366
Appendix A.11: Regression Statistics on SmartDrain™ Length 7.1 ft and Slope 9%.....	368
Appendix A.12: Regression Statistics on SmartDrain™ Length 7.1 ft and Slope 12%.....	370
Appendix A.13: Regression Statistics on SmartDrain™ Length 5.1 ft and Slope 0%.....	372
Appendix A.14: Regression Statistics on SmartDrain™ Length 5.1 ft and Slope 3%.....	374
Appendix A.15: Regression Statistics on SmartDrain™ Length 5.1 ft and Slope 12%.....	376
Appendix A.16: Regression Statistics on SmartDrain™ Length 3.1 ft and Slope 0%.....	378
Appendix A.17: Regression Statistics on SmartDrain™ Length 3.1 ft and Slope 3%.....	380

Appendix A.18: Regression Statistics on SmartDrain™ Length 3.1ft and Slope 12%.....	382
Appendix A.19: Regression Statistics on SmartDrain™ Length 1.1ft and Slope 0%.....	384
Appendix A.20: Regression Statistics on SmartDrain™ Length 1.1ft and Slope 3%.....	386
Appendix A.21: Regression Statistics on SmartDrain™ Length 1.1ft and Slope 12%.....	388
Appendix A.22: Regression Statistics on SmartDrain™ Clogging Test, Trial#1.....	390
Appendix A.23: Regression Statistics on SmartDrain™ Clogging Test, Trial#2.....	392
Appendix A.24: Regression Statistics on SmartDrain™ Clogging Test, Trial#3.....	394
Appendix A.25: Regression Statistics on SmartDrain™ Clogging Test, Trial#4.....	396
Appendix A.26: Regression Statistics on SmartDrain™ Clogging Test, Trial#5.....	398
Appendix A.27: Regression Statistics on SmartDrain™ Clogging Test, Trial#6.....	400
Appendix A.28: Regression Statistics on SmartDrain™ Clogging Test, Trial#7.....	402
Appendix A.29: Regression Statistics on SmartDrain™ Clogging Test, Trial#8.....	404
Appendix A.30: Regression Statistics on SmartDrain™ Clogging Test, Trial#9.....	406
Appendix A.31: Regression Statistics on SmartDrain™ Clogging Test, Trial#10.....	408
Appendix A.32: Regression Statistics on SmartDrain™ Clogging Test, Trial#11.....	410
Appendix A.33: Regression Statistics on SmartDrain™ Clogging Test, Trial#12.....	412
Appendix A.34: Regression Statistics on SmartDrain™ Clogging Test, Trial#13.....	414
Appendix A.35: Regression Statistics on SmartDrain™ Clogging Test, Trial#14.....	416
Appendix A.36: Regression Statistics on SmartDrain™ Clogging Test, Trial#15.....	418
Appendix A.37: Regression Statistics on SmartDrain™ Clogging Test, Trial#16.....	420
Appendix A.38: Regression Statistics on SmartDrain™ Clogging Test, Trial#17.....	422
Appendix A.39: Regression Statistics on SmartDrain™ Clogging Test, Trial#18.....	424
Appendix A.40: Regression Statistics on SmartDrain™ Clogging Test, Trial#19.....	426
Appendix A.41: Regression Statistics on SmartDrain™ Clogging Test, Trial#20.....	428

Appendix A.42: Regression Statistics on SmartDrain™ Clogging Test, Trial#21	430
Appendix A.43: Regression Statistics on SmartDrain™ Clogging Test, Trial#22	432
Appendix A.44: Regression Statistics on SmartDrain™ Clogging Test, Trial#23	434
Appendix A.45: Regression Statistics on SmartDrain™ Clogging Test, Trial#24	436
Appendix A.46: Regression Statistics on SmartDrain™ Clogging Test, Trial#25	438
Appendix A.47: Regression Statistics on SmartDrain™ Clogging Test, Trial#26	440
Appendix A.48: Regression Statistics on SmartDrain™ Clogging Test, Trial#27	442
Appendix A.49: Regression Statistics on SmartDrain™ Clogging Test, Trial#28	444
Appendix A.50: Regression Statistics on SmartDrain™ Clogging Test, Trial#29	446
Appendix A.51: Regression Statistics on SmartDrain™ Clogging Test, Trial#30	448
Appendix A.52: Regression Statistics on SmartDrain™ Clogging Test, Trial#31	450
Appendix A.53: Regression Statistics on SmartDrain™ Clogging Test, Trial#32	452
Appendix A.54: Regression Statistics on SmartDrain™ Biofouling Test, Trial#1	454
Appendix A.55: Regression Statistics on SmartDrain™ Biofouling Test, Trial#2	456
Appendix A.56: Regression Statistics on SmartDrain™ Biofouling Test, Trial#3	458
Appendix A.57: Regression Statistics on SmartDrain™ Biofouling Test, Trial#4	460
Appendix A.58: Regression Statistics on SmartDrain™ Biofouling Test, Trial#5	462
Appendix A.59: Regression Statistics on SmartDrain™ Biofouling Test, Trial#6	464
Appendix A.60: Regression Statistics on SmartDrain™ Biofouling Test, Trial#7	466
Appendix A.61: Example Calculation Showing Biofilter Facility Hydraulics and Design of Dewatering Options	468
Appendix A.62: An Example Calculation Showing a Biofilter Facility Hydraulics and Design of	471
Appendix A.63: Minimum No. of SmartDrain (SD) Required for a Biofilter Basin Having a Square Geometry	472

Appendix A. 64: Minimum No. of SmartDrain (SD) Required for a Biofilter Basin Having a Rectangular Geometry (Length: Width = 3:1)	473
Appendix A.65: Minimum No. of SmartDrain (SD) Required for a Biofilter Basin Having a Rectangular Geometry (Length: Width = 5:1)	474
Appendix A.66: Biofilter Basin Dewatering and Minimum No. of SmartDrain (SD) Required for a Biofilter Basin Based On SmartDrain Spacing.	475
APPENDIX B: STORMWATER BIOFILTRATION DEVICE PERFORMANCE TEST RESULTS	476
Appendix B.1: Biofilter Surface Infiltration Measurements at Location 1 Fitted with Horton Equation.....	476
Appendix B.2: Biofilter Surface Infiltration Measurements at Location 2 Fitted with Horton Equation.....	477
Appendix B.3: Biofilter Surface Infiltration Measurements at Location 3 Fitted with Horton Equation.....	478
Appendix B.4: Biofilter Surface Infiltration Measurements at Location 4 Fitted with Horton Equation.....	479
Appendix B.5: Biofilter Surface Infiltration Measurements after Rain Event 1 Fitted with Horton Equation.	480
Appendix B.6: Biofilter Surface Infiltration Measurements after Rain Event 2 Fitted with Horton Equation.	481
Appendix B.7: Biofilter Surface Infiltration Measurements after Rain Event 3 Fitted with Horton Equation.	482
Appendix B.8: Biofilter Surface Infiltration Measurements after Rain Event 4 Fitted with Horton Equation.	483
Appendix B.9: Biofilter Surface Infiltration Measurements after Rain Event 5 Fitted with Horton Equation.	484
Appendix B.10: Laboratory Infiltration Measurements Fitted with Horton Equations Using Biofilter Media Only.	485
Appendix B.11: Laboratory Infiltration Measurements Fitted with Horton Equations Using 10% Sand and 90% Biofilter Media.....	486
Appendix B.12: Laboratory Infiltration Measurements Fitted with Horton Equations Using 25% Sand and 75% Biofilter Media.....	487

Appendix B.13: Laboratory Infiltration Measurements Fitted with Horton Equations Using 50% Sand and 50% Biofilter Media.....	488
Appendix B.14: Laboratory Infiltration Measurements Fitted with Horton Equations Using Biofilter Media and Peat Mixture.....	489
Appendix B.15: Kruskal-Wallis Multiple Comparisons for the Saturated Infiltration Rates of Lab Compaction Tests Using Biofilter Media Only.....	490
Appendix B.16: Kruskal-Wallis Multiple Comparisons for the Saturated Infiltration Rates of Lab Compaction Tests Using 10% Sand and 90% Biofilter Media.....	492
Appendix B.17: Kruskal-Wallis Multiple Comparisons for the Saturated Infiltration Rates of Lab Compaction Tests Using 25% Sand and 75% Biofilter Media.....	494
Appendix B.18: Kruskal-Wallis Multiple Comparisons for the Saturated Infiltration Rates of Lab Compaction Tests Using 50% Sand and 50% Biofilter Media.....	496
APPENDIX C: SOIL MEDIA CHARACTERISTICS TEST RESULTS OF STORMWATER BIOINFILTRATION CONSTRUCTION SITES	497
Appendix C.1: Double-ring Infiltration Measurements at the Intersection of 15th St. E and 6th Ave. E. Fitted with Horton Equation.....	497
Appendix C.2: Double-ring Infiltration Measurements at Intersection of 17th Ave. E. and University Blvd E. Fitted with Horton Equation.....	498
Appendix C.3: Double-ring Infiltration Measurements at Intersection of 21th Ave. E. and University Blvd E. Fitted with Horton Equation.....	499
Appendix C.4: Double-ring Infiltration Measurements at Intersection of 25th Ave. E. and University Blvd E. Fitted with Horton Equation.....	500
Appendix C.5: Laboratory Infiltration Measurements Using Surface Soil from 15th St. E and 6th Ave. E. Fitted with Horton Equations.....	501
Appendix C.6: Laboratory Infiltration Measurements Using Surface Soil from 17th Ave. E and University Blvd E. Fitted with Horton Equations.....	502
Appendix C.7: Laboratory Infiltration Measurements Using Surface Soil from 21th Ave. E and University Blvd E. Fitted with Horton Equations.....	503
Appendix C.8: Laboratory Infiltration Measurements Using Surface Soil from 25th Ave. E and University Blvd E. Fitted with Horton Equations.....	504
Appendix C.9: Laboratory Infiltration Measurements Using Subsurface Soil from 15th St. E and 6th Ave. E. Fitted with Horton Equations.....	505

Appendix C.10: Laboratory Infiltration Measurements Using Subsurface Soil from 17th Ave. E and University Blvd E. Fitted with Horton Equations.	506
Appendix C.11: Laboratory Infiltration Measurements Using Subsurface Soil from 21th Ave. E and University Blvd E. Fitted with Horton Equations.	507
Appendix C.12: Laboratory Infiltration Measurements Using Subsurface Soil from 25th Ave. E and University Blvd E. Fitted with Horton Equations.	508
Appendix C.13: Kruskal-Wallis Multiple Comparisons for the Saturated Infiltration Rates of Lab Compaction Tests Using Surface Soil on 15th St. E and 6th Ave. E., Tuscaloosa, AL.	509
Appendix C.14: Kruskal-Wallis Multiple Comparisons for the Saturated Infiltration Rates of Lab Compaction Tests Using Surface Soil on 17th Ave. E. and University Blvd. E. (Tuscaloosa Physical Therapy), Tuscaloosa, AL.	511
Appendix C.15: Kruskal-Wallis Multiple Comparisons for the Saturated Infiltration Rates of Lab Compaction Tests Using Surface Soil on 21st Ave. E. and University Blvd. E. (Alberta Hand Carwash), Tuscaloosa, AL.	513
Appendix C.16: Kruskal-Wallis Multiple Comparisons for the Saturated Infiltration Rates of Lab Compaction Tests Using Surface Soil 25th Ave. E and University Blvd. E. (O'Reilly Auto Parts), Tuscaloosa, AL.	515
Appendix C.17: Kruskal-Wallis Multiple Comparisons for the Saturated Infiltration Rates of Lab Compaction Tests Using Surface Soils from Four Test Sites and Hand Compaction Conditions.	517
Appendix C.18: Kruskal-Wallis Multiple Comparisons for the Saturated Infiltration Rates of Lab Compaction Tests Using Surface Soils from Four Test Sites and Standard Proctor Compaction Conditions.	519
Appendix C.19: Kruskal-Wallis Multiple Comparisons for the Saturated Infiltration Rates of Lab Compaction Tests Using Surface Soils from Four Test Sites and Modified Proctor Compaction Conditions.	521
Appendix C.20: Kruskal-Wallis Multiple Comparisons for the Saturated Infiltration Rates of Lab Compaction Tests Using Subsurface Soil on 15th St. E and 6th Ave. E., Tuscaloosa, AL.	523
Appendix C.21: Kruskal-Wallis Multiple Comparisons for the Saturated Infiltration Rates of Lab Compaction Tests Using Subsurface Soil on 17th Ave. E. and University Blvd. E. (Tuscaloosa Physical Therapy), Tuscaloosa, AL.	525
Appendix C.22: Kruskal-Wallis Multiple Comparisons for the Saturated Infiltration Rates of Lab Compaction Tests Using Subsurface Soil on 21st Ave. E. and University Blvd E. (Alberta Hand Carwash), Tuscaloosa, AL.	527

Appendix C.23: Kruskal-Wallis Multiple Comparisons for the Saturated Infiltration Rates of Lab Compaction Tests Using Subsurface Soil 25th Ave. E and University Blvd E. (O’Reilly Auto Parts), Tuscaloosa, AL.	529
Appendix C.24: Kruskal-Wallis Multiple Comparisons for the Saturated Infiltration Rates of Lab Compaction Tests Using Surface Soils from Four Test Sites and Hand Compaction Conditions.....	531
Appendix C.25: Kruskal-Wallis Multiple Comparisons for the Saturated Infiltration Rates of Lab Compaction Tests Using Subsurface Soils from Four Test Sites and Standard Proctor Compaction Conditions.	533
Appendix C.26: Kruskal-Wallis Multiple Comparisons for the Saturated Infiltration Rates of Lab Compaction Tests Using Subsurface Soils from Four Test Sites and Modified Proctor Compaction Conditions.	535
Appendix C.27: Kruskal-Wallis Multiple Comparisons for the Saturated Infiltration Rates of Lab Compaction Tests Using Surface Soils from Four Test Sites and Hand Compaction Conditions, Combined Data.	537
Appendix C.28: Kruskal-Wallis Multiple Comparisons for the Saturated Infiltration Rates of Lab Compaction Tests Using Surface Soils from Four Test Sites, Standard and Modified Proctor Compaction Conditions with Combined Data.	539
Appendix C.29: Kruskal-Wallis Multiple Comparisons for the Saturated Infiltration Rates of Lab Compaction Tests Using Surface Soils from Four Test Sites, Standard and Modified Proctor Compaction Conditions with Combined Data.	541
Appendix C.30: Kruskal-Wallis Multiple Comparisons for the Saturated Infiltration Rates of Lab Compaction Tests Using Subsurface Soils from Four Test Sites, Hand Compaction Conditions with Combined Data.	543
Appendix C.31: Kruskal-Wallis Multiple Comparisons for the Saturated Infiltration Rates of Lab Compaction Tests Using Subsurface Soils from Four Test Sites, Standard and Modified Proctor Compaction Conditions with Combined Data.	545
Appendix C.32: Kruskal-Wallis Multiple Comparisons for the Saturated Infiltration Rates of Lab Compaction Tests Using Subsurface Soils from Four Test Sites, Hand, Standard, and Modified Proctor Compaction Conditions with Combined Data.	547
APPENDIX D: FLOWS CHANGES AND PARTICULATE RETENTION TESTS IN BIOFILTER MEDIA	549
Appendix D.1: Sand-Peat Mixture Nutrient Report	549
Appendix D.2: Lab Infiltration Measurements Using Sand and Peat Mixture (D50 = 340 um and Cu = 1.3)	553

Appendix D.3: Lab Infiltration Measurements Using Sand and Peat Mixture (D50 = 300 um and Cu = 3.5)	555
Appendix D.4: Lab Infiltration Measurements Using Sand and Peat Mixture (D50 = 300 um and Cu = 3.3)	557
Appendix D.5: Lab Infiltration Measurements Using Sand and Peat Mixture (D50 = 1500 um and Cu = 22)	559
Appendix D.6: Lab Infiltration Measurements Using Sand and Peat Mixture (D50 = 1500 um and Cu = 16)	561
Appendix D.7: Lab Infiltration Measurements Using Sand and Peat Mixture (D50 = 1500 um and Cu = 20)	563
Appendix D.8: Lab Infiltration Measurements Using Sand and Peat Mixture (D50 = 900 um and Cu = 11)	565
Appendix D.9: Lab Infiltration Measurements Using Sand and Peat Mixture (D50 = 850 um and Cu = 11)	567
Appendix D.10: Lab Infiltration Measurements Using Sand and Peat Mixture (D50 = 850 um and Cu = 11)	569
Appendix D.11: Lab Infiltration Measurements Using Sand and Peat Mixture (D50 = 900 um and Cu = 4)	571
Appendix D.12: Lab Infiltration Measurements Using Sand and Peat Mixture (D50 = 950 um and Cu = 4)	573
Appendix D.13: Lab Infiltration Measurements Using Sand and Peat Mixture (D50 = 1000 um and Cu = 4)	575
Appendix D.14: Lab Infiltration Measurements Using Sand and Peat Mixture (D50 = 1900 um and Cu = 2)	577
Appendix D.15: Lab Infiltration Measurements Using Sand and Peat Mixture (D50 = 1900 um and Cu = 2)	578
Appendix D.16: Lab Infiltration Measurements Using Sand and Peat Mixture (D50 = 1600 um and Cu = 2.5)	579
Appendix D.17: Lab Infiltration Measurements Using Kansas City Biofilte Media Fitted With Horton Equation.	581
Appendix D.18: Lab Infiltration Measurements Using Wisconsin Biofilte Media -1 Fitted With Horton Equation.	582

Appendix D.19: Lab Infiltration Measurements Using Wisconsin Biofilte Media -2 Fitted With Horton Equation.	583
Appendix D.20: Infiltration Test Through Peat (10, 25, and 50%) and Sand Mixture (D50 = 300 – 350 um) and Different Levels of Compaction.....	584
Appendix D.21: Infiltration Test Through Peat (10, 25, and 50%) and Sand Mixture (D50 = 1250 – 1500 um) and Different Levels of Compaction.....	588
Appendix D.22: Infiltration Test Through Peat (10, 25, and 50%) and Sand Mixture (D50 = 850 – 900 um) and Different Levels of Compaction.....	592
Appendix D.23: Infiltration Test Through Peat (10, 25, and 50%) and Sand Mixture (D50 = 900 – 975 um) and Different Levels of Compaction.....	596
Appendix D.24: Infiltration Test Through Peat (10, 25, and 50%) and Sand Mixture (D50 = 1625 – 1875 um) and Different Levels of Compaction.....	600
Appendix D. 25: Infiltration Data Used in Full 23 Factorial Designs for Sand-peat Mixture.	604
Appendix D. 26: Controlled Lab Column Test Sand-Peat Media (triplicate tests for each condition).....	607
Appendix D.27: 50% Peat and 50% Sand (Mixture D50 = 300 um and Cu = 3), Hand Compaction ($\rho = 0.74 \text{ g/cm}^3$), Low Concentration Regression Statics.	610
Appendix D.28: 50% Peat and 50% Sand (Mixture D50 = 300 um and Cu = 3), Hand Compaction ($\rho = 0.74 \text{ g/cm}^3$), High Concentration Regression Statics.....	610
Appendix D.29: 50% Peat and 50% Sand (Mixture D50 = 300 um and Cu = 3), Modified Proctor Compaction ($\rho = 1.03 \text{ g/cm}^3$), Low Concentration Regression Statics.	611
Appendix D.30: 50% Peat and 50% Sand (Mixture D50 = 300 um and Cu = 3), Modified Proctor Compaction ($\rho = 1.03 \text{ g/cm}^3$), High Concentration Regression Statics.....	611
Appendix D.31: 50% Peat and 50% Surface Soil (Mixture D50 = 325 um and Cu = 7), Hand Compaction ($\rho = 0.85 \text{ g/cm}^3$), Low Concentration Regression Statics.	612
Appendix D.32: 50% Peat and 50% Surface Soil (Mixture D50 = 325 um and Cu = 7), Hand Compaction ($\rho = 0.85 \text{ g/cm}^3$), High Concentration Regression Statics.....	612
Appendix D.33: 50% Peat and 50% Surface Soil (Mixture D50 = 325 um and Cu = 7), Modified Proctor Compaction ($\rho = 1.01 \text{ g/cm}^3$), Low Concentration Regression Statics..	613
Appendix D.34: 50% Peat and 50% Surface Soil (Mixture D50 = 325 um and Cu = 7), Modified Proctor Compaction ($\rho = 1.01 \text{ g/cm}^3$), High Concentration Regression Statics.	613

Appendix D.35: 10% Peat and 90% Sand (Mixture D50 = 1500 um and Cu = 22), Hand Compaction ($\rho = 1.61 \text{ g/cm}^3$), Low Concentration Regression Statics.	614
Appendix D.36: 10% Peat and 90% Sand (Mixture D50 = 1500 um and Cu = 22), Hand Compaction ($\rho = 1.61 \text{ g/cm}^3$), High Concentration Regression Statics.....	614
Appendix D.37: 10% Peat and 90% Sand (Mixture D50 = 1500 um and Cu = 22), Modified Proctor Compaction ($\rho = 1.63 \text{ g/cm}^3$), Low Concentration Regression Statics.	615
Appendix D.38: 10% Peat and 90% Sand (Mixture D50 = 1500 um and Cu = 22), Modified Proctor Compaction ($\rho = 1.63 \text{ g/cm}^3$), High Concentration Regression Statics.	615
Appendix D.39: 10% Peat and 90% Sand (Mixture D50 = 340 um and Cu = 1.3), Hand Compaction ($\rho = 1.28 \text{ g/cm}^3$), Low Concentration Regression Statics.	616
Appendix D.40: 10% Peat and 90% Sand (Mixture D50 = 340 um and Cu = 1.3), Hand Compaction ($\rho = 1.28 \text{ g/cm}^3$), High Concentration Regression Statics.....	616
Appendix D.41: 10% Peat and 90% Sand (Mixture D50 = 340 um and Cu = 1.3), Modified Proctor Compaction ($\rho = 1.35 \text{ g/cm}^3$), Low Concentration Regression Statics.	617
Appendix D.42: 10% Peat and 90% Sand (Mixture D50 = 340 um and Cu = 1.3), Modified Proctor Compaction ($\rho = 1.35 \text{ g/cm}^3$), High Concentration Regression Statics.....	617
Appendix D.43: Tuscaloosa Surface Soil (D50 = 270 um and Cu = 37), Hand Compaction ($\rho = 1.42 \text{ g/cm}^3$), Low Concentration Regression Statics.	618
Appendix D.44: Tuscaloosa Surface Soil (D50 = 270 um and Cu = 37), Hand Compaction ($\rho = 1.42 \text{ g/cm}^3$), High Concentration Regression Statics.	618
Appendix D.45: Tuscaloosa Surface Soil (D50 = 270 um and Cu = 37), Modified Proctor Compaction ($\rho = 1.67 \text{ g/cm}^3$), Low Concentration Regression Statics.	619
Appendix D.46: Tuscaloosa Surface Soil (D50 = 270 um and Cu = 37), Modified Proctor Compaction ($\rho = 1.67 \text{ g/cm}^3$), High Concentration Regression Statics.....	619
Appendix D.47: 50% Peat and 50% Sand (Mixture D50 = 1300 um and Cu = 20), Hand Compaction ($\rho = 1.1 \text{ g/cm}^3$), Low Concentration Regression Statics.	620
Appendix D.48: 50% Peat and 50% Sand (Mixture D50 = 1300 um and Cu = 20), Hand Compaction ($\rho = 1.1 \text{ g/cm}^3$), High Concentration Regression Statics.....	620
Appendix D.49: 50% Peat and 50% Sand (Mixture D50 = 1300 um and Cu = 20), Modified Proctor Compaction ($\rho = 1.1 \text{ g/cm}^3$), Low Concentration Regression Statics.	621
Appendix D.50: 50% Peat and 50% Sand (Mixture D50 = 1300 um and Cu = 20), Modified Proctor Compaction ($\rho = 1.1 \text{ g/cm}^3$), High Concentration Regression Statics.	621

Appendix D.51: 10% Peat and 90% Sand (Mixture D50 = 1900 um and Cu = 2), Hand Compaction ($\rho = 1.52 \text{ g/cm}^3$), Low Concentration Regression Statics.	622
Appendix D.52: 10% Peat and 90% Sand (Mixture D50 = 1900 um and Cu = 2), Hand Compaction ($\rho = 1.52 \text{ g/cm}^3$), High Concentration Regression Statics.....	622
Appendix D.53: 10% Peat and 90% Sand (Mixture D50 = 1900 um and Cu = 2), Modified Proctor Compaction ($\rho = 1.58 \text{ g/cm}^3$), Low Concentration Regression Statics.	623
Appendix D.54: 10% Peat and 90% Sand (Mixture D50 = 1900 um and Cu = 2), Modified Proctor Compaction ($\rho = 1.58 \text{ g/cm}^3$), High Concentration Regression Statics.....	623
Appendix D.55: 50% Peat and 50% Sand (Mixture D50 = 1600 um and Cu = 2.5), Hand Compaction ($\rho = 0.96 \text{ g/cm}^3$), Low Concentration Regression Statics.	624
Appendix D.56: 50% Peat and 50% Sand (Mixture D50 = 1600 um and Cu = 2.5), Hand Compaction ($\rho = 0.96 \text{ g/cm}^3$), High Concentration Regression Statics.....	624
Appendix D.57: 50% Peat and 50% Sand (Mixture D50 = 1600 um and Cu = 2.5), Modified Proctor Compaction ($\rho = 1.23 \text{ g/cm}^3$), Low Concentration Regression Statics.	625
Appendix D.58: 50% Peat and 50% Sand (Mixture D50 = 1600 um and Cu = 2.5), Modified Proctor Compaction ($\rho = 1.23 \text{ g/cm}^3$), High Concentration Regression Statics.....	625
Appendix D. 59: Particle Size Distribution Plots of Influent vs Effluent Concentrations ..	626
Appendix D.60: One-way ANOVA Comparison for Infiltration Rates Through 10% Peat and 90% Sand Mixture (D50 = 0.3 mm and Cu = 3).	628
Appendix D.61: One-way ANOVA Comparison for for Infiltration Rates Through 10% Peat and 90% Sand Mixture (D50 = 0.35 mm and Cu = 1).	633
Appendix D.62: One-way ANOVA Comparison for for Infiltration Rates Through Tuscaloosa Surface Soil (D50 = 0.3 mm and Cu = 37).....	635
Appendix D.63: One-way ANOVA Comparison for Infiltration Rates Through 50% Peat and 50% Tuscaloosa Surface Soil Mixture (D50 = 0.3 mm and Cu = 6.8).....	638
Appendix D.64: One-way ANOVA Comparison for Infiltration Rates Through 50% peat and 50% sand (D50 = 1.3 mm and Cu = 19).....	640
Appendix D.65: One-way ANOVA Comparison for Infiltration Rates Through 10% Peat and 90% Sand Mixture (D50 = 1.5 mm and Cu = 22).	642
Appendix D.66: One-way ANOVA Comparison for Infiltration Rates Through 50% Peat and 50% Sand Mixture (D50 = 1.6 mm and Cu = 2.5).	644
Appendix D.67: One-way ANOVA Comparison for Infiltration Rates Through 10% peat and 90% sand (D50 = 1.9 mm and Cu = 2).....	647

Appendix D.68: One-way ANOVA Comparison for Infiltration Rates Through Pea Gravel vs Coarse Gravel. Low Solid Concentration.	650
Appendix D.69: One-way ANOVA Comparison for Infiltration Rates Through Pea Gravel vs Coarse Gravel. High Solid Concentration.....	654
APPENDIX E:SAND-PEAT COLUMN AND SMARTDRAIN™ FIELD PERFORMANCE	658
Appendix E.1: Full-factorial Data Analysis for Peat-Sand Media Particle Retention Experiments.....	658
Appendix E.2: SmartDrain™ Field Performance Solid 12 to 30 um Particle Size Analysis.	663
Appendix E.3: SmartDrain™ Field Performance Solid 30 to 60um Particle Size Analysis.	665
Appendix E.4: SmartDrain™ Field Performance Solid 60 to 120um Particle Size Analysis.	666
Appendix E.5: SmartDrain™ Field Performance Solid 120 to 250um Particle Size Analysis.	667
Appendix E.6: SmartDrain™ Field Performance Solid 250 to 1180 um Particle Size Analysis.	668
Appendix E.7: Underdrain SmartDrain™ Field Performance Solid 0.45 to 3 um Particle Size Analysis.....	669
Appendix E.8: SmartDrain™ Field Performance Solid 3 to 12 um Particle Size Analysis	671
Appendix E.9: SmartDrain™ Field Performance Solid 12 to 30 um Particle Size Analysis.....	671
Appendix E.10: SmartDrain™ Field Performance Solid 30 to 60 um Particle Size Analysis.....	672
Appendix E.11: SmartDrain™ Field Performance Solid 60 to 120 um Particle Size Analysis.....	673
Appendix E.12: SmartDrain™ Field Performance Solid 120 to 250 um Particle Size Analysis.....	674
Appendix E.13: SmartDrain™ Field Performance Solid 250 to 1180 um Particle Size Analysis.....	674

Appendix E.14: SmartDrain™ Field Performance Solid > 1180 um Particle Size Analysis 676

Appendix E.15: SmartDrain™ Field Performance SSC Influent Vs. Underdrain 677

LIST OF TABLES

Table 1. Sand Filter Removal efficiencies (percent) (adapted from California Stormwater BMP Handbook 2003).....	16
Table 2. Soil Texture Effects on Bioretention Facility Design (Source: Atchison et al. 2004)....	23
Table 3. Example Underdrain Water Balance (WinSLAMM model calculations)	26
Table 4. Horton's Parameters for Different Types of Soil (Source: Akan 1993).....	33
Table 5. Parameters Used to Estimate Infiltration Rates (Source: Massman 2003).....	35
Table 6. Example Factorial Experimental Analysis for Field Project Investigating Infiltration into Disturbed Urban Soils (Source: Pitt et al. 1999a).....	52
Table 7. Factorial Experimental Design for two Factors and Four Experiments	53
Table 8. Laboratory Column Infiltration Test Results.....	61
Table 9. Outflow Balance of the Drain-Belt ® System during an Observation Period.....	74
Table 10. Design Values for Equation1	77
Table 11. Saturated Hydraulic Conductivity (in/hr) of Different Grain Size Sand (US EPA 1986)	78
Table 12. Design Values for Storage Volume Calculation.....	81
Table 13. Drainage Date and Exposure Period for the Algae in the Biofilter Device	88
Table 14. Linear Regression Analysis Results for SmartDrain™ Drainage Characteristics Test.93	
Table 15. Linear Regression Analysis Result for Clogging Tests.....	95
Table 16. Linear Regression Analysis Result for the Biofouling Tests.....	106
Table 17. Experimental Factors and their Levels.	108

Table 18. Flowrate Data Used in Full 2 ³ Factorial Designs.	109
Table 19. Estimated Effects and Coefficients for Q (L/s) (coded units).	111
Table 20. Unusual Observations for Q (L/s).....	111
Table 21. Effects and Half-Effects Results.....	114
Table 22. Standard Error Calculations for SmartDrain™ Flowrate Tests.....	116
Table 23. Two-Tailed T-Test for Clean Water (Trial #1) vs Dirty Water (Trial #32) for Clogging Tests.	119
Table 24. Experimental Factors and their Levels.	121
Table 25. Flowrate Data Used in Full 2 ² Factorial Designs	121
Table 26. Estimated Effects and Coefficients for Q (L/s) (coded units). Estimated Effects and Coefficients for Q (L/s) (coded units).....	122
Table 27. Unusual Observations for Q (L/s).....	123
Table 28. Effects and Half-Effects Results.....	125
Table 29. Two-tailed t-test for Clean (Trial#1) vs Dirty Water (Trial#7)	128
Table 30. Experimental Factors and their Levels	130
Table 31. Flowrate Data Used in Full 2 ² Factorial Designs	130
Table 32. Estimated Effects and Coefficients for Q (L/s) (coded units) for the Biofouling Tests	131
Table 33. Unusual Observations for Q (L/s).....	132
Table 34. Effects and Half-Effects Results.....	132
Table 35. Drainage Area and Land Use Breakdown	142
Table 36. Soil Media Characteristics Obtained from Four Locations along the Biofilter.....	148
Table 37. General Relationship of Soil Bulk Density to Root Growth on Soil Texture (USDA 2008).	151
Table 38. Summary of the Soil Nutrient Report for Shelby Park Biofilter Media (single composite analysis from four subsamples).....	152

Table 39. Critical Soil Test Values Used by the Auburn University Soil Testing Laboratory (Adams et al 1994).....	153
Table 40. Field Infiltration Tests using Small-Scale Infiltrimeters.	162
Table 41. Infiltration Measurement at Poned Locations in Biofilter.....	163
Table 42. Various Mixtures of Media and Filter Sand Used for Laboratory Infiltration Measurements.	167
Table 43. Laboratory Infiltration Tests Using Biofilter Media Only at Different Compaction Levels.....	170
Table 44. Laboratory Infiltration Tests Using a Mixture of 10% Filter Sand and 90% Biofilter Media at Different Compaction Levels.....	170
Table 45. Laboratory Infiltration Tests Using a Mixture of 25 % Filter Sand and 75% Biofilter Media at Different Compaction Levels.....	171
Table 46. Laboratory Infiltration Tests Using a Mixture of 50% Filter Sand and 50% Biofilter Media at Different Compaction Levels.....	171
Table 47. Laboratory Infiltration Tests Using Biofilter Soil and Peat at Different Compaction Levels.....	172
Table 48. Experimental Factors and their Levels.	174
Table 49. Infiltration Data Used In Full 2 ² Factorial Designs.	174
Table 50. Estimated Effects and Coefficients for Fc (in/hr) (coded units).....	176
Table 51. Shows the Results of the Effects and Half-Effects.	178
Table 52. Stand Error Calculations for Lab Infiltration Measurements Results.....	179
Table 53. Calculated Effects and Standard Errors for the 22 Factorial Design.....	180
Table 54. Analysis of Variance for Fc (in/hr) (coded units).....	181
Table 55. Various Mixtures of Biofilter Soil Media and Peat Used for Laboratory Infiltration Measurements.	189
Table 56. Soil Media Characteristics Obtained from the Surface of Bioinfiltration Sites.	205
Table 57. Soil Media Characteristics Obtained from the Subsurface of Bioinfiltration Sites....	206
Table 58. Summary of the Surface and Subsurface Soil Texture Reports for Bioinfiltration Sites.	212

Table 59. Summary of the Surface and Subsurface Soil Nutrient Report for Bioinfiltration Sites.	215
Table 60. Double-ring Infiltration Measurement at Bioinfiltration Sites.	217
Table 61. Borehole Infiltration Measurement at Bioinfiltration Sites.Horton's Parameter	218
Table 62. Laboratory Infiltration Tests Using Surface Soil on 15th St. E and 6th Ave. E. at Different Compaction Levels.....	221
Table 63. Laboratory Infiltration Tests Using Surface Soil on 17th Ave. E. and University Blvd. E. at Different Compaction Levels.	221
Table 64. Laboratory Infiltration Tests Using Surface Soil on 21st Ave. E. and University Blvd E. at Different Compaction Levels.	222
Table 65. Laboratory Infiltration Tests Using Surface Soil on 25th Ave. E and University Blvd E. at Different Compaction Levels.....	222
Table 66. Laboratory Infiltration Tests Using Subsurface Soil on 15 th St. E and 6 th Ave. E. at Different Compaction Levels.....	225
Table 67. Laboratory Infiltration Tests Using Subsurface Soil on 17th Ave. E. and University Blvd E at Different Compaction Levels.....	225
Table 68. Laboratory Infiltration Tests Using Subsurface Soil on 21st Ave. E. and University Blvd E. at Different Compaction Levels.....	226
Table 69. Laboratory Infiltration Tests Using Subsurface Soil from the Intersection of 25th Ave. E and University Blvd E. at Different Compaction Levels.	226
Table 70. Bioinfiltration Test Site Locations.....	231
Table 71. Kruskal-Wallis (KW) Multiple Comparisons of Combined Saturated Infiltration Rates Using Surface Soil.	239
Table 72. Kruskal-Wallis (KW) Multiple Comparisons of Combined Saturated Infiltration Rates Using Subsurface Soils.	240
Table 73. Filter Sand Components and Tuscaloosa Soil Media Characteristics	246
Table 74. Standard Biofilter Samples Characteristics	247
Table 75. Actual Biofilter Material Characteristics.....	249
Table 76. Analytical Methods and Detection Limits/Ranges	259

Table 77. Summary of the Sand and Peat Mixture Summary Nutrients and Other Constituents Report.....	262
Table 78. Test Mixture Descriptions (Fifteen Replicates in Each Test Series) (corresponding to the numbered samples on the box and whisker plot in Figure 121).	267
Table 79. Summary of Biofilter Media Texture Report.	268
Table 80. Kansas City and North Carolina Biofilter Media Nutrient and Other Constituent Concentrations.	269
Table 81. Laboratory Infiltration Tests Using North Carolina Biofilter Media.	271
Table 82. Laboratory Infiltration Tests Using Kansas City Soil Media.	272
Table 83. Laboratory Infiltration Tests Using Wisconsin Biofilter Media-1.	273
Table 84. Laboratory Infiltration Tests Using Wisconsin Biofilter Media-2.	274
Table 85. Test Mixture Descriptions (mixture: D50 = 300 to 340 um) Shown in Figure 125 ...	276
Table 86. Test Mixture Descriptions (mixture: D50 = 1600-1900 um).....	278
Table 87. Laboratory Column Infiltration Test Results.....	278
Table 88. Infiltration Data Used in Full 2 ⁴ Factorial Designs (showing replicates).....	280
Table 89. Estimated Effects and Coefficients for log (F _C) in/hr (coded).....	283
Table 90. Analysis of Variance for log (FC) -in/hr (coded units).	284
Table 91 shows the actual biofilter media characteristics and saturated infiltration rates through them.....	284
Table 92. Biofilter Media Characteristics.....	285
Table 93. Unusual Observations for log (F _C) in/hr.....	286
Table 94. Shows the Results of the Effects and Half-Effects.	289
Table 95. Calculated Flow Rates Using the Final Factorial Model.....	292
Table 96. Estimated Effects and Coefficients for Log F _C (in/hr) (coded units) and Using a Sand-peat Mixture.....	297
Table 97. Shows the Results of the Effects, Half-Effects, and Using a Sand-peat Mixture.....	298

Table 98. Calculated Infiltration Rates Using a Factorial Model Rate (in/hr).....	299
Table 99. Actual Biofilter Media Infiltration Rate (in/hr)	299
Table 100. Laboratory Column Coarse Media (average concentrations).....	305
Table 101. Approximate Flow Rates through the Coarse Media for the Different Tests.....	306
Table 102. Test Mixture Descriptions.	308
Table 103. Laboratory Column Coarse Media (average concentration).....	310
Table 104. Statistical Summary of Final Combined Results	311
Table 105. Land Use Description for McDonalds Site on 15th St. E and 6th Ave. E., Tuscaloosa, AL.	315
Table 106. Land Use Description for Selected Cedar Crest Neighborhood, Tuscaloosa, AL....	320
Table 107. Estimated Effects and Coefficients for SSC (mg/L) (coded units).....	325

LIST OF FIGURES

Figure 1. Cross-Section of a Bioinfiltration Stormwater Treatment Device (Source: VUSP).	18
Figure 2. Conventional Underdrain Effects on Water Balance (Robert Pitt, Unpublished).....	25
Figure 3. No Underdrain Effects on ` Balance (Robert Pitt, Unpublished).....	25
Figure 4. Example Restricted Underdrain Effects on Water Balance (WinSLAMM calculations).	26
Figure 5. Variables in the Green-Ampt Infiltration Model (Source: Chow 1988).	34
Figure 6. Probability Plots (Pitt et al. 1999a).....	52
Figure 7. Example Grouped Box and Whisker Plot of Influent vs. Effluent SSC Test Results from Sand and Peat Columns.....	55
Figure 8. Example of Linear Regression for Stage- discharge Relation Plots Using Different Length of Smartdrain™ Material.....	57
Figure 9. Probability Plot of The Residuals for Linear Regression of 9.4 ft.....	57
Figure 10. Production Function Plots for the Different Soil Infiltration Conditions Examined for Residential Drainage Area (Pitt et al 2013 in press).....	66
Figure 11. Close-Up Photograph of SmartDrain™ Material Showing the Microchannels (SmartDrain LLC).....	68
Figure 12. SmartDrain™ Installation at the University of Pennsylvania Shoemaker Plaza Project.	69
Figure 13. Biofilter Area Located on Shoemaker Plaza Landscape Project Soon after Planting (Source: Meliora Environmental Design, LLC, Photo Used with Permission).....	70
Figure 14. Detail of a Typical Section View of Biofilter Facility (Source: Meliora Environmental Design, LLC, Photo Used with Permission).....	71
Figure 15. The SmartDrain Belt ® System during Construction (Morhard 2006).....	72

Figure 16. Runoff Characteristics of the SmartDrain™ Belt ® System during an Observation Period (Morhard 2006).	73
Figure 17. Flow (L/min) of the Studied Drainage Systems during a Precipitation Event (Morhard 2006).	74
Figure 18. Scheme of Hooghoudt Equation.....	76
Figure 19. Underdrain Spacing vs Hydraulic Conductivity for 24-hr Drain Period.....	79
Figure 20. Underdrain Spacing vs Hydraulic Conductivity for 72-hr Drain Period.....	79
Figure 21. Cross-Section of a Typical Biofilter Facility.....	80
Figure 22. Drainage Rate vs Biofilter Basin Area	81
Figure 23. Pilot-Scale Biofilter Test to Measure Flow Rates as a Function of SmartDrain™ Length and Slope.	83
Figure 24. Particle Size Distributions of the Sand Filter Media Material and the U.S Sil-Co-Sil®250 (Fine Material on Graph) Used for the Clogging Test.	85
Figure 25. SmartDrain™ Clogging Test Setups with the Deep Water Pilot-Scale Biofilter.....	86
Figure 26. Pilot-scale Biofilter System Setups for SmartDrain™ Material Biofouling Test	89
Figure 27. Example of Stage- discharge Relation Plots for SmartDrain™ Length Equals 9.4 ft and Five Different Slopes (data combined for all slopes, as the slope was not found to significantly affect the discharge rates).	90
Figure 28. Stage-Discharge Relationship Plots For Different Lengths of SmartDrain™ Tested For Five Different Slopes Used to Determine the Drainage Characteristics of SmartDrain™ Belts.	92
Figure 29. Sil-Co-Sil®250 load (kg/m ²) vs. Equation Slope Coefficients for the Clogging Tests.	96
Figure 30. Turbidity Measurements Plots Taken from the Effluent of the Device during the Particulate Clogging Tests.	97
Figure 31. Probability Plot of Effluent Turbidity for the Particulate Clogging Tests (Trials 1, 16, and 32).	98
Figure 32. Box Plot Showing the Effluent Turbidity for Different Test Trials.	98
Figure 33. Moody diagram showing the Darcy-Weisbach friction factor plotted against Reynolds number for various roughness values.	100

Figure 34. Reynolds No. vs. Flowrate Relationships for the Particulate Clogging Tests (Overlay Graphs for Different Test Trials).....	102
Figure 35. Probability Plot of Effluent Turbidity for the Particulate Clogging Tests (Trial 1, 16, and 32).	102
Figure 36. Box Plot Showing Reynolds Number for Different Test Trials.....	103
Figure 37. Influent Turbidity (NTU) vs Flowrate for the Biofouling Tests.	104
Figure 38. Effluent Turbidity (NTU) vs Flowrate for the Biofouling Tests.....	104
Figure 39. Stage-discharge Relationship Plots for the Biofouling Tests.....	106
Figure 40. Equation Slope Coefficients vs Number of Trials for the Biofouling Tests.	107
Figure 41. Normal Probability Plots of the Effect.....	110
Figure 42. Main Effect Plots for SmartDrain™ Flowrate.....	112
Figure 43. Probability Plot of Flowrate for SmartDrain™ Length = 1.1ft (0.34 m) Slopes 0%, and 12%.	112
Figure 44. Interaction Plots for SmartDrain™ Flowrate.....	113
Figure 45. Scatter Plot of Observed Q (L/s) vs Fitted log (Q), L/s.....	117
Figure 46. Residuals Analysis Plot.....	118
Figure 47. Box and Whisker Plots of Flowrate Data Using Clean Water (Trial#1) and Dirt Water (Trial#32) for Particulate Clogging Tests.....	120
Figure 48. Normal Probability Plots of the Effect.....	122
Figure 49. Main Effect Plots for SmartDrain™ Flowrate.....	123
Figure 50. Interaction Plots for SmartDrain™ Flowrate.....	124
Figure 51. Scatter Plot of Observed vs. Fitted Flowrate (L/s).....	126
Figure 52. Residuals Analysis Plot.....	127
Figure 53. Box and Whisker Plots of Flowrate Data Using Clean Water (Trial#1) and Dirt Water (Trial#32) for Biofouling Tests.....	129
Figure 54. Normal Probability Plots of the Effect.....	131

Figure 55. Scatter Plot of Observed vs Fitted Flowrate (L/s).....	134
Figure 56. Residuals Analysis Plot.....	135
Figure 57. Cross-Section of a Typical Biofilter Facility.....	136
Figure 58. Three Dimensional Plots of No. of SmartDrains or Conventional Underdrains Required for Different Biofilter Area and Saturated Hydraulic ConductivityConductivities.	138
Figure 59. Flowsheet for the Field and Lab Infiltration Study at a Biofilter Facility.....	141
Figure 60. Aerial Photograph of Biofilter Location (Map by Google Map).	143
Figure 61. Drainage Areas Photographs Tributary to the Biofilter.	144
Figure 62. Photographs Showing the Infiltration Measurement Setup and In-Situ Soil Density Measurements at Shelby Park Biofilter.	146
Figure 63. A Close Up of Turf-Tec Infiltrometer (available from Turf-Tec International).....	147
Figure 64. Particle Size Distributions for the Biofilter Media from Four Locations along the Biofilter.....	149
Figure 65. Ponded Water on the Biofilter Surface Observed after Rainfall Event.....	157
Figure 66. Lab Column Construction for Infiltration Tests (Left to Right): Bottom of the Columns Secured With a Fiberglass Window Screen (Upper Left), Soil Media (Lower Left), and Media Compaction.....	160
Figure 67. Laboratory Column Setup.	161
Figure 68. Example Biofilter Surface Small-scale Infiltration Measurements Fitted With the Horton Equation.....	165
Figure 69. Example Actual Rain Event Ponded Infiltration Measurements Fitted With Horton Equation.	165
Figure 70. Box and Whisker Plots of the Different Test Conditions, Comparing Different Compaction Conditions with Varying Amounts of Sand Amendments (hand, standard proctor, and modified proctor compaction for each amendment condition).....	167
Figure 71. Example Laboratory Infiltration Measurements Fitted with Horton Equations.....	169
Figure 72. Example Laboratory Infiltration Measurements Fitted With Horton Equation, using Peat and Standard Proctor Compaction Method.....	173
Figure 73. Probability Plot to Identify Important Factors Affecting the Infiltration Rate through a Media Mixture.	175

Figure 74. Main Effects Plot for the Two Factors.	176
Figure 75. Interaction Plot between Different Factors.....	177
Figure 76. Observed vs Fitted Fc Values.....	182
Figure 77. Residuals Analysis Plot.....	183
Figure 78. Multiple Comparison Plots of Laboratory Infiltration Measurements Using Biofilter Media Only.....	185
Figure 79. Multiple Comparison Plots of Laboratory Infiltration Measurements Using 10% Sand and 90% Biofilter Media Mixture.....	186
Figure 80. Multiple Comparison Plots of Laboratory Infiltration Measurements Using 25% Sand and 75% Biofilter Media Mixture.....	187
Figure 81. Multiple Comparison Plots of Laboratory Infiltration Measurements Using 50% Sand and 50% Biofilter Media Mixture.....	188
Figure 82. Multiple Comparison Plots of Laboratory Infiltration Measurements Using Biofilter Soil Only vs Different Percentages of Peat Added to It.....	190
Figure 83. Flow Sheet for the Field and Lab Infiltration Study at Bioinfiltration Sites.....	197
Figure 84. Aerial Photograph of Bioinfiltration Site, McDonalds on 15th St. E and 6th Ave. E., Tuscaloosa, AL, Pre-Tornado (Map by Google Map).....	198
Figure 85. View of a Tornado Affected Area near McDonalds on 15th St. E and 6th Ave. E., Bioinfiltration Site.....	198
Figure 86. Aerial Photograph of Bioinfiltration Site, Double-ring and Borehole Infiltration Test Installation at McDonalds on 15th St. E and 6th Ave. E., Tuscaloosa, AL.....	200
Figure 87. Aerial Photograph of Bioinfiltration Site and Double-ring Infiltration Measurement Installation on 17th Ave. E. and University Blvd. E. (Tuscaloosa Physical Therapy).....	201
Figure 88. Aerial Photograph of Bioinfiltration Site, Double-ring Infiltration and Borehole Measurement Installations on 21st Ave. E. and University Blvd. E. (Alberta Hand Carwash). 202	
Figure 89. Aerial Photograph of Bioinfiltration Site, Double-ring Infiltration and Borehole Measurement Installations on 25th Ave. E. and University Blvd E. (O'Reilly Auto Parts).	203
Figure 90. Particle Size Distributions for the Surface Soil Media from Bioinfiltration Sites.	205
Figure 91. Particle Size Distributions for the Subsurface Soil Media from Bioinfiltration Study Sites.....	206

Figure 92. Borehole Marking, Borehole Drilling, Double-ring and Borehole Infiltration Measurement Installations at McDonalds on 15th St. and 6th Ave. Ave. E., Tuscaloosa, AL. .	208
Figure 93. Borehole Marking, Borehole Drilling, and Borehole Infiltration Measurement Installations on 21th Ave. and University Blvd E. (Alberta Hand Carwash).....	209
Figure 94. Laboratory Setup for Nine Soil Infiltration Test Columns.....	211
Figure 95. Example of Surface Infiltration Measurements Fitted With Horton Equation.....	216
Figure 96. Example of Borehole Infiltration Measurements Fitted With Horton Equation.	218
Figure 97. Example of Lab Infiltration Measurements Using Surface Soil Fitted with Horton’s Equation.	220
Figure 98. Example of Lab Infiltration Measurements Using Subsurface Soil Fitted With Horton Equation.	224
Figure 99. Multiple Comparison Plots of Laboratory Infiltration Measurements Using Surface Soil on 15th St. E and 6th Ave. E., Tuscaloosa, AL.....	228
Figure 100. Multiple Comparison Plots of Laboratory Infiltration Measurements Using Surface Soil on 17th Ave. E. and University Blvd. (Tuscaloosa Physical Therapy), Tuscaloosa, AL....	229
Figure 101. Multiple Comparison Plots of Laboratory Infiltration Measurements Using Surface Soils from Four Test Sites and Hand Compaction Tests.	230
Figure 102. Multiple Comparison Plots of Laboratory Infiltration Measurements Using Subsurface Soil on 15th St. E and 6th Ave. E., Tuscaloosa, AL.....	231
Figure 103. Multiple Comparison Plots of Laboratory Infiltration Measurements Using Subsurface Soil on 17th Ave. E. and University Blvd. (Tuscaloosa Physical Therapy), Tuscaloosa, AL.....	232
Figure 104. Multiple Comparison Plots of Laboratory Infiltration Measurements Using Subsurface Soils from Four Test Sites and Hand Compaction Tests.	233
Figure 105. Box and Whisker Plots Comparing Saturated Soil Infiltration Rates (in/hr).	235
Figure 106. Multiple Comparison Plots of Laboratory Infiltration Measurements using Surface Soil from Four Test Sites, Standard and Modified Proctor Compaction Conditions with Combined Data.	237
Figure 107. Multiple Comparisons Plots of Laboratory Infiltration Measurements using Subsurface Soil from Four Test Sites, Hand, Standard, and Modified Proctor Compaction Conditions with Combined Data.....	238

Figure 108. Sand Media Obtained from Atlanta Sand and Supply (From Upper Left to Upper Right), Sand from Ground Floor Sand Supplier, Northport, AL (Lower Left), Tuscaloosa Surface Soil and Tuscaloosa Subsurface Soils (Lower Middle and Lower Right).....	245
Figure 109. Particle Size Distributions of Filter Sand Components and Tuscaloosa Soil.....	246
Figure 110. Biofilter Media Mixtures (From Left To Right): North Carolina Biofilter Media, Kansas City Biofilter Media from Test Sites 1 and 2, and Wisconsin Biofilter Media from Test Sites 1 and 2.....	247
Figure 111. Particle Size Distributions of Actual Biofilter Material.....	248
Figure 112. Lab Column Infiltration Tests (Left To Right): Bottom of the Columns Secured with a Fiberglass Window Screen (Upper Left), Biofilter Media (Lower Left), and Media Compaction.....	250
Figure 113. Laboratory Column Setup for Infiltration Measurements.....	251
Figure 114. Particle Size Distribution of the Three Individual Components Used to Create the Solid Mixture and the Influent Water.....	253
Figure 115. Particle Size Distribution of the Solid Mixture (not including the river water component).....	254
Figure 116. Particle Size Distribution of the Coarse Media.....	255
Figure 117. USGS/Dekaport Teflon™ Cone Splitter.....	256
Figure 118. Flow Sheet for the Solids Analysis.....	258
Figure 119. Infiltration Measurements for 10% Peat and 90% Sand.....	265
Figure 120. Infiltration Measurements for 50% Peat and 50% Sand.....	265
Figure 121. Box and Whisker Plots of the Different Test Conditions, Comparing Different Compaction Conditions with Varying Amounts of Peat Amendments.....	266
Figure 122. Example of Laboratory Infiltration Test Results Using North Carolina Media.....	270
Figure 123. Example of Laboratory Infiltration Test Results Using Kansas City Media.....	271
Figure 124. Example of Laboratory Infiltration Test Results Using Wisconsin Biofilter Media.....	272
Figure 125. Multiple Comparison Plots of Laboratory Infiltration Measurements Using Sand and Peat Mixture (mixture D50 = 300 - 350 um) for Different Compaction Levels.....	276

Figure 126. Multiple Comparison Plots of Laboratory Infiltration Measurements Using Sand and Peat Mixture (mixture D50 = 1600 - 1900 um) for Different Compaction Levels.....	277
Figure 127. Probability Plot to Identify Important Factors Affecting the Infiltration Rate through a Media Mixture.....	282
Figure 128. Response Surface Plot for Uniformity and Texture vs Final Infiltration Rate for Low Organic Content Conditions.	285
Figure 129. Response Surface Plot for Uniformity and Texture vs Final Infiltration Rate for High Organic Content Conditions.	286
Figure 130. Main Effects Plot for the Four Factors.....	287
Figure 131. Interaction Plot between Different Factors.....	288
Figure 132. Observed vs Fitted log (Fc) Values.....	293
Figure 133. Residuals Analysis Plot.....	294
Figure 134. Probability Plot to Identify Important Factors Affecting the Infiltration Rate through a Sand-peat Mixture.....	296
Figure 135. Response Surface Plot for Uniformity and Texture vs Final Infiltration Rate for Standard Proctor Compaction Tests and Low Organic Content Conditions	297
Figure 136. Controlled Laboratory Column SSC Test Results, Series 1.....	302
Figure 137. Controlled Laboratory Column SSC Test Results, Series 2.....	303
Figure 138. Particle size Distribution Plot Using Sand and Peat (D50 = 300 um & Cu = 3.3) and Density = 1.03 g/cc	304
Figure 139. Controlled Lab Column SSC Test Results for Coarse Media.....	306
Figure 140. Example Grouped Box and Whisker Plot of Influent vs. Effluent SSC Test Results from Sand and Peat Columns.....	308
Figure 141. Grouped Box and Whisker Plot of Influent vs. Effluent SSC (mg/L) Test Results from Coarse Media Columns.....	310
Figure 142. Arial Photograph of McDonalds Site on 15th St. E and 6th Ave. E., Tuscaloosa, AL (During-construction)	314
Figure 143. Arial Photograph of McDonalds Site on 15th St. E and 6th Ave. E., Tuscaloosa, AL (Post-Development)	314
Figure 144. Biofiltration Control Practice.....	315

Figure 145. Biofilter Runoff Volume Reduction (McDonald’s Drainage Area).....	316
Figure 146. The Number of Surface Ponding Events Greater than 3 Days per 5 Years (clearly showing the need for an underdrain for these adverse soils).....	317
Figure 147. Years to Clog as a Function of Biofilter Size Compared to Paved Area.	318
Figure 148. Biofilter Performance for Soils Having 1 and 10 in/Hr Native Subsurface Infiltration Rates (commercial drainage area).....	319
Figure 149. Arial Photograph of Cedar Crest Neighborhood, Tuscaloosa, AL (Google Map)-1320	
Figure 150. Aerial Photograph of Cedar Crest Residential Neighborhood, Tuscaloosa, AL (Google Earth)-2	320
Figure 151. WinSLAMM Model Input for Grass Swale Control Practice.	321
Figure 152. Percent Annual Runoff Volume Infiltrated into Grass Swale	322
Figure 153. Percent Annual Particulate Solids Loading Trapping In Grass Swale	323
Figure 154. Probability Plot to Identify Significant Factors Affecting the Observed Effluent SSC Concentrations	324
Figure 155. SSC Line Performance Plots for SmartDrain™	327

CHAPTER 1

1. INTRODUCTION

Urbanization changes the natural hydrology of an area, including: increased volumetric flow rates of runoff, increased volume of runoff, decreased time for runoff to reach natural receiving water, reduced groundwater recharge; increased frequency and duration of high stream flows and wetlands inundation during and after wet weather, reduced stream flows and wetlands water levels during the dry season, and greater stream velocities (Ecology 2005). The most important cause of runoff increases in urban areas is the increased amount of the impervious areas of pavement and roof areas (Pitt et al. 2002). Increases in impervious urban surfaces also cause increases in the quantities of pollutants discharged to urban receiving waters (Booth 1991).

The primary methods to control stormwater discharges in urban areas is the use of stormwater control practices, or changes in development practices. State and Federal agencies implement different strategies to minimize the potential adverse impacts of stormwater runoff pollutants in urban areas by requiring new developments to employ these practices. Stormwater control practices include constructed wetlands, sand filters, wet ponds, and, more recently, bioretention areas. These controls rely on a wide range of hydrologic, physical, biological, and chemical processes to improve water quality and manage runoff. Many facilities, such as those involving infiltration, can serve a dual role by providing both flow control and stormwater treatment, depending on how these facilities are designed (Ecology 2005).

Biofilters (a bioretention device having an underdrain) are widely used in urban areas to reduce runoff volume, peak flows and stormwater discharges and impacts to receiving waters.

However, the performance of these devices is reduced by clogging of the filter media, which in turn can decrease the life span of the device. The drainage rates in biofiltration devices are usually controlled using an underdrain that is restricted with a small orifice or other flow-moderating component. These frequently fail, as effective orifices that are used for flow control are usually very small (< 10 mm). Small orifices allow slow releases of captured stormwater, but can easily clog due to their small size (Hunt 2006). A clogged orifice can affect plant communities inside the facility. Sediment deposition is considered to be the main cause of clogging of infiltration devices and can occur either at the surface of the system or at some depth where the soil is denser or finer (Bouwer 2002). Care also needs to be taken to prevent clogging at the underdrain; effluent with a high pH value can cause vegetative kill around the drain opening and causes clogging of the drain screens as described by Wukasch and Siddiqui (1996) as part of the extensive research to examine the reuse of waste materials in construction and repair of highways conducted by Purdue University, with the Indiana Department of Transportation and the U.S. Department of Transportation Federal Highway Administration.

Infiltration and bioinfiltration systems remove stormwater runoff pollutants primarily via physical filtration as stormwater passes through the underlying soil, but also via chemical adsorption and precipitation reactions (Herrera 2011). However, the performance of these systems can be affected by factors such as texture, structure and degree of compaction of the media during their construction.

Infiltration practices are becoming more common in many residential and other urban areas to compensate for the decreased natural infiltration areas associated with land development, but must consider local soil degradation conditions to be most effective (Pitt et al., 2002 and 2008). Infiltration facilities, which historically have included percolation ponds, dry

wells, infiltration galleries, and swales, are designed to capture and retain runoff and allow it to infiltrate rather than to discharge directly to surface water (Massman, 2003). Properly designed and constructed infiltration facilities can be one of the most effective flow control (and water quality treatment) stormwater control practices, and should be encouraged where conditions are appropriate (Ecology, 2005).

Infiltration facilities have the greatest runoff reduction capabilities of any stormwater control practices and are suitable for use in residential and other urban areas where measured soil permeability rates exceed locally determined critical values (such as 1/2 in/ hr as specified by VA DCR 2010). However, the design of these facilities is particularly challenging because of the large uncertainties associated with predictions of both short-term and long-term infiltration rates (Massman, 2003). Premature clogging by silt is usually responsible for early failures of infiltration devices, although compaction (during either construction or use) is also a recognized problem (Pitt et al., 2002 and 2008).

1.1 Research Objectives

Soil disturbance/compaction in urban areas occurs during construction cutting and filling operations, general grading operations, and other processes of running heavy equipment over the soil. After construction, continued compaction can occur with various site activities result in a significant reduction of soil infiltration performance compared to natural soil conditions. Knowing the likely effects of this soil compaction on urban hydrological conditions is critical for designing stormwater control practices. Restoring the infiltration capacity of a soil is also possible and can provide significant benefits in stormwater management. A pilot-scale study on the performance of a new underdrain for stormwater biofilter devices conducted in the first part

of this research. The objectives of this dissertation research work are focusing on five primary test series as follows:

- 1) More effective underdrains: The use of underdrains, while necessary to minimize long periods of standing water in poorly draining natural soils, can also decrease the performance of biofilter systems. Pilot-scale tests were conducted to determine the flow capacity and clogging potential of a newly developed underdrain material (SmartDrainTM) under severe service conditions.
- 2) Methods of characterizing site infiltration (double-ring infiltration tests, borehole tests, and actual infiltration rate tests during rain events).
- 3) Evaluate and compare surface and subsurface soil characteristics that are of the greatest interest in the design of stormwater management facilities (grass swales, bioinfiltration facilities, and rain gardens).
- 4) Examine the effects of different compaction levels (hand compaction, standard proctor compaction, and modified proctor compaction) on the infiltration rates through the soil media in a controlled laboratory column tests, along with benefits associated with adding sand, and other amendments, to the media mixture.
- 5) Evaluate changes in flow with changes in the various soil mixture characteristics, focusing on media density associated with compaction, particle size distribution (and uniformity), and amount of organic material (due to added peat).

During this dissertation research, small field double-ring infiltration measurements were conducted to determine the infiltration characteristics of the soils in typical areas where reconstruction with stormwater infiltration controls is planned. The test results were compared to

large pilot-scale borehole tests to identify if the small test methods can be accurately used for rapid field evaluations. Controlled laboratory column tests were also conducted on surface and subsurface soil samples under the three different compaction levels to see if depth of the test (and response to compaction) affected the infiltration results. Controlled laboratory column tests were conducted using various media to identify changes in flow with changes in the mixture characteristics, focusing on media density associated with compaction, particle size distribution (and uniformity), and amount of organic material (due to added peat). The results of the predicted performance of these mixtures were also verified using column tests (for different compaction conditions) of surface and subsurface soil samples obtained from Tuscaloosa, AL, along with biofilter media obtained from Kansas City, North Carolina, and Wisconsin. Statistical analyses conducted at several levels to establish the significant factors associated with field infiltration measurements (surface and subsurface method) and the laboratory column infiltration tests.

1.2 Dissertation Organization

This dissertation has eight chapters and contains: a literature review (chapter 2). Chapter 3 presents hypotheses and experimental design. Chapter 4 presents the performance of an alternative underdrain material (smartdrain™) for urban stormwater biofiltration systems. Chapter 5 assesses the impact of soil media characteristics on stormwater biofiltration device performance. Chapter 6 presents the soil media characteristics of proposed stormwater bioinfiltration construction sites. Laboratory column tests for predicting changes in flows and particulate retention with changes in biofilter media characteristics are presented in Chapter 7, and summary of the findings, applications, and conclusions of this research are presented in

Chapter 8. The appendices contain detailed soil nutrient report and the results of the statistical analyses.

The preliminary results of this dissertation research were published as book chapter, as articles in several conference proceedings, and presented at several local, national, and international conferences, including:

Book Chapter

Sileshi, R., R. Pitt, and S. Clark. 2013. Laboratory Column Test for Predicting Changes in Flow with Changes in Various Biofilter Mixture. *Stormwater and Urban Water Systems Modeling. Computational Hydraulics International*. Guelph, ON Canada (in press).

Published Conference Proceedings:

Pitt, R., Sileshi, R., Talebi, L., and Christian, C. 2013. Stormwater Management in the Aftermath of Natural Disasters. *World Environmental and Water Resources Congress 2013. ASCE-EWRI. Conference Proceedings*. Cincinnati, OH. May 22-23, 2013.

Sileshi, R., R. Pitt, and S. Clark. 2011. Impacts of Soil Texture, Structure, and Compaction on Bioinfiltration Device Performance: Results of Lab and Field Investigations. *Low Impact Development Symposium: Greening the Urban Environment 2011. Conference Post Proceedings*. Philadelphia, PA. Sept 25 – 28, 2011.

Sileshi, R., R. Pitt, S. Clark, and C. Christian. 2012. Laboratory and Field Studies of Soil Characteristics of Proposed Stormwater Bioinfiltration Sites. *Water Environment Federation (WEF) Stormwater Symposium 2012*. July 18-20, 2012. Baltimore, Maryland.

Sileshi, R., Pitt, R., and Clark, S. 2012. Assessing the Impact of Soil Media Characteristics on Stormwater Bioinfiltration Device Performance: Lab and Field Studies. *World Environmental and Water Resources Congress 2012. ASCE-EWRI. Conference Proceedings*. Albuquerque, NM. May 20-25, 2012.

Sileshi, R., R. Pitt, and S. Clark. 2011. Experimental Study on Particle Clogging of Biofilter Device in Urban Areas. *84th Annual Water Environment Federation Technical Exhibition and Conference. WEFTEC 2011*. Conference proceedings. Los Angeles, CA Oct 15-19, 2011.

Sileshi, R., R. Pitt, and S. Clark. 2011. Examining the Clogging Potential of Underdrain Material for Stormwater Biofilter. *World Environmental and Water Resources Congress 2011. ASCE-EWRI. Conference Proceedings*. Palm Springs, CA. May 2011, 3659-3668.

Sileshi, R., Pitt, R., and Clark, S. 2010. Enhanced biofilter treatment of urban stormwater by optimizing the hydraulic residence time in the media. *ASCE/ Watershed Management 2010. Conference Proceedings*. Madison, WI. Aug 23-27, 2010.

Sileshi, R., Pitt, R., and Clark, S. 2010. Enhanced biofilter treatment of stormwater by optimizing the residence time. *ASCE/ Low Impact Development Conference*. San Francisco, CA. April 11 - 14,

Conference Presentations and Posters:

Sileshi, R., R. Pitt, and S. Clark. 2013. Lab Column Particle Trapping Tests through Various Biofilter Mixtures. *Alabama Water Resources Conference 2013*. Orange Beach, AL. Sept 5-7, 2013 (Poster).

Sileshi, R., R. Pitt, and S. Clark. 2013. Effect of Compaction on Water Flow In Sand-Peat Columns. *Low Impact Development Symposium 2013*. Saint Paul, MN. Auguts18-21, 2013 (Poster).

Sileshi, R., Mary Collins, Hugh Sherer, Norman Pelak, Robert Pitt, Shirley Clark. 2013. Laboratory Column Study of Effect of Salt Loadings on Stormwater Biofilters Performance. *World Environmental and Water Resources Congress 2013. ASCE-EWRI*. Cincinnati, OH. May 19-23, 2013 (Poster).

Sileshi, R., R. Pitt, S. Clark, and C. Christian. 2013. Stormwater Management Studies in Areas Undergoing Reconstruction Following the Tornado that Hit Tuscaloosa, AL. *Alabama's Water Environmental Association (AWEA) 36th Annual Conference 2013*. Orange Beach, AL. April 7 - 10, 2013 (Presentation).

Sileshi, R., R. Pitt, and S. Clark. 2013. Laboratory Column Test for Predicting Changes in Flow with Changes in Various Biofilter Mixture. *Stormwater and Urban Water Systems Modeling. Computational Hydraulics International 2013*. Guelph, Ontario, Feb 21-22, 2013 (Presentation).

Sileshi, R., R. Pitt, and S. Clark. 2012. Evaluating the Influence of Soil Characteristics On Stormwater Biofilter Performance In Urban Areas. *American Water Resources Association (AWRA) Annual Water Resources Conference*. Jacksonville, FL. Nov 12-15, 2012 (Poster).

Sileshi, R., Mary Collins, Hugh Sherer, Norman Pelak, Robert Pitt, Shirley Clark. 2012. Impacts of Salt Loadings on the Performance of Stormwater Biofilters: Laboratory Column Experiments. *Alabama Water Resources Conference 2012*. Orange Beach, AL. Sept 5-7, 2012 (Poster).

- Sileshi, R., R. Pitt, S. Clark and C. Christian. 2012. Laboratory and field studies of soil characteristics of proposed stormwater bioinfiltration sites. *Water Environment Federation (WEF) Stormwater Symposium*. Baltimore, MD. July 18 – 20, 2012 (Presentation).
- Sileshi, R., R. Pitt, and S. Clark. 2012. Assessing the impact of soil media characteristics on stormwater bioinfiltration device performance: lab and field studies. *World Environmental and Water Resources Congress 2012. ASCE-EWRI*. Albuquerque, NM, May 20-25, 2012 (Presentation).
- Sileshi, R., R. Pitt, and S. Clark. 2011. Experimental Study on Particle Clogging of Biofilter Device in Urban Areas. *84th Annual Water Environment Federation Technical Exhibition and Conference. WEFTEC 2011*. Los Angeles, CA. Oct 15-19, 2011 (Poster).
- Sileshi, R., R. Pitt, and S. Clark. 2011. Impacts of Soil Texture, Structure, and Compaction on Bioinfiltration Device Performance: Results of Lab and Field Investigations. *Low Impact Development Symposium*. Philadelphia, PA. Sept 25-28, 2011 (Poster).
- Sileshi, R., R. Pitt, and S. Clark. 2011. Assessment of the Influence of Compactions on Biofilter Media Characteristics: Laboratory and Field Studies. *Alabama Water Resources Conference 2011*. Orange Beach, AL. Sept 7-9, 2011(Poster).
- Sileshi, R., R. Pitt, and S. Clark. 2011. Examining the clogging potential of underdrain material for stormwater biofilter. *World Environmental and Water Resources Congress 2011. ASCE-EWRI*. Palm Springs, CA, May 22-26, 2011 (Presentation).
- Sileshi, R., R. Pitt, and S. Clark. 2011. SmartDrain™ for Enhanced Biofiltration Controls. *Fox-Wolf Stormwater Conference*. Appleton, WI. May 11, 2011 (Presentation).
- Sileshi, R., R. Pitt, and S. Clark. 2010. Experimental Study on Underdrain Clogging of Stormwater Biofilters *American Water Resources Association (AWRA) Annual Water Resources Conference*. Philadelphia, PA. Nov 1-4, 2010 (Poster).
- Sileshi, R., R. Pitt, and S. Clark. 2010. Experimental Study on Newly Developed Underdrain Material for Biofiltration Devices. *Alabama Water Resources Conference*. Orange Beach, AL. Sept 8-10, 2010 (Poster).
- Sileshi, R., R. Pitt, and S. Clark. 2010. Enhanced biofilter treatment of urban stormwater by optimizing the hydraulic residence time in the media. *ASCE/EWRI, Watershed 2010: Innovations in Watershed Management under Land Use and Climate Change*. Madison, WI, Aug 23-27, 2010 (Presentation).
- Sileshi, R., R. Pitt, and S. Clark. 2010. Enhanced biofilter treatment of stormwater by optimizing the residence time. *International Low Impact Development Conference: Redefining Water in the City*. San Francisco, CA. April 11 – 14, 2010 (Presentation).

CHAPTER 2

2. LITERATURE REVIEW

2.1 Urban Stormwater Runoff Management

Rainfall that does not percolate into the ground or is lost by other abstractions (mostly evaporation, evapotranspiration and detention storage) becomes surface runoff, which either flows directly into surface waterways or is channeled into storm sewers in urban areas.

Stormwater runoff that flows over the land or impervious surfaces (rooftops, paved streets, highways, parking lots and building rooftops) may contain pollutants such as heavy metals, organic compounds, nutrients, bacteria and viruses, oils, fertilizers, pesticides, soil, trash, and animal wastes. These pollutants usually adversely affect the water quality and associated beneficial uses of receiving waters if proper treatment is not employed. However, the type and level of contaminants found in runoff depends on the nature of the activities in those areas.

Stormwater pollutants from critical source areas, such as gas stations, vehicle service areas, heavy equipment storage and maintenance areas, public works yards, auto recyclers/junkyards, large parking lots, bus or truck (fleet) storage areas, and vehicle and equipment washing/steam cleaning facilities may contain significantly larger pollutant loadings of hydrocarbons, toxic trace metals, nutrients, pathogens, and/or other toxicants and pollutants as compared to ‘normal’ runoff from most other areas (Bannerman et al.1993; Claytor and Schueler 1996; Woelkers 2006; Eriksson et al. 2007).

Flow control and water quality are the two critical aspects of urban stormwater runoff management (Herrera 2011). Currently, stormwater control practices are used in many areas to

reduce the impact of stormwater runoff. These practices are critical in controlling stormwater runoff near its sources, by reducing pollutant discharges, along with minimizing the impact of downstream flooding, and promoting groundwater recharge in urban areas.

2.2 Stormwater Filtration Techniques

Selecting the best media for a specific situation is critical when designing a biofilter or bioinfiltration stormwater control practice as the media affects the amount of runoff that is treated and the level of treatment that can be obtained. Selection of filtration media for pollutant removal capabilities needs to be based on the desired pollutant removal performance and the associated conditions, such as land use. Filtration research (Claytor and Schueler 1996; Urbonas 1999; Clark and Pitt 1999; and Clark 2000) has shown that stormwater filtration devices are limited in achieving the desired pollutant reduction goals by clogging caused by particulates in stormwater runoff. A clogging layer at the surface of the filters is the primary cause of the overall decline in the hydraulic performance of filters (Urbonas 1999; Hatt et al. 2008). Filtration performance depends on many factors such as the desired treatment flow rate, use with other controls, the source water quality (pollutant concentrations and type), media type, and the physical characteristics of the media (Clark and Pitt 1999; Minto 2005).

Filtration rates decrease dramatically as the filters approach the breakthrough condition. Clark (2000) reported four criteria that are used to measure filter performance (1) effluent water quality (traditionally, turbidity and suspended solids concentration; possibly particle counts by size and dissolved organic carbon concentration), (2) effluent heavy metal and/or organic concentrations (if applicable), (3) water production (unit filter run volume), and (4) head-loss development and time to backwash or media replacement if no backwash is used.

A comprehensive laboratory and bench scale study on the performance of various media (fine sand, activated carbon, peat moss, and compost media) for stormwater filtration by Clark (2000) indicated that clogging generally occurs before breakthrough of the pollutants. The clay-sized components in the incoming suspended solids are the controlling effect on media clogging. Hatt et al. (2008) recommend a maintenance frequency (i.e., scraping off the top 2–5 cm of the top layer of fine-media stormwater filters) of 2 years with inspections on alternate years. The expected lifespan therefore is at least 10 years, based on a recommendation by Urbonas (1999), who suggested that the whole media would need to be replaced after 5–10 scrapings because of clogging of lower pore spaces.

2.3 Sand Filters

Sand filters are depressions or ponds made of a layer of sand designed to treat urban stormwater. The concept of sand filtration for stormwater treatment was borrowed from wastewater treatment applications (Hunt 2004). Sand filters are usually two-chambered practices: the first is a settling chamber and the second is a filter bed filled with sand or another filtering medium. Runoff from a developed site is routed to the settling chamber-filter system, large particles settle out in the settling unit and finer particles and other pollutants are removed as runoff flows through the sand. The filtered water is then collected in underground pipes and returned back to the stream or channel. A sand filter operates much like an infiltration pond. However, instead of infiltrating into native soils, stormwater filters treat the stormwater by passing it through a constructed sand bed and then collecting it with an underdrain system. The treatment pathway in most sand filter is vertical (downward through the sand) rather than horizontal as it is in biofiltration swales and filter strips (King County 2009).

Sand filters are intended primarily for water quality enhancement (Shaver and Baldwin 1991). Sand filters treat to a higher level of total suspended solids (TSS) removal than many other water quality facilities (King County 2009). One of the main advantages of sand filters is their adaptability; they can be used on areas with thin soils, high evaporation rates, low infiltration rates, and in areas where groundwater is to be protected (Young et al. 1996). Sand filters require less land than other stormwater controls, such as ponds or wetland. However, they require high capital costs, frequent maintenance and provide little or no flood control benefits (Barrett et al. 1995). After clogging, even more of the flows are bypassed without receiving treatment (Urbonas 1999). Pretreatment techniques are applied to reduce flow velocities to the sand filter and remove debris, floatables, large particulate matter, and oils. The main differences among the different sand filter designs are location (i.e. above or below ground), the drainage area served, their filter surface areas, their land requirements, and the quantity of runoff they treat.

Sand filters can be used to actively treat stormwater runoff from intensely developed sites on appropriate sites such as gas stations, convenience stores, and small parking lots. There are several different sand filter types and designs, including surface sand filters, underground sand filters, perimeter sand filters, organic media filters, and multi-chambered treatment trains. The following are design variations for sand filtration devices:

2.3.1 Surface Sand Filter

The surface sand filter (sometimes referred to as the Austin sand filter system) has both the sediment chamber and the filter bed above ground. The surface sand filter is designed as an off-line practice; only the water quality volume is directed to the filter. The surface sand filter has been the most widely used and least expensive sand filter option. It is usually designed to

collect and treat the first 0.5 inches of runoff from drainage areas up to 50 acres that have both impervious and pervious surfaces. The City of Austin (1988) requires a minimum 18 inch sand layer. The Austin sand filtration system is recommended in regions where evaporation exceeds rainfall and a wet pond would be unlikely to maintain the required permanent pool (USEPA 1999a). Clogging was noted in Austin sand filters that were monitored in California when the TSS load to the system was between 5 and 7.5 kg/m² (1 to 1.5 lb/ft²) of the filter area (Barrett 2003).

Austin-style sand filters have demonstrated good metal (copper, lead, and zinc), TSS, and fecal coliform removals from stormwater runoff (Barrett 2003). However, the removal performance for pollutants in dissolved forms is poor, especially for nitrates (-74%) (Barrett 2003; Glick et al. 1998). The performance of sand filters can be enhanced with the use of peat, limestone, gravel, and/or topsoil mixtures. Sand filters mixed with peat have shown very good pollutant treatment performance (Galli 1990 and Clark and Pitt 1999). Sand-peat filters performed better as they age, suggesting that they develop a biofilm that will aid in retention of pollutants. Unfortunately, aged filters in conventional downflow mode also have significantly reduced treatment flow rates, resulting in increased bypasses (Urbonas 1999).

2.3.2 Underground Sand Filters

Underground sand filters (the Washington, D.C. sand filter) are a modification of the surface sand filter, where all of the filter components are underground. Like the surface sand filter, this practice is an off-line system that only receives flows during small rains. Underground sand filters are expensive to construct but consume very little space. The Washington, D.C. sand filter system is designed to handle runoff from completely impervious drainage areas of 1 acre or less. They are usually designed to accept the first 0.5 inch of runoff. The filter bed is 18 inches in

depth and may have a protective screen of gravel or permeable geotextile. The Washington, D.C. sand filters are ultra-urban stormwater controls best suited for use in situations where surface space is too constrained and/or real estate values are too high to allow the use of conventional retention ponds (USEPA 1999a).

2.3.3 Perimeter Sand Filters

Perimeter sand filter (Delaware sand filter) also include the basic design elements of a sediment chamber followed by a filter bed. In this design, flow enters the system through grates, usually at the edge of a parking lot. The perimeter sand filter is the only filtering option that is on-line; all flow enters the system, but a bypass to an overflow chamber prevents system flooding. One major advantage of the perimeter sand filter design is that it requires little hydraulic head and dedicated space and thus is a good option in areas of low relief. The Delaware sand filter system is designed to handle runoff from drainage areas of 5 acres or less. The filtration chamber contains a minimum 18 inch sand layer. The main difference between the Washington, D.C. and the Delaware sand filter is that the D.C. sand filter design has provisions for excluding floatable debris and petroleum sheens from reaching the filter media, which eventually would cause it to clog (Dzurik et al. 2003).

Bell et al. (1995) reported mass removal rates for sediment, Biological Oxygen Demand (BOD), total organic carbon, phosphorus and zinc ranging between 60 and 80 percent from a modified Delaware sand filter that collected runoff from a 0.7 acre section of a newly built parking lot located near National Airport in Alexandria, Virginia. The removals of total and soluble phosphorus were among the highest yet reported for a sand filter. The performance of these devices is sensitive to anaerobic conditions that can develop in the sand causing the release of previously captured metals and especially nutrients. Mass removal of total nitrogen was 47

percent, which reflected excellent removal of organic nitrogen (71 percent) coupled with negative removal of soluble nitrate (-53 percent) (Bell et al. 1995). Removal of oil and grease by sand filters has been reported to average between 55 and 84 percent in two similar Delaware sand filters located at a loading facility for a marine terminal in Seattle, Washington, suggesting sand filters can be an effective stormwater management practice for hydrocarbon hotspots (Horner and Horner 1995).

2.3.4 Organic Media Filter

Organic media filters are essentially the same as surface filters, with the sand replaced with or supplemented by another medium. Two examples are the peat/sand filter (Galli 1990) and the compost filter system. It is assumed that these systems will provide enhanced pollutant removal for many compounds because of the increased cation exchange capacity achieved by increasing organic matter content.

2.3.5 Multi-Chambered Treatment Train

The multi-chambered treatment train (MCTT) is essentially a “deluxe sand filter” (Pitt et al. 1995). This underground system consists of three chambers that are sized for specific runoff conditions at a site and contain complementary unit treatment processes (volatile pollutant stripping, floatable and gross solids removal, sorption booms, fine particle settling, plus ion exchange and sorption). Runoff enters into the first chamber where screening occurs, trapping large sediments and releasing highly volatile materials. The second chamber provides settling of fine sediments and further removal of volatile compounds and floatable hydrocarbons through the use of fine bubble diffusers and sorbent pads. The final chamber provides filtration by using a sand and peat (and sometimes granular activated carbon) mixed media for reduction of the remaining pollutants. The top of the filter is covered by a filter fabric that evenly distributes the

inflowing water and prevents channelization. Although this practice can achieve very high pollutant removal rates, it might be prohibitively expensive in many areas (USEPA 2005).

In general sand filters have been shown to be effective in removing many common pollutants, with the exception of nitrates. Percent removal rates for different type of sand filters and organic filters are presented in Table 1.

Table 1. Sand Filter Removal efficiencies (percent) (adapted from California Stormwater BMP Handbook 2003)

	Sand Filter (Glick et al,1998)	Compost Filter System		Multi-Chamber Treatment Train		
		Stewart, 1992	Leif,1999	Pitt et al., 1996	Pitt,1996	Grebe et al.,1998
TSS	89	95	85	85	83	98
TP	59	41	4	80	-	84
TN	17	-	-	-	-	-
Nitrate	-76	-34	-95	-	14	-
Metals	72-86	61-88	44-75	65-90	91-100	83-89
Bacteria	65	-	-	-	-	-

2.4 Biofiltration Systems

Biofilters and bioinfiltration systems are a natural advancement to the older sand and mixed media filters described above. They share many similar attributes to the sand filters but can be more easily integrated into the landscaping of a developed site. Biofilters are devices that contain underdrains and return treated water to the surface flows, but with usually significant detention times. Bioinfiltration systems rely more on infiltration into the natural underlying soils and therefore can be used to reduce the volume of runoff discharged to surface waters. These

devices are also most commonly used as relatively small devices that are placed throughout the watershed drainage area, and rarely used for larger outfall flows.

These devices can therefore be effective pollutant removal stormwater management devices and can also enhance stormwater infiltration for runoff volume reduction. Stormwater practices, particularly those installed in areas frequented by pedestrian traffic, not only need to be effective pollutant removers, but they must also maintain some aesthetic appeal (Hunt 2004). Most of the removal benefits of biofilters and bioinfiltration devices are through physical removal as the particulate-bound pollutants are trapped in the media (and through water infiltration into the natural soil surrounding the device if large underdrains are not used). The use of plants in these devices is an important aesthetic and treatment component, especially for nutrients and possibly other pollutants, as described by LeCoustumer et al. (2008) as part of the extensive biofilter research conducted by Monash University. Plants can enhance the treatment flow rate and time period before clogging by penetrating the surface clogging layer, allowing water to flow to deeper filter layers. Biochemical reactions may also be enhanced near the root zones of some plants.

A biofiltration system utilizes several treatment mechanisms for removing pollutants from stormwater runoff. However, separate sedimentation facilities are rarely used with biofilters. Surface ponding is a critical element for attenuating peak flow rates. Some large regional biofilters do have separate sediment facilities for pre-treatment. Likewise, sand filtration and biofiltration both remove pollutants through physical filtration. The primary difference between the two is that the presence of a biological community of plants and microorganism in a biofiltration system can provide additional treatment benefits (City of Austin 2011). Bio-infiltration combines sedimentation, filtration, adsorption and biological processes to treat and

infiltrate stormwater runoff as shown in Figure 1. Filtration occurs within the porous medium which is usually composed of soil, sand, gravel or a combination. As noted above, a biofilter would have an underdrain to capture much of the stormwater filtered through the media and return it to the surface flow.

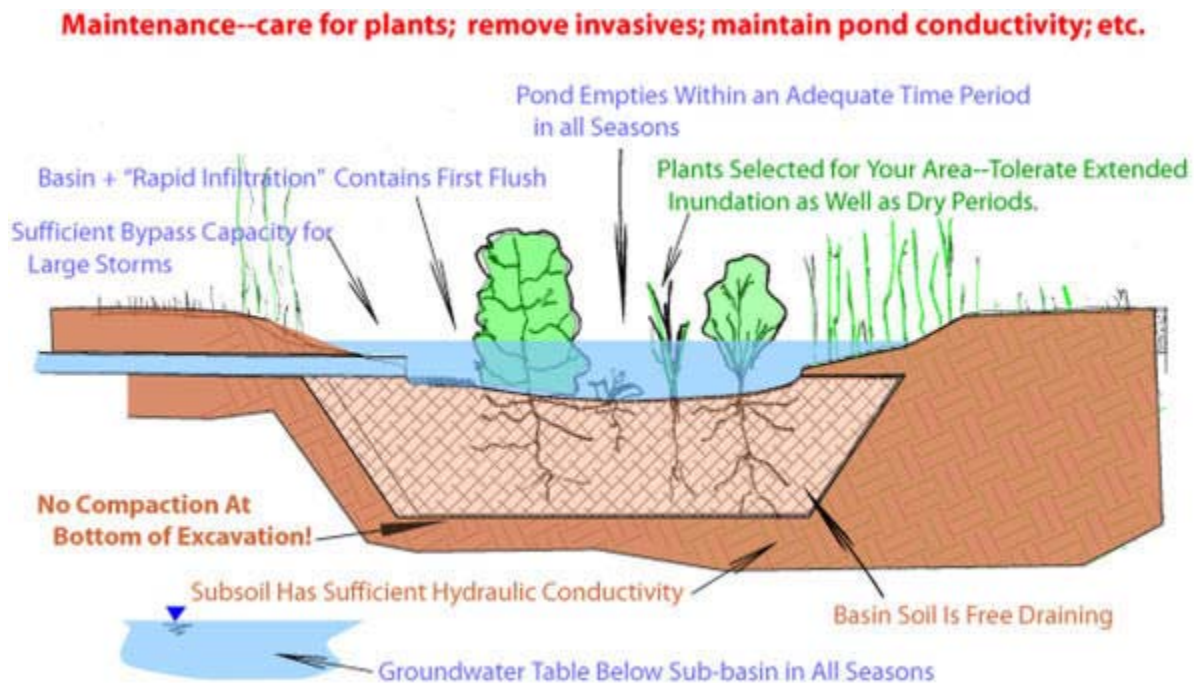


Figure 1. Cross-Section of a Bioinfiltration Stormwater Treatment Device (Source: VUSP).

Several studies have demonstrated the pollutant removal efficiency of stormwater biofilters (City of Austin 1988, Clark and Pitt 1999, Clark 2000, Winer 2000). With the exception of some highly mobile contaminants (such as chlorides), they can be designed for good pollutant removal. The removal of soluble forms of many stormwater pollutants is dependent on the residence time of the stormwater in the media, the stormwater characteristics,

and the media type. Besides water quality improvement, biofilters have been shown to effectively reduce runoff peak flow rates and runoff volumes (Hunt 2004, Gilroy and McCuena 2009, Hatt et al. 2009).

The effectiveness of a biofilter is commonly reduced through clogging of the media, through short-circuiting of infiltrating water through an underdrain, or by short resident/contact times of the stormwater and the treatment media. Clark (2000) found that failure of these systems is mostly caused by clogging, which can occur well before the contaminant removal capacity of the media is exceeded. Biofilter treatment performance is unlikely to be affected, for systems that are over-sized such that their detention storage volume compensates for reduced media conductivity by providing greater filter area and ponding volume (LeCoustumer et al. 2009).

Bioretention (bioinfiltration) is an urban stormwater treatment practice which combine various removal mechanisms using soil and plant complexes to manage stormwater runoff in small developments (0.25 – 2 acres) (Davis et al. 2001). Bioretention facilities can provide stormwater flow control in urban areas via detention, attenuation, and losses due to infiltration, interception, evaporation and transpiration (Herrera 2011). The healthy soil structure and vegetation associated with bioretention facilities promote infiltration, storage, and slow release of stormwater flows to more closely mimic natural conditions (City of Seattle 2009).

Bioretention facilities are a viable option for reducing the thermal pollution impacts of urban stormwater runoff (Jones and Hunt 2009).

The ability of bioretention areas to reduce runoff volumes may be this control practice's greatest asset compared to stormwater wetlands and wet ponds (Jones and Hunt 2009).

Installation of larger bioretention areas with respect to the watershed size does not seem to have substantial benefits with regard to temperature reduction; however, greater reductions in runoff

volume appears to have major implications for reducing the thermal load to cold water stream environments. Deeper bioretention areas may be better suited in regions where thermal pollution is a concern (Jones and Hunt 2009). Despite these concerns, underdrain depths between 35 inches (90 cm) and 47 inches (120 cm) appear to be practical for most applications. Bioretention areas should not be lined (although biofilters can be) and should be sited in locations with high underlying soil hydraulic conductivities when possible to encourage movement of stormwater runoff into the shallow groundwater. If a biofilter is installed at a potential stormwater pollutant hotspot, e.g. gas station or in karst topography, an impermeable liner should be installed to prevent runoff from potentially reaching and contaminating the aquifer (Georgia 2001, Jones and Hunt 2009).

2.4.1 Biofilter/Bioretention Media

The selection of appropriate fill media for biofilter and bioretention systems is of critical importance for stormwater treatment in urban areas. The primary media usually employed in these systems include soil, sand, and organic compost. Due to the differences in the physical properties (texture, structure) of these constituents, the percentage in the media mixture can affect the pollutant control and flow reduction performance of the system. Soil is made up of an extensive variety of substances, minerals, and rocks. It consists of four major components – minerals, organic materials, air and water. Sand (0.05-2 mm), silt (0.05- 0.002 mm), and clay (< 0.002 mm) are the three soil particle size fractions found in different amounts. The soil mix used for bioretention systems is central for determining flow control and water quality treatment performance. Soils with significant clay content should not be used for bioretention systems, because clay soils impede infiltration and might actually promote clogging (Prince George's County 2007). A typical soil restriction for use in bioretention facilities is that the soil must have

an infiltration rate sufficient to drain any pooled water within 48 hours after a storm event ends (Prince George's County 2007). This requires that the soil infiltration rate usually exceeds 0.5 in/hr.

The sand layer serves as a transition between the planting soil bed and the gravel layer and underdrain pipes for biofilter systems. Different sands, however, usually have different pollutant removal capacities and flow rates. Because of their coarse particle size and low clay content, sands usually result in a higher runoff treatment rate than soils. To ensure proper system operation, the sand layer must have a permeability rate at least twice as fast as the design permeability rate of the planting soil bed (New Jersey 2004).

Surface mulches have many benefits in the performance of biofilter/bioretention systems. It serves as a temporary soil stabilization or erosion control practice, controls weeds, prevents and reduces soil compaction; regulate soil temperatures and preserves soil moisture. A mulch layer can offer a nutrient-rich environment conducive to microbial growth, promoting degradation of petroleum-based products and other organic materials (US EPA 1999b). Unless the plants are in good health and the mulch layer is regularly replenished, the bioretention facility will not function as designed, and the longevity will be diminished. Fine sand or sandy loam is an effective filter media for biofiltration because they provide adequate support for plant growth and display minimal leaching (Henderson et al. 2007a).

Shallow bioretention media depths of 8 inches (20 cm) to 16 inches (40 cm) is sufficient for systems focused on metal capture (Li and Davis 2008c). Higher pollutant filtration and adsorption capacity results were found with higher silt, clay, and organic matter contents of the bioretention media, suggesting greater runoff storage capacity and longer media contact time for small events in thicker bioretention media layers. A greater thickness allows greater

opportunities for sorption, filtration, and/or biological processes to occur, promoting pollutant capture and biodegradation (Li and Davis 2009a). However, Hsieh and Davis (2005) emphasized that care should be taken when using organic matter in areas where nutrient discharges are of particular concern, because while it can be beneficial for removing certain pollutants (especially metals), organic matter decomposition may result in a net leaching of phosphorus from the media (Davis et al. 2001; Sun and Davis 2007).

2.4.2 Underdrains

Outlet control can be more consistent in providing the desired resident times needed for pollutant control. However, most outlet controls (underdrains) are difficult to size to obtain long residence times. Underdrains are perforated or porous pipes, installed in narrow trenches and surrounded by crushed stone or underdrain filter material that is both pervious to water and capable of protecting the pipe from infiltration by the surrounding soil. The primary purpose of the underdrain is to decrease the duration of ponding in facilities with less permeable native soils. Perforated pipe underdrains short-circuit natural infiltration, resulting in decreased runoff volume reduction. Underdrains are used to ensure adequate drawdown to prevent groundwater from entering the pavement, and to remove surface water that enters adjacent pavement.

Biofilters are designed with an underdrain connected to a stormwater collection system, while bioretention (bioinfiltration) devices do not have underdrains and discharge runoff into a permeable soil profile, while providing groundwater recharge (Prince George County 2002). The underlying soil is usually the main factor determining which configuration is used. In cases where existing soils have poor infiltration capacities, underdrains are typically used to discharge the filtered water back to the surface flows. The natural soils for bioinfiltration systems should have infiltration rates greater than 0.5 inches per hr if underdrains are not to be used; however,

when underdrains are not incorporated into the bioretention design, there is an increased risk of generating overflows during a storm event (Jones and Hunt 2009). Table 2 shows soil texture effects on bioretention/biofilter facility selections. The risk of infiltration failure is assumed to be minimal if the design infiltration rate of the native soil is determined to be at least 3.6 in/hr (Wisconsin DNR 2004).

Table 2. Soil Texture Effects on Bioretention Facility Design (Source: Atchison et al. 2004)

Soil Texture	Sat. Hydraulic conductivity(in/hr) ¹	Typical Design
Sand	3.6	Basic Bioretention
Loamy sand	1.63	Basic Bioretention
Sandy Loam	0.5	Basic Bioretention
Loam	0.24	Underdrain Recommended ²
Silt Loam	0.13	Underdrain Required
Sandy Clay Loam	0.11	Underdrain Required
Clay Loam	0.03	Not Recommended for infiltration ³
Silty Clay Loam	0.19	Underdrain Required
Sandy Clay	0.04	Not Recommended for infiltration ³
Silty Clay	0.07	Not Recommended for infiltration ³
Clay	0.07	Not Recommended for infiltration ³

1 Rawls et al.(1998)

2 Underdrain system recommended but may be capped initially;

3 Generally not feasibly to meet infiltration goals; however may be used for water-quality treatment if designed with an underdrain

Underdrains may have restricting orifices so that the design infiltration rate plus the underdrain flow rate equals the design drawdown rate. The required number of underdrain pipes is proportional to the surface area of the biofiltration device (Montgomery County Maryland 2005). According to the Montgomery County, Maryland stormwater manual, the number of underdrain pipes is determined by multiplying the surface area square footage by 0.05. This determines the linear feet of piping required. Use a minimum of two pipes whenever possible. For example, if the surface area of the biofiltration device is 450 square feet, then: $450 (0.05) =$

22.5 LF (This should be rounded to the nearest foot.). Thus, the requirement will be for two underdrain pipes, each about 12 feet long. Underdrain pipes should be placed a minimum of 5 feet apart.

2.4.3 Underdrain Effects on the Water Balance

Incorporating an underdrain increases the volume of water that can be captured and filtered through the root zone of the facility. However, the resulting flow through the underdrain still contributes to the volume discharged to downstream surface waters, reducing the retention and recharge capacity of the facility. The volume of water discharged through the underdrain can be easily approximated by comparing the flow rate through the underdrain with the observed drawdown rate when the facility is completely saturated (Atchison et al. 2006). Over the long term, the relative volumes associated with each of these rates are also approximately proportional to the design flow rates. For example, if the maximum underdrain flow rate is equal to half of the drawdown rate, just less than half of the stormwater infiltrating the surface of the facility will be discharged through the underdrain (Atchison et al. 2006).

Figures 2 through 4 illustrate underdrain effects on the water balance for a 0.75 inch rain from 1 acre of pavement, with 2.2 percent of the paved area as the biofilter surface, with natural loam soil (0.5 in/hr infiltration rate) and 2 ft of modified fill soil for water treatment and for groundwater protection. Orifice outlet controls that allow long residence times usually are very small and clog easily. This research examines a foundation drain material (SmartDrain™) that can be applied to biofiltration devices and provides another option for outlet control.

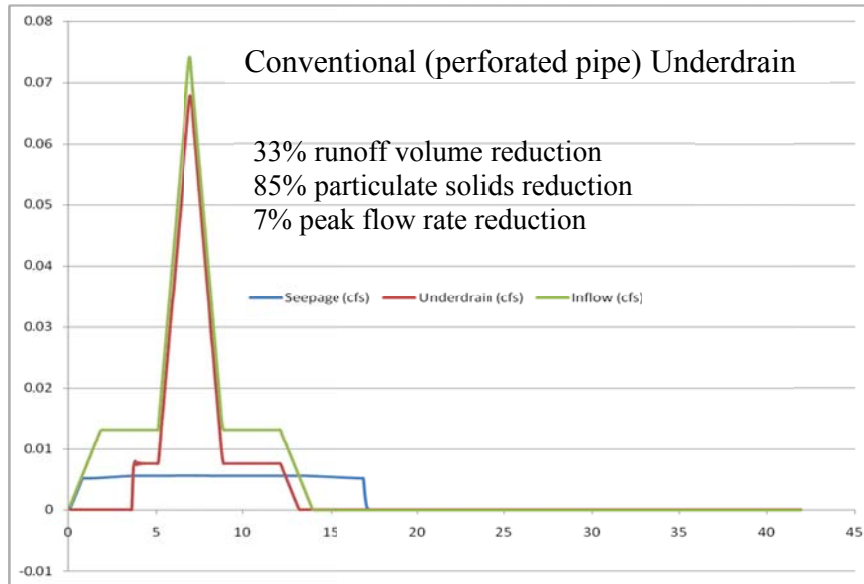


Figure 2. Conventional Underdrain Effects on Water Balance (Robert Pitt, Unpublished).

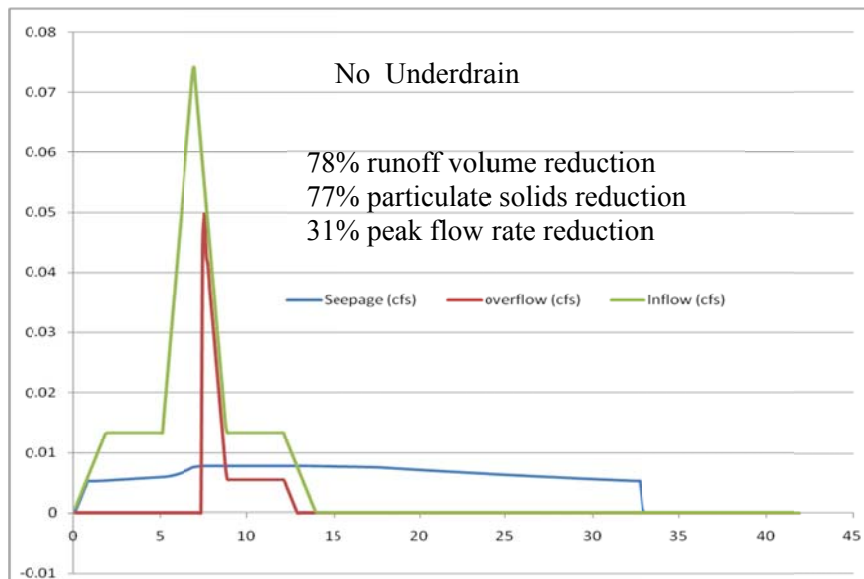


Figure 3. No Underdrain Effects on ` Balance (Robert Pitt, Unpublished).

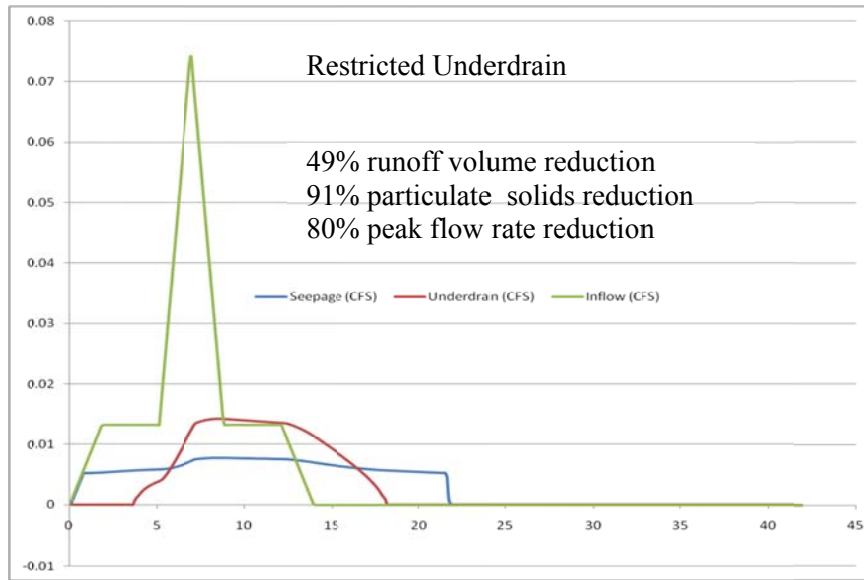


Figure 4. Example Restricted Underdrain Effects on Water Balance (WinSLAMM calculations).

Sandy-silt loam soils usually results in extended surface ponding, requiring an underdrain. Conventional underdrain (perforated pipe) reduces ponding, but also decreases infiltration opportunities. The SmartDrainTM also reduces ponding time, while providing additional infiltration.

Table 3. Example Underdrain Water Balance (WinSLAMM model calculations)

	Surface ponding (hrs)	Infiltration volume (ft ³)	Surface discharge (ft ³)	Subsurface (filtered) discharge to surface (ft ³)	Volume surface discharge reduction (percent)
No underdrain	56	115	126	0	48
Typical underdrain	20	51	118	72	21
SmartDrain TM	25	80	118	43	33

2.4.4 Biofilter/Bioretention Pollutant Removal

Several laboratory studies have demonstrated the ability of stormwater biofilter/bioretention facilities to reduce concentrations of heavy metals (copper, lead, and zinc) by more than 90 percent (Lau et al. 2000; Davis et al. 2001 and 2003; Hatt et al. 2007a and 2008; Sun and Davis 2007; Blecken et al. 2009a). Excellent total suspended solids (TSS) and metal reductions are associated with bioretention media filtration (Li and Davis 2008a, b) and strong metal (lead, copper, and zinc) adsorption onto the bioretention media (Li and Davis 2008c).

Bioretention facilities have also demonstrated good removal for total Kjeldahl nitrogen (TKN) and ammonia (NH_3), but poor nitrate removal (Davis et al. 2001 and 2006; Hsieh and Davis 2005; Hunt et al. 2006; Henderson et al. 2007a; Hsieh et al. 2007b; Passeport et al. 2009; Hatt et al. 2009), including in some cases, nitrate exportations by bioretention facilities. However, the presence of an internal water storage layer increases nitrite-nitrate as nitrogen ($\text{NO}_{2-3}\text{-N}$) removal significantly by increasing the contact time of the water with plant root systems (Kim et al. 2003; Hunt et al. 2006; Dietz and Clausen 2006).

2.5 Infiltration Mechanism

Infiltration is the process by which water originating from rainfall, snowmelt or irrigation arriving at the surface enters into the soil. Although infiltration may involve soil water movement in two or three dimensions, such as rainfall on a hillside, it is often treated as one dimensional vertical flow (Skaggs and Khaleel 1982). The infiltration of water into the surface soil is responsible for the largest abstraction (loss) of rainwater in urban areas (Pitt et al. 1999a). An understanding of the infiltration process and the factors that affect it is important not only in the determination of surface runoff but also in the subsurface movement and storage of water within a watershed (Skaggs and Khaleel 1982).

The infiltration rate, measured in inches per hour or centimeter per hour, is the rate at which water arriving at the soil surface enters the soil. The rate of infiltration depends on a number of factors, including the condition of the soil surface and its vegetative cover, the soil texture and structure, the current moisture content of the soil, the chemical nature of the soils, temperature of the air and of rain, rain intensity, the depth to ground water, the percentage of entrapped air in the soils, the atmospheric pressure, the biological activity in the soil, and the slope of the ground surface (Horton 1940, Johnson 1963, Willeke 1966, Chow et al. 1998). The initial moisture content of the soil is usually considered one of the more important factors influencing infiltration of water into a given soil profile (Morel-Seytoux 1978; Skaggs and Khaleel 1982).

2.5.1 Factors Affecting the Infiltration Process

Hydraulic conductivity, soil structure, surface and subsurface conditions of the soil affect the infiltration process. The hydraulic conductivity is a measure of the soil's ability to transmit water away from the infiltration area, and is therefore of critical importance to the infiltration rate since it expresses how easily water flows through soil. The hydraulic conductivity depends on the soil grain size, the structure of the soil matrix, and the type and amount of soil fluid (including entrapped air) present in the soil matrix. Soil texture, commonly used to designate the proportionate distribution of the different sizes of sand, silt, and clay that a soil comprises, directly affects the hydraulic conductivity, diffusivity and water holding capacity. Sandy soils have larger pores, a lower water holding capacity and a higher hydraulic conductivity, diffusivity and infiltration rate compared to clayey soils, which have smaller micropores.

Soil structure is the term used to refer to the arrangement or grouping of primary soil particles (sand, silt, clay and organic matter) into larger aggregates of various sizes and shapes. Soil structure is affected by the chemical composition of soil particles, amount of organic matter present, soil texture, water content, and activity of organisms such as earthworms, insects, fungi, plant roots and microbes. Soil structure determines porosity and infiltration; hence it determines water movement and availability to plants, and minimizes erosion. Soil structure also influences plant root development, both directly and indirectly (Angers and Caron 1998). One of the most significant plant-induced changes in soil structural is the formation of continuous macropores by penetrating roots. These macropores facilitate aeration and water movement and storage in the soil as well as decreasing resistance to further root growth. The larger the pores are, the more efficient they are at moving air and water through the soil.

Surface and subsurface conditions of the soil have a significant influence on infiltration rates (Aronovici 1954 and Johnson 1963). If all the soils are uniform or the deeper soils are more permeable than those near the surface, and the water table is a considerable distance below the surface, the infiltration rate is controlled by the soils near the surface (Johnson 1963). However, when the deeper soils are less permeable than the shallow soils, the shallow soils soon become saturated and the resultant infiltration rate is controlled by the less permeable soils at greater depth. Thus, the critical zone controlling the rate of infiltration is the least permeable zone. In natural soils, the infiltration rate in the early stages of a storm is generally high. The rate gradually decreases and reaches a nearly constant rate, generally within a few hours.

However, Horton (1939) described three main reasons why the infiltration capacity may decrease in the earlier stages of rain events: 1) Swelling of colloids and closing of soil-cracks and sun-checks. 2) In-washing of fine material to the surface-pores in the soil where surface erosion

occurs. Water entering the soil-pores is charged with fine material in suspension, which tends to clog the surface pores. Even though the surface soil is itself carried away, the clogging process still continues.3) Rain packing –Especially in the earlier stages of intense rains, direct impact of rain –drops on the soil compacts the soil-surface and decreases the infiltration capacity. Once the infiltration capacity of the soil has been reached, the excess water will first accumulate on the soil surface as surface storage, and when that storage capacity is exceeded, it becomes surface runoff. Neal (1938) reported exceptions where the infiltration capacities do not decrease in the earlier stages of rain events where the soil is already at its minimum infiltration-capacity and in some regions, where a moderate increase of infiltration capacity has been noted in the earlier stages of application of water to sprinkled plats. Pitt, et al (1999a) also noted increases in infiltration with time in disturbed urban soils, likely due to the extreme heterogeneity of the subsurface conditions and changes in hydraulic conductivity in the different soil layers. The water transmission rates, and hence the infiltration rates, could increase as the infiltrating water reached these more permeable subsurface layers.

The infiltration capacity of most soils allows low intensity rainfall to totally infiltrate, unless the soil voids become saturated or the underlying soil is much more compact than the top layer (Morel-Seytoux 1978). Pitt et al. (2002) described three mechanisms, by which the infiltration of rainfall into pervious surfaces is controlled: 1) the maximum possible rate of entry of the water through the soil/plant surface, 2) the rate of movement of the water through the vadose (unsaturated) zone, and 3) the rate of drainage from the vadose zone into the saturated zone. Under natural rainfall conditions water cannot in general enter the soil unless an equal volume of air escapes from the soil surface. During the infiltration process, there is a simultaneous downward flow of water and an upward current of air passing through the soil,

though not necessarily through the same soil pores (Horton 1940). Horton (1940) noted a marked rise of infiltration-capacity in the spring months (at about the time in the spring when earthworms, ants, beetles and other soil fauna become active) and a more rapid recession in the fall at about the time they become dormant. A quantitative estimate of infiltration rates through the infiltration media is critical in the design of most infiltration facilities. The size and geometry of the infiltration facilities are selected by comparing infiltration rates with estimates of runoff volumes calculated for specified precipitation events (Massman 2003).

2.5.2 Horton Equation

Horton (1939) defined the minimum infiltration capacity as the capacity of a soil – surface free from sun-checks and biological structures (perforations by earthworms, insects, and roots) which has been wetted to field moisture capacity long enough to permit full swelling of colloids and adjustment of the soil structure to a stable field condition. A soil surface may not fully meet these conditions during a rain because of under or over-packing, puddling of the soil surface (layering of fine silts or clays in areas where water had micro-ponded, allowing these fines to accumulate on the soil surface) and in-washing of fine material, or because of the presence of biological structures. If the rain intensity is less than the infiltration rate, then the rain will completely infiltrate, as it is not limited by the maximum infiltration capacity of the soil (Horton 1940). Horton's theory is based on the fact that infiltration is faster in dry soils since there are more void spaces in a dry soil surface compared to a moist or saturated soil. However, as rain continues and the ground becomes wetter, the infiltration rate decreases as these voids fill with water.

Horton (1939, 1940) derived a three-parameter empirical infiltration equation to describe the decline in the potential infiltration rate f_p as a function of time.

$$f_p = f_o + (f_o - f_c)e^{-kt}$$

Where f_o = the initial infiltration rate

f_c = the final (minimum) infiltration rate and

k = the decay constant.

The Horton empirical equation has been widely used over the years because it is simple to apply and has the advantage that, in the limit as time t approaches infinity, the infiltration rate does not become zero (Toebes 1962). Horton's equation generally provides a good fit to data (Turner, 2006). Horton's equation is applicable only when the effective rainfall intensity (i_e) is greater than the infiltration capacity at all times and that the infiltration rate decreases with time (Linsley et al. 1975, Bedient and Huber 1992). Horton's model recognizes that infiltration depends on several factors that are not explicitly accounted for, such as the initial moisture content and organic content of the soil, vegetation cover, and season (Linsley et al. 1982). Horton's model does not consider storage availability in the soil after varying amounts of infiltration have occurred, but only considers infiltration as a function of time (Akan 1993). The model does not consider subsurface flows and attributes control almost completely to surface conditions (Bevin, 2004). It is recommended that f_o , f_c , and k all be obtained through field data, but they are rarely measured locally. The use of published values in place of reliable field data is the cause of much concern by many researchers (Akan 1993). Typical values of f_o , f_c , and k are given in Table 4.

Table 4. Horton's Parameters for Different Types of Soil (Source: Akan 1993)

Soil Type	f_o (in/hr)	f_o (mm/hr)
Dry sandy soils with little to no vegetation	5	127
Dry loam soils with little to no vegetation	3	76
Dry clay soils with little to no vegetation	1	25
Dry sand soils with dense vegetation	10	254
Dry loam soils with dense vegetation	6	152
Dry clay soils with dense vegetation	2	51
Moist sandy soils with little to no vegetation	1.7	43
Moist loam soils with little to no vegetation	1	25
Moist clay soils with little to no vegetation	0.3	8
Moist sandy soils with dense vegetation	3.3	84
Moist loam soils with dense vegetation	2	51
Moist clay soils with little to no vegetation	0.7	18

Soil Type	f_c (in/hr)	f_c (mm/hr)	k (1/min)
Clay loam, silty clay loams	(0-0.05)	0-1.3	0.069
Sandy clay loam	(0.05-0.15)	1.3-3.8	0.069
Silt loam, loam	(0.15-0.30)	3.8-7.6	0.069
Sand, loamy sand, sandy loams	(0.30-0.45)	7.6-11.4	0.069

2.5.3 Green-Ampt Infiltration Model

Green and Ampt (1911) developed the first physically based infiltration equation by using Darcy's Law in conjunction with a set of assumptions regarding flow field geometry and material properties. Since it is theoretically based, it is often preferred over the more empirical Horton equation. The model was originally developed for ponded infiltration into a deep homogenous soil with uniform initial water content. The basic assumption behind the Green-Ampt equation is that water infiltrates into the soil as a piston flow resulting in a sharply-defined wetting front which separates the wetted and unwetted zones neglecting the depth of ponding at

the surface. The model calculates cumulative infiltration by assuming water flow into a vertical soil profile like a piston flow.

The Green-Ampt approach assumes the wetting front penetrates to a depth L at time t , separating the saturated soil with hydraulic conductivity K , and moisture content η from the soil which has moisture content i below the wetting front. The equation assumes ponded water with a depth of h_0 above the surface (Chow, 1998). The soil is assumed to be saturated above the wetting front (the water content is assumed to be equal to the porosity). Figure 5 below illustrates the variation in moisture content (η) with depth.

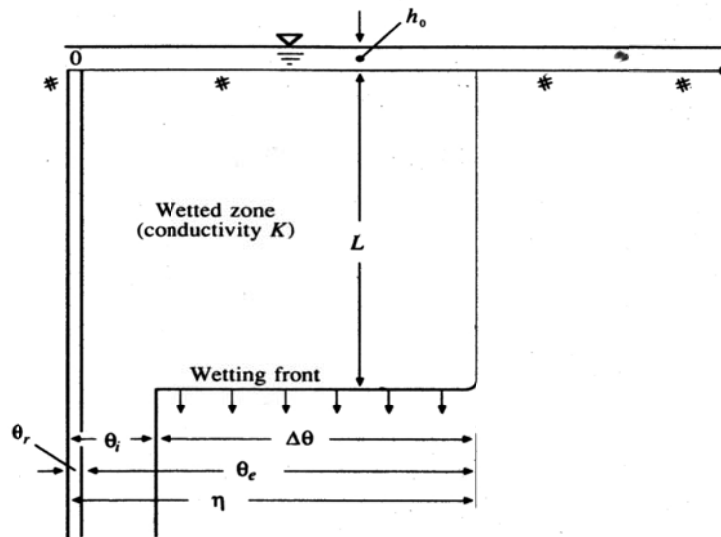


Figure 5. Variables in the Green-Ampt Infiltration Model (Source: Chow 1988).

The Green-Ampt infiltration equation involves three parameters which need to be estimated.

The rate of infiltration is approximated by the following expression:

$$f = k \frac{(h_0 + \psi + L)}{L}$$

Where

f = the infiltration rate at time t , cm/hr;

k = saturated hydraulic conductivity, cm/hr;

h_0 = depth of water in the pond or infiltration facility (L).

L = depth of the wetting front below the bottom of the pond (L), and

ψ = average capillary head at the wetting front (L). Approximately equal to the air entry pressure or bubbling pressure.

The initial infiltration rates are higher than the saturated hydraulic conductivity because of the relatively high gradients when the wetting front is shallow. As the depth of the wetting front increases, the gradient decreases and the infiltration rate approaches the saturated hydraulic conductivity, K . Table 5 summarizes the results for three different soil types that are often associated with stormwater infiltration facilities.

Table 5. Parameters Used to Estimate Infiltration Rates (Source: Massman 2003).

Input parameters	Sand	Loamy Sand	Sandy Loam
Capillary head at wetting front, inches(cm)	1.6 (4.10)	2.3 (5.80)	4.4 (11.20)
Saturated hydraulic Conductivity, in/min(cm/min)	0.20 (0.49)	0.1 (0.24)	0.03 (0.07)
Output description			
Time at which infiltration rate equals 1.5 times the saturated hydraulic conductivity (hrs)	0.05	0.1	0.9
Time at which infiltration rate equals 1.1 times the saturated hydraulic conductivity (hrs)	0.40	1.1	8.5

2.5.4 Measuring Infiltration Rates

A wide variety of infiltration testing methodologies and measuring instruments are available. Ring infiltrometers of large diameter are probably the most common field methods for obtaining data on infiltration rates. The double-ring infiltrometer test is a widely used technique for directly measuring field infiltration rates. Double-ring infiltrometers are often constructed

from thin walled hard-alloy, aluminum sheet or other material sufficiently strong to withstand hard driving several inches into the soil. The inner and outer cylinder diameters of the standard unit are 20 and 30 cm (8 and 12 inches), respectively, with a cylinder height of 50 cm (20 inches) (ASTM 2003). The edge of the cylinders should be beveled and kept sharp so that the soil disturbance is minimized. Rings set only a few inches into the soils may not indicate the permeability of the underlying materials (Musgrave 1935a). Guidelines on conducting double-ring infiltration tests are described by Bouwer (1986) and ASTM (2003).

The double-ring infiltrometer minimizes the error associated with the single-ring method because the outer ring helps to reduce the lateral movement of water in the soil from the inner ring. For uniform soils, the use of cylinders set 6 inches into the soil gave reliable results and showed that buffer rings were not needed if the infiltrometer was at least 18 inches in diameter (Lewis 1937).

There are two operational techniques used with single- or double-ring infiltrometers for measuring the infiltration of water into the soil: Constant head and falling head techniques. For constant head techniques, the water level in the inner ring is maintained at a fixed level and the volume of water used to maintain this level is measured. For the falling head technique, the time taken for the water level within the cylinder to decrease a certain amount is measured. The measurements normally are continued until the infiltration rate becomes constant. In many cases, the falling head test is preferred since less water and time are required to complete a test (Ali 2010).

The double-ring infiltrometer method is particularly applicable to relatively uniform fine-grained soils, with an absence of very plastic clays and gravel-size particles and with moderate to low resistance to ring penetration (ASTM 2003). This test method is difficult to use or the

resultant data may be unreliable, or both, in very pervious or impervious soils (soils with a hydraulic conductivity greater than about 10^{-2} cm/s (14 in/hr) or less than about 1×10^{-6} cm/s (0.01 in/hr) or in dry or stiff soils that most likely will fracture when the rings are installed.

2.6 Soil Compaction

Soil compaction is defined as the method of mechanically increasing the density of the soil (by compression) that results in reductions of the volume of air. It is the process by which soil grains are rearranged into closer contact to reduce void spaces. The usual effects of soil compaction results in increased bulk densities, decreased moisture holding capacities, restricted root penetration, impeded water infiltration, and fewer macropore spaces needed for adequate aeration, all often leading to a significant reduction in infiltration rates (Gregory et al., 2006; Pitt et al., 1999a, 2008; Thompson et al., 2008).

Infiltration tests conducted on many different soils having a wide range of texture and representative of the great soil and parent –material group at 68 field sites throughout the United States indicated that the infiltration rate decreases with increasing clay content and increases with increasing noncapillary porosity (Free et al.1940). Understanding the physical and hydrologic properties of different bioretention media mixtures as well as their response to compaction may increase the functional predictability of bioretention systems and thus improve their design (Pitt et al., 2002 and 2008; Thompson et al., 2008). Pitt et al. (1999a) conducted a series of 153 infiltration tests on disturbed urban soils near Birmingham and Mobile, Alabama. A double-ring infiltrometer with falling head was used to measure average infiltration rates at 5 min intervals for 2 hours. They used the two hour test to replicate typical two hour rain durations and the typical times needed to reach saturation. Pitt et al. (1999a) fitted the observed infiltration

rates to the Horton equation, but with limited success due to the wide scatter of the data for each soil condition and typically non-decreasing infiltration rates with time. These infiltration data were compared to site conditions to evaluate the effects of moisture content and compaction on infiltration rates in the disturbed urban soils. They found that sandy soils were mostly affected by compaction with moisture levels having little effect on infiltration rates, while clayey soils showed strong correlations for both soil moisture and soil compaction.

Pitt et al., (1999b) found substantial reductions in infiltration rates due to soil compaction, especially for clayey soils. The sandy soils were better able to withstand compaction, although their infiltration rates were still significantly reduced. Compaction was seen to have about the same effect as moisture saturation for clayey soils, with saturated and compacted clayey soils having very little effective infiltration rates (Pitt et al., 2008). Sandy soils can still provide substantial infiltration capacities, even when greatly compacted, in contrast to soils containing large amounts of clays that are very susceptible to compaction's detrimental effects. In a similar study, Gregory et al. (2006) examined the effects of compaction on infiltration rates at urban construction sites in north-central Florida. Infiltration was measured in noncompacted and compacted soils from three land types (natural forest, planted forest, and pasture sites). Although infiltration rates varied widely across the three land types, construction activity reduced infiltration rates by 70 to 99 percent at all sites.

Pitt et al. (1999a) measured mean final infiltration rates after 2 hours were to be 16 in/hr (410 mm/hr) for noncompacted sandy soils, 2.5 in/hr (64 mm/hr) for compacted sandy soils, 8.8 in/hr (220 mm/hr) for noncompacted and dry clayey soils, and 0.7 in/hr (20 mm/hr) for all other clayey soils. They noted large differences in the observed infiltration rates compared to traditional published values. Typically, published values are for undisturbed natural pasture or

wooded area soils and do not indicate effects associated with compaction associated with land development or other use.

Pitt et al.(1999a) defined compact soils as those soils having a cone index reading of greater than 300 psi (2068 kPa) on a cone penetrometer, while non-compacted soils have cone index readings of less than 300 psi (2068 kPa) at a depth of 75 mm (3 in). Very large errors in soil infiltration rates can easily be made if published soil maps are used in conjunction with most available models for typically disturbed urban soils, as these references ignore compaction (Pitt et al. 1999a, 2002, and 2008).

Full-scale tests provide the most reliable estimates of infiltration tests compared to other field and laboratory methods. Massman (2003) conducted full-scale "flood tests," in which infiltration tests at four infiltration facilities located in western Washington noted large differences in infiltration rates when the field values were compared to values estimated from air conductivity and grain size analyses. Massman (2003) illustrated that infiltration rates cannot be estimated solely on the basis of soil types (grain size texture) or saturated hydraulic conductivity, but other site-specific characteristics need to be considered to accurately design infiltration facilities.

2.7 Soil Amendments

Soil amendments (such as organic composts) improve soil infiltration rates and water holding characteristics and add protection to groundwater resources, especially from heavy metal contamination in urban areas (Pitt et al. 1999a and 1999b). Groundwater contamination problems were noted more often in commercial and industrial areas that incorporated subsurface infiltration and less often in residential areas where infiltration occurred through surface soil (Pitt et al. 1999a and Clark et al., 2006). However, stormwater runoff pretreatment practices can be applied to minimize groundwater contamination and to prolong the life of the infiltration device.

Compost was found to have a significant sorption and ion exchange capacity that was responsible for pollutant reductions in the infiltrating water (Pitt et al. 1999a). A significant increase in infiltration rates was noted in compost incorporated into the top 20 cm of a loam textured soil compared to unamended soils (Thompson et al. 2008). Adding compost has positive effects on aggregate stability, bulk density, porosity, infiltration rates, and total water holding capacity of soils. However, Weindorf et al. (2006) reported no treatment effects when compost was incorporated into a clay loam soil. Newly placed compost amendments may cause increased nutrient discharges until the material is better stabilized (usually within a couple of years). In addition to flow control benefits, amended soils in urban lawn can also have the benefits of reduced fertilizer requirements and help control disease and pest infestation in plants (US EPA 1997).

2.8 Need for Research

The literature summarized above has indicated that biofiltration devices are an effective option for the treatment and discharge of stormwater runoff from urban areas. However, the performance of these systems and other infiltration devices commonly is reduced through clogging of the media, use of substandard soils as part of the treatment media mixture, through short-circuiting of infiltrating water through an underdrain, or by short resident/contact times of the stormwater and the treatment media. In addition, few quantitative guidelines are available for the design of biofilters and bioinfiltration devices for specific treatment goals while minimizing operational problems.

Media selection is critical for biofilter performance as the media affects the amount of runoff that is treated and the level of treatment that can be obtained. Soil characteristics such as texture, structure and porosity (compaction) of the soil media used during construction of

stormwater treatment facilities and the underlying soils can have a significant impact on the performance of these systems. Appropriate hydraulic characteristics of the media, including treatment flow rate, clogging capacity, and water contact time, are needed to select the media and drainage system. Therefore, it is important to understand the media's ability to capture targeted pollutants with minimal clogging given the appropriate contact time, when predicting the performance of a biofilter device.

2.9 Dissertation Research

Based on the literature review and current biofilter issues, this dissertation research focused on the following outstanding questions pertaining to biofilter/bioinfiltration media:

1. More effective underdrains: The use of underdrains, while necessary to minimize long periods of standing water in poorly draining natural soils, can also decrease the performance of biofilter systems. Pilot-scale tests were conducted to determine the flow capacity and clogging potential of a newly developed underdrain material (SmartDrain™) under severe service conditions.
2. Restoration options of poorly operating biofilters: A common failure mechanism for biofilters is overly compacted media, as reflected in a large installation in Tuscaloosa. Restoration options include modifications to the media that enhance its resistance to compaction. Tests were conducted on amending the media and comparing field and laboratory performance measurements with actual event measurements. These parallel measurements were also used to illustrate the limitations of small-scale measurements when predicting full-scale performance.
3. Flow as a function of basic biofilter media characteristics: Media selection is critical for stormwater biofilter performance as the media affects the amount of runoff that is treated

and the level of treatment that can be obtained. A series of controlled laboratory column tests conducted using various media to identify changes in flow with changes in the mixture characteristics, focusing on media density associated with compaction, particle size distribution (and uniformity), and amount of organic material (due to added peat). The laboratory columns used in the tests had various mixtures of sand and peat. The results of the predicted performance of these mixtures were also verified using column tests (for different compaction conditions) of surface and subsurface soil samples obtained from Tuscaloosa, AL, along with biofilter media obtained from Kansas City, North Carolina, and Wisconsin.

4. Rapid response and scaling issues: Small scale, rapid, tests are needed to quickly inventory soil conditions in areas undergoing planning following natural disasters, or to meet short schedules associated with accelerated construction goals. Tests were conducted to determine the reliability of these rapid tests compared to pilot-scale or full-scale infiltration tests. This research included field-scale and laboratory studies of local soils in the Tuscaloosa, AL, area to provide insight into the existing soil characteristics at stormwater bioinfiltration sites in areas devastated by severe tornados that were undergoing reconstruction. The field studies include both small-scale infiltration tests along and larger pilot-scale borehole tests, plus controlled laboratory column tests that were examined the effects of compaction on the infiltration rates through the local soils obtained from bioinfiltration sites.

CHAPTER 3

3. HYPOTHESES AND EXPERIMENTAL DESIGN

The literature review has indicated that the performance of biofiltration systems is commonly reduced through clogging of the media, through short-circuiting of infiltrating water through an underdrain, or by short resident/contact times of the stormwater and the treatment media. Biofilters will experience a decline in hydraulic conductivity following construction mainly due to compaction. Knowledge of the physical and hydrologic characteristics of various stormwater biofiltration and bioretention soil mixtures, as well as their response to compaction during their construction, may increase the functional predictability of these facilities and thus improve their design. Pitt et al. (1999a) conducted a series of infiltration tests on disturbed urban soils near Birmingham and Mobile, AL and found substantial reductions in infiltration rates due to soil compaction, especially for clayey soils. Pitt et al. (1999a) noted a great difference in the observed infiltration rates from the published values. An infiltration study on sandy soils in north central Florida showed that even the lowest levels of compaction resulted in significantly lower infiltration rates and significant increased soil bulk density values associated with vehicular traffic during urban development construction (Gregory et al. 2006).

Laboratory and field studies conducted to examine the effects of soil-water, soil texture, and soil density (compaction) on water infiltration through historically disturbed urban soils suggests that the actual macro-structure conditions in the natural soils or the compaction levels obtained in the laboratory were unusually high compared to field condition(Pitt, *et al.* 1999a).

Massman (2003) reported that infiltration rates cannot be estimated solely on the basis of soil types (grain size texture) or saturated hydraulic conductivity but other site-specific characteristics need to be considered to accurately design infiltration facilities suggesting full-scale tests "flood tests," provide the most reliable estimates of infiltration tests compared to other field and laboratory methods.

3.1 Hypothesis

The main objective of this dissertation research was to examine the factors that affect the performance of stormwater biofilters and bioinfiltration stormwater treatment devices. This research also examined the flow capacity and clogging potential of a newly developed underdrain material (SmartDrain™) which offers promise as a low flow control device with minimal clogging potential after excessive loadings by fine ground silica particulates and biofouling experiments under controlled pilot-scale biofilter conditions.

The literature review and analyses indicated that the failure of biofiltration systems is mostly associated with clogging either at the surface, on buried geotextiles, or at the underdrain, or due to compacted media. The drainage rate in biofiltration devices is usually controlled using an underdrain that is restricted with a small orifice or other flow-moderating component, or through selection of media. Underdrains frequently fail as the orifices are usually very small (<10 mm) and are prone to clogging. Underdrains are used to ensure adequate drawdown, drain slopes, and prevent groundwater from entering the pavement, and remove surface water that enters the pavement. Sandy-silt loam soil results in extended surface ponding, requiring an underdrain. Media selection for rate control is not well understood, especially when using mixtures of materials. Scaling issues associated with different measurement methods is also

poorly understood when small-scale monitoring results are applied to designs. Finally, restoration options for failed biofilters need further exploration.

The following hypothesis statements for this dissertation research are based on the literature review and analyses and address these issues.

Hypothesis 1:

A restricted underdrain (such as the SmartDrain™) results in enhanced outlet control for bioinfiltration devices.

Prediction 1:

Biofilters (bioretention devices having an underdrain) are widely used in urban areas to reduce runoff volume, peak flows and stormwater pollutant impacts on receiving waters. The effectiveness of a biofilter is commonly reduced through clogging or compaction of the media, through short-circuiting of infiltrating water through an underdrain, or by short resident/contact times of the stormwater and the treatment media. A newly developed foundation drain material (SmartDrain™) can be used in bioinfiltration devices and provide an option for enhanced outlet control.

A typical biofilter that is 1 m deep, 1.5 m wide and 5 m long would require about 8 hours to drain using the SmartDrain™ material as the underdrain. This is a substantial residence time in the media and also provides significant retention of stormwater before being discharged to a combined sewer system. In addition, this slow drainage time will allow infiltration into the native underlying soil, with minimal short-circuiting to the underdrain. Even sandy-silt loam soils frequently used in bioretention devices can result in extended surface ponding, requiring an underdrain. Conventional underdrains (perforated pipe) reduce ponding, but also decrease

infiltration opportunities with much less detention times. The SmartDrain™ also reduces the ponding time but does not allow as much short-circuiting of the infiltration water.

Research Activities 1:

- a) Determine the particle size distributions of the sand filter media obtained from different local suppliers in Tuscaloosa, AL, to select the best bedding material for the underdrain.
- b) Examine the drainage characteristics of the SmartDrain™ material (such as length, slope, hydraulic head, and type of sand media) under a range of typical biofilter conditions using clean water.
- c) Examine the flow capacity and clogging potential of the SmartDrain™ material after excessive loadings by fine ground silica particulates and biofouling experiments under controlled conditions.
- d) Develop stage-discharge relationship plots for different lengths of SmartDrain™ material tested for different slopes with clean water and dirty water.
- e) Model different applicants of the SmarDrain™ to develop design curves for different biofilter design objectives and site conditions and to quantify performance attributes (water mass balances and residence times, for example) compared to conventional underdrains.

Critical Tests 1:

- a) Calculate Pearson's correlation coefficients to examine the strength and significance of the relationships between the drainage characteristics of the SmartDrain™ material (such as length, slope, hydraulic head, and type of sand media) and flow capacity.

- b) Assess the flow capacity and clogging potential of the SmartDrain™ material after excessive loadings by ground silica materials (Sil-Co-Sil250) and biofouling experiments under controlled conditions. Perform turbidity measurements (NTUs) from the influent and effluent of the pilot-scale biofilter device.
- c) Box-and-whisker plots were used to identify natural groupings of drainage characteristics that explain the variabilities in measured flowrate values.
- d) Stage-discharge relationship plots were shown for different lengths of SmartDrain™ material.
- e) Perform linear regression analyses to determine the intercept and slope terms of this stage - discharge relationship. The p-values of the estimated coefficients was used to determine if the coefficients were significant ($p < 0.05$).
- f) A complete two level and three factors (2^3 , SmartDrain™ length, slope, and head) factorial experiment was conducted to examine the effects of those factors, plus their interactions on the SmartDrain™ flowrates.
- g) An analysis of variance (ANOVA) table was constructed to determine the significant factors and their interactions needed to best predict SmartDrain™ flow performance.
- h) A final model was developed to predict the SmartDrain™ flowrate performance.

Hypothesis 2:

Amending biofilter media and landscaping soil can improve the infiltration capacity of the material and also reduce the impact of compaction on the infiltration rates.

Prediction 2:

Bioinfiltration devices are a potentially effective option for the treatment and discharge of stormwater runoff from urban areas. However, the performance of these systems and other infiltration devices are affected by soil characteristics such as texture, structure and porosity (compaction) of the soil media used during construction of the stormwater treatment facilities and the underlying soils. The usual effects of compaction are increased bulk density and soil strength; reduced porosity, moisture holding capacity infiltration rates, and evapotranspiration potential; and restricted root penetration and plant vigor due to reduced air available to plant roots and other soil organisms.

Soil compaction that occurs in stormwater treatment facilities during construction can cause significant reductions in infiltration capacities of the soils. Very large errors in soil infiltration rates can easily be made if published soil maps are used in conjunction with most available models for typically disturbed urban soils, as these tools ignore compaction. Infiltration rates cannot be estimated on the basis of soil types or saturated hydraulic conductivity but other site-specific characteristics need to be considered to accurately design infiltration facilities.

Research Activities 2:

- a) Conduct double -ring infiltrometer tests and soil compaction measurements to determine the in-situ characteristics of the media for a poorly operating biofilter facility located in Tuscaloosa, AL.
- b) Examine the effects of different compaction levels on the infiltration rates through the soil media obtained from the biofilter when mixed with varying amounts of filter sand and organic matter amendments during laboratory column experiments.
- c) Perform long-term and continuous monitoring in the biofilter during rains.

- d) Conduct surface double-ring infiltration tests and bore hole infiltration measurements in the field to determine the surface and subsurface infiltration characteristics (located at the depths at the bottom of bioinfiltration devices) in Tuscaloosa, AL, in areas devastated by the severe April 2011 tornados.
- e) Conduct controlled laboratory column tests using various media to identify changes in flow with changes in the mixture characteristics, focusing on media density associated with compaction, particle size distribution (and uniformity), and amount of organic material (due to added peat).
- f) Predicted performance of these mixtures were also verified using column tests (for different compaction conditions) of surface and subsurface soil samples obtained from Tuscaloosa, AL, along with biofilter media obtained from Kansas City, North Carolina, and Wisconsin.
- g) Examine the effects of different compaction levels on the infiltration rates through sand-peat mixture, surface and subsurface soil samples obtained from Tuscaloosa, AL, along with biofilter media obtained from Kansas City, North Carolina, and Wisconsin.

Critical Tests 2:

- a) Fit the observed surface infiltration rates measured within the poorly operating biofilter facility to the Horton equation, allowing the Horton coefficients to be determined for each test.
- b) Fit the observed infiltration rates that were measured through the soil media obtained from the biofilter when mixed with varying amounts of filter sand using laboratory column experiment, to the Horton equation, allowing the Horton coefficients to be determined for each test.

- c) Fit the observed surface and subsurface infiltration rates that were measured at the bioinfiltration facilities to the Horton equation, allowing the Horton coefficients to be determined for each test.
- d) Box-and-whisker plots were used to identify natural groupings of site characteristics that explain the variabilities in observed infiltration rates for surface and subsurface infiltration tests. These analyses identified the groupings of site characteristics that explain the variability in measured observed infiltration rate values.
- e) Perform analyses of variance and post-hoc tests for each field infiltration test (surface and subsurface) and laboratory column infiltration experiments to determine the difference within and between infiltration test methods and to verify the correlations.
- f) Compare Horton coefficients with site conditions to evaluate the effect of compaction on infiltration rates in urban soils.
- g) Kruskal-Wallis test was used to distinguish the difference in paired saturated infiltration rates for different percentages of sand and biofilter media and different levels of conditions. Similar tests were conducted for each field infiltration test (surface and subsurface) and laboratory column infiltration experiments to determine the difference within and between infiltration test methods and to verify the correlations.
- h) Full-factorial experimental design were used to determine the effects of media texture, uniformity of the media, organic content of the material, and compaction, plus their interactions, on the flowrate through the biofilter media.
- i) An analysis of variance (ANOVA) table was constructed to determine the significant factors and their interactions needed to best predict media flow performance. A final model was developed to predict the flowrate through the mixtures as a function of the

significant factors and their interactions. Based on these tests texture and uniformity of the media mixture have the greatest effect on the measured final infiltration rates of the media

3.2 Experimental Design

Full factorial analyses, as described by Box et al. (1978), was the primary tool used for the experimental designs of the various experiments and tests conducted during this research to identify the most important factors affecting the field and laboratory infiltration rates. The full factorial analyses was useful in identifying the effects of individual factors and the effects of factor interactions. Examples of the factors that were examined include soil compactness (hand compaction, standard proctor and modified proctor compaction) and soil location (surface and subsurface soils). Effects of the individual factors and their interactions were calculated using a table of contrasts with the averages of the differences between the sums of the final/observed infiltration rates when the factor was at its maximum value and at its minimum value.

Probability plots of calculated effects for individual factors and outliers (abnormal points) on the graph will indicate the most important factors and interactions affecting the observed/final infiltration rates on the type of compaction. This process were repeated for all selected individual observed/final infiltration rates. Residual analyses were conducted to ensure that the resulting model meets all the statistical test requirements. In an example of a 2^3 factorial design, Burton and Pitt (2002) described experiments investigating the effects of soil moisture, soil texture, and soil compaction on observed soil infiltration rates (Pitt *et al.* 1999a). Table 6 shows the calculations from 152 double-ring infiltration tests for the Horton (1939) equation final infiltration rate coefficient (f_c).

Table 6. Example Factorial Experimental Analysis for Field Project Investigating Infiltration into Disturbed Urban Soils (Source: Pitt et al. 1999a)

Moisture (Wet=+/Dry =-)	Texture(Clay=+/Sand =-)	Compacted (Yes=+/No =-)	Factorial Group	Average	Standard Error	Number
+	+	+	1	0.23	0.13	18
+	+	-	2	0.43	0.50	27
+	-	+	3	1.31	1.13	18
+	-	-	4	16.49	1.40	12
-	+	+	5	0.59	0.35	15
-	+	-	6	7.78	4.00	17
-	-	+	7	2.25	0.98	21
-	-	-	8	13.08	2.78	24
overall average					5.27	
calculated pooled S.E					1.90	

Factorial Group	Effects	Rank	Prob	$f_c = 5.27 \pm (T/2) \pm (C/2)$
C	-8.35	1	7.14	$f_c = 5.27 \pm (-6.02/2) \pm (-8.35/2)$
T	-6.02	2	21.43	T C
MT	-2.55	3	35.71	Calculated Values
M	-1.31	4	50.00	+ + -1.92
MC	0.66	5	64.29	+ - 6.43
MTC	2.83	6	78.57	- + 4.10
TC	4.66	7	92.86	- - 12.45

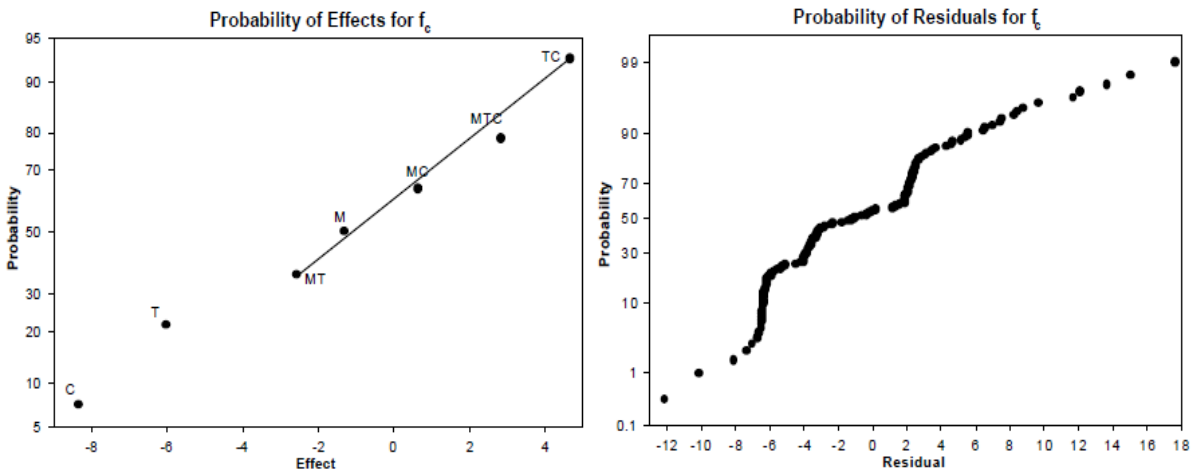


Figure 6. Probability Plots (Pitt et al. 1999a)

For this research the final/ initial infiltration rates through a soil media used for the laboratory column infiltration tests can be grouped according to the degree of compactness (hand and standard compaction, hand and modified compaction, standard and modified compaction), and surface and subsurface soils, in a 2² factorial test having four sample groups (Table 7).

C: Compaction (standard proctor: +; hand :-)

S: Soil media (surface: +; subsurface :-)

Table 7. Factorial Experimental Design for two Factors and Four Experiments

Test site #1 and Test site #2	
Compaction (Standard= +/Hand= -)	Soil media (Surface =+/Subsurface = -)
-	-
-	+
+	+
+	-

3.3 Quality Control (QC) and Quality Assurance (QA) Procedures

Quality control and quality assurance techniques were used during all parts of the research: for field surface and subsurface infiltration data collection, in-situ soil density measurements, laboratory column infiltration data collection, and statistical data analyses. Before placing the infiltrometer on the test sites where a measurement is to be made, the area is leveled and cleaned of debris and loose materials. In cases of field and laboratory infiltration tests, the measurements are recorded in a lab notebook, and later the information is entered into the spreadsheet. Once the database is completed, the main table is reviewed by columns corresponding to the change in water level (inch) and elapsed time (minute) since the beginning of the first measurement. Each row and column in the database are reviewed at least twice and

compared to information contained in the original lab notebook to identify possible errors associated with the transcription of the information. All soil sampling equipment and the drying dishes that are used for determining the soil moisture are washed and dried.

3.4 Data Analyses

This part of the research describes the experimental goals and the selected number of statistical tests and their data requirements that were used for data evaluation.

Basic Data Plots

There are several basic data plots that need to be prepared as data are collected and when all of the data are available. These plots are used for QA/QC analyses and to demonstrate basic data behavior.

3.4.1 Probability and Scatter plots

The probability plots indicate the possible range of the values expected, their likely probability distribution type, and the data variation. Probability plots should be supplemented with standard statistical tests that determine if the data is normally distributed. The majority of the graphs used in science are scatterplots. These plots should be made before any other analyses of the data are performed.

3.4.2 Grouped Box and Whisker Plots

Box-and-whisker plots are exploratory graphics used to show the distribution of a dataset. They are primarily used when differences between sample groups are of interest. Box-and-whisker plots indicate the range and major percentile locations of the data. If the 75 and 25 percentile lines of the boxes do not overlap on different box- and -whisker plots, then the data groupings are likely significantly different (at least at the 95 percent level). When large numbers

of data-sets are plotted, the relative overlapping or separation of the boxes is used to identify possible groupings of the separate sets. For this research, box- and -whisker plots were used to indicate the variabilities in the field and laboratory infiltration rate measurements. Figure 7 shows grouped box and whisker plot of influent vs. effluent SSC test results from sand and peat column (mixture $D_{50} = 0.3$ mm and $C_u = 3$)

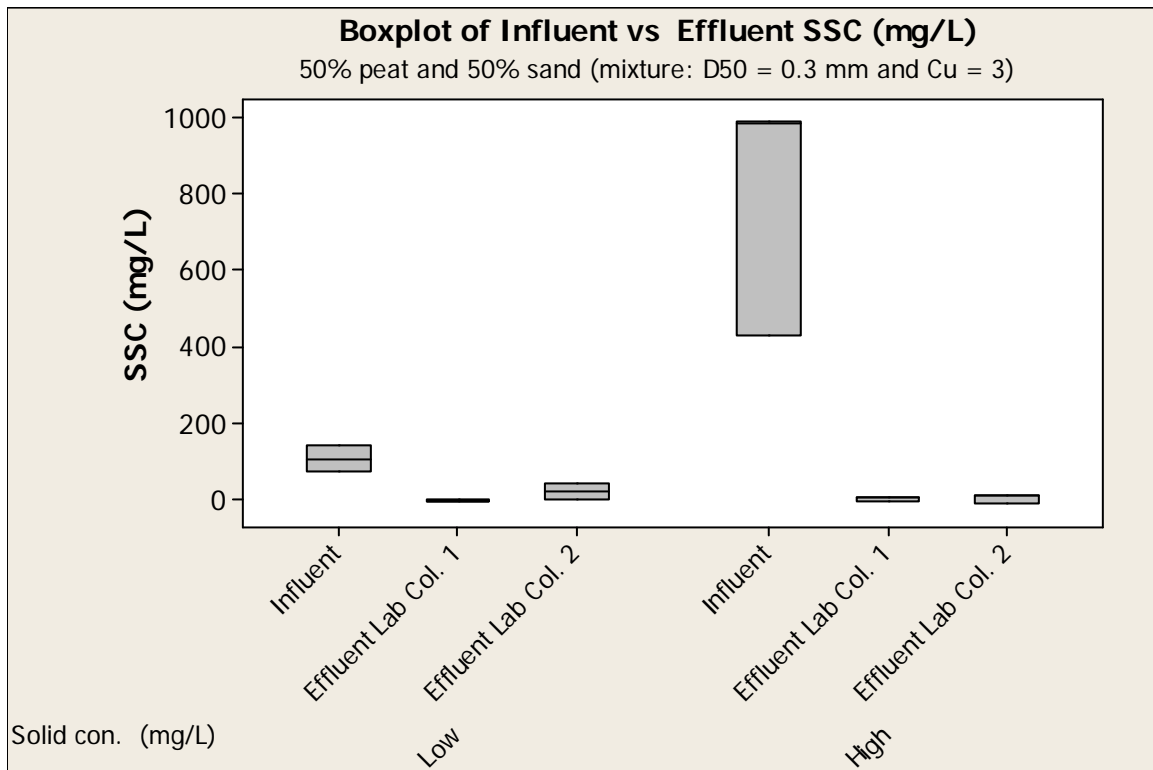


Figure 7. Example Grouped Box and Whisker Plot of Influent vs. Effluent SSC Test Results from Sand and Peat Columns.

3.4.3 Regression Analyses

Regression analyses are statistical tools that are used in various studies to explore an association between the independent and dependent variable, when graphed on a Cartesian coordinate system. Linear regression is used to examine the relationship between one dependent

and one independent variable. Linear regression is a parametric test, that is, for a given independent variable value, the possible values for the dependent variable are assumed to be normally distributed with constant variance around the regression line.

This dissertation research used simple linear regression ($y = b_0 + b_1x$) and nonlinear regression ($y = c + be^{-kx}$) analyses. Simple linear regression were used to predict stage and discharge relationships during drainage characteristics and clogging potential tests on SmartDrainTM material, for example. Nonlinear regression were used to fit the observed infiltration to Horton equations and determine the Horton's parameters (f_o, f_c , and k). Figure 8 is an example of linear regression for stage-discharge relation plots SmartDrainTM length 9.4 ft. Regression analyses evaluated the regression results by examining the coefficient of determination (R^2) and the results of the analysis of variance of the model (ANOVA). The coefficient of determination is a measure of how well the regression line represents the data. High R^2 values by themselves do not guarantee that the model has any predictive value; similarly, a seemingly low R^2 does not mean that the regression model is useless.

ANOVA and residual analyses were used to supplement the interpretation of the linear equation fit to the model. The analysis of residuals plays an important role in validating the regression model. The significance of the regression coefficients were determined by performing residual analyses for the fitted equations. Because the residuals are the unexplained variation of a model and are calculated as the differences between what is actually observed and what is predicted by the model (equation), their examination should confirm the validity of the fitted model. If the error term in the regression model satisfies the four assumptions (they must be independent, zero mean, constant variance, and normally distributed), then the model is considered valid. The normal probability plot of the residuals example shown in Figure 9 shows

that the residuals are normally distributed (Anderson Darling test for normality has a p-value greater than 0.05, indicating that the fitted data is normally distributed).

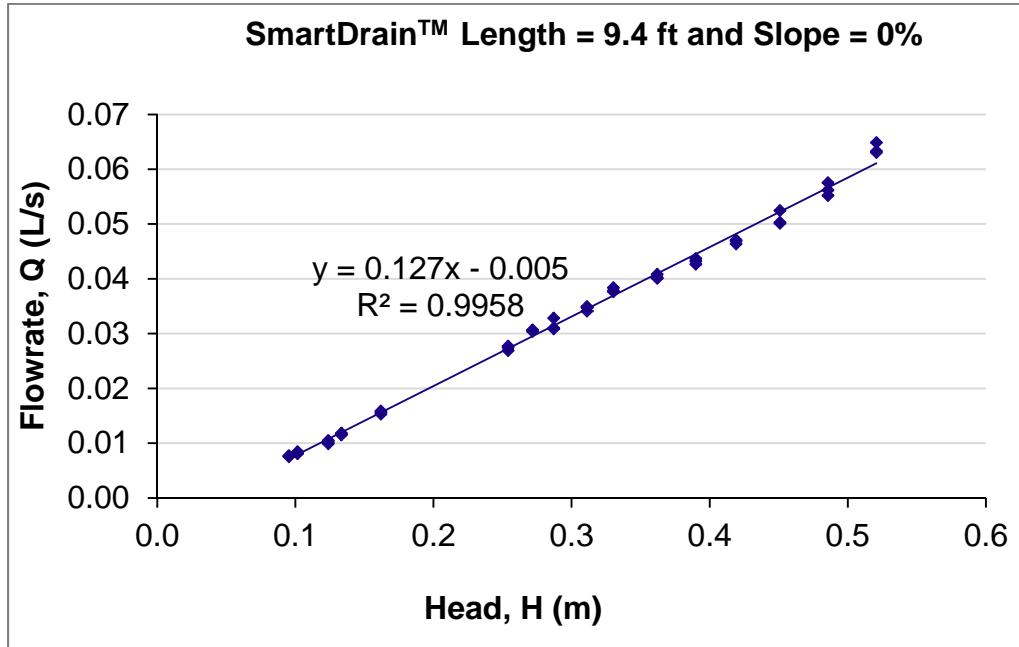


Figure 8. Example of Linear Regression for Stage- discharge Relation Plots Using Different Length of Smartdrain™ Material.

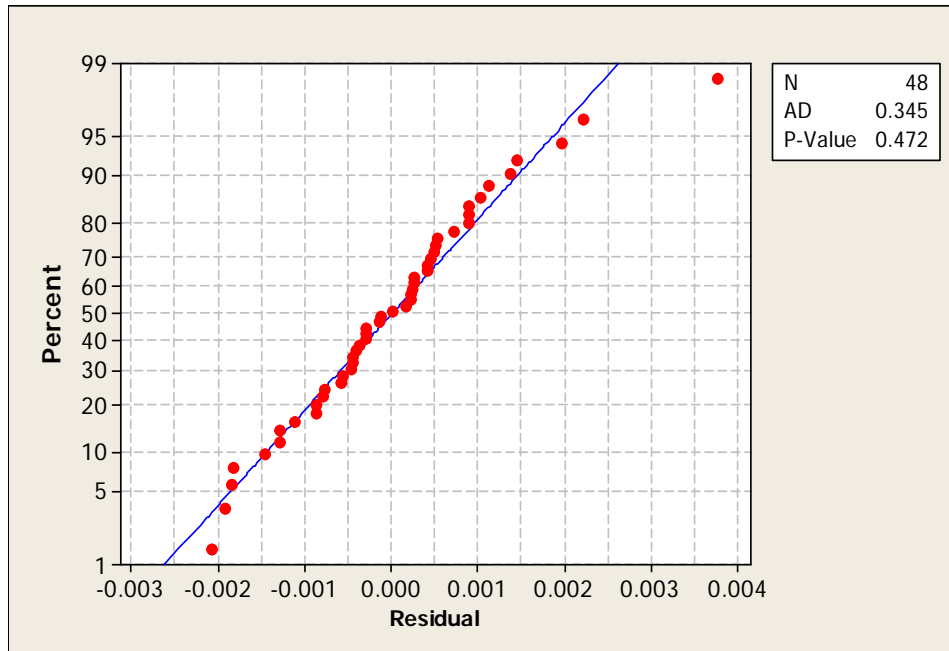


Figure 9. Probability Plot of The Residuals for Linear Regression of 9.4 ft

3.4.4 Analyses of Variance (ANOVA)

ANOVA is a statistical technique that can be used to test the hypothesis that the means among several means are equal, by comparing variance among groups relative to variance within groups (random error). ANOVA also requires that the sampled populations are normally distributed. However, ANOVA cannot identify which subsets of the data are different from the others, only that there is at least one subset that is statistically different from at least one other subset. A one-way ANOVA were used for multiple groupings with only one factor (independent variable such as degree of compaction) and several levels (observations) from each location. This design is essentially the same as an unpaired t-test: because a one-way ANOVA of two groups obtains exactly the same p-value as an unpaired t-test.

When evaluating data, the p-value is the probability of being wrong in concluding that there is a true association between the variables (i.e., the probability of falsely rejecting the null hypothesis, or committing a Type I error). The smaller the p-value, the more significant the relationship. Traditionally, you can conclude that the independent variable can be used to predict the dependent variable when $p < 0.05$.

The ANOVA test were used to test the significance of the regression coefficients, which highly depends on the number of data observations). When only few data observations are available, strong and important relationships may not be shown to be significant, or high R^2 values could occur with insignificant equation coefficients. Because it is not possible to determine how accurate predictions were based on the value of R^2 alone, this research evaluated the models by using the standard error of the estimate (ANOVA evaluation). An ANOVA table partition the variability of the responses and thus distinguish what can be explained by regression and what remains unexplained (i.e., error). The F critical value on the ANOVA table is the F

value that would result in a p-value equal to 0.05. The F is the ratio of the mean sum of squares (MS) of the “between group” and “within groups” values. The mean sum of squares is the sum of squares (SS) values divided by the degrees of freedom (df). A large F value resulting from an ANOVA suggested that there is a significant linear relationship between the response (endpoint) and the predictor variable. However, a significant F value will not be an indication that the regression equation used will be the “best fit” model. Calculation of the Pearson’s correlation (r), and the coefficient of determination (R^2) will indicate the fitness or strength of the regression.

3.4.5 Nonparametric Kurskal–Wallis ANOVA

One of the primary requirements for these multiple pairwise comparisons methods is that the data are normally distributed. When data are not normally distributed, there are two commonly used approaches. The first is to transform the data using logarithmic or square root transformations in an attempt to obtain a transformed normal distribution. One potential problem with this method is that the units of the transformed data may be difficult to interpret due to the logarithmic manipulation. The second method for dealing with non-normally distributed data is to use a non-parametric analysis having fewer data distribution requirements.

The Kruskal-Wallis test is usually represented as the nonparametric version of the parametric one-way ANOVA test. This test was used to determine if at least one group is significantly different from the other groups being compared. This test compares the population medians of the groups, instead of the population means used by ANOVA. The Kruskal-Wallis method tests the hypothesis that all population medians are equal (Gibbons, 1997). Multiple comparison tests were conducted using a MINITAB version 16 macro in a nonparametric setting (Orlich, 2010). comparison tests were conducted for the saturated infiltration rate among different levels of compaction and using surface and subsurface soil from different test sites.

Similar tests were conducted for the saturated infiltration rates for different levels of compaction and using different percentage of sand and biofilter media.

3.4.6 Post-hoc Tests

A post-hoc test was needed after an ANOVA test is completed in order to determine whether any two groups within the study are similar or different. Various post hoc tests such as Bonferroni *t*-test and Tukey's test were used to determine which groups differ from the rest if a significant difference was observed. These tests make pairwise comparisons between all pairs of means. Post hoc techniques were performed only after obtaining a significant F value. The post hoc procedure requires a larger difference between means to define where significance lies in the data. Box and whisker plots are also useful to supplement these statistical tests to graphically show potential data set groupings.

3.4.7 Statistical Significance Measures

This research used the p-value and the alpha level as statistical significance measures to quantify how confident we are that what is observed in the sample did not occur by chance and it is also true for the population. The p-value can be compared to the alpha level to determine whether the observed data are statistically significantly different from the null hypothesis. The alpha level sets the standard for how extreme the data must be before we can reject the null hypothesis whereas the p-value indicates how extreme the data are. The alpha level this research will accept to prove the hypothesis was set to be 0.05, meaning if the p-value is greater than alpha ($p > 0.05$), then we fail to reject the null hypothesis, and the result is statistically non-significant. If the p-value is less than or equal to the alpha ($p < 0.05$), then the null hypothesis can be rejected, and we say the result is statistically significant.

3.4.8 Factorial Experiment

A complete two level, four factors (2^4 , with varying texture, uniformity, organic content, and compaction) full-factorial experiment (Box et al. 1978) was conducted to examine the effects of these factors, plus their interactions, on the flowrate through the various sand-peat mixtures. The factors studied, and their low (-1) and high values (+1) used in the calculations, are shown in Table 8.

Table 8. Laboratory Column Infiltration Test Results.

Variable	Low value (-1)	High value (+1)
Median particle size of mixture (T), D_{50} (μm)	500	1000
Uniformity of the mixture (U)	4	6
Organic content of the mixture (O), %	10	25
Compaction level (C), hand/modified proctor	hand	modified proctor

Data analyses were performed using the statistical software package Minitab (version 16). Normal plots of the standardized effects, residual plots, main effects plots, and interaction plots were prepared to examine the effects of the factors and to determine their significance. An analysis of variance (ANOVA) table was constructed to determine the significant factors and their interactions needed to best predict media flow performance. Statistical hypothesis tests using a p-value of 0.05 (95% confidence) were used to determine whether the observed data were statistically significantly different from the null hypothesis.

Pooled Standard Error

The standard from replicate analyses can be used to identify significant factors (Box, et al 1987). If the calculated effect for a factor or interactions is much larger than the pooled standard

error from all of the tests (usually considered as 3 to 5 times larger, or more), then the effect can be considered to be significant. The standard error of the mean for each condition's mean is the standard deviation of the sample group divided by the square root of the sample size. The following equation was used to determine the pooled standard error.

$$S_p^2 = \frac{\sum_{i=1}^k (n_i - 1) s_i^2}{\sum_{i=1}^k (n_i - 1)}$$

where S_p^2 = the pooled variance

n_i = the sample size of the i^{th} sample

s_i^2 = the variance of the i^{th} sample

k = the number of samples being combined.

3.4.9 Model

To build an empirical model, factorial experiments were conducted to determine the effects of media texture (T), uniformity of the media (U), organic content (O) of the material, and compaction (C), plus their interactions, on the flowrate through the biofilter media. Based on these tests, factors were identified that can affect the flowrate through the biofilter media. An analysis of variance (ANOVA) table was constructed to determine the significant factors and their interactions needed to best predict media flow performance. A final factorial analysis model was developed to predict the flowrate through the mixtures as a function of media texture (T), media uniformity (U), compaction, TU, TO, TC, and UO.

CHAPTER 4

4. THE PERFORMANCE OF AN ALTERNATIVE UNDERDRAIN MATERIAL (SMARTDRAIN™) FOR URBAN STORMWATER BIOFILTRATION SYSTEMS

4.1 Introduction

In urban areas having soils with poor infiltration rates, water treated in biofilters is usually collected by an underdrain system to minimize the duration of standing water. The drainage rates in the biofilters are usually controlled using a restricted orifice or other flow-moderating component. These frequently fail, as orifices that are used for flow control are usually very small in order to provide sufficient contact time with the treatment media for water quality benefits, or to detain the water for a significant time when used as part of green infrastructure components in areas having combined sewers. If the orifices are large to minimize clogging, they are less effective for flow rate reductions or for maximizing water quality improvements.

The flow capacity and clogging potential of an alternative underdrain material based on a foundation drain material (SmartDrain™) were examined. Performance was examined for a range of material length and slopes using clean water in a pilot scale biofilter, and also after excessive loading by fine ground silica particulates and excessive biofouling. The results indicated that the SmartDrain™ material provides an alternative option for biofilter underdrains, showing minimal clogging while also providing desirable very low discharge rates.

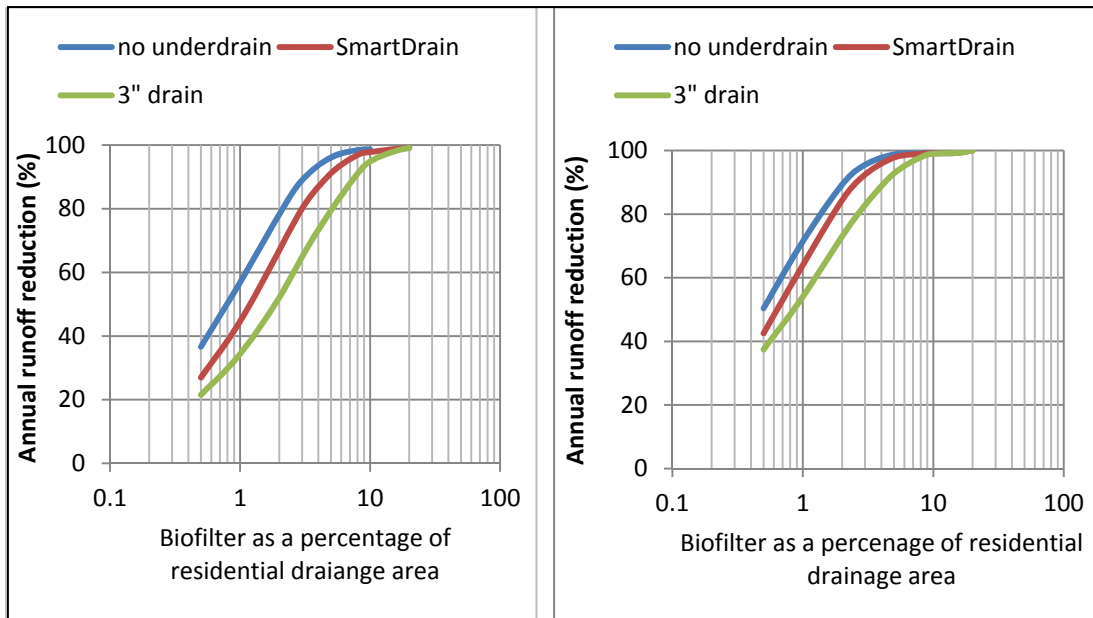
Biofilters are used in urban areas to reduce stormwater runoff volumes, peak flows, and pollutant discharges. In this research, biofilters are defined as stormwater infiltration devices that are excavated several feet deep, with a bottom coarse stone storage layer and an underdrain near

the top of this storage layer. Engineered soil or media (usually a sandy textured material, or the native soil, with amendments selected for the targeted contaminants) is placed on top of the storage layer. Shallow surface water ponding storage is also provided, along with a surface overflow device for discharging excess flows. Many studies have demonstrated the pollutant removal efficiency of stormwater biofilters (City of Austin 1988; Clark and Pitt 1999; Clark 2000; Winer 2000; Hunt et al. 2006, 2008; Brown and Hunt 2008; Li and Davis 2009; Hathaway et al. 2011; Zhang et al. 2011). With the exception of some highly mobile contaminants (such as chlorides), biofilters can be designed for good to excellent pollutant control and runoff volume reductions.

The effectiveness of a biofilter is commonly reduced through clogging of the media, through short-circuiting of infiltrating water through an underdrain, or by short resident/contact times of the stormwater and the treatment media. Care also needs to be taken to prevent clogging of the underdrain. As an example, Wukasch and Siddiqui (1996) report that effluent with a high pH can kill roots surface plants around the drain openings and cause clogging of the drain screens. Effluent from beneath new road construction using # 53 grade recycled concrete has been found to have a high pH. Due to its high pH the effluent from these drains was causing vegetative kill at the opening. In addition the drains were clogged due to sediment deposition causing the water to back up in the drains. Most underdrains with restricting orifices are usually installed with bypass valves to allow draining if the underdrains clog. Appropriate hydraulic characteristics of the filter media, including treatment flow rate, clogging capacity, and water contact time, are needed to select the media and underdrain system. This information, in combination with the media's ability to capture targeted pollutants with minimal clogging given the appropriate contact time, can be used to predict the performance of a biofilter.

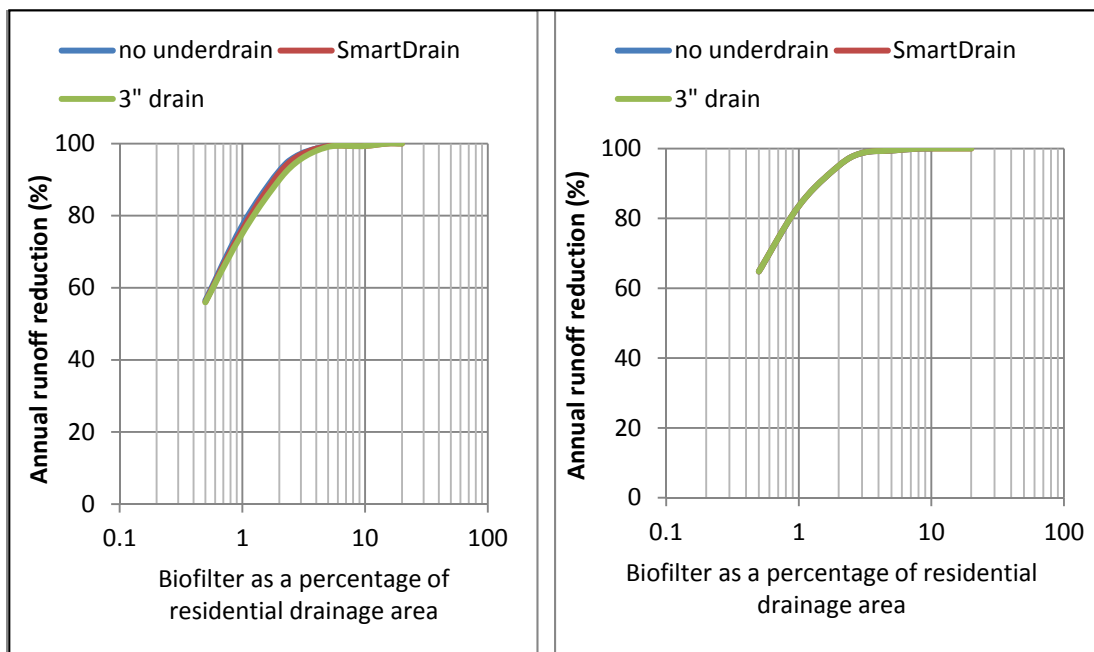
One feature of biofiltration devices that affects performance is the drainage time of the media. In many areas, biofilters are required to completely drain within 72 hours. If the underlying natural soil is restrictive, underdrains are commonly used to prevent nuisance and public safety issues. In most cases, the drainage rate is controlled using an underdrain that is restricted with a small orifice or other flow-moderating component. Outlet control is more consistent in providing the desired residence times needed for pollutant control compared to the natural media drainage rate. However, most outlet controls (underdrains) are difficult to size small enough to obtain desired long residence times. Perforated pipe underdrains with large flow capacities short-circuit the natural infiltration, resulting in decreased performance. A small orifice allows slow release of captured stormwater, but can easily clog due to its size (Hunt 2006).

Figures 10a through 10d are production function plots for different soil infiltration rates ranging from 0.2 (5) to 2.5 in/hr (63.5 mm/hr) (Pitt et al 2013 in press). For low infiltration rates, the use of underdrains reduces the performance of biofilters because the underdrains discharge subsurface ponding water before it can infiltrate (short-circuiting). The use of a SmartDrainTM results in an intermediate effect while also decreasing periods of long surface ponding. Gravel storage or underdrains have very little effect on performance when the native subsurface native infiltration rate is about 1 inch/hr (25 mm/hr), or greater.



a) Use of underdrains in soils having 0.2 in/hr (5 mm/hr)

b) Use of underdrains in soils having 0.5 in/hr (13 mm/hr)



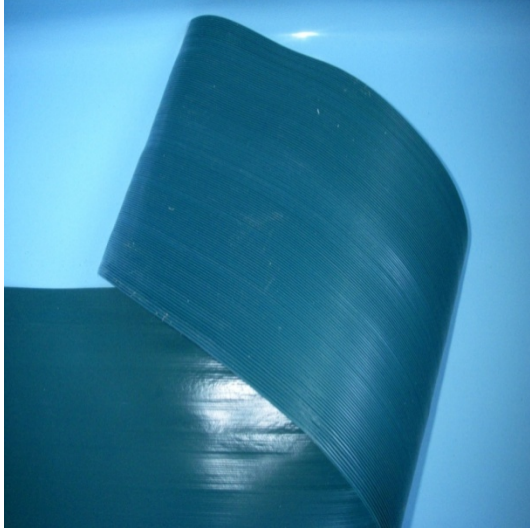
c) Use of underdrains in soils having 1 in/hr (25 mm/hr)

d) Use of underdrains in soils having 2.5 in/hr (63.5 mm/hr)

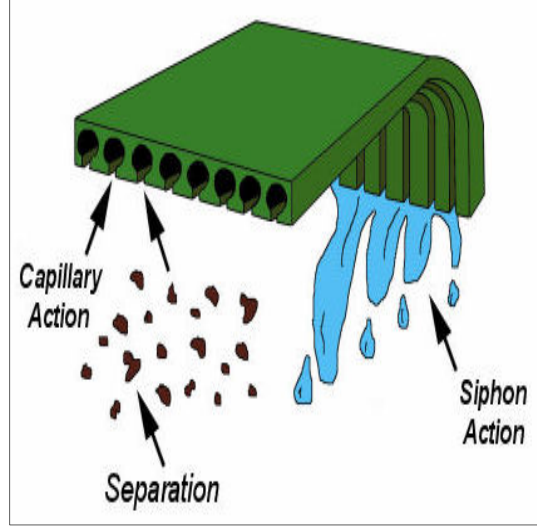
Figure 10. Production Function Plots for the Different Soil Infiltration Conditions Examined for Residential Drainage Area (Pitt et al 2013 in press).

4.2 SmartDrain™ Material Characteristics

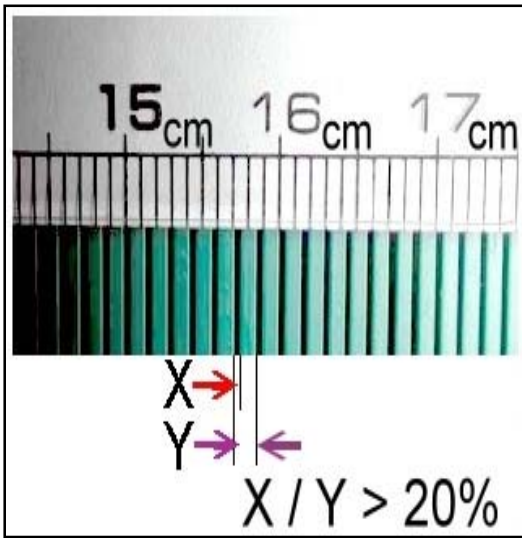
SmartDrains™ have been used extensively for subsurface foundation drainage in Asia, and to a lesser extent in the USA, Germany, Australia, Indonesia, and some other parts of the world. The laminar flow and capillary action of its micro siphons separates water and soil instead of relying on a filtering action, preventing the migration of soil fines that are the leading cause of conventional drainage system failure (Ming and Chun 2005). The carrying capacity of the slowly flowing water entering the SmartDrains™ (which also have very low Reynolds numbers) is very low and not capable of transporting most of the particulates into the underdrain material. They also utilize an initial siphoning action to initiate flow as the surrounding sand becomes saturated. SmartDrains™ are advertised as being almost completely maintenance free for the lifetime of the system with higher drainage efficiencies compared to conventional drainage systems. The SmartDrain™ consists of an 8 inch (20 cm) wide strip comprising microchannel inlet areas over 20% of the active drainage surface of the belt (Figure 11).



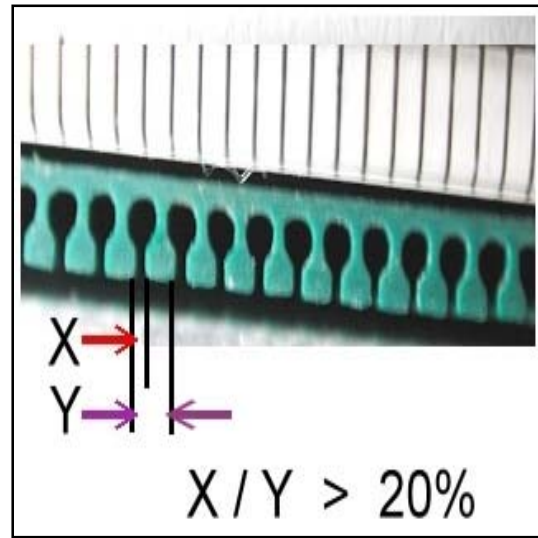
(a) SmartDrain™ Belt, 8 inch Wide Strip



(b) Capillary and Siphoning Properties



(c) X: Water Inlet Opening 0.3 mm



(d) Y: Pitch Spacing 1.5 mm

Figure 11. Close-Up Photograph of SmartDrain™ Material Showing the Microchannels (SmartDrain LLC).

4.3 Field Application of SmartDrain™

4.3.1 Biofilter Facility Using SmartDrain™ as Underdrain

SmartDrain™ belts were installed in the biofilter facilities integrated into a 2.75-acre landscaping development project located at the University of Pennsylvania. The biofilter units are installed in a greyfield area that was previously urbanized where stormwater drainage was a major issue (Figures 12 and 13). In addition to providing significant water quality benefits, the biofilter units can provide shade, improve the University's aesthetics, reduce irrigation needs, and reduce or eliminate the need for an underground storm drain system in the campus. The size of the drainage area for one biofilter area consist of 16,600 ft² (0.38 ac) asphalt walkways and 9,500 ft² (0.22 ac) planting.



Figure 12. SmartDrain™ Installation at the University of Pennsylvania Shoemaker Plaza Project.

(Source: Meliora Environmental Design, LLC, Photo Used with Permission).



Figure 13. Biofilter Area Located on Shoemaker Plaza Landscape Project Soon after Planting (Source: Meliora Environmental Design, LLC, Photo Used with Permission).

Figure 14 shows typical profile of the biofilter facility installed on the University of Pennsylvania campus. The approximate dimensions for each biofilter area is 45 feet (14 m) wide by 100 feet (30.5 m) in length (about 0.1 acre). The biofilter ponding area is designed to capture, detain and infiltrate the water quality volume (WQV) into an engineered soil mix consisting of a well mixed combination of a sandy loam and compost. The maximum ponding depths in biofilter -1 and 2 are 8.4 inch (22 cm) and 10.9 inch (28 cm) respectively. The biofilter areas have an average freeboard depth of 22 inches (56 cm) and a maximum depth of 46 inches (117cm).

The length of SmartDrain™ belt used for each biofilter area was about 80 ft (24 m) (4 belts @ approximately 20 ft (6 m) each). The SmartDrain™ belts were installed on top of a 4 inch (10 cm) layer of coarse sand, and another 4 inch layer of sand was placed on top of the belts (Figure 14). A 30 inch (0.8 m) layer of soil/planting mix was placed on top of the drainage layer.

The percent void space in the planting soil and coarse sand were 20% and 25% respectively. The sand layer acts as a bedding for the SmartDrain™ system. The outlet end of the SmartDrain™ was inserted into a slit cut in a 2 inch (5 cm) PVC underdrain collection pipe (Figures 14). The SmartDrain™ belts are always installed with the microchannels on the underside of the strips. The spacings between the SmartDrain™ belts for these installations were 20 ft (6 m). The underdrain collection pipe was connected to a down gradient storm drain outlet structure. A PVC 18 inch (0.45 m) or 24 inch (0.6 m) diameter overflow control structure w/domed grate was installed for overflows to the combined sewer system to prevent the surrounding area from flooding during storms that exceed the design capacity.

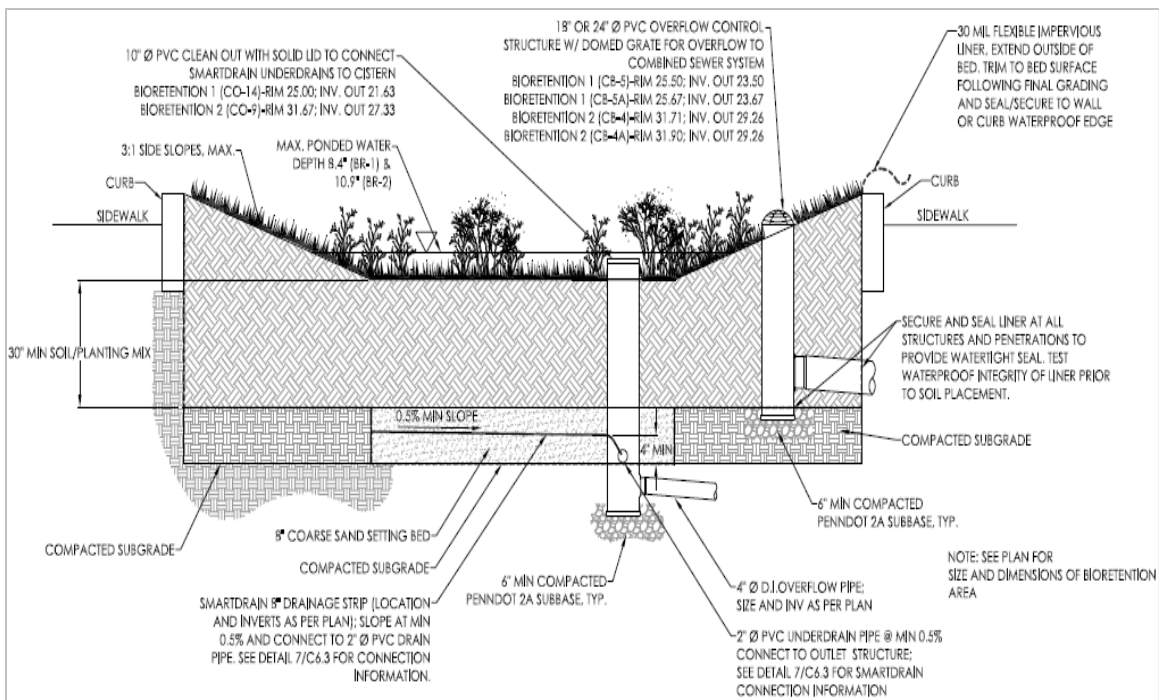


Figure 14. Detail of a Typical Section View of Biofilter Facility (Source: Meliora Environmental Design, LLC, Photo Used with Permission).

4.3.2 SmartDrain™ Drainage System Performance Installed in Sports Turf Facility

Field-scale studies were conducted to compare the performance of the SmartDrain™ belt sub-surface drainage system to the performance of a conventional drainage system at a sports turf facility in Germany (Morhard 2006). The SmartDrain™ system was installed on two equi-sized golf driving plots in German (Figure 15). The total size of the drainage area is 2,690 ft² (250 m²). The length of the Drain Belt® strips were about 43 ft (13 m) and the spacing between the belts was approximately 7 ft. The belts were placed on a drainage bed of 2 inch (5 cm) of coarse sand and covered with an additional 2 inch (5 cm) of coarse sand to complete the drainage layer. An 8 inch (20 cm) base course is placed on top of the drainage layer. The ends of the drain belt strips were connected to a central collection pipe with PVC connectors so the drain belt could empty into the pipe. The opposite ends of the drain belts were sealed with a sealant to prevent intrusion of particles from the open ends of the siphon channels.



Figure 15. The SmartDrain Belt® System during Construction (Morhard 2006).

The results of the field scale studies showed that 55% of the natural rainfall was removed during the observation period through the SmartDrain™ belt® system, whereas 38% of the rainfall was removed with the conventional drainage system (Figure 16).

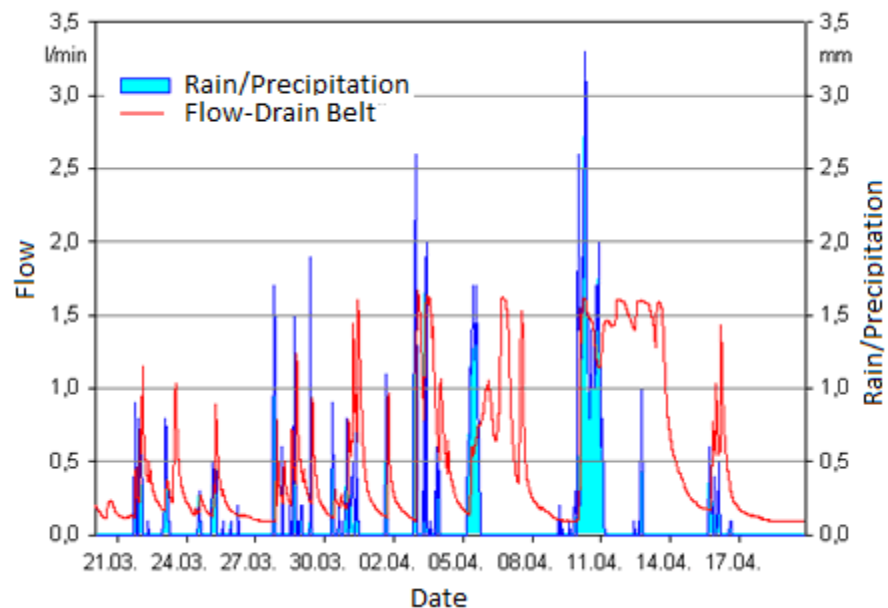


Figure 16. Runoff Characteristics of the SmartDrain™ Belt® System during an Observation Period (Morhard 2006).

Morhard (2006) observed a quick discharge of water at the end points of the SmartDrain™ belt collection pipes immediately after the onset of precipitation, whereas the conventional system took longer to begin draining. At the same time, the water flow increased for the SmartDrain™® system for a longer period. In addition, the discharged water was significantly increased in the experiment (Table 9). However, the drainage of the conventional system reacted more quickly to decreasing precipitation than the SmartDrain™ system, as shown in Figure 17.

Table 9. Outflow Balance of the Drain-Belt ® System during an Observation Period.

Precipitation (inch, mm)	Runoff (inch, mm)	
	SmartDrain™ belt system	Conventional system
5.4 (135.8)	-3 (-75.3)	-2 (-51.4)

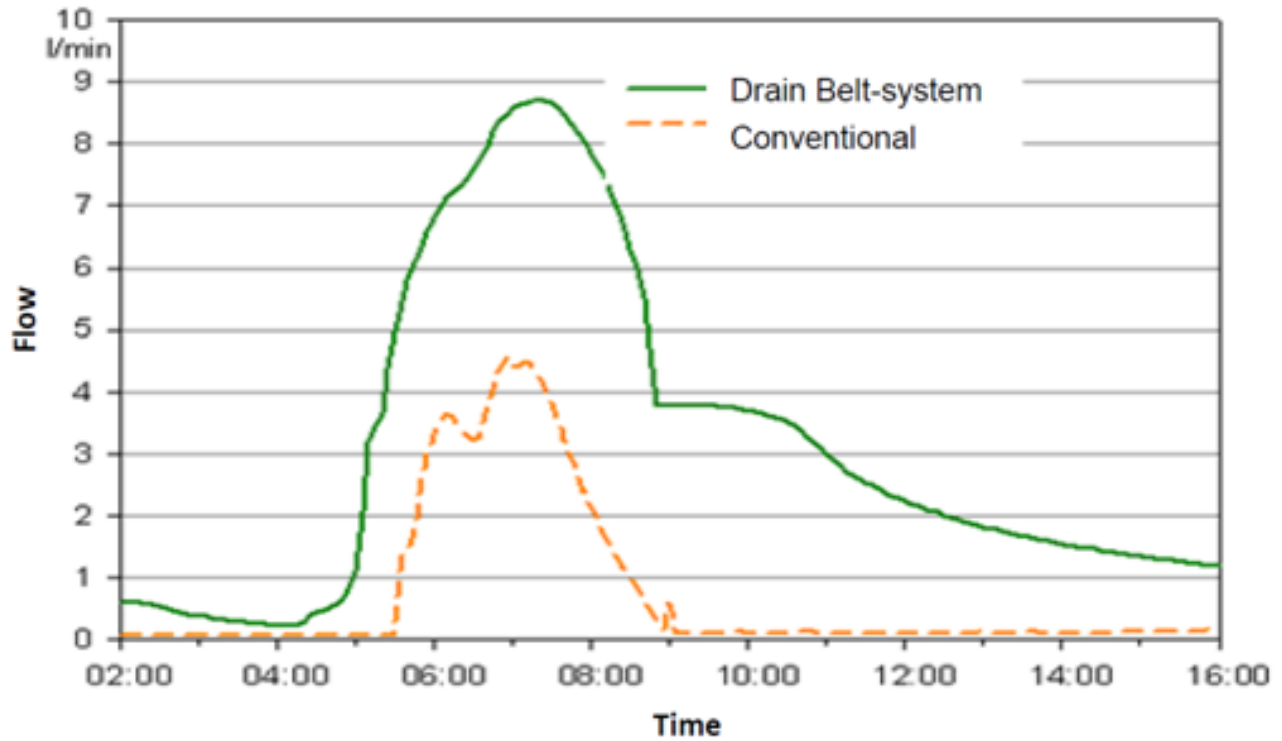


Figure 17. Flow (L/min) of the Studied Drainage Systems during a Precipitation Event (Morhard 2006).

4.3.3 Biofilter/Bioretention Facility Hydraulics and Design of Dewatering Facilities

The natural soils under bioinfiltration systems should have infiltration rates greater than 0.5 in/hr (13 mm/hr) if underdrains are not to be used; however, when underdrains are not incorporated into the biofilter design, there is an increased risk of generating overflows during a storm event (Jones and Hunt 2009). The water removal rate (inches per day) is commonly called the drainage coefficient (Encyclopedia of Water Science 2007). For subsurface drainage systems,

drainage coefficients are usually expressed as a depth of water removed per 24 hr over the drained area (in/day or mm/day), and for surface drainage systems, as a rate of flow per unit area drained. The drainage rate of a drainage system is affected by the soil properties, water table depth, depth of the drains, and the spacing between drains.

The depth of the drains below the ground surface determines the hydraulic head (h) of the water, driving flow to the drains (assuming saturated overlying soil), while the distance between the drains and the restrictive layer determine the cross-sectional area that is available for water flow. Hydraulic conductivity of the soil is an essential and invariably used parameter in all drain spacing equations (Raju et al. 2012). The Hooghoudt (1940) equation (Eqn. 3 and Figure 18) was used to test whether a biofilter facility which uses a SmartDrain™ as an underdrain meets the hydrologic criteria with regard to ponding time. Important soil properties needed to use Hooghoudt equation include the saturated hydraulic conductivity (K_s) and the depth to a restrictive layer (d_e).

The Hooghoudt equation is expressed as:

$$s = \sqrt{\frac{4 \cdot k_s (m^2 + 2 \cdot d_e \cdot m)}{q/24}}$$

Where:

- s spacing between drains (ft)
- q amount of water that the underdrain carries away (in/day),
- K_s average saturated hydraulic conductivity of the facility media (in/hr),
- d_e effective depth (ft),
- m depth of water, or head, created over the pipes (ft) (Irrigation Association, 2000).

A conversion factor of 24 is used to convert hours to days.

The values for the effective depth are determined from various figures and tables. The equation above is used to compute the drain spacing.

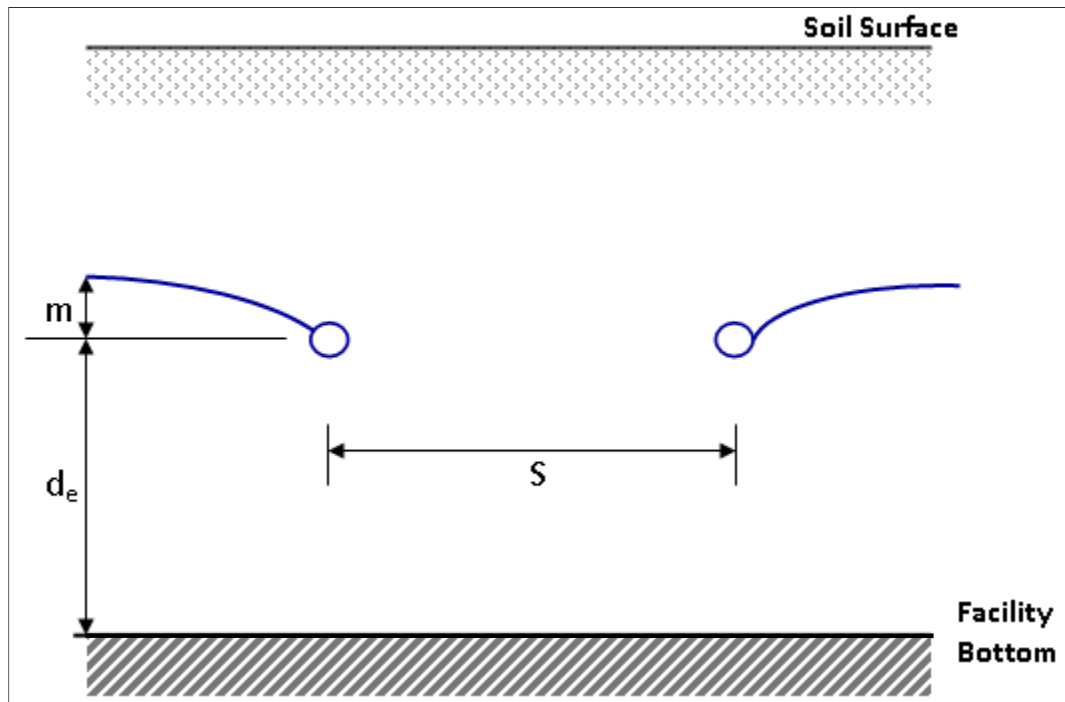


Figure 18. Scheme of Hooghoudt Equation

The value of q is determined by the amount of water that the underdrain must carry away in 24 hours (or whatever other time criterion is used). These time periods are used to minimize damage to the recommended plants in biofilters, to restrict breeding of mosquitoes, and to minimize the release of odors. An example rate of 30 in/day (76 cm/day) is chosen as the desired drainage rate by the underdrain. Table 10 shows the design values used for the equation, while Figures 19 and 20 shows the underdrain spacing vs saturated hydraulic conductivities for 24 hour and 72 hour drain periods. The graphs indicate that the underdrain spacing increases with

increases in saturated hydraulic conductivities of the biofilter media. The number of SmartDrain belts also decreases with increases in saturated hydraulic conductivities.

Table 10. Design Values for Equation 1

q (in/day)	de (ft)	m (ft)	Ks (in/hr)
30	0.5	0.5	30
		1	45
		1.5	60
		2	75
		3	100

Hydraulic Conductivity of Sand

The hydraulic conductivity is a measure of the soil's ability to transmit water away from the infiltration area, and is therefore of critical importance to the infiltration rate since it expresses how easily water flows through soil. The hydraulic conductivity of soil depends on the soil grain size and the type and amount of soil fluid (including entrapped air) present in the soil matrix. Sandy soils have larger pores, a lower water holding capacity and a higher hydraulic conductivity, diffusivity and infiltration rate compared to clayey soils, which have smaller micropores. Saturated hydraulic conductivity, K_s , describes water movement through saturated media. It has units with dimensions of length per time (m/s, cm/s, ft/day, in/hr). Table 11 shows saturated hydraulic conductivity of sand for different grain size.

Table 11. Saturated Hydraulic Conductivity (in/hr) of Different Grain Size Sand (US EPA 1986)

Grain size class	Degree of Sorting		
	Poor	Moderate	Well
medium sand	33.5	40	47
medium to coarse sand	37	47	-
medium to very coarse sand	42	49-56	-
coarse sand	40	54	67
coarse sand to very coarse sand	47	67	-
very coarse sand	54	74	94

*A hyphen indicates that no data are available

For a sand to be classified as well graded, $C_u \geq 6$ and $1 < C_c < 3$, where C_u and C_c are the coefficient of uniformity and coefficient of curvature respectively and were calculated using the following equations.

$$C_u = \frac{D_{60}}{D_{10}} \text{ and } C_c = \frac{D_{30}^2}{D_{10}D_{60}}, \text{ where } D_{60} \text{ is the grain diameter at 60\% passing, } D_{10} \text{ is the grain}$$

diameter at 10% passing, and D_{30} is the grain diameter at 30% passing

SmartDrain™ materials perform well when they are installed in coarse sand (0.5 – 2 mm grain size) and clean drainage sand (SmartDrain LLC). Fine and dirty sand mixtures will lead to decreased and slower performance. Washed concrete sand meeting sieve specification with everything passing the #10 sieve (2 mm) and no more than 10% passing the #40 sieve (0.42 mm) are recommended. SmartDrain™ will also work in any type of sand and native soil including clay (Matthew Nolan, SmartDrain LLC personal contact). Table 11 also indicated that the saturated hydraulic conductivity of a medium to very coarse sized sand ranges from 33 to 94 in/hr (recommend saturated hydraulic conductivity ranges for filter sand used for SmartDrain™ field application).

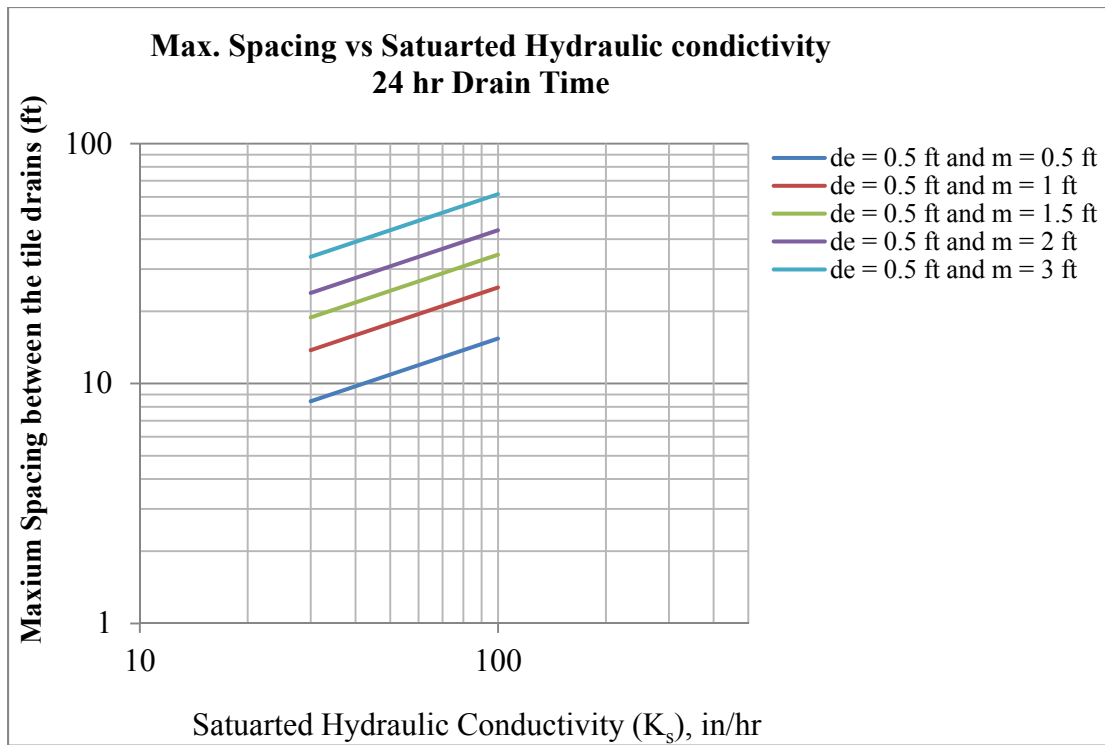


Figure 19. Underdrain Spacing vs Hydraulic Conductivity for 24-hr Drain Period

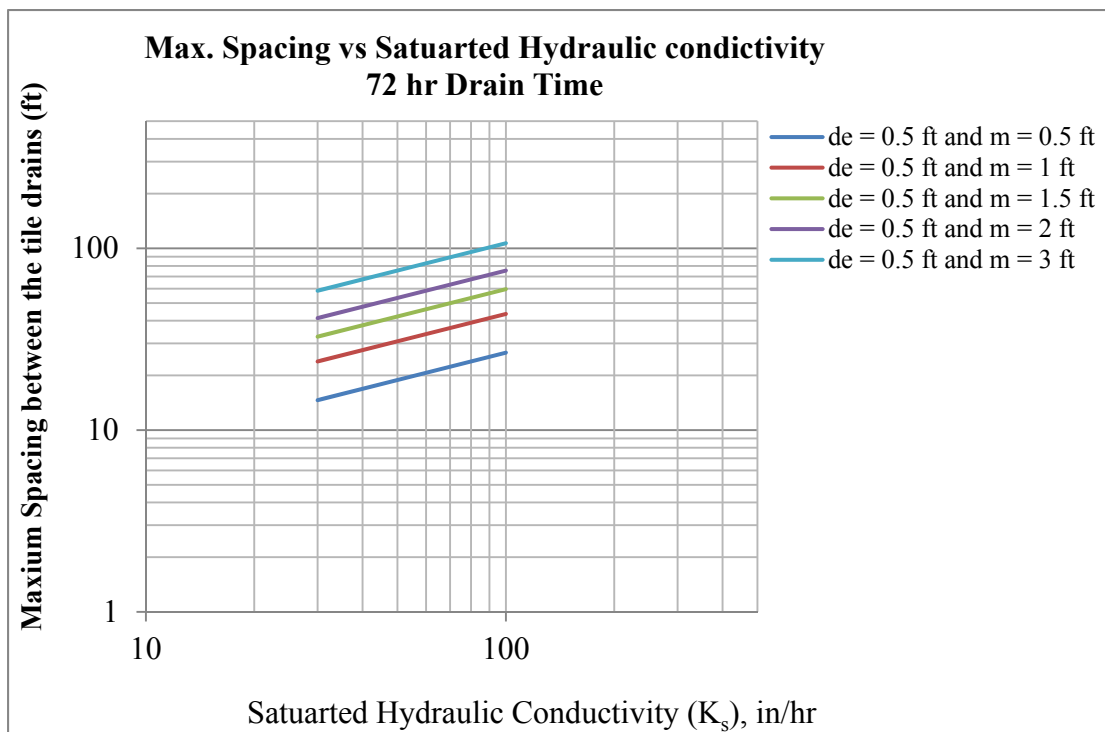


Figure 20. Underdrain Spacing vs Hydraulic Conductivity for 72-hr Drain Period

From Figure 19, the maximum spacing (ft) between underdrains for a 24 hour drain time in a biofilter facility that has a basin area of 100 ft², a saturated conductivity of a media of 45 in/hr, an effective depth (d_e) of 0.5 ft, head over the tile drains (m) of 0.5 ft, is approximately 10 ft apart. An example calculation showing a biofilter facility hydraulics and design of dewatering are shown in Appendix A.1.

Biofilter performance is dependent on the characteristics of the flow entering the device, the infiltration rate into the native soil, the filtering capacity and infiltration rate of the engineered media fill if used, the amount of rock fill storage, the size of the device and the outlet structures for the device (Pitt et al 2013 in press). The amended soil layer is critical to proper operation of the facility (Prince George's County, 1993). The storage volume of the biofilter facility is calculated using the porosity, facility area, and free storage. For these example calculations, the basin areas ranged from 100 (9 m²) to 10000 ft² (930 m²). The engineer media layer is 2 ft thick with a porosity of 0.44. The different media layer and porosity of each media were shown in Figure 21 and Table 12.

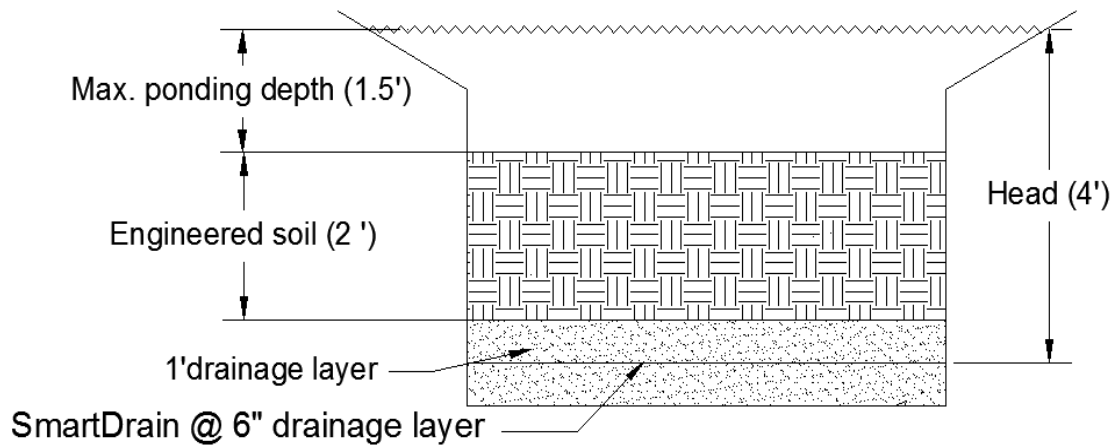


Figure 21. Cross-Section of a Typical Biofilter Facility

Figures 22 contain production function plots for different biofilter sizes. Pitt et al 2013 suggested that biofilters about 1 to 2% of the drainage area are expected to infiltrate a substantial amount of the annual runoff. For commercial areas, the amount of runoff is much greater and the biofilters would need to be at least twice as large for the same level of performance. Continuous simulations are needed to verify the biofilter performance for specific locations.

Table 12. Design Values for Storage Volume Calculation

Ponding depth (ft)	Engineered media depth (ft)	Drainage layer depth (ft)	Porosity of media mix (%)	Porosity of drainage layer (%)
1.5	2	1	0.44	0.3

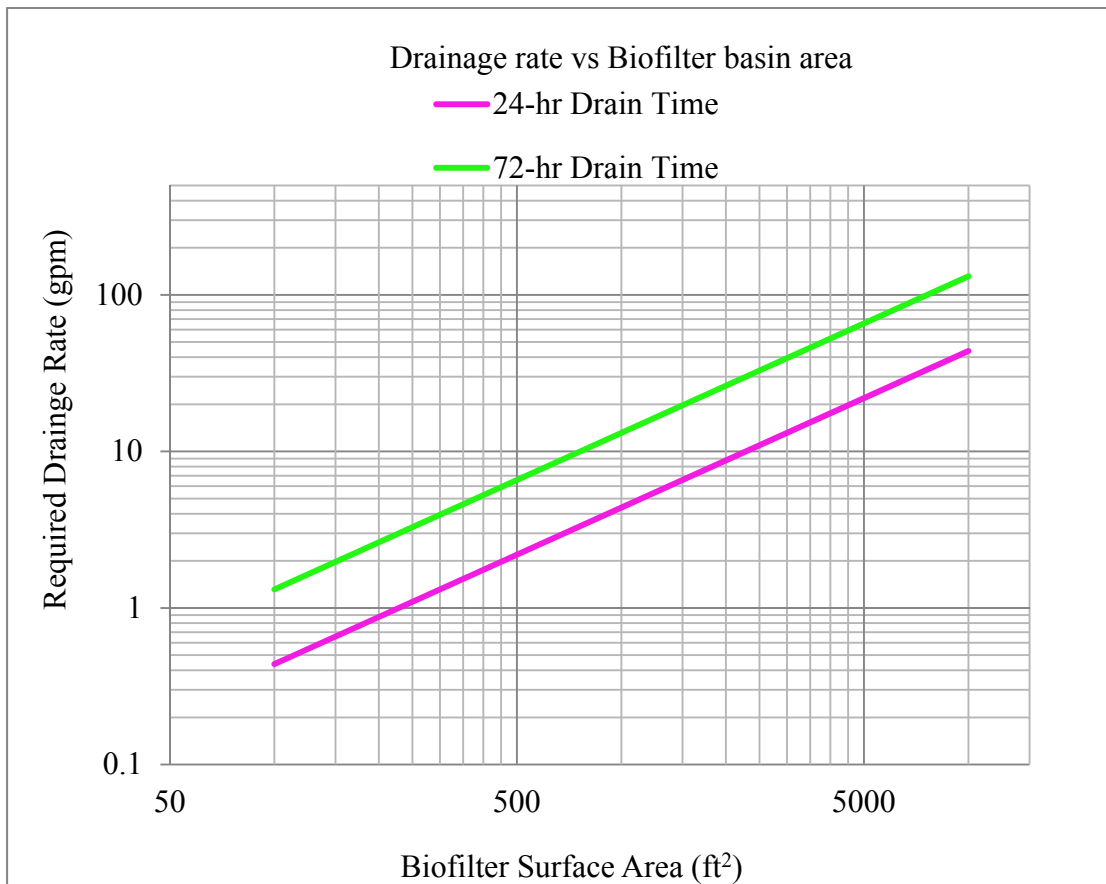


Figure 22. Drainage Rate vs Biofilter Basin Area

4.4 SmartDrain™ Material Performance Experiments under Controlled Pilot-Scale Biofilter Conditions

4.4.1 SmartDrain™ Material Drainage Characteristics Tests

The performance of an alternative underdrain material (SmartDrain™) that could be used as an underdrain option for stormwater biofiltration facilities was studied as a part of this dissertation research. It was found that the SmartDrains™ have minimal clogging potential while also providing very low discharge rates. SmartDrains™ also reduce the surface ponding time compared to no underdrains, while minimizing short-circuiting of the infiltration water. As an example, for a typical biofilter that is 3.3 ft (1 m) deep, 4.9 ft (1.5 m) wide and 16.4 ft (5 m) long, about 8 hours would be needed for complete drainage using a SmartDrain™, easily meeting typical 24 to 72 hr maximum ponded water drainage times usually specified for mosquito control. This also provides a substantial residence time in the media to optimize contaminant removal and also provides significant retention of the stormwater before being discharged to a combined sewer system. In addition, this slow drainage time encourages infiltration into the native underlying soil, with minimal short-circuiting to the underdrain.

The tests described below were conducted in three main phases: 1) basic flow tests using a pilot-scale biofilter to measure flow rates as a function of SmartDrain™ length and slope, 2) clogging tests conducted with deep water using ground silica to measure any reduction in flow capacity with increasing silt loadings, and to measure turbidity reductions with drainage, and 3) biofouling clogging tests with the deep water pilot-scale biofilter. These test setups and the results are described in the following sections.

Pilot-scale biofilter tests using a trough 10 ft (3 m) long and 2 ft (0.6 m) x 2 ft (0.6 m) in cross section (Figure 23) were used to test the variables affecting the drainage characteristics of

the SmartDrain™ material (such as length, slope, and hydraulic head). The outlet end of the SmartDrain™ was inserted into a slit cut in the PVC collection pipe and secured with screws and silicone sealant along the top of the strip (Figure 23a). The SmartDrain™ material is always installed with the microchannels on the underside of the strip. The SmartDrain™ directs the collected water into the PVC pipe, with a several inch drop to initiate the siphoning action. The PVC pipe was 2 inches (5 cm) in diameter and was placed 1 inch (2.5 cm) above the trough bottom. The SmartDrain™ was installed on top of a 4 inch (10 cm) layer of drainage sand with another 4 inch (10 cm) layer of the sand placed on top of the SmartDrain™ (Figure 23b). A hole was drilled through the side of the trough for an extension of this pipe. The pipe outlet was conveniently located so the flows could be measured and water samples collected for analyses (Figure 23c).

During the tests, the trough was initially filled with water to a maximum head of 22 inches (0.56 m) above the center of the pipe. A hydraulic jack and blocks were used to change the slope of the trough (Figure 23d). Tests were conducted for five different slopes, ranging from 0 to 12% and five different lengths of the SmartDrains™ ranging from 1.1 ft (0.3 m) to 9.4 ft (3 m). Each test was repeated several times and regression analyses were conducted to obtain equation coefficients for the stage vs. head relationships. The filter sand was purchased from a local supplier in Tuscaloosa, AL. The filter sand has a median particle size (D_{50}) of about 700 μm and a uniformity coefficient (C_u) of 3. The particle size distribution of the filter sand and the US Silica Sil-Co-Sil®250 ground silica that was used during the clogging tests are shown in Figure 24.



(a) SmartDrain™ Inserted into a Slit Cut in the PVC Collection Pipe and Secured with Screws and Silicone Sealant (before sand)



(b) SmartDrain™ showing underlayer of sand



(c) Flow Measurements



(d) A Hydraulic Jack and Blocks Used to Change the Slope of the Trough

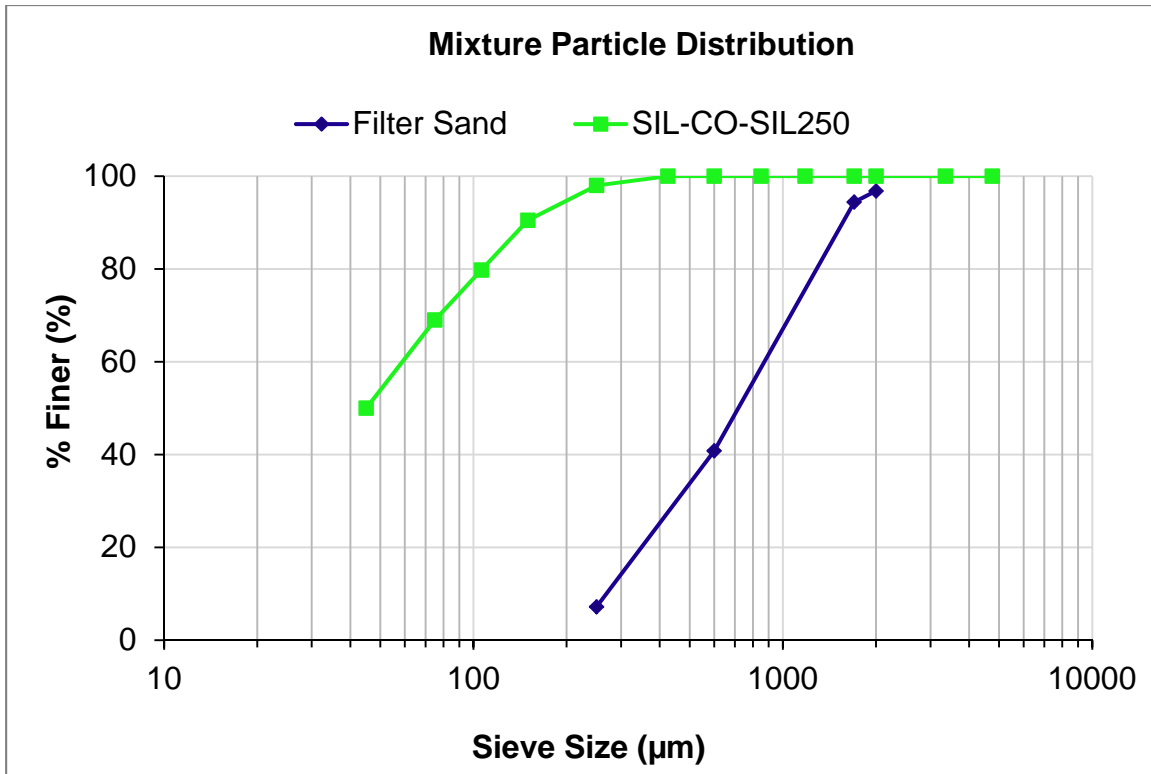


Figure 24. Particle Size Distributions of the Sand Filter Media Material and the U.S Sil-Co-Sil®250 (Fine Material on Graph) Used for the Clogging Test.

4.4.2 Testing the SmartDrain™ Belt for Potential Particulate Clogging

Sediment deposition in a biofilter is the main cause of clogging failure. This can occur at the surface of the system with the creation of a clogged layer or at some depth where the soil is denser or finer, and where they form a thin subsurface clogging layer (Bouwer 2002). The pilot-scale biofilter used for the clogging tests consisted of a tall formica-lined plywood box, 3 ft (0.9 m) x 2.8 ft (0.85 m) in cross sectional area and 4 ft (1.2 ft) tall (Figure 25a). The flow data obtained during these clogging tests (before silt was added to the test water) were also used to verify the basic performance relationships for deeper water. The SmartDrain™ installation procedures for the deep box were similar to the installation procedures described above, except that a shorter piece of SmartDrain™ was used (1.25 ft (0.4 m) long) (Figure 25a-25d).



Figure 25. SmartDrain™ Clogging Test Setups with the Deep Water Pilot-Scale Biofilter.

During these tests, the tank was initially filled with water to a maximum head of 4 ft (1.2 m) above the center of the pipe. Sil-Co-Sil[®]250 ground silica (provided by U.S. Silica Company), having a median particle size of about 45 μm (about 20% in the silt category of $<20 \mu\text{m}$), was mixed with the test water for the clogging tests at a concentration of 1000 mg/L. Many tests were conducted with time to measure any decrease in flow rate as the total accumulative fine sand and silt loading was increased.

4.4.3 Evaluating the Performance of SmartDrain[™] Material under Biofouling Conditions

Stormwater pretreatment techniques that reduce suspended solids, nutrients, and organic carbon can minimize clogging of stormwater biofilters (Bouwer 2002). However, Baveye, et al. (1998) described that even though these stormwater contaminants can be mostly removed from the water, clogging can still occur because of microbiological growths on surfaces of the infiltration device (biofouling). Accumulations of algae and bacterial flocs in the water, on the infiltrating soil surface; and growth of micro-organisms on and in the soil forms biofilms. The increased biomass can reduce the infiltration capacity of the filter media, and clog underdrain orifices (Bouwer 2002).

A series of tests were conducted to determine the flow capacity and clogging potential of the SmartDrain[™] material during biofouling experiments under controlled pilot-scale biofilter conditions. The tall pilot-scale biofilter described previously was used for these tests (Figure 25a) to determine if the stage-discharge relationships changed with biological growths. The SmartDrain[™] installation procedures were as described previously for the silica clogging tests.

The biofouling tests were conducted from mid-June to mid-October 2010 to maximize algal growth due to the presence of sunlight and warm conditions. During these tests, the tank was filled with tap water to produce a maximum head of 4 ft (1.2 m) above the center of the pipe.

The tank was left open to the sun for several weeks to promote the growth of the algae. Two different types of green algal were added to the test water from local ponds at the beginning of the tests, along with three to five capfuls of Miracle-Gro 12-4-8 all-purpose liquid fertilizer (nitrogen, phosphate and potassium), manufactured by the Scott Miracle-Gro Company to increase the algal mass and growth rates in the test biofilter (Figures 26b and 26c).

Seven biofouling trials were conducted, with several weeks between each drainage test (Table 13). The depth of the test water in the tank for the first five trials was 4 ft above the center of the pipe, and was reduced to 1.4 ft (0.43 m) for the last two trials to encourage algal growths near the filter sand surface and along the drainage strip. At the end of each biofouling test period, the test water was drained, resulting in seven stage - discharge relationships (Figure 26d). Regression analyses were conducted to obtain equation coefficients for these different conditions. Figure 26d shows the algae trapped on top of the filter sand after the water was completely drained from the tank after one of the tests.

Table 13. Drainage Date and Exposure Period for the Algae in the Biofilter Device

Trial No.	Date	Accumulative Exposure (days)
1	17-Jun-10	14
2	8-Jul-10	35
3	25-Jul-10	52
4	12-Aug-10	70
5	3-Sep-10	92
6	27-Sep-10	116
7	11-Oct-10	130



a) A Tall Formica-Lined Plywood Box Used for the Biofouling Test



(a) A Close-Up of Algae Floating in the Tank, Test in Deep water



c) Algae Floating in the Tank, Test in Shallow Water Depth



(d) Algae Trapped on Top of the Filter Sand

Figure 26. Pilot-scale Biofilter System Setups for SmartDrain™ Material Biofouling Test

4.5 Results and Discussion

4.5.1 SmartDrain™ Drainage Characteristics Tests

Tests were conducted to determine the variables affecting the drainage characteristics of the SmartDrain™ material as a function of length, slope, and hydraulic head. Two different lengths of the SmartDrain™ belt (9.4 ft (3 m) and 7.1 ft (2.2 m)) were tested at five different slopes (0%, 3%, 6%, 9%, and 12%). In addition, three different lengths of the SmartDrain™ (5.1 ft (1.6 m), 3.1ft (0.95 m), and 1.1ft (0.34 m)) were tested for three different slopes (0%, 3%, and 12%) to supplement the initial tests. Flowrate measurements were manually obtained at the discharge of the biofilter at 25 to 30 minute intervals until the water was completely drained from the trough, resulting in stage-discharge relationships (Figure 27).

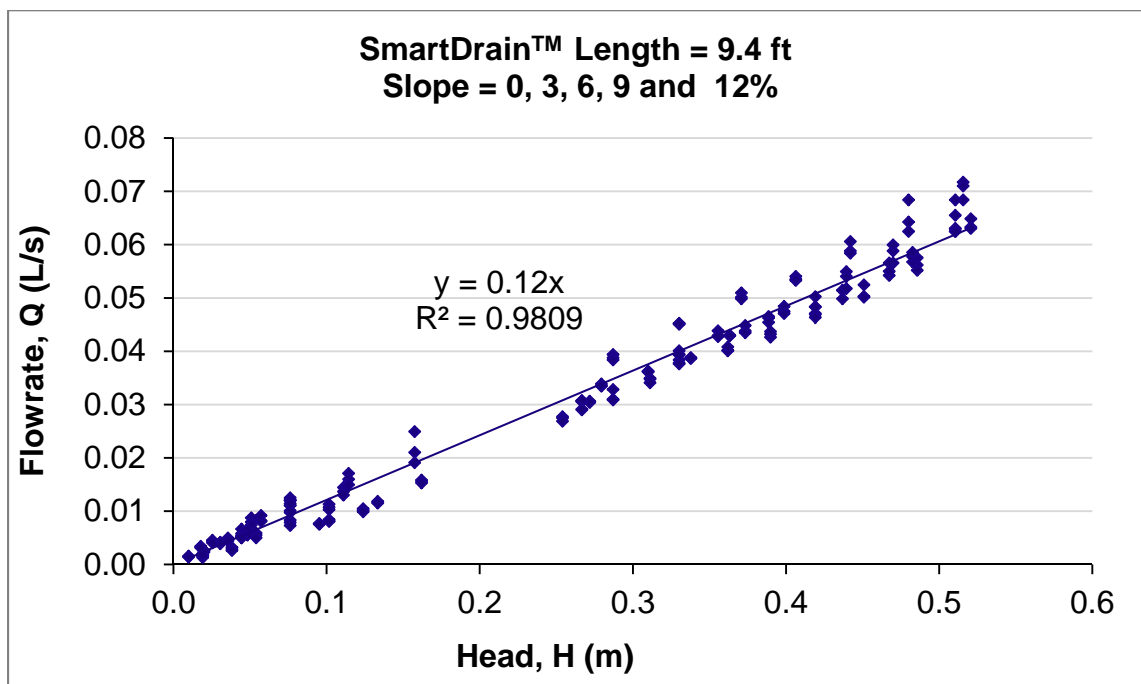


Figure 27. Example of Stage- discharge Relation Plots for SmartDrain™ Length Equals 9.4 ft and Five Different Slopes (data combined for all slopes, as the slope was not found to significantly affect the discharge rates).

The flows were measured by timing how long it took to fill a 0.5 L graduated cylinder, and depth of water in the pilot-scale biofilter was measured using a rule.

Regression analyses were evaluated by examining the coefficients of determination (R^2), the results of the analysis of variance of the model (ANOVA), and the residual behavior of the fitted model. The coefficient of determination is a measure of how well the regression line explains the variability of the data. High R^2 values by themselves do not guarantee that the model has any predictive value; similarly, a seemingly low R^2 does not mean that the regression model is useless. ANOVA analyses are therefore also needed (along with residual analyses) to evaluate the significance of the fitted regression equation.

Linear regression analyses were used to determine the intercept and slope terms of these stages vs. discharge relationships. The p-values of the estimated coefficients were used to determine if the coefficients were significant ($p < 0.05$). All of the five lengths tested for the given slopes showed that the slope coefficients were statistically significant ($p < 0.05$), while many of the intercept terms were not found to be significant on the stage-discharge relationship (Table 14). If the intercepts were not found to be significant, the regressions were re-analyzed forcing the intercept to be zero. Figure 28 shows stage-discharge relationship plots for shallow and deeper water (clean water and dirty water having the SilCoSil or algae contamination) for different lengths of SmartDrain™ belts tested for different conditions used to determine the drainage characteristics of SmartDrain™ belts. The SmartDrain™ stage-discharge relationships were represented by first-order linear equations and have flows generally corresponding to orifices in the size range of 0.1 to 0.2 inch (2.5 to 5 mm).

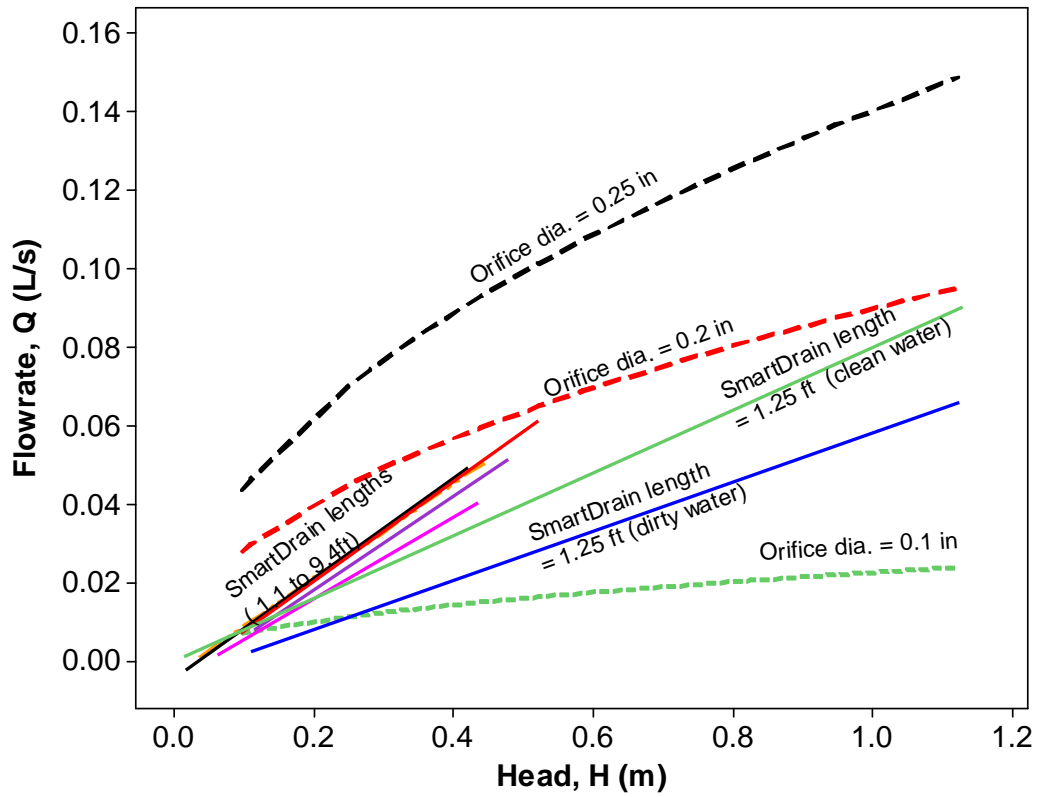


Figure 28. Stage-Discharge Relationship Plots For Different Lengths of SmartDrain™ Tested For Five Different Slopes Used to Determine the Drainage Characteristics of SmartDrain™ Belts.

Table 14. Linear Regression Analysis Results for SmartDrain™ Drainage Characteristics Test.

		SmartDrain™ length = 9.4 ft		SmartDrain™ length = 7.1 ft			
Slope (%)		<i>Coefficients</i>	<i>P-value</i>	<i>Coefficients</i>	<i>P-value</i>		
Intercept		-0.01	1.7E-16	-0.004	2.2E-08		
Slope	0	0.13	2.4E-56	0.13	5.9E-41		
Intercept		-0.001	0.0002	-0.003	8.9E-14		
Slope	3	0.12	2.8E-52	0.13	2.3E-61		
Intercept		0	#N/A	0	#N/A		
Slope	6	0.14	8E-66	0.11	2.9E-50		
Intercept		0	#N/A	0	#N/A		
Slope	9	0.12	4.8E-41	0.12	6.5E-49		
Intercept		0	#N/A	0	#N/A		
Slope	12	0.12	6.1E-41	0.12	7.3E-30		
		SmartDrain™ length = 5.1 ft		SmartDrain™ length = 3.1 ft		SmartDrain™ length = 1.1 ft	
Slope (%)		<i>Coefficients</i>	<i>P-value</i>	<i>Coefficients</i>	<i>P-value</i>	<i>Coefficients</i>	<i>P-value</i>
Intercept		-0.01	9.7E-19	-0.005	3.3E-13	-0.004	5.5E-19
Slope	0	0.12	8.2E-46	0.1	9.8E-46	0.12	1.9E-67
Intercept		-0.01	7.2E-15	-0.003	2.5E-16	-0.003	5.0E-08
Slope	3	0.11	2.3E-42	0.11	4.9E-67	0.12	1.8E-43
Intercept		0	#N/A	0	#N/A	0	#N/A
Slope	12	0.11	2E-43	0.11	4E-37	0.11	6.8E-60

Neither slope nor length had any apparent effect on the slope term, but slope seems to be important for the intercept (but not length). A complete two level and three factors (2^3 , SmartDrain™ length, slope, and head) factorial experiment (Box et al. 1978) was conducted and described in section 1.6 to examine the effects of those factors, plus their interactions on the SmartDrain™ flowrates.

The analysis of residuals plays an important role in validating the regression model. The significance of the regression coefficients is determined by performing residual analyses for the

fitted equations. Because the residuals are the unexplained variation of a model and are calculated as the differences between what is actually observed and what is predicted by the model (equation), their examination should confirm the validity of the fitted model. If the error term in the regression model satisfies the four regression assumptions (Matson and Huguenard 2007) (they must be independent, have zero mean, have constant variance, and be normally distributed), then the model is considered valid, if they explain a reasonable and sensible relationship between the dependent and independent variables (and not just a random relationship of factors). The detailed analyses including stage vs. discharge relationship plots, probability plots, ANOVA tests, and residual analyses comparing the different test conditions are included in Appendix A.2 through A.20.

4.5.2 SmartDrain™ Material Particulate Clogging Tests

Flow rate measurements were taken from the effluent of the device at 25 to 30 minute intervals until the water completely drained from the 4 ft (1.2 m) tall lined box used to verify the extrapolation of the stage-discharge relationships for deeper water. After these initial deep water tests using clean domestic tap water, ground silica was added to subsequent tests to measure clogging potential. About 0.95 kg of Sil-Co-Sil®250 was added to the filled tank for each trial (resulting in a solids concentration of about 1,000 mg/L), with a total of 30 kg used in total for the 32 separate test trials. The cumulative US Sil-Co-Sil®250 loading on the biofilter was the only variable changed throughout these tests. Very little reductions in flow rates were observed with time, even after the total 38 kg/m² load (The cumulative US Sil-Co-Sil®250 loadings (kg) per square meter of the biofilter area) on the biofilter (2 to 4 times the typical clogging load expected for biofilter media).

Linear regression analyses were used to determine the intercept and slope terms of these stages vs. discharge relationships for the 32 trials using dirty test water. The p-values of the estimated coefficients were used to determine if the coefficients were significant ($p < 0.05$). All of the 32 test trials showed that slope coefficients were statistically significant ($p < 0.05$), while many of the intercept terms were not found to be significant for the stage-discharge relationship (Table 15), similar to found for the clean water tests.

Table 15. Linear Regression Analysis Result for Clogging Tests.

	<i>Trial</i>	<i>Coefficients</i>	<i>P-value</i>	<i>Trial</i>	<i>Coefficients</i>	<i>P-value</i>	<i>Trial</i>	<i>Coefficients</i>	<i>P-value</i>
Intercept		0	#N/A		0	#N/A		-0.004	0.0007
Slope	1	0.08	2.5E-46	12	0.06	9.1E-50	23	0.06	5.8E-30
Intercept		-0.01	0.0003		-0.002	0.0024		-0.001	0.0382
Slope	2	0.08	1.3E-22	13	0.07	1.96E-33	24	0.06	5.3E-32
Intercept		0	#N/A		0	#N/A		-0.010	2.6E-08
Slope	3	0.07	1.2E-51	14	0.06	1.51E-45	25	0.07	1.8E-25
Intercept		0	#N/A		0	#N/A		-0.006	2.1E-08
Slope	4	0.07	1.82E-59	15	0.06	3.21E-33	26	0.06	4-34
Intercept		0	#N/A		0	#N/A		-0.003	0.01
Slope	5	0.07	6.7E-37	16	0.06	3.63E-47	27	0.06	3.6E-28
Intercept		0	#N/A		0	#N/A		-0.009	7.8E-07
Slope	6	0.07	1E-37	17	0.07	4.17E-43	28	0.07	4.4E-28
Intercept		0	#N/A		-0.001	0.0219		-0.007	6.2E-11
Slope	7	0.07	3.6E-43	18	0.07	1.0E-39	29	0.07	1.8E-34
Intercept		0	#N/A		-0.004	0.0004		-0.011	2.3E-06
Slope	8	0.07	5.6E-40	19	0.07	8.51E-29	30	0.07	6.1E-23
Intercept		0	#N/A		-0.003	0.0047		-0.004	0.0002
Slope	9	0.07	2.7E-38	20	0.07	2.5E-29	31	0.06	5.3E-31
Intercept		0	#N/A		-0.003	0.0003		-0.005	0.0008
Slope	10	0.07	2.5E-35	21	0.06	1.8E-35	32	0.06	1.5E-26
Intercept		0	#N/A		-0.003	4.2E-05			
Slope	11	0.06	8.4E-57	22	0.06	1.8E-40			

Figure 29 indicates Sil-Co-Sil[®]250 load (kg/m²) vs. equation slope coefficients for the 32 particulate clogging test trials. A mean flow rate reduction of about 25% was observed after adding about 15 kg/m² Sil-Co-Sil[®]250 to the biofilter. The flow rate did not appear to decrease any further with additional loading.

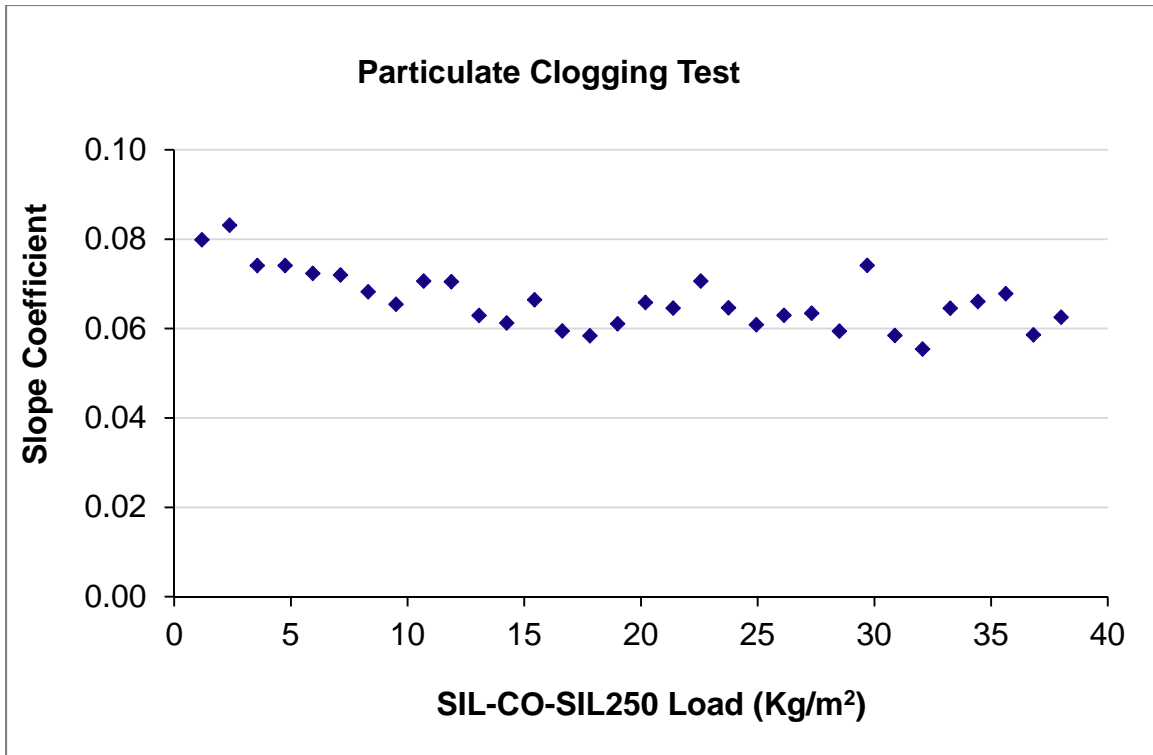


Figure 29. Sil-Co-Sil[®]250 load (kg/m²) vs. Equation Slope Coefficients for the Clogging Tests.

The detailed analyses including stages vs. discharge relationships plots, probability plots comparing the turbidity and flowrate for different test trials, ANOVA tests, and residual analyses for all test trials are included in Appendix A.21 through A.53.

Turbidity measurements of the effluent were also obtained at 25 to 30 minute intervals at the same time as the flowrate measurements until the water completely drained from the tank. The initial turbidity levels were about 1,000 NTU in the tank at the beginning of the test (and with

similar effluent water turbidity at the beginning of the tests when the flow rates and Reynolds values were the highest), but with significantly decreasing effluent turbidity values as the test progresses and the flow rates decreased (Figure 30).

The other SmartDrain™ clogging tests indicated that effluent turbidity is greater than influent turbidity during the first flush when the SmartDrain™ was opened with the maximum head on the drain and the tank full. It is expected that this short period of high turbidity water was due to the fine sediment in the Sil-Co-Sil® 250 that accumulated near the drain being washed out during the initial release at high velocity. As noted above, if more drain material was used to reduce these velocities (keeping it under 0.05 L/s per drain; for example), this would likely not be a problem.

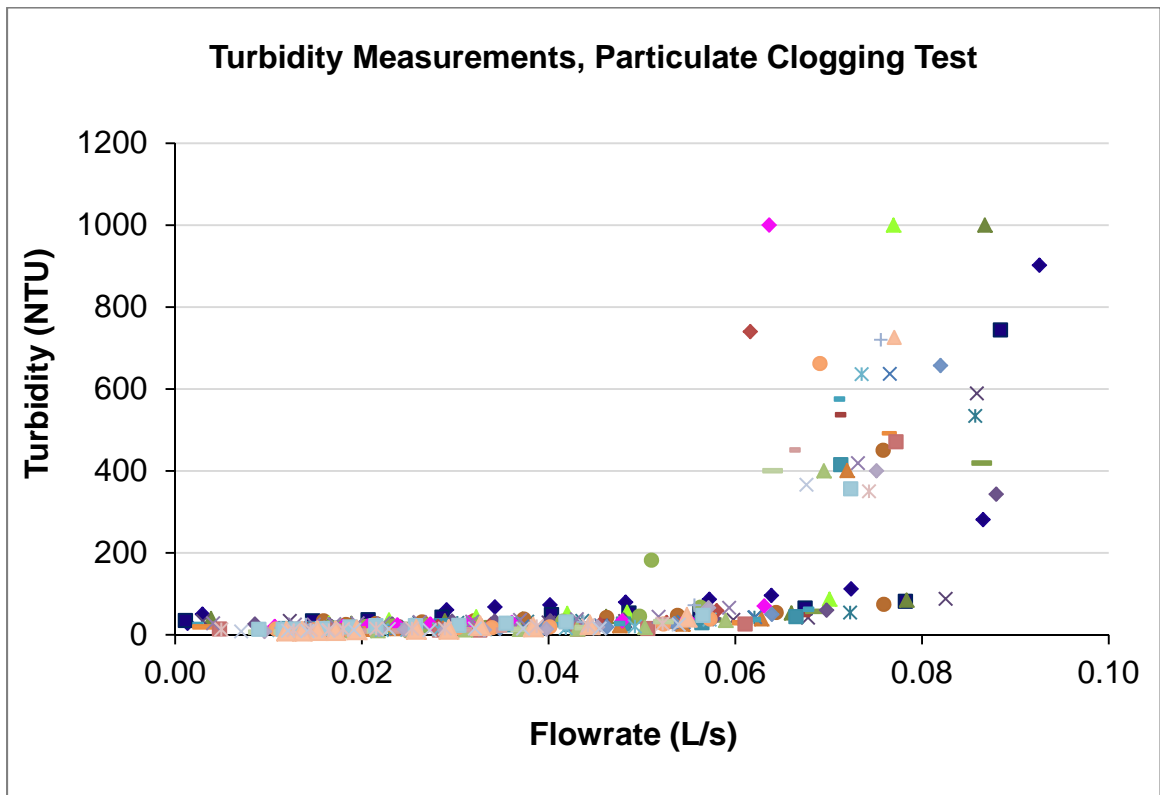


Figure 30. Turbidity Measurements Plots Taken from the Effluent of the Device during the Particulate Clogging Tests.

Figures 31 and 32 are probability plots and box plots of effluent turbidity for the particulate clogging tests for three different trials.

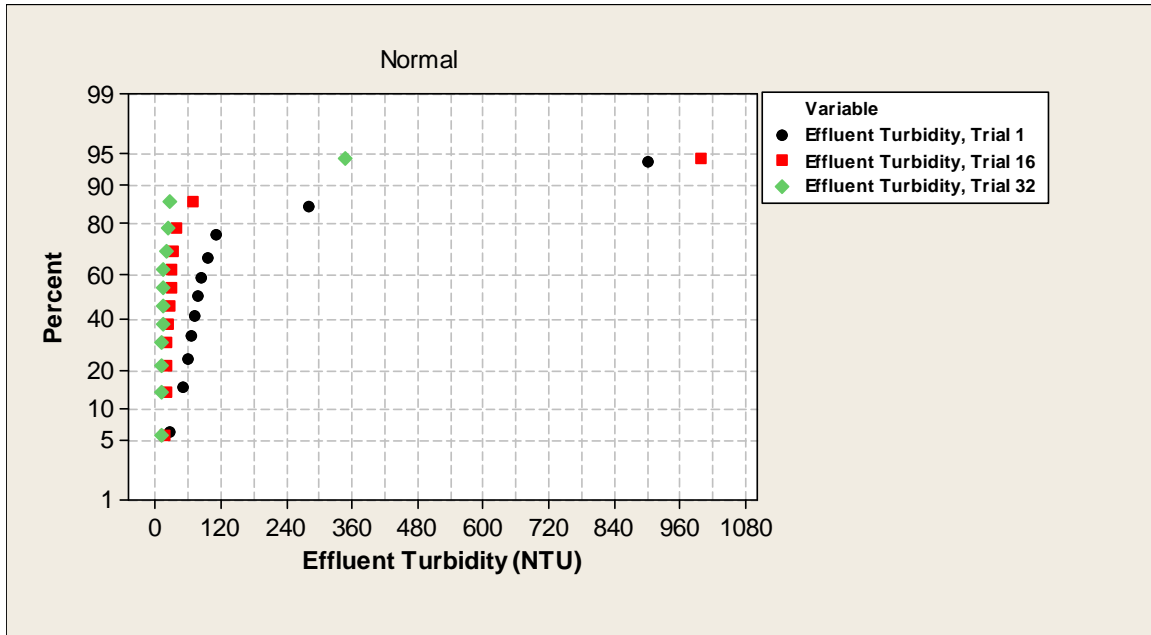


Figure 31. Probability Plot of Effluent Turbidity for the Particulate Clogging Tests (Trials 1, 16, and 32).

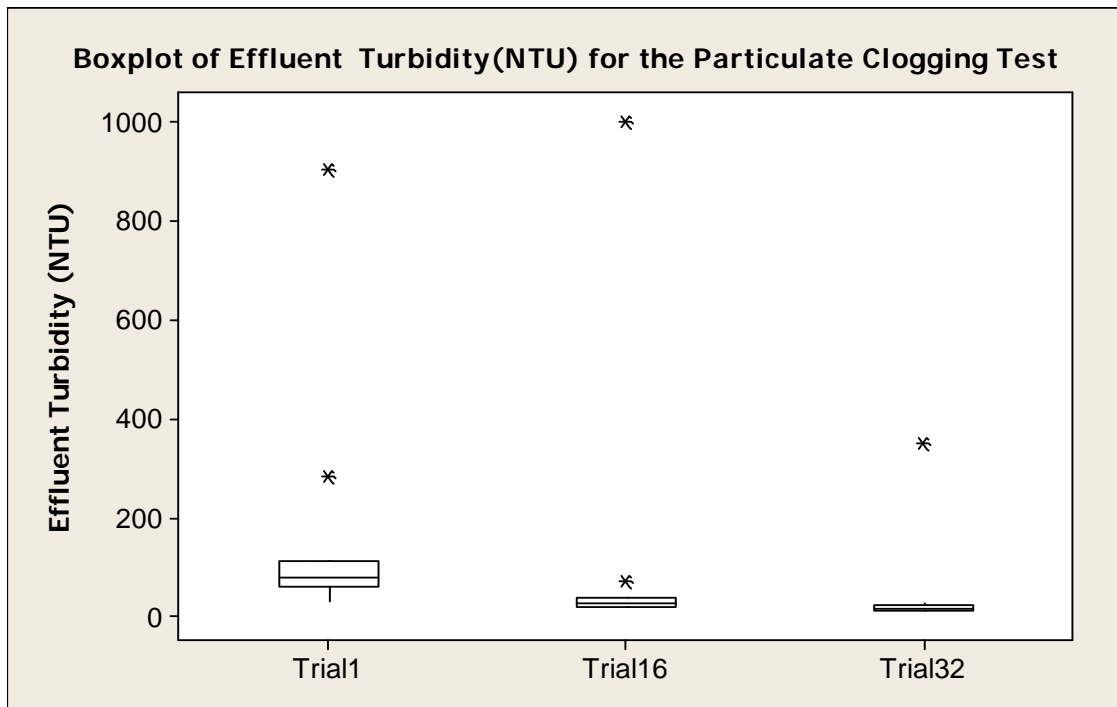


Figure 32. Box Plot Showing the Effluent Turbidity for Different Test Trials.

The average effluent turbidity values decrease as the test progresses.

4.5.3 Reynolds Number in a SmartDrain™ Belt

When water flows through a pipe, the internal roughness (ϵ) of the pipe wall can create local eddy currents within the water adding a resistance to flow of the water. Pipes with smooth walls have only a small effect on the frictional resistance. Pipes with rougher walls will create larger eddy currents which will sometimes have a significant effect on the frictional resistance. The resistance also increases quickly as the water velocity increases. The Reynolds number (Re) is a dimensionless number that gives a measure of the ratio of inertial forces to viscous forces and consequently quantifies the relative importance of these two types of forces for given flow conditions. The Reynolds number can be defined for a number of different situations where a fluid is in relative motion to a surface. These definitions generally include the fluid properties of density and viscosity, plus a velocity and a characteristic length or characteristic dimension.

Reynolds numbers are used to determine whether a flow will be laminar or turbulent. For general engineering purposes, if Re is high (> 4000), inertial forces dominate viscous forces and the flow in a round pipe is turbulent; if Re is low (< 2000), viscous forces dominate and the flow in a round pipe is laminar. The actual transition from laminar to turbulent flow may take place at various Reynolds numbers (i.e. $2000 < Re \leq 4000$), depending on how much the flow is disturbed by vibrations of the pipe, roughness of the entrance region, etc.

At high Re , the friction factor (f) depends only on ϵ/d ; defining the region referred to as fully turbulent flow. This is the region in the Moody diagram (Figure 33) where the lines for different ϵ/d become horizontal (ϵ is the equivalent roughness height and d is the pipe diameter). The Re_D at which this occurs depends on the pipe roughness (Kreith, 1999). Using the Moody diagram (Figure 33) to get f requires that Re and ϵ/d be known. Calculating Re is direct if the water temperature, velocity, and pipe diameter are known. The problem is obtaining a good

value for ϵ . Laminar flows in pipes is unusual. Most practical pipe flow problems are in the turbulent region. Since roughness may vary with time due to buildup of solid deposits or organic growths, f is also time dependent.

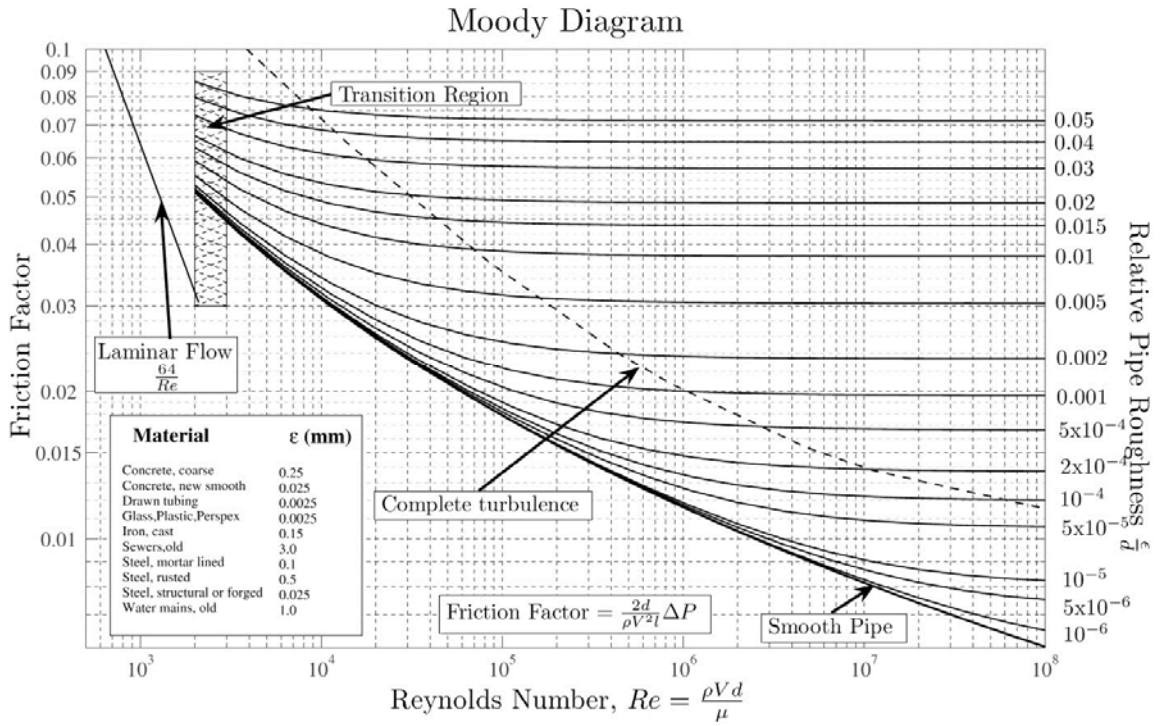


Figure 33. Moody diagram showing the Darcy-Weisbach friction factor plotted against Reynolds number for various roughness values.

Available: http://upload.wikimedia.org/wikipedia/commons/8/80/Moody_diagram.jpg

Reynolds numbers were also determined for each test trial during the clogging tests.

For flow in pipes or tubes, the Reynolds number is generally defined as:

$$Re = \frac{\rho VL}{\mu}$$

Where:

R_e Reynolds Number

ρ Density

V Velocity

L Characteristic length is pipe diameter or hydraulic radius

μ Dynamic viscosity of the fluid

The dynamic viscosity of water at room temperature (20° C), $\mu = 1.002 \times 10^{-3} \text{ N s/m}^2$

The density of water, $\rho = 1000 \text{ kg/m}^3$

Figure 34 shows the calculated Reynolds numbers vs observed turbidities during the “dirty water” tests. Since the only variable is water velocity, this relationship is linear. The earlier plot (Figure 30) indicated that particle transport issues were noted starting at about 0.05 L/s, which corresponds to a Reynolds number of about 350. The turbidity values quickly increases with higher flows (associated with higher heads) likely because the carrying capacity increased with the greater flow rates; therefore, if the flows were kept smaller (such as by using two parallel strips of SmartDrain™ instead on one), then this would not be an issue for heads of about 1m. In addition, it is expected that the particulate removal from filtering in finer sand or typical biofilter media would significantly reduce the delivery of material to the SmartDrain™. Certainly, faster flow rates from perforated pipes would cause more media erosion than the SmartDrain™. Figure 34 shows that the Reynolds number decreased due to decreasing flow rates with clogging.

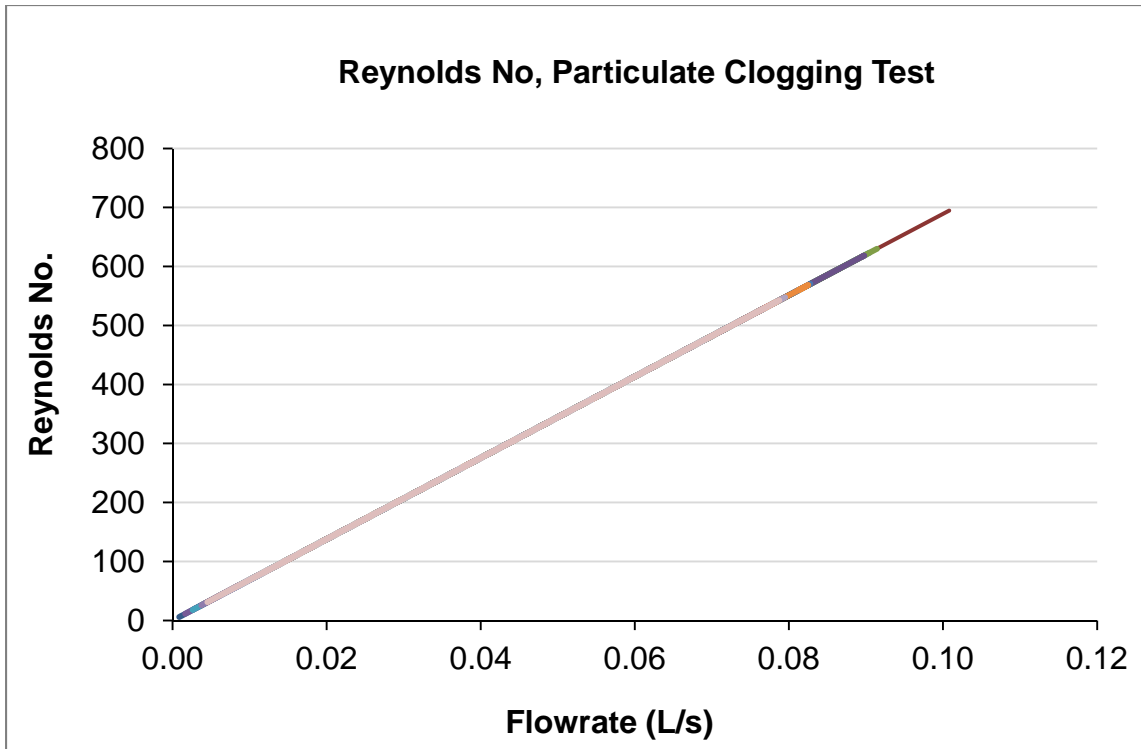


Figure 34. Reynolds No. vs. Flowrate Relationships for the Particulate Clogging Tests (Overlay Graphs for Different Test Trials).

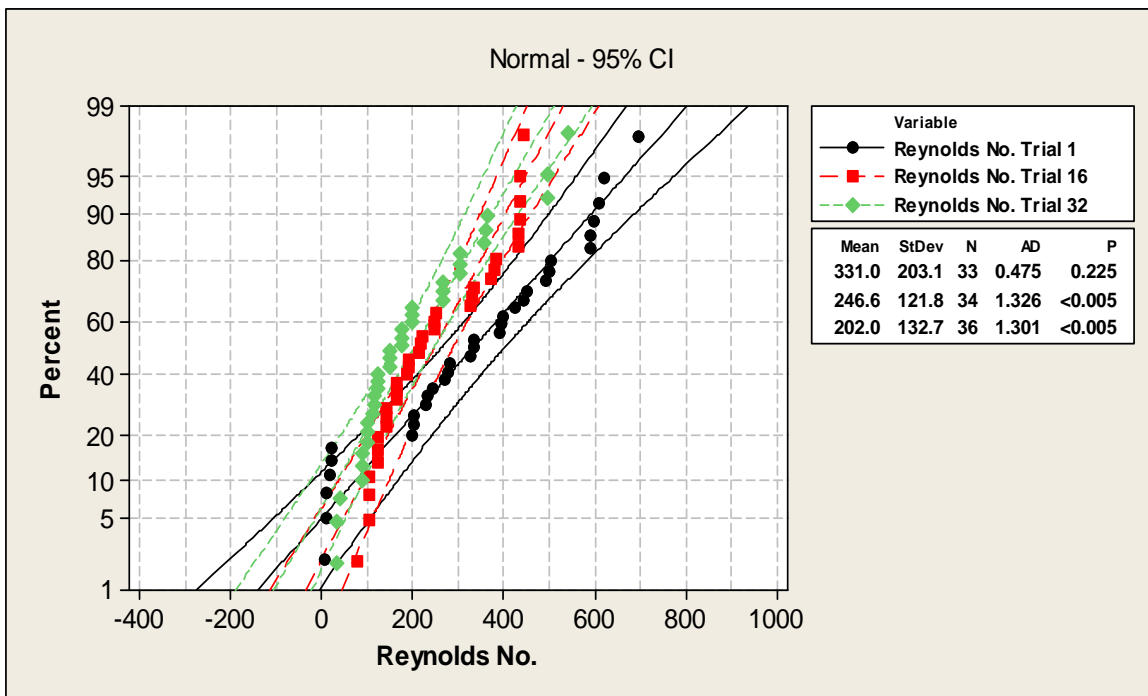


Figure 35. Probability Plot of Effluent Turbidity for the Particulate Clogging Tests (Trial 1, 16, and 32).

Figure 35 shows that the Reynolds No. using dirty water (trial 32) varied more than the Reynolds No. using clean water (trial 1), indicating better performance of the SmartDrain when the Reynolds No. was high or with a decrease in particulate loading.

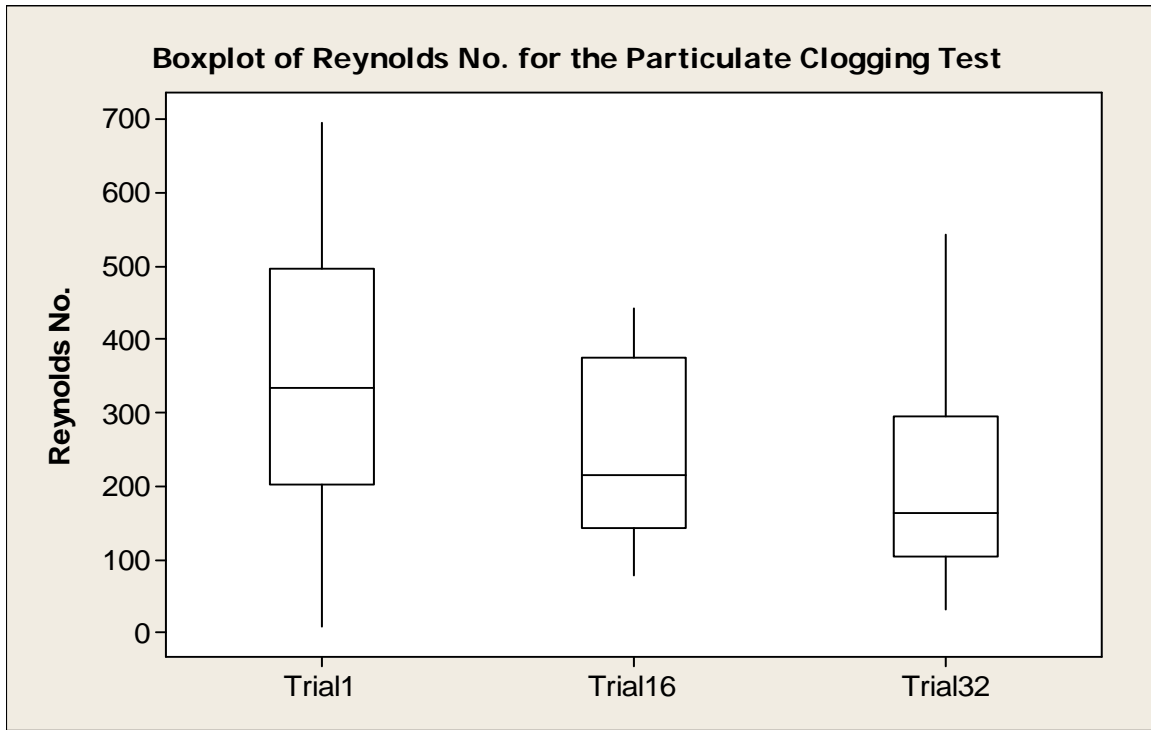


Figure 36. Box Plot Showing Reynolds Number for Different Test Trials.

4.5.4 SmartDrain™ Material Biofouling Tests

Flow rates and turbidity measurements were made for the test mixture inside the biofilter box and from both the effluent and influent of the device at 25 to 30 minute intervals until the water completely drained from the tank during the biofouling tests. The flows were measured by timing how long it took to fill a 0.5 L graduated cylinder. The influent turbidity (NTU) values in the tank increased as the water levels dropped for most of the trials (Figure 37). The effluent turbidity (NTU) values Reynolds numbers were also determined for each test trial during the biofouling tests (Figure 38).

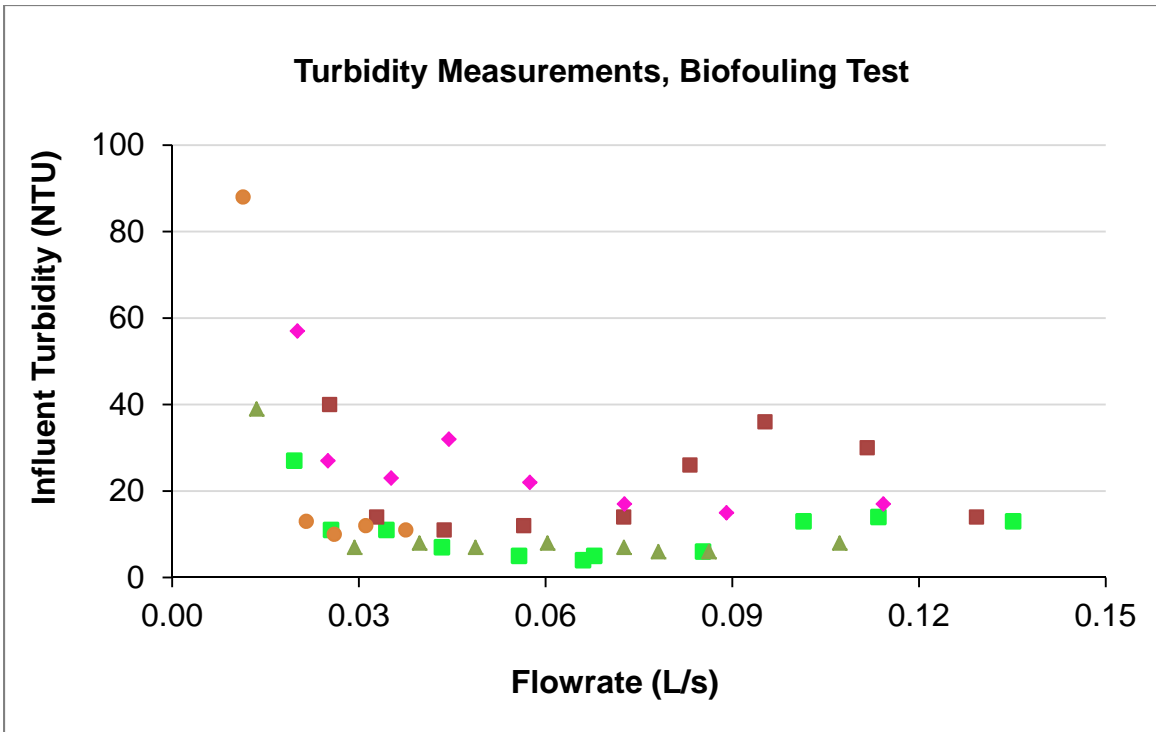


Figure 37. Influent Turbidity (NTU) vs Flowrate for the Biofouling Tests.

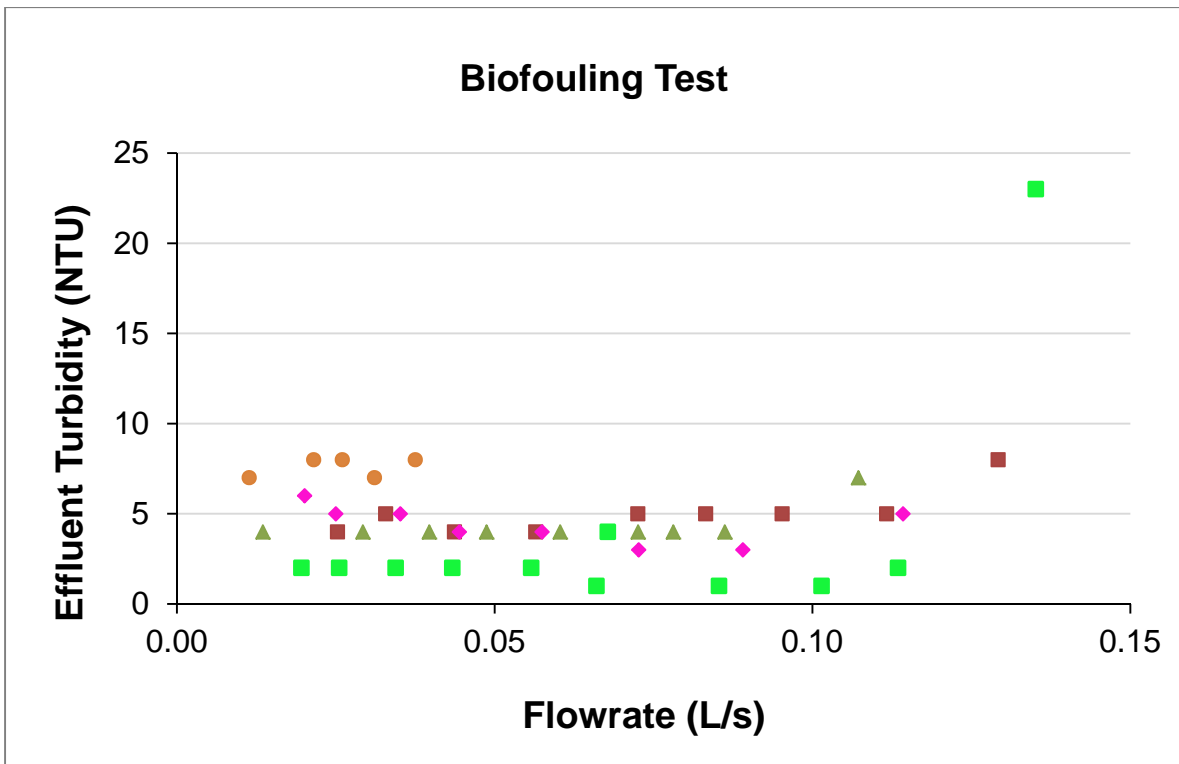


Figure 38. Effluent Turbidity (NTU) vs Flowrate for the Biofouling Tests.

Stage-discharge relationship plots (Figure 39) are shown for the seven different tests. Linear regression analyses were used to determine the intercept and slope terms of the resulting equations. The p-values of the estimated coefficients were used to determine if the coefficients were significant ($p < 0.05$). Stages vs. discharge relationships plots for the seven tests are included in Appendix A.54 through A.60. All of the seven trials tested for the biofouling experiments at various growth stages of algae in the tank showed that all slope coefficients were statistically significant ($p < 0.05$), while three of the intercept terms were not found to be significant on the stage-discharge relationship (Table 16). Detailed statistical results are included in Appendix A.54 through A.60.

The results indicated that the biofouling had only a small effect on the discharge rates, even though the algal growth was extensive. Figure 40 indicates equation slope coefficients vs. number of trials for the biofouling tests.

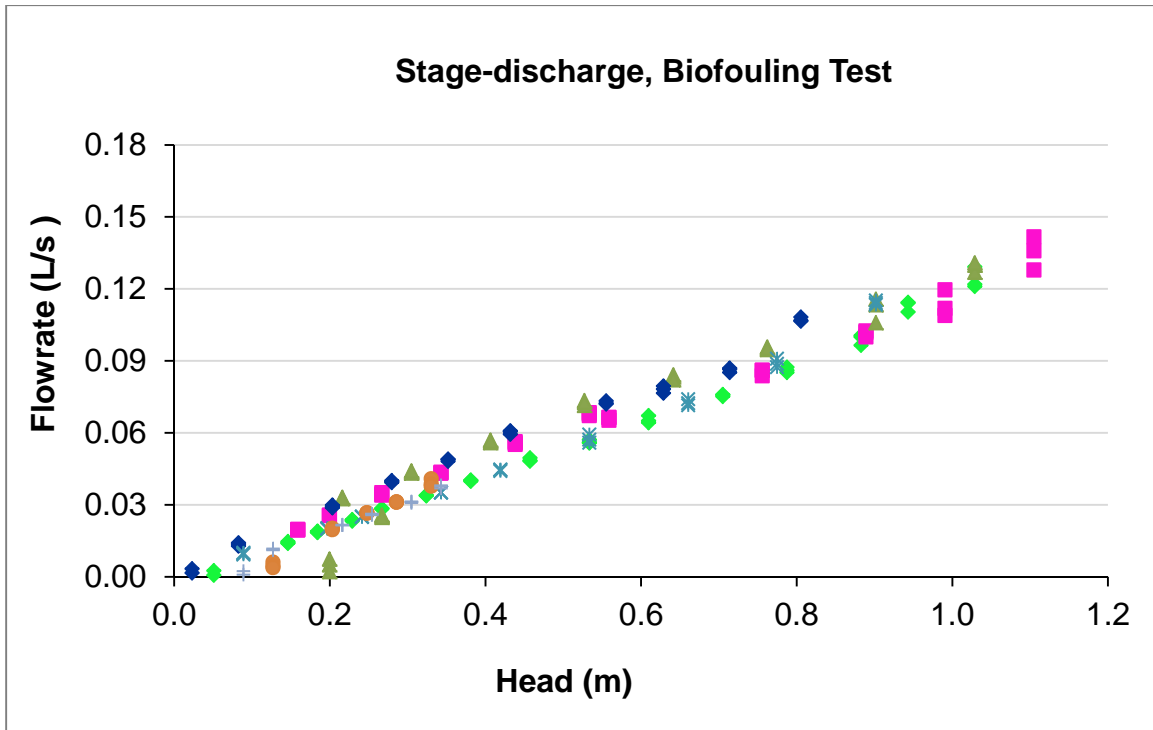


Figure 39. Stage-discharge Relationship Plots for the Biofouling Tests.

Table 16. Linear Regression Analysis Result for the Biofouling Tests.

Trial no.	Date	Coefficients		p-value	
		Intercept	Slope	Intercept	Slope
1	17-Jun-10	-0.005	0.12	1.85E-06	8.59E-47
2	8-Jul-10	0	0.119	#N/A	1.36E-42
3	25-Jul-10	0	0.126	#N/A	7.57E-30
4	12-Aug-10	0	0.130	#N/A	1.25E-36
5	3-Sep-10	-0.006	0.125	0.000985	3.07E-25
6	27-Sep-10	-0.015	0.165	1.61E-08	5.49E-14
7	11-Oct-10	-0.007	0.129	1.08E-05	1.14E-14

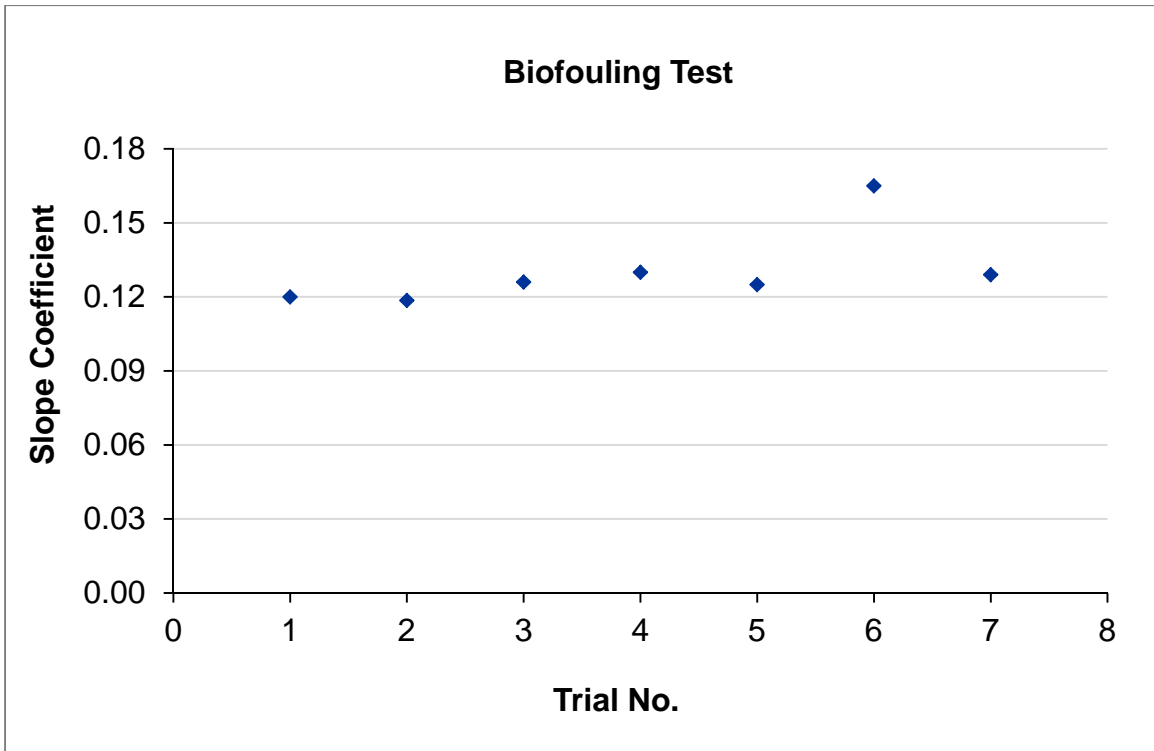


Figure 40. Equation Slope Coefficients vs Number of Trials for the Biofouling Tests.

4.6 Data Analyses

4.6.1 SmartDrain™ Drainage Characteristics Tests

Statistical analyses were conducted to determine the effects of SmartDrain™ length, slope, and head, plus their interactions on the SmartDrain™ flowrate performance. A complete two level and three factors (2^3 , SmartDrain™ length, slope, and head) factorial experiment (Box et al. 1978) was conducted to examine the effects of those factors, plus their interactions on the SmartDrain™ flowrates. The factors studied, and their low (-1) and high values (+1) used in the calculations, are shown in Table 17. The complete data set used in this factorial study is also summarized in Table 18. Experiments were performed in replicates of 3 to 12 for each flow rate. Statistical methods were used to summarize the data and to provide an empirical method to analyze factor interactions on the SmartDrain™ flowrate.

Table 17. Experimental Factors and their Levels.

Variable	Low value (-1)	High value (+1)
SmartDrain™ length, L (ft, m)	1.1 (0.34)	9.4 (3)
SmartDrain™ slope, S (%)	0	12
Head, H (inches, cm)	2 (5)	16.5 (42)

The data analyses were performed using the statistical software package Minitab (version 16). Normal plots of the standardized effects, residual plots, main effects plots, and interaction plots were prepared to examine the effects of the factors and to compare the significance of each effect. An analysis of variance (ANOVA) table was constructed to determine the significant factors and their interactions needed to best predict SmartDrain™ flow performance. Statistical hypothesis tests using a p-value of 0.05 (95% confidence) were used to determine whether the observed data were statistically significantly different from the null hypothesis.

Table 18. Flowrate Data Used in Full 2³ Factorial Designs.

Condition	Length (L)	Slope (S)	Head (H)	LS	LH	SH	LSH	Q (L/s)
1A	-	-	-	+	+	+	-	0.0018
1B	-	-	-	+	+	+	-	0.0015
1C	-	-	-	+	+	+	-	0.0012
2A	+	-	-	-	-	+	+	0.0041
2B	+	-	-	-	-	+	+	0.0041
2C	+	-	-	-	-	+	+	0.0041
3A	-	+	-	-	+	-	+	0.0064
3B	-	+	-	-	+	-	+	0.0061
3C	-	+	-	-	+	-	+	0.0059
3D	-	+	-	-	+	-	+	0.0035
3E	-	+	-	-	+	-	+	0.0033
3F	-	+	-	-	+	-	+	0.0032
4A	+	+	-	+	-	-	-	0.0066
4B	+	+	-	+	-	-	-	0.0065
4C	+	+	-	+	-	-	-	0.0055
4D	+	+	-	+	-	-	-	0.0054
4E	+	+	-	+	-	-	-	0.0051
4F	+	+	-	+	-	-	-	0.0050
5A	-	-	+	+	-	-	+	0.0537
5B	-	-	+	+	-	-	+	0.0528
5C	-	-	+	+	-	-	+	0.0526
5D	-	-	+	+	-	-	+	0.0480
5E	-	-	+	+	-	-	+	0.0472
6A	+	-	+	-	+	-	-	0.0649
6B	+	-	+	-	+	-	-	0.0633
6C	+	-	+	-	+	-	-	0.0631
6D	+	-	+	-	+	-	-	0.0562
6E	+	-	+	-	+	-	-	0.0552
6F	+	-	+	-	+	-	-	0.0575
6G	+	-	+	-	+	-	-	0.0503
6H	+	-	+	-	+	-	-	0.0525
6I	+	-	+	-	+	-	-	0.0502
6J	+	-	+	-	+	-	-	0.0471
6K	+	-	+	-	+	-	-	0.0469
6L	+	-	+	-	+	-	-	0.0464
7A	-	+	+	-	-	+	-	0.0559
7B	-	+	+	-	-	+	-	0.0551
7C	-	+	+	-	-	+	-	0.0549
7D	-	+	+	-	-	+	-	0.0523
7E	-	+	+	-	-	+	-	0.0516
7F	-	+	+	-	-	+	-	0.0520
7G	-	+	+	-	-	+	-	0.0469
7H	-	+	+	-	-	+	-	0.0464
7I	-	+	+	-	-	+	-	0.0466
8A	+	+	+	+	+	+	+	0.0625
8B	+	+	+	+	+	+	+	0.0684
8C	+	+	+	+	+	+	+	0.0625
8D	+	+	+	+	+	+	+	0.0566
8E	+	+	+	+	+	+	+	0.0542
8F	+	+	+	+	+	+	+	0.0550
8G	+	+	+	+	+	+	+	0.0503
8H	+	+	+	+	+	+	+	0.0484
8I	+	+	+	+	+	+	+	0.0483

Normal probability plots of effects were used to compare the relative magnitudes and the statistical significance of all main and interaction effects. These plots also indicated the direction of the effect. In Figure 41, the factors SmartDrain™ length and head have positive effects because they appear on the right side of the plot, meaning that when the low level changes to the high level of the factor, the flow response increases. Figure 41 shows that SmartDrain™ head (H) has the largest effect on the measured flowrates, followed by SmartDrain™ length. Slope was not found to be significant. The results of the factorial analyses are summarized in Table 19.

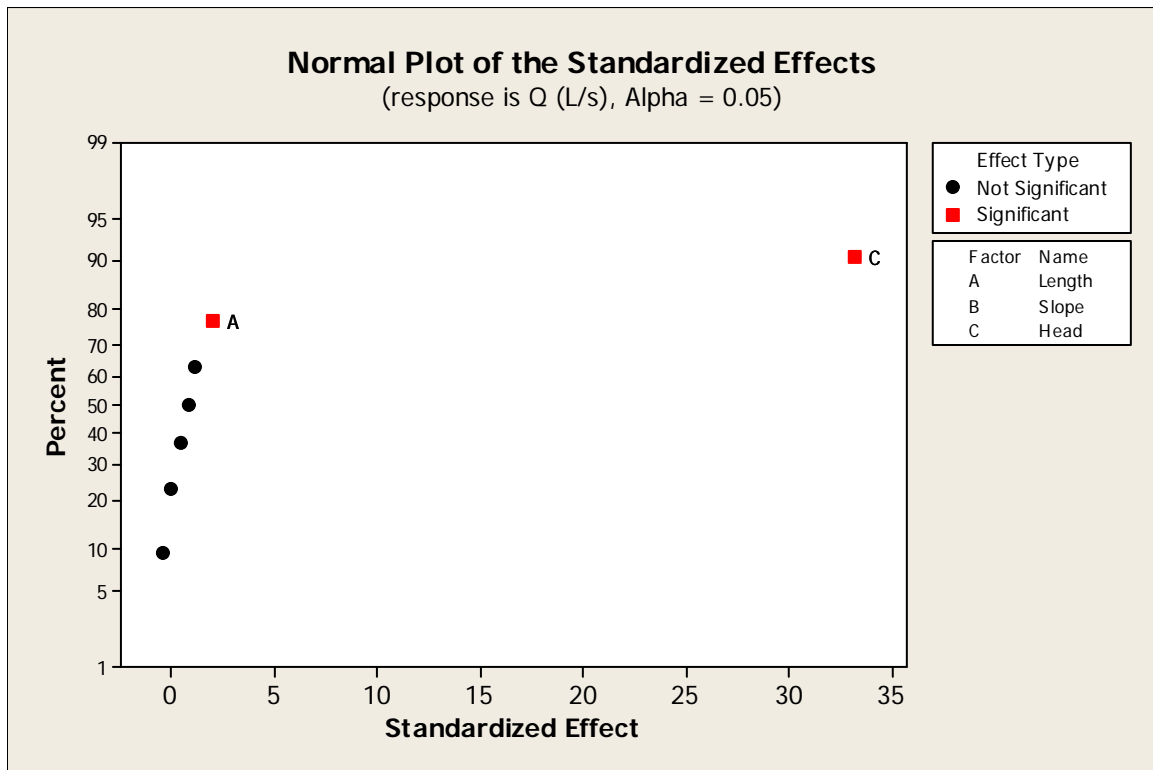


Figure 41. Normal Probability Plots of the Effect.

Table 19. Estimated Effects and Coefficients for Q (L/s) (coded units).

Term	Effect	Coef	SE Coef	T	P
Constant		0.0286	0.00074	38.6400	0.0000
Length	0.0030	0.0015	0.00074	2.0300	0.0480
Slope	0.0018	0.0009	0.00074	1.1800	0.2430
Head	0.0492	0.0246	0.00074	33.2200	0.0000
Length*Slope	-0.0001	0.0000	0.00074	-0.0400	0.9650
Length*Head	0.0012	0.0006	0.00074	0.8400	0.4070
Slope*Head	-0.0006	-0.0003	0.00074	-0.4300	0.6660
Length*Slope*Head	0.0007	0.0004	0.00074	0.5000	0.6190

S = 0.00482859 PRESS = 0.00130440
R-Sq = 96.50% R-Sq(pred) = 95.65% R-Sq(adj) = 95.96%

Table 20 indicates that observation 24 and 46 are unusual because their standardized residual is greater than 2. This could indicate that these observations are in error.

Table 20. Unusual Observations for Q (L/s).

Obs	StdOrder	Q (L/s)	Fit	SE Fit	Residual	St Resid
24	24	0.0649	0.0544	0.0014	0.0104	2.25R
46	46	0.0684	0.0562	0.0016	0.0122	2.67R

R denotes an observation with a large standardized residual.

The main effects plots are useful to compare magnitudes of main effects. Interaction plots can magnify or diminish the main effects of the parameters, their evaluation is extremely important. The main effect plots are obtained to examine the data means for the three factors. Figure 42 shows small increases in flowrates occurred with increases in SmartDrain™ length. However, significant increases in flowrates were observed with increases in head. Flowrates decreased with decreasing SmartDrain™ slope. Figure 43 shows probability plots of flowrate for SmartDrain™ length = 1.1ft, slopes 0% and 12%, indicating no apparent difference in flow rate as the slope changed.

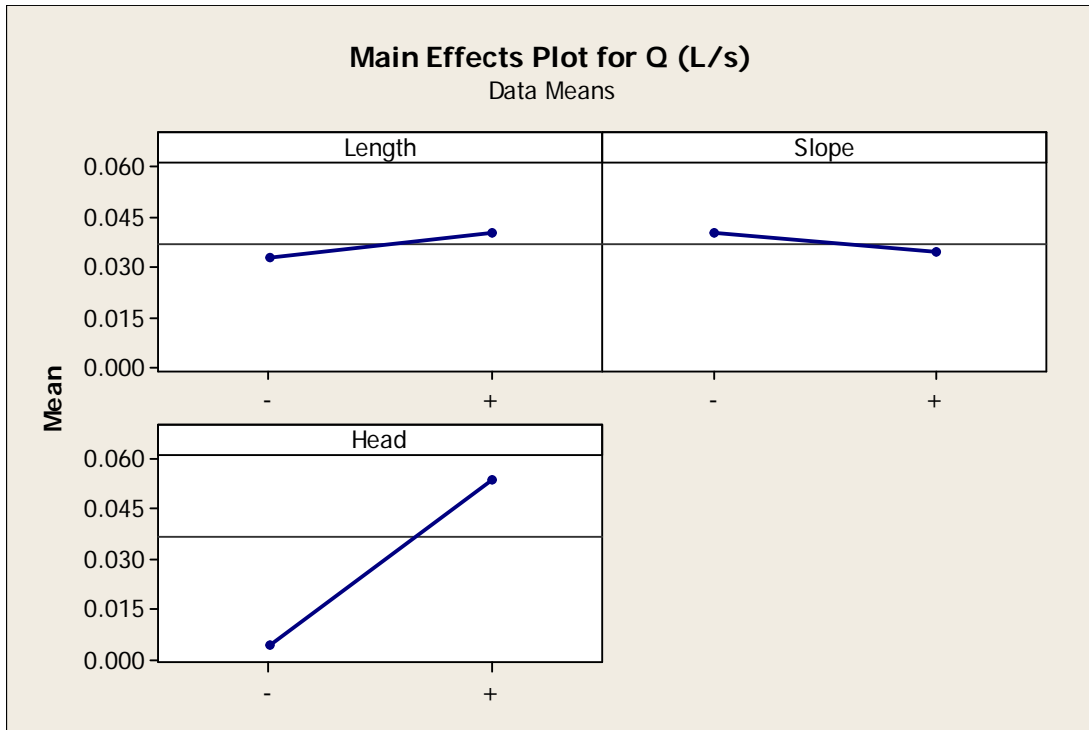


Figure 42. Main Effect Plots for SmartDrain™ Flowrate.

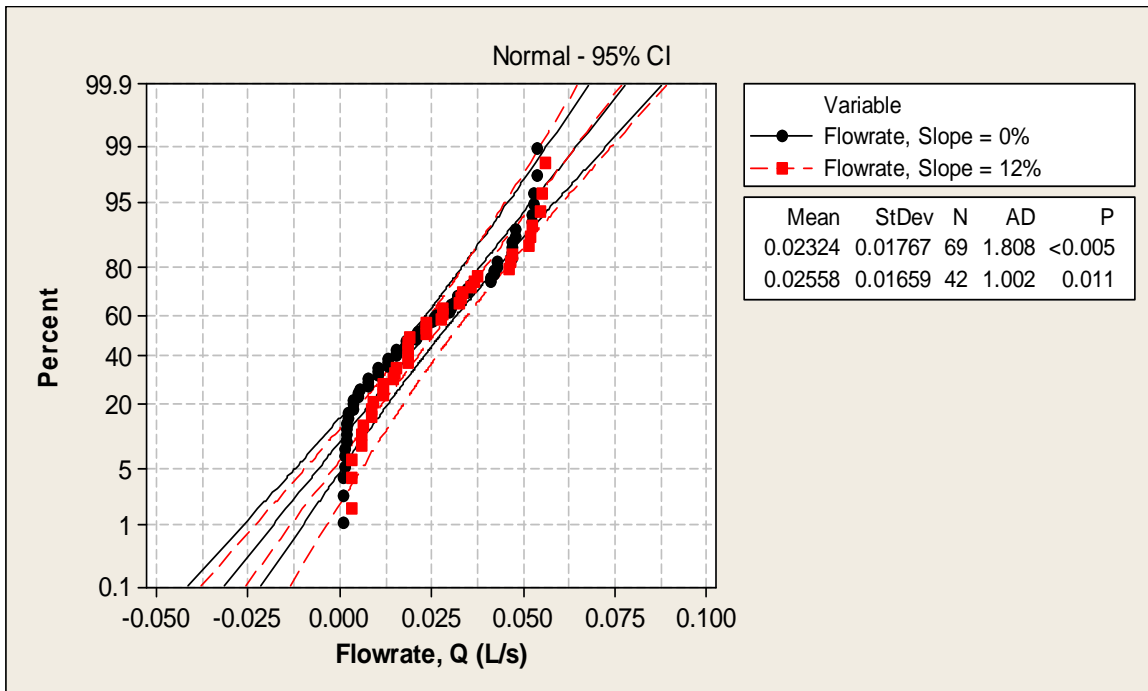


Figure 43. Probability Plot of Flowrate for SmartDrain™ Length = 1.1 ft (0.34 m) Slopes 0%, and 12%.

Figure 44 depicts interaction plots which are used to interpret significant interactions between the factors. The SmartDrain™ length vs. slope almost cross each other, indicating there may exist a significant interaction between these factors. In the other two plots, the lines for SmartDrain™ length vs. head and slope vs. head are approximately parallel, indicating an apparent lack of interaction between the two factors. These interaction plots suggest that mutual interactions between length vs. head and slope vs. head have negligible effects on the flowrate. The greater the departure of the lines from the parallel state, the higher the degree of interaction.

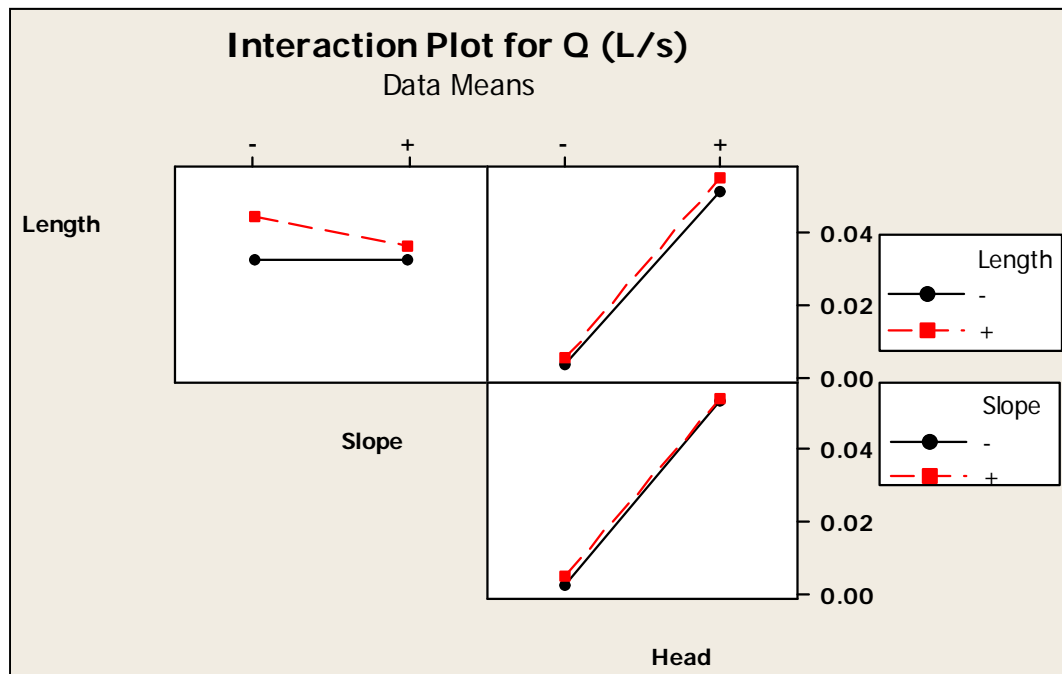


Figure 44. Interaction Plots for SmartDrain™ Flowrate

4.6.2 Model Fitting for Drainage Characteristics Tests

The effects and half-effects of the significant effects (main effects and interactions) were used to predict the SmartDrain™ flowrate performance. Table 21 shows the matrix (table of contrasts) representing factors (SmartDrain™ length, slope, and head) and their interactions. The results of the effects and half-effect are also shown in the table.

Table 21. Effects and Half-Effects Results.

Case	Length (L)	Slope (S)	Head (H)	LS	LH	SH	LSH	Q (L/s)
1	-	-	-	+	+	+	-	0.0015
2	+	-	-	-	-	+	+	0.0041
3	-	+	-	-	+	-	+	0.0047
4	+	+	-	+	-	-	-	0.0057
5	-	-	+	+	-	-	+	0.0509
6	+	-	+	-	+	-	-	0.0544
7	-	+	+	-	-	+	-	0.0513
8	+	+	+	+	+	+	+	0.0562
Y								0.0286
(grand)								
	L	S	H	LS	LH	SH	LSH	
Avg. Y@-1	0.0271	0.0277	0.004	0.0286	0.028	0.0289	0.0282	
Avg. Y@+1	0.0301	0.0295	0.0532	0.0286	0.0292	0.0283	0.029	
Δ	0.003	0.0018	0.0492	-0.0001	0.0012	-0.0006	0.0007	
$\Delta/2$	0.0015	0.0009	0.0246	0.0000	0.0006	-0.0003	0.0004	

As noted previously, the significant factors that affect the responses are head, SmartDrainTM length. Those factors have to be included in the prediction equation. The parameters slope, interactions of length and slope, interactions of length and head, interactions of slope and head, and the three-way interactions of these factors, have negligible effect (p-values greater than the chosen value of $\alpha = 0.05$) on the SmartDrainTM flowrate and a reduced model was created wherein these factors are ignored.

The prediction equation can be written in terms of the grand mean and half-effects, excluding the non-significant factors.

$$\hat{y} = \bar{y} + \left(\frac{\Delta L}{2}\right)L + \left(\frac{\Delta H}{2}\right)H$$

where: \hat{y} = predicted response (Y pred)
 \bar{y} = grand mean (Y grand)
 $\frac{\Delta}{2}$ = half-effects of each factor or interaction
 L = length (ft)
 H = head (in)

The final prediction equation is given as:

$$\hat{y} = 0.0286 + 0.0015L + 0.0246H$$

Table 22 shows the standard error of the mean (for each condition's mean). The number of flowrate measurements in a given population varied from 3 to 12. Within each sample population, there was no significant standard deviation. The standard error of the mean (for each condition's mean) is the standard deviation of the sample group divided by the square root of the sample size. The pooled standard error of the mean was computed to be 0.00483.

Table 22. Standard Error Calculations for SmartDrain™ Flowrate Tests.

Condition	1	2	3	4	5	6	7	8
Q (L/s)	0.0018	0.0041	0.0064	0.0066	0.0537	0.0649	0.0559	0.0625
	0.0015	0.0041	0.0061	0.0065	0.0528	0.0633	0.0551	0.0684
	0.0012	0.0041	0.0059	0.0055	0.0526	0.0631	0.0549	0.0625
			0.0035	0.0054	0.0480	0.0562	0.0523	0.0566
			0.0033	0.0051	0.0472	0.0552	0.0516	0.0542
			0.0032	0.0050		0.0575	0.0520	0.0550
						0.0503	0.0469	0.0503
						0.0525	0.0464	0.0484
						0.0502	0.0466	0.0483
						0.0471		
						0.0469		
						0.0464		
Standard Dev.	0.000	0.000	0.002	0.001	0.003	0.007	0.004	0.007
Square Root N	1.732	1.732	2.449	2.449	2.236	3.464	3.000	3.000
Standard Error	0.000	0.000	0.001	0.000	0.001	0.002	0.001	0.002
Average (L/s)	0.002	0.004	0.006	0.006	0.053	0.064	0.055	0.064

An ANOVA test was used to test the significance of the regression coefficients, which depends on the number of data observations. When only a few data observations are available, strong and important relationships may not be shown to be significant, or high R^2 values could occur with insignificant equation coefficients. The data were evaluated by using the p-value (the probability of obtaining a test statistic that is at least as extreme as the calculated value if there is actually no difference; the null hypothesis is true). The independent variable was used to predict the dependent variable when $p < 0.05$. A summary of statistical information about the model is also shown in Table 23. R^2 is a statistical measure of goodness of fit of a model whereas the adjusted R^2 is a statistic that is adjusted for the number of explanatory terms in a model. The value of R^2 and adjusted R^2 for the model are 96.5% and 95.96% respectively. Predicted R^2 is calculated from the PRESS (Prediction Error Sum of Squares) statistic. The predicted R^2 statistic is computed to be 95.65%. Larger values of predicted R^2 suggest models of greater predictive ability. This indicates that the model is expected to explain about 96.5% of the variability in new

data. Figure 45 shows a scatterplot of the observed and fitted Q (L/s) values, indicating very good fits of the observed with the predicted Q (L/s) values over a wide range of conditions.

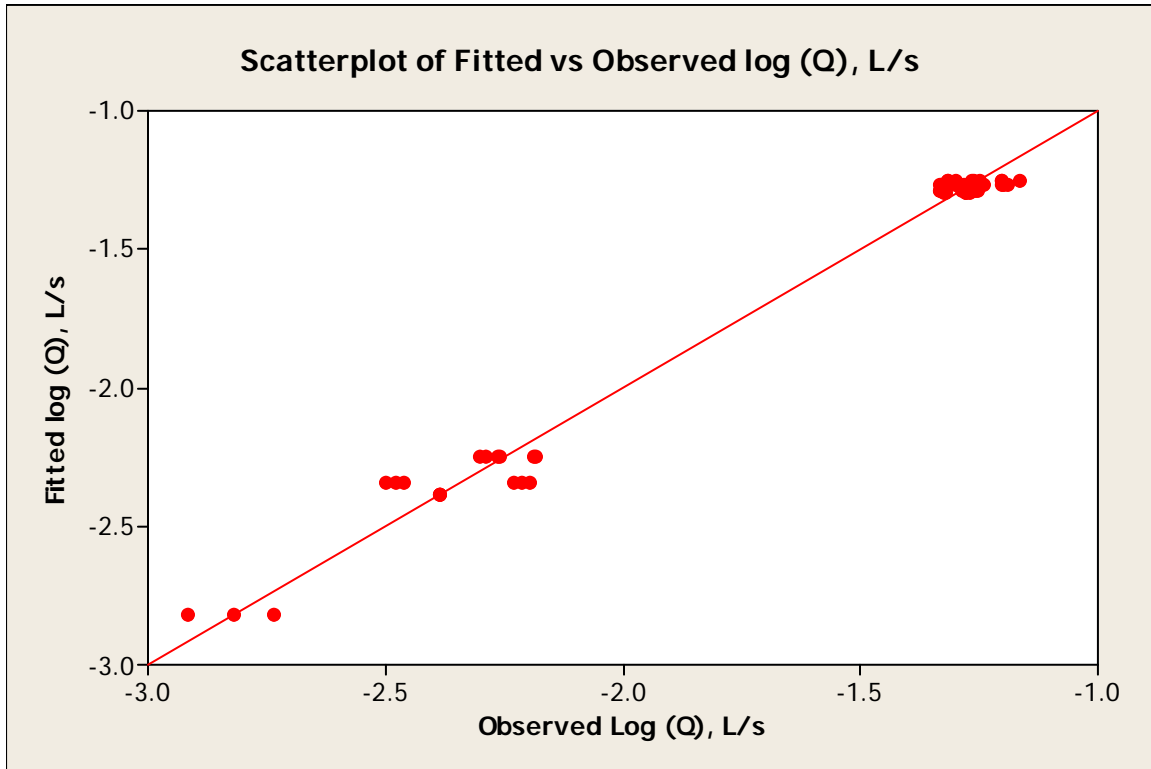


Figure 45. Scatter Plot of Observed Q (L/s) vs Fitted log (Q), L/s

Residual analyses were conducted to investigate the goodness of model fit. Residual plots were inspected to determine if the error term in the regression model satisfies the four assumptions (they must be independent, zero mean, constant variance, and normally distributed). To check the constant variance assumptions, the plots of residuals vs. the fitted values were inspected. To evaluate the normality of the residuals, normal probability plots and histograms of the residuals were also constructed. Anderson-Darling test statistic was also calculated to check for normality. The normal probability plot of the residuals shown in Figure 46 shows that the fitted data is normally distributed (Anderson-Darling test for normality has a p-value greater than

0.05, so the data are not significantly different from a normal distribution for the number of observations available). The zero mean of the residuals assumption was checked by examining the descriptive statistics and graphs of the residuals vs. fitted values and vs. the order of the observations. To determine if the residuals were independent of each other, graphs of the residuals vs. observation number were also examined.

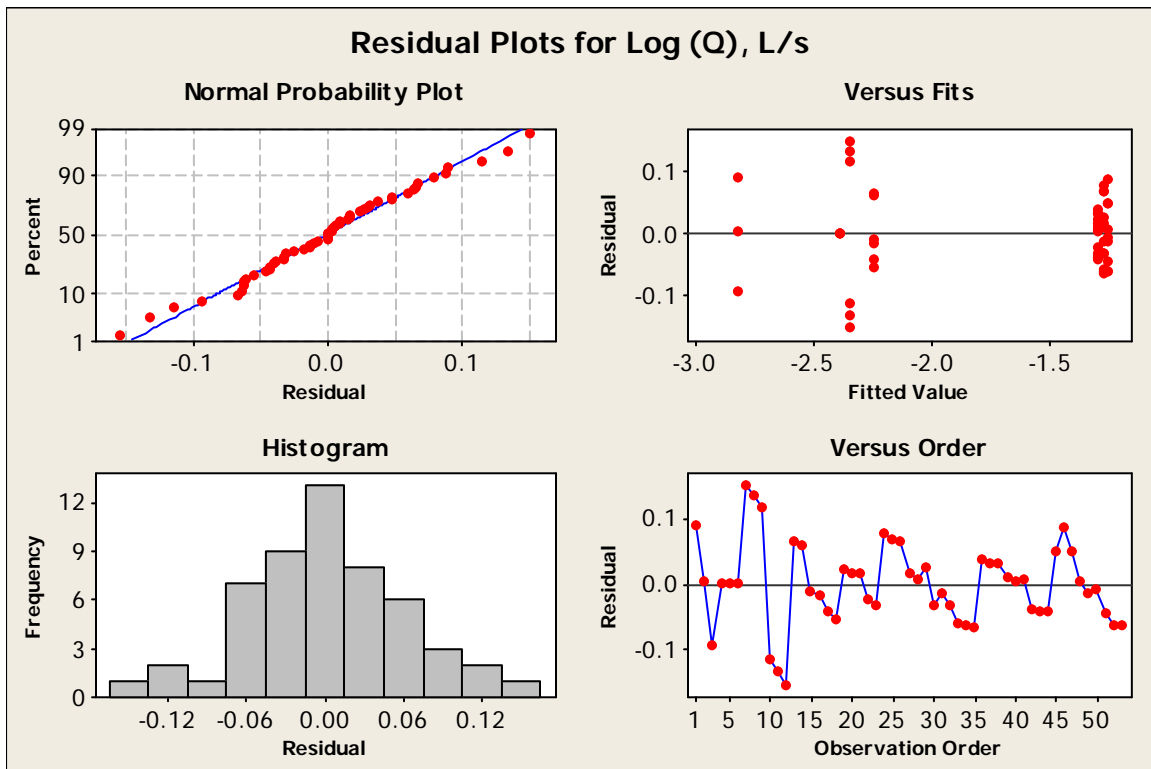


Figure 46. Residuals Analysis Plot.

The examination of the residual values vs. fitted values of the data indicated that there was a greater spread in the residuals for the higher fitted values. The model residual histogram was approximately bell shaped; the residuals were normally distributed and had zero mean, and were independent of each other. Model improvements should therefore focus on conditions that had high flowrate conditions.

4.6.3 SmartDrain™ Clogging Tests

Two-tailed *t* tests with 95% confidence intervals ($p = 0.05$ level) were performed to assess the significance of differences between flowrate measurements obtained on clean water (Trial #1) versus dirty water (Trial #32) during the clogging tests. The dirty water was obtained by adding a total of 30 kg of ground silica load for the 32 test trials, or 38 kg/m² total load (the cumulative US Sil-Co-Sil®250 loadings (kg) per square meter of the biofilter area). The difference between the two trial groups (clean and dirty water) was analyzed by comparing their mean flowrates. Table 23 indicates that the *p*-value is less than 0.05 indicating the two means are significantly different. Figure 47 depicts box and whisker plots of flowrate data using clean water and dirt water.

Table 23. Two-Tailed T-Test for Clean Water (Trial #1) vs Dirty Water (Trial #32) for Clogging Tests.

Trial#	N	Mean	StDev	SE Mean
1	33	0.0480	0.0295	0.0051
32	36	0.0293	0.0193	0.0032

Difference = μ Trial #1 - μ Trial #32

Estimate for difference: 0.01873

95% CI for difference: (0.00686, 0.03060)

T-Test of difference = 0 (vs not =): T-Value = 3.15 P-Value = 0.002 DF = 67

Both use Pooled StDev = 0.0247

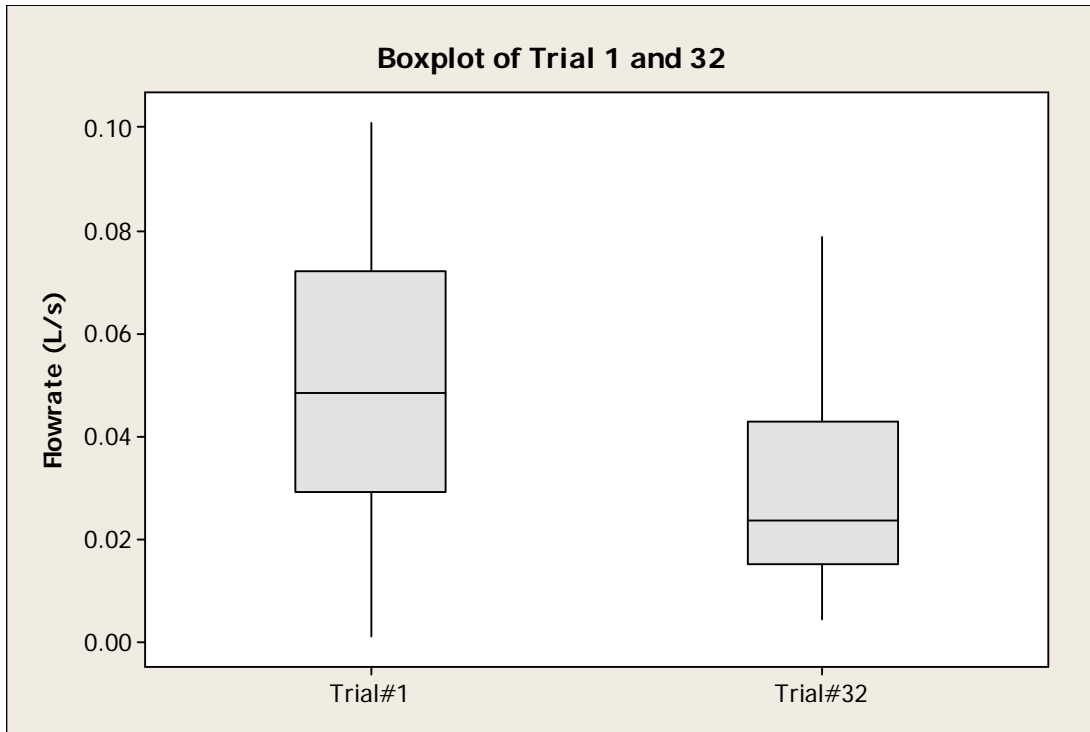


Figure 47. Box and Whisker Plots of Flowrate Data Using Clean Water (Trial#1) and Dirt Water (Trial#32) for Particulate Clogging Tests.

4.6.4 Statistical Analyses for SmartDrain™ Clogging Tests

Statistical analyses were conducted to determine the effects of particulate loading and head, plus their interactions on the SmartDrain™ flowrate performance. A complete two level and two factors (2^2 , particulate load and head) factorial experiment (Box et al. 1978) was conducted to examine the effects of those factors, plus their interactions on the SmartDrain™ flowrates. The factors studied, and their low (-1) and high values (+1) used in the calculations, are shown in Table 24. The complete data set used in this factorial study is also summarized in Table 25. Experiments were performed in replicates of 3 for each flow rate. Statistical methods were used to summarize the data and to provide an empirical method to analyze factor interactions on the SmartDrain™ flowrate.

Table 24. Experimental Factors and their Levels.

Variable	Low value (-1)	High value (+1)
Particulate loading, W (kg/m ²)	0 kg/m ²	32 kg/m ²
Head, H (inches, cm)	14 (36 cm)	44.5 (113 cm)

An analysis of variance (ANOVA) table was constructed to identify the significant factors and their interactions needed to best predict SmartDrain™ flow performance. Statistical hypothesis tests using a p-value of 0.05 (95% confidence) were used to determine whether the observed data were statistically significantly different from the null hypothesis.

Table 25. Flowrate Data Used in Full 2² Factorial Designs

Condition	Particulate loading	Head		Log (Q), L/s
	(W)	(H)	WH	
1A	-	-	+	-1.5338
1B	-	-	+	-1.5363
1C	-	-	+	-1.5393
2A	-	+	-	-0.9965
2B	-	+	-	-1.0607
2C	-	+	-	-1.0461
3A	+	-	-	-1.7452
3B	+	-	-	-1.7434
3C	+	-	-	-1.7463
4A	+	+	+	-1.1038
4B	+	+	+	-1.1418
4C	+	+	+	-1.1424

Normal probability plots of effects were used to compare the relative magnitudes and the statistical significance of all main and interaction effects. These plots also indicated the direction of the effect. In Figure 48, the main factor head has positive effects because it appear on the right side of the plot, meaning that when the low level changes to the high level of the factor, the flow response increases. Figure 48 shows that head (H) has the largest effect on the measured

flowrates, followed by particulate loading. The results of the factorial analyses are summarized in Table 26.

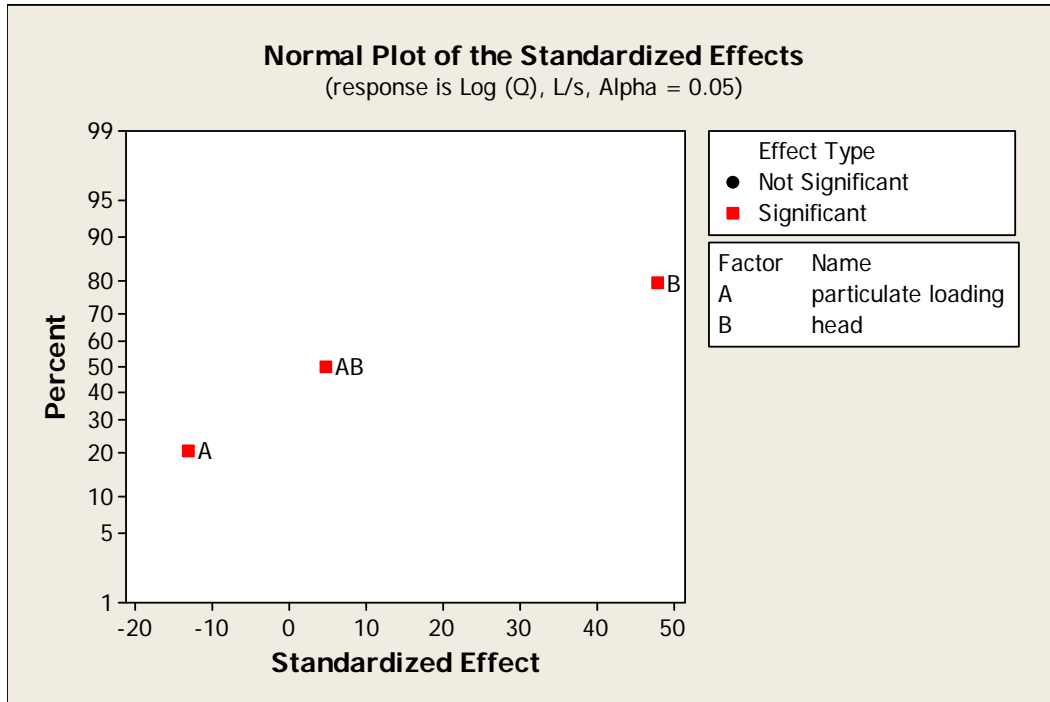


Figure 48. Normal Probability Plots of the Effect

Table 26. Estimated Effects and Coefficients for Q (L/s) (coded units). Estimated Effects and Coefficients for Q (L/s) (coded units)

Term	Effect	Coef	SE Coef	T	P
Constant		-1.361	0.006	-233.600	0.0000
W	-0.152	-0.076	0.006	-13.010	0.0000
H	0.559	0.279	0.006	47.940	0.0000
W*H	0.057	0.028	0.006	4.870	0.0010

S = 0.0202 press = 0.0073
R-sq = 99.68% R-sq(pred) = 99.28% R-sq(adj) = 99.56%
W- Particulate loading and H-head

Table 27 indicates that observation 4 is unusual because its standardized residual is greater than 2. This could indicate that the observation is an error.

Table 27. Unusual Observations for Q (L/s)

Obs	StdOrder	Log (Q), (L/s)	Fit	SE Fit	Residual	St Resid
4	4	-0.9965	-1.0344	0.0117	0.03793	2.30R

Figure 49 shows a decrease in flowrates occurred with increases in particulate loading. However, much larger increases in flowrates were observed with increases in head.

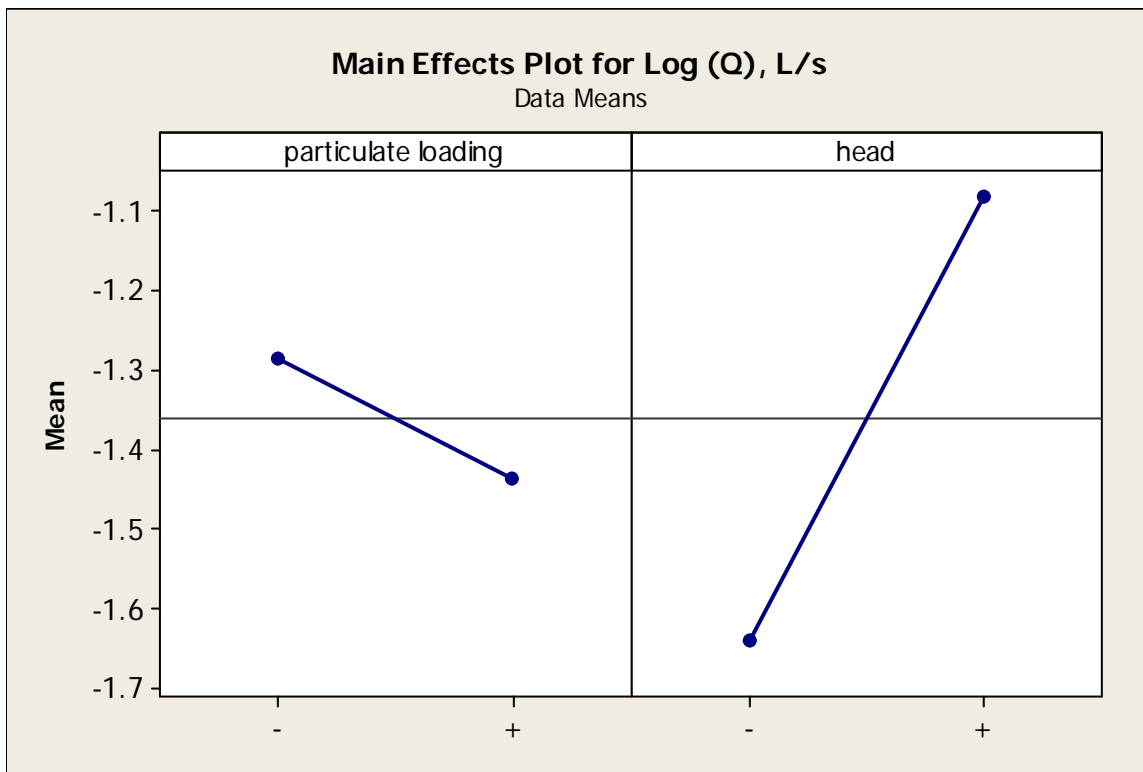


Figure 49. Main Effect Plots for SmartDrain™ Flowrate.

Figure 50 depicts interaction plots which are used to interpret significant interactions between the factors. In the plot, the line for particulate loading vs. head is approximately parallel,

indicating an apparent lack of interaction between the two factors. These interaction plots suggest that mutual interactions between these factors have negligible effects on the flowrate.

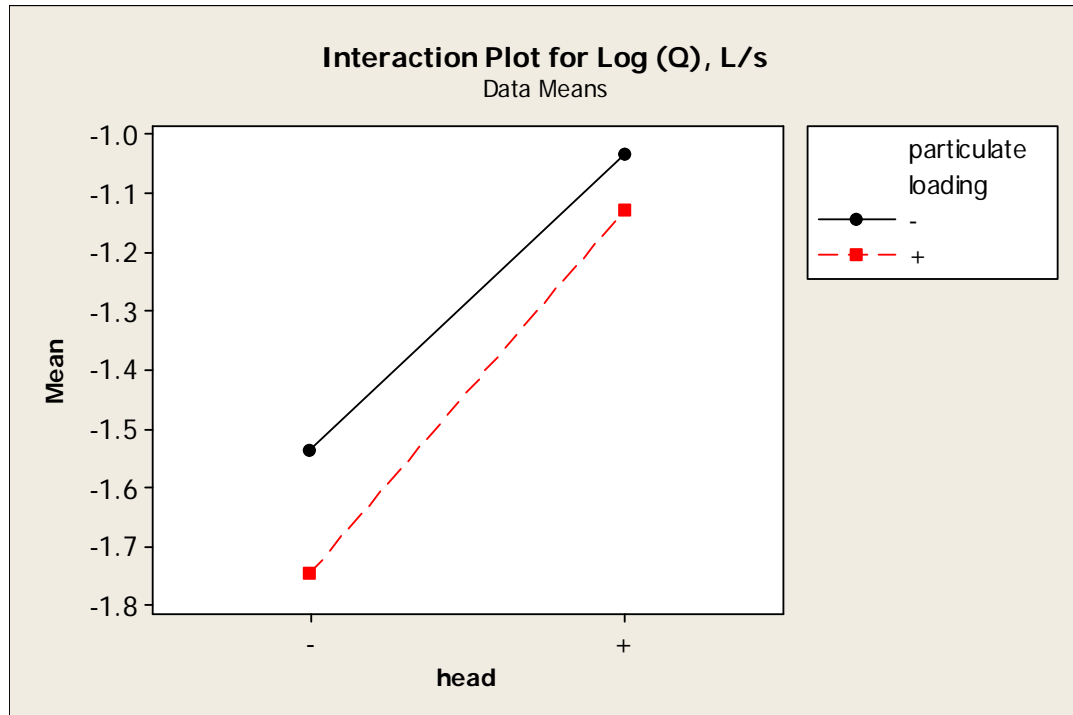


Figure 50. Interaction Plots for SmartDrain™ Flowrate.

4.6.5 Model Fitting for Clogging Tests

The effects and half-effects of the significant factors (main effects and interactions) were used to predict the SmartDrain™ flowrate performance. Table 28 shows the matrix (table of contrasts) representing factors (particulate loading and head) and their interactions. The results of the effects and half-effects are also shown in Table 28.

Table 28. Effects and Half-Effects Results.

Case	Particulate loading		Water depth		Log (Q), L/s
	W	H	WH		
1	-	-	+		-1.536468
2	-	+	-		-1.034438
3	+	-	-		-1.744969
4	+	+	+		-1.129319
				Y (grand)	-1.3612985
Avg. Y@-1	-1.285	-1.641	-1.390		
Avg. Y@+1	-1.437	-1.082	-1.333		
Δ	-0.152	0.559	0.057		
$\Delta/2$	-0.076	0.279	0.028		

As noted previously, the significant factors that affect the responses are particulate loading and head. Those factors have to be included in the prediction equation. The prediction equation can be written in terms of the grand mean and half-effects, excluding the non-significant factors.

$$\hat{y} = \bar{y} + \left(\frac{\Delta_W}{2}\right)W + \left(\frac{\Delta_H}{2}\right)H$$

- where:
- \hat{y} = predicted response (Ypred)
 - \bar{y} = grand mean (Ygrand)
 - $\frac{\Delta}{2}$ = half-effects of each factor or interaction
 - W = particulate loading
 - H = head (in)

The final prediction equation is given as:

$$\widehat{\log(y)} = -1.3613 - 0.076W + 0.28H + 0.028WH$$

A summary of statistical information about the model is also shown in Table 29. R^2 is a statistical measure of goodness of fit of a model whereas the adjusted R^2 is a statistic that is adjusted for the number of explanatory terms in a model. The value of R^2 and adjusted R^2 for the model are 99.68% and 99.56% respectively. Predicted R^2 is calculated from the PRESS

(Prediction Error Sum of Squares) statistic. The predicted R^2 statistic is computed to be 99.28%. Larger values of predicted R^2 suggest models of greater predictive ability. This indicates that the model is expected to explain about 99.28% of the variability in new data. Figure 51 shows a scatterplot of the observed and fitted Log (Q) values, indicating very good fits of the observed with the predicted Q (L/s) values over a wide range of conditions.

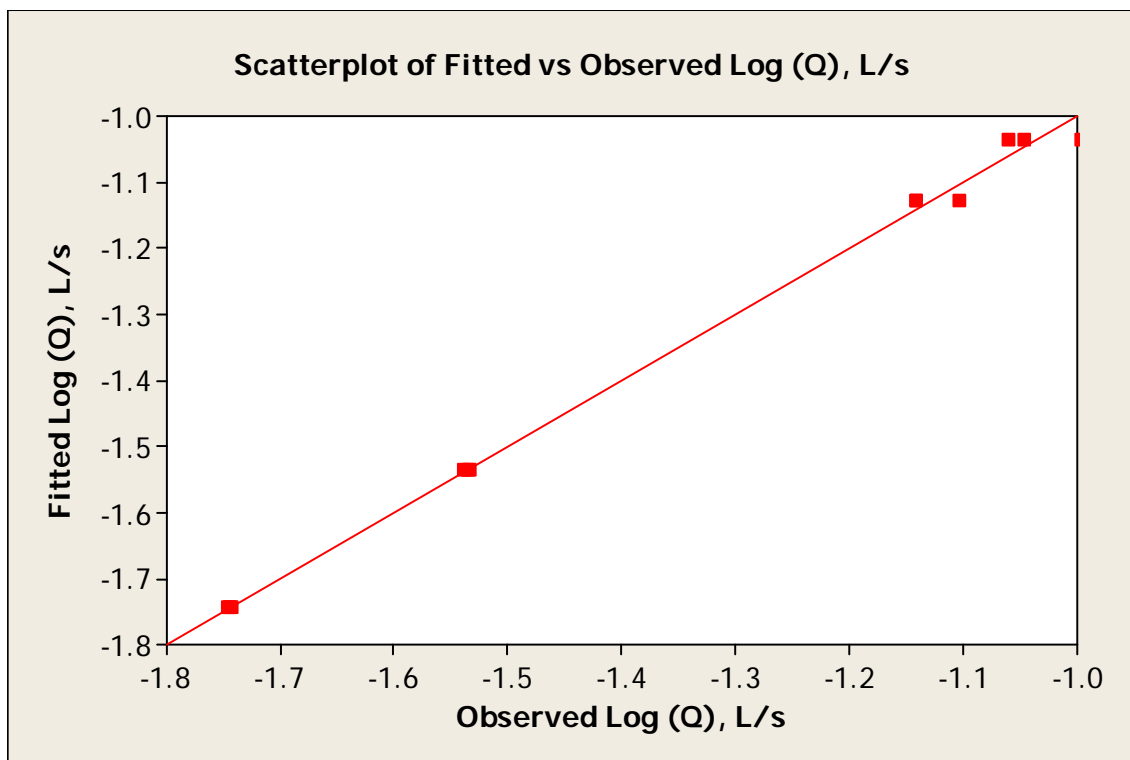


Figure 51. Scatter Plot of Observed vs. Fitted Flowrate (L/s)

The normal probability plot of the residuals shown in Figure 52 shows that the fitted data are normally distributed (Anderson-Darling test for normality has a p-value greater than 0.05, so the data are not significantly different from a normal distribution for the number of observations available). The zero mean of the residuals assumption was checked by examining the descriptive

statistics and graphs of the residuals vs. fitted values and vs. the order of the observations. To determine if the residuals were independent of each other, graphs of the residuals vs. observation number were also examined.

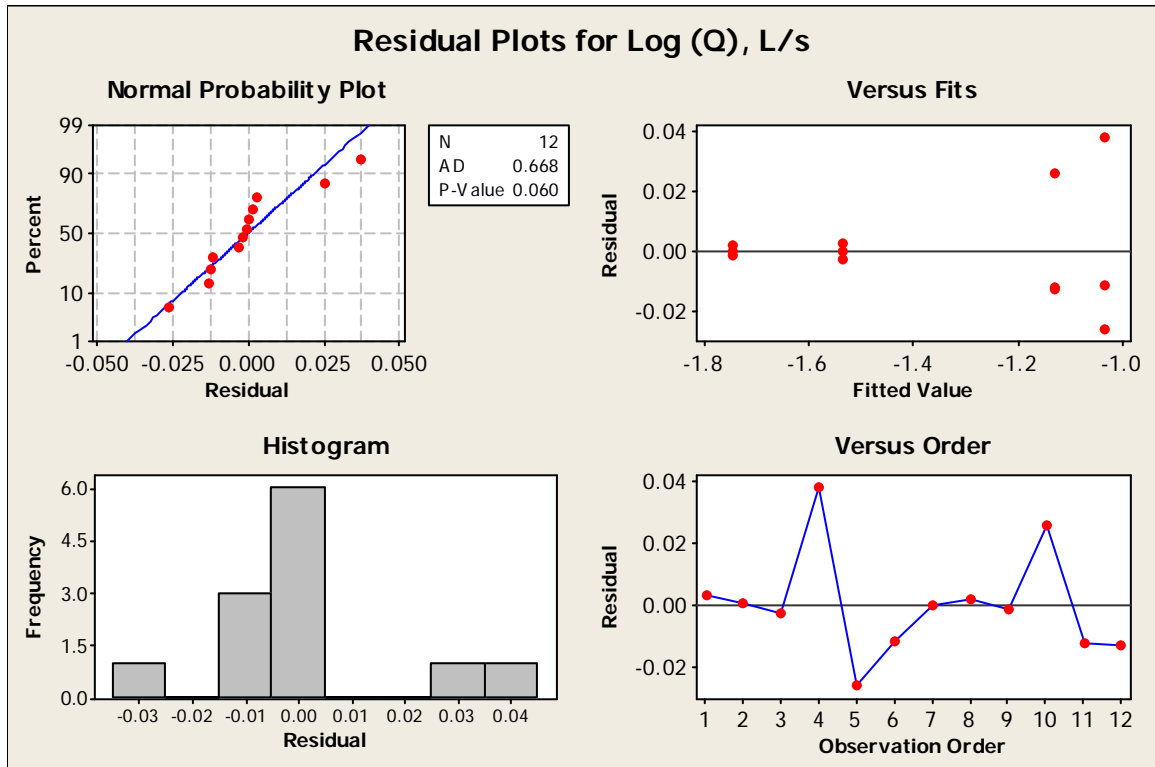


Figure 52. Residuals Analysis Plot

The examination of the residual values vs. fitted values of the data indicated that there was a greater spread in the residuals for the higher fitted values. The model residual histogram was approximately bell shaped; the residuals were normally distributed and had zero mean, and were independent of each other. Model improvements should therefore focus on conditions that had high flowrate conditions.

4.6.6 SmartDrain™ Biofouling Tests

Two-tailed t tests with 95% confidence intervals ($p = 0.05$ level) were performed to assess the significance of differences between flowrate measurements obtained on clean water

(Trial #1) versus dirty “green” water (Trial #7) for the biofouling test. The dirty green water was obtained by adding two different types of green algae and nutrients to the standing water and allowing the mixture to incubate in the summer sun for extended periods. Biofouling trials #1 and #7 were conducted at various algal growth stages in the device, with several weeks between each drainage test. The differences between the two trial groups (clean and dirty green water) were analyzed by comparing their mean flowrates. Table 29 indicates that the p-value is less than 0.05 indicating the two means are significantly different. Figure 53 depicts box and whisker plots of flowrate data using clean water and dirt water.

Table 29. Two-tailed t-test for Clean (Trial#1) vs Dirty Water (Trial#7)

Trial	N	Mean	StDev	SE Mean
1	44	0.0565	0.0363	0.0055
7	17	0.0227	0.0117	0.0028

Difference = μ Q (L/s) Trial #1 - μ Q (L/s) Trial #7

Estimate for difference: 0.03378

95% CI for difference: (0.02145, 0.04611)

T-Test of difference = 0 (vs not =): T-Value = 5.49 P-Value = 0.000 DF = 57

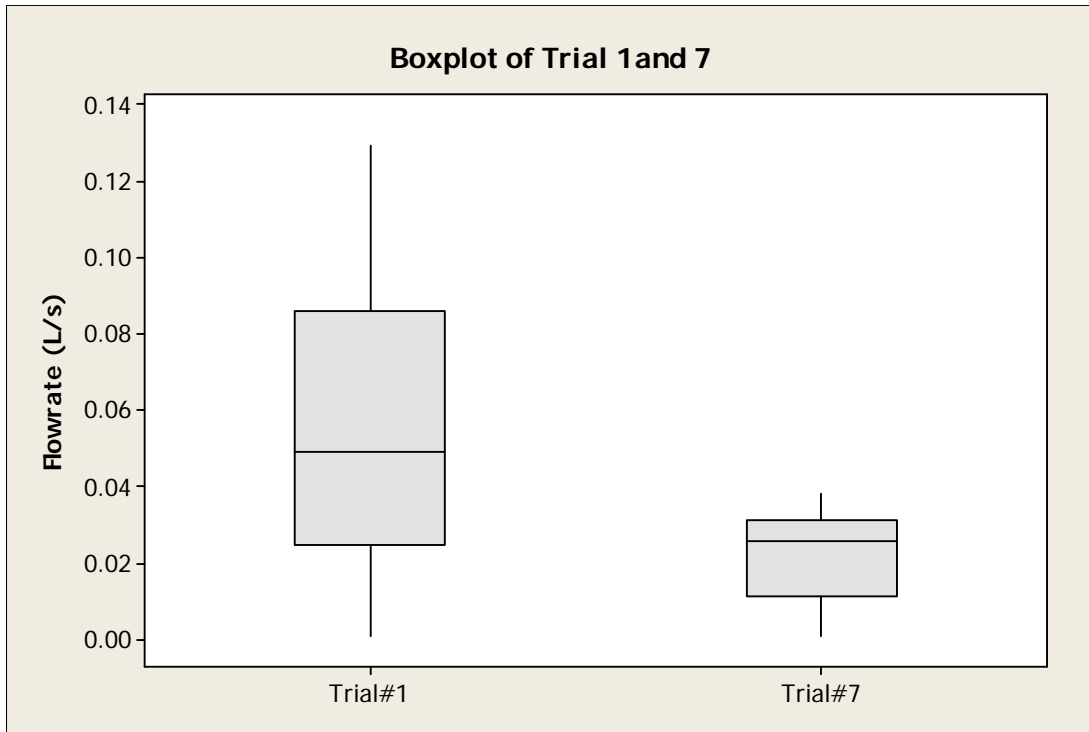


Figure 53. Box and Whisker Plots of Flowrate Data Using Clean Water (Trial#1) and Dirt Water (Trial#32) for Biofouling Tests.

4.6.7 Statistical Analyses for Biofouling Tests

Statistical analyses were conducted to determine the effects of algal loading and head, plus their interactions on the SmartDrain™ flowrate performance. A complete two level and two factors (2^2 , algal loading and head) factorial experiment (Box et al. 1978) was conducted to examine the effects of those factors, plus their interactions on the SmartDrain™ flowrates. The factors studied, and their low (-1) and high values (+1) used in the calculations, are shown in Table 30. The complete data set used in this factorial study is also summarized in Table 31. Experiments were performed in replicates of 3 for each flow rate. Statistical methods were used to summarize the data and to provide an empirical method to analyze factor interactions on the SmartDrain™ flowrate.

Table 30. Experimental Factors and their Levels

Variable	Low value (-1)	High value (+1)
Algal loading, L(trial number)	1	7
Head, H (inches)	14	44.5

An analysis of variance (ANOVA) table was constructed to determine the significant factors and their interactions needed to best predict SmartDrain™ flow performance. Statistical hypothesis tests using a p-value of 0.05 (95% confidence) were used to determine whether the observed data were statistically significantly different from the null hypothesis.

Table 31. Flowrate Data Used in Full 2² Factorial Designs

Condition	Algal loading	Head (in)	Log (Q), L/s
1A	-	-	-2.629
1B	-	-	-3.065
1C	-	-	-3.065
2A	-	+	-1.424
2B	-	+	-1.419
2C	-	+	-1.434
3A	+	-	-2.148
3B	+	-	-2.148
3C	+	-	-2.148
4A	+	+	-1.446
4B	+	+	-1.446
4C	+	+	-1.446

Normal probability plots of effects were used to compare the relative magnitudes and the statistical significance of all main and interaction effects. These plots also indicated the direction of the effect. In Figure 54, the main factor head has positive effects because it appear on the right side of the plot, meaning that when the low level changes to the high level of the factor, the flow response increases. Figure 54 shows that head (H) has the largest effect on the measured

flowrates, followed by algal loading. The results of the factorial analyses are summarized in Table 32.

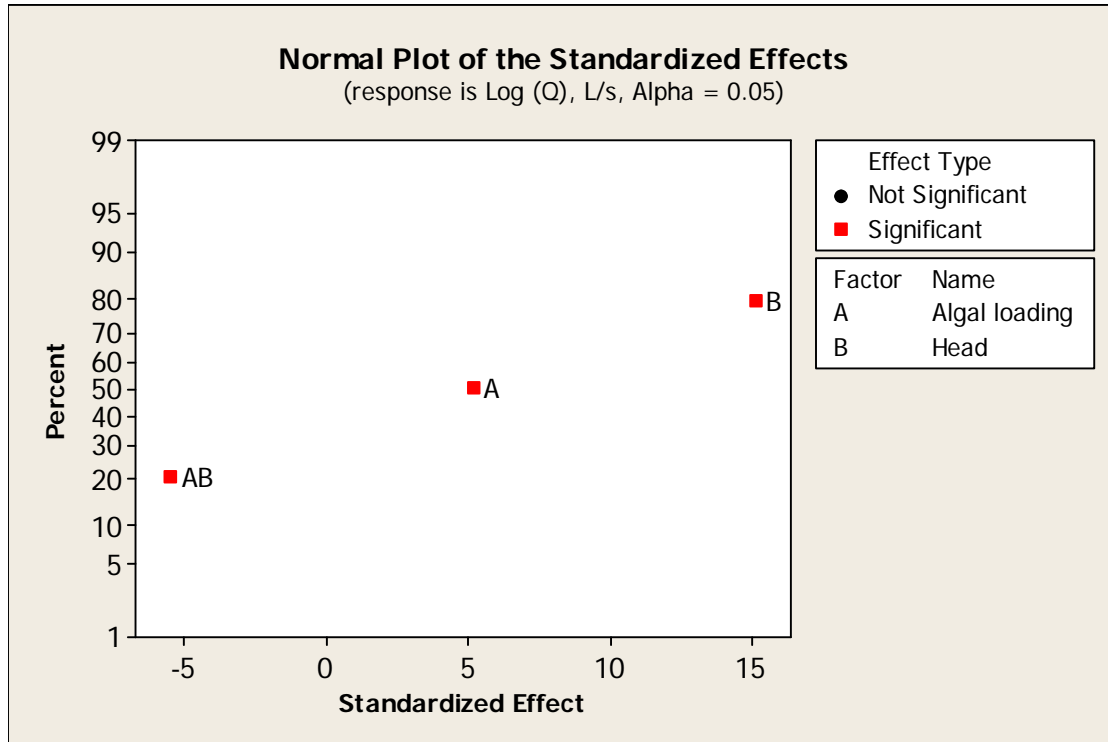


Figure 54. Normal Probability Plots of the Effect

Table 32. Estimated Effects and Coefficients for Q (L/s) (coded units) for the Biofouling Tests

Term	Effect	Coef	SE Coef	T	P
Constant		-1.985	0.0363	-54.690	0.000
L	0.376	0.188	0.0363	5.180	0.001
H	1.098	0.549	0.0363	15.130	0.000
L*H	-0.396	-0.198	0.0363	-5.460	0.001

S = 0.126

PRESS = 0.2844

R-Sq = 97.27%

R-Sq(pred) = 93.87%

R-Sq(adj) = 96.25%

L-algal loading and H-head

Table 33 indicates that observation 1 is unusual observation because its standardized residual is greater than 2. This could indicate that the observation is in error.

Table 33. Unusual Observations for Q (L/s)

Obs	StdOrder	Log (Q) ,L/s	Fit	SE Fit	Residual	St Resid
1	1	-2.62931	-2.9195	0.07257	0.29016	2.83R

4.6.8 Model Fitting for Biofouling Tests

The effects and half-effects of the significant factors (main effects and interactions) were used to predict the SmartDrain™ flowrate performance. Table 34 shows the matrix (table of contrasts) representing factors (algal loading and head) and their interactions. The results of the effects and half-effect are also shown in the table 34.

Table 34. Effects and Half-Effects Results.

Case	Algal loading		Head		Q (L/s)
	L	H	LH		
1	-	-	+		-2.9195
2	-	+	-		-1.4256
3	+	-	-		-2.1475
4	+	+	+		-1.4458
Y(grand) = -1.9846					
Avg. Y@-1	-2.173	-2.533	-1.787		
Avg. Y@+1	-1.797	-1.436	-2.183		
Δ	0.376	1.098	-0.396		
Δ/2	0.188	0.549	-0.198		

As noted previously, the significant factors that affect the responses are head, algal loading, and interactions of head and algal loading. Those factors have to be included in the prediction

equation. The prediction equation can be written in terms of the grand mean and half-effects, excluding the non-significant factors.

$$\hat{y} = \bar{y} + \left(\frac{\Delta_L}{2}\right)L + \left(\frac{\Delta_H}{2}\right)H + \left(\frac{\Delta_{HL}}{2}\right)LH$$

where: \hat{y} = predicted response (Ypred)

\bar{y} = grand mean (Y grand)

$\frac{\Delta}{2}$ = half-effects of each factor or interaction

L = algal loading

H = head (in)

The final prediction equation is given as:

$$\widehat{\log(y)} = -1.985 + 0.2L + 0.55H - 0.2LH$$

A summary of statistical information about the model is also shown in Table 32. R^2 is a statistical measure of goodness of fit of a model whereas the adjusted R^2 is a statistic that is adjusted for the number of explanatory terms in a model. The value of R^2 and adjusted R^2 for the model are 97.27% and 96.25% respectively. Predicted R^2 is calculated from the PRESS (Prediction Error Sum of Squares) statistic. The predicted R^2 statistic is computed to be 93.87%. Larger values of predicted R^2 suggest models of greater predictive ability. This indicates that the model is expected to explain about 93.87% of the variability in new data. Figure 55 shows a scatterplot of the observed and fitted Q (L/s) values, indicating very good fits of the observed with the predicted Q (L/s) values over a wide range of conditions.

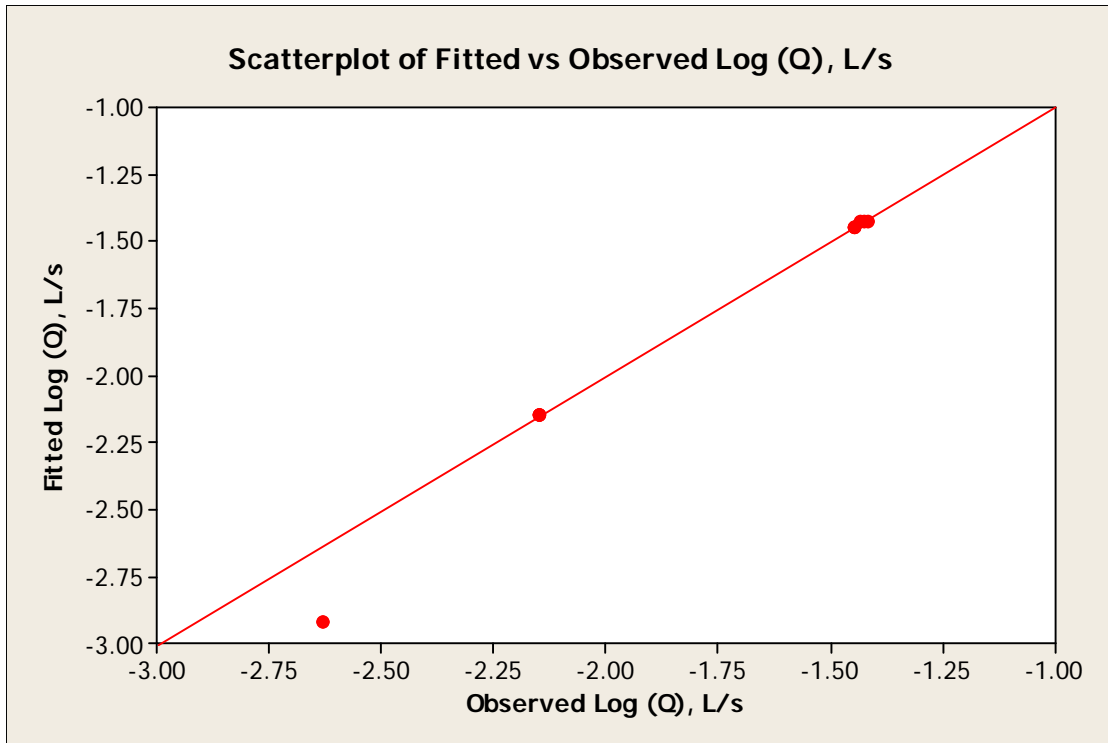


Figure 55. Scatter Plot of Observed vs Fitted Flowrate (L/s)

The normal probability plot of the residuals shown in Figure 56 shows that the fitted data are normally distributed (Anderson-Darling test for normality has a p-value greater than 0.05, so the data are not significantly different from a normal distribution for the number of observations available).

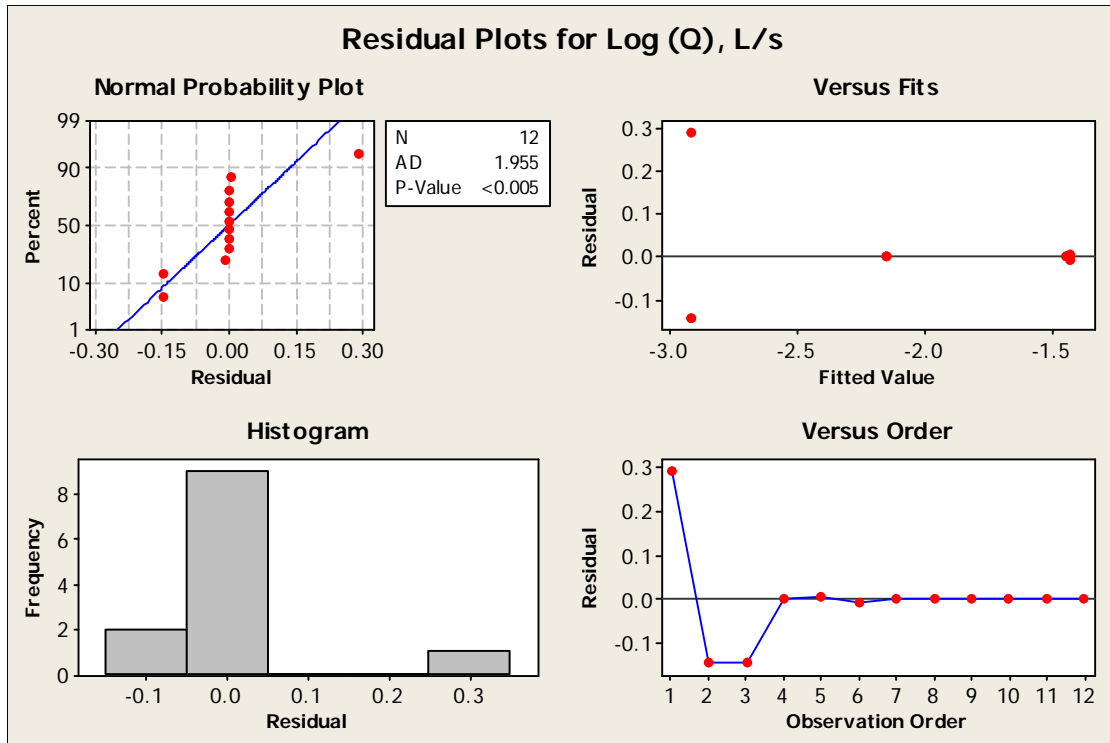


Figure 56. Residuals Analysis Plot

The examination of the residual values vs. fitted values of the data indicated that there was a greater spread in the residuals for the lower fitted values. The model residual histogram was approximately bell shaped; the residuals were normally distributed and had zero mean, and were independent of each other. Model improvements should therefore focus on conditions that had high flowrate conditions.

4.7 Chapter Summary

Material flow capacity and clogging potential tests, after excessive loadings by fine ground silica particulates and biofouling experiments indicated the SmartDrainsTM have minimal clogging potential while also providing very low discharge rates (preferred to encourage natural infiltration and to increase contact time with the media). SmartDrainsTM also reduce the surface

ponding time compared to no underdrains, while minimizing short-circuiting of the infiltration water. They also provide a substantial residence time in the media to optimize contaminant removal and also provide significant retention of the stormwater before being discharged to a combined sewer system. In addition, this slow drainage time encourages infiltration into the native underlying soil, with minimal short-circuiting to the underdrain.

Design guidance was developed to determine the number of SmartDrains required for different biofilter basin areas ranging from 100 to 10,000 ft² and with saturated conductivities (K_s) of the facility media ranging from 30 to 100 in/hr (recommend K_s ranges for filter sand used in SmartDrain™ field application). In contrast, typical K_s values for conventional underdrains range from 10 to 500 in/hr. The biofilter facility examined for these calculations has a 2 ft engineered soil layer, 1 ft medium to coarse sand layer, and a maximum ponding depth of 1.5 ft, as shown in Figure 57. The porosity of the engineered media and drainage layers are 0.44 and 0.3, respectively.

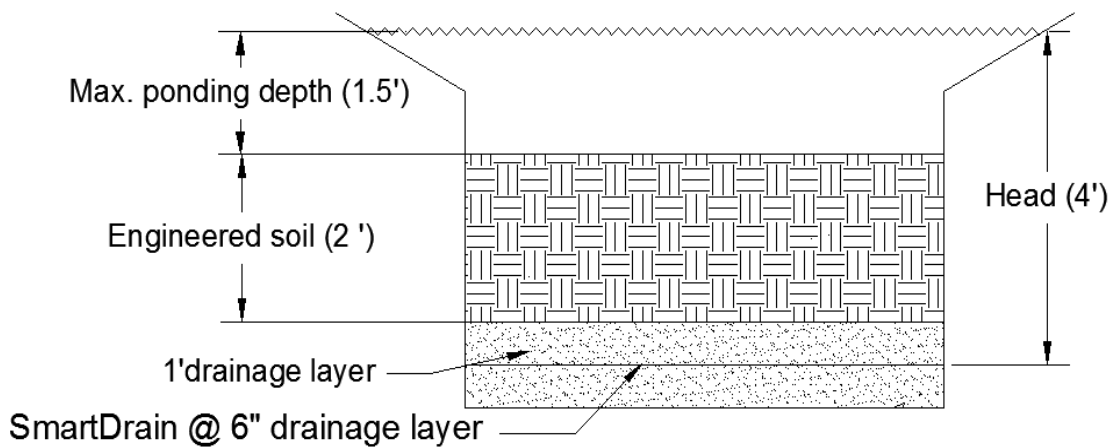


Figure 57. Cross-Section of a Typical Biofilter Facility

Figure 58 shows three dimensional plots of the required number of SmartDrain or conventional underdrains required for different biofilter sizes and saturated hydraulic conductivities. For low values of hydraulic conductivities of the media, the number of SmartDrain or conventional underdrains required in the field increases, as expected. Detailed design example calculations are attached in Appendix A.61 through A.66. These plots consider the number of underdrains needed for the basic infiltration rates of the devices, ensuring that the underdrains can carry away the infiltration water within the 24 or 72 hour time periods, and the spacing of the underdrains to insure that the water can reach the underdrains within the stated time, as shown in the basic equations earlier in the chapter.

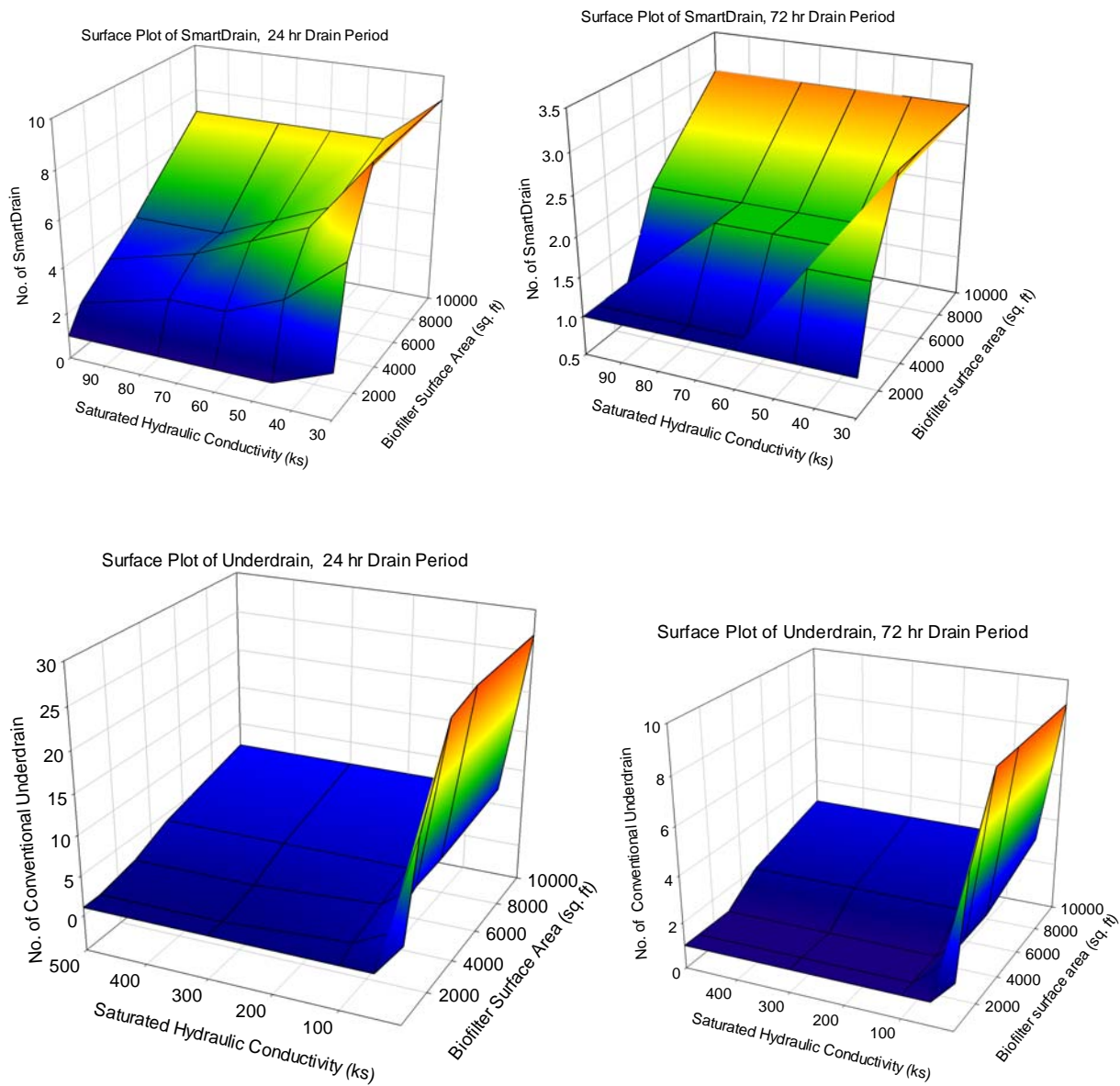


Figure 58. Three Dimensional Plots of No. of SmartDrains or Conventional Underdrains Required for Different Biofilter Area and Saturated Hydraulic Conductivities.

CHAPTER 5

5. ASSESSING THE IMPACT OF SOIL MEDIA CHARACTERISTICS ON STORMWATER BIOFILTRATION DEVICE PERFORMANCE

5.1 Introduction

Biofiltration devices are a potentially effective option for the treatment and disposal of stormwater runoff from urban areas. However, the performance of these systems, and other infiltration devices, are affected by factors such as texture, structure, and degree of compaction of the media during their construction. The effectiveness of a biofilter is commonly reduced through clogging of the media, through short-circuiting of infiltrating water through an underdrain, or by short resident/contact times of the stormwater in the treatment media. Vegetation in biofilters helps retain captured sediment and other pollutant, maintain infiltration capacity, and provides some bacteriological degradation opportunities in the root zone.

The infiltration rate is the rate at which water enters the soil at the surface. The rate of infiltration depends on a number of factors, including the condition of the soil surface and its vegetative cover, the properties of the soil, such as its porosity and hydraulic conductivity, and the current moisture content of the soil (Chow et al. 1988). The infiltration rate in a soil typically decreases during periods of rainfall as the soil becomes saturated. Infiltration practices have the greatest runoff volume reduction capability of any stormwater practice and are suitable for use in residential and other urban areas where measured soil infiltration rates are suitable. Many guidance manuals specify acceptable minimum infiltration rates, such as 0.5 in/hr (1 cm/hr) (VA DCR, 2010). Soil compaction that occurs in stormwater treatment facilities during construction

(or improper use) can cause significant reductions in infiltration capacities of the soils. Pitt et al. (2008) noted large detrimental effects of compaction on infiltration rates in both sandy and clayey soils. Infiltration rates were reduced to near zero values in soils having even small amounts of clay, if compacted. Large reductions in the infiltration rates in sandy soils with compaction were also reported, but several inches per hour rates were usually still observed, even with severe compaction (down from tens of inches per hour if uncompacted).

Laboratory and field-scale studies were conducted to provide insight on media characteristics of a biofilter facility located in Tuscaloosa, AL. Double ring infiltrometer tests and soil compaction measurements were conducted along a large biofilter to determine the in-situ characteristics of the media. In-situ soil density measurements were also taken in the same locations of the infiltration measurements. Infiltration measurements were also made during rain events. The effects of different compaction levels on the infiltration rates through the soil media were also examined during controlled laboratory column tests, along with benefits associated with adding different amounts of sand to the media mixture. Three levels of compaction were used to modify the density of the column media/sand samples during the tests: hand compaction, standard proctor compaction, and modified proctor compaction. Figure 59 shows the flow chart for this field and lab infiltration study of this biofiltration facility.

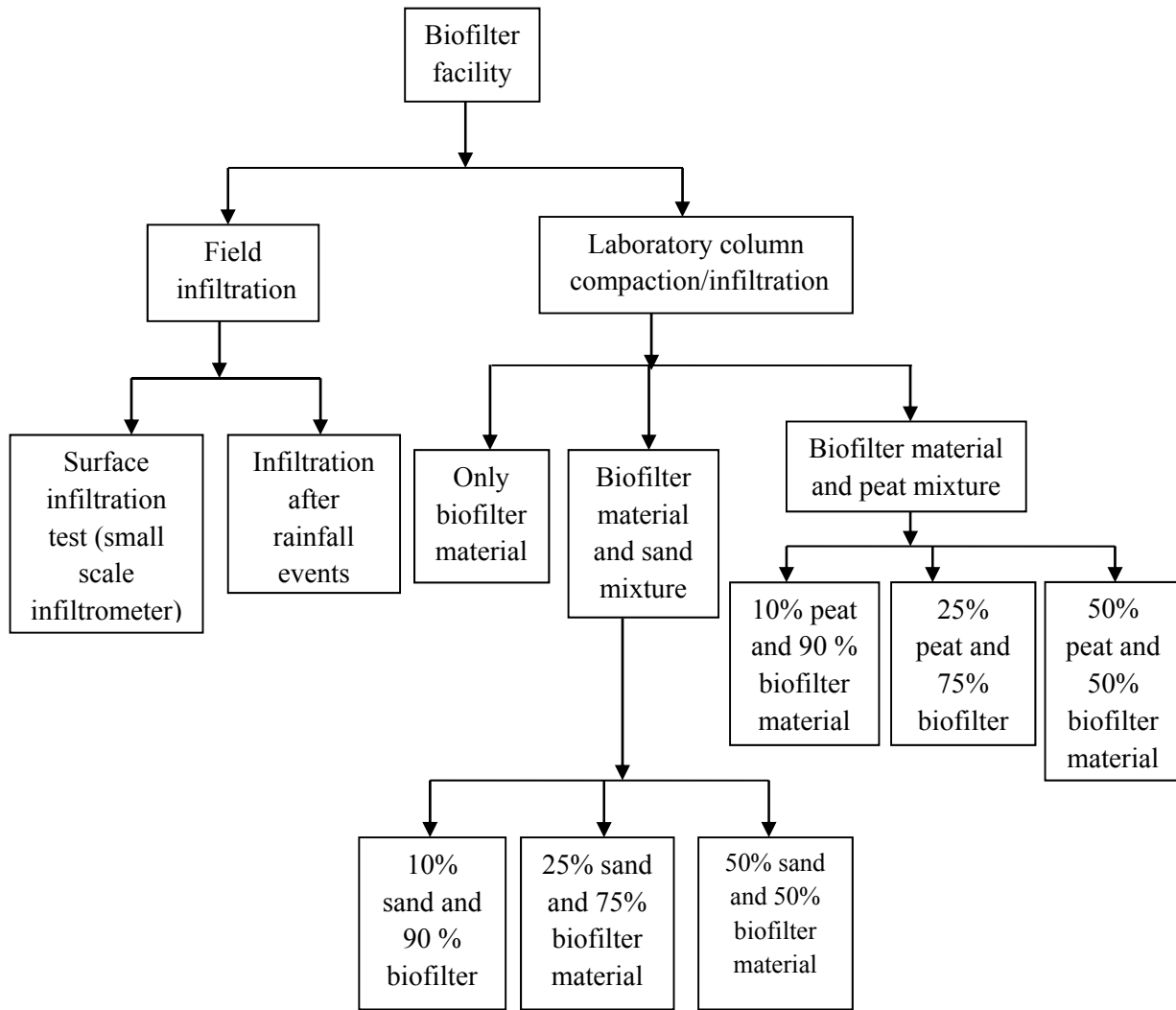


Figure 59. Flowsheet for the Field and Lab Infiltration Study at a Biofilter Facility.

5.2 Description of Test Site and Methodology

5.2.1 Description of Test Site

The biofilter facility selected for this study is about 300 ft (90 m) long and 30 ft (9 m) wide, being about 11% of the contributing paved and roofed source areas (7.8% of the total drainage area, including landscaped area). It is located in Shelby Park, adjacent to The University of Alabama, Tuscaloosa, rental car parking lot, from which it receives flow. The drainage area and land use for the study area are shown in Table 35

Table 35. Drainage Area and Land Use Breakdown

Drainage area	Area(ft ²)	Area(acre)	Land use (percent)
Paved vehicle parking area	65,250	1.50	55.6
Landscaped area	34,240	0.79	29.2
Roof area	17,860	0.41	15.2
Total	117,350	2.70	100

The biofilter receives flow from the rental car parking lot, driveways, and small landscaped areas. The 0.2 acre biofilter failed to function as expected soon after construction, with extended periods of standing water after rains and poorly established vegetation. The total drainage area tributary to the biofilter was approximately 2.7 acres. Figure 60 shows the location of the biofilter and Figure 61 are photographs of the drainage area tributary to the biofilter. The runoff sources within the drainage area were the University fleet maintenance and rental car service area. Runoff pollutants are expected to include bacteria, sediments and nutrients from the landscaped area, a variety of materials from the parked cars, possibly including oil and grease, metals, and spilled or leaked vehicle fluids, and zinc from the galvanized metal buildings. There

is no deicing chemical use at the site as the winters are generally mild with only rare snow or ice in the region. There were no other stormwater control practices at the site, except for the large biofilter.



Figure 60. Aerial Photograph of Biofilter Location (Map by Google Map).



Grass turf area in excellent condition



Disconnected roof from painted galvanized steel building draining to turf area.



Parking area



Parking lot edge and eroding soil

Figure 61. Drainage Areas Photographs Tributary to the Biofilter.

5.2.2 Field Infiltration Study at Biofiltration Facility

Turf-Tec Infiltrometers (Turf Tec 1989) were used to measure the infiltration rates at 12 test locations along the biofilter. These small devices have an inner chamber about 2.5 inches (64 mm) in diameter and an outer ring about 4.5 inches (110 mm) in diameter. The infiltrometers were gently pushed into the surface of the biofilter soil (having poor vegetation cover) until the “saturn” ring was against the soil surface (Figure 62). Relatively flat areas were selected in the biofilter to install the Turf-Tec infiltrometers and small obstacles such as stones and twigs were removed. Three infiltrometers were inserted within about 3 ft (1 m) from each other to measure the variability of the infiltration rates of the soil media in close proximity. Four clusters of three infiltrometer tests were conducted along the biofilter to examine variations along the biofilter length. After the soil was inspected and sealed around each ring to make sure that it was even and smooth, clean water was poured into the inner chamber and allowed to overflow and fill up the outer ring. The declining water level in the inner chamber were recorded during a period of one to two hours until the infiltration rates become constant.



Figure 62. Photographs Showing the Infiltration Measurement Setup and In-Situ Soil Density Measurements at Shelby Park Biofilter.

The rate of decline in the water level (corresponding to the infiltration rate) was measured by starting the timer immediately when the water was poured in the inner chamber, when pointer reached the beginning of the depth scale (Figure 63). Additional water was periodically added to the inner chamber and outer ring when the level in the inner chamber dropped to within about an inch of the ground surface to maintain pooled water. The change in water level and elapsed time were recorded since the beginning of the first measurement. The measurements were taken every five minutes at the beginning of the test and less frequently as the test progressed until the rate of infiltration was considered constant. The infiltration rate was calculated from the rate of fall of the water level in the inner chamber.



Figure 63. A Close Up of Turf-Tec Infiltrometer (available from Turf-Tec International)

<http://www.turf-tec.com/Instructions/IN2-W-Instructions.pdf>

5.2.3 Water Content and Density Measurements of the Soil Media

In-situ soil density measurements were also taken in the same general locations as the infiltration measurements. A small hole, about six inches (15 cm) deep and six inches (15 cm) wide, was carefully hand dug to avoid disturbance of the soil. The hole's side and bottom were also carefully smoothed. All of the soil excavated from each hole was placed into separate Ziploc plastic bags to retain soil moisture. Sand was then poured into the hole from a graduated cylinder to measure the volume of the holes, up to the top of the soil that was removed from the test hole in the biofilter. The excavated soil media was then transported to The University of Alabama environmental lab for further analyses. The soil media was weighed moist, dried at 105°C, and weighed again when dry. The dry density and moisture content (percent) of the soil media collected from each test locations were determined, as shown in Table 36. The density of the soil was determined by dividing the mass of oven-dried soil by the sand volume used to re-fill the hole. The soil moisture content (%) was determined by the ratio of the difference between the moist and the dry weights of the soil (corresponding to the water mass) to the mass of the oven-dried soil. The particle size distributions of the soil media excavated from the surface of the biofilter (determined using standard sieving procedures) are shown in Figure 64, and the median size and uniformity coefficient (the ratio of the 60th to the 10th percentile particle sizes) are also shown on Table 36 for the four test soil media samples.

Table 36. Soil Media Characteristics Obtained from Four Locations along the Biofilter.

Test locations	median size D ₅₀ (mm)	uniformity coefficient (C _u)	dry density (g/cm ³)	Moisture content (%)
1	3.0	38	2.18	9.2
2	0.5	17	2.32	5.6
3	0.3	5.6	1.80	8.0
4	0.7	12.5*	2.05	8.2

*estimated value as the 10th percentile particle size could not be reliably determined from the psd plot for this sample

According to Auburn’s laboratory tests, the biofilter media was classified as sandy clay loam, with 20% clay and 80% sand (3% organic matter content). Therefore, there is very little “bio” in this biofilter, indicating compacted media having adverse affects on plant growth.

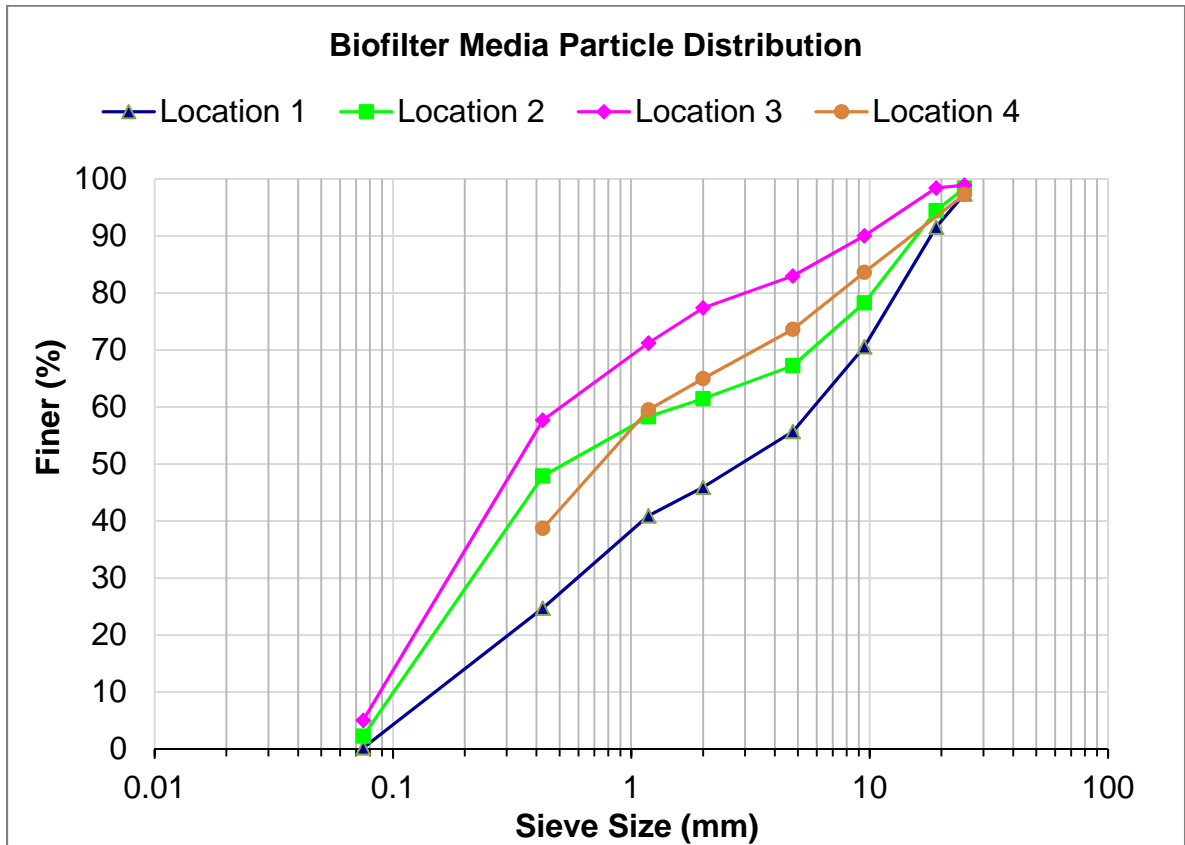


Figure 64. Particle Size Distributions for the Biofilter Media from Four Locations along the Biofilter.

5.2.4 Plant Nutrients

Soils vary greatly in water-holding capacity and infiltration rate. Silt, clay soils and those high in organic matter can hold much more water than sandy soils. Soils with high water-holding capacities require less frequent irrigation than soils with low water-holding capacities (Vegetable Crop Handbook 2010). Water should not be applied to soils at a rate greater than the holding

capacity base rate at which soils can absorb water. Recent research (Vegetable Crop Handbook 2010) indicates that maintaining soil moisture levels in a narrow range, just slightly below field capacity (75 to 90 % available soil moisture), maximizes crop growth.

Plants can contribute to treatment efficiency in biofilters both directly, through plant uptake and maintenance of soil porosity, as well as indirectly, through influence on soil microbial communities (Read et al. 2008; Hsieh and Davis 2005; Henderson et al. 2007a; Hatt et al. 2009). However, variations in pollutant removal (including metals) among plant species were noted (Read et al. 2008 and Henderson et al. 2007b). The choice of vegetation for biofilters should not only be based on their treatment performance, but also on their capacity to survive in potentially stressful growth conditions, such as drought periods and periodically inundation.

Soil test analyses results typically indicate whether a nutrient level in the soil is low, medium (moderate) or high (adequate). The nutrient rating depends on the soil group and the crop. Samples of the biofilter media were analyzed by the soil laboratory at Auburn University for selected nutrients and other basic characteristics. The biofilter media was classified as sandy clay loam, with 20% clay and 80% sand (3% organic matter content). According to the UA laboratory tests, the median size of the samples ranged from 300 to 3,000 μm , and *in-situ* density measurements indicated surface dry density values of about 2 g/cc, corresponding to severely compacted conditions (close to “modified” compaction conditions for this media). Poor vegetation growth also indicated compacted conditions, as indicated on Table 37. The soil analysis reports are summarized in Table 38.

High bulk density is an indicator of low soil porosity and compaction (USDA 2008). Densely compacted soil causes restrictions to root growth, and poor movement of air and water through the soil. Compaction can result in shallow plant rooting and restricted plant growth,

influencing crop yield and reducing vegetative cover available to protect soil from erosion.

Compacted media also has adverse affects on plant growth. Table 37 indicates that a bulk density value of sandy soil greater than 1.8 g/cm³ restricts root growth. The bulk density values of the biofilter soil (sandy clay loam) obtained from four locations along the biofilter surface have an average value of 2 g/cm³ (greater than the critical 1.8 g/cm³ value that affects plant growth) indicating very compacted media having adverse affects on plant growth. Very little “bio” in Shelby Park biofilter facility, indicating compacted media having adverse affects on plant growth.

Table 37. General Relationship of Soil Bulk Density to Root Growth on Soil Texture (USDA 2008).

Soil Texture	Ideal bulk densities for plant growth (g/cm ³)	Bulk densities that restrict toot growth (g/cm ³)
Sandy	<1.60	>1.80
Silty	<1.40	>1.65
Clayey	<1.10	>1.47

Table 38. Summary of the Soil Nutrient Report for Shelby Park Biofilter Media (single composite analysis from four subsamples).

Nutrient	ppm	Nutrient	ppm
Calcium (Ca)	525	Copper (Cu)	<0.1
Potassium (K)	30	Iron (Fe)	34
Magnesium (Mg)	137	Manganese (Mn)	31
Phosphorus (P)	12	Molybdenum (Mo)	<0.1
Aluminum (Al)	70	Sodium (Na)	31
Arsenic (As)	<0.1	Nickel (Ni)	<0.1
Boron (B)	0.2	Lead (Pb)	1
Barium (Ba)	9	Zinc (Zn)	6
Cadmium (Cd)	<0.1	Total Phosphorus (P)	149
Chromium (Cr)	<0.1		
Nutrient		percent	
Nitrogen (N)		0.06	
Carbon (C)		1.79	
Organic Matter (OM)		3.1	
Sodium Adsorption Ratio (SAR)		0.3	
pH		6.81	
H ₂ O availability (cm ³ /cm ³)		0.08	
Cation Exchange Capacity (CEC) (meq/100g)		4	

Auburn University’s Soil Testing Laboratory uses the critical soil test concentrations concept defined by the Soil Science Society of America where the critical concentration occurs when 95% of the maximum relative yield is achieved. Concentrations below the critical concentration are rated medium, low or very low, and fertilizers are generally recommended for that nutrient. Values above the critical concentration are rated high, very high, or extremely high and no fertilizer is generally recommended. The cutoff between a medium and high level is sometimes referred to as a ‘critical level’ and provides a value that indicates when fertilizer should (below critical level) or should not (above critical level) be added. The critical soil test

values as used by the Auburn University Soil Testing Laboratory vary from soil to soil and from crop to crop as shown in Table 39. As a general rule, no increased yield response is expected to a nutrient above its critical value.

Table 39. Critical Soil Test Values Used by the Auburn University Soil Testing Laboratory (Adams et al 1994).

Crop	Soil Group			
	1 Sandy soils (CEC 0-0.6)	2 Loam (CEC 0-0.6)	3 Clayey soils of Limestone Valleys & High org. matter soils(CEC 9.0+)-	4 Clays of Black Belt (CEC 9.0+)
Extractable P (ppm)				
P LEVEL 1. Peanuts, pine trees, blueberries & centipede grass	9.5	9.5	5.5	13.5
P LEVEL 2. All other crops	25	25	15	36
Extractable K (ppm)				
k LEVEL 1. Peanuts, pine trees, blueberries & centipede grass	20	30	40	60
k LEVEL 2. Corn, grasses, soybeans, fruits and nuts	40	60	80	95
k LEVEL 3. Cotton, legumes, gardens, lawns, shrubs, vegetables	60	90	120	120
Extractable Mg (ppm)				
All Crops	12.5	25	25	25
Extractable Ca (ppm)				
Peanuts	150	150	150	150
Peanuts, Tomatoes, peppers, fruits & nuts	250	250	250	250

Organic matter (OM) improves soil structure and soil tilth, and helps to provide a favorable medium for plant growth. Soils with large amounts of clay generally require large amounts of organic matter. Soils with a higher organic matter content will have a higher cation exchange capacity (CEC), higher water holding capacity, and better tilth than soils with a lower organic matter content. Soils in the Central Great Plains have organic contents ranging between 1 and 2% for cultivated soils, and about 1.5 to 3.0% for native grasslands (Bowman, 1996). Generally, healthy soil has between 3 and 5% organic material. The organic matter content of the biofilter soil is 3.1% indicating that it is favorable for plant growth.

The cation exchange capacity (CEC) of a soil is a measurement of its ability to bind or hold exchangeable cations. The biofilter soil had a CEC value 4.0 meq/100g and a pH value of 6.8. Typically CEC values, as defined by the Auburn University Soil Testing Laboratory (Mitchell and Huluka, 2011), vary from soil to soil, with sandy soils generally having CEC values ranging from 0 to 4.6 and loam soils having CEC values ranging from 4.6 to 9.0. According to the Alabama Cooperative Extension System, the ideal soil pH value for most crops ranges between 5.8 and 6.5 and for acid loving plants ranges between 5.0 and 5.7. When soil pH is outside of these optimal ranges, nutrients can be less available to plants, potentially resulting in deficiencies.

The biofilter soil had a phosphorus concentration value of 12 ppm. The critical phosphorus concentration for crops (peanuts, pine trees, blueberries and centipedegrass) grown in sandy soil in Alabama is 9.5 ppm, whereas for all other crops, is 25 ppm. The biofilter soil had potassium, magnesium, and calcium concentrations of 30, 137, and 525 ppm respectively. The critical magnesium level for all crops grown in sandy soil in Alabama as used by the Auburn University Soil Testing Laboratory is about 13 ppm, whereas the critical calcium level for crops

such as tomatoes, peppers, fruits and nuts grown in sandy soils is 250 ppm. The biofilter soil had a higher concentration of calcium for most crops grown in sandy and loam soils in Alabama.

Although the six micronutrients: boron (B), zinc (Zn), manganese (Mn), copper (Cu), molybdenum (Mo), iron (Fe), and chloride (Cl) in the soil are as important in plant nutrition as the primary and secondary nutrients, they are needed in much smaller quantities, and most Alabama soils contain adequate amounts for most crops (Adams and Mitchell 2000). Some crops may use between 20 and 200 lbs/acre of N, P, K, Ca, Mg and S, while using less than 1 lbs/acre of the micronutrients. Most Alabama soils have an abundance of minerals containing the micronutrients.

The following is a brief description of the Auburn Soil Testing Laboratory's recommendations for the micronutrient elements. Boron (B) is recommended for cotton, peanuts, clovers grown for seed, alfalfa, cauliflower, broccoli, root crops, apples, pears, and plums. Zinc (Zn) is recommended for corn on sandy soils where the pH is above 6.0 or for the first year after applying lime. It is also recommended for peaches, pecans, apples, and pears. Soil tests showing pH values above 7.0 along with Very High or Extremely High P indicate a probability that Zn deficiency may occur on some soils. Zinc toxicities could occur on sensitive crops such as peanuts where excessive Zn applications have caused high soil Zn levels (> 10 mg/kg extractable Zn) on sandy soils. Maintaining a soil pH above 6.0 may help to reduce Zn toxicity symptoms. Iron (Fe) is a common deficiency for only a few crops (e.g. soybeans) on the high pH soils of the Black Belt and for some specialty plants (e.g. azaleas, centipedegrass, and blueberries) where lime or phosphorus is excessive. Molybdenum (Mo) application to soybeans as a foliar or seed treatment at planting is recommended for all soils of North Alabama and for Black Belt soils. Manganese (Mn) is high in almost all Alabama soils and is not recommended for any crop.

Soybeans grown on sands with poor internal drainage, high organic content, and a pH above 6.0 may show Mn deficiency. Copper and chlorine have not been found to be deficient for any crop on Alabama soils. There is no need to supply these elements in fertilizers in Alabama.

The Sodium Adsorption Ratio (SAR) of a soil is a widely accepted index for characterizing soil sodicity. SAR describes the proportion of sodium to calcium and magnesium in soil solution (Sonon et al 2012). The sodium content of soil affects soil texture and pH. Soils with high concentrations of sodium relative to calcium and magnesium concentrations tend to be dispersed (with very poor drainage) and to have a high pH (Boyd et al. 2002).

Soils with an excess of sodium ions, compared to calcium and magnesium ions, remain in a dispersed condition, and are almost impermeable to rain or applied water. SAR has been documented to be causing premature failures of biofilters in northern communities (Pitt, R. 2011). These failures occur when snowmelt water is allowed to enter a biofilter that has clay in the soil mixture. The largest problem is associated with curb-cut biofilters or parking lot biofilters in areas with snowmelt entering these devices, especially if clay is present in the engineered backfill soil (Pitt, R. 2011). When the SAR rises above 12 to 15, serious physical soil problems arise and plants have difficulty absorbing water (Munshower, 1994). When SAR exceeds 12; soil pH usually will be above 8. The Shelby Park biofilter soil had a SAR value 0.3 and was not a problem.

5.2.5 Biofilter Surface Ponding

During rainfall events, if the runoff rate directed to the biofilter facility is greater than the infiltration capacity of the media in the biofilter, water will pond on the surface. Biofilters are designed with surface ponding storage to hold runoff during short periods of extensive rainfall for later infiltration. In most cases, design guidance restricts ponding to relatively short periods

after rains (such as 24 to 72 hrs) to minimize nuisance insect problems. Extended periods of surface ponding (several days) of water on the Shelby Park biofilter was often observed following heavy rainfall events (Figure 65).



Figure 65. Poned Water on the Biofilter Surface Observed after Rainfall Event.
(The Vegetation Cover Is Very Poor Indicating Likely Serious Compaction).

Infiltration rate measurements were manually recorded from biofilter ponded areas after five rainfall events between July 2010 and April 2011. Depth indicator scales were placed at 3 to 5 different locations in the biofilter in the ponded areas and measured every 30 min. at the beginning of the observation period for each event, and less frequently as the observations progressed, until the water completely infiltrated. The change in water level and elapsed time were recorded since the beginning of the first measurement. Measurements were taken only

during the daylight hours and it was therefore difficult to accurately predict the total drainage time for some events that were dry by the following morning. This method is time consuming, labor intensive, and greatly depends on operator care for accuracy, but was needed to verify the infiltrometer measurements using the Turf-Tec units during dry weather. These measurements were taken after the runoff ceased and the biofilter was fully saturated.

5.2.6 Laboratory Column Tests

Knowledge of physical and hydrologic properties of different bioretention mixtures, as well as their response to compaction, is essential for designing stormwater bioretention facilities in urban areas. Soil and media compaction that occurs in stormwater treatment facilities during construction (or improper use) can cause significant reductions in infiltration capacities of the soils. The effects of different compaction levels on the infiltration rates through the biofilter media (obtained from the biofilter) when mixed with varying amounts of filter sand was also examined during laboratory column experiments. Four-inch (100 mm) diameter PVC pipes (Charlotte Pipe TrueFit 4 in. PVC Schedule 40 Foam-Core Pipe) 3 ft (0.9 m) long, purchased from a local building supply store in Tuscaloosa, AL were used for these tests as shown in Figure 66. The bottom of the columns had a fiberglass window screen (about 1 mm openings) secured to contain the media and were placed in funnels.

The columns were filled with about 2 inch (5 cm) of cleaned pea gravel purchased from a local supplier. The columns had various mixtures of media and filter sand added on top of the gravel layer. The filter sand was purchased from a local supplier in Tuscaloosa, Alabama. It has a median particle size (D_{50}) of about 0.7 mm and a uniformity coefficient (C_u) of 3. To separate the gravel layer from the media layer, the coarse fiberglass window screen was placed over the gravel layer and then filled with the soil media brought from the biofilter, with varying amounts

of added filter sand (biofilter media alone; 10 % sand and 90 % biofilter soil; 25 % sand and 75 % biofilter soil; 50 % sand and 50 % biofilter soil) well mixed with the biofilter media. The media/sand layer was about 1.5 ft (0.46 m) thick.

Three levels of compaction were used to modify the density of the column media/sand samples during the tests: hand compaction, standard proctor compaction, and modified proctor compaction as shown in Figure 66. Both standard and modified proctor compactions follow ASTM standard (D 1140-54). The standard proctor compaction hammer is 24.4 kN and has a drop height of 12 in (300 mm). The modified proctor hammer is 44.5 kN and has a drop height of 18 in (460 mm). For the standard proctor setup, the hammer is dropped on the test soil 25 times on each of three soil layers, while for the modified proctor test, the heavier hammer was also dropped 25 times, but on each of five soil layers. The modified proctor test therefore results in much more compacted soil, and usually reflects the most compacted soil observed in the field. The hand compaction is done by gently hand pressing the media/sand material to place it into the test cylinder with as little compaction as possible, with no voids or channels. The hand compacted soil specimens therefore have the least amount of compaction. The densities were directly determined by measuring the weights and volume of the media/sand material added to each column.



Figure 66. Lab Column Construction for Infiltration Tests (Left to Right): Bottom of the Columns Secured With a Fiberglass Window Screen (Upper Left), Soil Media (Lower Left), and Media Compaction.

The infiltration through the biofilter media/sand was measured in each column using municipal tap water. The surface ponding depths in the columns ranged from 11 in (28 cm) to 14 in (36 cm), corresponding to the approximate maximum ponding depth at the Shelby Park biofilter. The freeboard depth above the media to the top of the columns was about 2 in (5 cm) to 3 in (7.5 cm). Infiltration rates in the media mixtures were determined by measuring the rates with time until apparent steady state rates were observed. The laboratory column setup for the infiltration measurements in the different media is shown in Figure 67.



Figure 67. Laboratory Column Setup.

5.3 Results

5.3.1 In-Situ Biofilter Infiltration Measurements Results

The small-scale double-ring infiltrometer tests (comprised of three separate setups each) conducted along the biofilter to examine variations in infiltration rates indicated that the average final infiltration rate and the coefficient of variation were about 5.7 in/hr (14.5 cm/hr) and 0.45 respectively, and ranged from 1.7 in/hr (4.3 cm/hr) to 10 in/hr (25.5 cm/hr) for the 12 separate tests (Table 40).

Table 40. Field Infiltration Tests using Small-Scale Infiltrimeters.

Horton's parameters				
Test site location	f_o (in/hr, cm/hr) and COV	f_c (in/hr, cm/hr) and COV	k (1/hr) and COV	dry density (g/cc)
1	(76, 190) and 1.37	(6, 15) and 0.42	13.8 (1.1)	2.2
2	(27, 67) and 0.76	(6, 15) and 0.65	7.2 (0.74)	2.3
3	(17, 43) and 0.31	(4.9, 12) and 0.14	8.4 (0.23)	1.8
4	(15, 38) and 0.19	(6, 15) and 0.62	6.6 (0.67)	2.1

In contrast, the measurements of the infiltration rates of the ponded water after actual rains indicated average saturated rates of only about 0.45 in/hr (1cm/hr) and coefficient of variation about 0.66. The actual rain event ponded average infiltration rates were about 25% of the lowest infiltrimeter measurements observed during the small scale tests. The actual event measurements were obtained with fully saturated conditions of the complete biofilter, while the small scale tests were only affected by saturated conditions in the close proximity of the test location. It is expected that the fully saturated conditions had a greater negative effects on the infiltration rates than the locally saturated conditions. Also, the compaction of the biofilter media extended to the bottom of the excavated trench, with possible increasing compaction with depth due to the media placement methods. Table 41 shows the infiltration rate measurements from biofilter ponded areas after five rainfall events.

Table 41. Infiltration Measurement at Pondered Locations in Biofilter.

Rain Event	Location	f_o (in/hr, cm/hr)	f_c (in/hr, cm/hr)	K (1/hr)
27-Jul-10	1	0.65 (1.7)	0.65 (1.7)	0.48
	2	2.7 (6.8)	1 (2.5)	0.54
	3	0.7 (1.9)	0.7 (1.9)	0.54
	4	1.3 (3.1)	0.25 (0.64)	0.78
	5	0.6 (1.6)	0.6 (1.6)	0.78
	mean COV	1.18 (3) 0.74	0.64 (1.6) 0.47	0.62 0.23
23-Nov-10	1	0.58 (1.5)	0.58 (1.5)	0.27
	2	148 (375)	0.17 (0.44)	7.55
	3	0.78 (2)	0.78 (2)	0.2
	4	21 (53)	0.2 (0.52)	6.12
	mean COV	42.5 (108) 1.67	0.43 (1.1) 0.68	3.54 1.09
	Feb 5-6, 2011	1	43.5 (111)	0.15 (0.4)
2		23.4 (59)	0.17 (0.43)	4.8
3		0.41 (1.0)	0.31 (0.8)	0.01
4		0.14 (0.4)	0.05 (0.12)	0.23
mean COV		17 (43) 1.24	0.1 (0.24) 0.63	2.8 1.12
9-Mar-11		1	1.5 (3.7)	0.2 (0.51)
	2	0.2 (0.5)	0.14 (0.36)	<0.001
	3	0.18 (0.45)	0.18 (0.45)	5.1
	4	0.6 (1.5)	0.6 (1.5)	3
	mean COV	0.6 (1.5) 1.01	0.2 (0.6) 0.74	2.7 0.77
	16-Apr-11	1	0.82 (2.1)	0.44 (1.12)
2		0.63 (1.6)	0.63 (1.6)	0.18
3		196.8 (500)	0.28 (0.7)	11.9
mean COV		66.1 (168) 1.71	0.45 (1.14) 0.40	4.2 1.60

The relationship between specifications on the assumed permeability of the planting mix and recommended infiltration rates of the in situ, or native, soil for biofilter design and cell sizing and performance is not very well quantified or discussed in many of the state guidelines (Carpenter 2010). Most states set biofilter cell drawdown times of 24 to 72 hours to avoid

standing water and potential mosquito larval habitat. Variables that can be influenced by maintenance include compaction, root growth and density, and surface clogging by fine particulates. The influence of an underdrain or highly pervious underlying soils is also critical and will often dictate design and performance of biofilter cells. Extended periods of surface ponding (more than 72 hours) of water in the Shelby Park biofilter was often observed following heavy rainfall events. Media compaction is likely the major problem associated with poor infiltration rates and poor plant growth at the Shelby Park biofilter facility.

Variations of final infiltration rates (about a factor of 2) were also observed in the small infiltrometers that were inserted within about a meter from each other at each test location along the biofilter, as shown in Figure 68. Figure 69 shows example actual rain event ponded infiltration measurements fitted with Horton's equation. Biofilter surface and actual rain event ponded infiltration measurements fitted with Horton's equation fitted are included in Appendix B.1 through B.9.

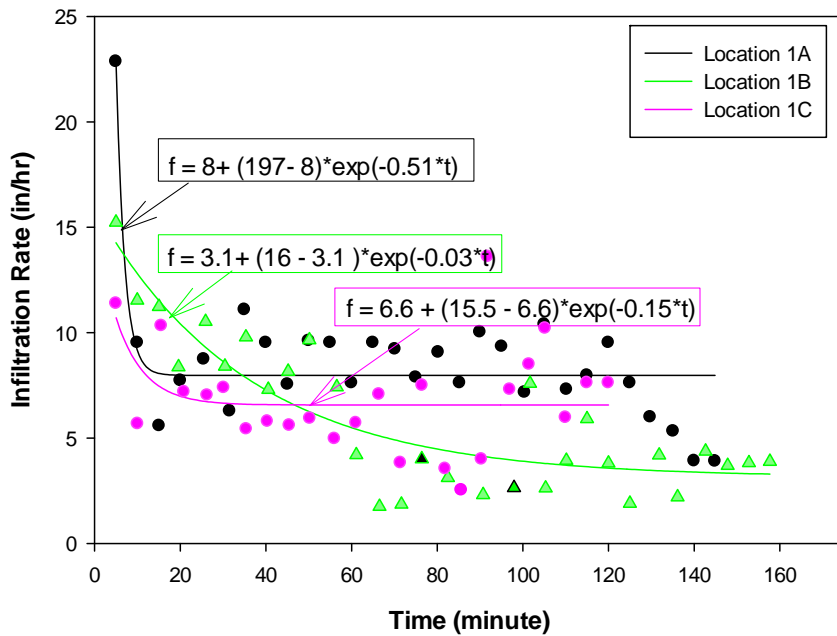


Figure 68. Example Biofilter Surface Small-scale Infiltration Measurements Fitted With the Horton Equation.

Biofilter Infiltration Test after One Rainfall Event

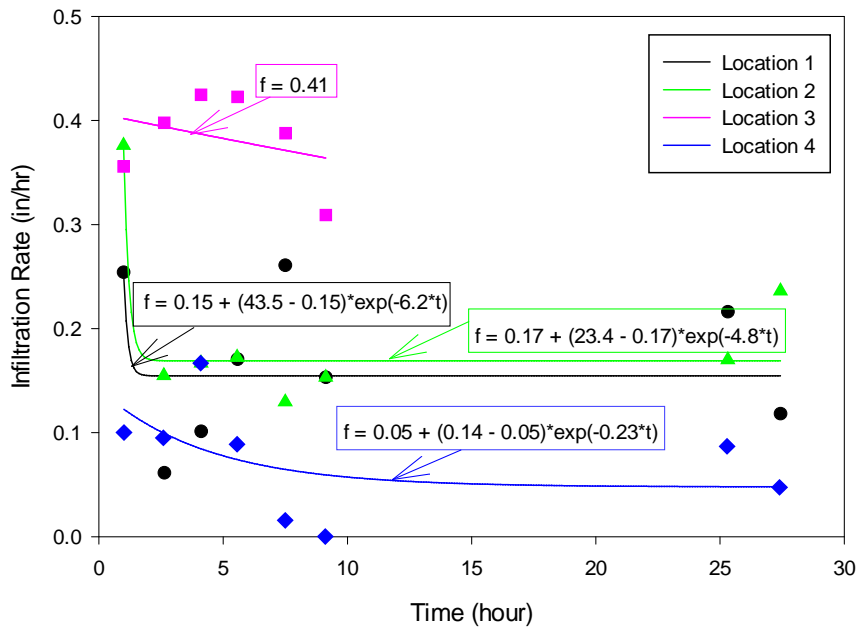


Figure 69. Example Actual Rain Event Poned Infiltration Measurements Fitted With Horton Equation.

The small-scale surface infiltration measurements did not include sufficient water to saturate the system and only indicated more favorable surface conditions. Therefore, care needs to be taken when using any surface infiltration method when evaluating an infiltration facility having deeply placed media or excavations. A trench or borehole infiltration test would be more reliable in this case, or more preferred in-situ measurements with pressure transducer recording depth sensors during actual rains.

5.3.2 Laboratory Infiltration Results

Biofilter media material obtained from the surface of the biofilter was brought to the laboratory for extended column testing. Figure 70 shows box and whisker plots of the infiltration rates for different test conditions, comparing different compaction conditions with varying amounts of sand amendments (Table 42).

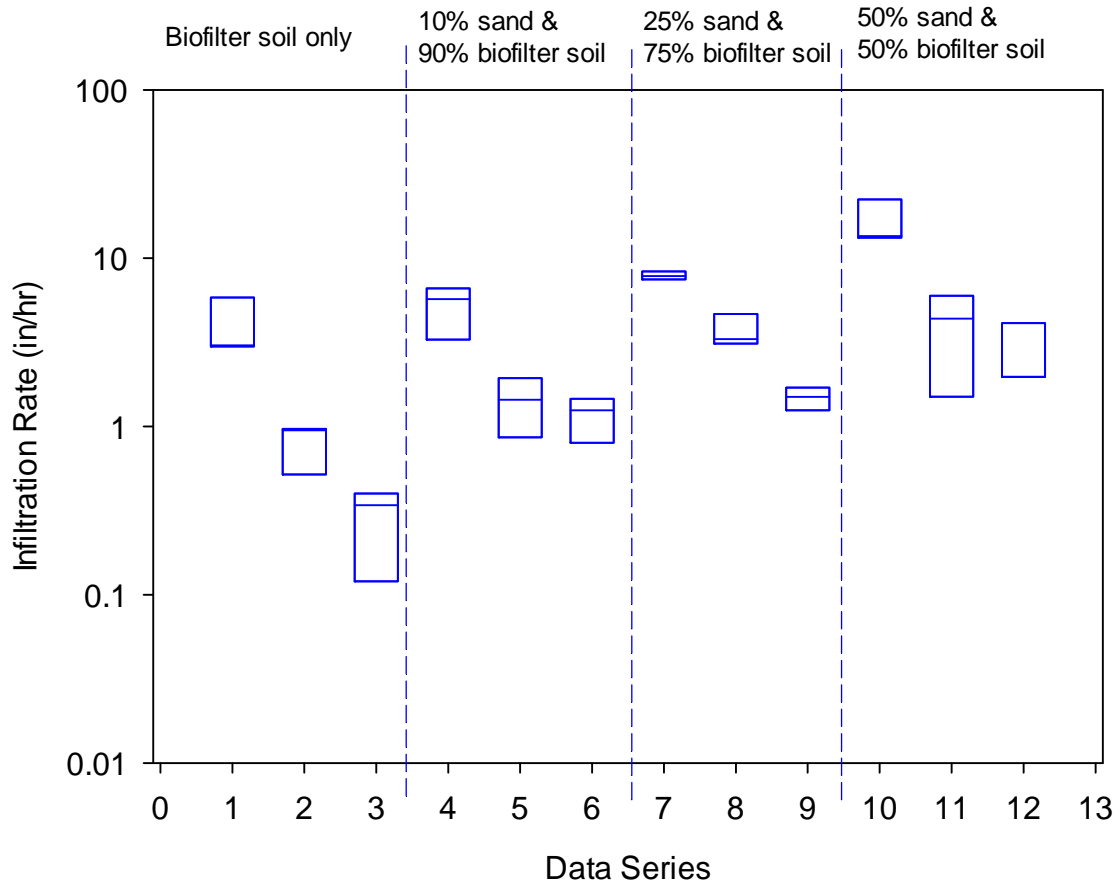


Figure 70. Box and Whisker Plots of the Different Test Conditions, Comparing Different Compaction Conditions with Varying Amounts of Sand Amendments (hand, standard proctor, and modified proctor compaction for each amendment condition).

Table 42. Various Mixtures of Media and Filter Sand Used for Laboratory Infiltration Measurements.

Data series	Compaction	percent (%) sand	percent (%) media
1	hand	0	100
2	standard proctor	0	100
3	modified proctor	0	100
4	hand	10	90
5	standard proctor	10	90
6	modified proctor	10	90
7	hand	25	75
8	standard proctor	25	75
9	modified proctor	25	75
10	hand	50	50
11	standard proctor	50	50
12	modified proctor	50	50

The box and whisker plots indicate the major benefits by adding sand to the media material, even at only 10%, for the most severely compacted material (increased from about 0.3 in/hr (0.8 cm/hr) to 1.2 in/hr (3.1 cm/hr)). Lower benefits were observed for the less-compacted conditions, at least until 50% sand was added. It is seen that the benefits of decreased compaction were much greater than the sand addition benefits. However, added sand prevented this media material from having severely reduced rates, even with severe compaction (averaging at least about 0.3 in/hr (0.8 cm/hr), with 0% sand, about 2.7 in/hr (6.9 cm/hr), with 50% sand.

For the laboratory tests, the average final infiltration rates through the biofilter soil only with increasing degrees of compaction were 4 in/hr (10.2 cm/hr), 0.8 in/hr (2 cm/hr), and 0.3 in/hr (0.8 cm/hr) using hand compaction, standard proctor compaction and modified proctor compaction methods, respectively. The final infiltration rates of the hand compacted biofilter soil were reduced by 80 and 93% using the standard proctor compaction and modified proctor compaction methods, respectively. Figure 71 shows example laboratory infiltration measurements fitted with the Horton equation.

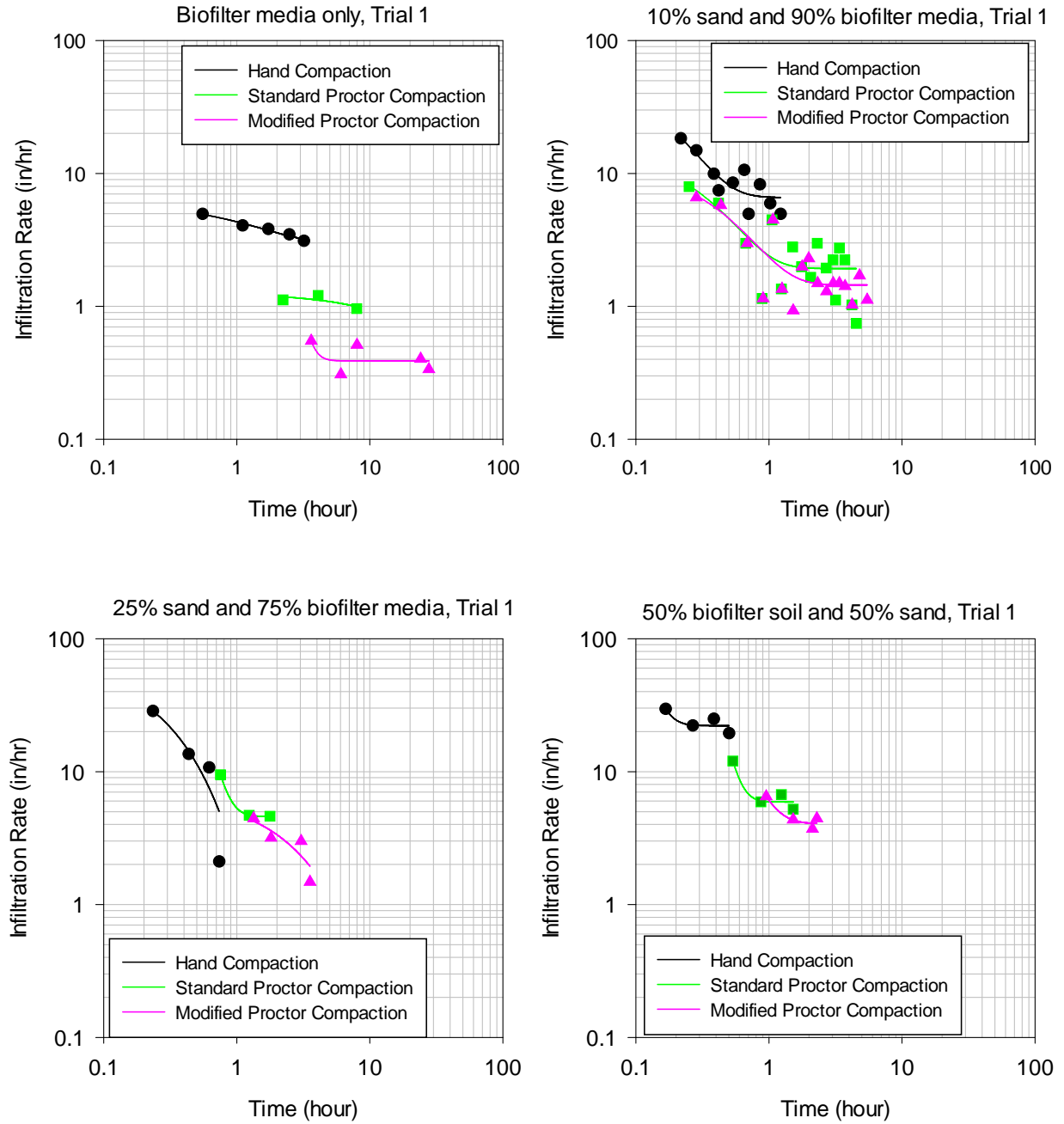


Figure 71. Example Laboratory Infiltration Measurements Fitted with Horton Equations

Laboratory infiltration measurements fitted with the Horton equation are shown in Appendix B.10 through B.14. Tables 43 through 46 summarize the column test results for the biofilter soil alone and with varying amounts of added sand, and for different compaction values.

Table 43. Laboratory Infiltration Tests Using Biofilter Media Only at Different Compaction Levels.

biofilter media only				
Compaction method	Test	f_o (in/hr, cm/hr)	f_c (in/hr, cm/hr)	k (1/hr)
hand (density = 1.54g/cc)	1	6.1 (15.5)	3.0 (7.6)	0.84
	2	8.2 (20.8)	3.0 (7.6)	2.46
	3	27.3 (69.4)	6.0 (15.3)	4.32
	mean	13.8 (35.2)	4.0 (10.2)	2.54
	COV	0.84	0.43	0.69
standard (density = 1.66g/cc)	1	1.3 (3.3)	1.0(2.5)	0.6
	2	1.2 (3.1)	1.0 (2.5)	1.38
	3	0.94 (2.4)	0.52 (1.3)	10.44
	mean	1.15 (2.9)	0.81 (2.1)	4.14
	COV	0.16	0.31	1.13
modified (density =1.94g/cc)	1	n/a	0.40 (1.02)	2.4
	2	0.5 (1.3)	0.34 (0.86)	0.9
	3	0.2 (0.51)	0.12 (0.3)	0.36
	mean	0.4 (0.9)	0.3 (0.73)	1.22
	COV	0.63	0.51	0.87

* n/a: values were beyond the data range and extrapolated results were unreasonable

Table 44. Laboratory Infiltration Tests Using a Mixture of 10% Filter Sand and 90% Biofilter Media at Different Compaction Levels.

10% sand and 90% biofilter media				
Compaction method	Test	f_o (in/hr, cm/hr)	f_c (in/hr ,cm/hr)	k (1/hr)
hand	1	64 (163)	6.6 (16.9)	7.21
	2	9.3 (23.7)	3.3 (8.4)	0.93
	3	9.9 (25.2)	5.7 (14.5)	1.57
	mean	27.7 (70.5)	5.2 (13.2)	3.24
	COV	1.13	0.33	1.07
standard	1	16.6 (42.1)	1.94 (4.9)	3.42
	2	3.01 (7.6)	1.45 (3.7)	2.25
	3	1.8 (4.5)	0.86 (2.2)	0.17
	mean	7.12 (18.1)	1.42 (3.6)	1.95
	COV	1.15	0.38	0.85
modified	1	12.4 (31.6)	1.46 (3.7)	2.51
	2	1.5 (3.8)	0.8 (2)	0.05
	3	1.4 (3.5)	1.25 (3.2)	0.02
	mean	5.1 (13)	1.2 (3)	0.86
	COV	1.24	0.3	1.66

Table 45. Laboratory Infiltration Tests Using a Mixture of 25 % Filter Sand and 75% Biofilter Media at Different Compaction Levels.

25% sand and 75% biofilter media				
Compaction method	Test	f_o (in/hr, cm/hr)	f_c (in/hr, cm/hr)	k (1/hr)
hand (density = 1.52g/cc)	1	65 (165)	7.5 (19.1)	3.47
	2	19 (49)	8.4 (21.2)	3.88
	3	25 (63)	7.8 (19.9)	4.58
	mean	36 (93)	7.9 (20.1)	3.98
	COV	0.68	0.05	0.14
standard (density = 1.71g/cc)	1	n/a	4.7 (11.9)	7.78
	2	6.6 (17)	3.3 (8.4)	1.04
	3	7.2 (18)	3.1 (7.9)	0.88
	mean	7 (17.5)	3.7 (9.4)	3.23
	COV	0.06	0.23	1.22
modified (density = 1.76 g/cc)	1	6.9 (17.5)	2 (3.8)	0.36
	2	3.0 (7.7)	1.7 (4.3)	0.09
	3	3.3 (8.4)	1.3 (3.2)	0.13
	mean	4.4 (11.2)	1.5 (3.8)	0.19
	COV	0.49	0.15	0.74

* n/a: values were beyond the data range and extrapolated results were unreasonable

Table 46. Laboratory Infiltration Tests Using a Mixture of 50% Filter Sand and 50% Biofilter Media at Different Compaction Levels.

50% sand and 50% biofilter media				
Compaction method	Test	f_o (in/hr, cm/hr)	f_c (in/hr, cm/hr)	k (1/hr)
hand (density = 1.63 g/cc)	1	n/a	22.4 (57)	35.7
	2	36 (91)	13.6 (34.4)	7.2
	3	41 (105)	13.3 (33.7)	5.7
	mean	38.5 (97.8)	16.4 (41.7)	16.2
	COV	0.1	0.32	1.1
standard (density = 1.70 g/cc)	1	n/a	6 (15.2)	11.8
	2	7.2 (18.4)	4.4 (11.1)	0.75
	3	7.8 (19.9)	1.5 (3.8)	0.36
	mean	7.5 (19.1)	4 (10.1)	4.3
	COV	0.06	0.57	1.5
modified (density = 1.77 g/cc)	1	n/a	4.1 (10.5)	4.01
	2	4.2 (10.6)	2.0 (5)	0.18
	3	2.6 (6.7)	2.0 (5)	0.05
	mean	3.4 (8.6)	2.7 (6.8)	1.41
	COV	0.32	0.46	1.53

Table 47 and Figure 72 summarize the column test results for the biofilter soil alone and with varying amounts of added peat, using the standard proctor compaction method. The major benefits by adding peat to the biofilter media material was noted during the test. The average final infiltration rate increased from 2.1 in/hr (5.4 cm/hr) to 3.6 in/hr (9.1 cm/hr) as the peat content increased from 10 to 50%, respectively. This indicated an average increase of 40% in infiltration. The peat amendment test indicated that the infiltration rates through the mixtures were extremely high for hand compaction conditions and they were very low for modified proctor compaction conditions, and as a result, no flow measurements were conducted.

Table 47. Laboratory Infiltration Tests Using Biofilter Soil and Peat at Different Compaction Levels.

Standard Proctor Compaction Test	Test	f_o (in/hr, cm/hr)	f_c (in/hr, cm/hr)	k (1/hr)
10% peat and 90% biofilter soil (density = 1.64 g/cc)	1	30 (76.3)	2.8 (7.1)	8.07
	2	6.4 (16.3)	1.9 (4.7)	5.3
	3	2.9 (7.3)	1.8 (4.5)	0.65
	mean	13.1 (33.3)	2.1 (5.4)	4.67
	COV	1.13	0.26	0.8
25% peat and 75% biofilter soil (density = 1.52 g/cc)	1	19.6 (49.7)	2.8 (7)	4.73
	2	12.2 (31.1)	2 (5.2)	12.37
	3	5 (12.7)	2 (5.2)	3.53
	mean	12.3 (31.2)	2.3 (5.8)	6.88
	COV	0.59	0.18	0.7
50% peat and 50% biofilter soil (density = 1.23 g/cc)	1	52 (130)	5.2 (13.1)	10.98
	2	5.6 (14.3)	3.5 (8.8)	3.16
	3	4.2 (10.5)	2.1 (5.4)	0.24
	mean	20.5 (52.1)	3.6 (9.1)	4.79
	COV	1.32	0.43	1.16

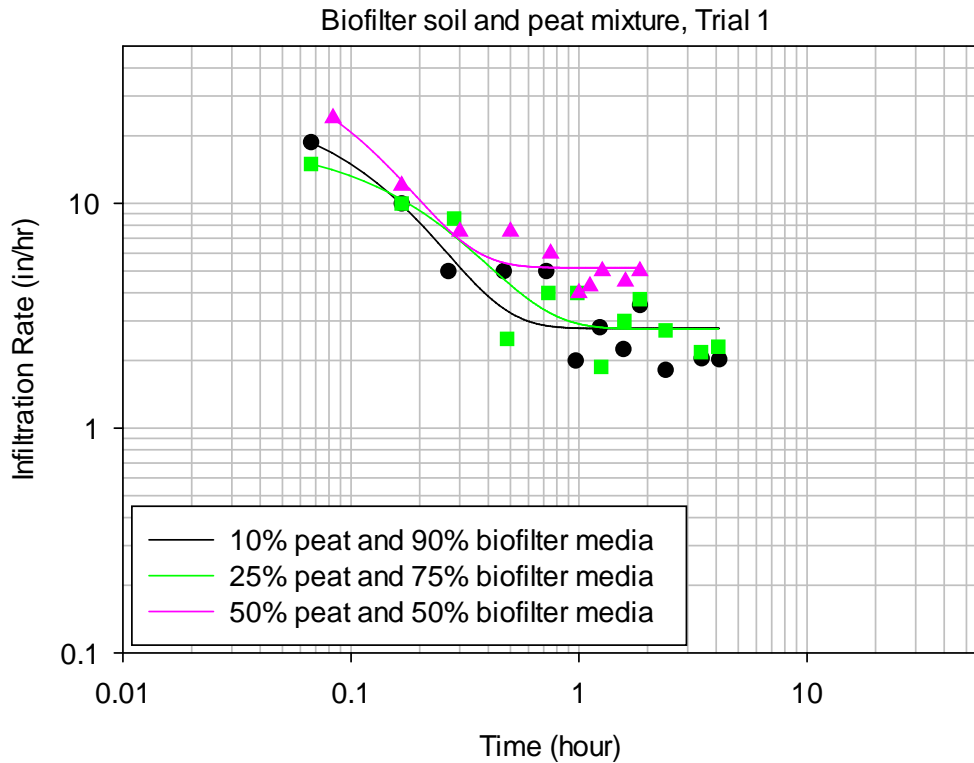


Figure 72. Example Laboratory Infiltration Measurements Fitted With Horton Equation, using Peat and Standard Proctor Compaction Method.

5.4 Statistical Analyses

Statistical analyses were conducted to determine the effects of sand and compaction, plus their interactions, on the infiltration rate through various mixtures of sand and biofilter media. A complete two level and 2 factors (2^2 , with varying sand and compaction) factorial experiment (Box et al. 1978) was used to examine the effects of those factors, plus their interactions, on the infiltration rate for the different sand and biofilter media mixtures. The factors studied, and their low (-1) and high values (+1) used in the calculations, are shown in Table 48. The complete data used in this factorial study are also summarized in Table 49. Experiments were performed in replicates of three for each infiltration measurements. Statistical methods are used to summarize

the data and to provide an efficient method to analyze factor interactions on the infiltration rates through the mixtures.

Table 48. Experimental Factors and their Levels.

Variable	Low value (-1)	High value (+1)
Percentage of sand in the mixture (S), %	10	50
Compaction level (C), hand/modified proctor	hand	modified proctor

The data analyses were performed using the statistical software package Minitab (version 16). Normal plots of the standardized effects, residual plots, main effects plots, and interaction plots were prepared to examine the effects of the factors and to compare the significance of each effect. An analysis of variance (ANOVA) table was constructed to determine the significant factors and their interactions needed to best predict media flow performance. Statistical hypothesis tests using a p-value of 0.05 (95% confidence) were used to determine whether the observed data were statistically significantly different from the null hypothesis.

Table 49. Infiltration Data Used In Full 2² Factorial Designs.

Case	% sand (S)	compaction (C)	Fc (in/hr)
1A	+	+	4.12
1B	+	+	1.98
1C	+	+	1.97
2A	+	-	22.43
2B	+	-	13.55
2C	+	-	13.26
3A	-	+	1.46
3B	-	+	0.80
3C	-	+	1.25
4A	-	-	6.63
4B	-	-	3.29
4C	-	-	5.72

Normal probability plots of effects are used to compare the relative magnitudes and the statistical significance of both main and interaction effects. These plots also indicate the direction of the effect; in Figure 73, the factor “sand” has positive effects because it appears on the right side of the plot, meaning that when the low level changes to the high level of the factor, the response increases. In Figure 73, “compaction” and the interaction of sand and compaction of the mixture appears on the left side of the plot, meaning that the factor has a negative effect. This indicates that when the low level changes to high, the response decreases.

Figure 73 shows that the percentage of sand and compaction of the media have the largest effects on the measured infiltration rates, followed by their interactions. The results of the factorial analyses are summarized in Table 50.

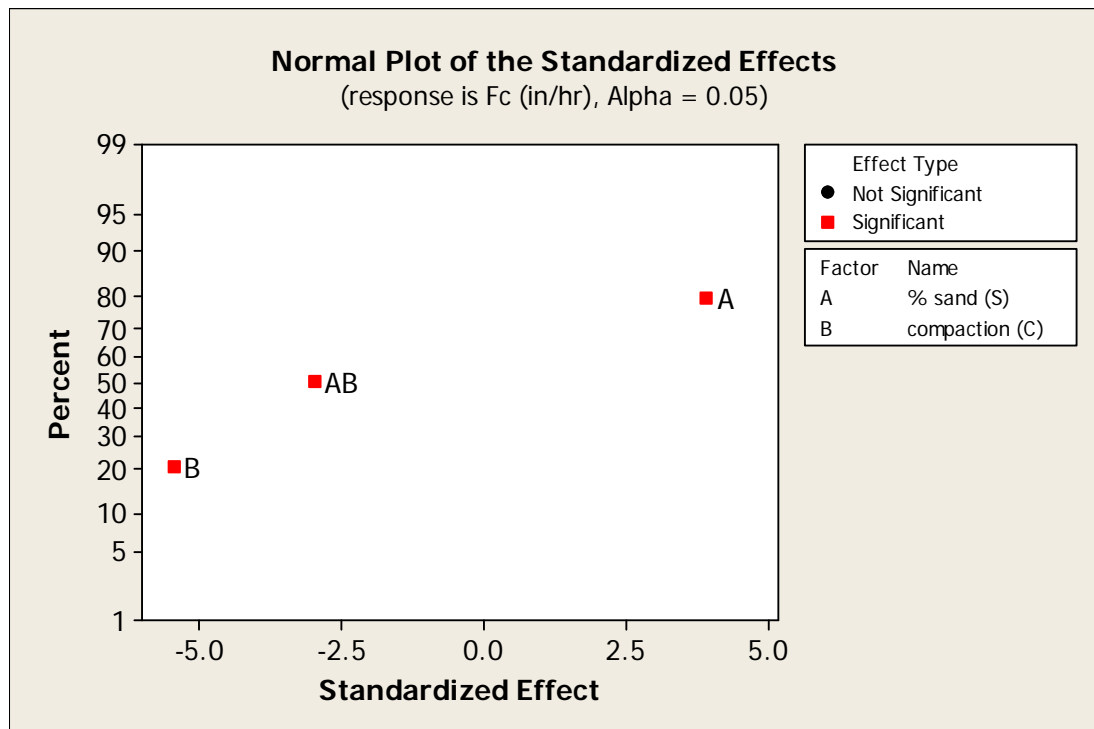


Figure 73. Probability Plot to Identify Important Factors Affecting the Infiltration Rate through a Media Mixture.

Table 50. Estimated Effects and Coefficients for Fc (in/hr) (coded units).

Term	Effect	Coef	SE Coef	T	P
Constant		6.37	0.81	7.83	0.000
% sand (S)	6.36	3.18	0.81	3.91	0.004
compaction (C)	-8.88	-4.44	0.81	-5.46	0.001
% sand (S)*compaction (C)	-4.84	-2.42	0.81	-2.97	0.018

S = 2.819 PRESS = 143.1

R-Sq = 87.1% R-Sq (pred) = 70.9% R-Sq(adj) = 82.2%

The main effects plots are useful to compare magnitudes of main effects. The main effect plots are obtained to examine the data means for the two factors. Figure 74 shows increases in infiltration rates occurred with increases in the percentage of sand in the mixture, whereas infiltration rates decreased with increase in media compaction.

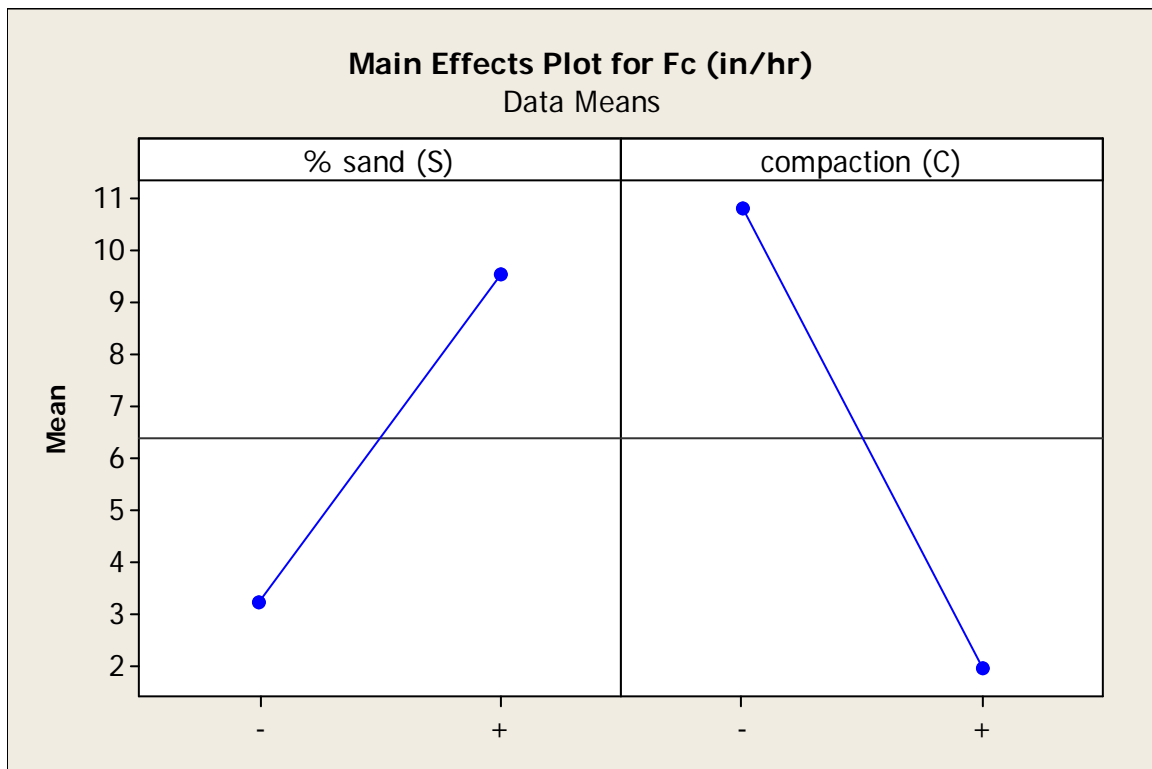


Figure 74. Main Effects Plot for the Two Factors.

Figure 75 depicts interaction plots which are used to interpret significant interactions between the factors. In the interaction plot, the lines in % sand vs. compaction are not parallel, indicating there exists an interaction between these factors. The greater the departure of the lines from the parallel state, the higher the degree of interaction.

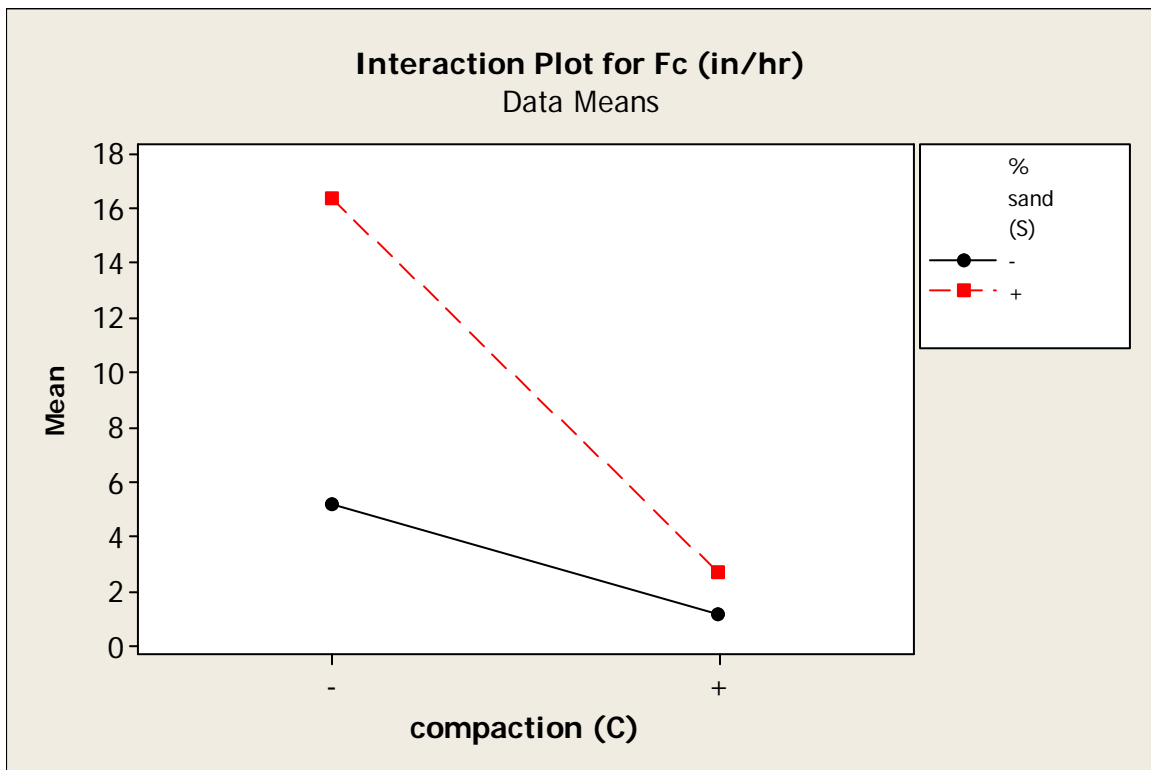


Figure 75. Interaction Plot between Different Factors.

5.4.1 Model Fitting

The effects and half-effects of the significant factors (main effects and interactions) were used to predict the infiltration rate performance of various mixtures. Table 51 shows the matrix (table of contrasts) representing factors (sand and compaction) and their interactions. The results of the effects and half-effect are also shown in the table.

Table 51. Shows the Results of the Effects and Half-Effects.

Case	S	C	SC	Fc (in/hr)	Identification	effects/SE
1	+	+	+	2.69	average	2.26
2	+	-	-	16.41	S	1.13
3	-	+	-	1.17	C	-1.58
4	-	-	+	5.21	SC	-0.86
Y (grand)				6.37		
Avg Y@-1	3.19	10.81	8.79			
Avg Y@+1	9.55	1.93	3.95			
Δ	6.36	-8.88	-4.84			
$\Delta/2$	3.18	-4.44	-2.42			

S: % sand and C: compaction

As noted previously, the significant factors and interactions that affect the responses are percent sand, compaction, and their interactions. Those factors and interactions have to be included in the prediction equation. These factors have significant effect (p-values greater less than the chosen value of $\alpha = 0.05$) on the infiltration rate and a model was created wherein these factors are included.

The prediction equation can be written in terms of the grand mean and half-effects, excluding the non-significant factors.

$$\hat{y} = \bar{y} + \left(\frac{\Delta_S}{2}\right)S + \left(\frac{\Delta_C}{2}\right)C + \left(\frac{\Delta_{SC}}{2}\right)SC$$

where:

\hat{y} = predicted response (Y pred)

\bar{y} = grand mean (Y grand)

$\frac{\Delta}{2}$ = half-effects of each factor or interaction

S = percent sand

C = compaction

The final prediction equation is given as:

$$\hat{y} = 6.37 + 3.18S - 4.44C - 2.42SC$$

5.4.2 Pooled Standard Error

The standard from replicate analyses can be used to identify significant factors (Box, et al 1987). If the calculated effect for a factor or interactions is much larger than the pooled standard error from all of the tests (usually considered as 3 to 5 times larger, or more), then the effect can be considered to be significant. The standard error of the mean for each condition's mean is the standard deviation of the sample group divided by the square root of the sample size. The following equation can be used to determine the pooled standard error. Table 52 show the data used to obtain the pooled standard error.

$$S_p^2 = \frac{\sum_{i=1}^k (n_i - 1) s_i^2}{\sum_{i=1}^k (n_i - 1)}$$

where S_p^2 = the pooled variance

n_i = the sample size of the i^{th} sample

s_i^2 = the variance of the i^{th} sample

k = the number of samples being combined.

The pooled standard error of the mean equals 2.82.

Table 52. Stand Error Calculations for Lab Infiltration Measurements Results

Condition	1	2	3	4
Fc (in/hr)	4.12	22.43	1.46	6.63
	1.98	13.55	0.80	3.29
	1.97	13.26	1.25	5.72
Standard Dev.	1.24	5.21	0.34	1.73
Square Root N	1.73	1.73	1.73	1.73
Standard Error	0.72	3.01	0.19	1.00
Average (in/hr)	2.69	16.41	1.17	5.21
$(n-1)*S_i^2$	3.08	54.31	0.23	5.98
$(n-1)$	2.00	2.00	2.00	2.00
Pooled Standard Error	2.82			

Table 53 compares the effects to the group standard errors (SE). As noted previously, the significant factors and interactions that affect the responses are percent sand, compaction, and their interactions (effects being at least 3 times the standard error values indicate the likely significant factors). No effects are significant at this traditional level, using SE as a measure of significance; therefore the following ANOVA test were conducted. Mixture compactions seem to have higher effects on the infiltration rates through the mixture than percent sand and their interactions.

Table 53. Calculated Effects and Standard Errors for the 22 Factorial Design

Effect	Estimate +/- Standard Error
Average	6.37 +/- 1.41
Main effects	
Sand, S	3.18 +/- 2.82
Compaction, C	-4.44 +/- 2.82
Two-Factor Interactions	
S x C	-2.42 +/- 2.82

An ANOVA test was also used to test the significance of the regression coefficients, which highly depends on the number of data observations (Table 54). When only a few data observations are available, strong and important relationships may not be shown to be significant, or high R^2 values could occur with insignificant equation coefficients. These data were evaluated using the p-value (the probability of obtaining a test statistic that is at least as extreme as the calculated value if there is actually no difference; the null hypothesis is true) calculated during the ANOVA tests. The independent variable was used to predict the dependent variable when $p < 0.05$,

Table 54. Analysis of Variance for Fc (in/hr) (coded units)

Source	DF	Seq SS	Adj SS	Adj MS	F	P
Main Effects	2	358.11	358.11	179.056	22.5	0.001
% sand (S)	1	121.38	121.38	121.381	15.3	0.004
compaction (C)	1	236.73	236.73	236.732	29.8	0.001
2-Way Interactions	1	70.27	70.27	70.272	8.84	0.018
% sand (S)*compaction (C)	1	70.27	70.27	70.272	8.84	0.018
Residual Error	8	63.59	63.59	7.949		
Pure Error	8	63.59	63.59	7.949		
Total	11	491.98				

A summary of statistical information about the model is also shown in Table 50. R^2 is a statistical measure of goodness of fit of a model whereas adjusted R^2 is a statistic that is adjusted for the number of explanatory terms in a model. The value of R^2 and adjusted R^2 for the model are 87.1% and 82.2% respectively. Predicted R^2 is calculated from the PRESS (Prediction Error Sum of Squares) statistic. The predicted R^2 statistic is computed to be 70.9%. Larger values of predicted R^2 suggest models of greater predictive ability. This indicates that the model is expected to explain about 70.9% of the variability in new data. Figure 76 shows a scatterplot of the observed and fitted Fc values, indicating very good fits of the observed with the predicted Fc values over a wide range of conditions.

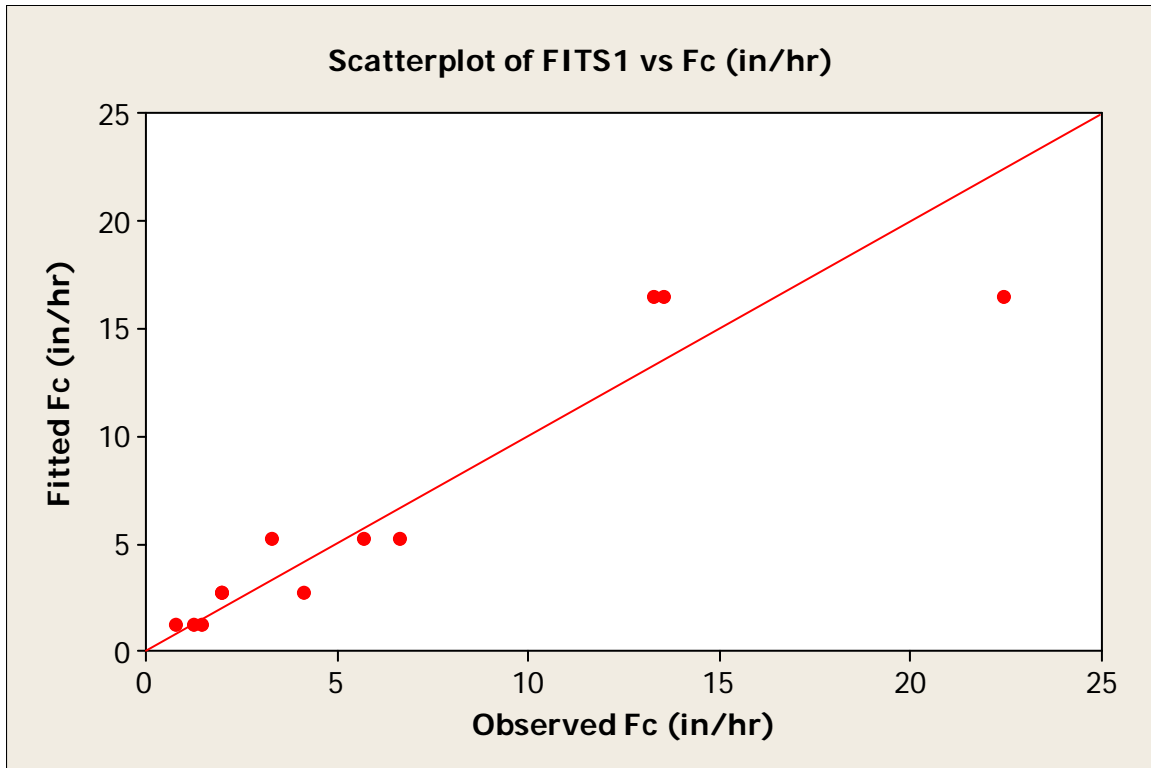


Figure 76. Observed vs Fitted Fc Values.

Residual analyses were conducted to investigate the goodness of model fit. Residual plots were inspected to determine if the error term in the regression model satisfies the four regression assumptions (Matson and Huguenard 2007) (they must be independent, zero mean, constant variance, and normally distributed). To check the constant variance assumptions, the plots of residuals vs. the fitted values were inspected. To evaluate the normality of the residuals, normal probability plots and histograms of the residuals were also constructed. The Anderson-Darling test statistic was also calculated to check for normality. The normal probability plot of the residuals shown in Figure 77 shows that the fitted data are normally distributed (Anderson-Darling test for normality has a p-value greater than 0.05, so the data are not significantly different from a normal distribution for the number of observations available). The zero mean of the residuals assumption was checked by examining the descriptive statistics and graphs of the

residuals vs. fitted values and vs. the order of the observations. To determine if the residuals were independent of each other, graphs of the residuals vs. observation number were also examined.

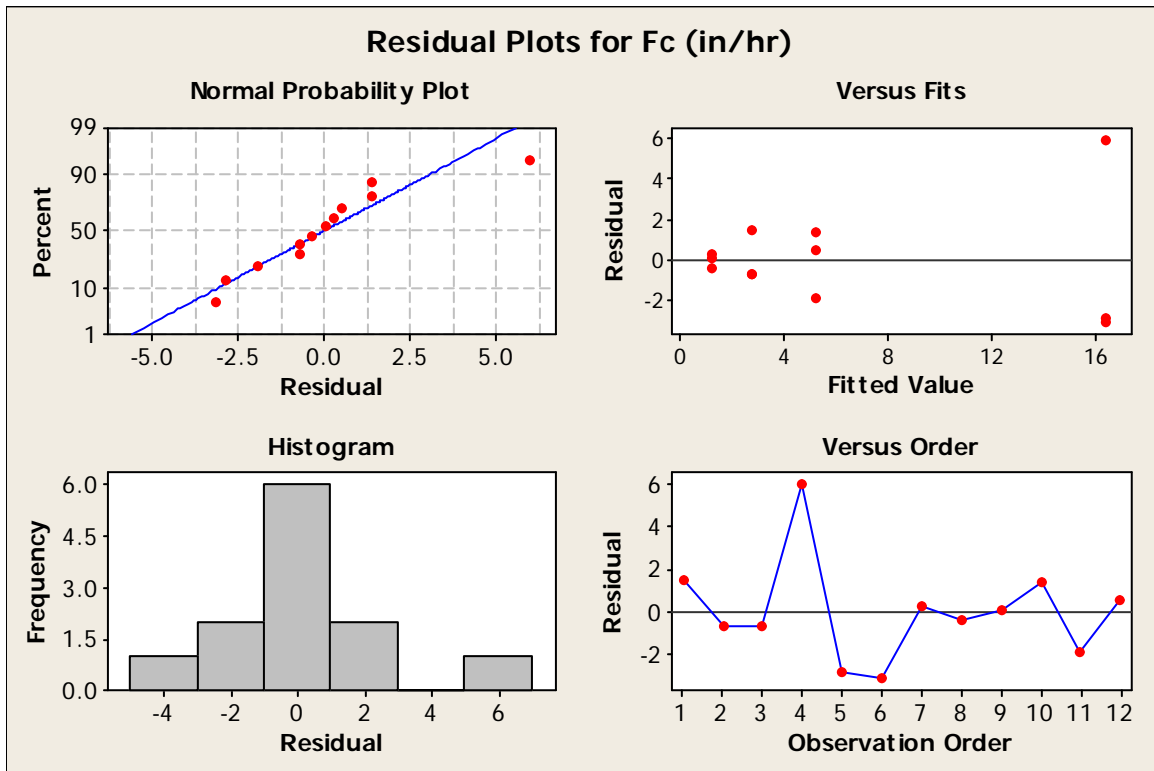


Figure 77. Residuals Analysis Plot.

The examination of the residual values vs. fitted values of the data indicated that there was a greater spread in the residuals for the higher fitted values. The model residual histogram was approximately bell shaped; the residuals were normally distributed and had zero mean, and were independent of each other. Model improvements should therefore focus on conditions that had high infiltration conditions.

5.5 Statistical Comparisons of Different Levels of Compaction

There are several statistical tests of multiple pairwise comparisons of groups available. The most commonly used approaches include: Least Significant Difference (LSD), Bonferroni Multiple Comparison, and the Tukey-Kramer test. The LSD (Least Significant Difference) test is a two-step test. First the ANOVA F-test is performed. If it is significant at level α (alpha), then all pairwise t-tests are carried out, each at level α (alpha). If the F-test is not significant, then the procedure terminates. The Bonferroni multiple comparison test is a conservative test, that is, the familywise error rate (FEWR) is not exactly equal to α (alpha), but is less than α (alpha) in most situations. It is easy to apply and can be used for any set of comparisons. The Tukey-Kramer test is an extension of the Tukey test to unbalanced designs. Unlike the Tukey test for balanced designs, it is not exact. The FWER of the Tukey-Kramer test may be less than α (alpha). It is less conservative for only slightly unbalanced designs and more conservative when differences among samples sizes are bigger.

One of the primary requirements for these multiple pairwise comparisons methods is that the data are normally distributed. When data are not normally distributed, there are two commonly used approaches. The first is to transform the data using logarithmic or square root transformations in an attempt to obtain a transformed normal distribution. One potential problem with this method is that the units of the transformed data may be difficult to interpret due to the logarithmic manipulation. The second method for dealing with non-normally distributed data is to use a non-parametric analysis having fewer data distribution requirements.

The Kruskal-Wallis test is usually represented as the nonparametric version of the parametric one-way ANOVA test. This test is used to determine if at least one group is significantly different from the other groups being compared. This test compares the population

medians of the groups, instead of the population means used by ANOVA. The Kruskal-Wallis method tests the hypothesis that all population medians are equal (Gibbons, 1997). The multiple comparison tests shown below were conducted using a MINITAB version 16 macro in a nonparametric setting (Orlich, 2010). The following figures describe the significance of the differences for the saturated infiltration rates for different levels of compaction and using different percentages of sand and biofilter media. Detailed calculation results are attached in Appendix B.16 through B.19.

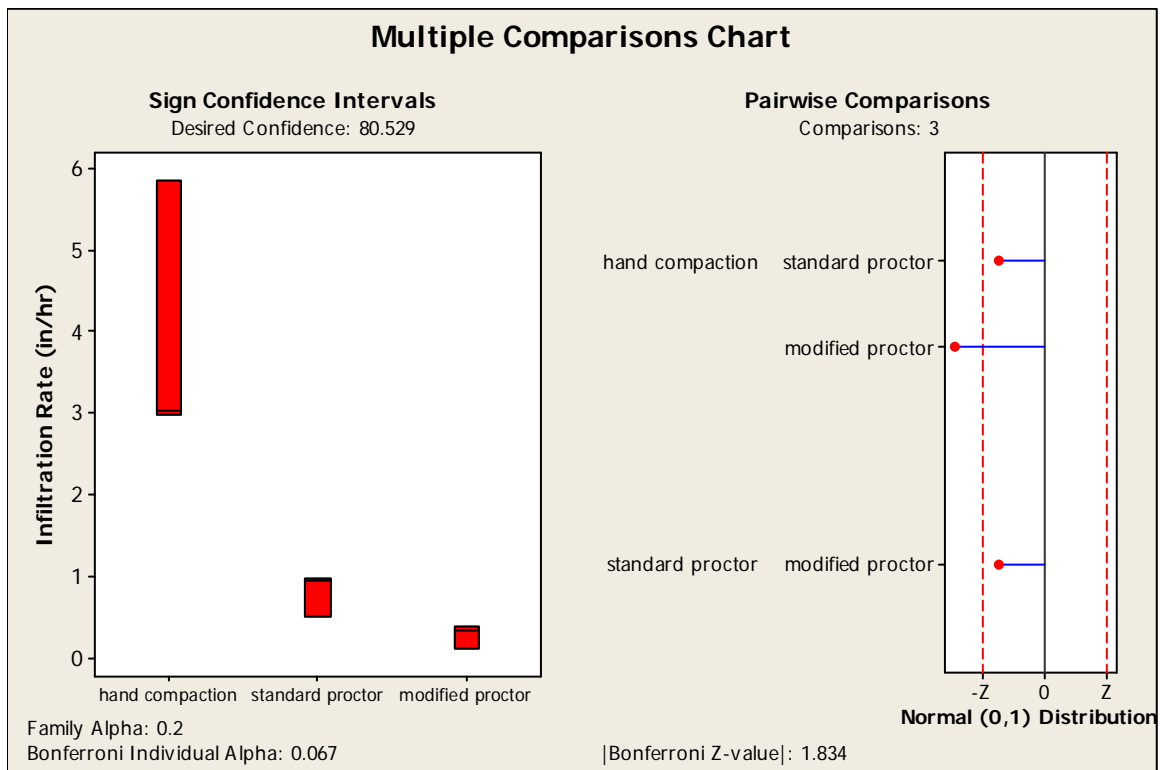


Figure 78. Multiple Comparison Plots of Laboratory Infiltration Measurements Using Biofilter Media Only.

The graph on the left of Figure 78 displays box plots of groups with their sign confidence intervals for the medians (red boxes in the each box plot). The graph on the right displays the

non absolute group mean rank standardized differences (Orlich, 2010). This latter plot shows the magnitude of the group differences and its direction. It also shows the positive and negative critical z-values and illustrates if a difference is likely statistically significant. From the above figures, it is seen that the saturated infiltration rate for hand compaction is larger than the saturated infiltration rates using standard proctor and modified proctor compaction method. This difference is also shown to be statistically significant since the standardized difference distance goes beyond the critical z-values compared to the other test groups. There are no significant differences noted between the saturated infiltration rate of standard proctor and modified proctor compaction methods.

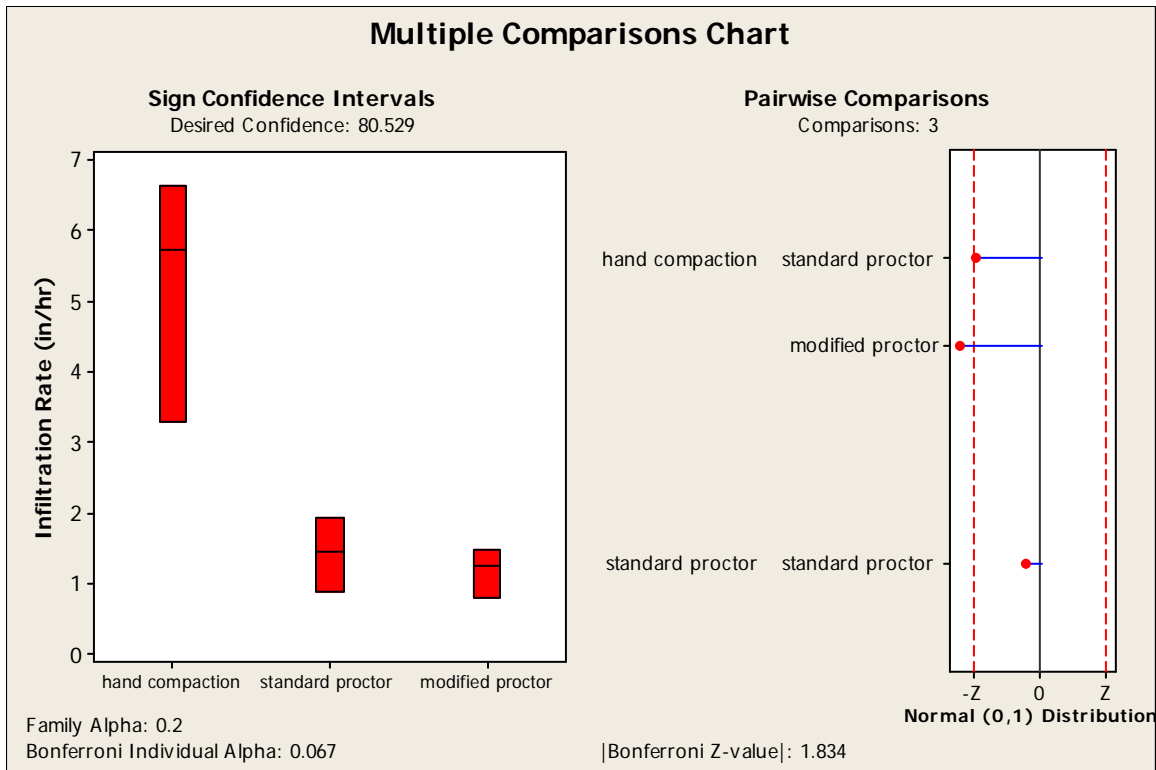


Figure 79. Multiple Comparison Plots of Laboratory Infiltration Measurements Using 10% Sand and 90% Biofilter Media Mixture.

A similar approach was used to distinguish the differences in paired saturated infiltration rates of hand compaction, standard proctor, and modified proctor compaction method for the 10% sand and 90% biofilter media mixtures. Figure 79 shows the multiple comparisons of saturated infiltration rates for 10% sand and 90% biofilter media mixture. The figure shows that there are statistically significant differences between saturated infiltration rates of hand compaction and modified proctor compaction. However, there are no statistically significant differences between saturated infiltration rates of standard proctor and modified proctor compaction conditions.

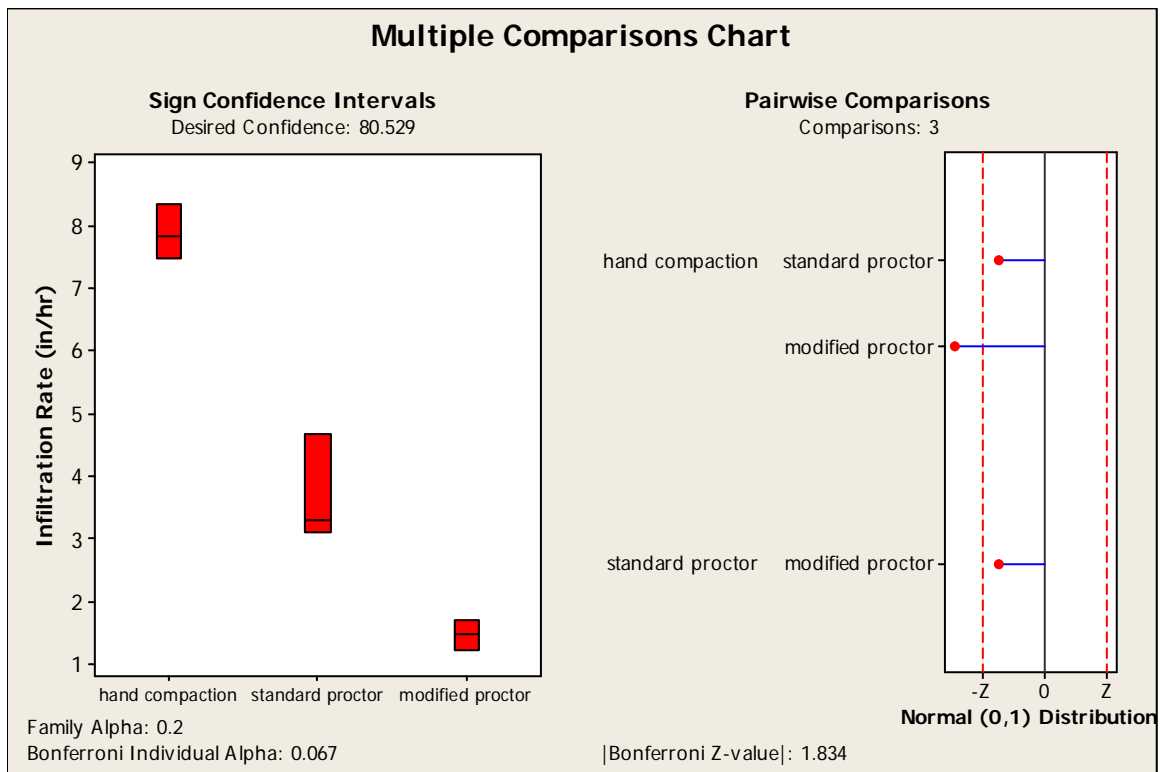


Figure 80. Multiple Comparison Plots of Laboratory Infiltration Measurements Using 25% Sand and 75% Biofilter Media Mixture.

A similar approach was used to distinguish the differences in paired saturated infiltration rates of hand compaction, standard proctor, and modified proctor compaction conditions for the 25% sand and 75% biofilter media mixtures. From Figure 80, it is seen that the saturated infiltration rate with hand compaction are larger than the saturated infiltration rates with standard proctor and modified proctor compaction. The figure shows that there are statistically significant differences between saturated infiltration rates for hand compaction and modified proctor conditions. However, there are no statistically significant differences between saturated infiltration rates for standard proctor and modified proctor compaction conditions.

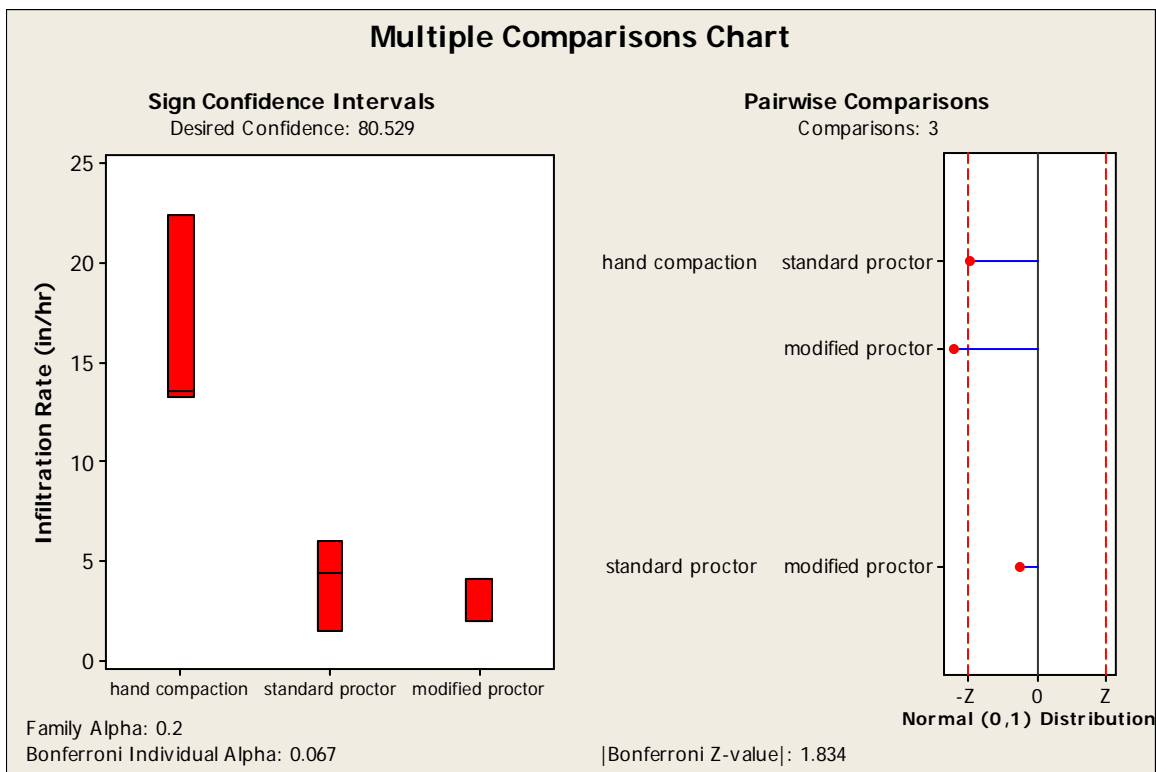


Figure 81. Multiple Comparison Plots of Laboratory Infiltration Measurements Using 50% Sand and 50% Biofilter Media Mixture.

A similar approach was used to distinguish the difference in paired saturated infiltration rates for hand compaction, standard proctor, and modified proctor compaction conditions for the 50% sand and 50% biofilter media mixture. Figure 81 shows the multiple comparisons of saturated infiltration rates for 50% sand and 50% biofilter media mixtures. The figure shows that there are statistically significant differences between saturated infiltration rates for hand compaction and modified proctor conditions. There are no significant differences in the saturated infiltration rates between standard proctor and modified proctor compaction conditions.

The Kruskal-Wallis test was used to distinguish the difference in paired saturated infiltration rates for different percentages of peat and biofilter media and standard proctor compaction conditions. Figure 82 shows the multiple comparisons of saturated infiltration rates with varying amounts of peat amendments (Table 55). The figure shows that there are statistically significant differences between saturated infiltration rates of biofilter soil vs 50% peat and 50% biofilter soil mixture. There are no significant differences in the saturated infiltration rates between biofilter soil only vs 10% peat and 90% biofilter soil mixture; 25% peat and 75% biofilter soil mixture; 50% peat and 50% biofilter soil mixture. Significant differences in the infiltration rates therefor require relatively large differences in peat additions.

Table 55. Various Mixtures of Biofilter Soil Media and Peat Used for Laboratory Infiltration Measurements.

Biofilter media			
1	2	3	4
biofilter soil only ($\rho = 1.66 \text{ g/cc}$)	10% peat and 90% biofilter soil ($\rho = 1.64 \text{ g/cc}$)	25% peat and 75% biofilter soil ($\rho = 1.52 \text{ g/cc}$)	25% peat and 75% biofilter soil ($\rho = 1.23 \text{ g/cc}$)
1.0	2.8	2.8	5.2
1.0	1.9	2.0	3.5
0.5	1.8	2.0	2.1

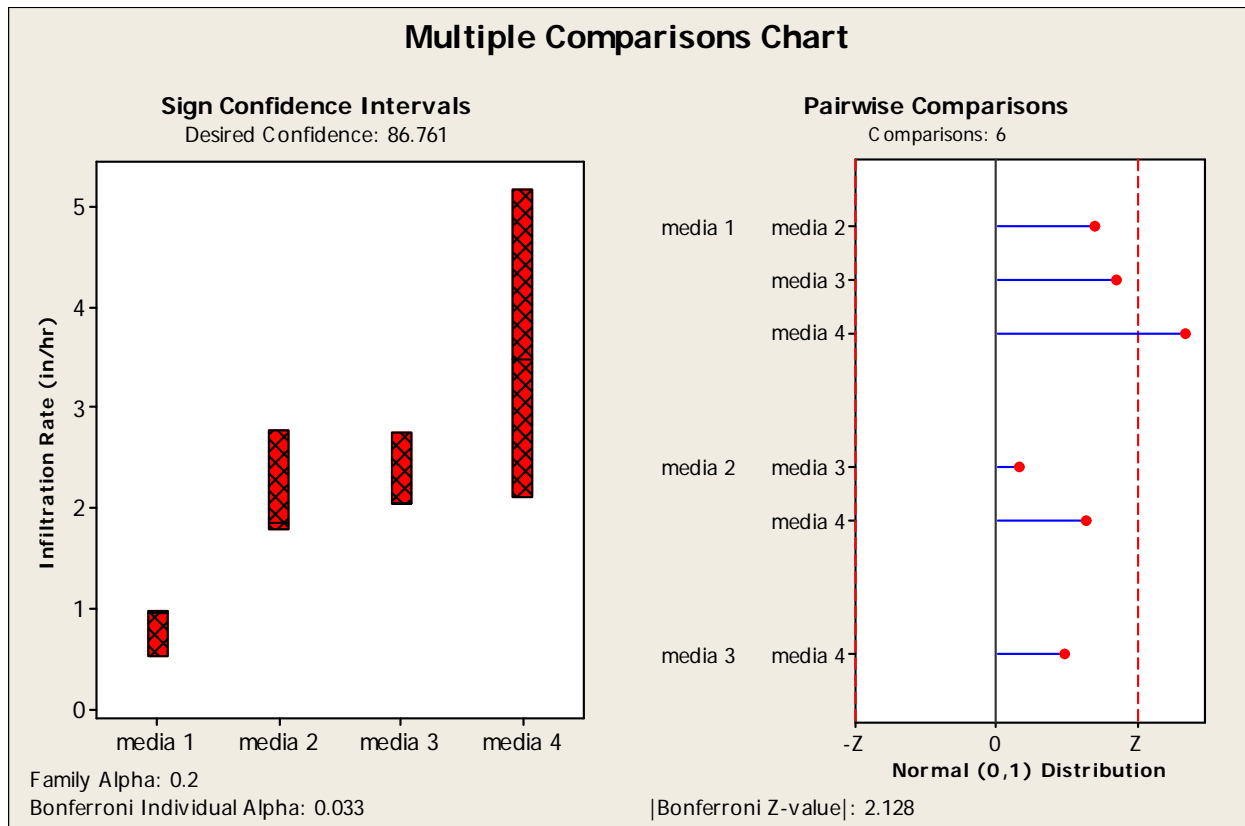


Figure 82. Multiple Comparison Plots of Laboratory Infiltration Measurements Using Biofilter Soil Only vs Different Percentages of Peat Added to It.

5.6 Chapter Summary

The laboratory column test results indicated that the infiltration rates through all mixtures of biofilter media and filter sand are greater than the infiltration rates through the biofilter media alone for the three levels of compaction (hand compaction, standard proctor, and modified proctor). The column test results for the biofilter soil alone and with varying amounts of added peat, using the standard proctor compaction method, also indicated benefits by adding peat to the biofilter media material. Mixing the biofilter media with filter sand and peat improved the infiltration capacity of the media and also reduced the impact of compaction on the infiltration rates. The mixture containing 50% biofilter media and 50% filter sand (the largest sand addition

tested) exhibited the highest infiltration rates, as expected (final saturated infiltration rates of 2.7 and 16.4 in/hr for the modified proctor and hand compaction tests respectively).

Peat amendment improves aeration and water holding capacity for plant roots, resulting in better growth. However, peat soils are more sensitive to compaction than other type of soils. Sand filters generally improve drainage by lending porosity to a mix and retain moisture. Sand amendment can add needed weight to peat and fill large pore spaces without impairing drainage. It is important that stormwater practice designers determine the subsoil characteristics before designing stormwater treatment facilities and consider the use of added amendments (sand and peat) to the soils.

The laboratory test results also demonstrated that soil compaction has dramatic effects on the infiltration rates; therefore care needs to be taken during the construction of biofilter stormwater treatment facilities to reduce detrimental compaction effects. The infiltration values from the ponded locations are very small compared to the laboratory and field test infiltration values, indicating fully saturated media under moderately to severely compacted conditions.

The in-situ infiltration measurements need to be evaluated carefully. The ponded water measurements in the biofilter were obtained after complete saturation. Also, ponding was not even throughout the biofilter, and preferentially pooled in areas having depressions and with low infiltration capacities. Because they were in depressions, silting may have also occurred in those areas. Long-term and continuous monitoring in a biofilter during rains is the best indication of performance, and these spot checks likely indicate the lowest values to occur. In fact, they were similar to the lowest infiltration rates observed with the small-scale infiltrometers and also corresponded to the compacted media column tests. Data from the infiltrometers also need to be cautiously evaluated as they also show very high rates that only occur during the initial portion

of the event under unsaturated conditions. Most of the infiltration in biofilters likely occurs after saturated conditions and the lowest rates observed may be most representative of actual field conditions.

CHAPTER 6

6. SOIL MEDIA CHARACTERISTICS OF PROPOSED STORMWATER BIOINFILTRATION CONSTRUCTION SITES

6.1 Introduction

Bioinfiltration devices are a potentially effective option for the treatment of stormwater runoff from urban areas, as well as a discharge location if groundwater and soil conditions are suitable. However, the performance of these systems is affected by characteristics of the treatment media and the underlying soils, such as texture, structure and porosity (compaction). Small scale, rapid, tests are needed to quickly inventory soil conditions in areas undergoing planning following natural disasters, or to meet short schedules associated with accelerated construction goals.

There are increasing interests in the use of infiltration practices for managing stormwater, as these systems promote groundwater recharge, reduce runoff peak flow rates and volumes, and can reduce pollutant discharges to surface water bodies. Infiltration practices recharge stormwater directly to groundwater and can potentially contaminate groundwater supplies with pollutants contained in the stormwater or mobilized from subsurface contamination. Infiltration practices are not appropriate in areas that contribute high concentrations of sediment, hydrocarbons, or other floatables without adequate pretreatment to protect the device (Connecticut 2004).

Infiltration practices are becoming more common in many residential and other urban areas to compensate for the decreased natural infiltration areas associated with land

development, but must also consider local soil conditions to be most effective (Pitt et al., 2002 and 2008). Infiltration facilities, which historically have included percolation ponds, dry wells, and infiltration galleries, are designed to capture and directly discharge the runoff to the groundwater rather than to discharge to surface water (Massman, 2003). Properly designed and constructed infiltration facilities can be one of the most effective flow control (and water quality treatment) stormwater control practices, and should be encouraged where conditions are appropriate (Ecology, 2005). However the performance of stormwater infiltration systems can be affected by factors such as texture, structure and degree of compaction of the media during their construction.

Infiltration facilities have the greatest runoff reduction capabilities of any stormwater control practices and are suitable for use in residential and other urban areas where measured soil infiltration rates are suitable. Many guidance manuals specify acceptable minimum infiltration rates, (such as 0.5 in/ hr, or 1cm/hr, as specified by VA DCR, 2010). However, the design of these facilities is particularly challenging because of the large uncertainties associated with predictions of both short-term and long-term infiltration rates (Massman, 2003). Infiltration rates cannot be estimated solely on the basis of soil types (grain size texture) or saturated hydraulic conductivity, but other site-specific characteristics need to be considered to accurately design infiltration facilities (Massman, 2003). Small-scale infiltrometers measure short-term infiltration rates which apply only to the initiation of the infiltration process (Philips, 2011). Factors such as infiltrate quality, frequency of infiltration system maintenance and site variability will affect long-term (design) infiltration rates.

Understanding the physical and hydrologic properties of different bioretention media mixtures, as well as their response to compaction, may increase the functional predictability of

bioretention systems and thus improve their design (Pitt et al., 2002 and 2008; Thompson et al., 2008). Premature clogging by silt is usually responsible for early failures of infiltration devices, although compaction (during either construction or use) is also a recognized problem (Pitt et al., 2002 and 2008). Pitt et al., (1999b) found substantial reductions in infiltration rates due to soil compaction, especially for clayey soils.

Compaction was seen to have about the same effect as moisture saturation for clayey soils, with saturated and compacted clayey soils having very little effective infiltration rates (Pitt et al., 1999b and 2008). Sandy soils can still provide substantial infiltration capacities, even when greatly compacted, in contrast to soils containing large amounts of clays that are very susceptible to compaction's detrimental effects. In a similar study, Gregory et al. (2006) examined the effects of compaction on infiltration rates at urban construction sites in north-central Florida. Infiltration was measured in noncompacted and compacted soils from three land types (natural forest, planted forest, and pasture sites). Although infiltration rates varied widely across the three land types, construction activity reduced infiltration rates by 70 to 99 percent at all sites.

Soil amendments (such as organic composts) improve soil infiltration rates and water holding characteristics and add protection to groundwater resources, especially from heavy metal contamination in urban areas (Pitt et al., 1999a and 1999b). Groundwater contamination problems were noted more often in commercial and industrial areas that incorporated subsurface infiltration and less often in residential areas where infiltration occurred through surface soil (Pitt et al., 1999a and Clark et al., 2006). However, pretreatment of stormwater runoff before infiltration can reduce groundwater contamination of many pollutants and also prolong the life of the infiltration device.

This chapter describes both laboratory and field-scale studies conducted to provide insight into the existing soil characteristics at typical potential stormwater bioinfiltration sites and how susceptible they are to compaction and how they respond to simple soil amendments. The test sites are located in areas which were severely affected by the April 27, 2011 tornado that devastated the city of Tuscaloosa, AL, and are undergoing reconstruction. During these studies, four surface double-ring infiltration tests (comprised of three separate setups each) and three large borehole infiltration measurements were conducted in the field to determine the surface infiltration characteristics and the subsurface infiltration characteristics (located at the depths at the bottom of proposed bioinfiltration devices). The effects of different compaction levels on the infiltration rates through the soil media were also examined during controlled laboratory column tests. Three levels of compaction were used to modify the density of the column media samples during the tests: hand compaction, standard proctor compaction, and modified proctor compaction. Figure 83 shows the flow sheet for these field and lab infiltration tests.

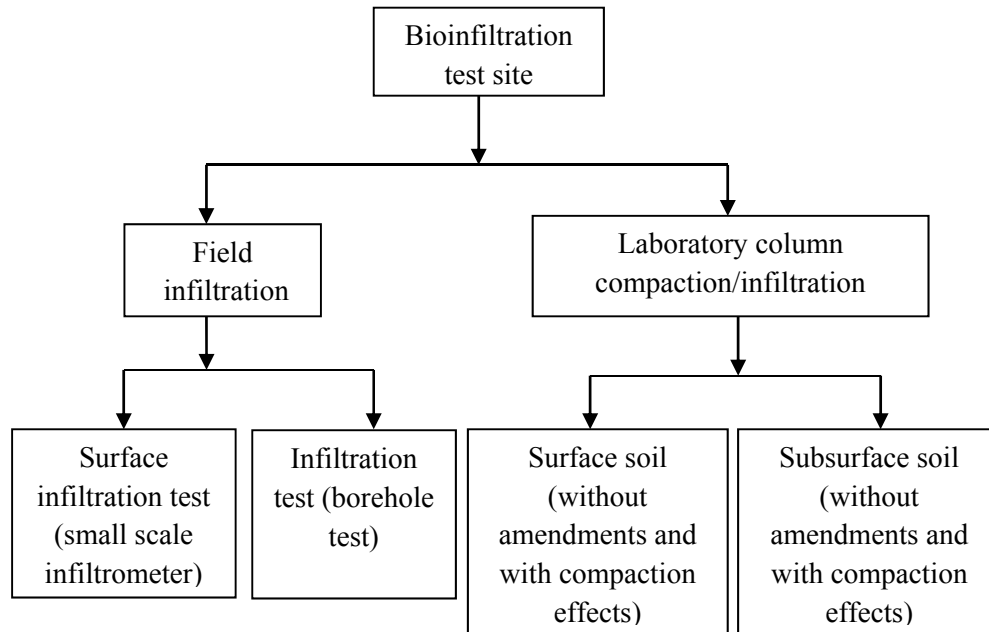


Figure 83. Flow Sheet for the Field and Lab Infiltration Study at Bioinfiltration Sites.

6.2 Description of Test Site and Methodology

6.2.1 Description of Test Sites

The proposed bioinfiltration test sites are located at:

- 1) McDonalds on 15th St. E and 6th Ave. E., Tuscaloosa, AL (Figure 84).
- 2) 17th Ave. E. and University Blvd E. (Tuscaloosa Physical Therapy), Tuscaloosa, AL.
- 3) 21st Ave. E. and University Blvd E. (Alberta Hand Carwash), Tuscaloosa, AL.
- 4) 25th Ave. E and University Blvd E. (O'Reilly Auto Parts), Tuscaloosa, AL.

The test sites are all located adjacent to fire hydrants for easy access to large quantities of water for the pilot-scale bore hole tests and are located on the city's right-of way.



Figure 84. Aerial Photograph of Bioinfiltration Site, McDonalds on 15th St. E and 6th Ave. E., Tuscaloosa, AL, Pre-Tornado (Map by Google Map).



Figure 85. View of a Tornado Affected Area near McDonalds on 15th St. E and 6th Ave. E., Bioinfiltration Site.

6.2.2 Field Surface Infiltration Study at Proposed Bioinfiltration Site

Four surface double-ring infiltration tests (comprised of three separate setups each) were conducted in the field to determine the surface infiltration characteristics. Turf-Tec infiltrometers (Turf Tec 1989) were used to measure the surface infiltration rates at four test locations where

reconstruction with stormwater infiltration controls are planned. These small devices have an inner chamber about 2.5 inches (64 mm) in diameter and an outer ring about 4.5 inches (110 mm) in diameter. The infiltrometers were gently pushed into the surface of the soil until the “saturn” ring was against the soil surface (Figure 86). Relatively flat areas were selected in the test sites to install the Turf-Tec infiltrometers and small obstacles such as stones and twigs were removed. Three infiltrometers were inserted within about 3ft (1 m) from each other to measure the variability of the infiltration rates of the soil media in close proximity. After the soil was inspected and sealed around each ring to make sure that it was even and smooth, clean water was poured into the inner chamber and allowed to overflow and fill up the outer ring (Figure 86). The decreasing water levels in the inner chamber were recorded during a period of one to two hours until the infiltration rates become constant.

The rate of decline in the water level (corresponding to the infiltration rate) was measured by starting the timer when the water was poured in the inner chamber with the pointer at the beginning of the depth scale. Additional water was periodically added to the inner chamber and outer ring when the level in the inner chamber dropped to within about an inch of the ground surface to maintain pooled water. The change in water level and elapsed time were recorded since the beginning of the first measurement. The measurements were taken every five minutes at the beginning of the test and less frequently as the test progressed until the rate of infiltration was considered constant. The tests were conducted for a period of one to two hours, until the infiltration rate become constant. The infiltration rate was calculated from the rate of fall of the water level in the inner chamber. Figure 86 through 89 shows the surface infiltration measurements at the sites selected for this study.



Figure 86. Aerial Photograph of Bioinfiltration Site, Double-ring and Borehole Infiltration Test Installation at McDonalds on 15th St. E and 6th Ave. E., Tuscaloosa, AL.



Figure 87. Aerial Photograph of Bioinfiltration Site and Double-ring Infiltration Measurement Installation on 17th Ave. E. and University Blvd. E. (Tuscaloosa Physical Therapy).



Figure 88. Aerial Photograph of Bioinfiltration Site, Double-ring Infiltration and Borehole Measurement Installations on 21st Ave. E. and University Blvd. E. (Alberta Hand Carwash).



Figure 89. Aerial Photograph of Bioinfiltration Site, Double-ring Infiltration and Borehole Measurement Installations on 25th Ave. E. and University Blvd E. (O'Reilly Auto Parts).

6.2.3 Water Content and Density Measurements of Surface Soil Media at Bioinfiltration Site

In-situ soil density measurements were also taken in the same general locations as the infiltration measurements. A small hole, about six inches (15 cm) deep and six inches (15 cm) wide, was carefully hand dug to avoid disturbance of the soil. The hole's side and bottom were also carefully smoothed. All of the soil excavated from each hole was placed into separate Ziploc plastic bags to retain soil moisture. Sand was then poured into the hole from a graduated cylinder to measure the volume of the holes, up to the top of the soil that was removed from the test hole in the bioinfiltration sites. The excavated soil media was then transported to The University of Alabama environmental lab for further analyses. The soil media was weighed moist, dried at 105°C, and weighed again when dry. The dry density and moisture content (percent) of the soil media collected from each test locations were determined, as shown in Table 56. The density of the soil was determined by dividing the mass of oven-dried soil by the sand volume used to re-fill the hole. The soil moisture content (%) was determined by the ratio of the difference between the moist and the dry weights of the soil (corresponding to the water mass) to the mass of the oven-dried soil. The particle size distributions of the soil media excavated from the surface and subsurface of the proposed stormwater bioinfiltration sites (determined using standard sieving procedures) are shown in Figure 90 and 91, and the median size and uniformity coefficient (the ratio of the 60th to the 10th percentile particle sizes) are also shown on Table 56 and 57 for the different test soil media samples.

Table 56. Soil Media Characteristics Obtained from the Surface of Bioinfiltration Sites.

Test locations	median size D ₅₀ (mm)	uniformity coefficient (C _u)	Dry bulk density (g/cm ³)	moisture content (%)
McDonalds on 15 th St. and 6 th Ave.	0.7	75	1.88	17.3
17 th Ave. E. and University Blvd E.	0.4	37	1.66	19.8
21 th Ave. E. and University Blvd E.	0.4	12	1.61	12.3
25 th Ave. E. and University Blvd E.	0.3	6	1.66	14.2

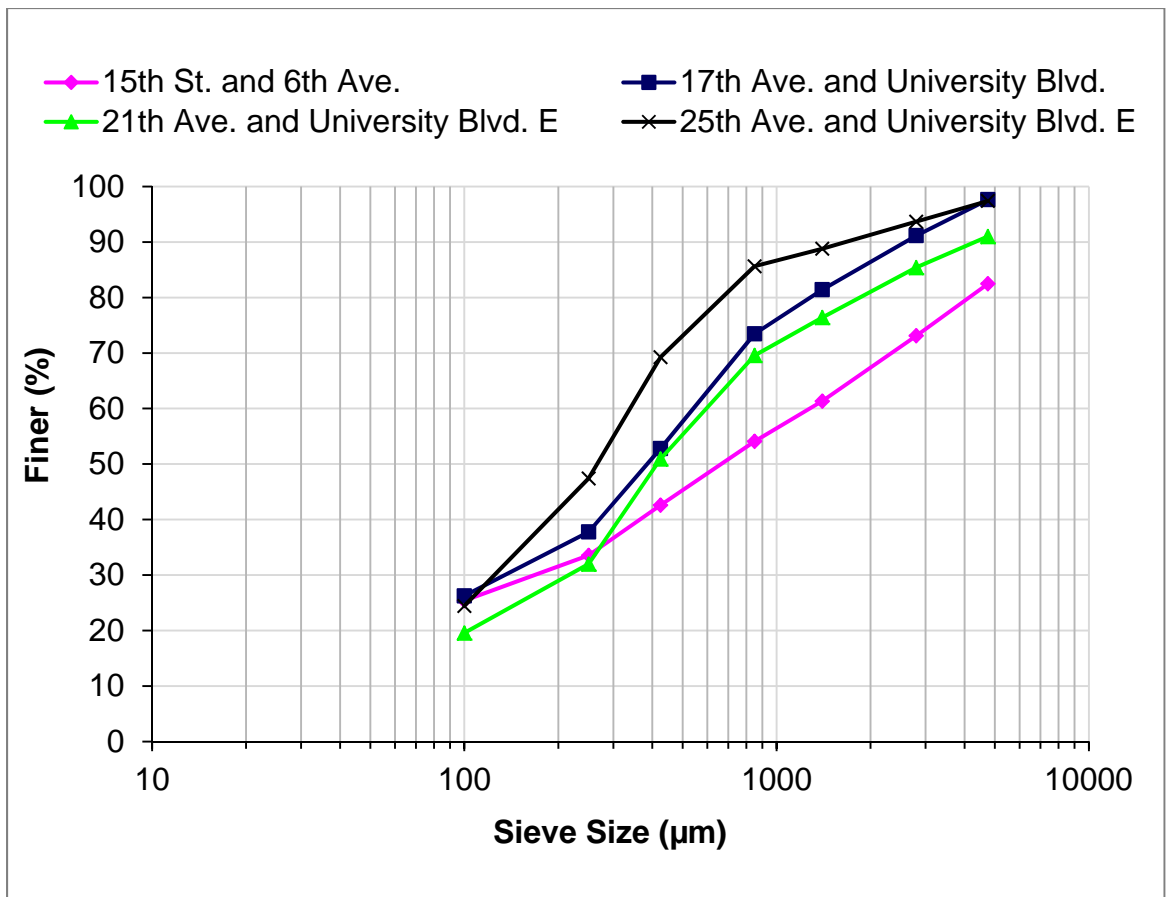


Figure 90. Particle Size Distributions for the Surface Soil Media from Bioinfiltration Sites.

Table 57. Soil Media Characteristics Obtained from the Subsurface of Bioinfiltration Sites.

Test locations	median size D ₅₀ (mm)	uniformity coefficient (C _u)
17 th Ave. E. and University Blvd E.	0.6	22.2
21 th Ave. E. and University Blvd E.	0.4	10.4
25 th Ave. E. and University Blvd E.	1.3	33.3

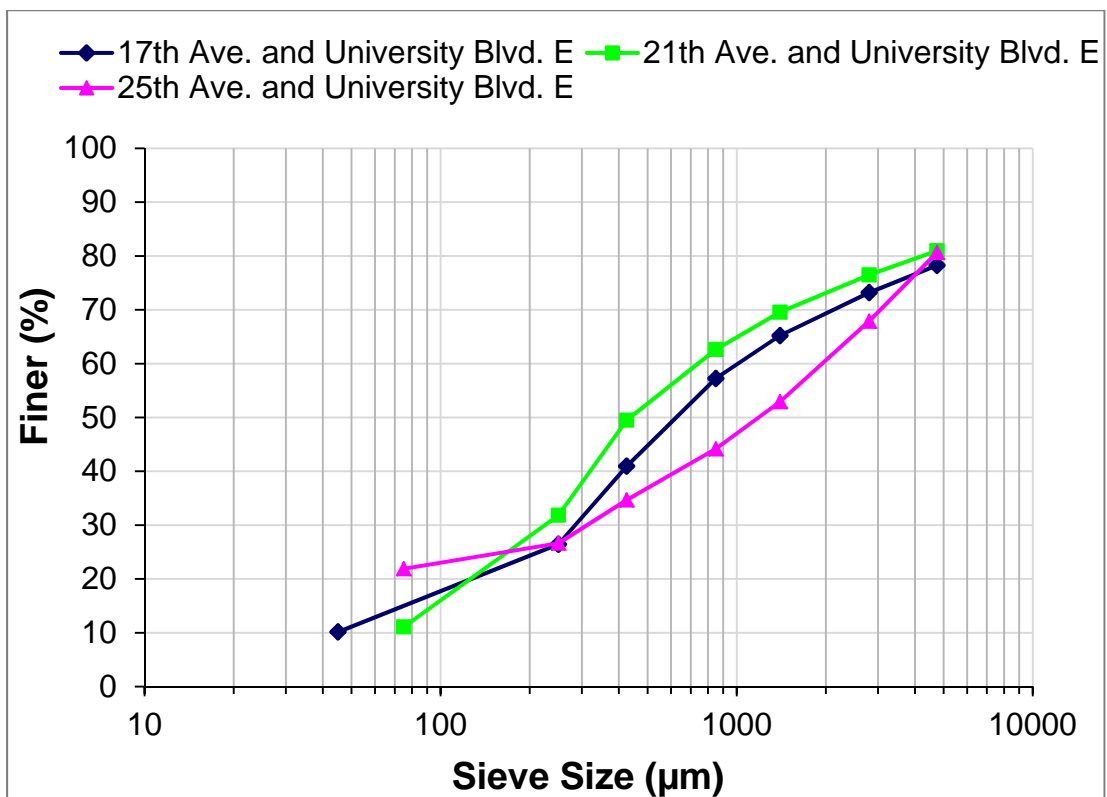


Figure 91. Particle Size Distributions for the Subsurface Soil Media from Bioinfiltration Study Sites.

6.2.4 Borehole Infiltration Tests

Large-scale borehole tests were also conducted at each location to indicate subsurface infiltration rates, especially under more typical saturated conditions. The borehole tests required boring a hole and placing a Sonotube cardboard concrete form into the hole to protect the hole sides. A 2 ft (0.6 m) to 3 ft (0.9m) diameter auger was used to create holes about 3 ft (0.9 m) to 4 ft (1.2 m) deep (depending on subsoil conditions) as shown in Figure 92 and 93. An approximate 5 ft (1.5 m) length of Sonotube was inserted in the boreholes to maintain structural integrity. The bare soil at the bottom of the tube was roughened to break up any smeared soil and back-filled with a few inches of coarse gravel to prevent the native soil erosion during water filling. During the tests, these boreholes were filled with water from the fire hydrants and the water elevations were measured with time until the infiltration rates reached an approximate steady rate.



Figure 92. Borehole Marking, Borehole Drilling, Double-ring and Borehole Infiltration Measurement Installations at McDonalds on 15th St. and 6th Ave. Ave. E., Tuscaloosa, AL.



Figure 93. Borehole Marking, Borehole Drilling, and Borehole Infiltration Measurement Installations on 21th Ave. and University Blvd E. (Alberta Hand Carwash).

6.3 Laboratory Column Tests

Controlled laboratory column tests were conducted using surface and subsurface soil samples collected at the borehole test locations for three different compaction levels (hand compaction, standard proctor compaction, and severe modified proctor compaction) to see if depth of the test and response to compaction affected the infiltration results.

Four-inch (100 mm) diameter PVC pipes (Charlotte Pipe TrueFit 4 in. PVC Schedule 40 Foam-Core Pipe) 3 ft (0.9 m) long, purchased from a local building supply store in Tuscaloosa, AL were used for these tests as shown in Figure 94. The bottom of the columns had a fiberglass window screen (about 1 mm openings) secured to contain the media and were placed in funnels. The columns were filled with about 2 inches (5 cm) of cleaned pea gravel purchased from a local supplier. To separate the gravel layer from the soil layer, the coarse fiberglass window screen was placed over the gravel layer and then filled with the soil media brought from the test sites. The media layer was about 1.5 ft (0.46 m) thick.

Three levels of compaction were used to modify the density of the column soil samples during the tests: hand compaction, standard proctor compaction, and modified proctor compaction. Both standard and modified proctor compactions follow ASTM standard (D 1140-54). The standard proctor compaction hammer is 24.4 kN and has a drop height of 12 in (300 mm). The modified proctor hammer is 44.5 kN and has a drop height of 18 in (460 mm). For the standard proctor setup, the hammer is dropped on the test soil 25 times on each of three soil layers, while for the modified proctor test, the heavier hammer was also dropped 25 times, but on each of five soil layers. The modified proctor test therefore results in much more compacted soil, and usually reflects the most compacted soil observed in the field. The hand compaction is done by gently hand pressing the soil media to place it into the test cylinder with as little compaction as possible, with no voids or channels. The hand compacted soil specimens therefore have the least amount of compaction. The densities were directly determined by measuring the weights and volume of the soil material added to each column. The infiltration rates through the soil media were measured in each column using municipal tap water. The surface ponding depths in the columns ranged from 11 in (28 cm) to 14 in (36 cm), corresponding to the approximate

maximum ponding depth at the site biofilter. The freeboard depth above the media to the top of the columns was about 2 in (5 cm) to 3 in (7.5 cm). Infiltration rates in the soil media were determined by measuring the rates with time until apparent steady state rates were observed. The laboratory column setup for the infiltration measurements in the different media is shown in Figure 94.



Figure 94. Laboratory Setup for Nine Soil Infiltration Test Columns.

6.4 Results

6.4.1 Surface and Subsurface Soil Nutrient Reports from Bioinfiltration Study Sites

Soils vary greatly in water-holding capacity and infiltration rate. Silt, clay soils and those high in organic matter can hold much more water than sandy soils. Soils with high water-holding capacities require less frequent irrigation than soils with low water-holding capacities (Vegetable Crop Handbook 2010). Planting soil should be capable of supporting a healthy vegetative cover.

Soil test analyses results typically indicate whether a nutrient level in the soil is low, medium (moderate) or high (adequate). The nutrient rating depends on the soil group and the crop. Samples of soil extracted from the surface and subsurface of the proposed bioinfiltration study sites were also delivered to Auburn University’s Soil Testing Laboratory, where soil texture (% sand, % silt, and % clay), organic matter, and general nutrients were also analyzed. Summary of the surface and subsurface soil texture and nutrient reports are shown in Tables 58 and 59. The surface and subsurface soils from the four bioinfiltration sites have clay content greater than 20% and 13% respectively, as shown in Table 58.

Table 58. Summary of the Surface and Subsurface Soil Texture Reports for Bioinfiltration Sites.

Surface Soil Texture Report					
Bioinfiltration study site location	Percent (%)			Textural Class	H ₂ O availability
	Sand	Silt	Clay		cm ³ /cm ³
McDonalds on 15 th St. and 6 th Ave.	42.5	30	27.5	Clay Loam	0.12
17 th Ave. and University Blvd E.	50	30	20	Loam	0.12
21 th Ave. and University Blvd E	58.75	17.5	23.75	Sandy Clay Loam	0.10
25 th Ave. and University Blvd E.	70	10	20	Sandy Clay Loam	0.09
Subsurface Soil Texture Report					
Bioinfiltration study site location	Percent (%)			Textural Class	H ₂ O availability
	Sand	Silt	Clay		(cm ³ /cm ³)
17 th Ave. and University Blvd E.	55.00	37.50	7.50	Sandy Loam	0.13
21 th Ave. and University Blvd E	67.50	22.50	10.00	Sandy Loam	0.10
25 th Ave. and University Blvd E.	52.50	25.00	22.50	Sandy Clay Loam	0.11

According to the UA laboratory tests, the median size of the surface soil samples ranged from 300 to 700 μm, and in-situ density measurements indicated surface dry density values of about 1.7 g/cm³, corresponding to severely compacted conditions (close to “modified”

compaction conditions for this media). The median size of the subsurface soil samples ranged from 400 to 1,300 μm .

Auburn University's Soil Testing Laboratory uses the critical soil test nutrient concentrations concept defined by the Soil Science Society of America where the critical concentration occurs when 95% of the maximum relative crop yield is achieved. Organic matter improves soil structure and soil tilth, and helps to provide a favorable medium for plant growth. Soils with large amounts of clay generally require large amounts of organic matter. Soils with a higher organic matter content will have a higher cation exchange capacity (CEC), higher water holding capacity, and better tilth than soils with a lower organic matter content. Soils in the Central Great Plains have organic contents ranging between 1 and 2% for cultivated soils, and about 1.5 to 3.0 % for native grasslands (Bowman, 1996). Generally, healthy soil has between 3 and 5% organic material. The organic matter content of the surface and subsurface soils from the test locations have an average value of 4.1% and 3.1% respectively, indicating the soil is in good condition.

The cation exchange capacity (CEC) of a soil is a measurement of its ability to bind or hold exchangeable cations. The surface and subsurface soil obtained from the test sites had an average CEC value of 12.5 meq/100g and 22.5 meq/100g respectively. The surface and subsurface soil obtained from the test sites had an average pH of 7.1 and 7.4 respectively. Typically CEC values, as defined by the Auburn University Soil Testing Laboratory (Mitchell and Huluka, 2011), vary from soil to soil, with sandy soils generally having CEC values ranging from 0 to 4.6 meq/100g and loam soils having CEC values ranging from 4.6 to 9.0 meq/100g. According to the Alabama Cooperative Extension System, the ideal soil pH value for most crops ranges between 5.8 and 6.5 and for acid loving plants ranges between 5.0 and 5.7. When soil pH

is outside of these optimal ranges, nutrients can be less available to plants, potentially resulting in deficiencies.

The surface soil obtained from the four bioinfiltration test sites had an average phosphorus concentration of 26 ppm and ranged from 12 to 52 ppm. The subsurface soil from the bioinfiltration sites had phosphorus concentration values of 10, 19, and < 0.1 ppm. The critical phosphorus concentration for crops (peanuts, pine trees, blueberries and centipedegrass) grown in sandy soil in Alabama is 9.5 ppm, whereas for all other crops, is 25 ppm. The surface soil had an average potassium, magnesium, and calcium concentrations of 101, 201, and 2,071 ppm respectively. The subsurface soil had an average potassium, magnesium, and calcium concentrations of 172, 293, and 3,752 ppm respectively. The critical magnesium level for all crops grown in sandy soil in Alabama as used by the Auburn University Soil Testing Laboratory is about 13 ppm, whereas the critical calcium level for crops such as tomatoes, peppers, fruits and nuts grown in sandy soils is 250 ppm. The surface soil had a higher concentration of calcium and magnesium for most crops grown in sandy and loam soils in Alabama. Sodium Adsorption Ratio (SAR) describes the proportion of sodium to calcium and magnesium in soil solution (Sonon et al 2012). The sodium content of soil affects soil texture and pH. The surface and subsurface soil obtained from the bioinfiltration study sites had an average SAR value of 0.23 and 0.9 respectively. An SAR value of 15 or greater indicates an excess of sodium will be adsorbed by the soil clay particles, potentially causing severe infiltration reductions (Curtis 2010). Summaries of surface and subsurface soil nutrient report are shown in Table 59.

Micronutrients, such as boron, zinc, manganese, copper, molybdenum, iron, and chloride, are needed in much smaller quantities, and most Alabama soils contain adequate amounts for most crops (Adams and Mitchell 2000). Some Alabama crops may use between 20 and 200

pounds per acre of N, P, K, Ca, Mg and S, they use less than 1 pound per acre of micronutrients (Adams and Mitchell 2000).

Table 59. Summary of the Surface and Subsurface Soil Nutrient Report for Bioinfiltration Sites.

Nutrient (ppm)	Surface Soil Nutrient Report				Subsurface Soil Nutrient Report		
	15 th St. and 6 th Ave.	17 th Ave. and University Blvd E.	21 th Ave. and University Blvd E.	25 th Ave. and University Blvd E.	17 th Ave. and University Blvd E.	21 th Ave. and University Blvd E.	25 th Ave. and University Blvd E.
Calcium (Ca)	4,054	1,198	1,835	1,197	1,419	3,966	5,872
Potassium (K)	77	113	114	100	204	190	121
Magnesium (Mg)	188	161	212	245	165	325	390
Phosphorus (P)	12	23	52	16	10	19	<0.1
Aluminum (Al)	101	155	183	118	231	228	29
Arsenic (As)	<0.1	<0.1	<0.1	<0.1	<0.1	<0.1	<0.1
Boron (B)	1.2	0.9	0.8	0.5	1	0.8	0.6
Barium (Ba)	8	9	9	9	4	4	4
Cadmium (Cd)	<0.1	<0.1	<0.1	<0.1	<0.1	<0.1	<0.1
Chromium (Cr)	<0.1	<0.1	<0.1	<0.1	<0.1	<0.1	<0.1
Copper (Cu)	<0.1	<0.1	<0.1	<0.1	4	4	4
Iron (Fe)	2	8	12	17	12	12	12
Manganese (Mn)	46	68	37	31	120	120	120
Molybdenum (Mo)	<0.1	<0.1	<0.1	<0.1	<0.1	<0.1	<0.1
Sodium (Na)	40	39	37	34	209	209	209
Nickel (Ni)	<0.1	<0.1	<0.1	<0.1	<0.1	<0.1	<0.1
Lead (Pb)	0.7	6	0.9	1	5	9	<0.1
Zinc (Zn)	9	51	9	9	30	125	1
Total Phosphorus (P)	223	354	273.3	193	235	205	164
	Nutrient (percent)				Nutrient (percent)		
Nitrogen (N)	0.18	0.23	0.15	0.15	0.14	0.11	0.08
Carbon (C)	3.51	2.77	1.9	1.24	1.52	1.71	2.59
Organic Matter (OM)	6	4.8	3.3	2.1	2.6	2.9	4.5
Sodium Adsorption Ratio (SAR)	0.2	0.3	0.2	0.2	1.40	0.79	0.59
pH	7.54	6.39	7.44	6.86	6.63	7.78	7.74
Cation Exchange Capacity (CEC) (meq/100g)	22.21	7.8	11.4	8.4	9.90	23.87	33.67

6.4.2 Field Surface and Subsurface Infiltration Test Results

Using the double ring infiltrometers, the saturated infiltration rates (of most significance when designing bioinfiltration stormwater controls) for all the test locations was found to average about 5.1 in/hr (13 cm/hr) for the 12 measurements and ranged from 2 in/hr (5 cm/hr) to 9 in/hr (23 cm/hr). The coefficient of variations was about 0.5. The variations of the observed surface infiltration rates among the test sites were relatively large, but all indicated large infiltration potentials. Variation of surface infiltration rates (about a factor of 2) were also observed along the bioinfiltration study site, as shown on Figure 95. Table 60 summarizes the double ring infiltrometer test results at different bioinfiltration study sites. Surface infiltration measurements fitted with Horton equation are shown in Appendix C.1 through C.5.

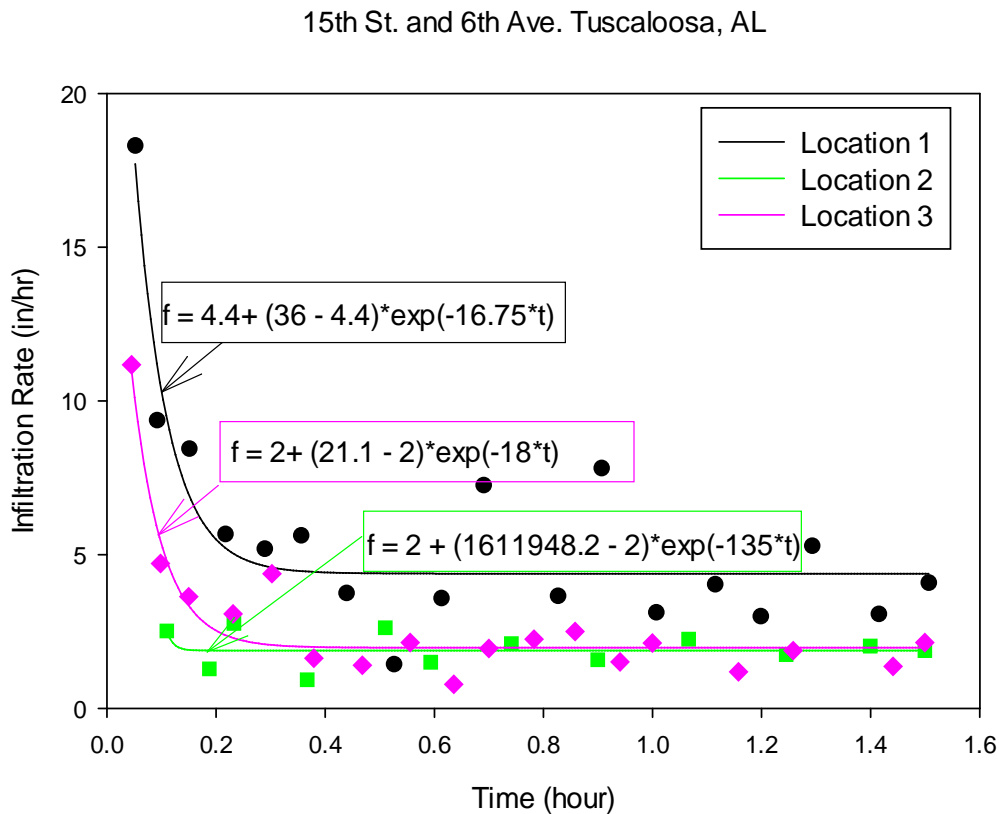


Figure 95. Example of Surface Infiltration Measurements Fitted With Horton Equation

Table 60. Double-ring Infiltration Measurement at Bioinfiltration Sites.

Horton's Parameter				
Test Site	Location	f_o (in/hr, cm/hr)	f_c (in/hr, cm/hr)	k (1/hr)
15 th St. and 6 th Ave. (density = 1.88 g/cc)	1	36 (91.2)	4.4 (11.1)	17
	2	n/a	1.9 (4.8)	135
	3	22 (56.2)	2 (5)	18
	mean	29 (73.7)	2.7 (7)	57
	COV	0.34	0.52	1.20
17 th Ave. and University Blvd E. (density = 1.66 g/cc)	1	9.5 (24.1)	6.5 (16.5)	2.0
	2	7.4 (18.8)	3.5 (8.8)	8.6
	3	101 (256)	2.9 (7.3)	44.4
	mean	39.2 (99.7)	4.3 (10.9)	18.4
	COV	1.36	0.46	1.24
21 th Ave. and University Blvd E. (density = 1.61 g/cc)	1	16.7 (42.5)	2.6 (6.6)	11
	2	17.1 (43.4)	8.2 (20.7)	13
	3	31 (78.6)	6.3 (16)	4.4
	mean	21.6 (54.8)	5.7 (14.4)	9.53
	COV	0.38	0.50	0.48
25 th Ave. and University Blvd E. (density = 1.66 g/cc)	1	26.3 (66.8)	9 (22.9)	0.69
	2	15.5 (39.4)	6.6 (16.8)	0.65
	3	36.3 (92.2)	7.4 (18.7)	16.91
	mean	26 (66.1)	7.7 (19.5)	6.08
	COV	0.40	0.16	1.54

* n/a values were beyond the data range

The average final infiltration rates and the coefficient of variation for the borehole infiltration tests were about 27.7 in/hr (70.4 cm/hr) and 0.4 respectively. The variations of the observed surface and subsurface infiltration rates along these test sites were also relatively large and showed larger infiltration potential. The initial rates from the subsurface tests were very large and are not indicative of actual rates that would be available for long during actual storm conditions. However, the long-term final rates measured at both the surface and subsurface locations indicated very good infiltration potentials. Obviously, care will need to be taken to prevent any compaction at the infiltration sites during construction. Table 61 summarizes the

subsurface infiltration test results at different bioinfiltration study sites. It is important that stormwater practice designers determine the subsoil characteristics before designing stormwater treatment facilities. Figure 96 shows subsurface infiltration measurements fitted with Horton equation.

Table 61. Borehole Infiltration Measurement at Bioinfiltration Sites.Horton's Parameter

Test Site Location	f_o (in/hr, cm/hr)	f_c (in/hr, cm/hr)	k (1/hr)
17 th Ave. and University Blvd E	n/a	15 (39)	22.5
21 th Ave. and University Blvd E	n/a	35(88)	4.8
25 th Ave. and University Blvd E	n/a	33 (84)	22.3
mean	n/a	28 (70)	16.5
COV	-	0.55	0.6

* n/a values were beyond the data range

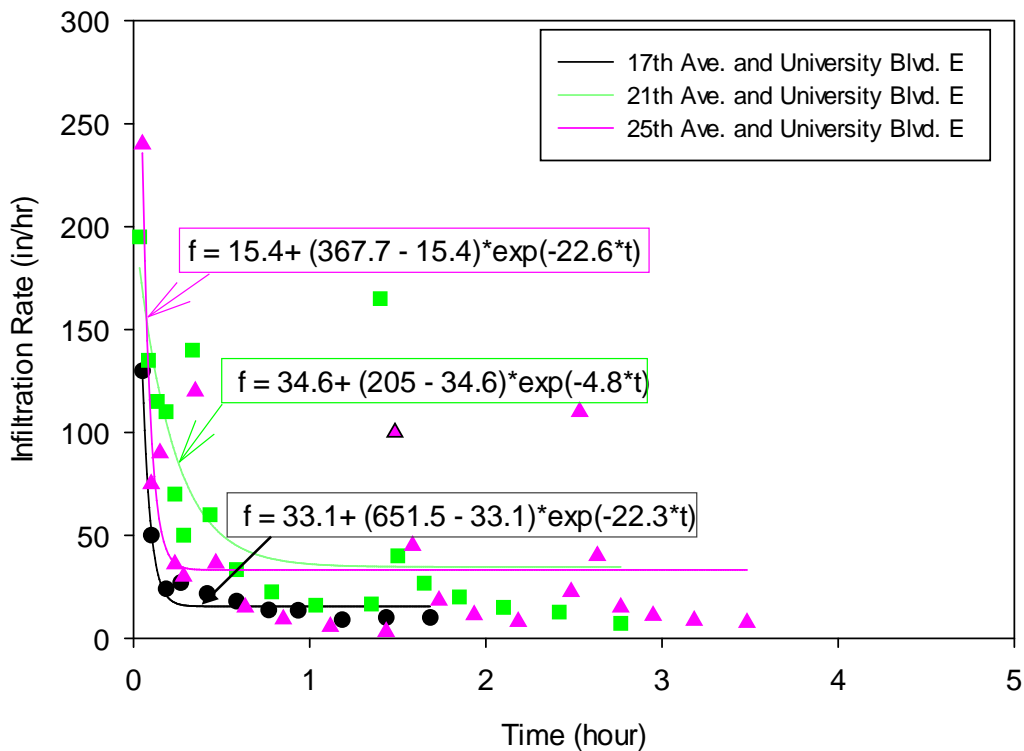


Figure 96. Example of Borehole Infiltration Measurements Fitted With Horton Equation.

6.4.3 Laboratory Column Infiltration Test Results Using Surface Soils

During the laboratory compaction/infiltration tests, the average final infiltration rates through the surface soil for the three levels of compaction were 9 in/hr (22.6 cm/hr), 1 in/hr (2.5 cm/hr), and 0.4 in/hr (1 cm/hr) using the hand compaction (little compaction), standard proctor compaction (typical compaction during construction activities) and modified proctor compaction methods (the most severe compaction level) respectively, at approximate 13 in. (330 mm) of head. The final infiltration rates of the hand compacted surface soil were reduced by 89 and 96 percent using standard proctor compaction and modified proctor compaction methods. The laboratory infiltration data for each individual test was fitted to the Horton's infiltration equation. Figure 97 shows examples of surface soil infiltration data fitted to the Horton's equation, and for different level of compaction values. The final saturated infiltration rates ranged from 2 to 20.6 in/hr and 0.1 to 1.7 in/hr for hand compaction and modified proctor compaction conditions respectively. This indicates that compaction had a significant impact on the infiltration rate of the soil. Laboratory infiltration measurements using surface soil fitted with the Horton's equations are shown in Appendix C.5 through C.8. Tables 62 through 65 summarize the column test results for the surface soil, and for different compaction values.

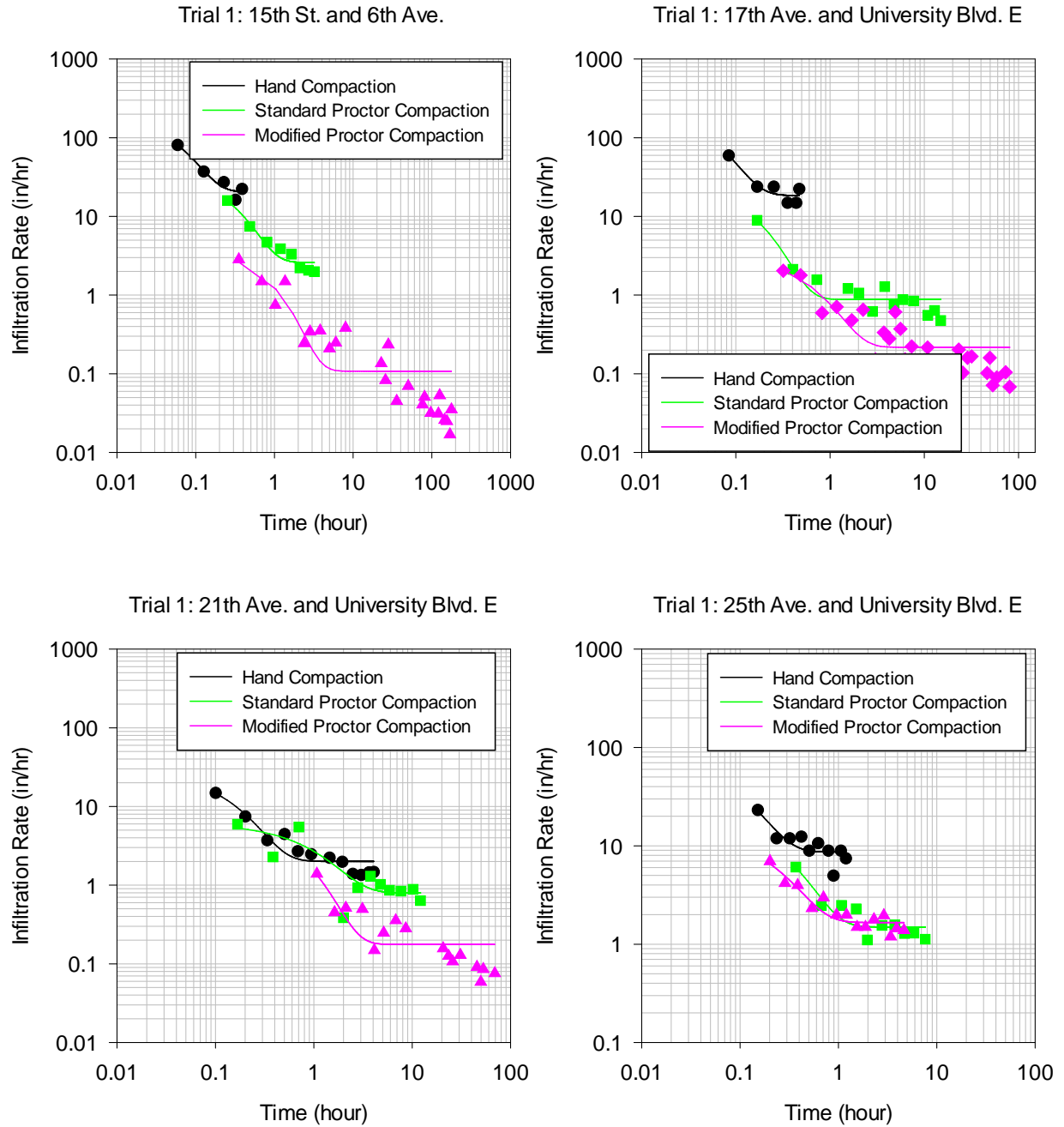


Figure 97. Example of Lab Infiltration Measurements Using Surface Soil Fitted with Horton's Equation.

Table 62. Laboratory Infiltration Tests Using Surface Soil on 15th St. E and 6th Ave. E. at Different Compaction Levels.

15 th St. and 6 th Ave. E				
Compaction method	Test	f _o (in/hr, cm/hr)	f _c (in/hr, cm/hr)	k (1/hr)
hand (density = 1.37 g/cc)	1	n/a	20.6 (52.3)	
	2	27 (70)	8.5 (21.6)	3.29
	3	133(338)	14.5 (36.8)	2.25
	mean	80	14.5 (36.9)	7.91
	COV	0.93	0.42	1.13
standard (density = 1.64 g/cc)	1	36 (92)	2.6 (6.6)	3.75
	2	n/a	1.6 (4.1)	18.36
	3	3.2 (8.2)	1.3 (3)	0.71
	mean	19.8 (50.3)	1.8 (4.6)	7.61
	COV	1.18	0.41	1.24
modified (density = 1.72 g/cc)	1	4 (10.2)	0.11(0.27)	1.23
	2	0.04 (0.11)	0.01(0.02)	0.01
	3	0.04 (09)	0.01(0.03)	0.03
	mean	1.4 (3.5)	0.04 (0.11)	0.42
	COV	1.68	1.36	1.66

* n/a values were beyond the data range

Table 63. Laboratory Infiltration Tests Using Surface Soil on 17th Ave. E. and University Blvd. E. at Different Compaction Levels.

17 th Ave. and University Blvd. E.				
Compaction method	Test	f _o (in/hr, cm/hr)	f _c (in/hr, cm/hr)	k (1/hr)
hand (density = 1.39 g/cc)	1	n/a	18.6 (47.1)	21.97
	2	62 (157)	11.3 (28.6)	15.14
	3	41 (104.3)	8.5 (21.6)	6.69
	mean	51 (130.6)	12.8 (32.4)	14.60
	COV	0.28	0.41	0.52
Standard (density = 1.64 g/cc)	1	29.6 (75.2)	0.9 (2.3)	7.59
	2	0.9 (2.3)	0.4 (0.94)	0.21
	3	0.6 (1.5)	0.1 (0.3)	0.03
	mean	10.4 (26.3)	0.5 (1.2)	2.61
	COV	1.61	0.88	1.65
Modified (density = 1.79 g/cc)	1	3.5 (8.9)	0.2 (0.6)	1.80
	2	0.3 (0.7)	0.09 (0.23)	0.37
	3	0.16 (0.4)	0.06 (0.16)	0.05
	mean	1.3 (3.4)	0.12 (0.31)	0.74
	COV	1.44	0.68	1.26

* n/a values were beyond the data range

Table 64. Laboratory Infiltration Tests Using Surface Soil on 21st Ave. E. and University Blvd E. at Different Compaction Levels.

21 th Ave. and University Blvd. E				
Compaction method	Test	f _o (in/hr, cm/hr)	f _c (in/hr, cm/hr)	k (1/hr)
Hand (density = 1.39 g/cc)	1	29.4 (74.6)	2 (5.1)	7.61
	2	8.6 (21.8)	1.5 (3.9)	3.95
	3	n/a	2 (5.2)	38.03
	mean	19 (48.2)	1.9 (4.7)	16.53
	COV	0.78	0.15	1.13
Standard (density = 1.52 g/cc)	1	6.2 (15.8)	0.8 (2)	1.05
	2	1 (2.4)	0.33 (0.84)	0.29
	3	2.1 (5.2)	0.3 (0.76)	0.19
	mean	3.1 (7.8)	0.5(1.2)	0.51
	COV	0.90	0.59	0.93
Modified (density = 1.59 g/cc)	1	7.2 (18.4)	0.2 (.45)	1.67
	2	0.12 (.32)	0.02 (0.06)	0.02
	3	0.03 (0.09)	0.01(0.04)	0.01
	mean	2.5 (6.3)	0.07 (0.18)	0.57
	COV	1.68	1.27	1.70

** n/a values were beyond the data range

Table 65. Laboratory Infiltration Tests Using Surface Soil on 25th Ave. E and University Blvd E. at Different Compaction Levels.

25 th Ave. and University Blvd. E				
Compaction method	Test	f _o (in/hr, cm/hr)	f _c (in/hr, cm/hr)	k (1/hr)
Hand (density = 1.42 g/cc)	1	83.7 (213)	8.7 (22.1)	11.16
	2	11 (28)	4.8 (12.1)	1.79
	3	18 (45.5)	5.9 (14.9)	4.13
	mean	36 (95.4)	6.5 (16.4)	5.69
	COV	1.07	0.32	0.86
Standard (density = 1.62 g/cc)	1	20 (51)	1.5 (16.4)	3.84
	2	1 (2.6)	1 (2.5)	0.03
	3	n/a	0.83	19.66
	mean	10.6 (26.8)	1.1 (2.5)	7.84
	COV	1.28	0.32	1.33
Modified (density = 1.67 g/cc)	1	14.5 (36.9)	1.7 (4.3)	4.78
	2	n/a	0.9 (2.4)	14.63
	3	3.7 (9.4)	1.1 (2.8)	3.16
	mean	9.1 (23.4)	1.2 (3.2)	7.52
	COV	0.84	0.31	0.82

* n/a values were beyond the data range

6.4.4 Laboratory Column Infiltration Test Results Using Subsurface Soils

During the laboratory compaction/infiltration tests, the average final infiltration through the subsurface soil for the three levels of compaction were 4.7, 1, and 0.1 in/hr using the hand compaction (little compaction), standard proctor compaction (typical compaction during construction activities) and modified proctor compaction methods (the most severe compaction level) respectively, at approximately 13 in (330 mm) of head. The final infiltration rates of the hand compacted subsurface soil were reduced by 82 and 98 percent using standard proctor compaction and modified proctor compaction methods. The laboratory infiltration data for each individual test was fitted to the Horton infiltration equation. Figure 98 shows example of subsurface soil infiltration data fitted with the Horton's equation. Laboratory infiltrations measurements using subsurface soil fitted with the Horton's equations are shown in Appendix C.9 through C.12. Tables 66 through 69 summarize the column test results for the subsurface

soil, and for different compaction values.

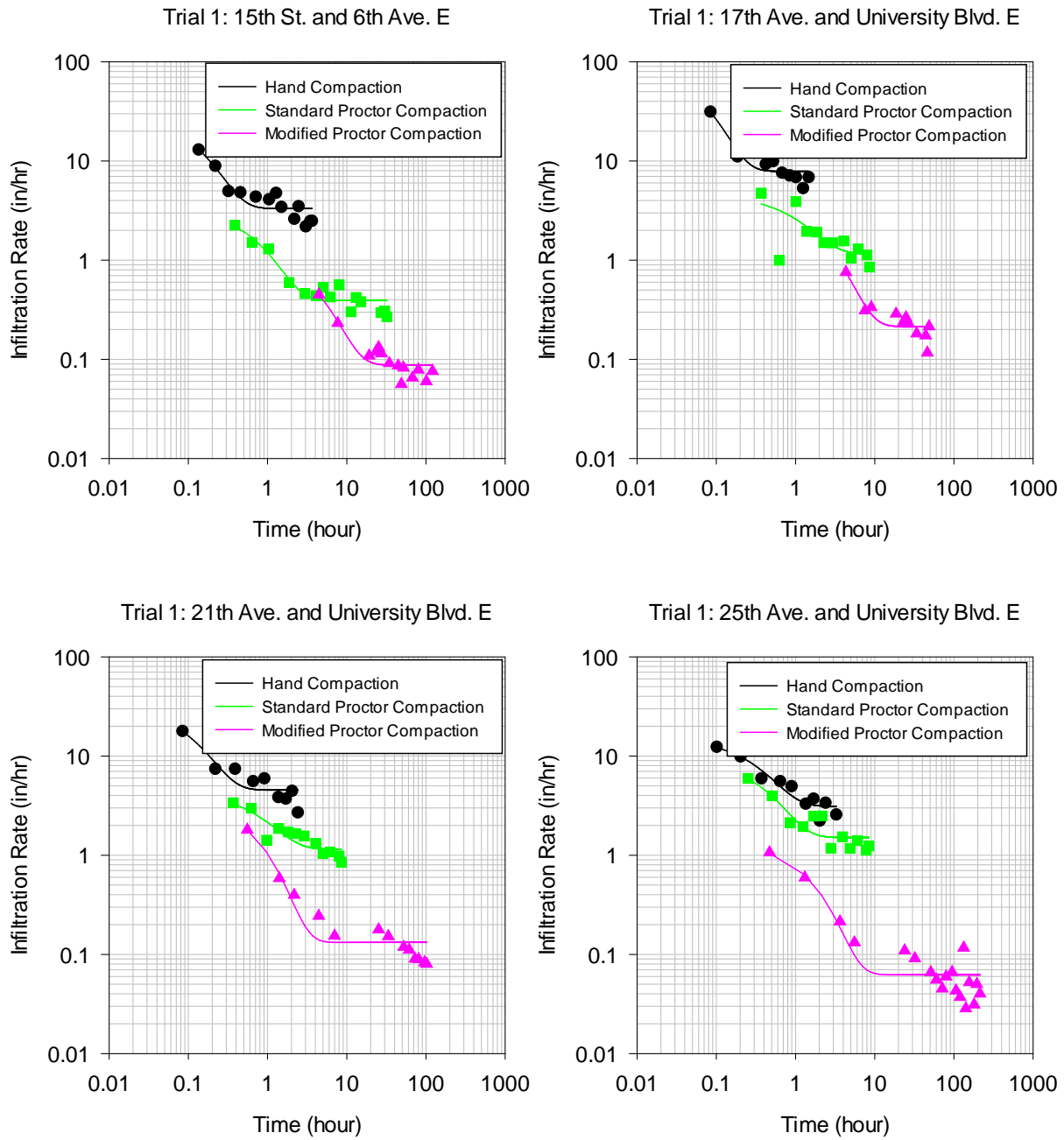


Figure 98. Example of Lab Infiltration Measurements Using Subsurface Soil Fitted With Horton Equation.

Table 66. Laboratory Infiltration Tests Using Subsurface Soil on 15th St. E and 6th Ave. E. at Different Compaction Levels.

15 th St. and 6 th Ave. E				
Compaction method	Test	f _o (in/hr, cm/hr)	f _c (in/hr, cm/hr)	k (1/hr)
hand (density = 1.42 g/cc)	1	29 (74.7)	3.3 (8.5)	7.33
	2	9.8 (24.9)	3.7 (9.3)	0.97
	3	27 (69)	4.9 (12.5)	11.61
	mean	22 (56.2)	3.9 (10.1)	6.64
	COV	0.48	0.21	0.81
Standard (density = 1.53 g/cc)	1	3.4 (8.7)	0.4 (1)	1.34
	2	0.5 (1.3)	0.3 (0.8)	0.01
	3	0.6 (1.4)	0.4 (1.1)	0.18
	mean	1.5 (3.8)	0.4 (1)	0.51
	COV	1.12	0.38	1.42
Modified (density = 1.66 g/cc)	1	1.3 (3.2)	0.09 (0.2)	0.26
	2	0.12 (0.3)	0.06 (0.16)	0.03
	3	0.2 (0.5)	0.07 (0.17)	0.05
	mean	0.5 (1.3)	0.07 (0.2)	0.12
	COV	1.23	0.18	1.1

Table 67. Laboratory Infiltration Tests Using Subsurface Soil on 17th Ave. E. and University Blvd E at Different Compaction Levels.

17 th Ave. and University Blvd. E				
Compaction method	Test	f _o (in/hr, cm/hr)	f _c (in/hr, cm/hr)	k (1/hr)
hand (density = 1.46 g/cc)	1	93.5 (237.6)	7.9 (20.1)	15.53
	2	22.3 (56.6)	6.4 (16.2)	3.85
	3	135 (343.3)	6.3 (16.1)	26.07
	mean	84 (212.5)	6.9 (17.4)	15.15
	COV	0.68	0.13	0.73
Standard (density = 1.70 g/cc)	1	4.7 (12)	1.2 (3)	0.91
	2	3.3 (8.5)	1.2 (3)	2.86
	3	1.5 (3.9)	0.8 (2)	0.22
	mean	3.2 (8.1)	1 (2.6)	1.33
	COV	0.5	0.23	1.03
modified (density = 1.77 g/cc)	1	3.6(9)	0.2(0.6)	0.43
	2	0.2 (0.6)	0.1(0.3)	0.06
	3	1.4 (3.6)	0.07(0.2)	2.8
	mean	1.7 (4.4)	0.13(0.33)	1.09
	COV	0.98	0.57	1.36

Table 68. Laboratory Infiltration Tests Using Subsurface Soil on 21st Ave. E. and University Blvd E. at Different Compaction Levels.

21 st Ave. and University Blvd. E				
Compaction method	Test	f _o (in/hr, cm/hr)	f _c (in/hr, cm/hr)	k (1/hr)
hand (density = 1.54 g/cc)	1	32 (81.9)	4.6 (11.6)	8.86
	2	20.6 (52.4)	5.8 (14.8)	3.57
	3	15 (37.3)	3.5 (8.9)	2.66
	mean	23 (57.2)	4.6 (11.8)	5.03
	COV	0.4	0.25	0.67
standard (density = 1.71 g/cc)	1	4.6 (11.7)	1.2 (2.9)	1.24
	2	1.5 (3.9)	0.4 (1)	0.161
	3	0.5 (1.3)	0.1 (0.3)	0.04
	mean	2.2 (5.6)	0.6 (1.4)	0.48
	COV	0.96	0.96	1.38
modified (density = 1.78 g/cc)	1	3.7 (9.4)	0.13 (0.34)	1.38
	2	0.13 (0.34)	0.04 (0.11)	0.014
	3	0.1 (0.27)	0.02 (0.04)	0.009
	mean	1.3(3.3)	0.06 (.16)	0.47
	COV	1.58	0.97	1.69

Table 69. Laboratory Infiltration Tests Using Subsurface Soil from the Intersection of 25th Ave. E and University Blvd E. at Different Compaction Levels.

25 th Ave. and University Blvd. E				
Compaction method	Test	f _o (in/hr, cm/hr)	f _c (in/hr, cm/hr)	k (1/hr)
hand (density = 1.38 g/cc)	1	15.4 (39.1)	3.14 (8)	2.97
	2	10.1(25.7)	3.1 (7.8)	1.08
	3	9.8 (24.8)	3.8 (9.7)	2.07
	mean	11.8 (29.8)	3.3 (8.5)	2.04
	COV	0.27	0.13	0.46
standard (density = 1.6 g/cc)	1	9.6 (24.3)	1.5 (3.9)	2.39
	2	3.4 (8.5)	1.4 (3.6)	0.65
	3	8.5 (21.6)	1.4 (3.7)	2.45
	mean	7.2 (18.2)	1.5 (3.7)	1.83
	COV	0.47	0.04	0.56
modified (density = 1.7 g/cc)	1	1.4 (3.6)	0.06 (0.16)	0.658
	2	0.06 (0.16)	0.01 (0.02)	0.003
	3	0.06 (0.14)	0.03 (0.07)	0.002
	mean	0.5 (1.3)	0.03 (0.08)	0.22
	COV	1.53	0.86	1.71

6.4.5 Comparisons of Different Levels of Compaction and Sample Locations

Statistical tests of multiple pairwise comparisons of groups that were considered during this research included: Least Significant Difference (LSD), Bonferroni Multiple Comparison, and the Tukey-Kramer test. The LSD (Least Significant Difference) test is a two-step test. First the ANOVA F-test is performed. If it is significant at level α (alpha), then all pairwise t-tests are carried out, each at level α (alpha) for normally distributed data. If the F-test is not significant, then the procedure terminates. The Bonferroni multiple comparison test is a conservative test, that is, the family-wise error rate (FEWR) is not exactly equal to α (alpha), but is less than α (alpha) in most situations. It is easy to apply and can be used for any set of comparisons. The Tukey-Kramer test is an extension of the Tukey test to unbalanced designs. Unlike the Tukey test for balanced designs, it is not exact. The FWER of the Tukey-Kramer test may be less than α (alpha). It is less conservative for only slightly unbalanced designs, and more conservative when differences among samples sizes are bigger.

One of the primary requirements for these multiple pairwise comparisons methods is that the data are normally distributed. When data are not normally distributed, there are two commonly used approaches. The first is to transform the data using logarithmic or square root transformations in an attempt to obtain a transformed normal distribution. One potential problem with this method is that the units of the transformed data may be difficult to interpret due to the logarithmic manipulation. The second method for dealing with non-normally distributed data is to use a non-parametric analysis having fewer data distribution requirements.

For these analyses, the Kruskal-Wallis test was used as it represents a nonparametric version of the parametric ANOVA test. This test is used to determine if at least one subgroup of data are significantly different from the other subgroups being compared. This test compares the

population medians of the groups, instead of the population means used by ANOVA. The Kruskal-Wallis method tests the hypothesis that all population medians are equal (Gibbons, 1997). The multiple comparison tests shown below were conducted using a MINITAB macro in a nonparametric setting (Orlich, 2010). The following figures describe the significance difference for the saturated infiltration rate among different levels of compaction and using surface and subsurface soil from four different test sites. Detailed calculation results are attached in the Appendix C.13 through C.32.

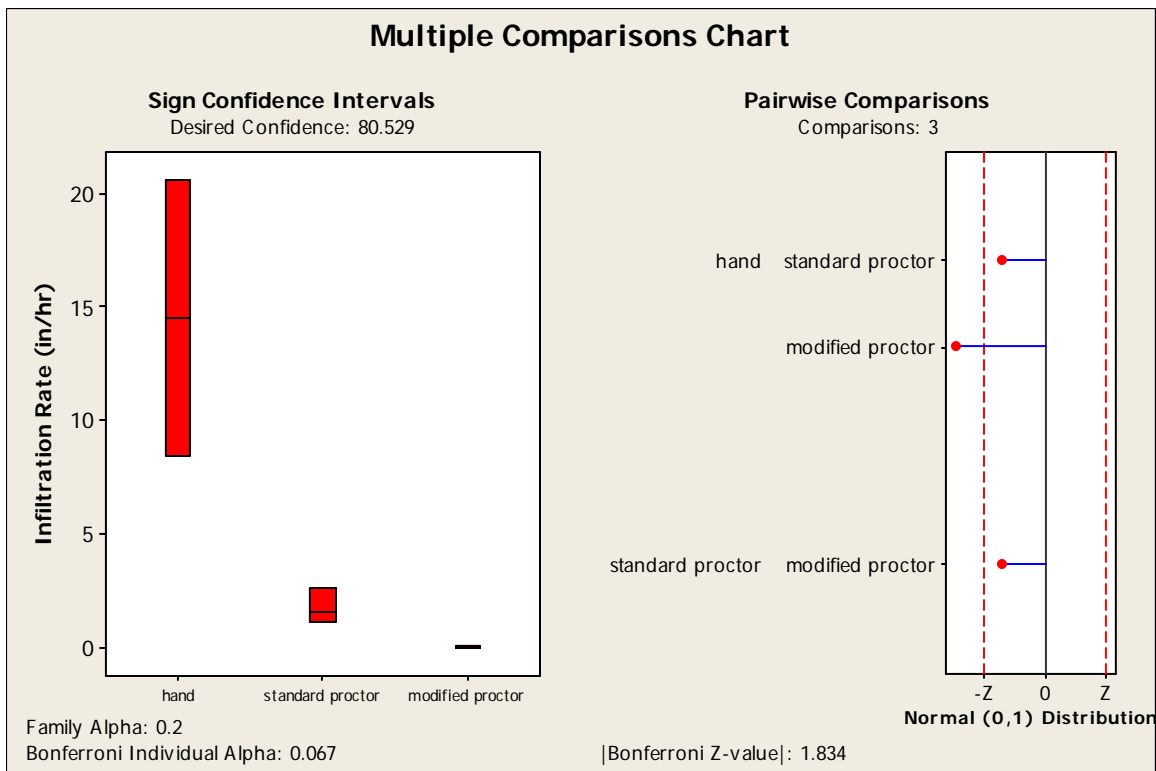


Figure 99. Multiple Comparison Plots of Laboratory Infiltration Measurements Using Surface Soil on 15th St. E and 6th Ave. E., Tuscaloosa, AL

The graph on the left of Figure 99 displays box plots of groups with their sign confidence intervals for the medians (red boxes in the each box plot). The graph on the right displays the non absolute group mean rank standardized differences (Orlich, 2010). This latter plot shows the

magnitude of the group differences and its direction. It also shows the positive and negative critical z-values and illustrates if a difference is likely statistically significant. From Figure 99, it is seen that the saturated infiltration rate using hand compaction is larger than the saturated infiltration rate using standard proctor and modified proctor compaction. This difference is also shown to be statistically significant since the standardized difference distance goes beyond the critical z-values compared to the other test groups. There are no significant differences noted between the saturated infiltration rate of standard proctor and modified proctor compaction methods, for the number of data observations available.

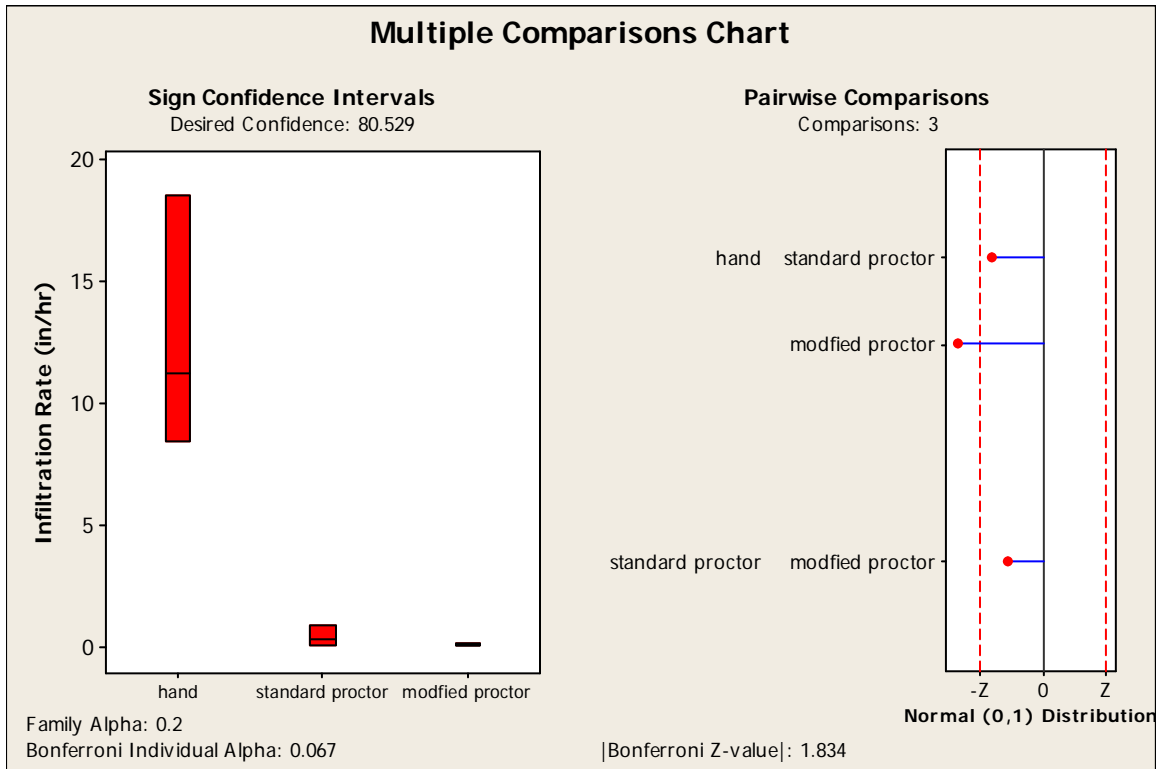


Figure 100. Multiple Comparison Plots of Laboratory Infiltration Measurements Using Surface Soil on 17th Ave. E. and University Blvd. (Tuscaloosa Physical Therapy), Tuscaloosa, AL

The same approach was used to identify any differences in paired saturated infiltration rates of hand compaction, standard proctor, and modified proctor compaction method using surface soil obtained from the intersection of 17th Ave. E. and University Blvd. (Tuscaloosa Physical Therapy), Tuscaloosa, AL. Figure 100 shows the multiple comparisons of saturated infiltration rates for the surface soil obtained from this site. The figure shows that there are statistically significant differences between saturated infiltration rates of hand compaction and modified proctor compaction. However, there are no statistically significant differences between saturated infiltration rates for standard proctor and modified proctor compaction conditions, based on the number of samples available.

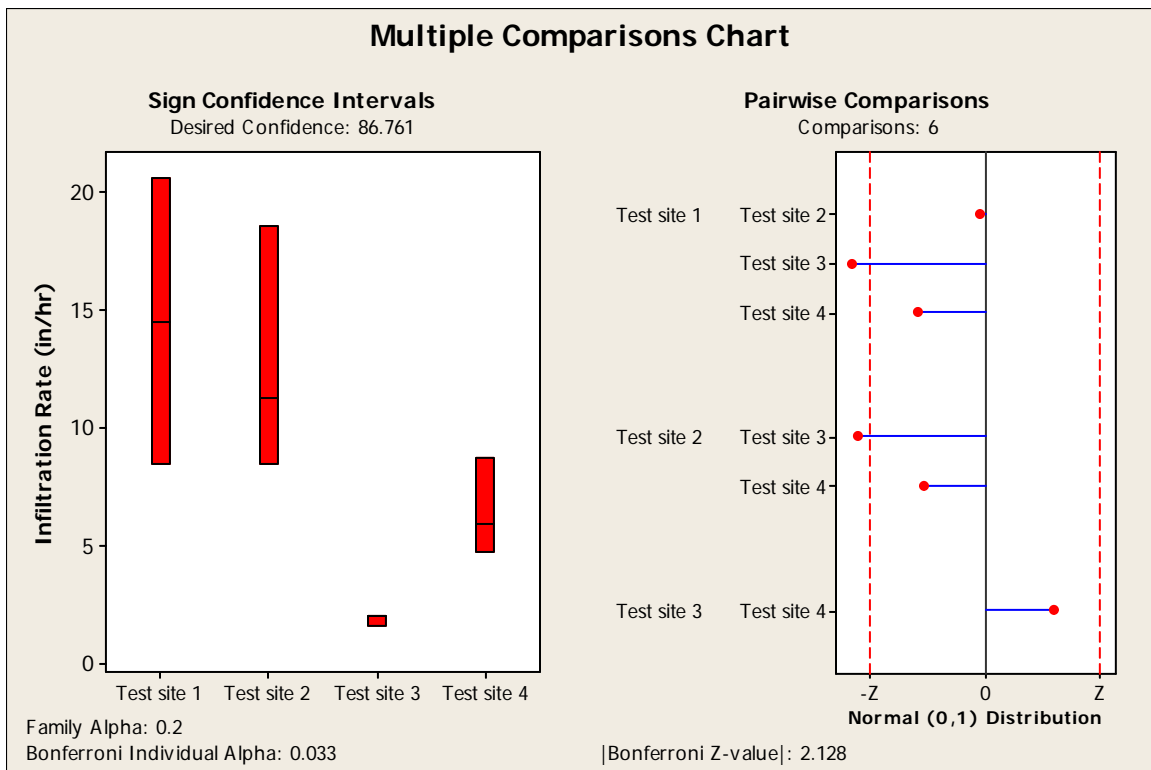


Figure 101. Multiple Comparison Plots of Laboratory Infiltration Measurements Using Surface Soils from Four Test Sites and Hand Compaction Tests.

Table 70. Bioinfiltration Test Site Locations

Test Site No.	Test Site Location
1	McDonalds on 15 th St. E and 6 th Ave. E., Tuscaloosa, AL
2	17 th Ave. E. and University Blvd E., Tuscaloosa, AL.
3	21 st Ave. E. and University Blvd E., Tuscaloosa, AL.
4	25 th Ave. E. and University Blvd E., Tuscaloosa, AL.

The same approach was used to distinguish the differences in paired saturated infiltration rates of hand compaction using surface soil obtained from the four bioinfiltration sites. Figure 101 shows the multiple comparisons of saturated infiltration rates for the surface soil obtained from the four bioinfiltration sites and hand compaction condition. The figure shows that there are statistically significant differences between saturated infiltration rates of surface soil from test site 1 versus 3, test site 2 versus 3. However, there are no statistically significant differences between saturated infiltration rates of surface soil from test site 1 versus 2, 1 versus 4, and 2 versus 4. Detailed calculation results are attached in Appendix C.19.

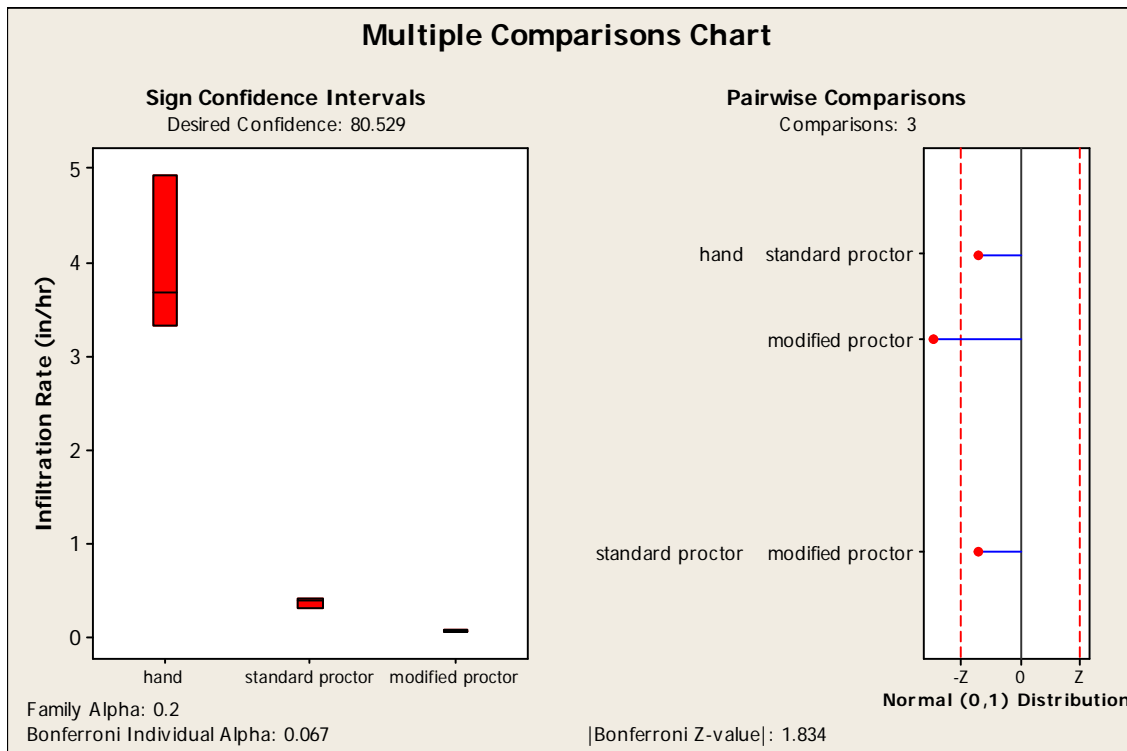


Figure 102. Multiple Comparison Plots of Laboratory Infiltration Measurements Using Subsurface Soil on 15th St. E and 6th Ave. E., Tuscaloosa, AL

The same approach was also used to distinguish the differences in paired saturated infiltration rates of hand compaction, standard proctor, and modified proctor compaction condition using subsurface soil obtained from the intersection of 15th St. E and 6th Ave. E., and 17th Ave. E. and University Blvd. (Tuscaloosa Physical Therapy), Tuscaloosa, AL. Figure 102 and 103 shows the multiple comparisons of saturated infiltration rates for the subsurface soil obtained from this site. The figure shows that there are statistically significant differences between saturated infiltration rates for hand compaction and modified proctor condition. However, there are no statistically significant differences in the saturated infiltration rates between standard proctor and modified proctor compaction conditions.

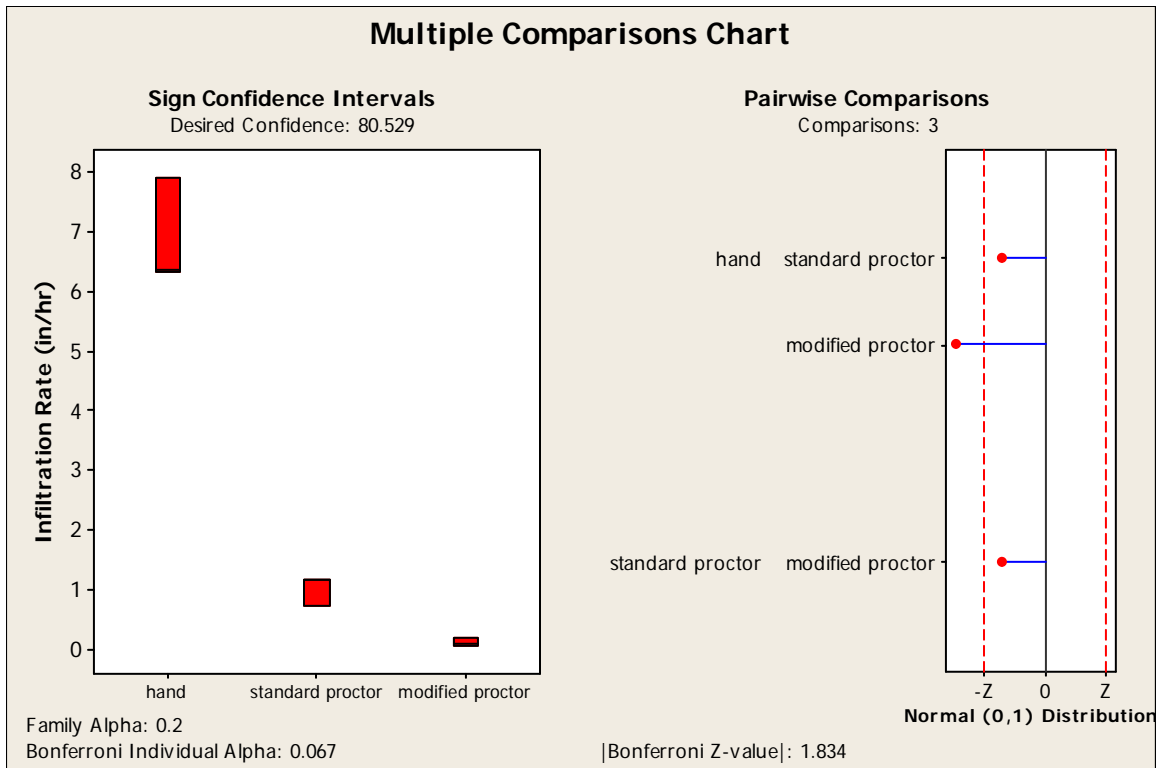


Figure 103. Multiple Comparison Plots of Laboratory Infiltration Measurements Using Subsurface Soil on 17th Ave. E. and University Blvd. (Tuscaloosa Physical Therapy), Tuscaloosa, AL

Figure 103 shows that there are statistically significant differences between saturated infiltration rates for hand compaction and modified proctor condition. However, there are no statistically significant differences in the saturated infiltration rates between standard proctor and modified proctor compaction conditions.

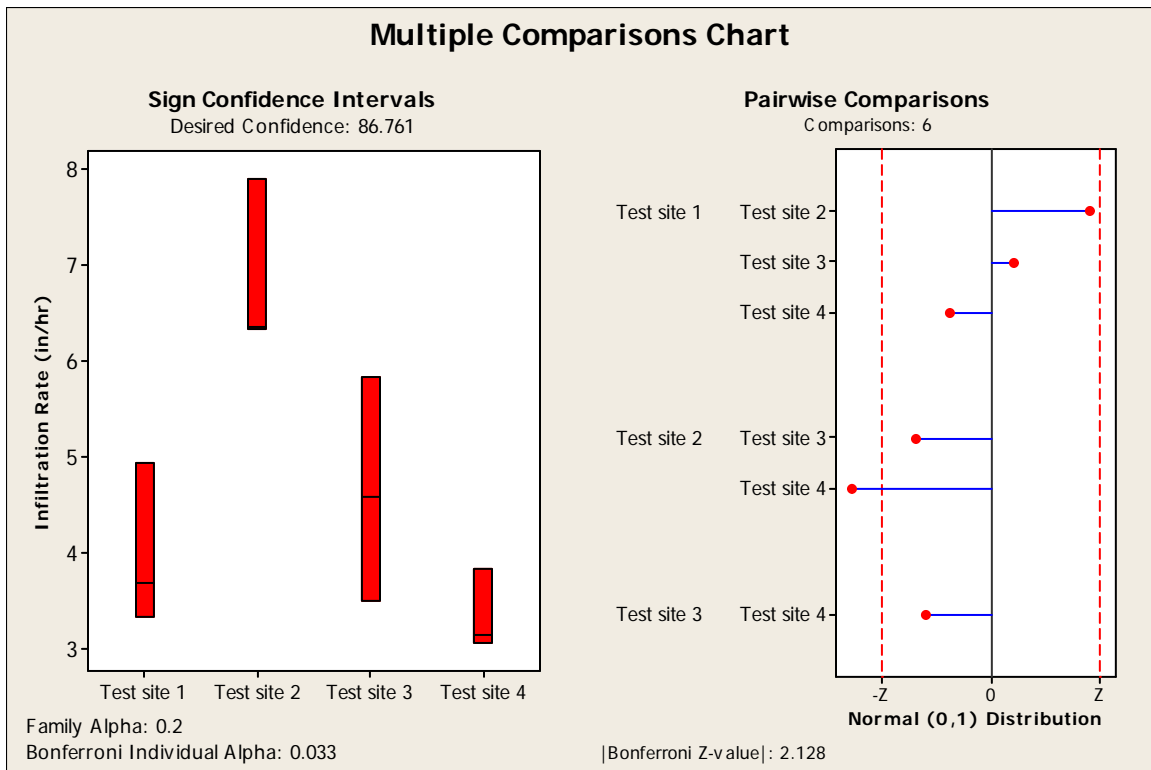


Figure 104. Multiple Comparison Plots of Laboratory Infiltration Measurements Using Subsurface Soils from Four Test Sites and Hand Compaction Tests.

The same approach was used to distinguish the differences in paired saturated infiltration rates of hand compaction method using subsurface soil obtained from the four bioinfiltration sites. Figure 104 shows the multiple comparisons of saturated infiltration rates for the subsurface soil obtained from this site. The figure shows that there are statistically significant differences between saturated infiltration rates of subsurface soil from test site 2 and 4, and using hand compaction condition. However, there are no statistically significant differences between saturated infiltration rates of subsurface soil from test site 1 versus 2, 1 versus 3, 1 versus 4, 2

versus 3, and 3 versus 4, and hand compaction conditions. Detailed calculation results are attached in Appendix C.30 through C.32.

6.5 Chapter Summary

Small-scale infiltrometers work well if surface characteristics are of the greatest interest (such as infiltration thru surface landscaped soils, as in turf areas, grass swales or in grass filters). Larger, conventional double-ring infiltrometers are not very practical in urban areas due to the excessive force needed to seat the units in most urban soils (usually requiring jacking from a heavy duty truck) and the length of time and large quantities of water needed for the tests. In addition, they also only measure surface soil conditions. Large-scale (deep) infiltration tests would be appropriate when subsurface conditions are of importance (as in bioinfiltration systems and deep rain gardens). Figure 105 shows box and whisker plots comparing the saturated soil infiltration rates (of most significance when designing bioinfiltration stormwater controls) for all test locations.

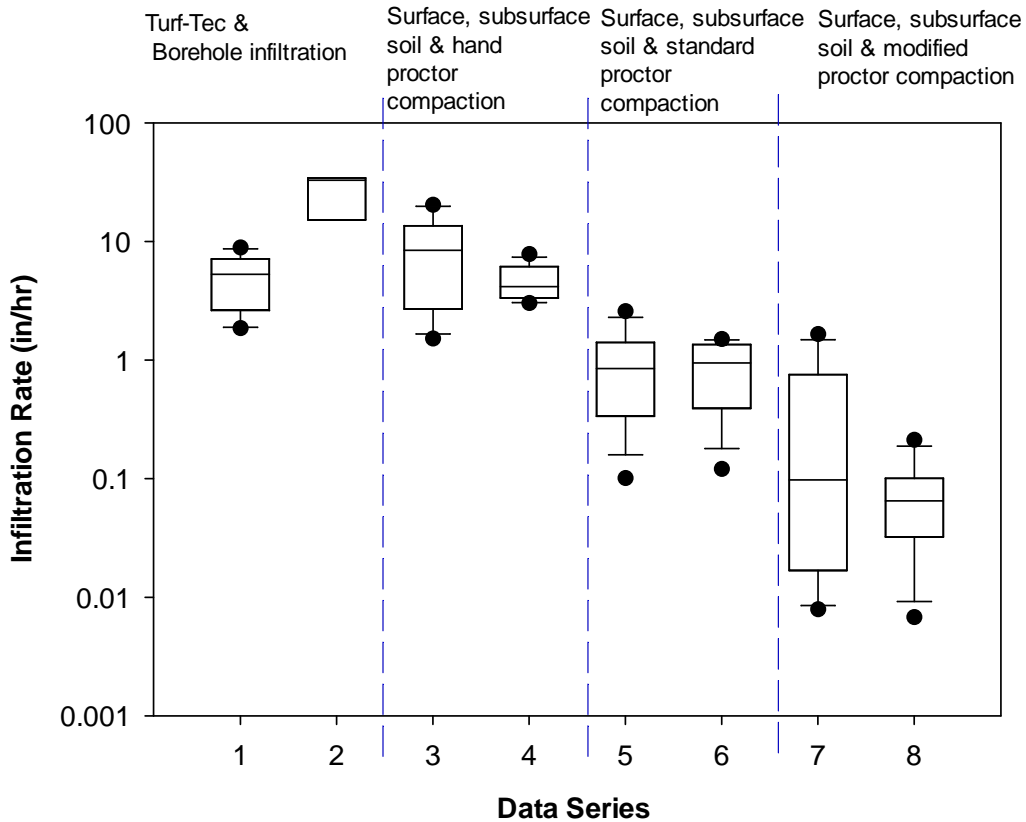


Figure 105. Box and Whisker Plots Comparing Saturated Soil Infiltration Rates (in/hr).

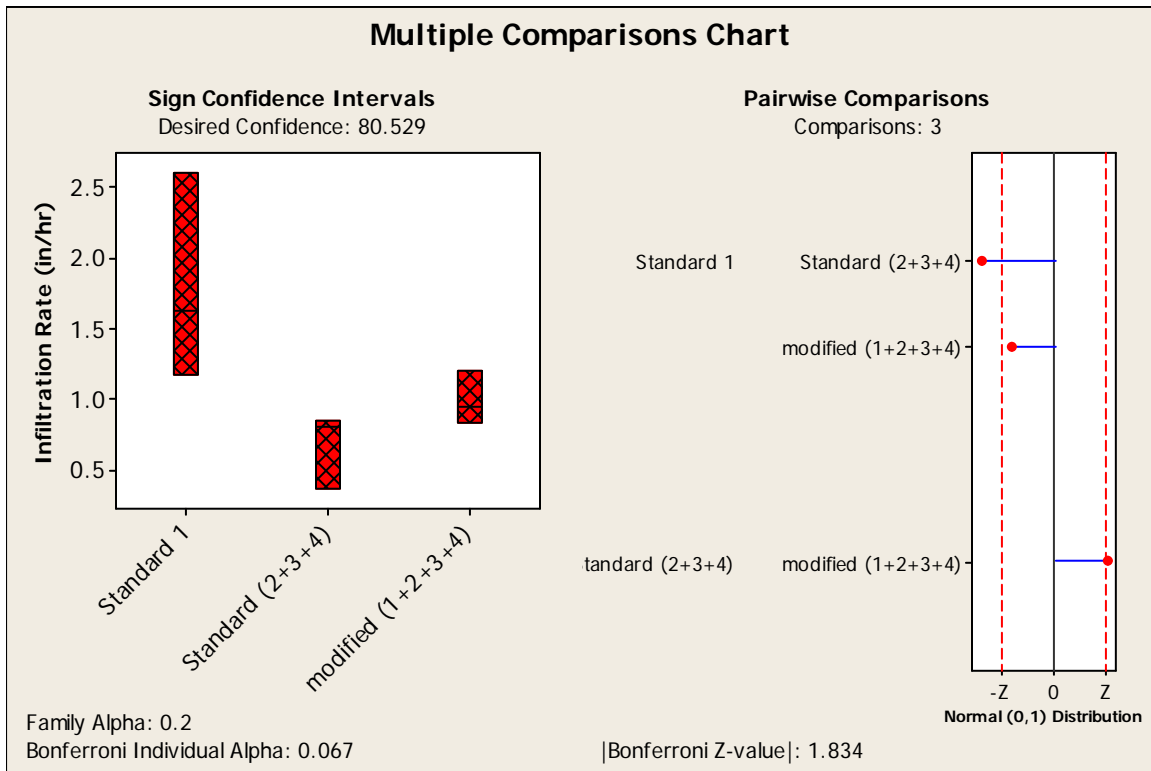
Test series descriptions (12 replicates in each test series except for the borehole tests which only included 3 observations):

- 1) Tur-Tec small double ring infiltrometer
- 2) Pilot-scale borehole infiltration tests
- 3) Surface soil composite sample with hand compaction
- 4) Subsurface soil composite sample with hand compaction
- 5) Surface soil composite sample with standard proctor compaction
- 6) Subsurface soil composite sample with standard proctor compaction
- 7) Surface soil composite sample with modified proctor compaction
- 8) Subsurface soil composite sample with modified proctor compaction

The borehole/Sonotube tests are relatively easy and fast to conduct, if a large borehole drill rig is available along with large volumes of water (such as from a close-by fire hydrant or a water truck). For infiltration facilities already in place, simple stage recording devices (small pressure transducers with data loggers) are very useful for monitoring during actual rain conditions. In many cases, disturbed urban soils have dramatically reduced infiltration rates, usually associated with compaction of the surface soils. These areas in Tuscaloosa were all originally developed more than 20 years ago and had standard turf grass covering. They were all isolated from surface disturbances, beyond standard landscaping maintenance. It is not likely that the tornado affected the soil structure. The soil profile (surface soils vs. subsurface soils from about 4 ft, or 1.2 m) did affect the infiltration rates at these locations. Due to the relatively high clay content, the compaction tests indicated similar severe losses in infiltration rates. Local measurements of the actual infiltration rates, as described above, can be a very useful tool in identifying problem areas and the need for more careful construction methods. Having accurate infiltration rates are also needed for proper design of stormwater bioinfiltration controls.

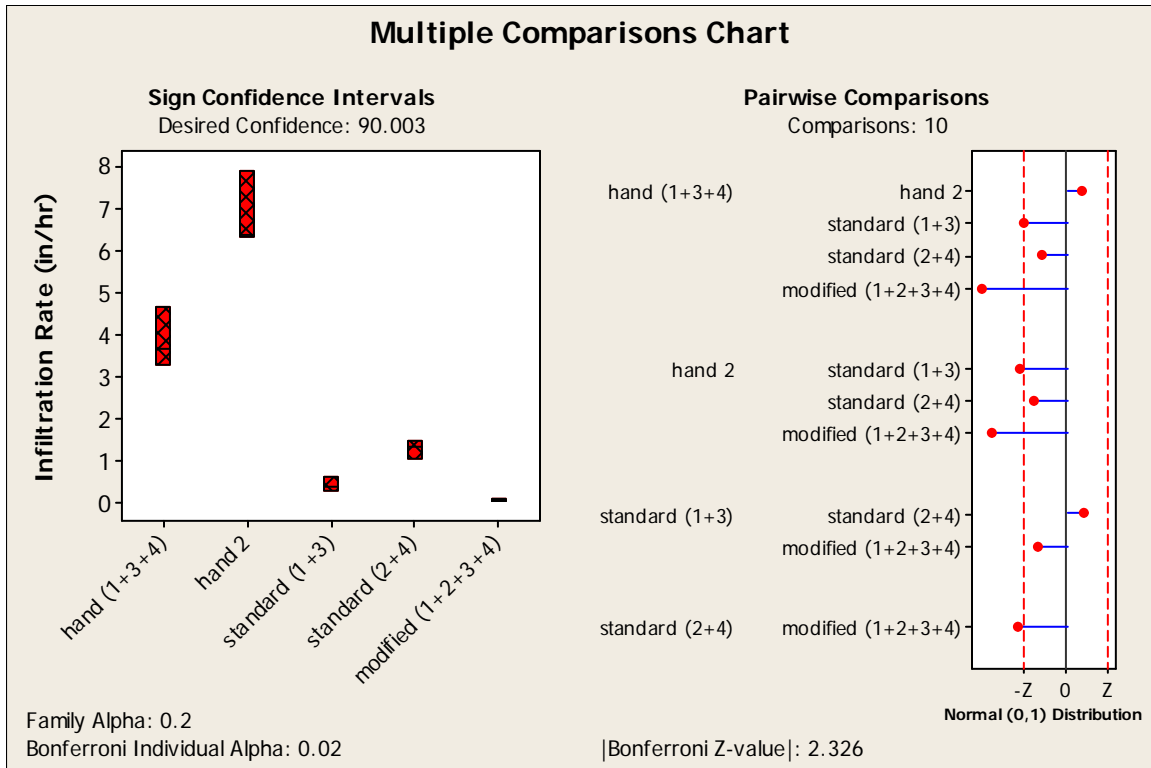
Multiple comparison tests were also conducted on overall test sites and the resulting conditions for the combined saturated infiltration rates. There are no significant differences between the different test locations saturated infiltration rates for standard proctor and modified proctor compaction conditions for each test sites. These data were therefore combined and similar tests were conducted with these combined data and for the different test sites. Figures 106 and 107 show example multiple comparisons of combined saturated infiltration rates for the surface and subsurface soils respectively. There are no statistically significant differences between the different test locations saturated infiltration rates using surface soil samples obtained from test sites 2, 3, and 4 and for the standard proctor compaction condition. Similar tests

indicated no statistically significant differences between saturated infiltration rates using surface soil samples obtained from all sites for modified proctor compaction conditions. Figure 106 is an example multiple comparison of combined saturated infiltration rates from these sites. Detailed calculation results are included in Appendix C.32.



*1, 2, 3, and 4 are test sites

Figure 106. Multiple Comparison Plots of Laboratory Infiltration Measurements using Surface Soil from Four Test Sites, Standard and Modified Proctor Compaction Conditions with Combined Data.



*1, 2, 3, and 4 are test sites

Figure 107. Multiple Comparisons Plots of Laboratory Infiltration Measurements using Subsurface Soil from Four Test Sites, Hand, Standard, and Modified Proctor Compaction Conditions with Combined Data.

The Kruskal-Wallis H statistic is an overall test statistic that is used to test the general hypothesis that all population medians are equal. The macro was used for multiple comparisons in a nonparametric setting for comparison amongst the individual groups. Tables 71 and 72 are summary tables showing overall groups of conditions and the resulting conditions for the combined groups.

Table 71. Kruskal-Wallis (KW) Multiple Comparisons of Combined Saturated Infiltration Rates Using Surface Soil.

Saturated infiltration rates between different levels of compaction				
Soil compaction test from different test site	KW test on the data	KW All Pairwise Comparisons	Z vs. Critical value	P-value
1	H = 7.2, p = 0.027	hand vs. modified proctor	2.53421 >= 1.834	0.0073
2	H = 6.49, p = 0.039	hand vs. modified proctor	2.53421 >= 1.834	0.0113
3	H = 7.2, p = 0.027	hand vs. modified proctor	2.68328 >= 1.834	0.0073
4	H = 5.6, p = 0.061	hand vs. standard proctor	2.23607 >= 1.834	0.0253
Saturated infiltration rates among the four test sites and different level of compactions				
hand compaction	H = 8.13, p = 0.043	Test site 1 vs. 3	2.49101 >= 2.128	0.0127
		Test site 2 vs. 3	2.37778 >= 2.128	0.0174
standard proctor	H = 8.28, p = 0.041	Test site 1 vs. 3	2.49101 >= 2.128	0.0127
modified proctor	H = 7.51, p = 0.057	Test site 1 vs. 2	2.26455 >= 2.128	0.0235
		Test site 1 vs. 4	2.60424 >= 2.128	0.0092
Saturated infiltration rates among different levels of compaction and using surface soil, combined data				
Soil compaction test using soil sample from different test sites	KW test on the data	KW All Pairwise Comparisons	Z vs. Critical value	P-value
hand compaction: test site 1 vs 2 vs (3+ 4)	H = 6.58, p = 0.037	test site 1 vs. 4	2.15728 >= 1.834	0.0427
		test site 2 vs. 4	2.02653 >= 1.834	
standard proctor: site 1 vs 2 vs (3+ 4) vs modified (1+2+3) vs 4	H = 6.28, p = 0.099	standard site 1 vs. standard site (2+3+4)	2.36320 >= 2.128	0.0181
H = 6.31, p = 0.098				
standard proctor site 1 vs site 2 vs site (3+ 4) vs modified site (1+2+3+ 4)	H = 7.98, p = 0.019	standard site1 vs. standard site (2+3+4)	2.60606 >= 1.834	0.0092
	H = 8.04, p = 0.018		1.89473 >= 1.834	
hand site (1+2) vs hand site (3+4) vs standard site1 vs standard site (2+3+4) vs modified site (1+2+3+ 4)	H = 30.15, p = 0.000	hand site (1+2) vs. standard site (2+3+4)	4.75126 >= 2.326	0.0000
		hand site (1+2) vs. modified site (1+2+3+4)	3.73168 >= 2.326	0.0002
		hand site (3+4) vs. standard site (2+3+4)	3.71754 >= 2.326	0.0002
		hand site (3+4) vs. modified site (1+2+3+4)	2.56791 >= 2.326	0.0102
	H = 30.23, p = 0.000			

* H: Kruskal-Wallis statistic test the general hypothesis

Table 72. Kruskal-Wallis (KW) Multiple Comparisons of Combined Saturated Infiltration Rates Using Subsurface Soils.

Saturated infiltration rates between different levels of compaction				
Soil compaction test from different test site	KW Test on the data	KW All Pairwise Comparisons	Z vs. Critical value	P-value
1	H = 7.2, p = 0.027	hand vs. modified proctor	2.68328 >= 1.834	0.0073
2	H = 7.2, p = 0.027	hand vs. modified proctor	2.68328 >= 1.834	0.0073
3	H = 6.49, p = 0.039	hand vs. modified proctor	2.53421 >= 1.834	0.0113
4	H = 7.2, p = 0.027	hand vs. standard proctor	2.68328 >= 1.834	0.0073
Saturated infiltration rates among the four test sites and for each level of compactions				
hand compaction	H = 7.82, p = 0.05	Test site 2 vs. 4	2.71746 >= 2.128	0.0066
		Test site 3 vs. 4	2.60424 >= 2.128	0.0092
standard proctor	H = 8.74, P = 0.033	Test site 1 vs. 2	2.37778 >= 2.128	0.0174
modified proctor	H = 5.97, P = 0.113	Test site 2 vs. 4	2.37778 >= 2.128	0.0174
Saturated infiltration rates among different levels of compaction and using subsurface soil				
Soil compaction from test using soil sample from different test sites	KW Test on the data	KW All Pairwise Comparisons	Z vs. Critical value	P-value
hand compaction test site (1+4) vs 2 vs 3	H = 7.19 and p = 0.027	hand site (1 + 4) vs hand site 2	2.68025 >= 1.834	0.00740
standard proctor compaction test site (1+3) vs (2+ 4) vs modified site (1+2) vs modified (3+4)	H = 19.62 and p = 0.000	standard site (2+4) vs. modified site (3+4)	4.12331 >= 2.128	0.00000
		standard site (2+4) vs. modified site (1+2)	3.06186 >= 2.128	0.00220
		standard site (1+3) vs. modified site (3+4)	2.65361 >= 2.128	0.00800
hand compaction test site (1 + 3+4) vs hand site 2 vs standard site (1+3) + standard site (2+4) modified site (1+2+3+4)	H = 32.41 and p = 0.000	hand site (1+3+4) vs. modified site (1+2+3+4)	4.80722 >= 2.326	0.00000
		hand site 2 vs. modified site (1+2+3+4)	4.16622 >= 2.326	0.00000
		standard site (2+4) vs. modified site (1+2+3+4)	2.78420 >= 2.326	0.00540
		hand site 2 vs. standard site (1+3)	2.63988 >= 2.326	0.00830
		hand site (1+3+4) vs. standard site (1+3)	2.46123 >= 2.326	0.01380

* H: Kruskal-Wallis statistic to test the general hypothesis

CHAPTER 7

7. LABORATORY COLUMN TESTS FOR PREDICTING CHANGES IN FLOWS AND PARTICULATE RETENTION WITH CHANGES IN BIOFILTER MEDIA CHARACTERISTICS

7.1 Introduction

Bioretention systems are widely used in urban areas to reduce stormwater runoff volume, peak flows and stormwater pollutant loads reaching receiving waters. However, the performances of bioretention systems, and other infiltration devices, are affected by factors such as texture, structure, and the degree of compaction of the media during their construction. The media used in bioretention systems is critical when determining water quality treatment and stormwater flow control performance of these systems. Premature clogging of filtration media by incoming sediment is also a major problem affecting the performance of stormwater biofiltration systems in urban areas. Appropriate hydraulic characteristics of the filter media, including treatment flow rate, and water contact time, are needed to select the media and drainage system.

Understanding the physical and hydrologic properties of different bioretention media mixtures as well as their responses to compaction may increase the functional predictability of bioretention systems and thus improve their design (Pitt et al., 2002 and 2008; Thompson et al., 2008). The usual effects of soil compaction include an increase in bulk density, decreased moisture holding capacities, restricted root penetration, impeded water infiltration, and fewer macropore spaces needed for adequate aeration, all often leading to a significant reduction in treatment performance (Gregory et al., 2006; Pitt et al., 2008; Thompson et al., 2008; Sileshi et al., 2012a and b).

Experiments conducted during this dissertation research and reported in this chapter included infiltration tests conducted on many different soils and media having a wide range of textures. The test conditions were representative of the great soil and parent material group at 68 field sites throughout the United States which indicated that the infiltration rate decreases with increasing clay content and increases with increasing noncapillary porosity (Free et al., 1940). Premature clogging by silt is usually responsible for early failures of infiltration devices, although compaction (during either construction or use) is also a recognized problem (Pitt et al., 2002 and 2008).

Substantial reductions in infiltration rates were noted due to soil compaction, especially for clayey soils, during prior research (Pitt et al., 1999b). Sandy soils are better able to withstand compaction, although their infiltration rates are still significantly reduced. Compaction was seen to have about the same effect as moisture saturation for clayey soils, with saturated and compacted clayey soils having very little effective infiltration rates (Pitt et al., 2008). Sandy soils can still provide substantial infiltration capacities, even when greatly compacted, in contrast to soils containing large amounts of clays that are very susceptible to compaction's detrimental effects. In a similar study that examined the effects of urban soil compaction on infiltration rates in north central Florida, Gregory et al. (2006) found a significant difference between the infiltration rates of a noncompacted pasture and wooded area, despite similar textural classification and mean bulk densities. The researchers conducted sixteen predevelopment infiltration and sixteen bulk density and gravimetric soil moisture content measurements on four wooded lots. Eighteen post development infiltration tests were carried out on a naturally wooded lot and two planted forest lots (six for each lot). The authors did not quantify the organic matter

of the test soils; however it was assumed that there were differences in organic content between these test sites.

Soil amendments (such as organic composts) improve soil infiltration rates and water holding characteristics and add protection to groundwater resources, especially from heavy metal contamination in urban areas (Pitt et al., 1999a and 1999b). However, organic composts may degrade and cause increased nutrient and other contaminant releases until they become further stabilized. Groundwater contamination problems were noted more often in commercial and industrial areas that incorporated subsurface infiltration and less often in residential areas where infiltration occurred through surface soils (Pitt et al., 1999a and Clark et al., 2006). Pretreatment of stormwater runoff before infiltration can reduce groundwater contamination of many pollutants and also prolong the life of infiltration devices.

Compost has significant pollutant sorption and ion exchange capacities that can also reduce groundwater contamination potential of the infiltrating water (Pitt et al., 1999b). However, newly placed compost amendments may cause increased nutrient discharges until the material is better stabilized (usually within a couple of years). In addition to flow control benefits, amended soils in urban lawns can also have the benefits of reduced fertilizer requirements and help control disease and pest infestation in plants (US EPA, 1997).

This chapter describes a series of controlled laboratory column tests conducted using various media to identify changes in flow with changes in the mixture characteristics, focusing on media density associated with compaction, particle size distribution (and uniformity), and amount of organic material (due to added peat). The laboratory columns used in the tests had various mixtures of sand and peat. The results of the predicted performance of these mixtures were also verified using column tests (for different compaction conditions) of surface and

subsurface soil samples obtained from Tuscaloosa, AL, along with biofilter media obtained from Kansas City, North Carolina, and Wisconsin. Three levels of compaction were used to modify the density of the media layer during the tests: hand compaction (least compacted), standard proctor compaction, and modified proctor compaction (most compacted). Statistical analyses and a full-factorial experimental design were used to determine the effects of media texture, uniformity of the media, organic content of the material, and compaction, plus their interactions, on the flowrate through the biofilter media. Model fitting was performed on the time series plots to predict the flowrate through the mixtures as a function of the significant factors and their interactions.

7.2 Description of Various Media and Test Methodology

Controlled laboratory column tests using various sand-peat mixtures, along with Tuscaloosa surface and subsurface soils and biofilter media from several installations were used to develop equations that could be used to predict changes in flow with changes in the mixtures, focusing on media density associated with compaction, particle size distribution (and uniformity), and amount of organic material. The sand media were obtained from suppliers in Tuscaloosa, AL and Atlanta, GA. Figure 108 show the four different filter sand components and the Tuscaloosa surface and subsurface soils used during these tests.



Figure 108. Sand Media Obtained from Atlanta Sand and Supply (From Upper Left to Upper Right), Sand from Ground Floor Sand Supplier, Northport, AL (Lower Left), Tuscaloosa Surface Soil and Tuscaloosa Subsurface Soils (Lower Middle and Lower Right).

The median size of the filter sand components used in the sand-peat mixtures ranged from 300 to 2,000 μm , and the uniformity coefficients ranged from 1.5 to 3. Figure 109 and Table 73 show the particle size distribution plots of the media components and their characteristics.

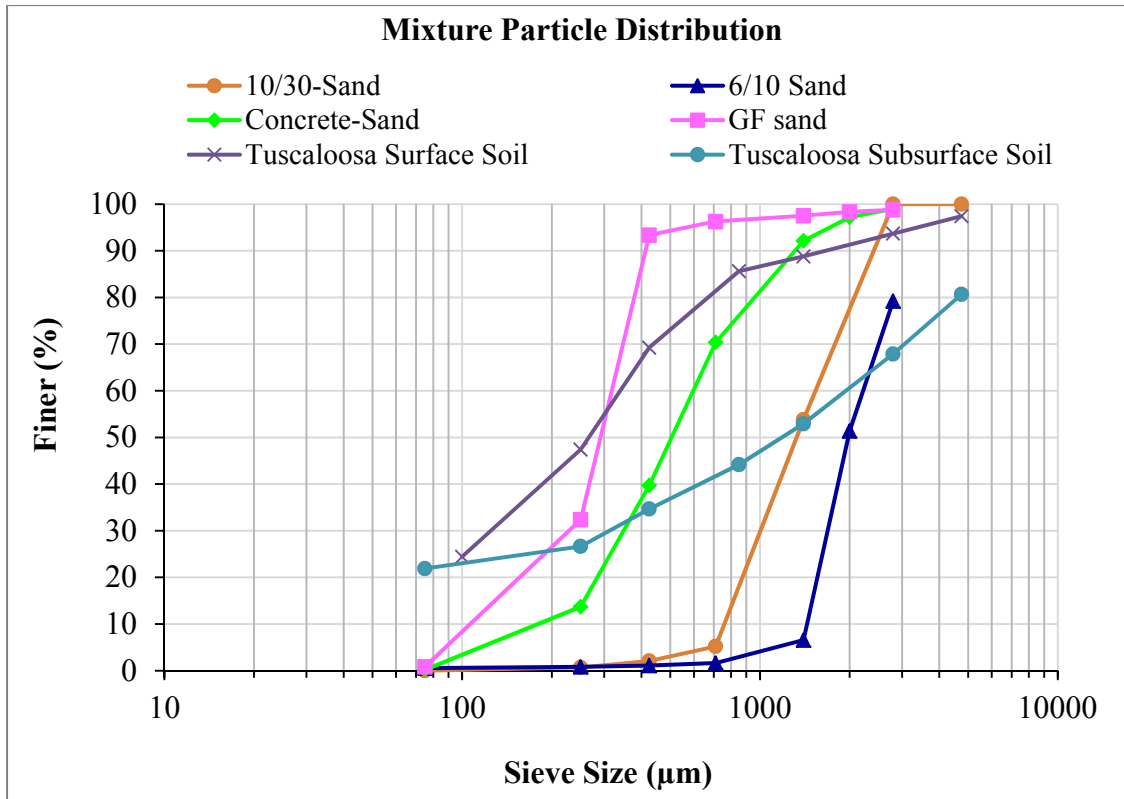


Figure 109. Particle Size Distributions of Filter Sand Components and Tuscaloosa Soil.

Table 73. Filter Sand Components and Tuscaloosa Soil Media Characteristics

Media	D ₅₀ (mm)	C _u
10/30 sand from Atlanta, GA	1.3	2
Concrete sand from Atlanta, GA	0.5	3
6/10 sand from Atlanta, GA	2	1.4
Sand from Ground Floor (GF), Northport, AL	0.3	3
Tuscaloosa Surface Soil 25 th Ave. E. and University Blvd E	0.3	6
Tuscaloosa Subsurface Soil 25 th Ave. E. and University Blvd E	1.3	33

Controlled laboratory column tests were also conducted using actual biofilter media mixtures from Kansas City, North Carolina, and Wisconsin. Figure 110 and Table 74 show these biofilter samples and their characteristics used during the tests.



Figure 110. Biofilter Media Mixtures (From Left To Right): North Carolina Biofilter Media, Kansas City Biofilter Media from Test Sites 1 and 2, and Wisconsin Biofilter Media from Test Sites 1 and 2.

Table 74. Standard Biofilter Samples Characteristics

Composition by Volume (%)					
North Carolina biofilter material (source: NCDENR 2007)		Kansas City biofilter material (source: APWA/MARC 2012)		Wisconsin biofilter material (source : WDNR 2006)	
Planting Soil (%)	85-88	Planting Soil (%)	30	Sand (%)	70-85
Fine (silt and clay) (%)	8-12	Organic Compost (%)	20	Organic Compost (%)	15-30
Organic matter (%)	3-5	Sand (%)	50		

The median sizes of the biofilter media mixtures ranged from 400 to 2,000 μm and the uniformity coefficients ranged from 5 to 40. Figure 111 and Table 75 show the particle size distribution plots and characteristics for the biofilter media mixtures. The plot shows that the Kansas City biofilter materials are relatively coarse and has a larger uniformity coefficient than the other media mixtures (uniformity coefficient = D_{60}/D_{10} , where D_{60} is the particle size associated with the 60th percentile and the D_{10} is the particle size associated with the 10th percentile).

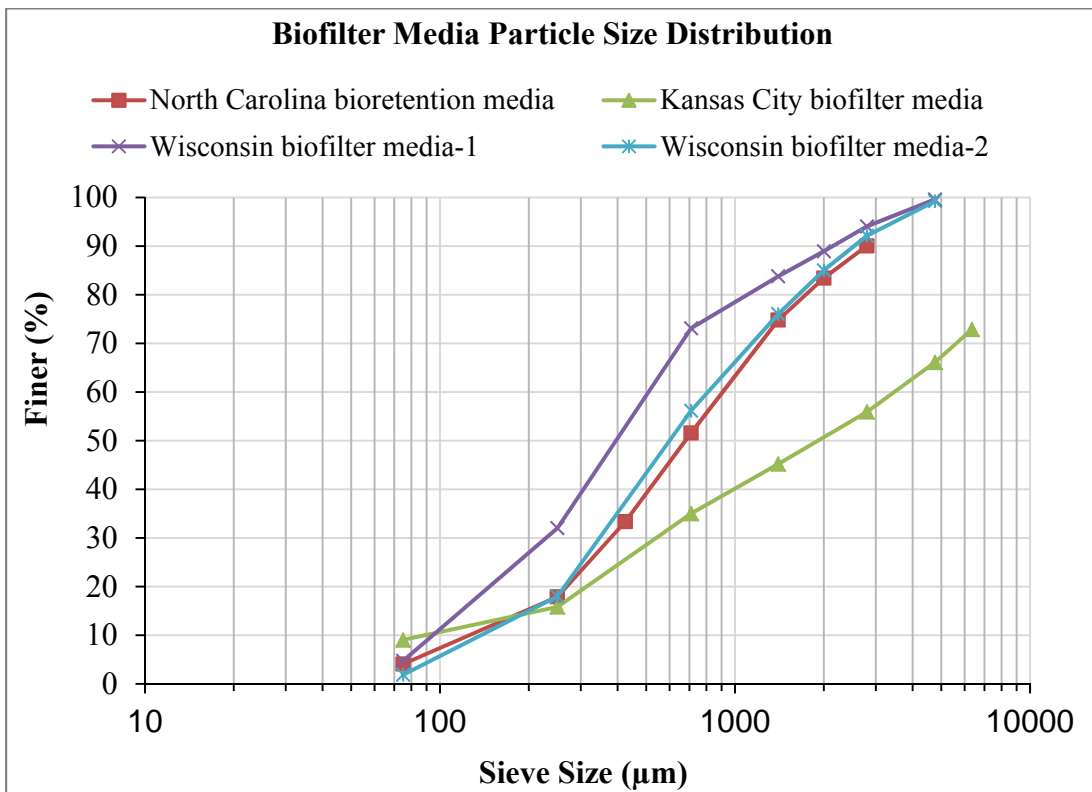


Figure 111. Particle Size Distributions of Actual Biofilter Material.

Table 75. Actual Biofilter Material Characteristics.

Media	D ₅₀ (mm)	C _u
Kansas City biofilter material	2	40
North Carolina biofilter material	0.7	6
Wisconsin USGS bio mix (85-88% sand, 3-5% pine bark, 8-12% silt and clay)*	0.4	5.6
Wisconsin Neenah mix (86% sand, 11% peat moss, and 3% Imbrium)*	0.6	5.3

* Wisconsin biofilter sample mixture percentages from Roger Bannerman (2012).

According to Imbrium Systems Company, Imbrium (Sorbtive™ MEDIA) is an oxide-coated, high surface area reactive engineered media that performs absorption, surface complexation and filtration of stormwater for total phosphorus removal. It is applied as part of a variety of stormwater control measures to capture high levels of TP, as well as Total Suspended Solids (TSS), and other sediment –associated pollutants.

7.2.1 Laboratory Column Flow Tests

The effects of different compaction levels on the infiltration rates through various sand-peat mixtures, and soil, were examined during laboratory column testing in The University of Alabama environmental engineering laboratories. A Four inch (100 mm) diameter PVC pipe (Charlotte Pipe TrueFit 100 mm PVC Schedule 40 Foam-Core Pipe) purchased from a local building supply store in Tuscaloosa, AL was used to construct the columns for these tests. Laboratory columns, each 3 ft (0.9 m) long, were constructed as shown in Figure 112. The columns were filled with about 2 inches (5 cm) of cleaned pea gravel purchased from local suppliers. To separate the gravel layer from the media layer, a permeable fiberglass screen was placed over the gravel layer and then filled with the different media listed in the previous section. The media layer was about 1.5 ft (0.5 m) thick. The bottom of the columns had a secured fiberglass window screen to contain the media.



Figure 112. Lab Column Infiltration Tests (Left To Right): Bottom of the Columns Secured with a Fiberglass Window Screen (Upper Left), Biofilter Media (Lower Left), and Media Compaction.

Three levels of compaction were used to modify the density of the media in the columns during the tests (Figure 113): hand compaction, standard proctor compaction, and modified proctor compaction. Both standard and modified proctor compaction follow ASTM standard (D 1140-54). The standard proctor compaction hammer is 24.4 kN and has a drop height of 12 in (300 mm). The modified proctor hammer is 44.5 kN and has a drop height of 18 in (460 mm). For the standard proctor setup, the hammer is dropped on the test media 25 times on each of three media layers, while for the modified proctor test, the heavier hammer was also dropped 25 times, but on each of five thinner media layers. The modified proctor test therefore results in much more compacted media, and usually reflects the most compacted soil observed in the field. Hand compaction is done by gently hand pressing the media material into the test columns with as little compaction as possible, but with no voids or channels. The hand compacted media

specimens therefore have the least amount of compaction. The densities were directly determined by measuring the weights and volume of the media material added to each column.

The infiltration rates through the mixture media were measured in each column using municipal tap water. The surface ponding depths in the columns ranged from 11 - 14 inches (28 - 36 cm), generally corresponding to maximum ponded water depths in biofilters. The freeboard depths above the media to the top of the columns were about 2 - 3 inches (50 - 75 mm).

Infiltration rates in the media were determined by measuring the time it took the infiltrated water to fill known volumes in the containers under the columns. These measurements were conducted every several minutes and repeated until apparent steady state infiltration rates were observed.

The laboratory column setups for the infiltration measurements in the different media are shown in Figure 113.



Figure 113. Laboratory Column Setup for Infiltration Measurements.

7.2.2 Laboratory Column Particle Trapping Tests

Particle trapping tests were also performed for the sand-peat media mixtures and the Tuscaloosa surface and subsurface soils, using challenge water. The test sediment in the challenge water was based on a mixture of fine ground silica particulates (Sil-Co-SiL[®] 250), medium sand, and coarse sand mixed with the Black Warrior River water to result in a wide range of particle sizes. The silica mixture added to the water (coarse sand: medium sand: fine Sil-Co-Sil 250 = 10: 15: 75 by mass) resulted in a generally uniform particle size distribution ranging from about 20 µm to 2,000 µm. Black Warrior River water was used as the test water to provide the smaller particles which are less than 20 µm in the challenge water mixture. Figure 114 shows the particle size distribution of the three individual silica sand components used to create the test mixture. The resulting concentrations of sediment in the influent challenge water were about 100 and 1,000 mg/L during the experiments. The influent dirty water samples were composited for analysis for each batch, while the column effluents were separated for suspended sediment concentration (SSC), total dissolved solids (TDS), particle size distribution (PSD), turbidity, and conductivity analyses. Figure 115 shows the particle size distribution of the solid mixture used during the test.

The solids mixtures were poured into graduated plastic containers having 10 gallon volumes and filled with Black Warrior River water. This influent mixture was then split into 10 1gallon capacity containers for the 10 columns. A gallon of the challenge water was then poured into each lab column that was filled with various media mixtures. Effluent samples were collected from the bottom of the columns at the beginning, middle, and end of the drainage time and composited in clean 1L bottles for the lab analysis to ensure that all of the sediment and all particle sizes entered the sampling bottles. Each experiment was repeated three times.

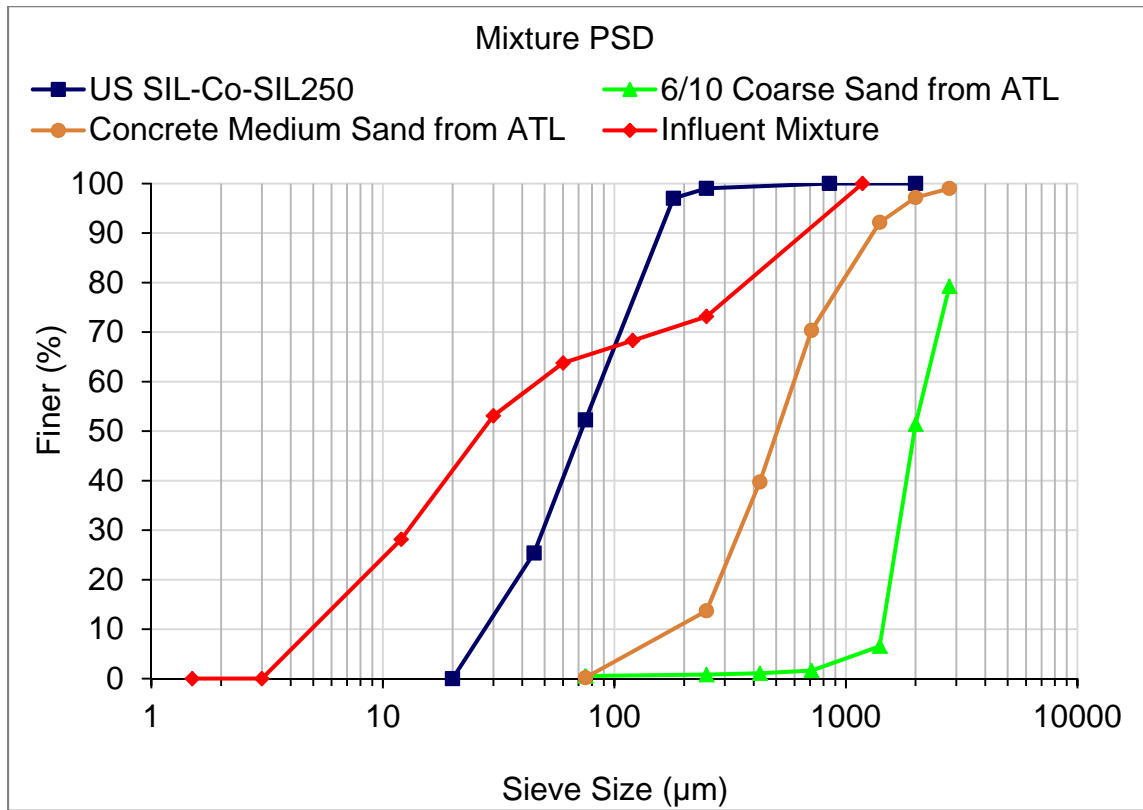


Figure 114. Particle Size Distribution of the Three Individual Components Used to Create the Solid Mixture and the Influent Water.

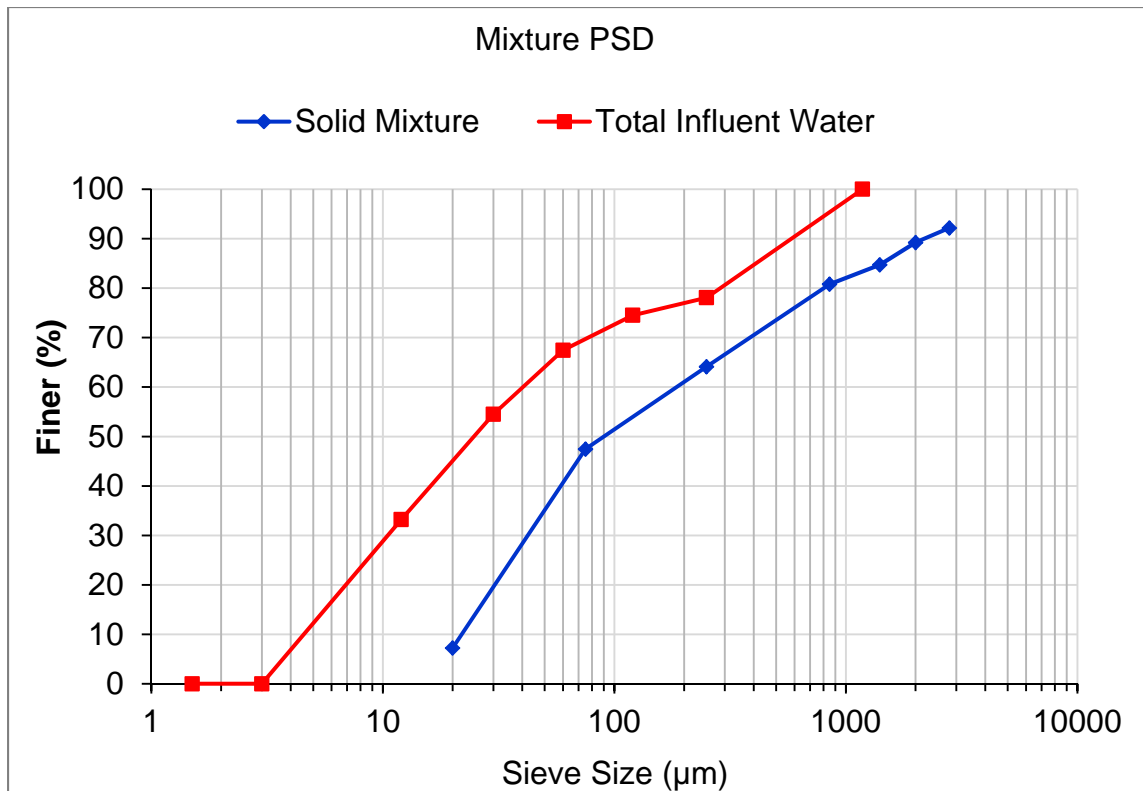


Figure 115. Particle Size Distribution of the Solid Mixture (not including the river water component).

The influent water (solid mixture added to the River water) has a median size of 25 µm. The solid mixture alone has a median size of 90 µm. Figure 115 shows that about 45 % of the influent water is finer than 20 µm, reflecting the presence of fine particles in the Black Warrior River water used in the tests.

Laboratory column particle trapping tests were also performed using pea gravel and coarse gravel media representing coarse drainage layer or storage layer materials used in biofilters, green roofs, or under porous pavements. The laboratory column construction was described in section 4.2.2. The columns were filled with 1.5 ft (0.5 m) of pea gravel and coarse gravel media purchased from a local supplier in Tuscaloosa, AL. A total of four lab columns were constructed during the tests (two columns filled with pea gravel with 0.25 and 1 inch

orifices at the bottom to provide two different treatment flow rates corresponding to underdrain flow rates, and two columns filled with coarse gravel, also with 0.25 and 1 inch orifices. Figure 116 shows the particle size distributions of these coarse media used for these tests. The pea gravel and coarse gravel have median sizes (D_{50}) of 7.5 and 9.5 mm respectively. The pea gravel and coarse gravel have uniformity coefficients (uniformity coefficient = D_{60}/D_{10} , where D_{60} is the particle size associated with the 60th percentile and the D_{10} is the particle size associated with the 10th percentile) of 1.5 and 2 respectively.

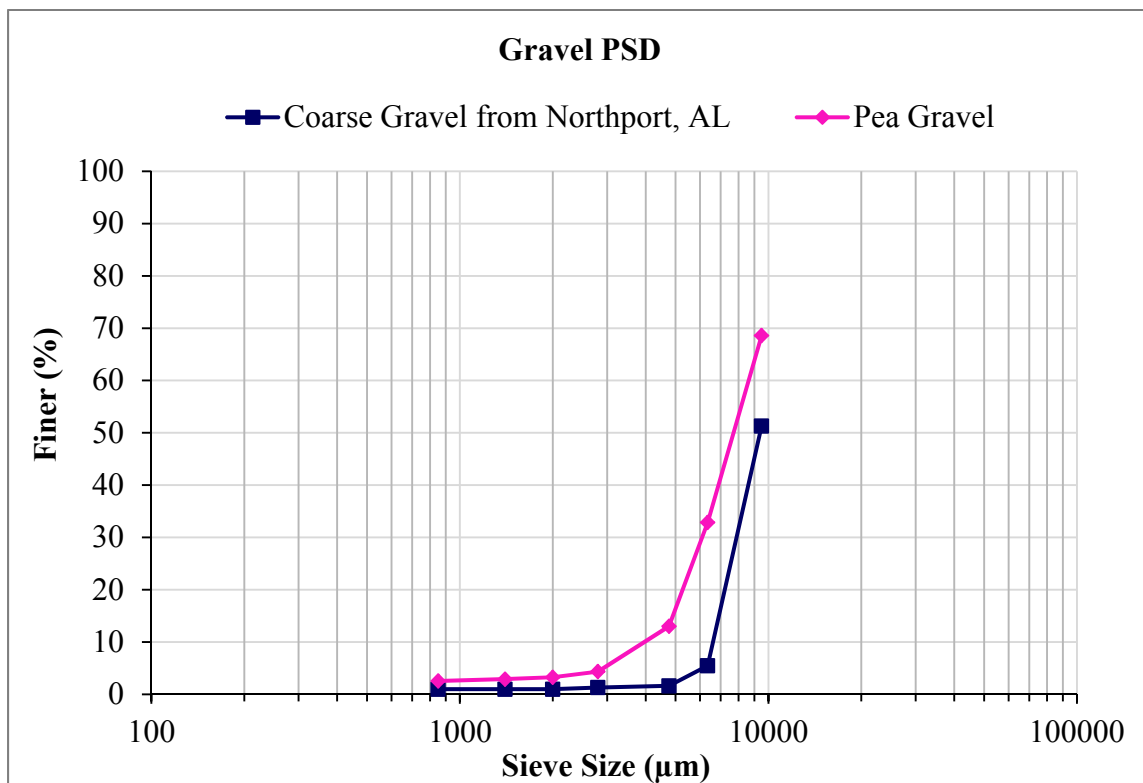


Figure 116. Particle Size Distribution of the Coarse Media.

The concentrations of the sediment in the challenge water during the low and high concentration tests were 100 and 1,000 mg/L. As for the other particle retention tests, the influent

dirty water samples were composited for analysis for each batch, while the effluent samples were separately analyzed for each column for suspended sediment concentration (SSC), total dissolved solids (TDS), particle size distribution (PSD), turbidity, and conductivity analyses.

7.2.3 Particle Trapping Test Sample Analysis

The influent dirty water samples and the treated effluent water samples obtained from laboratory column tests were analyzed. Three test replicates were conducted for approximately low and high concentrations. A total of 96 samples were analyzed during the tests. Before conducting the analyses, each sample was split into 10 equal volumes of about 100 mL each using a USGS/Dekaport cone splitter, as shown in Figure 117.

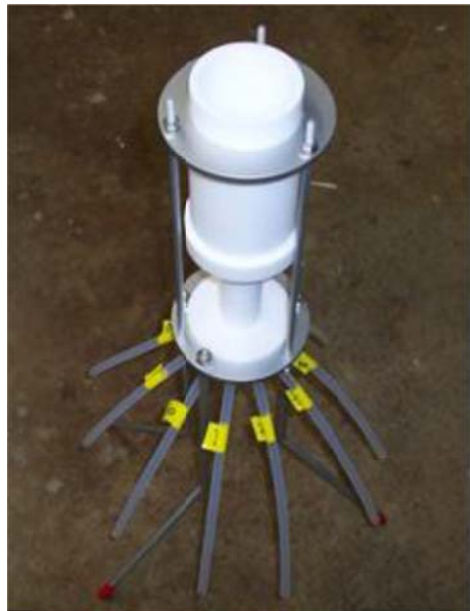


Figure 117. USGS/Dekaport Teflon™ Cone Splitter

7.2.4 Laboratory Solids Analysis (Figure 118 shows the solids analysis flow sheet).

- 1) Ten 250 mL capacity graduate cylinders (short versions) were placed under each tube of the splitter in order to measure the volume of each subsample (needed for SSC calculations).
- 2) 1 L bottle sample water was carefully poured to the splitter. The initial volume was noted for each split. The sample bottle was then rinsed and poured into the splitter several times to ensure that the large particles that tend to catch near the bottle lip were rinsed into the splitter. Then the additional water added was noted in order to adjust the calculated concentrations.
- 3) Two subsamples were poured through a 3-inch stainless steel Tyler #60 sieve to remove particles larger than 250 μm from the subsample water. One of these was used for solids analyses to determine the fraction of the particle solids having particles smaller than 250 μm , while the other was used for the Coulter Counter particle-size-distribution analyses.
- 4) The initial particle size distribution was created using the software provided by Coulter that overlaps the different results from the different Coulter Counter aperture tubes. Each aperture tube can quantify particles at high resolution using many bins in the range of approximately 2% to 60% of the aperture size (e.g., 30 μm tube – 0.6 μm to 18 μm ; 140 μm tube – 2.8 μm to 84 μm ; 40 μm tube – 8 μm to 240 μm). Each of the tubes' data substantially overlaps the adjacent tubes' data providing sufficient duplication of particle diameters for the software overlap. Three-inch stainless steel Tyler sieves were used to pre-sieve the subsamples before analyses by each aperture to minimize clogging; the sieve size selected was the smallest commercially available sieve that exceeds the maximum analytical range of each tube, while still being smaller than the tube aperture

itself (e.g., 30- μm tube – 20- μm sieve [Tyler #625], 140- μm tube – 106- μm sieve [Tyler #150], 400- μm tube – 250- μm sieve [Tyler #60]). The sample is pipetted through the sieve and directly into the Coulter Counter vessel.

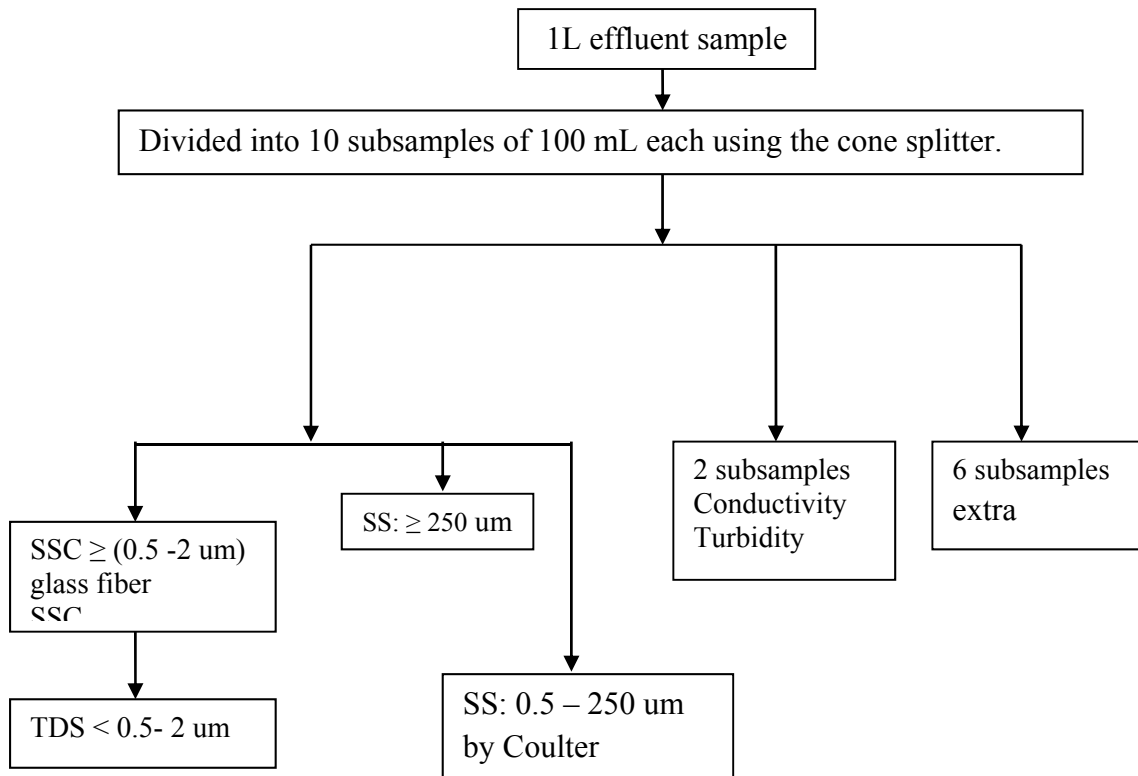


Figure 118. Flow Sheet for the Solids Analysis

The constituents analyzed as a part of the particle trapping experiments include (Table 76 indicates analytical methods and detection limits for these constituents):

- Suspended sediment concentration (SSC)
- Total dissolved solids (TDS) (< 0.45 μm particles)
- Turbidity (continuous and for samples)
- Conductivity analyses (continuous and for samples)
- Particle size distribution (PSD) (by sieves and Coulter Counter)

Table 76. Analytical Methods and Detection Limits/Ranges

Constituents	Analytical Methods	Detection Limit/Ranges
SSC	ASTM D3977-97 B	N.A
TDS	EPA Method 160.1	N.A
Turbidity (laboratory)	EPA Method 180.1 (Standard Method 2130.B.)	0 to 4,000 NTU
Conductivity (laboratory)	EPA Method 120.1 (Standard Method 2510.B.)	0 to 199,900 $\mu\text{S}/\text{cm}$

7.2.5 Suspended Sediment Concentration (ASTM, 1997)

1. Nominal 0.45 to 2 μm pore size glass fiber filter paper (Whatman) with wrinkled side up is placed on the filtration apparatus using a pair of tweezers. Vacuum is applied and the filter paper is washed three times with about 20 mL of DI water. After continuous suction, all traces of water was filtered through the filter paper. The filter paper was removed and placed on an aluminum dish which was washed before with DI water. The aluminum dish was placed in the oven and left for complete evaporation of water at 105 $^{\circ}\text{C}$ for approximate 24 hours.
2. The filtration apparatus was washed before and after washing every filter paper.
3. After 24 hours, the aluminum dishes were removed from the oven and placed inside desiccators.
4. The complete split subsamples (approximately 100 mL) from the cone splitter, were then filtered thru the cleaned and weighed filter. The filtered water volume was measured directly during the sub sampling process and the filter is dried and weighed, as described below.
5. In addition to the sieve analysis, particle size distributions were measured using the Coulter Counter for the smaller particles (about 2 to 250 μm).

Suspended Sediment Concentrations were calculated by the following equation.

$$\text{Suspended Sediment Concentrations} = (\text{Weight of Aluminum dish before filtration (mg)} - \text{Weight of Aluminum dish after filtration (mg)}) / \text{Volume (L)}$$

7.2.6 Total Dissolved Solid (TDS) Analysis Procedure (Standard Method, 2005)

1. Cleaned crucibles were removed from the desiccators and weighed.
2. After the filtration using the nominal 0.45 to 2 μm glass fiber filter, the water which was filtered by the filter is transferred into the crucibles
3. The flask was washed with DI water and transferred into the crucibles to make sure all the solids were transferred into the crucible.
4. The crucibles were placed in the oven at 105 °C for approximately 24 hours
5. The crucibles were removed after 24 hours and placed in the desiccators for cooling.
6. After cooling the crucibles were weighed.

Total Dissolved Solids (TDS) were calculated by the following equation.

$$\text{Total Dissolved Solids} = (\text{Weight of empty crucible (mg)} - \text{Weight of crucible after evaporation (mg)}) / \text{Volume (L)}$$

7.3 Results and Discussions

7.3.1 Sand-Peat Mixture Nutrient and Other Constituents Report

Samples of different sand and sand-peat mixtures representing a wide range of median sizes, uniformities, and organic content were delivered to Auburn University's Soil Testing Laboratory, where texture (% sand, % silt, and % clay), organic matter, major ions, heavy metals, cation exchange capacity, general nutrients, and sodium adsorption ratios were also analyzed. According to the AU laboratory tests, the median size of the sand and peat mixture samples ranged from 300 to 1,900 μm . The reports for these analyses are shown in Appendix D.1, while a summary is shown below in Table 77.

Table 77. Summary of the Sand and Peat Mixture Summary Nutrients and Other Constituents Report

Sample ID	Cation Exchange Capacity (meq/100g)	pH	Organic Matter (%)	Sodium Adsorption Ratio (SAR)
Sand from Northport, AL	0.036	4.80	0.2	2.3
10% peat & 90% sand from Northport, AL	0.042	4.51	1.0	1.8
25% peat & 75% sand from Northport, AL	0.048	4.05	2.7	1.9
50% peat & 50% sand from, Northport, AL	0.071	3.81	9.9	0.4
10/30 sand from ATL, GA	0.007	4.85	0.1	3.4
10% peat, 45% sand from Northport, & 45% 10/30 sand	0.039	4.04	0.9	2.3
25% peat, 37.5% sand from Northport, & 37.5% 10/30 sand	0.059	3.86	2.0	2.0
50% peat, 25% sand from Northport, & 25% 10/30 sand	0.087	3.69	7.1	1.3
Concrete sand from ATL, GA	0.040	4.75	0.1	1.8
10% peat, 45% concrete sand, & 45% 10/30 sand	0.048	4.28	0.8	1.9
25% peat, 37.5% concrete sand, & 37.5% 10/30 sand	0.059	3.95	2.3	0.4
50% peat, 25% concrete sand, & 25% 10/30 sand	0.085	4.03	4.9	1.3
6/10 sand from ATL, GA	0.049	5.10	0.1	2.5
10% peat, 45% sand from Northport & 45% 6/10 sand	0.073	4.61	0.8	2.4
25% peat, 37.5% sand from Northport & 37.5% 6/10 sand	0.077	4.19	1.5	1.7
50% peat, 25% sand from Northport & 25% 6/10 sand	0.099	3.85	6.8	1.4
10% peat, 45% 10/30 sand, & 45% 6/10 sand	0.067	4.19	0.4	2.5
25% peat, 37.5% 10/30 sand, & 37.5% 6/10 sand	0.068	4.03	1.6	2.0
50% peat, 25% 10/30 sand, & 25% 6/10 sand	0.085	3.89	6.2	2.5

Organic matter improves soil structure and soil tilth, and helps to provide a favorable medium for plant growth. Soils with large amounts of clay generally require large amounts of

organic matter. Soils with a higher organic matter content will have a higher cation exchange capacity (CEC), higher water holding capacity, and better tilth than soils with a lower organic matter content. The cation exchange capacity (CEC) of a soil is a measurement of its ability to bind or hold exchangeable cations. The different sand and peat mixtures had an average CEC value of 0.06 meq/100g and ranged from 0.01 to 0.1 meq/100g. Increases in the CEC values were noted with increase in the percentage of peat in the mixture. The sand and peat mixture had an average pH of 4.2 and ranged from 3.7 to 5.1 respectively. The pH values decrease with an increase in the percentage of peat in the mixture. According to the Alabama Cooperative Extension System, the ideal soil pH value for most crops ranges between 5.8 and 6.5 and for acid loving plants ranges between 5.0 and 5.7. The sand-peat mixtures had a pH values outside this range. When soil pH is outside of these optimal ranges, nutrients can be less available to plants, potentially resulting in deficiencies.

Soils in the Central Great Plains have organic content ranging between 1 and 2% for cultivated soils, and about 1.5 to 3.0% for native grasslands (Bowman, 1996). Generally, healthy soil has between 3 and 5% organic material. The different sand and peat mixtures tested had an average organic content of 2.6% and ranged from 0.1 to 10%.

The sodium content of soil affects soil texture and pH. The sand and peat mixture had an average sodium adsorption ratio (SAR) of 2 and ranged from 0.4 to 3.4. A SAR value of 15 or greater indicates an excess of sodium will be adsorbed by the soil clay particles, potentially causing severe infiltration reductions (Curtis 2010).

The sand and peat mixtures have an average phosphorus concentration of 0.6 ppm. The critical phosphorus concentration for crops (peanuts, pine trees, blueberries and centipedegrass) grown in sandy soil in Alabama is 9.5 ppm, whereas for all other crops, is 25 ppm indicating the

sand peat mixtures had lower phosphorus concentrations than growing media, which support the minimal expected leaching of phosphorus from the media when treating stormwater (in contrast of media mixtures that have large amounts of compost, for example). The sand and peat mixture had an average potassium, magnesium, and calcium concentrations of 1.5, 0.7, and 1.1 ppm respectively. The critical magnesium level for all crops grown in sandy soil in Alabama as used by the Auburn University Soil Testing Laboratory is about 13 ppm, whereas the critical calcium level for crops such as tomatoes, peppers, fruits and nuts grown in sandy soils is 250 ppm. The sand and peat mixture had a lower concentration of potassium, calcium and magnesium for most crops grown in sandy and loam soils in Alabama.

Micronutrients, such as boron, zinc, manganese, copper, molybdenum, iron, and chloride, are needed in much smaller quantities, and most Alabama soils contain adequate amounts for most crops (Adams and Mitchell 2000). The sand and peat mixture had an average boron, zinc, manganese, copper, molybdenum concentration of less than 0.2 ppm. Some Alabama crops may use between 20 (10 ppm) and 200 (100 ppm) pounds per acre of N, P, K, Ca, Mg and S, they use less than 1 pound per acre of micronutrients (Adams and Mitchell 2000).

7.3.2 Infiltration Results for Sand and Peat Mixture Tests

Infiltration data for different test trials using different sand-peat mixtures were fitted to the Horton equation by using multiple nonlinear regressions to estimate f_c (the saturated mixture infiltration rate, the critical value used for biofilter design) based on the observed data. The average infiltration rates of the saturated mixtures indicated that the infiltration rates through the mixtures increased with increases in the percentage of peat. Examples of Horton's plots of the different test trials are shown in Figures 119 and 120.

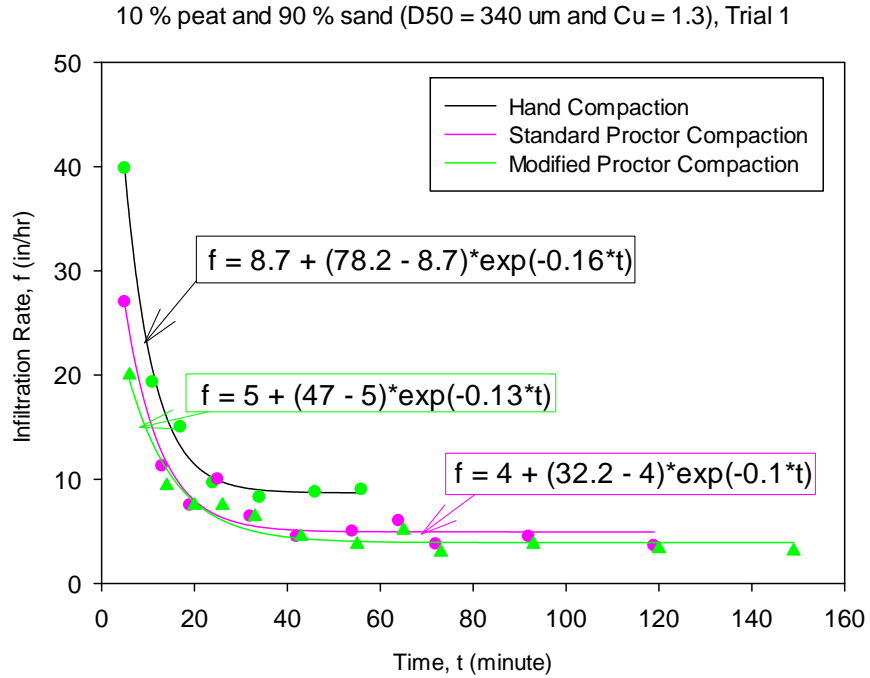


Figure 119. Infiltration Measurements for 10% Peat and 90% Sand.

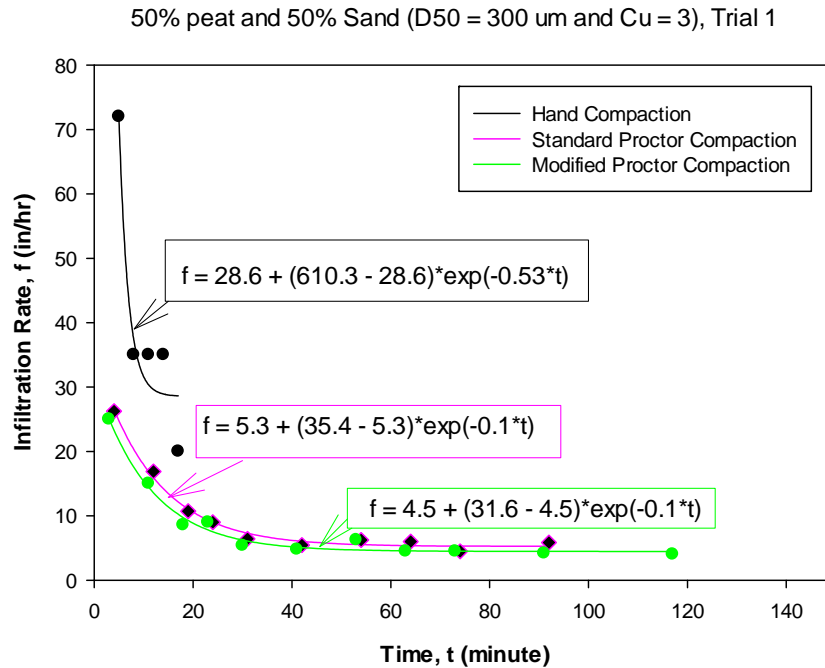


Figure 120. Infiltration Measurements for 50% Peat and 50% Sand.

Laboratory infiltrations measurements using sand-peat mixtures fitted with the Horton's equations are shown in Appendix D.2 through D.16.

Figure 121 shows box and whisker plots of the final infiltration rates for the different test conditions, comparing different compaction conditions with varying amounts of peat amendments. The infiltration rates (in/hr) appear to increase with increases in the percentage of peat (a later discussion presents the statistical test results). Four different sand media mixtures were used for the test series for full factorial tests and other analyses. Table 78 shows the sand-peat mixtures used during the tests. Fifteen replicates are available for each test series. The median sizes of the sand and peat mixtures ranged from 300 to 2,000 μm and the uniformity coefficients ranged from 2 to 22.

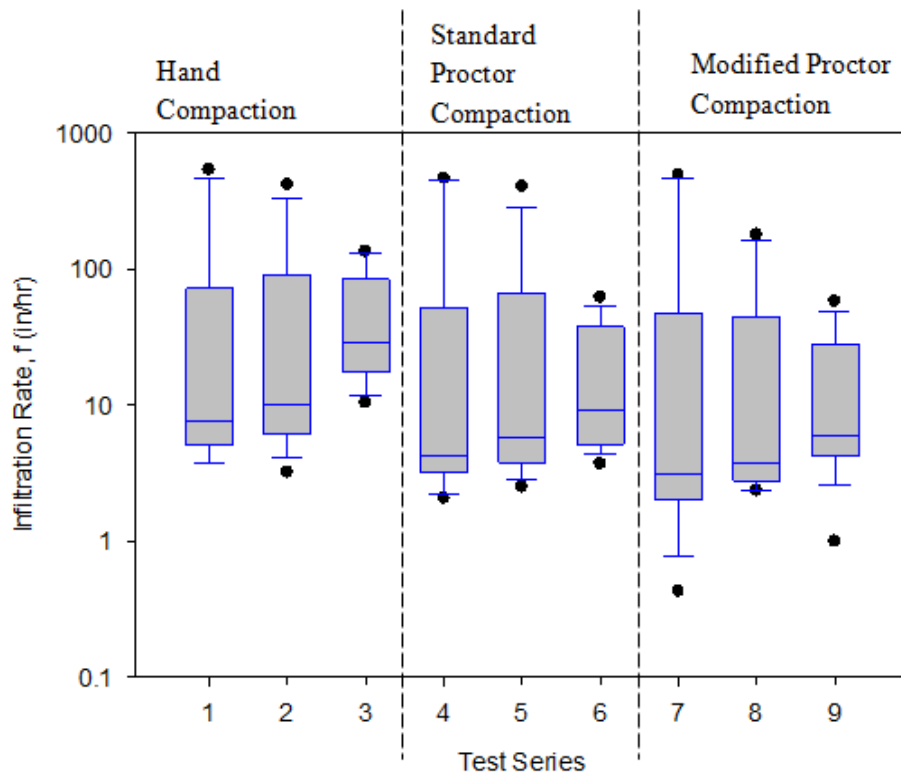


Figure 121. Box and Whisker Plots of the Different Test Conditions, Comparing Different Compaction Conditions with Varying Amounts of Peat Amendments.

Table 78. Test Mixture Descriptions (Fifteen Replicates in Each Test Series) (corresponding to the numbered samples on the box and whisker plot in Figure 121).

Data series	Mixture
1	10% peat and 90% sand with hand compaction
2	25% peat and 75% sand with hand compaction
3	50% peat and 50% sand with hand compaction
4	10% peat and 90% sand with standard proctor compaction
5	25% peat and 75% sand with standard proctor compaction
6	50% peat and 50% sand with standard proctor compaction
7	10% peat and 90% sand with modified proctor compaction
8	25% peat and 75% sand with modified proctor compaction
9	50% peat and 75% sand with modified proctor compaction

7.3.3 Biofilter Media Nutrient and Other Constituents Report

Samples of treatment media from Kansas City and North Carolina biofilters were also analyzed by Auburn University’s Soil Testing Laboratory (Wisconsin biofilter media samples were also delivered to the laboratory for these chemical analyses but the results are not available for this dissertation). Summaries of the biofilter media texture and soils laboratory reports are shown in Tables 79 and 80. The media from the Kansas City and North Carolina biofilter sites have clay contents of 10 and 7.5% respectively. According to the AU laboratory tests, the median size of the media from these North Carolina and Kansas City biofilter sites are 700 um and 2,000 um, respectively.

Organic matter improves soil structure and soil tilth, and helps to provide a favorable medium for plant growth. Soils with large amounts of clay generally require large amounts of organic matter. The organic matter content of the Kansas City biofilter media has a value of 15%, indicating the soil is in good condition, whereas the organic content of the North Carolina biofilter media has a value of 1.5%.

The media obtained from the Kansas City biofilter sites had CEC and pH values of 0.83 meq/100g and 7.4 respectively. The media obtained from the North Carolina site had CEC and pH values of 0.09 meq/100g and 5.2 respectively. As described by the Auburn University Soil Testing Laboratory (Mitchell and Huluka, 2011), these characteristics vary from soil to soil, with sandy soils generally having CEC values ranging from 0 to 4.6 meq/100g and loam soils having CEC values ranging from 4.6 to 9.0 meq/100g. The sodium content of soil affects soil texture and pH, and high sodium (in the presence of low calcium and magnesium, as defined by the sodium adsorption ratio, or SAR) can cause severe flow restrictions if affected by snowmelt waters. The biofilter media obtained from both biofilter sites had a SAR value of about 1.5, well below typical problematic levels.

Table 79. Summary of Biofilter Media Texture Report.

Biofilter Media from	Sand (%)	Silt (%)	Clay (%)	Textural Class
Kansas City	58.75	31.25	10.00	Sandy Loam
North Carolina	90.00	2.50	7.50	Sand

Table 80. Kansas City and North Carolina Biofilter Media Nutrient and Other Constituent Concentrations.

Nutrient (ppm)	Kansas City	North Carolina
Calcium (Ca)	5,903	219
Potassium (K)	304	56
Magnesium (Mg)	266	45
Phosphorus (P)	69	4
Aluminum (Al)	3	19
Arsenic (As)	1.0	0.9
Boron (B)	1	0.2
Barium (Ba)	14	6
Cadmium (Cd)	<0.1	<0.1
Chromium (Cr)	<0.1	<0.1
Copper (Cu)	0	3
Iron (Fe)	1	12
Manganese (Mn)	13	48
Molybdenum (Mo)	<0.1	<0.1
Sodium (Na)	155	32
Nickel (Ni)	0.3	0.1
Lead (Pb)	<0.1	<0.1
Zinc (Zn)	1	1
Total Phosphorus (P)	1009	66
Nutrient (percent)		
Nitrogen (N)	0.74	0.02
Carbon (C)	8.59	0.86
Sulfur (S)	0.18	0.03
Organic Matter (OM)	14.8	1.5
Sodium Adsorption Ratio (SAR)	1.50	1.60
Moisture (%)	44.40	15.90
pH	7.41	5.2
H ₂ O availability (cm ³ /cm ³)	0.12	0.07
Cation Exchange Capacity (CEC) (meq/100g)	0.83	0.09

7.3.4 Infiltration Results using Biofilter Media

Infiltration data obtained during tests using biofilter media from North Carolina, Wisconsin, and Kansas City were fitted to the Horton equation by using multiple nonlinear regressions to estimate f_c (the saturated soil infiltration rate). As an example, the average

infiltration rates for the saturated North Carolina biofilter media ranged from 7.4 in/hr (19 cm/hr) to 1.9 in/hr (4.8) for the hand and modified proctor compaction tests, respectively, while the average infiltration rates for the saturated Kansas City biofilter media ranged from 0.55 in/hr (1.4 cm/hr) to 0.13 in/hr (0.33 cm/hr) for the hand and modified proctor compaction tests, respectively. Horton's plots of the different test trials, comparing different compaction conditions using North Carolina, Kansas City, and Wisconsin media are shown in Figure 122, 123, and 124, respectively. The saturated soil infiltration rates for hand, standard proctor, and modified proctor compaction using North Carolina and Wisconsin media are greater than the saturated soil infiltration rates through the Kansas City biofilter material for the three levels of compaction. Table 81 through 84 summarizes the laboratory column infiltration test results for the biofilter material, and for the different compaction values. Laboratory infiltration measurements using actual biofilter media fitted with the Horton's equation are shown in Appendix D.17 and 18 .

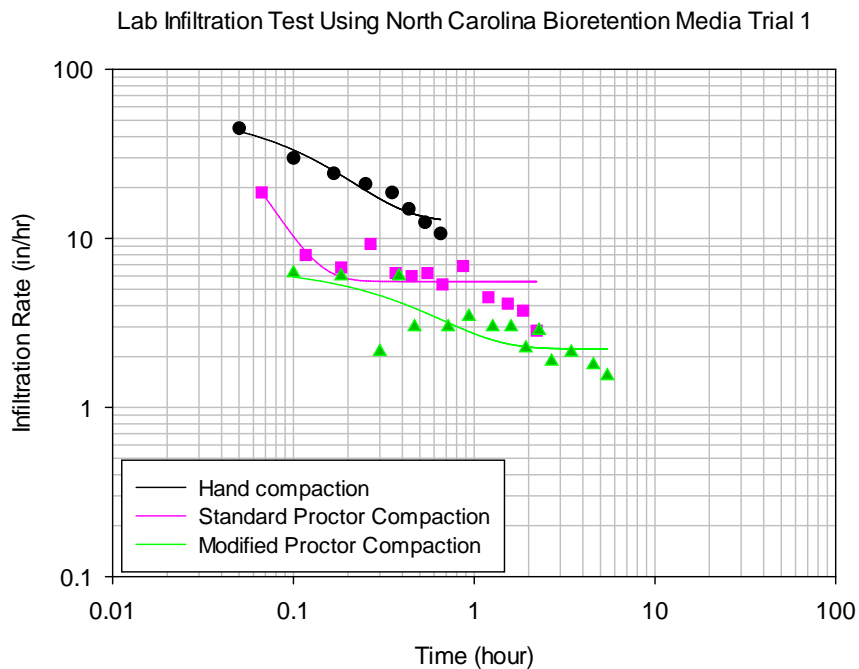


Figure 122. Example of Laboratory Infiltration Test Results Using North Carolina Media.

Table 81. Laboratory Infiltration Tests Using North Carolina Biofilter Media.

North Carolina Biofilter Media				
Compaction method	Test	f_0 (in/hr, cm/hr)	f_c (in/hr, cm/hr)	k (1/hr)
hand (density = 1.24 g/cc)	1	57 (144.8)	12.7 (32.1)	7.60
	2	28.6 (72.6)	6.6 (16.6)	6.07
	3	17.4 (44.2)	2.8 (7.1)	2.77
	mean	34.3 (87.2)	7.3 (18.6)	5.48
	COV	0.6	0.7	0.45
Standard (density = 1.34 g/cc)	1	107 (273)	5.6 (14.2)	30.73
	2	29 (73.6)	3.5 (9)	10.48
	3	14.3 (36.3)	2.6 (6.6)	4.85
	mean	50.2 (128)	4 (10)	15.35
	COV	1	0.4	0.89
Modified (density = 1.36 g/cc)	1	6.8 (17.4)	2.2 (5.7)	2.20
	2	8.8 (22.3)	1.8 (4.6)	3.92
	3	6.5 (16.6)	1.6 (4.1)	3.67
	mean	7.4 (18.8)	1.9 (4.8)	3.26
	COV	0.17	0.17	0.28

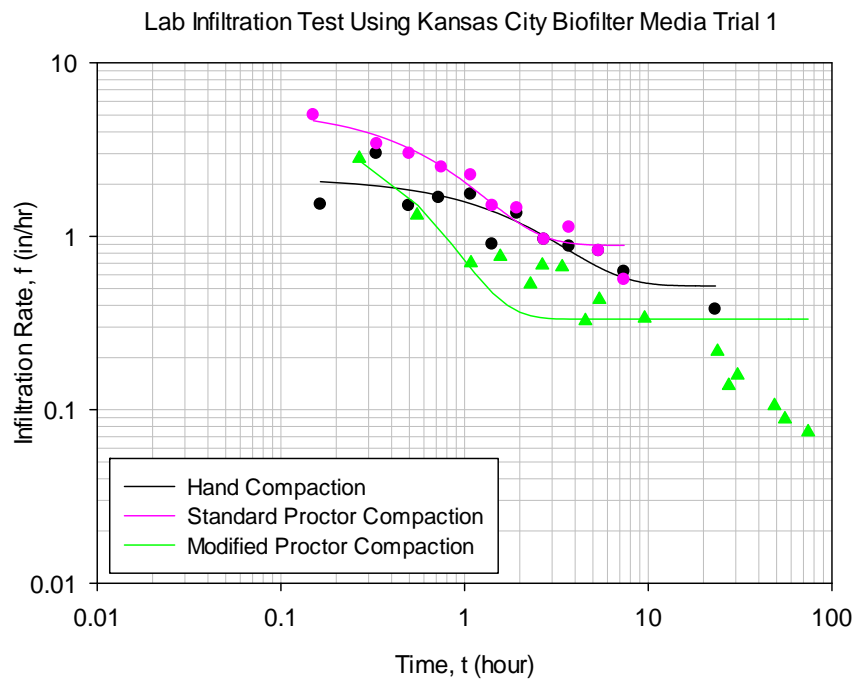


Figure 123. Example of Laboratory Infiltration Test Results Using Kansas City Media.

Table 82. Laboratory Infiltration Tests Using Kansas City Soil Media.

Kansas City Biofilter Media				
Compaction method	Test	f_o (in/hr, cm/hr)	f_c (in/hr, cm/hr)	k (1/hr)
hand (density = 1.1 g/cc)	1	2.2 (5.6)	0.5 (1.3)	0.45
	2	2.4 (6.2)	0.8 (1.9)	0.70
	3	0.9 (2.2)	0.4 (0.9)	0.21
	mean	1.8 (4.6)	0.6 (1.4)	0.45
	COV	0.47	0.36	0.54
standard (density = 1.13 g/cc)	1	5.5 (14)	0.9 (2.2)	1.40
	2	6.4 (16.4)	0.7 (1.7)	5.51
	3	0.9 (2.2)	0.4 (0.9)	0.57
	mean	4.3 (10.9)	0.6 (1.6)	2.49
	COV	0.70	0.41	1.06
modified (density = 1.1 g/cc)	1	4.98 (12.65)	0.33 (0.84)	59.4
	2	0.10 (0.26)	0.03 (0.08)	0.33
	3	0.34 (0.86)	0.04 (0.1)	0.12
	mean	1.81 (4.59)	0.13 (0.34)	19.9
	COV	1.52	1.27	1.73

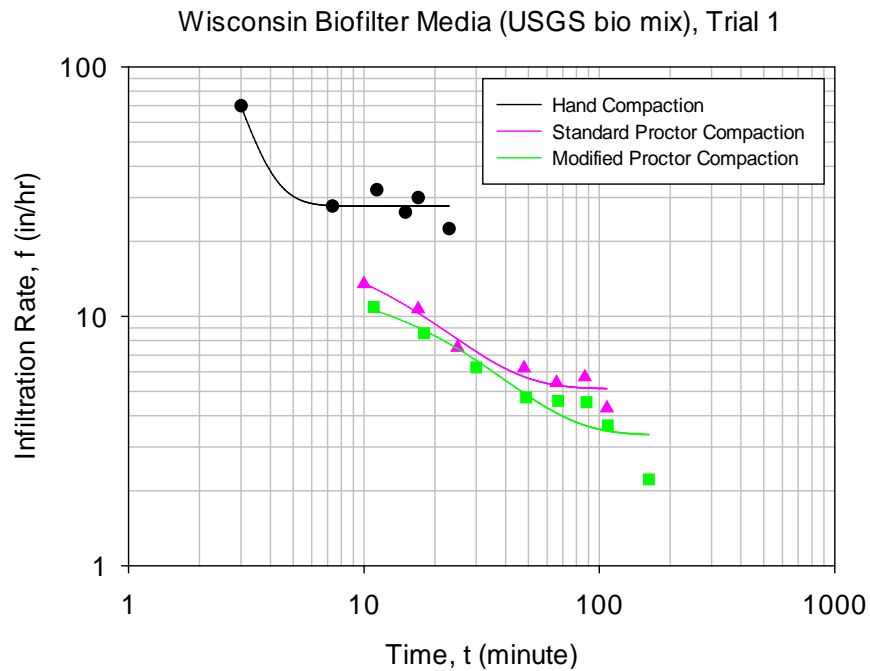


Figure 124. Example of Laboratory Infiltration Test Results Using Wisconsin Biofilter Media.

It is obvious that the saturated soil infiltration rates through the North Carolina biofilter media are greater than the saturated soil infiltration rates through the Kansas City biofilter material for the three levels of compaction. The North Carolina and Kansas City biofilter media had percent fine (silt + clay) values of 10 and 40% respectively. The effect of compaction on infiltration rates is more pronounced for media and soils that have greater percentages of fines (silt + clay), as indicated by the actual Kansas City biofilter media. Compaction affected the Kansas City biofilter material more than North Carolina biofilter media, which had 90% sand.

Table 83. Laboratory Infiltration Tests Using Wisconsin Biofilter Media-1.

Wisconsin Biofilter Media-1 (USGS Bio Mix)				
Compaction method	Test	f_o (in/hr, cm/hr)	f_c (in/hr, cm/hr)	k (1/min)
hand (density = 1.51 g/cc)	1	2,736 (6,950)	27.7 (70.4)	1.39
	2	84.3 (214)	30 (76.2)	0.06
	3	85.2 (216)	17.5 (44.4)	0.11
	mean	969 (2,460)	25.1 (63.6)	0.52
	COV	1.6	0.3	1.44
standard (density = 1.74 g/cc)	1	22.1 (56)	5.1 (13)	0.07
	2	12.7 (32.3)	5.2 (13.2)	0.04
	3	27 (68.5)	7.5 (19)	0.12
	mean	20.6 (52.2)	5.9 (15.1)	0.08
	COV	0.4	0.2	0.58
modified (density = 1.8 g/cc)	1	14.8 (37.6)	3.4 (8.5)	0.04
	2	12.6 (32)	4 (10.2)	0.09
	3	23.9 (60.6)	5.3 (13.4)	0.09
	mean	17.1 (43.4)	4.20 (10.7)	0.07
	COV	0.3	0.2	0.38

Table 84. Laboratory Infiltration Tests Using Wisconsin Biofilter Media-2.

Wisconsin Biofilter Media-2 (Neenah Mix)				
Compaction method	Test	f_o (in/hr, cm/hr)	f_c (in/hr, cm/hr)	k (1/min)
hand (density = 1.7 g/cc)	1	126 (321)	2.5 (6.5)	0.10
	2	138 (351)	29.6 (75.1)	0.69
	3	76.4 (194)	29.5 (74.9)	0.18
	mean	114 (289)	20.5 (52.1)	0.32
	COV	0.29	0.76	1.00
standard (density = 1.8 g/cc)	1	385 (978)	31.6 (80.3)	0.70
	2	32.8 (83.2)	13.1 (33.2)	0.05
	3	52 (132)	18.6 (47.4)	0.15
	mean	157 (398)	21.1 (53.6)	0.30
	COV	1.26	0.45	1.17
modified (density = 1.81 g/cc)	1	138 (351)	29.6 (75.1)	0.69
	2	24.5 (62.3)	13.6 (34.7)	0.07
	3	24.5 (62.3)	12.3 (31.2)	0.02
	mean	62.4 (158)	18.5 (47)	0.26
	COV	1.05	0.52	1.45

7.3.5 Comparisons of Different Levels of Compaction and Percentage of Peat in the Sand- Peat Mixture.

Kruskal-Wallis multiple pairwise comparison tests were used to determine if at least one subgroup of data were significantly different from the other subgroups being compared. This test compares the population medians of the groups, instead of the population means used by ANOVA and it represents a nonparametric version of the parametric ANOVA test. The Kruskal-Wallis method tests the hypothesis that all population medians are equal (Gibbons, 1997). The multiple comparison tests shown below were conducted using a MINITAB version 16 macro in a nonparametric setting (Orlich, 2010). The following figures describe the significance of the differences for the saturated infiltration rates (F_c) for different levels of compaction and different sand and peat mixtures. Detailed calculations and results are attached in Appendix D. The graph

on the left of Figure 125 shows box plots of groups with their sign confidence intervals for the medians (red boxes in the each box plot). The graph on the right displays the non absolute group mean rank standardized differences (Orlich, 2010). This latter plot shows the magnitude of the group differences and its direction. It also shows the positive and negative critical z-values and illustrates if a difference is likely statistically significant. Table 85 shows the test mixture descriptions used during this test.

From Figure 125, it is seen that the saturated infiltration rate using 50% sand and 50% peat mixture and hand compaction was larger than the saturated infiltration rates using 10, 25, and 50% peat added to the sand media for standard proctor and modified proctor compaction tests. This difference is also shown to be statistically significant for some of the mixtures since the standardized difference distance goes beyond the critical z-values compared to the other test groups. There are significant differences noted between saturated infiltration rate using test mixture 3 and hand compaction vs. test mixture 8 and modified proctor compaction; test mixture 3 and hand compaction vs. test mixture 7 and modified proctor compaction method; saturated infiltration rate using test mixture 1 and hand compaction vs. test mixture 8 and modified proctor compaction. There were no significant differences noted between the saturated infiltration rates of samples subjected to the standard proctor vs. the modified proctor compaction procedures, for the number of data observations available.

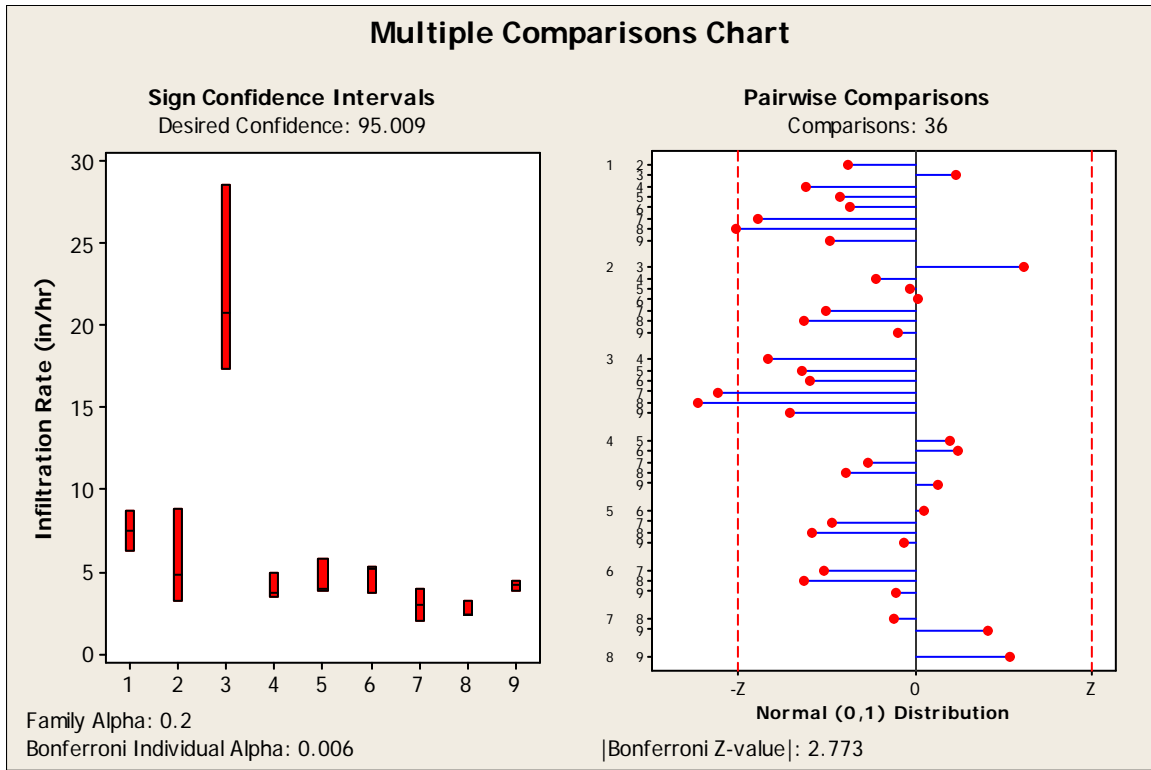


Figure 125. Multiple Comparison Plots of Laboratory Infiltration Measurements Using Sand and Peat Mixture (mixture $D_{50} = 300 - 350$ um) for Different Compaction Levels.

Table 85. Test Mixture Descriptions (mixture: $D_{50} = 300$ to 340 um) Shown in Figure 125

Data series	Mixture
1	10% peat and 90% sand with hand compaction (mixture : $D_{50} = 340$ um and $C_u = 1.3$)
2	25% peat and 75% sand with hand compaction (mixture : $D_{50} = 300$ um and $C_u = 3.5$)
3	50% peat and 50% sand with hand compaction (mixture : $D_{50} = 300$ um and $C_u = 3.3$)
4	10% peat and 90% sand with standard proctor compaction (mixture : $D_{50} = 340$ um and $C_u = 1.3$)
5	25% peat and 75% sand with standard proctor compaction (mixture : $D_{50} = 300$ um and $C_u = 3.5$)
6	50% peat and 50% sand with standard proctor compaction (mixture : $D_{50} = 300$ um and $C_u = 3.3$)
7	10% peat and 90% sand with modified proctor compaction (mixture : $D_{50} = 340$ um and $C_u = 1.3$)
8	25% peat and 75% sand with modified proctor compaction (mixture : $D_{50} = 300$ um and $C_u = 3.5$)
9	50% peat and 50% sand with modified proctor compaction (mixture : $D_{50} = 300$ um and $C_u = 3.3$)

The same approach was used to distinguish the differences in paired saturated infiltration rates for hand, standard proctor, and modified proctor compaction for sand and peat mixtures having median sizes ranging from 1,600 to 1,900 um. Table 86 shows the test mixture

descriptions used during these tests. Figure 126 shows the multiple comparisons of saturated infiltration rates of observed data. Figure 126 shows that there are statistically significant differences between saturated infiltration rates of test mixture 4 vs. 9, test mixture 1 vs. 9, and 7 vs. 9. However, there are no significant differences noted between the saturated infiltration rates of standard proctor and modified proctor compaction methods, for the number of data observations available. Detailed calculations and results are included in Appendix D.

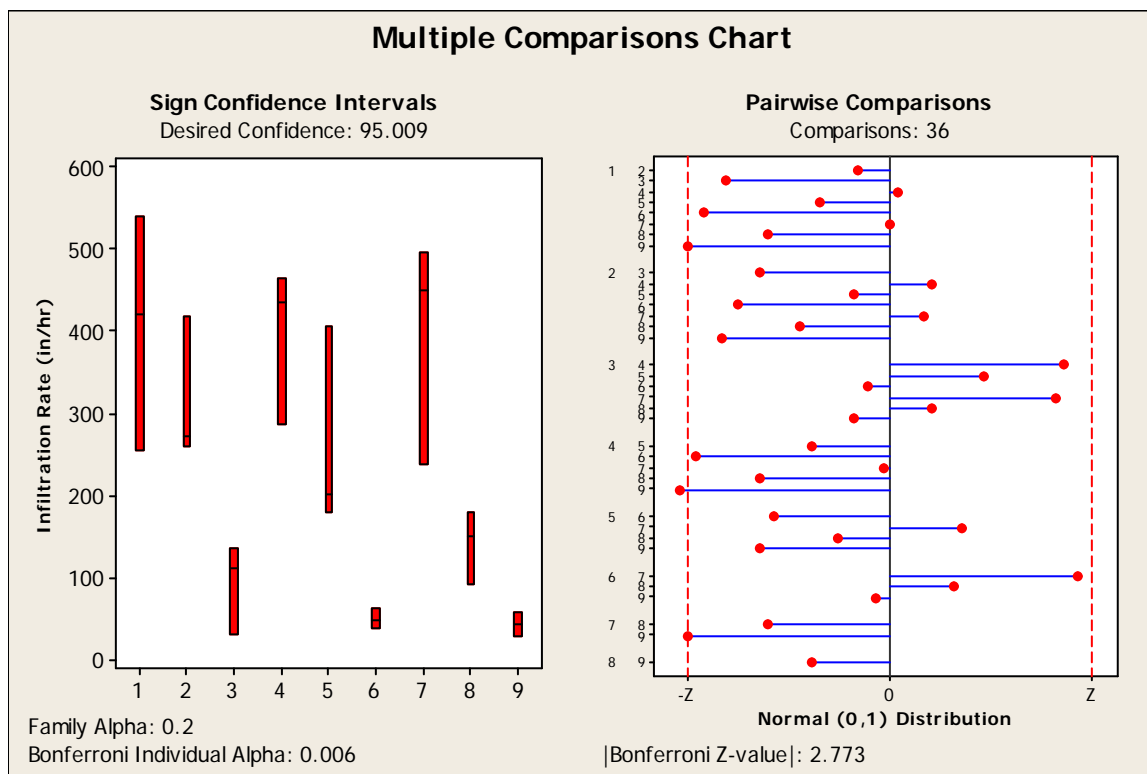


Figure 126. Multiple Comparison Plots of Laboratory Infiltration Measurements Using Sand and Peat Mixture (mixture $D_{50} = 1600 - 1900$ um) for Different Compaction Levels.

Table 86. Test Mixture Descriptions (mixture: D₅₀ = 1600-1900 um)

Data series	Mixture
1	10% peat and 90% sand with hand compaction (mixture : D ₅₀ = 1875 um and C _u = 2.1)
2	25% peat and 75% sand with hand compaction (mixture : D ₅₀ = 1875 um and C _u = 2)
3	50% peat and 50% sand with hand compaction (mixture : D ₅₀ = 1625 um and C _u = 2.5)
4	10% peat and 90% sand with standard proctor compaction (mixture : D ₅₀ = 1875 um and C _u = 2.1)
5	25% peat and 75% sand with standard proctor compaction (mixture : D ₅₀ = 1875 um and C _u = 2)
6	50% peat and 50% sand with standard proctor compaction (mixture : D ₅₀ = 1625 um and C _u = 2.5)
7	10% peat and 90% sand with modified proctor compaction (mixture : D ₅₀ = 1875 um and C _u = 2.1)
8	25% peat and 75% sand with modified proctor compaction (mixture : D ₅₀ = 1875 um and C _u = 2)
9	50% peat and 50% sand with modified proctor compaction (mixture : D ₅₀ = 1625 um and C _u = 2.5)

7.3.6 Statistical Analyses of Infiltration Rates Through Sand-Peat Mixture and Tuscaloosa Soil

Statistical analyses were conducted to determine the effects of texture, uniformity, amount of organic material, and compaction, plus their interactions, on the flowrate through the various mixtures of sand and peat on flow rate. A complete two level, four factors (2⁴, with varying texture, uniformity, organic content, and compaction) full-factorial experiment (Box et al. 1978) was conducted to examine the effects of these factors, plus their interactions, on the flowrate through the various sand-peat mixtures. The factors studied, and their low (-1) and high values (+1) used in the calculations, are shown in Table 87. The complete data used in this factorial study are also summarized in Table 88, showing the log₁₀ transformed f_c rates for each experiment. Experiments were performed in replicates of 3 to 17 for each infiltration measurement.

Table 87. Laboratory Column Infiltration Test Results.

Variable	Low value (-1)	High value (+1)
Median particle size of mixture (T), D ₅₀ (µm)	500	1000
Uniformity of the mixture (U)	4	6
Organic content of the mixture (O), %	10	25
Compaction level (C), hand/modified proctor	hand	modified proctor

Data analyses were performed using the statistical software package Minitab (version 16). Normal plots of the standardized effects, residual plots, main effects plots, and interaction plots were prepared to examine the effects of the factors and to determine their significance. An analysis of variance (ANOVA) table was constructed to determine the significant factors and their interactions needed to best predict media flow performance. Statistical hypothesis tests using a p-value of 0.05 (95% confidence) were used to determine whether the observed data were statistically significantly different from the null hypothesis.

Table 88. Infiltration Data Used in Full 2⁴ Factorial Designs (showing replicates).

Case	Case	T Texture	U Uniformity	O Organic	C Compaction	log (Fc), in/hr
1	1A	+	+	+	+	0.78
2	1B	+	+	+	+	0.00
3	1C	+	+	+	+	0.57
4	2A	+	+	+	-	1.20
5	2B	+	+	+	-	0.91
6	2C	+	+	+	-	-0.07
7	3A	+	+	-	+	0.49
8	3B	+	+	-	+	0.30
9	3C	+	+	-	+	0.00
10	3D	+	+	-	+	0.22
11	3E	+	+	-	+	-0.03
12	3F	+	+	-	+	0.04
13	4A	+	+	-	-	0.76
14	4B	+	+	-	-	-0.28
15	4C	+	+	-	-	-0.32
16	4D	+	+	-	-	0.94
17	4E	+	+	-	-	0.68
18	4F	+	+	-	-	0.77
19	5A	+	-	+	+	1.76
20	5B	+	-	+	+	1.63
21	5C	+	-	+	+	1.45
22	6A	+	-	+	-	2.13
23	6B	+	-	+	-	1.49
24	6C	+	-	+	-	2.05
25	7A	+	-	-	+	2.69
26	7B	+	-	-	+	2.65
27	7C	+	-	-	+	2.37
28	8A	+	-	-	-	2.73
29	8B	+	-	-	-	2.40
30	8C	+	-	-	-	2.62
31	9A	-	+	+	+	0.63
32	9B	-	+	+	+	0.31
33	9C	-	+	+	+	0.27
34	10A	-	+	+	-	1.44
35	10B	-	+	+	-	1.03
36	10C	-	+	+	-	1.21
37	11A	-	+	-	+	0.22
38	11B	-	+	-	+	-0.03
39	11C	-	+	-	+	0.04
40	11D	-	+	-	+	-0.66
41	11E	-	+	-	+	-1.05
42	11F	-	+	-	+	-1.21
43	11G	-	+	-	+	-0.75
44	11H	-	+	-	+	-1.63
45	11I	-	+	-	+	-1.83
46	11J	-	+	-	+	-0.88
47	11K	-	+	-	+	-1.37
48	11L	-	+	-	+	-1.82
49	11M	-	+	-	+	-0.40
50	11N	-	+	-	+	-0.47
51	11O	-	+	-	+	-0.92
52	11P	-	+	-	+	0.63
53	11Q	-	+	-	+	0.31
54	11R	-	+	-	+	0.27

Case	Case	T	U	O	C	log (Fc), in/hr
55	12A	-	+	-	-	0.94
56	12B	-	+	-	-	0.68
57	12C	-	+	-	-	0.77
58	12D	-	+	-	-	1.27
59	12E	-	+	-	-	1.05
60	12F	-	+	-	-	0.93
61	12G	-	+	-	-	0.31
62	12H	-	+	-	-	0.19
63	12I	-	+	-	-	0.31
64	12J	-	+	-	-	0.66
65	12K	-	+	-	-	0.77
66	12L	-	+	-	-	0.54
67	12M	-	+	-	-	0.48
68	12N	-	+	-	-	0.48
69	12O	-	+	-	-	0.78
70	12P	-	+	-	-	1.44
71	12Q	-	+	-	-	1.03
72	12R	-	+	-	-	1.08
73	13A	-	-	+	+	0.65
74	13B	-	-	+	+	0.62
75	13C	-	-	+	+	0.58
76	14A	-	-	+	-	1.46
77	14B	-	-	+	-	1.32
78	14C	-	-	+	-	1.24
79	15A	-	-	-	+	0.60
80	15B	-	-	-	+	0.48
81	15C	-	-	-	+	0.30
82	16A	-	-	-	-	0.94
83	16B	-	-	-	-	0.80
84	16C	-	-	-	-	0.88

Normal probability plots of effects were used to compare the relative magnitudes and the statistical significance of both main and interaction effects. These plots also indicate the direction of the effect. As an example, in Figure 127, the factors media texture, the interaction of uniformity and organic content, and the interaction of texture and compaction of the material have positive effects because they appear on the right side of the plot, meaning that when the low level changes to the high level of the factor, the flow rate response increases. In Figure 127, media uniformity, the interaction of texture and uniformity of the material, compaction, and the

interaction of texture and compaction appears on the left side of the plot, meaning that the factor has a negative effect. This indicates that when the low level changes to high, the flow rate response decreases. Figure 127 shows that media texture and uniformity have the highest effects on the measured infiltration rates. The results of the factorial analyses are summarized in Table 89.

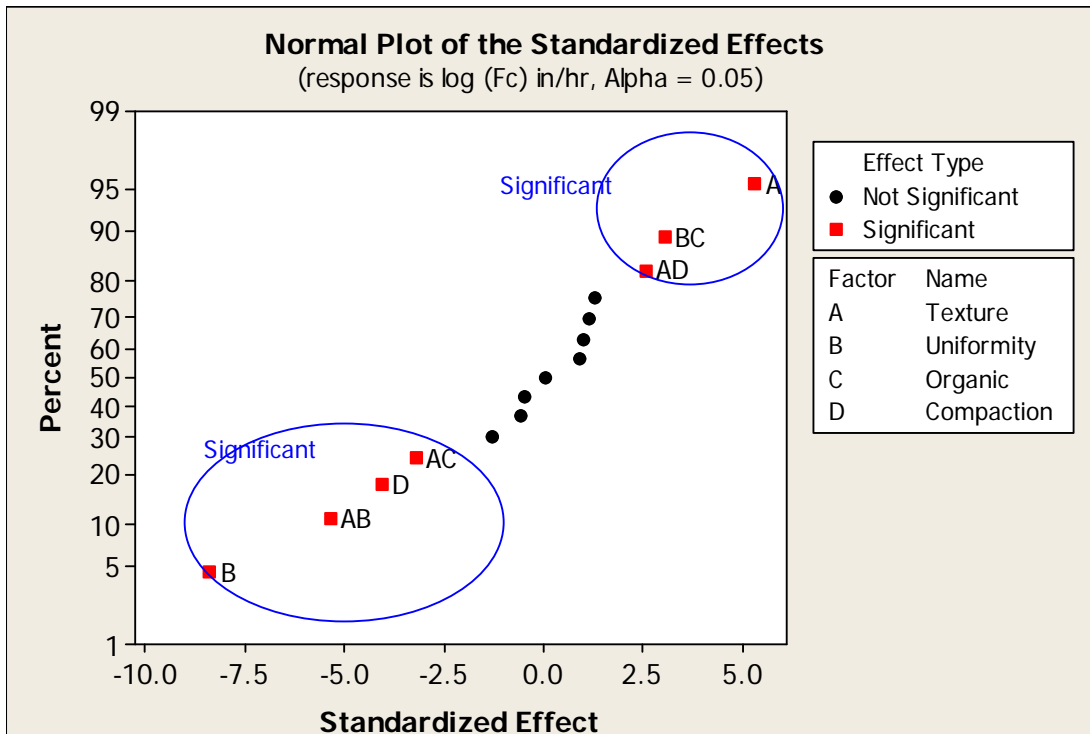


Figure 127. Probability Plot to Identify Important Factors Affecting the Infiltration Rate through a Media Mixture

Table 89. Estimated Effects and Coefficients for log (F_c) in/hr (coded).

Term	Effect	Coef	SE Coef	T	P
Constant		0.964	0.063	15.260	0.000
T	0.669	0.335	0.063	5.290	0.000
U	-1.060	-0.530	0.063	-8.390	0.000
O	0.126	0.063	0.063	1.000	0.321
C	-0.516	-0.258	0.063	-4.080	0.000
T*U	-0.676	-0.338	0.063	-5.340	0.000
T*O	-0.408	-0.204	0.063	-3.220	0.002
T*C	0.325	0.162	0.063	2.570	0.012
U*O	0.384	0.192	0.063	3.040	0.003
U*C	-0.162	-0.081	0.063	-1.280	0.204
O*C	0.004	0.002	0.063	0.030	0.976
T*U*O	0.163	0.081	0.063	1.290	0.203
T*U*C	0.113	0.056	0.063	0.890	0.377
T*O*C	-0.062	-0.031	0.063	-0.490	0.623
U*O*C	0.145	0.073	0.063	1.150	0.254
T*U*O*C	-0.075	-0.038	0.063	-0.590	0.554

S = 0.479695 PRESS = 20.23

R-Sq = 80.45% R-Sq(pred) = 74.74% R-Sq(adj) = 76.14%

T: texture, U: uniformity, O: organic content, and C: compaction.

According to Table 89, the significant factors and interactions that affect the long-term infiltration rates are texture, uniformity of the mixture, compaction, interactions of texture and uniformity, interactions of texture and organic content of the material, interactions of texture and compaction, and interactions of uniformity and organic content of the material. Texture and uniformity had the greatest effects, but all those listed above were significant at least at the 0.05 level. Table 90 indicates that 3- way and 4- way interactions of the factors have no effect on the infiltration rates through the media. Figures 128 and 129 are response surface plots for all of the texture (median particle size) and uniformity data vs. observed final flow rates illustrating these relationships. Figure 128 is for the low organic content conditions while Figure 129 is for the high organic content conditions. While the organic content was important in the interactions, it had lower effects on the flow rates through the mixtures compared to other factors tested.

Table 90. Analysis of Variance for log (FC) -in/hr (coded units).

Source	DF	Seq SS	Adj SS	Adj MS	F	p
Main Effects	4	47.872	29.743	7.436	32.310	0.000
T	1	11.902	6.447	6.447	28.020	0.000
U	1	21.662	16.192	16.192	70.370	0.000
O	1	0.418	0.230	0.230	1.000	0.321
C	1	13.891	3.829	3.829	16.640	0.000
2-Way Interactions	6	15.222	11.659	1.943	8.440	0.000
T*U	1	5.495	6.571	6.571	28.560	0.000
T*O	1	2.380	2.392	2.392	10.390	0.002
T*C	1	4.339	1.516	1.516	6.590	0.012
U*O	1	2.036	2.120	2.120	9.210	0.003
U*C	1	0.916	0.379	0.379	1.650	0.204
O*C	1	0.056	0.000	0.000	0.000	0.976
3-Way Interactions	4	1.219	1.026	0.256	1.110	0.357
T*U*O	1	0.381	0.381	0.381	1.660	0.203
T*U*C	1	0.405	0.182	0.182	0.790	0.377
T*O*C	1	0.113	0.056	0.056	0.240	0.623
U*O*C	1	0.321	0.304	0.304	1.320	0.254
4-Way Interactions	1	0.081	0.081	0.081	0.350	0.554
T*U*O*C	1	0.081	0.081	0.081	0.350	0.554
Residual Error	68	15.647	15.647	0.230		
Pure Error	68	15.647	15.647	0.230		
Total	83	80.042				

T: texture, U: uniformity, O: organic content, and C: compaction

Table 91 shows the actual biofilter media characteristics and saturated infiltration rates through them.

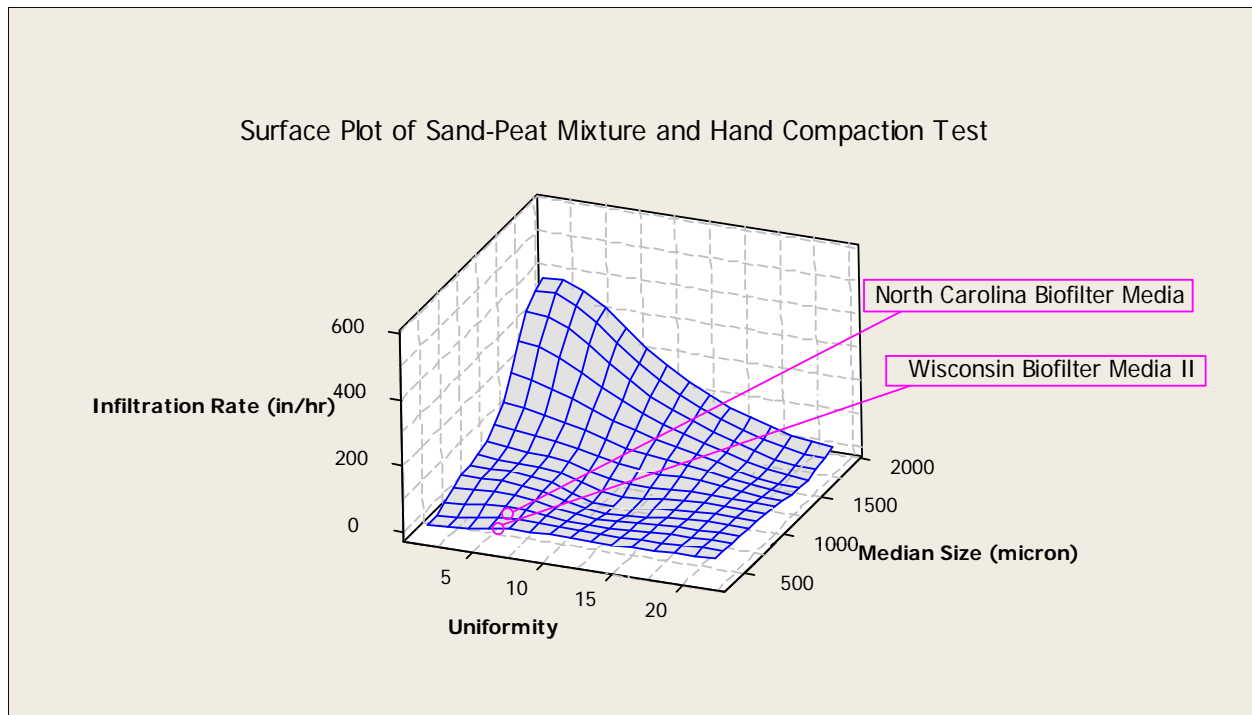


Figure 128. Response Surface Plot for Uniformity and Texture vs Final Infiltration Rate for Low Organic Content Conditions.

Table 92. Biofilter Media Characteristics

Biofilter Media	Percent (%) organic matter (OM)	Uniformity (C_u)	Median size D_{50} (um)
Kansas City	15	40	2000
North Carolina	1.5	6	700
ShelbyPark biofilter	3	20	1100
Wisconsin I	3 - 5	6	400
Wisconsin II	11 % Peat moss & 3% Imbrium	5	600

Laboratory Infiltration Rates (in/hr) Through Biofilter Media				
Compaction	Wisconsin		North Carolina	Kansas City
	I	II		
hand	25.1	20.5	18.7	0.55
standard proctor	5.9	21.1	3.9	0.63
modified proctor	4.2	18.5	1.9	0.13

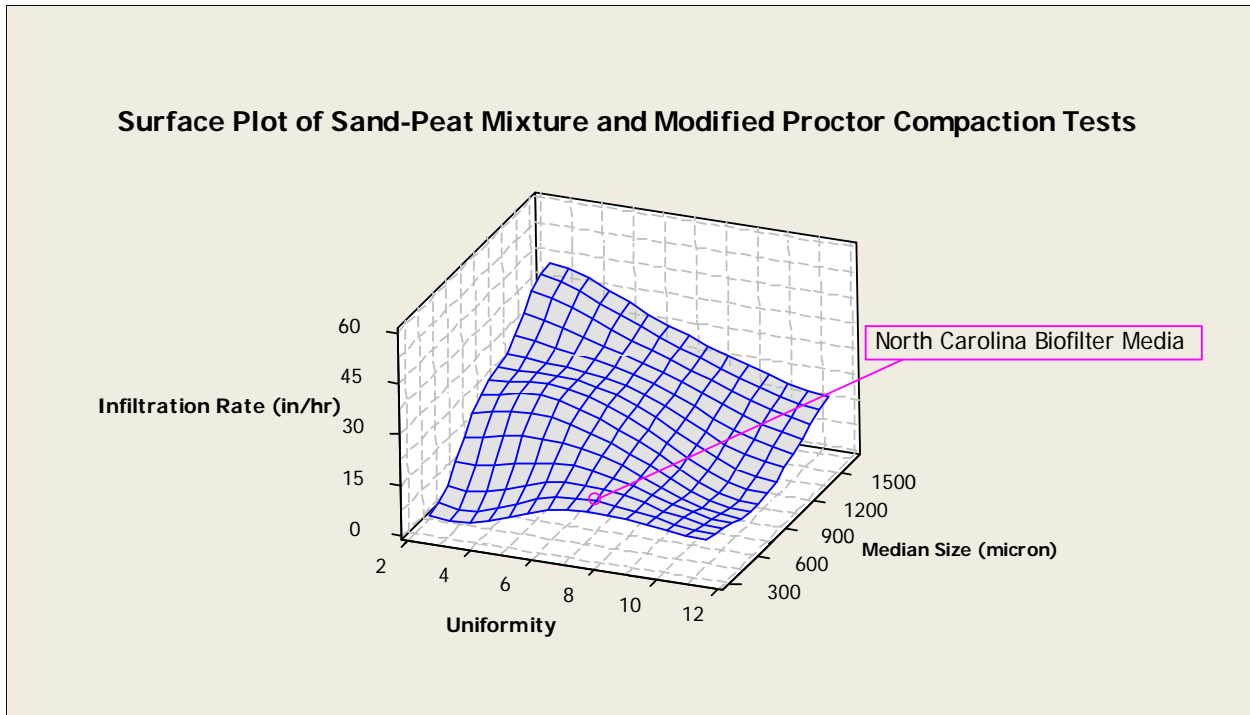


Figure 129. Response Surface Plot for Uniformity and Texture vs Final Infiltration Rate for High Organic Content Conditions.

Table 92 indicates that observations 44, 45, 48, 52 and 53 are unusual observation because their standardized residuals are greater than 2. This could indicate that these observations were in error, or affected by unmeasured conditions.

Table 93. Unusual Observations for log (Fc) in/hr

Obs	StdOrder	log (Fc)- in/hr	Fit	SE Fit	Residual	St Resid*
44	44	-1.62709	-0.641	0.11307	-0.9861	-2.12R
45	45	-1.82974	-0.641	0.11307	-1.1887	-2.55R
48	48	-1.82391	-0.641	0.11307	-1.1829	-2.54R
52	52	0.62519	-0.641	0.11307	1.26622	2.72R
53	53	0.3061	-0.641	0.11307	0.94713	2.03R

*R denotes an observation with a large standardized residual.

The main effects plots are useful to compare magnitudes of the main effects. The main effect plots examine the data means for the four factors. Figure 130 shows increases in

infiltration rates that occurred with increases in media texture and organic content, whereas infiltration rates decreased with increasing uniformity and compaction of the mixture, as expected.

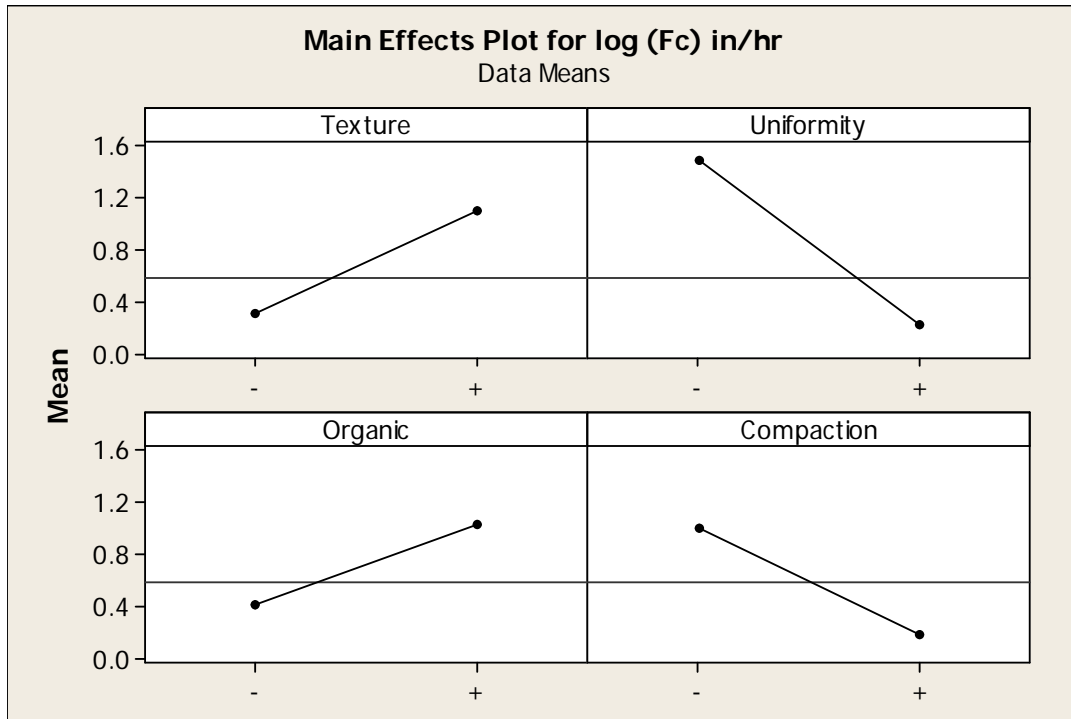


Figure 130. Main Effects Plot for the Four Factors.

Figure 131 are interaction plots which were used to interpret significant interactions between the factors. In the interaction plots, the lines in texture vs. uniformity, texture vs. organic content, texture vs. compaction, and uniformity vs. organic content, cross each other, indicating there exists interactions between these factors. Figure 131 also shows that uniformity vs. compaction, and organic content vs. compaction, are approximately parallel, indicating a lack of interaction between the sets of factors. These interaction plots suggest that mutual interactions between these factors have negligible effects on the infiltration rates. The greater the departure of the lines from the parallel state, the higher the degree of interaction.

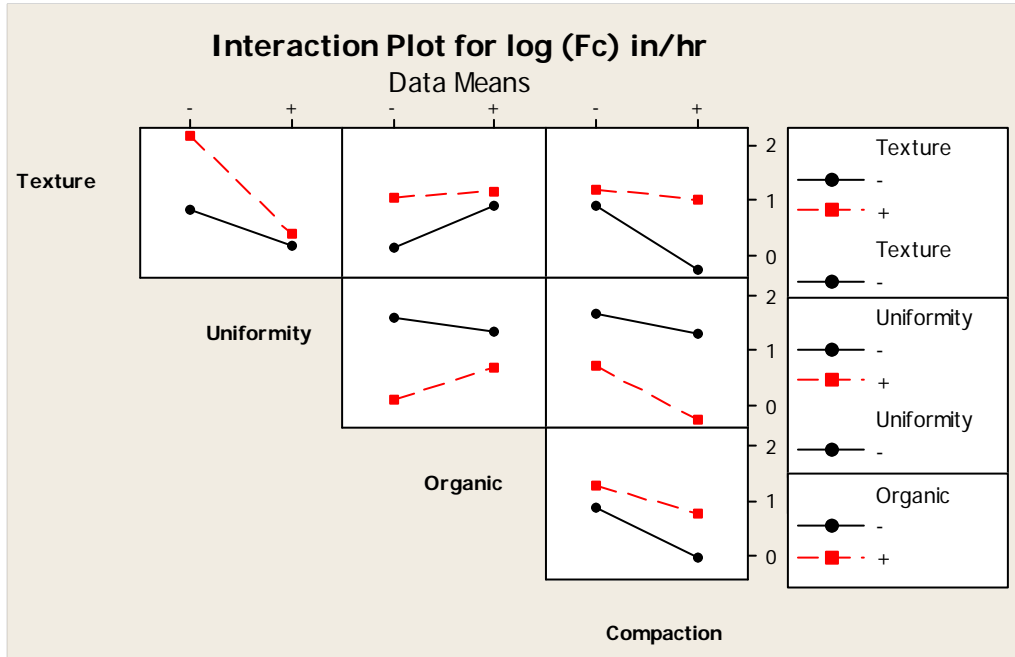


Figure 131. Interaction Plot between Different Factors.

7.3.7 Model Fitting

The effects and half-effects of the significant factors (main effects and interactions) were used to predict the flowrate performance of various mixtures. Table 93 shows the matrix (table of contrasts) representing factors (texture, uniformity, organic content, and compaction) and their interactions. The results of the effects and half-effect are also shown in the table.

Table 94. Shows the Results of the Effects and Half-Effects.

Case	Main Effects				Two interactions					
	T	U	O	C	TU	TO	TC	UO	UC	OC
1	+	+	+	+	+	+	+	+	+	+
2	+	+	+	-	+	+	-	+	-	-
3	+	+	-	+	+	-	+	-	+	-
4	+	+	-	-	+	-	-	-	-	+
5	+	-	+	+	-	+	+	-	-	+
6	+	-	+	-	-	+	-	-	+	-
7	+	-	-	+	-	-	+	+	-	-
8	+	-	-	-	-	-	-	+	+	+
9	-	+	+	+	-	-	-	+	+	+
10	-	+	+	-	-	-	+	+	-	-
11	-	+	-	+	-	+	-	-	+	-
12	-	+	-	-	-	+	+	-	-	+
13	-	-	+	+	+	-	-	-	-	+
14	-	-	+	-	+	-	+	-	+	-
15	-	-	-	+	+	+	-	+	-	-
16	-	-	-	-	+	+	+	+	+	+

	T	U	O	C	TU	TO	TC	UO	UC	OC
Avg Y										
@ -1	0.72	1.52	1.02	1.31	1.41	1.21	0.94	0.90	1.13	1.08
Avg Y										
@ +1	1.39	0.60	1.09	0.80	0.70	0.90	1.17	1.21	0.98	1.03
Δ	0.67	-0.92	0.07	-0.51	-0.70	-0.32	0.23	0.32	-0.15	-0.05
$\Delta/2$	0.33	-0.46	0.03	-0.26	-0.35	-0.16	0.12	0.16	-0.07	-0.02

T: texture, U: uniformity, O: organic content, and C: compaction.

Case	Three and four interactions					log (Fc) (in/hr)
	TUO	TUC	TOC	UOC	TUOC	
1	+	+	+	+	+	0.55
2	+	-	-	-	-	0.91
3	-	+	-	-	-	0.21
4	-	-	+	+	+	0.64
5	-	-	+	-	-	1.64
6	-	+	-	+	+	1.97
7	+	-	-	+	+	2.60
8	+	+	+	-	-	2.61
9	-	-	-	+	-	0.43
10	-	+	+	-	+	1.26
11	+	-	+	-	+	-0.13
12	+	+	-	+	-	0.89
13	+	+	-	-	+	0.62
14	+	-	+	+	-	1.35
15	-	+	+	+	-	0.48
16	-	-	-	-	+	0.88
					Y (grand)	1.06
	TUO	TUC	TOC	UOC	TUOC	
Avg Y @ -1	0.94	1.04	1.06	1.00	1.06	
Avg Y @ +1	1.18	1.07	1.05	1.11	1.05	
Δ	0.24	0.03	-0.01	0.11	-0.02	
$\Delta/2$	0.12	0.02	-0.01	0.06	-0.01	

T: texture, U: uniformity, O: organic content, and C: compaction

As noted previously, the significant factors and interactions that affect the responses are texture, uniformity, compaction, interactions of texture and uniformity, interactions of texture and organic content of the material, interactions of texture and compaction, and uniformity and organic content of the material. These significant factors and interactions are therefore included in the complete prediction equation. The parameters organic content, interactions of uniformity and compaction, interactions of organic content and compaction, and all the three-way and four-

way interactions of these factors, have negligible effects (p-values greater than the chosen value of $\alpha = 0.05$) on the flowrate and a reduced model was created wherein these factors are ignored.

The prediction equation can be written in terms of the grand mean and half-effects, excluding the non-significant factors.

$$\hat{y} = \bar{y} \pm \left(\frac{\Delta T}{2}\right) T \pm \left(\frac{\Delta U}{2}\right) U \pm \left(\frac{\Delta C}{2}\right) C \pm \left(\frac{\Delta TU}{2}\right) TU \pm \left(\frac{\Delta TO}{2}\right) TO \pm \left(\frac{\Delta TC}{2}\right) TC \pm \left(\frac{\Delta UO}{2}\right) UO \quad (1)$$

where: \hat{y} = predicted response (Y pred)

\bar{y} = grand mean (Y grand)

$\frac{\Delta}{2}$ = half-effects of each factor or interaction

T = texture

U = uniformity of the mixture

C = compaction

O = organic content of the material

The final prediction equation is given as:

$$\widehat{\log(y)} = 1.1 + 0.33T - 0.46U - 0.26C - 0.35TU - 0.16TO + 0.12TC + 0.16UO$$

Table 94 shows example calculations how the above equation can be used. The test results also indicated that the expected ranges of infiltration for the sand and peat mixture ranged from 0.9 to 501 in/hr. The measured values during the laboratory tests agree with these predictions, ranging from 0.01 to 540 in/hr. The highest infiltration rates were noted in sand-peat mixtures that had 90% coarse sand media and 10% peat amendment.

$$\widehat{\log(y)} = 1.1 \pm \left(\frac{\Delta_T}{2}\right)T \pm \left(\frac{\Delta_U}{2}\right)U \pm \left(\frac{\Delta_C}{2}\right)C \pm \left(\frac{\Delta_{TU}}{2}\right)TU \pm \left(\frac{\Delta_{TO}}{2}\right)TO \pm \left(\frac{\Delta_{TC}}{2}\right)TC \pm \left(\frac{\Delta_{UO}}{2}\right)UO$$

$$\widehat{\log(y)} = 1.1 \pm (0.33)T \pm (-0.46)U \pm (-0.26)C \pm (-0.35)TU \pm (-0.16)TO \pm (0.12)TC \pm (0.16)UO$$

Table 95. Calculated Flow Rates Using the Final Factorial Model.

Factorial Group	Effect	Case	T	U	C	TU	TO	TC	UO	Calculated values of $\widehat{\log(y)}$	Calculated flow rate y (in/hr)
T	0.67	1	+	+	+	+	+	+	+	0.48	3.02
U	-0.92	2	+	+	-	+	+	-	+	0.76	5.75
C	-0.52	3	+	+	+	+	-	+	-	0.48	3.02
TU	-0.70	4	+	+	-	+	-	-	-	0.76	5.75
TO	-0.32	5	+	-	+	-	+	+	-	1.78	60.26
TC	0.23	6	+	-	-	-	+	-	-	2.06	114.82
UO	0.32	7	+	-	+	-	-	+	+	2.42	263.03
		8	+	-	-	-	-	-	+	2.70	501.19
		9	-	+	+	-	-	-	+	0.60	3.98
		10	-	+	-	-	-	+	+	1.36	22.91
		11	-	+	+	-	+	-	-	-0.04	0.91
		12	-	+	-	-	+	+	-	0.72	5.25
		13	-	-	+	+	-	-	-	0.50	3.16
		14	-	-	-	+	-	+	-	1.26	18.20
		15	-	-	+	+	+	-	+	0.50	3.16
		16	-	-	-	+	+	+	+	1.26	18.20

An ANOVA test was used to test the significance of the regression coefficients, which highly depends on the number of data observations. When only a few data observations are available, strong and important relationships may not be shown to be significant, or high R^2 values could occur with insignificant equation coefficients. The data were evaluated by using the p-value (the probability of obtaining a test statistic that is at least as extreme as the calculated value if there is actually no difference; the null hypothesis is true). The independent variable was used to predict the dependent variable when $p < 0.05$. A summary of statistical information about the model is also shown in Table 89. R^2 is a statistical measure of goodness of fit of a model

whereas adjusted R^2 is a statistic that is adjusted for the number of explanatory terms in a model. The value of R^2 and adjusted R^2 for the model are 80.5% and 76.1% respectively. Predicted R^2 is calculated from the PRESS (Prediction Error Sum of Squares) statistic. The predicted R^2 statistic is computed to be 74.7%. Larger values of predicted R^2 suggest models of greater predictive ability. This indicates that the model is expected to explain about 75% of the variability in new data. Figure 132 shows a scatterplot of the observed and fitted log (Fc) values, indicating very good fits of the observed with the predicted log Fc values over a wide range of conditions.

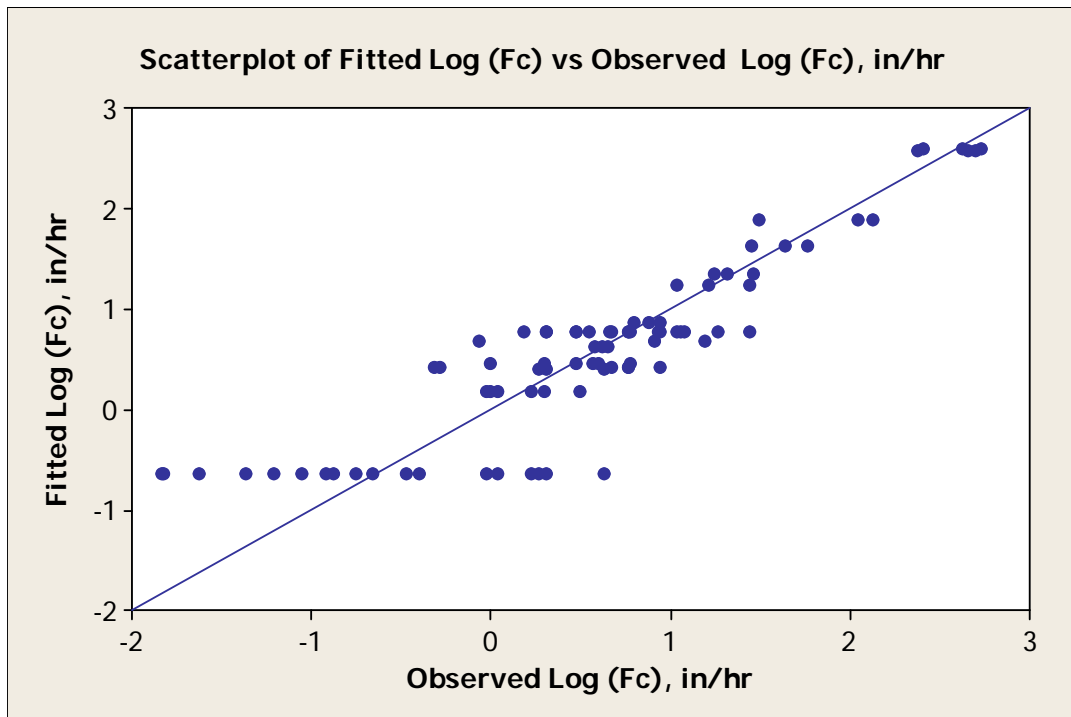


Figure 132. Observed vs Fitted log (Fc) Values.

Residual analyses were conducted to investigate the goodness of model fit. Residual plots were inspected to determine if the error term in the regression model satisfies the four

assumptions (they must be independent, zero mean, constant variance, and normally distributed). To check the constant variance assumptions, the plots of residuals vs. the fitted values were inspected. To evaluate the normality of the residuals, normal probability plots and histograms of the residuals were also constructed. The Anderson-Darling test statistic was also calculated to check for normality. The normal probability plot of the residuals shown in Figure 133 shows that the fitted data is normally distributed (Anderson-Darling test for normality has a p-value greater than 0.05, so the data are not significantly different from a normal distribution for the number of observations available). The zero mean of the residuals assumption was checked by examining the descriptive statistics and graphs of the residuals vs. fitted values and vs. the order of the observations. To determine if the residuals were independent of each other, graphs of the residuals vs. observation number were also examined.

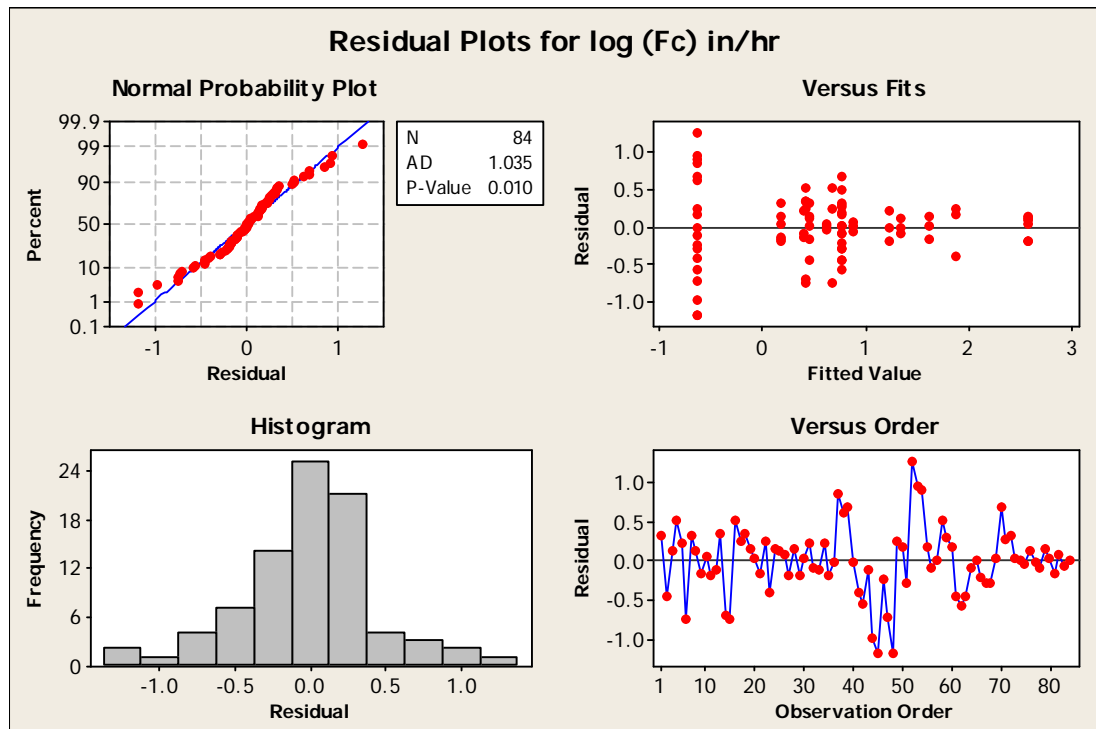


Figure 133. Residuals Analysis Plot.

The examination of the residual values vs. fitted values of the data indicated that there was a greater spread in the residuals for the lower fitted values than for the higher fitted values, implying greater errors for low flow observations. The model residual histogram was approximately bell shaped, the residuals were normally distributed and had zero mean, and were independent of each other. Model improvements should therefore focus on conditions that had low infiltration conditions where the largest errors were observed.

7.3.8 Statistical Analyses of Infiltration Rates through Sand-Peat Mixture Only

Statistical analyses were conducted to determine the effects of texture, uniformity, and compaction, plus their interactions, on the flowrate through the various mixtures of sand and peat on flow rate. A complete two level, four factors (23, with varying texture, uniformity, organic content, and compaction) full-factorial experiment (Box et al. 1978) was conducted to examine the effects of these factors, plus their interactions, on the flowrate through the various sand-peat mixtures. A final factorial analysis model was developed. The final model was verified using the actual Kansas City, North Carolina, and Wisconsin biofilter media test data. The complete data used in this factorial study are summarized in Appendix D.

Data analyses were performed using the statistical software package Minitab (version 16). Normal plots of the standardized effects, residual plots were prepared to examine the effects of the factors and to determine their significance. An analysis of variance (ANOVA) table was constructed to determine the significant factors and their interactions needed to best predict media flow performance. Statistical hypothesis tests using a p-value of 0.05 (95% confidence) were used to determine whether the observed data were statistically significantly different from the null hypothesis. Normal probability plots of effects were used to compare the relative magnitudes and the statistical significance of both main and interaction effects. Figure 134 shows

that media texture, uniformity and their interactions have significant effects on the measured infiltration rates. These significant factors and their interactions are therefore included in the final factorial analysis model. The model can be written in terms of the grand mean and half-effects, excluding the non-significant factors. The model was verified using the actual biofilter media test results. The results of the factorial analyses are summarized in Appendix E.

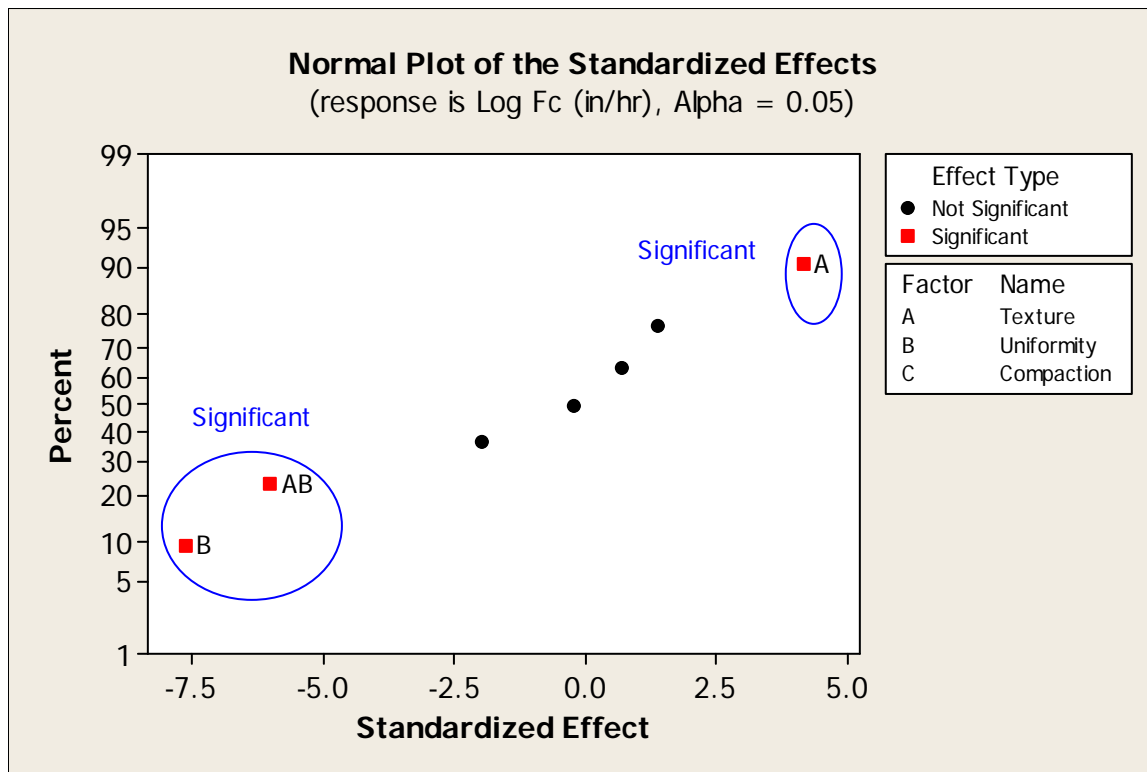


Figure 134. Probability Plot to Identify Important Factors Affecting the Infiltration Rate through a Sand-peat Mixture.

Table 96. Estimated Effects and Coefficients for Log Fc (in/hr) (coded units) and Using a Sand-peat Mixture.

Term	Effect	Coef	SE	T	P
			Coef		
Constant		0.9889	0.06619	14.94	0.000
Texture	0.5501	0.275	0.06619	4.16	0.000
Uniformity	-1.011	-0.5055	0.06619	-7.64	0.000
Compaction	-0.2589	-0.1295	0.06619	-1.96	0.059
Texture*Uniformity	-0.7945	-0.3972	0.06619	-6.00	00.000
Texture*Compaction	0.1835	0.0917	0.06619	1.39	0.175
Uniformity*Compaction	0.0945	0.0473	0.06619	0.71	0.48
Texture*Uniformity*Compaction	-0.0285	-0.0142	0.06619	-0.22	0.831

S = 0.410142 PRESS = 8.26827
R-Sq = 80.52% R-Sq(pred) = 71.84% R-(adj) 76.51%

Figure 135 shows a response surface plot for uniformity and texture vs final infiltration rate for standard proctor compaction method and low organic content conditions.

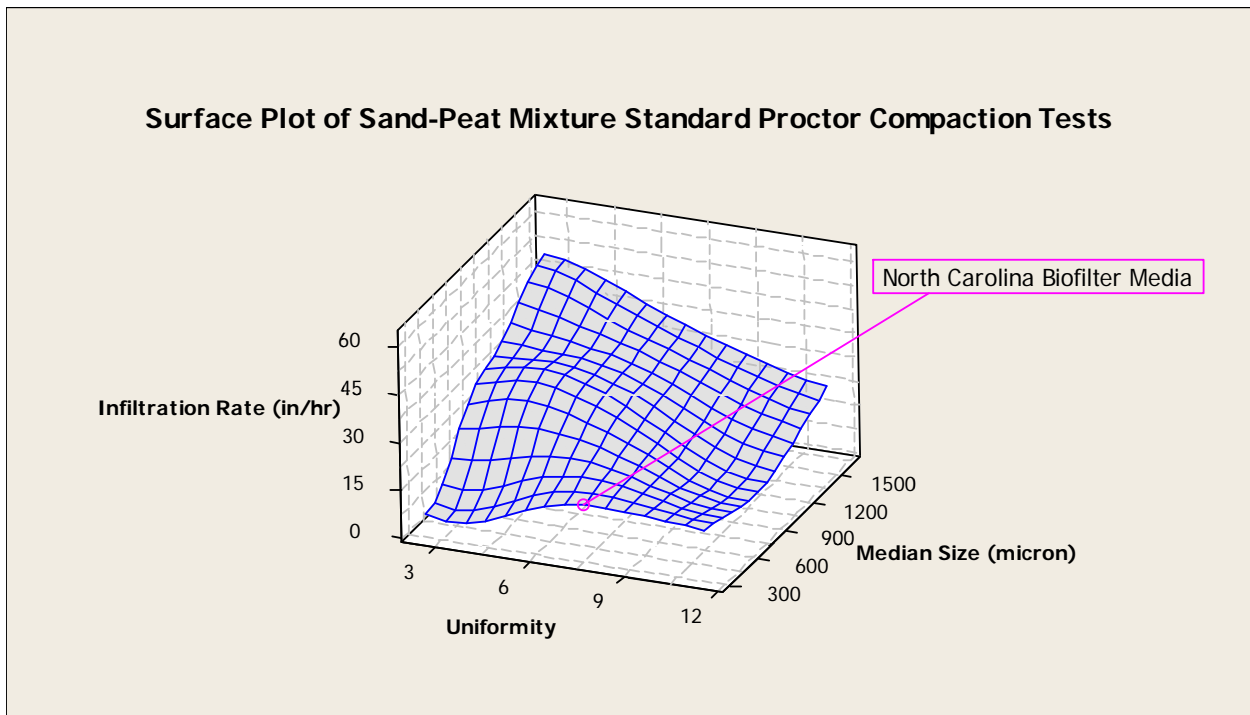


Figure 135. Response Surface Plot for Uniformity and Texture vs Final Infiltration Rate for Standard Proctor Compaction Tests and Low Organic Content Conditions

Table 96 shows the matrix (table of contrasts) representing factors (texture, uniformity, organic content, and compaction) and their interactions. The results of the effects and half-effect are also shown in the table.

Table 97. Shows the Results of the Effects, Half-Effects, and Using a Sand-peat Mixture

Case	Texture (T)	Uniformity (U)	Compaction(C)	TU	TC	UC	TUC	Log(Fc), in/hr
1	-	-	-	+	+	+	-	1.10
2	+	-	-	-	-	+	+	2.24
3	-	+	-	-	+	-	+	0.77
4	+	+	-	+	-	-	-	0.37
5	-	-	+	+	-	-	+	0.54
6	+	-	+	-	+	-	-	2.10
7	-	+	+	-	-	+	-	0.45
8	+	+	+	+	+	+	+	0.36

	T	U	C	TU	TC	UC	Y (grand) TUC	0.9889
Avg. Y@-1	0.71	1.49	1.12	1.39	0.90	0.94	1.00	
Avg. Y@+1	1.26	0.48	0.86	0.59	1.08	1.04	0.97	
Δ	0.55	-1.01	-0.26	-0.79	0.18	0.09	-0.03	
Δ/2	0.28	-0.51	-0.13	-0.40	0.09	0.05	-0.01	

T: texture, U: uniformity, and C: compaction.

The prediction equation can be written in terms of the grand mean and half-effects, excluding the non-significant factors.

$$\widehat{\log(y)} = \bar{y} \pm \left(\frac{\Delta_T}{2}\right)T \pm \left(\frac{\Delta_U}{2}\right)U \pm \frac{\Delta_{TU}}{2}TU$$

$$\widehat{\log(y)} = 1 + 0.28T - 0.51U - 0.4TU$$

where: $\widehat{\log(y)}$ = predicted response (log(y))
 \bar{y} = grand mean (Y grand)
 $\frac{\Delta}{2}$ = half-effects of each factor or interaction
T = texture
U = uniformity of the mixture
O = organic content of the material

An example showing how the above equation can be used is given in Table 97. The test results also indicated that the expected ranges of infiltration for the mixture ranged from 2.3 to 155 in/hr. Table 98 shows the actual biofilter media infiltration rates.

Table 98. Calculated Infiltration Rates Using a Factorial Model Rate (in/hr)

Factorial Group	Effect	Case	T	U	TU	Calculated values $\log(\bar{y})$	Calculated values \bar{y} (in/hr)
T	0.28	1	-	-	+	0.83	6.76
U	-0.51	2	+	-	-	2.19	154.88
TU	-0.40	3	-	+	-	0.61	4.07
		4	+	+	+	0.37	2.34

T: texture, U: uniformity, O: organic content, and C: compaction.

Table 99. Actual Biofilter Media Infiltration Rate (in/hr)

Compaction	Actual Biofilter Media Infiltration Rate (in/hr)				
	Kansas City	North Carolina	ShelbyPark	Wisconsin I	Wisconsin II
Hand	0.55	18.7	4	25.1	20.5
Standard Proctor	0.63	3.9	0.81	5.9	21.1
Modified Proctor	0.13	1.9	0.3	4.2	18.5

The measured infiltration rates through actual Kansas City biofilter media ranged from 0.13 to 0.63 in/hr. The Kansas City media infiltration rates are outside the expected ranges of infiltration rates obtained using the final factorial model. The infiltration rates through North Carolina and Wisconsin biofilter media ranged from 2 to 25 in/hr. The actual North Carolina and Wisconsin biofilter mixture had infiltration rate values inside the range of infiltration rates obtained using the factorial model.

7.4 Particle Trapping Tests

7.4.1 Particle Trapping Tests for Sand and Peat Mixtures

Influent dirty water and effluent treated water were analyzed for suspended sediment concentration (SSC), total dissolved solids (TDS), particle size distribution (PSD), turbidity, and conductivity. Table 99 shows the controlled laboratory column test results for low and high influent solids concentration conditions. Three test replicates were conducted for approximately low and high concentrations. A total of 96 samples were analyzed during the tests. Statistical tests were used to evaluate and compare the performance data collected during these tests. The tests were conducted in some of the sand-peat columns (selected to represent the overall range of conditions observed) and Tuscaloosa surface soil for hand and modified proctor compaction conditions. The media size of the sand-peat mixtures used during these tests ranged from 270 to 1,500 μm and the uniformity coefficients ranged from 1.3 to 20. Figures 136 and 137 show the simple SSC line performance plots of these controlled tests for the high and low influent SSC concentration conditions. The results of the PSD plots of influent and effluent are summarized in Appendix D58.

Table 99. Controlled Lab Column Test Sand-Peat Media (average concentrations from triplicate tests for each condition).

		Low concentration tests				High concentration tests			
Mixture	Influent	SSC (mg/L)	TDS (mg/L)	Turbidity (NTU)	Conductivity (µS/cm)	SSC (mg/L)	TDS (mg/L)	Turbidity (NTU)	Conductivity (µS/cm)
		103	148	20	188	798	132	137	190
10% peat & 90% sand: (D ₅₀ = 340 µm and C _u = 1.3)	hand compaction (ρ = 1.28 g/cm ³)	6	96	3	125	7	86	1	129
	modified proctor (ρ = 1.35 g/cm ³)	N/A	120	1	126	3	88	1	131
Surface soil (D ₅₀ = 270 µm and C _u = 37)	hand compaction: (ρ = 1.42 g/cm ³)	2	267	2	338	9	220	2	324
	modified proctor (ρ = 1.67 g/cm ³)	8	351	1	453	15	328	1	434
50% peat & 50% sand (D ₅₀ = 300 µm and C _u = 3)	hand compaction: (ρ = 0.74 g/cm ³)	N/A	143	3	172	3	100	2	154
	modified proctor: ρ = 1.03 g/cm ³)	39	156	2	159	1	106	2	150
50% peat & 50% surface soil (D ₅₀ = 325 µm and C _u = 7)	hand compaction: (ρ = 0.85 g/cm ³)	10	266	5	266	5	119	9	146
	modified proctor: ρ = 1.01 g/cm ³)	7	471	4	420	1	175	5	179
10% peat and 90% sand (D ₅₀ = 1.5 mm, and C _u = 22)	hand compaction: (ρ = 1.61 g/cm ³)	1	50	2	133	N/A	90	1	128
	modified proctor: ρ = 1.63 g/cm ³)	7	58	2	136	5	100	1	130
Mixture	Influent	57	119	24	139	439	159	94	205
50% peat & 50% sand (D ₅₀ = 1.3 mm, C _u = 20)	hand compaction (ρ = 1.1 g/cm ³)	N/A	147	3	139	N/A	108	2	156
	modified proctor (ρ = 1.1 g/cm ³)	74	178	2	139	N/A	122	1	160
10% peat & 90% sand (D ₅₀ = 1.9 mm, C _u = 2)	hand compaction (ρ = 1.52 g/cm ³)	74	102	118	139	86	135	101	135
	modified proctor (ρ = 1.58 g/cm ³)	52	102	75	139	71	148	84	150
50% peat & 50% sand (D ₅₀ = 1.6 mm, C _u = 2.5)	hand compaction (ρ = 0.96 g/cm ³)	25	271	42	139	12	150	10	175
	modified proctor (ρ = 1.23 g/cm ³)	22	281	45	139	8	140	8	176

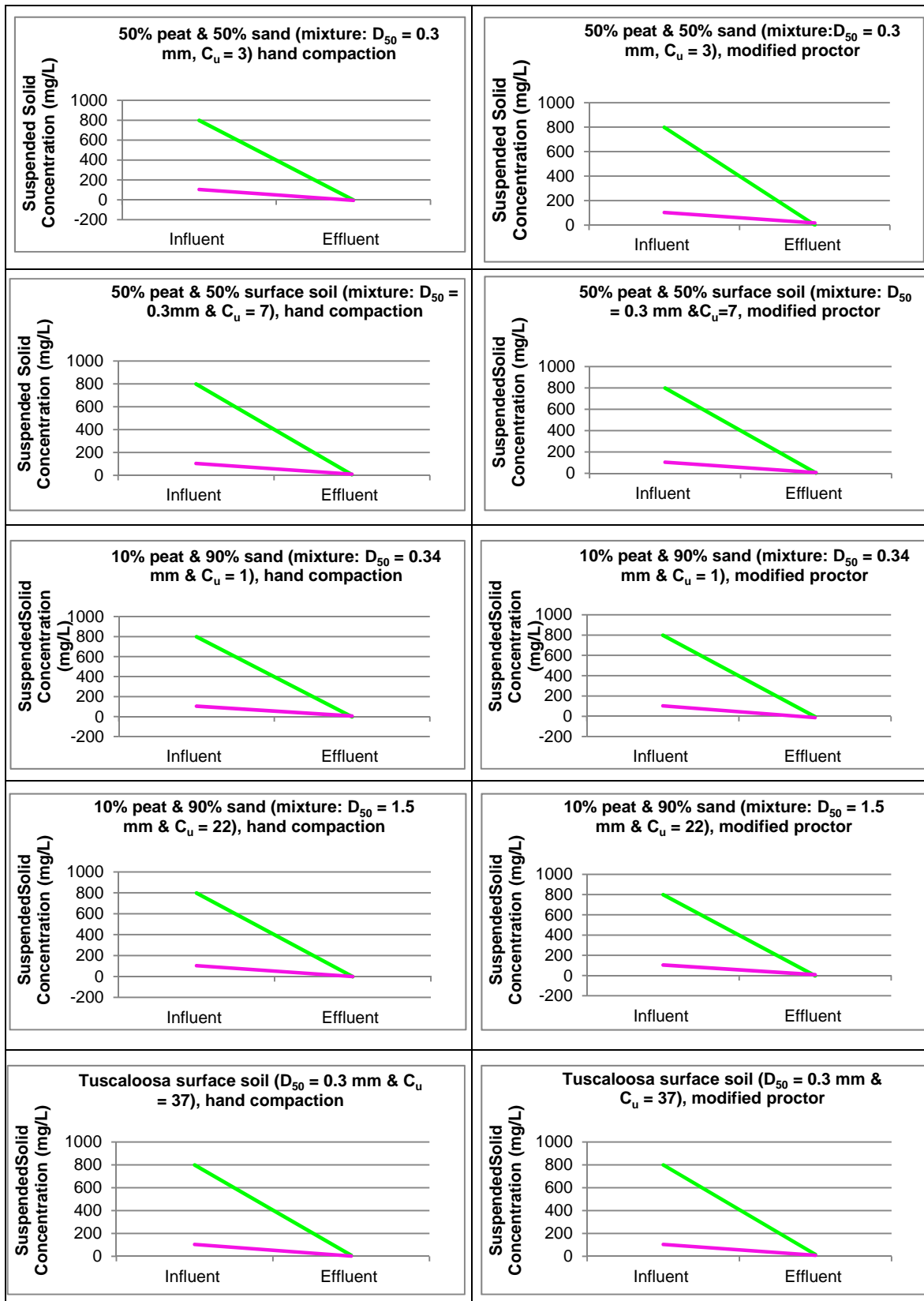


Figure 136. Controlled Laboratory Column SSC Test Results, Series 1.

The particle trapping experiments using sand-peat mixture indicated that reductions occurred for most lab columns, with relatively consistent effluent SSC conditions.

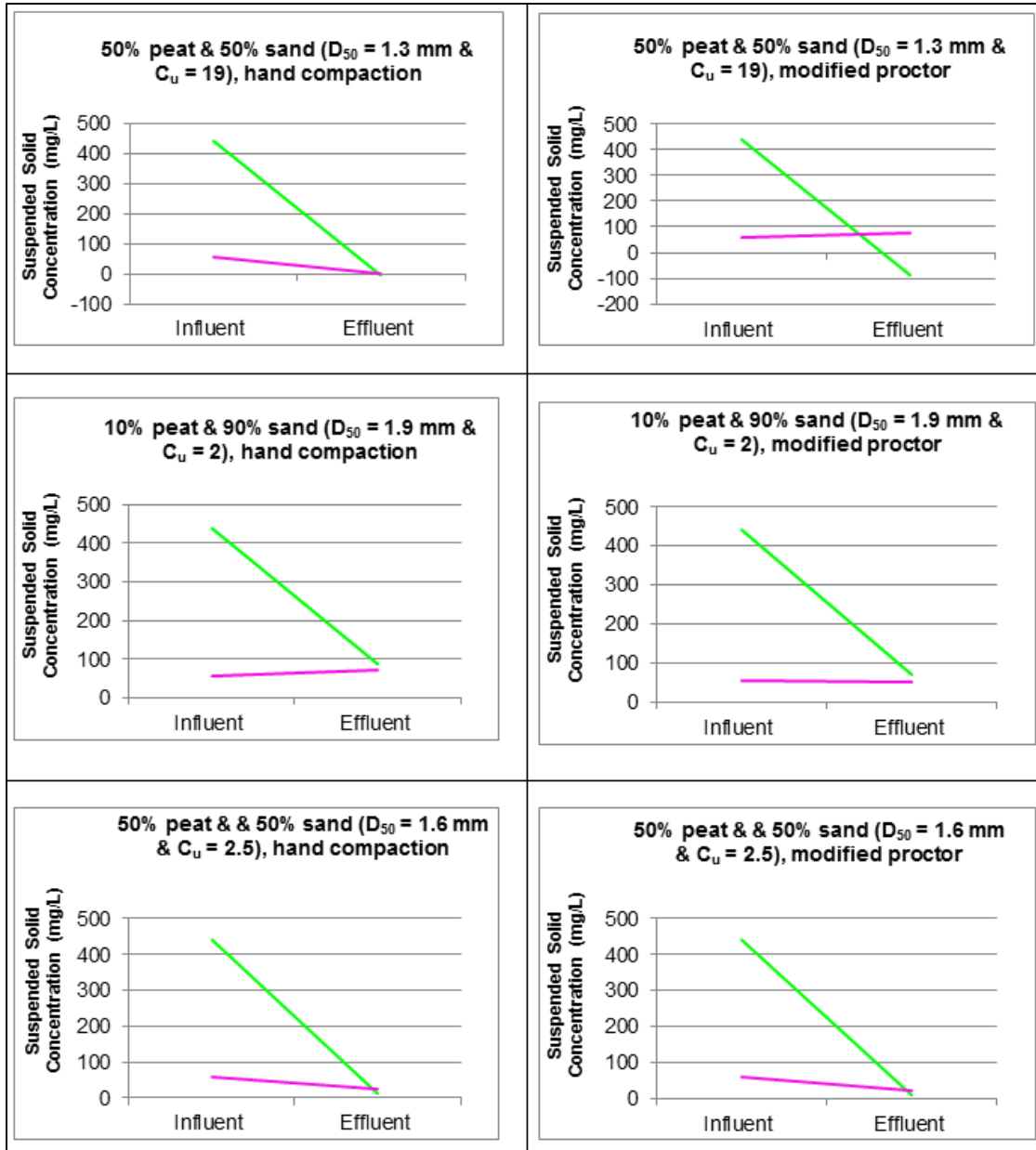


Figure 137. Controlled Laboratory Column SSC Test Results, Series 2.

Figure 138 shows an example SSC particle size distribution plot for the low, high solids, and accumulative concentration tests using the 50% sand and 50% peat mixture. The results of the PSD plots are summarized in Appendix D58. A table of the raw data observations for all the tests and regression analyses for influent vs. effluent concentration for each mixture and particle size are given in Appendix D.25 and Appendix D.26 through D.57 respectively.

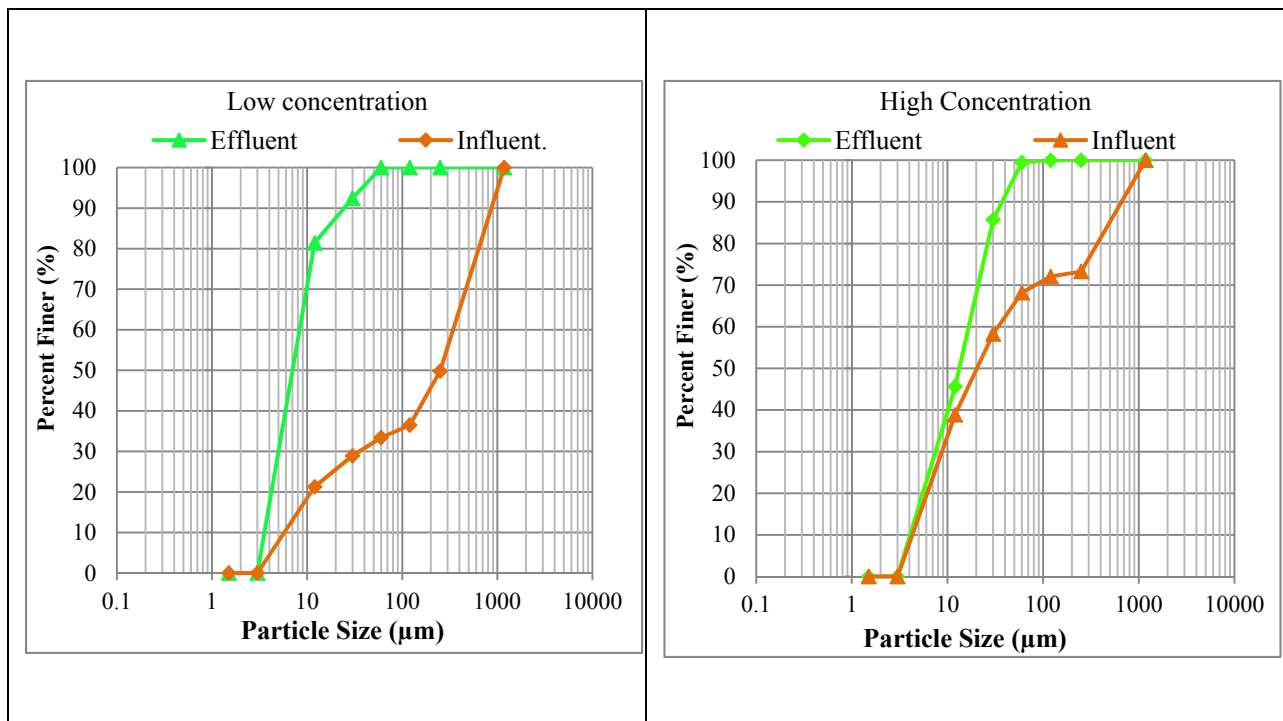


Figure 138. Particle size Distribution Plot Using Sand and Peat ($D_{50} = 300 \mu\text{m}$ & $C_u = 3.3$) and Density = 1.03 g/cc

7.4.2 Particle Trapping Test Results for Coarse Media

Similar tests were conducted using the coarse media and for low and high solids concentrations, as summarized in Table 100. These results show that the effluent concentrations are larger than the influent concentration for many columns, indicating continued releases of fine

silts from these materials, even after the extensive media washing before the tests. Tests were conducted using two different controlled flow rates, as uncontrolled flows would be very high for these coarse materials. The orifices used to reduce the flows corresponded to the likely range of conditions associated with underdrains that are used with these materials. Table 101 shows flow rates through the coarse media for low and high concentrations. Figure 139 show the simple SSC line performance plots of these controlled tests for the two different solids concentrations and two different flow rates. These line plots illustrate the poor particle retention for these coarse materials.

Table 100. Laboratory Column Coarse Media (average concentrations)

	Influent	Effluent			
		0.25 inch dia. orifice and pea gravel	1 inch dia. orifice and pea gravel	0.25 inch dia. orifice and coarse gravel	1 inch dia. orifice and coarse gravel
Low Concentration Tests					
SSC (mg/L)	57	199	164	101	95
TDS (mg/L)	119	134	114	120	118
Turbidity (NTU)	24	21	24	30	21
Conductivity (μ S/cm)	139	158	161	156	157
High Concentration Tests					
SSC (mg/L)	439	712	899	642	693
TDS (mg/L)	159	166	141	131	152
Turbidity (NTU)	94	183	202	173	189
Conductivity (μ S/cm)	205	209	208	203	205

Table 101. Approximate Flow Rates through the Coarse Media for the Different Tests

Solid concentration (mg/L)	Trial	Pea gravel		Coarse gravel	
		0.25 in orifice dia.	1 in orifice dia.	0.25 in orifice dia.	1 in orifice dia.
		Q (L/s, gal/min)	Q (L/s, gal/min)	Q (L/s, gal/min)	Q (L/s, gal/min)
Low	1	0.29 (4.66)	0.29 (4.76)	0.29 (4.66)	0.38 (6.05)
	2	0.35 (5.55)			
High	1	0.39 (6.16)	0.39 (5.55)	0.39 (6.16)	0.32 (5.04)
	2	0.35 (5.55)	0.32 (5.04)	0.32 (5.04)	
	3	0.32 (5.04)	0.35 (5.04)	0.35 (5.55)	

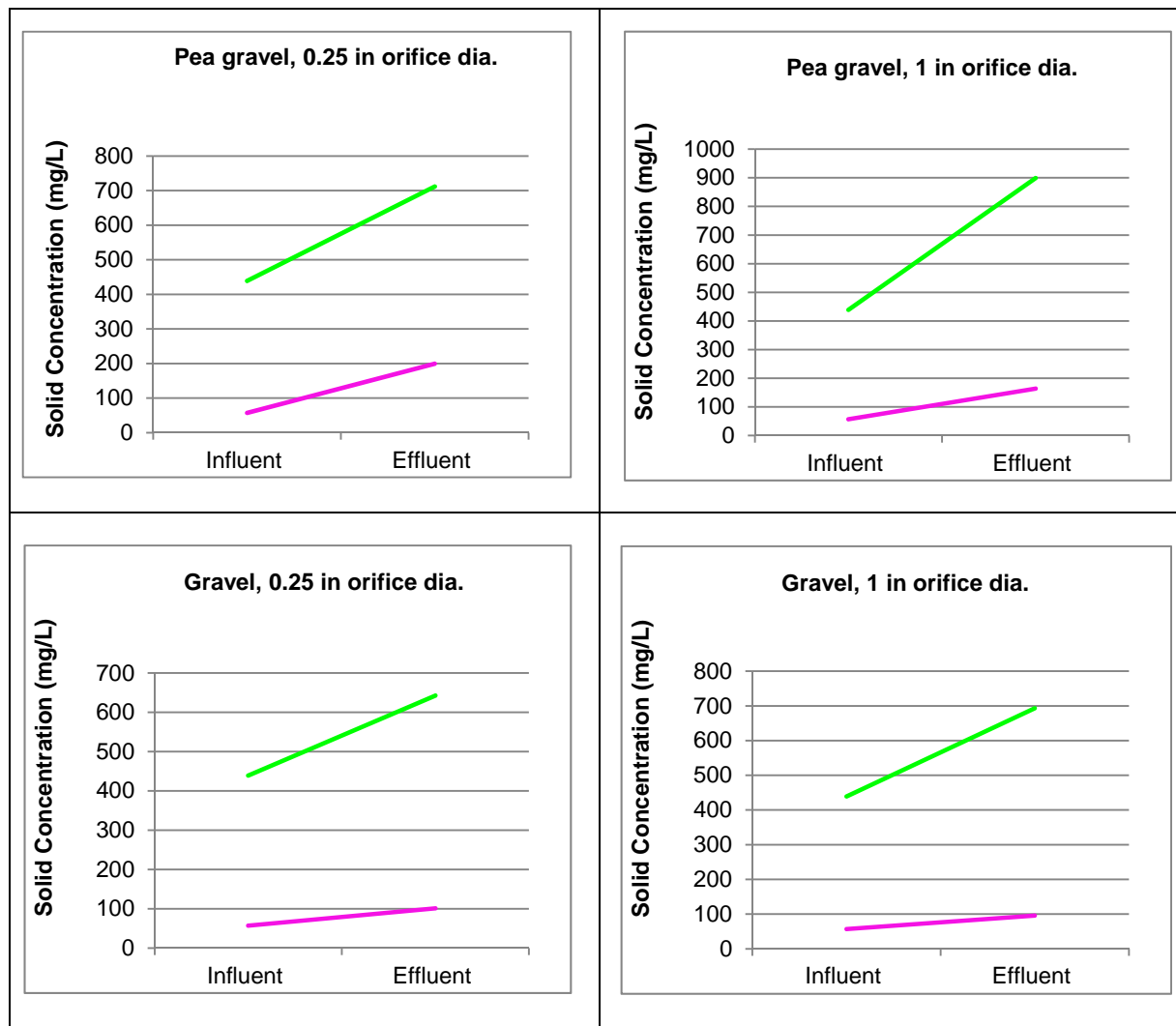


Figure 139. Controlled Lab Column SSC Test Results for Coarse Media

7.4.3 Statistical Analysis for the Particle Trapping Experiment

A number of statistical tests were used to evaluate and compare the performance data collected during these particle trapping tests. Grouped box and whisker plots were used to examine the influent and effluent flows for the different lab columns. Grouped comparison tests indicated that at least one of the groups were significantly different from at least one other; they do not indicate which. In an attempt to supplement the visual presentations of the grouped box and whisker plots, a standard one-way analysis of variance (ANOVA) test was conducted to determine whether group means are different from one another. ANOVA doesn't specifically identify which sets of data are different from any other (Pitt 2007).

Tukey's multiple comparison tests were used to determine which means amongst a set of means differ from the rest. These tests identify differences in sample groupings, but similarities (to combine data) are probably also important to know. Figure 140 shows an example of a grouped box and whisker plot that shows significant differences in influent vs. effluent values from a laboratory column having a mixture of 50% sand and 50% peat (mixture $D_{50} = 0.3$ mm and $C_u = 3$). Table 102 shows mixture descriptions used during the test.

A one-way ANOVA test was conducted to supplement grouped box and whisker plots and determine whether group influent and effluent means are different from one another. If the ANOVA test results indicated that there was no statistical difference in the mean values, the mean values from the different groups were combined and a one-way ANOVA tests was conducted again. The one-way ANOVA test for the low and high solids concentration conditions indicated that there was no statistical difference between. the mean effluent SSC from lab columns 1 vs. 2 and lab columns 3 vs. 4 for both low and high solid concentrations. Therefore, the effluent concentrations were not dependent on the influent concentrations in the range tested.

These mean values were combined and a one-way ANOVA tests were conducted again. Detailed calculation results are attached in the Appendix G.

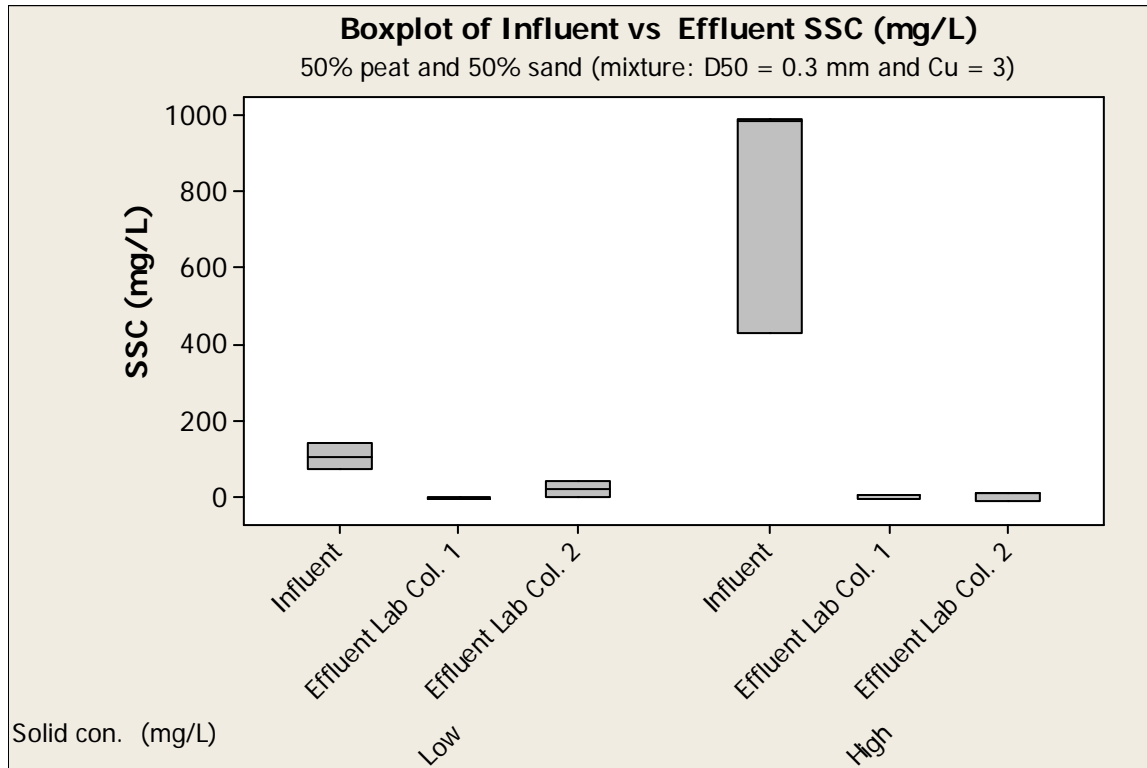


Figure 140. Example Grouped Box and Whisker Plot of Influent vs. Effluent SSC Test Results from Sand and Peat Columns.

Table 102. Test Mixture Descriptions.

Mixture	Lab column	Compaction
50% peat and 50% sand	1	hand ($\rho = 0.74 \text{ g/cc}$)
	2	modified proctor ($\rho = 1.03 \text{ g/cc}$)

Similar statistical tests were conducted to examine the influent and effluent flows from the coarse media lab columns having 0.25 and 1 inches orifice flows. Figure 141 is the grouped box

and whisker plot for the SSC data. Table 103 shows descriptions of the coarse media used during the tests. A one-way ANOVA test was conducted to determine whether group influent and effluent means were significantly different from one another. If the ANOVA test results indicated that there was no statistical difference in the mean values, the mean values from the different groups were combined and a one-way ANOVA tests was repeated. The one-way ANOVA test for the low solids concentration tests indicated that there were no statistically significant differences between the effluent SSC values from lab columns 1, 2, and 4. These mean values were combined and a one-way ANOVA test was conducted again. Table 104 shows a statistical summary for the final combined results. The one-way ANOVA results for the high solids concentration tests indicated that there were no statistically significant differences between the effluent SSC values from lab columns 1, 2, 3, and 4. Detailed calculation results are attached in the Appendix G.

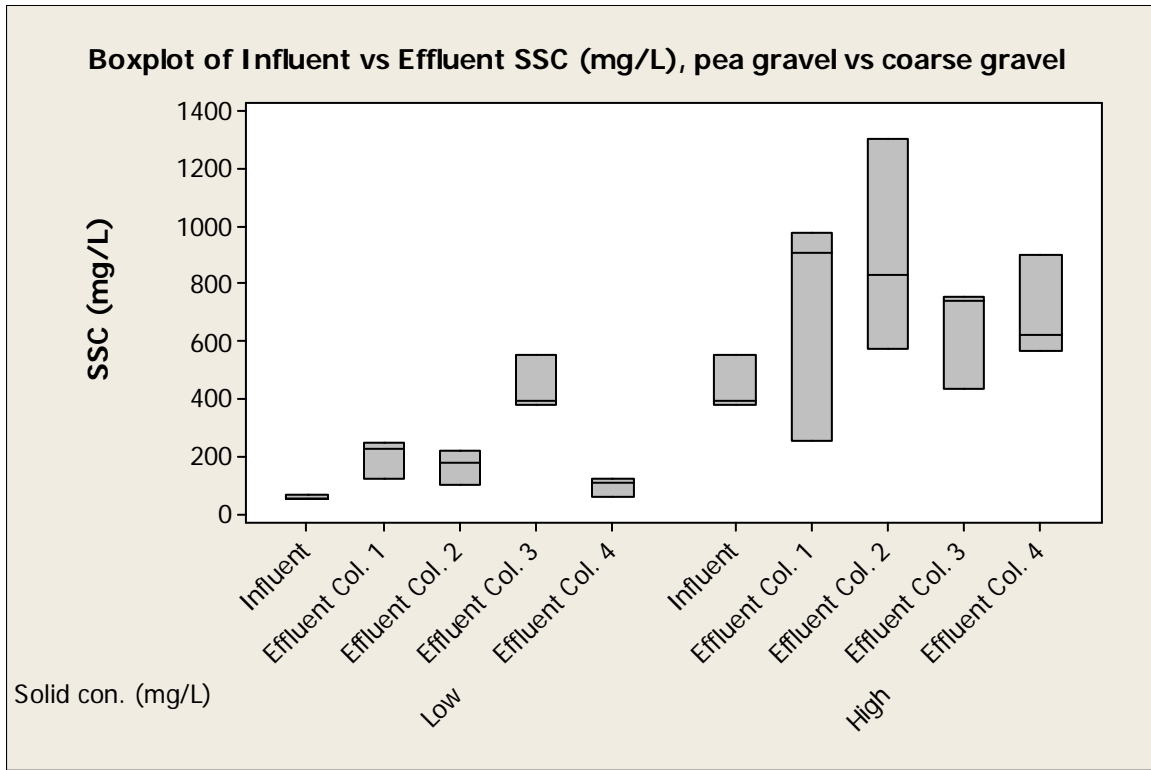


Figure 141. Grouped Box and Whisker Plot of Influent vs. Effluent SSC (mg/L) Test Results from Coarse Media Columns.

Table 103. Laboratory Column Coarse Media (average concentration)

Column No.	Media	Orifice dia. (inch)
1	Pea gravel	0.25
2	Pea gravel	1
3	Coarse gravel	0.25
4	Coarse gravel	1

Table 104. Statistical Summary of Final Combined Results

Mixture	D ₅₀ and C _u	F test results and p values for particle trapping tests	F test results and p values for particle trapping tests with combined effluent data
10% peat & 90% sand from Northport, AL	350 mm and 1	F = 12.78 and P = 0.001	F = 42.53 and P = 0.000
Tuscaloosa Surface Soil	300 mm and 37	F = 12.43 and P = 0.001	F = 41.40 and P = 0.000
50% Peat and 50% Tuscaloosa Surface Soil	300 mm and 6.8	F = 12.56 and P = 0.001	F = 41.84 and P = 0.000
50% Peat and 50% Sand	1300 mm and 19	F = 13.98 and P = 0.000	F = 27.75 and P = 0.000
10% Peat and 90% Sand	1500 mm and 22	F = 12.70 and P = 0.001	F = 42.30 and P = 0.000
50% Peat and 50% Sand	1600 mm and 2.5	F = 53.01 and P = 0.000	F = 161.01 and P = 0.000
10% Peat and 90% Sand	1900 mm and 2	F = 38.05 and P = 0.000	F = 109.26 and P = 0.000
50% Peat and 50% Sand	300 mm and 3	F = 12.58 and P = 0.001	F = 41.80 and P = 0.000
Pea gravel vs coarse gravel	Pea gravel D ₅₀ = 7.5 mm coarse gravel D ₅₀ = 9.5 mm	F = 18.65 and P = 0.000	F = 28.66 and P = 0.000
Pea gravel vs coarse gravel		F = 1.1 and P = 0.408	F = 3.23 and P = 0.095

7.5 Chapter Summary

The results of the full-factorial analyses indicated that texture and uniformity of the media mixture have the greatest effect on the measured final infiltration rates of the media, followed by interactions of texture and uniformity; compaction; interactions of texture and organic content of the material; and interactions of uniformity and organic content of the material. The organic matter in the biofilter media does not have a significant effect by itself on the infiltration rate compared to the other factors (texture, uniformity, and compaction). However the organic matter serves as a reservoir of nutrients and water in the biofilter media and increases water infiltration into the media.

Compaction did not significantly affect the infiltration rates for the mixtures having large amounts of sand and little peat; however infiltration studies conducted previously indicated that compaction significantly affected typical soil infiltration rates having normal organic content, especially if high in fines (Sileshi et al., 2012a). These test results also indicated that the

infiltration rates through all sand-peat mixture columns were greater than the infiltration rates through only soil media for the three levels of compaction (modified proctor, standard proctor and hand compaction). However, mixing the soil media with filter sand or peat improved the infiltration capacity of the media and also reduced the impact of compaction on the infiltration rates. Soil compaction has dramatic effects on the infiltration rates of most underlying soils; therefore care needs to be taken during stormwater treatment facilities construction in urban areas to reduce detrimental compaction effects. Overall, mixing the soil media with filter sand or peat improved the infiltration capacity of the media and also reduced the impact of compaction on the infiltration rates.

The particle trapping experiments using sand-peat mixture and Tuscaloosa surface soil columns indicated that reductions occurred for most lab columns, with relatively consistent effluent SSC conditions. However, particulate trapping and retention in the coarse materials was poor.

CHAPTER 8

8 APPLICATIONS AND CONCLUSIONS

8.1 Typical Biofilter as Modeled using Research Results for a Commercial Area in Tuscaloosa

This discussion incorporates the findings of the dissertation research in example applications in the Tuscaloosa, AL, area. Production function plots were developed for alternative stormwater control options for small scale commercial areas (McDonalds and Krispy Kreme) in Tuscaloosa, AL, both having almost complete impervious material (roofs and paved parking and driveway areas) covers. The area sustained heavy damage by the April 27, 2011 tornado that devastated the city of Tuscaloosa. Figures 142 and 143 show during-construction and post development aerial photographs. The drainage area and land use for the study area are shown in Table 105.



Figure 142. Aerial Photograph of McDonalds Site on 15th St. E and 6th Ave. E., Tuscaloosa, AL (During-construction)

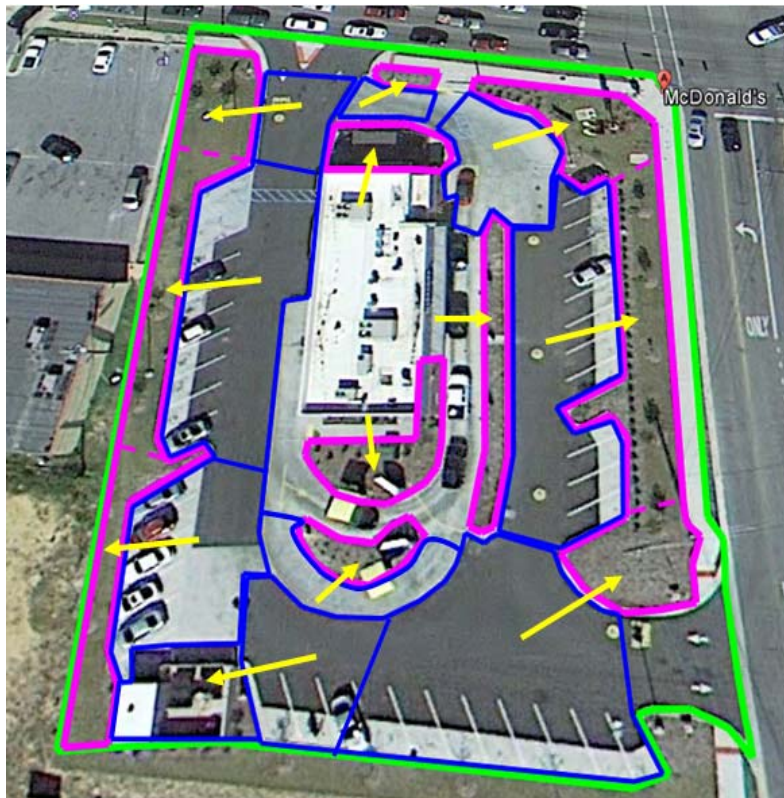


Figure 143. Aerial Photograph of McDonalds Site on 15th St. E and 6th Ave. E., Tuscaloosa, AL (Post-Development)

Table 105. Land Use Description for McDonalds Site on 15th St. E and 6th Ave. E., Tuscaloosa, AL.

Paved (ac)	Landscape (ac)	Roof (ac)	Total area (ac)
0.78	0.3	0.09	1.17

Figure 144 shows a typical biofilter as modeled using the research results for a commercial area in Tuscaloosa. The engineered media infiltration rate and porosity of the biofilter are 11.2 in/hr and 0.32 respectively.

Biofiltration Control Device

Drainage System Control Practice

Device Properties **Biofilter Number 1**

Top Area (sf)	170
Bottom Area (sf)	85
Total Depth (ft)	4.50
Typical Width (ft) (Cost est. only)	10.00
Native Soil Infiltration Rate (in/hr)	1.000
Native Soil Infiltration Rate COV	N/A
Infil. Rate Fraction-Bottom (0-1)	1.00
Infil. Rate Fraction-Sides (0-1)	1.00
Rock Filled Depth (ft)	1.00
Rock Fill Porosity (0-1)	0.30
Engineered Media Type	Media Data
Engineered Media Infiltration Rate	11.22
Engineered Media Infiltration Rate COV	N/A
Engineered Media Depth (ft)	2.00
Engineered Media Porosity (0-1)	0.32
Percent solids reduction due to Engineered Media (0 -100)	N/A
Inflow Hydrograph Peak to Average Flow Ratio	3.80
Number of Devices in Source Area or Upstream Drainage System	1

Media Data

Engineered Media Infiltration Rate	11.22
Engineered Media Infiltration Rate COV	N/A
Engineered Media Depth (ft)	2.00
Engineered Media Porosity (0-1)	0.32
Percent solids reduction due to Engineered Media (0 -100)	N/A

Evaporation

Month	Evapotranspiration (in/day)	Evaporation (in/day)
Jan		0.04
Feb		0.05
Mar		0.07
Apr		0.10
May		0.16
Jun		0.19
Jul		0.19
Aug		0.16
Sep		0.14
Oct		0.10
Nov		0.06
Dec		0.04

Biofilter Geometry Schematic

10.00'

4.50'

4.25'

2.00'

1.00'

Top of Engineered Media

Top of Rock Fill

Figure 144. Biofiltration Control Practice.

Figure 145 shows the production function plots created using the WinSLAMM model for 5 years of Tuscaloosa rain data for paved areas in Tuscaloosa comparing native soil infiltration rates of 0.1, 1, and 10 in/hr. The plot shows how large a biofilter device would need to be for different native soil infiltration rates to infiltrate different fractions of the annual runoff. This plot is for paved areas; for example, an area with a native soil infiltration rate of 0.1 in/hr would require a biofilter area (without underdrain) to be about 8% of the paved source area for about 70% annual runoff volume reductions. Whereas an area with a native soil infiltration rate of 0.1 in/hr, with conventional underdrains or SmartDrains, results in about 15 and 50% annual runoff reduction respectively for the same sized biofilters (8% of the paved source area)..

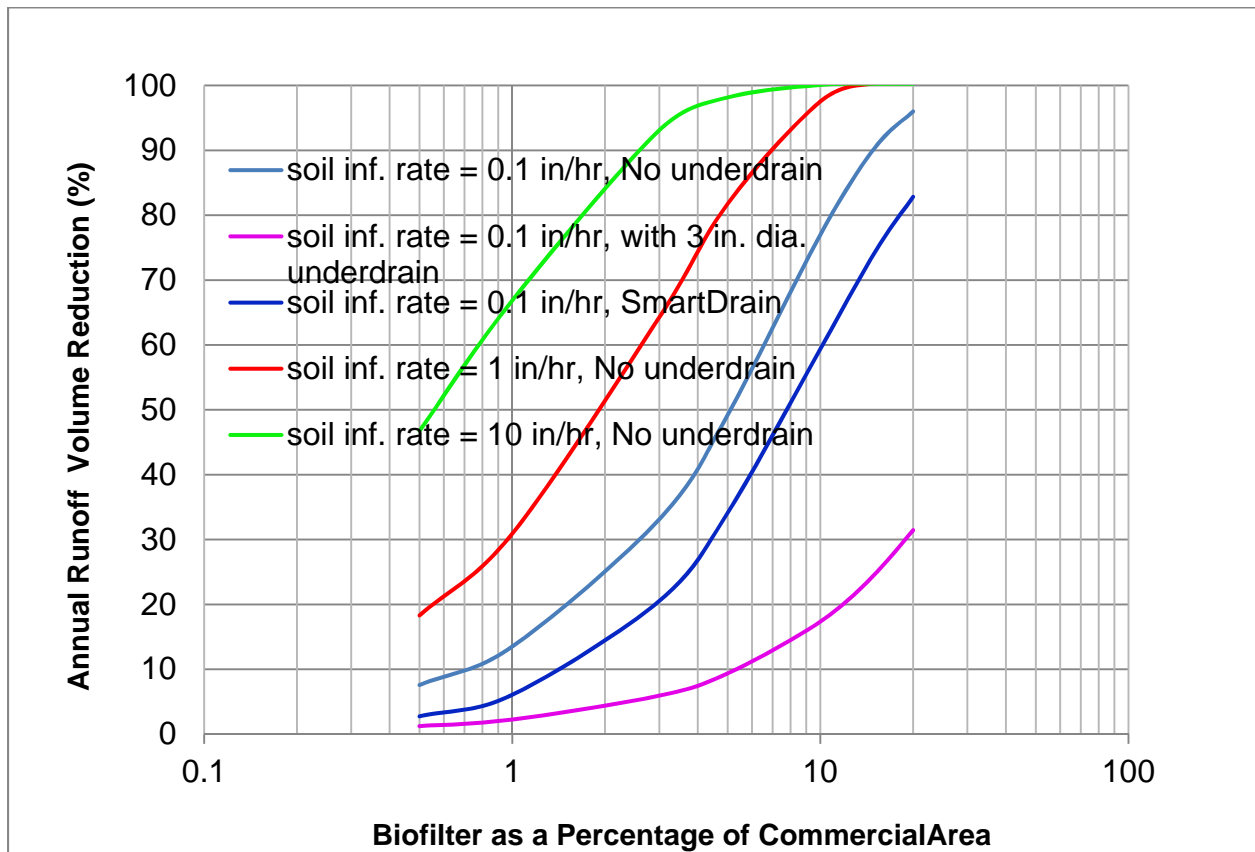


Figure 145. Biofilter Runoff Volume Reduction (McDonald’s Drainage Area).

Figure 146 shows the number of surface ponding events greater than 3 days (the typical maximum allowable period to minimize nuisance conditions such as breeding of mosquitoes) for a biofilter installed in an area that has a native soil infiltration rate of 0.1 in/hr.

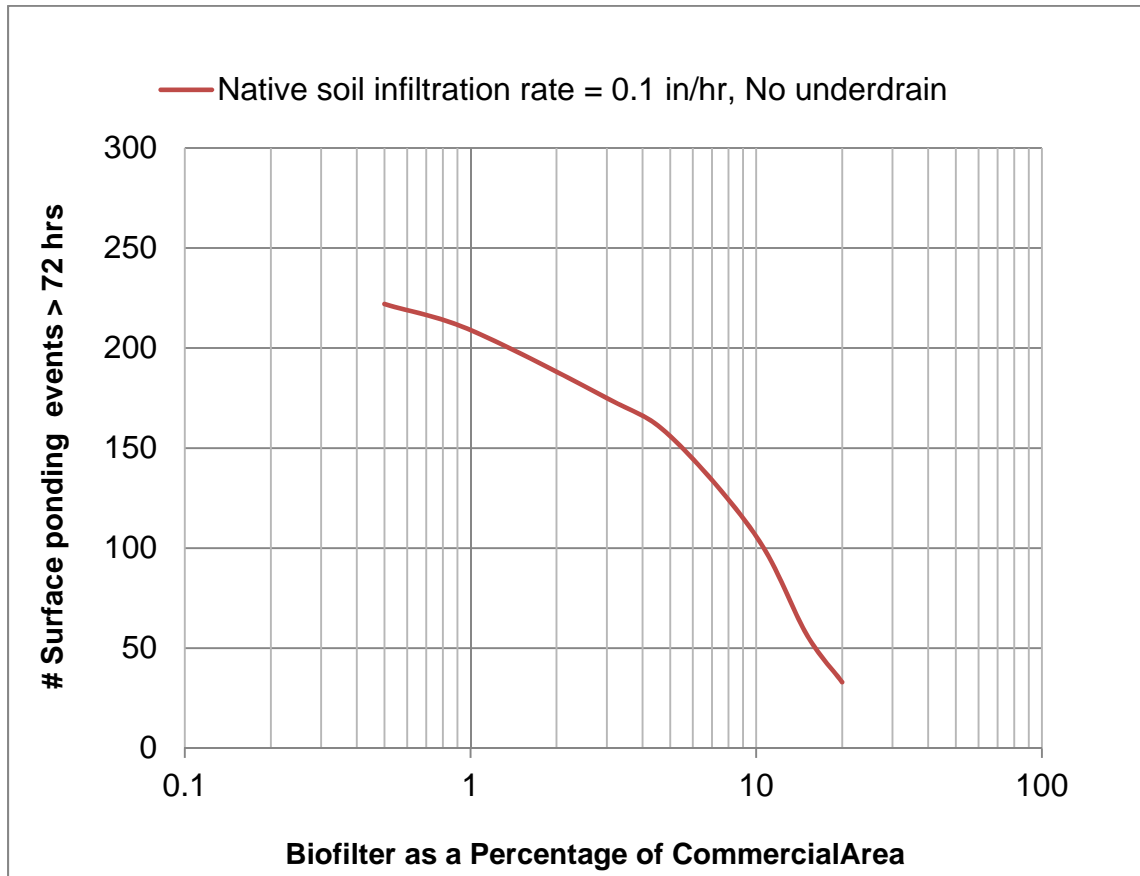


Figure 146. The Number of Surface Ponding Events Greater than 3 Days per 5 Years (clearly showing the need for an underdrain for these adverse soils).

This plot is for paved commercial area and the native soil infiltration rate is 0.1 in/hr. A biofilter area (without underdrain) to be about 4% of the paved source area has 165 surface ponding events per 5 years lasting over three day periods, clearly indicating the need for an underdrain to reduce the surface ponding durations.

Figures 147 and 148 show biofilter performance plots for an area having subsurface infiltration rates of 0.1, 1, and 10 in/hr. Figure 147 shows that 3% of the commercial area as a biofilter (with a conventional underdrain) would provide 2 to 8 years before clogging (reaching 10 to 25 kg/m² solids loading), whereas the same biofilter area using a SmartDrain underdrain would provide 7 to 18 years before clogging. The results indicated that the use of underdrain, while necessary to minimize long periods of standing water in poorly draining natural soils, can also decrease the performance of a biofilter system by short-circuiting water that would otherwise infiltrate. However, the additional water passing through the treatment media should result in increased sediment control. Conventional underdrains (perforated large diameter pipes) reduce ponding, but also decrease infiltration opportunities. The SmartDrainTM also reduces ponding time, while providing additional infiltration when underdrain are required.

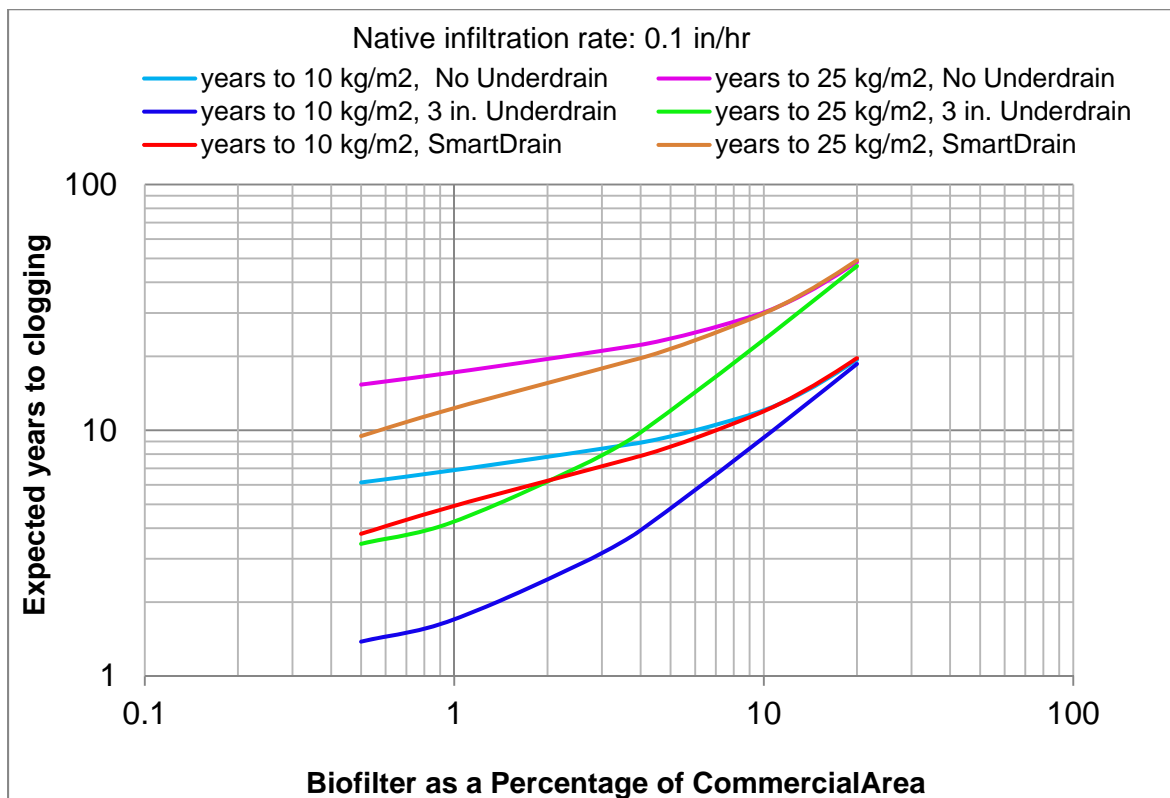


Figure 147. Years to Clog as a Function of Biofilter Size Compared to Paved Area.

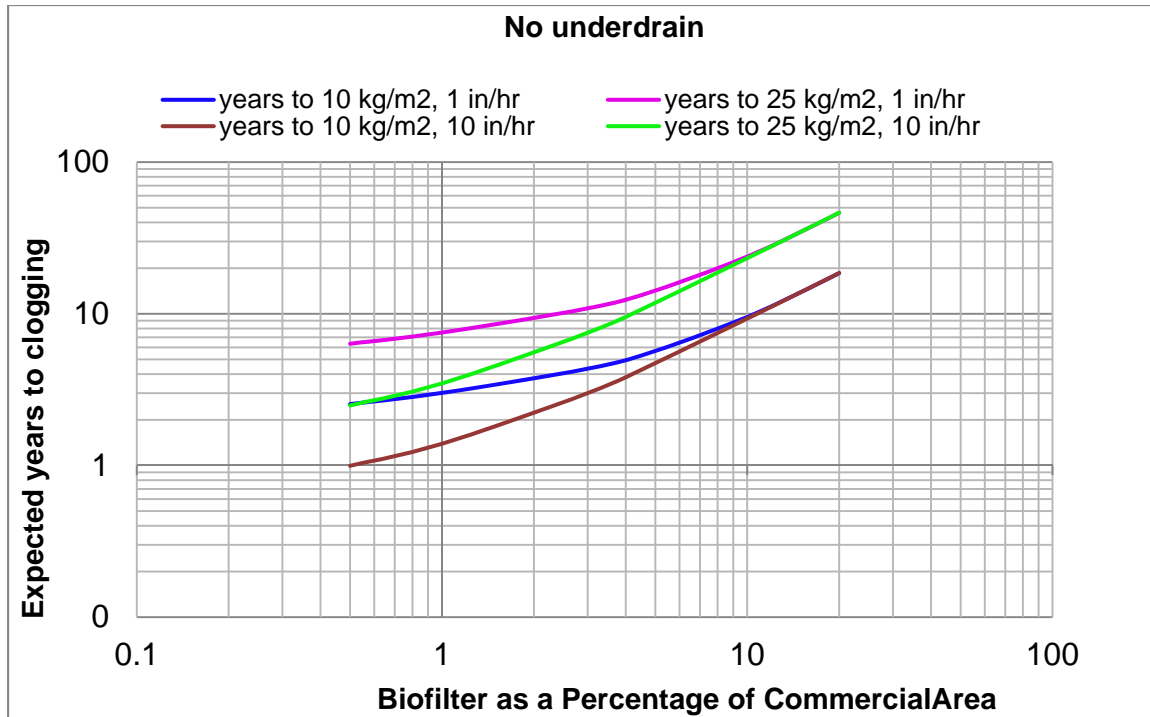


Figure 148. Biofilter Performance for Soils Having 1 and 10 in/Hr Native Subsurface Infiltration Rates (commercial drainage area).

8.2 Typical Grass Swale as Modeled using Research Results for a Residential Area in Tuscaloosa

Production function plots were developed for alternative stormwater control option (a grass swale) for a medium density residential area in Tuscaloosa, AL. The area is located in the Cedar Crest neighborhood in Tuscaloosa, AL, that sustained partial roof removals by the April 27, 2011 tornado that devastated the city of Tuscaloosa. Figures 149 and 150 show during and post development aerial photographs showing drainage grass swales. The drainage area and land use for the study area are shown in Table 106.



Figure 149. Aerial Photograph of Cedar Crest Neighborhood, Tuscaloosa, AL (Google Map)-1



Figure 150. Aerial Photograph of Cedar Crest Residential Neighborhood, Tuscaloosa, AL (Google Earth)-2

Table 106. Land Use Description for Selected Cedar Crest Neighborhood, Tuscaloosa, AL.

Paved (ac)	Landscape (ac)	Roof (ac)	Total area (ac)
0.35	4.91	0.98	6.24

Figure 151 is the WinSLAMM model input for grass swales at Cedar Crest neighborhood in Tuscaloosa.

Grass Swales

Drainage System Control Practice **Grass Swale Number 1**

Grass Swale Data	
Total Drainage Area (ac)	6.240
Fraction of Drainage Area Served by Swales (0-1)	1.00
Swale Density (ft/ac)	16.03
Total Swale Length (ft)	100
Average Swale Length to Outlet (ft)	100
Typical Bottom Width (ft)	2.0
Typical Swale Side Slope (___ ft H : 1 ft V)	3.0
Typical Longitudinal Slope (ft/ft, V/H)	0.020
Swale Retardance Factor	D
Typical Grass Height (in)	4.0
Swale Dynamic Infiltration Rate (in/hr)	0.100
Typical Swale Depth (ft) for Cost Analysis (Optional)	0.0

Select infiltration rate by soil type

- Sand - 4 in/hr
- Loamy sand - 1.25 in/hr
- Sandy loam - 0.5 in/hr
- Loam - 0.25 in/hr
- Silt loam - 0.15 in/hr
- Sandy clay loam - 0.1 in/hr
- Clay loam - 0.05 in/hr
- Silty clay loam - 0.025 in/hr
- Sandy clay - 0.025 in/hr
- Silty clay - 0.02 in/hr
- Clay - 0.01 in/hr

Use Total Swale Length Instead of Swale Density for Infiltration Calculations

Total area served by swales (acres): 6.240
Total area (acres): 6.240

Select Particle Size Distribution File **Particle Size Distribution File Name**

C:\WinSLAMM Files\NURP.CPZ

View Retardance Table

Select Swale Density by Land Use

- Low density residential - 240 ft/ac
- Medium density residential - 350 ft/ac
- High density residential - 375 ft/ac
- Strip commercial - 410 ft/ac
- Shopping center - 90 ft/ac
- Industrial - 260 ft/ac
- Freeways (shoulder only) - 480 ft/ac
- Freeways (center and shoulder) - 540 ft/ac

Copy Swale Data Paste Swale Data Delete Cancel Continue

Control Practice #: 1 CP Index #: 1

Figure 151. WinSLAMM Model Input for Grass Swale Control Practice.

Figures 152 and 153 were created using a WinSLAMM model and 5 years of Tuscaloosa rain data for medium density residential areas in Tuscaloosa.

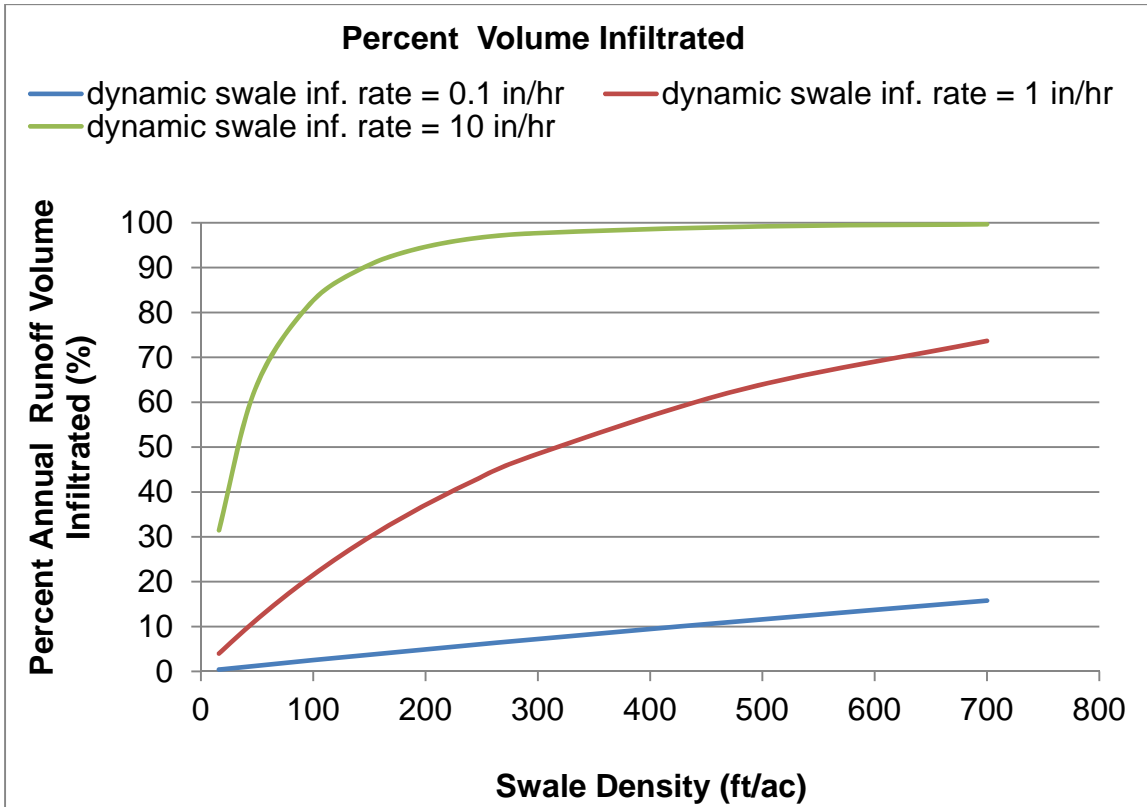


Figure 152. Percent Annual Runoff Volume Infiltrated into Grass Swale

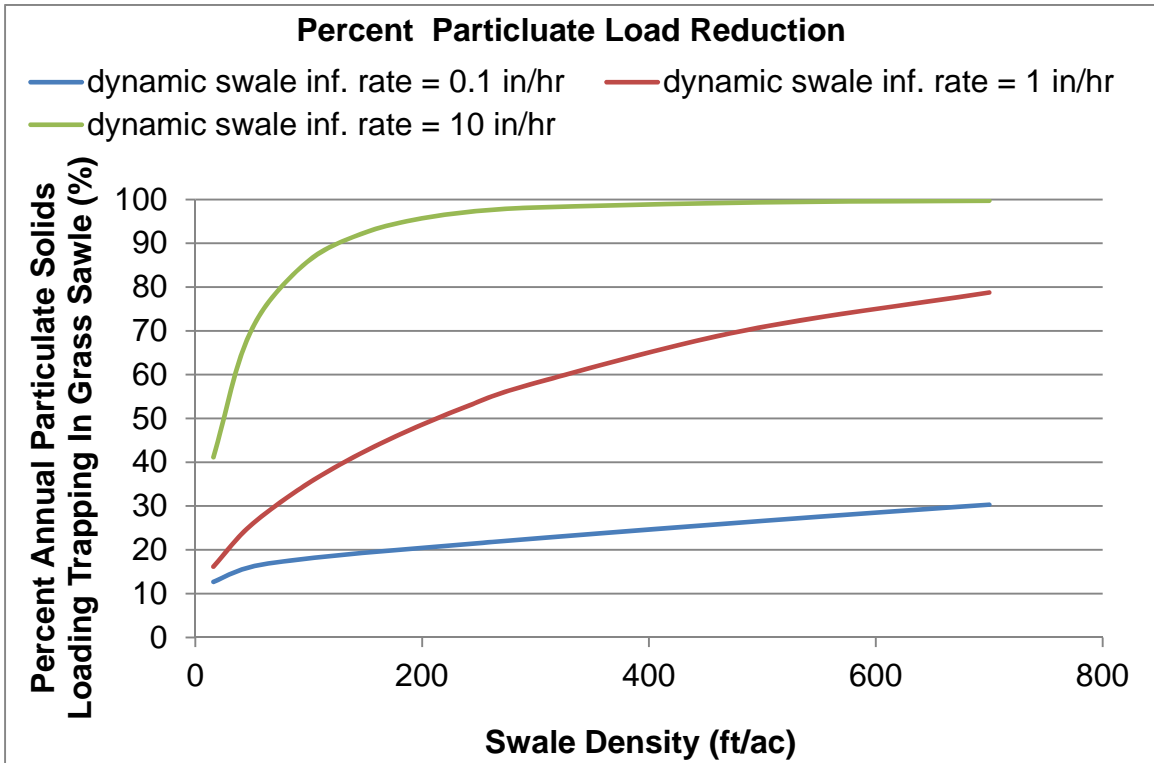


Figure 153. Percent Annual Particulate Solids Loading Trapping In Grass Swale

8.3 Factorial Statistical Analyses of Sand-Peat Mixture Column Experiments to Identify Significant Factors Affecting Particulate Removal Performance

Complete two level, three factor (2^3) experiments and statistical analyses were conducted to determine the effects of texture, uniformity, and compaction, plus their interactions, on effluent SSC water quality from various mixtures of sand and peat biofilter media. A final factorial model was developed and the complete data used in this factorial study are presented in Appendix E.

Data analyses were performed using the statistical software package Minitab (version 16). Normal plots of the standardized effects along with residual plots were prepared to examine the effects of the factors and to determine their significance. An analysis of variance (ANOVA)

table was constructed to identify the significant factors and interactions. Normal probability plots of effects were used to compare the relative magnitudes and the statistical significance of both main and interaction effects. Figure 154 shows that media texture, uniformity, and their interactions have significant effects on the observed effluent SSC concentration. These significant factors and their interactions are therefore included in the final factorial analysis model. The model can be written in terms of the grand mean and half-effects, excluding the non-significant factors. Table 107 summarizes the results of the factorial analyses.

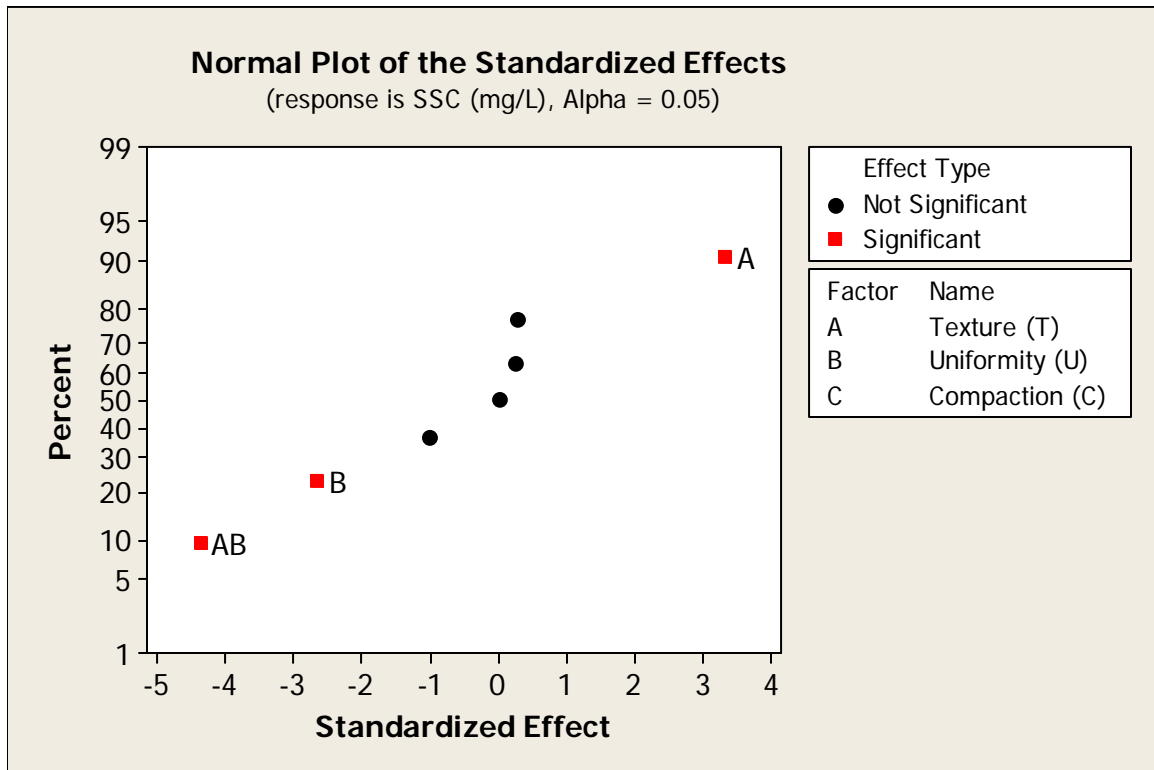


Figure 154. Probability Plot to Identify Significant Factors Affecting the Observed Effluent SSC Concentrations

Table 107. Estimated Effects and Coefficients for SSC (mg/L) (coded units)

Term	Effect	Coef	SE Coef	T	P
Constant		9.47	3.049	3.11	0.003
T	20.34	10.17	3.049	3.34	0.001
U	-16.12	-8.06	3.049	-2.64	0.01
C	1.54	0.77	3.049	0.25	0.801
T*U	-26.58	-13.29	3.049	-4.36	0.000
T*C	0.03	0.01	3.049	0.00	0.997
U*C	-6.22	-3.11	3.049	-1.02	0.312
T*U*C	1.74	0.87	3.049	0.28	0.777

S = 23.0981 PRESS = 38822.2

R-Sq = 44.87% R-Sq(pred) = 33.14% R-Sq(adj) = 38.43%

T: texture, U: uniformity, and C: compaction.

The final prediction equation is given as:

$$\text{Effluent SSC (mg/L)} = 9.47 + 10.2T - 8.1U - 13.3TU$$

As noted previously, Appendix E also includes the residual analyses for this overall equation.

8.4 SmartDrain™ Underdrain SSC and Particle Size Data and Analyses from Full-Scale Biofilter Monitoring in Kansas City

Full-scale underdrain samples from SmartDrain™ installations associated with the Kansas City National Green Infrastructure Demonstration Project were also evaluated. Seventy rain events were monitored during this three year monitoring project, with six yielding flows in the underdrains. The other events all had complete infiltration of the stormwater with no surface over-flows or underdrain flows. Influent water and underdrain treated water samples for these six events were analysed for suspended sediment concentration (SSC) and particle size distributions (PSD). Statistical tests were used to evaluate and compare the performance data collected during these tests. The tests results indicate that the average influent SSC reduction was 65% (ranged from 45 to 88%) in the underdrains compared to the influent concentrations, with the effluent

SSC concentrations averaging about 66 mg/L, with little variation. The data indicated that significant reductions occurred for all particle size ranges, except for the smallest particles (0.45 to 4 μm). It is likely that fines from the media mixture were washed into the underdrain during these events. Figure 155 shows the SSC line performance plots of these tests for different particle sizes. The results of the PSD plots of influent and effluent are summarized from Appendix E7 to E15.

The expected ranges of effluent SSC concentration (mg/L) using the column factorial equation ranged from - 6 to 41 mg/L whereas the effluent SSC concentrations averaged about 66 mg/L for the Kansas City biofilter (outside the range of estimated effluent SSC from the lab column tests). The predicted effluent SSC for the Kansas City biofilter material using the factorial equation based on its texture and uniformity conditions was -1.7 mg/L. It was way off likely due to the soil components in the Kansas City media (not pure sand mixtures) and adverse washing of fines occurred in the field decreasing the performance.

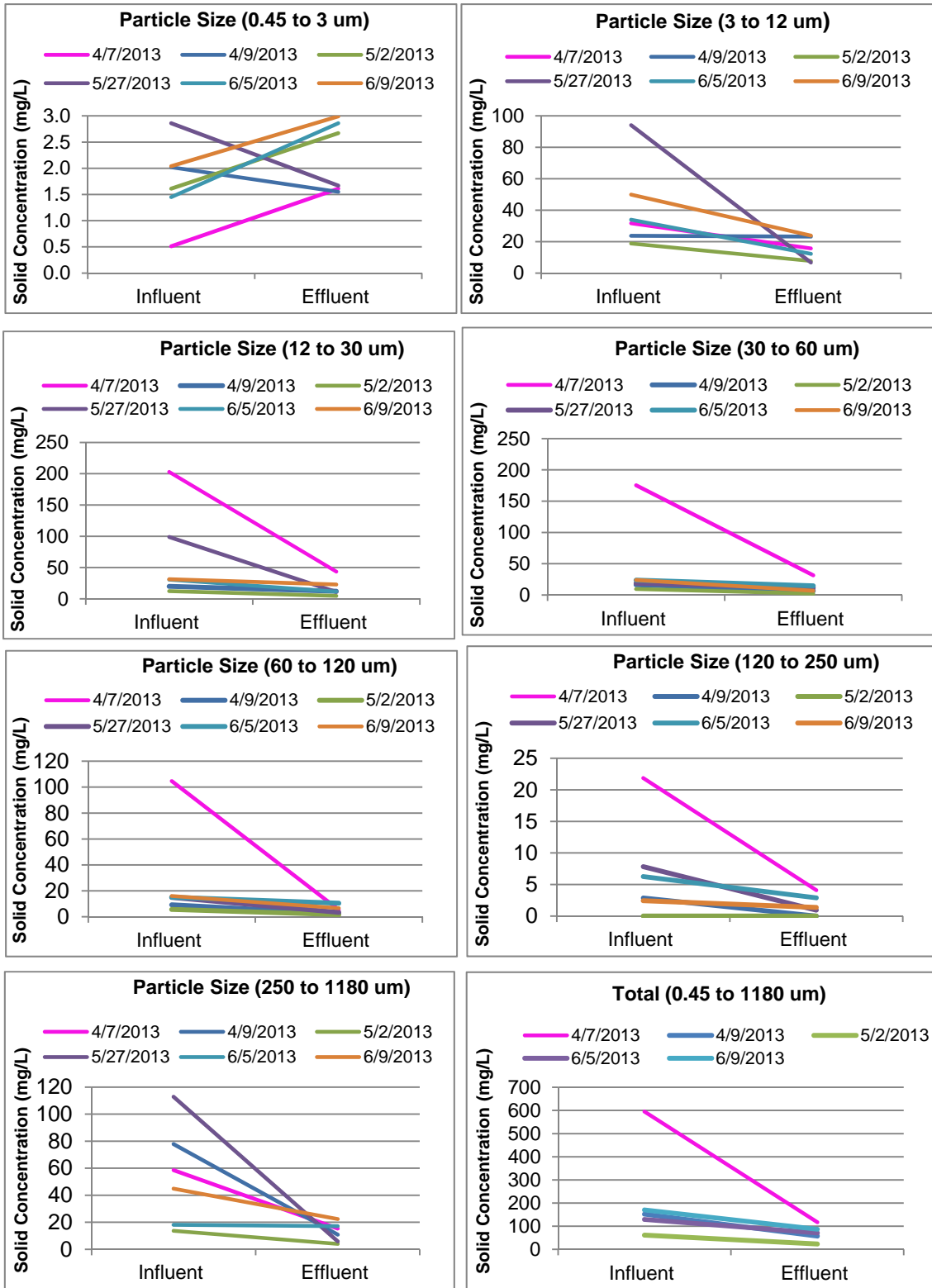


Figure 155. SSC Line Performance Plots for SmartDrain™

8.4 Research Summary

The goals of this dissertation researches were divided into four phases, as shown in the main dissertation chapters: i) to determine the flow capacity and clogging potential of a newly developed underdrain material (SmartDrain™) under severe service conditions; ii) to characterize site infiltration (double-ring infiltration tests, borehole tests, and actual infiltration rate tests during rain events); iii) to evaluate, compare surface and subsurface soil characteristics that are of the greatest interest in the design of stormwater management facilities (grass swales, bioinfiltration facilities, and rain gardens); iv) to evaluate changes in flow and particulate trapping with changes in the various soil mixture characteristics, focusing on media density associated with compaction, particle size distribution (and uniformity), and amount of organic material (due to added peat).

8.5 Dissertation Research Hypothesis

The hypotheses of this dissertation are:

Hypothesis 1:

A restricted underdrain (such as the SmartDrain™) results in enhanced outlet control for bioinfiltration devices.

During Phase I of this research, the flow capacity and clogging potential of a newly developed underdrain material (SmartDrain™) under severe service conditions were examined. The particle size distributions of the sand filter media obtained from different local suppliers in Tuscaloosa, AL were determined to select the best bedding material for the underdrain. The drainage characteristics of the SmartDrain™ material (such as length, slope, hydraulic head, and type of sand media) under a range of typical biofilter conditions using clean water were also examined. The flow capacity and clogging potential of the SmartDrain™ material after excessive

loadings by fine ground silica particulates and biofouling experiments under controlled conditions were examined to identify the most significant factors affecting drainage characteristics of this material.

A complete two level and three factors (2^3 , SmartDrainTM length, slope, and head) factorial experiment was conducted to examine the effects of those factors, plus their interactions on the SmartDrainTM flowrates. An analysis of variance (ANOVA) table was constructed to determine the significant factors and their interactions needed to best predict SmartDrainTM flow performance. SmartDrainTM head (H) has the largest effect on the measured flowrates, followed by SmartDrainTM length. Slope was not found to be significant. The significant factors that affect the responses are head, SmartDrainTM length. Those factors were included in the prediction equation. The parameters slope, interactions of length and slope, interactions of length and head, interactions of slope and head, and the three-way interactions of these factors, have negligible effect (p-values greater than the chosen value of $\alpha = 0.05$) on the SmartDrainTM flowrate and a reduced model was created wherein these factors are ignored.

Two-tailed t tests with 95% confidence intervals ($p = 0.05$ level) were performed to assess the significance of differences between flowrate measurements obtained on clean water versus dirty water during the clogging and biofouling tests. The differences between the two trial groups (clean and dirty water) were analyzed for each test by comparing their mean flowrates. The result indicates that the p-value is less than 0.05 indicating the two means are significantly different for both tests.

Hypothesis 2:

Amending biofilter media and landscaping soil can improve the infiltration capacity of the material and also reduce the impact of compaction on the infiltration rates.

Data to test this hypothesis were collected during several research phases. During Phase II of this dissertation research, double – ring infiltrometer tests and soil compaction measurements were conducted to determine the in-situ characteristics of the media for a poorly operating biofilter facility located in Tuscaloosa, AL. The effects of different compaction levels on the infiltration rates through the soil media obtained from the biofilter when mixed with varying amounts of filter sand and organic matter amendments were examined during laboratory column experiments. Long-term and continuous monitoring in the biofilter was performed during rains.

During Phase III of this research, surface double-ring infiltration tests and subsurface bore hole infiltration measurements in the field were also conducted to determine the surface and subsurface infiltration characteristics (located at the depths at the bottom of bioinfiltration devices) in Tuscaloosa, AL, in areas devastated by the severe April 2011 tornados.

During Phase IV of this research, controlled laboratory column tests were also conducted using various media to identify changes in flow and particle trapping with changes in the mixture characteristics, focusing on media density associated with compaction, particle size distribution (and uniformity), and amount of organic material (due to added peat). The performance of these mixtures were predicted and also verified using column tests (for different compaction conditions) of surface and subsurface soil samples obtained from Tuscaloosa, AL, along with biofilter media obtained from Kansas City, North Carolina, and Wisconsin.

A complete two level, four factors (2^4 , with varying texture, uniformity, organic content, and compaction) full-factorial experiment was conducted to examine the effects of these factors, plus their interactions, on the flowrate through the various sand-peat mixtures. An analysis of variance (ANOVA) table was constructed to determine the significant factors and their

interactions needed to best predict media flow performance. The significant factors and interactions that affect the responses are texture, uniformity, compaction, interactions of texture and uniformity, interactions of texture and organic content of the material, interactions of texture and compaction, and uniformity and organic content of the material. These significant factors and interactions are therefore included in the complete prediction equation.

The parameters organic content, interactions of uniformity and compaction, interactions of organic content and compaction, and all the three-way and four-way interactions of these factors, have negligible effects (p-values greater than the chosen value of $\alpha = 0.05$) on the flowrate and a reduced model was created wherein these factors are ignored.

Kruskal-Wallis nonparametric version of the parametric ANOVA test of multiple pairwise comparisons of saturated infiltration rate of different levels of compaction and sample locations were conducted. There are no significant differences noted between the saturated infiltration rate of standard proctor and modified proctor compaction methods, for the number of data observations available.

8.6 Summary of Dissertation Research Finding

The research found that:

SmartDrainsTM have minimal clogging potential while also providing very low discharge rates (preferred to encourage natural infiltration and to increase contact time with the media).

SmartDrainsTM also reduce the surface ponding time compared to no underdrains, while minimizing short-circuiting of the infiltration water. As an example, for a typical biofilter that is 3.3 ft (1 m) deep, 4.9 ft (1.5 m) wide and 16.4 ft (5 m) long, about 8 hours would be needed for complete drainage using a SmartDrainTM, easily meeting typical 24 to 72 hr maximum ponded water drainage times usually specified for mosquito control. This also provides a substantial

residence time in the media to optimize contaminant removal and also provides significant retention of the stormwater before being discharged to a combined sewer system. In addition, this slow drainage time encourages infiltration into the native underlying soil, with minimal short-circuiting to the underdrain. The laboratory column test results indicated that the infiltration rates through all mixtures of biofilter media and filter sand were greater than the infiltration rates through the biofilter media alone for the three levels of compaction (hand compaction, standard proctor, and modified proctor). The column test results for the biofilter soil alone and with varying amounts of added peat, using the standard proctor compaction method, also indicated benefits by adding peat to the biofilter media material. Mixing the biofilter media with filter sand and peat improved the infiltration capacity of the media and also reduced the impact of compaction on the infiltration rates. The mixture containing 50% biofilter media and 50% filter sand (the largest sand addition tested) exhibited the highest infiltration rates, as expected (final saturated infiltration rates of 2.7 to 16.4 in/hr for the replicated tests).

Peat amendments improve aeration and water holding capacity for plant roots, resulting in better growth. However, peat soils are more sensitive to compaction than other type of soils. Sand amendments decrease compaction effects by providing support in the mixture, preventing complete infiltration failure under adverse conditions. Sand filters generally improve drainage by lending porosity to a mix and retain moisture. Sand amendment can add needed weight to peat and fill large pore spaces without impairing drainage. It is important that stormwater practice designers determine the subsoil characteristics before designing stormwater treatment facilities and consider the use of added amendments (sand and peat) to the soils.

The laboratory test results also demonstrated that soil compaction has dramatic adverse effects on the infiltration rates; therefore care needs to be taken during the construction of

biofilter stormwater treatment facilities to reduce detrimental compaction effects. The infiltration values from the ponded locations are very small compared to the laboratory and field test infiltration values, indicating fully saturated media under moderately to severely compacted conditions.

The in-situ infiltration measurements need to be evaluated carefully. The ponded water measurements in the biofilter were obtained after complete saturation. Also, ponding was not even throughout the biofilter, and preferentially pooled in areas having depressions and with low infiltration capacities. Because they were in depressions, silting may have also occurred in those areas. Long-term and continuous monitoring in a biofilter during rains is the best indication of performance, and these spot checks likely indicate the lowest values that may occur. In fact, they were similar to the lowest infiltration rates observed with the small-scale infiltrometers and also corresponded to the compacted media column tests. Data from the infiltrometers can show very high rates that only occur during the initial portion of the event under unsaturated conditions and do not reflect long-term infiltration that occurs during the complete event period. Most of the infiltration in biofilters likely occurs after saturated conditions and the lowest rates observed may be most representative of actual field conditions.

Small-scale infiltrometers work well if surface characteristics are of the greatest interest (such as infiltration thru surface landscaped soils, as in turf areas, grass swales or in grass filters). Larger, conventional double-ring infiltrometers are not very practical in urban areas due to the excessive force needed to seat the units in most urban soils (usually requiring jacking from a heavy duty truck) and the length of time and large quantities of water needed for the tests. In addition, they also only measure surface soil conditions. Large-scale (deep) infiltration tests

would be appropriate when subsurface conditions are of importance (as in bioinfiltration systems and deep rain gardens).

The borehole/Sonotube tests were relatively easy and fast to conduct, as a large borehole drill rig was available along with large volumes of water from close-by fire hydrants. For infiltration facilities already in place, simple stage recording devices (small pressure transducers with data loggers) are very useful for monitoring during actual rain conditions. In many cases, disturbed urban soils have dramatically reduced infiltration rates, usually associated with compaction of the surface soils. These areas in Tuscaloosa were all originally developed more than 20 years ago and had standard turf grass covering. They were all isolated from unusual surface disturbances and had standard landscaping maintenance. It is not likely that the tornado affected the soil structure. The soil profile (surface soils vs. subsurface soils from about 4 ft, or 1.2 m) did affect the infiltration rates at these locations. Due to the relatively high clay content, the compaction tests indicated similar severe losses in infiltration rates with increasing soil density. Local measurements of the actual infiltration rates, as described above, can be a very useful tool in identifying problem areas and the need for more careful construction methods. Having accurate infiltration rates are also needed for proper design of stormwater bioinfiltration controls.

The results of the full-factorial analyses of infiltration and particulate trapping with a wide range of sand mixtures indicated that texture and uniformity of the media mixture have the greatest effect on the measured final infiltration rates of the media, followed by interactions of texture and uniformity; compaction; interactions of texture and organic content of the material; and interactions of uniformity and organic content of the material. The organic matter in the biofilter media did not have a significant effect by itself on the infiltration rate compared to the

other factors (texture, uniformity, and compaction). However the organic matter serves as a reservoir of nutrients and water in the biofilter media and increases water infiltration into the media.

Compaction did not significantly affect the infiltration rates for the mixtures having large amounts of sand and little peat; however infiltration studies conducted previously indicated that compaction significantly affected typical soil infiltration rates having normal organic content, especially if high in fines (Sileshi et al., 2012a). These test results also indicated that the infiltration rates through all sand-peat mixture columns were greater than the infiltration rates through only soil media for the three levels of compaction (modified proctor, standard proctor and hand compaction). However, mixing the soil media with filter sand or peat improved the infiltration capacity of the media and also reduced the impact of compaction on the infiltration rates. Soil compaction has dramatic effects on the infiltration rates of most underlying soils; therefore care needs to be taken during stormwater treatment facilities construction in urban areas to reduce detrimental compaction effects. Overall, mixing the soil media with filter sand or peat improved the infiltration capacity of the media and also reduced the impact of compaction on the infiltration rates.

The particle trapping experiments using sand-peat mixtures and Tuscaloosa surface soils indicated that reductions occurred during most of the lab column experiments, with relatively consistent effluent SSC effluent conditions. However, particulate trapping was rather poor for the coarse materials.

REFERENCES

- Adams, J.F., Mitchell, C.C. and Bryant, H.H. (1994). Soil test Fertilizer Recommendations for Alabama Crops.
- Adams, J.F. and Mitchell, C.C. (2000). Soil Test Nutrient Recommendations for Alabama Crops. This document last modified May 1, 2000.
<http://www.ag.auburn.edu/agrn/croprecs/aboutNutrients.html>
- Akan, A.O. (1993). *Urban Stormwater Hydrology: A Guide to Engineering Calculations*. Lancaster: Technomic Publishing Company, Inc.
- Ali, M.H. (2010). *Fundamentals of Irrigation and on-farm water management. Vol. 1*. Springer New York, NY.
- American Society of Testing and Materials. (1996). *Annual Book of ASTM Standards*. West Conshohocken, PA: ASTM, vol. 04.08, 1994.
- American Society for Testing and Materials. (1999). D 3977-97, *Standard Test Method for Determining Sediment Concentration in Water Sample*. Annual Book of Standards, Water and Environmental Technology, 1999, Volume 11.02, p 389–394.
- American Society of Testing and Materials. (2003). D3385-03, *Standard Test Method for Infiltration Rate of Soils in Field Using Double-ring Infiltrometer*. In Annual Book of ASTM Standards 04.08. West Conshohocken, Penn.: ASTM.
- Angers, D. E. and J. Caron. (1998). Plant -induced Changes in Soil Structure: Processes and Feedbacks. *Biogeochemistry* 42:55-72.
- Aronovici, V. S. (1954). The application of the ring infiltrometer to diagnosis of irrigation problems in southern California: *Transactions-American Geophysical Union* 35: 813-820.
- Atchison , Dustin, Ken Potter, and Linda Severson. (2006). *Water Resources Institute "Stormwater bioretention facilities"*. University of Wisconsin System Publication No. WIS-WRI-06-01. <http://aqua.wisc.edu/publications/PDFs/stormwaterbioretention.pdf>
- Bannerman, R. T., Owens, D. W., Dodds, R. B., and Hornewer, N. J. (1993). Sources of pollutants in Wisconsin stormwater. *Water Science Technology* 28: 241–259.
- Bannerman, Roger. (2012). North American Stormwater and Erosion Control Association. What are we learning about selecting a soil media for bioretention systems?
<http://www.nasecawi.org/wp-content/uploads/D2-3-Bannerman-Engineered-Soil.pdf>

- Bennett, S., and Kerchkof, T., Shea-Keenan, M., Szlaga, P. (2007). Proposed Stormwater Bioretention Facility. Michigan State University: Biosystems Engineering.
- Barrett, M. E., S. Tenney, J. F. Malina, R. J. Charbeneau, G. H. Ward. (1995). *An Evaluation of Highway Runoff Filtration Systems*. Technical Report CRWR 265, Center for Research in Water Resources, The University of Texas at Austin.
- Barrett, M.B. (2003). Performance, Cost, and Maintenance Requirements of Austin Sand Filters. *Journal of Water Resources Planning and Management* 129:3(234).
- Baveye, P., Vandevivere, P., Hoyle, B.L., DeLeo, P.C., and Lozada, D.S. (1998). Environmental Impact and Mechanisms of the Biological Clogging of Saturated Soils and Aquifer Materials. *Critical Reviews in Environmental Science and Technology*, 28(2), 123-191.
- Bedient, P.B., and Huber, W.C. (1992). *Hydrology and Floodplain Analysis*. New York: Addison Wesley Publishing Company.
- Bell, W., L. Stokes, L. J. Gavan., T. N. Nguyen. (1995). *Assessment of the Pollutant Removal Efficiencies of Delaware Sand Filter BMPs*. Department of Transportation and Environmental Services. Alexandria, VA. 140 pp.
- Bevin, K. J. (2004). Robert E. Horton's perceptual model of infiltration process. *Hydrological Processes* 18: 3447-3460
- Blecken, G.-T., Zinger, Y., Deletic, A., Fletcher, T.D., Viklander, M. (2009a). Influence of intermittent wetting and drying conditions on heavy metal removal by stormwater biofilters. *Water Research* 43: 4590–4598.
- Booth, D. B. (1991). Urbanization and the natural drainage system: Impacts, solutions, and prognoses. *Northwest Environmental Journal* 7(1):93-118.
- Bouwer, H. (1986). Intake rate: cylinder infiltrometer. Pages 825-843 in A. Klute ed. *Methods of Soil Analysis, Part 1. Physical and Mineralogical Methods-Agronomy Monograph No. 9: 2nd ed.* Madison, WI: *American Society of Agronomy /Soil Science society of America*.
- Bouwer, H. (2002). Artificial recharge of groundwater. *Hydrogeology and engineering Hydrogeology Journal* 10:121-142.
- Bowman, Rudy and Mike Petersen. (1996). *Soil organic matter levels in the central Great Plains*. USDA-ARS, Akron, CO and USDA-NRCS, Greeley, CO.
- Boyd, C.E., Wood, W.C., Thunjai, T. (2002). Pond Soil Characteristics and Dynamics of Soil Organic Matter and Nutrients. Edited by: K. McElwee, K. Lewis, M. Nidiffer, and P. Buitrago (Editors), Nineteenth Annual Technical Report. Pond Dynamics/Aquaculture CRSP, Oregon State University, Corvallis, Oregon.
<http://pdacrsp.oregonstate.edu/pubs/technical/19tchhtml/9PDR2.html>
- Box, G. E. P., Hunter, W. G., and Hunter, J. S. (1978). *Statistics for experimenters*, J Wiley, New York.

- Brown, R.A., and Hunt, W.H. (2008). Bioretention Performance in the Upper Coastal Plain of North Carolina. Low Impact Development for Urban Ecosystem and Habitat Protection. November 2008, 1-10.
- Bruce R. Hoskins. (1997). *Soil Testing Handbook for Professionals in Agriculture, Horticulture, Nutrient and Residuals Management*, Third Edition.
- Burton, G.A. and R. Pitt. (2002). *Handbook for Evaluating Stormwater Runoff Effects, a Tool Box of Procedures and Methods to Assist Watershed Managers*. CRC/Lewis Publishers, New York.
- Chow, V.T., D.R. Maidment, and L.W. Mays. (1988). *Applied Hydrology*. McGraw-Hill, Inc.
- City of Austin, Texas (1988). *Design Guidelines for Water Quality Control Basins*. Environmental Criteria Manual.
- City of Austin, Texas. (2011). *Environmental Criteria Manual*. Section 1.6.7(C)
Available Online:
[http://austintech.amlegal.com/nxt/gateway.dll/Texas/environ/cityofaustintexasenvironmentalcriteria?f=templates\\$fn=default.htm\\$3.0\\$vid=amlegal:austin_environment\\$anc=](http://austintech.amlegal.com/nxt/gateway.dll/Texas/environ/cityofaustintexasenvironmentalcriteria?f=templates$fn=default.htm$3.0$vid=amlegal:austin_environment$anc=)
- City of Seattle. (2009). *Environmentally Critical Areas Best Available Science Review*. Submitted per RCW 36.70A and WAC 365-195-900 through WAC 365-195-925 and in support of revisions to the following development regulations. Stormwater Code (SMC 22.800-22.808) and Grading Code (SMC 22.170).
- Clar, M. L., Billy J. Barfield, Thomas P. O'Connor. (2004). *Stormwater Best Management Practice Design Guide Volume 1*. General considerations. EPA/600/r-04/121. National risk management research laboratory office of research and development U.S. environmental protection Cincinnati, OH 45268.
- Clark, S. C., D.F. Lawler, and R.S. Cushing. (1992). Contact filtration: particle size and ripening. *Journal of the American Water Works Association* 84 (12): 61-71.
- Clark, S. and R. Pitt. (1999). *Stormwater Treatment at Critical Areas, Vol. 3: Evaluation of Filtration Media for Stormwater Treatment*. U.S. Environmental Protection Agency, Water Supply and Water Resources Division, National Risk Management Research Laboratory. EPA/600/R-00/016, Cincinnati, Ohio.
- Clark, S. E. (2000). *Urban Stormwater Filtration: Optimization of Design Parameters and a Pilot-Scale Evaluation*. Ph.D. Dissertation, University of Alabama at Birmingham, Birmingham, AL.
- Clark, S.E., Baker, K.H., Mikula, J.B., Burkhardt, C.S., Lator, M.M. (2006). Infiltration vs. surface water discharge: Guidance for stormwater managers. Water Environment Research Foundation. Project No. 03-SW-4. 220 pages.

- Connecticut Stormwater Quality Manual. (2004). Connecticut Department of Environmental Protection. Volume 1.
- Curtis E. Swift. (2010). Sodium Adsorption Ratio (SAR). Colorado State University Cooperative Extension Area Extension Agent (Horticulture). Last updated: 11/01/2010.
<http://www.colostate.edu/Depts/CoopExt/TRA/PLANTS/sar.html>
- Claytor, R. and T. Schueler. (1996). *Design of stormwater filtering systems*. Prepared for Chesapeake Bay Research Consortium in cooperation with U.S. EPA Region V, Chesapeake Bay Research Consortium.
- Davis, A.P., Shokouhian, M., Sharma, H., Minami, C. (2001). Laboratory Study of Biological Retention for Urban Stormwater Management. *Water Environment Research* 73(1): 5-14
- Davis, A.P., Shokouhian, M., Sharma, H., Minami, C., Winogradoff, D. (2003). Water Quality Improvement through Bioretention: Lead, Copper, and Zinc Removal. *Water Environment Research* 75(1):73-82.
- Davis, A.P., Shokouhian, M., Sharma, H., Minami, C. (2006). Water quality improvement through bioretention media: nitrogen and phosphorus removal. *Water Environment Research* 78 (3): 284.
- Dietz, M.E. and Clausen, J.C. (2006). Saturation to Improve Pollutant Retention in a Rain Garden. *Environmental Science & Technology*, 40(4): 1335-1340.
- Dinkins, Courtney and Clain Jones. (2007). *Interpretation of Soil Test Reports for Agriculture*. A Self-Learning Resource from Montana State University Extension.
- Dzurik, A. A., Ahmad, H., Benner, A., Ethers, E., Michalowski, P. (2003). *Design and Monitoring of Delaware Sand filter for the treatment of Treatment of Stormwater Runoff*. Department of Civil Engineering Florida State University Tallahassee, FL. Prepared for Florida Department of Environmental Protection DEP Contract No. WMD 669.
- Ecology. (2005). *Stormwater Management Manual for Western Washington*. Olympia, WA. Washington State Department of Ecology Water Quality Program. Publication Numbers 05-10-029 through 05-10-033. <http://www.ecy.wa.gov/pubs/0510029.pdf>
- Encyclopedia of Water Science. (2007). Second Edition (Print Version). Stanley W. Trimble. CRC Press. Pages 166–168.
- Eriksson, E., Baun, A., Scholes, L., Ledin, A., Ahlman, S., Revitt, M., Noutsopoulos, C., Mikkelsen, P.S. (2007). Selected stormwater priority pollutants – a European perspective. *Science of the Total Environment* : 383(1-3), 41-51.
- Free, G. R., Browning, G. M., and Musgrave, G. W. (1940). *Relative infiltration and related physical characteristics of certain soils*: United State Department of Agriculture, Washington, D.C. Technical Bulletin No. 729.

- Galli, J. (1990). *Peat-Sand Filters: A Proposed Stormwater Management Practice for Urbanized Areas*, Department of Environmental Programs, Metropolitan Washington Council of Governments, Washington, DC.
- Georgia Stormwater Management Manual. (2001). Volume 2 -Technical Manual. Section 3.2.3 Bioretention Areas.
- Gibbons, J. D. (1997). *Nonparametric Methods for Quantitative Analysis* (3rd ed.). Columbus, OH: American Sciences Press.
- Gilroy, K.L. and McCuena, R.H. (2009). Spatio-temporal effects of low impact development practices. *Journal of Hydrology* 367:228-236.
- Glick, R., Chang, G. C., and Barrett, M. E.(1998). *Monitoring and evaluation of stormwater quality control basins*. Watershed management: Moving from theory to implementation, Denver, Colorado, 369-376.
- Greb, S., S. Corsi, and R. Waschbush. (1998). *Evaluation of Stormceptor and Multi-Chamber Treatment Train as Urban Retrofit Strategies*. Presented at Retrofit Opportunities for Water Resource Protection in Urban Environments, A National Conference. The Westin Hotel, Chicago, IL, February 10–12, 1998.
- Green W. H., and G.A. Ampt. (1911). Studies on soil physics, part I, the flow of air and water through soils. *Journal of Agricultural Science* 4(1): 1-24.
- Gregory, J. H., Dukes, M. D., Jones, P. H., and Miller, G. L. (2006). Effect of urban soil compaction on infiltration rate. *J. Soil Water Conserv.*, 61(3), 117-123.
- Hathaway, J.M., Hunt, W.F. , Graves, A.K., Wright, J.D. (2011). Field Evaluation of Bioretention Indicator Bacteria Sequestration in Wilmington, North Carolina. *J. Environ. Eng.*, 137 (12), 1103–1113.
- Hatt, B.E., Deletic A, Fletcher TD. (2007a). Stormwater reuse: designing biofiltration systems for reliable treatment. *Water Science Technology* 55(4):201-209.
- Hatt, B.E., Tim D. Fletcher, and Ana Deletic. (2008). Hydraulic and Pollutant Removal Performance of Fine Media Stormwater Filtration Systems. *Environmental Science Technology* 42 (7): 2535-2541.
- Hatt, B.E., Fletcher, T.D., Deletic, A. (2009). Hydrologic and pollutant removal performance of stormwater biofiltration systems at the field scale. *Journal of hydrology* 365: 310-321.
- Henderson, C., Greenway, M., Phillips, I. (2007a). Removal of dissolved nitrogen, phosphorus and carbon from stormwater by biofiltration mesocosms. *Water Science and Technology* 55 (4):183-191.
- Henderson, C., Greenway, M., Phillips, I. (2007b). *Sorption behaviour of nutrients in loamy-sand bioretention media subject to different conditions (vegetation, enrichment and incubation time)*. In: Paper presented at the Conference on Rainwater and Urban Design, Sydney, Australia, 21–23 August, 2007.

- Herrera, Esteban. (2005). *Soil Test Interpretations*. Guide A-122. Cooperative Extension Service College of Agriculture and Home Economics.
- Herrera. (2011). Best Available Science for Stormwater Management Alternatives. Available Online:http://sanjuanco.com/cdp/docs/CAO/SECOND_DRAFT_Stormwater_Alternatives_2011-04-19.pdf
- Horner, R. R., and C. R. Horner. (1995). *Design, Construction, and Evaluation of a Sand Filter Stormwater Treatment System*. Part II. Performance monitoring .Report to Alaska Marine Lines, Seattle WA.
- Horton, R.E. (1939). Analysis of runoff plat experiments with varying infiltration capacity, *Transactions – American Geophysical Union* 20: 693-711.
- Horton, R.E. (1940). An Approach toward physical Interpretation of infiltration –capacity. *Soil Science Society of America proceeding* 5: 399-417.
- Hsieh, C., and A. P. Davis. (2005). Evaluation and optimization of bioretention media for treatment of urban stormwater runoff. *Journal of Environmental Engineering* 131(11): 1521-1531.
- Hsieh, C.H., Davis, A.P., Needelman, B.A. (2007b). Nitrogen removal from urban stormwater runoff through layered bioretention columns. *Water Environment Research* 79: 2404–2411.
- Hunt, W.F. (2004). *Pollutant Removal Evaluation and Hydraulic Characterization for Bioretention Stormwater after Treatment Devices*. Ph.D. Dissertation, Pennsylvania State University, PA.
- Hunt, W., Smith, J., Jadlocki, S., Hathaway, J., and Eubanks, P. (2008). Pollutant Removal and Peak Flow Mitigation by a Bioretention Cell in Urban Charlotte, N.C. *J. Environ Eng.*, 134(5), 403-408.
- Hunt, W.F., Jarrett, A. R, Smith, J. T., and Sharkey, L. J. (2006). Evaluating Bioretention Hydrology and Nutrient Removal at Three Field Sites in North Carolina. *Journal of Irrigation and Drainage Engineering* 132(6): 600-606.
- Hunt, W.F. (2006). *Urban waterways Maintenance of Stormwater Wetlands and Wet Ponds report*. North Carolina Cooperative Extension Service. AGW-588-07. E07-45831. Available Online: <http://www.bae.ncsu.edu/stormwater/PublicationFiles/WetlandMaintenance2006.pdf>
- Hooghoudt, SB. (1940). Contributions to the knowledge of some physical quantities of the ground, Algemeene consideration of the problem of detailed drainage and infiltration by the middle of parallel loop income drains, ditches, canals and ditches. *Encrypt Landb, Ent Algemeene Country Printing, The Hauge* 46: 515-707.

- Imbrium Systems: Sorbtive™ MEDIA: A Breakthrough in Total Phosphorus Removal: The science behind Sorbtive™ MEDIA.
<http://www.imbriumsystems.com/pdf/SorbitiveMEDIATechBrief.pdf>
- Irrigation Association. (2000). Landscape Drainage Design. The Irrigation Association, Falls Church, VA.
- Johnson, A.I. (1963). *A field method for the measurement of infiltration*. US Geological Survey Water-Supply paper 1544-F.
- Jones, M. P. and Hunt, W. (2009). Bioretention Impact on Runoff Temperature in Trout Sensitive Waters. *Journal of Environmental Engineering* 135(8): 577-585.
- Kim, H., Eric A Seagren, Allen P Davis. (2003). Engineered Bioretention for Removal of Nitrate from Stormwater Runoff. *Water Environment Research* 75(4): 355-367.
- King County, Washington. (2009). Surface Water Design Manual. Seattle, WA.
 Available Online: <http://your.kingcounty.gov/dnrp/library/water-and-land/stormwater/surface-water-design-manual/SWDM-2009.pdf>
- Kreith, F.; Berger, S.A.; et. al. (1999). “Fluid Mechanics” *Mechanical Engineering Handbook* Ed. Frank Kreith. Boca Raton: CRC Press LLC, 1999
<http://www.itiomar.it/pubblca/dispense/MECHANICAL%20ENGINEERING%20HANDBOOK/Ch03.pdf>
- Lau, Y.L., Marsalek, J., Rochfort, Q., (2000). Use of a biofilter for treatment of heavy metals in highway runoff. *Water Quality Research Journal of Canada* 35 (3):563–580.
- LeCoustumer, S., T.D. Fletcher, A. Deletic, and M. Potter. (2008). *Hydraulic Performance of Biofilter Systems for Stormwater Management: Lessons from a Field Study*. Facility for Advancing Water Biofiltration, Department of Civil Engineering, Institute for Sustainable Water Resources, Monash University, Melbourne, Vic., 3800, Australia.
 Available Online: <http://www.monash.edu.au/fawb/publications/fawb-biofilter-field-infiltration-study.pdf>
- LeCoustumer S., Fletcher T. D., Deletic A., Barraud S., Lewis J.F. (2009). Hydraulic performance of biofilter systems for stormwater management: Influences of design and operation. *Journal of Hydrology* 376(1-2):16-23.
- Leif, T. (1999). *Compost Stormwater Filter Evaluation*. Snohomish County, Washington, Department of Public Works, Everett, WA.
- Lewis, M. R. (1937). The rate of infiltration of water in irrigation-practice: *Transactions-American Geophysical Union* 18: 361-368.
- Li, H., and Davis, A.P. (2008a). Urban Particle Capture in Bioretention Media. I: Laboratory and Field Studies. *Journal of Environmental Engineering* 134(6): 409-418.

- Li, H., and Davis, A.P. (2008b). Urban Particle Capture in Bioretention Media. II: Theory and Model Development. *Journal of Environmental Engineering* 134(6): 419-432.
- Li, H., and Davis, A.P. (2008c). Heavy Metal Capture and Accumulation in Bioretention Media. *Environmental Science & Technology* 42(14): 5247-5253.
- Li, H., and Davis, A. P. (2009a). Water Quality Improvement through Reductions of Pollutant Loads Using Bioretention. *Journal of Environmental Engineering* 135(8): 567-576.
- Linsley, R.K., Jr., J.B. Franzini.(1975). *Water Resource Engineering*, 2nd ed., McGraw-Hill, New York.
- Linsley, R.K., Jr., M.A. Kohler, and J. L .H. Paulhus. (1982). *Hydrology for Engineers*, 3rd ed., McGraw-Hill, New York.
- Low Impact Development (LID) Manual for Michigan: A Design Guide for Implementors and Reviewers. (2008). Chapter 7, page 141.
<http://library.semcog.org/InmagicGenie/DocumentFolder/LIDManualWeb.pdf>
- Massman, J.W. (2003). *Implementation of infiltration ponds research. Final Research Report, Research Project Agreement No. Y8265*. Washington State Department of Transportation. Available
 Online:<http://www.wsdot.wa.gov/research/reports/fullreports/578.1.pdf>
- Matson, Jack E.and Huguenard, Brian R. (2007). Evaluating Aptness of a Regression Model. *Journal of Statistics Education* Volume 15, Number 2.
<http://www.amstat.org/publications/jse/v15n2/datasets.matson.html>
- Mid-America Regional Council and American Public Works Association (APWA/MARC) (2012). Manual of Best Management Practices for Stormwater Quality, APWA/MARC Kansas City, MO.
http://kcmetro.apwa.net/chapters/kcmetro/specs/2012%20BMP%20Manual%20May-15-2012_CombinedDraft.pdf
- Ming, H.Y. and Chun, H.M. (2005). Percolation Research & Application of Smart Drain™ Belt in Chun-In Reservoir. <http://www.neimagazine.com/story.asp?sc=2031862>
- Minton, G.R. (2005). *Stormwater Treatment: Biological, Chemical & Engineering Principles. Resource Planning Associates*. Sheridan Books, Inc., Seattle, WA.
- Mitchell, C. C. and Gobena Huluka. (2011). *Timely information agriculture & natural resources. Agronomy and Soils Series*. Alabama Cooperative Extension System.
- Montgomery County Maryland. (2005). Department of Permitting Services Water Resources Section Revised.
- Morel-Seytoux, H. J. (1978). Derivation of equations for variable rainfall infiltration. *Water Resource . Research* 14(4): 561–568.

- Morhard, J. (2006). Analysis of the drainage of sports grounds with the Drain Belt ® (Smart Drain) System, *Rasen-Turf-Gazon* 37, 152-154
- Munshower, F.F. (1994). *Practical Handbook of Disturbed Land Revegetation*. Publication: Lewis Publishers, Boca Raton, Florida
- Musgrave, G. W. (1935a). A device for measuring precipitation waters lost from the soil surface runoff, percolation, evaporation, and transpiration: *Soil Science* 40: 391-401.
- Neal, J.H.(1938). *The effect of the degree of slope and rainfall characteristics on runoff and soil erosion*, Research Bulletin. Vol. 280, Missouri Agricultural Experiment Station.
- New Jersey. (2004). *Stormwater Best Management Practices Manual*. New Jersey Department of Environmental Protection Division of Watershed Management.
http://www.njstormwater.org/bmp_manual/NJ_SWBMP_9.1%20print.pdf
- North Carolina Division of Water Quality (NCDENR) Stormwater Best management Practices Manual. (2007). Chapter 12. Bioretention: Chapter Revised 07-02-07.
http://www.ncsu.edu/ehs/environ/DWQ_StormwaterBMPmanual_001%5B1%5D.pdf
- Orlich, S. (2010). Kruskal-Wallis Multiple Comparisons with a MINITAB Macro. (Minitab, Inc.).
- Passeport, E., Hunt, W.F., Line, D.E., Smith, R.A., Brown, R. A. (2009). Field study of the ability of two grassed bioretention cells to reduce stormwater runoff pollution. *Journal of Irrigation and Drainage Engineering* 135(4): 505-510.
- Philips, C.E. and Kitch, W.A. (2011). *A Review of Methods for Characterization of Site Infiltration with Design Recommendations*; Proceedings: 43rd Symposium on Engineering Geology and Geotechnical Engineering, University of Las Vegas, NV, March 23-25
- Pitt, R., Sileshi, R., Talebi, L., and Christian, C. (2013). Stormwater Management in the Aftermath of Natural Disasters,” ASCE/EWRI, Proceedings of the 2013 World Environmental and Water Resources Congress, May 22-23, 2013.
- Pitt, R. (1996). *The Control of Toxicants at Critical Source Areas*. Presented at the ASCE/Engineering Foundation Conference, Snowbird, UT, August 1996.
- Pitt, R., M. Lilburn, and S. Burian. (1997). *Storm Drainage Design for the Future: Summary of Current U.S. EPA Research*. American Society of Civil Engineers Technical Conference, Gulf Shores, AL, July 1997.
- Pitt, R., J. Lantrip, R. Harrison, C. Henry, and D. Hue. (1999a). *Infiltration through Disturbed Urban Soils and Compost-Amended Soil Effects on Runoff Quality and Quantity*. EPA 600-R-00-016. U.S. Environmental Protection Agency. National Risk Management Research Laboratory. Office of Research and Development. Cincinnati, OH: 231 pp.

- Pitt, R., S. Clark, and R. Field. (1999b). Groundwater Contamination Potential from Stormwater Infiltration Practices. *Urban Water* 1(3): 217-236.
- Pitt, R., Chen, S.-E., Clark, S.E. (2002). *Compacted Urban Soils Effects on Infiltration and Bioretention Stormwater Control Designs*. Conf. proceedings. 9th International Conference on Urban Drainage (9ICUD). Portland, Oregon.
- Pitt, R. Module 5: Statistical Analyses. April 5, 2007
<http://rpitt.eng.ua.edu/Class/ExperimentalDesignFieldSampling/Module%205/M5%20Statistical%20Analyses.pdf>
- Pitt, R., Chen, S.-E., Clark, S.E., Swenson, J., and Ong, C.K. (2008). Compaction's Impacts on Urban Stormwater Infiltration. *Journal of Irrigation and Drainage Engineering* 134(5): 652-658.
- Robert Pitt. (2009). QUALITY ASSURANCE PROJECT PLAN (QAPP) Presence and Treatability of Emerging Contaminants in Wet Weather Flows March 31, 2009.
- Pitt, R. (2011). Lincoln, Nebraska, Retrofit Stormwater Management Options: Performance and Relative Costs. Prepared for the City of Lincoln, Nebraska. July 29
- Prince George's County. (1993). Environmental Service Department of Environmental Resources The Prince George's County, Maryland.
- Prince George's County. (2002). *Bioretention Manual*. Department of Environmental Resources. Programs & Planning Division, Prince George's County, Maryland, USA.
- Prince George's County. (2007). *Bioretention Manual*. Department of Environmental Resources. Environmental Services Division, Prince George's County, Maryland, USA.
- Raju MM, Kumar A, Bisht D, Kumar Y, Sarkar A. (2012). Representative Hydraulic Conductivity and its Effect of Variability in the Design of Drainage System. Volume 1 (12). Open Access Scientific Reports
<http://www.omicsonline.org/scientific-reports/IDSE-SR-576.pdf>
- Rawls, W. J.; D. Gimenez, and R. Grossman. (1998). Use of soil texture, bulk density, and slope of the water retention curve to predict saturated hydraulic conductivity. *Proc. ASAE* 41(4):983-88
- Read, J., Wevill, T., Fletcher, T.D., Deletic, A. (2008). Variation among plant species in pollutant removal from stormwater in biofiltration systems. *Water Research* 42 (4-5):893-902.
- Robertson, B., R Pitt, A Ayyoubi, and R Field. (1995). *A Multi-Chambered Stormwater Treatment Train*. In *Proceedings of the Engineering Foundation Conference: Stormwater NPDES-Related Monitoring Needs*, Mt. Crested Butte, Colorado, August 7-12, 1994, American Society of Civil Engineers, New York, New York.

- Shaver, E. and R. Baldwin. (1991). *Sand Filter Design for Water Quality Treatment*. Delaware Department of Natural Resources and Environmental Control. Dover, DE.
- Sileshi, R., Pitt, R., Clark, S., and Christian, C. (2012a). Laboratory and Field Studies of Soil Characteristics of Proposed Stormwater Bioinfiltration Sites, Water Environment Federation (WEF) Stormwater Symposium 2012. July 18-20, 2012. Baltimore, Maryland.
- Sileshi R., Pitt R., and Clark S. (2012b). Assessing the Impact of Soil Media Characteristics on Stormwater Bioinfiltration Device Performance: Lab and Field Studies, ASCE/EWRI, Proceedings of the 2012. World Environmental and Water Resources Congress, May 2012, 3505-3516
- Skaggs, R. W., and R. Khaleel. (1982). *Chapter 4: Infiltration, In Hydrology of Small Watersheds*. St Joseph, Michigan: American Society of Agricultural Engineers.
- SmartDrain LLC. SmartDrain Installation Instructions General Guidelines. http://www.smartdrain.com/pdf/sd_horizontal_guide.pdf
- Sonon, L.S., Saha, U., and Kissel, D.E. (2012). Soil Salinity Testing, Data Interpretation and Recommendations. The University of Georgia Cooperative Extension. College of Agricultural and Environmental Sciences; College of Family and Consumer Sciences. http://www.caes.uga.edu/applications/publications/files/pdf/C%201019_1.PDF
- South Eastern U.S. (2009). Vegetable Crop Handbook.
- Sun, X., Davis, A.P. (2007). Heavy metal fates in laboratory bioretention systems. *Chemosphere* 66 (9):1601–1609.
- Thompson, A.M., A.C. Paul, and N.J. Balster. (2008). Physical and Hydraulic Properties of Engineered Soil Media for Bioretention Basins. *Transactions of the American Society of Agricultural Engineers* 51(2): 499-514.
- Toebes, C. (1962). A Note on the Use of Infiltration Equations in Infiltration Analysis. Presented at the Hydrology Symposium Tenth New Zealand Science Congress, Christchurch, 13-17 August, 1962. http://www.hydrologynz.org.nz/downloads/20080527-035423-JoHNZ_1962_v1_2_Toebes.pdf
- Turf Tec International. (1989). *Turf Tec instructions*, Oakland Park, Fla.
- Turner, Ellen. (2006). Comparison of Infiltration Equations and Their Field Validation with Rainfall Simulation. Master Thesis, University of Maryland College Park.
- United States Department of Agriculture (USDA), Natural Resource Conservation Service (NRCS). (1986). *Urban Hydrology for Small Watersheds*. Technical Release 55. 2nd Edition. Washington, D.C.

- United States Department of Agriculture (USDA), Natural Resource Conservation Service (NRCS). (2008). Soil Quality Indicators. http://soils.usda.gov/sqi/assessment/files/bulk_density_sq_physical_indicator_sheet.pdf
- United States Environmental Protection Agency (US EPA). (1986). Saturated hydraulic conductivity, Saturated Leachate Conductivity, and Intrinsic Permeability. Method 9100. <http://www.epa.gov/osw/hazard/testmethods/sw846/pdfs/9100.pdf>
- Winer, R. (2000). National Pollutant Removal Performance Database for Stormwater Treatment Practices: 2nd Edition. Center for Watershed Protection. Ellicott City, MD.
- United States Environmental Protection Agency (US EPA). (1993). Environmental Monitoring Systems Laboratory. Cincinnati, Ohio. "Method 180.1: Determination of Turbidity by Nephelometry; Revision 2.0." August 1993.
- United States Environmental Protection Agency (US EPA). (1996). *Protecting Natural Wetlands: A Guide to Stormwater Best Management Practices*. EPA-843-B-96-001. Office of Water (4502F) Washington, D.C.
- United States Environmental Protection Agency (US EPA). (1997). *Innovative Uses of Compost: Erosion Control, Turf Remediation, and Landscaping*. US EPA Fact Sheet EPA 530-F-97-043.
- United States Environmental Protection Agency (US EPA). (1999a). *Stormwater Technology Fact Sheet: Sand Filters*. EPA 832-F-99-007. Office of Water, Washington D.C. Available Online: http://water.epa.gov/scitech/wastetech/upload/2002_06_28_mtb_sandfltr.pdf
- United States Environmental Protection Agency (US EPA). (1999b). *Preliminary Data Summary of Urban Stormwater Best Management Practices*. Office of Water, EPA 821-R-99-012, Washington D.C. Available Online: http://water.epa.gov/scitech/wastetech/guide/stormwater/upload/2006_10_31_guide_stormwater_usw_c.pdf
- United States Environmental Protection Agency (US EPA). (2004). *National Pollutant Discharge Elimination System Compliance Inspection Manual (Appendix U)*. EPA 305-X-04-001. Office of Enforcement and Compliance Assurance. Washington, D.C.: 802 pp.
- United States Environmental Protection Agency (USEPA). (2005). *National Management Measures To Control Nonpoint Source Pollution From Urban Areas*. Office of Water Washington, DC 20460 (4503F) EPA-841-B-05-004. Available Online: <http://www.scribd.com/doc/19828532/Urban-Stormwater-Manual>
- Urbonas, B. (1999). Design of a Sand Filter for Stormwater Quality Enhancement. *Water Environment Research* 71(1):102-113.

- Vegetable Crop Handbook for Southeastern United States .(2010).
<https://sites.aces.edu/group/commhort/vegetable/Vegetable/2010%20Southeast%20Veg%20Guide%20Part%201%20-%20Introduction.pdf>
- Villanova Urban Stormwater Partnership (VUSP):
http://www3.villanova.edu/VUSP/bmp_research/bio_traffic/bio_des_comp.htm
- Virginia Department of Conservation and Recreation (VDCR). (2010). *Stormwater Design Specification No. 8 Infiltration Practices Version 1.7*
<http://www.cwp.org/cbstp/Resources/d2s4a-dcr-bmp-infiltration.pdf>
- Weindorf, D. C., R. E. Zartman, and B. L. Allen. (2006). Effect of compost on soil properties in Dallas, Texas. *Compost Science and Utilization* 14(1): 59-67.
- Willeke, G.E.(1966). Time in Urban Hydrology. *Journal of the Hydraulics Division Proceedings of the American Society of Civil Engineers*: 13-29.
- Winer, R. (2000). *National Pollutant Removal Performance Database for Stormwater Treatment Practices*: 2nd Edition. Center for Watershed Protection. Ellicott City, MD
- Wisconsin Department of Natural Resources. (2004). DNR Technical Standard 1002. *Site Evaluation for Stormwater Infiltration*. Available Online:
<http://dnr.wi.gov/runoff/pdf/stormwater/techstds/post/dnr1002-Infiltration.pdf>
- Wisconsin Department of Natural Resources (WDNR). (2006). Conservation Practice Standard. Bioretention For Infiltration (1004)
<http://dnr.wi.gov/topic/stormwater/documents/Bioretention1004.pdf>
- Wukasz, R.J. and Siddiqui, A. (1996). *Remediation of hazardous effluent emitted from beneath newly constructed road systems and clogging of underdrain systems*. School of Civil Engineering , Purdue University ,Project No. SPR-2116, and File No. 4-7-3.
Available Online:
<http://docs.lib.purdue.edu/cgi/viewcontent.cgi?article=1653&context=jtrp>
- Young, G. K., S. Stein, P. Cole, T. Kammer, F. Graziano and F. Bank. (1996). *Evaluation and management of Highway Runoff Water Quality*, U.S. Department of Transportation, Federal Highway Administration, Publication No. FHWA-PD-96-032.
- Zhang, L., Seagren, E.A, Davis, A.P., and Karns, J.S. (2011). Long-Term Sustainability of Escherichia Coli Removal in Conventional Bioretention Media. *J. Environ Eng.*, 137(8), 669-677.

APPENDIX A: SMARTDRAIN™ PERFORMANCE CHARACTERISTICS TEST

Appendix A.1: Example Calculation Showing Biofilter Facility Hydraulics and Design of Dewatering Facilities.

The design parameters used for this calculation are given in Tables 1 and 2.

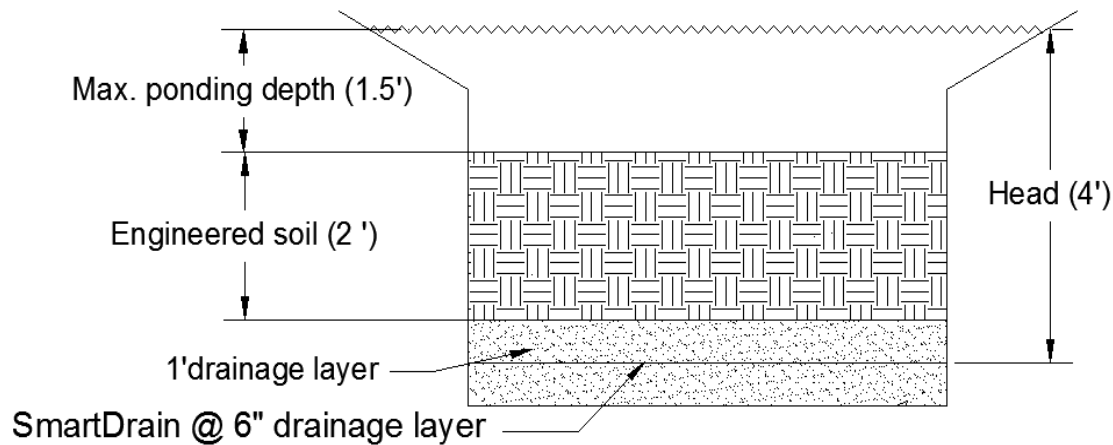


Table 1. Design parameters used for example calculations

Biofilter surface area (ft ²)	Ponding depth (ft)	Engineered media depth (ft)	Drainage layer (ft)	Porosity of media mix (%)	Porosity of drainage layer (%)
100	1.5	2	1	0.44	0.3

$$\begin{aligned}
 \text{Biofilter storage volume (ft}^3\text{)} &= \text{Ponding storage (ft}^3\text{)} + \text{Engineered media storage (ft}^3\text{)} + \\
 &\quad \text{Drainage layer storage (ft}^3\text{)} \\
 &= \text{surface area} * \text{ponding depth} + \text{surface area} * \text{engineered media depth} * \text{engineered} \\
 &\quad \text{media porosity} + 0.5 * \text{surface area} * \text{drainage layer} * \text{drainage layer porosity}
 \end{aligned}$$

Note: Smartdrain is installed at the center of drainage layer.

Required drainage rate = storage volume / drain time

$$\begin{aligned}
 \text{Storage volume} &= 100 \text{ ft}^2 * 1.5 \text{ ft} + 100 \text{ ft}^2 * 2 \text{ ft} * 0.44 + 100 \text{ ft}^2 * 0.5 \text{ ft} * 0.3 \\
 &= 253 \text{ ft}^3
 \end{aligned}$$

$$\text{Required drainage rate} = 253 \text{ ft}^3 / (24 \text{ hr} * 3600 \text{ s/hr}) = 0.003 \text{ cfs}$$

Design of Dewatering Using SmartDrain

$$s = \sqrt{\frac{4 \cdot k_s (m^2 + 2 \cdot d_e \cdot m)}{q/24}}$$

Where:

- s spacing between drains (ft)
- q amount of water that the underdrain carries away (in/day),
- K_s average saturated hydraulic conductivity of the facility media (in/hr),
- d_e effective depth (ft),
- m depth of water, or head, created over the pipes (ft) (Irrigation Association, 2000).

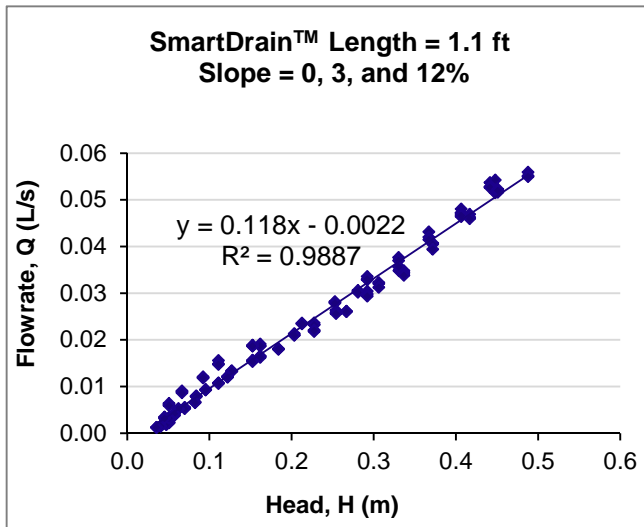
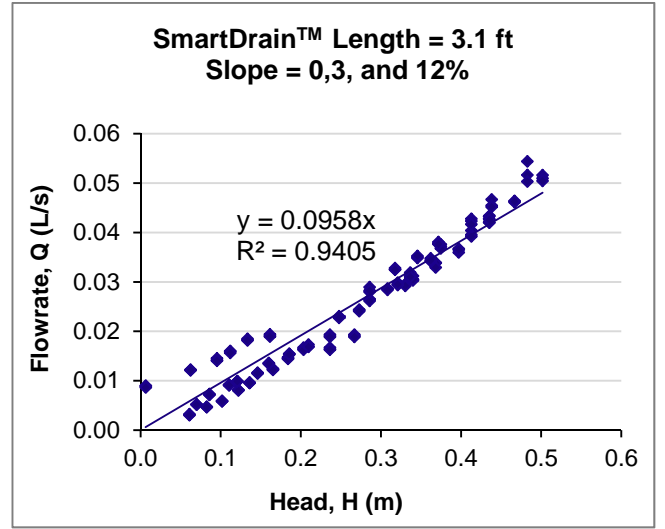
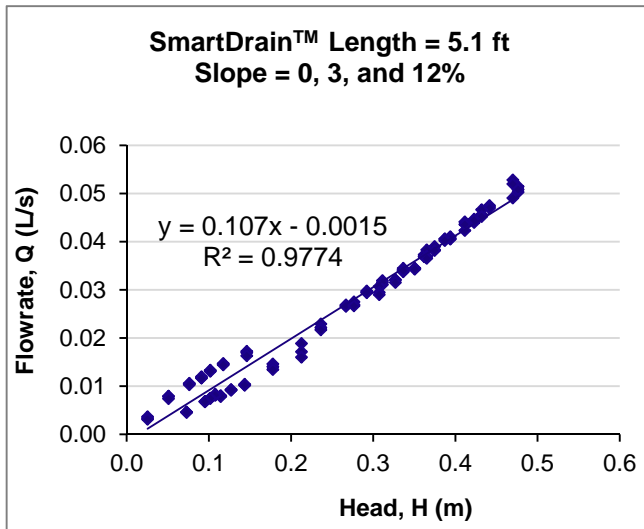
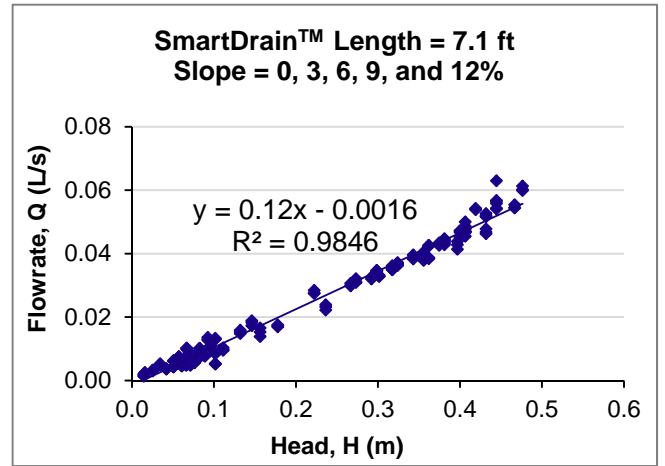
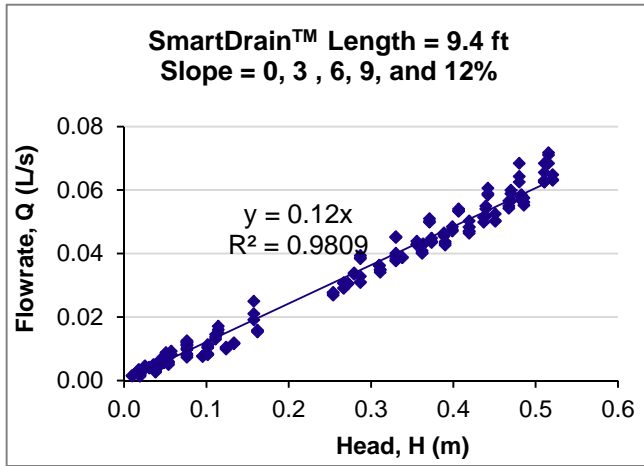
The maximum spacing between underdrains using the design parameters given in table 2:

Table 2. Design Values for Equation

d_e (ft)	m (ft)	q (in/day)	K_s (in/hr)
0.5	0.5	30	45

$$S = \sqrt{\frac{4 \cdot 45 \text{ in/hr} \left((0.5 \text{ ft})^2 + 2 \cdot 0.5 \text{ ft} \cdot 0.5 \text{ ft} \right)}{30 \text{ in/day} / 24}} = 10 \text{ ft}$$

Appendix A.2: Stage- discharge Relation Plots Summary for Different SmartDrain™ Lengths and Slopes

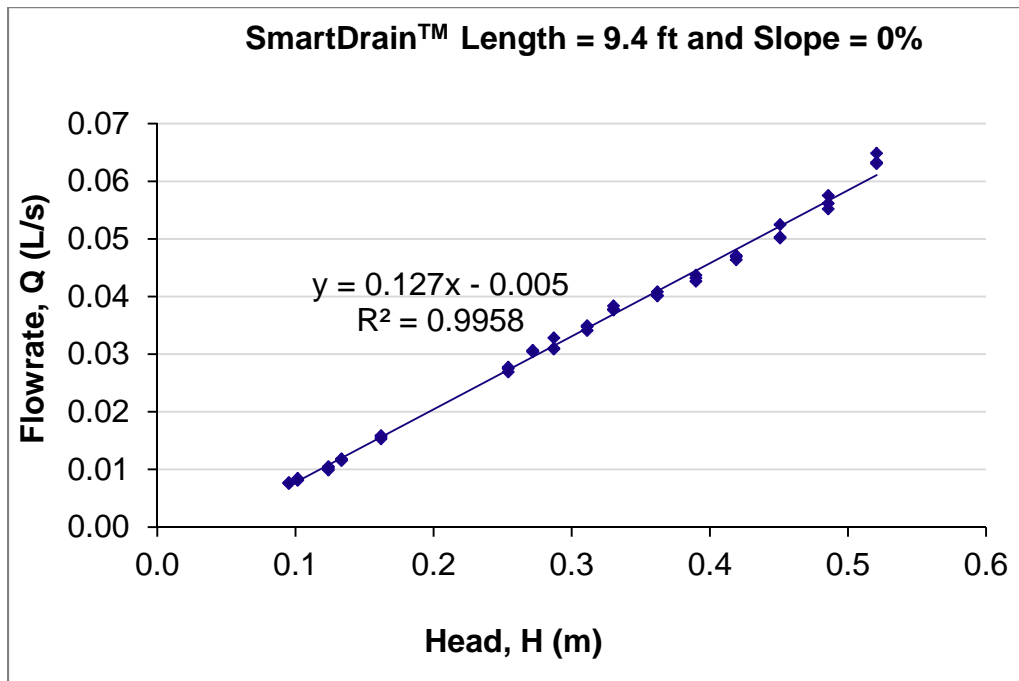


Appendix A.3: Regression Statistics on SmartDrain™ Length 9.4 ft and Slope 0%

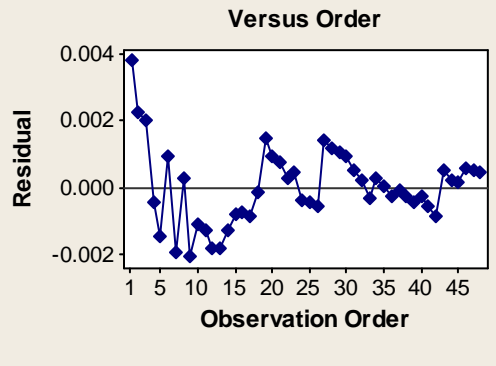
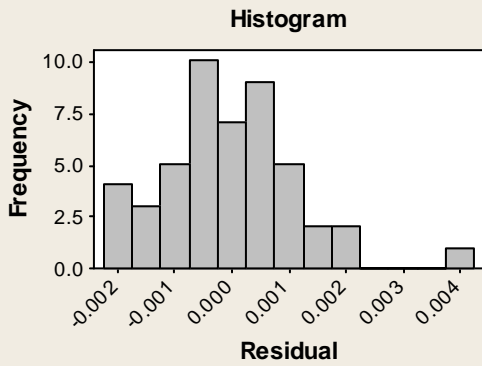
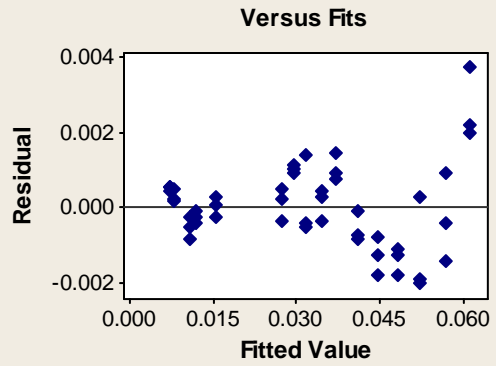
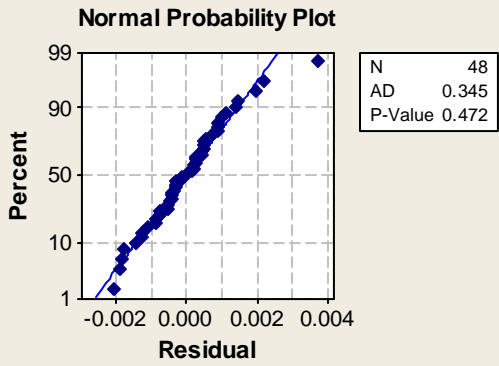
<i>Regression Statistics</i>	
Multiple R	0.998
R Square	0.996
Adjusted R Square	0.996
Standard Error	0.001
Observations	48

ANOVA					
	<i>df</i>	<i>SS</i>	<i>MS</i>	<i>F</i>	<i>Significance F</i>
Regression	1	0.0142	0.01421	10939.636	2.36333E-56
Residual	46	0.0001	1.3E-06		
Total	47	0.0143			

	<i>Coefficients</i>	<i>Standard Error</i>	<i>t Stat</i>	<i>P-value</i>	<i>Lower 95%</i>	<i>Upper 95%</i>
Intercept	-0.0049	0.0004	-12.5838	1.681E-16	-0.0057	-0.0041
Slope	0.1268	0.0012	104.5927	2.363E-56	0.1243	0.1292



Residual Plots for Flowrate, Q (L/s) (SmartDrain Length = 9.4 ft and Slope = 0%)

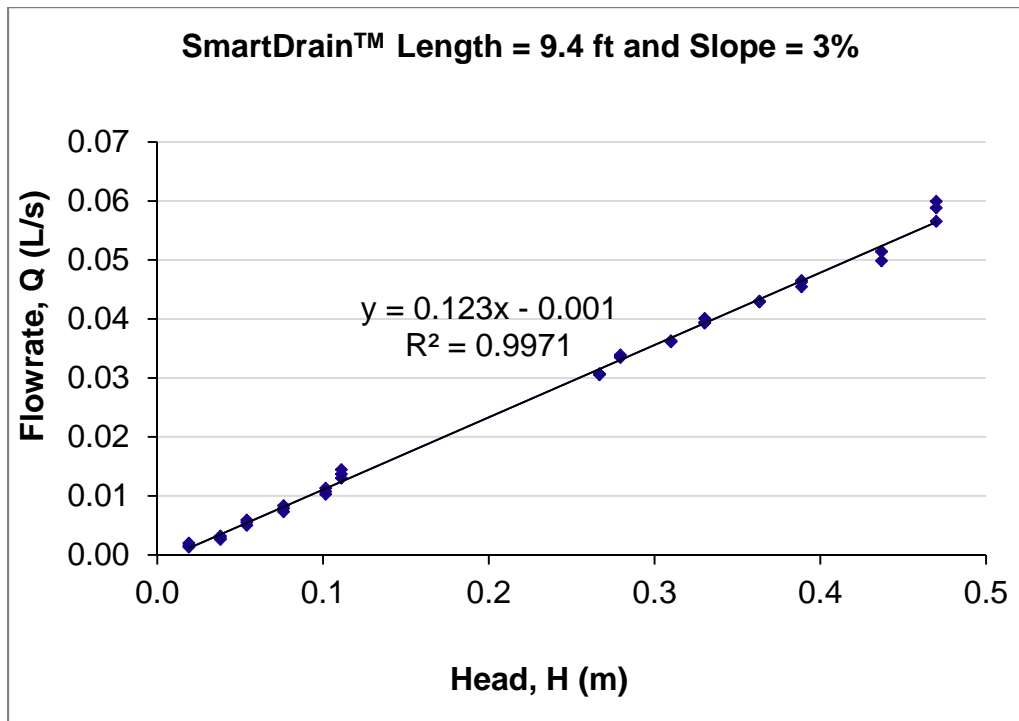


Appendix A.4: Regression Statistics on SmartDrain™ Length 9.4 ft and Slope 3%

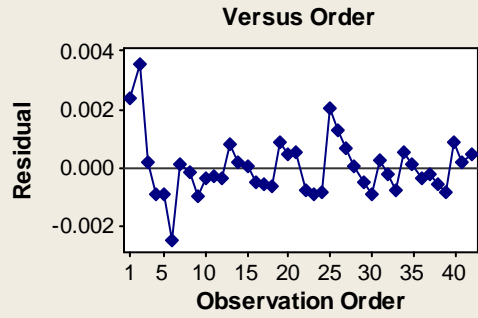
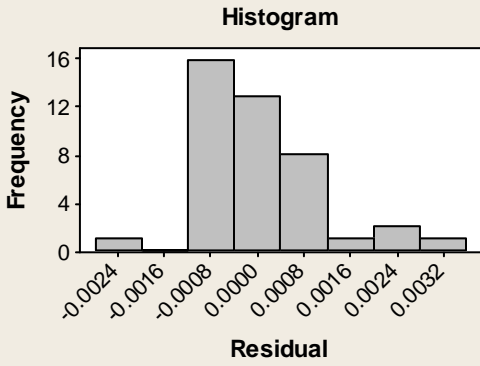
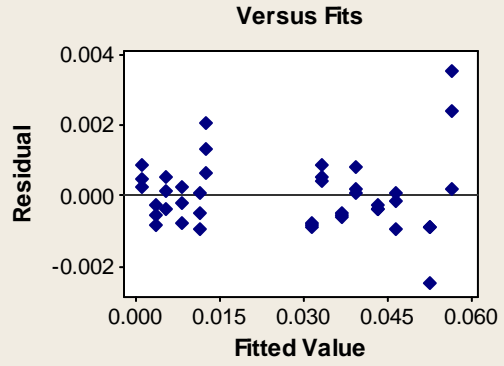
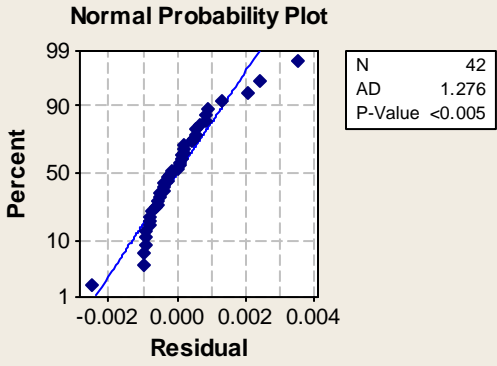
<i>Regression Statistics</i>	
Multiple R	0.999
R Square	0.997
Adjusted R Square	0.997
Standard Error	0.001
Observations	42

ANOVA					
	<i>df</i>	<i>SS</i>	<i>MS</i>	<i>F</i>	<i>Significance F</i>
Regression	1	0.0149	0.014881	13606.145	2.75298E-52
Residual	40	0.0000	1.09E-06		
Total	41	0.0149			

	<i>Coefficients</i>	<i>Standard Error</i>	<i>t Stat</i>	<i>P-value</i>	<i>Lower 95%</i>	<i>Upper 95%</i>
Intercept	-0.0012	0.0003	-4.1318	0.0002	-0.0018	-0.0006
Slope	0.1226	0.0011	116.6454	2.753E-52	0.1205	0.1247



Residual Plots for Flowrate, Q (L/s) (SmartDrain Length = 9.4 ft and Slope = 3%)



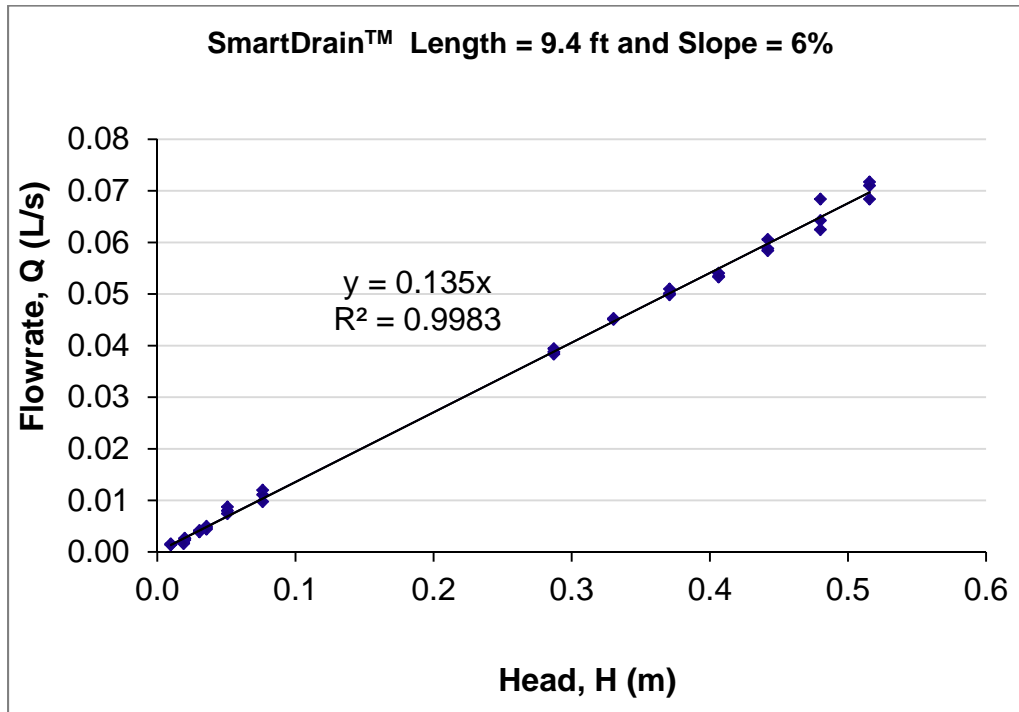
Appendix A.5: Regression Statistics on SmartDrain™ Length 9.4 ft and Slope 6%

<i>Regression Statistics</i>	
Multiple R	1.000
R Square	0.999
Adjusted R Square	0.975
Standard Error	0.001
Observations	42

ANOVA					
	<i>df</i>	<i>SS</i>	<i>MS</i>	<i>F</i>	<i>Significance F</i>
Regression	1	0.0657	0.065664	55411.662	1.82496E-64
Residual	41	0.0000	1.19E-06		
Total	42	0.0657			

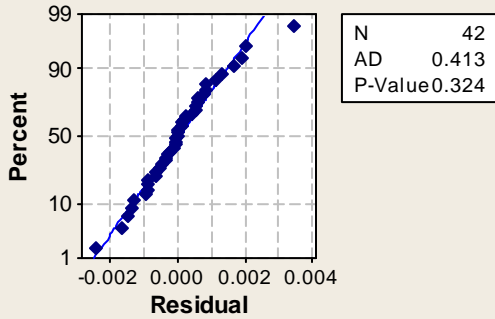
	<i>Coefficients</i>	<i>Standard Error</i>	<i>t Stat</i>	<i>P-value</i>	<i>Lower 95%</i>	<i>Upper 95%</i>
Intercept	0	#N/A	#N/A	#N/A	#N/A	#N/A
Slope	0.1352	0.0006	235.3968	8.03E-66	0.1341	0.1364

* the intercept term was determined to be not significant during the initial analyses and was therefore eliminated from the model and the regression and ANOVA reanalyzed.

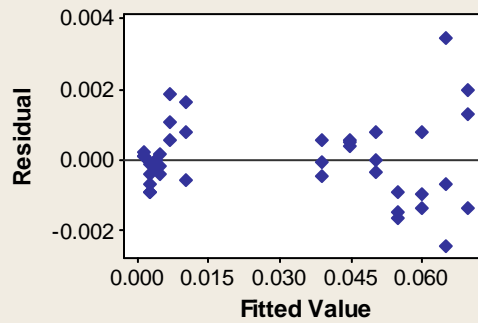


Residual Plots for Flowrate, Q (L/s) (SmartDrain Length = 9.4 ft and Slope = 6%)

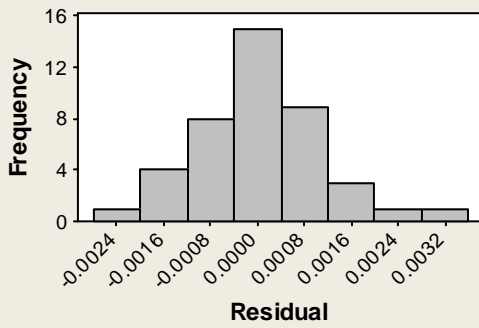
Normal Probability Plot



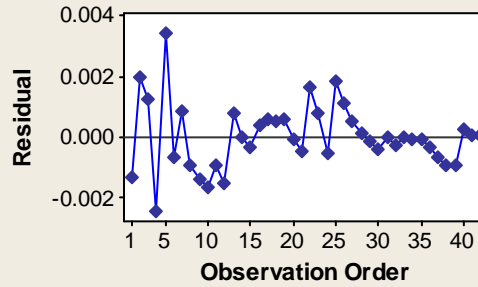
Versus Fits



Histogram



Versus Order



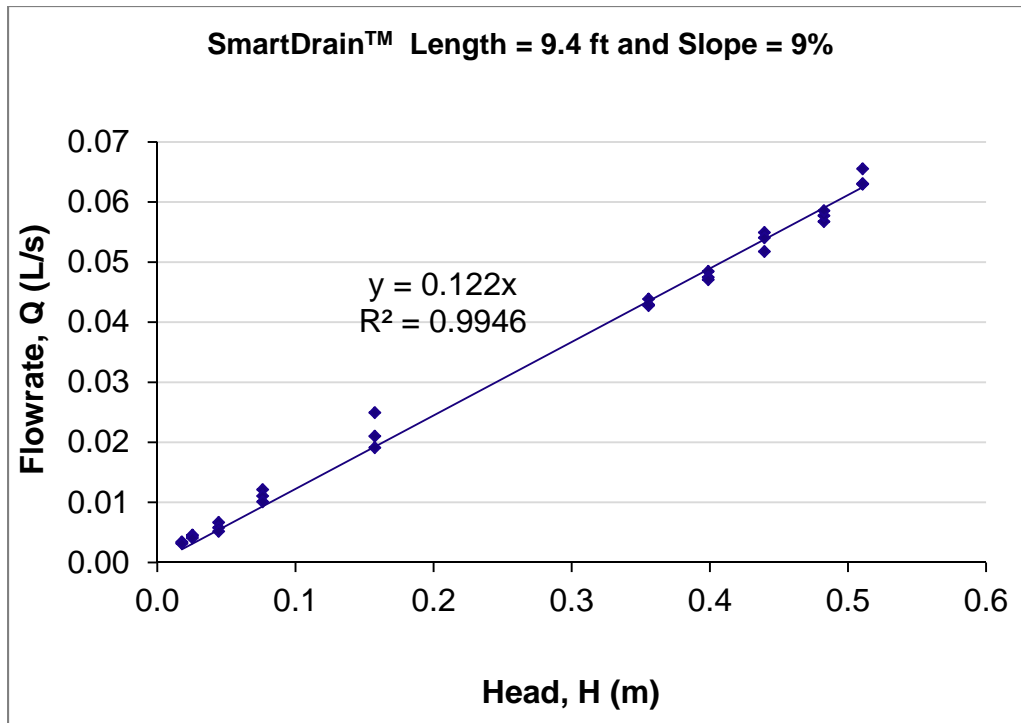
Appendix A.6: Regression Statistics on SmartDrain™ Length 9.4 ft and Slope 9%

<i>Regression Statistics</i>	
Multiple R	0.999
R Square	0.998
Adjusted R Square	0.964
Standard Error	0.002
Observations	30

ANOVA					
	<i>df</i>	<i>SS</i>	<i>MS</i>	<i>F</i>	<i>Significance F</i>
Regression	1	0.0452	0.045161	15295.978	6.91617E-40
Residual	29	0.0001	2.95E-06		
Total	30	0.0452			

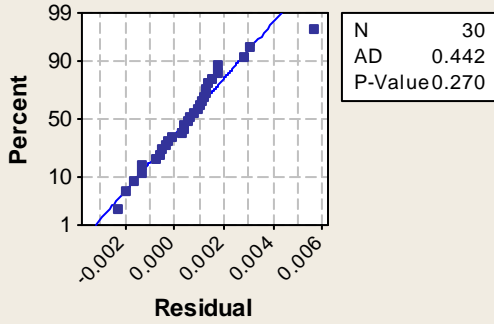
	<i>Coefficients</i>	<i>Standard Error</i>	<i>t Stat</i>	<i>P-value</i>	<i>Lower 95%</i>	<i>Upper 95%</i>
Intercept	0.0000	#N/A	#N/A	#N/A	#N/A	#N/A
Slope	0.1223	0.0010	123.6769	4.829E-41	0.1203	0.1244

* the intercept term was determined to be not significant during the initial analyses and was therefore eliminated from the model and the regression and ANOVA reanalyzed.

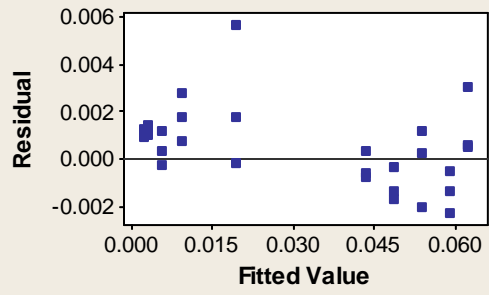


Residual Plots for Flowrate, Q (L/s) (SmartDrain length = 9.4 ft and Slope = 9%)

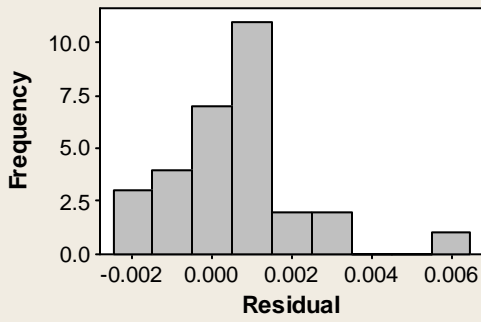
Normal Probability Plot



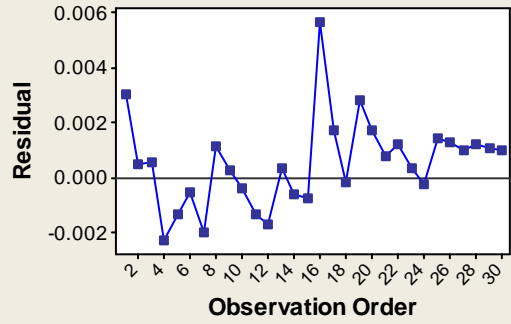
Versus Fits



Histogram



Versus Order



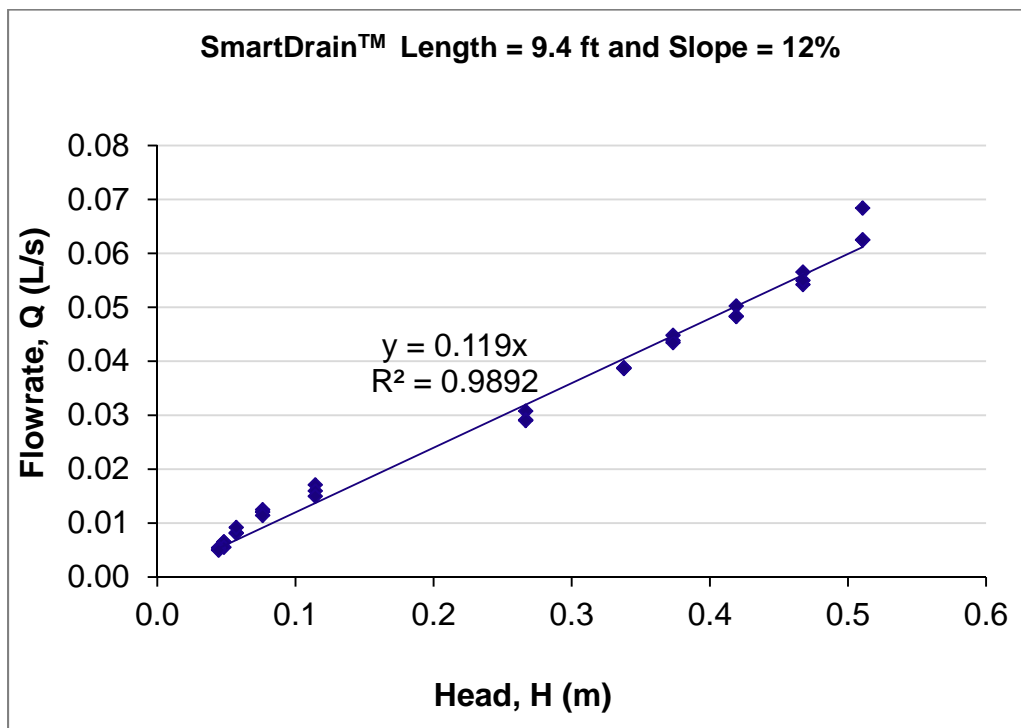
Appendix A.7: Regression Statistics on SmartDrain™ Length 9.4 ft, Slope 12% and Probability Analysis Detail

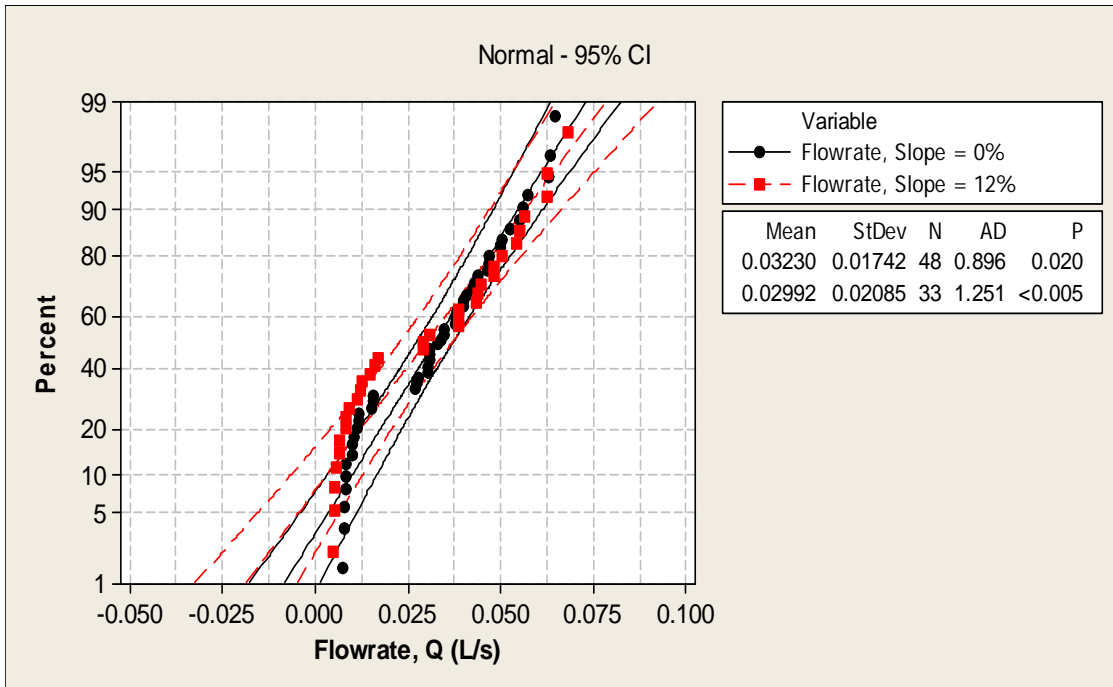
<i>Regression Statistics</i>	
Multiple R	0.998
R Square	0.997
Adjusted R Square	0.965
Standard Error	0.002
Observations	33

ANOVA					
	<i>df</i>	<i>SS</i>	<i>MS</i>	<i>F</i>	<i>Significance F</i>
Regression	1	0.0433	0.043289	9199.3612	6.43665E-40
Residual	32	0.0002	4.71E-06		
Total	33	0.0434			

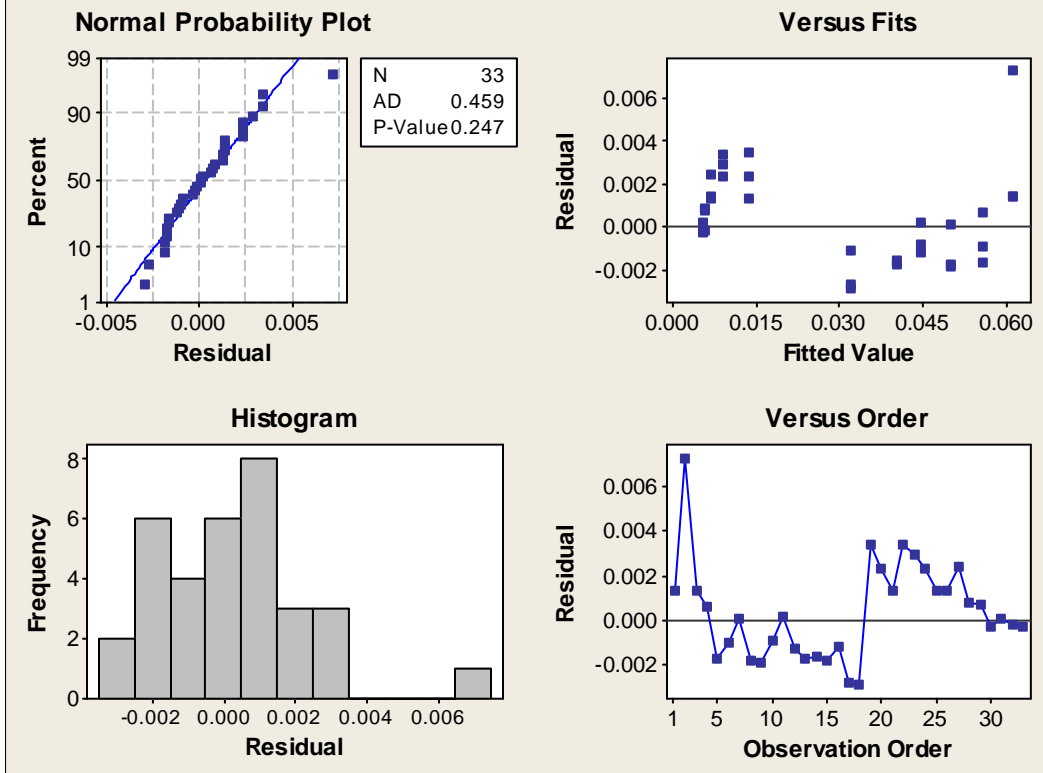
	<i>Coefficients</i>	<i>Standard Error</i>	<i>t Stat</i>	<i>P-value</i>	<i>Lower 95%</i>	<i>Upper 95%</i>
Intercept	0.0000	#N/A	#N/A	#N/A	#N/A	#N/A
Slope	0.1198	0.0012	95.9133	6.093E-41	0.1172	0.1223

* the intercept term was determined to be not significant during the initial analyses and was therefore eliminated from the model and the regression and ANOVA reanalyzed.





Residual Plots for Flowrate, Q (L/s) (SmartDrain length = 9.4 ft and Slope = 12%)

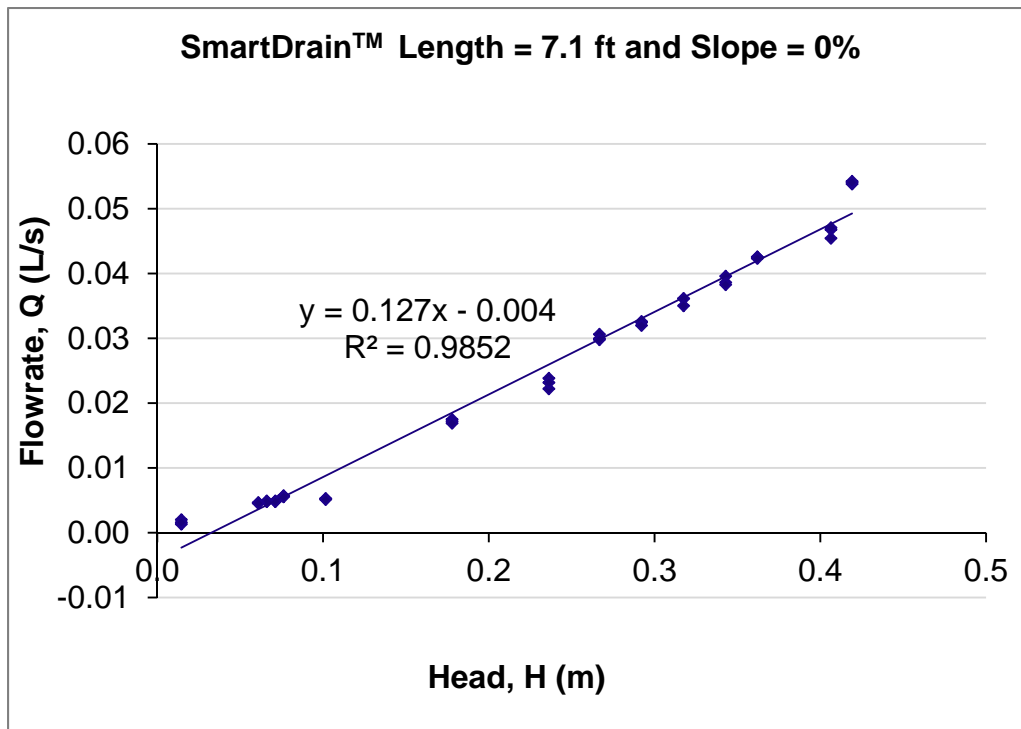


Appendix A.8: Regression Statistics on SmartDrain™ Length 7.1 ft and Slope 0%

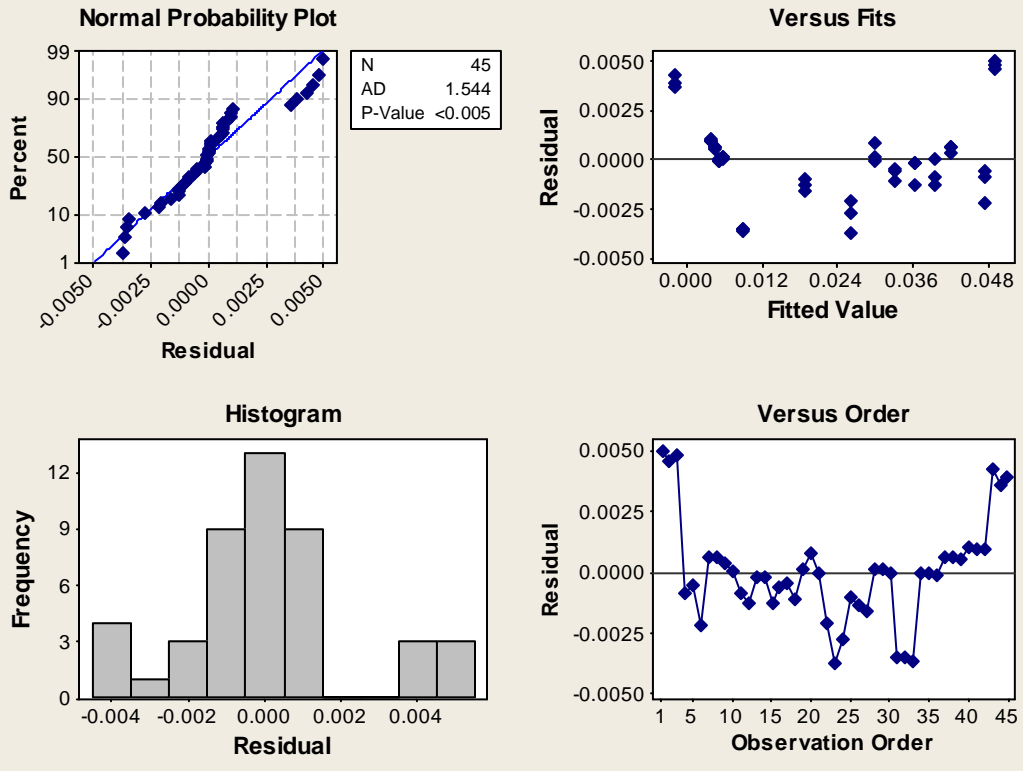
<i>Regression Statistics</i>	
Multiple R	0.993
R Square	0.985
Adjusted R Square	0.985
Standard Error	0.002
Observations	45

ANOVA					
	<i>df</i>	<i>SS</i>	<i>MS</i>	<i>F</i>	<i>Significance F</i>
Regression	1	0.0134	0.013446	2855.5071	5.86954E-41
Residual	43	0.0002	4.71E-06		
Total	44	0.0136			

	<i>Coefficients</i>	<i>Standard Error</i>	<i>t Stat</i>	<i>P-value</i>	<i>Lower 95%</i>	<i>Upper 95%</i>
Intercept	-0.0041	0.0006	-6.8397	2.197E-08	-0.0054	-0.0029
Slope	0.1274	0.0024	53.4369	5.87E-41	0.1226	0.1322



Residual Plots for Flowrate, Q (L/s) (SmartDrain Length = 7.1 ft and Slope = 0%)

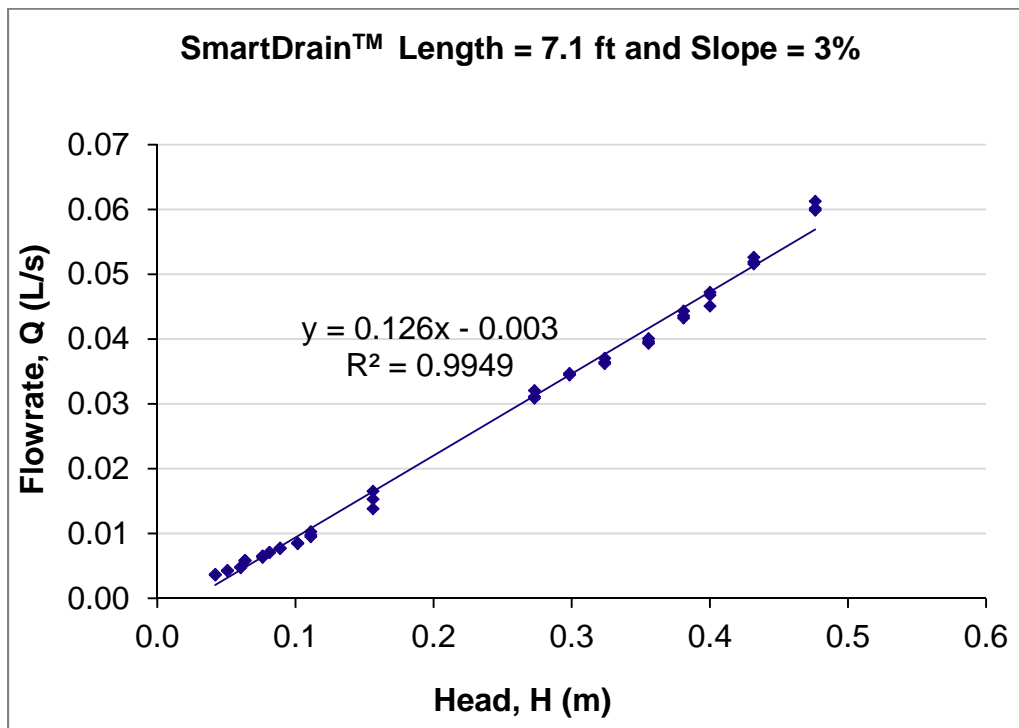


Appendix A.9: Regression Statistics on SmartDrain™ Length 7.1 ft and Slope 3%

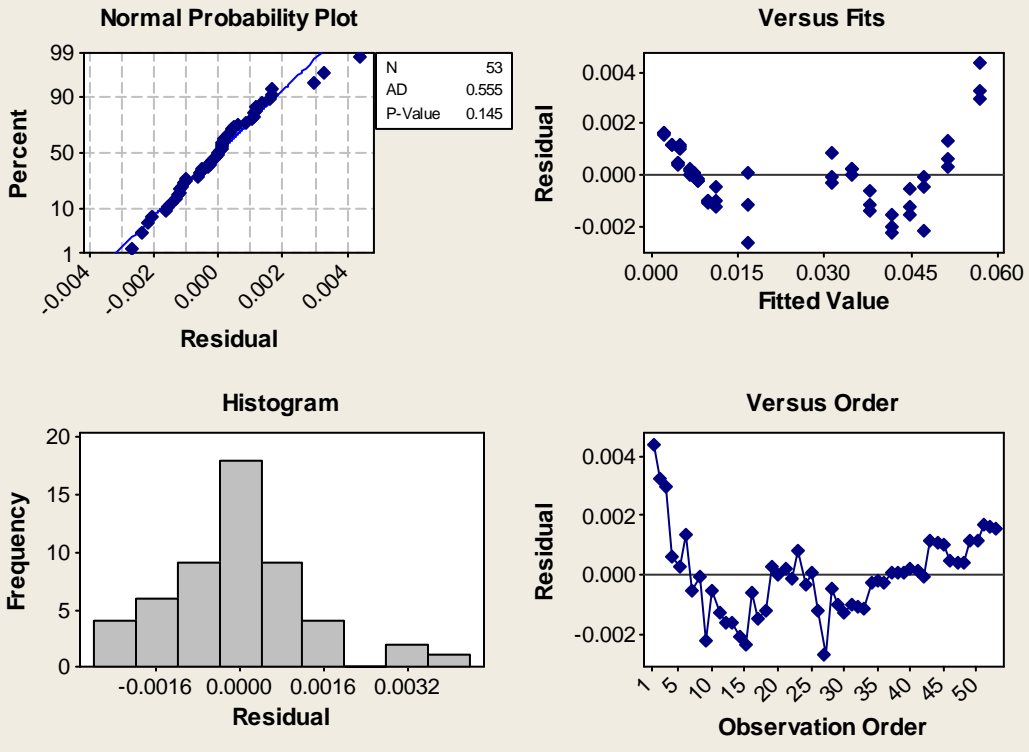
<i>Regression Statistics</i>	
Multiple R	0.997
R Square	0.995
Adjusted R Square	0.995
Standard Error	0.001
Observations	54

ANOVA					
	<i>df</i>	<i>SS</i>	<i>MS</i>	<i>F</i>	<i>Significance F</i>
Regression	1	0.0192	0.019245	10213.544	2.30711E-61
Residual	52	0.0001	1.88E-06		
Total	53	0.0193			

	<i>Coefficients</i>	<i>Standard Error</i>	<i>t Stat</i>	<i>P-value</i>	<i>Lower 95%</i>	<i>Upper 95%</i>
Intercept	-0.0032	0.0003	-10.0438	8.936E-14	-0.0039	-0.0026
Slope	0.1263	0.0012	101.0621	2.307E-61	0.1237	0.1288



Residual Plots for Flowrate, Q (L/s) (SmartDrain Length = 7.1 ft and Slope = 3%)



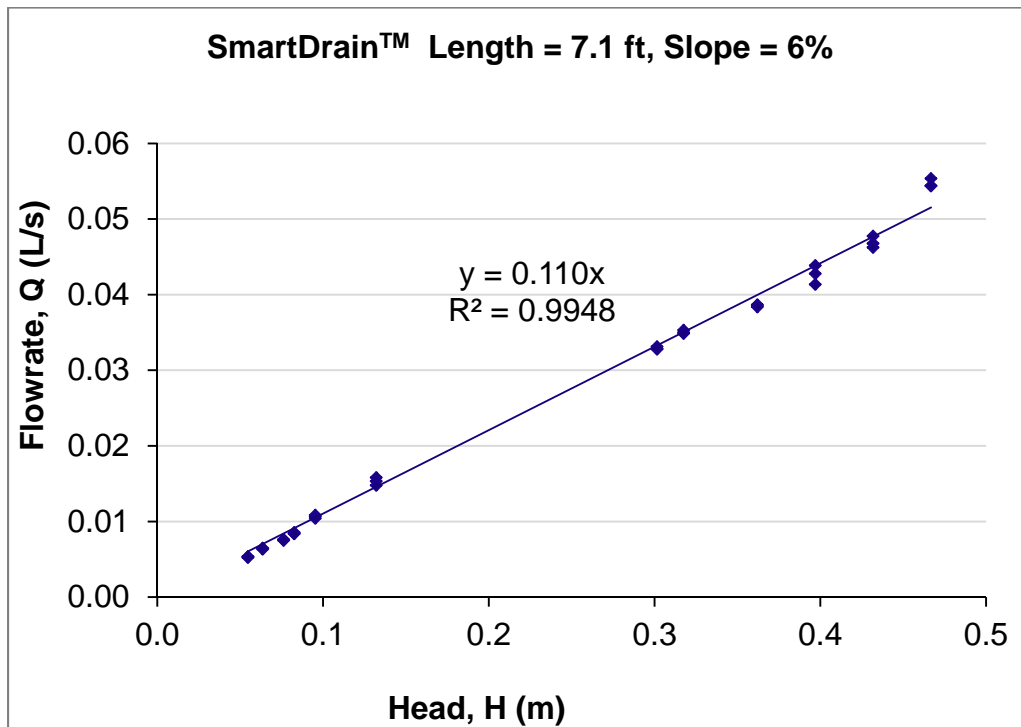
Appendix A.10: Regression Statistics on SmartDrain™ Length 7.1 ft and Slope 6%

<i>Regression Statistics</i>	
Multiple R	0.999
R Square	0.998
Adjusted R Square	0.970
Standard Error	0.001
Observations	36

ANOVA					
	<i>df</i>	<i>SS</i>	<i>MS</i>	<i>F</i>	<i>Significance F</i>
Regression	1	0.0340	0.034033	21085.396	4.45548E-49
Residual	35	0.0001	1.61E-06		
Total	36	0.0341			

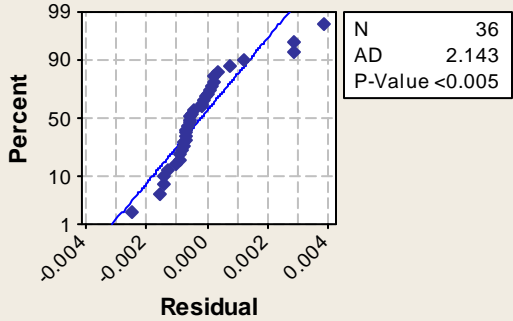
	<i>Coefficients</i>	<i>Standard Error</i>	<i>t Stat</i>	<i>P-value</i>	<i>Lower 95%</i>	<i>Upper 95%</i>
Intercept	0.0000	#N/A	#N/A	#N/A	#N/A	#N/A
Slope	0.1104	0.0008	145.2081	2.924E-50	0.1089	0.1119

* the intercept term was determined to be not significant during the initial analyses and was therefore eliminated from the model and the regression and ANOVA reanalyzed.

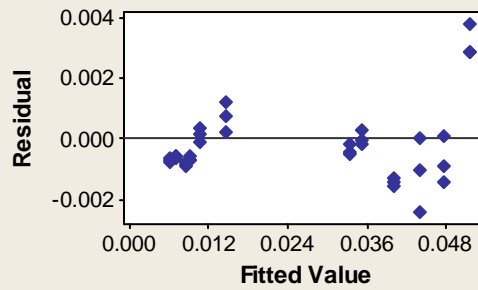


Residual Plots for Flowrate, Q (L/s) (SmartDrain length = 7.1 ft and Slope = 6%)

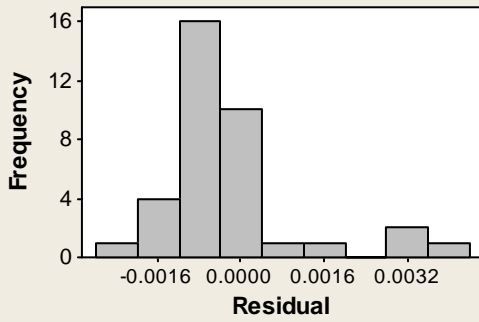
Normal Probability Plot



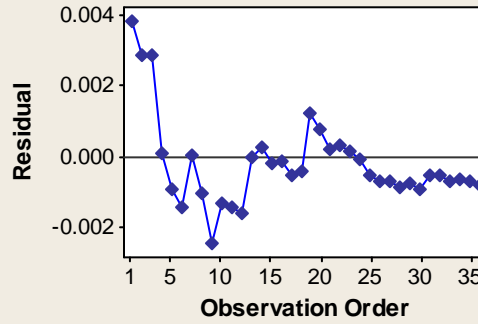
Versus Fits



Histogram



Versus Order



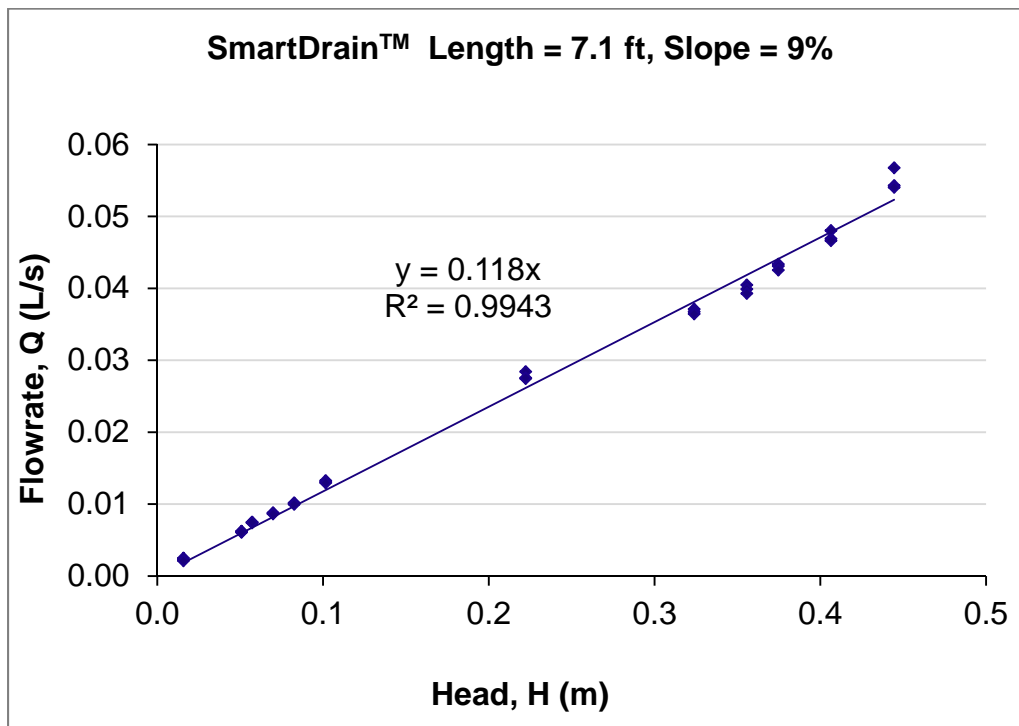
Appendix A.11: Regression Statistics on SmartDrain™ Length 7.1 ft and Slope 9%

<i>Regression Statistics</i>	
Multiple R	0.999
R Square	0.998
Adjusted R Square	0.969
Standard Error	0.001
Observations	36

ANOVA					
	<i>df</i>	<i>SS</i>	<i>MS</i>	<i>F</i>	<i>Significance F</i>
Regression	1	0.0338	0.033755	17651.186	9.10291E-48
Residual	35	0.0001	1.91E-06		
Total	36	0.0338			

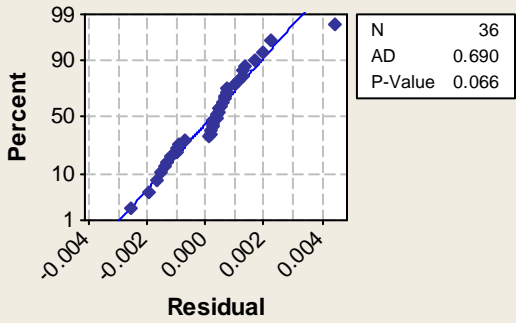
	<i>Coefficients</i>	<i>Standard Error</i>	<i>t Stat</i>	<i>P-value</i>	<i>Lower 95%</i>	<i>Upper 95%</i>
Intercept	0.0000	#N/A	#N/A	#N/A	#N/A	#N/A
Slope	0.1177	0.0009	132.8578	6.528E-49	0.1159	0.1195

* the intercept term was determined to be not significant during the initial analyses and was therefore eliminated from the model and the regression and ANOVA reanalyzed.

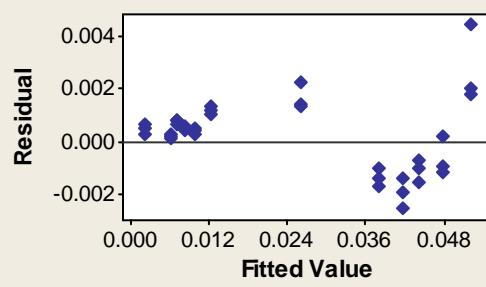


Residual Plots for Flowrate, Q (L/s) (SmartDreain Length = 7.1 ft and Slope = 9%)

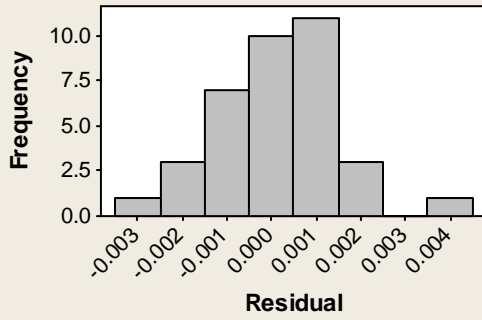
Normal Probability Plot



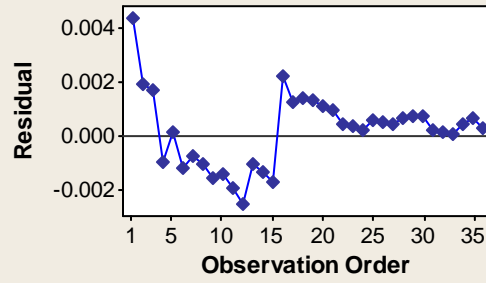
Versus Fits



Histogram



Versus Order



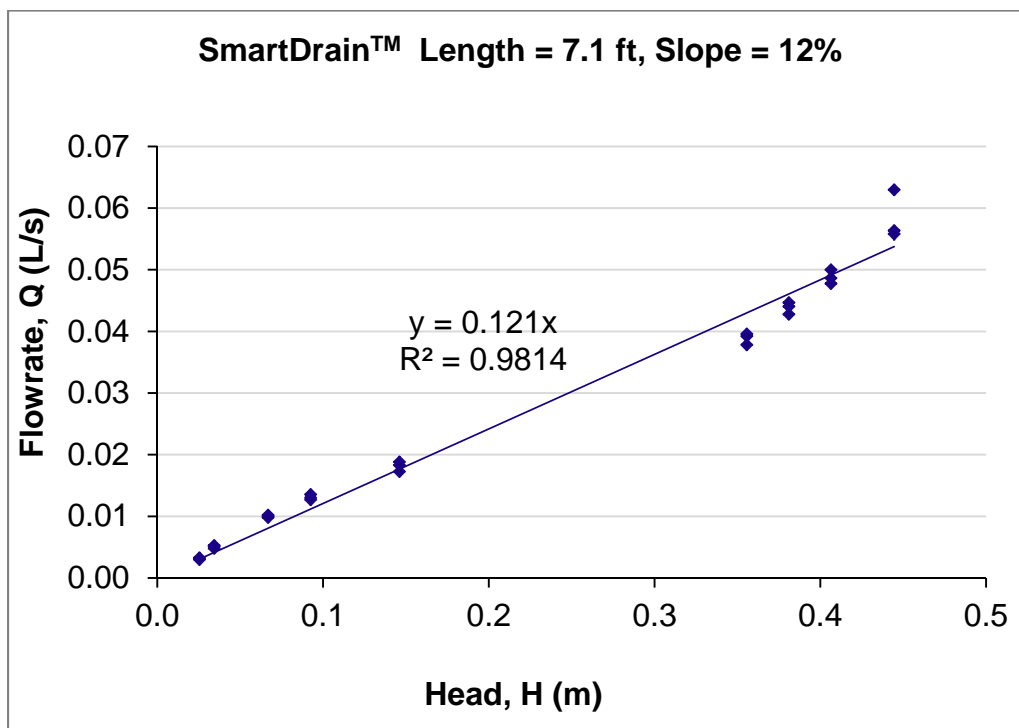
Appendix A.12: Regression Statistics on SmartDrain™ Length 7.1 ft and Slope 12%

<i>Regression Statistics</i>	
Multiple R	0.997
R Square	0.993
Adjusted R Square	0.955
Standard Error	0.003
Observations	27

ANOVA					
	<i>df</i>	<i>SS</i>	<i>MS</i>	<i>F</i>	<i>Significance F</i>
Regression	1	0.0294	0.02942	3900.4952	5.62966E-29
Residual	26	0.0002	7.54E-06		
Total	27	0.0296			

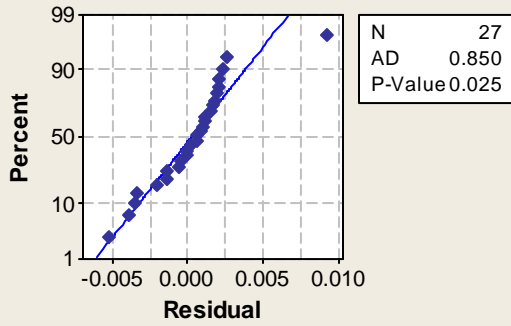
	<i>Coefficients</i>	<i>Standard Error</i>	<i>t Stat</i>	<i>P-value</i>	<i>Lower 95%</i>	<i>Upper 95%</i>
Intercept	0.0000	#N/A	#N/A	#N/A	#N/A	#N/A
Slope	0.1209	0.0019	62.4539	7.315E-30	0.1170	0.1249

* the intercept term was determined to be not significant during the initial analyses and was therefore eliminated from the model and the regression and ANOVA reanalyzed.

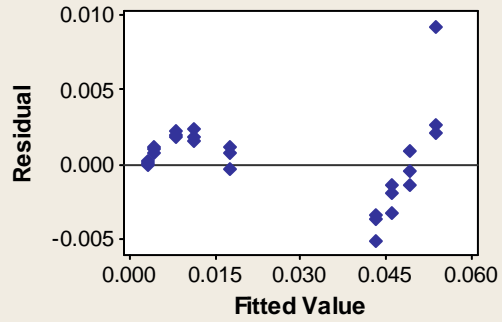


Residual Plots for Flowrate, Q (L/s) (SmartDrain Length = 7.1 ft and Slope = 12%)

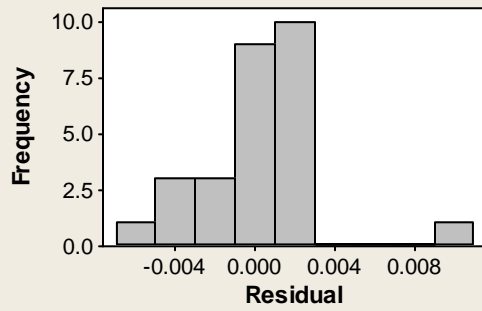
Normal Probability Plot



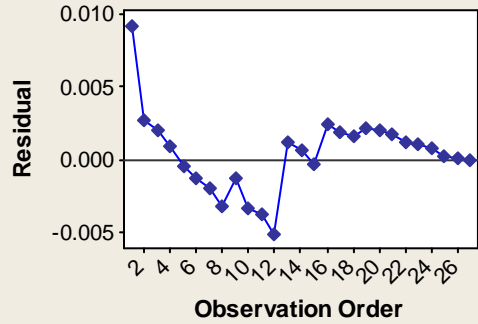
Versus Fits



Histogram



Versus Order

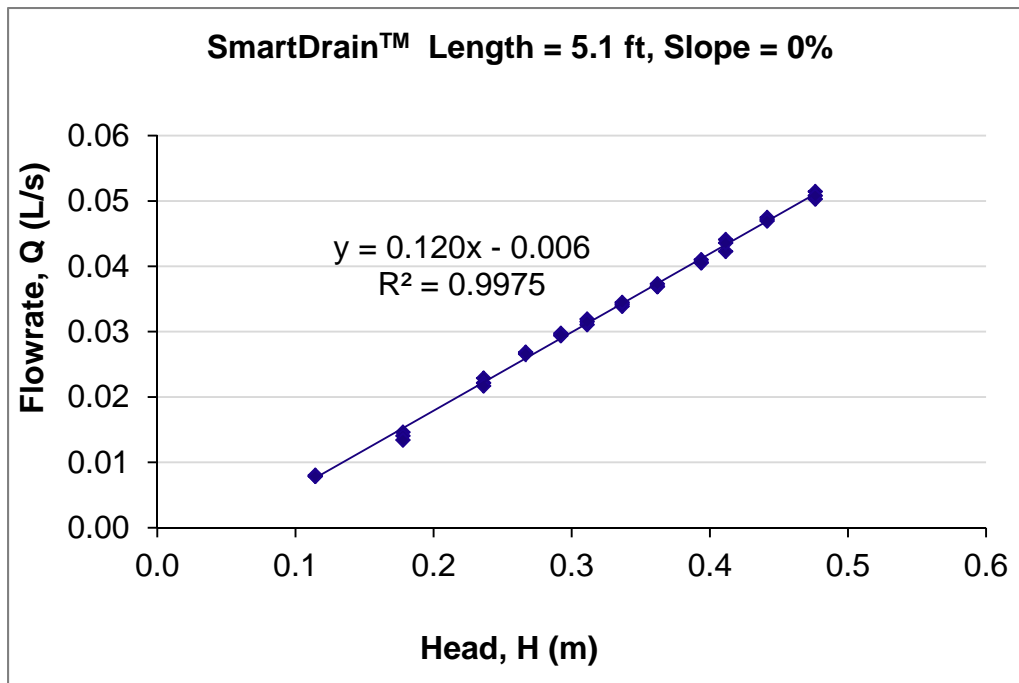


Appendix A.13: Regression Statistics on SmartDrain™ Length 5.1 ft and Slope 0%

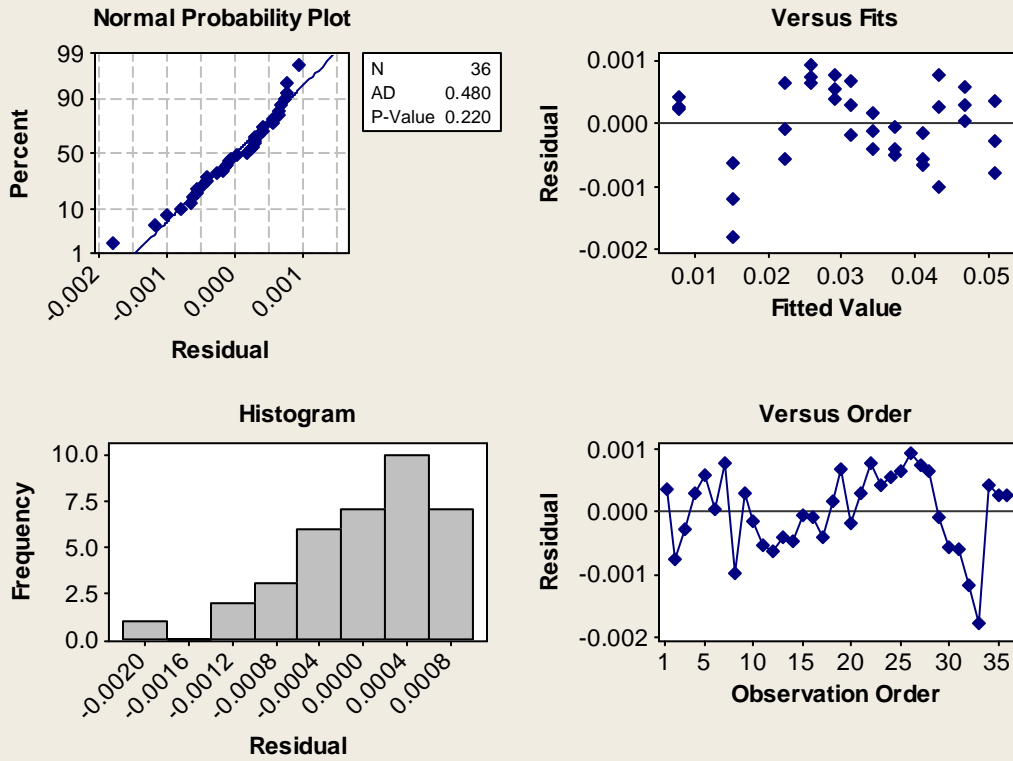
<i>Regression Statistics</i>	
Multiple R	0.999
R Square	0.997
Adjusted R Square	0.997
Standard Error	0.001
Observations	36

ANOVA					
	<i>df</i>	<i>SS</i>	<i>MS</i>	<i>F</i>	<i>Significance F</i>
Regression	1	0.0055	0.005549	13536.906	8.20943E-46
Residual	34	0.0000	4.1E-07		
Total	35	0.0056			

	<i>Coefficients</i>	<i>Standard Error</i>	<i>t Stat</i>	<i>P-value</i>	<i>Lower 95%</i>	<i>Upper 95%</i>
Intercept	-0.0061	0.0003	-17.7168	9.655E-19	-0.0068	-0.0054
Slope	0.1201	0.0010	116.3482	8.209E-46	0.1180	0.1222



Residual Plots for Flowrate, Q (L/s) (SmartDrain Length = 5.1 ft and Slope = 0%)

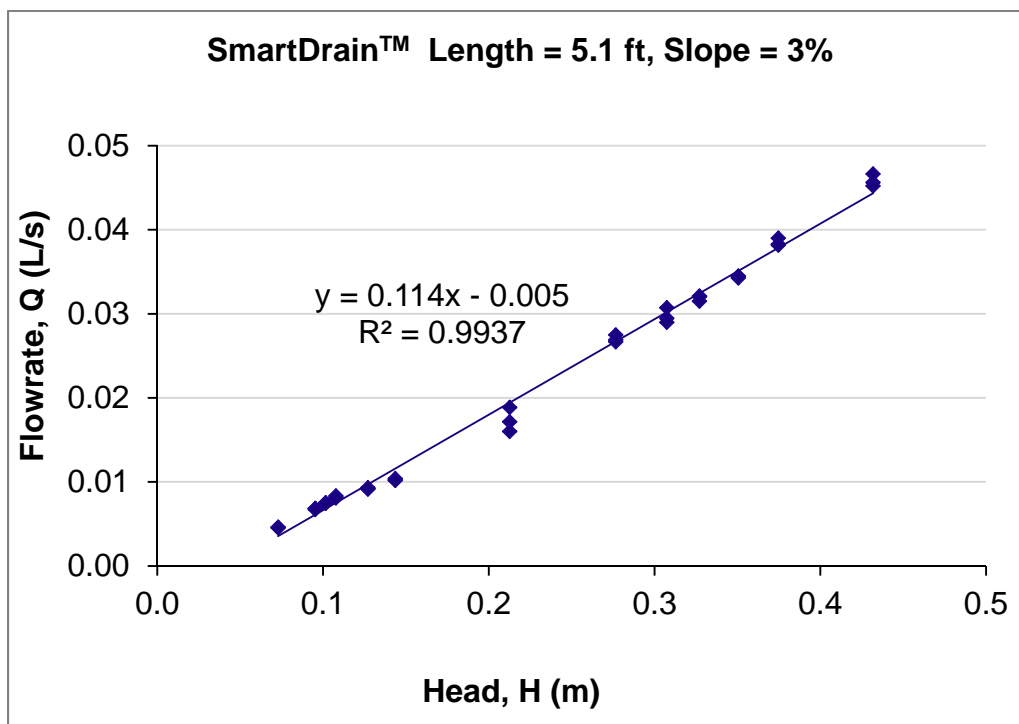


Appendix A.14: Regression Statistics on SmartDrain™ Length 5.1 ft and Slope 3%

<i>Regression Statistics</i>	
Multiple R	0.997
R Square	0.994
Adjusted R Square	0.994
Standard Error	0.001
Observations	39

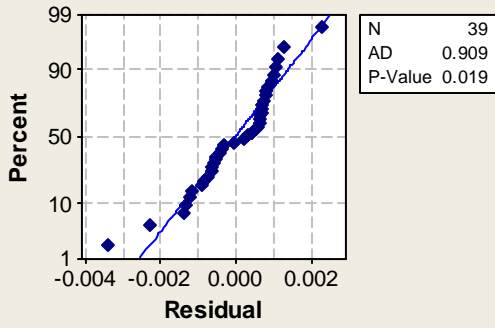
ANOVA					
	<i>df</i>	<i>SS</i>	<i>MS</i>	<i>F</i>	<i>Significance F</i>
Regression	1	0.0072	0.007214	5865.7291	2.30916E-42
Residual	37	0.0000	1.23E-06		
Total	38	0.0073			

	<i>Coefficients</i>	<i>Standard Error</i>	<i>t Stat</i>	<i>P-value</i>	<i>Lower 95%</i>	<i>Upper 95%</i>
Intercept	-0.0047	0.0004	-12.5194	7.19E-15	-0.0055	-0.0040
Slope	0.1137	0.0015	76.5880	2.309E-42	0.1107	0.1167

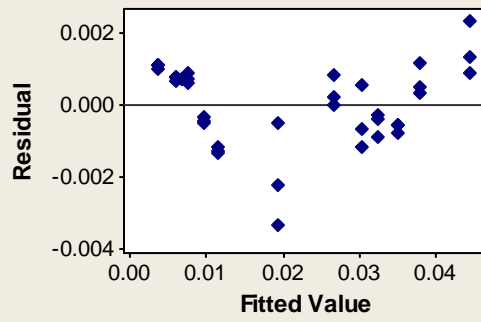


Residual Plots for Flowrate, Q (L/s) (SmartDrain Length = 5.1 ft and Slope = 3%)

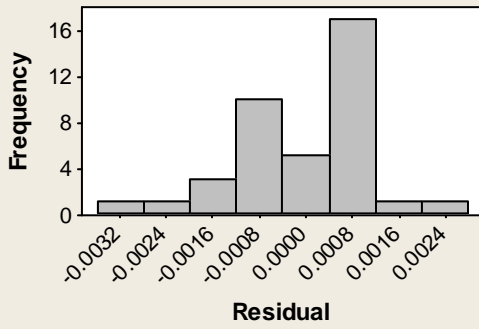
Normal Probability Plot



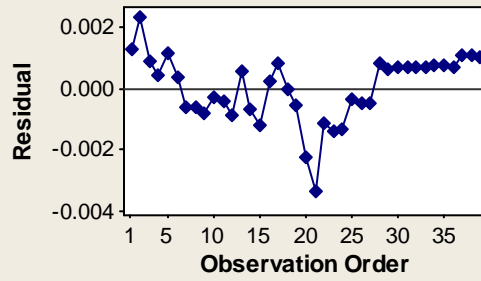
Versus Fits



Histogram



Versus Order



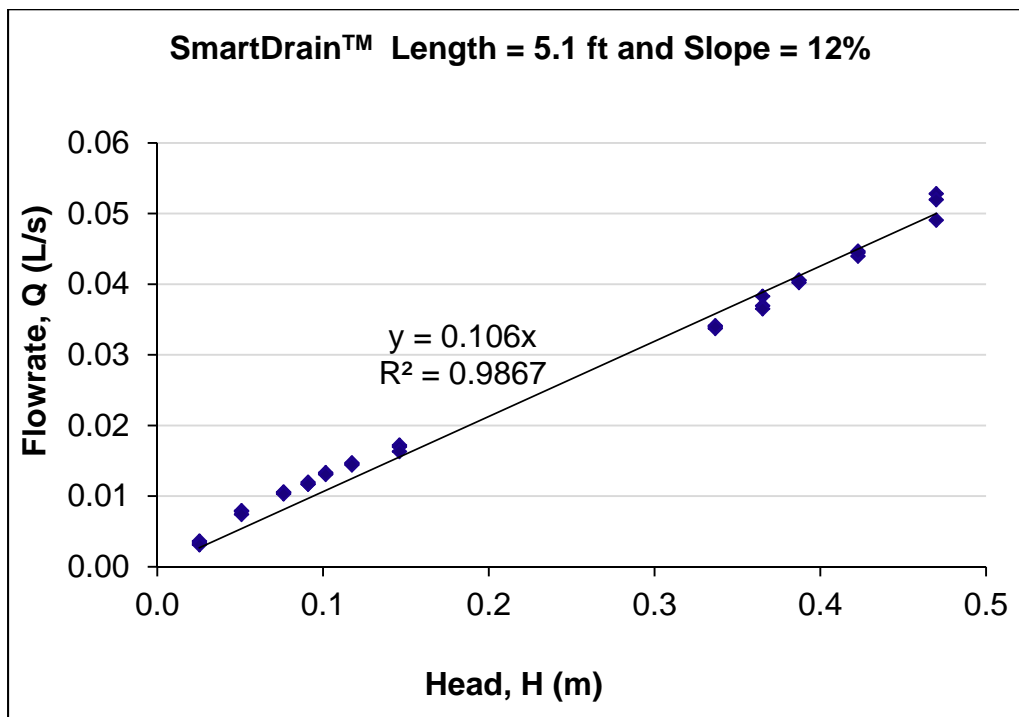
Appendix A.15: Regression Statistics on SmartDrain™ Length 5.1 ft and Slope 12%

<i>Regression Statistics</i>	
Multiple R	0.998
R Square	0.996
Adjusted R Square	0.967
Standard Error	0.002
Observations	36

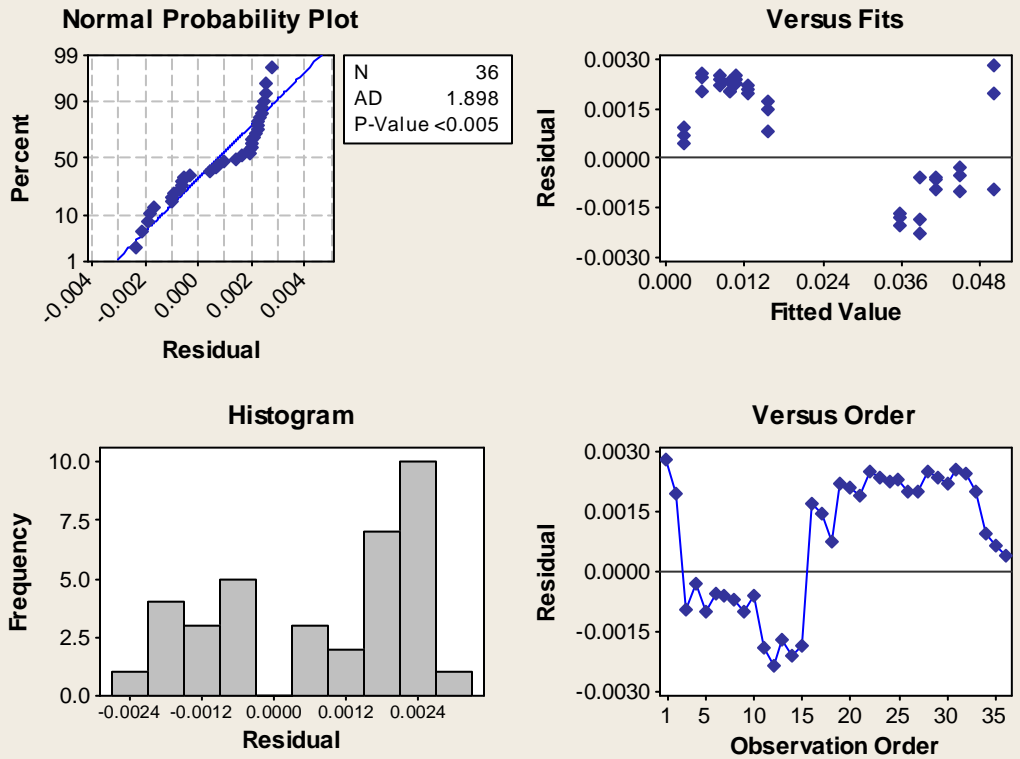
ANOVA					
	<i>df</i>	<i>SS</i>	<i>MS</i>	<i>F</i>	<i>Significance F</i>
Regression	1	0.0292	0.029182	8571.3862	1.89612E-42
Residual	35	0.0001	3.4E-06		
Total	36	0.0293			

	<i>Coefficients</i>	<i>Standard Error</i>	<i>t Stat</i>	<i>P-value</i>	<i>Lower 95%</i>	<i>Upper 95%</i>
Intercept	0.0000	#N/A	#N/A	#N/A	#N/A	#N/A
Slope	0.1064	0.0011	92.5818	1.947E-43	0.1041	0.1088

* the intercept term was determined to be not significant during the initial analyses and was therefore eliminated from the model and the regression and ANOVA reanalyzed.



Residual Plots for Flowrate, Q (L/s) (SmartDrain Length = 5.1 ft and Slope = 12%)

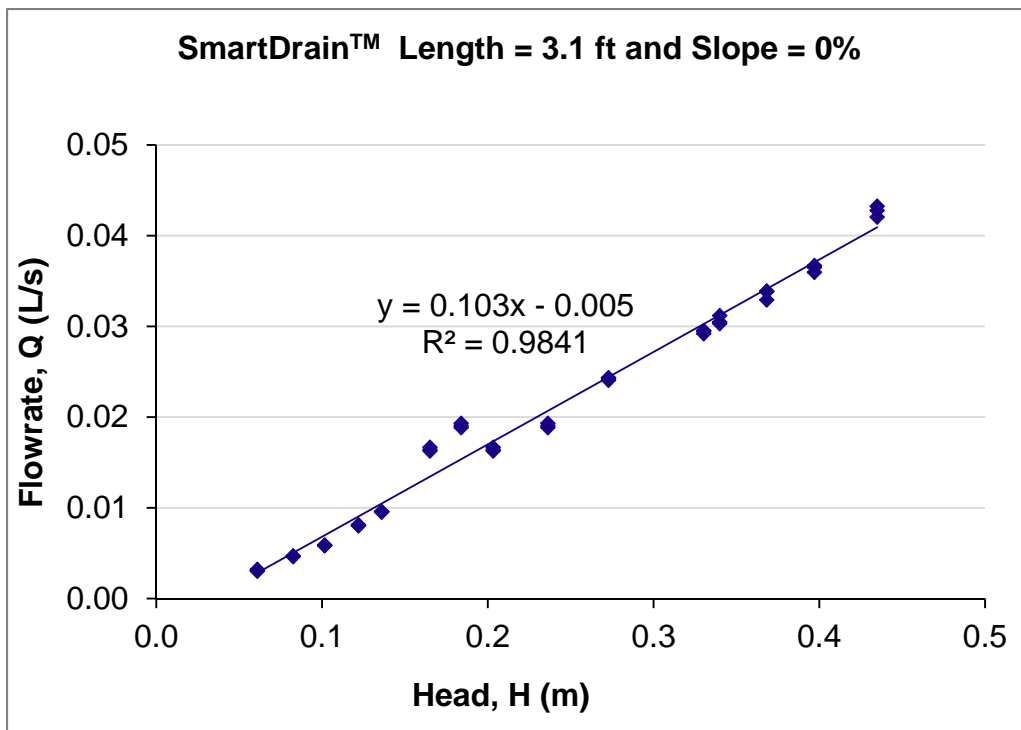


Appendix A.16: Regression Statistics on SmartDrain™ Length 3.1 ft and Slope 0%

<i>Regression Statistics</i>	
Multiple R	0.992
R Square	0.984
Adjusted R Square	0.984
Standard Error	0.001
Observations	51

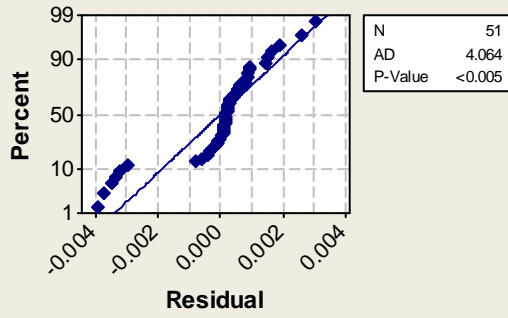
ANOVA					
	<i>df</i>	<i>SS</i>	<i>MS</i>	<i>F</i>	<i>Significance F</i>
Regression	1	0.0067	0.006685	3032.4857	9.8435E-46
Residual	49	0.0001	2.2E-06		
Total	50	0.0068			

	<i>Coefficients</i>	<i>Standard Error</i>	<i>t Stat</i>	<i>P-value</i>	<i>Lower 95%</i>	<i>Upper 95%</i>
Intercept	-0.0048	0.0005	-9.8602	3.206E-13	-0.0057	-0.0038
Slope	0.1033	0.0019	55.0680	9.844E-46	0.0996	0.1071

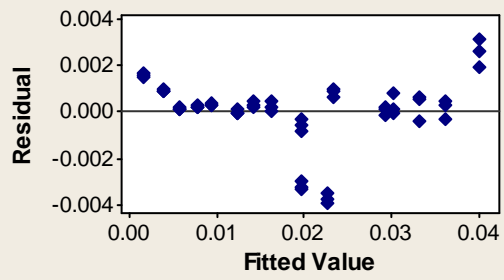


Residual Plots for Flowrate, Q (L/s) (SmartDrain Length = 3.1 ft and Slope = 0%)

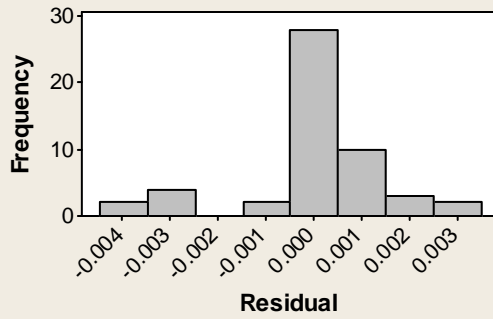
Normal Probability Plot



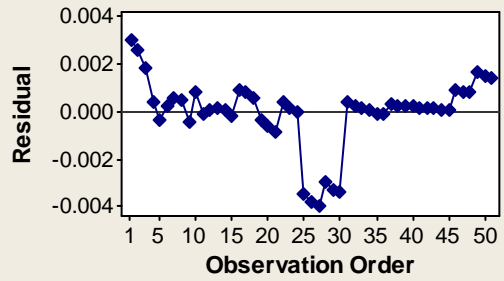
Versus Fits



Histogram



Versus Order

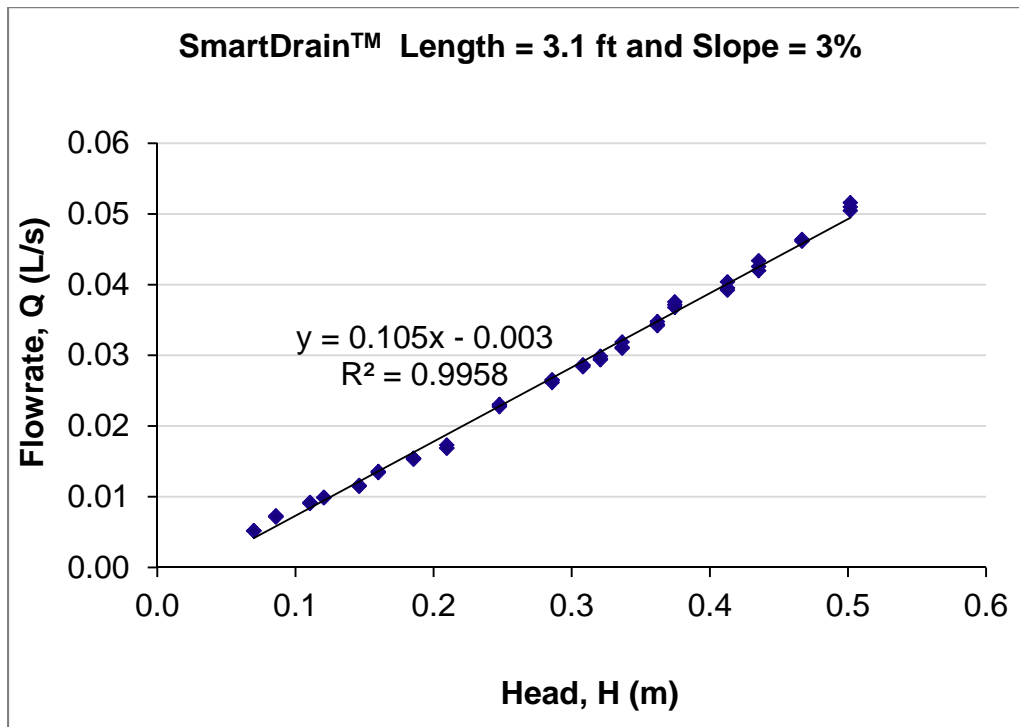


Appendix A.17: Regression Statistics on SmartDrain™ Length 3.1ft and Slope 3%

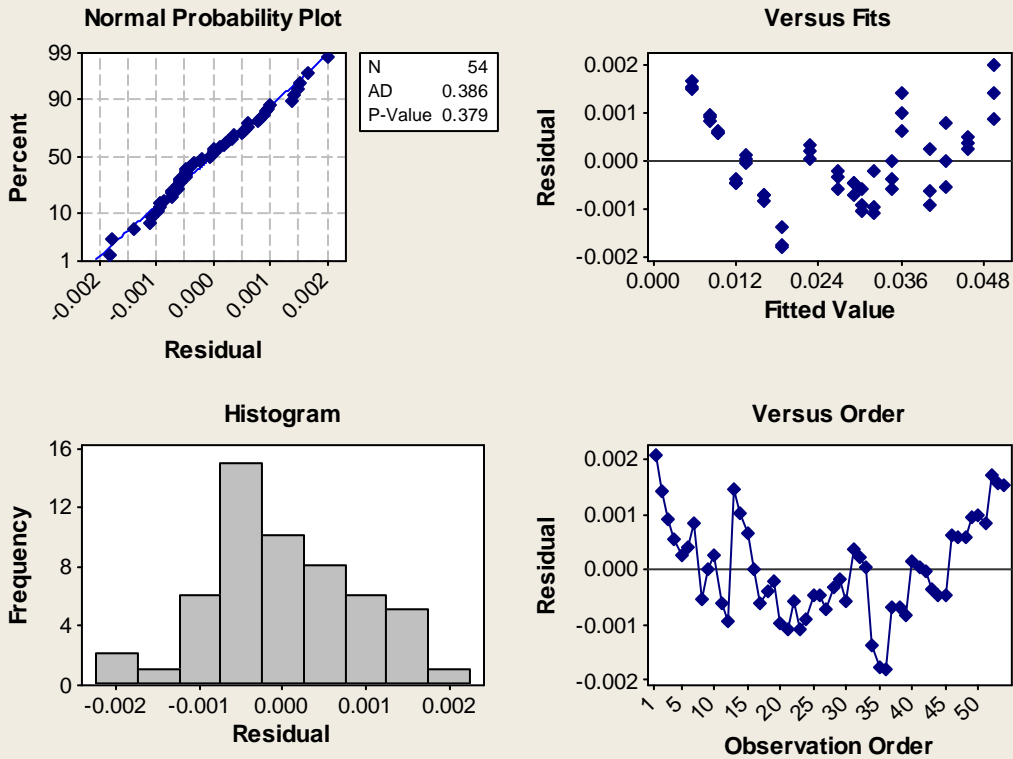
<i>Regression Statistics</i>	
Multiple R	0.998
R Square	0.996
Adjusted R Square	0.996
Standard Error	0.001
Observations	57

ANOVA					
	<i>df</i>	<i>SS</i>	<i>MS</i>	<i>F</i>	<i>Significance F</i>
Regression	1	0.0109	0.010859	13023.08	4.84933E-67
Residual	55	0.0000	8.34E-07		
Total	56	0.0109			

	<i>Coefficients</i>	<i>Standard Error</i>	<i>t Stat</i>	<i>P-value</i>	<i>Lower 95%</i>	<i>Upper 95%</i>
Intercept	-0.0032	0.0003	-11.5490	2.502E-16	-0.0037	-0.0026
Slope	0.1049	0.0009	114.1187	4.849E-67	0.1031	0.1068



Residual Plots for Flowrate, Q (L/s) (SmartDrain Length = 3.1 ft and Slope = 3%)



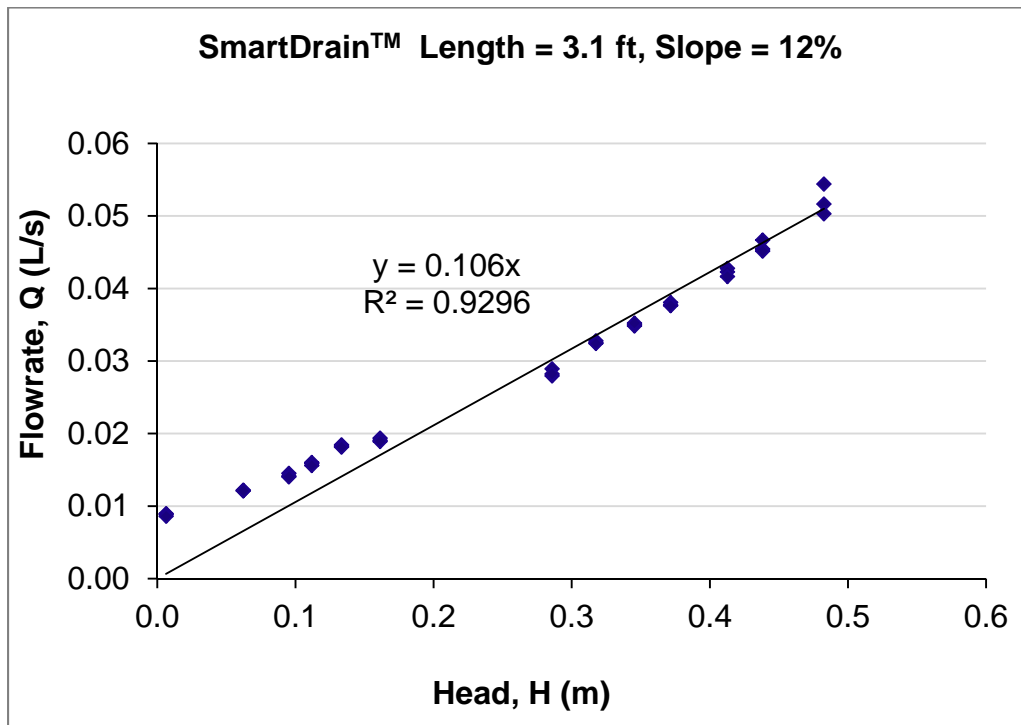
Appendix A.18: Regression Statistics on SmartDrain™ Length 3.1 ft and Slope 12%

<i>Regression Statistics</i>	
Multiple R	0.993
R Square	0.986
Adjusted R Square	0.960
Standard Error	0.004
Observations	39

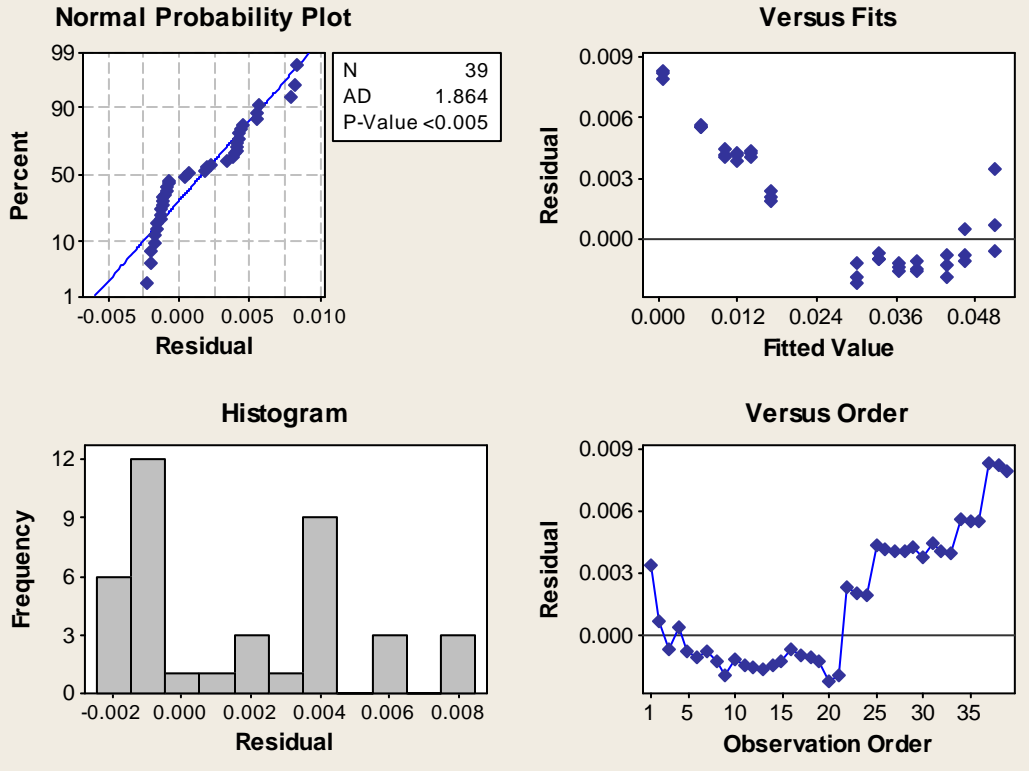
ANOVA					
	<i>df</i>	<i>SS</i>	<i>MS</i>	<i>F</i>	<i>Significance F</i>
Regression	1	0.0370	0.037005	2773.6648	2.12031E-36
Residual	38	0.0005	1.33E-05		
Total	39	0.0375			

	<i>Coefficients</i>	<i>Standard Error</i>	<i>t Stat</i>	<i>P-value</i>	<i>Lower 95%</i>	<i>Upper 95%</i>
Intercept	0.0000	#N/A	#N/A	#N/A	#N/A	#N/A
Slope	0.1057	0.0020	52.6656	3.959E-37	0.1016	0.1097

* the intercept term was determined to be not significant during the initial analyses and was therefore eliminated from the model and the regression and ANOVA reanalyzed.



Residual Plots for Flowrate, Q (L/s) (SmartDrain Length = 3.1 ft and Slope = 12%)

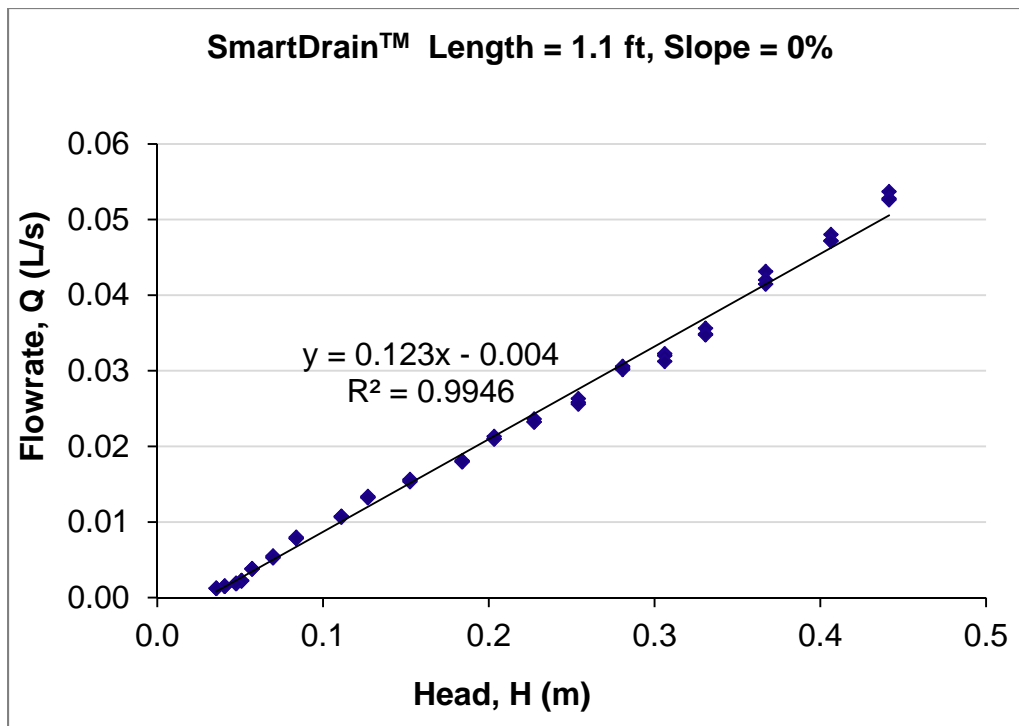


Appendix A.19: Regression Statistics on SmartDrain™ Length 1.1 ft and Slope 0%

<i>Regression Statistics</i>	
Multiple R	0.997
R Square	0.995
Adjusted R Square	0.994
Standard Error	0.001
Observations	60

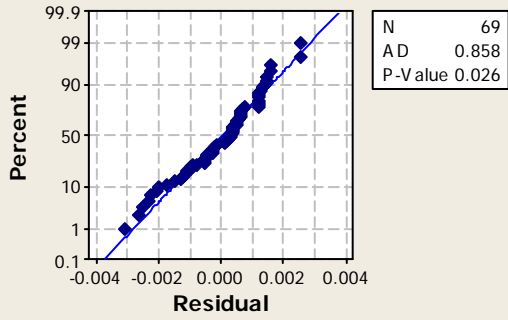
ANOVA					
	<i>df</i>	<i>SS</i>	<i>MS</i>	<i>F</i>	<i>Significance F</i>
Regression	1	0.01485	0.014852	10648.429	1.99165E-67
Residual	58	0.00008	1.39E-06		
Total	59	0.01493			

	<i>Coefficients</i>	<i>Standard Error</i>	<i>t Stat</i>	<i>P-value</i>	<i>Lower 95%</i>	<i>Upper 95%</i>
Intercept	-0.0036	0.0003	-13.10897	5.456E-19	-0.0041	-0.0030
Slope	0.1226	0.0012	103.1912	1.992E-67	0.1202	0.1250

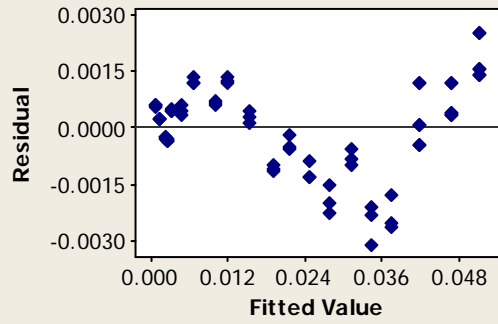


Residual Plots for Flowrate, Q (L/s) (SmartDrain Length = 1.1 ft and Slope = 0%)

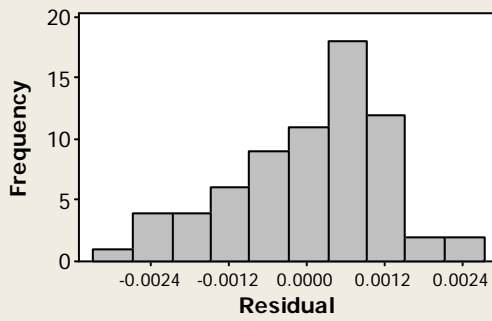
Normal Probability Plot



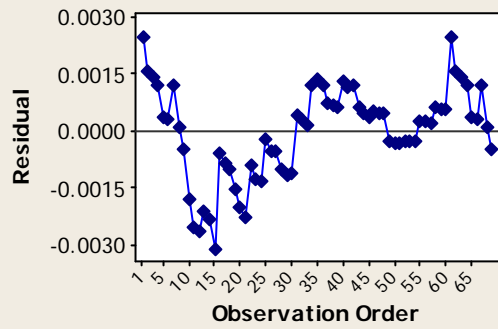
Versus Fits



Histogram



Versus Order

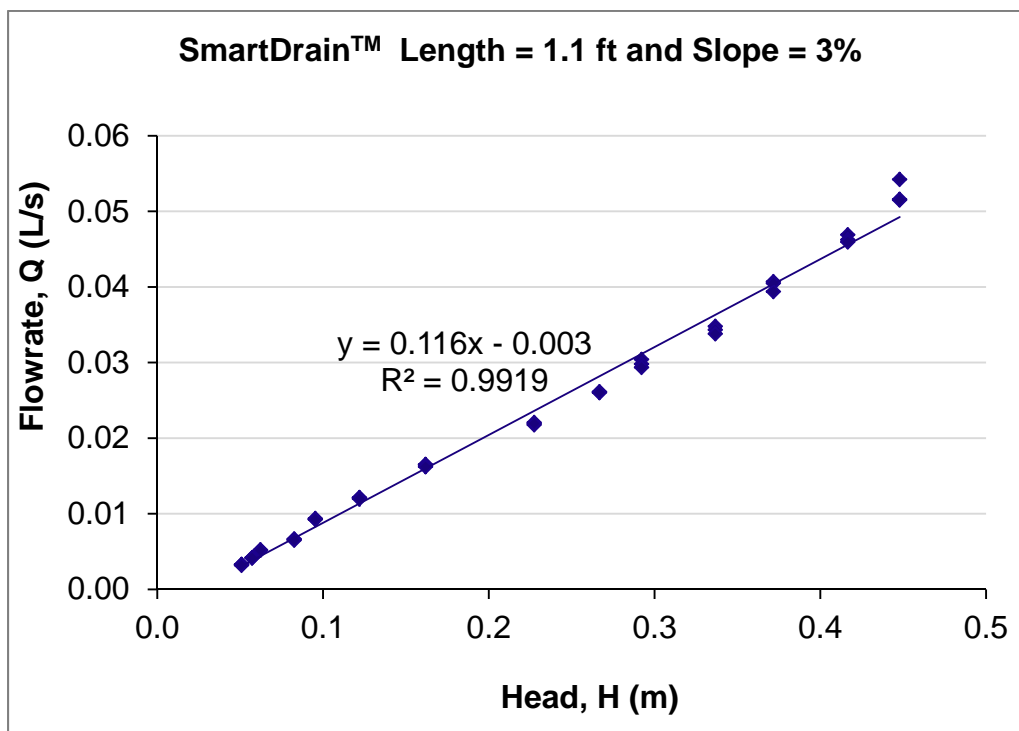


Appendix A.20: Regression Statistics on SmartDrain™ Length 1.1 ft and Slope 3%

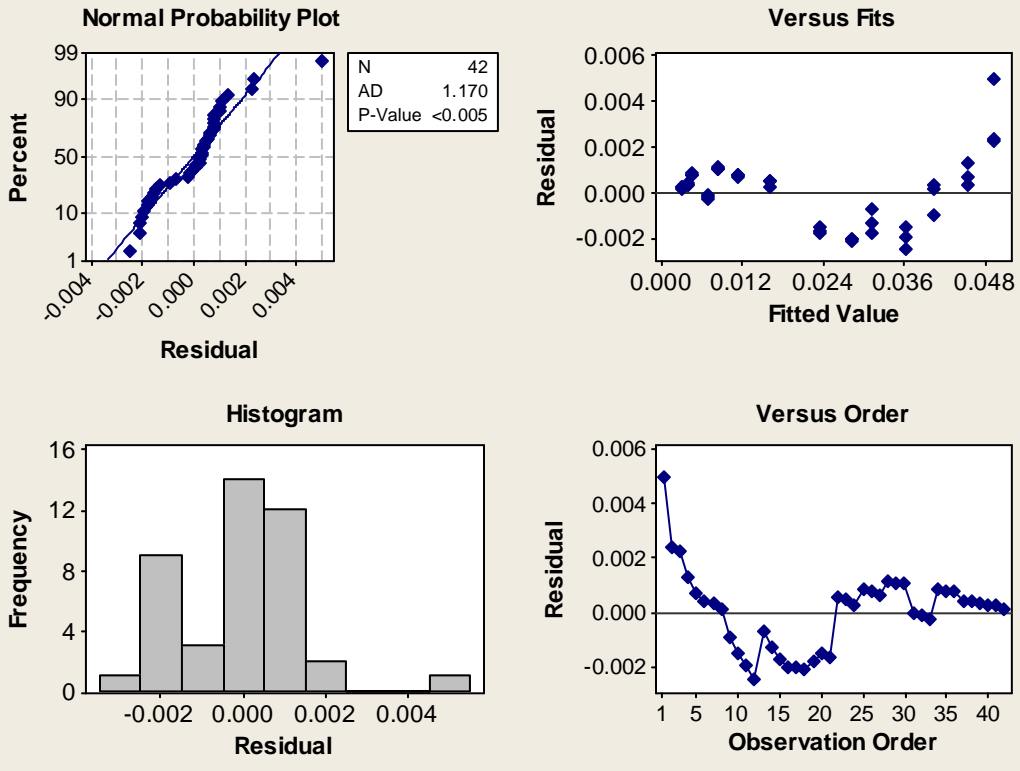
<i>Regression Statistics</i>	
Multiple R	0.996
R Square	0.992
Adjusted R Square	0.992
Standard Error	0.001
Observations	42

ANOVA					
	<i>df</i>	<i>SS</i>	<i>MS</i>	<i>F</i>	<i>Significance F</i>
Regression	1	0.01060	0.010603	4906.1542	1.80186E-43
Residual	40	0.00009	2.16E-06		
Total	41	0.01069			

	<i>Coefficients</i>	<i>Standard Error</i>	<i>t Stat</i>	<i>P-value</i>	<i>Lower 95%</i>	<i>Upper 95%</i>
Intercept	-0.0028	0.0004	-6.6938	5.018E-08	-0.0037	-0.0020
Slope	0.1163	0.0017	70.0439	1.802E-43	0.1129	0.1196



Residual Plots for Flowrate, Q (L/s) (SmartDrain Length = 1.1 ft and Slope = 3%)



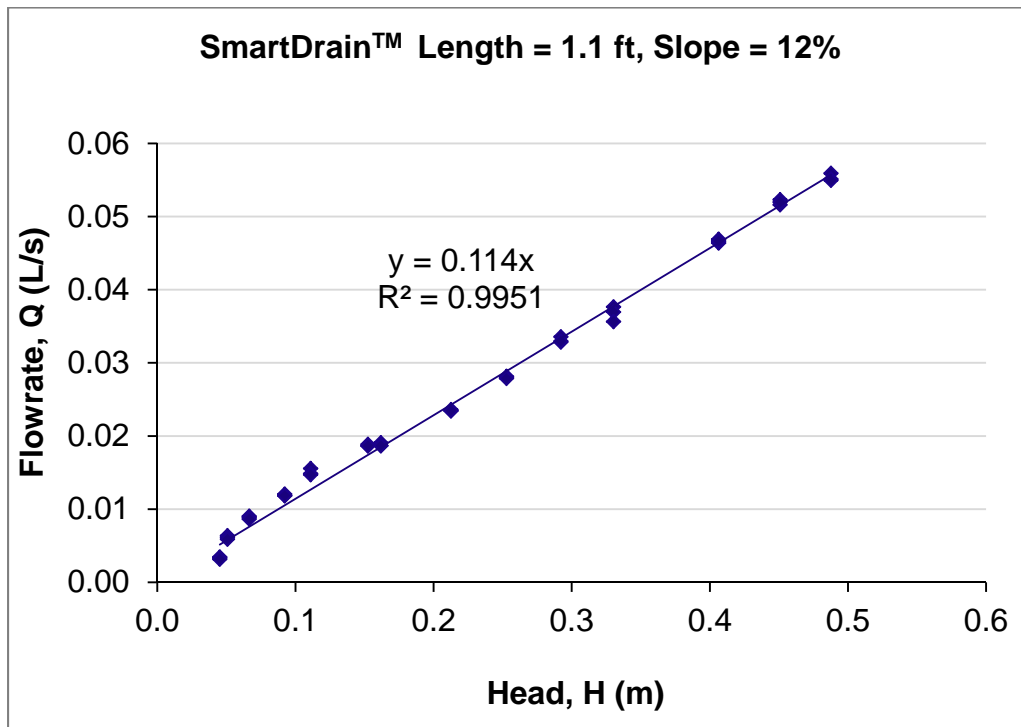
Appendix A.21: Regression Statistics on SmartDrain™ Length 1.1ft and Slope 12%

<i>Regression Statistics</i>	
Multiple R	0.999
R Square	0.999
Adjusted R Square	0.974
Standard Error	0.001
Observations	42

ANOVA					
	<i>df</i>	<i>SS</i>	<i>MS</i>	<i>F</i>	<i>Significance F</i>
Regression	1	0.0387	0.038717	28449.335	1.11183E-58
Residual	41	0.0001	1.36E-06		
Total	42	0.0388			

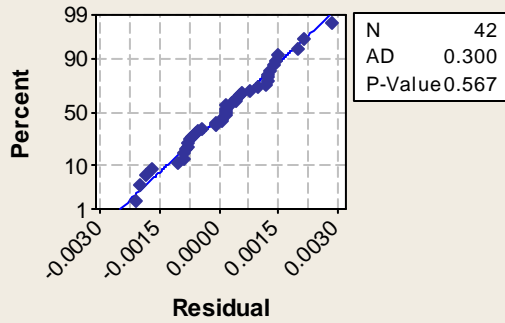
	<i>Coefficients</i>	<i>Standard Error</i>	<i>t Stat</i>	<i>P-value</i>	<i>Lower 95%</i>	<i>Upper 95%</i>
Intercept	0	#N/A	#N/A	#N/A	#N/A	#N/A
Slope	0.1142	0.0007	168.6693	6.823E-60	0.1129	0.1156

* the intercept term was determined to be not significant during the initial analyses and was therefore eliminated from the model and the regression and ANOVA reanalyzed.

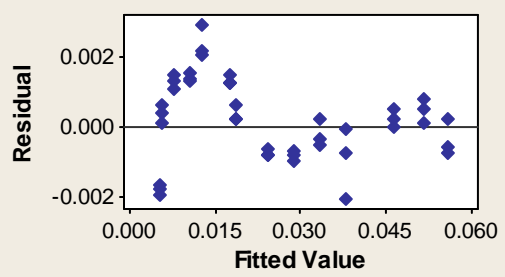


Residual Plots for Flowrate, Q (L/s) (SmartDrain Length = 1.1 ft and Slope = 12%)

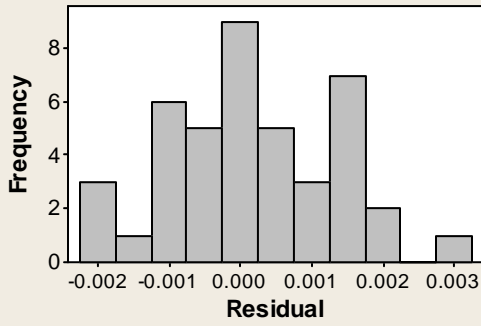
Normal Probability Plot



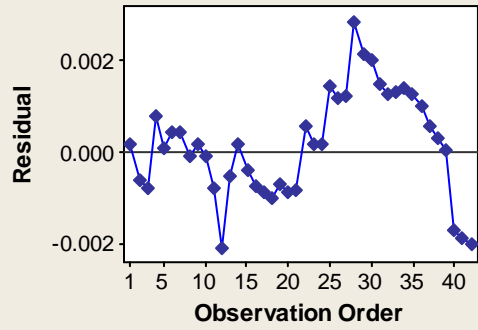
Versus Fits



Histogram



Versus Order



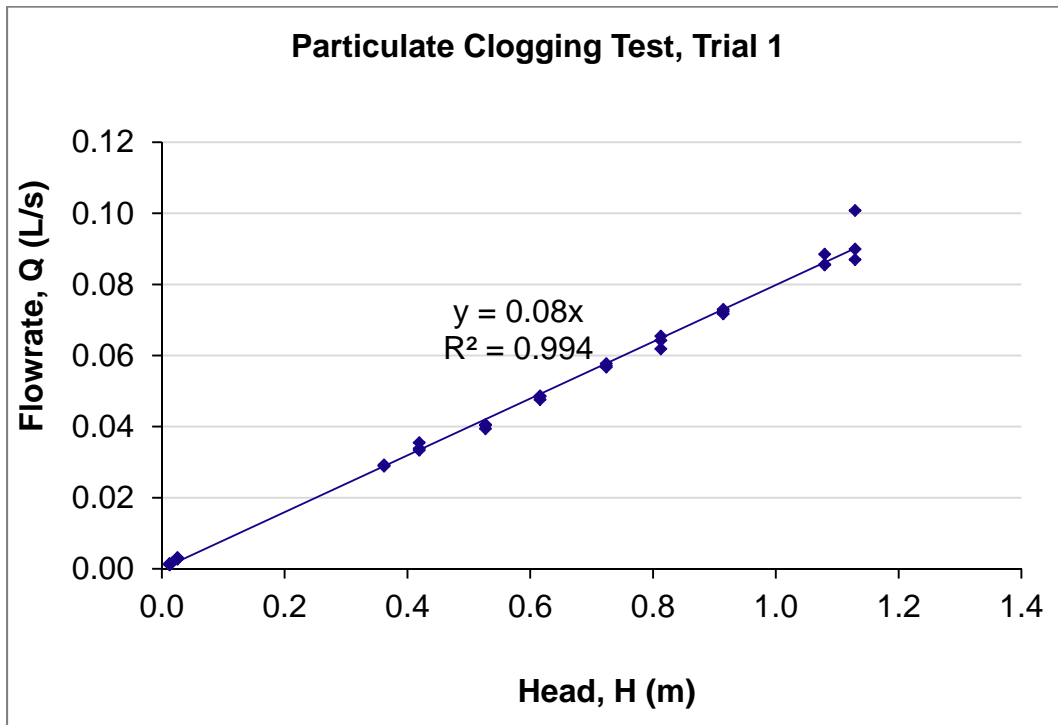
Appendix A.22: Regression Statistics on SmartDrain™ Clogging Test, Trial#1.

<i>Regression Statistics</i>	
Multiple R	0.9992
R Square	0.9984
Adjusted R Square	0.9672
Standard Error	0.0023
Observations	33

ANOVA					
	<i>df</i>	<i>SS</i>	<i>MS</i>	<i>F</i>	<i>Significance F</i>
Regression	1	0.1038	0.1038	20018.5085	3.85986E-45
Residual	32	0.0002	5.18547E-06		
Total	33	0.1040			

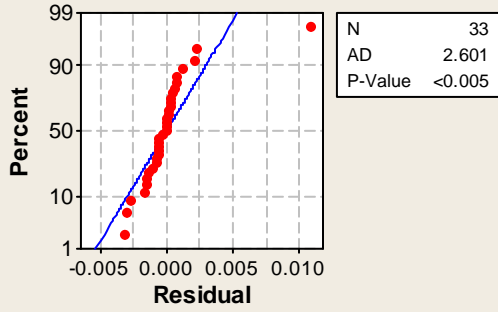
	<i>Coefficients</i>	<i>Standard Error</i>	<i>t Stat</i>	<i>P-value</i>	<i>Lower 95%</i>	<i>Upper 95%</i>
Intercept	0	#N/A	#N/A	#N/A	#N/A	#N/A
Slope	0.0799	0.0006	141.4868	2.4814E-46	0.0787	0.0810

* the intercept term was determined to be not significant during the initial analyses and was therefore eliminated from the model and the regression and ANOVA reanalyzed.

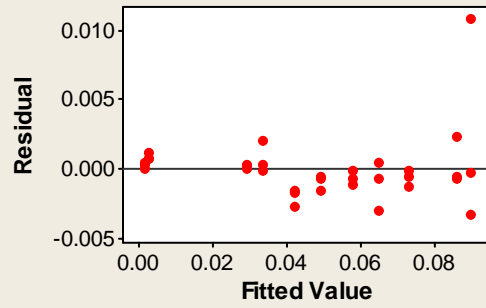


Residual Plots for Flowrate, Q (L/s), Clogging Test Trial 1

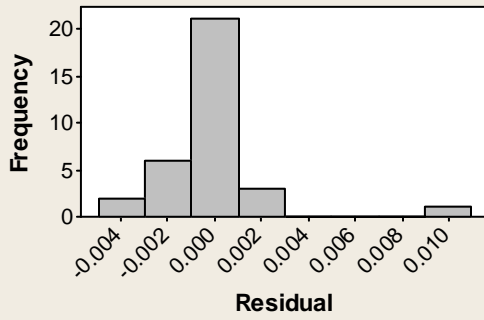
Normal Probability Plot



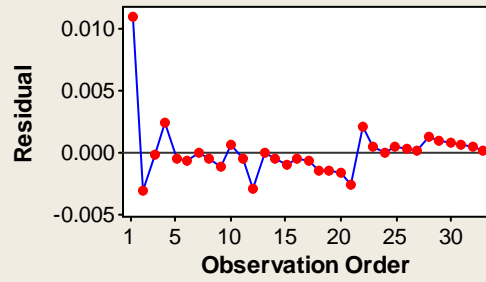
Versus Fits



Histogram



Versus Order

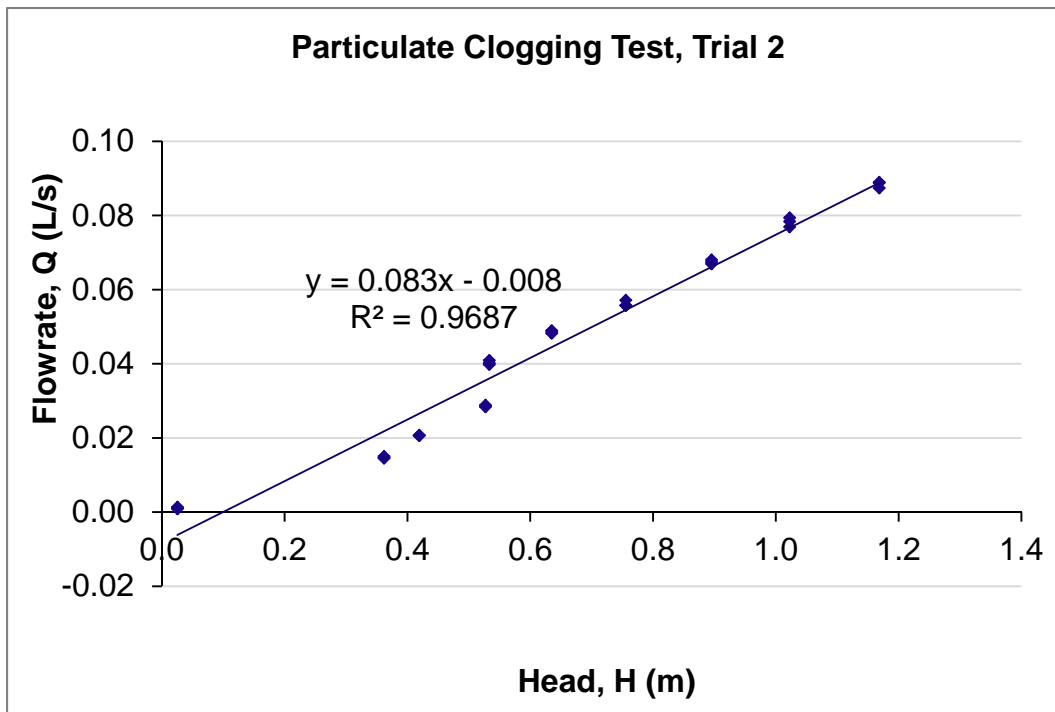


Appendix A.23: Regression Statistics on SmartDrain™ Clogging Test, Trial#2.

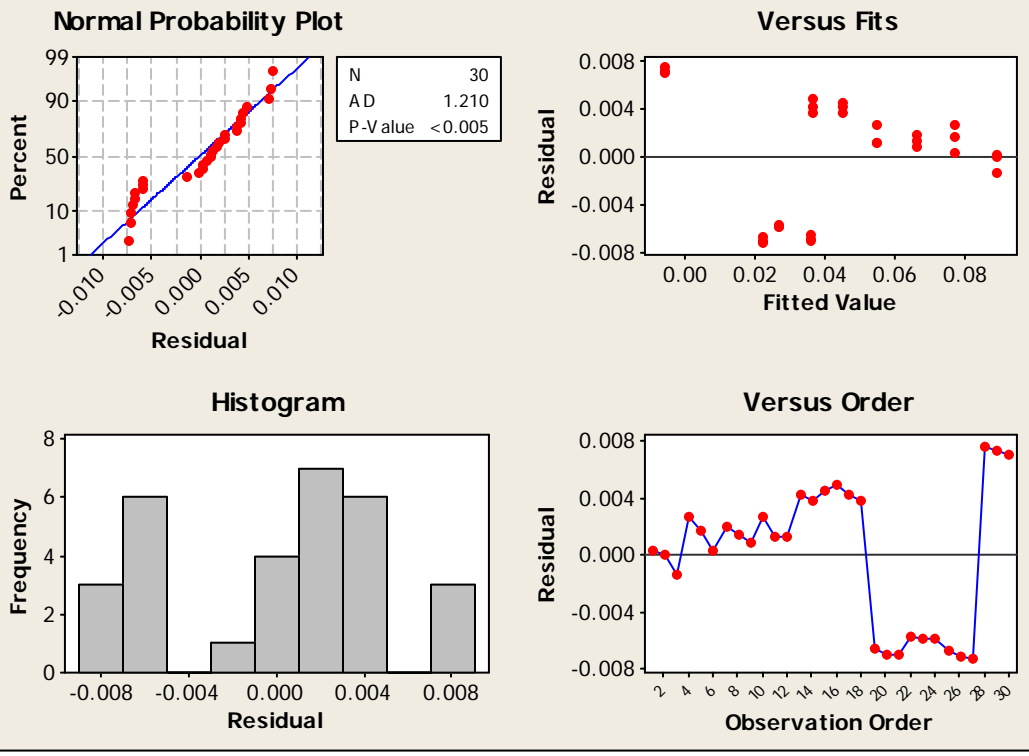
<i>Regression Statistics</i>	
Multiple R	0.9842
R Square	0.9687
Adjusted R Square	0.9676
Standard Error	0.0050
Observations	30

ANOVA					
	<i>df</i>	<i>SS</i>	<i>MS</i>	<i>F</i>	<i>Significance F</i>
Regression	1	0.0214	0.0214	866.2981	1.31943E-22
Residual	28	0.0007	2.46748E-05		
Total	29	0.0221			

	<i>Coefficients</i>	<i>Standard Error</i>	<i>t Stat</i>	<i>P-value</i>	<i>Lower 95%</i>	<i>Upper 95%</i>
Intercept	-0.0083	0.0020	-4.1276	0.0003	-0.0124	-0.0042
Slope	0.0831	0.0028	29.4329	1.3194E-22	0.0773	0.0889



Residual Plots for Flowrate, Q (L/s), Clogging Test Trial 2



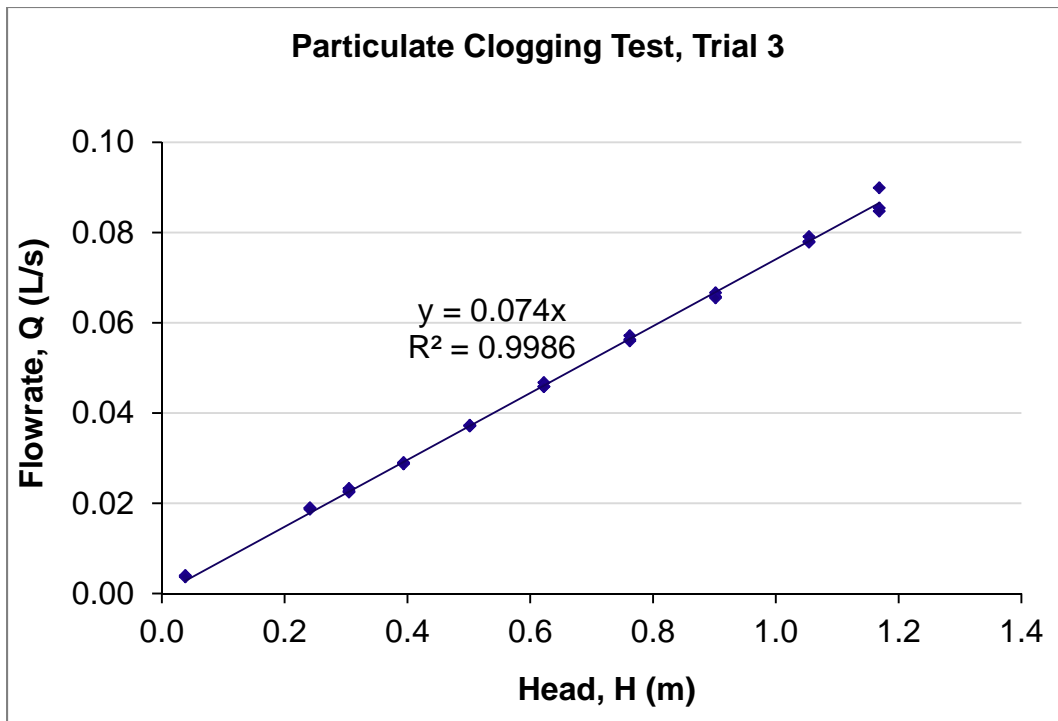
Appendix A.24: Regression Statistics on SmartDrain™ Clogging Test, Trial#3.

<i>Regression Statistics</i>	
Multiple R	0.9998
R Square	0.9996
Adjusted R Square	0.9652
Standard Error	0.0010
Observations	30

ANOVA					
	<i>df</i>	<i>SS</i>	<i>MS</i>	<i>F</i>	<i>Significance F</i>
Regression	1	0.0793	0.079314178	82466.4223	4.02551E-50
Residual	29	0.0000	9.61775E-07		
Total	30	0.0793			

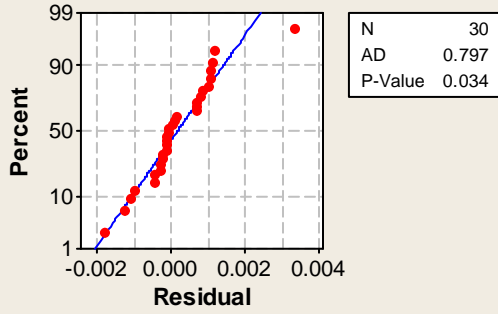
	<i>Coefficients</i>	<i>Standard Error</i>	<i>t Stat</i>	<i>P-value</i>	<i>Lower 95%</i>	<i>Upper 95%</i>
Intercept	0	#N/A	#N/A	#N/A	#N/A	#N/A
Slope	0.0741	0.0003	287.1697	1.2123E-51	0.0736	0.0746

* the intercept term was determined to be not significant during the initial analyses and was therefore eliminated from the model and the regression and ANOVA reanalyzed.

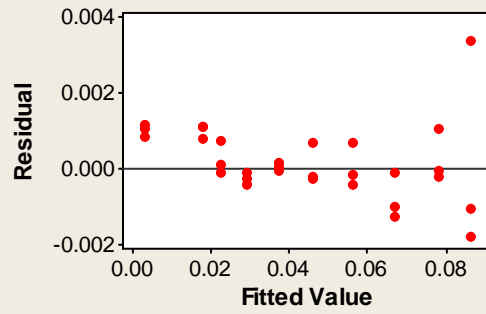


Residual Plots for Flowrate, Q (L/s), Clogging Test Trial 3

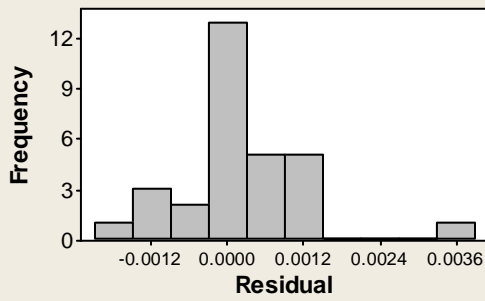
Normal Probability Plot



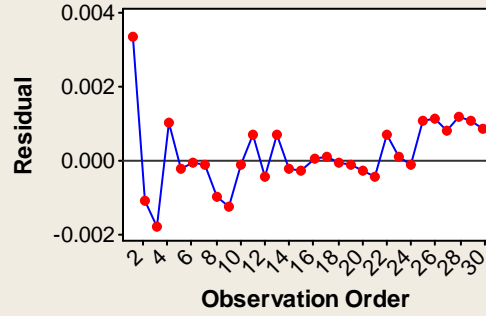
Versus Fits



Histogram



Versus Order



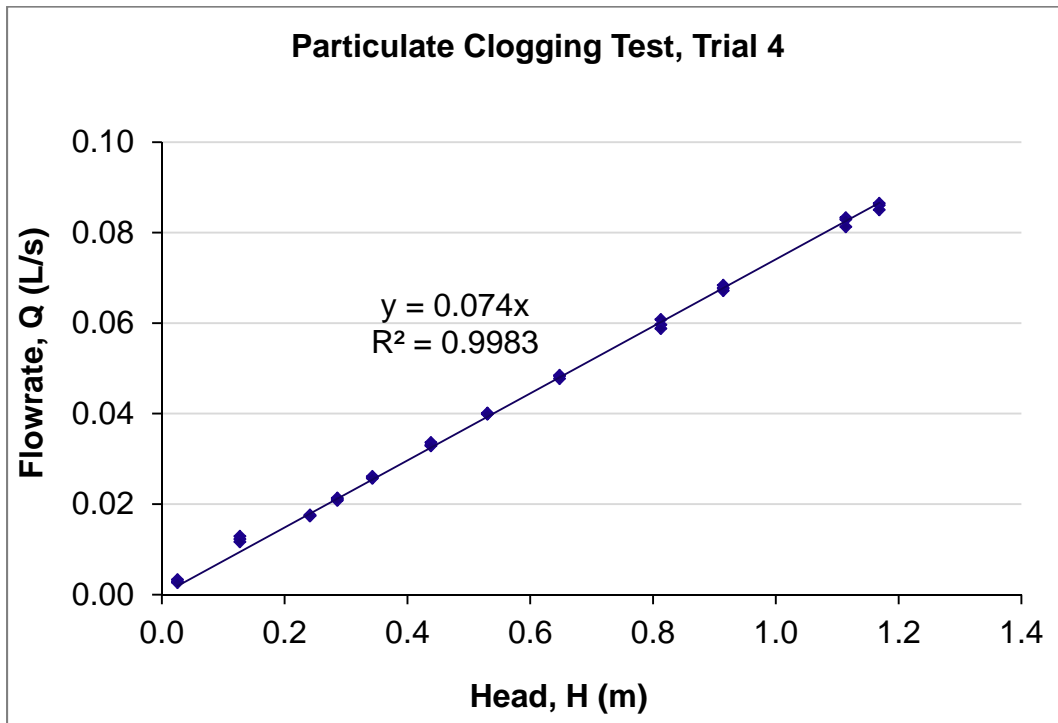
Appendix A.25: Regression Statistics on SmartDrain™ Clogging Test, Trial#4.

<i>Regression Statistics</i>	
Multiple R	0.9998
R Square	0.9995
Adjusted R Square	0.9709
Standard Error	0.0011
Observations	36

ANOVA					
	<i>df</i>	<i>SS</i>	<i>MS</i>	<i>F</i>	<i>Significance F</i>
Regression	1	0.0868	0.0868	70886.284	5.07166E-58
Residual	35	0.0000	1.22493E-06		
Total	36	0.0869			

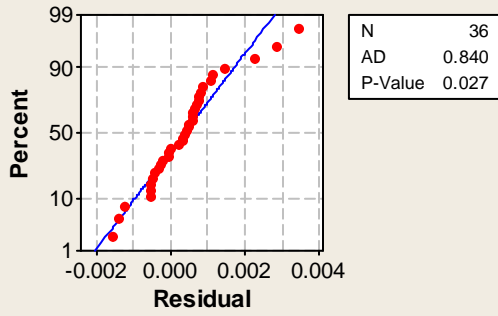
	<i>Coefficients</i>	<i>Standard Error</i>	<i>t Stat</i>	<i>P-value</i>	<i>Lower 95%</i>	<i>Upper 95%</i>
Intercept	0	#N/A	#N/A	#N/A	#N/A	#N/A
Slope	0.0741	0.0003	266.2448	1.8176E-59	0.0735	0.0747

* the intercept term was determined to be not significant during the initial analyses and was therefore eliminated from the model and the regression and ANOVA reanalyzed.

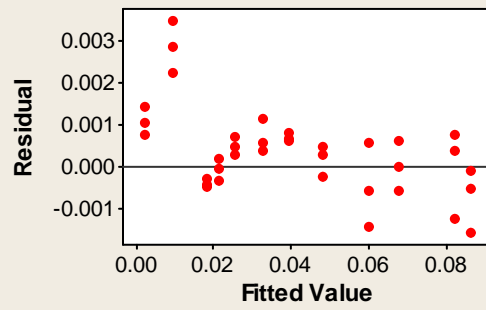


Residual Plots for Flowrate, Q (L/s), Clogging Test Trial 4

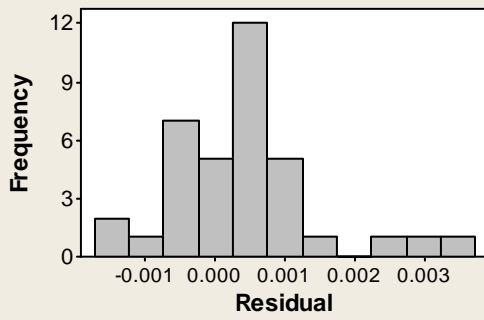
Normal Probability Plot



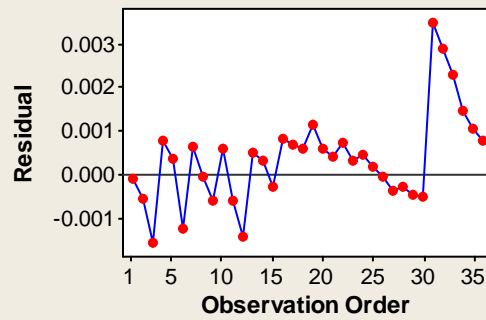
Versus Fits



Histogram



Versus Order



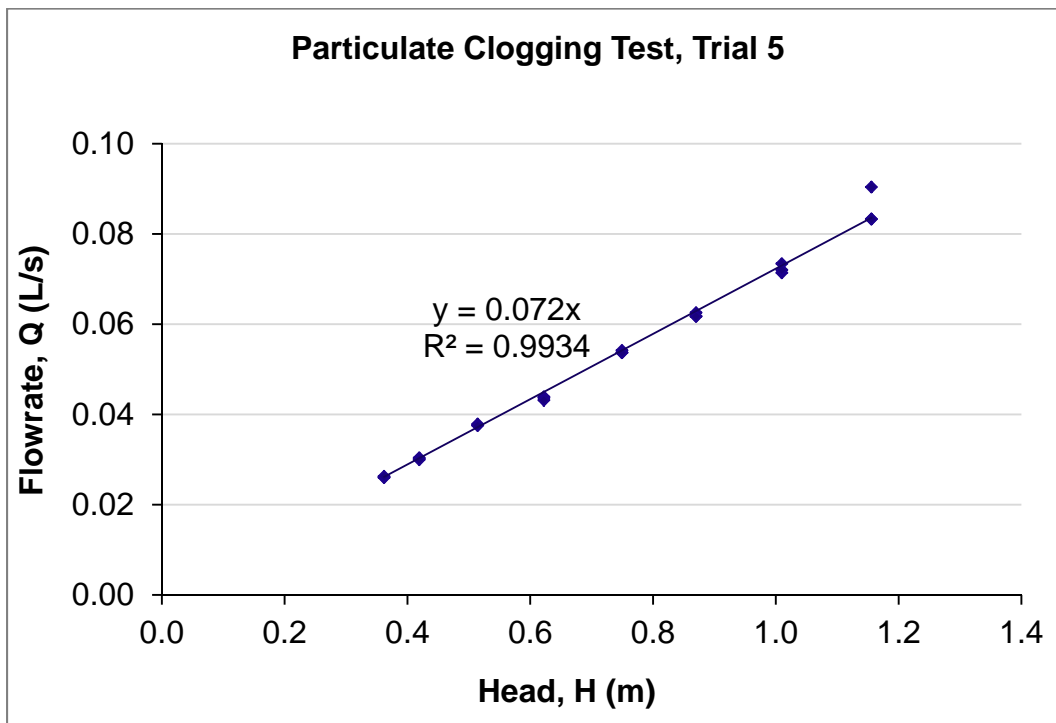
Appendix A.26: Regression Statistics on SmartDrain™ Clogging Test, Trial#5.

<i>Regression Statistics</i>	
Multiple R	0.9996
R Square	0.9992
Adjusted R Square	0.9557
Standard Error	0.0016
Observations	24

ANOVA					
	<i>df</i>	<i>SS</i>	<i>MS</i>	<i>F</i>	<i>Significance F</i>
Regression	1	0.0727	0.0727	27475.7022	1.44658E-35
Residual	23	0.0001	2.64614E-06		
Total	24	0.0728			

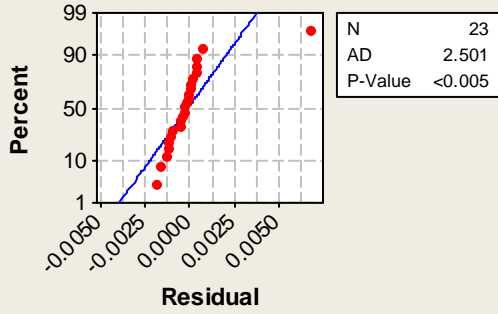
	<i>Coefficients</i>	<i>Standard Error</i>	<i>t Stat</i>	<i>P-value</i>	<i>Lower 95%</i>	<i>Upper 95%</i>
Intercept	0	#N/A	#N/A	#N/A	#N/A	#N/A
Slope	0.0723	0.0004	165.7580	6.6727E-37	0.0714	0.0732

* the intercept term was determined to be not significant during the initial analyses and was therefore eliminated from the model and the regression and ANOVA reanalyzed.

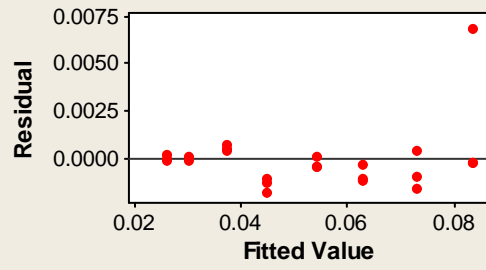


Residual Plots for Flowrate, Q (L/s), Clogging Test Trial 5

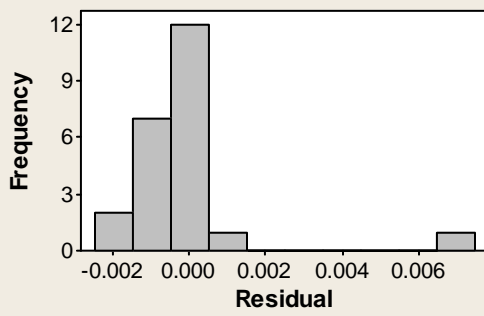
Normal Probability Plot



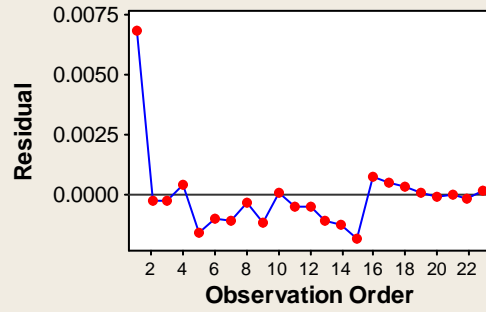
Versus Fits



Histogram



Versus Order



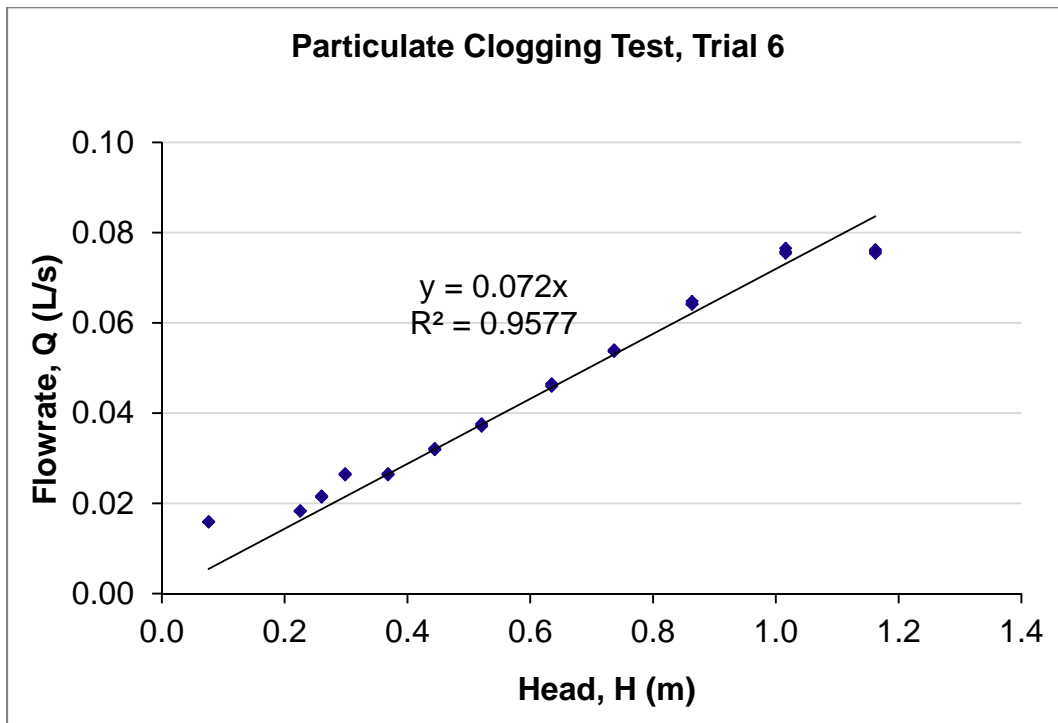
Appendix A.27: Regression Statistics on SmartDrain™ Clogging Test, Trial#6.

<i>Regression Statistics</i>	
Multiple R	0.9957
R Square	0.9914
Adjusted R Square	0.9628
Standard Error	0.0043
Observations	36

ANOVA					
	<i>df</i>	<i>SS</i>	<i>MS</i>	<i>F</i>	<i>Significance F</i>
Regression	1	0.0760	0.0760	4019.6965	6.86128E-37
Residual	35	0.0007	1.89138E-05		
Total	36	0.0767			

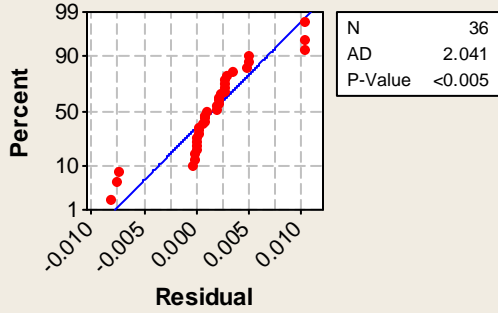
	<i>Coefficients</i>	<i>Standard Error</i>	<i>t Stat</i>	<i>P-value</i>	<i>Lower 95%</i>	<i>Upper 95%</i>
Intercept	0	#N/A	#N/A	#N/A	#N/A	#N/A
Slope	0.0720	0.0011	63.4011	1.0245E-37	0.0697	0.0743

* the intercept term was determined to be not significant during the initial analyses and was therefore eliminated from the model and the regression and ANOVA reanalyzed.

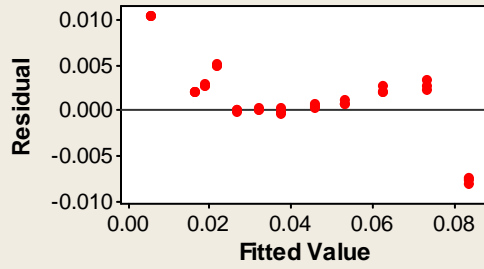


Residual Plots for Flowrate, Q (L/s), Clogging Test Trial 6

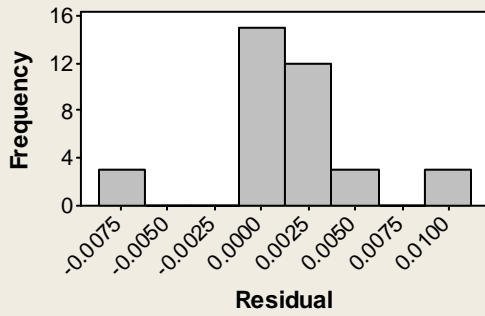
Normal Probability Plot



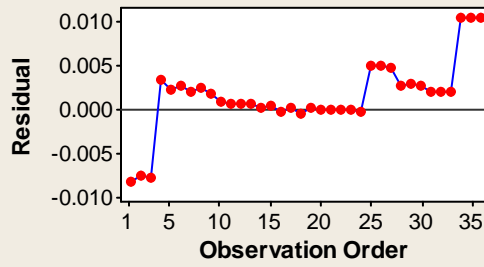
Versus Fits



Histogram



Versus Order



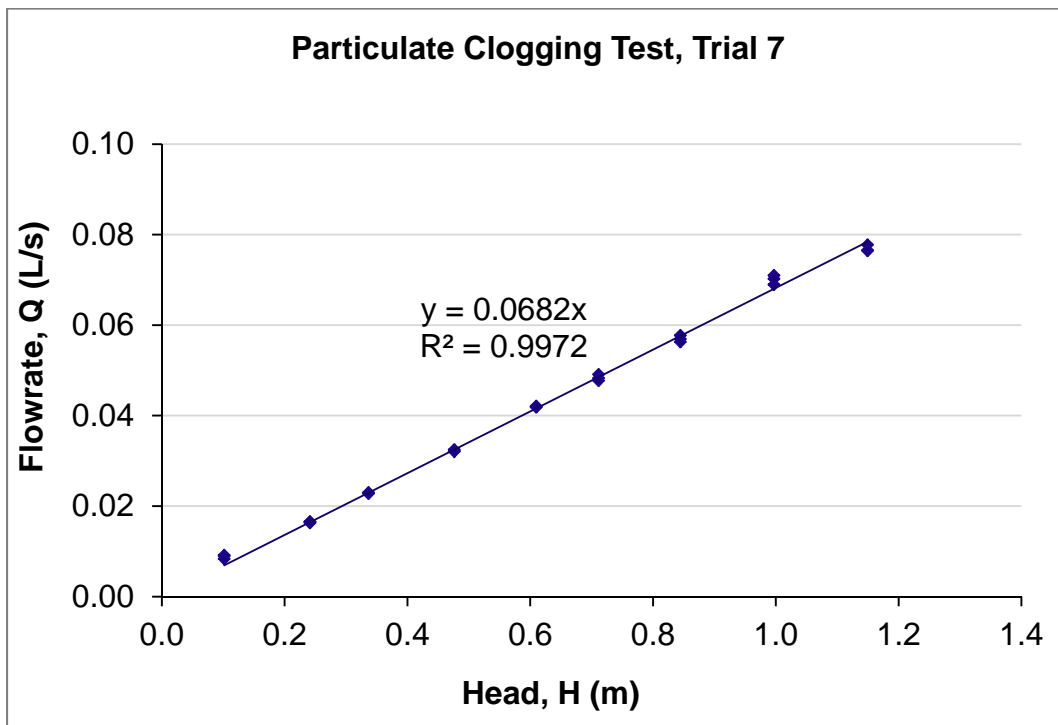
Appendix A.28: Regression Statistics on SmartDrain™ Clogging Test, Trial#7.

<i>Regression Statistics</i>	
Multiple R	0.9997
R Square	0.9994
Adjusted R Square	0.9609
Standard Error	0.0012
Observations	27

ANOVA					
	<i>df</i>	<i>SS</i>	<i>MS</i>	<i>F</i>	<i>Significance F</i>
Regression	1	0.0603	0.0603	41436.4549	8.96278E-42
Residual	26	0.0000	1.45413E-06		
Total	27	0.0603			

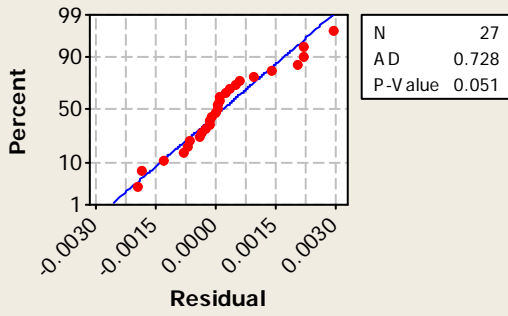
	<i>Coefficients</i>	<i>Standard Error</i>	<i>t Stat</i>	<i>P-value</i>	<i>Lower 95%</i>	<i>Upper 95%</i>
Intercept	0	#N/A	#N/A	#N/A	#N/A	#N/A
Slope	0.0682	0.0003	203.5595	3.5937E-43	0.0675	0.0689

* the intercept term was determined to be not significant during the initial analyses and was therefore eliminated from the model and the regression and ANOVA reanalyzed.

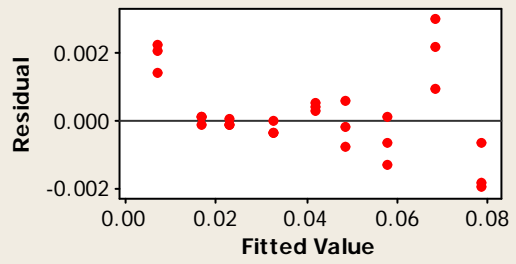


Residual Plots for Flowrate, Q (L/s), Clogging Test Trial 7

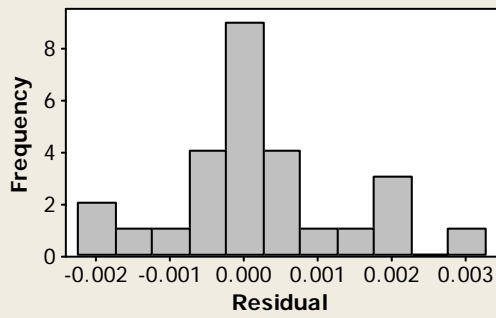
Normal Probability Plot



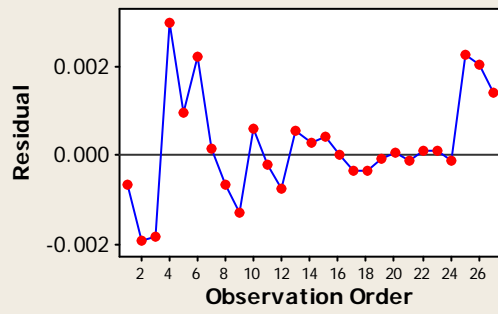
Versus Fits



Histogram



Versus Order



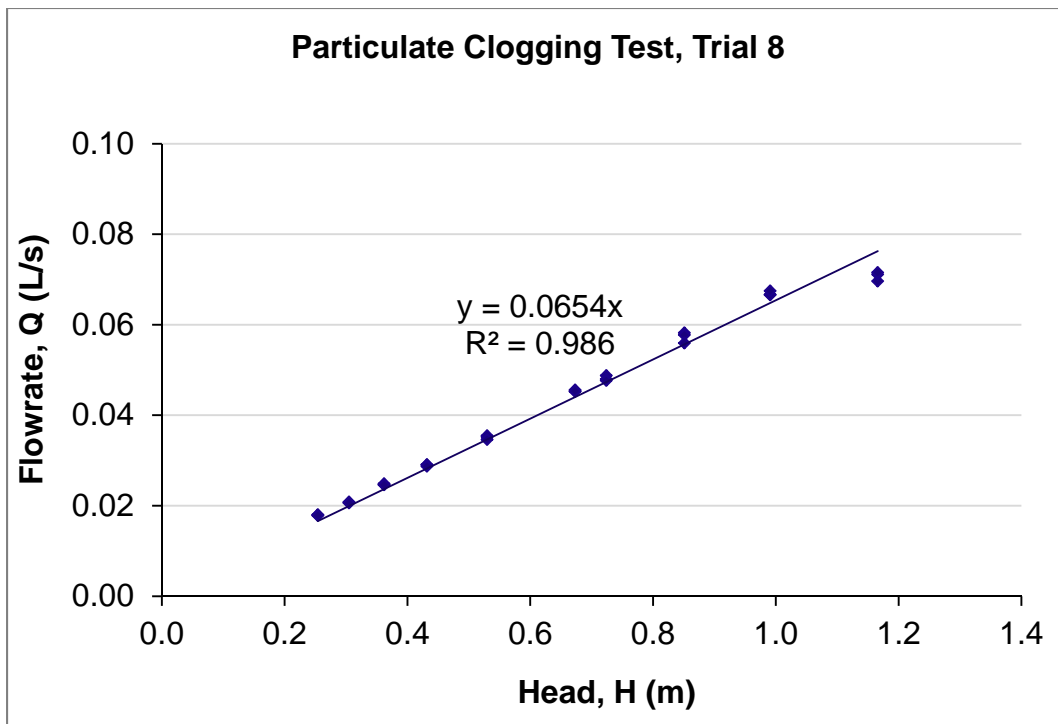
Appendix A.29: Regression Statistics on SmartDrain™ Clogging Test, Trial#8.

<i>Regression Statistics</i>	
Multiple R	0.9989
R Square	0.9978
Adjusted R Square	0.9633
Standard Error	0.0022
Observations	30

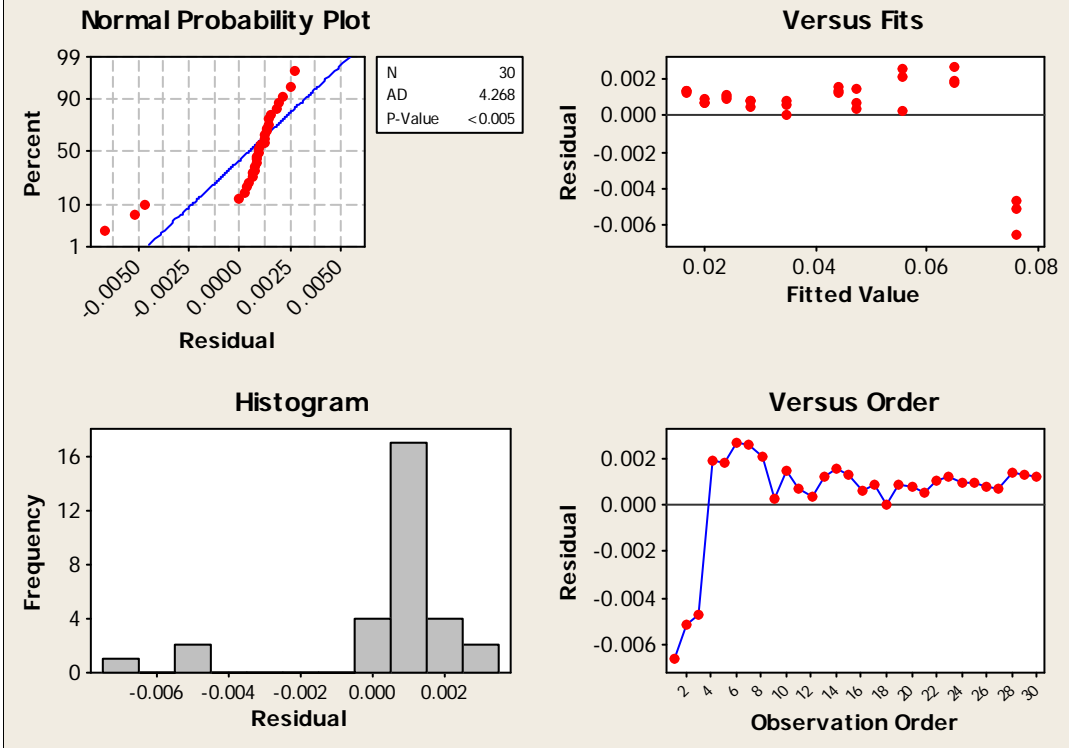
ANOVA					
	<i>df</i>	<i>SS</i>	<i>MS</i>	<i>F</i>	<i>Significance F</i>
Regression	1	0.0616	0.0616	12918.947	7.32474E-39
Residual	29	0.0001	4.76779E-06		
Total	30	0.0617			

	<i>Coefficients</i>	<i>Standard Error</i>	<i>t Stat</i>	<i>P-value</i>	<i>Lower 95%</i>	<i>Upper 95%</i>
Intercept	0	#N/A	#N/A	#N/A	#N/A	#N/A
Slope	0.0654	0.0006	113.6615	5.563E-40	0.0642	0.0666

* the intercept term was determined to be not significant during the initial analyses and was therefore eliminated from the model and the regression and ANOVA reanalyzed.



Residual Plots for Flowrate, Q (L/s), Clogging Test Trial 8



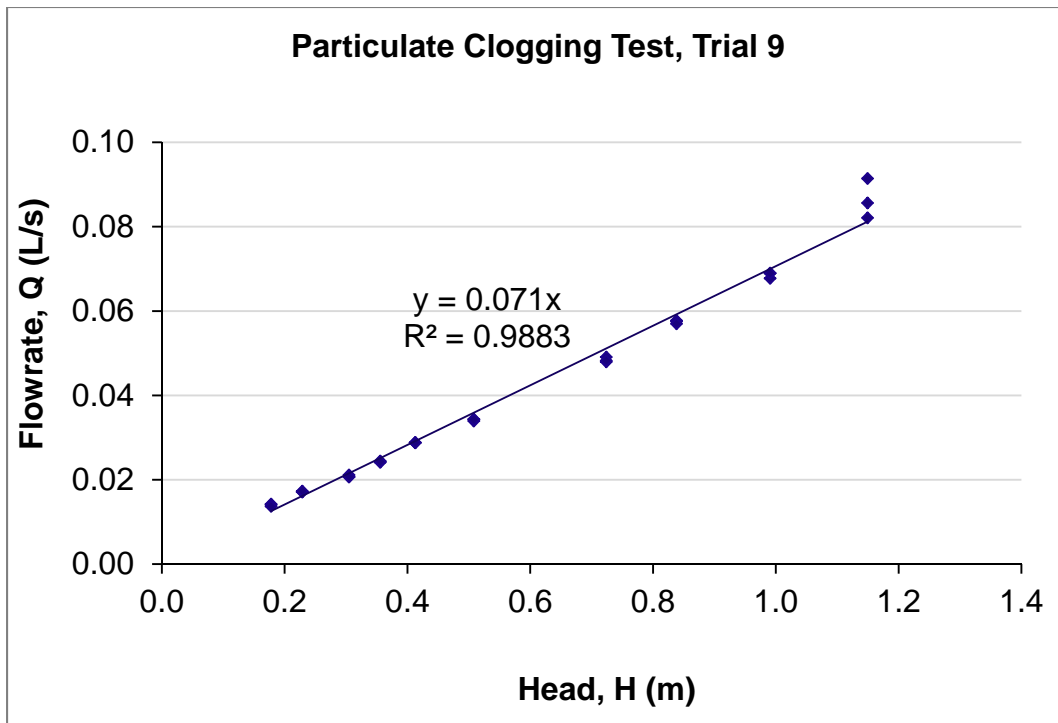
Appendix A.30: Regression Statistics on SmartDrain™ Clogging Test, Trial#9.

<i>Regression Statistics</i>	
Multiple R	0.9985
R Square	0.9971
Adjusted R Square	0.9626
Standard Error	0.0025
Observations	30

ANOVA					
	<i>df</i>	<i>SS</i>	<i>MS</i>	<i>F</i>	<i>Significance F</i>
Regression	1	0.0638	0.0638	9867.9896	3.15385E-37
Residual	29	0.0002	6.46266E-06		
Total	30	0.0640			

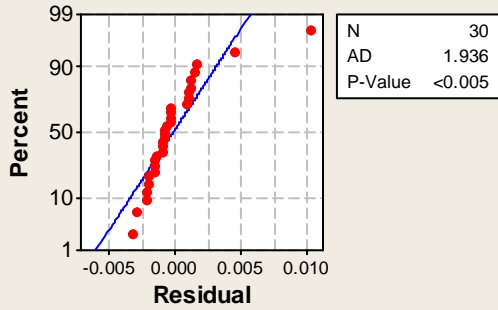
	<i>Coefficients</i>	<i>Standard Error</i>	<i>t Stat</i>	<i>P-value</i>	<i>Lower 95%</i>	<i>Upper 95%</i>
Intercept	0	#N/A	#N/A	#N/A	#N/A	#N/A
Slope	0.0706	0.0007	99.3378	2.7389E-38	0.0692	0.0721

* the intercept term was determined to be not significant during the initial analyses and was therefore eliminated from the model and the regression and ANOVA reanalyzed.

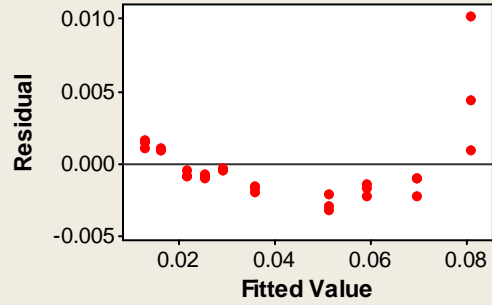


Residual Plots for Flowrate, Q (L/s), Clogging Test Trial 9

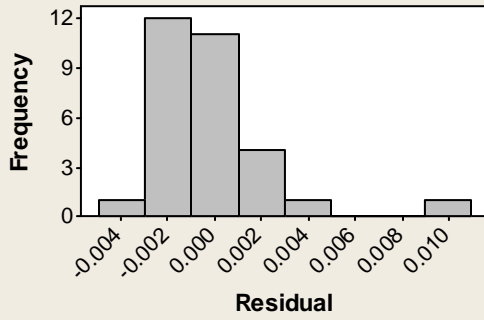
Normal Probability Plot



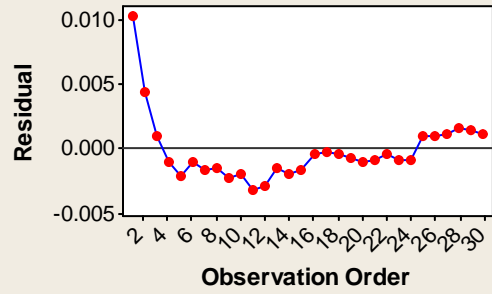
Versus Fits



Histogram



Versus Order



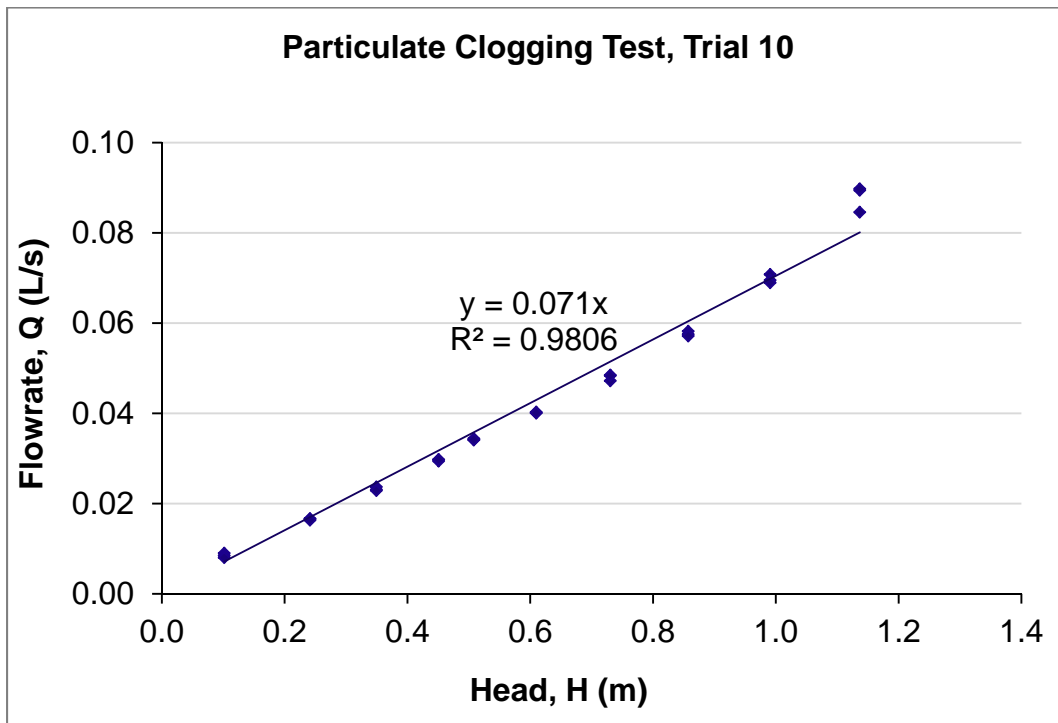
Appendix A.31: Regression Statistics on SmartDrain™ Clogging Test, Trial#10.

<i>Regression Statistics</i>	
Multiple R	0.9977
R Square	0.9953
Adjusted R Square	0.9608
Standard Error	0.0033
Observations	30

ANOVA					
	<i>df</i>	<i>SS</i>	<i>MS</i>	<i>F</i>	<i>Significance F</i>
Regression	1	0.0680	0.0680	6161.2911	2.25239E-34
Residual	29	0.0003	1.10438E-05		
Total	30	0.0684			

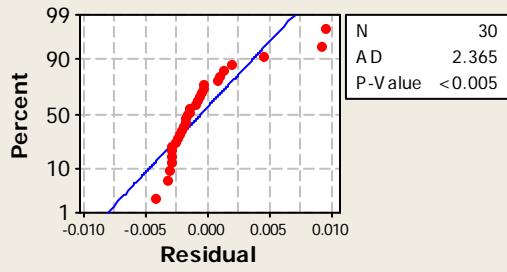
	<i>Coefficients</i>	<i>Standard Error</i>	<i>t Stat</i>	<i>P-value</i>	<i>Lower 95%</i>	<i>Upper 95%</i>
Intercept	0	#N/A	#N/A	#N/A	#N/A	#N/A
Slope	0.0705	0.0009	78.4939	2.4712E-35	0.0687	0.0723

* the intercept term was determined to be not significant during the initial analyses and was therefore eliminated from the model and the regression and ANOVA reanalyzed.

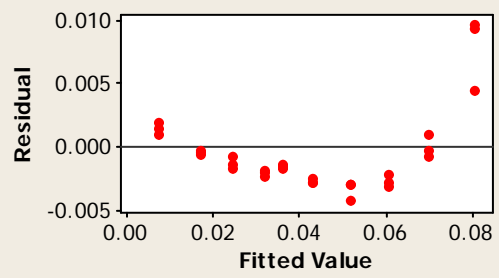


Residual Plots for Flowrate, Q (L/s), Clogging Test Trial 10

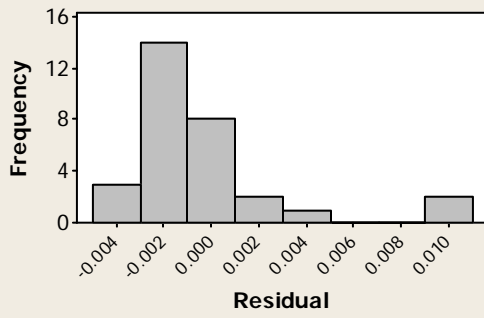
Normal Probability Plot



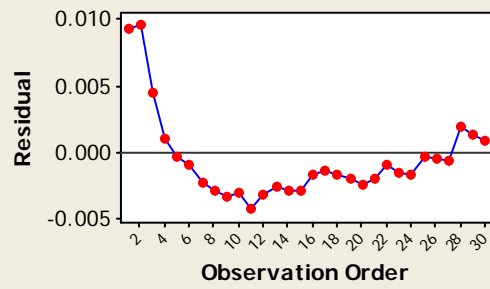
Versus Fits



Histogram



Versus Order

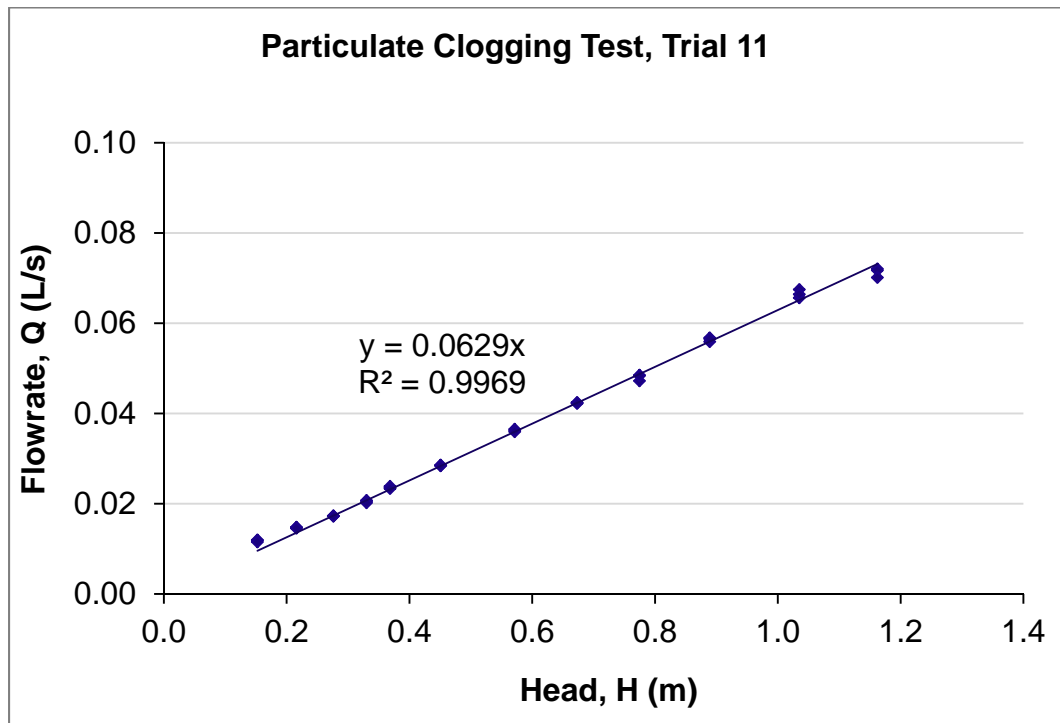


Appendix A.32: Regression Statistics on SmartDrain™ Clogging Test, Trial#11.

<i>Regression Statistics</i>	
Multiple R	0.9996
R Square	0.9993
Adjusted R Square	0.9707
Standard Error	0.0011
Observations	36

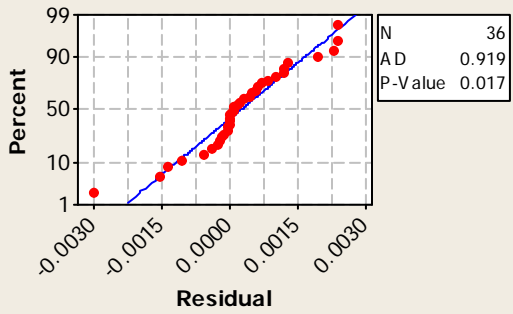
ANOVA					
	<i>df</i>	<i>SS</i>	<i>MS</i>	<i>F</i>	<i>Significance F</i>
Regression	1	0.0616	0.0616	49930.2465	1.9547E-55
Residual	35	0.0000	1.23366E-06		
Total	36	0.0616			

	<i>Coefficients</i>	<i>Standard Error</i>	<i>t Stat</i>	<i>P-value</i>	<i>Lower 95%</i>	<i>Upper 95%</i>
Intercept	0	#N/A	#N/A	#N/A	#N/A	#N/A
Slope	0.0629	0.0003	223.4508	8.3454E-57	0.0624	0.0635

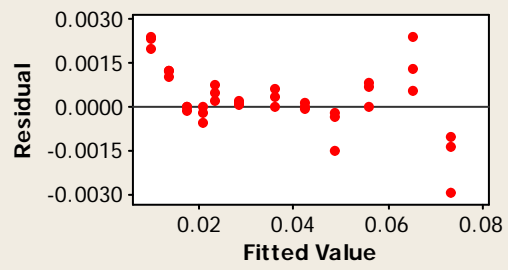


Residual Plots for Flowrate, Q (L/s), Clogging Test Trial 11

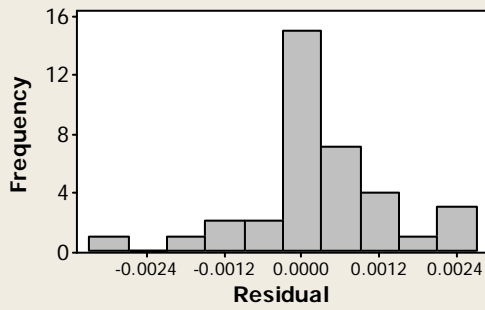
Normal Probability Plot



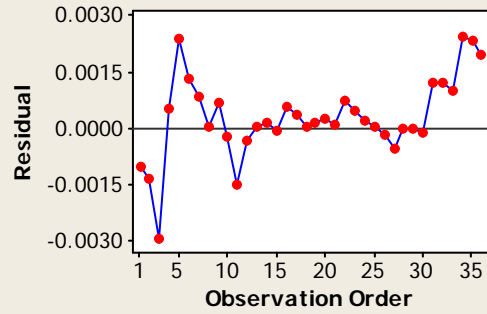
Versus Fits



Histogram



Versus Order



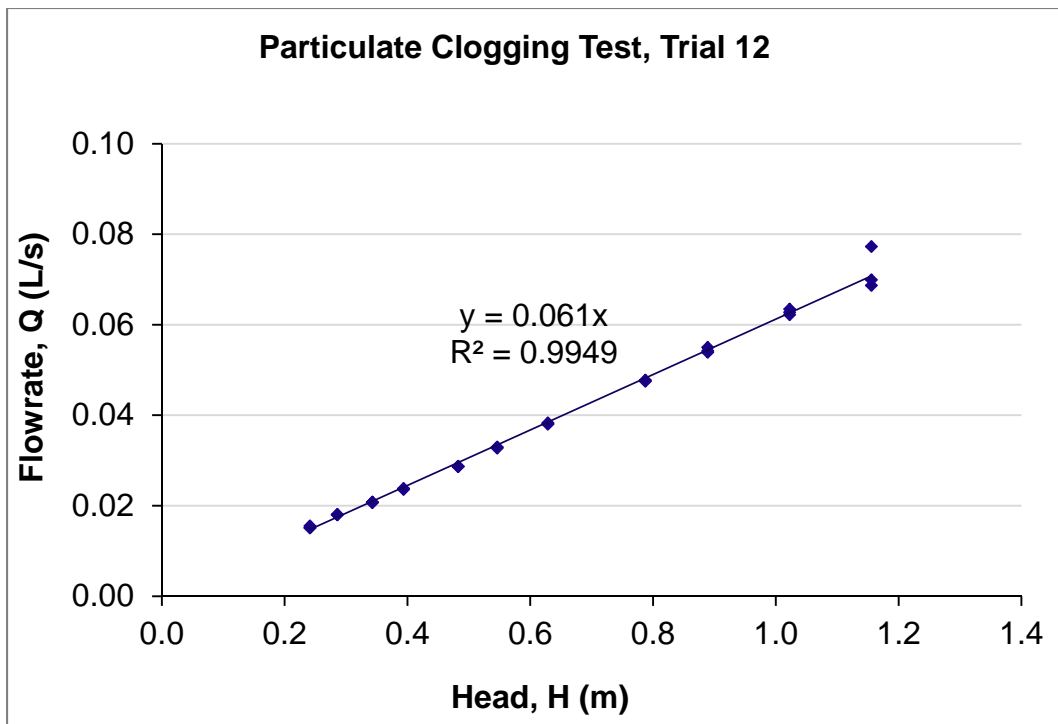
AppendixA.33: Regression Statistics on SmartDrain™ Clogging Test, Trial#12.

<i>Regression Statistics</i>	
Multiple R	0.9995
R Square	0.9990
Adjusted R Square	0.9678
Standard Error	0.0013
Observations	33

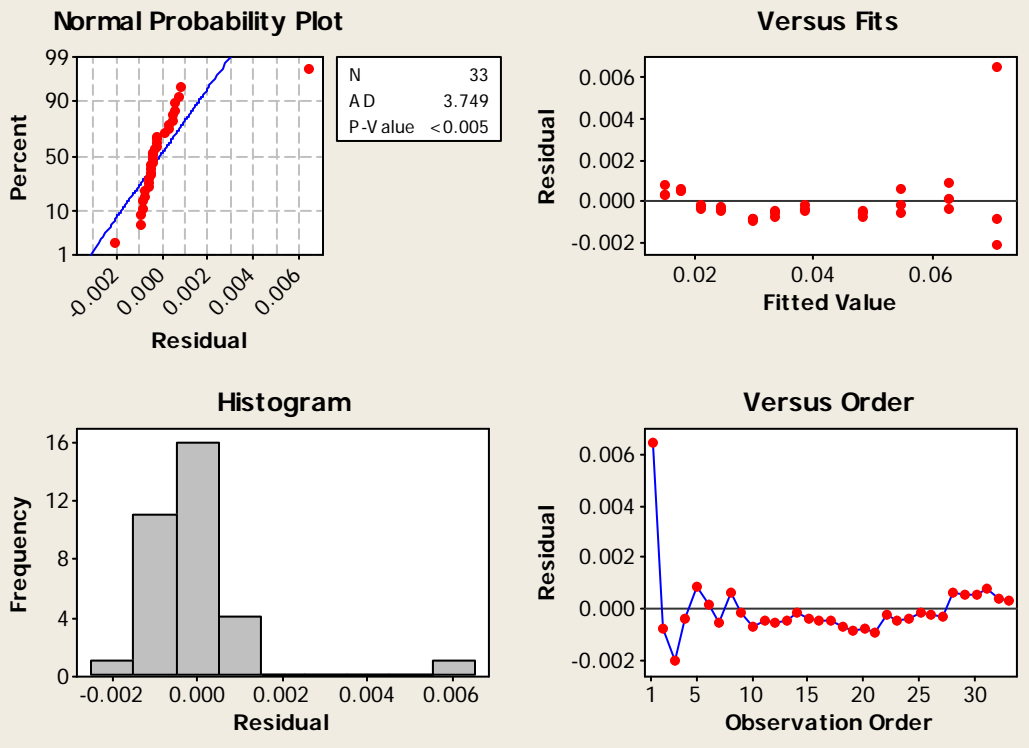
ANOVA					
	<i>df</i>	<i>SS</i>	<i>MS</i>	<i>F</i>	<i>Significance F</i>
Regression	1	0.0577	0.0577	32839.2352	1.8139E-48
Residual	32	0.0001	1.75816E-06		
Total	33	0.0578			

	<i>Coefficients</i>	<i>Standard Error</i>	<i>t Stat</i>	<i>P-value</i>	<i>Lower 95%</i>	<i>Upper 95%</i>
Intercept	0	#N/A	#N/A	#N/A	#N/A	#N/A
Slope	0.0613	0.0003	181.2160	9.1099E-50	0.0606	0.0619

* the intercept term was determined to be not significant during the initial analyses and was therefore eliminated from the model and the regression and ANOVA reanalyzed.



Residual Plots for Flowrate, Q (L/s), Clogging Test Trial 12

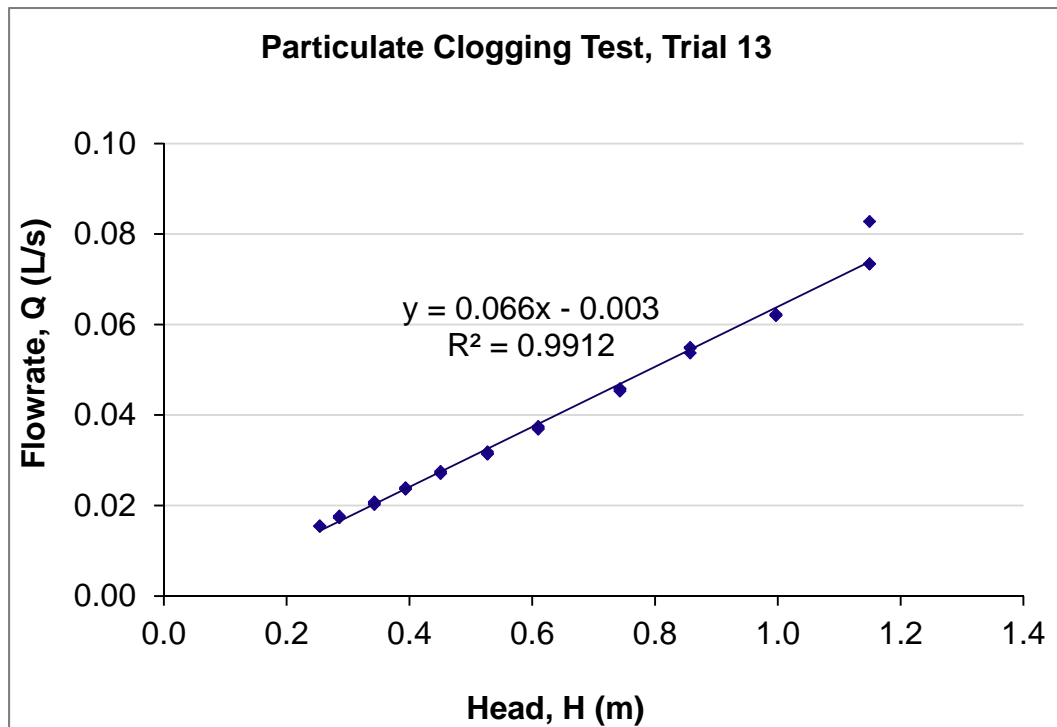


Appendix A.34: Regression Statistics on SmartDrain™ Clogging Test, Trial#13.

<i>Regression Statistics</i>	
Multiple R	0.9956
R Square	0.9912
Adjusted R Square	0.9909
Standard Error	0.0018
Observations	33

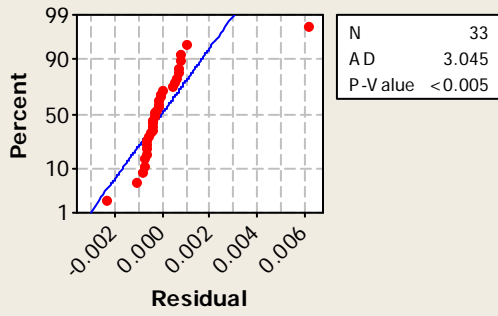
ANOVA					
	<i>df</i>	<i>SS</i>	<i>MS</i>	<i>F</i>	<i>Significance F</i>
Regression	1	0.0119	0.0119	3493.0378	1.95676E-33
Residual	31	0.0001	3.41315E-06		
Total	32	0.0120			

	<i>Coefficients</i>	<i>Standard Error</i>	<i>t Stat</i>	<i>P-value</i>	<i>Lower 95%</i>	<i>Upper 95%</i>
Intercept	-0.0025	0.0007	-3.3032	0.0024	-0.0040	-0.0009
Slope	0.0664	0.0011	59.1019	1.9568E-33	0.0641	0.0687

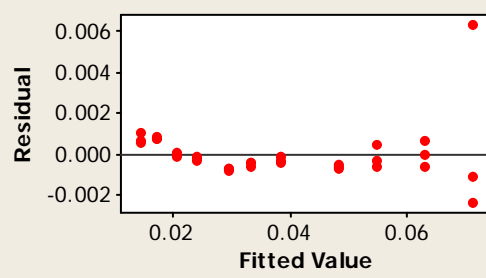


Residual Plots for Flowrate, Q (L/s), Clogging Test Trial 13

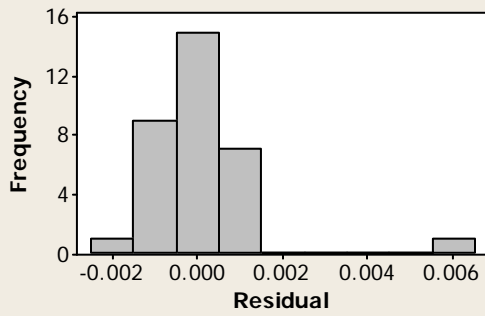
Normal Probability Plot



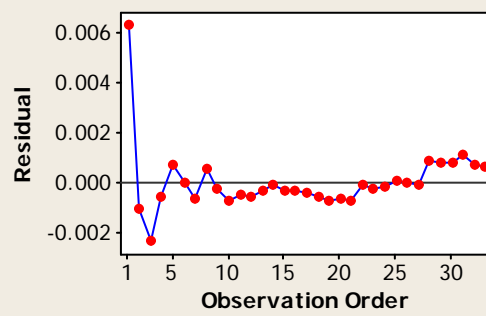
Versus Fits



Histogram



Versus Order



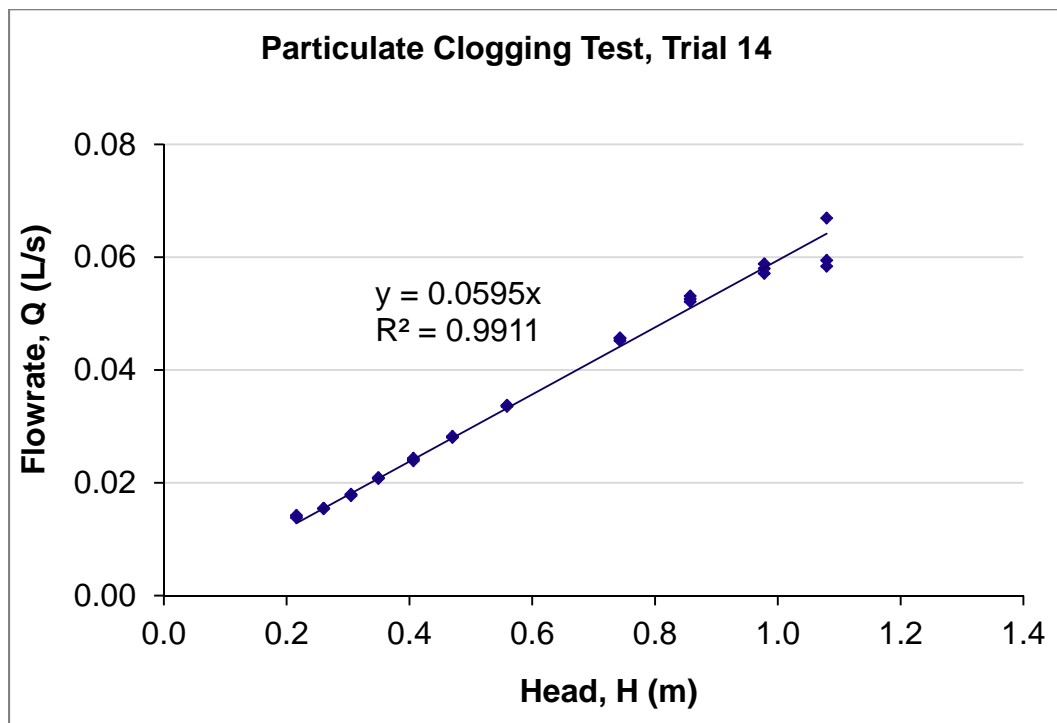
Appendix A.35: Regression Statistics on SmartDrain™ Clogging Test, Trial#14.

<i>Regression Statistics</i>	
Multiple R	0.9991
R Square	0.9982
Adjusted R Square	0.9670
Standard Error	0.0016
Observations	33

ANOVA					
	<i>df</i>	<i>SS</i>	<i>MS</i>	<i>F</i>	<i>Significance F</i>
Regression	1	0.0470	0.0470	17877.8258	2.22166E-44
Residual	32	0.0001	2.63151E-06		
Total	33	0.0471			

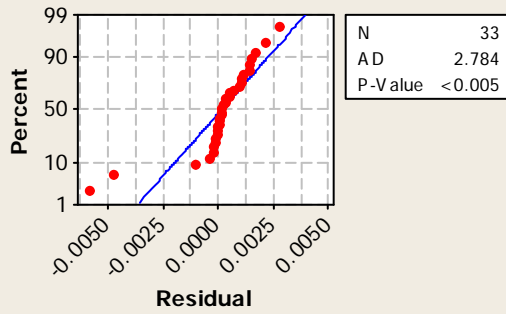
	<i>Coefficients</i>	<i>Standard Error</i>	<i>t Stat</i>	<i>P-value</i>	<i>Lower 95%</i>	<i>Upper 95%</i>
Intercept	0	#N/A	#N/A	#N/A	#N/A	#N/A
Slope	0.0595	0.0004	133.7080	1.511E-45	0.0586	0.0604

* the intercept term was determined to be not significant during the initial analyses and was therefore eliminated from the model and the regression and ANOVA reanalyzed.

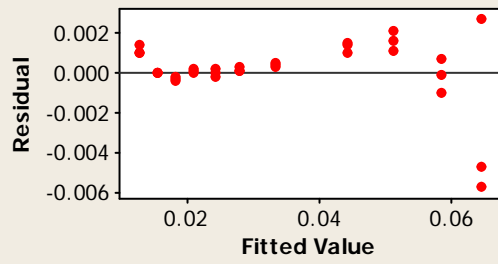


Residual Plots for Flowrate, Q (L/s), Clogging Test Trial 14

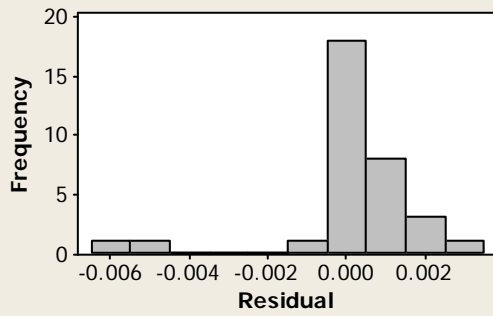
Normal Probability Plot



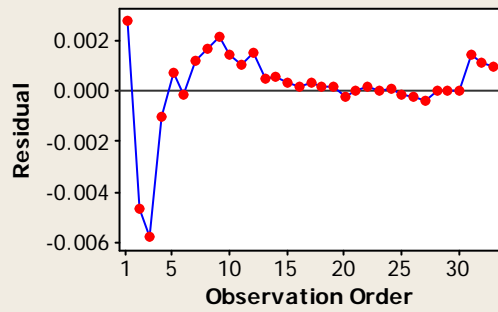
Versus Fits



Histogram



Versus Order



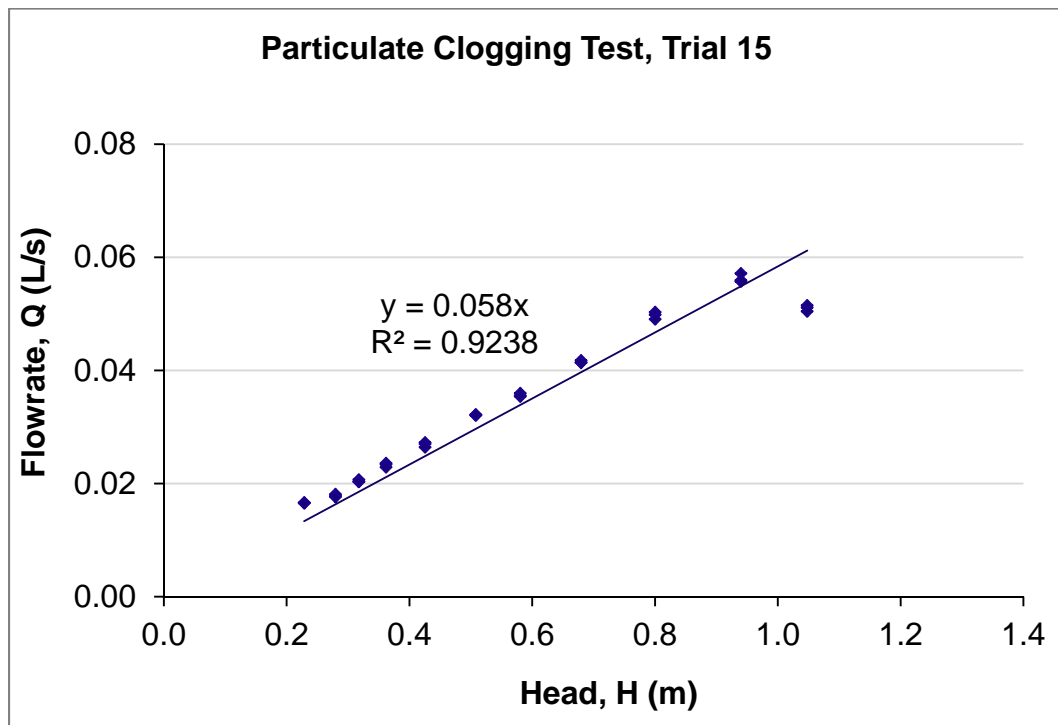
Appendix A.36: Regression Statistics on SmartDrain™ Clogging Test, Trial#15.

<i>Regression Statistics</i>	
Multiple R	0.9947
R Square	0.9895
Adjusted R Square	0.9582
Standard Error	0.0038
Observations	33

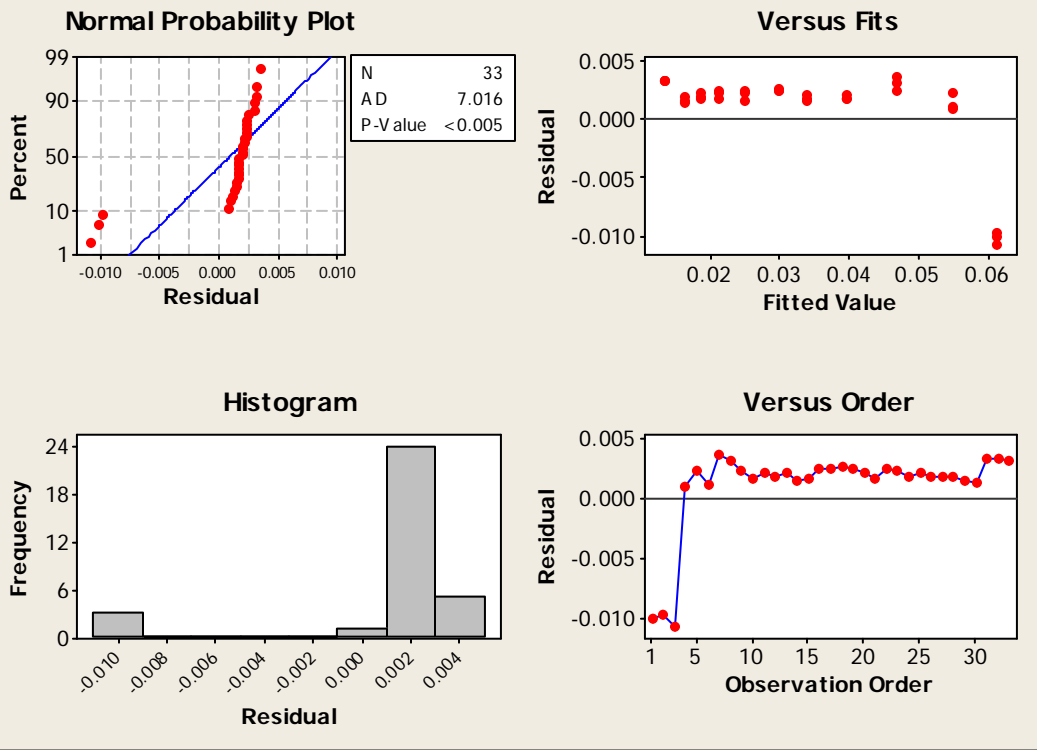
ANOVA					
	<i>df</i>	<i>SS</i>	<i>MS</i>	<i>F</i>	<i>Significance F</i>
Regression	1	0.0432	0.0432	3007.2720	1.95093E-32
Residual	32	0.0005	1.43599E-05		
Total	33	0.0436			

	<i>Coefficients</i>	<i>Standard Error</i>	<i>t Stat</i>	<i>P-value</i>	<i>Lower 95%</i>	<i>Upper 95%</i>
Intercept	0	#N/A	#N/A	#N/A	#N/A	#N/A
Slope	0.0584	0.0011	54.8386	3.2079E-33	0.0562	0.0606

* the intercept term was determined to be not significant during the initial analyses and was therefore eliminated from the model and the regression and ANOVA reanalyzed.



Residual Plots for Flowrate, Q (L/s), Clogging Test Trial 15



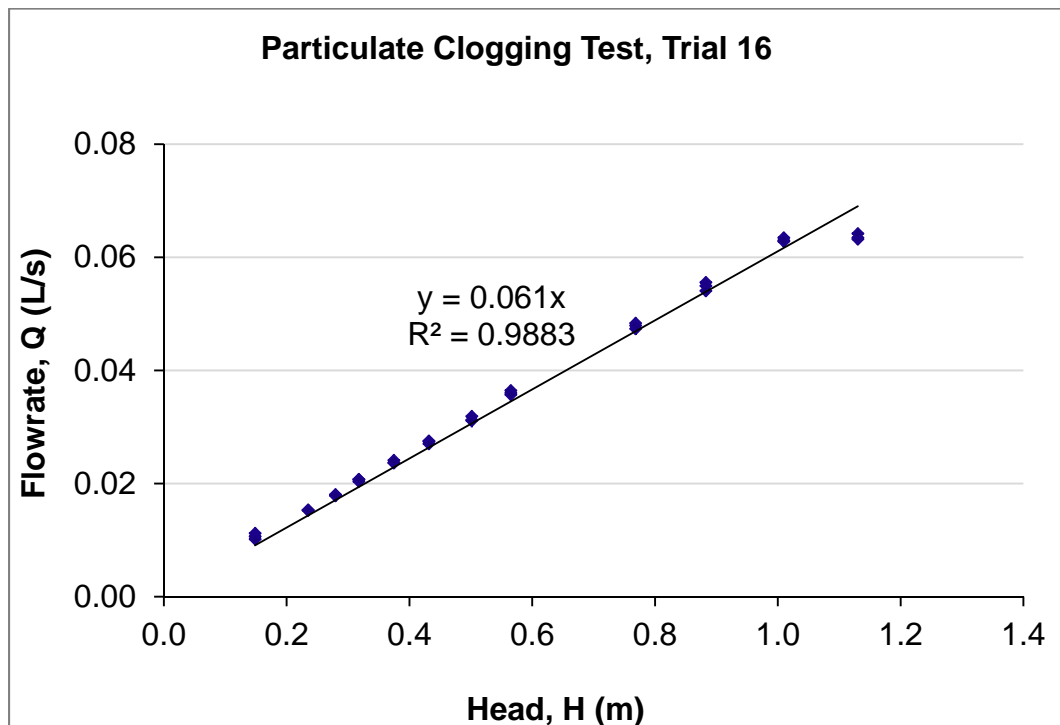
Appendix A.37: Regression Statistics on SmartDrain™ Clogging Test, Trial#16.

<i>Regression Statistics</i>	
Multiple R	0.9988
R Square	0.9975
Adjusted R Square	0.9689
Standard Error	0.0020
Observations	36

ANOVA					
	<i>df</i>	<i>SS</i>	<i>MS</i>	<i>F</i>	<i>Significance F</i>
Regression	1	0.0539	0.0539	14023.7729	4.50884E-46
Residual	35	0.0001	3.84592E-06		
Total	36	0.0541			

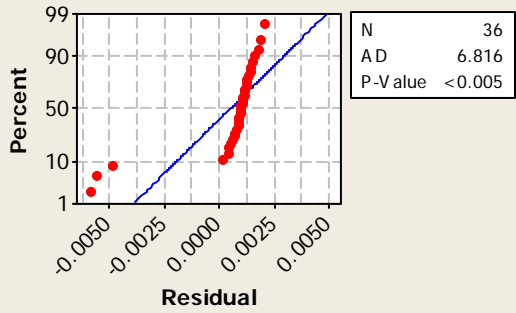
	<i>Coefficients</i>	<i>Standard Error</i>	<i>t Stat</i>	<i>P-value</i>	<i>Lower 95%</i>	<i>Upper 95%</i>
Intercept	0	#N/A	#N/A	#N/A	#N/A	#N/A
Slope	0.0611	0.0005	118.4220	3.626E-47	0.0600	0.0621

* the intercept term was determined to be not significant during the initial analyses and was therefore eliminated from the model and the regression and ANOVA reanalyzed.

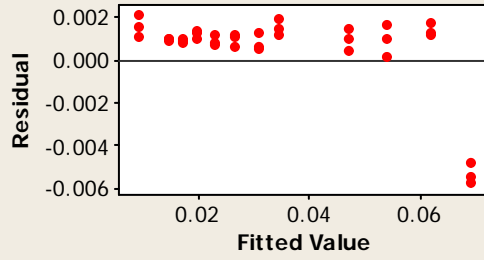


Residual Plots for Flowrate, Q (L/s), Clogging Test Trial 16

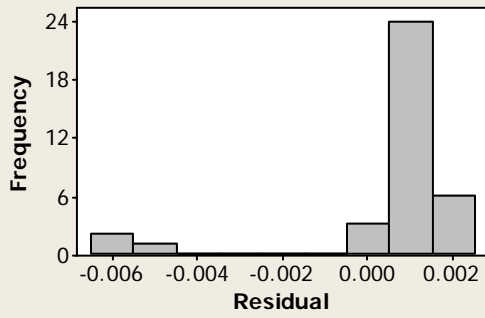
Normal Probability Plot



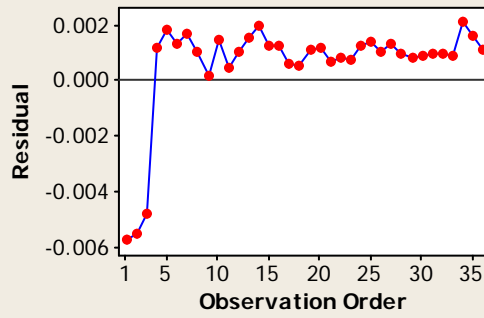
Versus Fits



Histogram



Versus Order



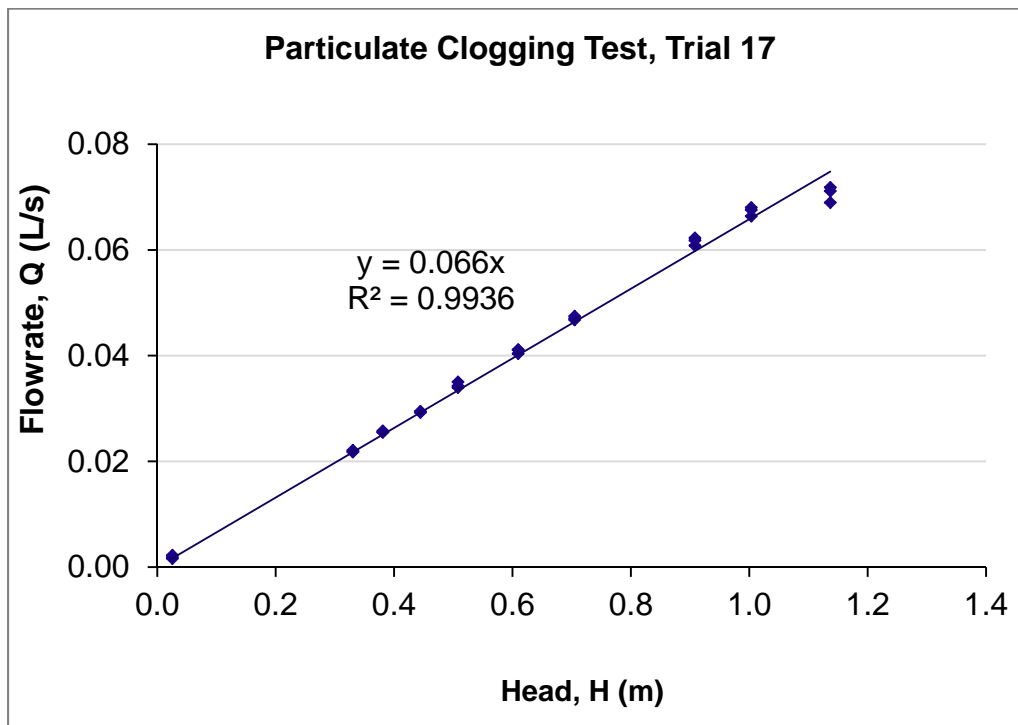
Appendix A.38: Regression Statistics on SmartDrain™ Clogging Test, Trial#17.

<i>Regression Statistics</i>	
Multiple R	0.9993
R Square	0.9986
Adjusted R Square	0.9642
Standard Error	0.0017
Observations	30

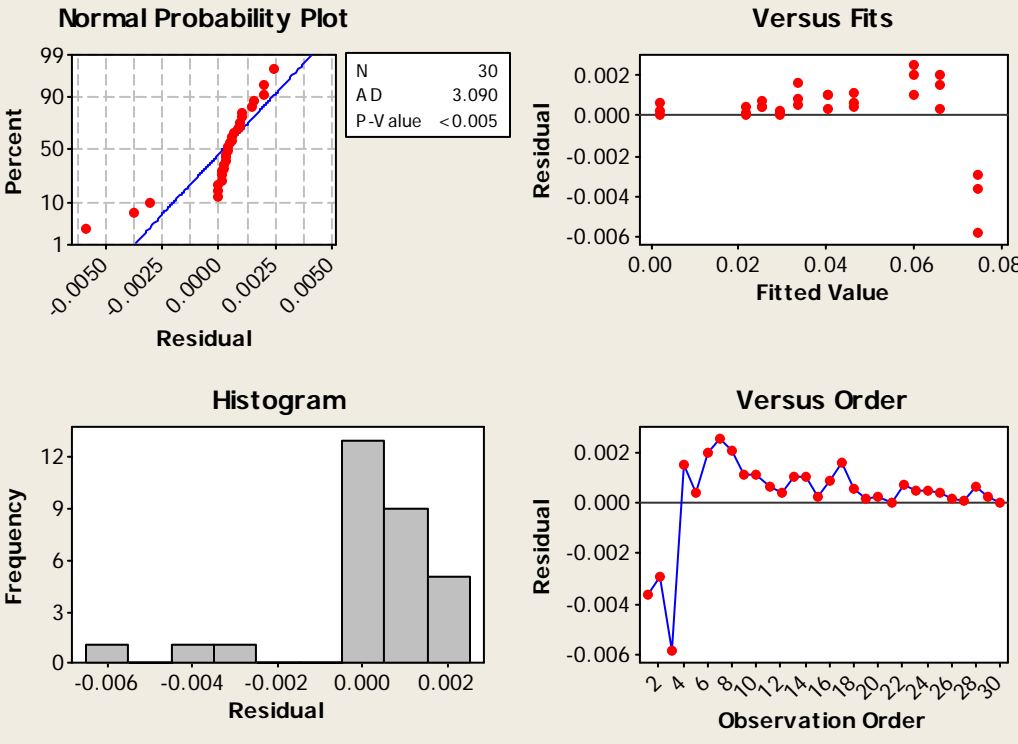
ANOVA					
	<i>df</i>	<i>SS</i>	<i>MS</i>	<i>F</i>	<i>Significance F</i>
Regression	1	0.0611	0.0611	21238.4078	7.0347E-42
Residual	29	0.0001	2.87786E-06		
Total	30	0.0612			

	<i>Coefficients</i>	<i>Standard Error</i>	<i>t Stat</i>	<i>P-value</i>	<i>Lower 95%</i>	<i>Upper 95%</i>
Intercept	0	#N/A	#N/A	#N/A	#N/A	#N/A
Slope	0.0658	0.0005	145.7340	4.1705E-43	0.0649	0.0667

* the intercept term was determined to be not significant during the initial analyses and was therefore eliminated from the model and the regression and ANOVA reanalyzed.



Residual Plots for Flowrate, Q (L/s), Clogging Test Trial 17

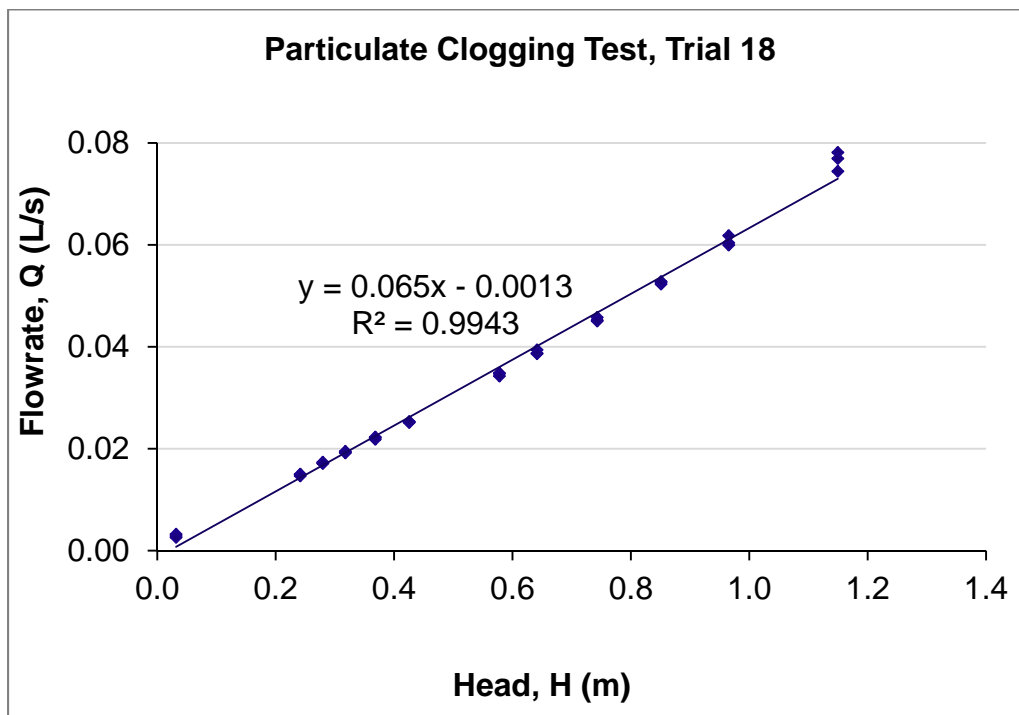


Appendix A.39: Regression Statistics on SmartDrain™ Clogging Test, Trial#18.

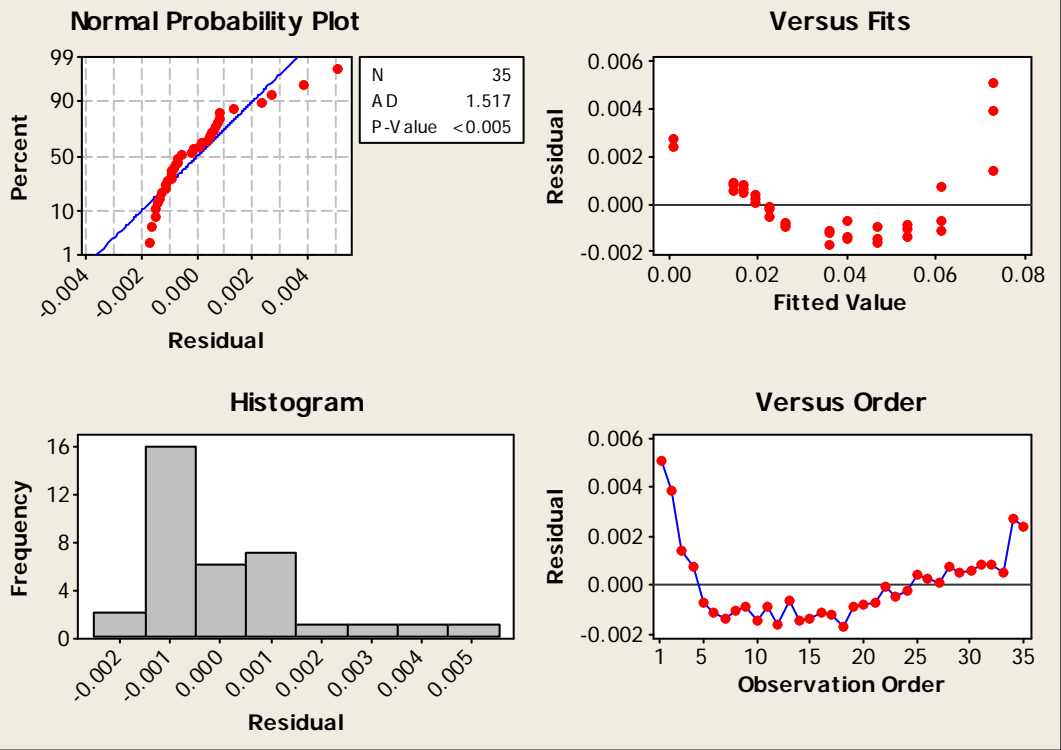
<i>Regression Statistics</i>	
Multiple R	0.9971
R Square	0.9943
Adjusted R Square	0.9941
Standard Error	0.0016
Observations	36

ANOVA					
	<i>df</i>	<i>SS</i>	<i>MS</i>	<i>F</i>	<i>Significance F</i>
Regression	1	0.0151	0.0151	5917.6034	1.00126E-39
Residual	34	0.0001	2.55436E-06		
Total	35	0.0152			

	<i>Coefficients</i>	<i>Standard Error</i>	<i>t Stat</i>	<i>P-value</i>	<i>Lower 95%</i>	<i>Upper 95%</i>
Intercept	-0.0013	0.0005	-2.4032	0.0219	-0.0024	-0.0002
Slope	0.0646	0.0008	76.9260	1.0013E-39	0.0629	0.0663



Residual Plots for Flowrate, Q (L/s), Clogging Test Trial 18

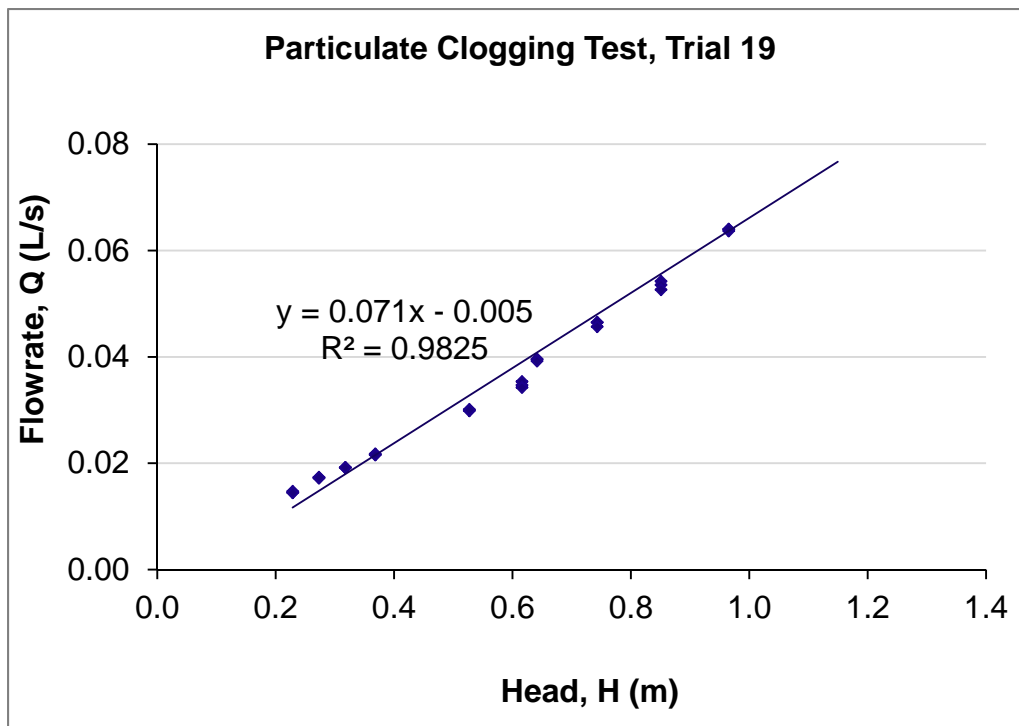


Appendix A.40: Regression Statistics on SmartDrain™ Clogging Test, Trial#19.

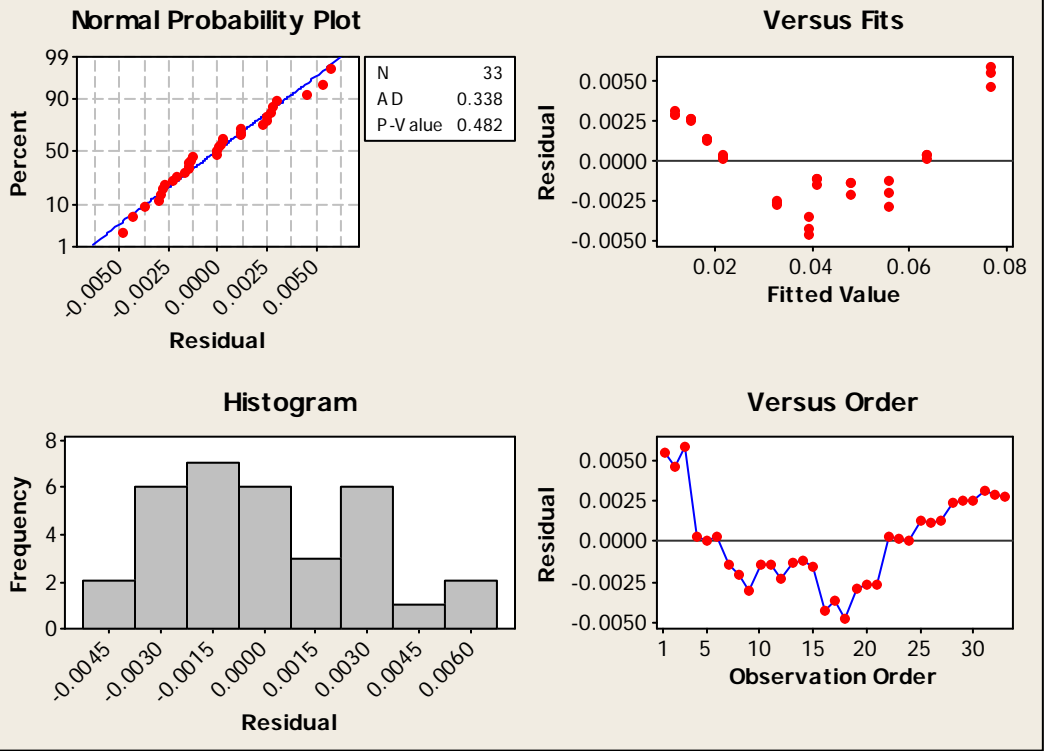
<i>Regression Statistics</i>	
Multiple R	0.9912
R Square	0.9825
Adjusted R Square	0.9819
Standard Error	0.0028
Observations	33

ANOVA					
	<i>df</i>	<i>SS</i>	<i>MS</i>	<i>F</i>	<i>Significance F</i>
Regression	1	0.0135	0.0135	1738.7909	8.50504E-29
Residual	31	0.0002	7.77488E-06		
Total	32	0.0138			

	<i>Coefficients</i>	<i>Standard Error</i>	<i>t Stat</i>	<i>P-value</i>	<i>Lower 95%</i>	<i>Upper 95%</i>
Intercept	-0.0045	0.0011	-3.9361	0.0004	-0.0068	-0.0022
Slope	0.0706	0.0017	41.6988	8.505E-29	0.0672	0.0741



Residual Plots for Flowrate, Q (L/s), Clogging Test Trial 19

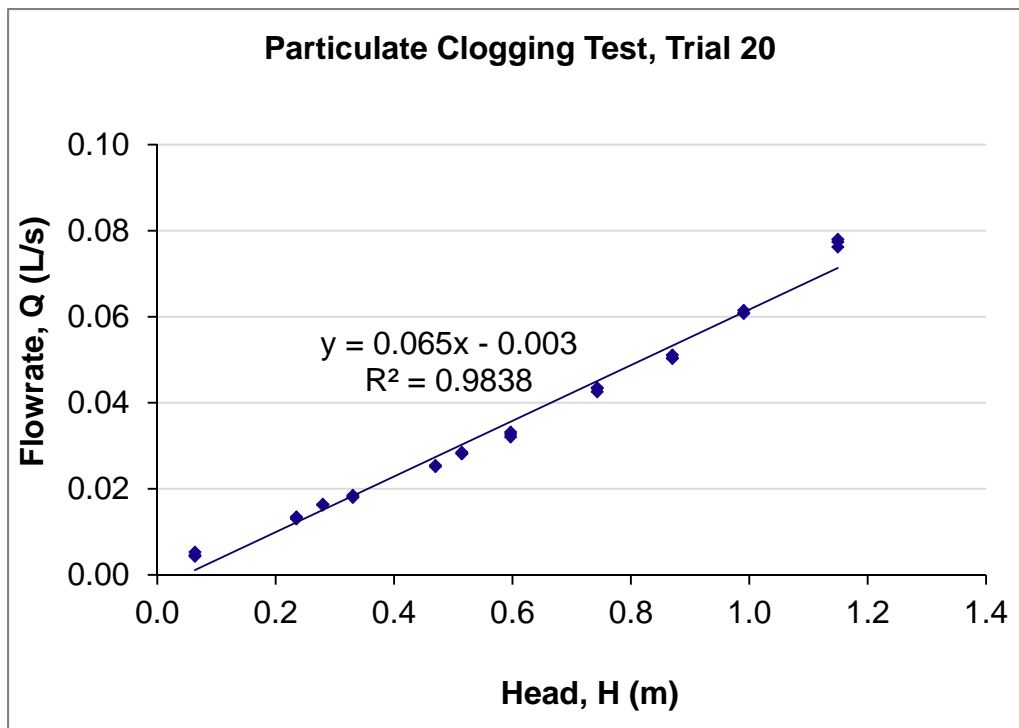


Appendix A.41: Regression Statistics on SmartDrain™ Clogging Test, Trial#20.

<i>Regression Statistics</i>	
Multiple R	0.9919
R Square	0.9838
Adjusted R Square	0.9833
Standard Error	0.0028
Observations	33

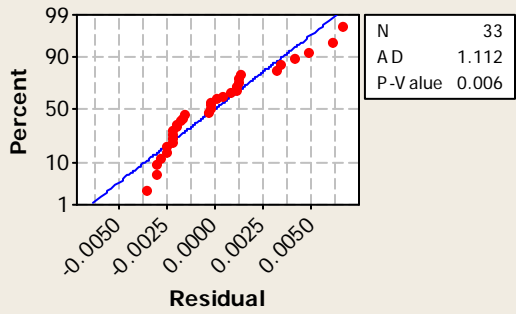
ANOVA					
	<i>df</i>	<i>SS</i>	<i>MS</i>	<i>F</i>	<i>Significance F</i>
Regression	1	0.0145	0.0145	1883.6340	2.51109E-29
Residual	31	0.0002	7.69963E-06		
Total	32	0.0147			

	<i>Coefficients</i>	<i>Standard Error</i>	<i>t Stat</i>	<i>P-value</i>	<i>Lower 95%</i>	<i>Upper 95%</i>
Intercept	-0.0030	0.0010	-3.0454	0.0047	-0.0050	-0.0010
Slope	0.0646	0.0015	43.4009	2.5111E-29	0.0616	0.0677

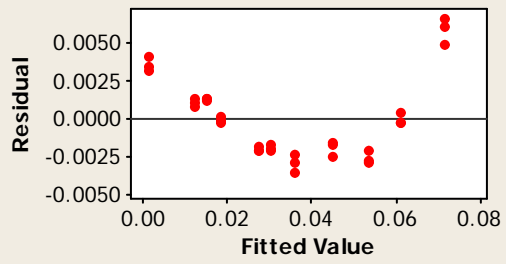


Residual Plots for Flowrate, Q (L/s), Clogging Test Trial 20

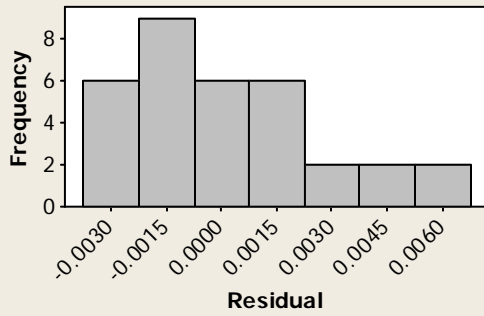
Normal Probability Plot



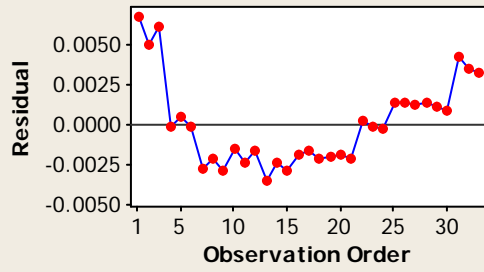
Versus Fits



Histogram



Versus Order

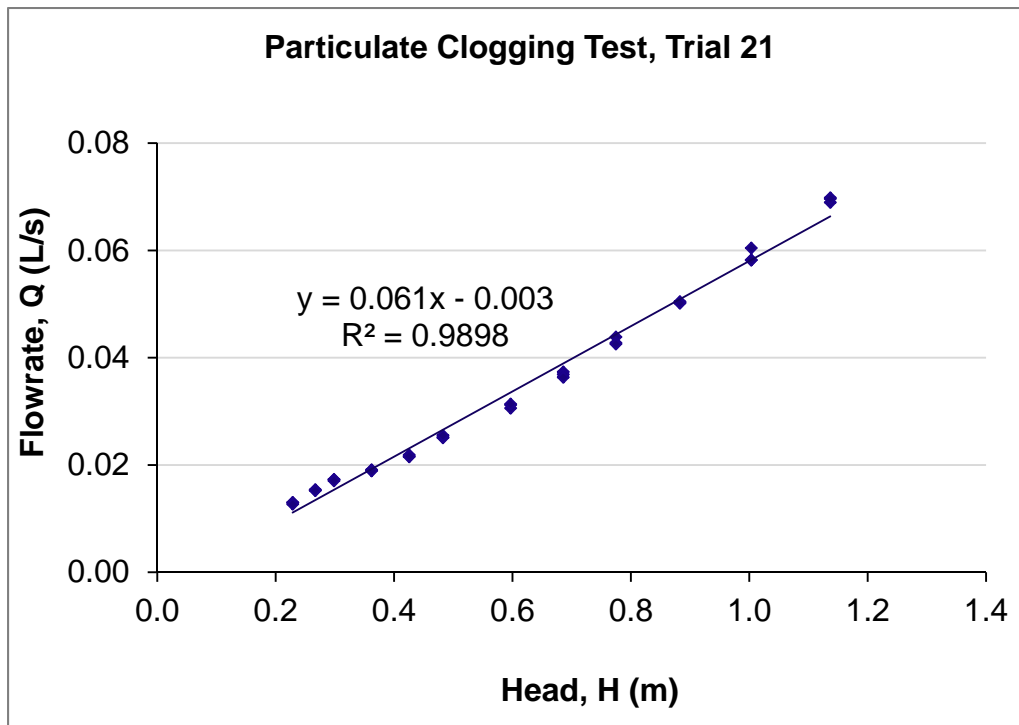


Appendix A.42: Regression Statistics on SmartDrain™ Clogging Test, Trial#21.

<i>Regression Statistics</i>	
Multiple R	0.9949
R Square	0.9898
Adjusted R Square	0.9895
Standard Error	0.0018
Observations	36

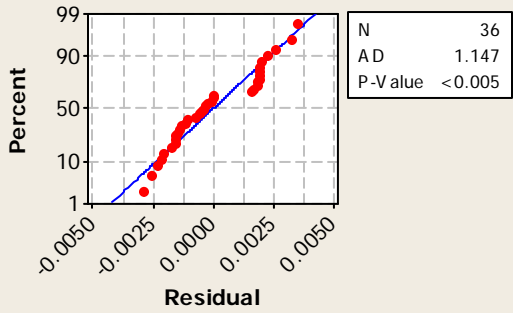
ANOVA					
	<i>df</i>	<i>SS</i>	<i>MS</i>	<i>F</i>	<i>Significance F</i>
Regression	1	0.0112	0.0112	3307.9775	1.82888E-35
Residual	34	0.0001	3.38758E-06		
Total	35	0.0113			

	<i>Coefficients</i>	<i>Standard Error</i>	<i>t Stat</i>	<i>P-value</i>	<i>Lower 95%</i>	<i>Upper 95%</i>
Intercept	-0.0028	0.0007	-3.9914	0.0003	-0.0042	-0.0014
Slope	0.0608	0.0011	57.5150	1.8289E-35	0.0587	0.0630

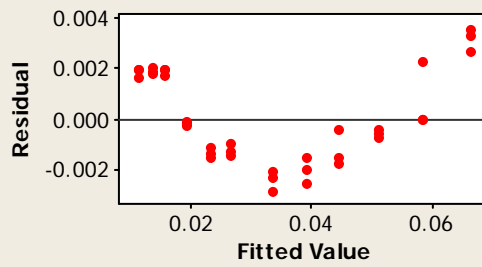


Residual Plots for Flowrate, Q (L/s), Clogging Test Trial 21

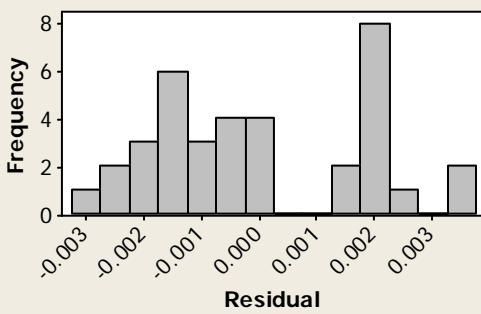
Normal Probability Plot



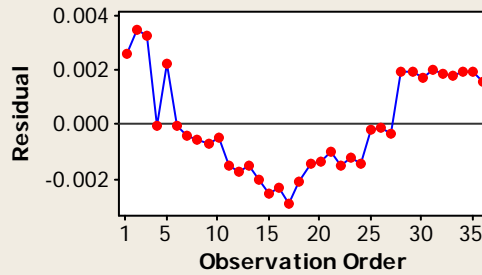
Versus Fits



Histogram



Versus Order

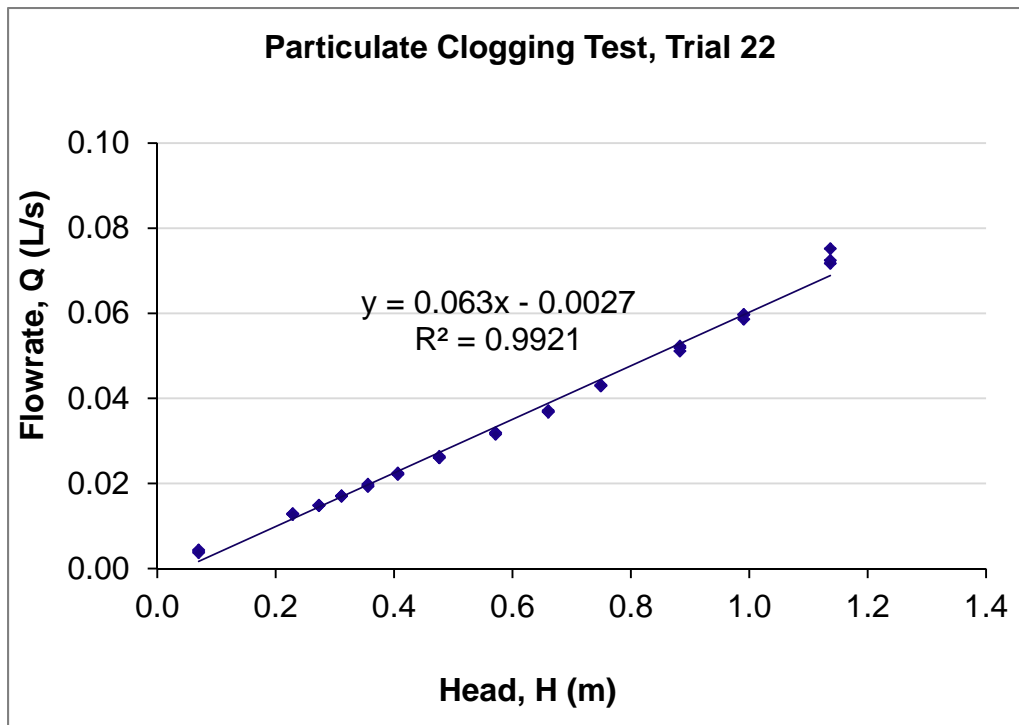


Appendix A.43: Regression Statistics on SmartDrain™ Clogging Test, Trial#22.

<i>Regression Statistics</i>	
Multiple R	0.9960
R Square	0.9921
Adjusted R Square	0.9919
Standard Error	0.0018
Observations	39

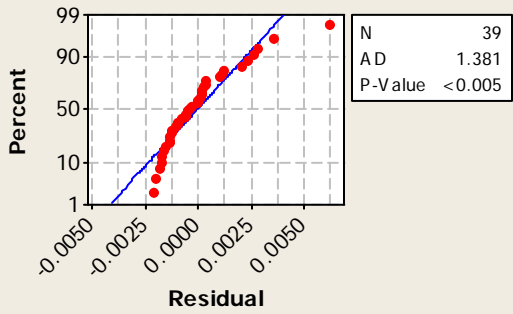
ANOVA					
	<i>df</i>	<i>SS</i>	<i>MS</i>	<i>F</i>	<i>Significance F</i>
Regression	1	0.0147	0.0147	4627.5130	1.80037E-40
Residual	37	0.0001	3.16947E-06		
Total	38	0.0148			

	<i>Coefficients</i>	<i>Standard Error</i>	<i>t Stat</i>	<i>P-value</i>	<i>Lower 95%</i>	<i>Upper 95%</i>
Intercept	-0.0027	0.0006	-4.6449	4.2017E-05	-0.0039	-0.0015
Slope	0.0630	0.0009	68.0258	1.8004E-40	0.0611	0.0649

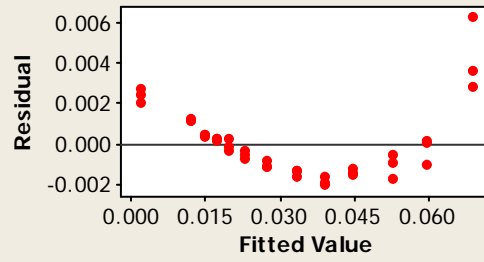


Residual Plots for Flowrate, Q (L/s), Clogging Test Trial 22

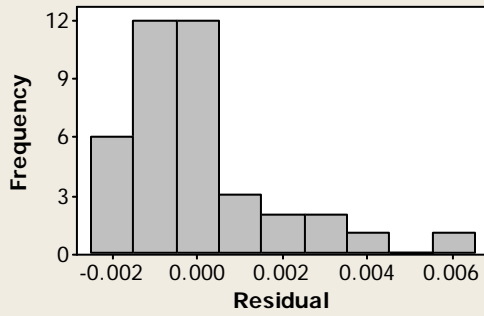
Normal Probability Plot



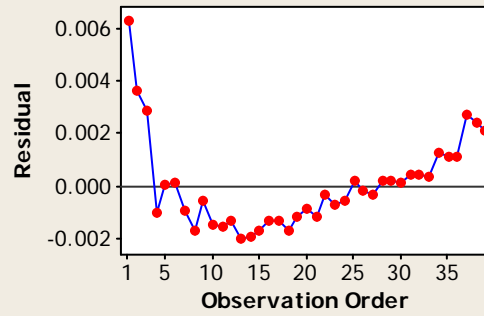
Versus Fits



Histogram



Versus Order

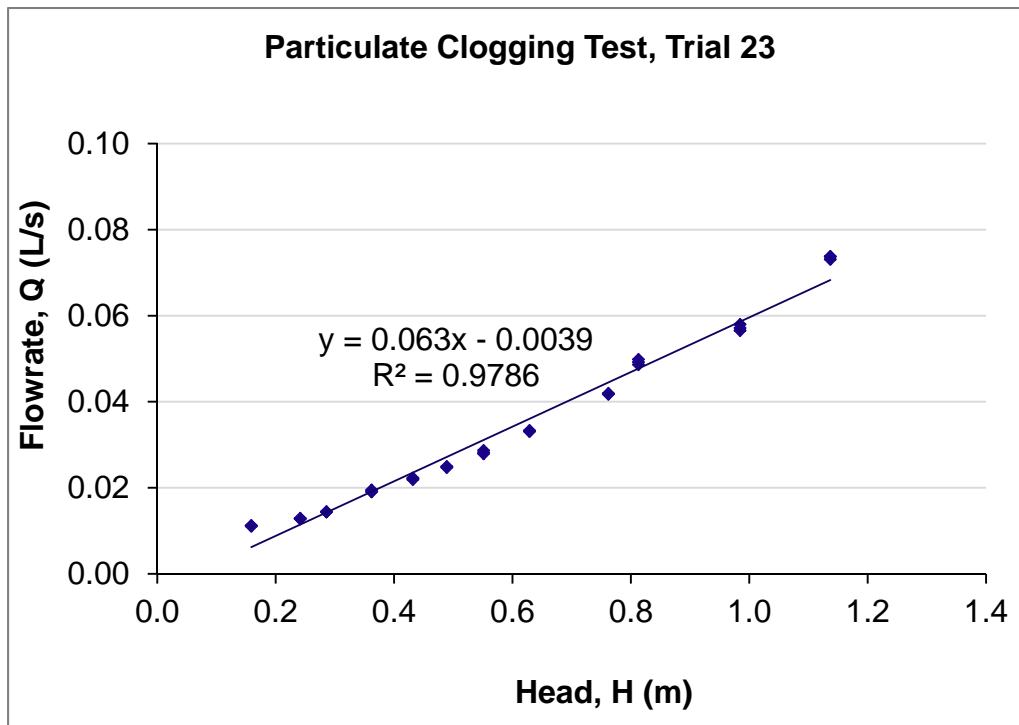


Appendix A.44: Regression Statistics on SmartDrain™ Clogging Test, Trial#23.

<i>Regression Statistics</i>	
Multiple R	0.9892
R Square	0.9786
Adjusted R Square	0.9779
Standard Error	0.0028
Observations	36

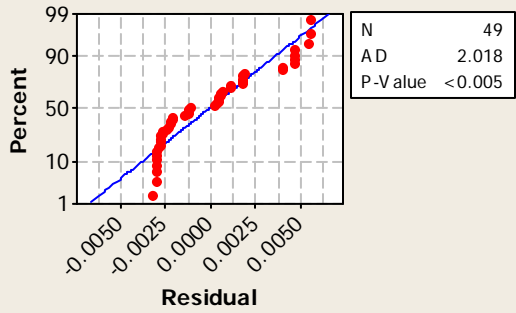
ANOVA					
	<i>df</i>	<i>SS</i>	<i>MS</i>	<i>F</i>	<i>Significance F</i>
Regression	1	0.0123	0.0123	1552.7705	5.80563E-30
Residual	34	0.0003	7.92672E-06		
Total	35	0.0126			

	<i>Coefficients</i>	<i>Standard Error</i>	<i>t Stat</i>	<i>P-value</i>	<i>Lower 95%</i>	<i>Upper 95%</i>
Intercept	-0.0039	0.0010	-3.7417	0.0007	-0.0060	-0.0018
Slope	0.0634	0.0016	39.4052	5.8056E-30	0.0602	0.0667

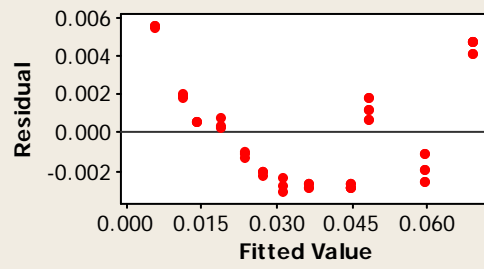


Residual Plots for Flowrate, Q (L/s), Clogging Test Trial 23

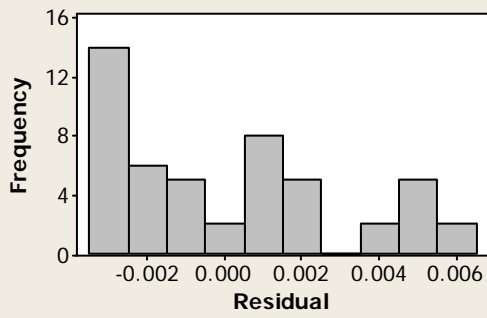
Normal Probability Plot



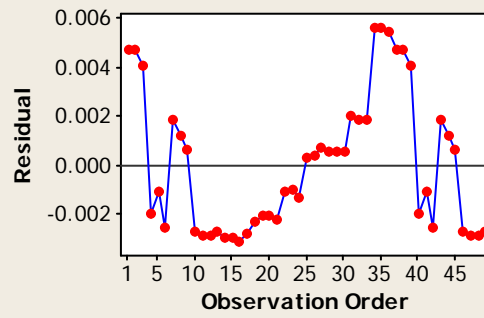
Versus Fits



Histogram



Versus Order

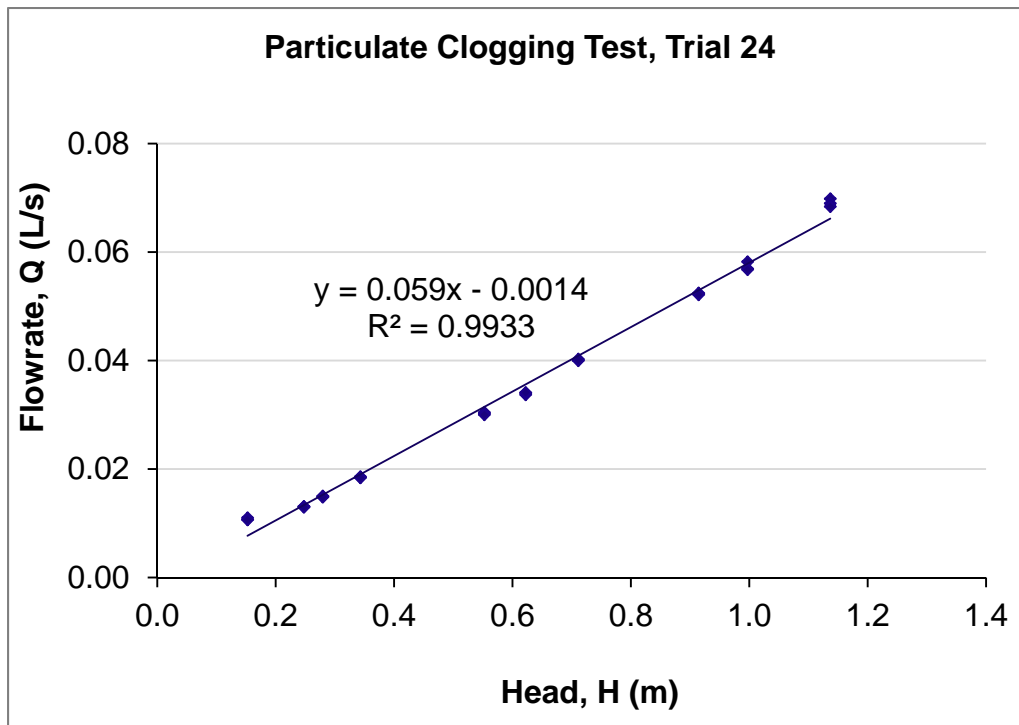


Appendix A.45: Regression Statistics on SmartDrain™ Clogging Test, Trial#24.

<i>Regression Statistics</i>	
Multiple R	0.9967
R Square	0.9933
Adjusted R Square	0.9931
Standard Error	0.0016
Observations	30

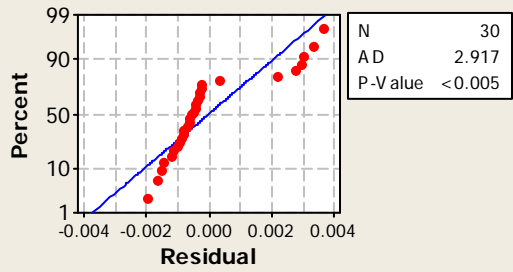
ANOVA					
	<i>df</i>	<i>SS</i>	<i>MS</i>	<i>F</i>	<i>Significance F</i>
Regression	1	0.0111	0.0111	4161.9398	5.31063E-32
Residual	28	0.0001	2.67827E-06		
Total	29	0.0112			

	<i>Coefficients</i>	<i>Standard Error</i>	<i>t Stat</i>	<i>P-value</i>	<i>Lower 95%</i>	<i>Upper 95%</i>
Intercept	-0.0014	0.0006	-2.1753	0.0382	-0.0026	-0.0001
Slope	0.0594	0.0009	64.5131	5.3106E-32	0.0575	0.0613

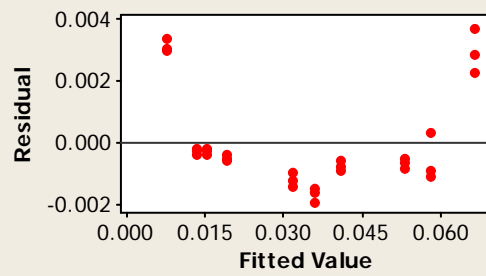


Residual Plots for Flowrate, Q (L/s), Clogging Test Trial 24

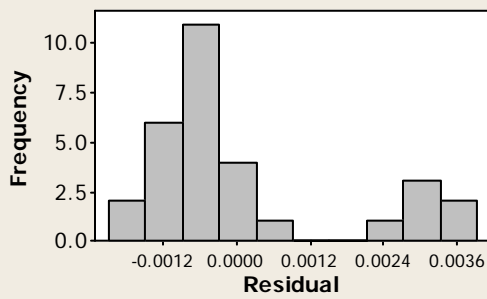
Normal Probability Plot



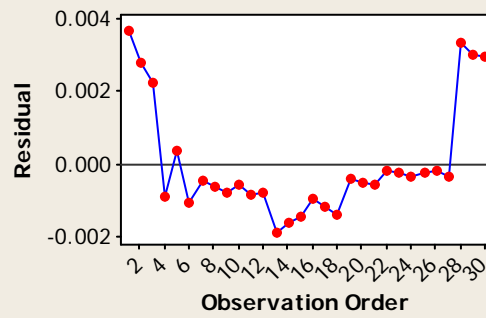
Versus Fits



Histogram



Versus Order

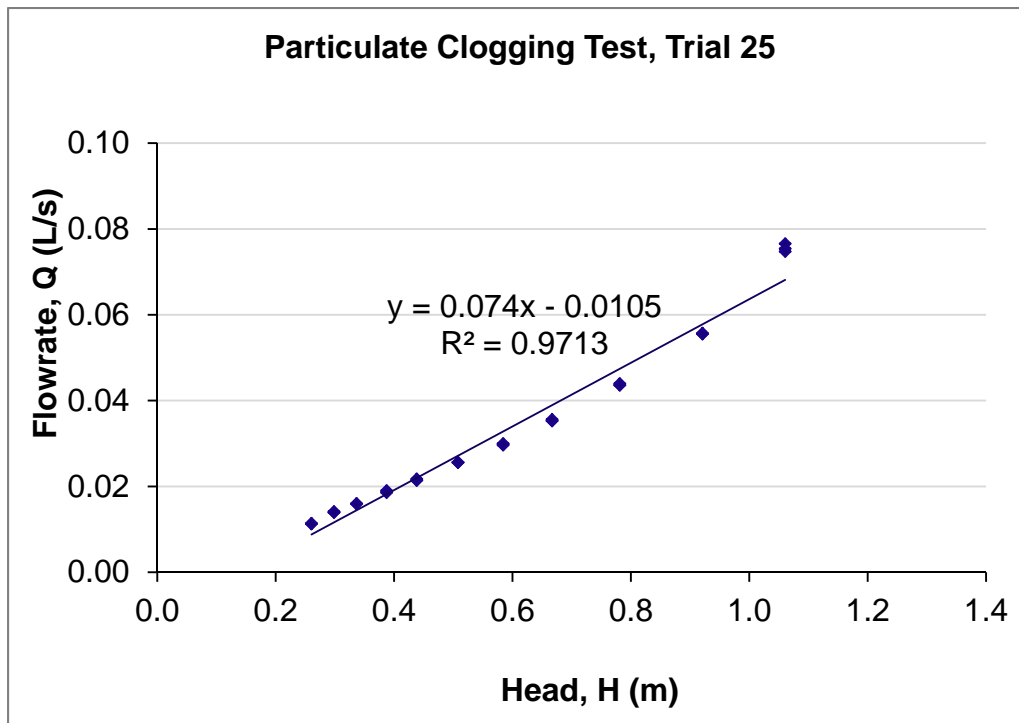


Appendix A.46: Regression Statistics on SmartDrain™ Clogging Test, Trial#25.

<i>Regression Statistics</i>	
Multiple R	0.9855
R Square	0.9713
Adjusted R Square	0.9704
Standard Error	0.0033
Observations	33

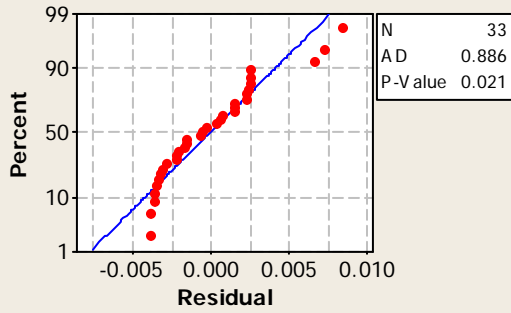
ANOVA					
	<i>df</i>	<i>SS</i>	<i>MS</i>	<i>F</i>	<i>Significance F</i>
Regression	1	0.0115	0.0115	1048.4743	1.81975E-25
Residual	31	0.0003	1.09547E-05		
Total	32	0.0118			

	<i>Coefficients</i>	<i>Standard Error</i>	<i>t Stat</i>	<i>P-value</i>	<i>Lower 95%</i>	<i>Upper 95%</i>
Intercept	-0.0105	0.0014	-7.3849	2.5763E-08	-0.0134	-0.0076
Slope	0.0742	0.0023	32.3802	1.8197E-25	0.0695	0.0788

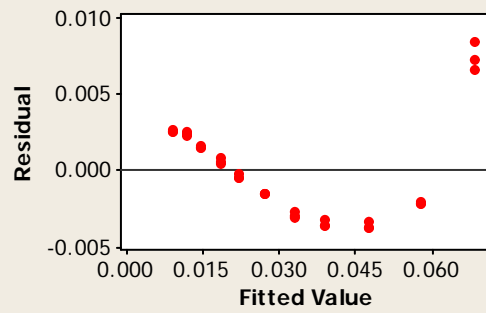


Residual Plots for Flowrate, Q (L/s), Clogging Test Trial 25

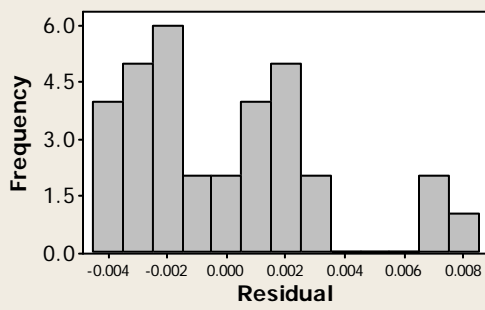
Normal Probability Plot



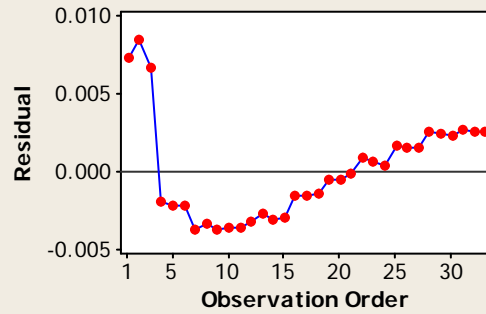
Versus Fits



Histogram



Versus Order

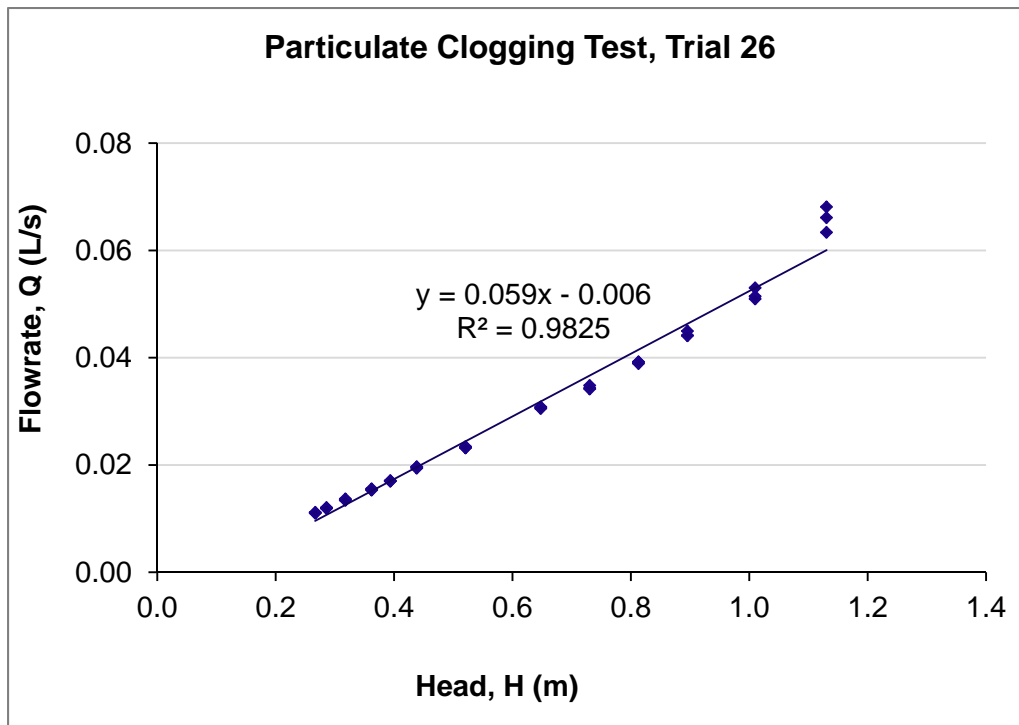


Appendix A.47: Regression Statistics on SmartDrain™ Clogging Test, Trial#26.

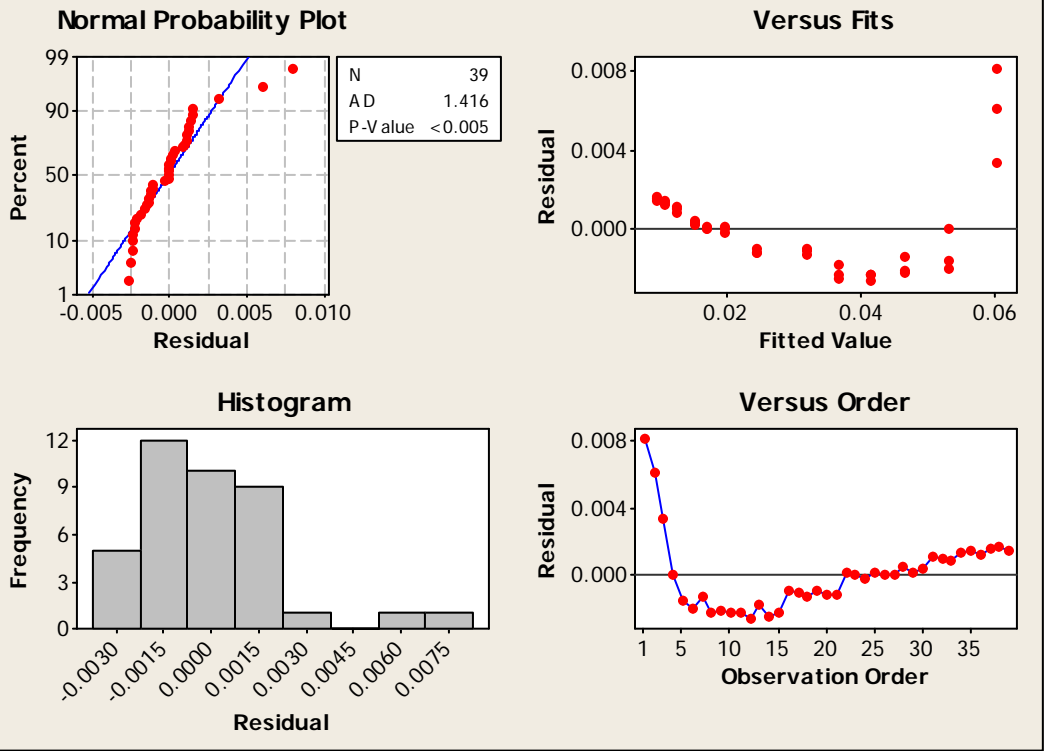
<i>Regression Statistics</i>	
Multiple R	0.9912
R Square	0.9825
Adjusted R Square	0.9821
Standard Error	0.0022
Observations	39

ANOVA					
	<i>df</i>	<i>SS</i>	<i>MS</i>	<i>F</i>	<i>Significance F</i>
Regression	1	0.0105	0.0105	2080.6903	3.99771E-34
Residual	37	0.0002	5.03768E-06		
Total	38	0.0107			

	<i>Coefficients</i>	<i>Standard Error</i>	<i>t Stat</i>	<i>P-value</i>	<i>Lower 95%</i>	<i>Upper 95%</i>
Intercept	-0.0060	0.0008	-7.0960	2.1126E-08	-0.0078	-0.0043
Slope	0.0585	0.0013	45.6146	3.9977E-34	0.0559	0.0611



Residual Plots for Flowrate, Q (L/s), Clogging Test Trial 26

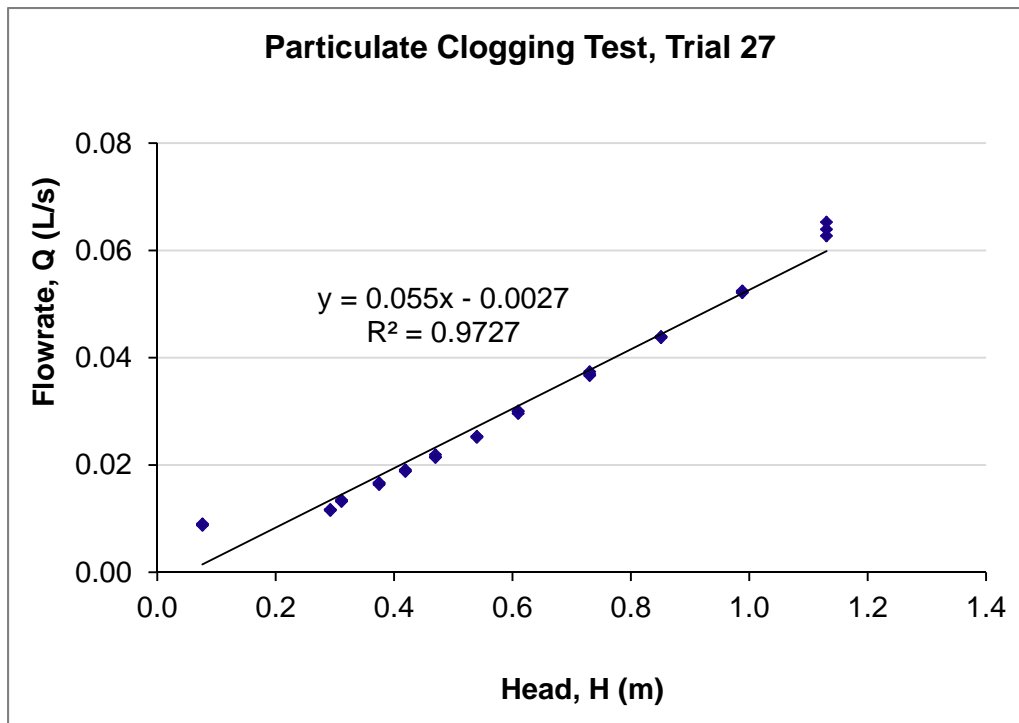


Appendix A.48: Regression Statistics on SmartDrain™ Clogging Test, Trial#27.

<i>Regression Statistics</i>	
Multiple R	0.9863
R Square	0.9727
Adjusted R Square	0.9719
Standard Error	0.0028
Observations	36

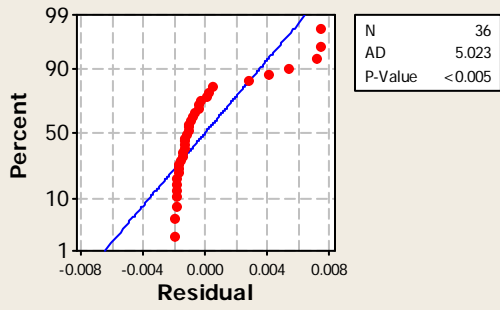
ANOVA					
	<i>df</i>	<i>SS</i>	<i>MS</i>	<i>F</i>	<i>Significance F</i>
Regression	1	0.0097	0.0097	1211.3068	3.58199E-28
Residual	34	0.0003	8.01595E-06		
Total	35	0.0100			

	<i>Coefficients</i>	<i>Standard Error</i>	<i>t Stat</i>	<i>P-value</i>	<i>Lower 95%</i>	<i>Upper 95%</i>
Intercept	-0.0027	0.0010	-2.7027	0.0107	-0.0048	-0.0007
Slope	0.0554	0.0016	34.8038	3.582E-28	0.0522	0.0586

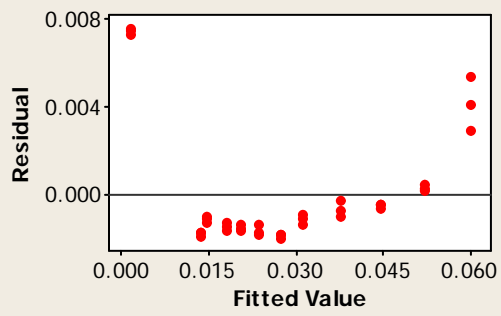


Residual Plots for Flowrate, Q (L/s), Clogging Test Trial 27

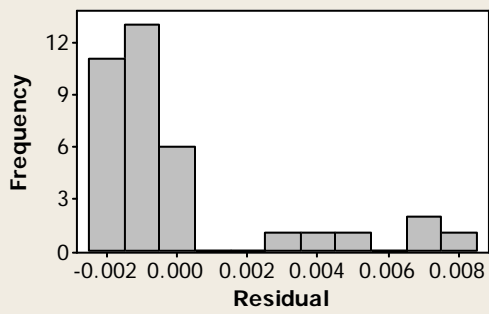
Normal Probability Plot



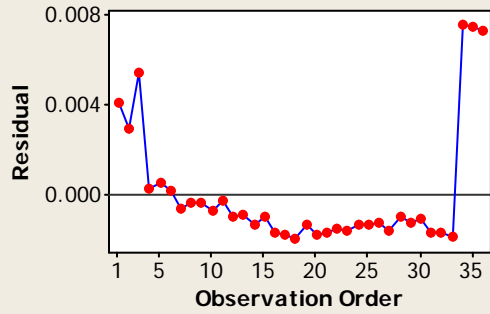
Versus Fits



Histogram



Versus Order

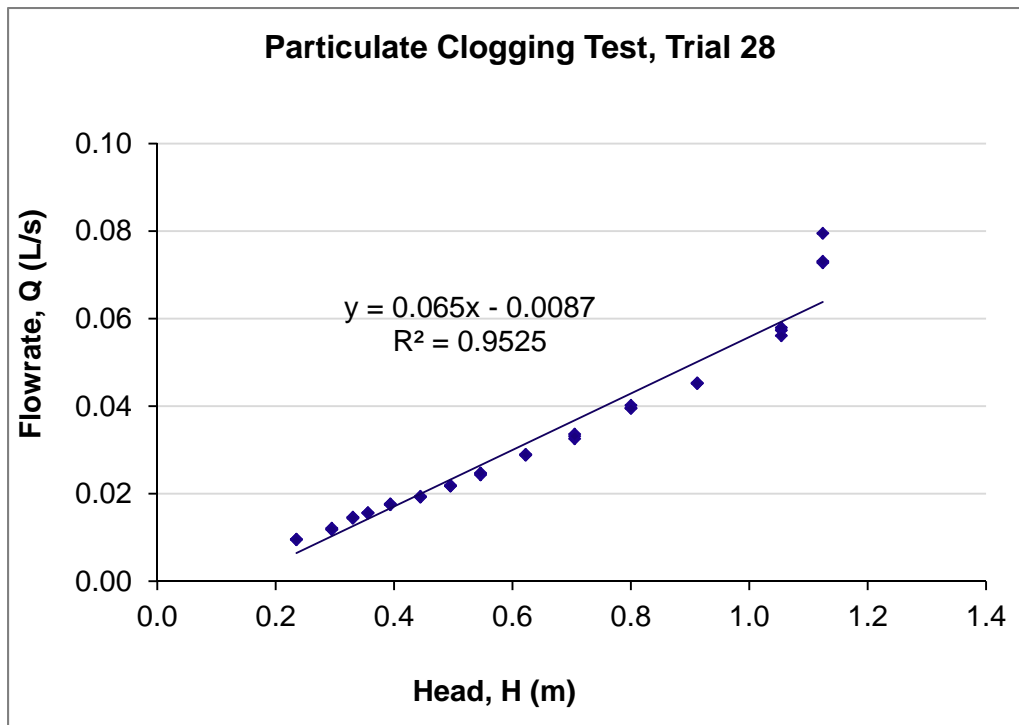


Appendix A.49: Regression Statistics on SmartDrain™ Clogging Test, Trial#28.

<i>Regression Statistics</i>	
Multiple R	0.9759
R Square	0.9525
Adjusted R Square	0.9513
Standard Error	0.0041
Observations	42

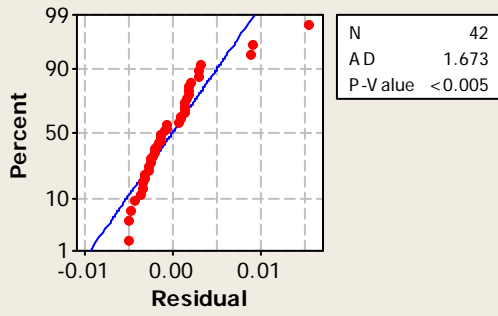
ANOVA					
	<i>df</i>	<i>SS</i>	<i>MS</i>	<i>F</i>	<i>Significance F</i>
Regression	1	0.0134	0.0134	801.6109	4.43842E-28
Residual	40	0.0007	0.0000		
Total	41	0.0140			

	<i>Coefficients</i>	<i>Standard Error</i>	<i>t Stat</i>	<i>P-value</i>	<i>Lower 95%</i>	<i>Upper 95%</i>
Intercept	-0.0087	0.0015	-5.8470	7.7552E-07	-0.0117	-0.0057
Slope	0.0645	0.0023	28.3127	4.4384E-28	0.0599	0.0691

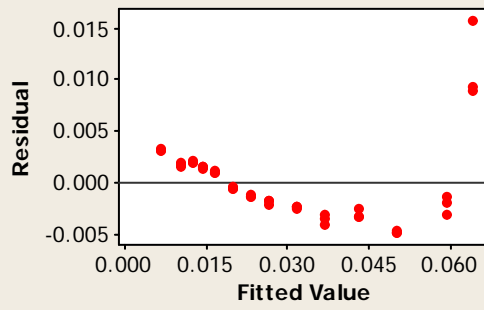


Residual Plots for Flowrate, Q (L/s), Clogging Test Trial 28

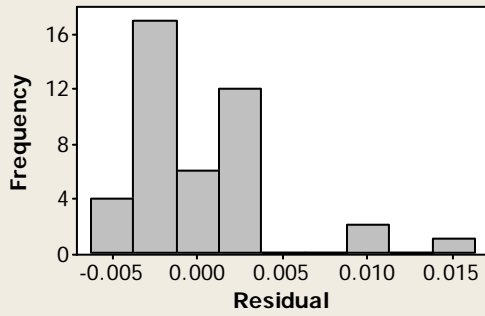
Normal Probability Plot



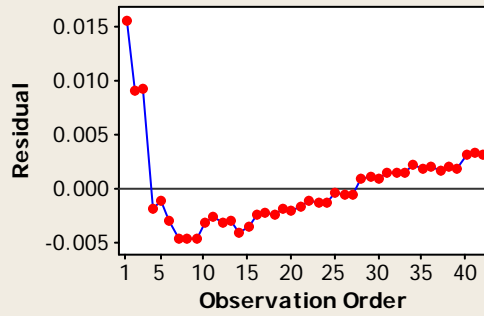
Versus Fits



Histogram



Versus Order

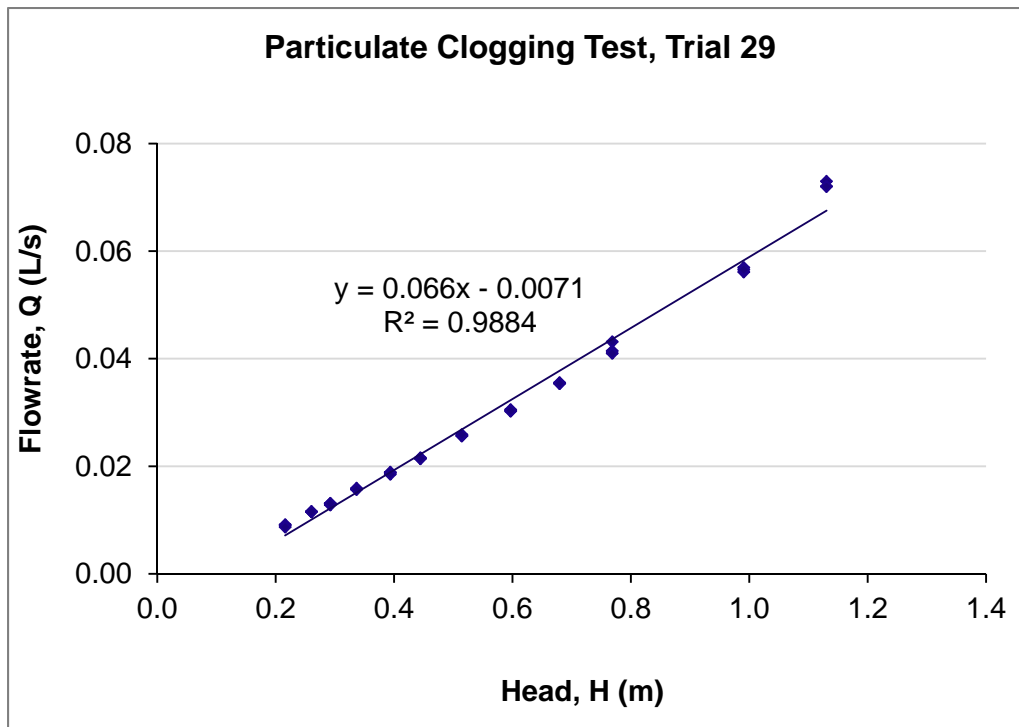


Appendix A.50: Regression Statistics on SmartDrain™ Clogging Test, Trial#29.

<i>Regression Statistics</i>	
Multiple R	0.9942
R Square	0.9884
Adjusted R Square	0.9880
Standard Error	0.0021
Observations	36

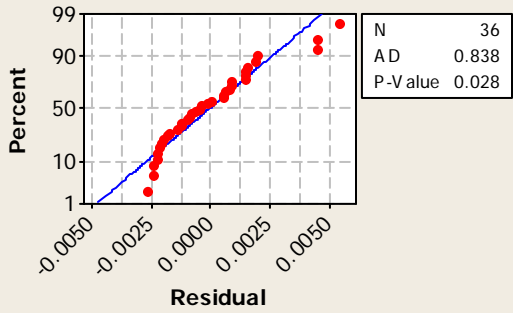
ANOVA					
	<i>df</i>	<i>SS</i>	<i>MS</i>	<i>F</i>	<i>Significance F</i>
Regression	1	0.0123	0.0123	2885.6502	1.81939E-34
Residual	34	0.0001	0.0000		
Total	35	0.0125			

	<i>Coefficients</i>	<i>Standard Error</i>	<i>t Stat</i>	<i>P-value</i>	<i>Lower 95%</i>	<i>Upper 95%</i>
Intercept	-0.0071	0.0008	-9.3569	6.2221E-11	-0.0087	-0.0056
Slope	0.0660	0.0012	53.7182	1.8194E-34	0.0635	0.0685

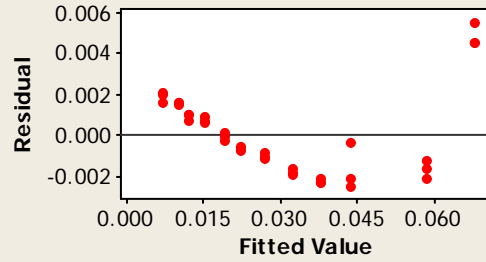


Residual Plots for Flowrate, Q (L/s), Clogging Test Trial 29

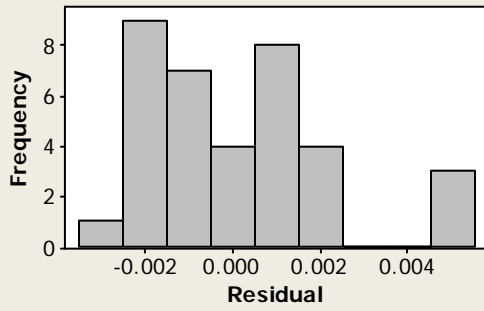
Normal Probability Plot



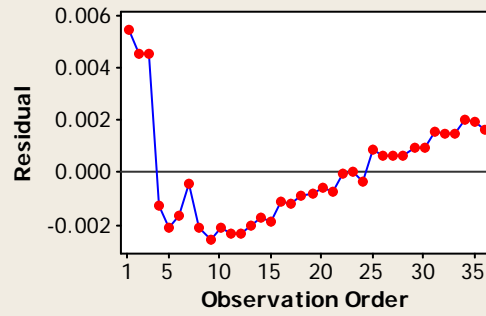
Versus Fits



Histogram



Versus Order

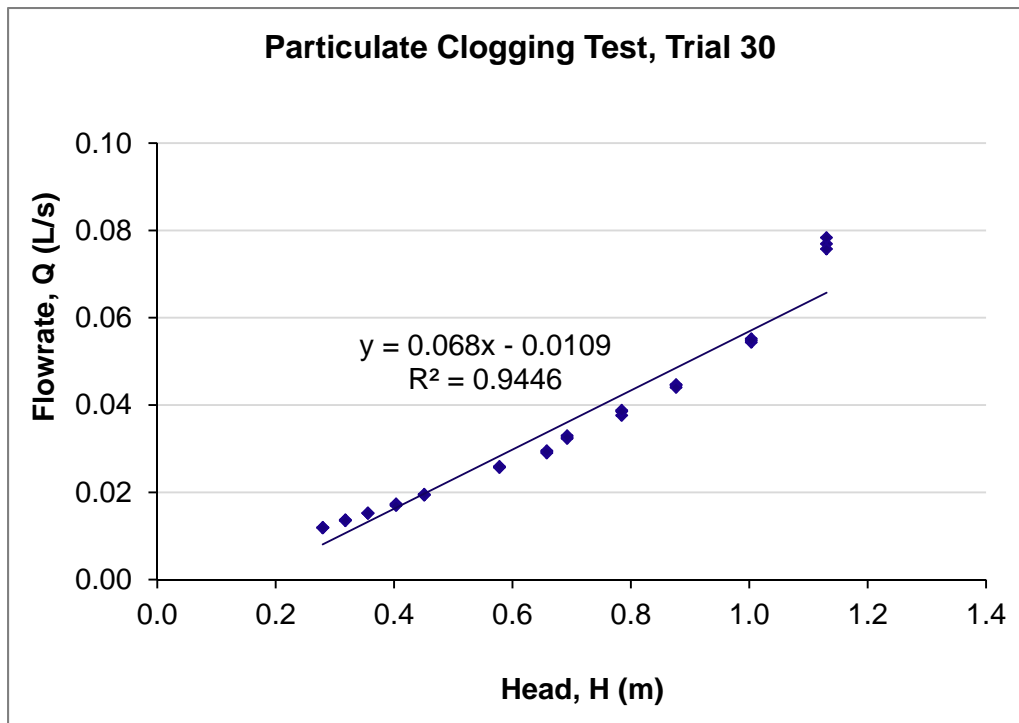


Appendix A.51: Regression Statistics on SmartDrain™ Clogging Test, Trial#30.

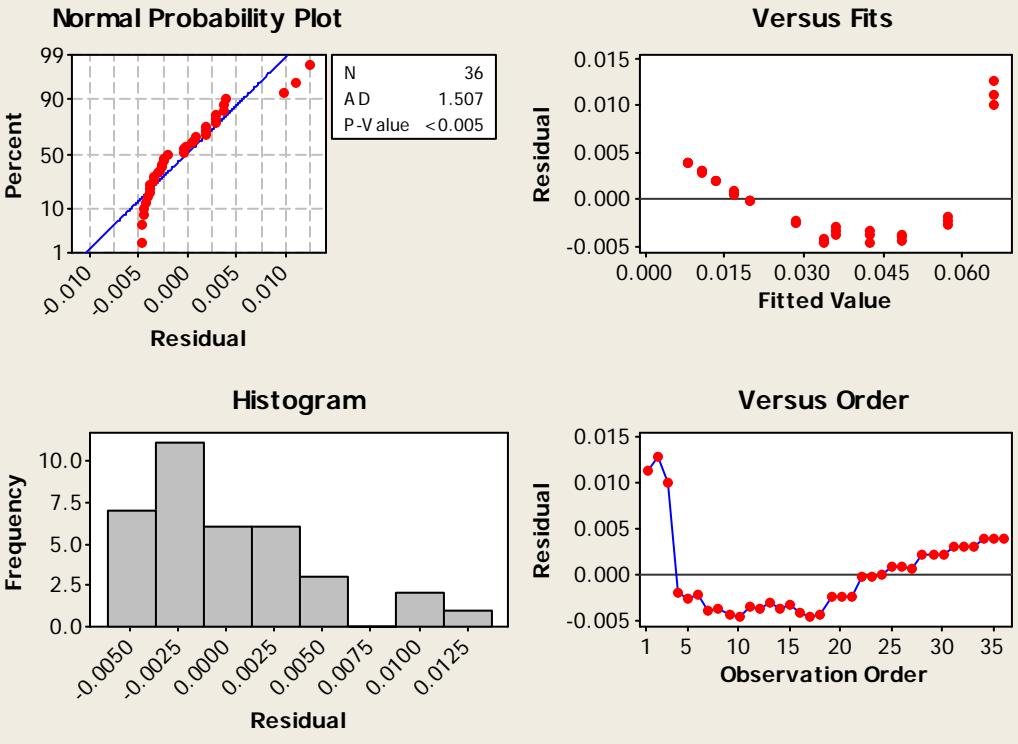
<i>Regression Statistics</i>	
Multiple R	0.9719
R Square	0.9446
Adjusted R Square	0.9430
Standard Error	0.0045
Observations	36

ANOVA					
	<i>df</i>	<i>SS</i>	<i>MS</i>	<i>F</i>	<i>Significance F</i>
Regression	1	0.0119	0.0119	579.7561	6.07982E-23
Residual	34	0.0007	2.047E-05		
Total	35	0.0126			

	<i>Coefficients</i>	<i>Standard Error</i>	<i>t Stat</i>	<i>P-value</i>	<i>Lower 95%</i>	<i>Upper 95%</i>
Intercept	-0.0109	0.0019	-5.6691	2.3181E-06	-0.0148	-0.0070
Slope	0.0678	0.0028	24.0781	6.0798E-23	0.0621	0.0735



Residual Plots for Flowrate, Q (L/s), Clogging Test Trial 30

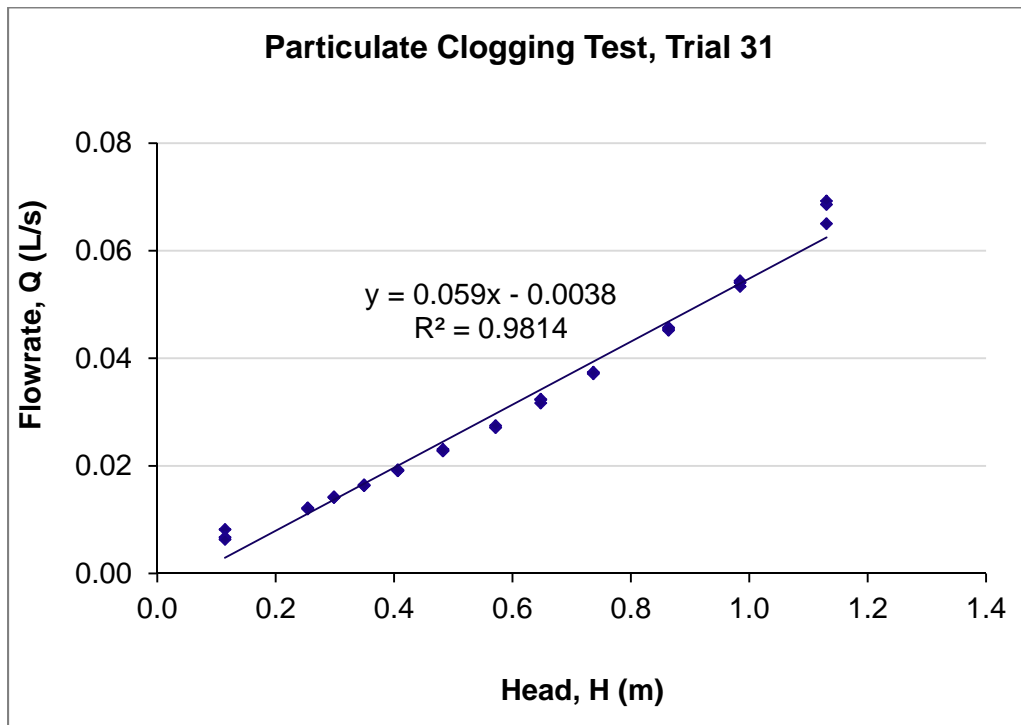


Appendix A.52: Regression Statistics on SmartDrain™ Clogging Test, Trial#31.

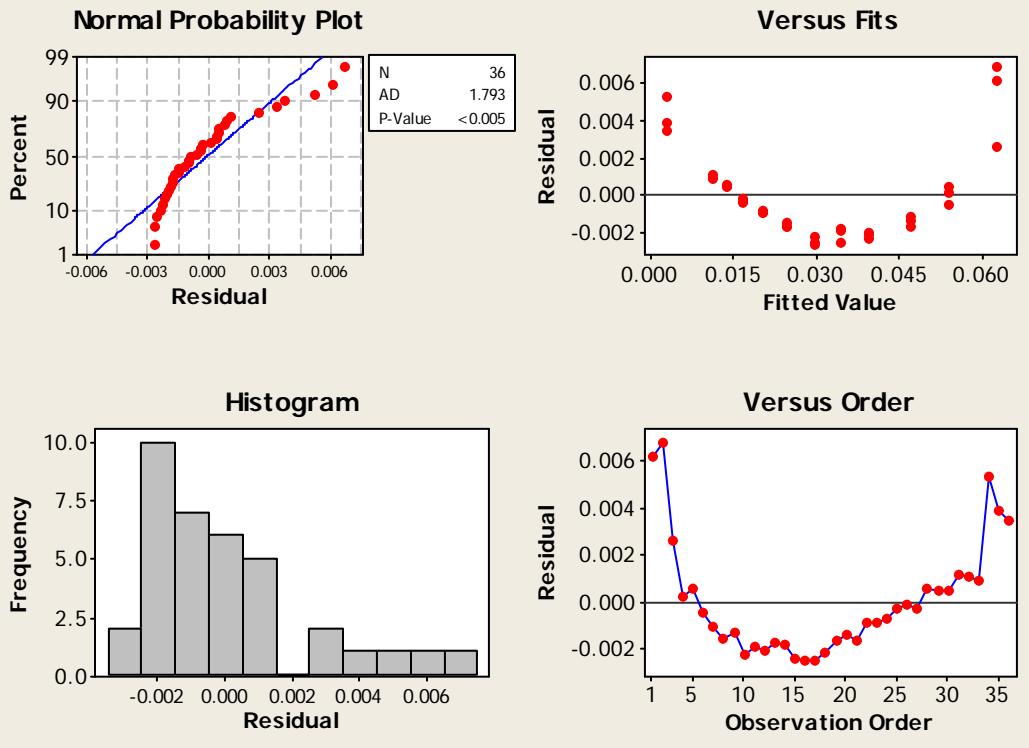
<i>Regression Statistics</i>	
Multiple R	0.9907
R Square	0.9814
Adjusted R Square	0.9808
Standard Error	0.0025
Observations	36

ANOVA					
	<i>df</i>	<i>SS</i>	<i>MS</i>	<i>F</i>	<i>Significance F</i>
Regression	1	0.0110	0.0110	1792.8036	5.28736E-31
Residual	34	0.0002	6.15118E-06		
Total	35	0.0112			

	<i>Coefficients</i>	<i>Standard Error</i>	<i>t Stat</i>	<i>P-value</i>	<i>Lower 95%</i>	<i>Upper 95%</i>
Intercept	-0.0038	0.0009	-4.2537	0.0002	-0.0056	-0.0020
Slope	0.0586	0.0014	42.3415	5.2874E-31	0.0558	0.0614



Residual Plots for Flowrate, Q (L/s), Clogging Test Trial 31

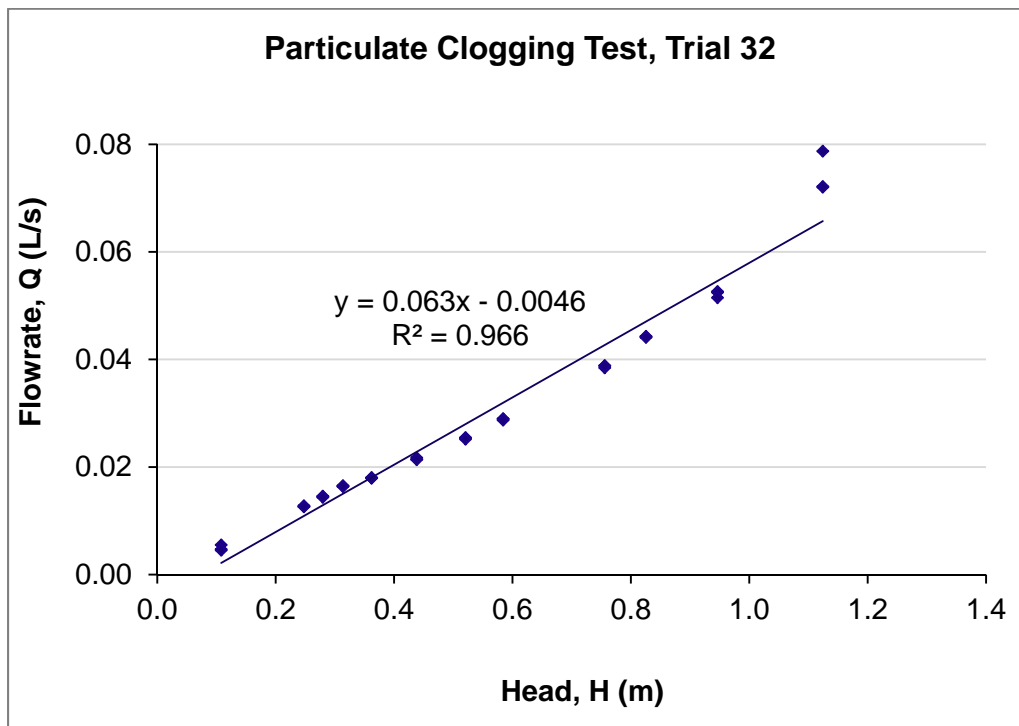


Appendix A.53: Regression Statistics on SmartDrain™ Clogging Test, Trial#32.

<i>Regression Statistics</i>	
Multiple R	0.9829
R Square	0.9660
Adjusted R Square	0.9650
Standard Error	0.0036
Observations	36

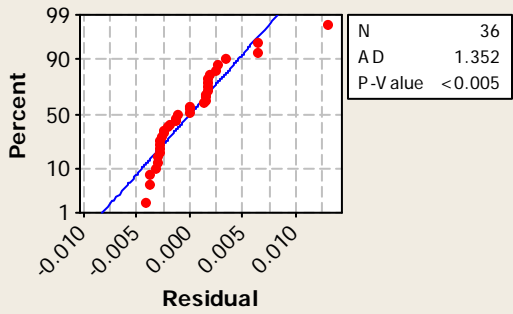
ANOVA					
	<i>df</i>	<i>SS</i>	<i>MS</i>	<i>F</i>	<i>Significance F</i>
Regression	1	0.0125	0.0125	966.0182	1.49659E-26
Residual	34	0.0004	0.0000		
Total	35	0.0130			

	<i>Coefficients</i>	<i>Standard Error</i>	<i>t Stat</i>	<i>P-value</i>	<i>Lower 95%</i>	<i>Upper 95%</i>
Intercept	-0.0046	0.0012	-3.6790	0.0008	-0.0071	-0.0021
Slope	0.0625	0.0020	31.0808	1.4966E-26	0.0584	0.0666

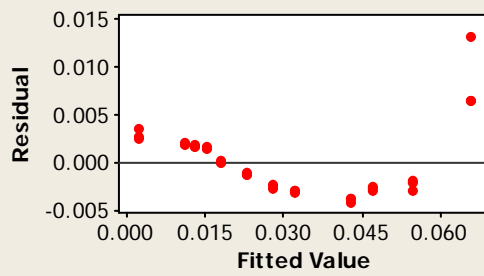


Residual Plots for Flowrate, Q (L/s), Clogging Test Trial 32

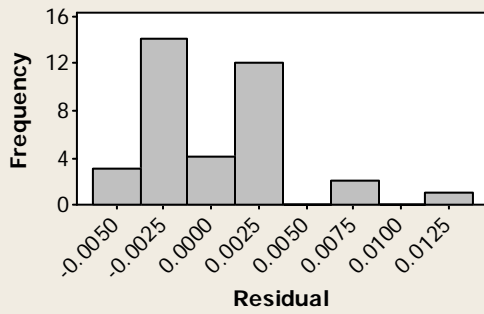
Normal Probability Plot



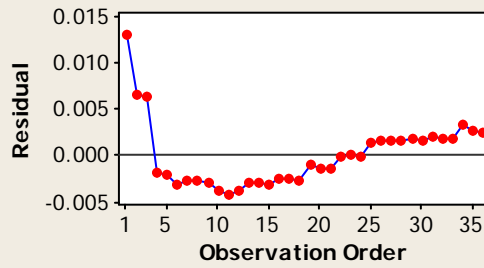
Versus Fits



Histogram



Versus Order

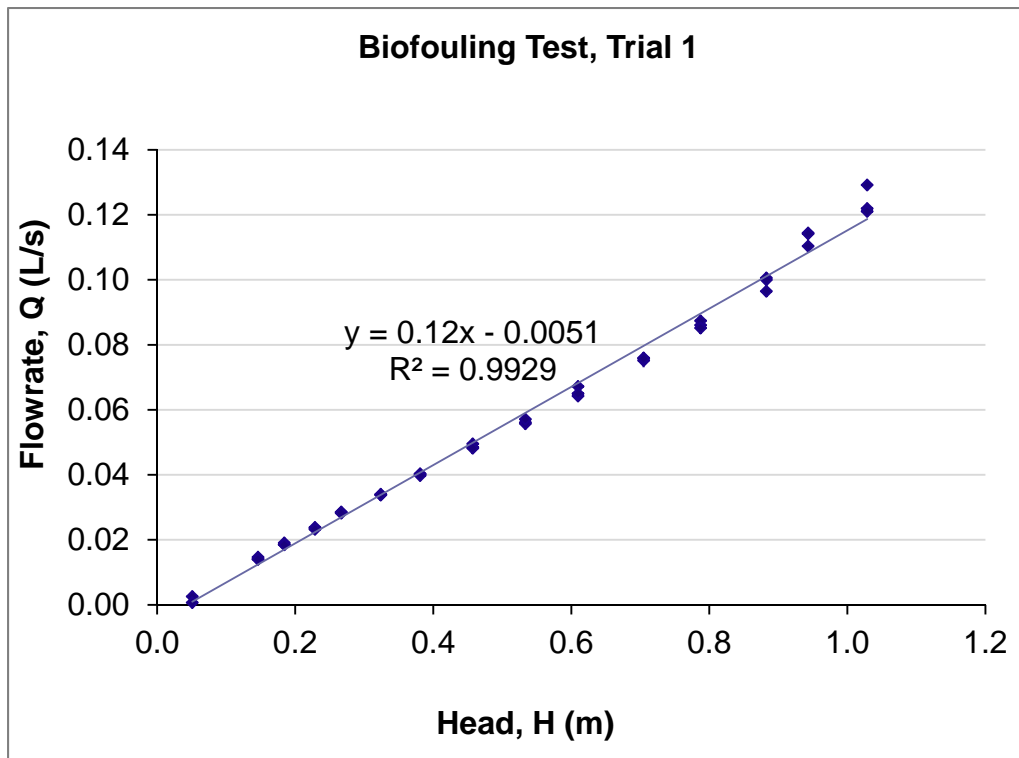


Appendix A.54: Regression Statistics on SmartDrain™ Biofouling Test, Trial#1.

<i>Regression Statistics</i>	
Multiple R	0.9965
R Square	0.9929
Adjusted R Square	0.9928
Standard Error	0.0031
Observations	44

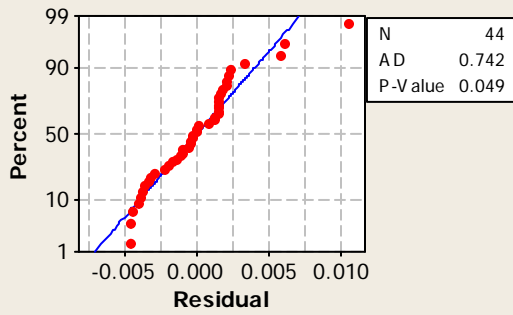
ANOVA					
	<i>df</i>	<i>SS</i>	<i>MS</i>	<i>F</i>	<i>Significance F</i>
Regression	1	0.0562	0.0562	5894.11811	8.58784E-47
Residual	42	0.0004	9.5E-06		
Total	43	0.0566			

	<i>Coefficients</i>	<i>Standard Error</i>	<i>t Stat</i>	<i>P-value</i>	<i>Lower 95%</i>	<i>Upper 95%</i>
Intercept	-0.0051	0.0009	-5.5343	1.85E-06	-0.0070	-0.0033
Slope	0.1203	0.0016	76.7732	8.59E-47	0.1172	0.1235

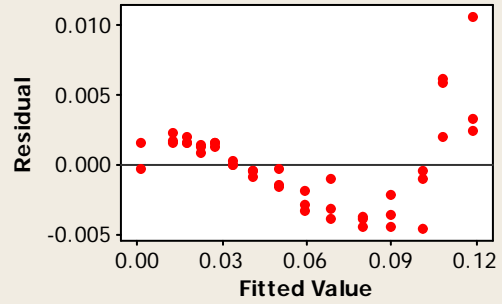


Residual Plots for Flowrate, Q (L/s), Biofouling Test Trial 1

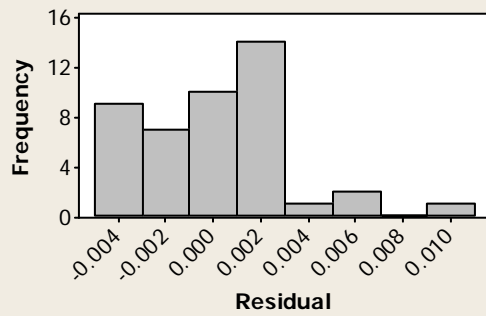
Normal Probability Plot



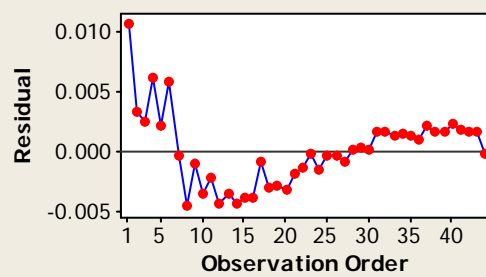
Versus Fits



Histogram



Versus Order



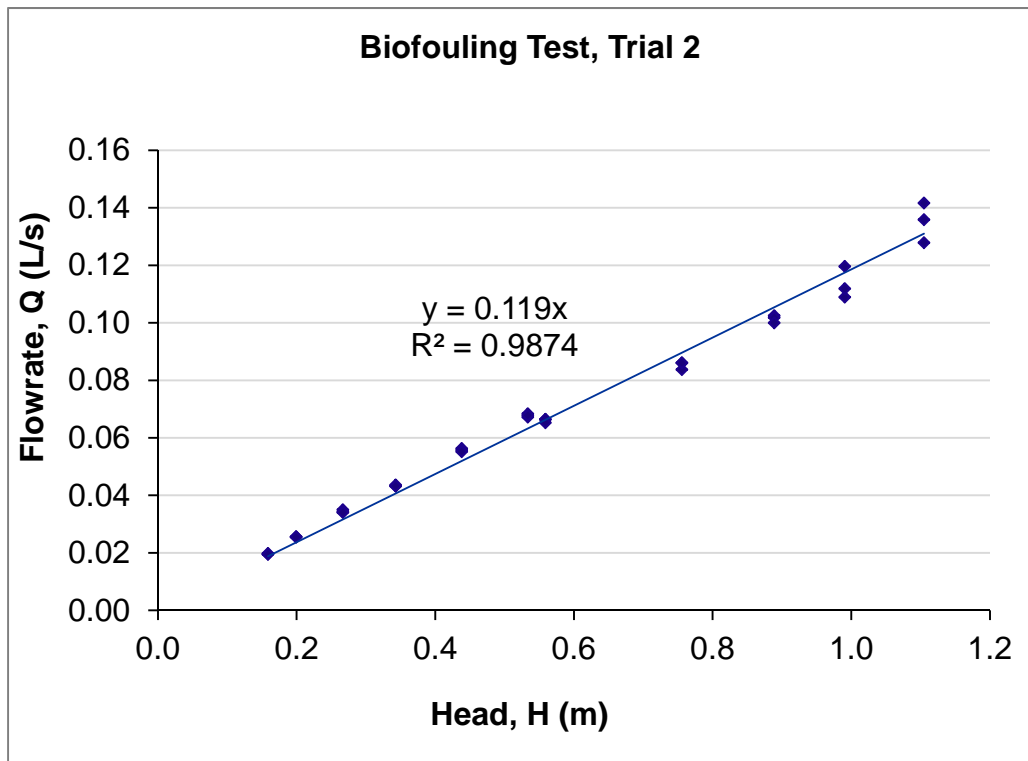
Appendix A.55: Regression Statistics on SmartDrain™ Biofouling Test, Trial#2.

<i>Regression Statistics</i>	
Multiple R	0.9986
R Square	0.9973
Adjusted R Square	0.9660
Standard Error	0.0041
Observations	33

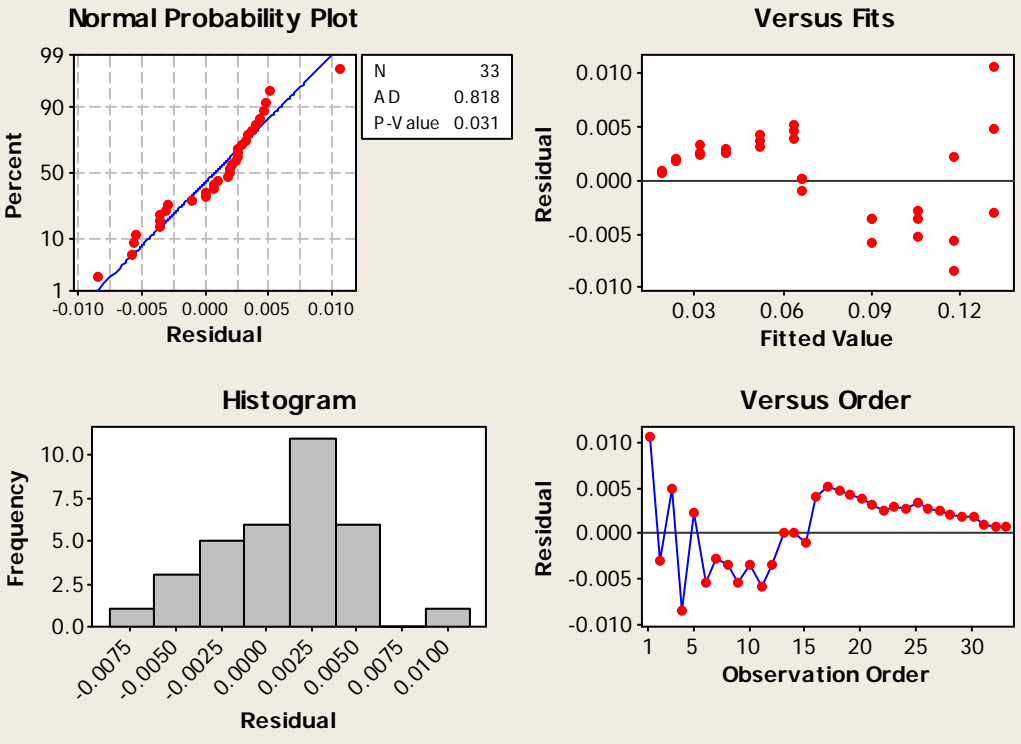
ANOVA					
	<i>df</i>	<i>SS</i>	<i>MS</i>	<i>F</i>	<i>Significance F</i>
Regression	1	0.1942	0.1942327	11675.77722	1.61669E-41
Residual	32	0.0005	1.664E-05		
Total	33	0.1948			

	<i>Coefficients</i>	<i>Standard Error</i>	<i>t Stat</i>	<i>P-value</i>	<i>Lower 95%</i>	<i>Upper 95%</i>
Intercept	0	#N/A	#N/A	#N/A	#N/A	#N/A
Slope	0.1186	0.0011	108.0545	1.3594E-42	0.1163	0.1208

* the intercept term was determined to be not significant during the initial analyses and was therefore eliminated from the model and the regression and ANOVA reanalyzed.



Residual Plots for Flowrate, Q (L/s), Biofouling Test Trial 2



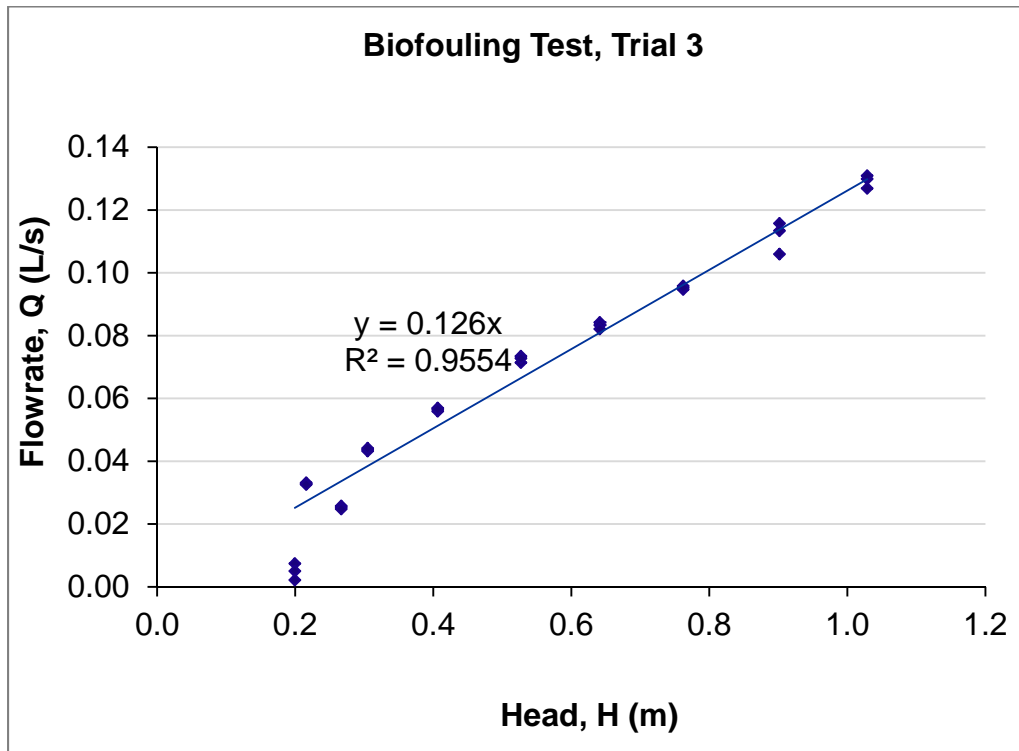
Appendix A.56: Regression Statistics on SmartDrain™ Biofouling Test, Trial#3.

<i>Regression Statistics</i>	
Multiple R	0.9944
R Square	0.9888
Adjusted R Square	0.9543
Standard Error	0.0081
Observations	30

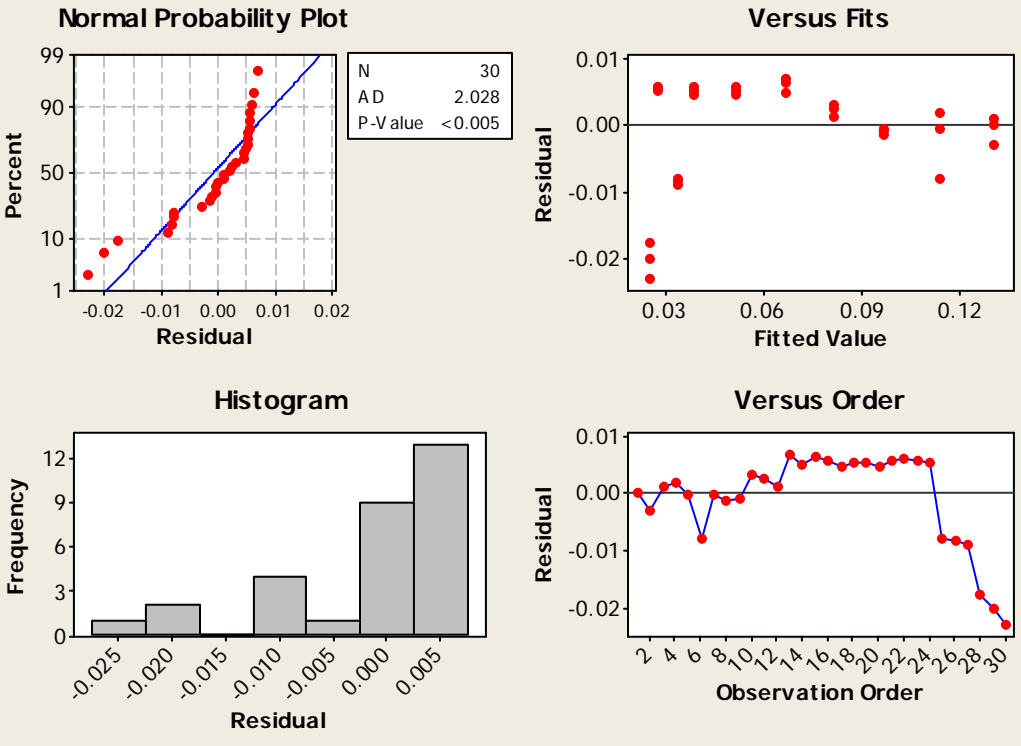
ANOVA					
	<i>df</i>	<i>SS</i>	<i>MS</i>	<i>F</i>	<i>Significance F</i>
Regression	1	0.1700	0.16997	2561.81292	4.47859E-29
Residual	29	0.0019	6.6E-05		
Total	30	0.1719			

	<i>Coefficients</i>	<i>Standard Error</i>	<i>t Stat</i>	<i>P-value</i>	<i>Lower 95%</i>	<i>Upper 95%</i>
Intercept	0	#N/A	#N/A	#N/A	#N/A	#N/A
h(m)	0.1262	0.0025	50.6144	7.5724E-30	0.1211	0.1313

* the intercept term was determined to be not significant during the initial analyses and was therefore eliminated from the model and the regression and ANOVA reanalyzed.



Residual Plots for Flowrate, Q (L/s), Biofouling Test Trial 3



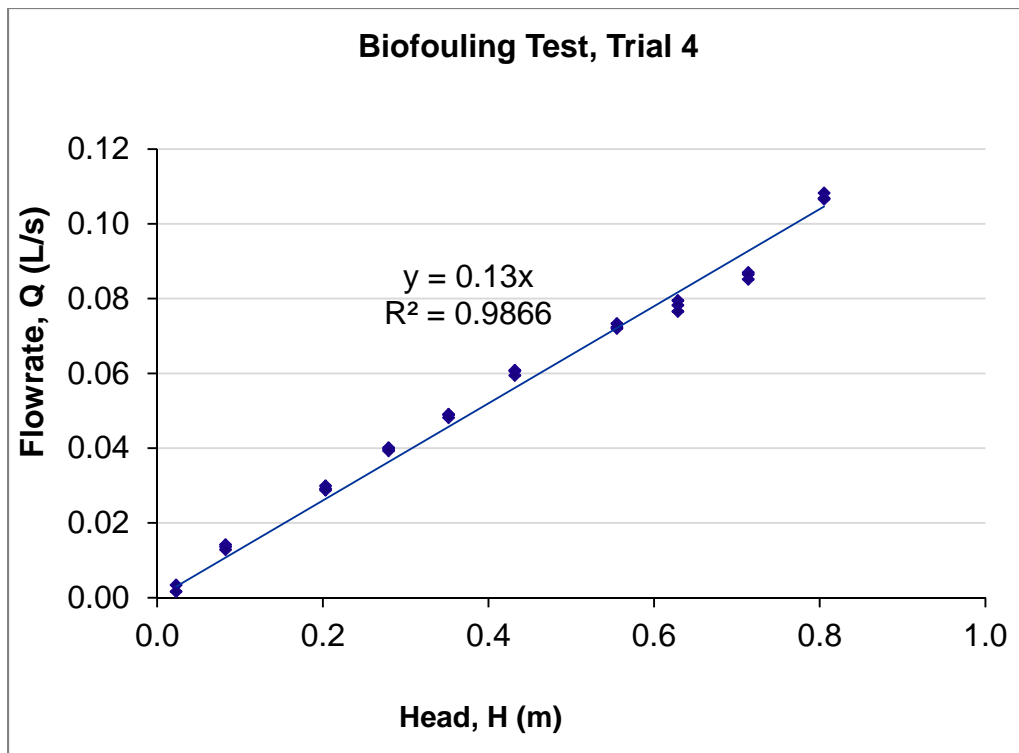
Appendix A.57: Regression Statistics on SmartDrain™ Biofouling Test, Trial#4.

<i>Regression Statistics</i>	
Multiple R	0.9984
R Square	0.9969
Adjusted R Square	0.9612
Standard Error	0.0036
Observations	29

ANOVA					
	<i>df</i>	<i>SS</i>	<i>MS</i>	<i>F</i>	<i>Significance F</i>
Regression	1	0.1164	0.1164	8943.1698	1.39139E-35
Residual	28	0.0004	1.302E-05		
Total	29	0.1168			

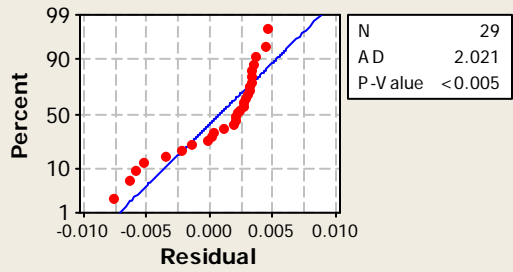
	<i>Coefficients</i>	<i>Standard Error</i>	<i>t Stat</i>	<i>P-value</i>	<i>Lower 95%</i>	<i>Upper 95%</i>
Intercept	0	#N/A	#N/A	#N/A	#N/A	#N/A
X Variable 1	0.1300	0.0014	94.5683	1.2458E-36	0.1272	0.1328

* the intercept term was determined to be not significant during the initial analyses and was therefore eliminated from the model and the regression and ANOVA reanalyzed.

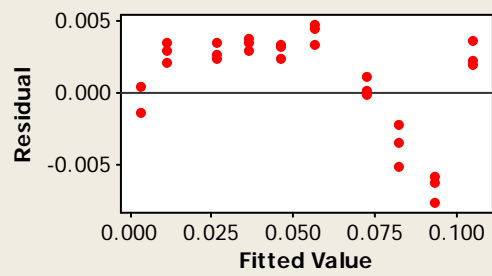


Residual Plots for Flowrate, Q (L/s), Biofouling Test Trial 4

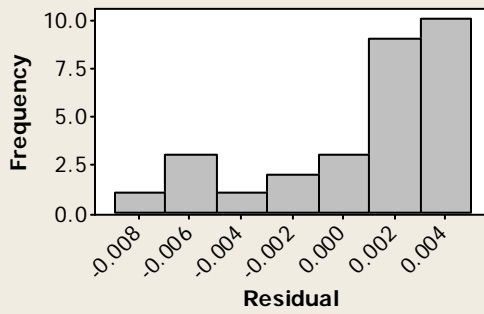
Normal Probability Plot



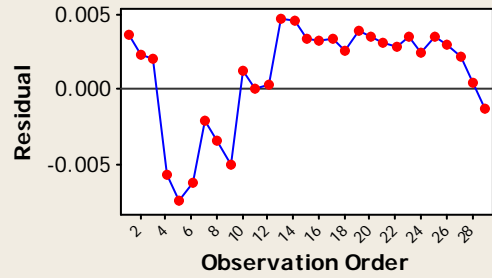
Versus Fits



Histogram



Versus Order

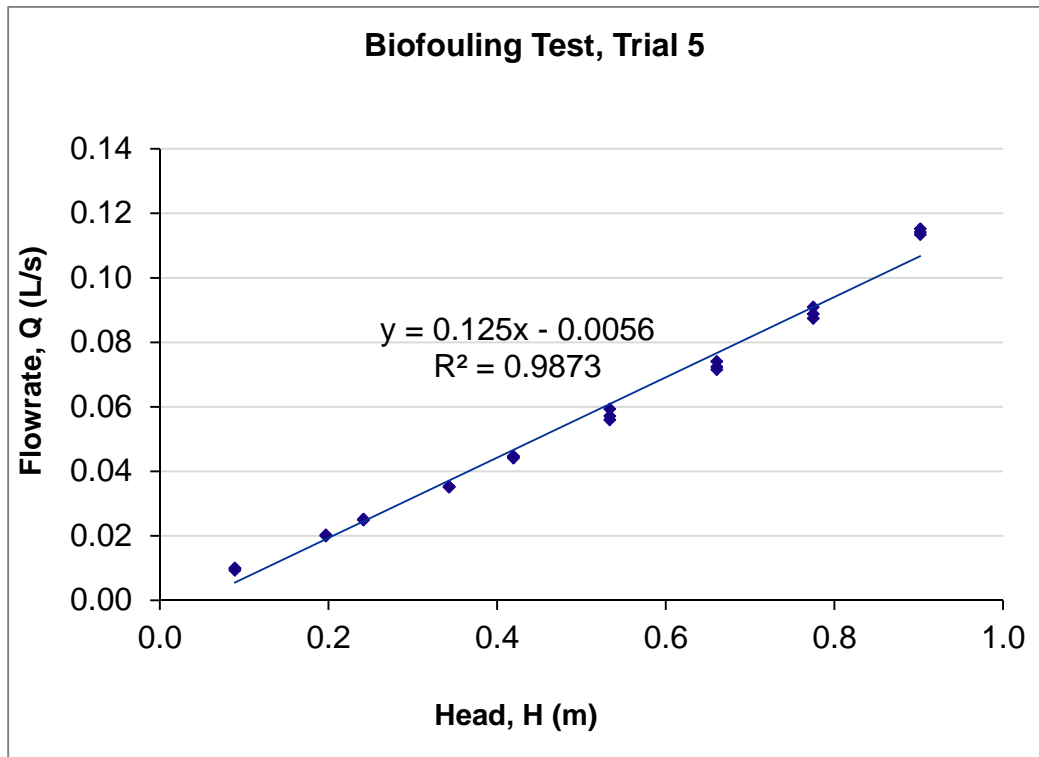


Appendix A.58: Regression Statistics on SmartDrain™ Biofouling Test, Trial#5.

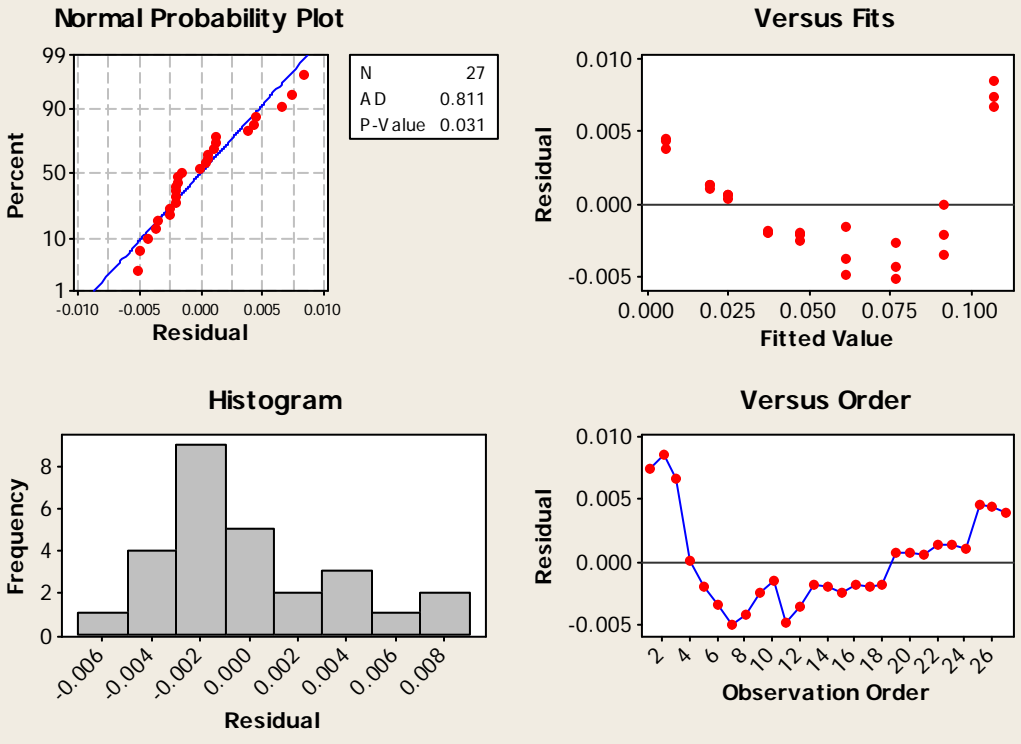
<i>Regression Statistics</i>	
Multiple R	0.9936
R Square	0.9873
Adjusted R Square	0.9868
Standard Error	0.0038
Observations	27

ANOVA					
	<i>df</i>	<i>SS</i>	<i>MS</i>	<i>F</i>	<i>Significance F</i>
Regression	1	0.0284	0.02839	1947.56518	3.07291E-25
Residual	25	0.0004	1.5E-05		
Total	26	0.0288			

	<i>Coefficients</i>	<i>Standard Error</i>	<i>t Stat</i>	<i>P-value</i>	<i>Lower 95%</i>	<i>Upper 95%</i>
Intercept	-0.0056	0.0015	-3.7310	0.00099	-0.0087	-0.0025
h(m)	0.1246	0.0028	44.1312	3.0729E-25	0.1188	0.1304



Residual Plots for Flowrate, Q (L/s), Biofouling Test Trial 5

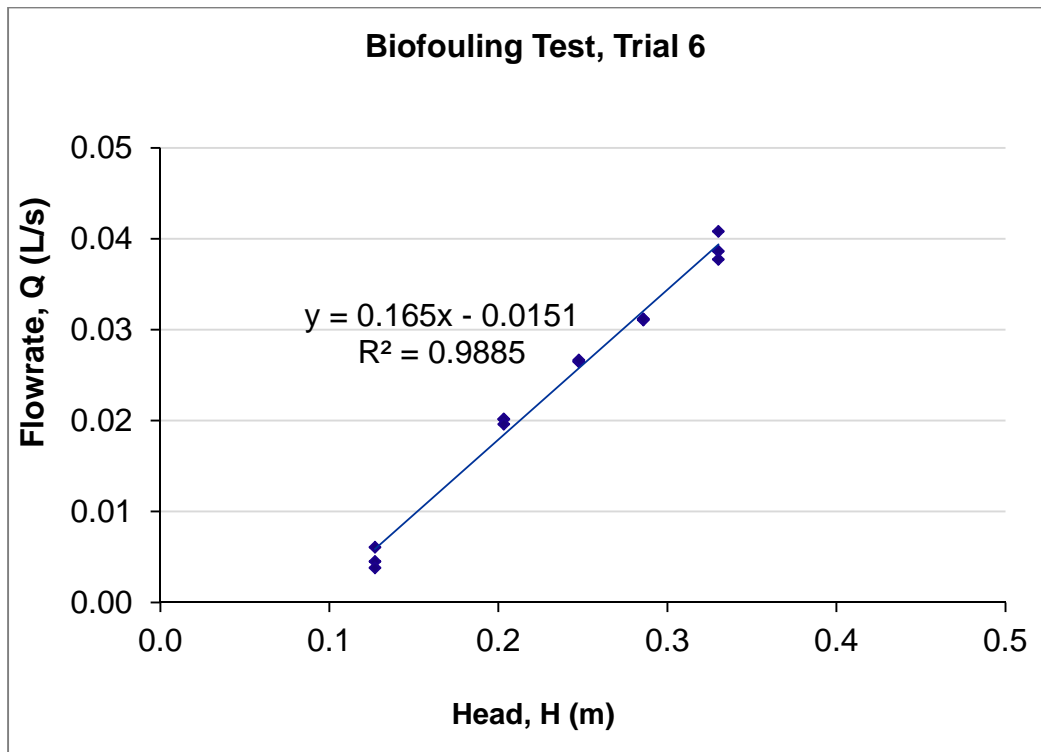


Appendix A.59: Regression Statistics on SmartDrain™ Biofouling Test, Trial#6.

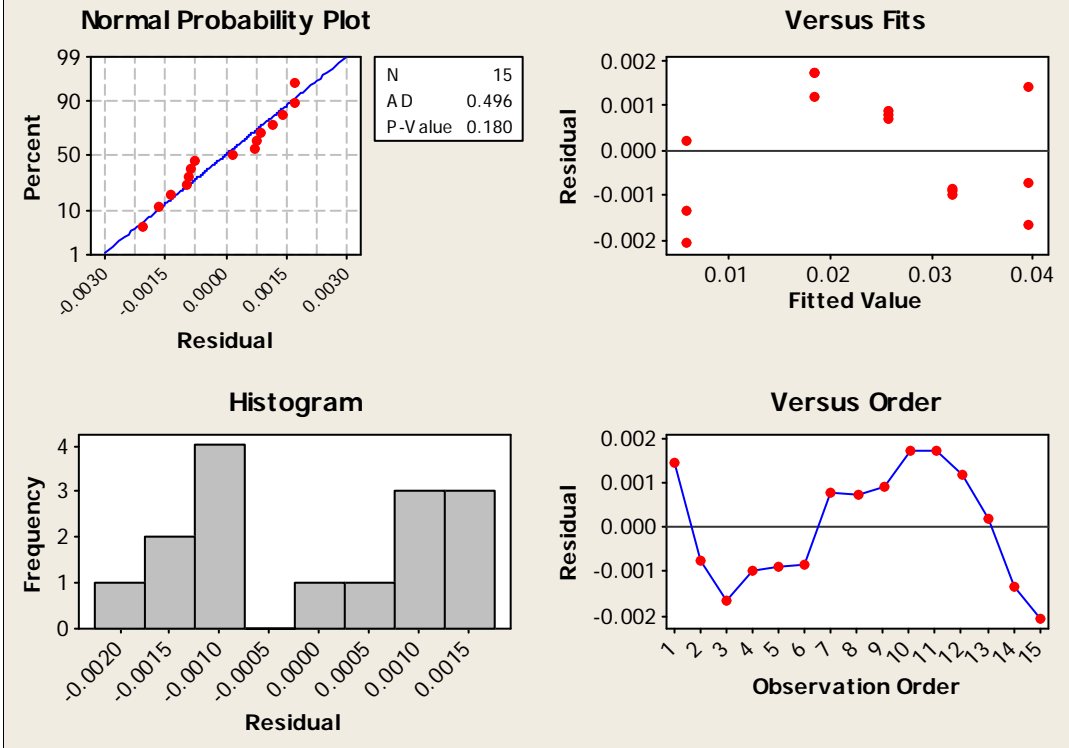
<i>Regression Statistics</i>	
Multiple R	0.9942
R Square	0.9885
Adjusted R Square	0.9876
Standard Error	0.0013
Observations	15

ANOVA					
	<i>df</i>	<i>SS</i>	<i>MS</i>	<i>F</i>	<i>Significance F</i>
Regression	1	0.0020	0.0020	1114.87105	5.49225E-14
Residual	13	0.0000	1.8E-06		
Total	14	0.0020			

	<i>Coefficients</i>	<i>Standard Error</i>	<i>t Stat</i>	<i>P-value</i>	<i>Lower 95%</i>	<i>Upper 95%</i>
Intercept	-0.0151	0.0012	-12.2638	1.6093E-08	-0.0177	-0.0124
h(m)	0.1649	0.0049	33.3897	5.4923E-14	0.1543	0.1756



Residual Plots for Flowrate, Q (L/s), Biofouling Test Trial 6

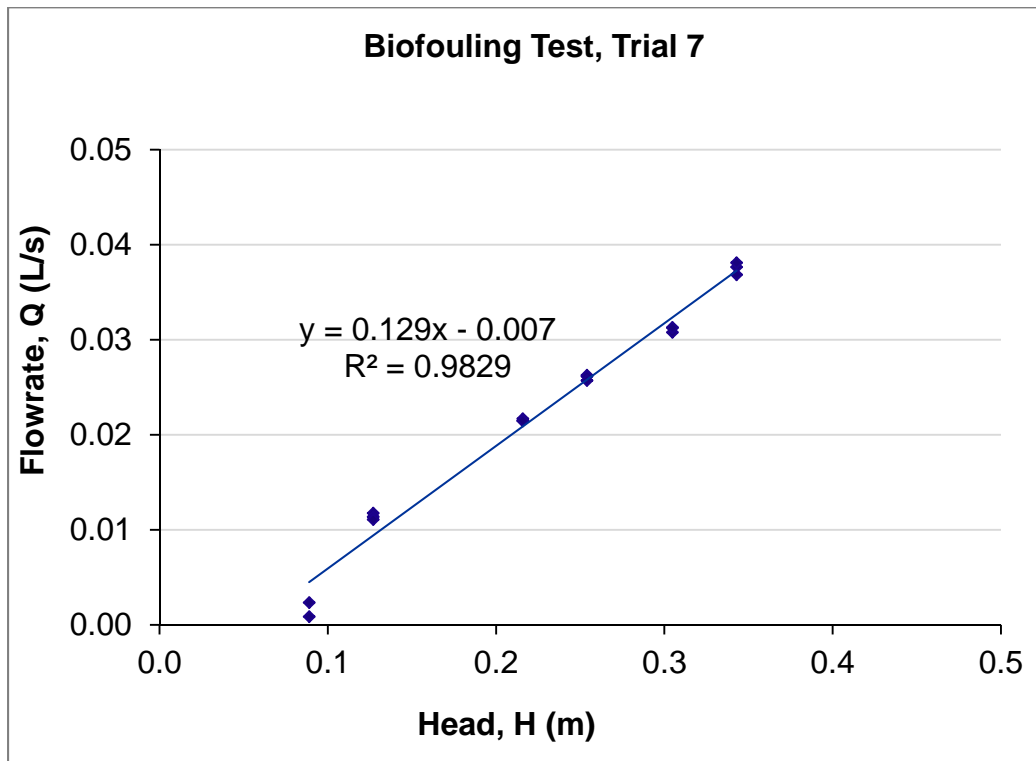


Appendix A.60: Regression Statistics on SmartDrain™ Biofouling Test, Trial#7.

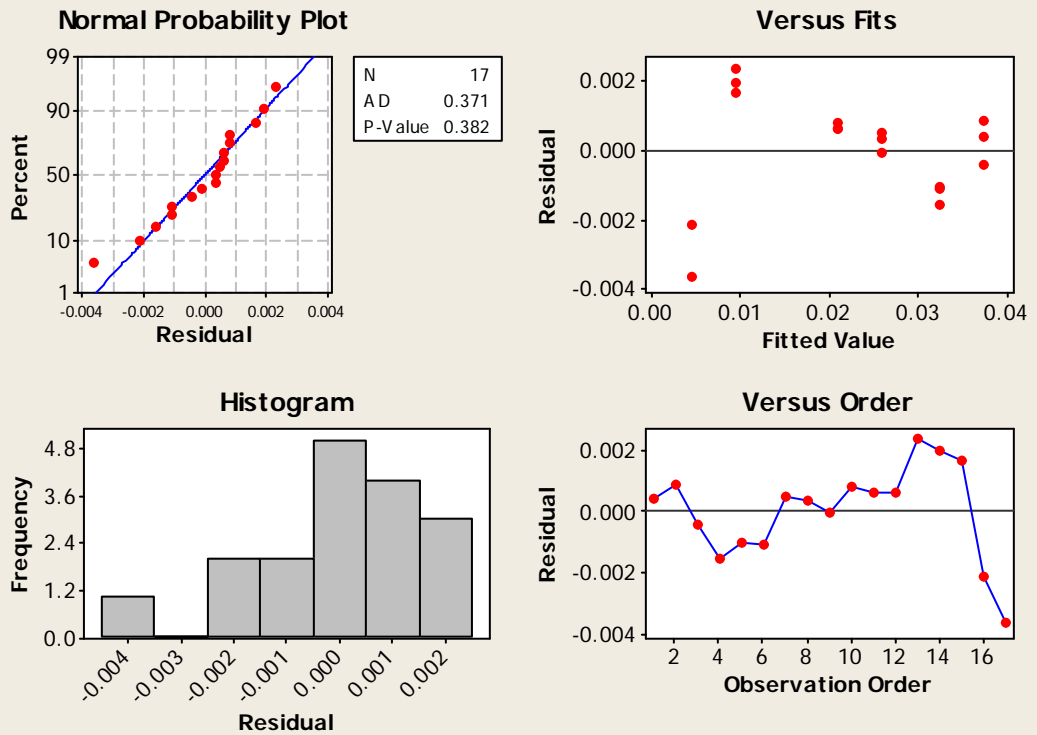
<i>Regression Statistics</i>	
Multiple R	0.9914
R Square	0.9829
Adjusted R Square	0.9818
Standard Error	0.0016
Observations	17

ANOVA					
	<i>df</i>	<i>SS</i>	<i>MS</i>	<i>F</i>	<i>Significance F</i>
Regression	1	0.0021	0.00215	862.2037	1.14129E-14
Residual	15	0.00004	2.5E-06		
Total	16	0.0022			

	<i>Coefficients</i>	<i>Standard Error</i>	<i>t Stat</i>	<i>P-value</i>	<i>Lower 95%</i>	<i>Upper 95%</i>
Intercept	-0.0070	0.0011	-6.4565	1.082E-05	-0.0093	-0.0047
h(m)	0.1291	0.0044	29.3633	1.1413E-14	0.1197	0.1384



Residual Plots for Flowrate, Q (L/s), Biofouling Test Trial 7



Appendix A.61: Example Calculation Showing Biofilter Facility Hydraulics and Design of Dewatering Options

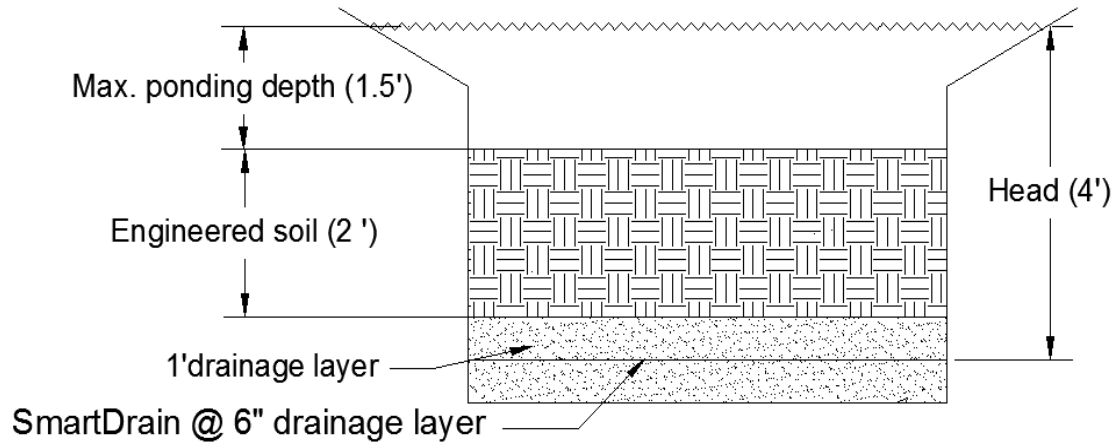


Figure 1. Example biofilter profile

$$\begin{aligned} \text{Biofilter storage volume (ft}^3\text{)} &= \text{Ponding storage (ft}^3\text{)} + \text{Engineered media storage (ft}^3\text{)} + \\ &\quad \text{Drainage layer storage (ft}^3\text{)} \\ &= \text{surface area} * \text{ponding depth} + \text{surface area} * \text{engineered media depth} * \text{engineered} \\ &\quad \text{media porosity} + 0.5 * \text{surface area} * \text{drainage layer} * \text{drainage layer porosity} \end{aligned}$$

Note: SmartDrain is installed at the center of drainage layer.

The final factorial model from the SmartDrain characteristics tests:

$$Q \left(\frac{L}{s} \right) = 0.0286 + 0.0015 * L + 0.0246 * H$$

Where: Q (L/s) = Predicted flowrate

L = SmartDrain length (ft)

H = SmartDrain head (in)

Example calculations for the biofilter shown in Fig. 1 and design parameters given in table 1.

Table1. Design parameters used for example calculations

Biofilter surface area (ft ²)	Ponding depth (ft)	Engineered media depth (ft)	Drainage layer (ft)	Porosity of media mix (%)	Porosity of drainage layer (%)
100	1.5	2	1	0.44	0.3

Required drainage rate = storage volume /drain time,

$$\begin{aligned} \text{Storage volume} &= 100 \text{ ft}^2 \cdot 1.5 \text{ ft} + 100 \text{ ft}^2 \cdot 2 \text{ ft} \cdot 0.44 + 100 \text{ ft}^2 \cdot 0.5 \text{ ft} \cdot 0.3 \\ &= 253 \text{ ft}^3 \end{aligned}$$

$$\text{Required drainage rate} = 253 \text{ ft}^3 / (24 \text{ hr} \cdot 3600 \text{ s/hr}) = 0.003 \text{ cfs}$$

Assume the 100 ft² biofilter has a square geometry:

$$\text{SmartDrain length} = \sqrt{\text{biofilter surface area}} = 10 \text{ ft}$$

SmartDrain drainage rate:

$$Q \left(\frac{L}{s} \right) = 0.0286 + 0.0015 * L + 0.0246 * H$$

Given: SmartDrain length = 10 ft

$$\text{Head} = 4 \text{ ft} = 48 \text{ in}$$

$$Q = 0.0286 + 0.0015 \cdot 10 + 0.0246 \cdot 4 \cdot 12 = 1.22 \text{ L/s}$$

$$Q = 0.0353 \cdot Q \text{ (L/s)} = 0.043 \text{ cfs}$$

$$\text{Minimum No. of SmartDrain} = 0.003 \text{ cfs} / 0.043 \text{ cfs} \sim 1 \text{ (Roundup to even number)}$$

Design of Dewatering Using SmartDrain

$$s = \sqrt{\frac{4 \cdot k_s (m^2 + 2 \cdot d_e \cdot m)}{q/24}}$$

Where:

- s spacing between drains (ft)
- q amount of water that the underdrain carries away (in/day),
- K_s average saturated hydraulic conductivity of the facility media (in/hr),
- d_e effective depth (ft),

m depth of water, or head, created over the pipes (ft) (Irrigation Association, 2000).

The maximum spacing between tile drains using the design parameters given in table 2:

Table 2. Design values for the Dewatering Equation

d_e (ft)	m (ft)	q (in/day)	K_s (in/hr)
0.5	0.5	30	30

$$S = \sqrt{\frac{4 * 30 \text{ in/hr} ((0.5 \text{ ft})^2 + 2 * 0.5 \text{ ft} * 0.5 \text{ ft})}{30 \text{ in/day} / 24}} = 8 \text{ ft}$$

Minimum No. of SmartDrain for 100 ft² biofilter having a square geometry in example 1

$$\begin{aligned} &= \left(\frac{\text{Biofilter length}}{\text{SmartDrain spacing}} \right) * \left(\frac{\text{Biofilter width}}{\text{SmartDrain spacing}} \right) \\ &= \left(\frac{10 \text{ ft}}{8 \text{ ft}} \right) * \left(\frac{10 \text{ ft}}{8 \text{ ft}} \right) = 2 \end{aligned}$$

Use the largest No. of SmartDrain indicated by either option!

Therefore, for a 100 ft² biofilter having a square geometry (10 ft by 10 ft), two SmartDrain strips are required. A complete design example for various biofilter sizes, hydraulic conductivities, and 24 hour drain period were summarized in Appendix F2-F6.

Appendix A.62: An Example Calculation Showing a Biofilter Facility Hydraulics and Design of Dewater Using SmartDrain (SD).

surface area (ft ²)	Ponding depth (ft)	Engineered media layer (ft)	Porosity of media mix (%)	Drainage layer (ft)	Porosity of drainage layer (%)	Head above SD (ft)	Storage volume (ft ³)	Drainage time 24 hr	Required drainage rate (cfs)
100	1.5	2	0.44	1	0.3	4	253	24	0.003
100	1.5	2	0.44	1	0.3	4	253	24	0.003
100	1.5	2	0.44	1	0.3	4	253	24	0.003
100	1.5	2	0.44	1	0.3	4	253	24	0.003
100	1.5	2	0.44	1	0.3	4	253	24	0.003
1000	1.5	2	0.44	1	0.3	4	2530	24	0.029
1000	1.5	2	0.44	1	0.3	4	2530	24	0.029
1000	1.5	2	0.44	1	0.3	4	2530	24	0.029
1000	1.5	2	0.44	1	0.3	4	2530	24	0.029
1000	1.5	2	0.44	1	0.3	4	2530	24	0.029
3000	1.5	2	0.44	1	0.3	4	7590	24	0.088
3000	1.5	2	0.44	1	0.3	4	7590	24	0.088
3000	1.5	2	0.44	1	0.3	4	7590	24	0.088
3000	1.5	2	0.44	1	0.3	4	7590	24	0.088
3000	1.5	2	0.44	1	0.3	4	7590	24	0.088
5000	1.5	2	0.44	1	0.3	4	12650	24	0.146
5000	1.5	2	0.44	1	0.3	4	12650	24	0.146
5000	1.5	2	0.44	1	0.3	4	12650	24	0.146
5000	1.5	2	0.44	1	0.3	4	12650	24	0.146
5000	1.5	2	0.44	1	0.3	4	12650	24	0.146
10000	1.5	2	0.44	1	0.3	4	25300	24	0.293
10000	1.5	2	0.44	1	0.3	4	25300	24	0.293
10000	1.5	2	0.44	1	0.3	4	25300	24	0.293
10000	1.5	2	0.44	1	0.3	4	25300	24	0.293
10000	1.5	2	0.44	1	0.3	4	25300	24	0.293

Appendix A.63: Minimum No. of SmartDrain (SD) Required for a Biofilter Basin Having a Square Geometry

SD length (ft)	Q (L/s), from factorial design	Q (gpm)	Q (cfs)	Drain volume (cf)/SM = [Q*t]	Min. No. of SD	Example max. spacing (= sqrt. (A)/min No. of SD)
10	1.22	19.41	0.043	3734.32	1	10
10	1.22	19.41	0.043	3734.32	1	10
10	1.22	19.41	0.043	3734.32	1	10
10	1.22	19.41	0.043	3734.32	1	10
10	1.22	19.41	0.043	3734.32	1	10
32	1.26	19.92	0.044	3833.24	1	32
32	1.26	19.92	0.044	3833.24	1	32
32	1.26	19.92	0.044	3833.24	1	32
32	1.26	19.92	0.044	3833.24	1	32
32	1.26	19.92	0.044	3833.24	1	32
55	1.29	20.47	0.046	3939.15	2	27
55	1.29	20.47	0.046	3939.15	2	27
55	1.29	20.47	0.046	3939.15	2	27
55	1.29	20.47	0.046	3939.15	2	27
55	1.29	20.47	0.046	3939.15	2	27
71	1.32	20.85	0.046	4012.07	4	18
71	1.32	20.85	0.046	4012.07	4	18
71	1.32	20.85	0.046	4012.07	4	18
71	1.32	20.85	0.046	4012.07	4	18
71	1.32	20.85	0.046	4012.07	4	18
100	1.36	21.55	0.048	4146.06	7	14
100	1.36	21.55	0.048	4146.06	7	14
100	1.36	21.55	0.048	4146.06	7	14
100	1.36	21.55	0.048	4146.06	7	14
100	1.36	21.55	0.048	4146.06	7	14

Appendix A. 64: Minimum No. of SmartDrain (SD) Required for a Biofilter Basin Having a Rectangular Geometry (Length: Width = 3:1)

Width (ft)	Length (ft)	Head above SD (ft)	Q (L/s), from Factorial design	Q (cfs)	Drain volume (cf)/SM = [Q*t], cf	Min. No. of SD	Example max. spacing (= Sqrt. (A)/min No. of SD)
6	17	4	1.24	0.044	3767.812	1	17
6	17	4	1.24	0.044	3767.812	1	17
6	17	4	1.24	0.044	3767.812	1	17
6	17	4	1.24	0.044	3767.812	1	17
6	17	4	1.24	0.044	3767.812	1	17
18	55	4	1.29	0.046	3939.150	1	55
18	55	4	1.29	0.046	3939.150	1	55
18	55	4	1.29	0.046	3939.150	1	55
18	55	4	1.29	0.046	3939.150	1	55
18	55	4	1.29	0.046	3939.150	1	55
32	95	4	1.35	0.048	4122.584	2	47
32	95	4	1.35	0.048	4122.584	2	47
32	95	4	1.35	0.048	4122.584	2	47
32	95	4	1.35	0.048	4122.584	2	47
32	95	4	1.35	0.048	4122.584	2	47
41	122	4	1.39	0.049	4248.879	3	41
41	122	4	1.39	0.049	4248.879	3	41
41	122	4	1.39	0.049	4248.879	3	41
41	122	4	1.39	0.049	4248.879	3	41
41	122	4	1.39	0.049	4248.879	3	41
58	173	4	1.47	0.052	4480.966	6	29
58	173	4	1.47	0.052	4480.966	6	29
58	173	4	1.47	0.052	4480.966	6	29
58	173	4	1.47	0.052	4480.966	6	29
58	173	4	1.47	0.052	4480.966	6	29

Appendix A.65: Minimum No. of SmartDrain (SD) Required for a Biofilter Basin Having a Rectangular Geometry (Length: Width = 5:1)

Width (ft)	Length (ft)	Head above SD (ft)	Q (L/s), from factorial design	Q (cfs)	Drain volume (cf)/SM = [Q*t]	Min. No. of SD	Example max. spacing (= Sqrt. (A)/min No. of SD)
4	22	4	1.24	0.044	3790.87	1	22
4	22	4	1.24	0.044	3790.87	1	22
4	22	4	1.24	0.044	3790.87	1	22
4	22	4	1.24	0.044	3790.87	1	22
4	22	4	1.24	0.044	3790.87	1	22
14	71	4	1.32	0.046	4012.07	1	71
14	71	4	1.32	0.046	4012.07	1	71
14	71	4	1.32	0.046	4012.07	1	71
14	71	4	1.32	0.046	4012.07	1	71
14	71	4	1.32	0.046	4012.07	1	71
24	122	4	1.39	0.049	4248.88	2	61
24	122	4	1.39	0.049	4248.88	2	61
24	122	4	1.39	0.049	4248.88	2	61
24	122	4	1.39	0.049	4248.88	2	61
24	122	4	1.39	0.049	4248.88	2	61
32	158	4	1.45	0.051	4411.93	3	53
32	158	4	1.45	0.051	4411.93	3	53
32	158	4	1.45	0.051	4411.93	3	53
32	158	4	1.45	0.051	4411.93	3	53
32	158	4	1.45	0.051	4411.93	3	53
45	224	4	1.54	0.055	4711.55	6	37
45	224	4	1.54	0.055	4711.55	6	37
45	224	4	1.54	0.055	4711.55	6	37
45	224	4	1.54	0.055	4711.55	6	37
45	224	4	1.54	0.055	4711.55	6	37

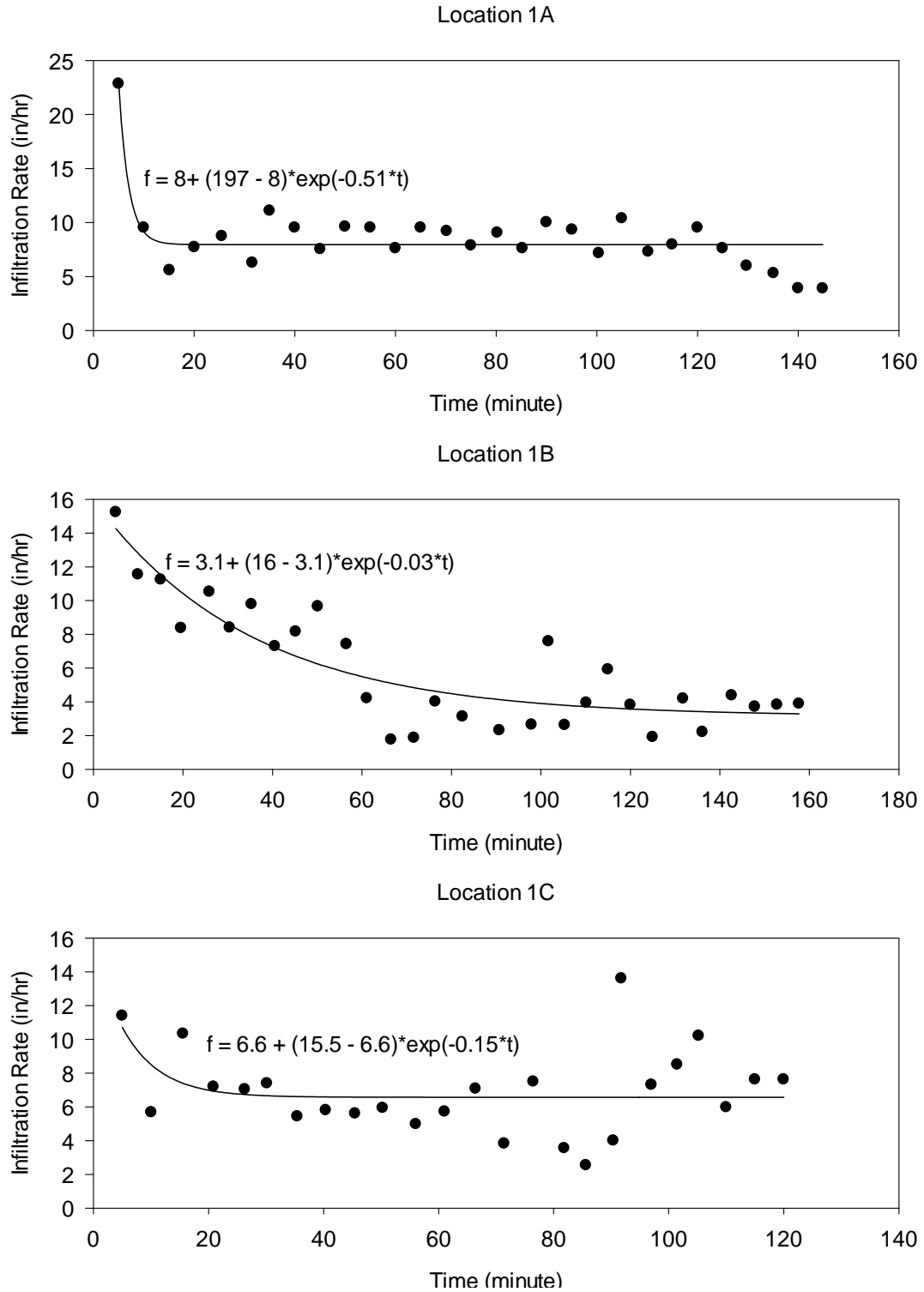
Appendix A.66: Biofilter Basin Dewatering and Minimum No. of SmartDrain (SD) Required for a Biofilter Basin Based On SmartDrain Spacing.

q - the amount of water that the underdrain carries away (in/day)	K_s -the average saturated hydraulic conductivity of the facility media (in/hr)	de-the difference in elevation between the tile drain and the impermeable layer (ft)	m-head, created over the tiles (ft)	S-the max. spacing between tile drains (ft)	Min. number of SD for square geometry	Min. number of SD for rectangular geometry length: width (3:1)	Min. number of SD for rectangular geometry length: width (5:1)
30	30	0.5	0.5	8	2	2	2
30	45	0.5	0.5	10	1	1	1
30	60	0.5	0.5	12	1	1	1
30	75	0.5	0.5	13	1	1	1
30	100	0.5	0.5	15	1	1	1
30	30	0.5	1.0	14	6	6	6
30	45	0.5	1.0	17	4	4	4
30	60	0.5	1.0	19	3	3	3
30	75	0.5	1.0	22	3	3	3
30	100	0.5	1.0	25	2	2	2
30	30	0.5	1.5	19	9	9	9
30	45	0.5	1.5	23	6	6	6
30	60	0.5	1.5	27	5	5	5
30	75	0.5	1.5	30	4	4	4
30	100	0.5	1.5	34	3	3	3
30	30	0.5	2.0	24	9	9	9
30	45	0.5	2.0	29	6	6	6
30	60	0.5	2.0	34	5	5	5
30	75	0.5	2.0	38	4	4	4
30	100	0.5	2.0	44	3	3	3
30	30	0.5	3.0	34	9	9	9
30	45	0.5	3.0	41	6	6	6
30	60	0.5	3.0	48	5	5	5
30	75	0.5	3.0	53	4	4	4
30	100	0.5	3.0	62	3	3	3

Note: The largest number of SmartDrain was selected for the final model.

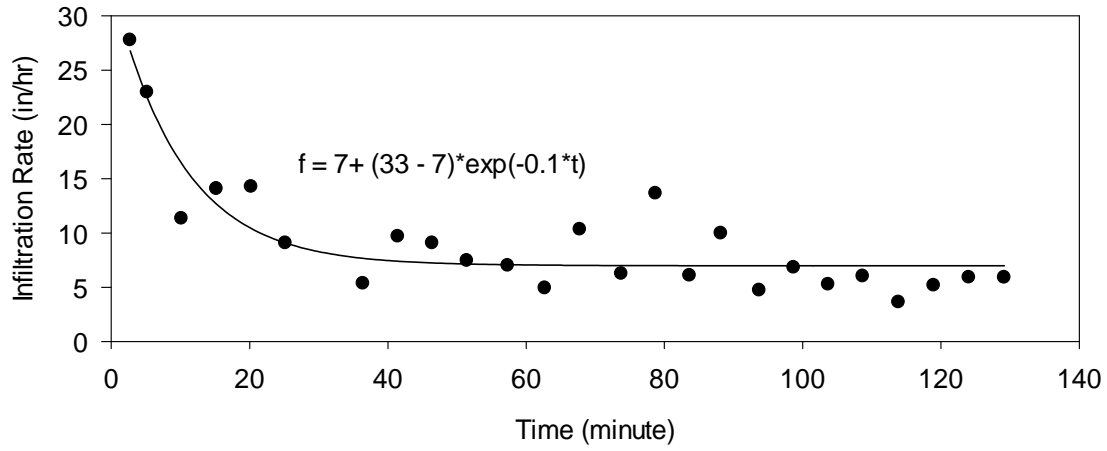
APPENDIX B: STORMWATER BIOFILTRATION DEVICE PERFORMANCE TEST RESULTS

Appendix B.1: Biofilter Surface Infiltration Measurements at Location 1 Fitted with Horton Equation.

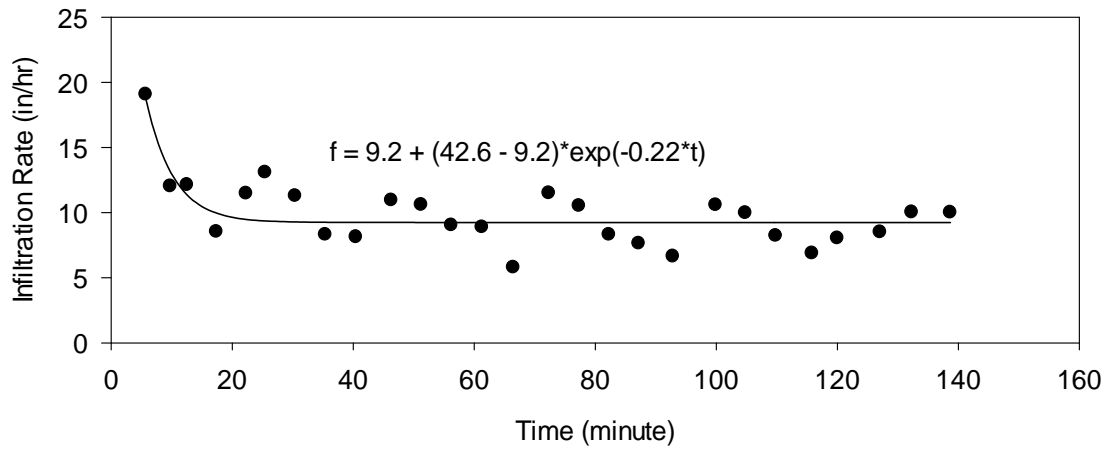


Appendix B.2: Biofilter Surface Infiltration Measurements at Location 2 Fitted with Horton Equation.

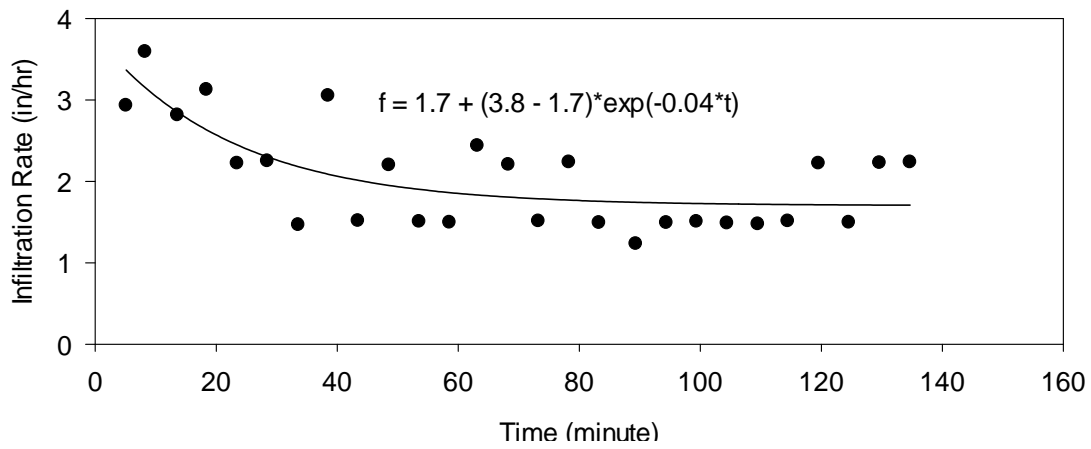
Location 2A



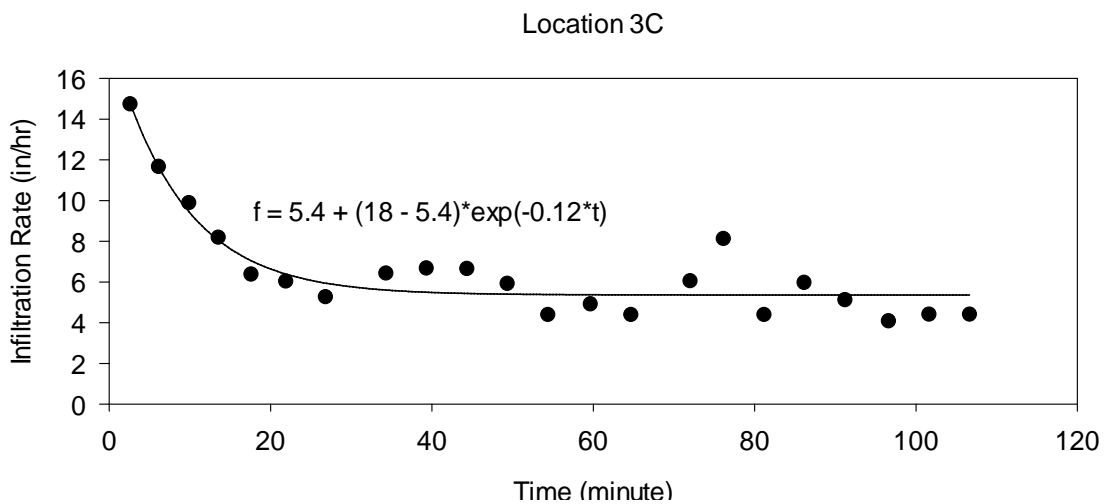
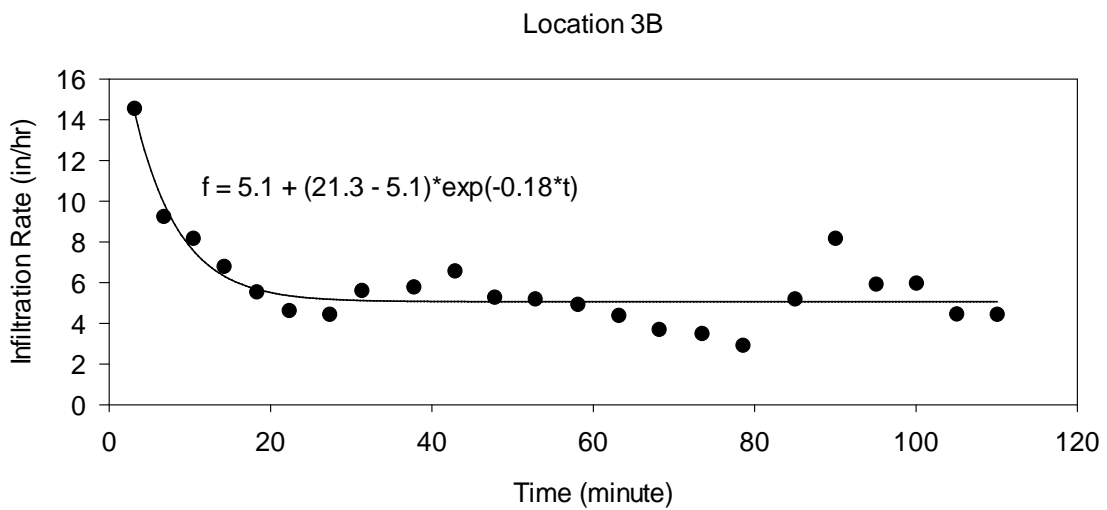
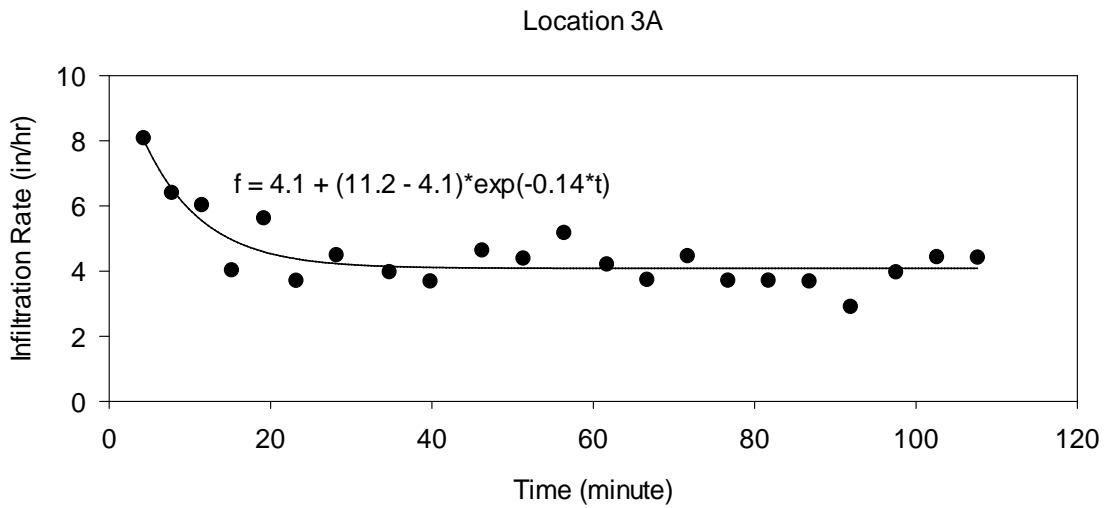
Location 2B



Location 2C

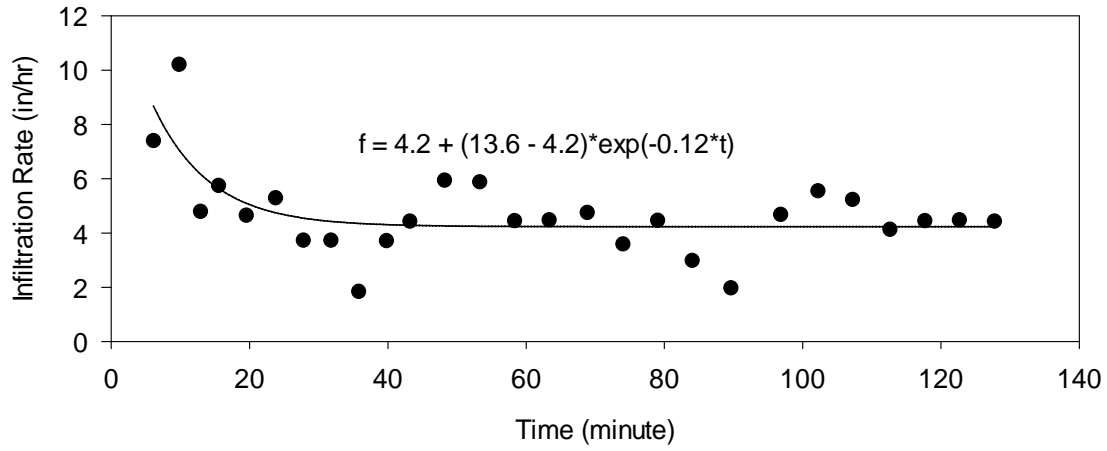


Appendix B.3: Biofilter Surface Infiltration Measurements at Location 3 Fitted with Horton Equation.

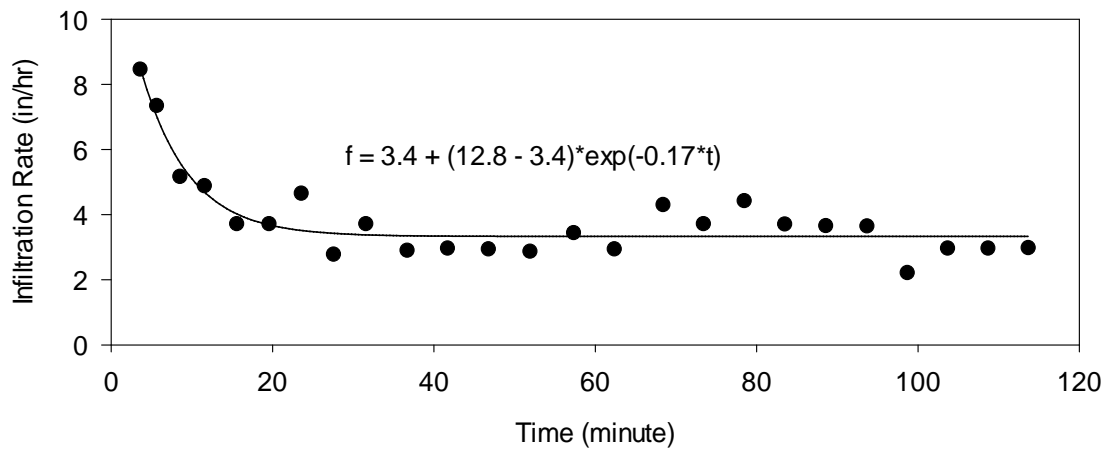


Appendix B.4: Biofilter Surface Infiltration Measurements at Location 4 Fitted with Horton Equation.

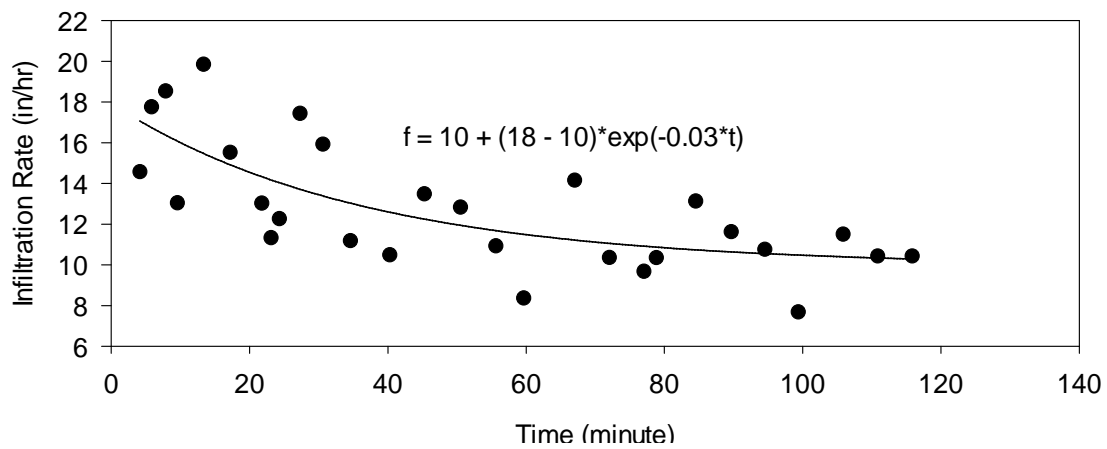
Location 4A



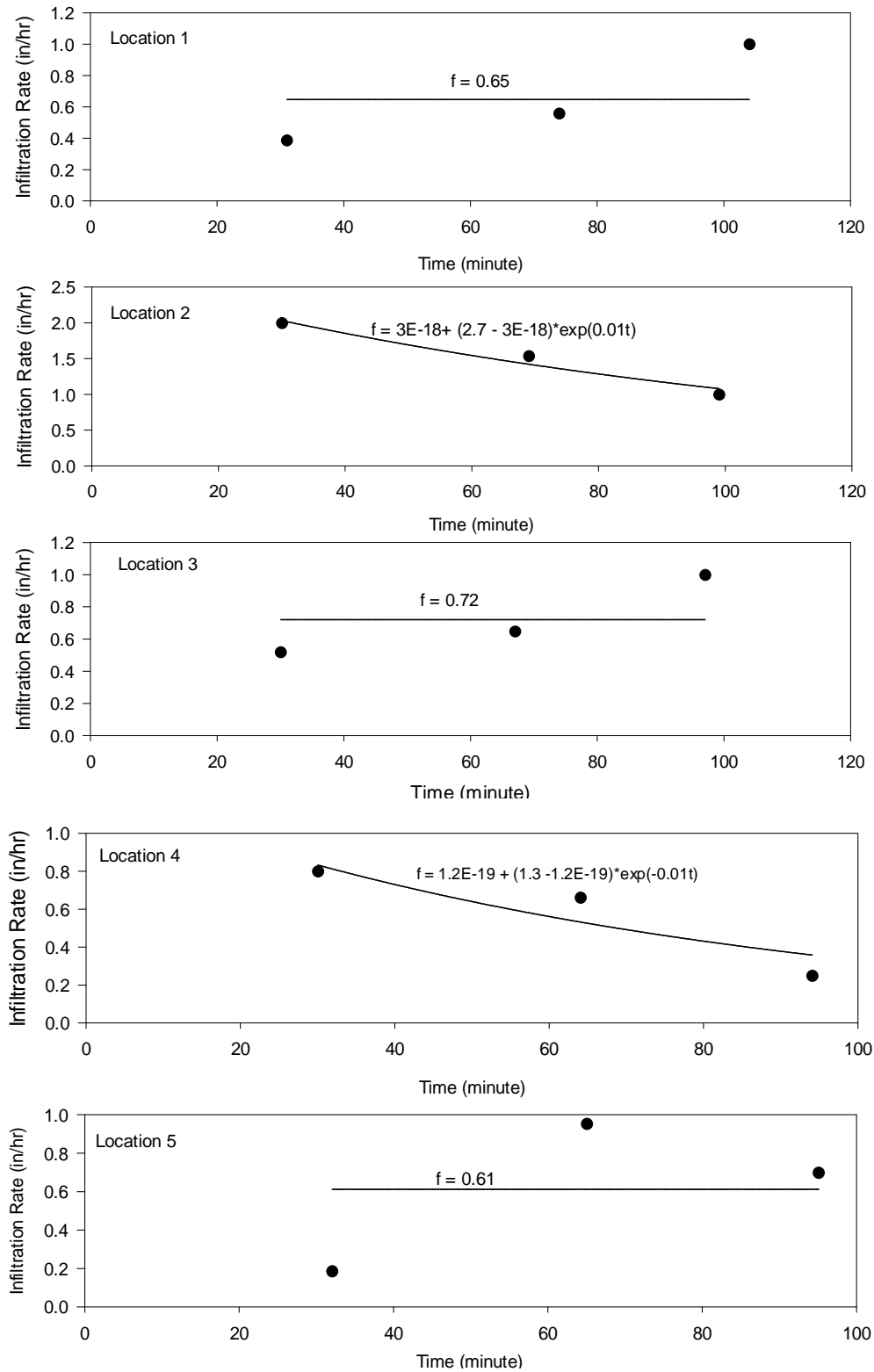
Location 4B



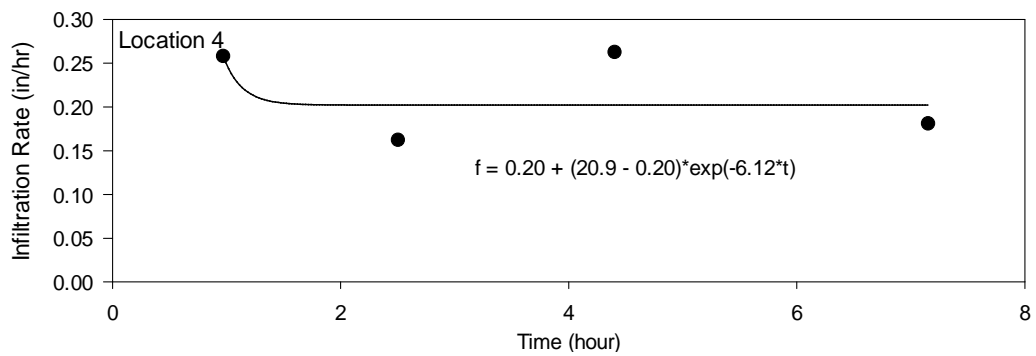
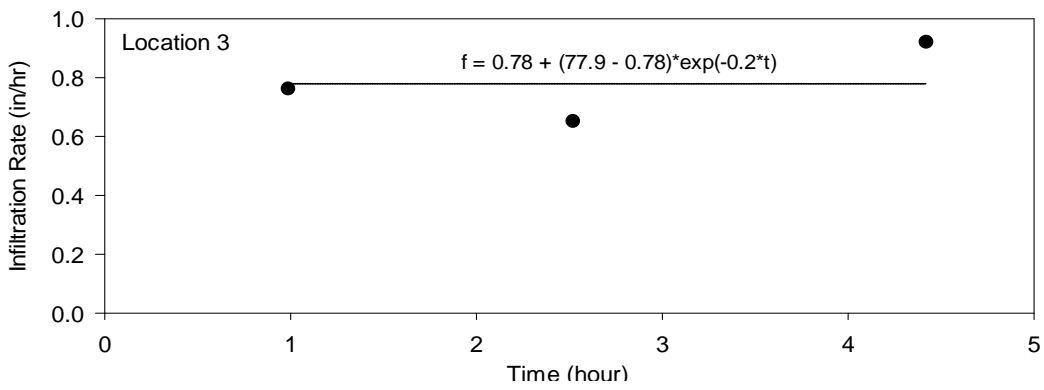
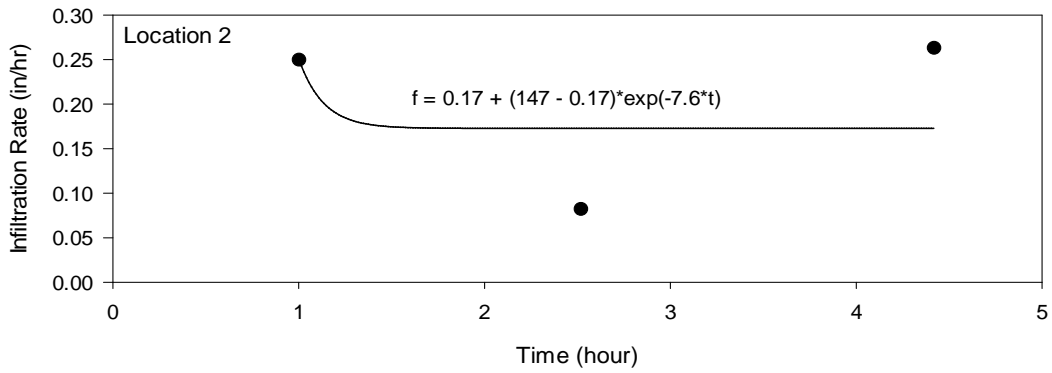
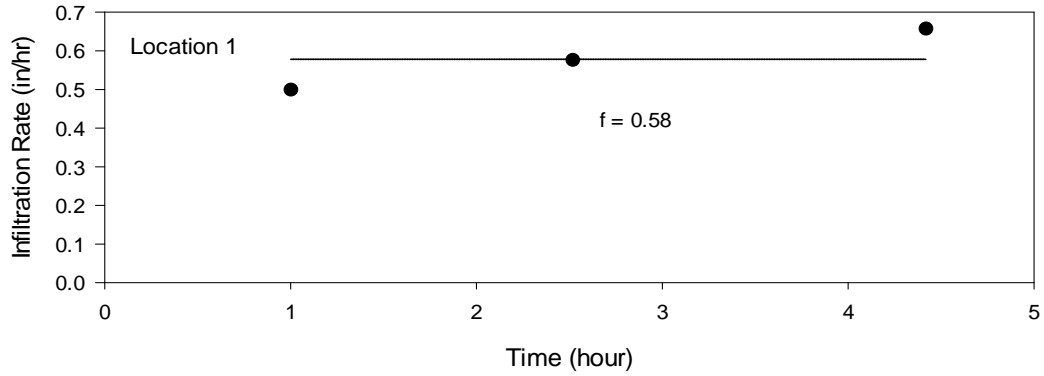
Location 4C



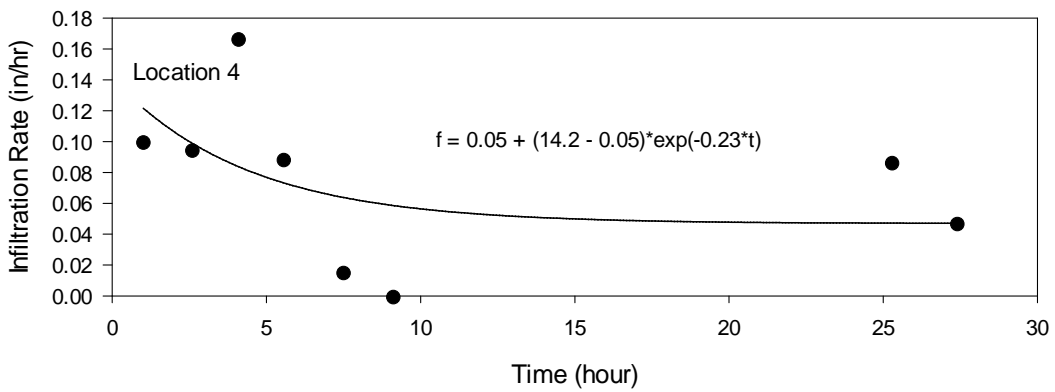
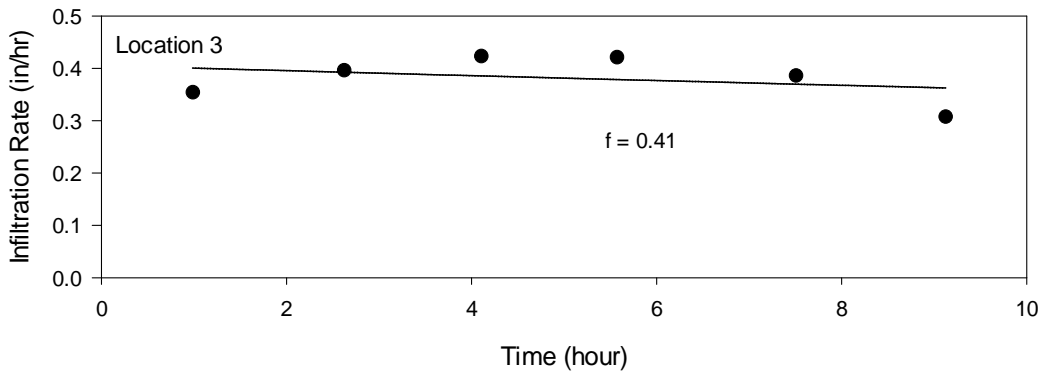
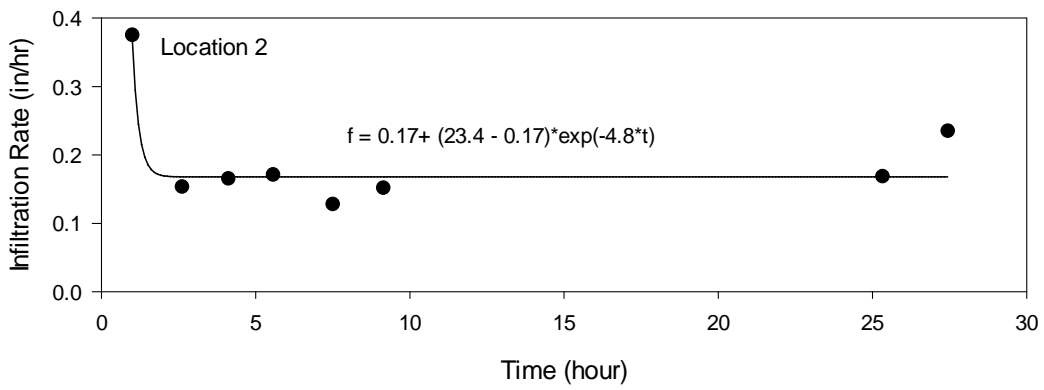
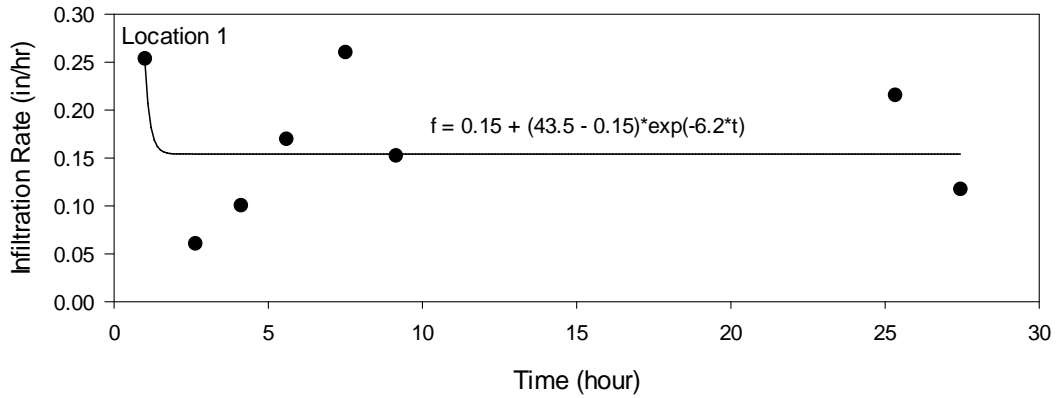
Appendix B.5: Biofilter Surface Infiltration Measurements after Rain Event 1 Fitted with Horton Equation.



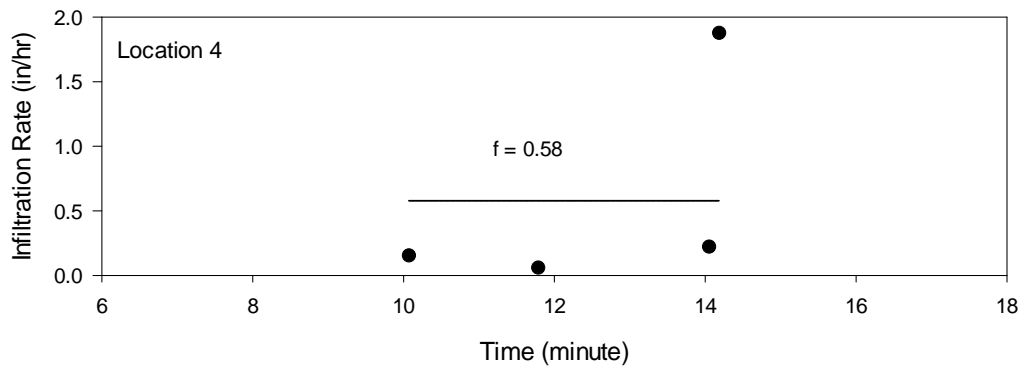
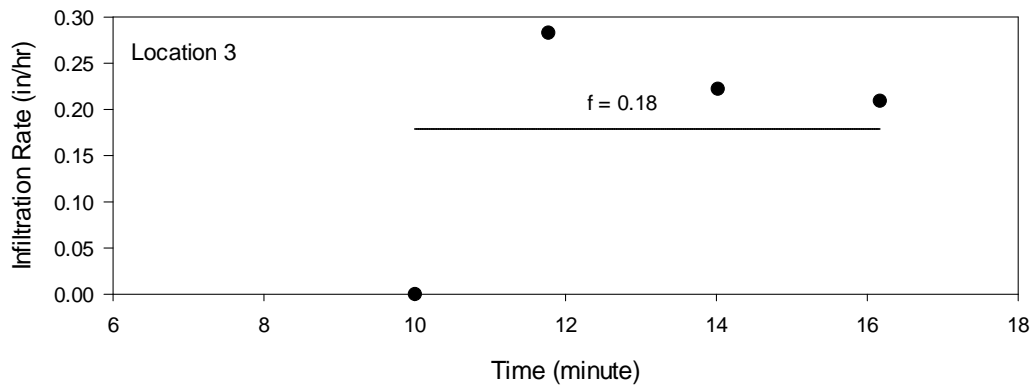
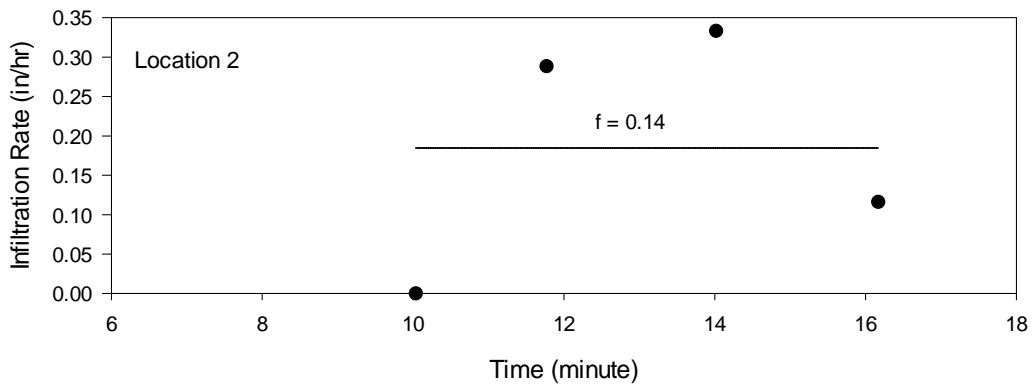
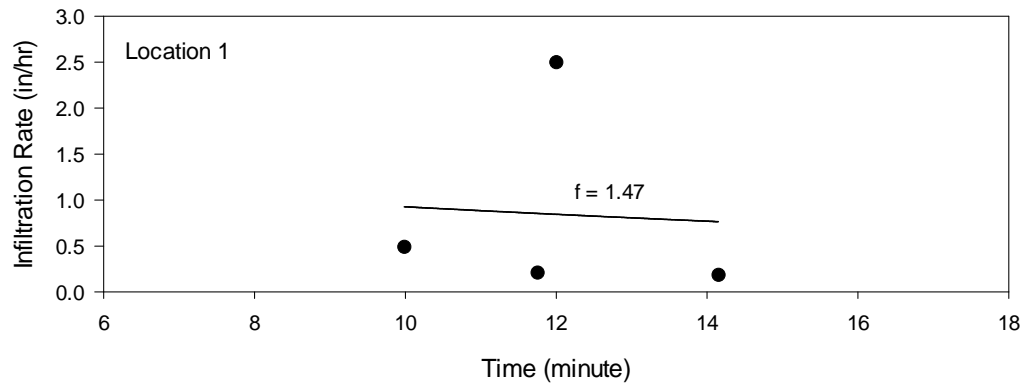
Appendix B.6: Biofilter Surface Infiltration Measurements after Rain Event 2 Fitted with Horton Equation.



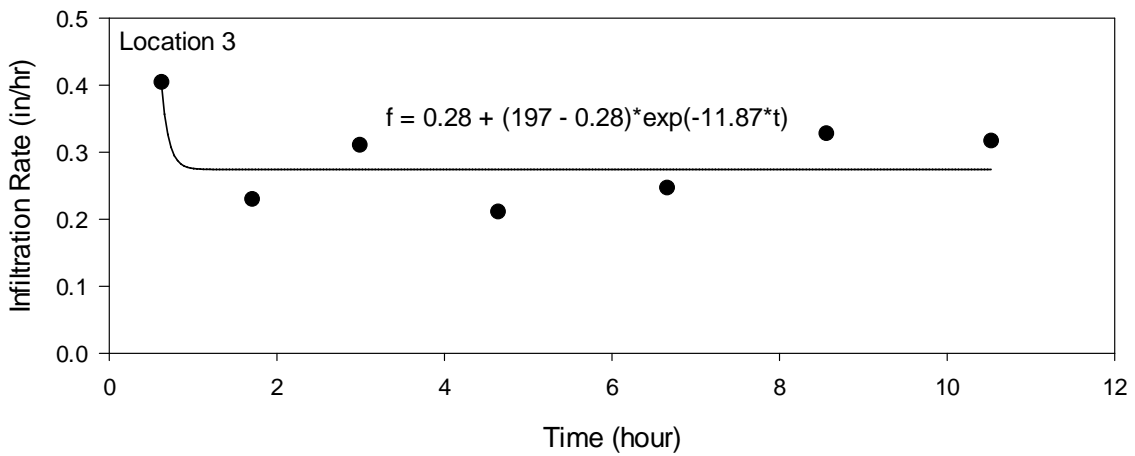
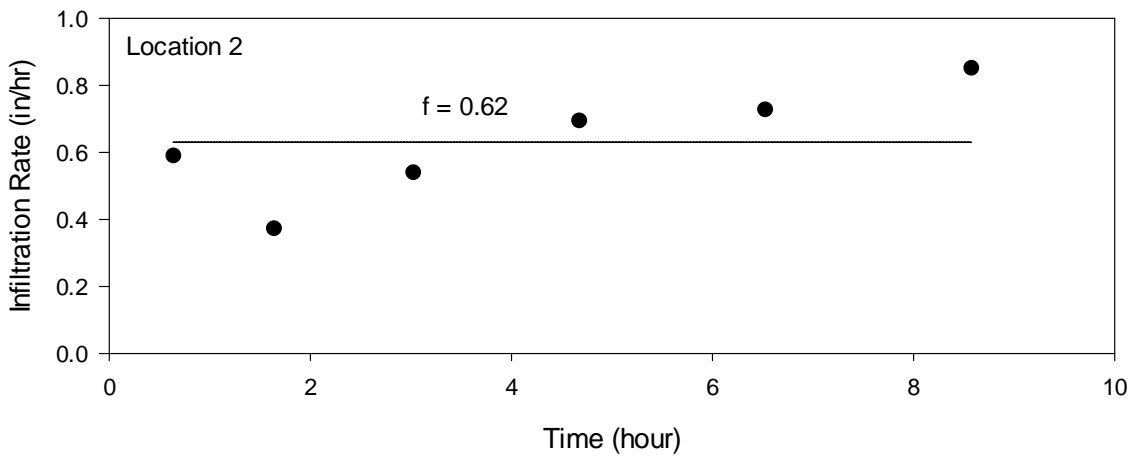
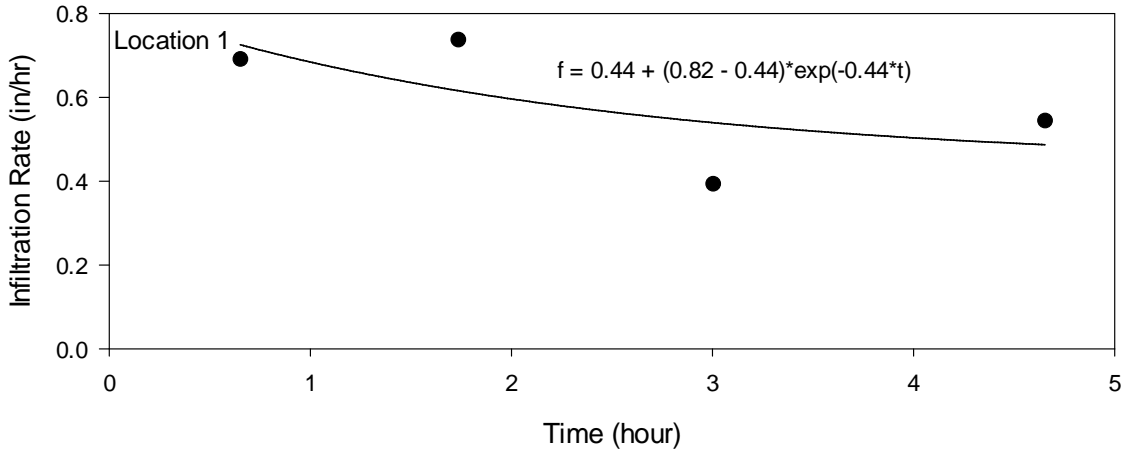
Appendix B.7: Biofilter Surface Infiltration Measurements after Rain Event 3 Fitted with Horton Equation.



Appendix B.8: Biofilter Surface Infiltration Measurements after Rain Event 4 Fitted with Horton Equation.

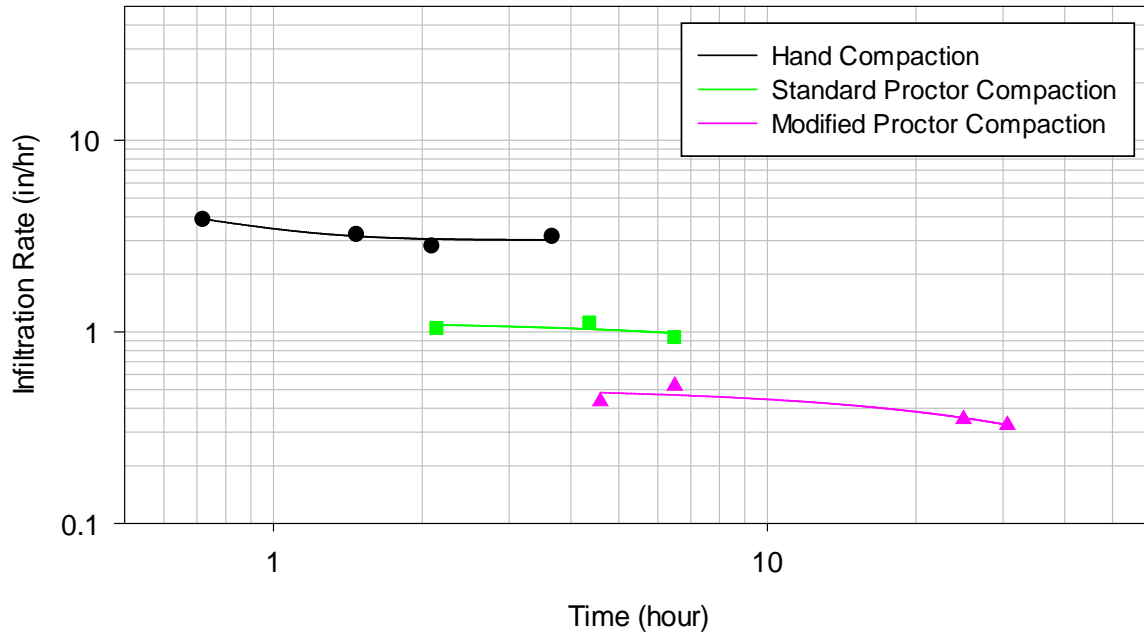


Appendix B.9: Biofilter Surface Infiltration Measurements after Rain Event 5 Fitted with Horton Equation.

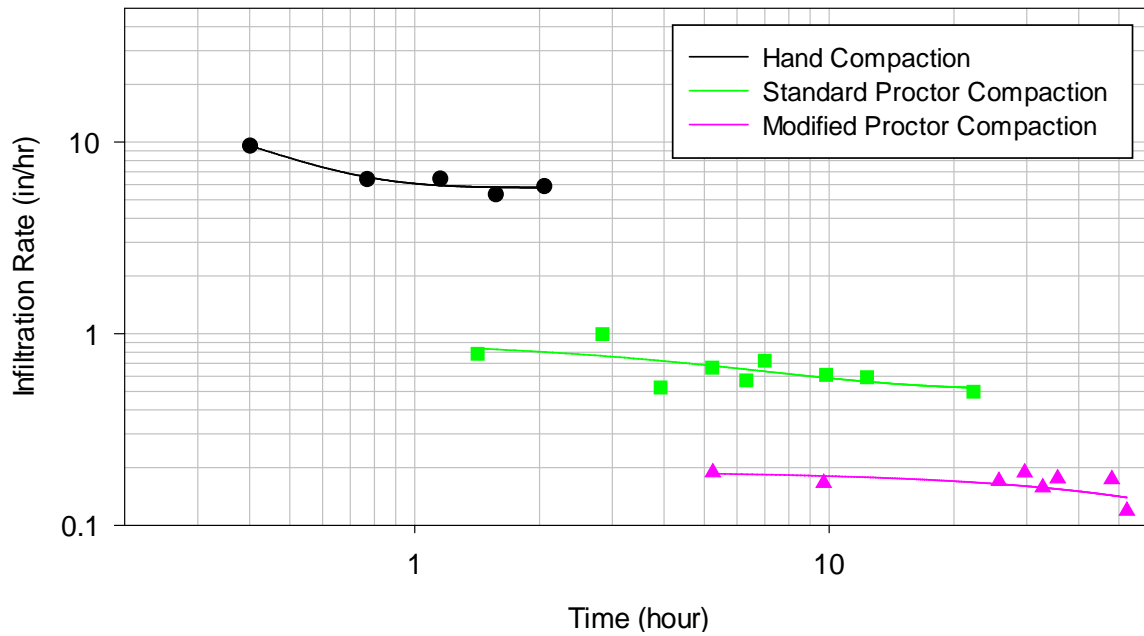


Appendix B.10: Laboratory Infiltration Measurements Fitted with Horton Equations Using Biofilter Media Only.

Biofilter media only, Trial 2

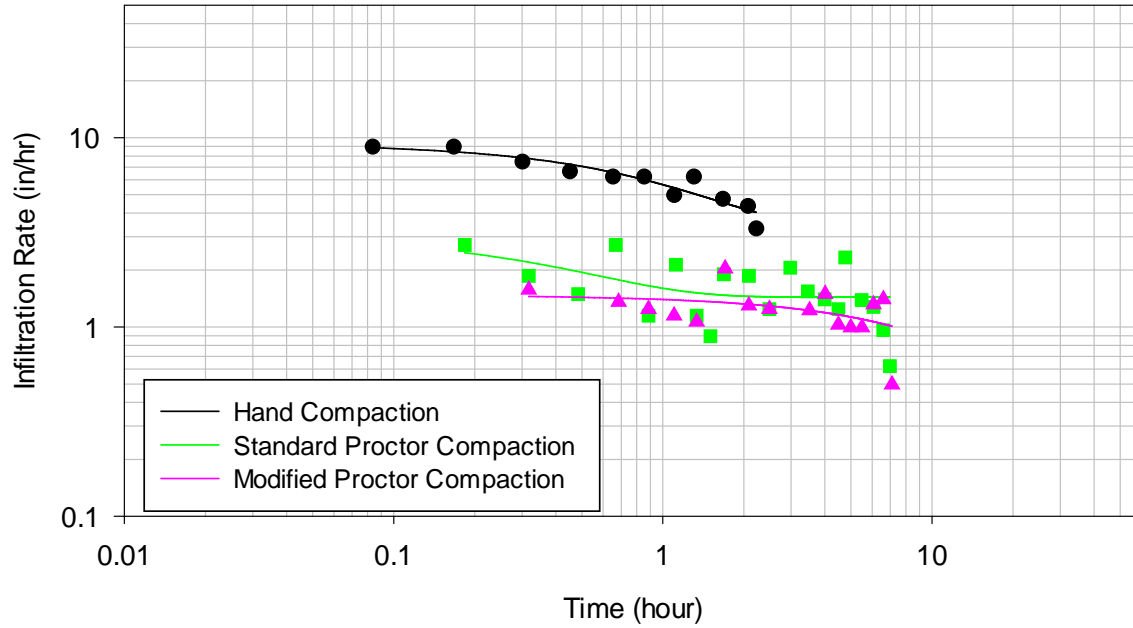


Biofilter media only, Trial 3

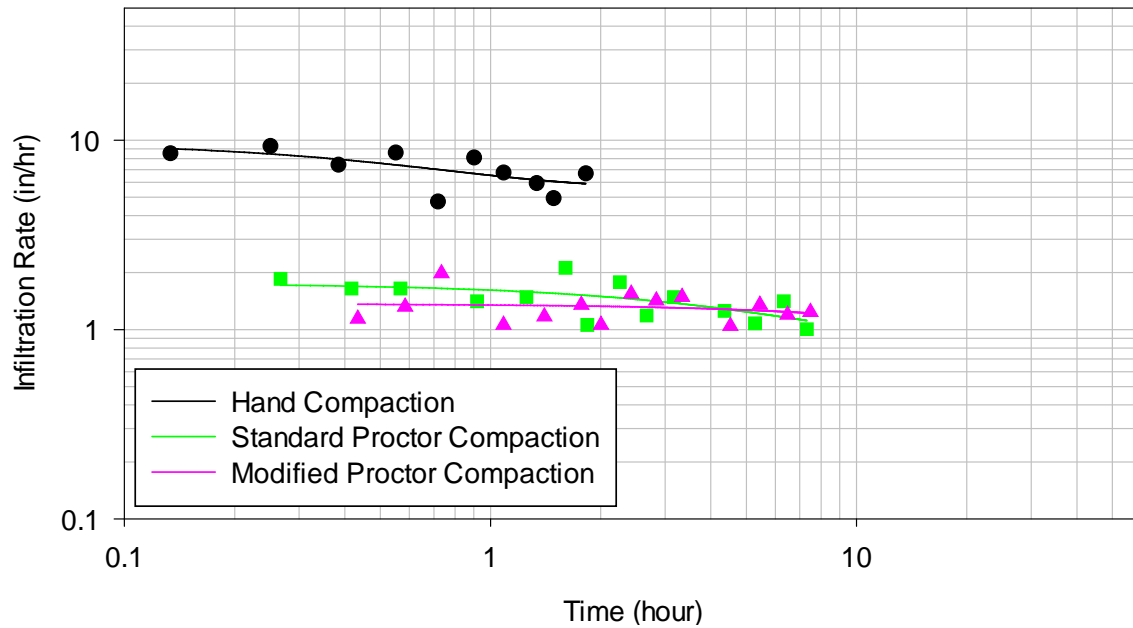


Appendix B.11: Laboratory Infiltration Measurements Fitted with Horton Equations Using 10% Sand and 90% Biofilter Media.

10% sand and 90% biofilter media, Trial 2

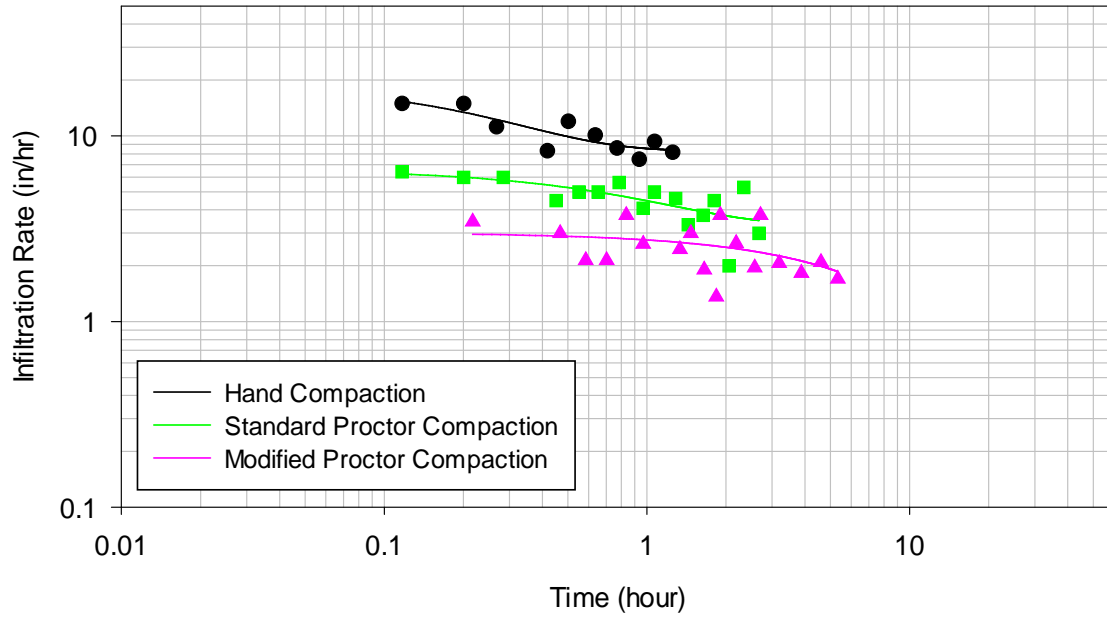


10% sand and 90% biofilter media, Trial 3

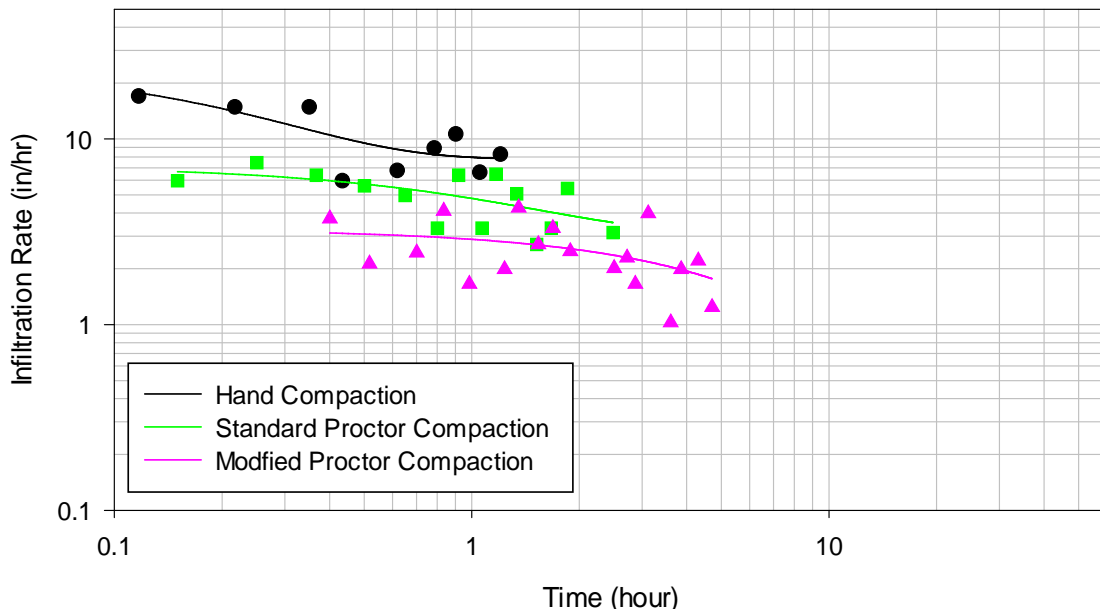


Appendix B.12: Laboratory Infiltration Measurements Fitted with Horton Equations Using 25% Sand and 75% Biofilter Media.

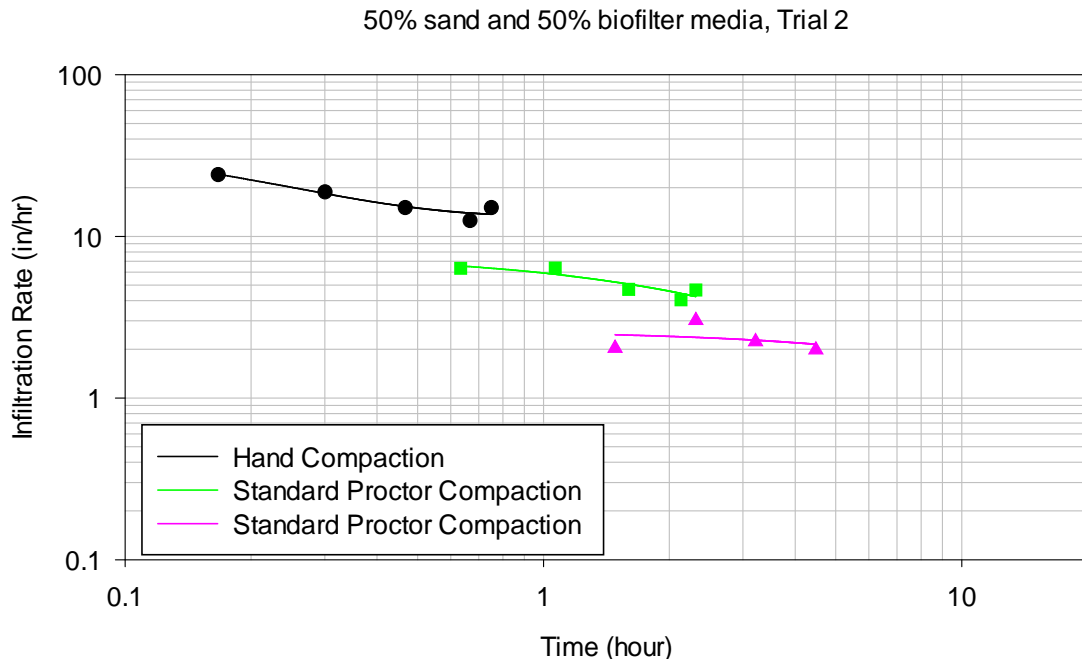
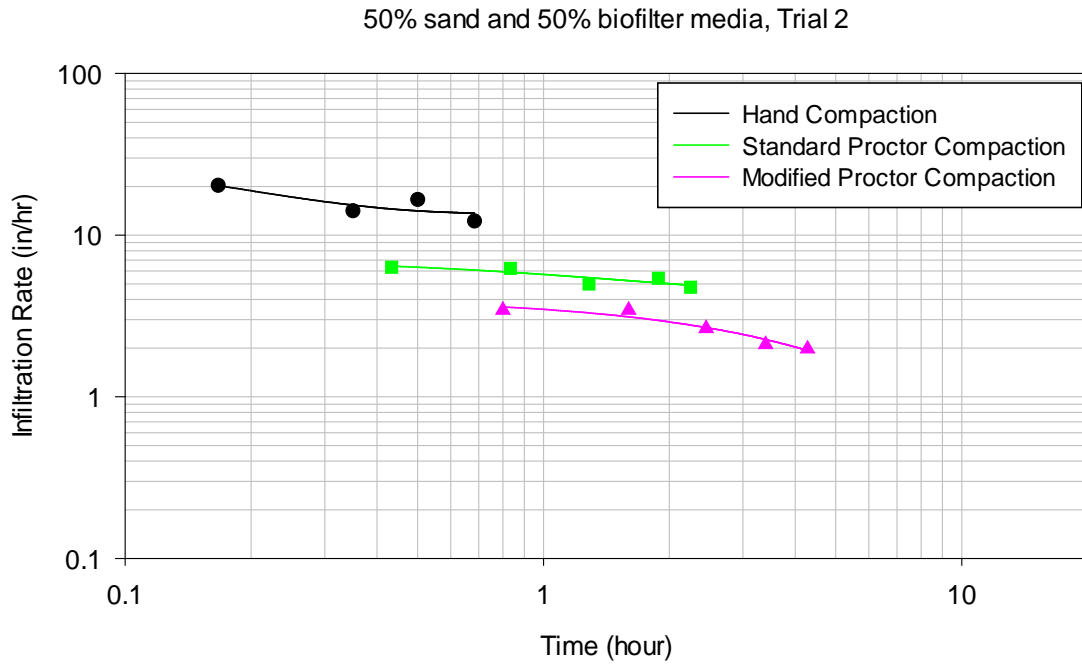
25% sand and 75% biofilter media, Trial 2



25% sand and 75% biofilter media, Trial 3

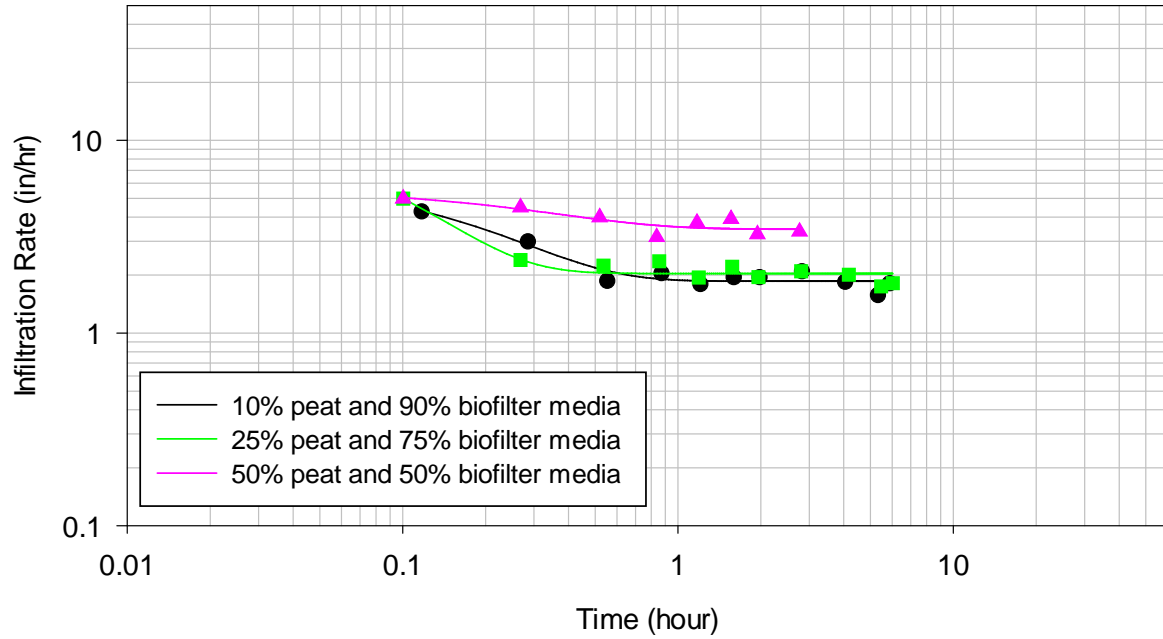


Appendix B.13: Laboratory Infiltration Measurements Fitted with Horton Equations Using 50% Sand and 50% Biofilter Media.

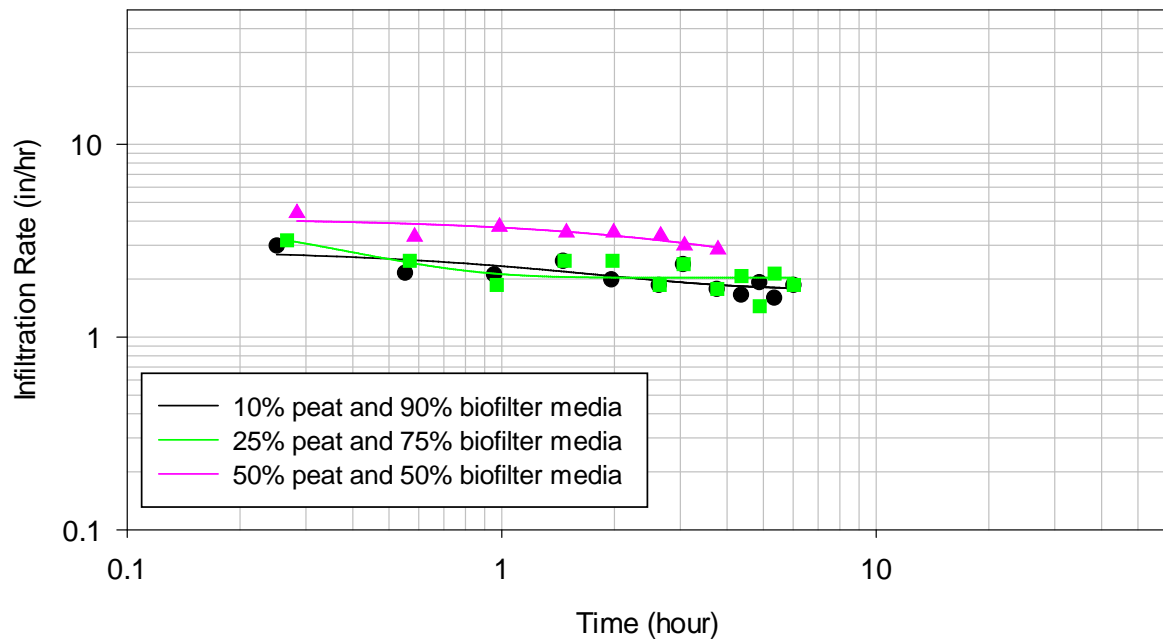


Appendix B.14: Laboratory Infiltration Measurements Fitted with Horton Equations Using Biofilter Media and Peat Mixture.

Lab Compaction Test Using Biofilter Soil and Peat Mixture, Trial 2



Lab Compaction Test Using Biofilter Soil and Peat Mixture, Trial 3



Appendix B.15: Kruskal-Wallis Multiple Comparisons for the Saturated Infiltration Rates of Lab Compaction Tests Using Biofilter Media Only.

Kruskal-Wallis: Multiple Comparisons

Kruskal-Wallis Test on the data

Group	N	Median	Ave Rank	Z
hand compaction	3	3.0410	8.0	2.32
standard proctor	3	0.9500	5.0	0.00
modified proctor	3	0.3400	2.0	-2.32
Overall	9		5.0	

H = 7.20 DF = 2 P = 0.027

* NOTE * One or more small samples

Kruskal-Wallis: All Pairwise Comparisons

Comparisons:	3
Family Alpha:	0.2
Bonferroni Individual Alpha:	0.067
Bonferroni Z-value (2-sided):	1.834

Standardized Absolute Mean Rank Differences
 $|\bar{R}(i) - \bar{R}(j)| / \text{Stdev}$

Rows: Group i = 1, ..., n
 Columns: Group j = 1, ..., n

1. Table of Z-values

hand compaction	0.00000		*	*
standard proctor	1.34164	0.00000	*	*
modified proctor	2.68328	1.34164	0	

2. Table of P-values

hand compaction	1.00000		*	*
standard proctor	0.17971	1.00000	*	*
modified proctor	0.00729	0.17971	1	

Sign Confidence Intervals controlled at a family error rate of 0.2

Desired Confidence: 80.529

Sign confidence interval for median

	N	Median	Achieved Confidence	Confidence Interval		Position
				Lower	Upper	
hand compaction	3	3.041	0.7500	2.996	5.850	1

standard proctor	3	0.9500	0.7500	0.5200	0.9700	1
modified proctor	3	0.3400	0.7500	0.1200	0.4000	1

The highest attainable confidence has been achieved.
The highest attainable confidence has been achieved.
The highest attainable confidence has been achieved.

Kruskal-Wallis: Conclusions

The following groups showed significant differences:

Groups	Z vs. Critical value	P-value
hand compaction vs. modified proctor	2.68328 >= 1.834	0.0073

Appendix B.16: Kruskal-Wallis Multiple Comparisons for the Saturated Infiltration Rates of Lab Compaction Tests Using 10% Sand and 90% Biofilter Media.

Kruskal-Wallis: Multiple Comparisons

Kruskal-Wallis Test on the data

Group	N	Median	Ave Rank	Z
hand compaction	3	5.720	8.0	2.32
standard proctor compaction	3	1.445	4.0	-0.77
modified proctor compaction	3	1.250	3.0	-1.55
Overall	9		5.0	

H = 5.60 DF = 2 P = 0.061

* NOTE * One or more small samples

Kruskal-Wallis: All Pairwise Comparisons

 Comparisons: 3
 Family Alpha: 0.2
 Bonferroni Individual Alpha: 0.067
 Bonferroni Z-value (2-sided): 1.834

Standardized Absolute Mean Rank Differences
 $|Rbar(i)-Rbar(j)| / Stdev$

Rows: Group i = 1,...,n
 Columns: Group j = 1,...,n

1. Table of Z-values

hand compaction	0.00000		*	*
standard proctor compaction	1.78885	0.000000	*	*
modified proctor compaction	2.23607	0.447214	0	

2. Table of P-values

hand compaction	1.00000		*	*
standard proctor compaction	0.07364	1.00000	*	*
modified proctor compaction	0.02535	0.65472	1	

 Sign Confidence Intervals controlled at a family error rate of 0.2

Desired Confidence: 80.529

Sign confidence interval for median

N	Median	Achieved Confidence	Confidence Interval		Position
			Lower	Upper	

hand compaction	3	5.720	0.7500	3.288	6.633	1
standard proctor compaction	3	1.445	0.7500	0.864	1.937	1
modified proctor compaction	3	1.250	0.7500	0.800	1.461	1

The highest attainable confidence has been achieved.
The highest attainable confidence has been achieved.
The highest attainable confidence has been achieved.

Kruskal-Wallis: Conclusions

The following groups showed significant differences:

Groups

hand compaction vs. modified proctor compaction

Z vs. Critical value	P-value
2.23607 >= 1.834	0.0253

Appendix B.17: Kruskal-Wallis Multiple Comparisons for the Saturated Infiltration Rates of Lab Compaction Tests Using 25% Sand and 75% Biofilter Media.

Kruskal-Wallis: Multiple Comparisons

Kruskal-Wallis Test on the data

Group	N	Median	Ave Rank	Z
hand compaction	3	7.843	8.0	2.32
standard proctor	3	3.311	5.0	0.00
modified proctor	3	1.500	2.0	-2.32
Overall	9		5.0	

H = 7.20 DF = 2 P = 0.027

* NOTE * One or more small samples

Kruskal-Wallis: All Pairwise Comparisons

Comparisons:	3
Family Alpha:	0.2
Bonferroni Individual Alpha:	0.067
Bonferroni Z-value (2-sided):	1.834

Standardized Absolute Mean Rank Differences
 $|Rbar(i) - Rbar(j)| / Stdev$

Rows: Group i = 1, ..., n
 Columns: Group j = 1, ..., n

1. Table of Z-values

hand compaction	0.00000		*	*
standard proctor	1.34164	0.00000	*	
modified proctor	2.68328	1.34164	0	

2. Table of P-values

hand compaction	1.00000		*	*
standard proctor	0.17971	1.00000	*	
modified proctor	0.00729	0.17971	1	

Sign Confidence Intervals controlled at a family error rate of 0.2

Desired Confidence: 80.529

Sign confidence interval for median

	N	Median	Achieved Confidence	Confidence Interval		Position
				Lower	Upper	
hand compaction	3	7.843	0.7500	7.500	8.346	1

standard proctor	3	3.311	0.7500	3.111	4.665	1
modified proctor	3	1.500	0.7500	1.250	1.705	1

The highest attainable confidence has been achieved.
The highest attainable confidence has been achieved.
The highest attainable confidence has been achieved.

Kruskal-Wallis: Conclusions

The following groups showed significant differences:

Groups	Z vs. Critical value	P-value
hand compaction vs. modified proctor	2.68328 >= 1.834	0.0073

Appendix B.18: Kruskal-Wallis Multiple Comparisons for the Saturated Infiltration Rates of Lab Compaction Tests Using 50% Sand and 50% Biofilter Media.

Kruskal-Wallis: All Pairwise Comparisons

```
-----
Comparisons:                3
Family Alpha:               0.2
Bonferroni Individual Alpha: 0.067
Bonferroni Z-value (2-sided): 1.834
-----
```

Standardized Absolute Mean Rank Differences
 $|Rbar(i)-Rbar(j)| / Stdev$

Rows: Group i = 1,...,n
 Columns: Group j = 1,...,n

1. Table of Z-values

```
hand compaction    0.00000    *  *
standard proctor  1.78885    0.000000  *
modified proctor   2.23607    0.447214  0
```

2. Table of P-values

```
hand compaction    1.00000    *  *
standard proctor   0.07364    1.00000  *
modified proctor   0.02535    0.65472  1
```

 Sign Confidence Intervals controlled at a family error rate of 0.2

Desired Confidence: 80.529

Sign confidence interval for median

	N	Median	Achieved Confidence	Confidence Interval		Position
				Lower	Upper	
hand compaction	3	13.55	0.7500	13.26	22.43	1
standard proctor	3	4.379	0.7500	1.507	5.997	1
modified proctor	3	1.980	0.7500	1.970	4.124	1

The highest attainable confidence has been achieved.
 The highest attainable confidence has been achieved.
 The highest attainable confidence has been achieved.

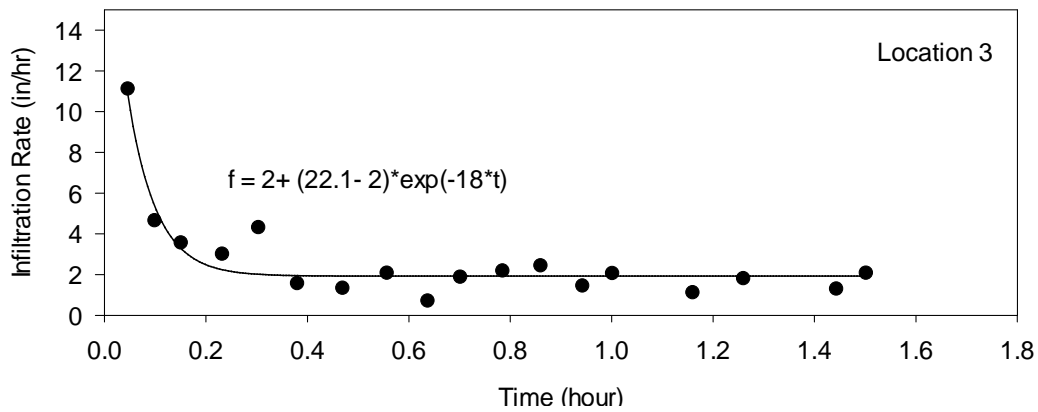
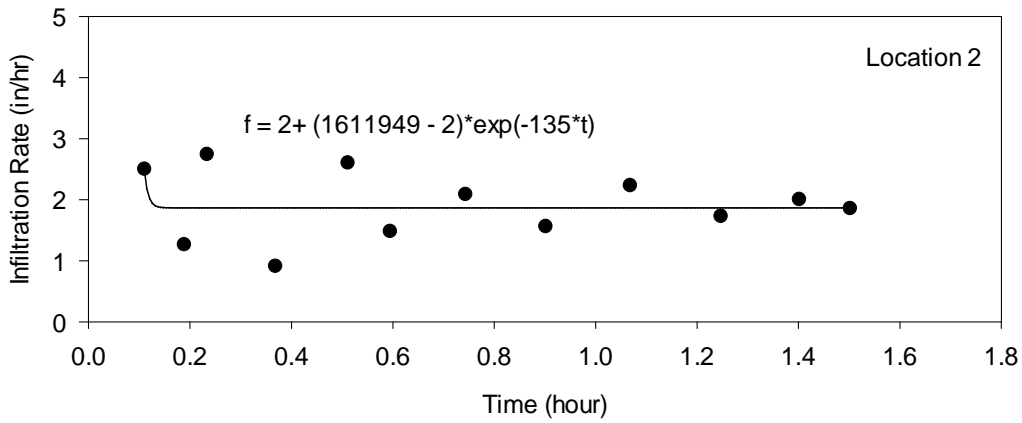
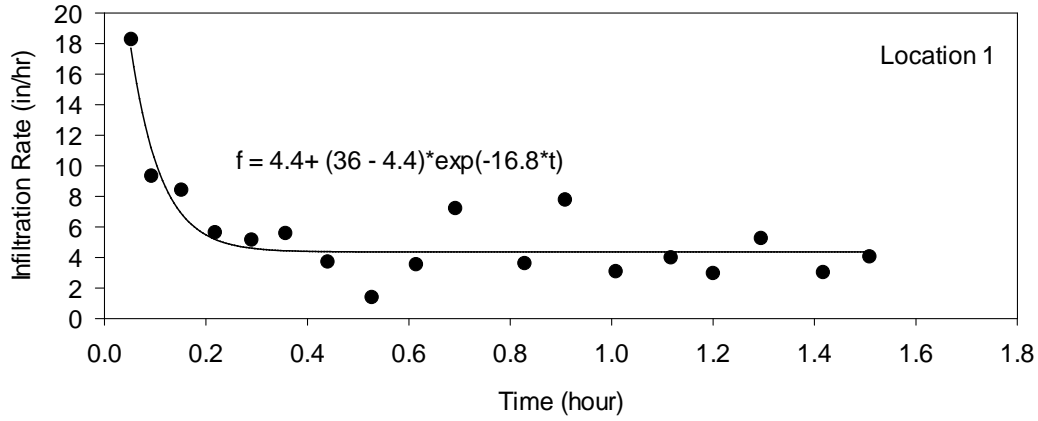
Kruskal-Wallis: Conclusions

The following groups showed significant differences:

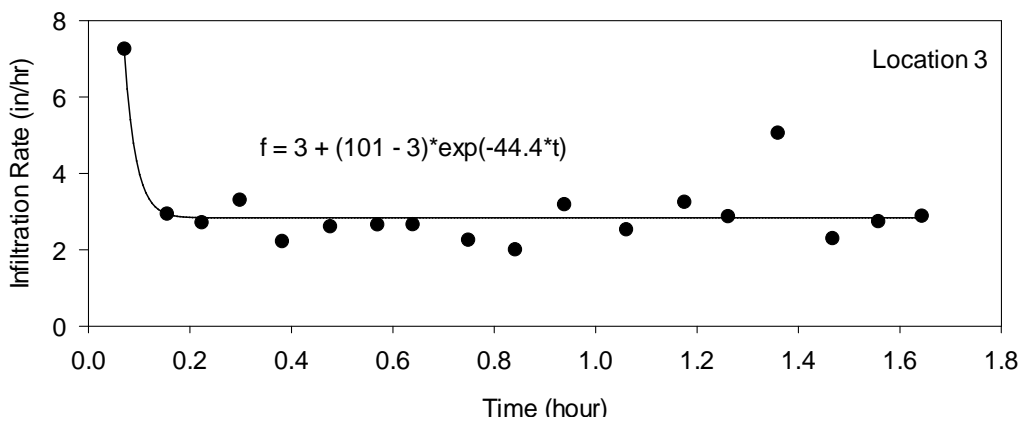
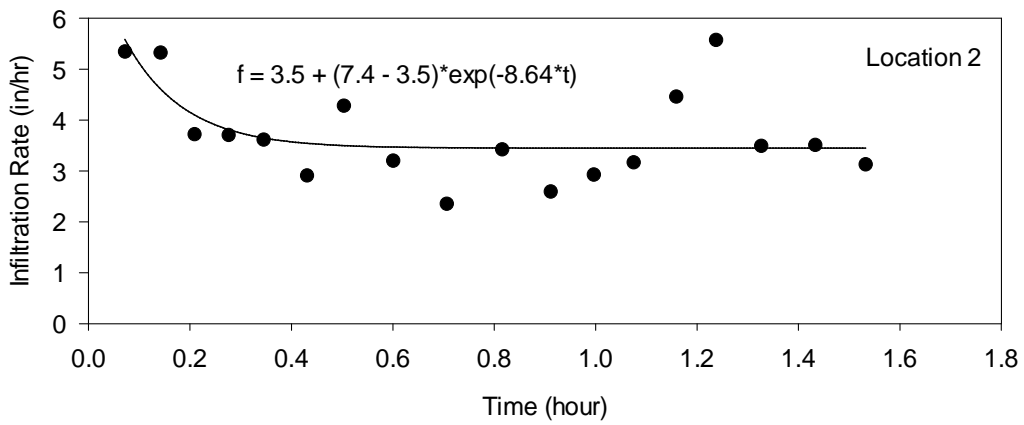
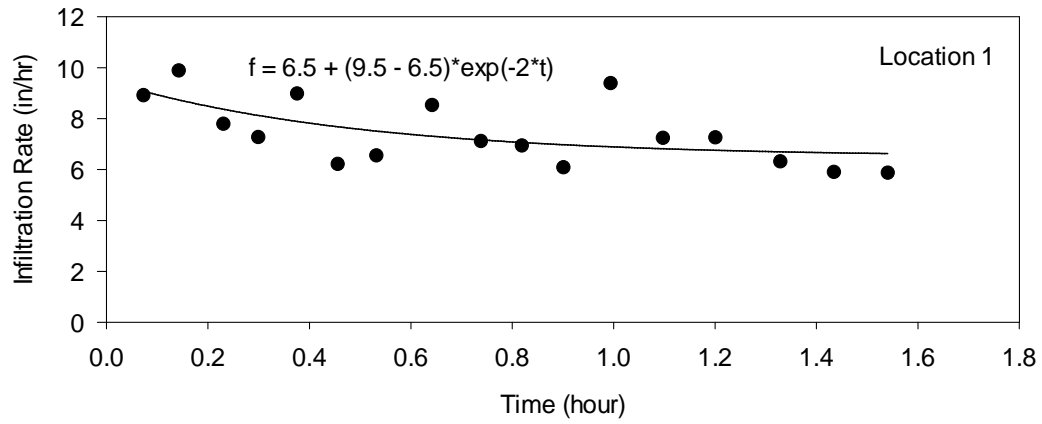
Groups	Z vs. Critical value	P-value
hand compaction vs. modified proctor	2.23607 >= 1.834	0.0253

APPENDIX C: SOIL MEDIA CHARACTERISTICS TEST RESULTS OF STORMWATER BIOINFILTRATION CONSTRUCTION SITES

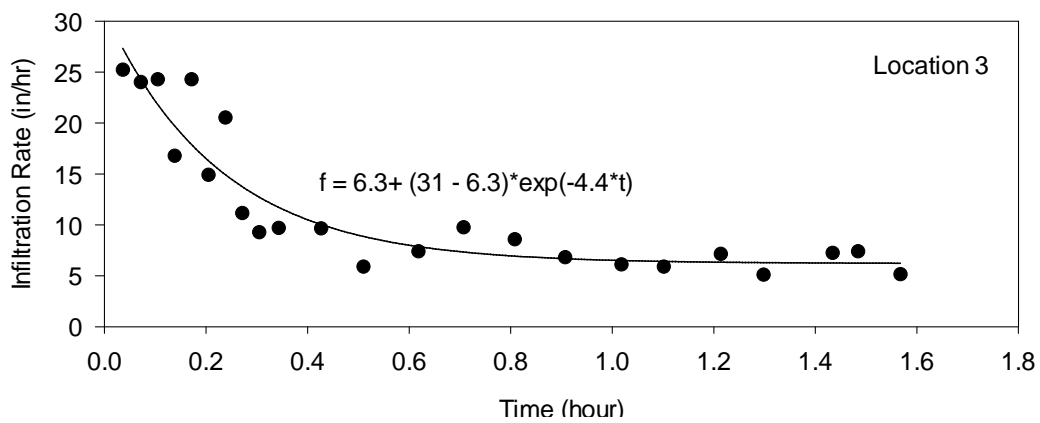
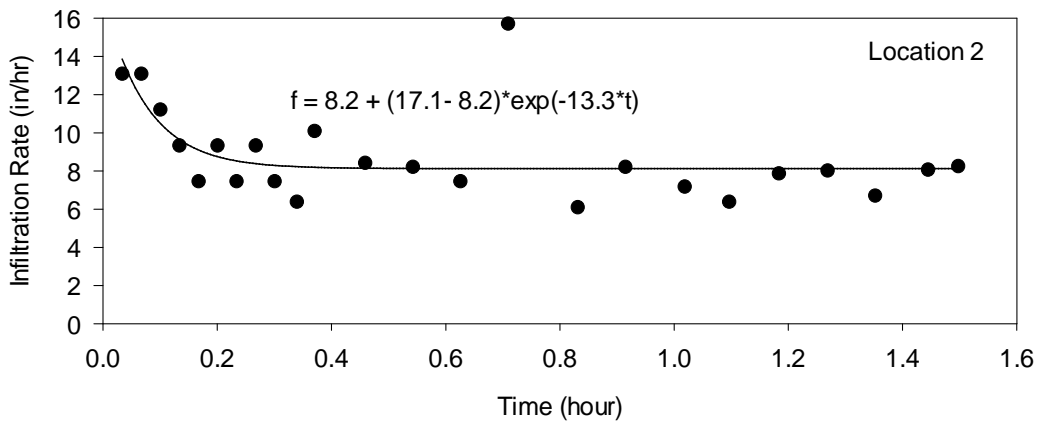
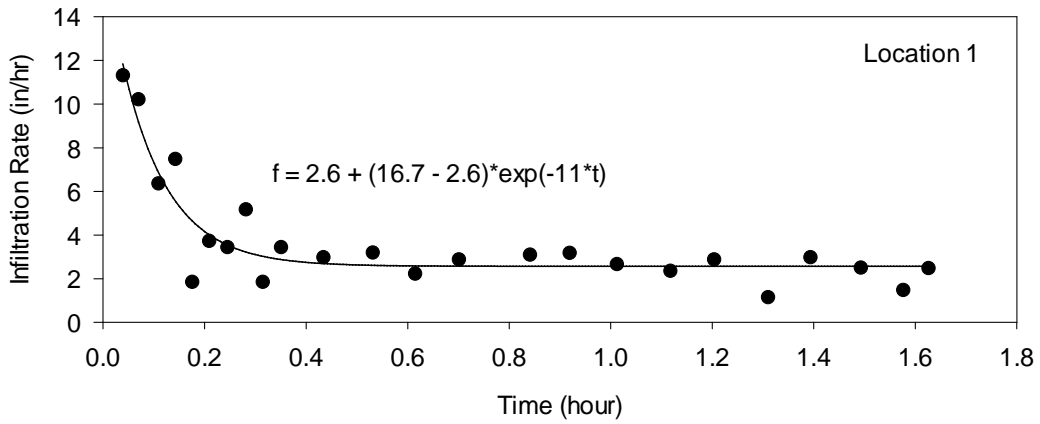
Appendix C.1: Double-ring Infiltration Measurements at the Intersection of 15th St. E and 6th Ave. E. Fitted with Horton Equation.



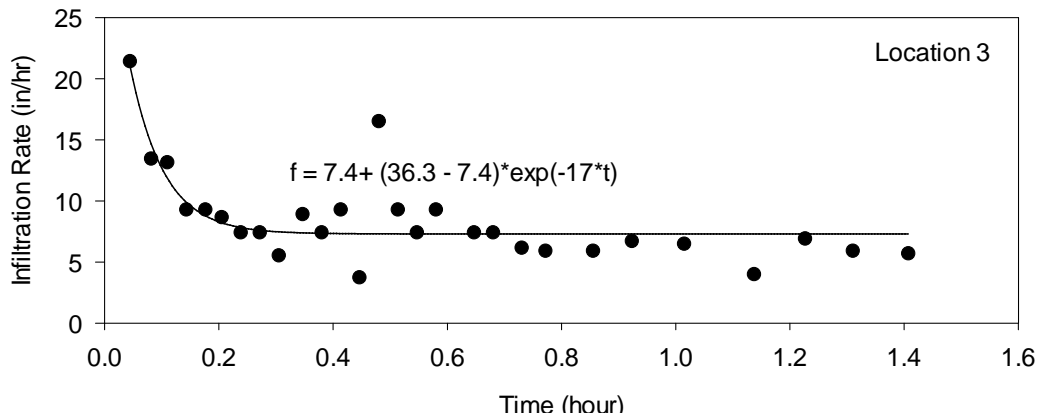
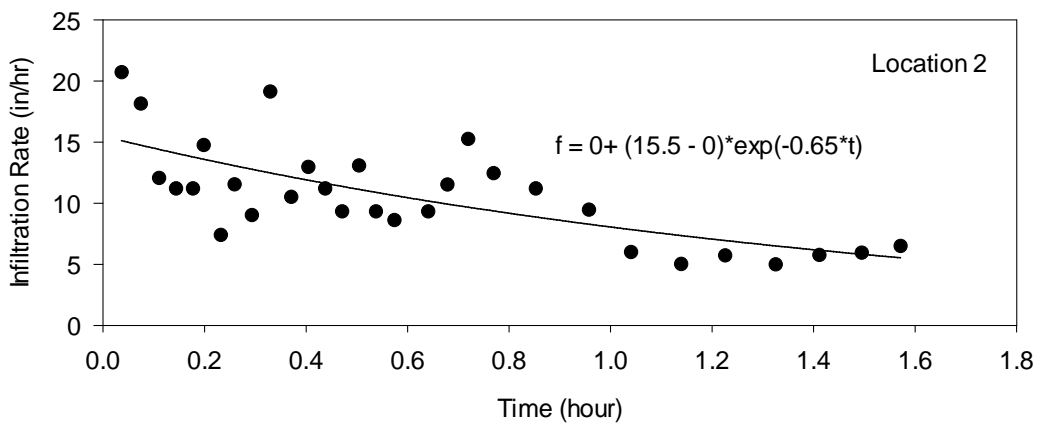
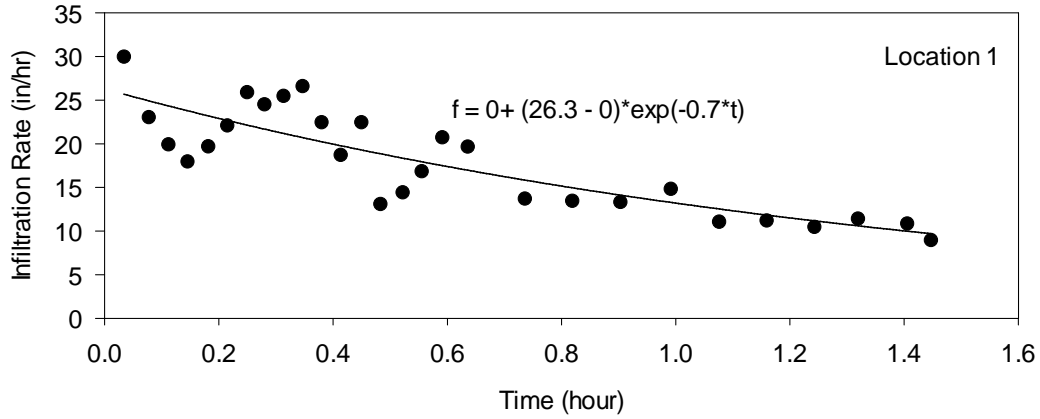
Appendix C.2: Double-ring Infiltration Measurements at Intersection of 17th Ave. E. and University Blvd E. Fitted with Horton Equation.



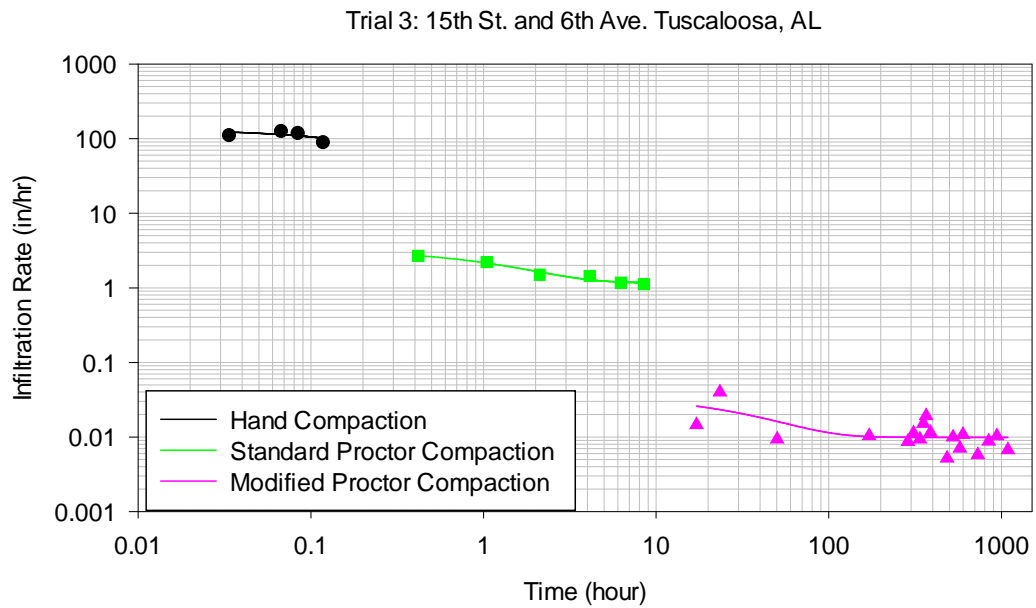
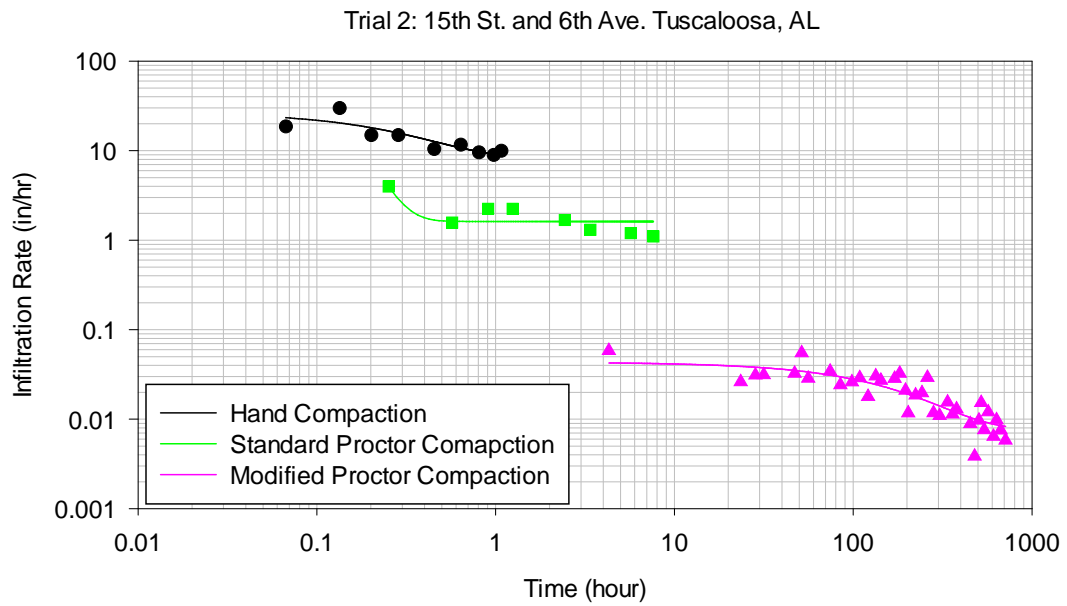
Appendix C.3: Double-ring Infiltration Measurements at Intersection of 21th Ave. E. and University Blvd E. Fitted with Horton Equation.



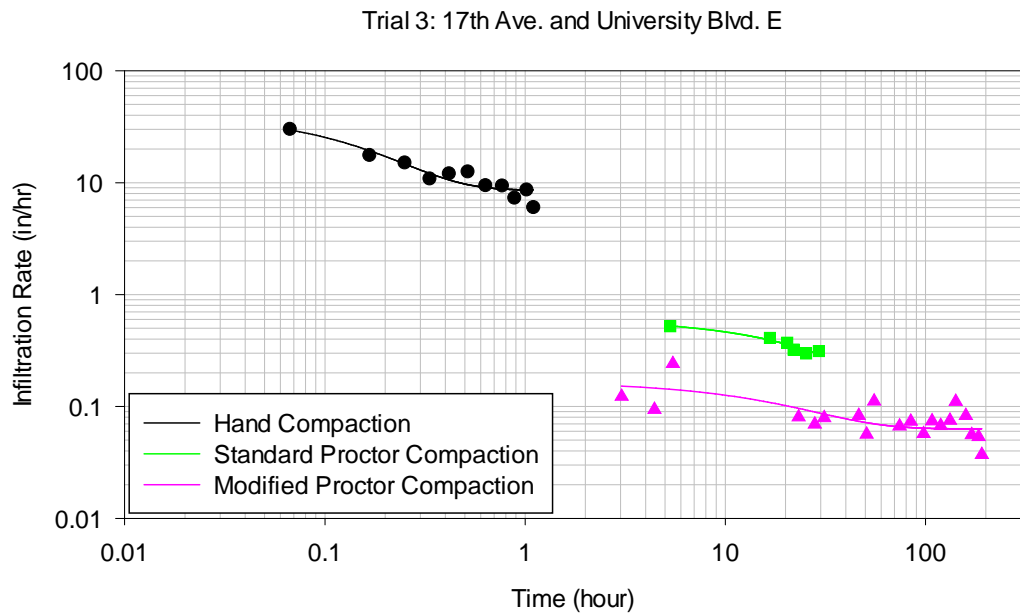
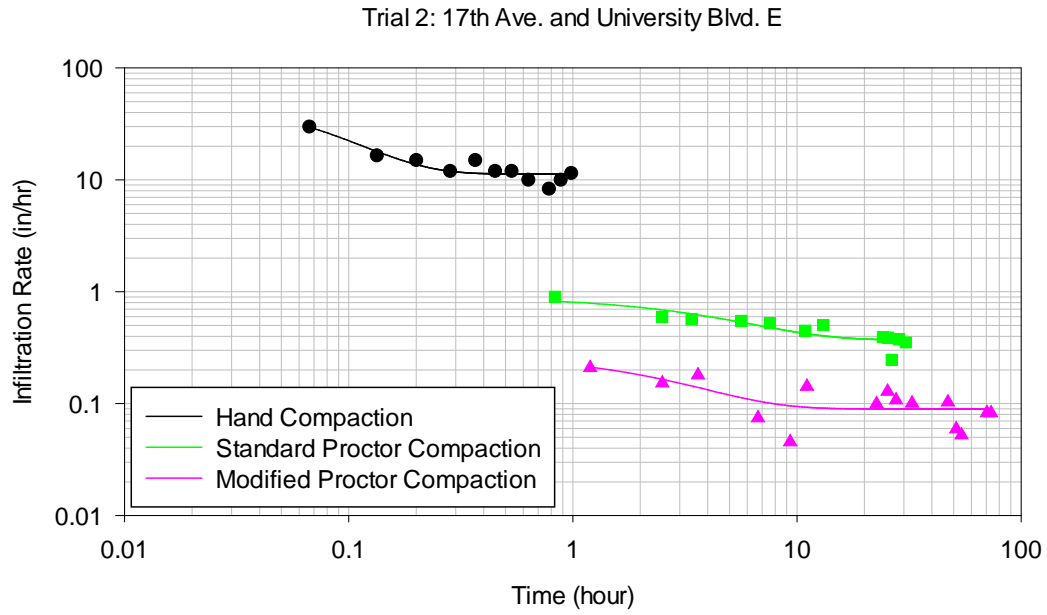
Appendix C.4: Double-ring Infiltration Measurements at Intersection of 25th Ave. E. and University Blvd E. Fitted with Horton Equation.



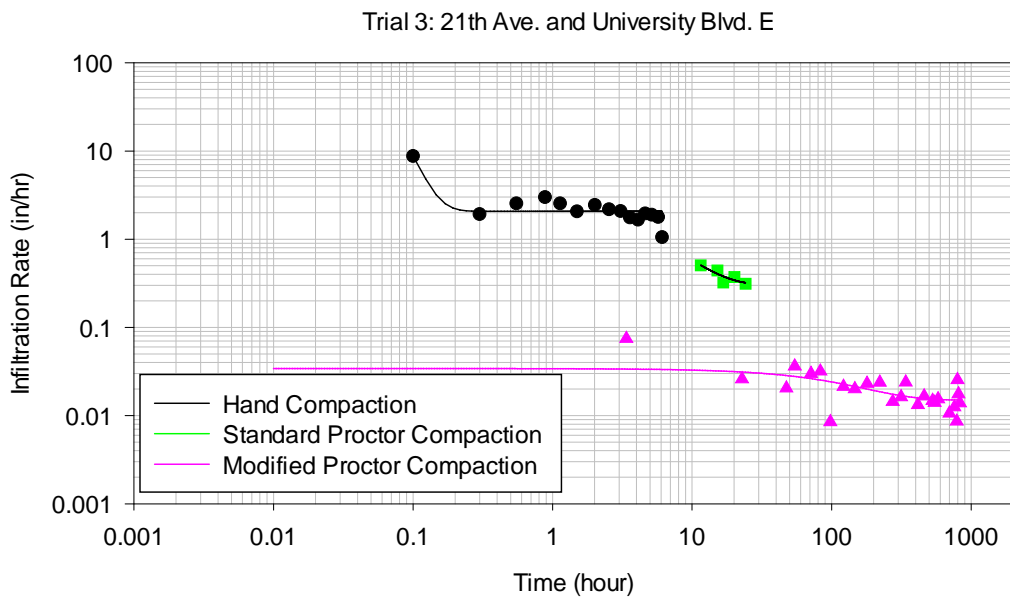
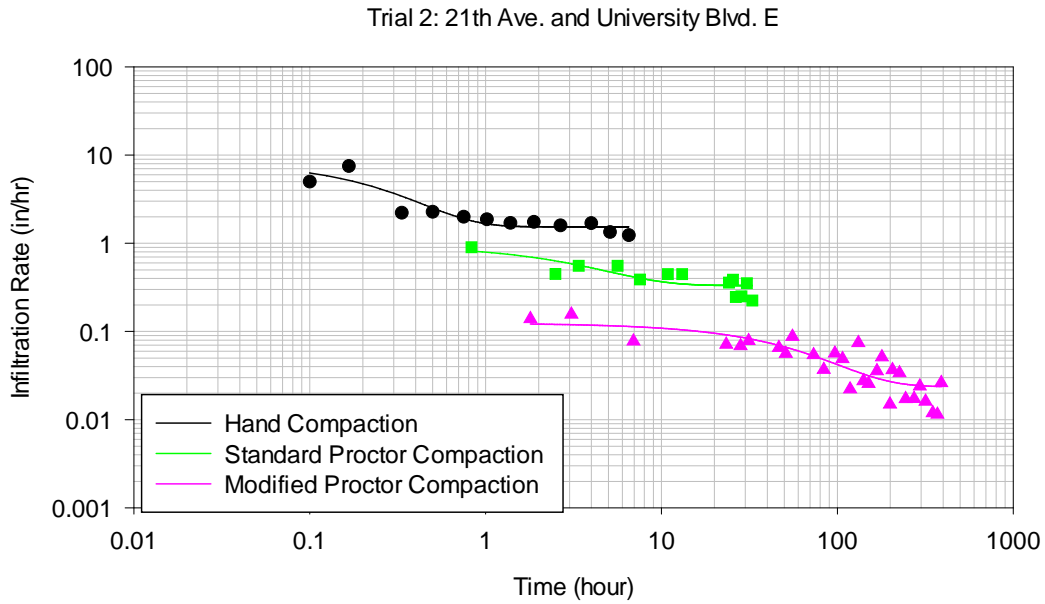
Appendix C.5: Laboratory Infiltration Measurements Using Surface Soil from 15th St. E and 6th Ave. E. Fitted with Horton Equations.



Appendix C.6: Laboratory Infiltration Measurements Using Surface Soil from 17th Ave. E and University Blvd E. Fitted with Horton Equations.

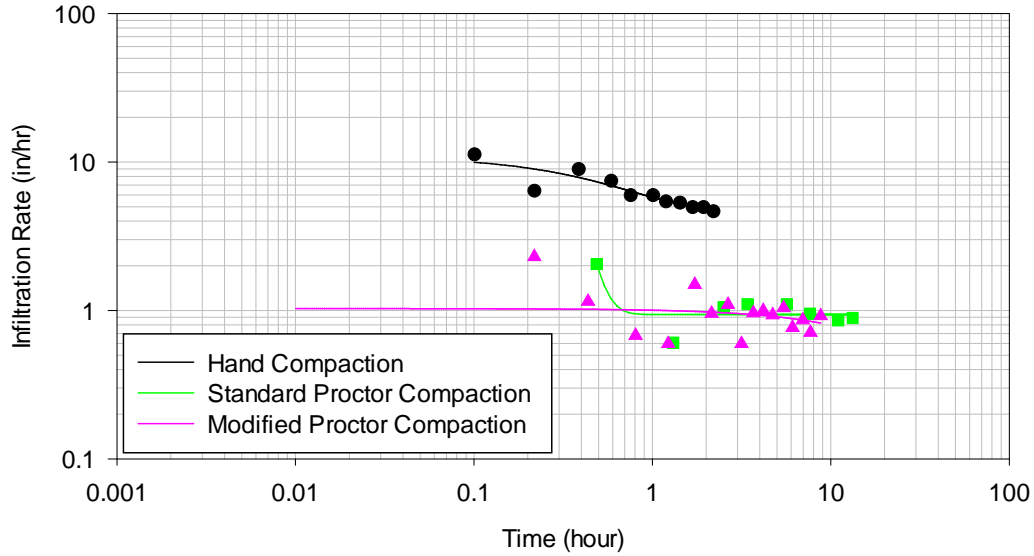


Appendix C.7: Laboratory Infiltration Measurements Using Surface Soil from 21th Ave. E and University Blvd E. Fitted with Horton Equations.

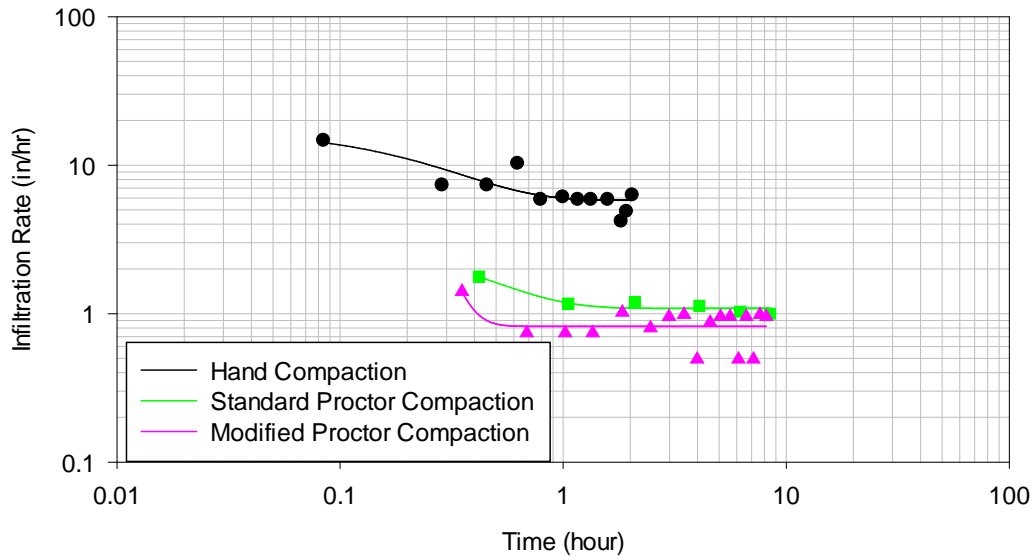


Appendix C.8: Laboratory Infiltration Measurements Using Surface Soil from 25th Ave. E and University Blvd E. Fitted with Horton Equations.

Trial 2: 25th Ave. and University Blvd. E

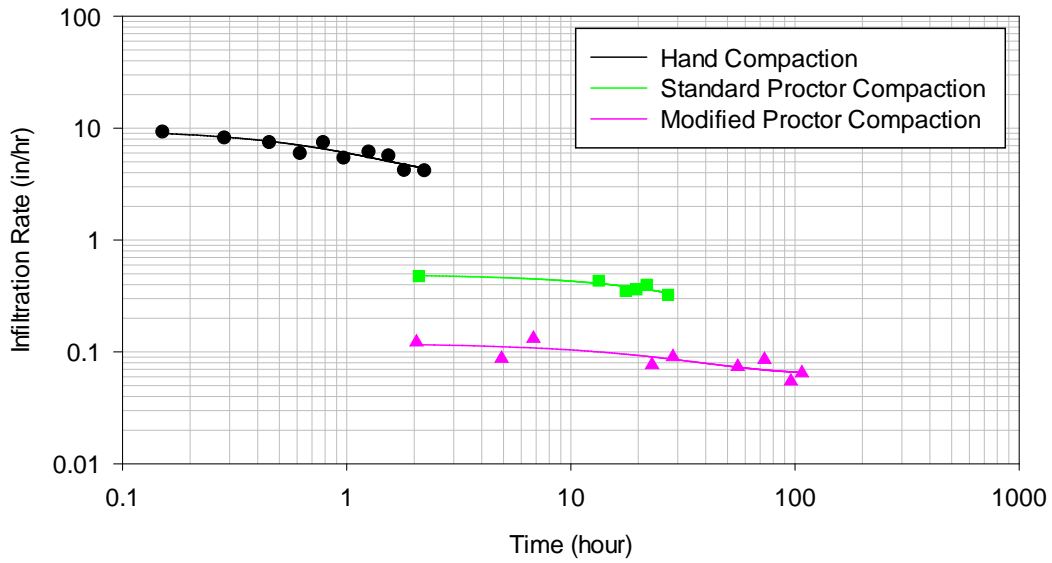


Trial 3: 25th Ave. and University Blvd. E

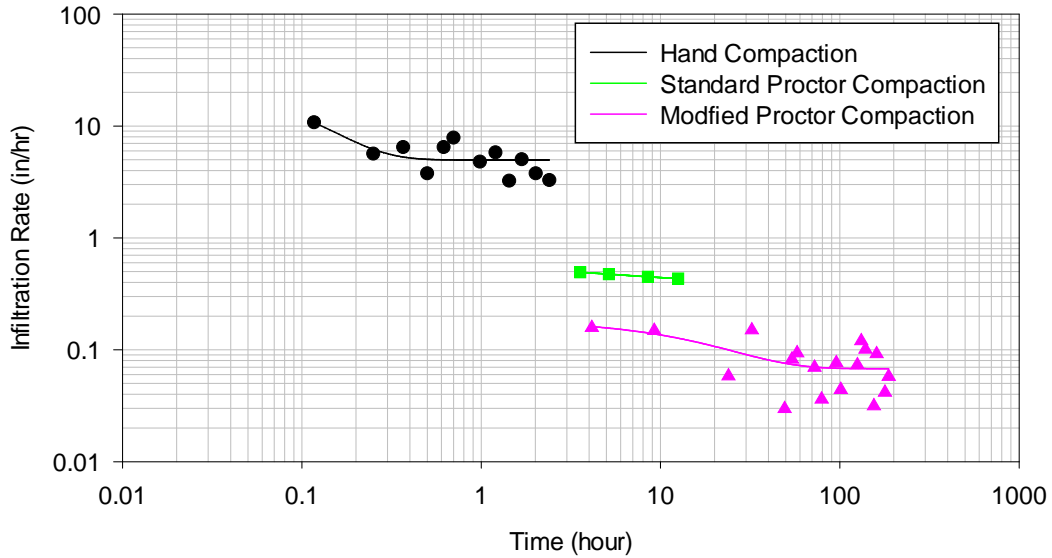


Appendix C.9: Laboratory Infiltration Measurements Using Subsurface Soil from 15th St. E and 6th Ave. E. Fitted with Horton Equations.

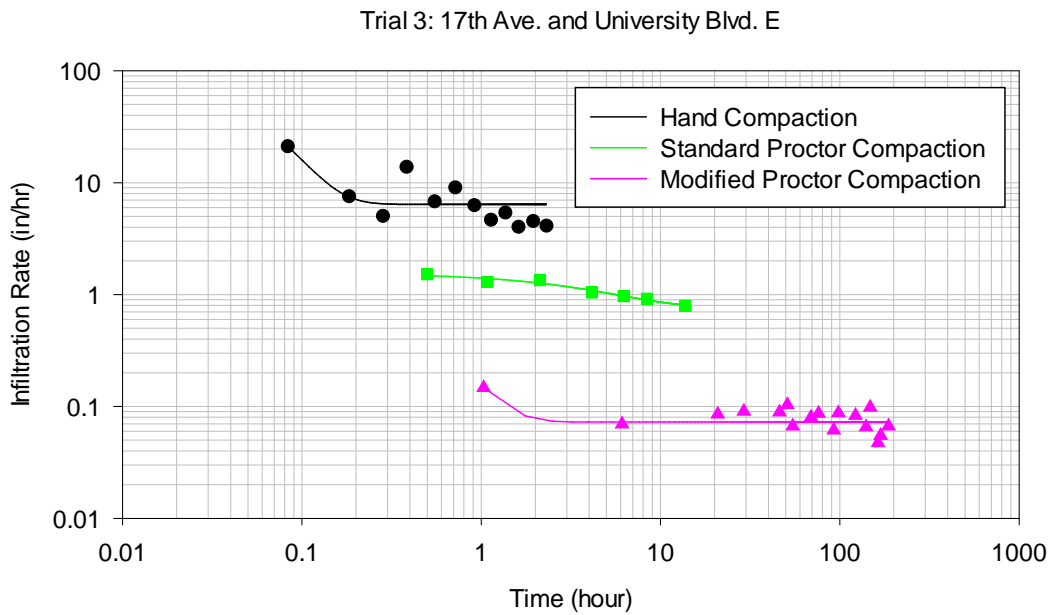
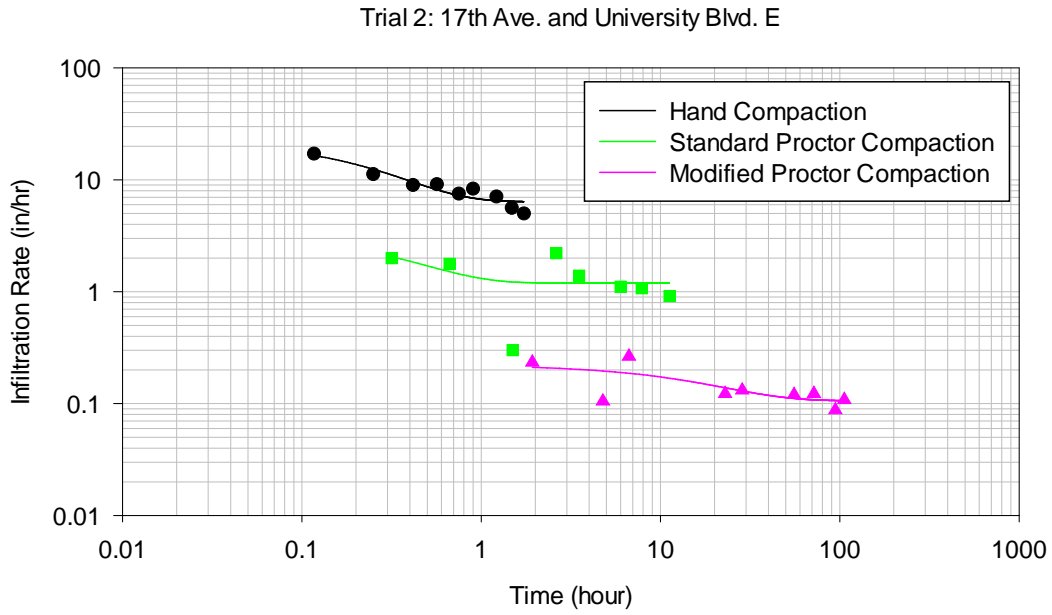
Trial 2: 15th St. and 6th Ave. E



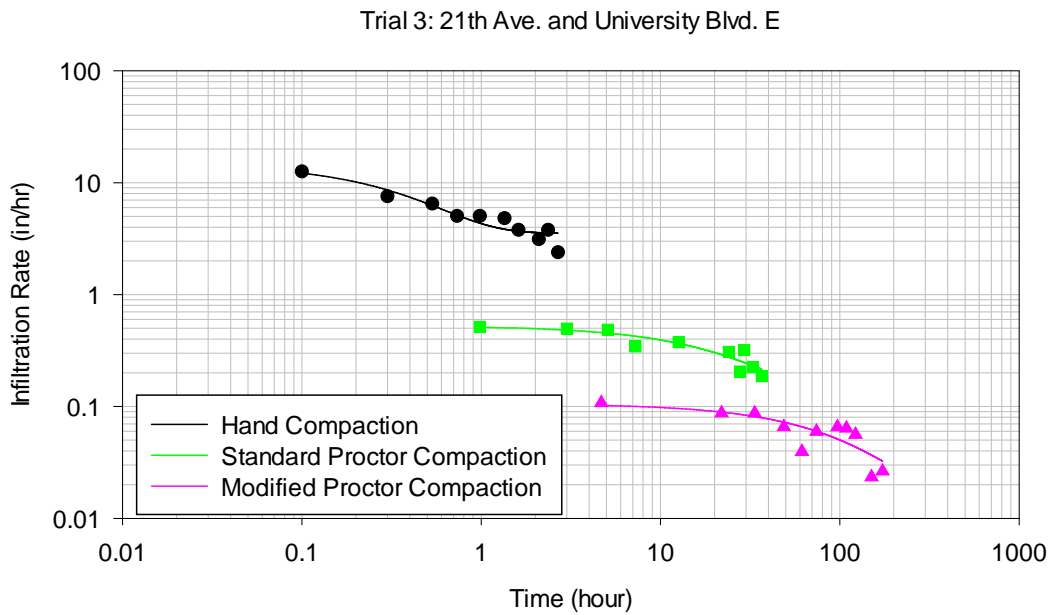
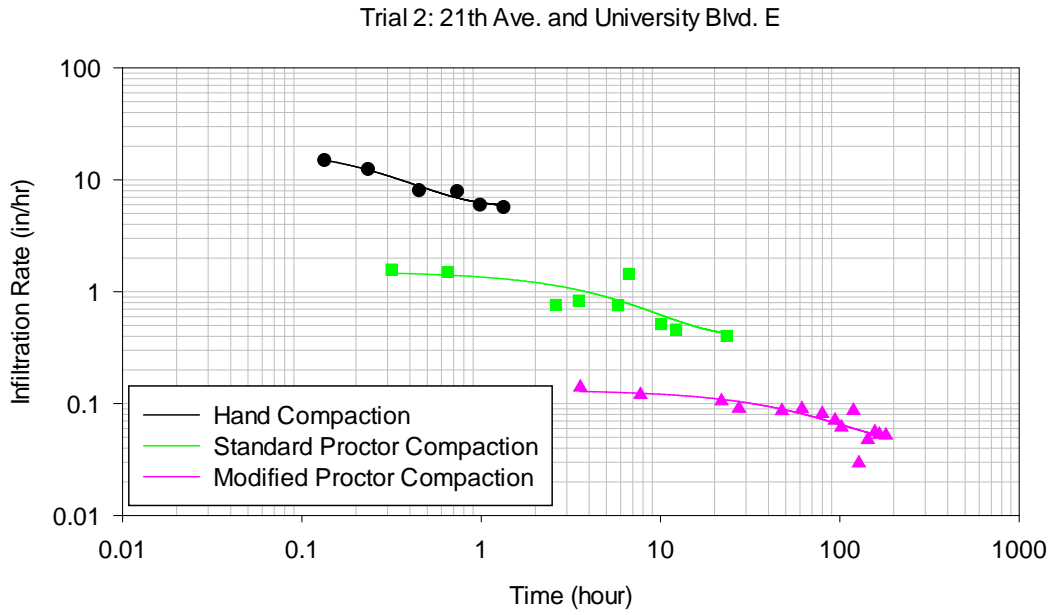
Trial 3: 15th St. and 6th Ave. E



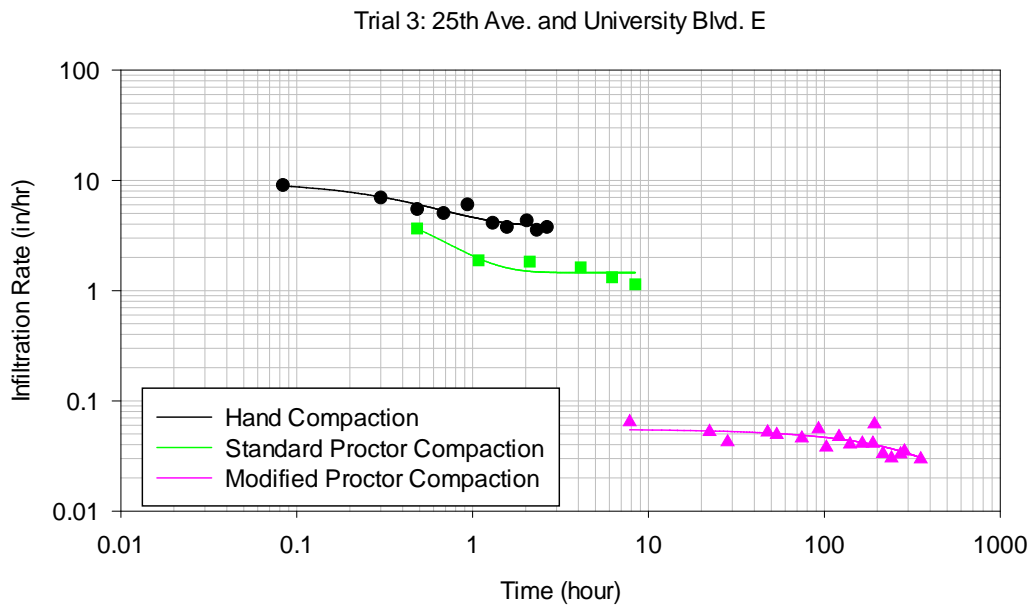
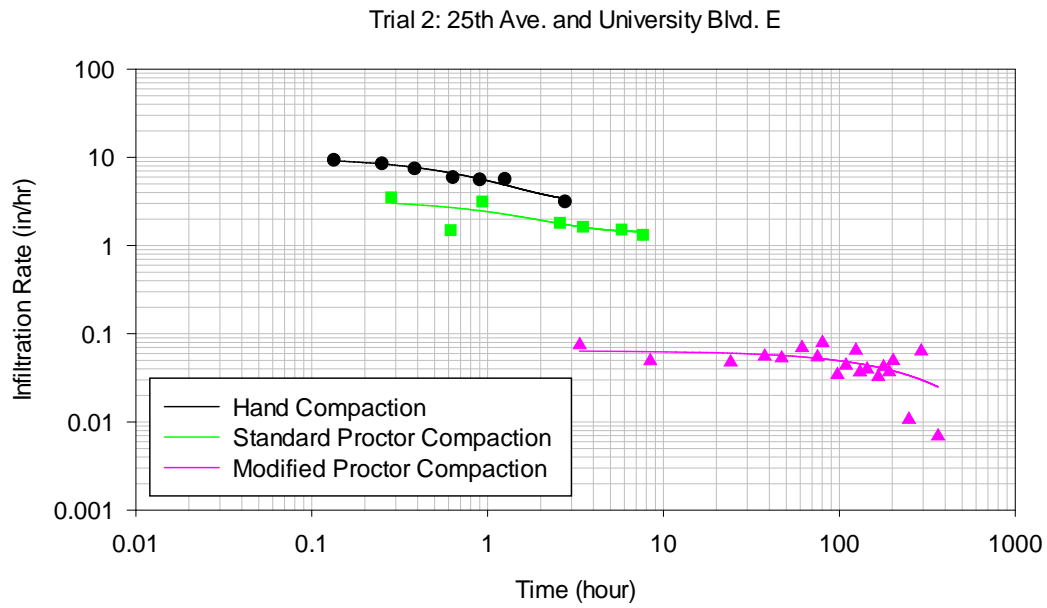
Appendix C.10: Laboratory Infiltration Measurements Using Subsurface Soil from 17th Ave. E and University Blvd E. Fitted with Horton Equations.



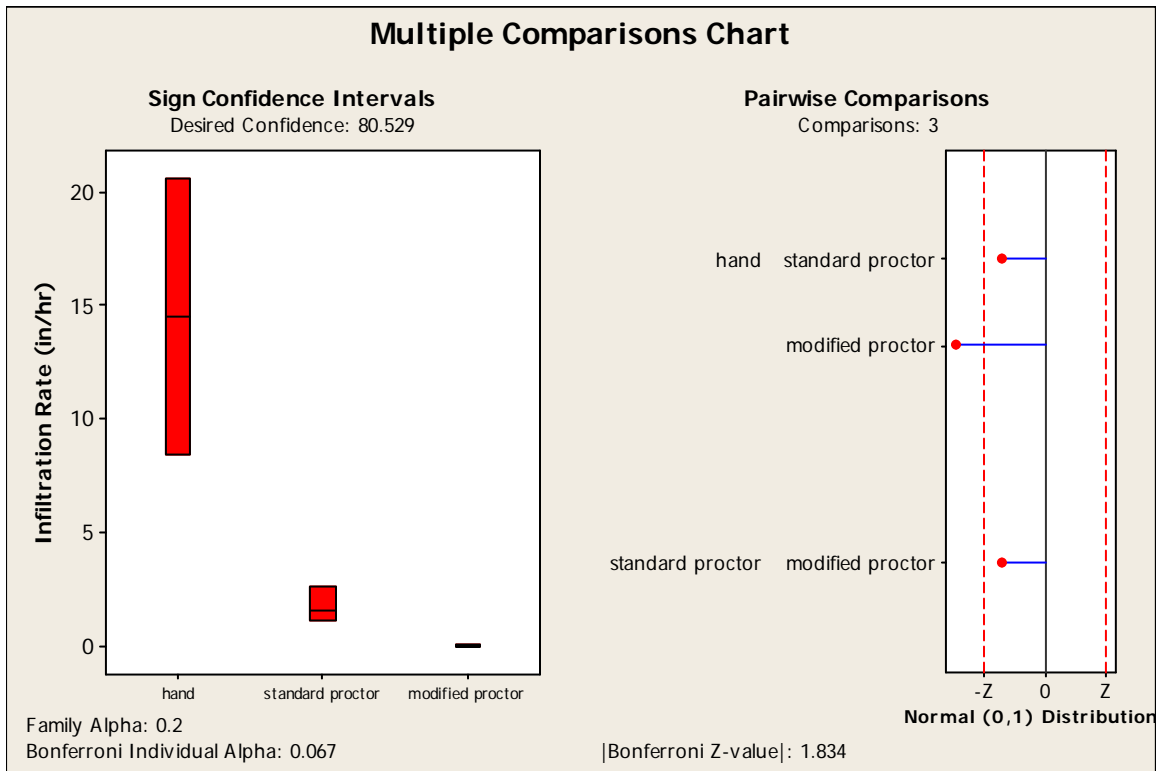
Appendix C.11: Laboratory Infiltration Measurements Using Subsurface Soil from 21th Ave. E and University Blvd E. Fitted with Horton Equations.



Appendix C.12: Laboratory Infiltration Measurements Using Subsurface Soil from 25th Ave. E and University Blvd E. Fitted with Horton Equations.



Appendix C.13: Kruskal-Wallis Multiple Comparisons for the Saturated Infiltration Rates of Lab Compaction Tests Using Surface Soil on 15th St. E and 6th Ave. E., Tuscaloosa, AL.



Kruskal-Wallis: Multiple Comparisons

Kruskal-Wallis Test on the data

Group	N	Median	Ave Rank	Z
hand	3	14.50000	8.0	2.32
standard proctor	3	1.62700	5.0	0.00
modified proctor	3	0.01000	2.0	-2.32
Overall	9		5.0	

H = 7.20 DF = 2 P = 0.027

* NOTE * One or more small samples

Kruskal-Wallis: All Pairwise Comparisons

Comparisons: 3
 Family Alpha: 0.2
 Bonferroni Individual Alpha: 0.067
 Bonferroni Z-value (2-sided): 1.834

 Standardized Absolute Mean Rank Differences
 $|Rbar(i)-Rbar(j)| / Stdev$

Rows: Group i = 1,...,n
 Columns: Group j = 1,...,n

1. Table of Z-values

hand	0.00000		*	*
standard proctor	1.34164	0.00000	*	
modified proctor	2.68328	1.34164	0	

2. Table of P-values

hand	1.00000		*	*
standard proctor	0.17971	1.00000	*	
modified proctor	0.00729	0.17971	1	

 Sign Confidence Intervals controlled at a family error rate of 0.2

Desired Confidence: 80.529

Sign confidence interval for median

	N	Median	Achieved Confidence	Confidence Interval		Position
				Lower	Upper	
hand	3	14.50	0.7500	8.48	20.59	1
standard proctor	3	1.627	0.7500	1.181	2.611	1
modified proctor	3	0.0100	0.7500	0.0080	0.1080	1

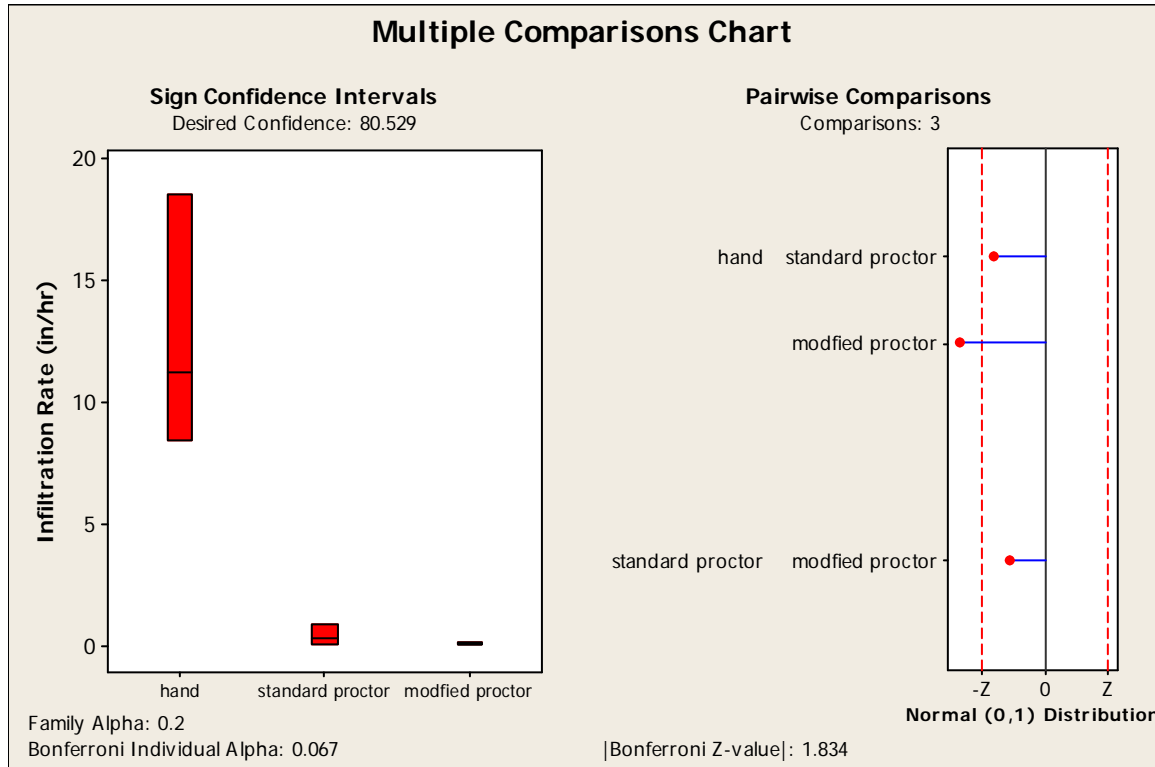
The highest attainable confidence has been achieved.
 The highest attainable confidence has been achieved.
 The highest attainable confidence has been achieved.

Kruskal-Wallis: Conclusions

The following groups showed significant differences:

Groups	Z vs. Critical value	P-value
hand vs. modified proctor	2.68328 >= 1.834	0.0073

Appendix C.14: Kruskal-Wallis Multiple Comparisons for the Saturated Infiltration Rates of Lab Compaction Tests Using Surface Soil on 17th Ave. E. and University Blvd. E. (Tuscaloosa Physical Therapy), Tuscaloosa, AL.



Kruskal-Wallis: Multiple Comparisons

Kruskal-Wallis Test on the data

Group	N	Median	Ave Rank	Z
hand	3	11.25200	8.0	2.32
standard proctor	3	0.36900	4.7	-0.26
modified proctor	3	0.08900	2.3	-2.07
Overall	9		5.0	

H = 6.49 DF = 2 P = 0.039

* NOTE * One or more small samples

Kruskal-Wallis: All Pairwise Comparisons

Comparisons:	3
Family Alpha:	0.2
Bonferroni Individual Alpha:	0.067
Bonferroni Z-value (2-sided):	1.834

Standardized Absolute Mean Rank Differences
 $|Rbar(i)-Rbar(j)| / Stdev$

Rows: Group i = 1,...,n
 Columns: Group j = 1,...,n

1. Table of Z-values

hand	0.00000		*	*
standard proctor	1.49071	0.00000	*	*
modified proctor	2.53421	1.04350	0	

2. Table of P-values

hand	1.00000		*	*
standard proctor	0.13604	1.00000	*	*
modified proctor	0.01127	0.29672	1	

Sign Confidence Intervals controlled at a family error rate of 0.2

Desired Confidence: 80.529

Sign confidence interval for median

	N	Median	Achieved Confidence	Confidence Interval		Position
				Lower	Upper	
hand	3	11.25	0.7500	8.50	18.55	1
standard proctor	3	0.3690	0.7500	0.1020	0.8860	1
modified proctor	3	0.0890	0.7500	0.0620	0.2180	1

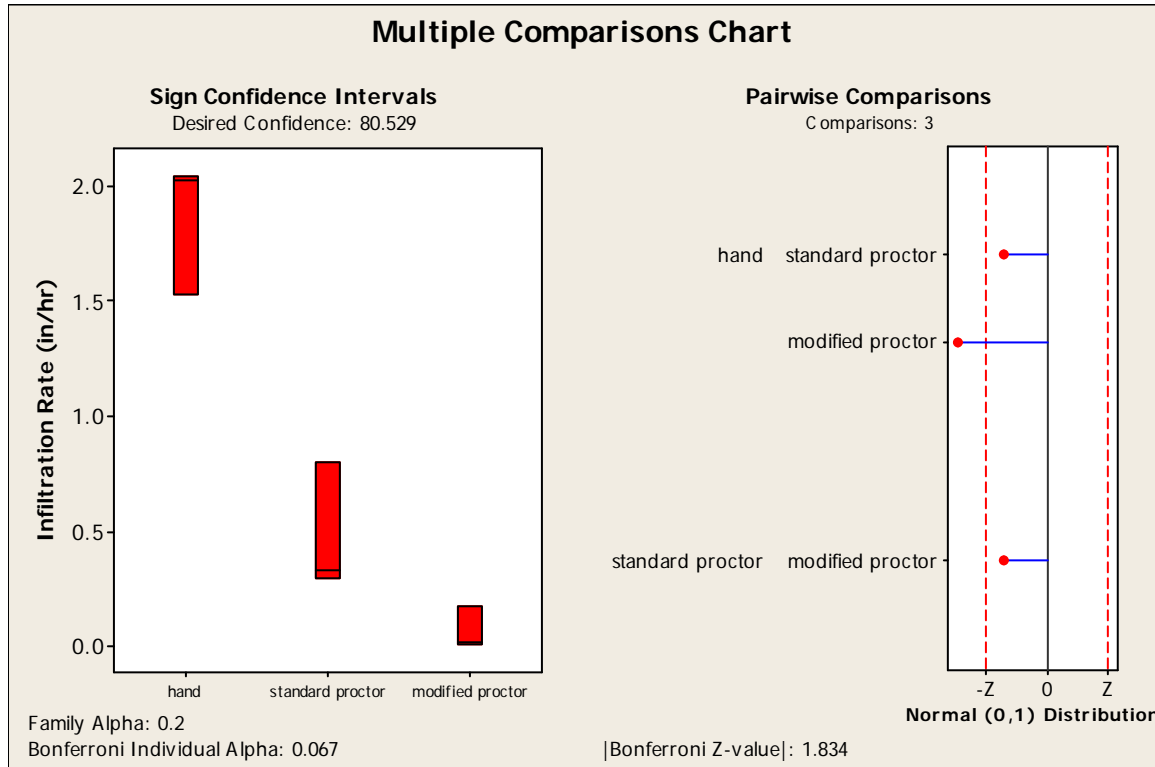
The highest attainable confidence has been achieved.
 The highest attainable confidence has been achieved.
 The highest attainable confidence has been achieved.

Kruskal-Wallis: Conclusions

The following groups showed significant differences:

Groups	Z vs. Critical value	P-value
hand vs. modified proctor	2.53421 >= 1.834	0.0113

Appendix C.15: Kruskal-Wallis Multiple Comparisons for the Saturated Infiltration Rates of Lab Compaction Tests Using Surface Soil on 21st Ave. E. and University Blvd. E. (Alberta Hand Carwash), Tuscaloosa, AL.



Kruskal-Wallis: Multiple Comparisons

Kruskal-Wallis Test on the data

Group	N	Median	Ave Rank	Z
hand	3	2.02200	8.0	2.32
standard proctor	3	0.33160	5.0	0.00
modified proctor	3	0.02360	2.0	-2.32
Overall	9		5.0	

H = 7.20 DF = 2 P = 0.027

* NOTE * One or more small samples

Kruskal-Wallis: All Pairwise Comparisons

Comparisons: 3
Family Alpha: 0.2
Bonferroni Individual Alpha: 0.067

Bonferroni Z-value (2-sided): 1.834

Standardized Absolute Mean Rank Differences
|Rbar(i)-Rbar(j)| / Stdev

Rows: Group i = 1,...,n
Columns: Group j = 1,...,n

1. Table of Z-values

hand	0.00000		*	*
standard proctor	1.34164	0.00000	*	*
modified proctor	2.68328	1.34164	0	

2. Table of P-values

hand	1.00000		*	*
standard proctor	0.17971	1.00000	*	*
modified proctor	0.00729	0.17971	1	

Sign Confidence Intervals controlled at a family error rate of 0.2

Desired Confidence: 80.529

Sign confidence interval for median

				Confidence		
	N	Median	Achieved	Interval		Position
			Confidence	Lower	Upper	
hand	3	2.022	0.7500	1.535	2.043	1
standard proctor	3	0.3316	0.7500	0.2975	0.8050	1
modified proctor	3	0.0236	0.7500	0.0148	0.1780	1

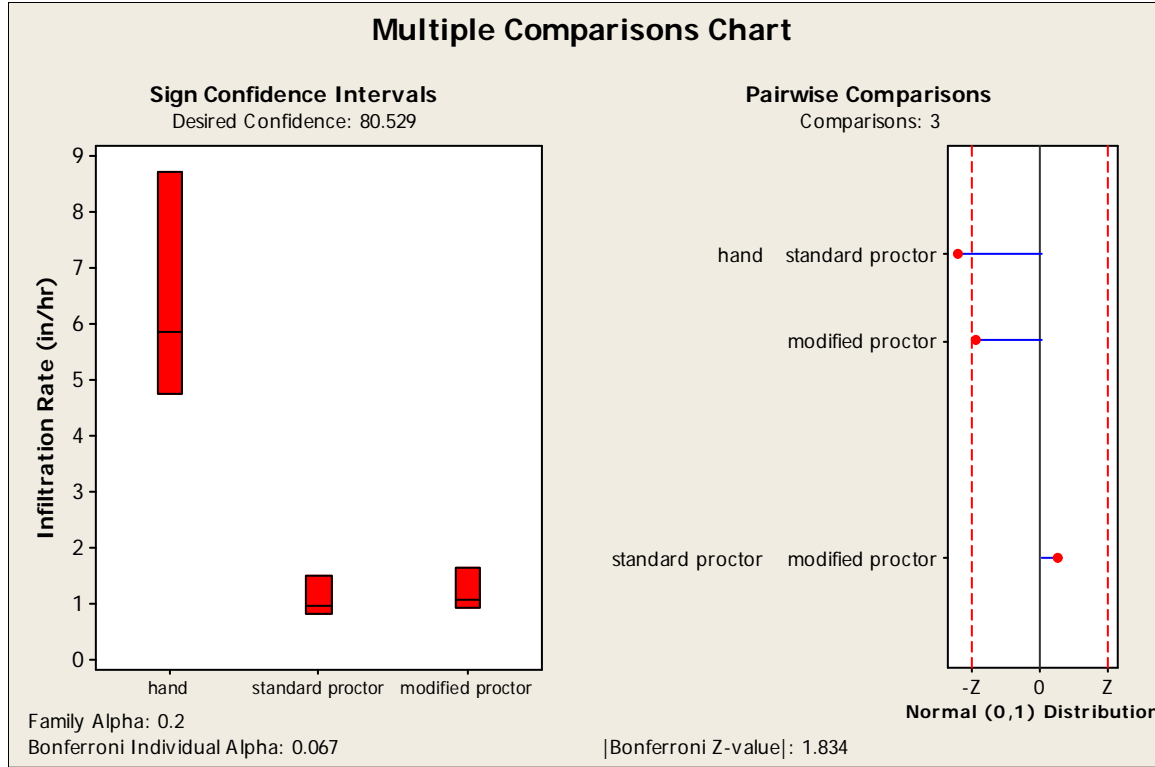
The highest attainable confidence has been achieved.
The highest attainable confidence has been achieved.
The highest attainable confidence has been achieved.

Kruskal-Wallis: Conclusions

The following groups showed significant differences:

Groups	Z vs. Critical value	P-value
hand vs. modified proctor	2.68328 >= 1.834	0.0073

Appendix C.16: Kruskal-Wallis Multiple Comparisons for the Saturated Infiltration Rates of Lab Compaction Tests Using Surface Soil 25th Ave. E and University Blvd. E. (O'Reilly Auto Parts), Tuscaloosa, AL.



Kruskal-Wallis: Multiple Comparisons

Kruskal-Wallis Test on the data

Group	N	Median	Rank	Ave	Z
hand	3	5.874	8.0	5.874	2.32
standard proctor	3	1.000	3.0	1.000	-1.55
modified proctor	3	1.100	4.0	1.100	-0.77
Overall	9		5.0	5.0	

H = 5.60 DF = 2 P = 0.061

* NOTE * One or more small samples

Kruskal-Wallis: All Pairwise Comparisons

Comparisons: 3
 Family Alpha: 0.2
 Bonferroni Individual Alpha: 0.067
 Bonferroni Z-value (2-sided): 1.834

Standardized Absolute Mean Rank Differences
|Rbar(i)-Rbar(j)| / Stdev

Rows: Group i = 1,...,n
Columns: Group j = 1,...,n

1. Table of Z-values

hand	0.00000		*	*
standard proctor	2.23607	0.000000	*	
modified proctor	1.78885	0.447214	0	

2. Table of P-values

hand	1.00000		*	*
standard proctor	0.02535	1.00000	*	
modified proctor	0.07364	0.65472	1	

Sign Confidence Intervals controlled at a family error rate of 0.2

Desired Confidence: 80.529

Sign confidence interval for median

				Confidence		
	N	Median	Achieved	Lower	Upper	Position
			Confidence			
hand	3	5.874	0.7500	4.749	8.715	1
standard proctor	3	1.000	0.7500	0.832	1.507	1
modified proctor	3	1.100	0.7500	0.944	1.672	1

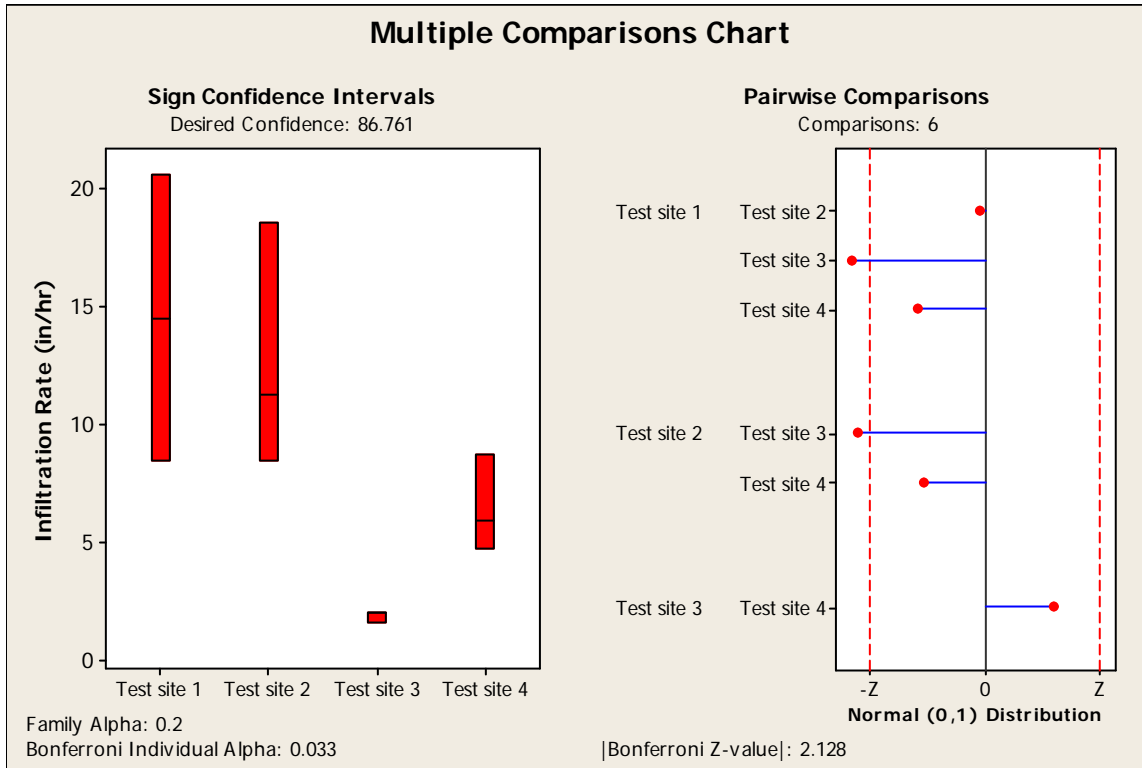
The highest attainable confidence has been achieved.
The highest attainable confidence has been achieved.
The highest attainable confidence has been achieved.

Kruskal-Wallis: Conclusions

The following groups showed significant differences:

Groups	Z vs. Critical value	P-value
hand vs. standard proctor	2.23607 >= 1.834	0.0253

Appendix C.17: Kruskal-Wallis Multiple Comparisons for the Saturated Infiltration Rates of Lab Compaction Tests Using Surface Soils from Four Test Sites and Hand Compaction Conditions.



Kruskal-Wallis: Multiple Comparisons

Kruskal-Wallis Test on the data

Group	N	Median	Ave Rank	Z
Test site 1	3	14.500	9.3	1.57
Test site 2	3	11.252	9.0	1.39
Test site 3	3	2.022	2.0	-2.50
Test site 4	3	5.874	5.7	-0.46
Overall	12		6.5	

H = 8.13 DF = 3 P = 0.043

* NOTE * One or more small samples

Kruskal-Wallis: All Pairwise Comparisons

Comparisons: 6
 Family Alpha: 0.2
 Bonferroni Individual Alpha: 0.033
 Bonferroni Z-value (2-sided): 2.128

 Standardized Absolute Mean Rank Differences
 $|Rbar(i)-Rbar(j)| / Stdev$

Rows: Group i = 1,...,n
 Columns: Group j = 1,...,n

1. Table of Z-values

Test site 1	0.00000		*	*	*
Test site 2	0.11323	0.00000		*	*
Test site 3	2.49101	2.37778	0.00000		*
Test site 4	1.24550	1.13228	1.24550	0	

2. Table of P-values

Test site 1	1.00000		*	*	*
Test site 2	0.90985	1.00000		*	*
Test site 3	0.01274	0.01742	1.00000		*
Test site 4	0.21295	0.25752	0.21295	1	

 Sign Confidence Intervals controlled at a family error rate of 0.2

Desired Confidence: 86.761

Sign confidence interval for median

	N	Median	Confidence Interval		Position
			Achieved Confidence	Lower Upper	
Test site 1	3	14.50	0.7500	8.48 20.59	1
Test site 2	3	11.25	0.7500	8.50 18.55	1
Test site 3	3	2.022	0.7500	1.535 2.043	1
Test site 4	3	5.874	0.7500	4.749 8.715	1

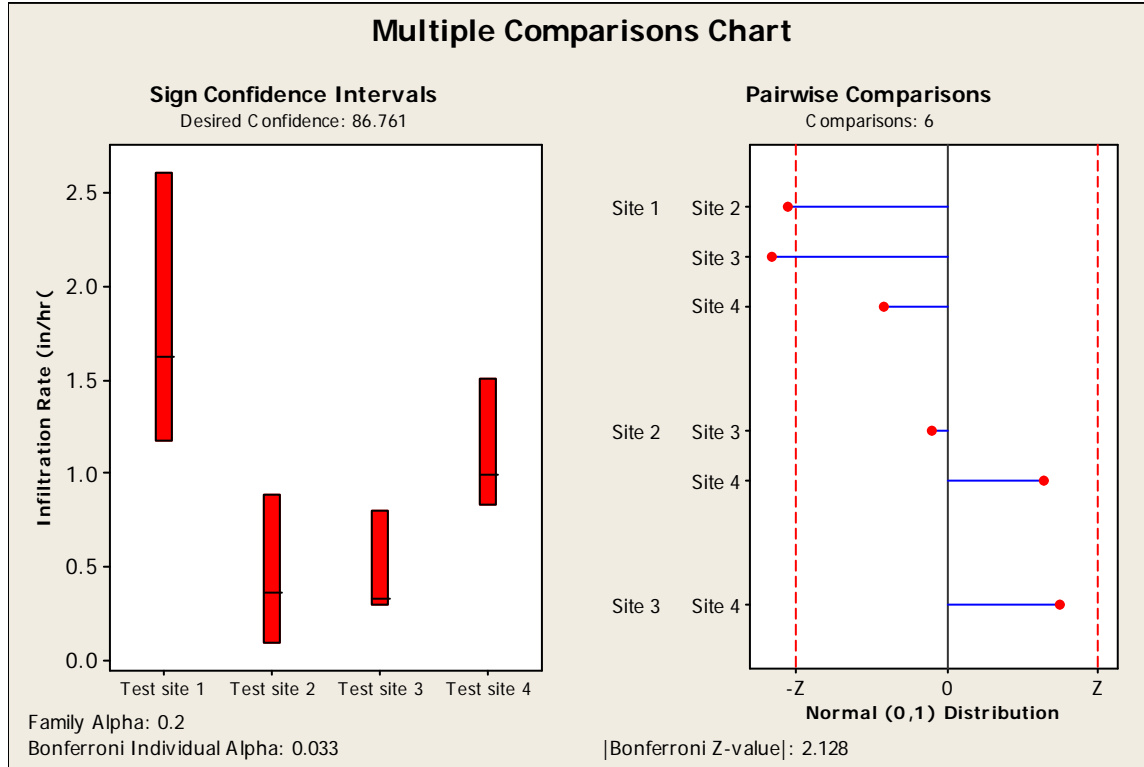
The highest attainable confidence has been achieved.
 The highest attainable confidence has been achieved.
 The highest attainable confidence has been achieved.
 The highest attainable confidence has been achieved.

Kruskal-Wallis: Conclusions

The following groups showed significant differences:

Groups	Z vs. Critical value	P-value
Test site 1 vs. Test site 3	2.49101 >= 2.128	0.0127
Test site 2 vs. Test site 3	2.37778 >= 2.128	0.0174

Appendix C.18: Kruskal-Wallis Multiple Comparisons for the Saturated Infiltration Rates of Lab Compaction Tests Using Surface Soils from Four Test Sites and Standard Proctor Compaction Conditions.



Kruskal-Wallis: Multiple Comparisons

Kruskal-Wallis Test on the data

Group	N	Median	Ave Rank	Z
Site 1	3	1.6270	10.7	2.31
Site 2	3	0.3690	4.0	-1.39
Site 3	3	0.3316	3.3	-1.76
Site 4	3	1.0000	8.0	0.83
Overall	12		6.5	

H = 8.28 DF = 3 P = 0.041

* NOTE * One or more small samples

Kruskal-Wallis: All Pairwise Comparisons

Comparisons:	6
Family Alpha:	0.2
Bonferroni Individual Alpha:	0.033
Bonferroni Z-value (2-sided):	2.128

Standardized Absolute Mean Rank Differences
|Rbar(i)-Rbar(j)| / Stdev

Rows: Group i = 1,...,n
Columns: Group j = 1,...,n

1. Table of Z-values

Site 1	0.00000		*	*	*
Site 2	2.26455	0.00000		*	*
Site 3	2.49101	0.22646	0.00000		*
Site 4	0.90582	1.35873	1.58519	0	

2. Table of P-values

Site 1	1.00000		*	*	*
Site 2	0.02354	1.00000		*	*
Site 3	0.01274	0.82085	1.00000		*
Site 4	0.36503	0.17423	0.11292	1	

Sign Confidence Intervals controlled at a family error rate of 0.2

Desired Confidence: 86.761

Sign confidence interval for median

		Achieved		Confidence Interval		Position
	N	Median	Confidence	Lower	Upper	
Site 1	3	1.627	0.7500	1.181	2.611	1
Site 2	3	0.3690	0.7500	0.1020	0.8860	1
Site 3	3	0.3316	0.7500	0.2975	0.8050	1
Site 4	3	1.000	0.7500	0.832	1.507	1

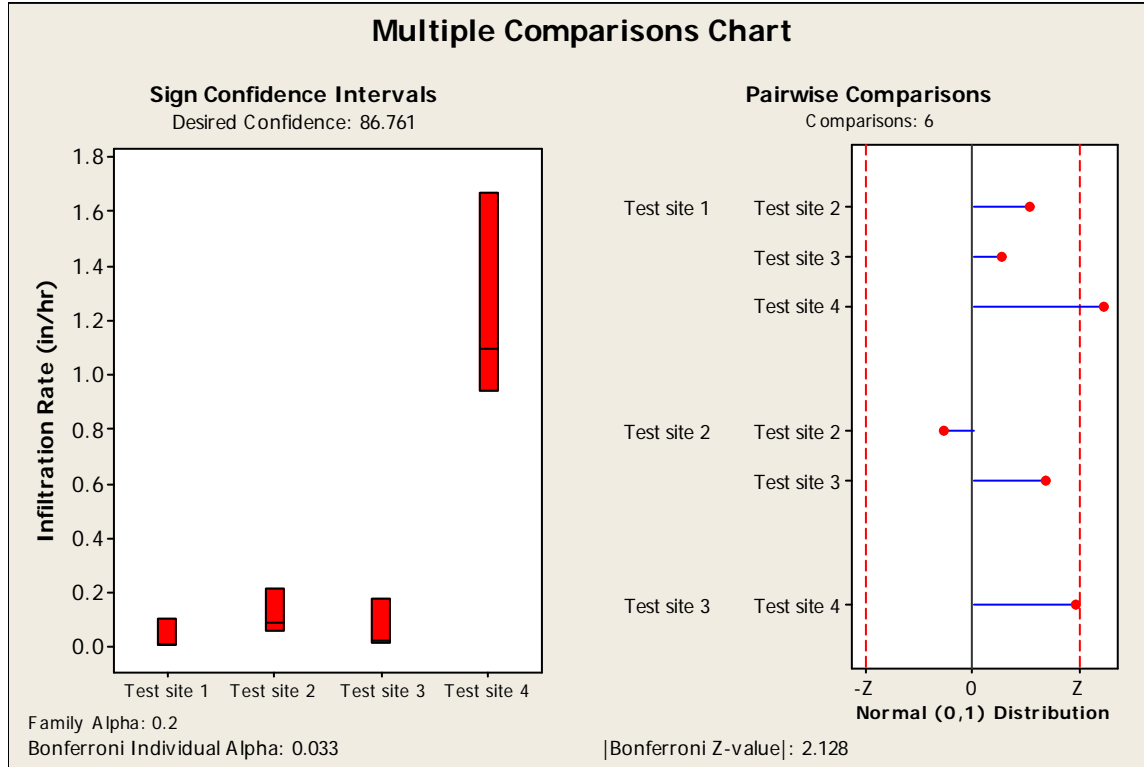
The highest attainable confidence has been achieved.
The highest attainable confidence has been achieved.
The highest attainable confidence has been achieved.
The highest attainable confidence has been achieved.

Kruskal-Wallis: Conclusions

The following groups showed significant differences:

Groups	Z vs. Critical value	P-value
Site 1 vs. Site 3	2.49101 >= 2.128	0.0127
Site 1 vs. Site 2	2.26455 >= 2.128	0.0235

Appendix C.19: Kruskal-Wallis Multiple Comparisons for the Saturated Infiltration Rates of Lab Compaction Tests Using Surface Soils from Four Test Sites and Modified Proctor Compaction Conditions.



Kruskal-Wallis: Multiple Comparisons

Kruskal-Wallis Test on the data

Group	N	Median	Ave Rank	Z
Site 1	3	0.01000	3.3	-1.76
Site 2	3	0.08900	6.7	0.09
Site 3	3	0.02360	5.0	-0.83
Site 4	3	1.10000	11.0	2.50
Overall	12		6.5	

H = 7.51 DF = 3 P = 0.057

* NOTE * One or more small samples

Kruskal-Wallis: All Pairwise Comparisons

Comparisons:	6
Family Alpha:	0.2
Bonferroni Individual Alpha:	0.033
Bonferroni Z-value (2-sided):	2.128

Standardized Absolute Mean Rank Differences
|Rbar(i)-Rbar(j)| / Stdev

Rows: Group i = 1,...,n
Columns: Group j = 1,...,n

1. Table of Z-values

Site 1	0.00000		*	*	*
Site 2	1.13228	0.00000		*	*
Site 3	0.56614	0.56614	0.00000		*
Site 4	2.60424	1.47196	2.03810	0	

2. Table of P-values

Site 1	1.00000		*	*	*
Site 2	0.25752	1.00000		*	*
Site 3	0.57130	0.57130	1.00000		*
Site 4	0.00921	0.14103	0.04154	1	

Sign Confidence Intervals controlled at a family error rate of 0.2

Desired Confidence: 86.761

Sign confidence interval for median

	N	Median	Achieved Confidence	Confidence Interval		Position
				Lower	Upper	
Site 1	3	0.0100	0.7500	0.0080	0.1080	1
Site 2	3	0.0890	0.7500	0.0620	0.2180	1
Site 3	3	0.0236	0.7500	0.0148	0.1780	1
Site 4	3	1.100	0.7500	0.944	1.672	1

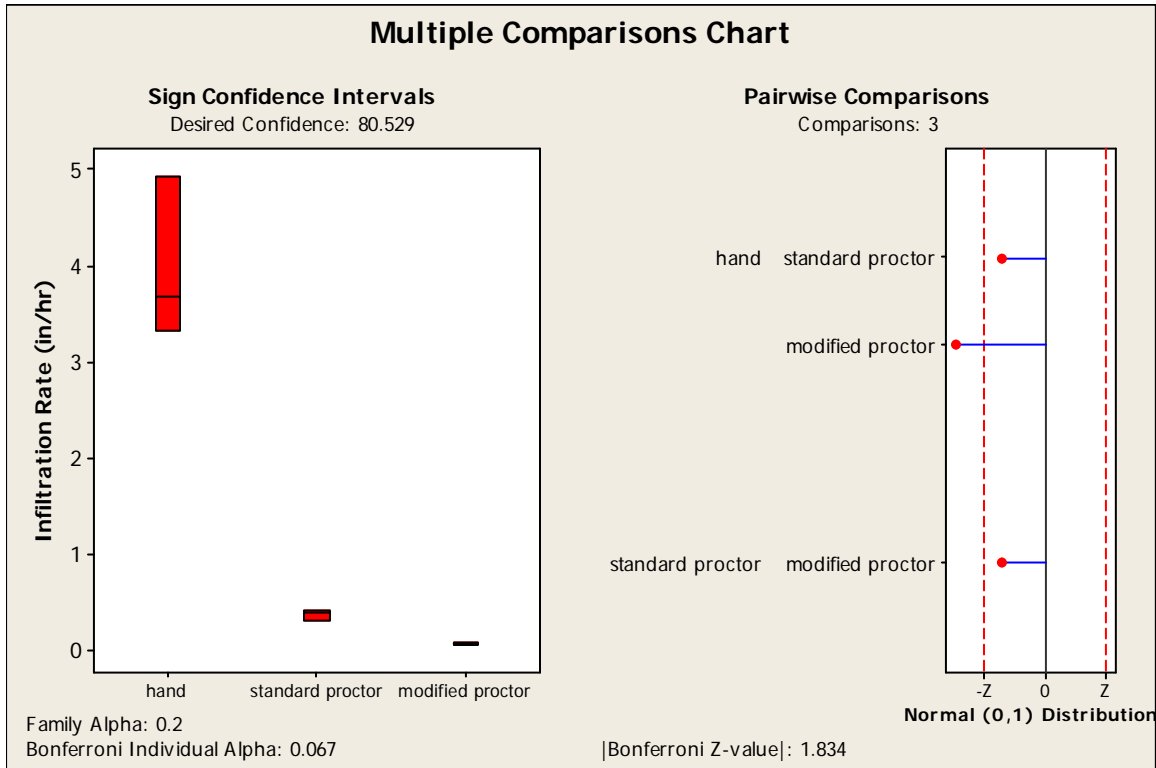
The highest attainable confidence has been achieved.
The highest attainable confidence has been achieved.
The highest attainable confidence has been achieved.
The highest attainable confidence has been achieved.

Kruskal-Wallis: Conclusions

The following groups showed significant differences:

Groups	Z vs. Critical value	P-value
Site 1 vs. Site 4	2.60424 >= 2.128	0.0092

Appendix C.20: Kruskal-Wallis Multiple Comparisons for the Saturated Infiltration Rates of Lab Compaction Tests Using Subsurface Soil on 15th St. E and 6th Ave. E., Tuscaloosa, AL.



Kruskal-Wallis: Multiple Comparisons

Kruskal-Wallis Test on the data

Group	N	Median	Ave Rank	Z
hand	3	3.67500	8.0	2.32
standard proctor	3	0.39400	5.0	0.00
modified proctor	3	0.06700	2.0	-2.32
Overall	9		5.0	

H = 7.20 DF = 2 P = 0.027

* NOTE * One or more small samples

Kruskal-Wallis: All Pairwise Comparisons

Comparisons: 3
 Family Alpha: 0.2
 Bonferroni Individual Alpha: 0.067
 Bonferroni Z-value (2-sided): 1.834

Standardized Absolute Mean Rank Differences
 $|Rbar(i)-Rbar(j)| / Stdev$

Rows: Group i = 1,...,n
 Columns: Group j = 1,...,n

1. Table of Z-values

hand	0.00000		*	*
standard proctor	1.34164	0.00000	*	*
modified proctor	2.68328	1.34164	0	

2. Table of P-values

hand	1.00000		*	*
standard proctor	0.17971	1.00000	*	*
modified proctor	0.00729	0.17971	1	

Sign Confidence Intervals controlled at a family error rate of 0.2

Desired Confidence: 80.529

Sign confidence interval for median

	N	Median	Achieved Confidence	Confidence Interval		Position
				Lower	Upper	
hand	3	3.675	0.7500	3.333	4.929	1
standard proctor	3	0.3940	0.7500	0.3200	0.4140	1
modified proctor	3	0.06700	0.7500	0.06400	0.08800	1

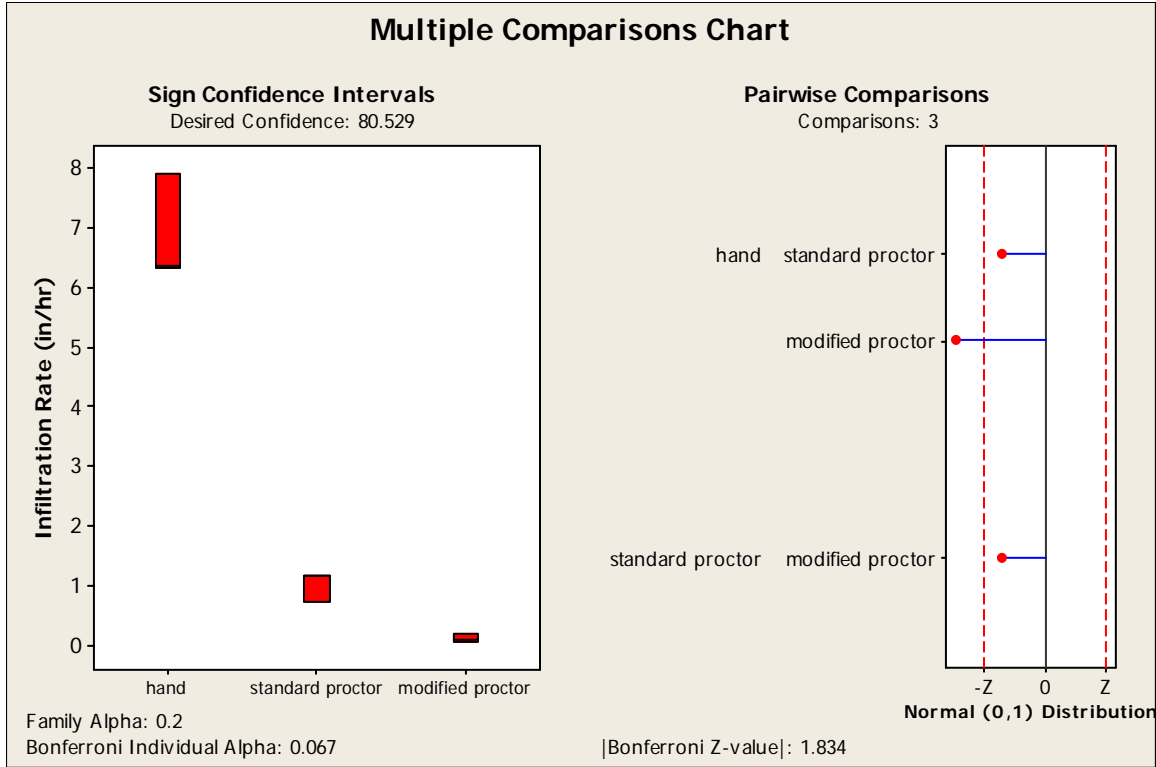
The highest attainable confidence has been achieved.
 The highest attainable confidence has been achieved.
 The highest attainable confidence has been achieved.

Kruskal-Wallis: Conclusions

The following groups showed significant differences:

Groups	Z vs. Critical value	P-value
hand vs. modified proctor	2.68328 >= 1.834	0.0073

Appendix C.21: Kruskal-Wallis Multiple Comparisons for the Saturated Infiltration Rates of Lab Compaction Tests Using Subsurface Soil on 17th Ave. E. and University Blvd. E. (Tuscaloosa Physical Therapy), Tuscaloosa, AL.



Kruskal-Wallis: Multiple Comparisons

Kruskal-Wallis Test on the data

Group	N	Median	Ave Rank	Z
hand	3	6.3650	8.0	2.32
standard proctor	3	1.1630	5.0	0.00
modified proctor	3	0.1060	2.0	-2.32
Overall	9		5.0	

H = 7.20 DF = 2 P = 0.027

* NOTE * One or more small samples

Kruskal-Wallis: All Pairwise Comparisons

Comparisons: 3
 Family Alpha: 0.2
 Bonferroni Individual Alpha: 0.067
 Bonferroni Z-value (2-sided): 1.834

Standardized Absolute Mean Rank Differences
|Rbar(i)-Rbar(j)| / Stdev

Rows: Group i = 1,...,n
Columns: Group j = 1,...,n

1. Table of Z-values

hand	0.00000		*	*
standard proctor	1.34164	0.00000	*	*
modified proctor	2.68328	1.34164	0	

2. Table of P-values

hand	1.00000		*	*
standard proctor	0.17971	1.00000	*	*
modified proctor	0.00729	0.17971	1	

Sign Confidence Intervals controlled at a family error rate of 0.2

Desired Confidence: 80.529

Sign confidence interval for median

				Confidence Interval		
	N	Median	Achieved Confidence	Lower	Upper	Position
hand	3	6.365	0.7500	6.331	7.903	1
standard proctor	3	1.163	0.7500	0.757	1.192	1
modified proctor	3	0.1060	0.7500	0.0720	0.2150	1

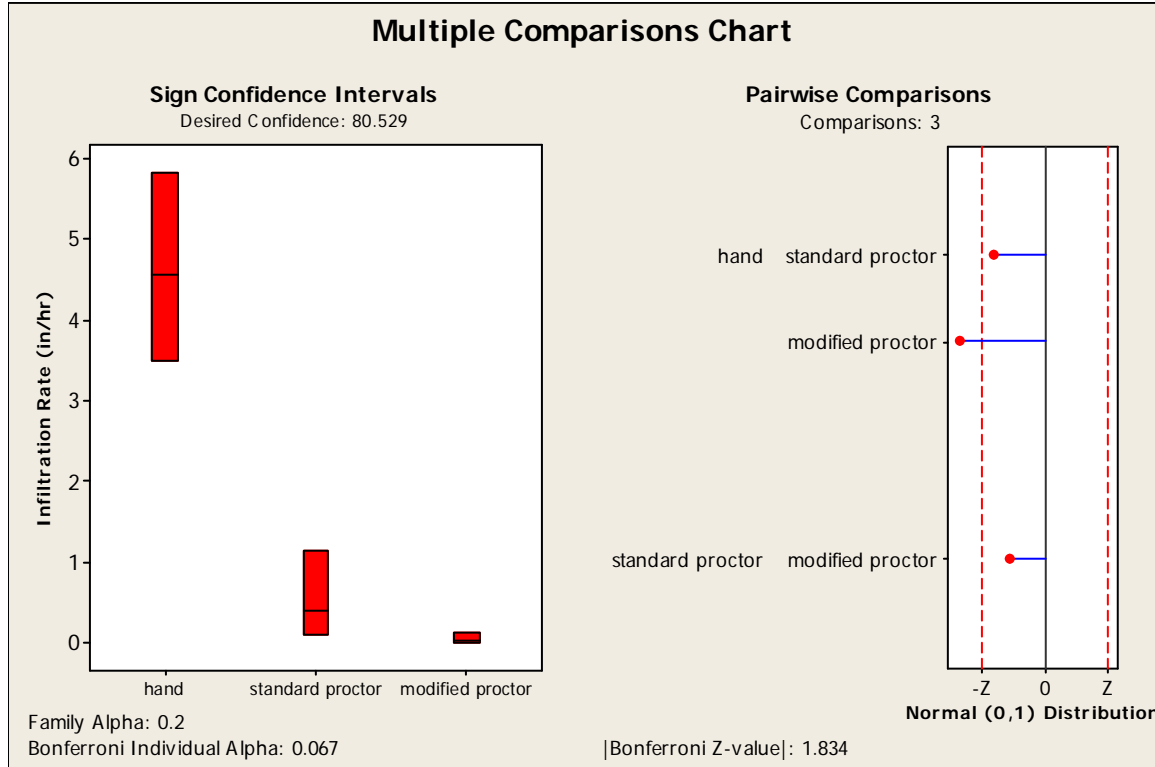
The highest attainable confidence has been achieved.
The highest attainable confidence has been achieved.
The highest attainable confidence has been achieved.

Kruskal-Wallis: Conclusions

The following groups showed significant differences:

Groups	Z vs. Critical value	P-value
hand vs. modified proctor	2.68328 >= 1.834	0.0073

Appendix C.22: Kruskal-Wallis Multiple Comparisons for the Saturated Infiltration Rates of Lab Compaction Tests Using Subsurface Soil on 21st Ave. E. and University Blvd E. (Alberta Hand Carwash), Tuscaloosa, AL.



Kruskal-Wallis: Multiple Comparisons

Kruskal-Wallis Test on the data

Group	N	Median	Ave Rank	Z
hand	3	4.57600	8.0	2.32
standard proctor	3	0.40000	4.7	-0.26
modified proctor	3	0.04300	2.3	-2.07
Overall	9		5.0	

H = 6.49 DF = 2 P = 0.039

* NOTE * One or more small samples

Kruskal-Wallis: All Pairwise Comparisons

Comparisons: 3
Family Alpha: 0.2
Bonferroni Individual Alpha: 0.067
Bonferroni Z-value (2-sided): 1.834

Standardized Absolute Mean Rank Differences
|Rbar(i)-Rbar(j)| / Stdev

Rows: Group i = 1,...,n
Columns: Group j = 1,...,n

1. Table of Z-values

hand	0.00000		*	*
standard proctor	1.49071	0.00000	*	*
modified proctor	2.53421	1.04350	0	

2. Table of P-values

hand	1.00000		*	*
standard proctor	0.13604	1.00000	*	*
modified proctor	0.01127	0.29672	1	

Sign Confidence Intervals controlled at a family error rate of 0.2

Desired Confidence: 80.529

Sign confidence interval for median

			Achieved	Confidence Interval		Position
	N	Median	Confidence	Lower	Upper	
hand	3	4.576	0.7500	3.494	5.825	1
standard proctor	3	0.400	0.7500	0.122	1.154	1
modified proctor	3	0.0430	0.7500	0.0150	0.1330	1

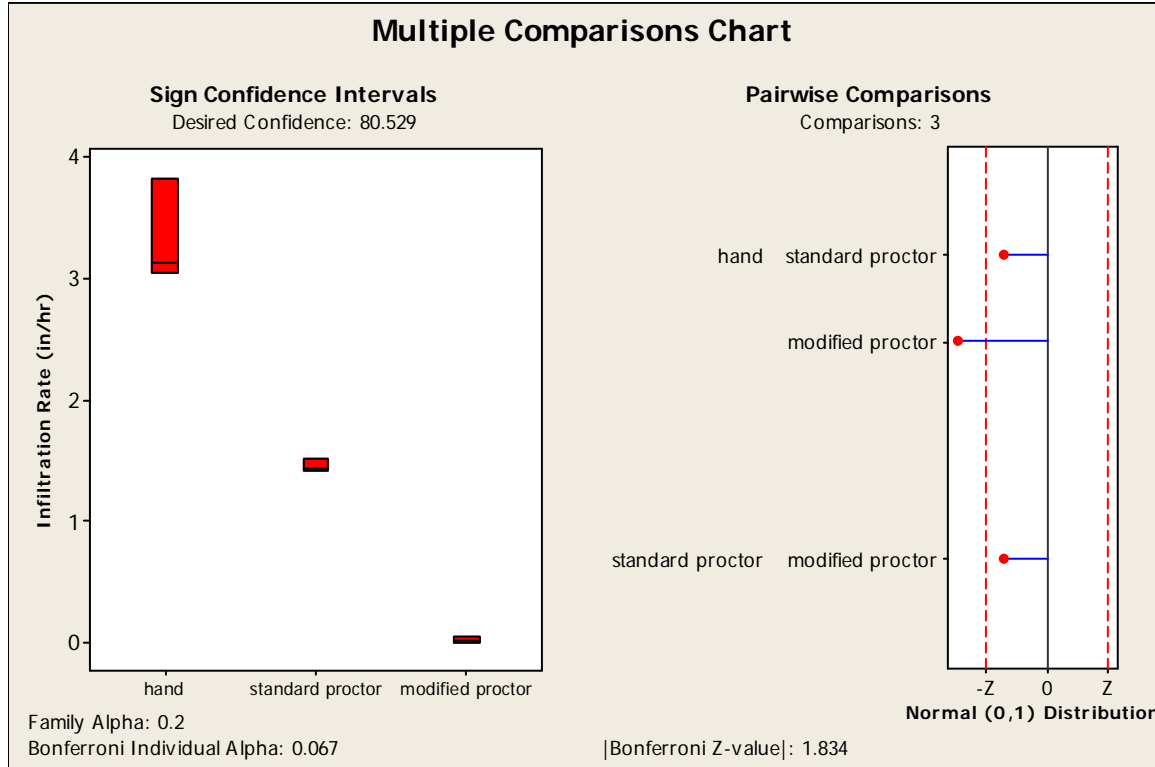
The highest attainable confidence has been achieved.
The highest attainable confidence has been achieved.
The highest attainable confidence has been achieved.

Kruskal-Wallis: Conclusions

The following groups showed significant differences:

Groups	Z vs. Critical value	P-value
hand vs. modified proctor	2.53421 >= 1.834	0.0113

Appendix C.23: Kruskal-Wallis Multiple Comparisons for the Saturated Infiltration Rates of Lab Compaction Tests Using Subsurface Soil 25th Ave. E and University Blvd E. (O'Reilly Auto Parts), Tuscaloosa, AL.



Kruskal-Wallis: Multiple Comparisons

Kruskal-Wallis Test on the data

Group	N	Median	Ave Rank	Z
hand	3	3.13800	8.0	2.32
standard proctor	3	1.44100	5.0	0.00
modified proctor	3	0.02920	2.0	-2.32
Overall	9		5.0	

H = 7.20 DF = 2 P = 0.027

* NOTE * One or more small samples

Kruskal-Wallis: All Pairwise Comparisons

Comparisons: 3
 Family Alpha: 0.2
 Bonferroni Individual Alpha: 0.067
 Bonferroni Z-value (2-sided): 1.834

 Standardized Absolute Mean Rank Differences
 $|Rbar(i)-Rbar(j)| / Stdev$

Rows: Group i = 1,...,n
 Columns: Group j = 1,...,n

1. Table of Z-values

hand	0.00000		*	*
standard proctor	1.34164	0.00000	*	
modified proctor	2.68328	1.34164	0	

2. Table of P-values

hand	1.00000		*	*
standard proctor	0.17971	1.00000	*	
modified proctor	0.00729	0.17971	1	

 Sign Confidence Intervals controlled at a family error rate of 0.2

Desired Confidence: 80.529

Sign confidence interval for median

	N	Median	Achieved Confidence	Confidence Interval		Position
				Lower	Upper	
hand	3	3.138	0.7500	3.057	3.834	1
standard proctor	3	1.441	0.7500	1.421	1.520	1
modified proctor	3	0.02920	0.7500	0.00688	0.06300	1

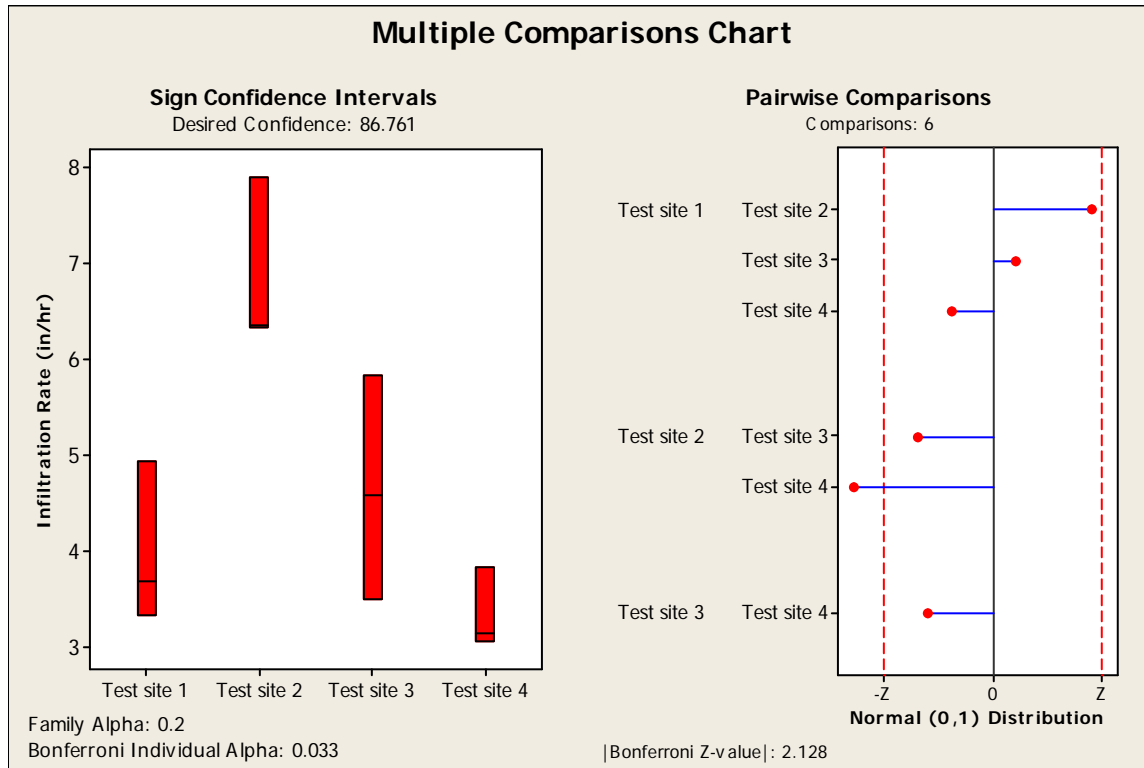
The highest attainable confidence has been achieved.
 The highest attainable confidence has been achieved.
 The highest attainable confidence has been achieved.

Kruskal-Wallis: Conclusions

The following groups showed significant differences:

Groups	Z vs. Critical value	P-value
hand vs. modified proctor	2.68328 >= 1.834	0.0073

Appendix C.24: Kruskal-Wallis Multiple Comparisons for the Saturated Infiltration Rates of Lab Compaction Tests Using Surface Soils from Four Test Sites and Hand Compaction Conditions.



Kruskal-Wallis: Multiple Comparisons

Kruskal-Wallis Test on the data

Group	N	Median	Ave Rank	Z
Test site 1	3	3.675	5.3	-0.65
Test site 2	3	6.365	11.0	2.50
Test site 3	3	4.576	6.7	0.09
Test site 4	3	3.138	3.0	-1.94
Overall	12		6.5	

H = 7.82 DF = 3 P = 0.050

* NOTE * One or more small samples

Kruskal-Wallis: All Pairwise Comparisons

Comparisons: 6
Family Alpha: 0.2
Bonferroni Individual Alpha: 0.033
Bonferroni Z-value (2-sided): 2.128

Standardized Absolute Mean Rank Differences
 $|Rbar(i)-Rbar(j)| / Stdev$

Rows: Group i = 1,...,n
 Columns: Group j = 1,...,n

1. Table of Z-values

Test site 1	0.00000		*	*	*
Test site 2	1.92487	0.00000		*	*
Test site 3	0.45291	1.47196	0.00000	*	
Test site 4	0.79259	2.71746	1.24550	0	

2. Table of P-values

Test site 1	1.00000		*	*	*
Test site 2	0.05425	1.00000		*	*
Test site 3	0.65061	0.14103	1.00000	*	
Test site 4	0.42801	0.00658	0.21295	1	

Sign Confidence Intervals controlled at a family error rate of 0.2

Desired Confidence: 86.761

Sign confidence interval for median

	N	Median	Confidence		Position
			Achieved	Interval	
Test site 1	3	3.675	0.7500	3.333 4.929	1
Test site 2	3	6.365	0.7500	6.331 7.903	1
Test site 3	3	4.576	0.7500	3.494 5.825	1
Test site 4	3	3.138	0.7500	3.057 3.834	1

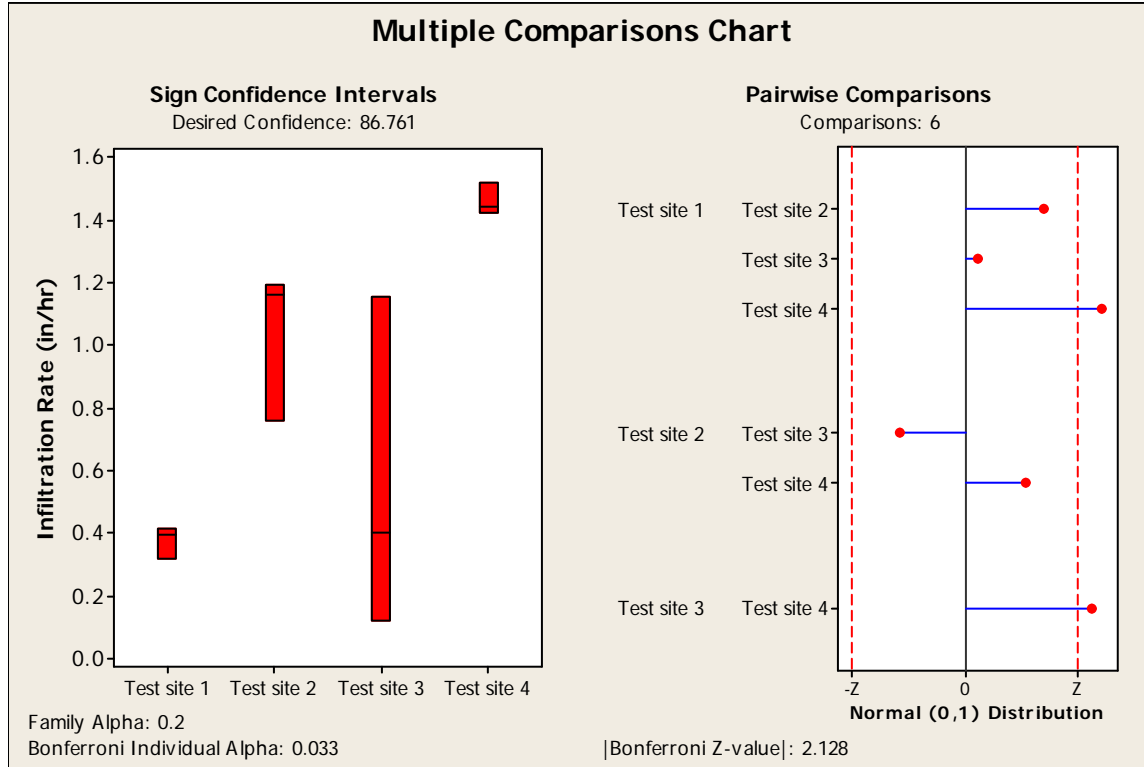
The highest attainable confidence has been achieved.
 The highest attainable confidence has been achieved.
 The highest attainable confidence has been achieved.
 The highest attainable confidence has been achieved.

Kruskal-Wallis: Conclusions

The following groups showed significant differences:

Groups	Z vs. Critical value	P-value
Test site 2 vs. Test site 4	2.71746 >= 2.128	0.0066

Appendix C.25: Kruskal-Wallis Multiple Comparisons for the Saturated Infiltration Rates of Lab Compaction Tests Using Subsurface Soils from Four Test Sites and Standard Proctor Compaction Conditions.



Kruskal-Wallis: Multiple Comparisons

Kruskal-Wallis Test on the data

Group	N	Median	Ave Rank	Z
Test site 1	3	0.3940	3.3	-1.76
Test site 2	3	1.1630	7.7	0.65
Test site 3	3	0.4000	4.0	-1.39
Test site 4	3	1.4410	11.0	2.50
Overall	12		6.5	

H = 8.74 DF = 3 P = 0.033

* NOTE * One or more small samples

Kruskal-Wallis: All Pairwise Comparisons

Comparisons: 6
 Family Alpha: 0.2
 Bonferroni Individual Alpha: 0.033
 Bonferroni Z-value (2-sided): 2.128

 Standardized Absolute Mean Rank Differences
 $|Rbar(i)-Rbar(j)| / Stdev$

Rows: Group i = 1,...,n
 Columns: Group j = 1,...,n

1. Table of Z-values

Test site 1	0.00000		*	*	*
Test site 2	1.47196	0.00000		*	*
Test site 3	0.22646	1.24550	0.00000	*	
Test site 4	2.60424	1.13228	2.37778	0	

2. Table of P-values

Test site 1	1.00000		*	*	*
Test site 2	0.14103	1.00000		*	*
Test site 3	0.82085	0.21295	1.00000	*	
Test site 4	0.00921	0.25752	0.01742	1	

 Sign Confidence Intervals controlled at a family error rate of 0.2

Desired Confidence: 86.761

Sign confidence interval for median

	N	Median	Achieved Confidence	Confidence Interval		Position
				Lower	Upper	
Test site 1	3	0.3940	0.7500	0.3200	0.4140	1
Test site 2	3	1.163	0.7500	0.757	1.192	1
Test site 3	3	0.400	0.7500	0.122	1.154	1
Test site 4	3	1.441	0.7500	1.421	1.520	1

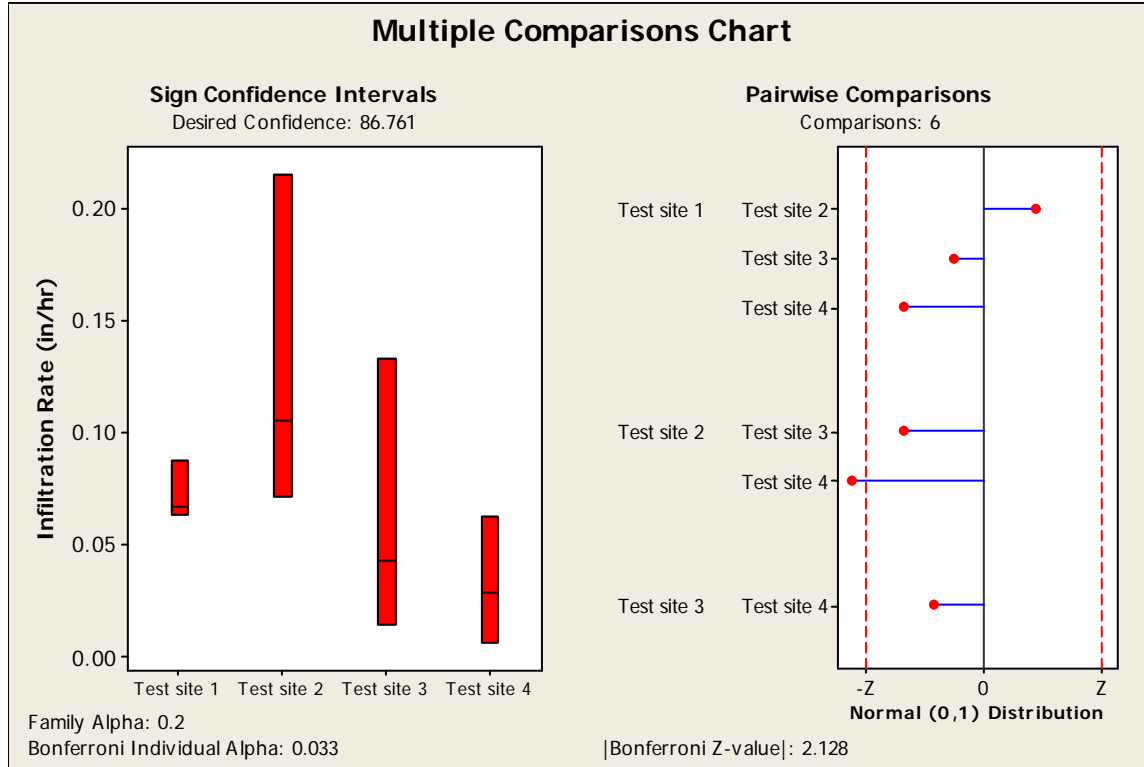
The highest attainable confidence has been achieved.
 The highest attainable confidence has been achieved.
 The highest attainable confidence has been achieved.
 The highest attainable confidence has been achieved.

Kruskal-Wallis: Conclusions

The following groups showed significant differences:

Groups	Z vs. Critical value	P-value
Test site 1 vs. Test site 4	2.60424 >= 2.128	0.0092
Test site 3 vs. Test site 4	2.37778 >= 2.128	0.0174

Appendix C.26: Kruskal-Wallis Multiple Comparisons for the Saturated Infiltration Rates of Lab Compaction Tests Using Subsurface Soils from Four Test Sites and Modified Proctor Compaction Conditions.



Kruskal-Wallis: Multiple Comparisons

Kruskal-Wallis Test on the data

Group	N	Median	Ave Rank	Z
Test site 1	3	0.06700	7.3	0.46
Test site 2	3	0.10600	10.0	1.94
Test site 3	3	0.04300	5.7	-0.46
Test site 4	3	0.02920	3.0	-1.94
Overall	12		6.5	

H = 5.97 DF = 3 P = 0.113

* NOTE * One or more small samples

Kruskal-Wallis: All Pairwise Comparisons

Comparisons: 6
 Family Alpha: 0.2
 Bonferroni Individual Alpha: 0.033
 Bonferroni Z-value (2-sided): 2.128

 Standardized Absolute Mean Rank Differences
 $|Rbar(i)-Rbar(j)| / Stdev$

Rows: Group i = 1,...,n
 Columns: Group j = 1,...,n

1. Table of Z-values

Test site 1	0.00000		*	*	*
Test site 2	0.90582	0.00000		*	*
Test site 3	0.56614	1.47196	0.000000		*
Test site 4	1.47196	2.37778	0.905822	0	

2. Table of P-values

Test site 1	1.00000		*	*	*
Test site 2	0.36503	1.00000		*	*
Test site 3	0.57130	0.14103	1.00000		*
Test site 4	0.14103	0.01742	0.36503	1	

 Sign Confidence Intervals controlled at a family error rate of 0.2

Desired Confidence: 86.761

Sign confidence interval for median

	N	Median	Achieved Confidence	Confidence Interval		Position
				Lower	Upper	
Test site 1	3	0.06700	0.7500	0.06400	0.08800	1
Test site 2	3	0.1060	0.7500	0.0720	0.2150	1
Test site 3	3	0.0430	0.7500	0.0150	0.1330	1
Test site 4	3	0.02920	0.7500	0.00688	0.06300	1

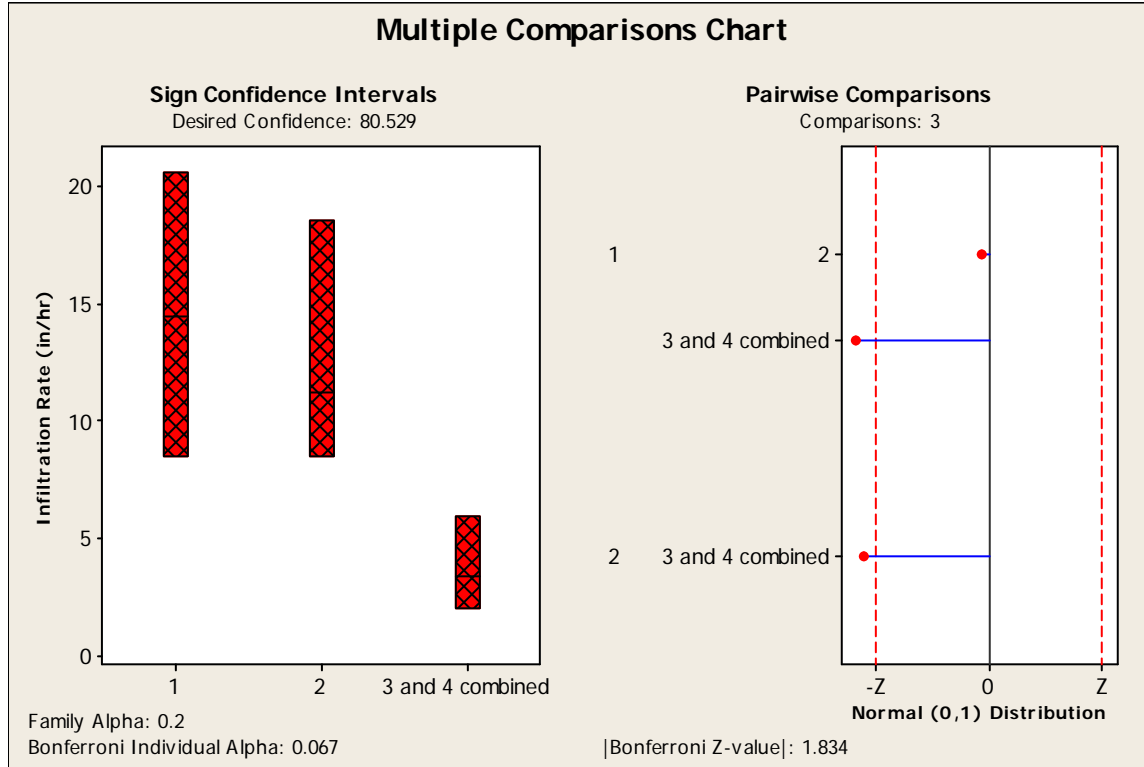
The highest attainable confidence has been achieved.
 The highest attainable confidence has been achieved.
 The highest attainable confidence has been achieved.
 The highest attainable confidence has been achieved.

Kruskal-Wallis: Conclusions

The following groups showed significant differences:

Groups	Z vs. Critical value	P-value
Test site 2 vs. Test site 4	2.37778 >= 2.128	0.0174

Appendix C.27: Kruskal-Wallis Multiple Comparisons for the Saturated Infiltration Rates of Lab Compaction Tests Using Surface Soils from Four Test Sites and Hand Compaction Conditions, Combined Data.



*1, 2, 3, and 4 are test sites

Kruskal-Wallis: Multiple Comparisons

Kruskal-Wallis Test on the data

Group	N	Median	Ave Rank	Z
1	3	14.500	9.3	1.57
2	3	11.252	9.0	1.39
3 and 4 combined	6	3.396	3.8	-2.56
Overall	12		6.5	

H = 6.58 DF = 2 P = 0.037

* NOTE * One or more small samples

Kruskal-Wallis: All Pairwise Comparisons

Comparisons:	3
Family Alpha:	0.2
Bonferroni Individual Alpha:	0.067
Bonferroni Z-value (2-sided):	1.834

 Standardized Absolute Mean Rank Differences
 $|Rbar(i)-Rbar(j)| / Stdev$

Rows: Group i = 1,...,n
 Columns: Group j = 1,...,n

1. Table of Z-values

1	0.00000		*	*
2	0.11323	0.00000	*	
3 and 4 combined	2.15728	2.02653	0	

2. Table of P-values

1	1.00000		*	*
2	0.90985	1.00000	*	
3 and 4 combined	0.03098	0.04271	1	

 Sign Confidence Intervals controlled at a family error rate of 0.2
 Desired Confidence: 80.529

Sign confidence interval for median

	N	Median	Achieved Confidence	Confidence Interval		Position
				Lower	Upper	
1	3	14.50	0.7500	8.48	20.59	1
2	3	11.25	0.7500	8.50	18.55	1
3 and 4 combined	6	3.396	0.7813	2.022	5.874	2
			0.8053	2.008	5.955	NLI
			0.9688	1.535	8.715	1

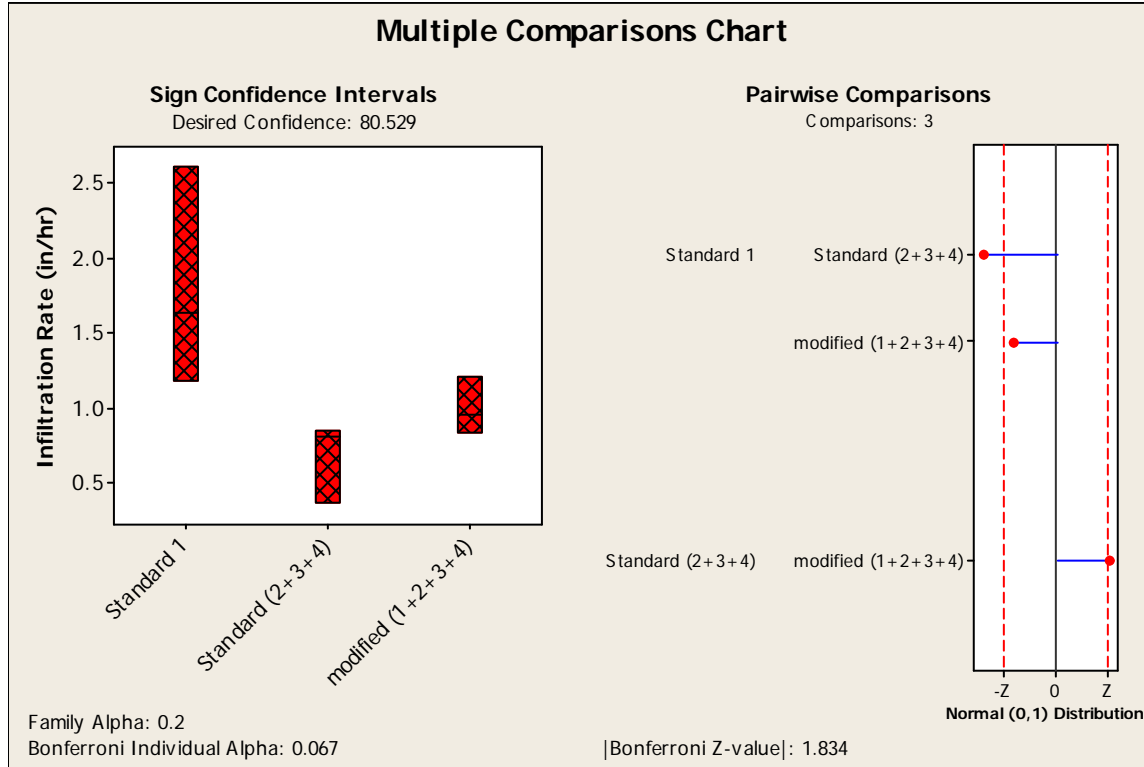
The highest attainable confidence has been achieved.
 The highest attainable confidence has been achieved.

Kruskal-Wallis: Conclusions

The following groups showed significant differences:

Groups	Z vs. Critical value	P-value
1 vs. 3 and 4 combined	2.15728 >= 1.834	0.0310
2 vs. 3 and 4 combined	2.02653 >= 1.834	0.0427

Appendix C.28: Kruskal-Wallis Multiple Comparisons for the Saturated Infiltration Rates of Lab Compaction Tests Using Surface Soils from Four Test Sites, Standard and Modified Proctor Compaction Conditions with Combined Data.



*1, 2, 3, and 4 are test sites

Kruskal-Wallis: Multiple Comparisons

Kruskal-Wallis Test on the data

Group	N	Median	Ave Rank	Z
Standard 1	3	1.6270	27.3	2.10
Standard (2+3+4)	13	0.8050	11.7	-2.38
modified (1+2+3+4)	16	0.9430	18.3	1.11
Overall	32		16.5	

H = 7.98 DF = 2 P = 0.019

H = 8.04 DF = 2 P = 0.018 (adjusted for ties)

* NOTE * One or more small samples

Kruskal-Wallis: All Pairwise Comparisons

Comparisons: 3
Ties: 20
Family Alpha: 0.2

Bonferroni Individual Alpha: 0.067
 Bonferroni Z-value (2-sided): 1.834

 Standardized Absolute Mean Rank Differences
 $|Rbar(i)-Rbar(j)| / Stdev$

Rows: Group i = 1,...,n
 Columns: Group j = 1,...,n

1. Table of Z-values

Standard 1	0.00000		*	*
Standard (2+3+4)	2.59673	0.00000	*	
modified (1+2+3+4)	1.52315	1.88794	0	

 Adjusted for Ties in the Data

1. Table of Z-values

Standard 1	0.00000		*	*
Standard (2+3+4)	2.60606	0.00000	*	
modified (1+2+3+4)	1.52862	1.89473	0	

2. Table of P-values

Standard 1	1.00000		*	*
Standard (2+3+4)	0.00916	1.00000	*	
modified (1+2+3+4)	0.12636	0.05813	1	

 Sign Confidence Intervals controlled at a family error rate of 0.2

Desired Confidence: 80.529

Sign confidence interval for median

	N	Median	Achieved Confidence	Confidence Interval		Position
				Lower	Upper	
Standard 1	3	1.627	0.7500	1.181	2.611	1
Standard (2+3+4)	13	0.8050	0.7332	0.3690	0.8320	5
			0.8053	0.3601	0.8449	NLI
			0.9077	0.3316	0.8860	4
modified (1+2+3+4)	16	0.943	0.7899	0.832	1.181	6
			0.8053	0.830	1.199	NLI
			0.9232	0.805	1.507	5

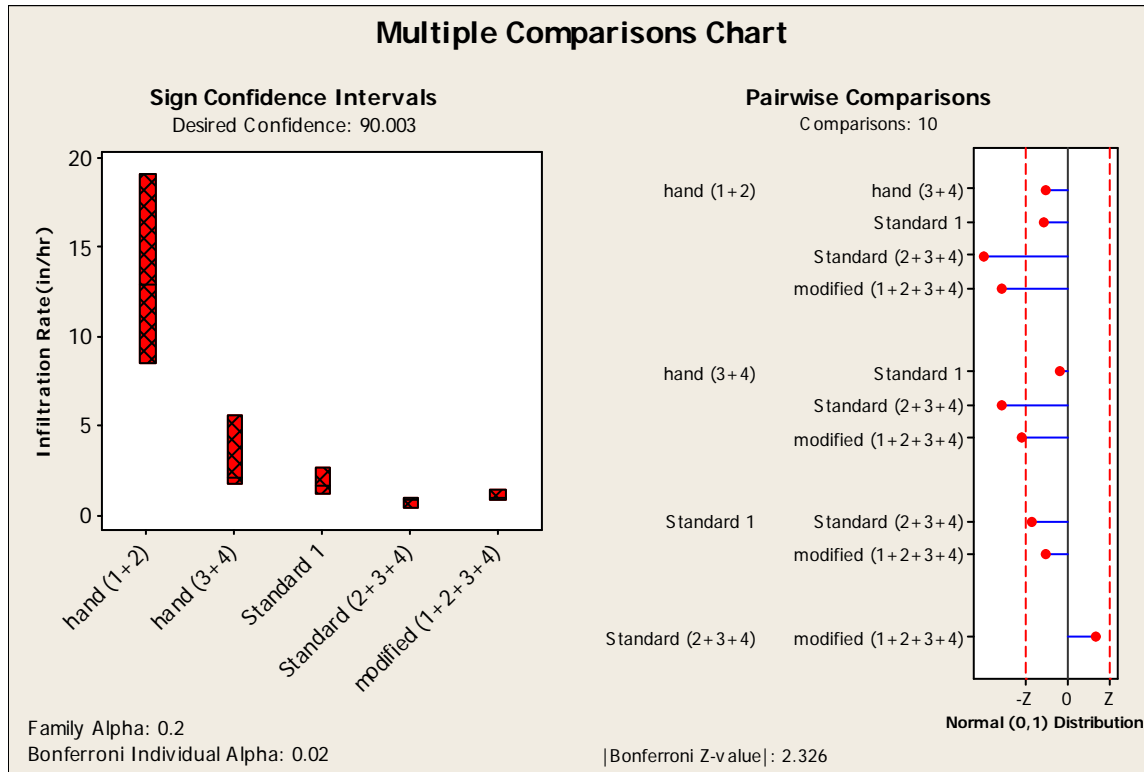
The highest attainable confidence has been achieved.

Kruskal-Wallis: Conclusions

The following groups showed significant differences (adjusted for ties):

Groups	Z vs. Critical value	p-value
Standard 1 vs. Standard (2+3+4)	2.60606 >= 1.834	0.0092
Standard (2+3+4) vs. modified (1+2+3+4)	1.89473 >= 1.834	0.0581

Appendix C.29: Kruskal-Wallis Multiple Comparisons for the Saturated Infiltration Rates of Lab Compaction Tests Using Surface Soils from Four Test Sites, Standard and Modified Proctor Compaction Conditions with Combined Data.



*1, 2, 3, and 4 are test sites

Kruskal-Wallis: Multiple Comparisons

Kruskal-Wallis Test on the data

Group	N	Median	Ave Rank	Z
hand (1+2)	6	12.8760	43.2	3.85
hand (3+4)	8	2.0323	34.1	2.46
Standard 1	3	1.6270	29.7	0.82
Standard (2+3+4)	13	0.8050	11.7	-3.73
modified (1+2+3+4)	16	0.9430	19.2	-1.58
Overall	46		23.5	

H = 30.15 DF = 4 P = 0.000
H = 30.23 DF = 4 P = 0.000 (adjusted for ties)

* NOTE * One or more small samples

Kruskal-Wallis: All Pairwise Comparisons

Comparisons:	10
Ties:	22
Family Alpha:	0.2
Bonferroni Individual Alpha:	0.02
Bonferroni Z-value (2-sided):	2.326

Standardized Absolute Mean Rank Differences
 $|\bar{R}(i) - \bar{R}(j)| / \text{Stdev}$

Rows: Group i = 1, ..., n
 Columns: Group j = 1, ..., n

1. Table of Z-values

hand (1+2)	0.00000		*	*	*	*
hand (3+4)	1.24729	0.00000		*	*	*
Standard 1	1.42237	0.49062	0.00000		*	*
Standard (2+3+4)	4.74525	3.71284	2.08621	0.00000		*
modified (1+2+3+4)	3.72696	2.56466	1.23719	1.49403	0	

Adjusted for Ties in the Data

1. Table of Z-values

hand (1+2)	0.00000		*	*	*	*
hand (3+4)	1.24887	0.00000		*	*	*
Standard 1	1.42417	0.49124	0.00000		*	*
Standard (2+3+4)	4.75126	3.71754	2.08885	0.00000		*
modified (1+2+3+4)	3.73168	2.56791	1.23876	1.49593	0	

2. Table of P-values

hand (1+2)	1.00000		*	*	*	*
hand (3+4)	0.21171	1.00000		*	*	*
Standard 1	0.15440	0.62326	1.00000		*	*
Standard (2+3+4)	0.00000	0.00020	0.03672	1.00000		*
modified (1+2+3+4)	0.00019	0.01023	0.21544	0.13467	1	

 Sign Confidence Intervals controlled at a family error rate of 0.2

Desired Confidence: 90.003

Sign confidence interval for median

	N	Median	Confidence Interval		Position
			Achieved Confidence	Lower Upper	
hand (1+2)	6	12.88	0.7813	8.50 18.55	2
			0.9000	8.50 19.08	NLI
			0.9688	8.48 20.59	1
hand (3+4)	8	2.032	0.7109	2.022 4.749	3
			0.9000	1.691 5.514	NLI
			0.9297	1.535 5.874	2
Standard 1	3	1.627	0.7500	1.181 2.611	1
			0.9000	0.3690 0.8320	5
Standard (2+3+4)	13	0.8050	0.7332	0.3351 0.8809	NLI
			0.9077	0.3316 0.8860	4
			0.9000	0.832 1.181	6
modified (1+2+3+4)	16	0.943	0.7899	0.814 1.404	NLI
			0.9000	0.814 1.404	NLI
			0.9232	0.805 1.507	5

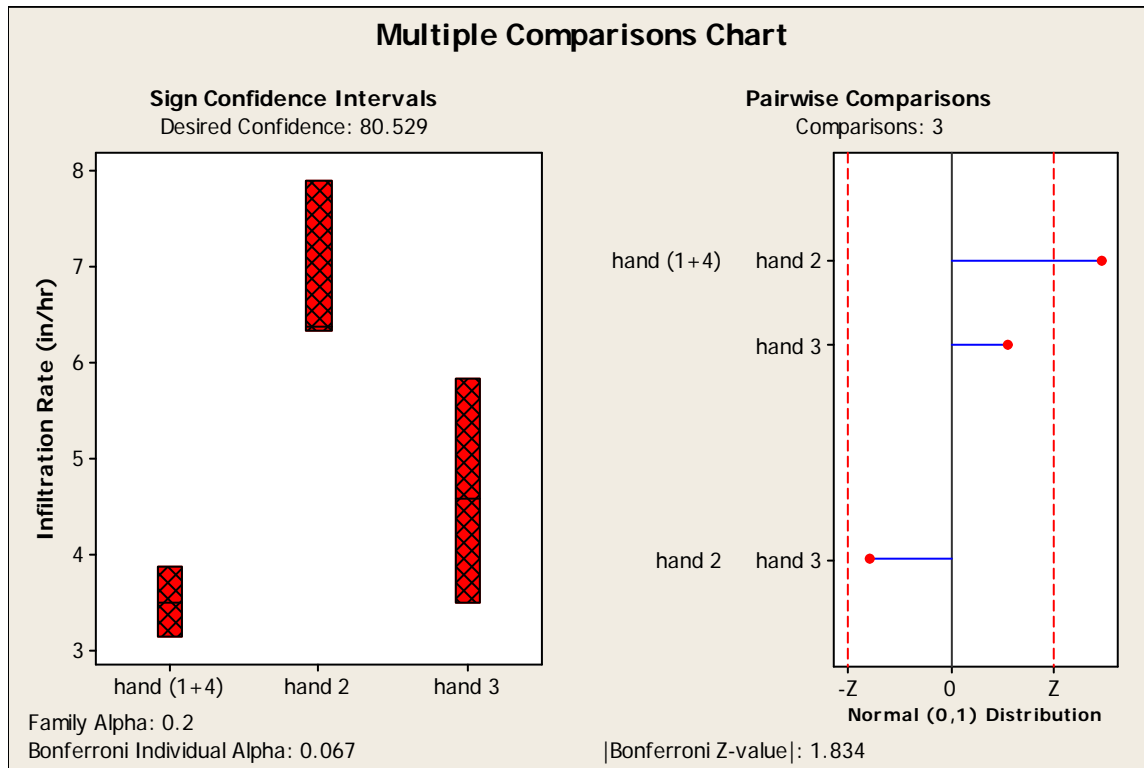
The highest attainable confidence has been achieved.

Kruskal-Wallis: Conclusions

The following groups showed significant differences (adjusted for ties):

Groups	Z vs. Critical value	P-value
hand (1+2) vs. Standard (2+3+4)	4.75126 >= 2.326	0.0000
hand (1+2) vs. modified (1+2+3+4)	3.73168 >= 2.326	0.0002
hand (3+4) vs. Standard (2+3+4)	3.71754 >= 2.326	0.0002
hand (3+4) vs. modified (1+2+3+4)	2.56791 >= 2.326	0.0102

Appendix C.30: Kruskal-Wallis Multiple Comparisons for the Saturated Infiltration Rates of Lab Compaction Tests Using Subsurface Soils from Four Test Sites, Hand Compaction Conditions with Combined Data.



*1, 2, 3, and 4 are test sites

Kruskal-Wallis: Multiple Comparisons

Kruskal-Wallis Test on the data

Group	N	Median	Ave Rank	Z
hand (1+4)	6	3.504	4.2	-2.24
hand 2	3	6.365	11.0	2.50
hand 3	3	4.576	6.7	0.09
Overall	12		6.5	

H = 7.19 DF = 2 P = 0.027

* NOTE * One or more small samples

Kruskal-Wallis: All Pairwise Comparisons

Comparisons: 3
Family Alpha: 0.2
Bonferroni Individual Alpha: 0.067
Bonferroni Z-value (2-sided): 1.834

 Standardized Absolute Mean Rank Differences
 $|Rbar(i)-Rbar(j)| / Stdev$

Rows: Group i = 1,...,n
 Columns: Group j = 1,...,n

1. Table of Z-values

hand (1+4)	0.00000		*	*
hand 2	2.68025	0.00000	*	
hand 3	0.98058	1.47196	0	

2. Table of P-values

hand (1+4)	1.00000		*	*
hand 2	0.00736	1.00000	*	
hand 3	0.32680	0.14103	1	

Sign Confidence Intervals controlled at a family error rate of 0.2

Desired Confidence: 80.529

Sign confidence interval for median

	N	Median	Confidence		Position
			Achieved Confidence	Interval	
hand (1+4)	6	3.504	0.7813	3.138 3.834	2
			0.8053	3.136 3.865	NLI
			0.9688	3.057 4.929	1
hand 2	3	6.365	0.7500	6.331 7.903	1
hand 3	3	4.576	0.7500	3.494 5.825	1

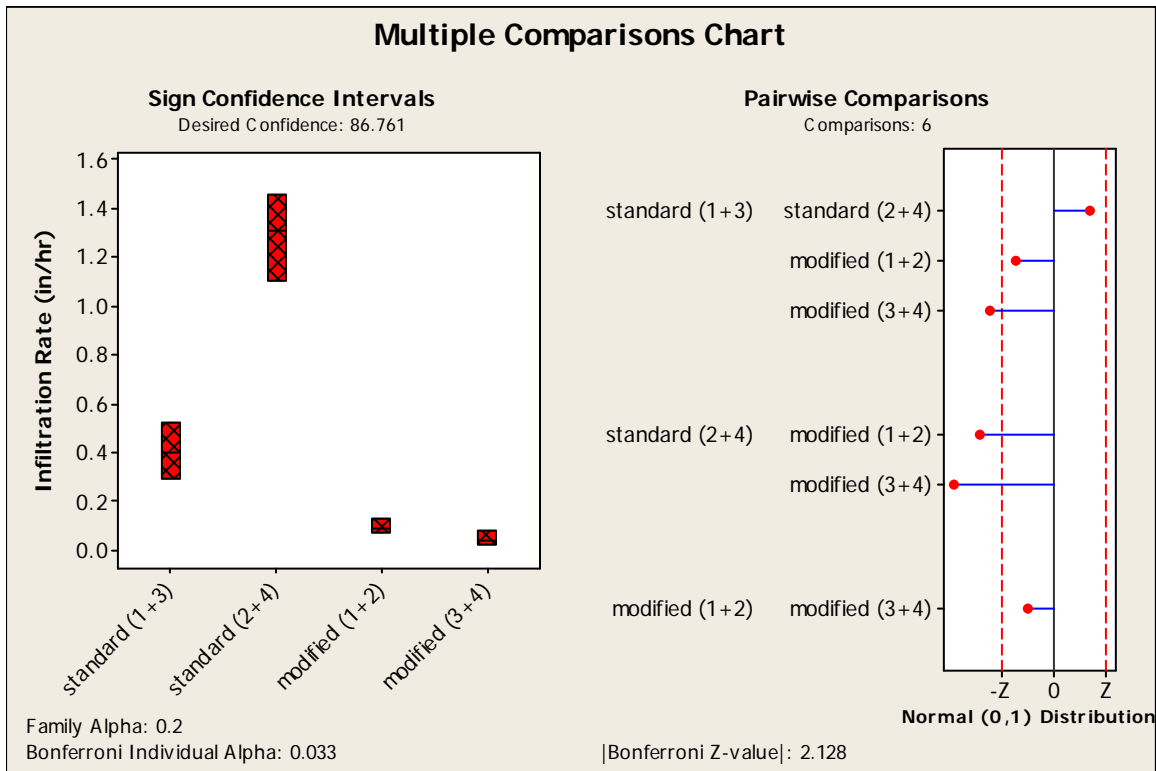
The highest attainable confidence has been achieved.
 The highest attainable confidence has been achieved.

Kruskal-Wallis: Conclusions

The following groups showed significant differences:

Groups	Z vs. Critical value	P-value
hand (1+4) vs. hand 2	2.68025 >= 1.834	0.0074

Appendix C.31: Kruskal-Wallis Multiple Comparisons for the Saturated Infiltration Rates of Lab Compaction Tests Using Subsurface Soils from Four Test Sites, Standard and Modified Proctor Compaction Conditions with Combined Data.



*1, 2, 3, and 4 are test sites

Kruskal-Wallis: Multiple Comparisons

Kruskal-Wallis Test on the data

Group	N	Median	Ave Rank	Z
standard (1+3)	6	0.39700	15.3	1.13
standard (2+4)	6	1.30650	21.3	3.53
modified (1+2)	6	0.08000	8.8	-1.47
modified (3+4)	6	0.03610	4.5	-3.20
Overall	24		12.5	

H = 19.62 DF = 3 P = 0.000

Kruskal-Wallis: All Pairwise Comparisons

Comparisons: 6
 Family Alpha: 0.2
 Bonferroni Individual Alpha: 0.033
 Bonferroni Z-value (2-sided): 2.128

Standardized Absolute Mean Rank Differences
 $|\bar{R}(i) - \bar{R}(j)| / \text{Stdev}$

Rows: Group i = 1, ..., n
Columns: Group j = 1, ..., n

1. Table of Z-values

standard (1+3)	0.00000		*	*	*
standard (2+4)	1.46969	0.00000		*	*
modified (1+2)	1.59217	3.06186	0.00000		*
modified (3+4)	2.65361	4.12331	1.06145	0	

2. Table of P-values

standard (1+3)	1.00000		*	*	*
standard (2+4)	0.14164	1.00000		*	*
modified (1+2)	0.11135	0.00220	1.00000		*
modified (3+4)	0.00796	0.00004	0.28849	1	

Sign Confidence Intervals controlled at a family error rate of 0.2

Desired Confidence: 86.761

Sign confidence interval for median

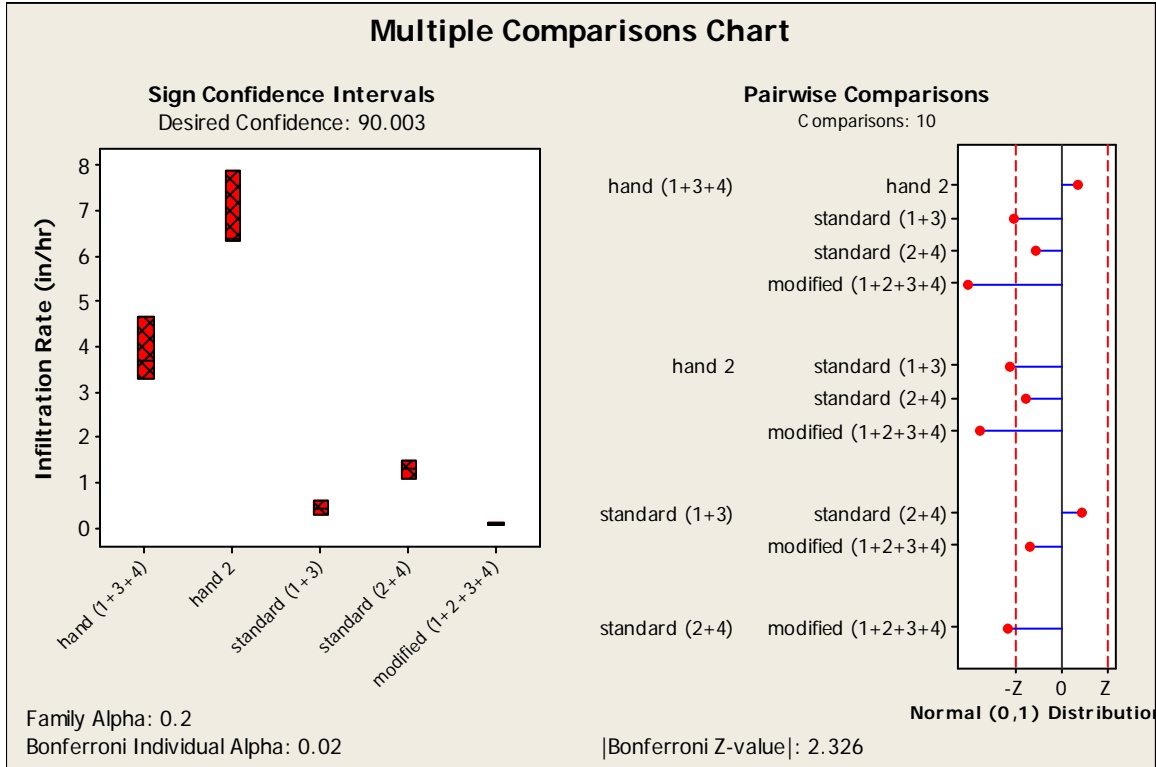
	N	Median	Achieved Confidence	Confidence Interval		Position
				Lower	Upper	
standard (1+3)	6	0.397	0.7813	0.320	0.414	2
			0.8676	0.291	0.522	NLI
			0.9688	0.122	1.154	1
standard (2+4)	6	1.307	0.7813	1.163	1.441	2
			0.8676	1.104	1.453	NLI
			0.9688	0.757	1.520	1
modified (1+2)	6	0.0800	0.7813	0.0670	0.1060	2
			0.8676	0.0666	0.1219	NLI
			0.9688	0.0640	0.2150	1
modified (3+4)	6	0.0361	0.7813	0.0150	0.0630	2
			0.8676	0.0138	0.0732	NLI
			0.9688	0.0069	0.1330	1

Kruskal-Wallis: Conclusions

The following groups showed significant differences:

Groups	Z vs. Critical value	P-value
standard (2+4) vs. modified (3+4)	4.12331 >= 2.128	0.0000
standard (2+4) vs. modified (1+2)	3.06186 >= 2.128	0.0022
standard (1+3) vs. modified (3+4)	2.65361 >= 2.128	0.0080

Appendix C.32: Kruskal-Wallis Multiple Comparisons for the Saturated Infiltration Rates of Lab Compaction Tests Using Subsurface Soils from Four Test Sites, Hand, Standard, and Modified Proctor Compaction Conditions with Combined Data.



*1, 2, 3, and 4 are test sites

Kruskal-Wallis: Multiple Comparisons

Kruskal-Wallis Test on the data

Group	N	Median	Ave Rank	Z
hand (1+3+4)	9	3.67500	29.0	3.45
hand 2	3	6.36500	35.0	2.83
standard (1+3)	6	0.39700	15.3	-0.81
standard (2+4)	6	1.30650	21.3	0.72
modified (1+2+3+4)	12	0.06550	6.7	-4.77
Overall	36		18.5	

H = 32.41 DF = 4 P = 0.000

* NOTE * One or more small samples

Kruskal-Wallis: All Pairwise Comparisons

Comparisons: 10
Family Alpha: 0.2
Bonferroni Individual Alpha: 0.02

Bonferroni Z-value (2-sided): 2.326

 Standardized Absolute Mean Rank Differences
 $|Rbar(i)-Rbar(j)| / Stdev$

Rows: Group i = 1,...,n
 Columns: Group j = 1,...,n

1. Table of Z-values

hand (1+3+4)	0.00000	*	*	*	*
hand 2	0.85424	0.00000	*	*	*
standard (1+3)	2.46123	2.63988	0.00000	*	*
standard (2+4)	1.38069	1.83449	0.98639	0.00000	*
modified (1+2+3+4)	4.80722	4.16622	1.64521	2.78420	0

2. Table of P-values

hand (1+3+4)	1.00000	*	*	*	*
hand 2	0.39297	1.00000	*	*	*
standard (1+3)	0.01385	0.00829	1.00000	*	*
standard (2+4)	0.16737	0.06658	0.32394	1.00000	*
modified (1+2+3+4)	0.00000	0.00003	0.09993	0.00537	1

 Sign Confidence Intervals controlled at a family error rate of 0.2

Desired Confidence: 90.003

Sign confidence interval for median

	N	Median	Achieved Confidence	Confidence Interval		Position
				Lower	Upper	
hand (1+3+4)	9	3.675	0.8203	3.333	4.576	3
			0.9000	3.280	4.672	NLI
			0.9609	3.138	4.929	2
hand 2	3	6.365	0.7500	6.331	7.903	1
			0.7813	0.320	0.414	2
standard site (1+3)	6	0.397	0.9000	0.269	0.604	NLI
			0.9688	0.122	1.154	1
			0.7813	1.163	1.441	2
standard (2+4)	6	1.307	0.9000	1.059	1.461	NLI
			0.9688	0.757	1.520	1
			0.8540	0.0430	0.0880	4
modified (1+2+3+4)	12	0.0655	0.9000	0.0402	0.0916	NLI
			0.9614	0.0292	0.1060	3

The highest attainable confidence has been achieved.

Kruskal-Wallis: Conclusions

The following groups showed significant differences:

Groups	Z vs. Critical value	P-value
hand (1+3+4) vs. modified (1+2+3+4)	4.80722 >= 2.326	0.0000
hand 2 vs. modified (1+2+3+4)	4.16622 >= 2.326	0.0000
standard (2+4) vs. modified (1+2+3+4)	2.78420 >= 2.326	0.0054
hand 2 vs. standard (1+3)	2.63988 >= 2.326	0.0083
hand (1+3+4) vs. standard (1+3)	2.46123 >= 2.326	0.0138

APPENDIX D: FLOWS CHANGES AND PARTICULATE RETENTION TESTS IN BIOFILTER MEDIA

Appendix D.1: Sand-Peat Mixture Nutrient Report

Units: ppm , %, & meq/100g in soil		Extraction Method: Saturated Paste						
Sample	ppm	ppm	ppm	ppm	ppm	ppm	ppm	ppm
ID	Ca	K	Mg	P	Al	As	B	Ba
ID	Calcium	Potassium	Magnesium	Phosphorus	Aluminum	Arsenic	Boron	Barium
Sand from Northport, AL	0.2	1.3	0.2	<0.1	<0.1	<0.1	<0.1	<0.1
10% peat & 90% sand from Northport, AL	0.6	2.0	0.3	0.3	<0.1	0.2	<0.1	<0.1
25% peat & 75% sand from Northport, AL	1.0	2.0	0.5	<0.1	<0.1	0.1	<0.1	<0.1
50% peat & 50% sand from, Northport, AL	1.5	2.4	1.0	0.3	0.2	<0.1	<0.1	<0.1
10/30 sand from ATL, GA	<0.1	0.2	<0.1	1.6	<0.1	0.2	<0.1	<0.1
10% peat, 45% sand from Northport, & 45% 10/30 sand	0.4	1.6	0.2	<0.1	<0.1	0.3	<0.1	<0.1
25% peat, 37.5% sand from Northport, & 37.5% 10/30 sand	1.5	1.8	0.6	0.4	0.2	0.2	<0.1	<0.1
50% peat, 25% sand from Northport, & 25% 10/30 sand	1.9	2.0	1.4	0.9	1.3	<0.1	<0.1	<0.1
Concrete sand from ATL, GA	0.5	0.5	0.1	0.2	0.9	0.3	<0.1	<0.1
10% peat, 45% concrete sand , & 45% 10/30 sand	1.0	0.7	0.4	<0.1	7.0	<0.1	<0.1	<0.1
25% peat, 37.5% concrete sand , & 37.5% 10/30 sand	1.3	0.8	0.5	<0.1	2.0	0.3	<0.1	<0.1
50% peat, 25% concrete sand , & 25% 10/30 sand	1.9	1.0	1.2	0.4	2.5	<0.1	<0.1	<0.1
6/10 sand from ATL, GA	0.2	1.0	0.1	0.5	0.1	0.1	<0.1	<0.1
10% peat, 45% sand from Northport & 45% 6/10 sand	0.5	2.7	0.4	<0.1	0.5	0.2	<0.1	<0.1
25% peat, 37.5% sand from Northport & 37.5% 6/10 sand	1.5	2.3	0.7	<0.1	0.5	<0.1	<0.1	<0.1
50% peat, 25% sand from Northport & 25% 6/10 sand	2.4	2.3	1.5	<0.1	1.0	0.3	<0.1	<0.1
10% peat, 45% 10/30 sand, & 45% 6/10 sand	0.5	1.4	0.5	0.4	5.6	<0.1	<0.1	<0.1
25% peat, 37.5% 10/30 sand, & 37.5% 6/10 sand	1.5	0.9	0.9	0.5	3.6	<0.1	<0.1	<0.1
50% peat, 25% 10/30 sand, & 25% 6/10 sand	1.7	0.9	1.5	0.6	2.3	0.2	<0.1	<0.1

Units: ppm								
	ppm	ppm	ppm	ppm	ppm	ppm	ppm	ppm
Sample	Cd	Cr	Cu	Fe	Mn	Mo	Na	Ni
ID	Cadmium	Chromium	Copper	Iron	Manganese	Molybdenum	Sodium	Nickel
Sand from Northport, AL	<0.1	<0.1	<0.1	<0.1	<0.1	<0.1	6.9	<0.1
10% peat & 90% sand from Northport, AL	<0.1	<0.1	<0.1	<0.1	<0.1	<0.1	7.1	<0.1
25% peat & 75% sand from Northport, AL	<0.1	<0.1	<0.1	<0.1	<0.1	<0.1	7.8	<0.1
50% peat & 50% sand from, Northport, AL	<0.1	<0.1	<0.1	0.1	<0.1	<0.1	11.4	<0.1
10/30 sand from ATL, GA	<0.1	<0.1	<0.1	<0.1	<0.1	<0.1	1.6	<0.1
10% peat, 45% sand from Northport, & 45% 10/30 sand	<0.1	<0.1	<0.1	<0.1	<0.1	<0.1	7.2	<0.1
25% peat, 37.5% sand from Northport, & 37.5% 10/30 sand	<0.1	<0.1	<0.1	0.1	<0.1	<0.1	9.7	<0.1
50% peat, 25% sand from Northport, & 25% 10/30 sand	<0.1	<0.1	0.2	1.1	<0.1	<0.1	14.1	<0.1
Concrete sand from ATL, GA	<0.1	<0.1	<0.1	<0.1	<0.1	<0.1	8.1	<0.1
10% peat, 45% concrete sand, & 45% 10/30 sand	<0.1	<0.1	<0.1	1.7	<0.1	<0.1	8.7	<0.1
25% peat, 37.5% concrete sand, & 37.5% 10/30 sand	<0.1	<0.1	0.1	0.6	<0.1	<0.1	10.7	<0.1
50% peat, 25% concrete sand, & 25% 10/30 sand	<0.1	<0.1	0.3	0.8	<0.1	<0.1	14.4	<0.1
6/10 sand from ATL, GA	<0.1	<0.1	<0.1	<0.1	<0.1	<0.1	10.3	<0.1
10% peat, 45% sand from Northport & 45% 6/10 sand	<0.1	<0.1	<0.1	0.2	<0.1	<0.1	14.0	<0.1
25% peat, 37.5% sand from Northport & 37.5% 6/10 sand	<0.1	<0.1	<0.1	0.3	<0.1	<0.1	13.2	<0.1
50% peat, 25% sand from Northport & 25% 6/10 sand	<0.1	<0.1	0.2	0.9	<0.1	<0.1	15.9	<0.1
10% peat, 45% 10/30 sand, & 45% 6/10 sand	<0.1	<0.1	<0.1	2.9	<0.1	<0.1	13.1	<0.1
25% peat, 37.5% 10/30 sand, & 37.5% 6/10 sand	<0.1	<0.1	0.2	1.8	<0.1	<0.1	11.7	<0.1
50% peat, 25% 10/30 sand, & 25% 6/10 sand	<0.1	<0.1	0.3	1.0	<0.1	<0.1	14.3	<0.1

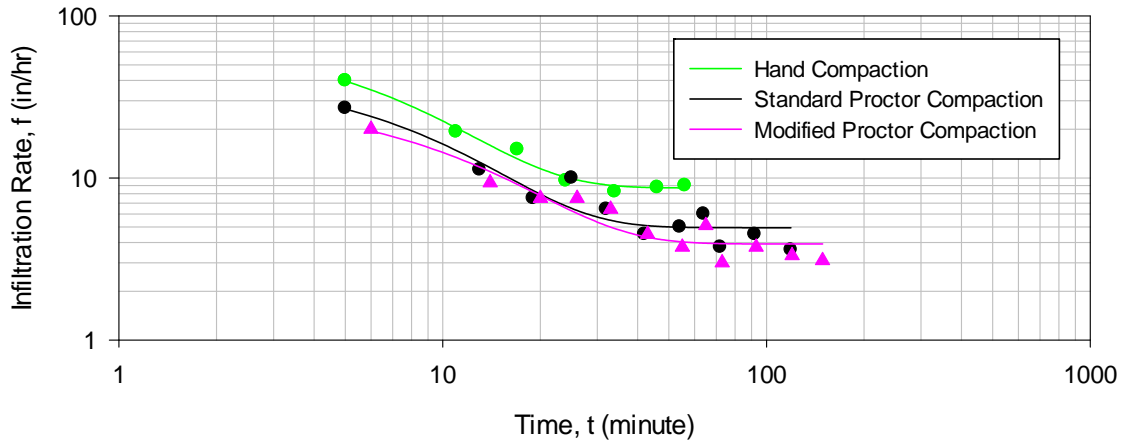
Units: ppm and meq/100g in soil					
	ppm	ppm	ppm	meq/100g	
Sample	Pb	Zn	Tot. P	CEC	
ID	Lead	Zinc	Total Phosphorus	Cation Exchange Capacity	pH
Sand from Northport, AL	<0.1	<0.1	166	0.036	4.80
10% peat & 90% sand from Northport, AL	<0.1	<0.1	131	0.042	4.51
25% peat & 75% sand from Northport, AL	<0.1	0.1	100	0.048	4.05
50% peat & 50% sand from, Northport, AL	<0.1	<0.1	176	0.071	3.81
10/30 sand from ATL, GA	<0.1	<0.1	<0.1	0.007	4.85
10% peat, 45% sand from Northport, & 45% 10/30 sand	<0.1	<0.1	96	0.039	4.04
25% peat, 37.5% sand from Northport, & 37.5% 10/30 sand	<0.1	0.2	72	0.059	3.86
50% peat, 25% sand from Northport, & 25% 10/30 sand	<0.1	0.1	58	0.087	3.69
Concrete sand from ATL, GA	<0.1	0.1	28	0.040	4.75
10% peat, 45% concrete sand, & 45% 10/30 sand	<0.1	<0.1	<0.1	0.048	4.28
25% peat, 37.5% concrete sand, & 37.5% 10/30 sand	<0.1	<0.1	<0.1	0.059	3.95
50% peat, 25% concrete sand, & 25% 10/30 sand	<0.1	<0.1	34	0.085	4.03
6/10 sand from ATL, GA	<0.1	<0.1	<0.1	0.049	5.10
10% peat, 45% sand from Northport & 45% 6/10 sand	<0.1	<0.1	89	0.073	4.61
25% peat, 37.5% sand from Northport & 37.5% 6/10 sand	<0.1	0.2	<0.1	0.077	4.19
50% peat, 25% sand from Northport & 25% 6/10 sand	<0.1	<0.1	172	0.099	3.85
10% peat, 45% 10/30 sand, & 45% 6/10 sand	<0.1	0.1	<0.1	0.067	4.19
25% peat, 37.5% 10/30 sand, & 37.5% 6/10 sand	<0.1	0.1	<0.1	0.068	4.03
50% peat, 25% 10/30 sand, & 25% 6/10 sand	<0.1	0.1	48	0.085	3.89

Units: %					
	%	%	%	%	
Sample	N	C	S	OM	SAR
ID	Nitrogen	Carbon	Sulfur	Organic Matter	Sodium Adsorption Ratio
Sand from Northport, AL	0.14	0.13	0.012	0.2	2.3
10% peat & 90% sand from Northport, AL	0.064	0.60	0.008	1.0	1.8
25% peat & 75% sand from Northport, AL	0.068	1.57	0.011	2.7	1.9
50% peat & 50% sand from, Northport, AL	0.139	5.73	0.030	9.9	0.4
10/30 sand from ATL, GA	0.040	0.05	0.013	0.1	3.4
10% peat, 45% sand from Northport, & 45% 10/30 sand	0.034	0.51	0.012	0.9	2.3
25% peat, 37.5% sand from Northport, & 37.5% 10/30 sand	0.042	1.19	0.012	2.0	2.0
50% peat, 25% sand from Northport, & 25% 10/30 sand	0.11	4.12	0.019	7.1	1.3
Concrete sand from ATL, GA	0.019	0.06	0.007	0.1	1.8
10% peat, 45% concrete sand, & 45% 10/30 sand	0.048	0.47	0.008	0.8	1.9
25% peat, 37.5% concrete sand, & 37.5% 10/30 sand	0.043	1.34	0.009	2.3	0.4
50% peat, 25% concrete sand, & 25% 10/30 sand	0.090	2.84	0.013	4.9	1.3
6/10 sand from ATL, GA	0.020	0.04	0.009	0.1	2.5
10% peat, 45% sand from Northport & 45% 6/10 sand	0.029	0.46	0.008	0.8	2.4
25% peat, 37.5% sand from Northport & 37.5% 6/10 sand	0.027	0.87	0.010	1.5	1.7
50% peat, 25% sand from Northport & 25% 6/10 sand	0.104	3.95	0.017	6.8	1.4
10% peat, 45% 10/30 sand, & 45% 6/10 sand	0.016	0.25	0.005	0.4	2.5
25% peat, 37.5% 10/30 sand, & 37.5% 6/10 sand	0.027	0.93	0.007	1.6	2.0
50% peat, 25% 10/30 sand, & 25% 6/10 sand	0.077	3.62	0.013	6.2	2.5

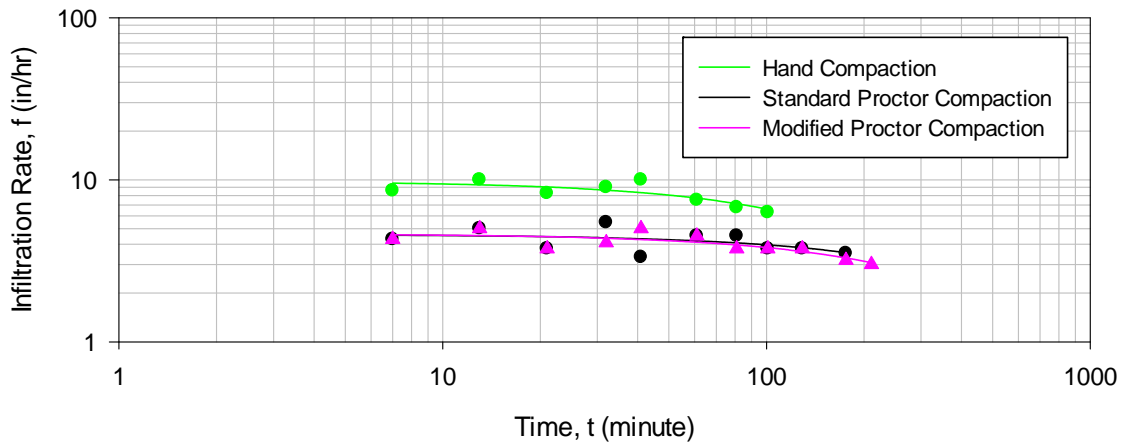
Appendix D.2: Lab Infiltration Measurements Using Sand and Peat Mixture ($D_{50} = 340$ um and $C_u = 1.3$)

10% Peat and 90% Sand from Ground Floor Sand Supplier Northport, AL (GF) Sand (Mixture $D_{50} = 340$ um and $C_u = 1.3$)				
Compaction	Trial	f_o (in/hr)	f_c (in/hr)	k (1/min)
hand 1.28 g/cm^3	1	78.1	8.7	0.16
	2	16.1	6.3	0.004
	3	17.9	7.5	0.004
	mean	37.4	7.5	0.06
	COV	0.9	0.2	1.61
Compaction	Trial	f_o (in/hr)	f_c (in/hr)	k (1/min)
standard proctor 1.29 g/cm^3	1	46.9	5.0	0.13
	2	8.1	3.5	0.002
	3	5.8	3.7	0.020
	mean	20.3	4.1	0.05
	COV	1.1	0.2	1.37
Compaction	Trial	f_o (in/hr)	f_c (in/hr)	k (1/min)
modified proctor 1.35 g/cm^3	1	32.2	4.0	0.10
	2	7.6	3.0	0.002
	3	4.4	2.0	0.01
	mean	14.7	3.0	0.04
	COV	1.0	0.3	1.46

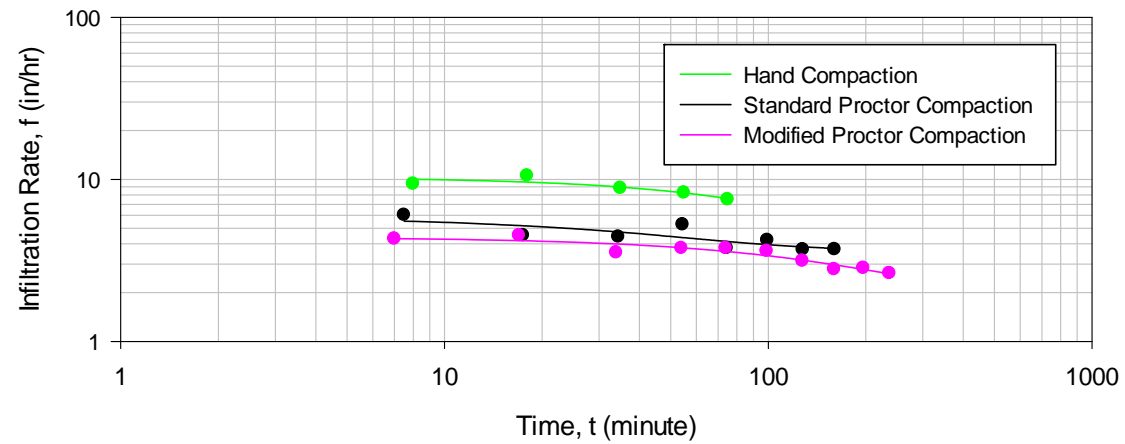
10 % peat and 90 % sand (D50 = 340 um and Cu = 1.3), Trial 1



10 % peat and 90 % sand (D50 = 340 um and Cu = 1.3), Trial 2



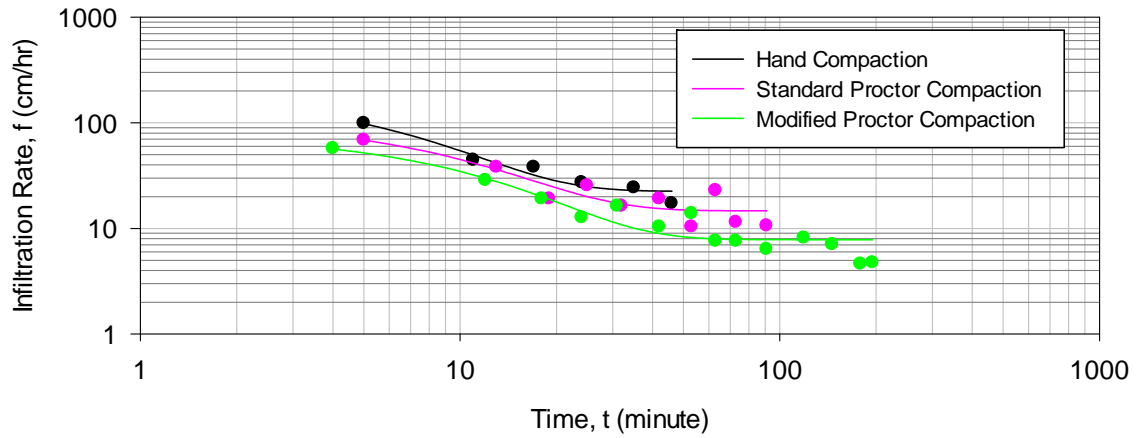
10 % peat and 90 % sand (D50 = 340 um and Cu = 1.3), Trial 3



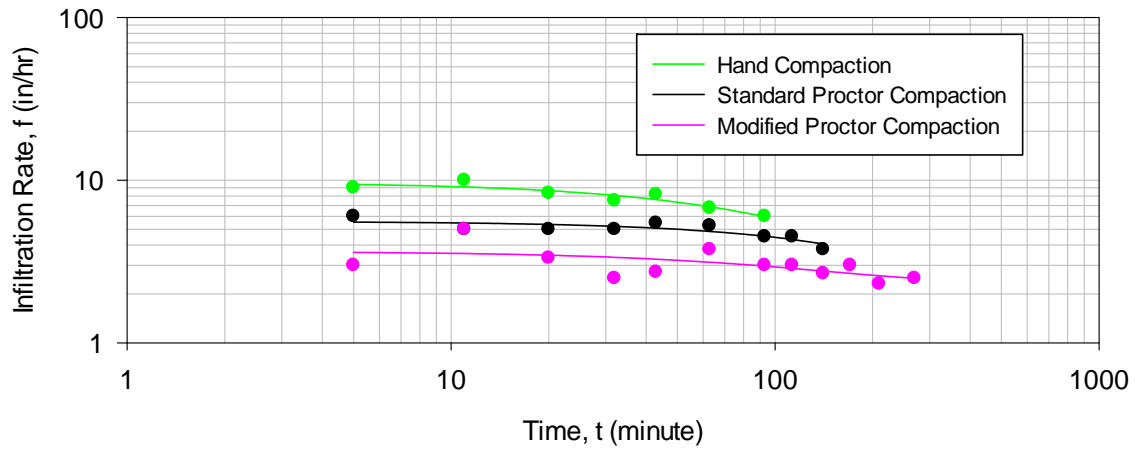
Appendix D.3: Lab Infiltration Measurements Using Sand and Peat Mixture ($D_{50} = 300 \text{ um}$ and $C_u = 3.5$)

25% Peat and 75% Sand from Ground Floor (GF) Sand Supplier Northport, AL (Mixture $D_{50} = 300 \text{ um}$ and $C_u = 3.5$)				
Compaction	Trial	f_o (in/hr)	f_c (in/hr)	k (1/min)
hand 1.14 g/cm^3	1	79.3	8.9	0.17
	2	9.7	3.2	0.01
	3	9.4	4.8	0.01
	mean	32.8	5.6	0.06
	COV	1.2	0.5	1.46
Compaction	Trial	f_o (in/hr)	f_c (in/hr)	k (1/min)
standard proctor 1.1 g/cm^3	1	43.7	5.8	0.12
	2	9.4	3.8	0.002
	3	9.1	4.0	0.001
	mean	20.7	4.5	0.04
	COV	1.0	0.2	1.67
Compaction	Trial	f_o (in/hr)	f_c (in/hr)	k (1/min)
modified proctor 1.2 g/cm^3	1	31.9	3.3	0.100
	2	3.7	2.3	0.01
	3	5.7	2.4	0.001
	mean	13.8	2.7	0.04
	COV	1.1	0.2	1.48

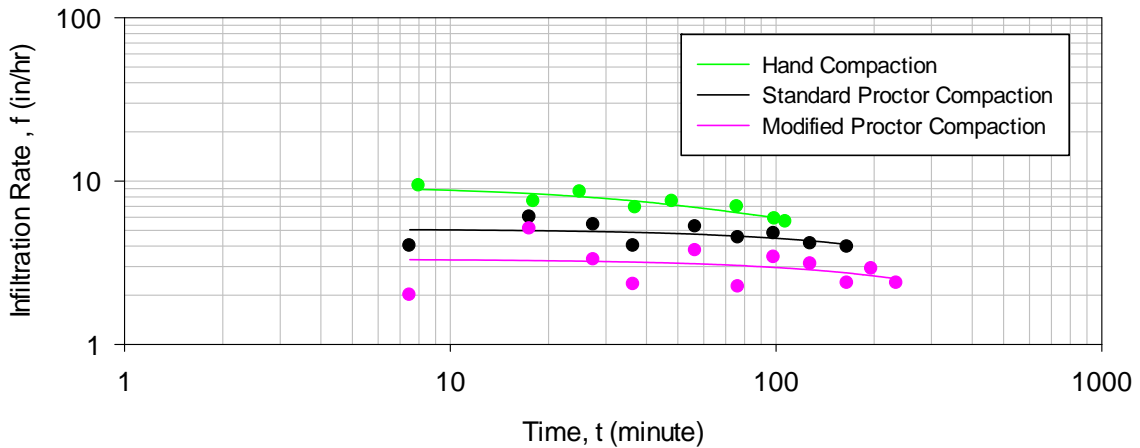
25% peat and 75 % sand (D50 = 300 um and Cu = 3.5), Trial 1



25% peat and 75 % sand (D50 = 300 um and Cu = 3.5), Trial 2



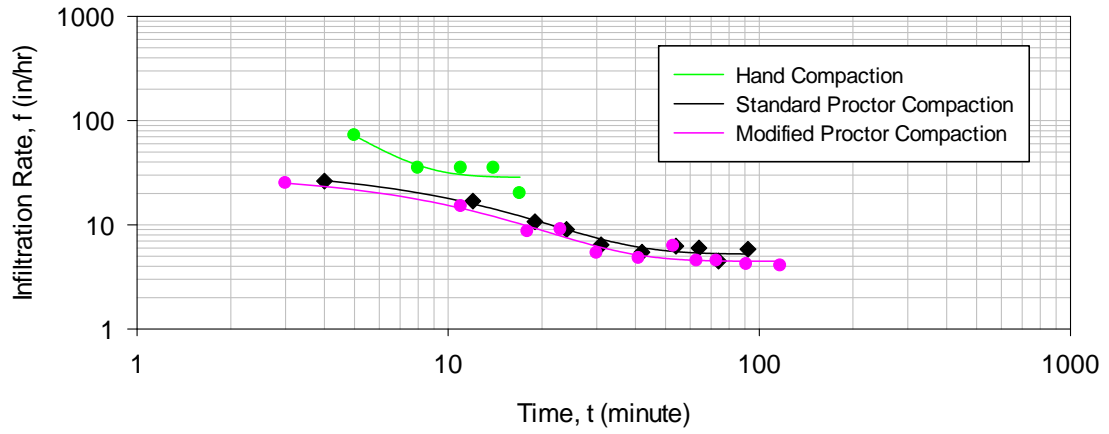
25% peat and 75 % sand (D50 = 300 um and Cu = 3.5), Trial 3



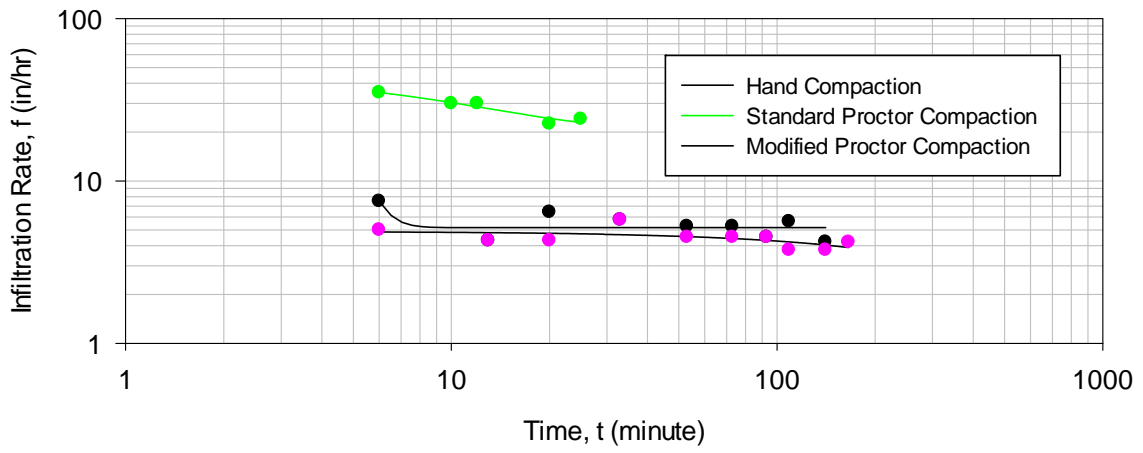
Appendix D.4: Lab Infiltration Measurements Using Sand and Peat Mixture ($D_{50} = 300 \text{ um}$ and $C_u = 3.3$).

50% peat and 50% Sand from Ground Floor (GF) Sand Supplier Northport, AL (Mixture $D_{50} = 300 \text{ um}$ and $C_u = 3.3$)				
Compaction	Trial	f_o (in/hr)	f_c (in/hr)	k (1/min)
hand 0.74 g/cm^3	1	n/a	28.6	0.53
	2	47.0	20.8	0.10
	3	48.4	17.4	0.01
	mean	47.7	22.3	0.21
	COV	0.02	0.3	1.30
Compaction	Trial	f_o (in/hr)	f_c (in/hr)	k (1/min)
standard proctor 0.96 g/cm^3	1	35.4	5.3	0.10
	2	n/a	5.2	1.10
	3	5.7	3.7	0.01
	mean	20.6	4.7	0.40
	COV	1.0	0.2	1.50
Compaction	Trial	f_o (in/hr)	f_c (in/hr)	k (1/min)
modified proctor 1.03 g/cm^3	1	31.6	4.5	0.100
	2	9.1	4.2	0.001
	3	6.2	3.8	0.050
	mean	15.6	4.2	0.05
	COV	0.9	0.1	0.98

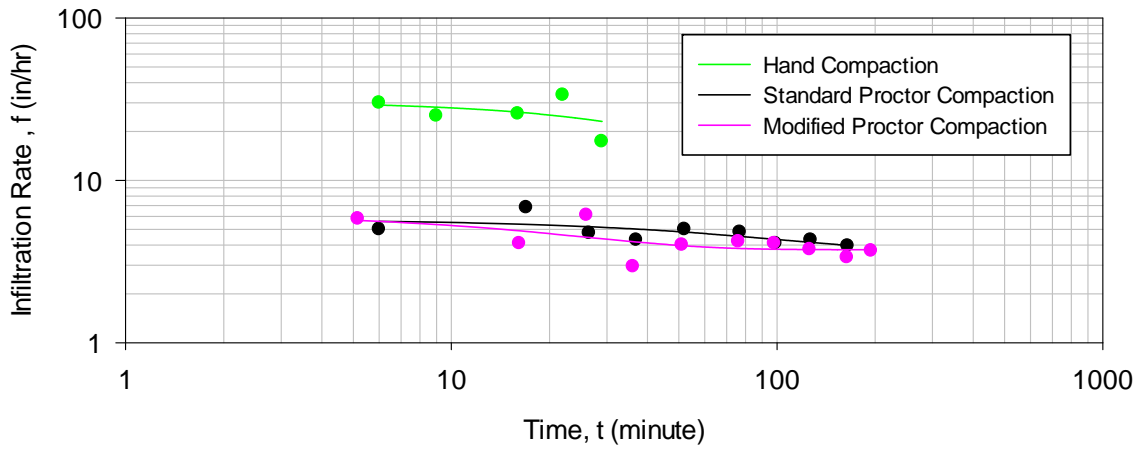
50 % peat and 50 % sand (D50 = 300 um and Cu = 3.3), Trial 1



50 % peat and 50 % sand (D50 = 300 um and Cu = 3.3), Trial 2



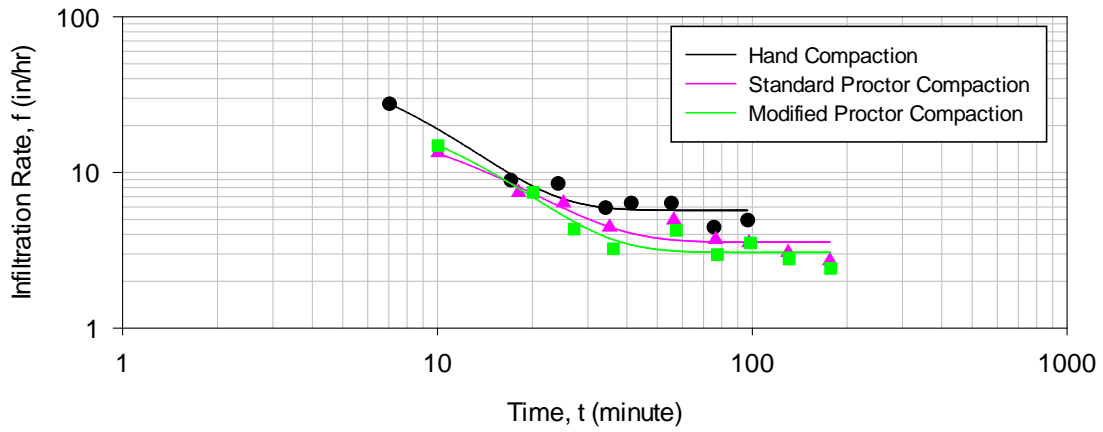
50 % peat and 50 % sand (D50 = 300 um and Cu = 3.3), Trial 3



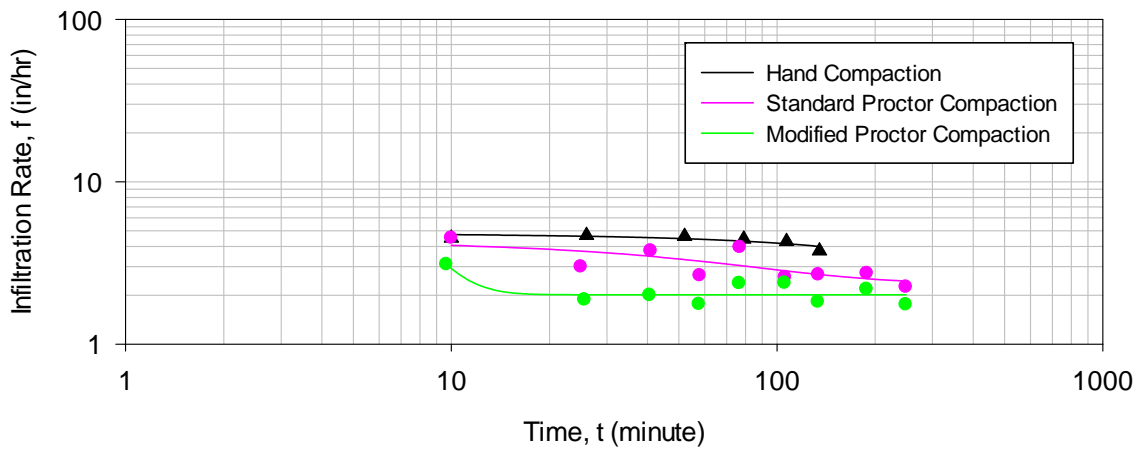
Appendix D.5: Lab Infiltration Measurements Using Sand and Peat Mixture ($D_{50} = 1500$ um and $C_u = 22$).

10% Peat, 45% Sand from Ground Floor (GF) Sand Supplier Northport, AL, and 45% 6/10 Sand from ATL, GA (Mixture $D_{50} = 1500$ um and $C_u = 22$)				
Compaction	Trial	f_o (in/hr)	f_c (in/hr)	k (1/min)
hand 1.61 g/cm ³	1	77.4	5.8	0.17
	2	8.5	3.8	0.001
	3	8.4	3.8	0.002
	mean	31.5	4.4	0.06
	COV	1.3	0.3	1.69
Compaction	Trial	f_o (in/hr)	f_c (in/hr)	k (1/min)
standard proctor 1.64 g/cm ³	1	28.6	3.6	0.10
	2	4.2	2.3	0.014
	3	5.2	2.1	0.001
	mean	12.7	2.7	0.04
	COV	1.1	0.3	1.40
Compaction	Trial	f_o (in/hr)	f_c (in/hr)	k (1/min)
modified proctor 1.63 g/cm ³	1	40.0	3.1	0.10
	2	177	2.0	0.53
	3	2.1	1.0	0.001
	mean	73.0	2.0	0.21
	COV	1.3	0.5	1.34

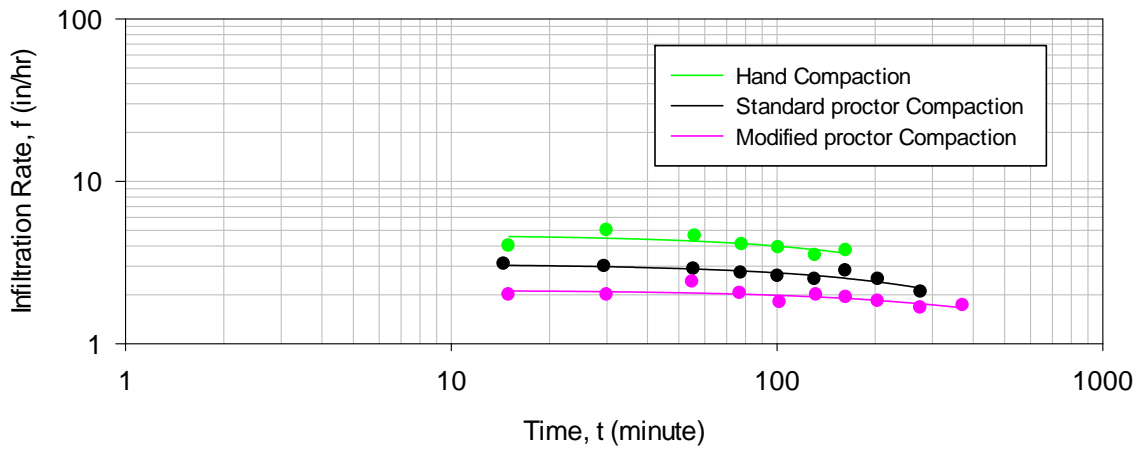
10% peat and 90% sand (D50 = 1500 um and Cu = 22), Trial 1



10% peat and 90% sand (D50 = 1500 um and Cu = 22), Trial 2



10% peat and 90% sand (D50 = 1500 um and Cu = 22), Trial 3

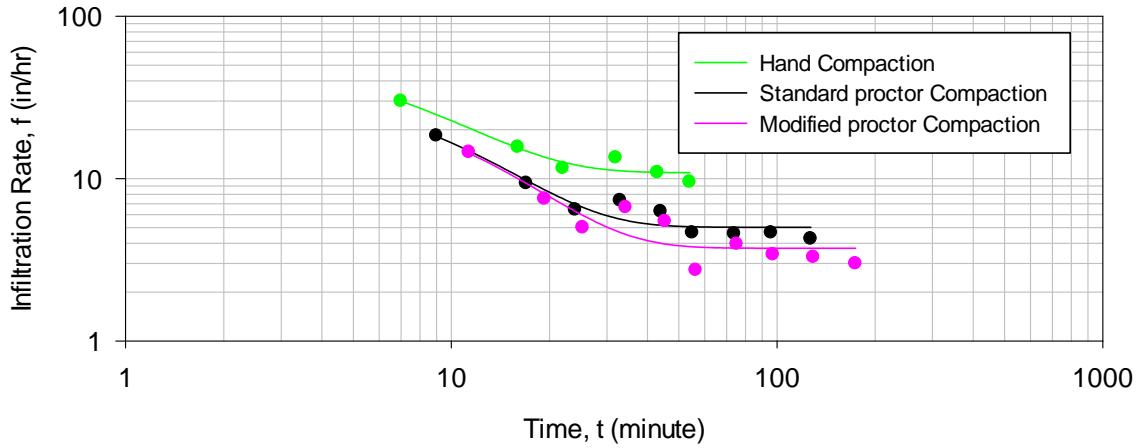


Appendix D.6: Lab Infiltration Measurements Using Sand and Peat Mixture ($D_{50} = 1500 \text{ um}$ and $C_u = 16$).

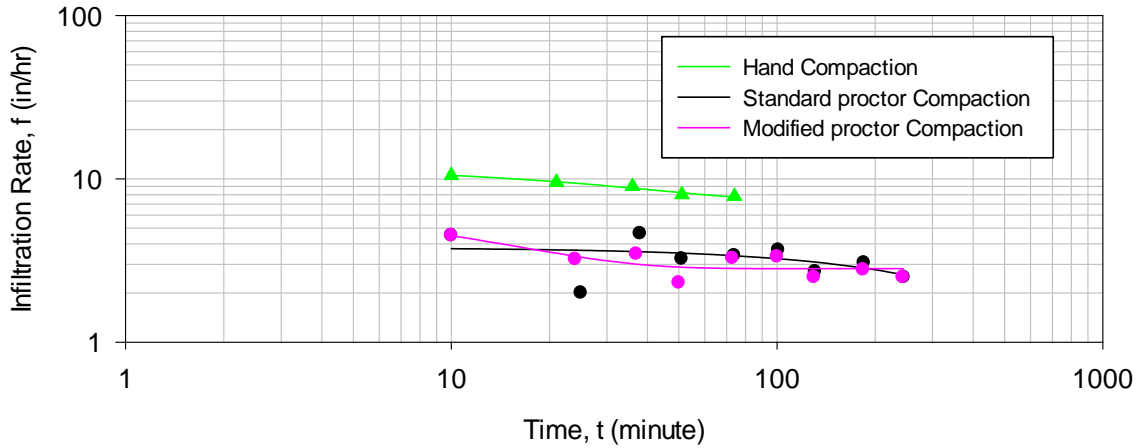
25% Peat, 37.5% Sand from Ground Floor Sand Supplier Northport, AL, and 37.5% 6/10 Sand from ATL, GA (Mixture $D_{50} = 1500 \text{ um}$ and $C_u = 16$)				
Compaction	Trial	f_o (in/hr)	f_c (in/hr)	k (1/min)
hand 1.46 g/cm ³	1	69.0	11.0	0.16
	2	11.6	7.2	0.03
	3	17.3	6.2	0.01
	mean	32.6	8.1	0.07
	COV	1.0	0.3	1.27
Compaction	Trial	f_o (in/hr)	f_c (in/hr)	k (1/min)
standard proctor 1.5 g/cm ³	1	46.7	5.0	0.13
	2	6.3	2.5	0.002
	3	n/a	3.1	0.510
	mean	26.5	3.5	0.21
	COV	1.1	0.4	1.23
Compaction	Trial	f_o (in/hr)	f_c (in/hr)	k (1/min)
modified proctor 1.52 g/cm ³	1	41.4	3.7	0.100
	2	6.5	2.8	0.08
	3	5.9	2.4	0.001
	mean	17.9	3.0	0.06
	COV	1.1	0.2	0.87

* n/a values were beyond the data range

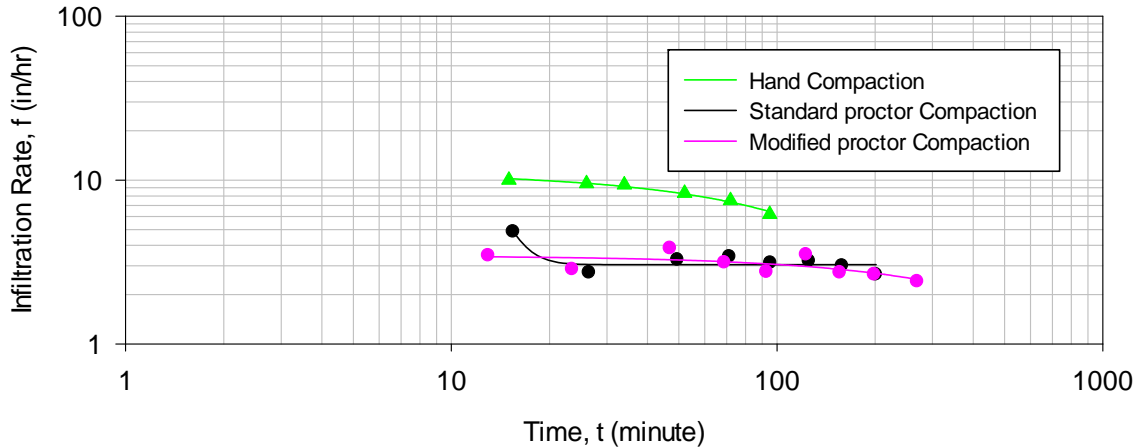
25% peat and 75% sand (D50 = 1500 um and Cu = 16), Trial 1



25% peat and 75% sand (D50 = 1500 um and Cu = 16), Trial 2



25% peat and 75% sand (D50 = 1500 um and Cu = 16), Trial 3

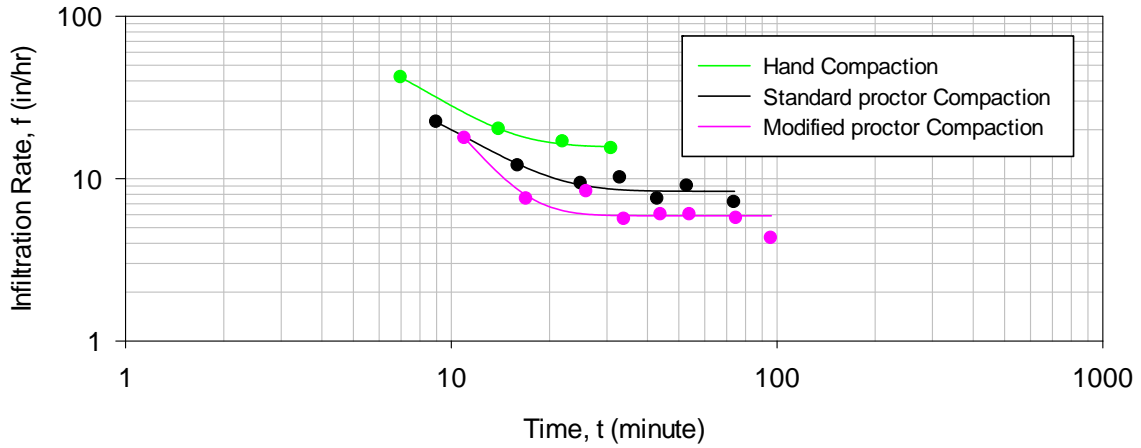


Appendix D.7: Lab Infiltration Measurements Using Sand and Peat Mixture ($D_{50} = 1500$ um and $C_u = 20$).

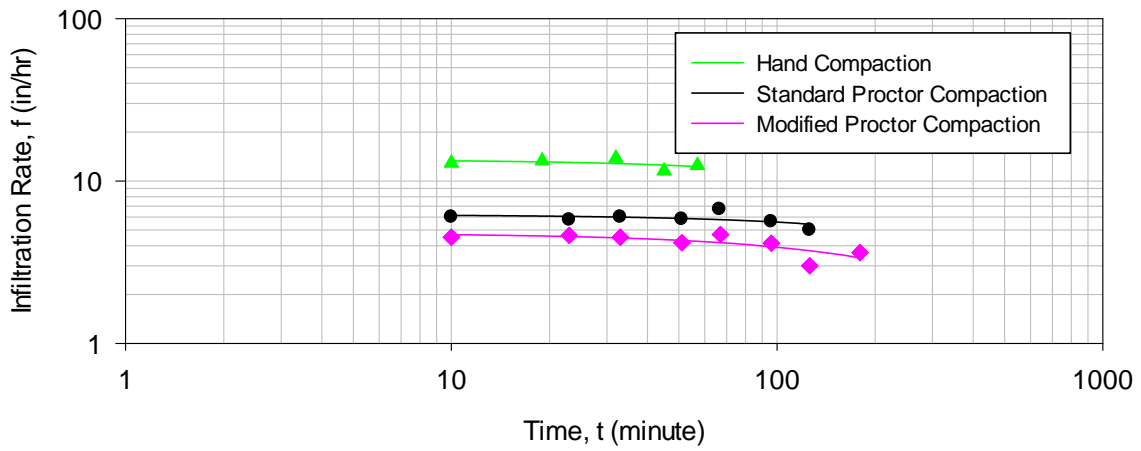
50% Peat, 25% Sand from Ground Floor (GF) Sand Supplier Northport, AL, and 25% of 6/10 Sand from ATL, GA (Mixture $D_{50} = 1500$ um and $C_u = 20$)				
Compaction	Trial	f_o (in/hr)	f_c (in/hr)	k (1/min)
hand 1.08 g/cm ³	1	n/a	15.7	0.25
	2	26.1	12.5	0.002
	3	22.6	10.5	0.004
	mean	71.7	12.9	0.09
	COV	1.1	0.2	1.67
Compaction	Trial	f_o (in/hr)	f_c (in/hr)	k (1/min)
standard proctor 1.11 g/cm ³	1	78.9	8.4	0.2
	2	11.2	5.0	0.001
	3	10.9	4.8	0.001
	mean	33.7	6.1	0.07
	COV	1.2	0.3	1.71
Compaction	Trial	f_o (in/hr)	f_c (in/hr)	k (1/min)
modified proctor 1.06 g/cm ³	1	n/a	6.0	0.30
	2	4.8	1.0	0.003
	3	6.5	3.7	0.09
	mean	5.6	3.6	0.13
	COV	0.2	0.7	1.17

* n/a values were beyond the data range

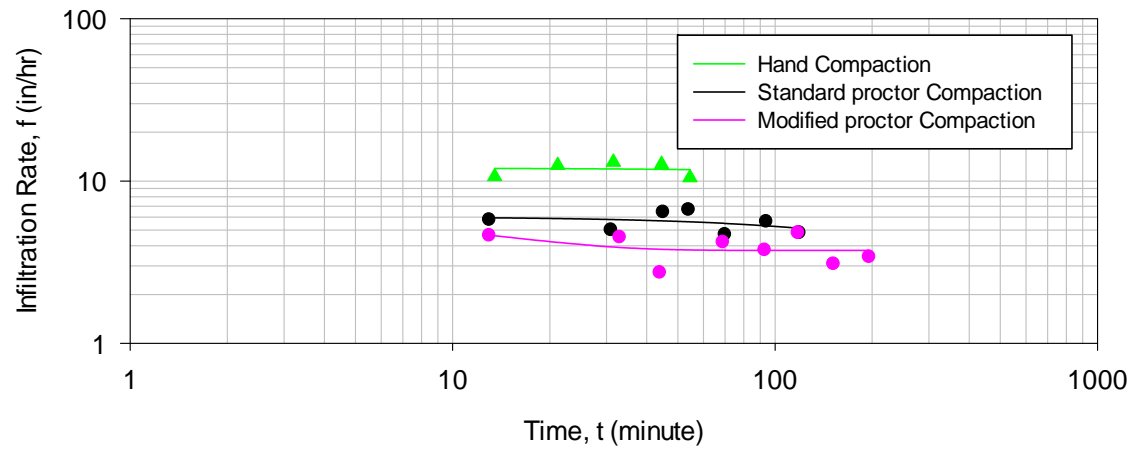
50% peat and 50% sand (D50 = 1500 um and Cu = 20), Trial 1



50% peat and 50% sand (D50 = 1500 um and Cu = 20), Trial 2



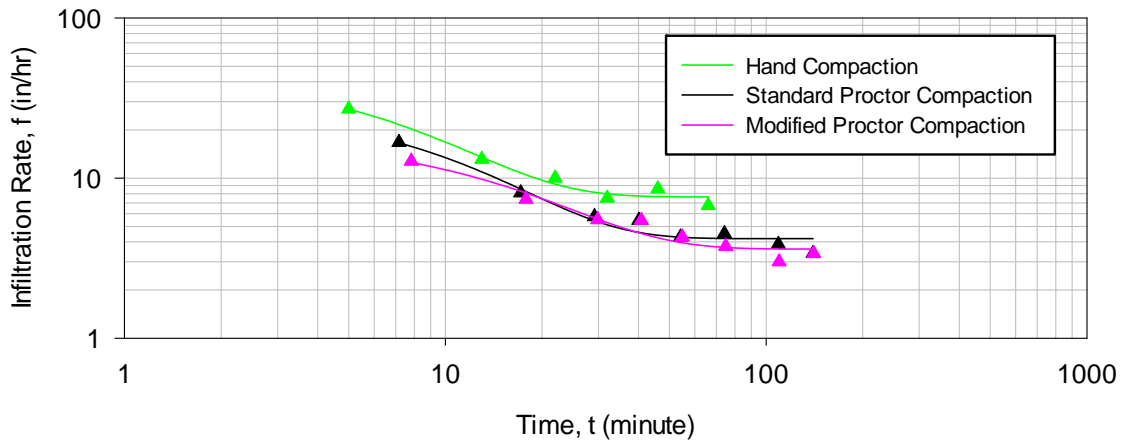
50% peat and 50% sand (D50 = 1500 um and Cu = 20), Trial 3



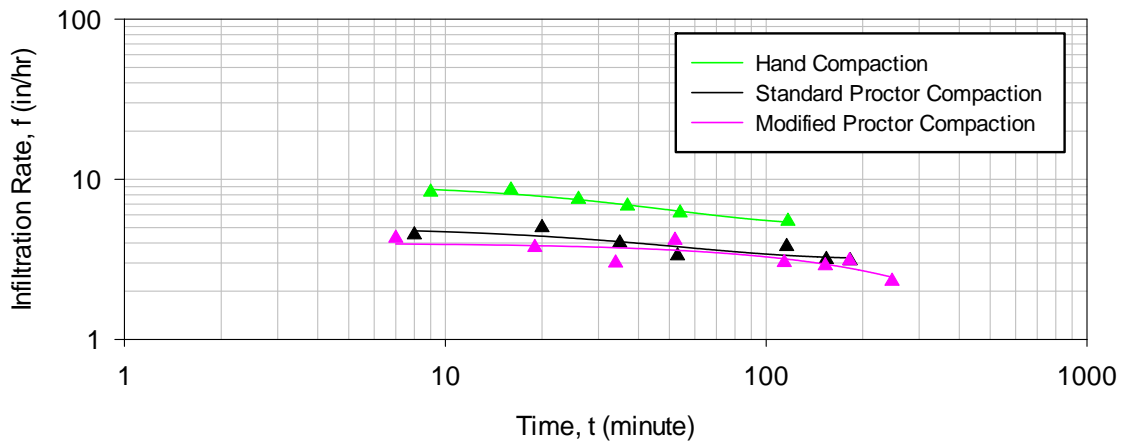
Appendix D.8: Lab Infiltration Measurements Using Sand and Peat Mixture ($D_{50} = 900$ μm and $C_u = 11$).

10% Peat, 45% Sand from Ground Floor Sand Supplier Northport, AL, and 45% of 10/30 Sand from ATL, GA (Mixture $D_{50} = 900$ μm and $C_u = 11$)				
Compaction	Trial	f_o (in/hr)	f_c (in/hr)	k (1/min)
hand 1.57 g/cm ³	1	48.2	7.60	0.15
	2	9.5	5.2	0.02
	3	9.0	5.0	0.03
	mean	22.2	5.9	0.07
	COV	1.0	0.2	1.09
Compaction	Trial	f_o (in/hr)	f_c (in/hr)	k (1/min)
standard proctor 1.66 g/cm ³	1	30.6	4.2	0.11
	2	5.1	3.2	0.02
	3	6.9	2.9	0.002
	mean	14.2	3.4	0.04
	COV	1.0	0.2	1.32
Compaction	Trial	f_o (in/hr)	f_c (in/hr)	k (1/min)
modified proctor 1.64 g/cm ³	1	19.0	3.6	0.070
	2	6.3	2.3	0.002
	3	6.2	2.6	0.002
	mean	10.5	2.8	0.02
	COV	0.7	0.2	1.59

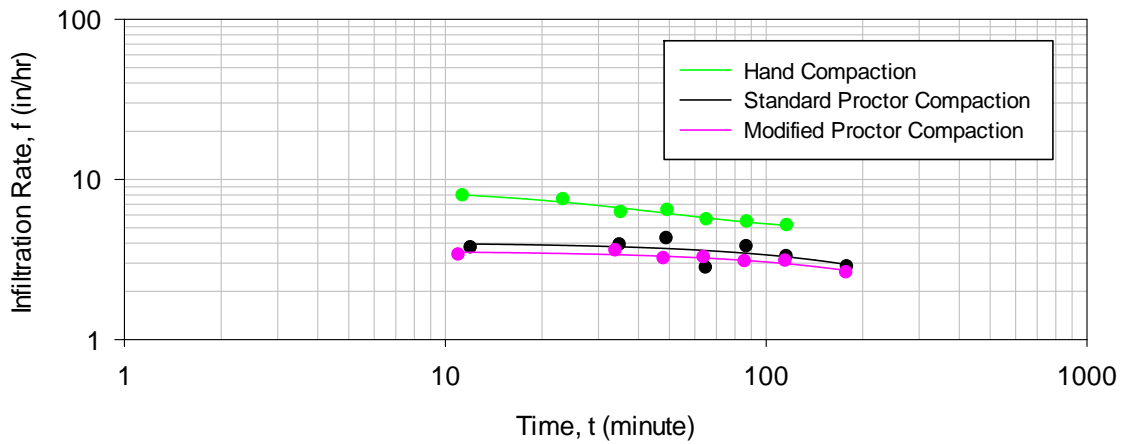
10% peat and 90% sand (D50 = 900 um and Cu = 11), Trial 1



10% peat and 90% sand (D50 = 900 um and Cu = 11), Trial 2



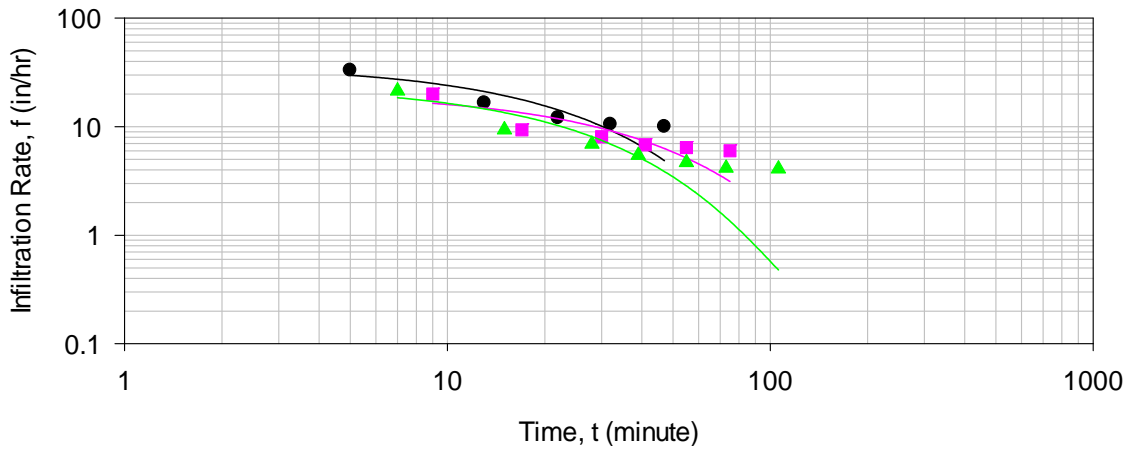
10% peat and 90% sand (D50 = 900 um and Cu = 11), Trial 3



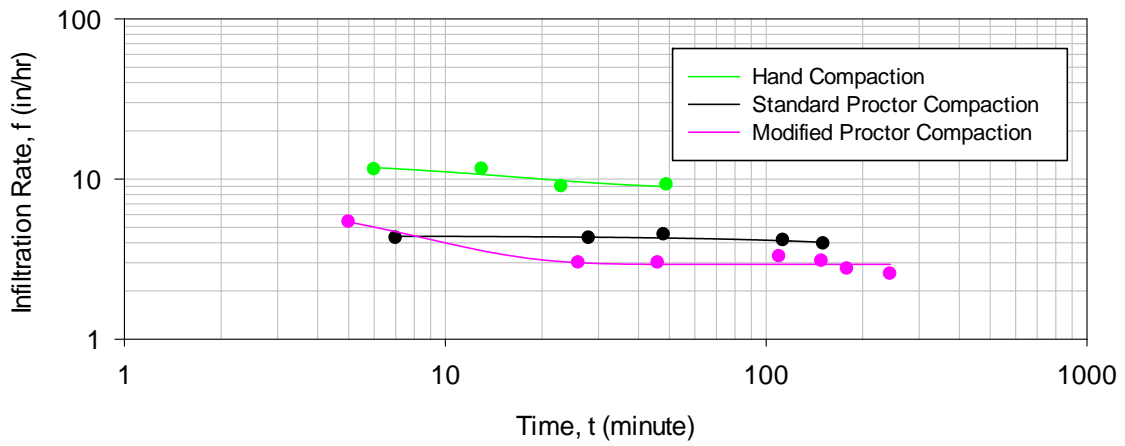
Appendix D.9: Lab Infiltration Measurements Using Sand and Peat Mixture ($D_{50} = 850$ um and $C_u = 11$).

25% Peat, 37.5% Sand from Ground Floor Sand Supplier Northport, AL, and 37.5% 10/30 Sand from ATL, GA (Mixture $D_{50} = 850$ um and $C_u = 11$)				
Compaction hand 1.43 g/cm ³	Trial	f_o (in/hr)	f_c (in/hr)	k (1/min)
	1	60.3	10.2	0.16
	2	13.2	8.8	0.07
	3	12.5	5.5	0.02
	mean	28.7	8.2	0.08
COV	1.0	0.3	0.85	
Compaction	Trial	f_o (in/hr)	f_c (in/hr)	k (1/min)
standard proctor 1.49 g/cm ³	1	79.3	6.7	0.2
	2	8.3	3.9	0.001
	3	5.3	3.5	0.020
	mean	31.0	4.7	0.07
	COV	1.4	0.4	1.50
Compaction	Trial	f_o (in/hr)	f_c (in/hr)	k (1/min)
modified proctor 1.48 g/cm ³	1	50.2	4.8	0.14
	2	8.7	3.0	0.17
	3	6.7	2.9	0.002
	mean	21.8	3.6	0.10
	COV	1.1	0.3	0.86

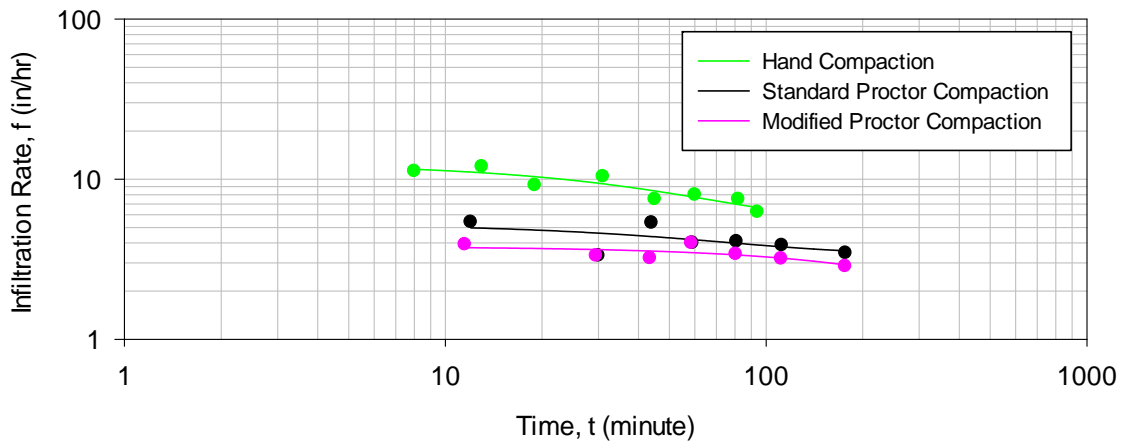
25% peat and 75% sand (D50 = 850 um and Cu = 11), Trial 1



25% peat and 75% sand (D50 = 850 um and Cu = 11), Trial 2



25% peat and 75% sand (D50 = 850 um and Cu = 11), Trial 3

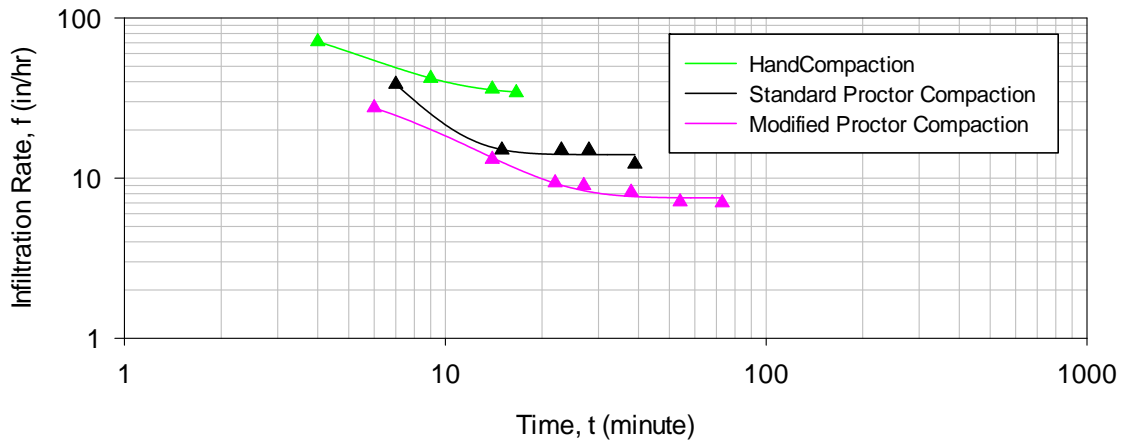


Appendix D.10: Lab Infiltration Measurements Using Sand and Peat Mixture ($D_{50} = 850 \text{ um}$ and $C_u = 11$).

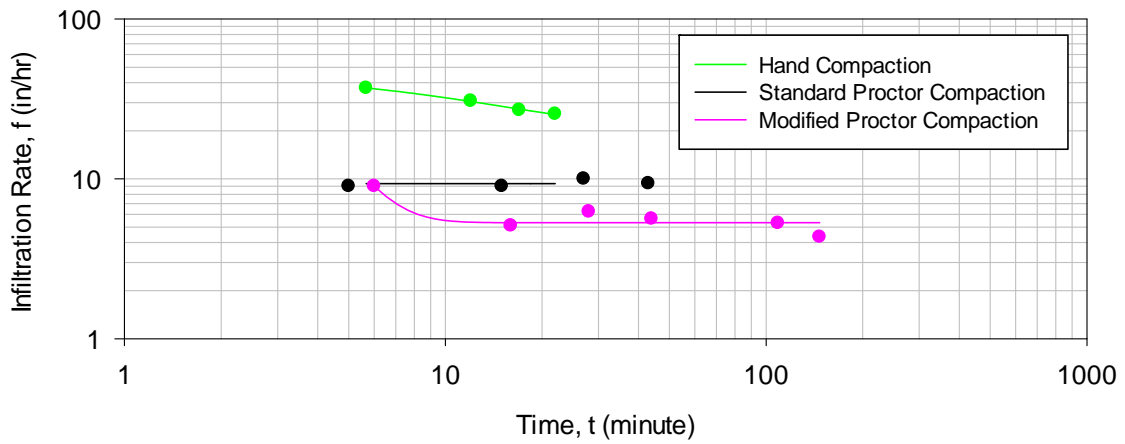
50% Peat, 25% Sand from Ground Floor (GF) Sand Supplier Northport, AL, and 25% 10/30 Sand from ATL, GA (Mixture $D_{50} = 850 \text{ mm}$ and $C_u = 11$)				
Compaction	Trial	f_o (in/hr)	f_c (in/hr)	k (1/min)
hand 0.95 g/cm^3	1	n/a	33.6	0.30
	2	47.0	21.5	0.1
	3	43.0	23.0	0.13
	mean	45	26.0	0.18
	COV	0.1	0.3	0.61
Compaction	Trial	f_o (in/hr)	f_c (in/hr)	k (1/min)
standard proctor 1.02 g/cm^3	1	n/a	14.0	0.4
	2	13.8	9.3	1.40E-17
	3	8.4	8.0	0.07
	mean	11.1	10.4	0.16
	COV	0.3	0.3	1.36
Compaction	Trial	f_o (in/hr)	f_c (in/hr)	k (1/min)
modified proctor 1.17 g/cm^3	1	57.0	7.5	0.15
	2	n/a	5.3	0.76
	3	10.1	4.5	0.002
	mean	33.6	5.8	0.30
	COV	1.0	0.3	1.32

* n/a values were beyond the data range

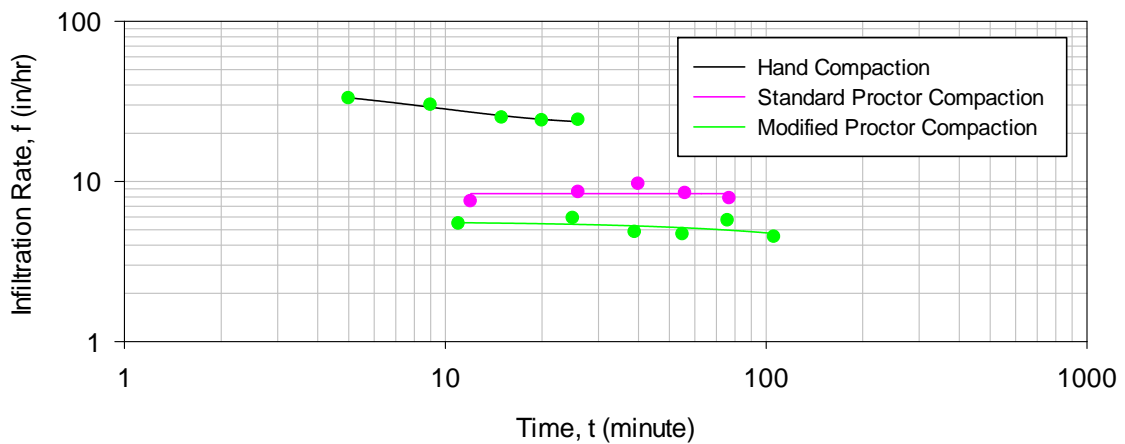
50% peat and 50% sand (D50 = 850 um and Cu = 11), Trial 1



50% peat and 50% sand (D50 = 850 um and Cu = 11), Trial 2



50% peat and 50% sand (D50 = 850 um and Cu = 11), Trial 3

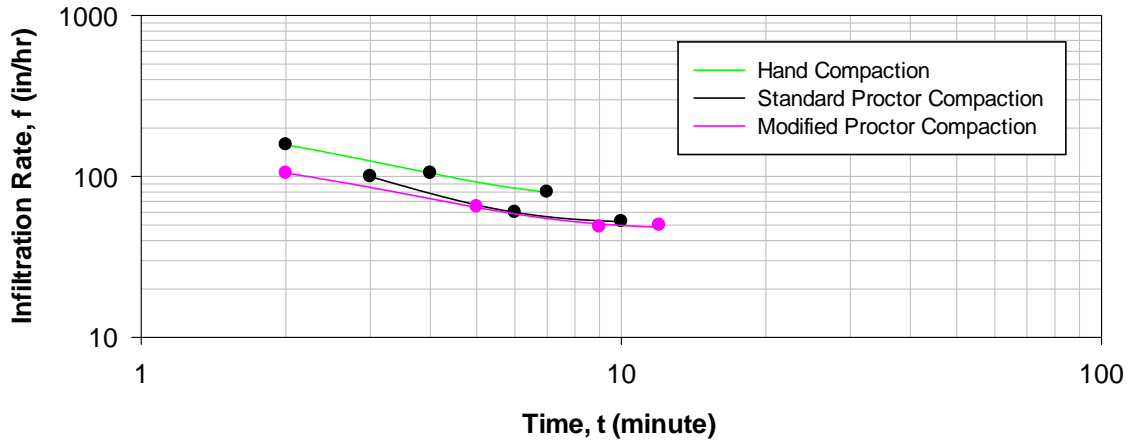


Appendix D.11: Lab Infiltration Measurements Using Sand and Peat Mixture ($D_{50} = 900$ um and $C_u = 4$).

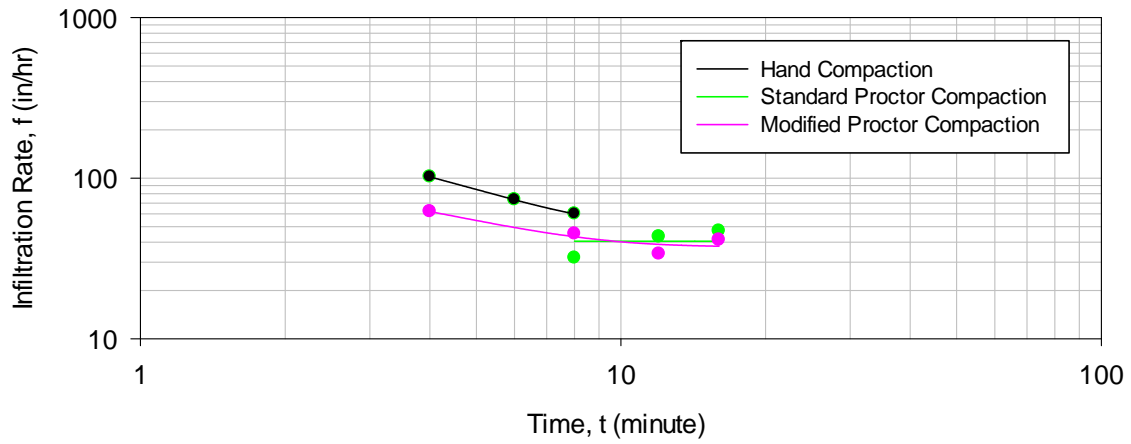
10% Peat, 45% Concrete Sand from ATL, GA, and 45% of 10/30 Sand from ATL, GA (Mixture $D_{50} = 900$ um and $C_u = 4$)				
Compaction	Trial	f_o (in/hr)	f_c (in/hr)	k (1/min)
hand 1.70 g/cm ³	1	n/a	72.2	0.5
	2	n/a	48.0	0.4
	3	n/a	67.2	0.6
	mean	-	62.5	0.5
	COV	-	0.2	0.2
Compaction	Trial	f_o (in/hr)	f_c (in/hr)	k (1/min)
standard proctor 1.80 g/cm ³	1	n/a	51.7	0.6
	2	72.5	40.6	0.1
	3	n/a	44.1	1.9
	mean	72.5	45.5	0.9
	COV	-	0.1	1.1
Compaction	Trial	f_o (in/hr)	f_c (in/hr)	k (1/min)
modified proctor 1.82 g/cm ³	1	n/a	47.5	0.4
	2	n/a	37.5	0.4
	3	77.6	0.4	0.1
	mean	77.6	28.5	0.3
	COV	-	0.9	0.7

* n/a values were beyond the data range

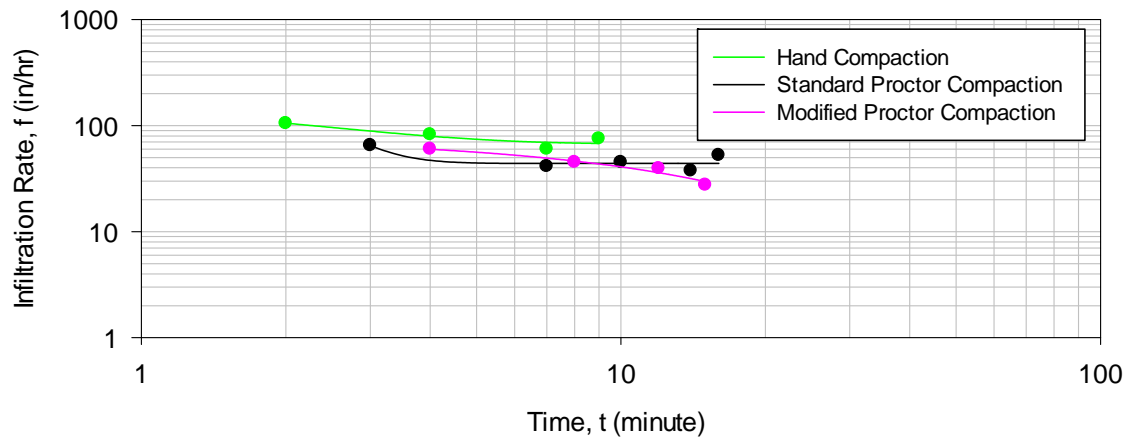
10% peat and 90% sand (D50 = 900 um and Cu = 4), Trial 1



10% peat and 90% sand (D50 = 900um and Cu = 4), Trial 2



10% peat and 90% sand (D50 = 900 um and Cu = 4), Trial 3

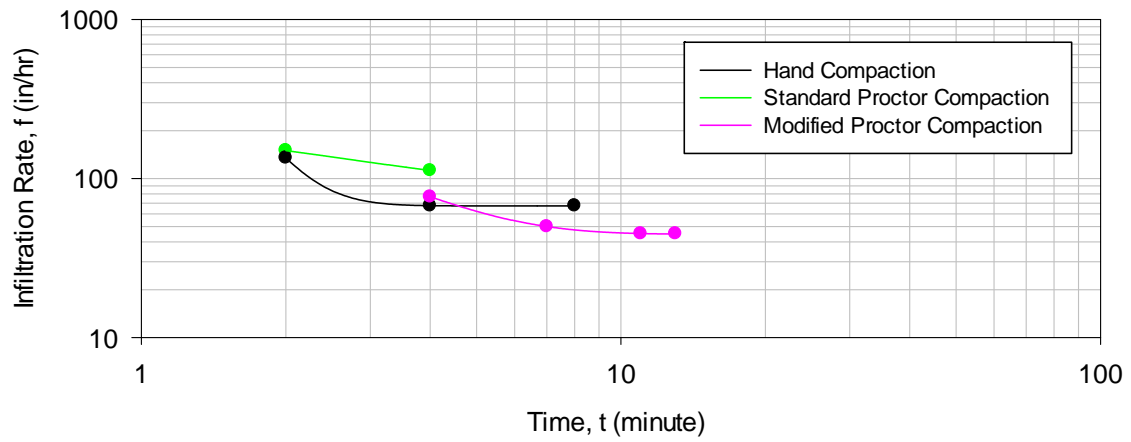


Appendix D.12: Lab Infiltration Measurements Using Sand and Peat Mixture ($D_{50} = 950 \text{ um}$ and $C_u = 4$).

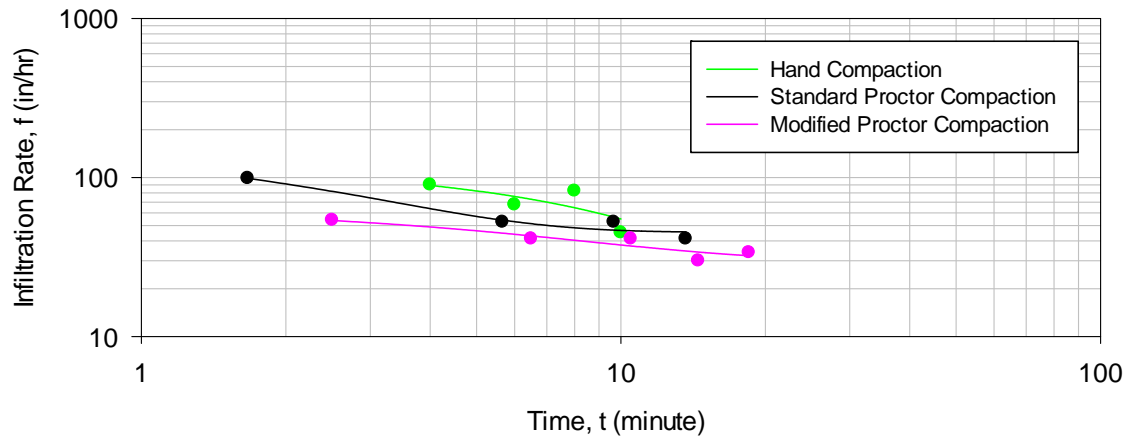
25% Peat, 37.5% Concrete Sand from ATL, GA, and 37.5% of 10/30 Sand from ATL, GA (Mixture $D_{50} = 950 \text{ um}$ and $C_u = 4$)				
Compaction hand 1.50 g/cm ³	Trial	f_o (in/hr)	f_c (in/hr)	k (1/min)
	1	n/a	91.0	0.5
	2	n/a	67.2	185.3
	3	95.1	44.1	0.1
	mean	95.1	67.4	62.0
Compaction	COV	-	0.3	1.7
standard proctor 1.60 g/cm ³	Trial	f_o (in/hr)	f_c (in/hr)	k (1/min)
	1	n/a	67.4	2.8
	2	n/a	45.4	0.5
	3	n/a	41.0	0.5
	mean	n/a	51.3	1.3
Compaction	COV	-	0.3	1.1
modified proctor 1.67 g/cm ³	Trial	f_o (in/hr)	f_c (in/hr)	k (1/min)
	1	n/a	44.7	0.6
	2	64.5	30.2	0.2
	3	n/a	32.8	0.8
	mean	64.5	35.9	0.5
	COV	-	0.2	0.6

* n/a values were beyond the data range

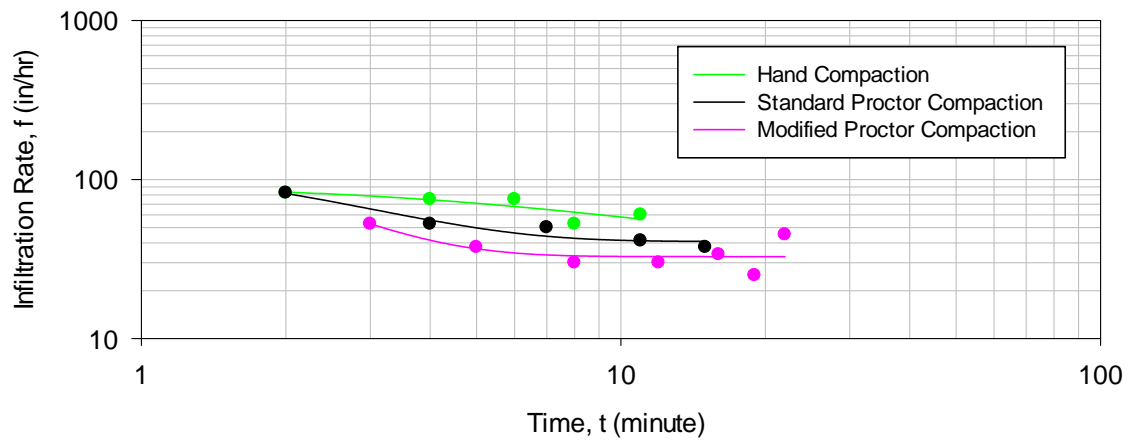
25% peat and 75% sand (D50 = 950 um and Cu = 4), Trial 1



25% peat and 75% sand (D50 = 950 um and Cu = 4), Trial 2



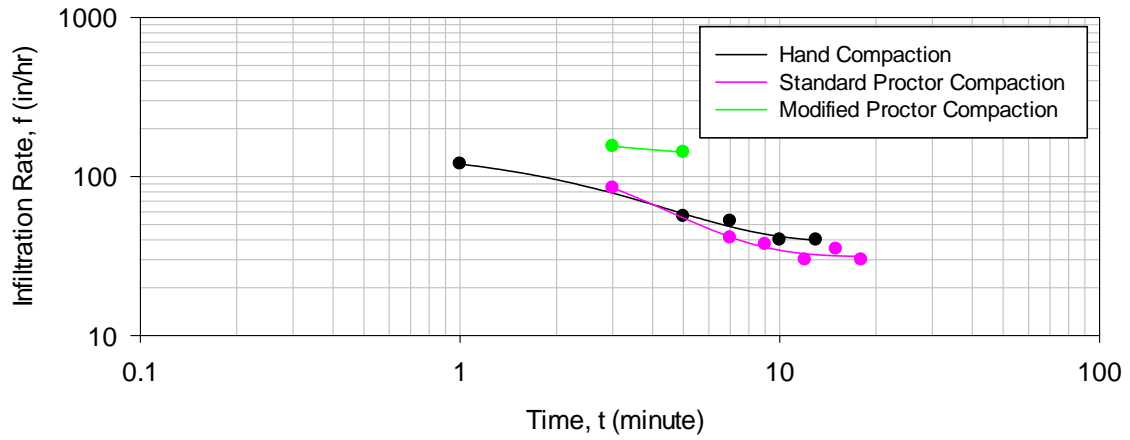
25% peat and 25% sand (D50 = 950 um and Cu = 4), Trial 3



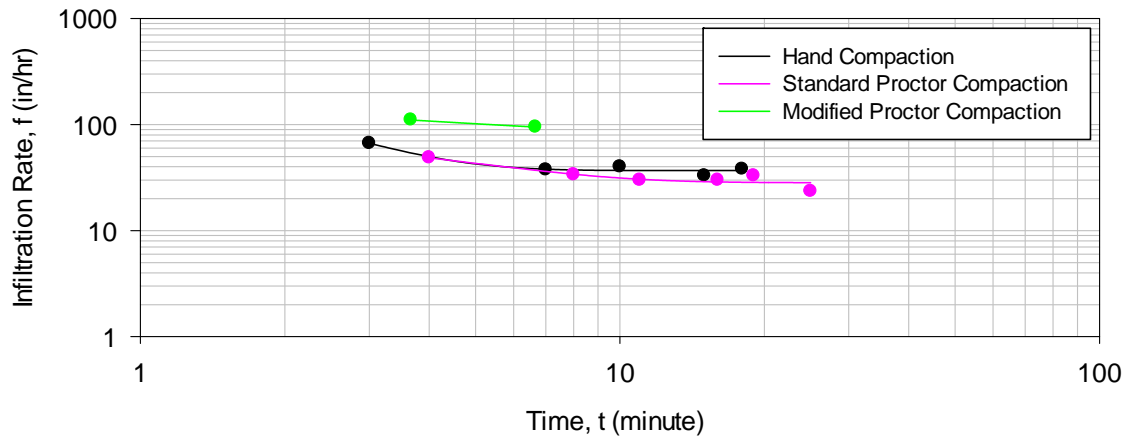
Appendix D.13: Lab Infiltration Measurements Using Sand and Peat Mixture ($D_{50} = 1000 \text{ um}$ and $C_u = 4$).

50% Peat, 25% Concrete Sand from ATL, GA, and 25% of 10/30 Sand from ATL, GA (Mixture $D_{50} = 1000 \text{ um}$ and $C_u = 4$)				
Compaction	Trial	f_o (in/hr)	f_c (in/hr)	k (1/min)
hand 1.13 g/cm ³	1	n/a	132	0.4
	2	n/a	84.3	0.3
	3	n/n	80.0	0.1
	mean	n/a	98.8	0.3
	COV	-	0.3	0.7
Compaction	Trial	f_o (in/hr)	f_c (in/hr)	k (1/min)
standard proctor 1.31 g/cm ³	1	n/a	38.7	0.4
	2	n/a	36.8	0.8
	3	n/a	30.5	0.5
	mean	-	35.3	0.6
	COV	-	0.1	0.4
Compaction	Trial	f_o (in/hr)	f_c (in/hr)	k (1/min)
modified proctor 1.32 g/cm ³	1	n/a	31.4	0.4
	2	100.9	28.4	0.3
	3	n/a	25.5	1.8
	mean	101	28.4	0.8
	COV	-	0.1	1.0

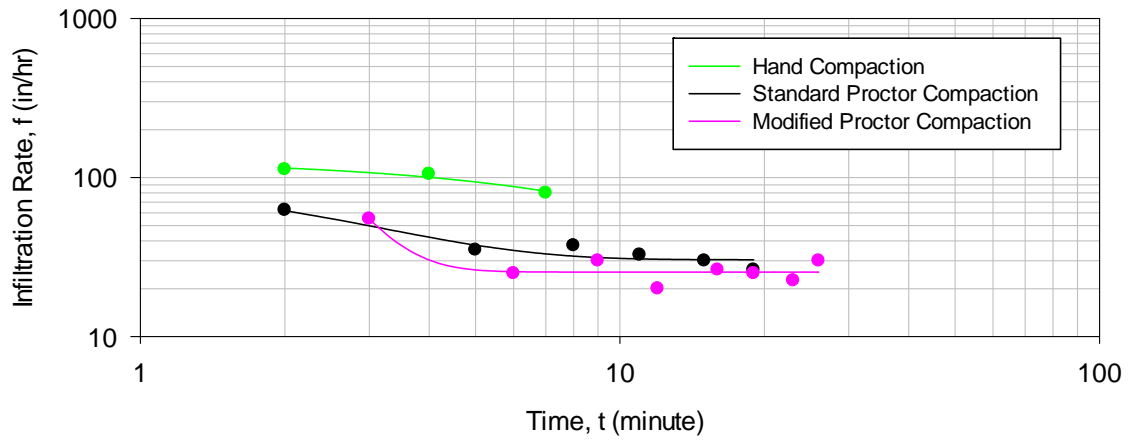
50% peat and 50% sand (D50 = 975 um and Cu = 4), Trial 1



50% peat and 50% sand (D50 = 975 um and Cu = 4), Trial 2



50% peat and 50% sand (D50 = 975 um and Cu = 4), Trial 3



Appendix D.14: Lab Infiltration Measurements Using Sand and Peat Mixture ($D_{50} = 1900$ um and $C_u = 2$).

10% Peat, 45% 6/10 Sand from ATL, GA, and 45% of 10/30 Sand from ATL, GA (Mixture $D_{50} = 1900$ um and $C_u = 2$)				
Compaction	Trial	f_o (in/hr)	f_c (in/hr)	k (1/min)
hand 1.52 g/cm ³	1	n/a	540	-
	2	n/a	254	1.1
	3	n/a	420	-
	mean	n/a	405	1.1
	COV	-	0.4	
Compaction	Trial	f_o (in/hr)	f_c (in/hr)	k (1/min)
standard proctor 1.54 g/cm ³	1	n/a	465	-
	2	n/a	435	-
	3	n/a	287	1.0
	mean	n/a	396	1.0
	COV	-	0.2	-
Compaction	Trial	f_o (in/hr)	f_c (in/hr)	k (1/min)
modified proctor 1.58 g/cm ³	1	n/a	495	-
	2	n/a	450	-
	3	n/a	237	1
	mean	n/a	394	1.00
	COV	-	0.3	-

* n/a values were beyond the data range (f_c values are very high because of the coarse sand media used during the tests).

Appendix D.15: Lab Infiltration Measurements Using Sand and Peat Mixture ($D_{50} = 1900 \text{ um}$ and $C_u = 2$).

25% Peat, 37.5% 6/10 Sand from ATL, GA, and 37.5% of 10/30 Sand from ATL, GA (Mixture $D_{50} = 1900 \text{ um}$ and $C_u = 2$)				
Compaction	Trial	f_o (in/hr)	f_c (in/hr)	k (1/min)
hand 1.38 g/cm ³	1	n/a	272	1.0
	2	n/a	418	0.5
	3	n/a	261	1.0
	mean	n/a	317	0.8
	COV	-	0.3	0.4
Compaction	Trial	f_o (in/hr)	f_c (in/hr)	k (1/min)
standard proctor 1.46 g/cm ³	1	-	405	-
	2	n/a	179	0.7
	3	n/a	201	2.0
	mean	-	262	1.4
	COV	-	0.5	0.7
Compaction	Trial	f_o (in/hr)	f_c (in/hr)	k (1/min)
modified proctor 1.47 g/cm ³	1	n/a	180	0.2
	2	n/a	91	0.2
	3	n/a	150	0.7
	mean	n/a	140	0.4
	COV	-	0.3	0.8

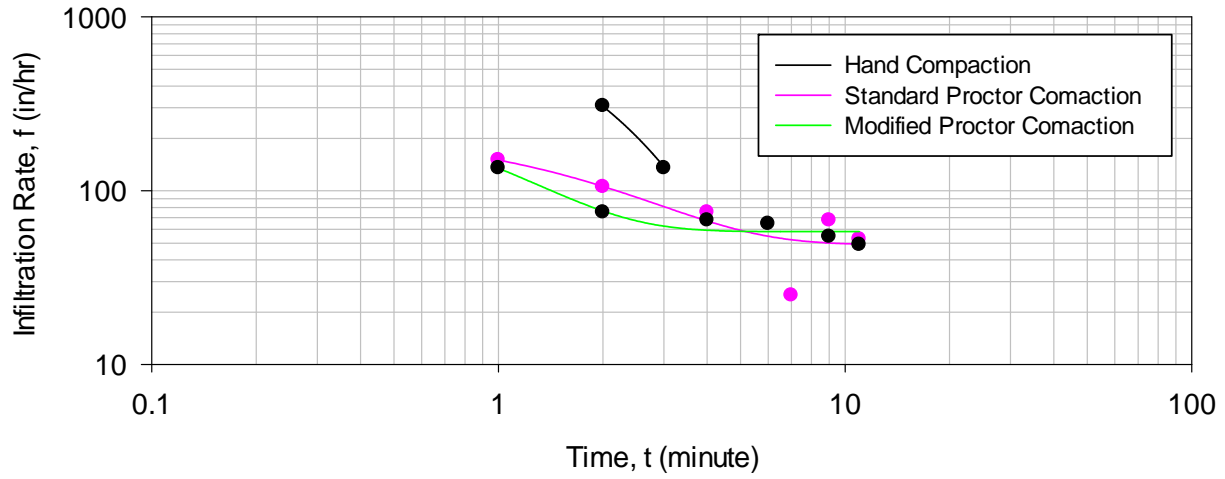
* n/a values were beyond the data range (f_c values are very high because of the coarse sand media used during the tests).

Appendix D.16: Lab Infiltration Measurements Using Sand and Peat Mixture ($D_{50} = 1600 \text{ um}$ and $C_u = 2.5$).

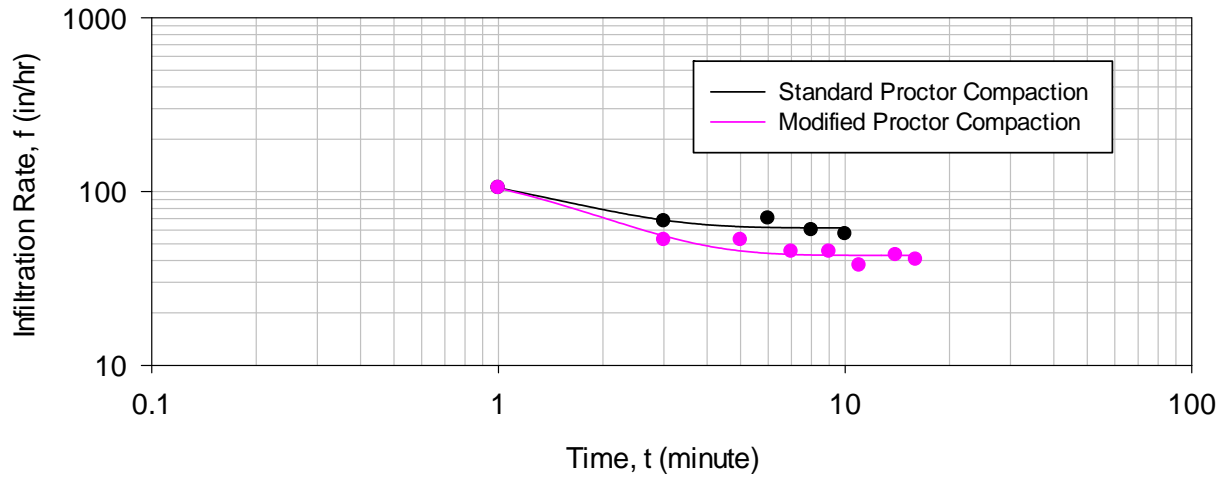
50% Peat, 25% 6/10 Sand from ATL, GA, and 25% of 10/30 Sand from ATL, GA (Mixture $D_{50} = 1600 \text{ um}$ and $C_u = 2.5$)				
Compaction	Trial	f_o (in/hr)	f_c (in/hr)	k (1/min)
hand 0.96 g/cm^3	1	n/a	135	0.8
	2	n/a	30.8	1.0
	3	n/a	111	0.6
	mean	n/a	92.3	0.8
	COV	-	06	0.2
Compaction	Trial	f_o (in/hr)	f_c (in/hr)	k (1/min)
standard proctor 1.18 g/cm^3	1	n/a	49	0.6
	2	n/a	62	0.9
	3	n/a	38	0.6
	mean	-	50	0.7
	COV	-	0.2	0.3
Compaction	Trial	f_o (in/hr)	f_c (in/hr)	k (1/min)
modified proctor 1.23 g/cm^3	1	n/a	58	1.4
	2	n/a	43	0.8
	3	n/a	29	0.5
	mean	n/a	43	0.9
	COV	-	0.3	0.5

* n/a values were beyond the data range

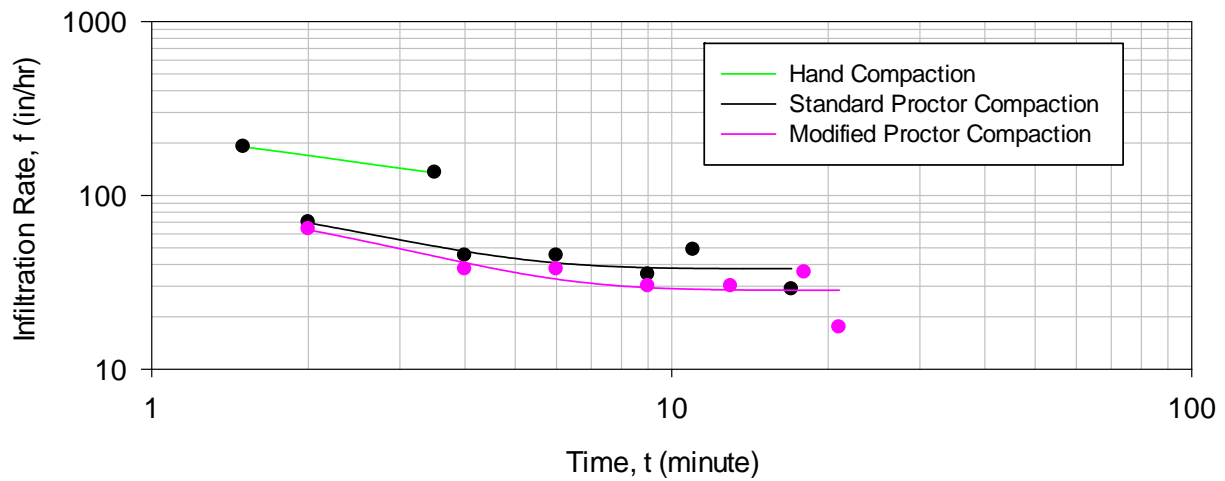
50% peat and 50% sand (D50 = 1.9 mm and Cu = 2), Trial 1



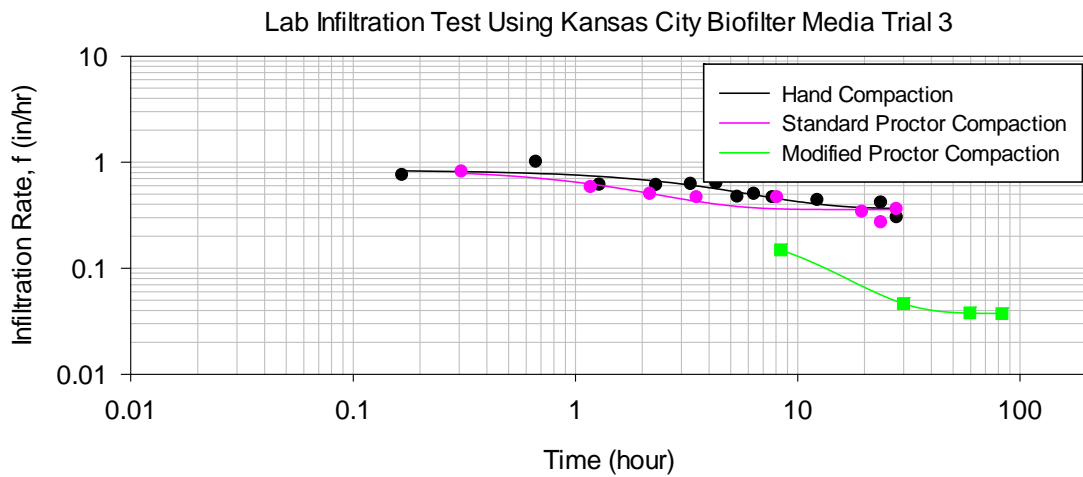
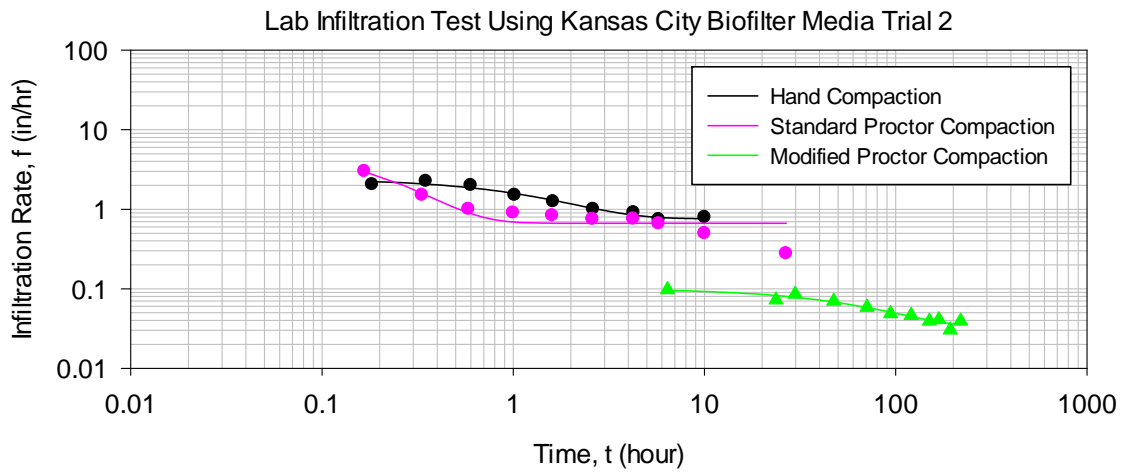
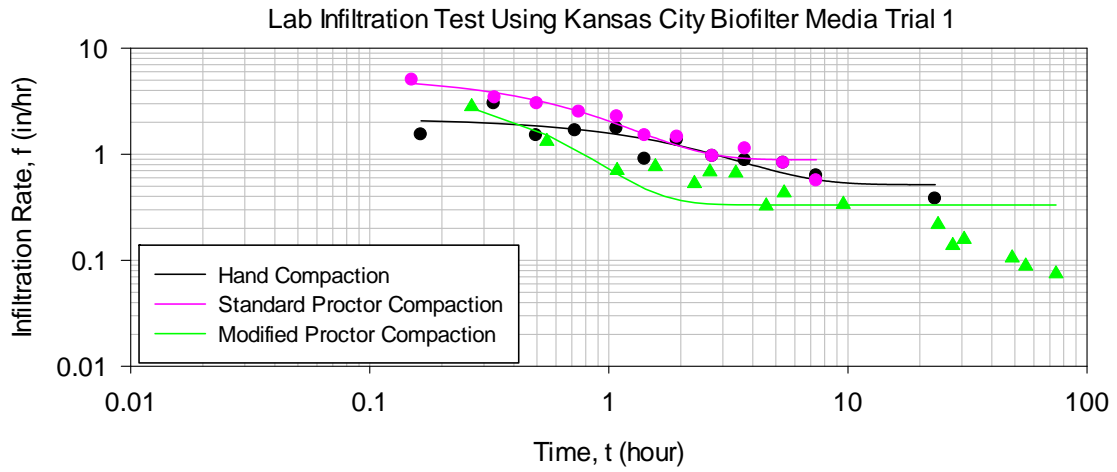
50% peat and 50% sand (D50 = 1.9 mm and Cu = 2), Trial 2



50% peat and 50% sand (D50 = 1.6 mm and Cu = 2.5), Trial 3

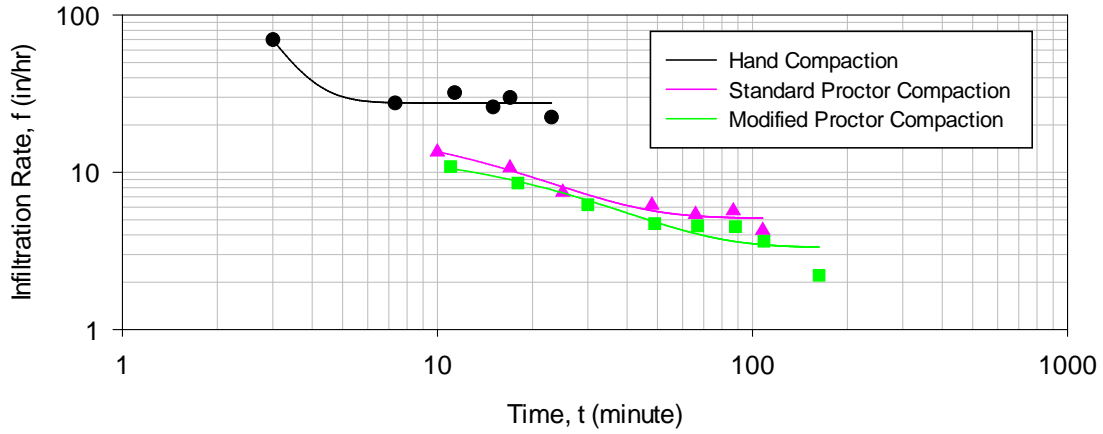


Appendix D.17: Lab Infiltration Measurements Using Kansas City Biofilte Media Fitted With Horton Equation.

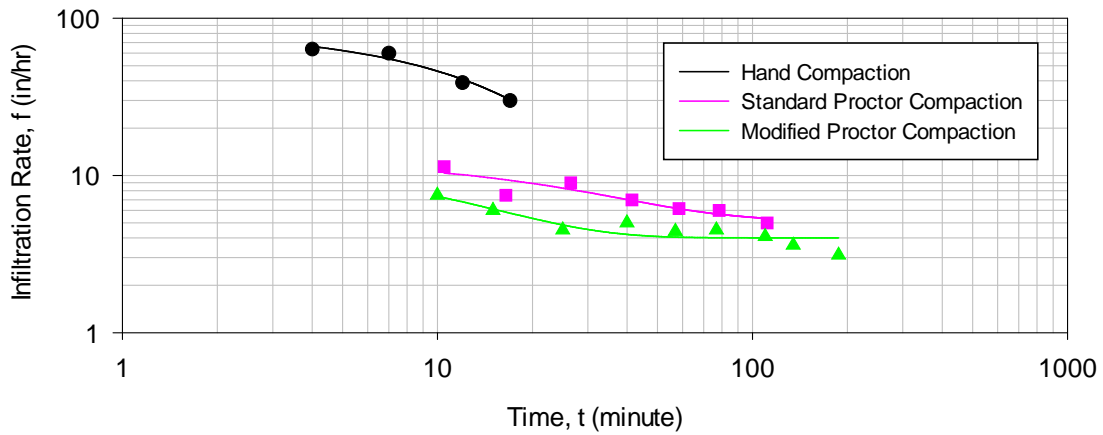


Appendix D.18: Lab Infiltration Measurements Using Wisconsin Biofilter Media -1 Fitted With Horton Equation.

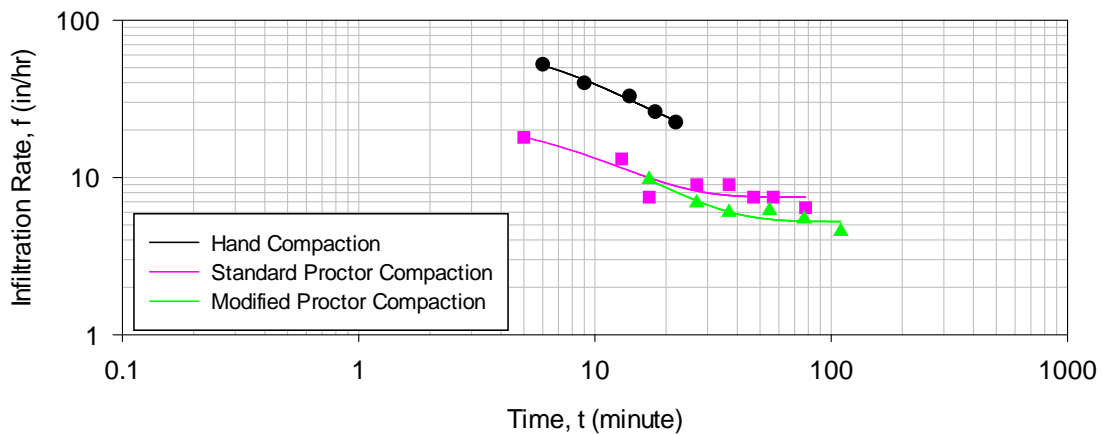
Wisconsin Biofilter Media (USGS bio mix), Trial 1



Wisconsin Biofilter Media (USGS bio mix), Trial 2

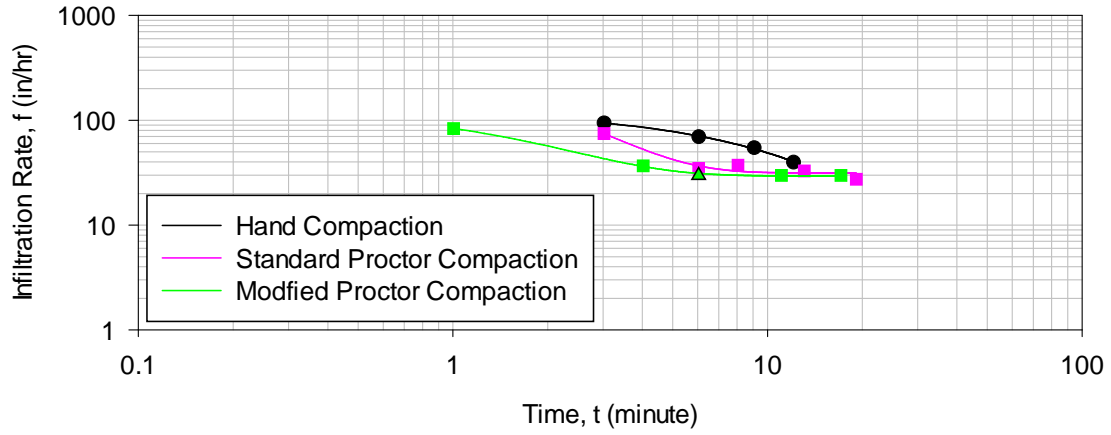


Wisconsin Biofilter Media (USGS bio mix), Trial 3

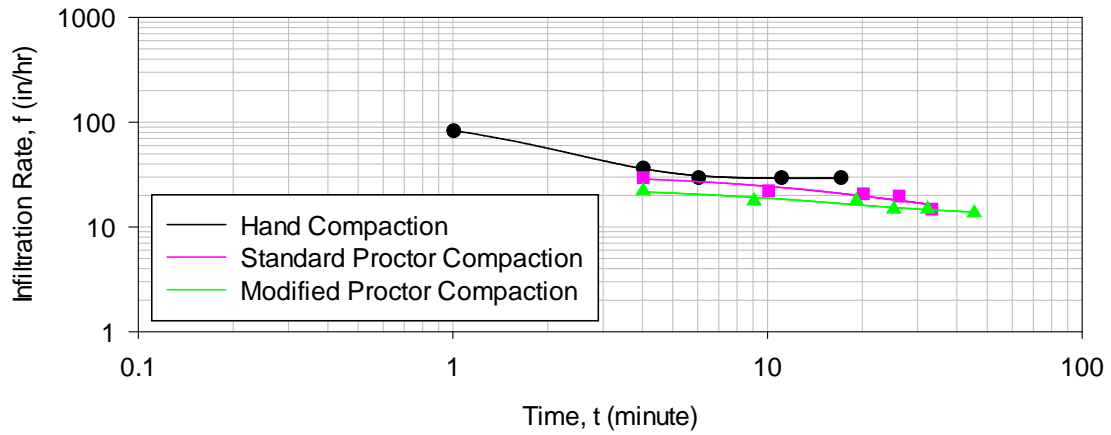


Appendix D.19: Lab Infiltration Measurements Using Wisconsin Biofilte Media -2 Fitted With Horton Equation.

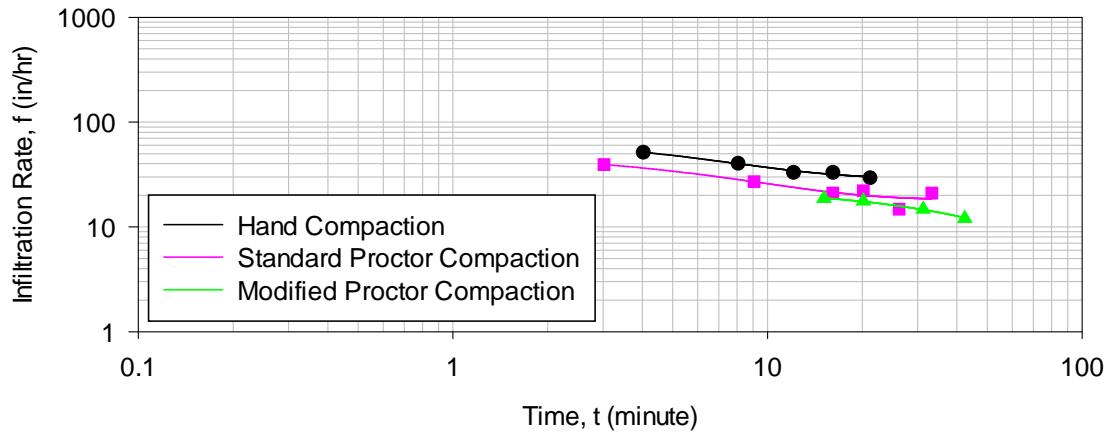
Wisconsin Biofilter Media 2 (Neenah mix), Trial 1



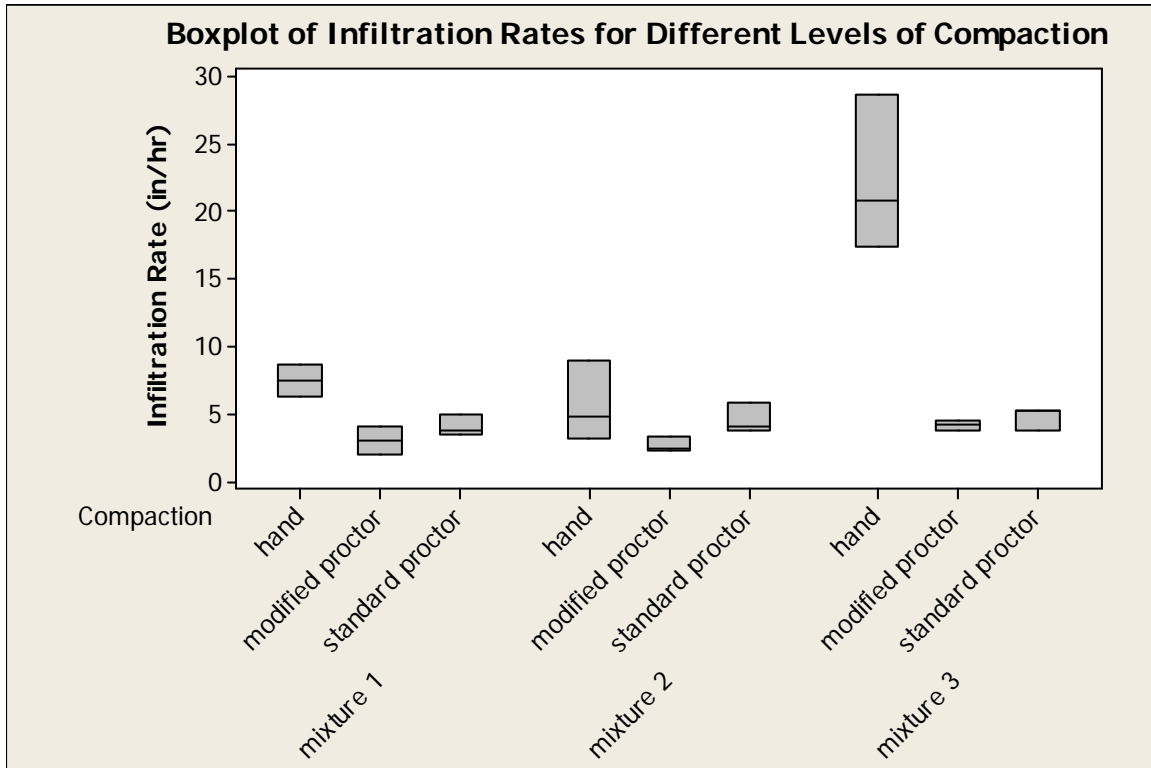
Wisconsin Biofilter Media 2 (Neenah mix), Trial 2



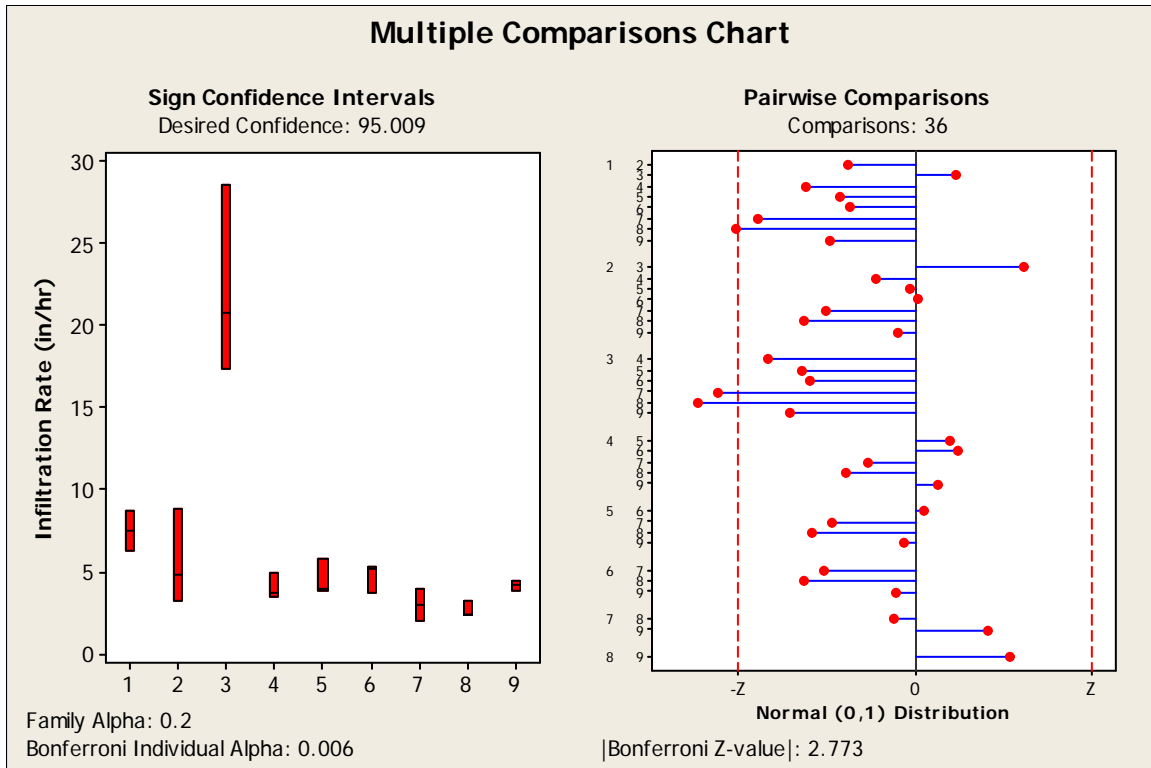
Wisconsin Biofilter Media 2 (Neenah mix), Trial 3



Appendix D.20: Infiltration Test Through Peat (10, 25, and 50%) and Sand Mixture (D50 = 300 – 350 um) and Different Levels of Compaction.



Component	Mixture No.	Columns	D ₅₀ (um)	C _u
peat and sand from Ground Floor (GF) Landscape Supply, Northport, AL	1	10% peat and 90% GF sand	340	1.3
	2	25% peat & 75% GF sand	300	3.5
	3	50% peat and 50% GF sand	300	3.3



Data series	Mixture
1	10% peat and 90% sand with hand compaction (mixture : $D_{50} = 340$ um and $C_u = 1.3$)
2	25% peat and 75% sand with hand compaction (mixture : $D_{50} = 300$ um and $C_u = 3.5$)
3	50% peat and 50% sand with hand compaction (mixture : $D_{50} = 300$ um and $C_u = 3.3$)
4	10% peat and 90% sand with standard proctor compaction (mixture : $D_{50} = 340$ um and $C_u = 1.3$)
5	25% peat and 75% sand with standard proctor compaction (mixture : $D_{50} = 300$ um and $C_u = 3.5$)
6	50% peat and 50% sand with standard proctor compaction (mixture : $D_{50} = 300$ um and $C_u = 3.3$)
7	10% peat and 90% sand with modified proctor compaction (mixture : $D_{50} = 340$ um and $C_u = 1.3$)
8	25% peat and 75% sand with modified proctor compaction (mixture : $D_{50} = 300$ um and $C_u = 3.5$)
9	50% peat and 50% sand with modified proctor compaction (mixture : $D_{50} = 300$ um and $C_u = 3.3$)

Kruskal-Wallis: Conclusions

The following groups showed significant differences (adjusted for ties):

Groups	Z vs. Critical value	P-value
3 vs. 8	3.44769 \geq 2.773	0.0006
3 vs. 7	3.11321 \geq 2.773	0.0019
1 vs. 8	2.83019 \geq 2.773	0.0047

50% peat and 50% sand with hand compaction (mixture: $D_{50} = 300$ um and $C_u = 3.3$) vs 25% peat and 75% sand with modified proctor compaction (mixture: $D_{50} = 300$ um and $C_u = 3.5$).

Kruskal-Wallis: Multiple Comparisons

Kruskal-Wallis Test on the data

Group	N	Median	Ave Rank	Z
1	3	7.500	22.0	1.85
2	3	4.800	15.0	0.23
3	3	20.800	26.0	2.78
4	3	3.700	10.8	-0.73
5	3	4.000	14.3	0.08
6	3	5.200	15.2	0.27
7	3	3.000	5.8	-1.89
8	3	2.400	3.7	-2.39
9	3	4.200	13.2	-0.19
Overall	27		14.0	

H = 18.79 DF = 8 P = 0.016
H = 18.81 DF = 8 P = 0.016 (adjusted for ties)

* NOTE * One or more small samples

Kruskal-Wallis: All Pairwise Comparisons

Comparisons: 36
Ties: 3
Family Alpha: 0.2
Bonferroni Individual Alpha: 0.006
Bonferroni Z-value (2-sided): 2.773

Standardized Absolute Mean Rank Differences
 $|\bar{R}(i) - \bar{R}(j)| / \text{Stdev}$

Rows: Group i = 1, ..., n
Columns: Group j = 1, ..., n

1. Table of Z-values

1	0.00000	*	*	*	*	*	*	*	*
2	1.08012	0.00000	*	*	*	*	*	*	*
3	0.61721	1.69734	0.00000	*	*	*	*	*	*
4	1.72305	0.64293	2.34027	0.00000	*	*	*	*	*
5	1.18299	0.10287	1.80021	0.54006	0.00000	*	*	*	*
6	1.05441	0.02572	1.67162	0.66865	0.12859	0.00000	*	*	*
7	2.49457	1.41445	3.11178	0.77152	1.31158	1.44016	0.00000	*	*
8	2.82889	1.74877	3.44611	1.10584	1.64590	1.77449	0.33432	0.00000	*
9	1.36301	0.28289	1.98023	0.36004	0.18002	0.30861	1.13156	1.46588	0

Adjusted for Ties in the Data

1. Table of Z-values

1	0.00000	*	*	*	*	*	*	*	*
2	1.08062	0.00000	*	*	*	*	*	*	*

3	0.61750	1.69811	0.00000	*	*	*	*	*	*	*
4	1.72384	0.64323	2.34134	0.00000	*	*	*	*	*	*
5	1.18353	0.10292	1.80103	0.54031	0.00000	*	*	*	*	*
6	1.05489	0.02573	1.67239	0.66895	0.12865	0.00000	*	*	*	*
7	2.49571	1.41510	3.11321	0.77187	1.31218	1.44082	0.00000	*	*	*
8	2.83019	1.74957	3.44769	1.10635	1.64666	1.77530	0.33448	0.00000	*	*
9	1.36364	0.28302	1.98113	0.36021	0.18010	0.30875	1.13208	1.46655	0	*

2. Table of P-values

1	1.00000	*	*	*	*	*	*	*	*	*
2	0.27987	1.00000	*	*	*	*	*	*	*	*
3	0.53691	0.08949	1.00000	*	*	*	*	*	*	*
4	0.08474	0.52008	0.01921	1.00000	*	*	*	*	*	*
5	0.23660	0.91803	0.07170	0.58898	1.00000	*	*	*	*	*
6	0.29148	0.97947	0.09445	0.50352	0.89764	1.00000	*	*	*	*
7	0.01257	0.15704	0.00185	0.44019	0.18946	0.14963	1.00000	*	*	*
8	0.00465	0.08019	0.00057	0.26858	0.09963	0.07585	0.73802	1.00000	*	*
9	0.17268	0.77716	0.04758	0.71869	0.85707	0.75751	0.25760	0.14250	1	*

Sign Confidence Intervals controlled at a family error rate of 0.2

Desired Confidence: 95.009

Sign confidence interval for median

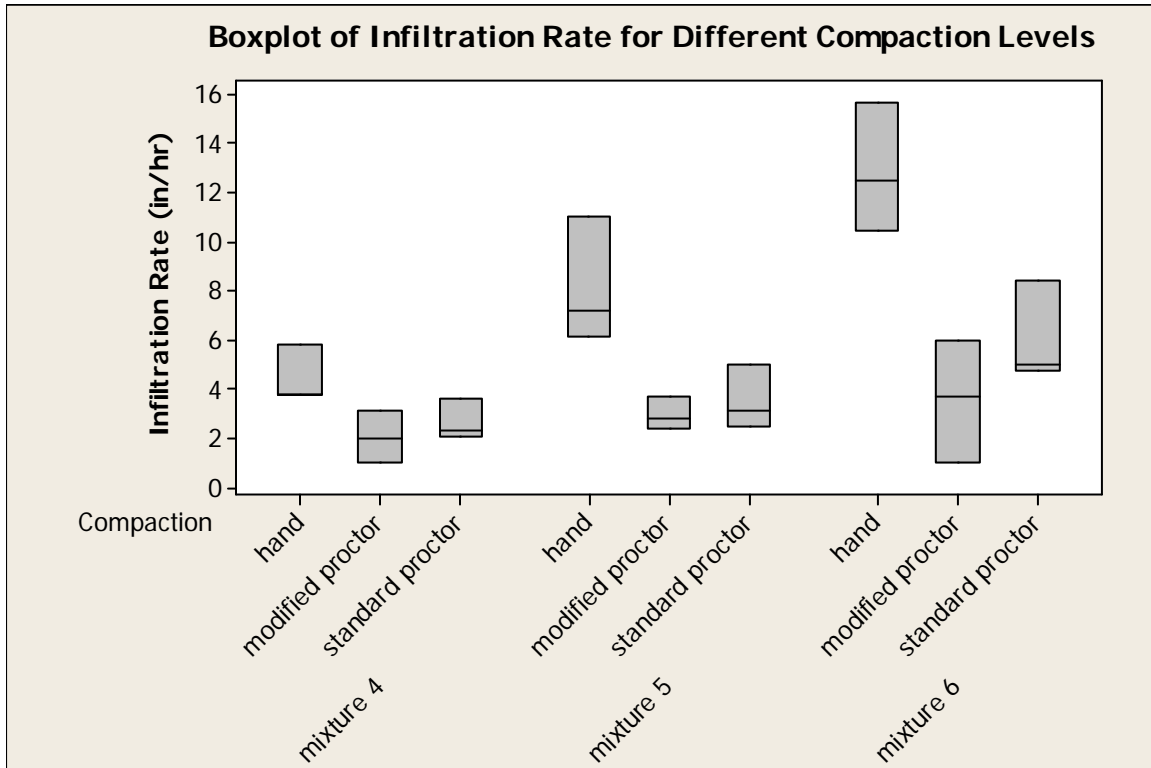
	N	Median	Achieved Confidence	Confidence Interval		Position
				Lower	Upper	
1	3	7.500	0.7500	6.300	8.700	1
2	3	4.800	0.7500	3.200	8.900	1
3	3	20.80	0.7500	17.40	28.60	1
4	3	3.700	0.7500	3.500	5.000	1
5	3	4.000	0.7500	3.800	5.800	1
6	3	5.200	0.7500	3.700	5.300	1
7	3	3.000	0.7500	2.000	4.000	1
8	3	2.400	0.7500	2.347	3.300	1
9	3	4.200	0.7500	3.800	4.500	1

Kruskal-Wallis: Conclusions

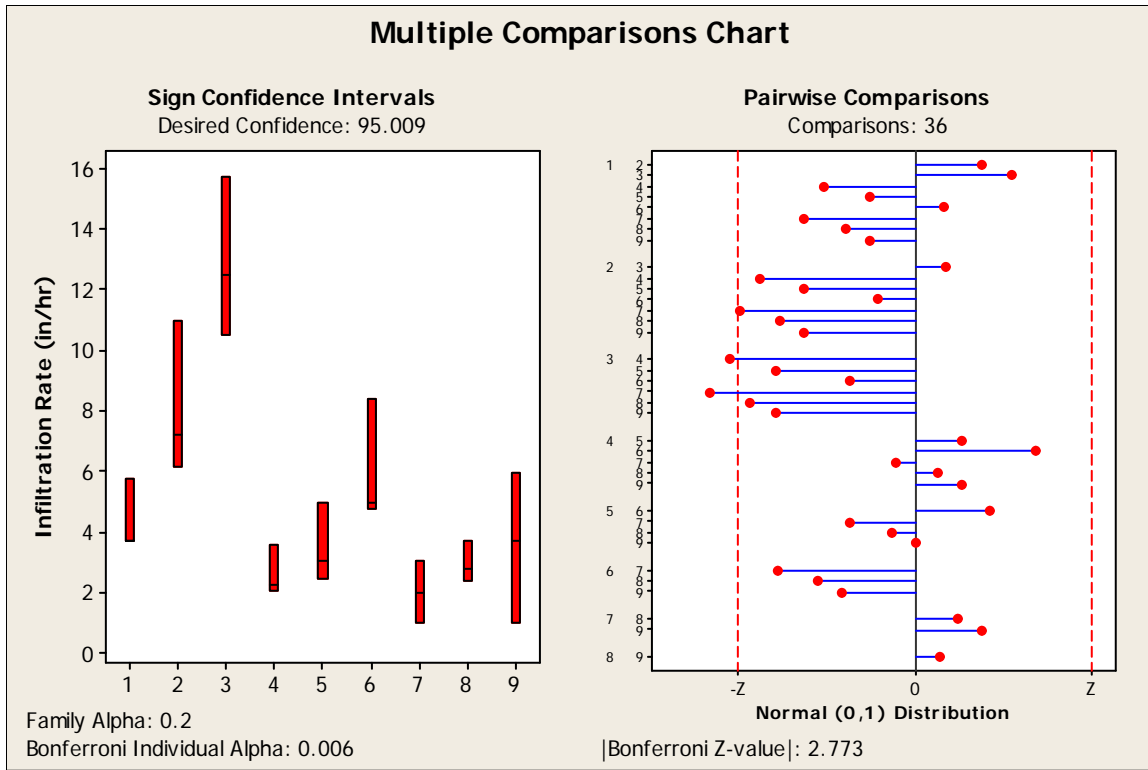
The following groups showed significant differences (adjusted for ties):

Groups	Z vs. Critical value	P-value
3 vs. 8	3.44769 >= 2.773	0.0006
3 vs. 7	3.11321 >= 2.773	0.0019
1 vs. 8	2.83019 >= 2.773	0.0047

Appendix D.21: Infiltration Test Through Peat (10, 25, and 50%) and Sand Mixture ($D_{50} = 1250 - 1500 \text{ um}$) and Different Levels of Compaction.



Component	Mixture No.	Columns	D_{50} (um)	C_u
peat, sand from Ground Floor (GF) Landscape Supply, Northport, AL, and 6/10 Sand from Atlanta, GA	4	10% peat, 45% GF sand, and 45% of 6/10 sand	1500	21.9
	5	25% peat, 37.5% GF sand, and 37.5% of 6/10 sand	1500	16.2
	6	50% peat, 25% GF sand, and 25% of 6/10 sand	1250	19.4



Data series	Mixture
1	10% peat and 90% sand with hand compaction (mixture : $D_{50} = 1500$ um and $C_u = 22$)
2	25% peat and 75% sand with hand compaction (mixture : $D_{50} = 1500$ um and $C_u = 16$)
3	50% peat and 50% sand with hand compaction (mixture : $D_{50} = 1250$ um and $C_u = 19$)
4	10% peat and 90% sand with standard proctor compaction (mixture : $D_{50} = 1500$ um and $C_u = 22$)
5	25% peat and 75% sand with standard proctor compaction (mixture : $D_{50} = 1500$ um and $C_u = 16$)
6	50% peat and 50% sand with standard proctor compaction (mixture : $D_{50} = 1250$ um and $C_u = 19$)
7	10% peat and 90% sand with modified proctor compaction (mixture : $D_{50} = 1500$ um and $C_u = 22$)
8	25% peat and 75% sand with modified proctor compaction (mixture : $D_{50} = 1500$ um and $C_u = 16$)
9	50% peat and 50% sand with modified proctor compaction (mixture : $D_{50} = 1250$ um and $C_u = 19$)

Kruskal-Wallis: Multiple Comparisons

Kruskal-Wallis Test on the data

Group	N	Median	Ave Rank	Z
1	3	3.750	16.0	0.46
2	3	7.200	22.7	2.01
3	3	12.500	25.7	2.70
4	3	2.300	6.7	-1.70
5	3	3.100	11.3	-0.62
6	3	5.000	18.8	1.12
7	3	2.000	4.7	-2.16
8	3	2.800	8.8	-1.20
9	3	3.700	11.3	-0.62
Overall	27		14.0	

H = 20.02 DF = 8 P = 0.010
H = 20.05 DF = 8 P = 0.010 (adjusted for ties)

* NOTE * One or more small samples

Kruskal-Wallis: All Pairwise Comparisons

Comparisons: 36
Ties: 5
Family Alpha: 0.2
Bonferroni Individual Alpha: 0.006
Bonferroni Z-value (2-sided): 2.773

Standardized Absolute Mean Rank Differences
 $|\bar{R}(i) - \bar{R}(j)| / \text{Stdev}$

Rows: Group i = 1, ..., n
Columns: Group j = 1, ..., n

1. Table of Z-values

1	0.00000	*	*	*	*	*	*	*	*
2	1.02869	0.00000	*	*	*	*	*	*	*
3	1.49160	0.46291	0.00000	*	*	*	*	*	*
4	1.44016	2.46885	2.93176	0.00000	*	*	*	*	*
5	0.72008	1.74877	2.21168	0.72008	0.00000	*	*	*	*
6	0.43719	0.59150	1.05441	1.87736	1.15728	0.00000	*	*	*
7	1.74877	2.77746	3.24037	0.30861	1.02869	2.18596	0.00000	*	*
8	1.10584	2.13453	2.59744	0.33432	0.38576	1.54303	0.64293	0.000000	*
9	0.72008	1.74877	2.21168	0.72008	0.00000	1.15728	1.02869	0.385758	0

Adjusted for Ties in the Data

1. Table of Z-values

1	0.00000	*	*	*	*	*	*	*	*
2	1.02947	0.00000	*	*	*	*	*	*	*
3	1.49274	0.46326	0.00000	*	*	*	*	*	*
4	1.44126	2.47074	2.93400	0.00000	*	*	*	*	*
5	0.72063	1.75011	2.21337	0.72063	0.00000	*	*	*	*

6	0.43753	0.59195	1.05521	1.87879	1.15816	0.00000	*	*	*
7	1.75011	2.77958	3.24285	0.30884	1.02947	2.18763	0.00000	*	*
8	1.10669	2.13616	2.59942	0.33458	0.38605	1.54421	0.64342	0.000000	*
9	0.72063	1.75011	2.21337	0.72063	0.00000	1.15816	1.02947	0.386053	0

2. Table of P-values

1	1.00000	*	*	*	*	*	*	*	*	*
2	0.30326	1.00000	*	*	*	*	*	*	*	*
3	0.13551	0.64318	1.00000	*	*	*	*	*	*	*
4	0.14951	0.01348	0.00335	1.00000	*	*	*	*	*	*
5	0.47114	0.08010	0.02687	0.47114	1.00000	*	*	*	*	*
6	0.66173	0.55389	0.29133	0.06027	0.24680	1.00000	*	*	*	*
7	0.08010	0.00544	0.00118	0.75744	0.30326	0.02870	1.00000	*	*	*
8	0.26843	0.03267	0.00934	0.73794	0.69946	0.12254	0.51995	1.00000	*	*
9	0.47114	0.08010	0.02687	0.47114	1.00000	0.24680	0.30326	0.69946	1	*

Sign Confidence Intervals controlled at a family error rate of 0.2

Desired Confidence: 95.009

Sign confidence interval for median

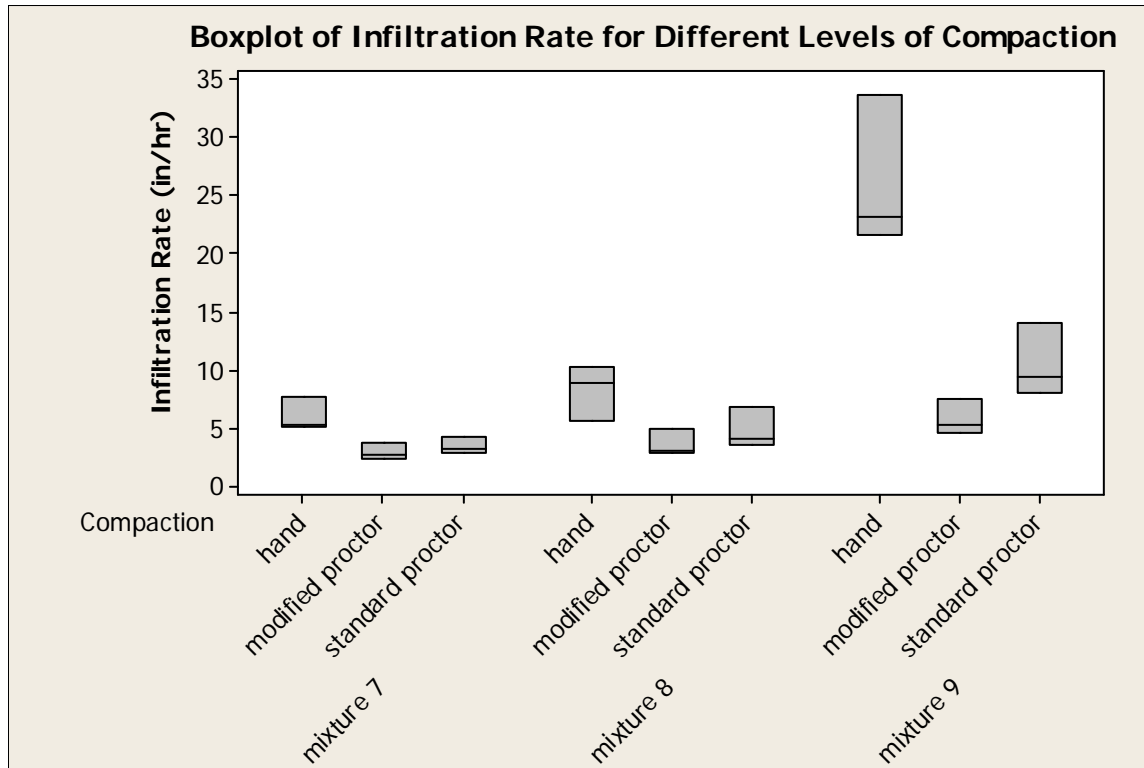
N	Median	Achieved Confidence	Confidence Interval		Position	
			Lower	Upper		
1	3	3.750	0.7500	3.750	5.800	1
2	3	7.20	0.7500	6.18	11.00	1
3	3	12.50	0.7500	10.50	15.70	1
4	3	2.300	0.7500	2.083	3.600	1
5	3	3.100	0.7500	2.500	5.000	1
6	3	5.000	0.7500	4.800	8.400	1
7	3	2.000	0.7500	1.000	3.100	1
8	3	2.800	0.7500	2.408	3.700	1
9	3	3.700	0.7500	1.000	6.000	1

Kruskal-Wallis: Conclusions

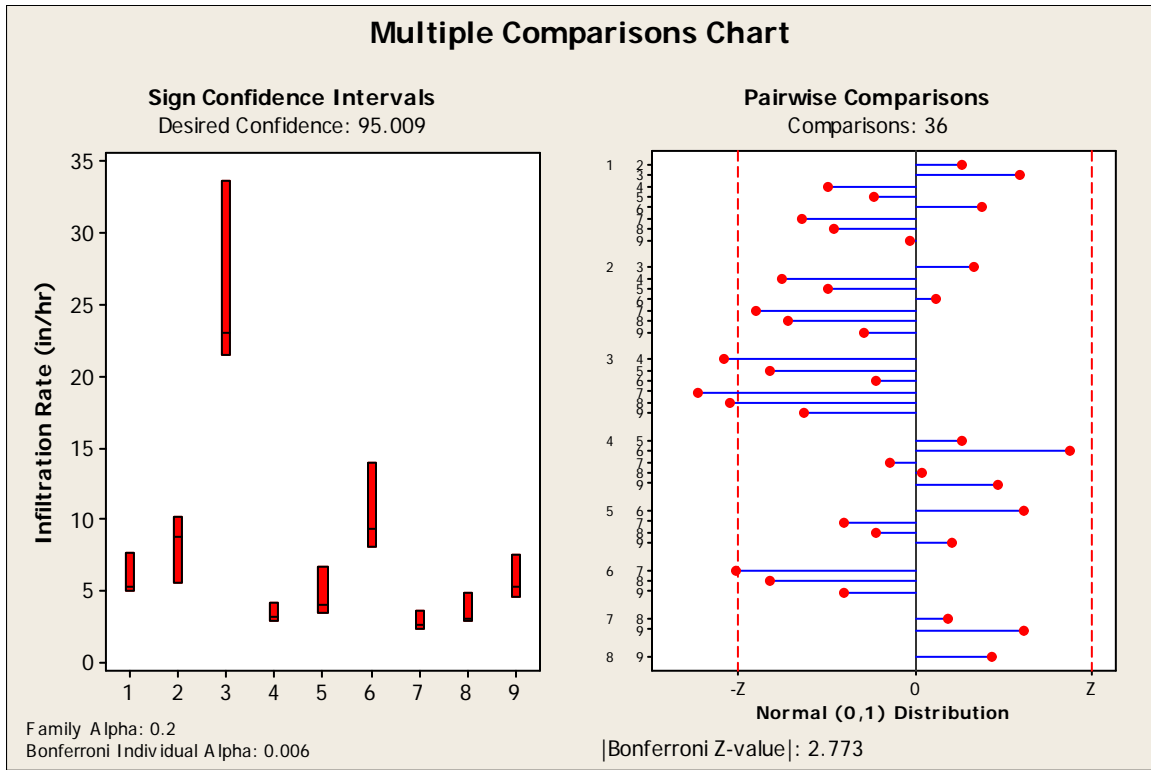
The following groups showed significant differences (adjusted for ties):

Groups	Z vs. Critical value	P-value
3 vs. 7	3.24285 >= 2.773	0.0012
3 vs. 4	2.93400 >= 2.773	0.0033
2 vs. 7	2.77958 >= 2.773	0.0054

Appendix D.22: Infiltration Test Through Peat (10, 25, and 50%) and Sand Mixture ($D_{50} = 850 - 900 \text{ um}$) and Different Levels of Compaction.



Component	Mixture No.	Columns	D_{50} (um)	C_u
peat, sand from Ground Floor (GF) Landscape Supply, Northport, AL, and 10/30 sand from Atlanta, GA	7	10% peat, 45% GF sand, and 45% of 10/30 sand	900	11.4
	8	25% peat, 37.5% GF sand, and 37.5% of 10/30 sand	850	11.4
	9	50% peat, 25% GF sand, and 25% of 10/30 sand	850	11.4



Data series	Mixture
1	10% peat and 90% sand with hand compaction (mixture : $D_{50} = 900$ um and $C_u = 11$)
2	25% peat and 75% sand with hand compaction (mixture : $D_{50} = 850$ um and $C_u = 11$)
3	50% peat and 50% sand with hand compaction (mixture : $D_{50} = 850$ um and $C_u = 11$)
4	10% peat and 90% sand with standard proctor compaction (mixture : $D_{50} = 900$ um and $C_u = 11$)
5	25% peat and 75% sand with standard proctor compaction (mixture : $D_{50} = 850$ um and $C_u = 11$)
6	50% peat and 50% sand with standard proctor compaction (mixture : $D_{50} = 850$ um and $C_u = 11$)
7	10% peat and 90% sand with modified proctor compaction (mixture : $D_{50} = 900$ um and $C_u = 11$)
8	25% peat and 75% sand with modified proctor compaction (mixture : $D_{50} = 850$ um and $C_u = 11$)
9	50% peat and 50% sand with modified proctor compaction (mixture : $D_{50} = 850$ um and $C_u = 11$)

Kruskal-Wallis: Multiple Comparisons

Kruskal-Wallis Test on the data

Group	N	Median	Ave Rank	Z
1	3	5.200	15.3	0.31
2	3	8.800	20.0	1.39
3	3	23.000	26.0	2.78
4	3	3.200	6.3	-1.77
5	3	3.947	11.0	-0.69
6	3	9.300	22.0	1.85
7	3	2.619	3.7	-2.39
8	3	3.000	7.0	-1.62
9	3	5.300	14.7	0.15
Overall	27		14.0	

H = 22.37 DF = 8 P = 0.004

* NOTE * One or more small samples

Kruskal-Wallis: All Pairwise Comparisons

```
-----
Comparisons:                36
Family Alpha:               0.2
Bonferroni Individual Alpha: 0.006
Bonferroni Z-value (2-sided): 2.773
-----
```

Standardized Absolute Mean Rank Differences
 $|\bar{R}(i) - \bar{R}(j)| / \text{Stdev}$

Rows: Group i = 1, ..., n
 Columns: Group j = 1, ..., n

1. Table of Z-values

1	0.00000	*	*	*	*	*	*	*	*
2	0.72008	0.00000	*	*	*	*	*	*	*
3	1.64590	0.92582	0.00000	*	*	*	*	*	*
4	1.38873	2.10881	3.03463	0.00000	*	*	*	*	*
5	0.66865	1.38873	2.31455	0.72008	0.00000	*	*	*	*
6	1.02869	0.30861	0.61721	2.41742	1.69734	0.00000	*	*	*
7	1.80021	2.52029	3.44611	0.41148	1.13156	2.82889	0.00000	*	*
8	1.28586	2.00594	2.93176	0.10287	0.61721	2.31455	0.51434	0.00000	*
9	0.10287	0.82295	1.74877	1.28586	0.56578	1.13156	1.69734	1.18299	0

2. Table of P-values

1	1.00000	*	*	*	*	*	*	*	*
2	0.47147	1.00000	*	*	*	*	*	*	*
3	0.09978	0.35454	1.00000	*	*	*	*	*	*
4	0.16491	0.03496	0.00241	1.00000	*	*	*	*	*
5	0.50372	0.16491	0.02064	0.47147	1.00000	*	*	*	*
6	0.30363	0.75762	0.53709	0.01563	0.08963	1.00000	*	*	*
7	0.07183	0.01173	0.00057	0.68072	0.25782	0.00467	1.00000	*	*
8	0.19849	0.04486	0.00337	0.91807	0.53709	0.02064	0.60701	1.00000	*
9	0.91807	0.41054	0.08033	0.19849	0.57154	0.25782	0.08963	0.23681	1

Sign Confidence Intervals controlled at a family error rate of 0.2

Desired Confidence: 95.009

Sign confidence interval for median

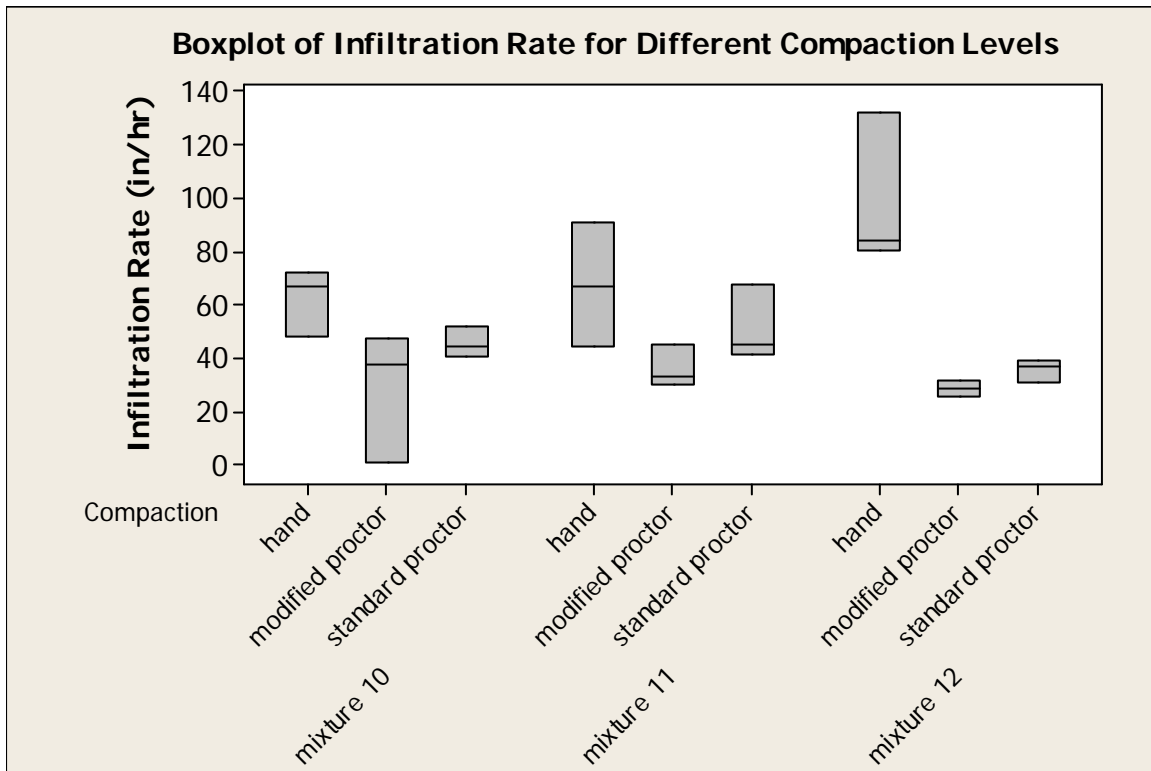
			Achieved	Confidence		
	N	Median	Confidence	Lower	Upper	Position
1	3	5.200	0.7500	5.000	7.600	1
2	3	8.80	0.7500	5.50	10.20	1
3	3	23.00	0.7500	21.50	33.60	1
4	3	3.200	0.7500	2.857	4.200	1
5	3	3.947	0.7500	3.500	6.700	1
6	3	9.30	0.7500	8.00	14.00	1
7	3	2.619	0.7500	2.308	3.600	1
8	3	3.000	0.7500	2.862	4.800	1
9	3	5.300	0.7500	4.500	7.500	1

Kruskal-Wallis: Conclusions

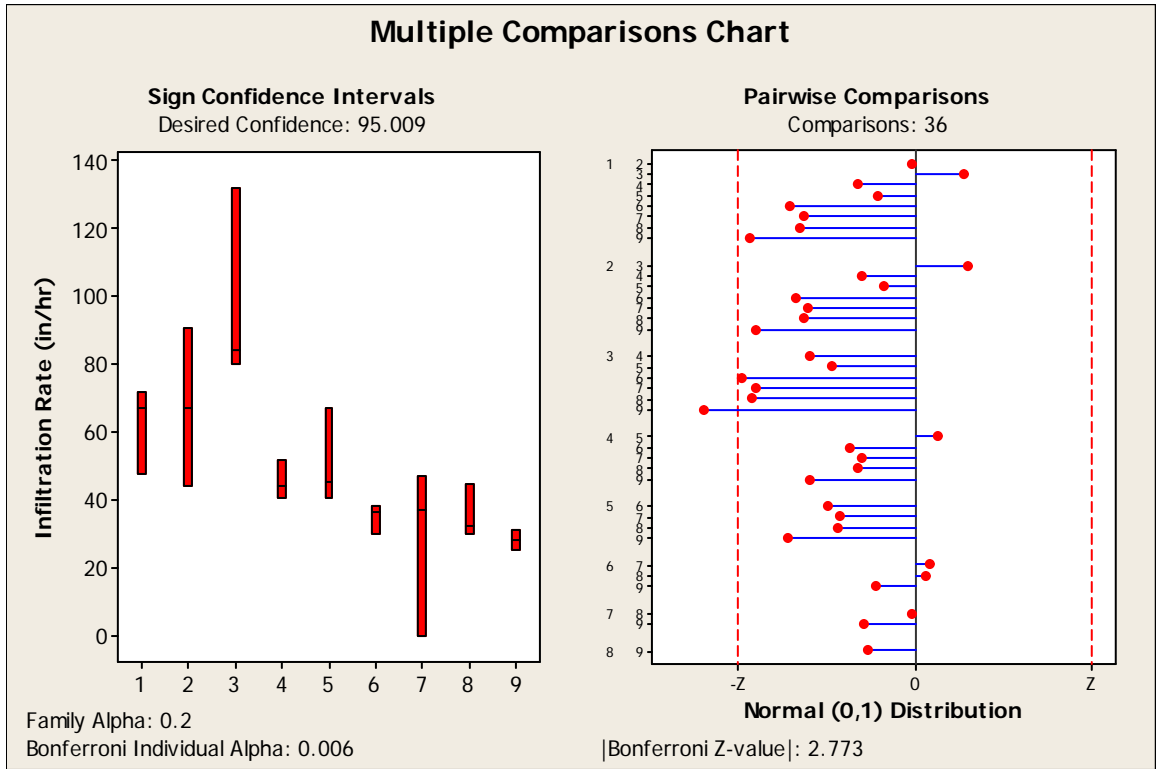
The following groups showed significant differences:

Groups	Z vs. Critical value	P-value
3 vs. 7	3.44611 >= 2.773	0.0006
3 vs. 4	3.03463 >= 2.773	0.0024
3 vs. 8	2.93176 >= 2.773	0.0034
6 vs. 7	2.82889 >= 2.773	0.0047

Appendix D.23: Infiltration Test Through Peat (10, 25, and 50%) and Sand Mixture (D50 = 900 – 975 um) and Different Levels of Compaction.



Component	Mixture No.	Columns	D ₅₀ (um)	C _u
peat, concrete sand from Atlanta, GA, and 10/30 sand from Atlanta, GA	10	10% peat, 45% concrete sand, and 45% of 10/30 sand	900	3.8
	11	25% peat, 37.5% concrete sand, and 37.5% of 10/30 sand	950	4
	12	50% peat, 25% concrete sand, and 25% of 10/30 sand	975	4.3



Data series	Mixture
1	10% peat and 90% sand with hand compaction (mixture : $D_{50} = 900$ um and $C_u = 3.8$)
2	25% peat and 75% sand with hand compaction (mixture : $D_{50} = 950$ um and $C_u = 4$)
3	50% peat and 50% sand with hand compaction (mixture : $D_{50} = 975$ um and $C_u = 4.3$)
4	10% peat and 90% sand with standard proctor compaction (mixture : $D_{50} = 900$ um and $C_u = 3.8$)
5	25% peat and 75% sand with standard proctor compaction (mixture : $D_{50} = 950$ um and $C_u = 4$)
6	50% peat and 50% sand with standard proctor compaction (mixture : $D_{50} = 975$ um and $C_u = 4.3$)
7	10% peat and 90% sand with modified proctor compaction (mixture : $D_{50} = 900$ um and $C_u = 3.8$)
8	25% peat and 75% sand with modified proctor compaction (mixture : $D_{50} = 950$ um and $C_u = 4$)
9	50% peat and 50% sand with modified proctor compaction (mixture : $D_{50} = 975$ um and $C_u = 4.3$)

Kruskal-Wallis Test on the data

Group	N	Median	Ave Rank	Z
1	3	67.20	20.5	1.50
2	3	67.20	20.0	1.39
3	3	84.30	25.3	2.62
4	3	44.10	14.5	0.12
5	3	45.40	16.7	0.62
6	3	36.80	7.7	-1.47
7	3	37.50	9.0	-1.16
8	3	32.80	8.7	-1.23
9	3	28.40	3.7	-2.39
Overall	27		14.0	

H = 19.73 DF = 8 P = 0.011
H = 19.74 DF = 8 P = 0.011 (adjusted for ties)
* NOTE * One or more small samples

Kruskal-Wallis: All Pairwise Comparisons

Comparisons: 36
Ties: 2
Family Alpha: 0.2
Bonferroni Individual Alpha: 0.006
Bonferroni Z-value (2-sided): 2.773

Standardized Absolute Mean Rank Differences
 $|\bar{R}(i) - \bar{R}(j)| / \text{Stdev}$

Rows: Group i = 1, ..., n
Columns: Group j = 1, ..., n

1. Table of Z-values

1	0.00000	*	*	*	*	*	*	*	*
2	0.07715	0.00000	*	*	*	*	*	*	*
3	0.74580	0.82295	0.00000	*	*	*	*	*	*
4	0.92582	0.84867	1.67162	0.00000	*	*	*	*	*
5	0.59150	0.51434	1.33730	0.33432	0.00000	*	*	*	*
6	1.98023	1.90307	2.72603	1.05441	1.38873	0.000000	*	*	*
7	1.77449	1.69734	2.52029	0.84867	1.18299	0.205738	0.000000	*	*
8	1.82592	1.74877	2.57172	0.90010	1.23443	0.154303	0.051434	0.000000	*
9	2.59744	2.52029	3.34324	1.67162	2.00594	0.617213	0.822951	0.771517	0

Adjusted for Ties in the Data

1. Table of Z-values

1	0.00000	*	*	*	*	*	*	*	*
2	0.07718	0.00000	*	*	*	*	*	*	*
3	0.74603	0.82320	0.00000	*	*	*	*	*	*
4	0.92610	0.84893	1.67213	0.00000	*	*	*	*	*
5	0.59168	0.51450	1.33770	0.33443	0.00000	*	*	*	*
6	1.98083	1.90366	2.72686	1.05473	1.38915	0.000000	*	*	*
7	1.77503	1.69786	2.52106	0.84893	1.18335	0.205801	0.000000	*	*
8	1.82648	1.74931	2.57251	0.90038	1.23480	0.154350	0.051450	0.000000	*
9	2.59823	2.52106	3.34426	1.67213	2.00656	0.617402	0.823203	0.771752	0

2. Table of P-values

1	1.00000	*	*	*	*	*	*	*	*
---	---------	---	---	---	---	---	---	---	---

2	0.93848	1.00000	*	*	*	*	*	*	*	*
3	0.45565	0.41039	1.00000	*	*	*	*	*	*	*
4	0.35439	0.39592	0.09450	1.00000	*	*	*	*	*	*
5	0.55407	0.60690	0.18099	0.73806	1.00000	*	*	*	*	*
6	0.04761	0.05696	0.00639	0.29155	0.16479	1.00000	*	*	*	*
7	0.07589	0.08954	0.01170	0.39592	0.23667	0.83695	1.00000	*	*	*
8	0.06778	0.08024	0.01010	0.36792	0.21690	0.87733	0.95897	1.00000	*	*
9	0.00937	0.01170	0.00083	0.09450	0.04480	0.53697	0.41039	0.44026	1	*

Sign Confidence Intervals controlled at a family error rate of 0.2

Desired Confidence: 95.009

Sign confidence interval for median

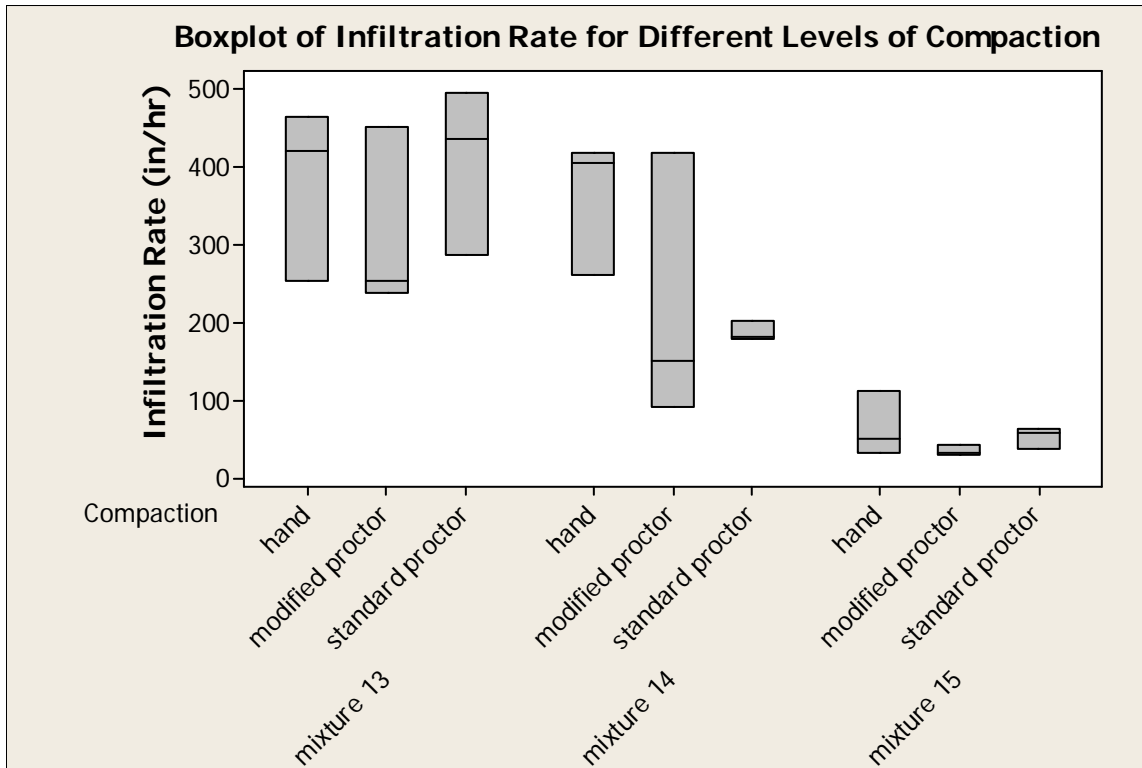
	N	Median	Achieved Confidence	Confidence Interval		Position
				Lower	Upper	
1	3	67.20	0.7500	48.00	72.20	1
2	3	67.20	0.7500	44.10	91.00	1
3	3	84.3	0.7500	80.0	132.0	1
4	3	44.10	0.7500	40.63	51.70	1
5	3	45.40	0.7500	41.00	67.40	1
6	3	36.80	0.7500	30.50	38.70	1
7	3	37.50	0.7500	0.43	47.50	1
8	3	32.80	0.7500	30.20	44.70	1
9	3	28.40	0.7500	25.50	31.40	1

Kruskal-Wallis: Conclusions

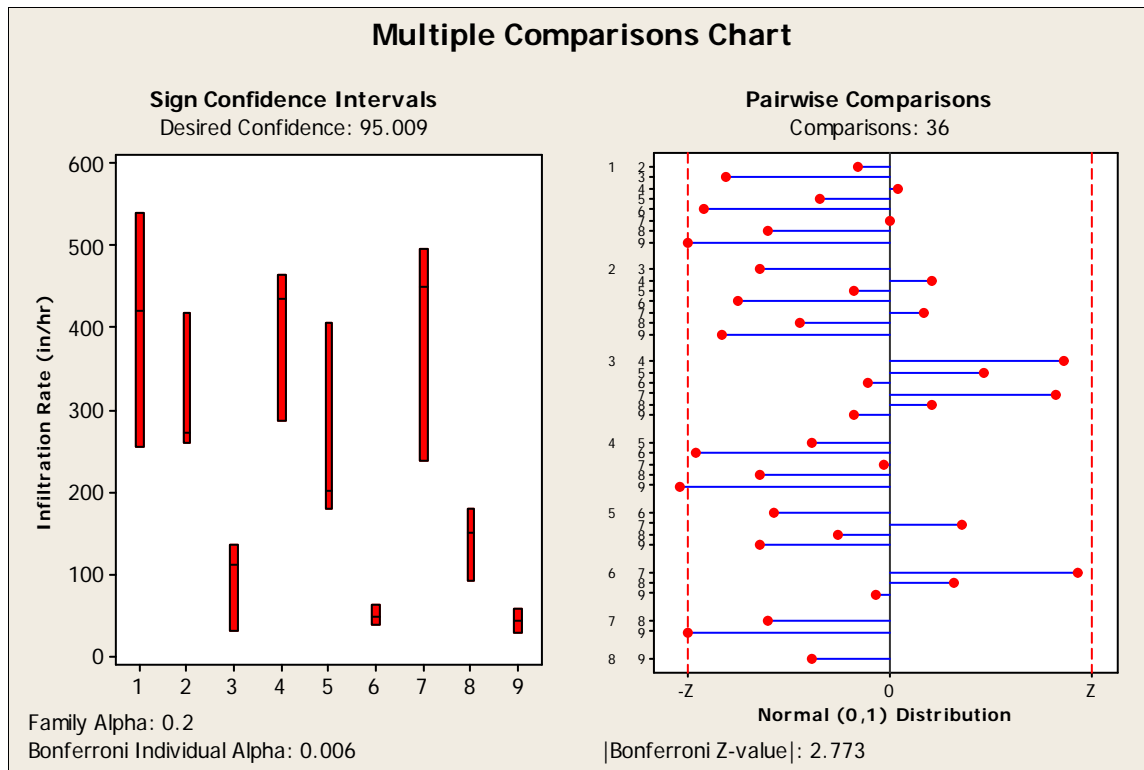
The following groups showed significant differences (adjusted for ties):

Groups	Z vs. Critical value	P-value
3 vs. 9	3.34426 >= 2.773	0.0008

Appendix D.24: Infiltration Test Through Peat (10, 25, and 50%) and Sand Mixture ($D_{50} = 1625 - 1875 \text{ um}$) and Different Levels of Compaction.



Component	Mixture No.	Columns	D_{50} (μm)	C_u
Peat, 6/10 sand from Atlanta, GA and 10/30 sand Atlanta, GA	13	10% peat, 45% 6/10 sand from ATL, GA, and 45% of 10/30 sand from ATL, GA	1875	2.1
	14	25% peat, 37.5% 6/10 sand, and 37.5% of 10/30 sand	1875	2
	15	50% peat, 25% 6/10 sand, and 25% of 10/30 sand	1625	2.5



Data series	Mixture
1	10% peat and 90% sand with hand compaction (mixture : $D_{50} = 1875$ um and $C_u = 2.1$)
2	25% peat and 75% sand with hand compaction (mixture : $D_{50} = 1875$ um and $C_u = 2$)
3	50% peat and 50% sand with hand compaction (mixture : $D_{50} = 1625$ um and $C_u = 2.5$)
4	10% peat and 90% sand with standard proctor compaction (mixture : $D_{50} = 1875$ um and $C_u = 2.1$)
5	25% peat and 75% sand with standard proctor compaction (mixture : $D_{50} = 1875$ um and $C_u = 2$)
6	50% peat and 50% sand with standard proctor compaction (mixture : $D_{50} = 1625$ um and $C_u = 2.5$)
7	10% peat and 90% sand with modified proctor compaction (mixture : $D_{50} = 1875$ um and $C_u = 2.1$)
8	25% peat and 75% sand with modified proctor compaction (mixture : $D_{50} = 1875$ um and $C_u = 2$)
9	50% peat and 50% sand with modified proctor compaction (mixture : $D_{50} = 1625$ um and $C_u = 2.5$)

Kruskal-Wallis: Multiple Comparisons

Kruskal-Wallis Test on the data

Group	N	Median	Ave Rank	Z
1	3	420.00	21.7	1.77
2	3	272.00	18.7	1.08
3	3	111.00	7.0	-1.62
4	3	435.00	22.3	1.93
5	3	201.00	15.3	0.31
6	3	49.00	5.0	-2.08
7	3	450.00	21.7	1.77
8	3	150.00	10.7	-0.77
9	3	43.00	3.7	-2.39
Overall	27		14.0	

H = 21.83 DF = 8 P = 0.005

* NOTE * One or more small samples

Kruskal-Wallis: All Pairwise Comparisons

 Comparisons: 36
 Family Alpha: 0.2
 Bonferroni Individual Alpha: 0.006
 Bonferroni Z-value (2-sided): 2.773

Standardized Absolute Mean Rank Differences
 $|Rbar(i) - Rbar(j)| / Stdev$

Rows: Group i = 1, ..., n
 Columns: Group j = 1, ..., n

1. Table of Z-values

1	0.00000	*	*	*	*	*	*	*	*
2	0.46291	0.00000	*	*	*	*	*	*	*
3	2.26312	1.80021	0.00000	*	*	*	*	*	*
4	0.10287	0.56578	2.36598	0.00000	*	*	*	*	*
5	0.97725	0.51434	1.28586	1.08012	0.00000	*	*	*	*
6	2.57172	2.10881	0.30861	2.67459	1.59447	0.00000	*	*	*
7	0.00000	0.46291	2.26312	0.10287	0.97725	2.57172	0.00000	*	*
8	1.69734	1.23443	0.56578	1.80021	0.72008	0.87439	1.69734	0.00000	*
9	2.77746	2.31455	0.51434	2.88033	1.80021	0.20574	2.77746	1.08012	0

2. Table of P-values

1	1.00000	*	*	*	*	*	*	*	*
2	0.64343	1.00000	*	*	*	*	*	*	*
3	0.02363	0.07183	1.00000	*	*	*	*	*	*
4	0.91807	0.57154	0.01798	1.00000	*	*	*	*	*
5	0.32844	0.60701	0.19849	0.28009	1.00000	*	*	*	*
6	0.01012	0.03496	0.75762	0.00748	0.11083	1.00000	*	*	*
7	1.00000	0.64343	0.02363	0.91807	0.32844	0.01012	1.00000	*	*
8	0.08963	0.21704	0.57154	0.07183	0.47147	0.38191	0.08963	1.00000	*
9	0.00548	0.02064	0.60701	0.00397	0.07183	0.83700	0.00548	0.28009	1

 Sign Confidence Intervals controlled at a family error rate of 0.2

Desired Confidence: 95.009

Sign confidence interval for median

		Confidence		Interval		
N	Median	Achieved Confidence	Lower	Upper	Position	
1	3	420.0	0.7500	254.0	540.0	1
2	3	272.0	0.7500	261.0	417.8	1
3	3	111.0	0.7500	30.8	135.0	1
4	3	435.0	0.7500	287.0	465.0	1
5	3	201.0	0.7500	179.2	405.0	1
6	3	49.00	0.7500	38.00	62.00	1
7	3	450.0	0.7500	237.0	495.0	1
8	3	150.0	0.7500	91.0	180.0	1
9	3	43.00	0.7500	28.50	58.20	1

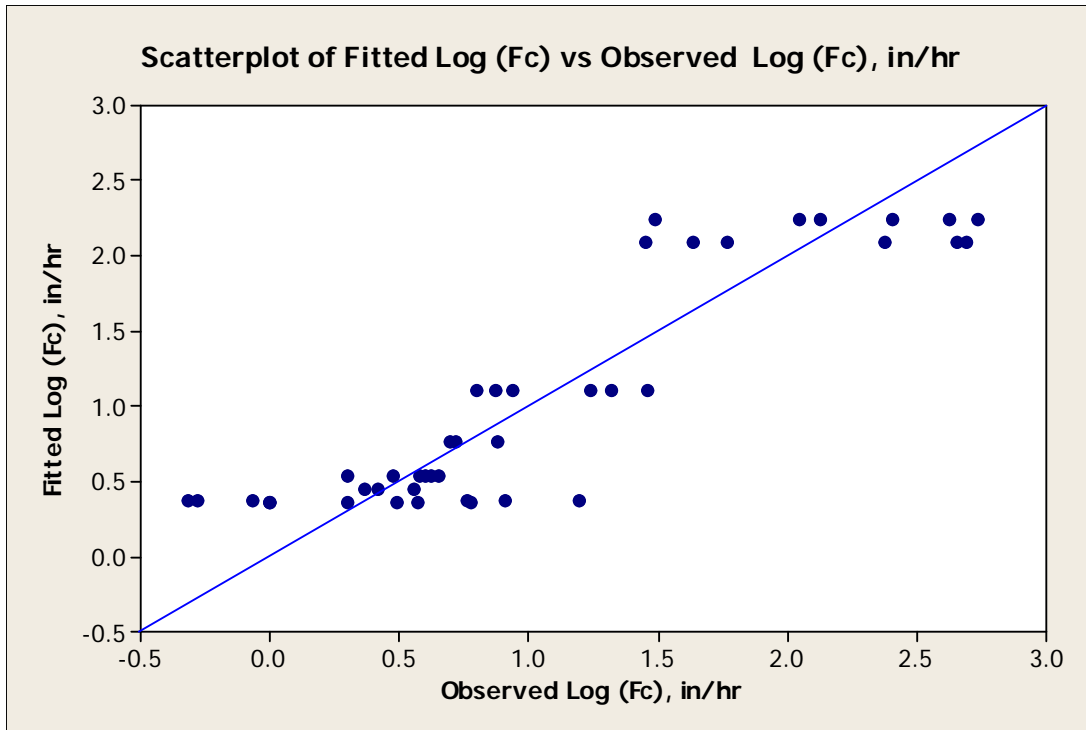
Kruskal-Wallis: Conclusions

The following groups showed significant differences:

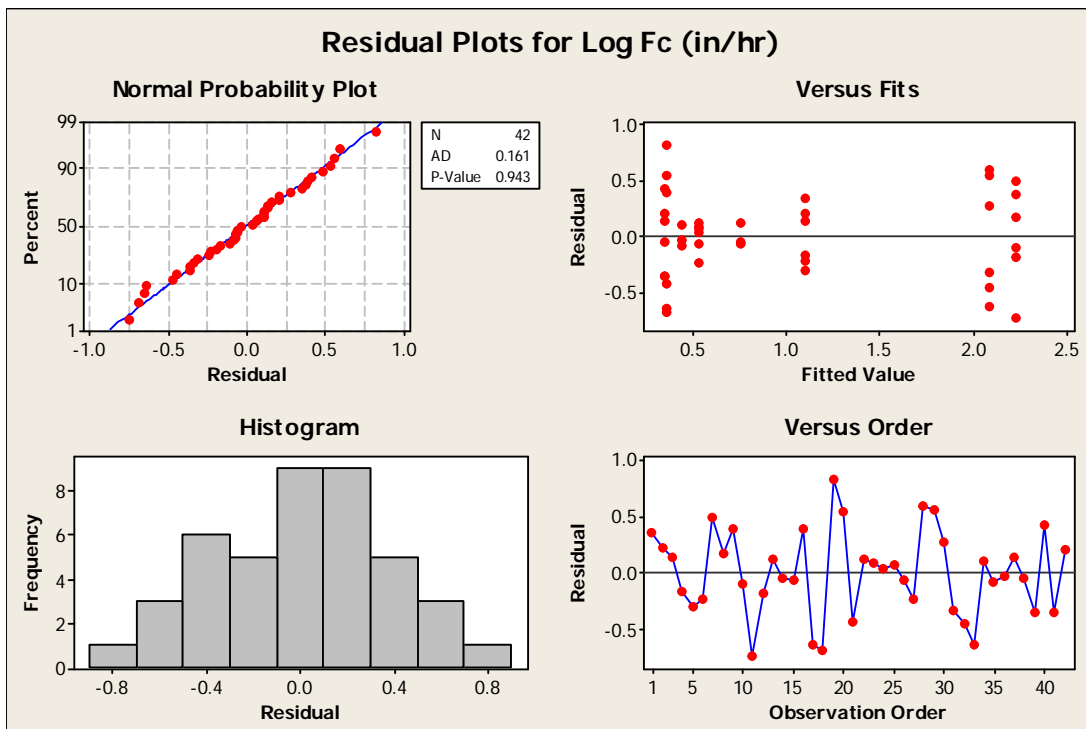
Groups	Z vs. Critical value	P-value
4 vs. 9	2.88033 >= 2.773	0.0040
1 vs. 9	2.77746 >= 2.773	0.0055
7 vs. 9	2.77746 >= 2.773	0.0055

Appendix D. 25: Infiltration Data Used in Full 23 Factorial Designs for Sand-peat Mixture.

Condition	Texture	Uniformity	Compaction					log (Fc) in/hr
	T	U	C	TU	TC	UC	TUC	
1A	-	-	-	+	+	+	-	1.46
1B	-	-	-	+	+	+	-	1.32
1C	-	-	-	+	+	+	-	1.24
1D	-	-	-	+	+	+	-	0.94
1E	-	-	-	+	+	+	-	0.80
1F	-	-	-	+	+	+	-	0.88
2A	+	-	-	-	-	+	+	2.73
2B	+	-	-	-	-	+	+	2.40
2C	+	-	-	-	-	+	+	2.62
2D	+	-	-	-	-	+	+	2.13
2E	+	-	-	-	-	+	+	1.49
2F	+	-	-	-	-	+	+	2.05
3A	-	+	-	-	+	-	+	0.88
3B	-	+	-	-	+	-	+	0.72
3C	-	+	-	-	+	-	+	0.70
4A	+	+	-	+	-	-	-	0.76
4B	+	+	-	+	-	-	-	-0.28
4C	+	+	-	+	-	-	-	-0.32
4D	+	+	-	+	-	-	-	1.20
4E	+	+	-	+	-	-	-	0.91
4F	+	+	-	+	-	-	-	-0.07
5A	-	-	+	+	-	-	+	0.65
5B	-	-	+	+	-	-	+	0.62
5C	-	-	+	+	-	-	+	0.58
5D	-	-	+	+	-	-	+	0.60
5E	-	-	+	+	-	-	+	0.48
5F	-	-	+	+	-	-	+	0.30
6A	+	-	+	-	+	-	-	2.69
6B	+	-	+	-	+	-	-	2.65
6C	+	-	+	-	+	-	-	2.37
6D	+	-	+	-	+	-	-	1.76
6E	+	-	+	-	+	-	-	1.63
6F	+	-	+	-	+	-	-	1.45
7A	-	+	+	-	-	+	-	0.56
7B	-	+	+	-	-	+	-	0.36
7C	-	+	+	-	-	+	-	0.42
8A	+	+	+	+	+	+	+	0.49
8B	+	+	+	+	+	+	+	0.30
8C	+	+	+	+	+	+	+	0.00
8D	+	+	+	+	+	+	+	0.78
8E	+	+	+	+	+	+	+	0.00
8F	+	+	+	+	+	+	+	0.57



Observed vs Fitted log (Fc) Values.



Residuals Analysis Plot.

Analysis of Variance for Log Fc (in/hr) (coded units)

Source	DF	Seq SS	Adj SS	Adj MS	F	P
Main Effects	3	17.063	11.667	3.889	23.12	0.000
Texture	1	2.718	2.905	2.905	17.27	0.000
Uniformity	1	13.688	9.813	9.813	58.34	0.000
Compaction	1	0.658	0.644	0.644	3.83	0.059
2-Way Interactions	3	6.567	6.555	2.185	12.99	0.000
Texture*Uniformity	1	6.060	6.060	6.060	36.02	0.000
Texture*Compaction	1	0.428	0.323	0.323	1.92	0.175
Uniformity*Compaction	1	0.079	0.086	0.086	0.51	0.480
3-Way Interactions	1	0.008	0.008	0.008	0.05	0.831
Texture*Uniformity*Compaction	1	0.008	0.008	0.008	0.05	0.831
Residual Error	34	5.719	5.719	0.168		
Pure Error	34	5.719	5.719	0.168		
Total	41	29.357				

Unusual Observations for Log Fc (in/hr)

Obs	StdOrder	Log Fc (in/hr)	Fit	SE Fit	Residual	St Resid
11	11	1.48855	2.23745	0.16744	-0.7489	-2.00R
19	19	1.1959	0.36587	0.16744	0.83003	2.22R

R denotes an observation with a large standardized residual.

Appendix D. 26: Controlled Lab Column Test Sand-Peat Media (triplicate tests for each condition).

Low Solid Concentration								
Trial No.	Influent	50% peat & 50% sand (D ₅₀ = 300 um & C _u = 37) hand compaction (ρ = 0.74 g/cm ³)	50% peat & 50% sand (D ₅₀ = 300 um & C _u = 37) modified proctor compaction (ρ = 1.03 g/cm ³)	50% peat & 50% surface soil (D ₅₀ = 325 um & C _u = 7) hand compaction (ρ = 0.85 g/cm ³)	50% peat & 50% surface soil (D ₅₀ = 325 um & C _u = 7) modified proctor compaction (ρ = 1.01 g/cm ³)	10% peat & 90% sand (D ₅₀ = 1500 um & C _u = 22) (hand compaction (ρ = 1.61 g/cm ³)	10% peat and 90% sand (D ₅₀ = 1500 um & C _u = 22) modified proctor compaction (ρ = 1.63 g/cm ³)	
1	SSC (mg/L)	137.0	ND	39.0	4.8	9.0	ND	13.3
	TDS (mg/L)	163.3	176.7	188.3	323.3	691.7	1.7	5.0
	Turbidity (NTU)	25.6	3.9	2.0	4.5	3.1	3.8	3.6
	Conductivity (μs/cm)	188.8	174.5	162.5	336.0	608.0	133.2	134.0
2	SSC (mg/L)	69.5	ND	ND	14.3	4.9	1.0	1.0
	TDS (mg/L)	132.4	109.3	123.0	208.6	249.5	99.0	111.4
	Turbidity (NTU)	14.8	3.1	1.4	5.9	4.4	0.8	0.6
	Conductivity (μs/cm)	186.7	168.8	154.9	196.6	232.0	132.0	139.0
High Solid Concentration								
1	SSC	426.3	ND	6.7	3.6	1.1	ND	5.0
	TDS	129.5	99.0	110.5	123.6	188.4	106.0	90.0
	Turbidity (NTU)	120.0	1.8	1.7	8.7	5.2	1.1	1.2
	Conductivity (μs/cm)	190.9	162.8	148.9	153.9	205.0	126.8	131.4
2	SSC	982.7	4.5	6.0	6.3	1.0	0.0	ND
	TDS	134.5	102.7	119.0	111.6	171.3	84.3	117.1
	Turbidity (NTU)	150.0	2.1	2.0	9.5	4.4	1.2	0.8
	Conductivity (μs/cm)	182.6	134.0	153.6	141.5	164.7	129.1	133.3
3	SSC	985.8	1.0	ND	5.0	1.9	ND	ND
	TDS	131.1	98.0	89.0	121.0	165.0	79.6	93.3
	Turbidity (NTU)	141.0	1.4	2.4	8.0	4.5	0.4	0.4
	Conductivity (μs/cm)	196.5	166.3	148.6	142.8	167.8	127.4	124.3

Low Solid Concentration						
Trial No.	Influent	10% peat & 90% sand (D ₅₀ = 340 um & C _u = 1.3) hand compaction (ρ = 1.28 g/cm ³)	10% peat & 90% sand (D ₅₀ = 340 um & C _u = 1.3) modified proctor compaction (ρ = 1.35 g/cm ³)	Surface soil (D ₅₀ = 270 um & C _u = 37) hand compaction (ρ = 1.42 g/cm ³)	Surface soil (D ₅₀ = 270 um & C _u = 37) modified proctor compaction (ρ = 1.67 g/cm ³)	
1	SSC (mg/L)	137.0	4.0	ND	3.2	12.0
	TDS (mg/L)	163.3	101.7	132.7	301.7	364.0
	Turbidity (NTU)	25.6	3.8	1.3	2.0	1.2
	Conductivity (μs/cm)	188.8	124.7	125.4	359.0	460.0
2	SSC (mg/L)	69.5	7.6	ND	1.0	4.0
	TDS (mg/L)	132.4	89.5	107.6	231.4	338.0
	Turbidity (NTU)	14.8	1.5	0.4	1.5	0.6
	Conductivity (μs/cm)	186.7	125.7	126.9	316.0	445.0
High Solid Concentration						
1	SSC	426.3	ND	3.0	5.7	15.6
	TDS	129.5	77.1	78.0	202.9	365.6
	Turbidity (NTU)	120.0	0.6	0.7	1.3	1.2
	Conductivity (μs/cm)	190.9	127.5	129.7	321.0	444.0
2	SSC	982.7	6.7	ND	7.8	24.8
	TDS	134.5	96.2	98.0	241.2	341.0
	Turbidity (NTU)	150.0	0.5	0.4	2.2	2.2
	Conductivity (μs/cm)	182.6	131.6	132.3	331.0	467.0
3	SSC	985.8	ND	ND	12.7	3.3
	TDS	131.1	84.2	87.4	215.7	276.7
	Turbidity (NTU)	141.0	0.8	0.4	1.5	0.7
	Conductivity (μs/cm)	196.5	129.3	130.1	321.0	392.0

Low Solid Concentration								
Trial No.	Influent	50% peat , 50% sand (D ₅₀ = 300 um & C _u = 3) hand compaction (ρ = 1.1 g/cm3)	50% peat & 50% sand (D ₅₀ = 300 um & C _u = 3) modified proctor compaction (ρ = 1.1 g/cm3)	10% peat & 90% sand (D ₅₀ = 1900 um & C _u = 2) hand compaction (ρ = 1.52 g/cm3)	10% peat & 90% sand (D ₅₀ = 1900 um & C _u = 2) modified proctor compaction (ρ = 1.58 g/cm3)	50 % peat & 50% sand (D ₅₀ = 1600 um & C _u = 2.5) hand compaction (ρ = 0.96 g/cm3)	50 % peat & 50% sand (D ₅₀ = 1600 um & C _u = 2.5) modified proctor compaction (ρ = 1.23 g/cm3)	
1	SSC (mg/L)	62	ND	ND	57.0	61.8	53.0	25.5
	TDS (mg/L)	124	150	180	96	99	300	345
	Turbidity (NTU)	22.6	-	2.76	75.8	55.8	78.2	74.2
	Conductivity (μs/cm)	176.9	170.8	178.6	111.6	136.7	199.2	206
2	SSC (mg/L)	55	2.2	3.6	73.0	22.9	4.8	20.0
	TDS (mg/L)	136	154.4	191.8	102.0	87.6	312.4	286.7
	Turbidity (NTU)	26.3	2.23	2.26	112	40	30.4	37.6
	Conductivity (μs/cm)	119.8	134.6	155.6	95.4	89.7	144	137.8
3	SSC (mg/L)	54	ND	234.0	91.0	70.0	16.0	19.6
	TDS (mg/L)	98	136.0	162.0	108.0	119.0	200.00	210.28
	Turbidity (NTU)	24.5	3.9	1.78	167	129	18.7	22.4
	Conductivity (μs/cm)	121.4	111.6	119.3	90.4	93.2	125.8	121.2
High Solid Concentration								
1	SSC (mg/L)	549	ND	ND	92.6	84.9	15.0	11.4
	TDS (mg/L)	165	71.00	ND	130.53	153.77	173.00	144.76
	Turbidity (NTU)	94.0	3.26	2.15	108	89.6	12	9.6
	Conductivity (μs/cm)	213	123.4	122	128.6	145.9	163.9	163.1
2	SSC (mg/L)	378	ND	ND	65.7	42.9	6.7	7.0
	TDS (mg/L)	155	120.95	132.38	129.52	143.81	144.76	144.00
	Turbidity (NTU)	84.0	1.65	1.29	78.2	62.8	8.44	8.5
	Conductivity (μs/cm)	190.3	170.5	169.9	132.4	145.9	177.3	180.6
3	SSC (mg/L)	390	ND	ND	98.9	83.8	15.2	5.8
	TDS (mg/L)	157	132.38	111.58	145.26	146.67	133.33	132.04
	Turbidity (NTU)	104.0	1.44	0.84	117	101	10.2	6.78
	Conductivity (μs/cm)	212	174.2	187.5	145	157.7	182.9	184.4

Appendix D.27: 50% Peat and 50% Sand (Mixture $D_{50} = 300$ μm and $C_u = 3$), Hand Compaction ($\rho = 0.74$ g/cm^3), Low Concentration Regression Statics.

<i>Regression Statistics</i>	
Multiple R	1
R Square	1
Adjusted R Square	65535
Standard Error	0
Observations	2

ANOVA					
	<i>df</i>	<i>SS</i>	<i>MS</i>	<i>F</i>	<i>Significance F</i>
Regression	1	1.143114	1.143114	#NUM!	#NUM!
Residual	0	0	65535		
Total	1	1.143114			

	<i>Coefficients</i>	<i>Standard Error</i>	<i>t Stat</i>	<i>P-value</i>	<i>Lower 95%</i>	<i>Upper 95%</i>
Intercept	-3.596728	0	65535	#NUM!	-3.596727999	-3.59673
X Variable 1	-0.02240831	0	65535	#NUM!	-0.022408311	-0.02241

Appendix D.28: 50% Peat and 50% Sand (Mixture $D_{50} = 300$ μm and $C_u = 3$), Hand Compaction ($\rho = 0.74$ g/cm^3), High Concentration Regression Statics.

<i>Regression Statistics</i>	
Multiple R	0.089007
R Square	0.007922
Adjusted R Square	-0.49208
Standard Error	1025.331
Observations	3

ANOVA					
	<i>df</i>	<i>SS</i>	<i>MS</i>	<i>F</i>	<i>Significance F</i>
Regression	1	16790.36	16790.36	0.015971	0.919971
Residual	2	2102606	1051303		
Total	3	2119396			

	<i>Coefficients</i>	<i>Standard Error</i>	<i>t Stat</i>	<i>P-value</i>	<i>Lower 95%</i>	<i>Upper 95%</i>
Intercept	0	#N/A	#N/A	#N/A	#N/A	#N/A
X Variable 1	12.22619	96.74426	0.126376	0.910993	-404.031	428.4832

Appendix D.29: 50% Peat and 50% Sand (Mixture $D_{50} = 300 \text{ um}$ and $C_u = 3$), Modified Proctor Compaction ($\rho = 1.03 \text{ g/cm}^3$), Low Concentration Regression Statics.

<i>Regression Statistics</i>	
Multiple R	1
R Square	1
Adjusted R Square	65535
Standard Error	0
Observations	2

ANOVA					
	<i>df</i>	<i>SS</i>	<i>MS</i>	<i>F</i>	<i>Significance F</i>
Regression	1	968	968	#NUM!	#NUM!
Residual	0	0	65535		
Total	1	968			

	<i>Coefficients</i>	<i>Standard Error</i>	<i>t Stat</i>	<i>P-value</i>	<i>Lower 95%</i>	<i>Upper 95%</i>
Intercept	-50.3352152	0	65535	#NUM!	-50.33521524	-50.3352
X Variable 1	0.652081863	0	65535	#NUM!	0.652081863	0.652082

Appendix D.30: 50% Peat and 50% Sand (Mixture $D_{50} = 300 \text{ um}$ and $C_u = 3$), Modified Proctor Compaction ($\rho = 1.03 \text{ g/cm}^3$), High Concentration Regression Statics.

<i>Regression Statistics</i>	
Multiple R	0.101917
R Square	0.010387
Adjusted R Square	-0.48961
Standard Error	1024.056
Observations	3

ANOVA					
	<i>df</i>	<i>SS</i>	<i>MS</i>	<i>F</i>	<i>Significance F</i>
Regression	1	22014.46	22014.46	0.020992	0.908399
Residual	2	2097382	1048691		
Total	3	2119396			

	<i>Coefficients</i>	<i>Standard Error</i>	<i>t Stat</i>	<i>P-value</i>	<i>Lower 95%</i>	<i>Upper 95%</i>
Intercept	0	#N/A	#N/A	#N/A	#N/A	#N/A
X Variable 1	-10.4539	72.15163	-0.14489	0.898083	-320.897	299.9895

Appendix D.31: 50% Peat and 50% Surface Soil (Mixture $D_{50} = 325 \text{ um}$ and $C_u = 7$), Hand Compaction ($\rho = 0.85 \text{ g/cm}^3$), Low Concentration Regression Statics.

<i>Regression Statistics</i>						
Multiple R		1				
R Square		1				
Adjusted R Square						
Standard Error	65535					
Observations		2				

ANOVA					
	<i>df</i>	<i>SS</i>	<i>MS</i>	<i>F</i>	<i>Significance F</i>
Regression	1	45.35147	45.35147	#NUM!	#NUM!
Residual	0	0	65535		
Total	1	45.35147			

	<i>Coefficients</i>	<i>Standard Error</i>	<i>t Stat</i>	<i>P-value</i>	<i>Lower 95%</i>	<i>Upper 95%</i>
Intercept	24.09853144	0	65535	#NUM!	24.09853144	24.09853
X Variable 1	-0.14114326	0	65535	#NUM!	-0.14114326	-0.14114

Appendix D.32: 50% Peat and 50% Surface Soil (Mixture $D_{50} = 325 \text{ um}$ and $C_u = 7$), Hand Compaction ($\rho = 0.85 \text{ g/cm}^3$), High Concentration Regression Statics.

<i>Regression Statistics</i>						
Multiple R		0.985973				
R Square		0.972143				
Adjusted R Square		0.472143				
Standard Error	171.8141					
Observations		3				

ANOVA					
	<i>df</i>	<i>SS</i>	<i>MS</i>	<i>F</i>	<i>Significance F</i>
Regression	1	2060356	2060356	69.79507	0.075841
Residual	2	59040.17	29520.08		
Total	3	2119396			

	<i>Coefficients</i>	<i>Standard Error</i>	<i>t Stat</i>	<i>P-value</i>	<i>Lower 95%</i>	<i>Upper 95%</i>
Intercept	0	#N/A	#N/A	#N/A	#N/A	#N/A
X Variable 1	162.4095	19.44012	8.354344	0.014027	78.76537	246.0536

Appendix D.33: 50% Peat and 50% Surface Soil (Mixture $D_{50} = 325 \text{ um}$ and $C_u = 7$), Modified Proctor Compaction ($\rho = 1.01 \text{ g/cm}^3$), Low Concentration Regression Statics.

<i>Regression Statistics</i>						
Multiple R		1				
R Square		1				
Adjusted R Square						
Standard Error	65535					
Observations		2				

ANOVA					
	<i>df</i>	<i>SS</i>	<i>MS</i>	<i>F</i>	<i>Significance F</i>
Regression	1	8.593128	8.593128	#NUM!	#NUM!
Residual	0	0	65535		
Total	1	8.593128			

	<i>Coefficients</i>	<i>Standard Error</i>	<i>t Stat</i>	<i>P-value</i>	<i>Lower 95%</i>	<i>Upper 95%</i>
Intercept	0.582935369	0	65535	#NUM!	0.582935369	0.582935
X Variable 1	0.061438428	0	65535	#NUM!	0.061438428	0.061438

Appendix D.34: 50% Peat and 50% Surface Soil (Mixture $D_{50} = 325 \text{ um}$ and $C_u = 7$), Modified Proctor Compaction ($\rho = 1.01 \text{ g/cm}^3$), High Concentration Regression Statics.

<i>Regression Statistics</i>						
Multiple R		0.947889				
R Square		0.898493				
Adjusted R Square		0.398493				
Standard Error	327.9741					
Observations		3				

ANOVA					
	<i>df</i>	<i>SS</i>	<i>MS</i>	<i>F</i>	<i>Significance F</i>
Regression	1	1904262	1904262	17.70303	0.14855
Residual	2	215134	107567		
Total	3	2119396			

	<i>Coefficients</i>	<i>Standard Error</i>	<i>t Stat</i>	<i>P-value</i>	<i>Lower 95%</i>	<i>Upper 95%</i>
Intercept	0	#N/A	#N/A	#N/A	#N/A	#N/A
X Variable 1	569.1585	135.2725	4.207497	0.052111	-12.8719	1151.189

Appendix D.35: 10% Peat and 90% Sand (Mixture $D_{50} = 1500 \text{ um}$ and $C_u = 22$), Hand Compaction ($\rho = 1.61 \text{ g/cm}^3$), Low Concentration Regression Statics.

<i>Regression Statistics</i>	
Multiple R	1
R Square	1
Adjusted R Square	
Standard Error	65535
Observations	2

ANOVA					
	<i>df</i>	<i>SS</i>	<i>MS</i>	<i>F</i>	<i>Significance F</i>
Regression	1	7.810658	7.810658	#NUM!	#NUM!
Residual	0	0	65535		
Total	1	7.810658			

	<i>Coefficients</i>	<i>Standard Error</i>	<i>t Stat</i>	<i>P-value</i>	<i>Lower 95%</i>	<i>Upper 95%</i>
Intercept	5.024700071	0	65535	#NUM!	5.024700071	5.0247
X Variable 1	-0.05857445	0	65535	#NUM!	-0.058574453	-0.05857

Appendix D.36: 10% Peat and 90% Sand (Mixture $D_{50} = 1500 \text{ um}$ and $C_u = 22$), Hand Compaction ($\rho = 1.61 \text{ g/cm}^3$), High Concentration Regression Statics.

<i>Regression Statistics</i>	
Multiple R	0.735574
R Square	0.54107
Adjusted R Square	0.04107
Standard Error	697.372
Observations	3

ANOVA					
	<i>df</i>	<i>SS</i>	<i>MS</i>	<i>F</i>	<i>Significance F</i>
Regression	1	1146741	1146741	2.35796	0.36748
Residual	2	972655.3	486327.6		
Total	3	2119396			

	<i>Coefficients</i>	<i>Standard Error</i>	<i>t Stat</i>	<i>P-value</i>	<i>Lower 95%</i>	<i>Upper 95%</i>
Intercept	0	#N/A	#N/A	#N/A	#N/A	#N/A
X Variable 1	-347.737	226.4557	-1.53557	0.264426	-1322.1	626.6228

Appendix D.37: 10% Peat and 90% Sand (Mixture $D_{50} = 1500 \text{ um}$ and $C_u = 22$), Modified Proctor Compaction ($\rho = 1.63 \text{ g/cm}^3$), Low Concentration Regression Statics.

<i>Regression Statistics</i>					
Multiple R		1			
R Square		1			
Adjusted R Square					
Standard Error	65535				
Observations		2			

ANOVA					
	<i>df</i>	<i>SS</i>	<i>MS</i>	<i>F</i>	<i>Significance F</i>
Regression	1	76.64399	76.64399	#NUM!	#NUM!
Residual	0	0	65535		
Total	1	76.64399			

	<i>Coefficients</i>	<i>Standard Error</i>	<i>t Stat</i>	<i>P-value</i>	<i>Lower 95%</i>	<i>Upper 95%</i>
Intercept	-11.8042813	0	65535	#NUM!	-11.80428135	-11.8043
X Variable 1	0.183486239	0	65535	#NUM!	0.183486239	0.183486

Appendix D.38: 10% Peat and 90% Sand (Mixture $D_{50} = 1500 \text{ um}$ and $C_u = 22$), Modified Proctor Compaction ($\rho = 1.63 \text{ g/cm}^3$), High Concentration Regression Statics.

<i>Regression Statistics</i>					
Multiple R	0.551161				
R Square	0.303779				
Adjusted R Square					
Standard Error	-0.19622				
Observations	858.9439				

ANOVA					
	<i>df</i>	<i>SS</i>	<i>MS</i>	<i>F</i>	<i>Significance F</i>
Regression	1	643827.1	643827.1	0.872649	0.521664
Residual	2	1475569	737784.6		
Total	3	2119396			

	<i>Coefficients</i>	<i>Standard Error</i>	<i>t Stat</i>	<i>P-value</i>	<i>Lower 95%</i>	<i>Upper 95%</i>
Intercept	0	#N/A	#N/A	#N/A	#N/A	#N/A
X Variable 1	-64.1358	68.65638	-0.93416	0.448839	-359.54	231.2687

Appendix D.39: 10% Peat and 90% Sand (Mixture $D_{50} = 340 \text{ um}$ and $C_u = 1.3$), Hand Compaction ($\rho = 1.28 \text{ g/cm}^3$), Low Concentration Regression Statics.

<i>Regression Statistics</i>	
Multiple R	1
R Square	1
Adjusted R Square	
Standard Error	65535
Observations	2

ANOVA					
	<i>df</i>	<i>SS</i>	<i>MS</i>	<i>F</i>	<i>Significance F</i>
Regression	1	6.548753	6.548753	#NUM!	#NUM!
Residual	0	0	65535		
Total	1	6.548753			

	<i>Coefficients</i>	<i>Standard Error</i>	<i>t Stat</i>	<i>P-value</i>	<i>Lower 95%</i>	<i>Upper 95%</i>
Intercept	11.34791814	0	65535	#NUM!	11.34791814	11.34792
X Variable 1	-0.05363444	0	65535	#NUM!	-0.053634439	-0.05363

Appendix D.40: 10% Peat and 90% Sand (Mixture $D_{50} = 340 \text{ um}$ and $C_u = 1.3$), Hand Compaction ($\rho = 1.28 \text{ g/cm}^3$), High Concentration Regression Statics.

<i>Regression Statistics</i>	
Multiple R	0.252746
R Square	0.06388
Adjusted R Square	
Standard Error	-0.43612
Observations	995.9941
	3

ANOVA					
	<i>df</i>	<i>SS</i>	<i>MS</i>	<i>F</i>	<i>Significance F</i>
Regression	1	135387.9	135387.9	0.136479	0.774714
Residual	2	1984009	992004.3		
Total	3	2119396			

	<i>Coefficients</i>	<i>Standard Error</i>	<i>t Stat</i>	<i>P-value</i>	<i>Lower 95%</i>	<i>Upper 95%</i>
Intercept	0	#N/A	#N/A	#N/A	#N/A	#N/A
X Variable 1	-29.1918	79.01832	-0.36943	0.747254	-369.18	310.7966

Appendix D.41: 10% Peat and 90% Sand (Mixture $D_{50} = 340 \text{ um}$ and $C_u = 1.3$), Modified Proctor Compaction ($\rho = 1.35 \text{ g/cm}^3$), Low Concentration Regression Statics.

<i>Regression Statistics</i>	
Multiple R	1
R Square	1
Adjusted R Square	
Standard Error	65535
Observations	2

ANOVA					
	<i>df</i>	<i>SS</i>	<i>MS</i>	<i>F</i>	<i>Significance F</i>
Regression	1	262.2149	262.2149	#NUM!	#NUM!
Residual	0	0	65535		
Total	1	262.2149			

	<i>Coefficients</i>	<i>Standard Error</i>	<i>t Stat</i>	<i>P-value</i>	<i>Lower 95%</i>	<i>Upper 95%</i>
Intercept	-47.4048887	0	65535	#NUM!	-47.40488869	-47.4049
X Variable 1	0.339385385	0	65535	#NUM!	0.339385385	0.339385

Appendix D.42: 10% Peat and 90% Sand (Mixture $D_{50} = 340 \text{ um}$ and $C_u = 1.3$), Modified Proctor Compaction ($\rho = 1.35 \text{ g/cm}^3$), High Concentration Regression Statics.

<i>Regression Statistics</i>	
Multiple R	0.844254
R Square	0.712764
Adjusted R Square	
Standard Error	0.212764
Observations	551.7094

ANOVA					
	<i>df</i>	<i>SS</i>	<i>MS</i>	<i>F</i>	<i>Significance F</i>
Regression	1	1510630	1510630	4.962921	0.268605
Residual	2	608766.5	304383.3		
Total	3	2119396			

	<i>Coefficients</i>	<i>Standard Error</i>	<i>t Stat</i>	<i>P-value</i>	<i>Lower 95%</i>	<i>Upper 95%</i>
Intercept	0	#N/A	#N/A	#N/A	#N/A	#N/A
X Variable 1	-101.115	45.38848	-2.22776	0.155746	-296.406	94.17616

Appendix D.43: Tuscaloosa Surface Soil ($D_{50} = 270 \text{ um}$ and $C_u = 37$), Hand Compaction ($\rho = 1.42 \text{ g/cm}^3$), Low Concentration Regression Statics.

<i>Regression Statistics</i>	
Multiple R	1
R Square	1
Adjusted R Square	65535
Standard Error	0
Observations	2

ANOVA					
	<i>df</i>	<i>SS</i>	<i>MS</i>	<i>F</i>	<i>Significance F</i>
Regression	1	2.432146	2.432146	#NUM!	#NUM!
Residual	0	0	65535		
Total	1	2.432146			

	<i>Coefficients</i>	<i>Standard Error</i>	<i>t Stat</i>	<i>P-value</i>	<i>Lower 95%</i>	<i>Upper 95%</i>
Intercept	-1.32006091	0	65535	#NUM!	-1.320060914	-1.32006
X Variable 1	0.032685808	0	65535	#NUM!	0.032685808	0.032686

Appendix D.44: Tuscaloosa Surface Soil ($D_{50} = 270 \text{ um}$ and $C_u = 37$), Hand Compaction ($\rho = 1.42 \text{ g/cm}^3$), High Concentration Regression Statics.

<i>Regression Statistics</i>	
Multiple R	0.973754
R Square	0.948198
Adjusted R Square	0.448198
Standard Error	234.2966
Observations	3

ANOVA					
	<i>df</i>	<i>SS</i>	<i>MS</i>	<i>F</i>	<i>Significance F</i>
Regression	1	2009607	2009607	36.60826	0.104275
Residual	2	109789.8	54894.9		
Total	3	2119396			

	<i>Coefficients</i>	<i>Standard Error</i>	<i>t Stat</i>	<i>P-value</i>	<i>Lower 95%</i>	<i>Upper 95%</i>
Intercept	0	#N/A	#N/A	#N/A	#N/A	#N/A
X Variable 1	88.4958	14.62625	6.050476	0.026246	25.5641	151.4275

Appendix D.45: Tuscaloosa Surface Soil ($D_{50} = 270 \text{ um}$ and $C_u = 37$), Modified Proctor Compaction ($\rho = 1.67 \text{ g/cm}^3$), Low Concentration Regression Statics.

<i>Regression Statistics</i>						
Multiple R						1
R Square						1
Adjusted R Square						
Standard Error					65535	
Observations						2

ANOVA						
	<i>df</i>	<i>SS</i>	<i>MS</i>	<i>F</i>	<i>Significance F</i>	
Regression	1	32	32	#NUM!	#NUM!	
Residual	0	0	65535			
Total	1	32				

	<i>Coefficients</i>	<i>Standard Error</i>	<i>t Stat</i>	<i>P-value</i>	<i>Lower 95%</i>	<i>Upper 95%</i>
Intercept	-4.24276641	0	65535	#NUM!	-4.242766408	-4.24277
X Variable 1	0.118560339	0	65535	#NUM!	0.118560339	0.11856

Appendix D.46: Tuscaloosa Surface Soil ($D_{50} = 270 \text{ um}$ and $C_u = 37$), Modified Proctor Compaction ($\rho = 1.67 \text{ g/cm}^3$), High Concentration Regression Statics.

<i>Regression Statistics</i>						
Multiple R						0.799393
R Square						0.639029
Adjusted R Square						
Standard Error					0.139029	
Observations					618.482	

ANOVA						
	<i>df</i>	<i>SS</i>	<i>MS</i>	<i>F</i>	<i>Significance F</i>	
Regression	1	1354356	1354356	3.540616	0.310981	
Residual	2	765039.9	382520			
Total	3	2119396				

	<i>Coefficients</i>	<i>Standard Error</i>	<i>t Stat</i>	<i>P-value</i>	<i>Lower 95%</i>	<i>Upper 95%</i>
Intercept	0	#N/A	#N/A	#N/A	#N/A	#N/A
X Variable 1	39.54101	21.01398	1.881653	0.200607	-50.8749	129.9569

Appendix D.47: 50% Peat and 50% Sand (Mixture $D_{50} = 1300 \text{ um}$ and $C_u = 20$), Hand Compaction ($\rho = 1.1 \text{ g/cm}^3$), Low Concentration Regression Statics.

<i>Regression Statistics</i>	
Multiple R	0.384887
R Square	0.148138
Adjusted R Square	-0.35186
Standard Error	64.56478
Observations	3

ANOVA					<i>Significance</i>
	<i>df</i>	<i>SS</i>	<i>MS</i>	<i>F</i>	<i>F</i>
Regression	1	1449.838	1449.838	0.347799	0.660781
Residual	2	8337.222	4168.611		
Total	3	9787.061			

	<i>Coefficients</i>	<i>Standard Error</i>	<i>t Stat</i>	<i>P-value</i>	<i>Lower 95%</i>	<i>Upper 95%</i>
Intercept	0	#N/A	#N/A	#N/A	#N/A	#N/A
X Variable 1	-6.8456	11.60774	-0.58974	0.615113	-56.7897	43.09847

Appendix D.48: 50% Peat and 50% Sand (Mixture $D_{50} = 1300 \text{ um}$ and $C_u = 20$), Hand Compaction ($\rho = 1.1 \text{ g/cm}^3$), High Concentration Regression Statics.

<i>Regression Statistics</i>	
Multiple R	0.853029
R Square	0.727659
Adjusted R Square	0.227659
Standard Error	284.9789
Observations	3

ANOVA					<i>Significance</i>
	<i>df</i>	<i>SS</i>	<i>MS</i>	<i>F</i>	<i>F</i>
Regression	1	433980.6	433980.6	5.343734	0.259921
Residual	2	162426	81212.98		
Total	3	596406.5			

	<i>Coefficients</i>	<i>Standard Error</i>	<i>t Stat</i>	<i>P-value</i>	<i>Lower 95%</i>	<i>Upper 95%</i>
Intercept	0	#N/A	#N/A	#N/A	#N/A	#N/A
X Variable 1	-54.9596	23.77503	-2.31165	0.146971	-157.255	47.3361

Appendix D.49: 50% Peat and 50% Sand (Mixture $D_{50} = 1300 \text{ um}$ and $C_u = 20$), Modified Proctor Compaction ($\rho = 1.1 \text{ g/cm}^3$), Low Concentration Regression Statics.

<i>Regression Statistics</i>	
Multiple R	0.518042
R Square	0.268367
Adjusted R Square	-0.23163
Standard Error	59.83534
Observations	3

ANOVA					
	<i>df</i>	<i>SS</i>	<i>MS</i>	<i>F</i>	<i>Significance F</i>
Regression	1	2626.524	2626.524	0.733611	0.549106
Residual	2	7160.536	3580.268		
Total	3	9787.061			

	<i>Coefficients</i>	<i>Standard Error</i>	<i>t Stat</i>	<i>P-value</i>	<i>Lower 95%</i>	<i>Upper 95%</i>
Intercept	0	#N/A	#N/A	#N/A	#N/A	#N/A
X Variable 1	0.218582	0.255201	0.856511	0.481958	-0.87946	1.316622

Appendix D.50: 50% Peat and 50% Sand (Mixture $D_{50} = 1300 \text{ um}$ and $C_u = 20$), Modified Proctor Compaction ($\rho = 1.1 \text{ g/cm}^3$), High Concentration Regression Statics.

<i>Regression Statistics</i>	
Multiple R	0.775169
R Square	0.600887
Adjusted R Square	0.100887
Standard Error	344.9879
Observations	3

ANOVA					
	<i>df</i>	<i>SS</i>	<i>MS</i>	<i>F</i>	<i>Significance F</i>
Regression	1	358373.2	358373.2	3.011117	0.332824
Residual	2	238033.4	119016.7		
Total	3	596406.5			

	<i>Coefficients</i>	<i>Standard Error</i>	<i>t Stat</i>	<i>P-value</i>	<i>Lower 95%</i>	<i>Upper 95%</i>
Intercept	0	#N/A	#N/A	#N/A	#N/A	#N/A
X Variable 1	-2.54336	1.465697	-1.73526	0.224831	-8.84975	3.763024

Appendix D.51: 10% Peat and 90% Sand (Mixture $D_{50} = 1900 \text{ um}$ and $C_u = 2$), Hand Compaction ($\rho = 1.52 \text{ g/cm}^3$), Low Concentration Regression Statics.

<i>Regression Statistics</i>						
Multiple R		0.970772				
R Square		0.942398				
Adjusted R Square		0.442398				
Standard Error		16.78926				
Observations		3				

ANOVA						
	<i>df</i>	<i>SS</i>	<i>MS</i>	<i>F</i>	<i>Significance F</i>	
Regression	1	9223.302	9223.302	32.72075	0.11018	
Residual	2	563.7586	281.8793			
Total	3	9787.061				

	<i>Coefficients</i>	<i>Standard Error</i>	<i>t Stat</i>	<i>P-value</i>	<i>Lower 95%</i>	<i>Upper 95%</i>
Intercept	0	#N/A	#N/A	#N/A	#N/A	#N/A
X Variable 1	0.739652	0.129305	5.720205	0.029228	0.183297	1.296007

Appendix D.52: 10% Peat and 90% Sand (Mixture $D_{50} = 1900 \text{ um}$ and $C_u = 2$), Hand Compaction ($\rho = 1.52 \text{ g/cm}^3$), High Concentration Regression Statics.

<i>Regression Statistics</i>						
Multiple R		0.982447				
R Square		0.965201				
Adjusted R Square		0.465201				
Standard Error		101.8682				
Observations		3				

ANOVA						
	<i>df</i>	<i>SS</i>	<i>MS</i>	<i>F</i>	<i>Significance F</i>	
Regression	1	575652.3	575652.3	55.47318	0.084967	
Residual	2	20754.26	10377.13			
Total	3	596406.5				

	<i>Coefficients</i>	<i>Standard Error</i>	<i>t Stat</i>	<i>P-value</i>	<i>Lower 95%</i>	<i>Upper 95%</i>
Intercept	0	#N/A	#N/A	#N/A	#N/A	#N/A
X Variable 1	5.036944	0.676278	7.448032	0.017553	2.127152	7.946735

Appendix D.53: 10% Peat and 90% Sand (Mixture $D_{50} = 1900 \text{ um}$ and $C_u = 2$), Modified Proctor Compaction ($\rho = 1.58 \text{ g/cm}^3$), Low Concentration Regression Statics.

<i>Regression Statistics</i>	
Multiple R	0.933985
R Square	0.872329
Adjusted R Square	0.372329
Standard Error	24.99529
Observations	3

ANOVA					
	<i>df</i>	<i>SS</i>	<i>MS</i>	<i>F</i>	<i>Significance F</i>
Regression	1	8537.532	8537.532	13.66521	0.16819
Residual	2	1249.529	624.7643		
Total	3	9787.061			

	<i>Coefficients</i>	<i>Standard Error</i>	<i>t Stat</i>	<i>P-value</i>	<i>Lower 95%</i>	<i>Upper 95%</i>
Intercept	0	#N/A	#N/A	#N/A	#N/A	#N/A
X Variable 1	0.961375	0.260067	3.696648	0.066015	-0.1576	2.080353

Appendix D.54: 10% Peat and 90% Sand (Mixture $D_{50} = 1900 \text{ um}$ and $C_u = 2$), Modified Proctor Compaction ($\rho = 1.58 \text{ g/cm}^3$), High Concentration Regression Statics.

<i>Regression Statistics</i>	
Multiple R	0.975507
R Square	0.951614
Adjusted R Square	0.451614
Standard Error	120.1203
Observations	3

ANOVA					
	<i>df</i>	<i>SS</i>	<i>MS</i>	<i>F</i>	<i>Significance F</i>
Regression	1	567548.7	567548.7	39.33419	0.100659
Residual	2	28857.78	14428.89		
Total	3	596406.5			

	<i>Coefficients</i>	<i>Standard Error</i>	<i>t Stat</i>	<i>P-value</i>	<i>Lower 95%</i>	<i>Upper 95%</i>
Intercept	0	#N/A	#N/A	#N/A	#N/A	#N/A
X Variable 1	5.942882	0.947572	6.271698	0.024493	1.865811	10.01995

Appendix D.55: 50% Peat and 50% Sand (Mixture $D_{50} = 1600 \text{ um}$ and $C_u = 2.5$), Hand Compaction ($\rho = 0.96 \text{ g/cm}^3$), Low Concentration Regression Statics.

<i>Regression Statistics</i>	
Multiple R	0.803176
R Square	0.645092
Adjusted R Square	
Standard Error	41.6744
Observations	3

ANOVA					<i>Significance</i>
	<i>df</i>	<i>SS</i>	<i>MS</i>	<i>F</i>	<i>F</i>
Regression	1	6313.55	6313.55	3.635256	0.307515
Residual	2	3473.511	1736.755		
Total	3	9787.061			

	<i>Coefficients</i>	<i>Standard Error</i>	<i>t Stat</i>	<i>P-value</i>	<i>Lower 95%</i>	<i>Upper 95%</i>
Intercept	0	#N/A	#N/A	#N/A	#N/A	#N/A
X Variable 1	1.42995	0.749987	1.906635	0.196824	-1.79698	4.656882

Appendix D.56: 50% Peat and 50% Sand (Mixture $D_{50} = 1600 \text{ um}$ and $C_u = 2.5$), Hand Compaction ($\rho = 0.96 \text{ g/cm}^3$), High Concentration Regression Statics.

<i>Regression Statistics</i>	
Multiple R	0.965382
R Square	0.931963
Adjusted R Square	
Standard Error	142.4387
Observations	3

ANOVA					<i>Significance</i>
	<i>df</i>	<i>SS</i>	<i>MS</i>	<i>F</i>	<i>F</i>
Regression	1	555829	555829	27.39587	0.120181
Residual	2	40577.57	20288.79		
Total	3	596406.5			

	<i>Coefficients</i>	<i>Standard Error</i>	<i>t Stat</i>	<i>P-value</i>	<i>Lower 95%</i>	<i>Upper 95%</i>
Intercept	0	#N/A	#N/A	#N/A	#N/A	#N/A
X Variable 1	33.28686	6.359606	5.234106	0.034618	5.923678	60.65003

Appendix D.57: 50% Peat and 50% Sand (Mixture $D_{50} = 1600 \text{ um}$ and $C_u = 2.5$), Modified Proctor Compaction ($\rho = 1.23 \text{ g/cm}^3$), Low Concentration Regression Statics.

<i>Regression Statistics</i>	
Multiple R	0.99812
R Square	0.996243
Adjusted R Square	0.496243
Standard Error	4.287985
Observations	3

ANOVA

	<i>df</i>	<i>SS</i>	<i>MS</i>	<i>F</i>	<i>Significance F</i>
Regression	1	9750.287	9750.287	530.2868	0.027628
Residual	2	36.77363	18.38682		
Total	3	9787.061			

	<i>Coefficients</i>	<i>Standard Error</i>	<i>t Stat</i>	<i>P-value</i>	<i>Lower 95%</i>	<i>Upper 95%</i>
Intercept	0	#N/A	#N/A	#N/A	#N/A	#N/A
X Variable 1	2.605781	0.113157	23.02796	0.00188	2.118905	3.092658

Appendix D.58: 50% Peat and 50% Sand (Mixture $D_{50} = 1600 \text{ um}$ and $C_u = 2.5$), Modified Proctor Compaction ($\rho = 1.23 \text{ g/cm}^3$), High Concentration Regression Statics.

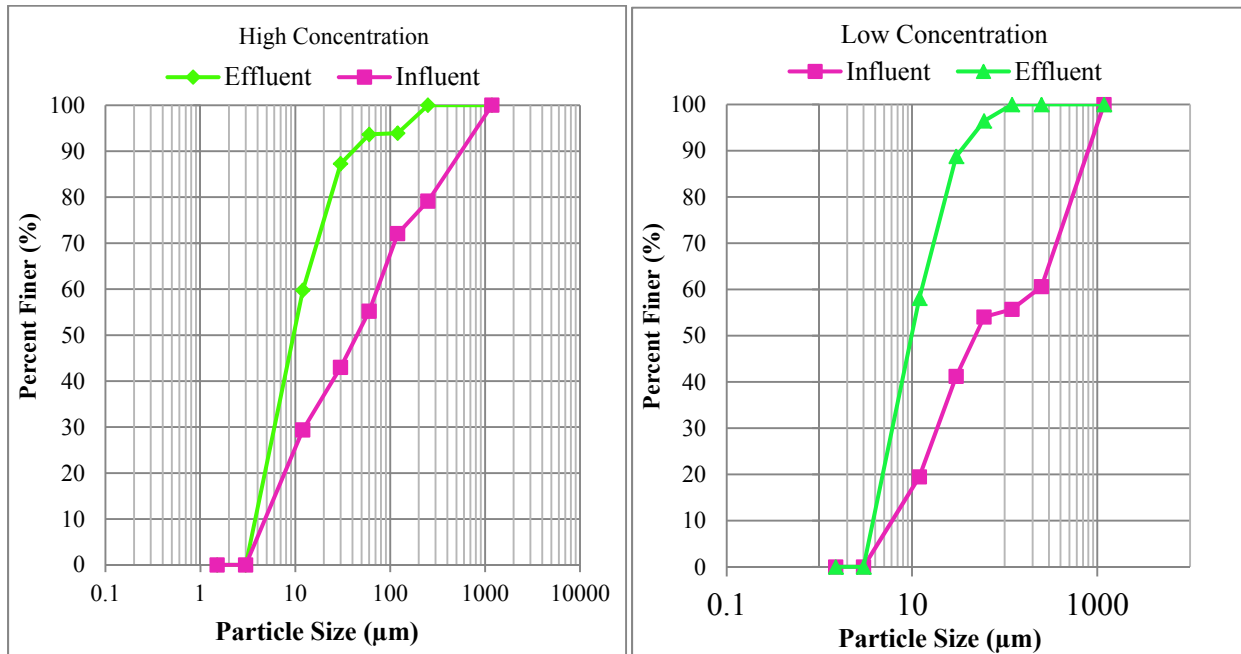
<i>Regression Statistics</i>	
Multiple R	0.991756
R Square	0.98358
Adjusted R Square	0.48358
Standard Error	69.97495
Observations	3

ANOVA

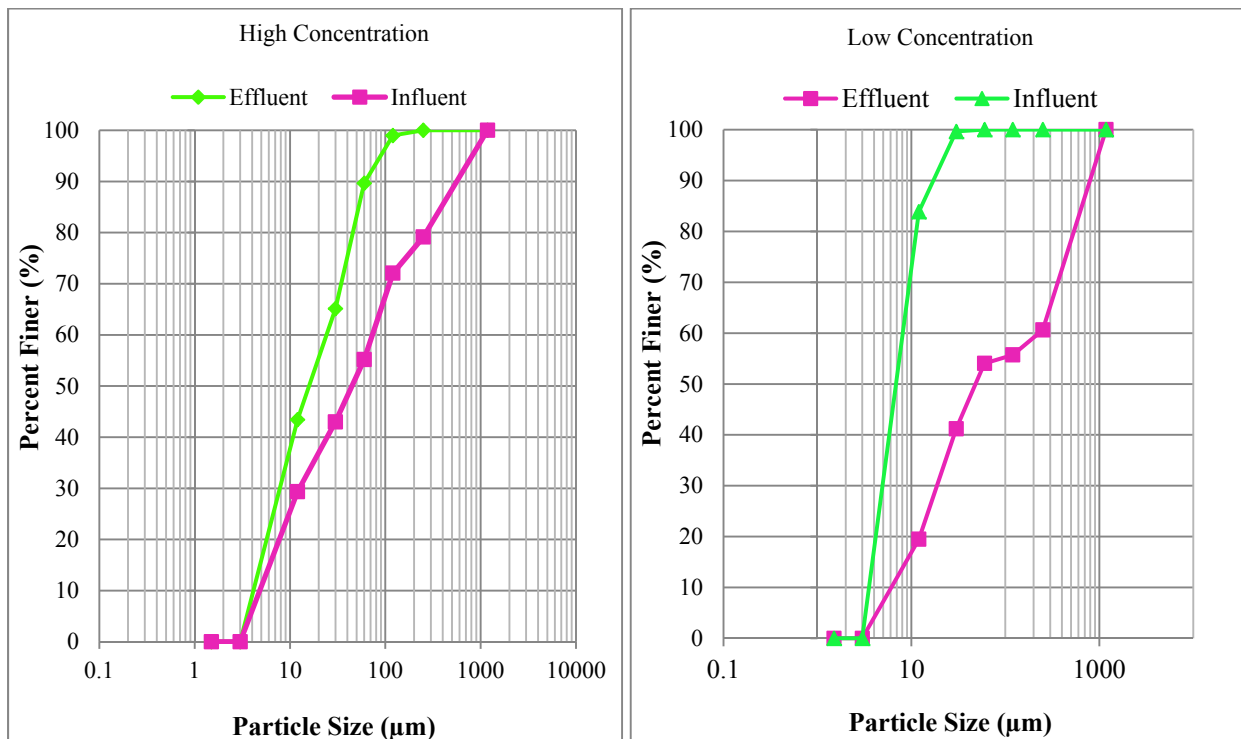
	<i>df</i>	<i>SS</i>	<i>MS</i>	<i>F</i>	<i>Significance F</i>
Regression	1	586613.5	586613.5	119.8028	0.058002
Residual	2	9792.986	4896.493		
Total	3	596406.5			

	<i>Coefficients</i>	<i>Standard Error</i>	<i>t Stat</i>	<i>P-value</i>	<i>Lower 95%</i>	<i>Upper 95%</i>
Intercept	0	#N/A	#N/A	#N/A	#N/A	#N/A
X Variable 1	52.41199	4.788474	10.94545	0.008244	31.80885	73.01513

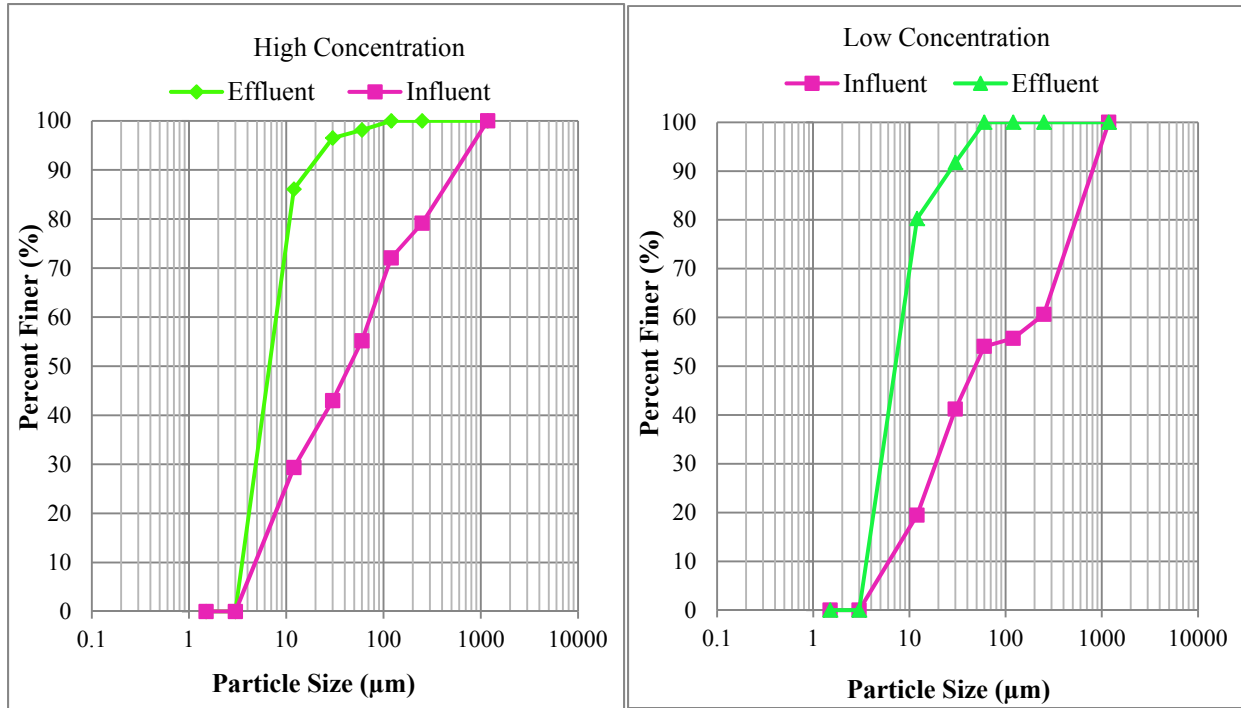
Appendix D. 59: Particle Size Distribution Plots of Influent vs Effluent Concentrations
 50% Peat and 50% Tuscaloosa Surface Soil ($D_{50} = 325 \mu\text{m}$ & $C_u = 7$) and Density = 0.85g/cc



50% Peat and 50% Tuscaloosa Surface Soil ($D_{50} = 325 \mu\text{m}$ & $C_u = 7$) and Density = 1.01g/cc

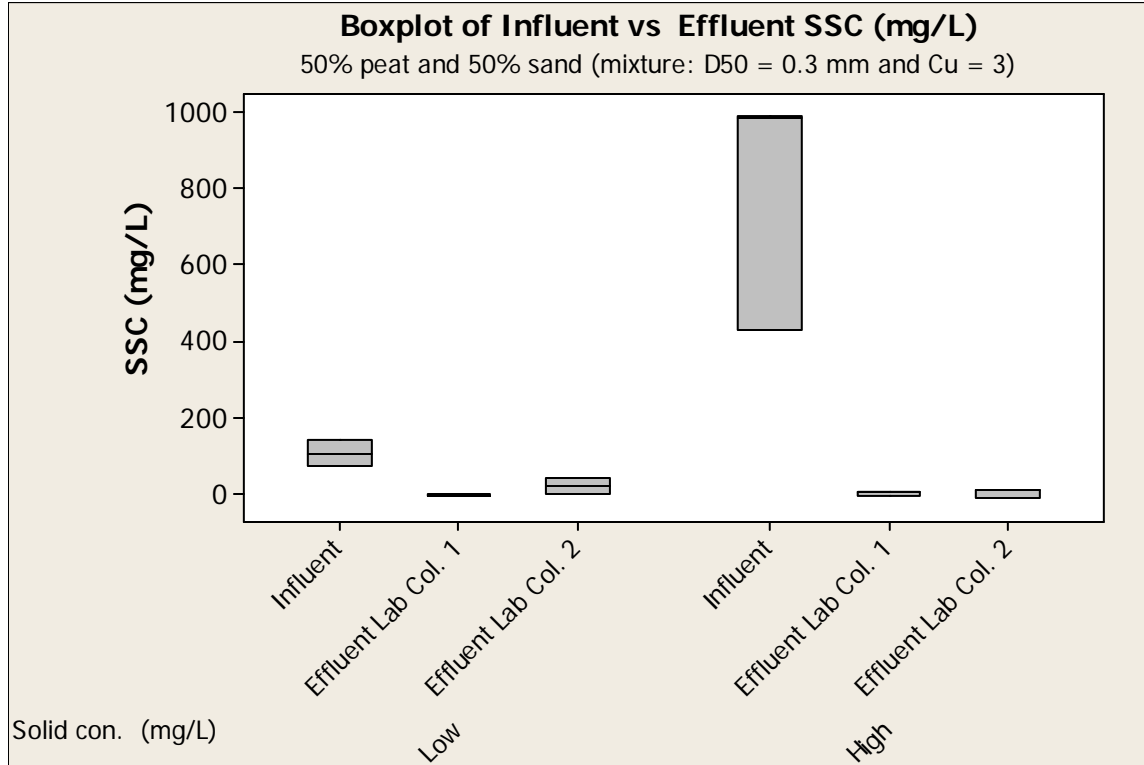


10% Peat and 90% Sand ($D_{50} = 340 \mu\text{m}$ & $C_u = 1.3$) and Density = 1.28 g/cc



Appendix D.60: One-way ANOVA Comparison for Infiltration Rates Through 10% Peat and 90% Sand Mixture ($D_{50} = 0.3$ mm and $C_u = 3$).

Mixture	Lob column	Compaction
50% peat and	1	hand ($\rho = 0.74$ g/cc)
50% Sand	2	modified proctor ($\rho = 1.03$ g/cc)



Source	DF	SS	MS	F	P
Factor	5	1475748	295150	12.58	0.001
Error	9	211113	23457		
Total	14	1686862			

S = 153.2 R-Sq = 87.48% R-Sq(adj) = 80.53%

Level	N	Mean	StDev	Individual 95% CIs For Mean Based on Pooled StDev
Influent-1	2	103.3	47.7	(-----*-----)
Effluent Lab Col. 1	2	-5.9	1.1	(-----*-----)
Effluent Lab Col. 2	2	17.0	31.1	(-----*-----)
Influent-2	3	798.3	322.1	(-----*-----)
Effluent Lab Col. 1*	3	-1.3	7.3	(-----*-----)
Effluent Lab Col. 2*	3	0.6	10.0	(-----*-----)

Pooled StDev = 153.2

Grouping Information Using Tukey Method

	N	Mean	Grouping
Influent-2	3	798.3	A
Influent-1	2	103.3	B
Effluent Lab Col. 2	2	17.0	B
Effluent Lab Col. 2*	3	0.6	B
Effluent Lab Col. 1*	3	-1.3	B
Effluent Lab Col. 1	2	-5.9	B

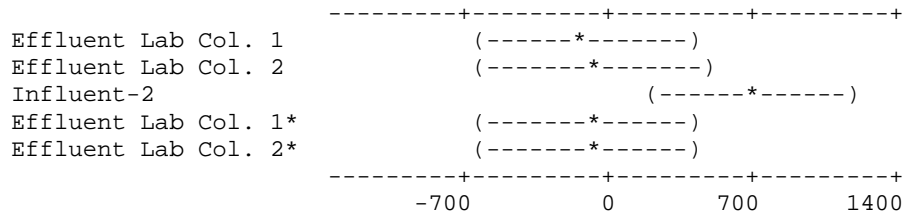
Means that do not share a letter are significantly different.

Tukey 95% Simultaneous Confidence Intervals
All Pairwise Comparisons

Individual confidence level = 99.38%

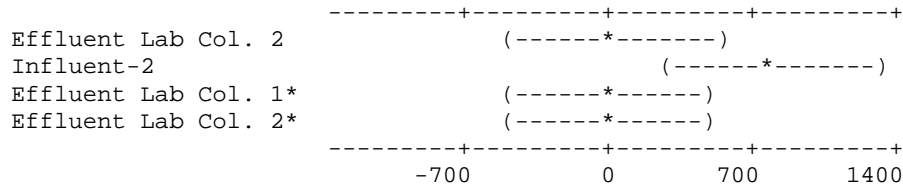
Influent-1 subtracted from:

	Lower	Center	Upper
Effluent Lab Col. 1	-652.8	-109.2	434.5
Effluent Lab Col. 2	-629.9	-86.3	457.4
Influent-2	198.7	695.0	1191.3
Effluent Lab Col. 1*	-600.9	-104.6	391.7
Effluent Lab Col. 2*	-599.0	-102.7	393.6



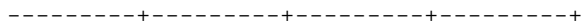
Effluent Lab Col. 1 subtracted from:

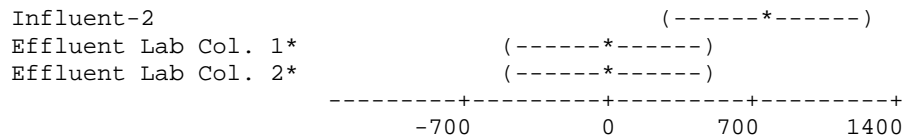
	Lower	Center	Upper
Effluent Lab Col. 2	-520.7	22.9	566.6
Influent-2	307.9	804.2	1300.5
Effluent Lab Col. 1*	-491.7	4.6	500.9
Effluent Lab Col. 2*	-489.8	6.5	502.8



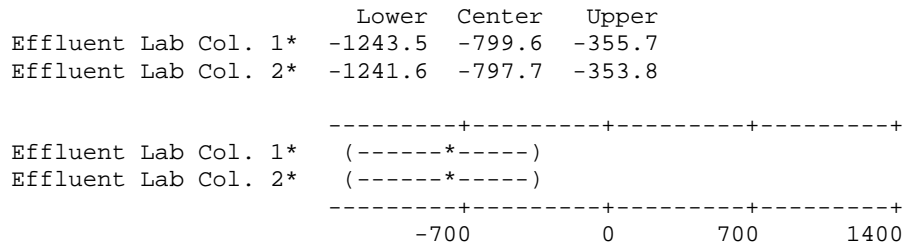
Effluent Lab Col. 2 subtracted from:

	Lower	Center	Upper
Influent-2	285.0	781.3	1277.6
Effluent Lab Col. 1*	-514.6	-18.3	478.0
Effluent Lab Col. 2*	-512.7	-16.4	479.8

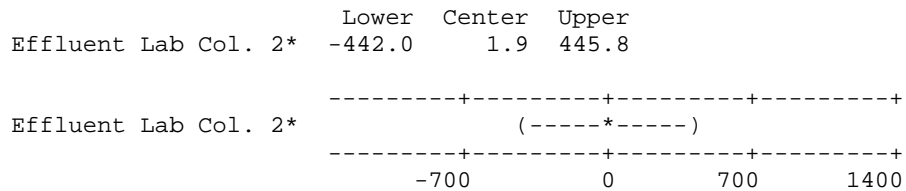




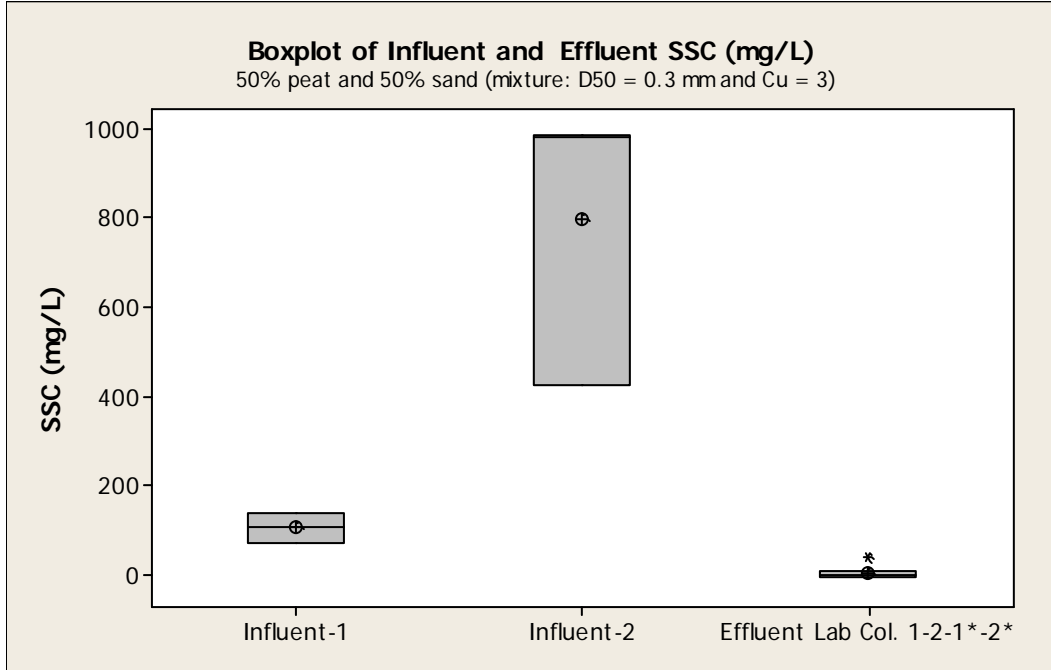
Influent-2 subtracted from:



Effluent Lab Col. 1* subtracted from:



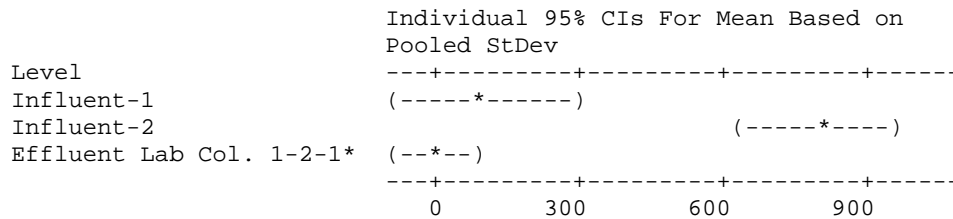
One-way ANOVA Comparison for Infiltration Rates Through 50% Peat and 50% Sand Mixture ($D_{50} = 0.3 \text{ mm}$ and $C_u = 3$) with Combined Data.



Source	DF	SS	MS	F	P
Factor	2	1475133	737567	41.80	0.000
Error	12	211728	17644		
Total	14	1686862			

S = 132.8 R-Sq = 87.45% R-Sq(adj) = 85.36%

Level	N	Mean	StDev
Influent-1	2	103.3	47.7
Influent-2	3	798.3	322.1
Effluent Lab Col. 1-2-1*	10	2.0	14.5



Pooled StDev = 132.8

Grouping Information Using Tukey Method

	N	Mean	Grouping
Influent-2	3	798.3	A

Influent-1	2	103.3	B
Effluent Lab Col. 1-2-1*-2*	10	2.0	B

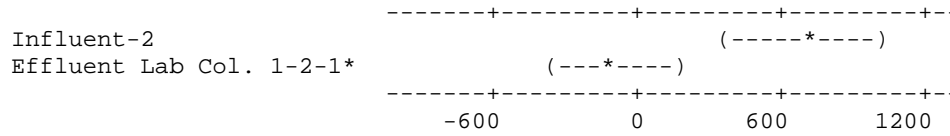
Means that do not share a letter are significantly different.

Tukey 95% Simultaneous Confidence Intervals
All Pairwise Comparisons

Individual confidence level = 97.94%

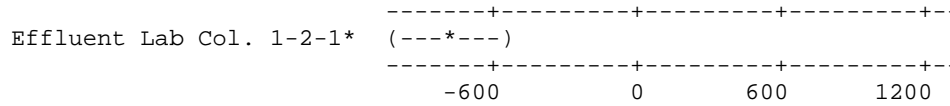
Influent-1 subtracted from:

	Lower	Center	Upper
Influent-2	371.8	695.0	1018.3
Effluent Lab Col. 1-2-1*	-375.6	-101.3	173.0



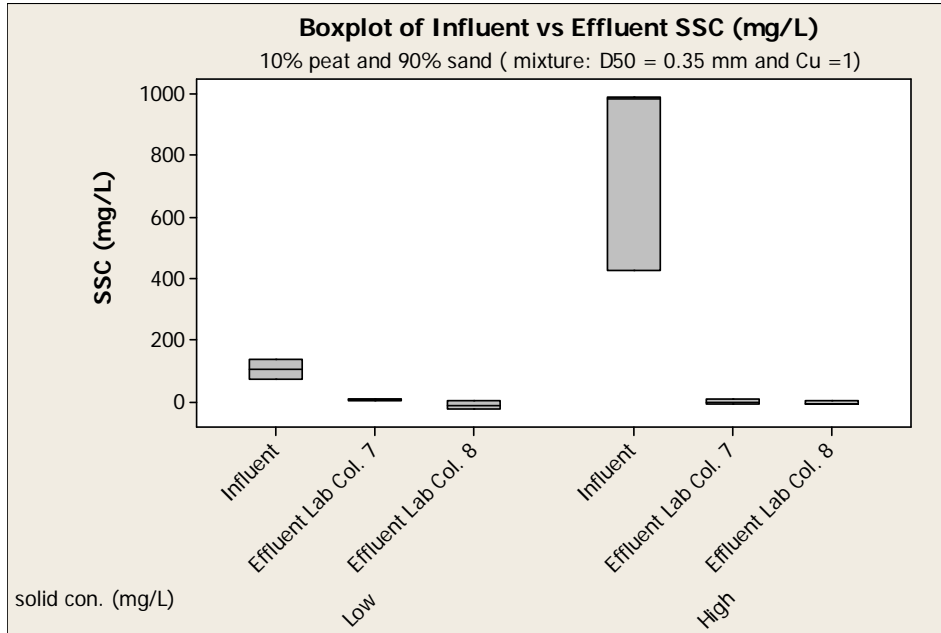
Influent-2 subtracted from:

	Lower	Center	Upper
Effluent Lab Col. 1-2-1*	-1029.4	-796.3	-563.2



Appendix D.61: One-way ANOVA Comparison for for Infiltration Rates Through 10% Peat and 90% Sand Mixture ($D_{50} = 0.35$ mm and $C_u = 1$).

Mixture	Lob column	Compaction
10% peat and 90% Sand	7	hand ($\rho = 1.28$ g/cc)
	8	modified proctor ($\rho = 1.35$ g/cc)



Source	DF	SS	MS	F	P
Factor	5	1493596	298719	12.78	0.001
Error	9	210341	23371		
Total	14	1703936			

S = 152.9 R-Sq = 87.66% R-Sq(adj) = 80.80%

Level	N	Mean	StDev	Individual 95% CIs For Mean Based on Pooled StDev
Influent-1	2	103.3	47.7	(-----*-----)
Effluent Lab Col. 7	2	5.8	2.6	(-----*-----)
Effluent Lab Col. 8	2	-12.4	16.2	(-----*-----)
Influent-2	3	798.3	322.1	(-----*-----)
Effluent Lab Col. 7*	3	-1.9	8.6	(-----*-----)
Effluent Lab Col. 8*	3	-4.5	6.6	(-----*-----)

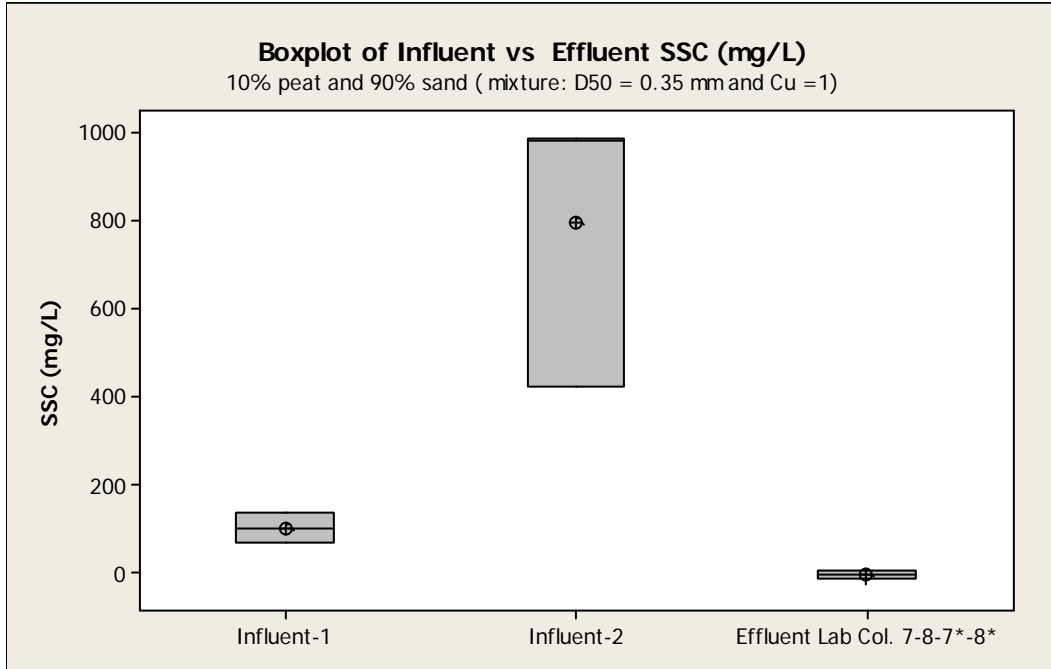
Pooled StDev = 152.9

***7 and *8 1000 mg/L solid concentration columns**

Grouping Information Using Tukey Method	N	Mean	Grouping
Influent-2	3	798.3	A
Influent-1	2	103.3	B
Effluent Lab Col. 7	2	5.8	B
Effluent Lab Col. 7*	3	-1.9	B
Effluent Lab Col. 8*	3	-4.5	B
Effluent Lab Col. 8	2	-12.4	B

Means that do not share a letter are significantly different.

One-way ANOVA Comparison for for Infiltration Rates Through 10% Peat and 90% Sand Mixture ($D_{50} = 0.35$ mm and $C_u = 1$) with Combined Data.



Source	DF	SS	MS	F	P
Factor	2	1493256	746628	42.53	0.000
Error	12	210681	17557		
Total	14	1703936			

S = 132.5 R-Sq = 87.64% R-Sq(adj) = 85.57%

Level	N	Mean	StDev
Influent-1	2	103.3	47.7
Influent-2	3	798.3	322.1
Effluent Lab Col. 7-8-7*-8*	10	-3.2	9.7

Individual 95% CIs For Mean Based on Pooled StDev

Level	CI Lower	CI Upper
Influent-1	(-----*-----)	(-----*-----)
Influent-2	(--*--)	(-----*-----)
Effluent Lab Col. 7-8-7*-8*	(--*--)	(-----*-----)

0 300 600 900

Pooled StDev = 132.5

*7 and *8 1000 mg/L solid concentration columns

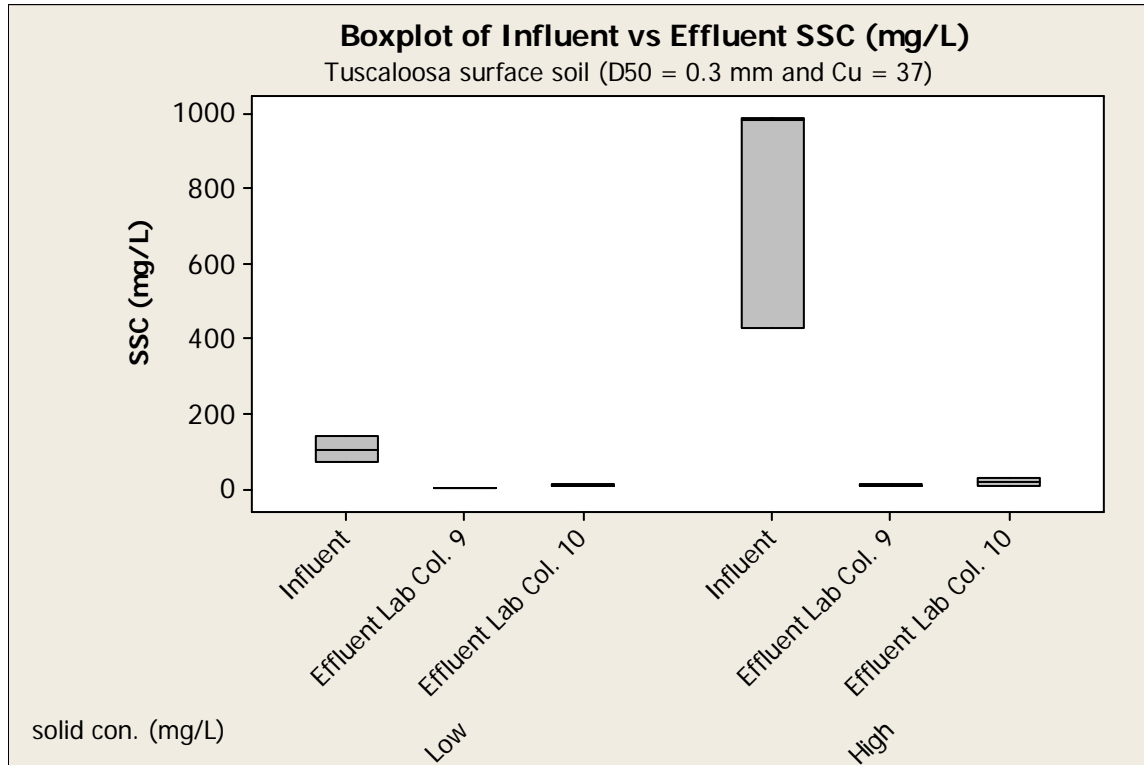
Grouping Information Using Tukey Method

Level	N	Mean	Grouping
Influent-2	3	798.3	A
Influent-1	2	103.3	B
Effluent Lab Col. 7-8-7*-8*	10	-3.2	B

Means that do not share a letter are significantly different.

Appendix D.62: One-way ANOVA Comparison for for Infiltration Rates Through Tuscaloosa Surface Soil ($D_{50} = 0.3$ mm and $C_u = 37$).

Mixture	Lob column	Compaction
Tuscaloosa	9	hand ($\rho = 1.42$ g/cc)
Surface Soil	10	modified proctor ($\rho = 1.67$ g/cc)



Source	DF	SS	MS	F	P
Factor	5	1451227	290245	12.43	0.001
Error	9	210128	23348		
Total	14	1661355			

S = 152.8 R-Sq = 87.35% R-Sq(adj) = 80.33%

Level	N	Mean	StDev
Influent-1	2	103.3	47.7
Effluent Lab Col. 9	2	2.1	1.6
Effluent Lab Col. 10	2	8.0	5.7
Influent-2	3	798.3	322.1
Effluent Lab Col. 9*	3	8.8	3.6
Effluent Lab Col. 10*	3	14.6	10.7

*9 and *10 1000 mg/L solid concentration columns

Individual 95% CIs For Mean Based on Pooled StDev

Level	CI
Influent-1	(-----*-----)
Effluent Lab Col. 9	(-----*-----)
Effluent Lab Col. 10	(-----*-----)
Influent-2	(-----*-----)
Effluent Lab Col. 9*	(-----*-----)

Effluent Lab Col. 10* (----*----)

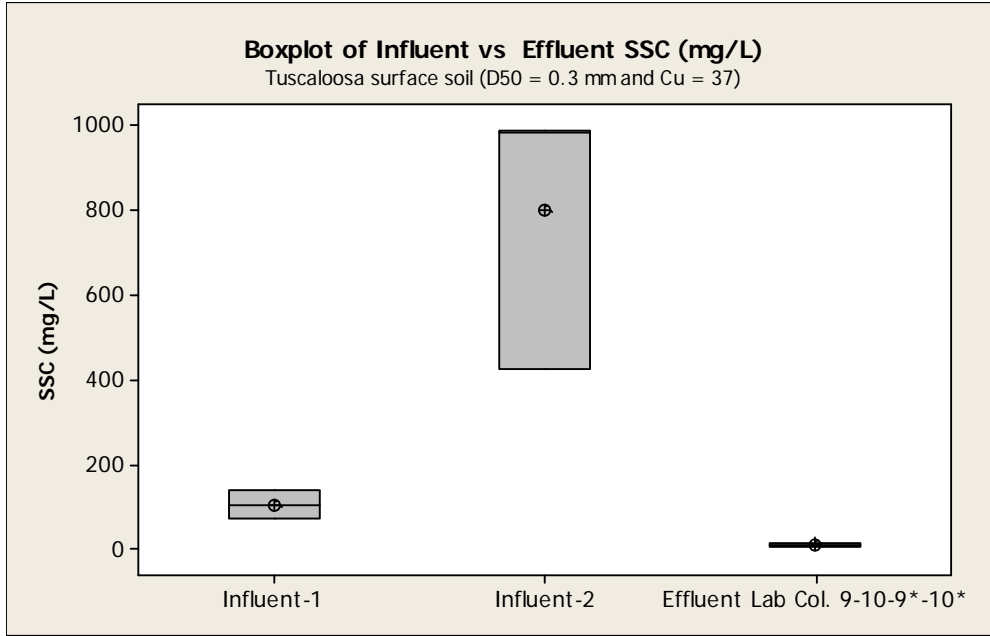
Pooled StDev = 152.8

Grouping Information Using Tukey Method

	N	Mean	Grouping
Influent-2	3	798.3	A
Influent-1	2	103.3	B
Effluent Lab Col. 10*	3	14.6	B
Effluent Lab Col. 9*	3	8.8	B
Effluent Lab Col. 10	2	8.0	B
Effluent Lab Col. 9	2	2.1	B

Means that do not share a letter are significantly different.

One-way ANOVA Comparison for Infiltration Rates Through Tuscaloosa Surface Soil (D50 = 0.3 mm and Cu = 37) with Combined Data.

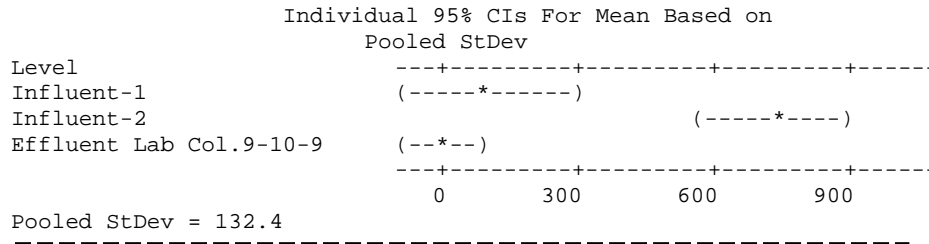


Source	DF	SS	MS	F	P
Factor	2	1451036	725518	41.40	0.000
Error	12	210319	17527		
Total	14	1661355			

S = 132.4 R-Sq = 87.34% R-Sq(adj) = 85.23%

Level	N	Mean	StDev
Influent-1	2	103.3	47.7
Influent-2	3	798.3	322.1
Effluent Lab Col. 9-10-9*10*	10	9.0	7.3

*9 and *10 1000 mg/L solid concentration columns

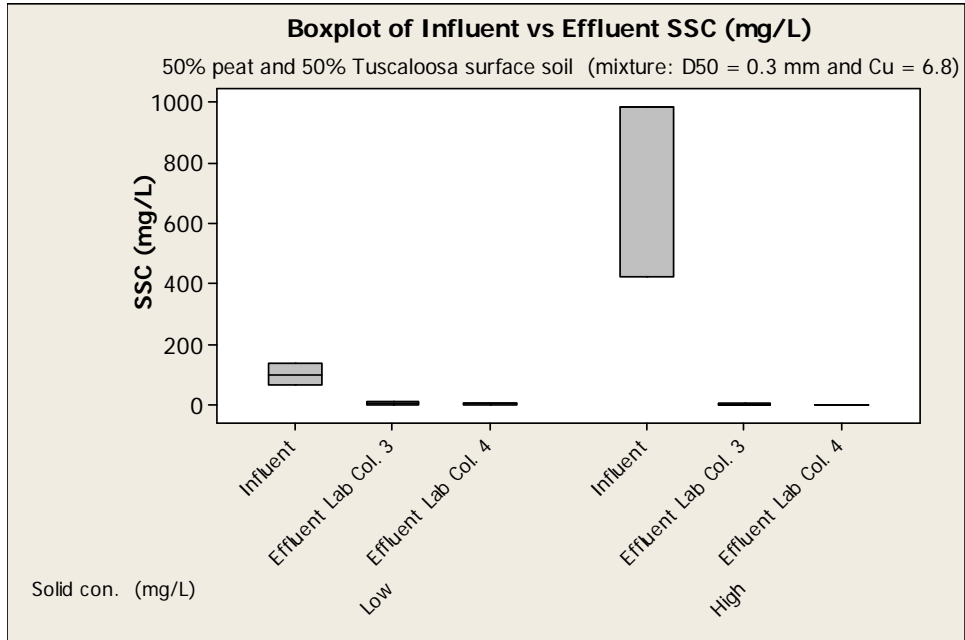


Grouping Information Using Tukey Method

Level	N	Mean	Grouping
Influent-2	3	798.3	A
Influent-1	2	103.3	B
Effluent Lab Col. 9-10-9*-10*	10	9.0	B

Means that do not share a letter are significantly different.

Appendix D.63: One-way ANOVA Comparison for Infiltration Rates Through 50% Peat and 50% Tuscaloosa Surface Soil Mixture ($D_{50} = 0.3$ mm and $C_u = 6.8$).



Mixture	Lob column	Compaction
50% peat and 50% Tuscaloosa Surface Soil	3	hand ($\rho = 0.85$ g/cc)
	4	modified proctor ($\rho = 1.01$ g/cc)

Source	DF	SS	MS	F	P
Factor	5	1464199	292840	12.56	0.001
Error	9	209895	23322		
Total	14	1674093			

S = 152.7 R-Sq = 87.46% R-Sq(adj) = 80.50%

Individual 95% CIs For Mean Based on Pooled StDev

Level	N	Mean	StDev
Influent-1	2	103.3	47.7
Effluent Lab Col. 3	2	9.5	6.7
Effluent Lab Col. 4	2	6.9	2.9
Influent-2	3	798.3	322.1
Effluent Lab Col. 3*	3	5.0	1.3
Effluent Lab Col. 4*	3	1.3	0.5

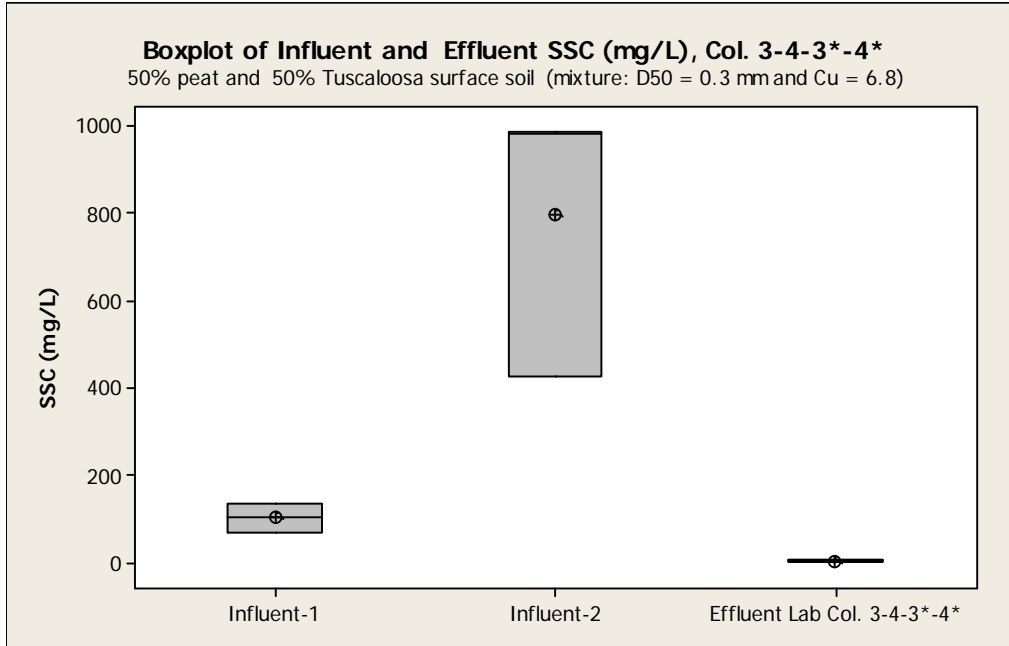
Pooled StDev = 152.7
 3* and 4* 1000 mg/L solid concentration columns

Grouping Information Using Tukey Method

	N	Mean	Grouping
Influent-2	3	798.3	A
Influent-1	2	103.3	B
Effluent Lab Col. 3	2	9.5	B
Effluent Lab Col. 4	2	6.9	B
Effluent Lab Col. 3*	3	5.0	B
Effluent Lab Col. 4*	3	1.3	B

Means that do not share a letter are significantly different.

One-way ANOVA Comparison for 50% Peat and 50% Tuscaloosa Surface Soil Mixture ($D_{50} = 0.3 \text{ mm}$ and $C_u = 6.8$) with Combined Data.

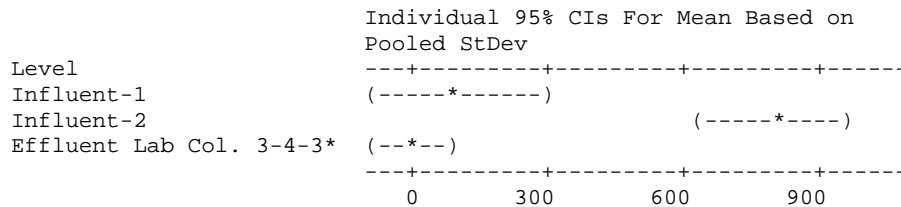


Source	DF	SS	MS	F	P
Factor	2	1464110	732055	41.84	0.000
Error	12	209983	17499		
Total	14	1674093			

S = 132.3 R-Sq = 87.46% R-Sq(adj) = 85.37%

Level	N	Mean	StDev
Influent-1	2	103.3	47.7
Influent-2	3	798.3	322.1
Effluent Lab Col. 3-4-3*-4*	10	5.2	4.0

3* and 4* 1000 mg/L solid concentration columns



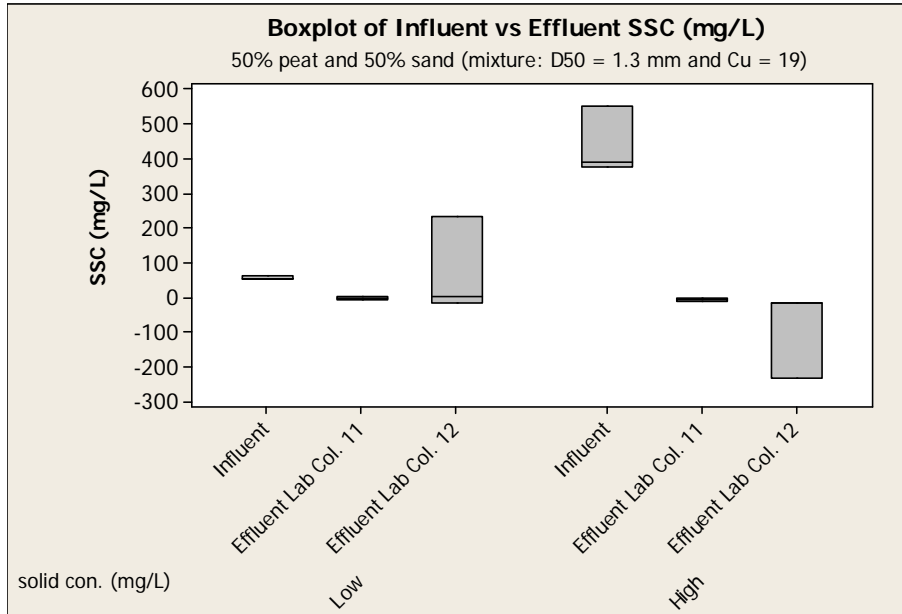
Pooled StDev = 132.3

Grouping Information Using Tukey Method	N	Mean	Grouping
Influent-2	3	798.3	A
Influent-1	2	103.3	B
Effluent Lab Col. 3-4-3*-4*	10	5.2	B

Means that do not share a letter are significantly different.

Appendix D.64: One-way ANOVA Comparison for Infiltration Rates Through 50% peat and 50% sand ($D_{50} = 1.3$ mm and $C_u = 19$)

Mixture	Lob column	Compaction
50% peat and 50% sand	11	hand ($\rho = 1.1$ g/cc)
	12	modified proctor ($\rho = 1.1$ g/cc)

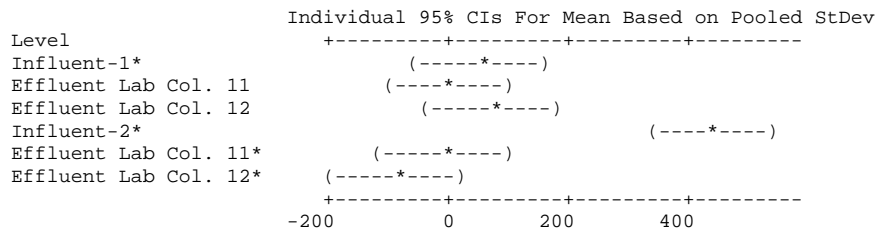


Source	DF	SS	MS	F	P
Factor	5	515373	103075	13.98	0.000
Error	12	88464	7372		
Total	17	603837			

S = 85.86 R-Sq = 85.35% R-Sq(adj) = 79.25%

Level	N	Mean	StDev
Influent-1*	3	57.01	4.33
Effluent Lab Col. 11	3	-1.26	3.62
Effluent Lab Col. 12	3	74.45	138.46
Influent-2*	3	439.01	95.46
Effluent Lab Col. 11*	3	-5.25	5.52
Effluent Lab Col. 12*	3	-88.76	126.03

11* and 12* 1000 mg/L solid concentration columns



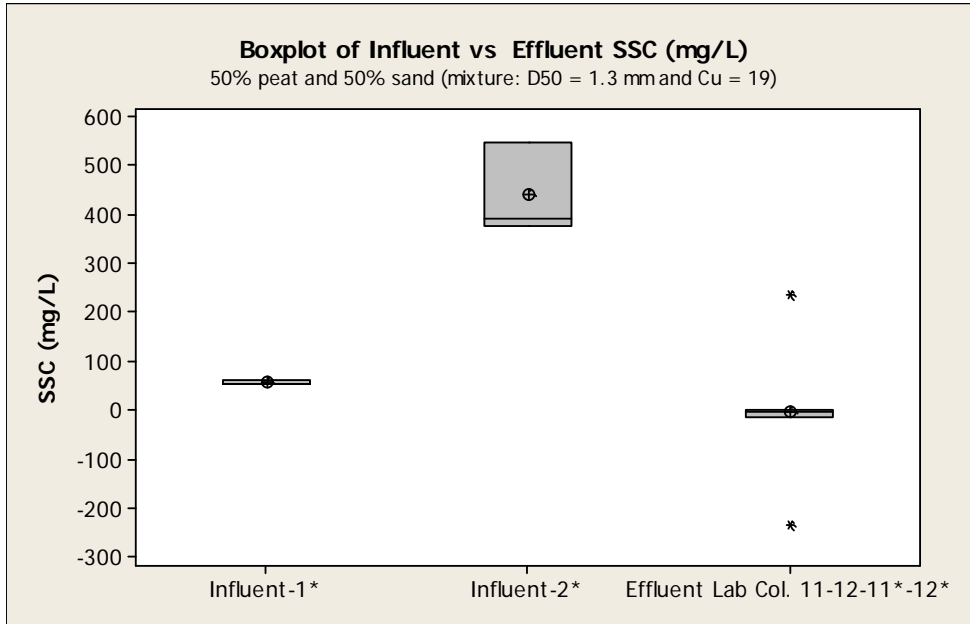
Pooled StDev = 85.86

Grouping Information Using Tukey Method

Level	N	Mean	Grouping
Influent-2*	3	439.01	A
Effluent Lab Col. 12	3	74.45	B
Influent-1*	3	57.01	B
Effluent Lab Col. 11	3	-1.26	B
Effluent Lab Col. 11*	3	-5.25	B
Effluent Lab Col. 12*	3	-88.76	B

Means that do not share a letter are significantly different.

One-way ANOVA Comparison for 50% Peat and 50% Sand ($D_{50} = 1.3$ mm and $C_u = 19$) with Combined Data.

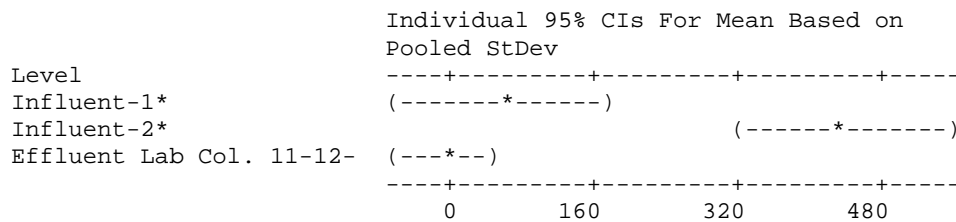


Source	DF	SS	MS	F	P
Factor	2	475349	237675	27.75	0.000
Error	15	128488	8566		
Total	17	603837			

S = 92.55 R-Sq = 78.72% R-Sq(adj) = 75.88%

Level	N	Mean	StDev
Influent-1*	3	57.01	4.33
Influent-2*	3	439.01	95.46
Effluent Lab Col. 11-12- 11*12*	12	-5.20	100.10

11* and 12* 1000 mg/L solid concentration columns



Pooled StDev = 92.55

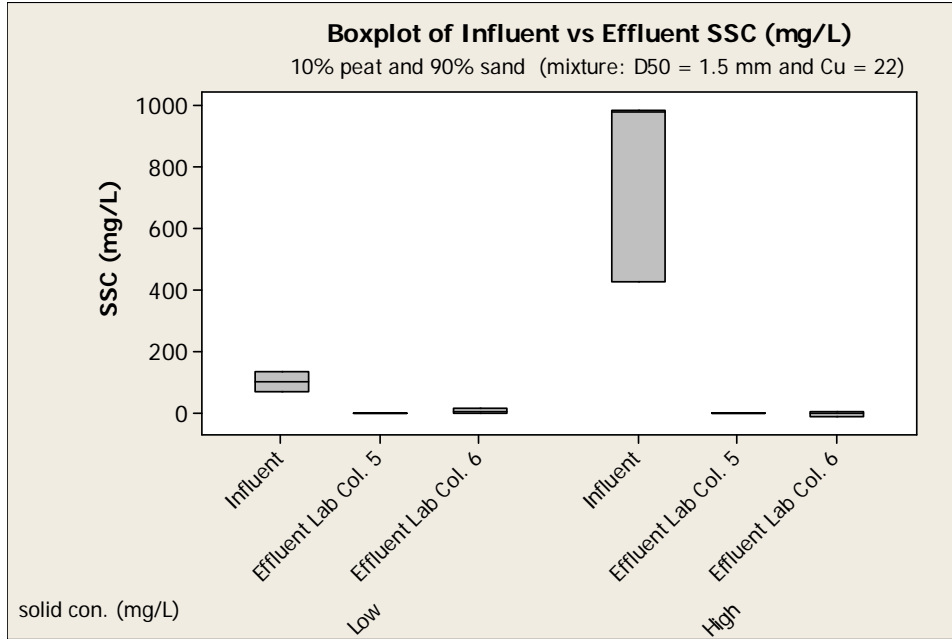
Grouping Information Using Tukey Method

	N	Mean	Grouping
Influent-2*	3	439.01	A
Influent-1*	3	57.01	B
Effluent Lab Col. 11-12-11*-12*	12	-5.20	B

Means that do not share a letter are significantly different.

Appendix D.65: One-way ANOVA Comparison for Infiltration Rates Through 10% Peat and 90% Sand Mixture (D50 = 1.5 mm and Cu = 22).

Mixture	Lob column	Compaction
	5	hand ($\rho = 1.61 \text{ g/cc}$)
10% peat and 90% Sand	6	modified proctor ($\rho = 1.63 \text{ g/cc}$)



Source	DF	SS	MS	F	P
Factor	5	1481804	296361	12.70	0.001
Error	9	210064	23340		
Total	14	1691868			

S = 152.8 R-Sq = 87.58% R-Sq(adj) = 80.69%

Level	N	Mean	StDev	Individual 95% CIs For Mean Based on Pooled StDev
Influent-1	2	103.3	47.7	(-----*-----)
Effluent Lab Col. 5	2	-1.0	2.8	(-----*-----)
Effluent Lab Col. 6	2	7.1	8.8	(-----*-----)
Influent-2	3	798.3	322.1	(-----*-----)
Effluent Lab Col. 5*	3	-1.3	1.5	(-----*-----)
Effluent Lab Col. 6*	3	-2.5	8.3	(-----*-----)

0 350 700 1050

Pooled StDev = 152.8

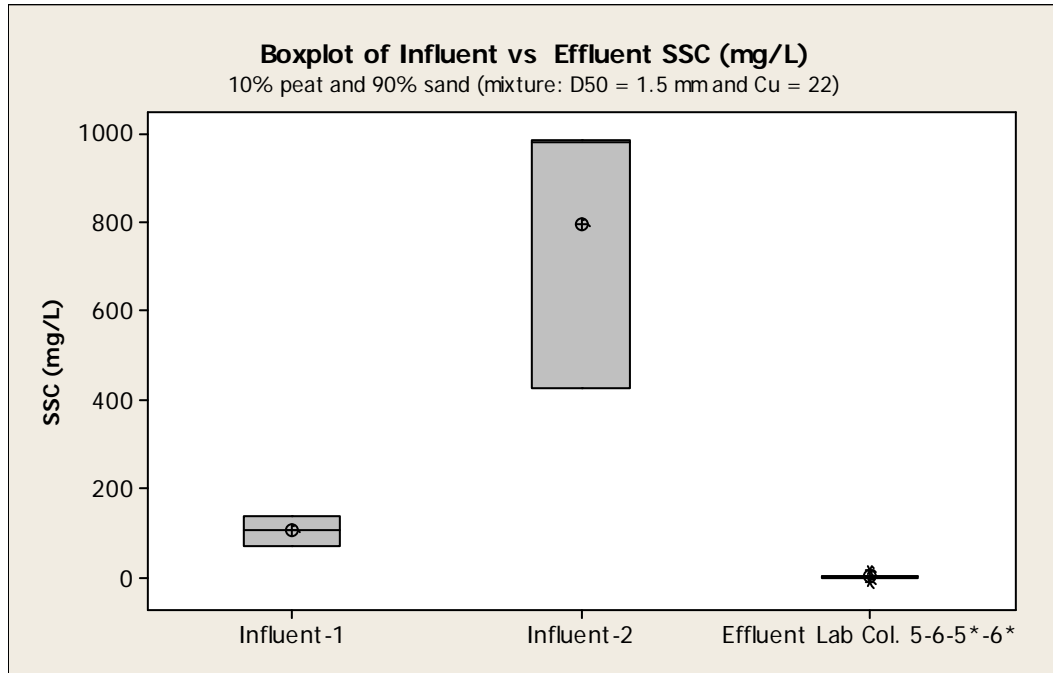
5* and 6* 1000 mg/L solid concentration columns

Grouping Information Using Tukey Method

	N	Mean	Grouping
Influent-2	3	798.3	A
Influent-1	2	103.3	B
Effluent Lab Col. 6	2	7.1	B
Effluent Lab Col. 5	2	-1.0	B
Effluent Lab Col. 5*	3	-1.3	B
Effluent Lab Col. 6*	3	-2.5	B

Means that do not share a letter are significantly different.

One-way ANOVA Comparison for 10% Peat and 90% Sand Mixture ($D_{50} = 1.5 \text{ mm}$ and $C_u = 22$) with Combined Data.

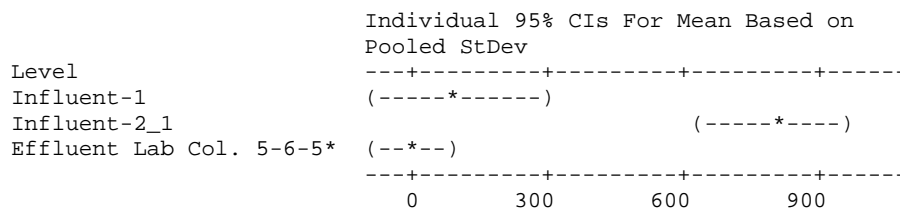


Source	DF	SS	MS	F	P
Factor	2	1481677	740838	42.30	0.000
Error	12	210191	17516		
Total	14	1691868			

S = 132.3 R-Sq = 87.58% R-Sq(adj) = 85.51%

Level	N	Mean	StDev
Influent-1	2	103.3	47.7
Influent-2_1	3	798.3	322.1
Effluent Lab Col. 5-6-5*-6*	10	0.1	6.3

5* and 6* 1000 mg/L solid concentration columns



Pooled StDev = 132.3
 5* and 6* 1000 mg/L solid concentration columns

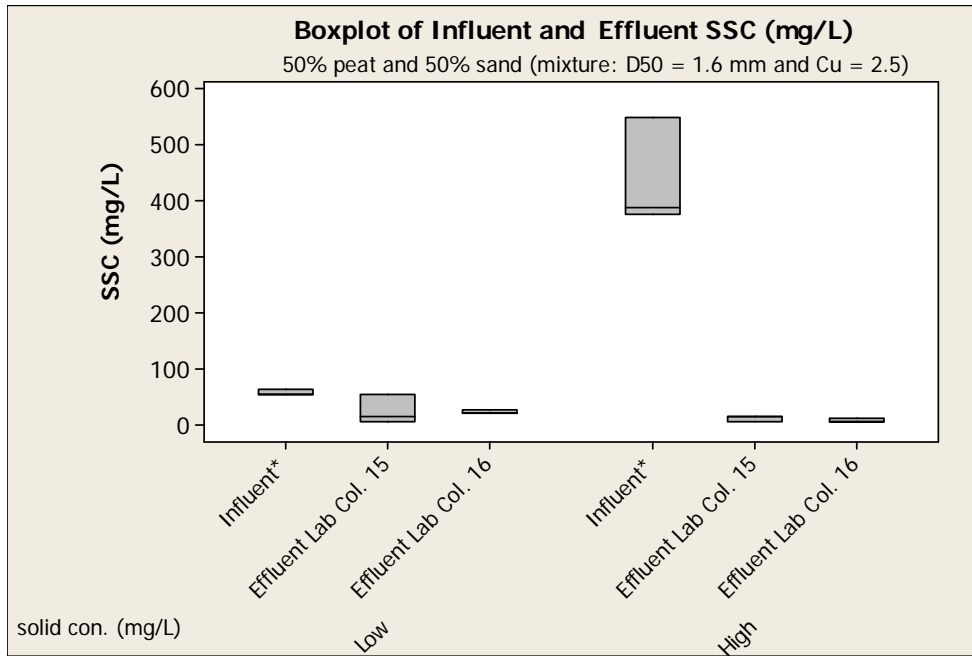
Grouping Information Using Tukey Method

Level	N	Mean	Grouping
Influent-2_1	3	798.3	A
Influent-1	2	103.3	B
Effluent Lab Col. 5-6-5*-6*	10	0.1	B

Means that do not share a letter are significantly different.

Appendix D.66: One-way ANOVA Comparison for Infiltration Rates Through 50% Peat and 50% Sand Mixture ($D_{50} = 1.6 \text{ mm}$ and $C_u = 2.5$).

Mixture	Lob column	Compaction
50% peat and 50% sand	15 16	hand ($\rho = 0.96 \text{ g/cc}$) modified proctor ($\rho = 1.23 \text{ g/cc}$)

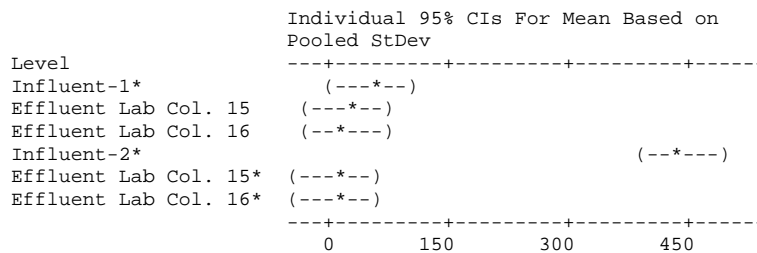


Source	DF	SS	MS	F	P
Factor	5	433492	86698	53.01	0.000
Error	12	19625	1635		
Total	17	453117			

S = 40.44 R-Sq = 95.67% R-Sq(adj) = 93.86%

Level	N	Mean	StDev
Influent-1*	3	57.01	4.33
Effluent Lab Col. 15	3	24.59	25.24
Effluent Lab Col. 16	3	21.71	3.29
Influent-2*	3	439.01	95.46
Effluent Lab Col. 15*	3	12.30	4.88
Effluent Lab Col. 16*	3	8.08	2.95

15* and 16* 1000 mg/L solid concentration columns



Pooled StDev = 40.44

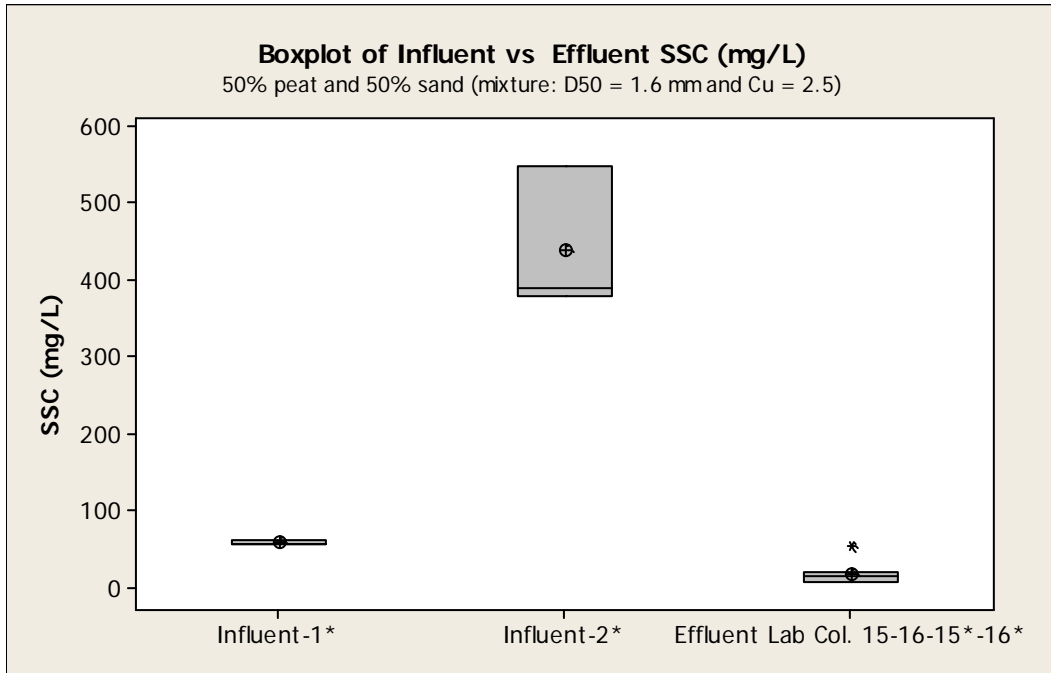
Grouping Information Using Tukey Method

N Mean Grouping

Influent-2*	3	439.01	A
Influent-1*	3	57.01	B
Effluent Lab Col. 15	3	24.59	B
Effluent Lab Col. 16	3	21.71	B
Effluent Lab Col. 15*	3	12.30	B
Effluent Lab Col. 16*	3	8.08	B

Means that do not share a letter are significantly different.

One-way ANOVA Comparison for 50% peat and 50% Sand Mixture ($D_{50} = 1.6$ mm and $C_u = 2.5$).



Source	DF	SS	MS	F	P
Factor	2	432950	216475	161.01	0.000
Error	15	20167	1344		
Total	17	453117			

S = 36.67 R-Sq = 95.55% R-Sq(adj) = 94.96%

Level	N	Mean	StDev
Influent-1*	3	57.01	4.33
Influent-2*	3	439.01	95.46
Effluent Lab Col. 15-16-15*-16*	12	16.67	13.15

15* and 16* 1000 mg/L solid concentration columns

Individual 95% CIs For Mean Based on Pooled StDev

Level	95% CI
Influent-1*	(--*--)
Influent-2*	(--*--)
Effluent Lab Col. 15-16-	(*--)

0 150 300 450

Pooled StDev = 36.67

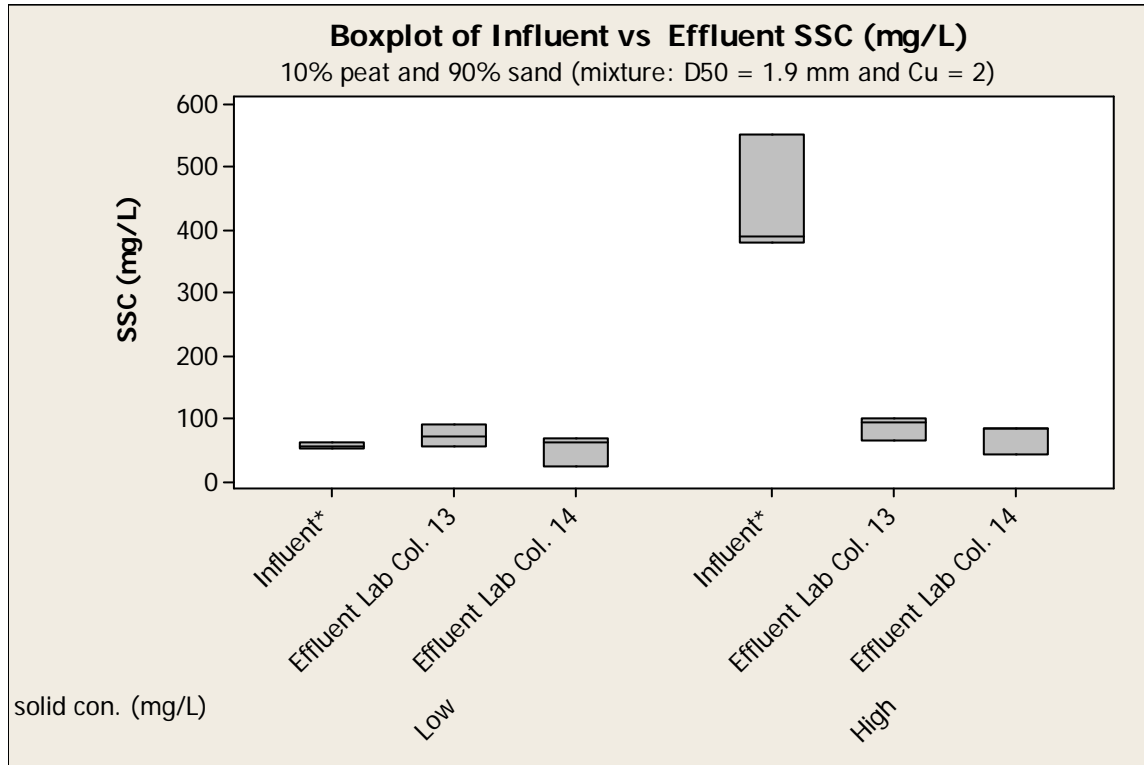
Grouping Information Using Tukey Method

	N	Mean	Grouping
Influent-2*	3	439.01	A
Influent-1*	3	57.01	B
Effluent Lab Col. 15-16-15*-16*	12	16.67	B

Means that do not share a letter are significantly different.

Appendix D.67: One-way ANOVA Comparison for Infiltration Rates Through 10% peat and 90% sand ($D_{50} = 1.9$ mm and $C_u = 2$).

Mixture	Lob column	Compaction
10% peat and 90% sand	13 14	hand ($\rho = 1.52$ g/cc) modified proctor ($\rho = 1.58$ g/cc)



Source	DF	SS	MS	F	P
Factor	5	346906	69381	38.05	0.000
Error	12	21882	1824		
Total	17	368788			

S = 42.70 R-Sq = 94.07% R-Sq(adj) = 91.59%

Level	N	Mean	StDev
Influent-1*	3	57.01	4.33
Effluent Lab Col. 13	3	73.67	17.01
Effluent Lab Col. 14	3	51.54	25.18
Influent-2*	3	439.01	95.46
Effluent Lab Col. 13*	3	85.76	17.65
Effluent Lab Col. 14*	3	70.52	23.97

13* and 14* 1000 mg/L solid concentration columns

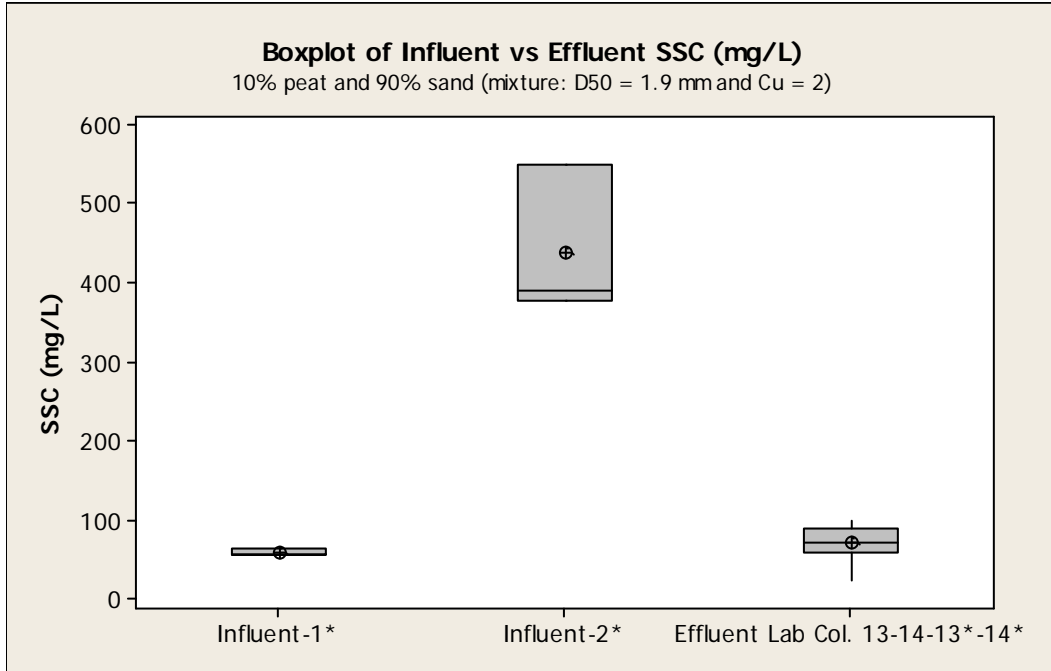
Level	Individual 95% CIs For Mean Based on Pooled StDev
Influent-1*	(---*--)
Effluent Lab Col. 13	(---*--)
Effluent Lab Col. 14	(---*--)
Influent-2*	(---*--)

```

Effluent Lab Col. 13*  (---*-- )
Effluent Lab Col. 14*  (---*-- )
+-----+-----+-----+-----+
0         150        300        450
Pooled StDev = 42.70
Grouping Information Using Tukey Method
N      Mean  Grouping
Influent-2*      3  439.01  A
Effluent Lab Col. 13*  3  85.76  B
Effluent Lab Col. 13  3  73.67  B
Effluent Lab Col. 14*  3  70.52  B
Influent-1*      3  57.01  B
Effluent Lab Col. 14  3  51.54  B
Means that do not share a letter are significantly different.
-----

```

One-way ANOVA Comparison for 10% peat and 90% sand ($D_{50} = 1.9$ mm and $C_u = 2$) with Combined Data.



Source	DF	SS	MS	F	P
Factor	2	345099	172549	109.26	0.000
Error	15	23690	1579		
Total	17	368788			

S = 39.74 R-Sq = 93.58% R-Sq(adj) = 92.72%

Level	N	Mean	StDev
Influent-1*	3	57.01	4.33
Influent-2*	3	439.01	95.46
Effluent Lab Col. 13-14-13*-14*	12	70.37	22.21

13* and 14* 1000 mg/L solid concentration columns

Individual 95% CIs For Mean Based on Pooled StDev

Level	Lower CI	Upper CI
Influent-1*	(---*---)	
Influent-2*		(---*---)
Effluent Lab Col. 13-14-	(-*-)	

-----+-----+-----+-----+
120 240 360 480

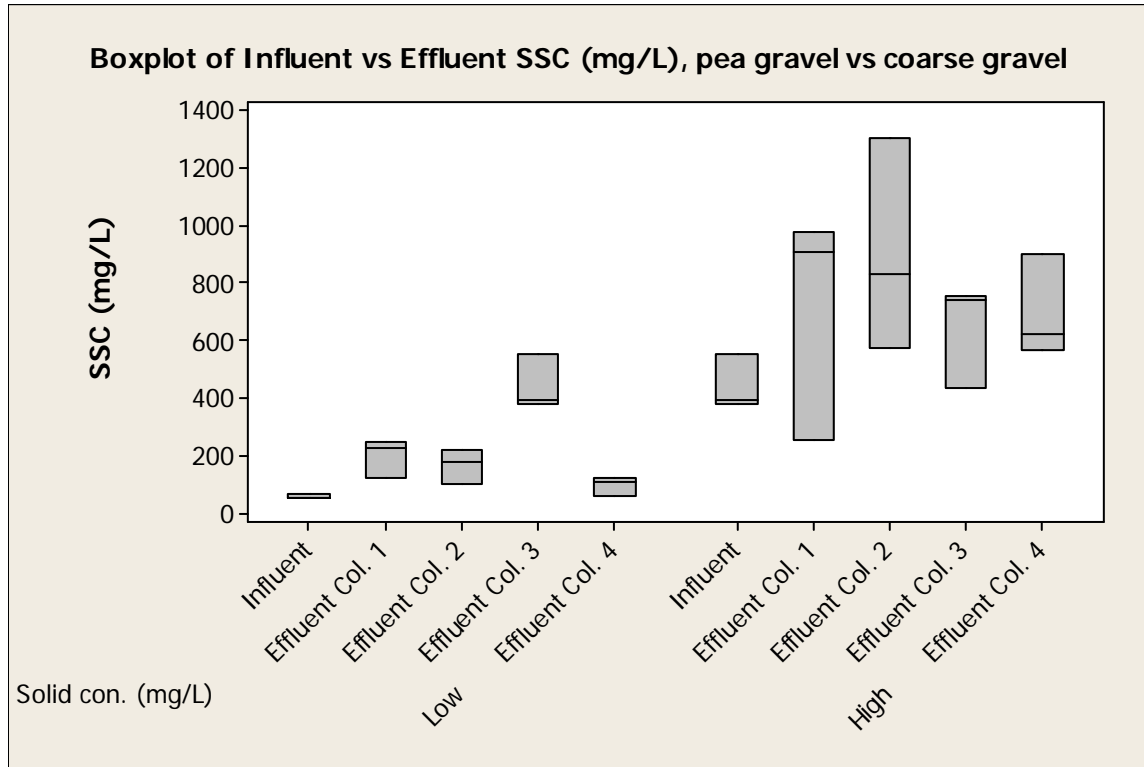
Pooled StDev = 39.74

Grouping Information Using Tukey Method

Level	N	Mean	Grouping
Influent-2*	3	439.01	A
Effluent Lab Col. 13-14-13*-14*	12	70.37	B
Influent-1*	3	57.01	B

Means that do not share a letter are significantly different.

Appendix D.68: One-way ANOVA Comparison for Infiltration Rates Through Pea Gravel vs Coarse Gravel. Low Solid Concentration.



Source	DF	SS	MS	F	P
Factor	4	268143	67036	18.65	0.000
Error	10	35941	3594		
Total	14	304083			

S = 59.95 R-Sq = 88.18% R-Sq(adj) = 83.45%

Level	N	Mean	StDev	Individual 95% CIs For Mean Based on Pooled StDev
Influent-1	3	57.01	4.33	(---*---)
Effluent Lab Col. 1	3	199.21	66.33	(---*---)
Effluent Lab Col. 3	3	439.01	95.46	(---*---)
Effluent Lab Col. 2	3	164.01	58.02	(---*---)
Effluent Lab Col. 4	3	95.48	32.73	(---*---)

Pooled StDev = 59.95

Grouping Information Using Tukey Method

Level	N	Mean	Grouping
Effluent Lab Col. 3	3	439.01	A

Effluent Lab Col. 1	3	199.21	B
Effluent Lab Col. 2	3	164.01	B
Effluent Lab Col. 4	3	95.48	B
Influent-1	3	57.01	B

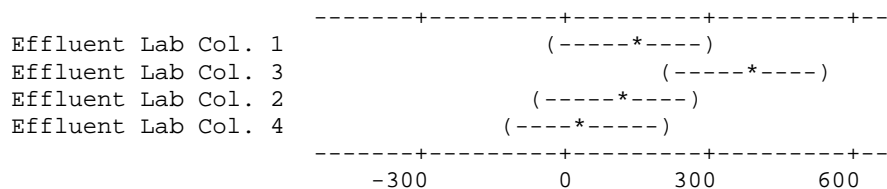
Means that do not share a letter are significantly different.

Tukey 95% Simultaneous Confidence Intervals
All Pairwise Comparisons

Individual confidence level = 99.18%

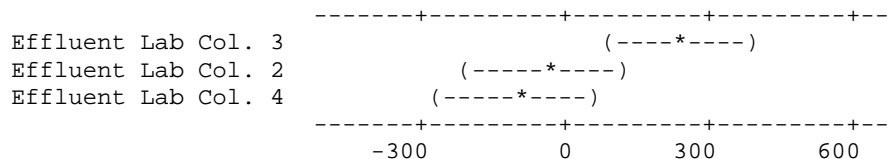
Influent-1 subtracted from:

	Lower	Center	Upper
Effluent Lab Col. 1	-18.74	142.21	303.16
Effluent Lab Col. 3	221.05	382.00	542.95
Effluent Lab Col. 2	-53.95	107.00	267.95
Effluent Lab Col. 4	-122.47	38.47	199.42



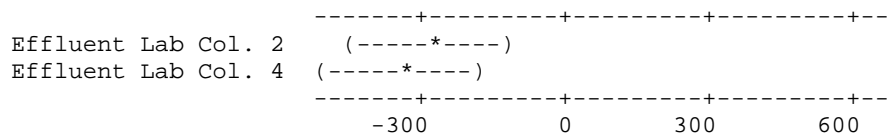
Effluent Lab Col. 1 subtracted from:

	Lower	Center	Upper
Effluent Lab Col. 3	78.84	239.79	400.74
Effluent Lab Col. 2	-196.15	-35.21	125.74
Effluent Lab Col. 4	-264.68	-103.73	57.22



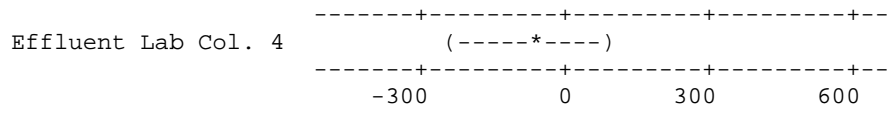
Effluent Lab Col. 3 subtracted from:

	Lower	Center	Upper
Effluent Lab Col. 2	-435.95	-275.00	-114.05
Effluent Lab Col. 4	-504.47	-343.52	-182.58

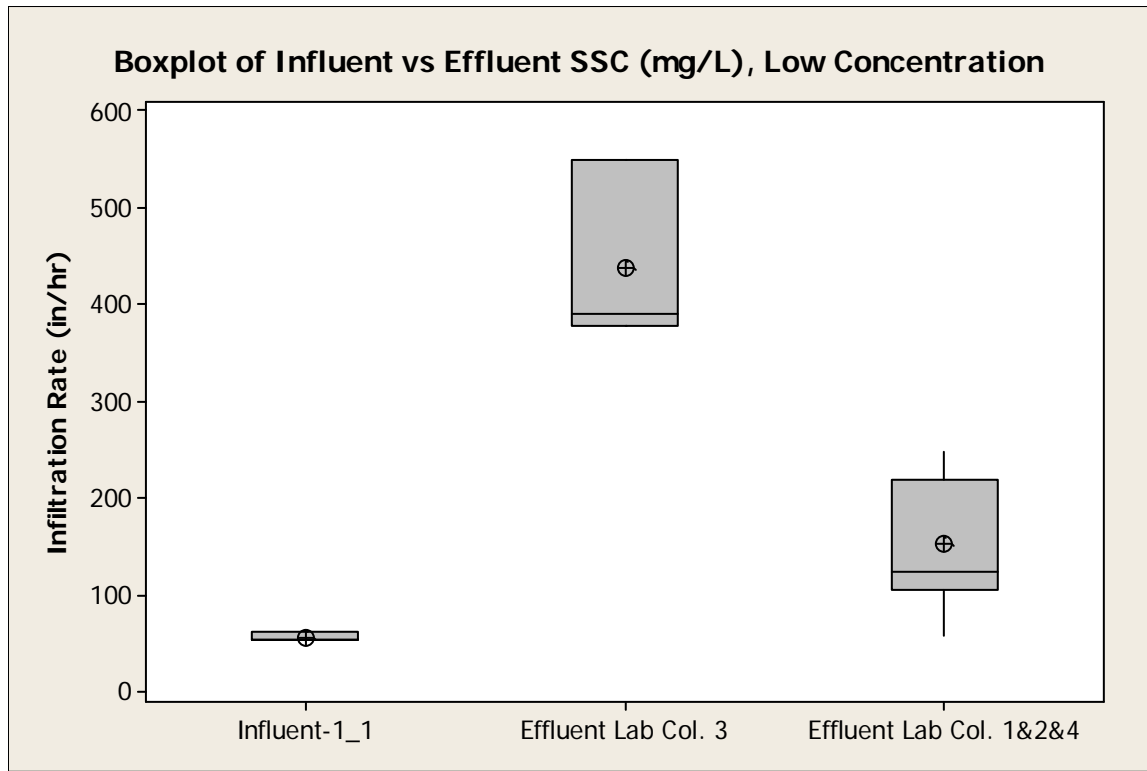


Effluent Lab Col. 2 subtracted from:

	Lower	Center	Upper
Effluent Lab Col. 4	-229.48	-68.53	92.42



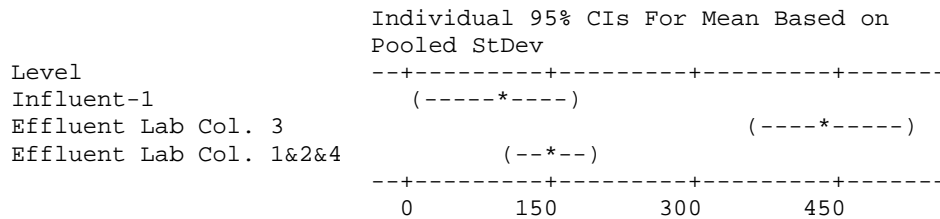
One-way ANOVA Comparison for Pea Gravel vs Coarse Gravel with Combined Data.



Source	DF	SS	MS	F	P
Factor	2	251447	125723	28.66	0.000
Error	12	52637	4386		
Total	14	304083			

S = 66.23 R-Sq = 82.69% R-Sq(adj) = 79.81%

Level	N	Mean	StDev
Influent-1	3	57.01	4.33
Effluent Lab Col. 3	3	439.01	95.46
Effluent Lab Col. 1&2&4	9	152.90	65.55



Pooled StDev = 66.23

Grouping Information Using Tukey Method

	N	Mean	Grouping
Effluent Lab Col. 3	3	439.01	A
Effluent Lab Col. 1&2&4	9	152.90	B
Influent-1	3	57.01	B

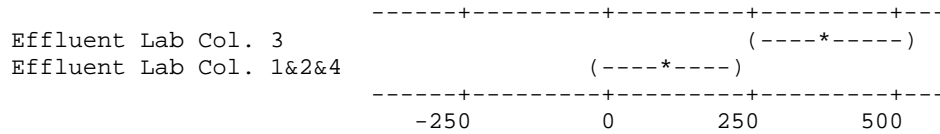
Means that do not share a letter are significantly different.

Tukey 95% Simultaneous Confidence Intervals
All Pairwise Comparisons

Individual confidence level = 97.94%

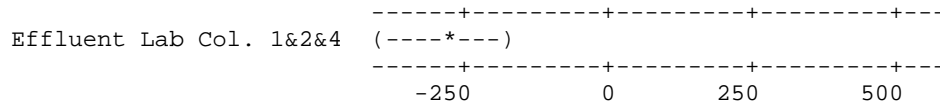
Influent-1_1 subtracted from:

	Lower	Center	Upper
Effluent Lab Col. 3	237.84	382.00	526.16
Effluent Lab Col. 1&2&4	-21.81	95.89	213.60



Effluent Lab Col. 3 subtracted from:

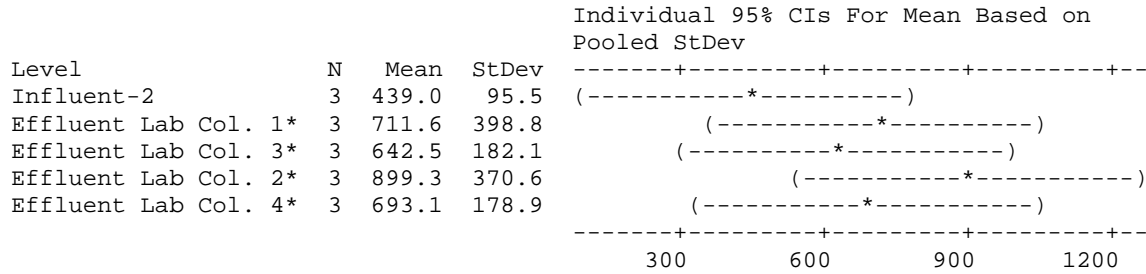
	Lower	Center	Upper
Effluent Lab Col. 1&2&4	-403.81	-286.10	-168.40



Appendix D.69: One-way ANOVA Comparison for Infiltration Rates Through Pea Gravel vs Coarse Gravel. High Solid Concentration.

Source	DF	SS	MS	F	P
Factor	4	326147	81537	1.10	0.408
Error	10	741272	74127		
Total	14	1067419			

S = 272.3 R-Sq = 30.55% R-Sq(adj) = 2.78%



Pooled StDev = 272.3

Grouping Information Using Tukey Method

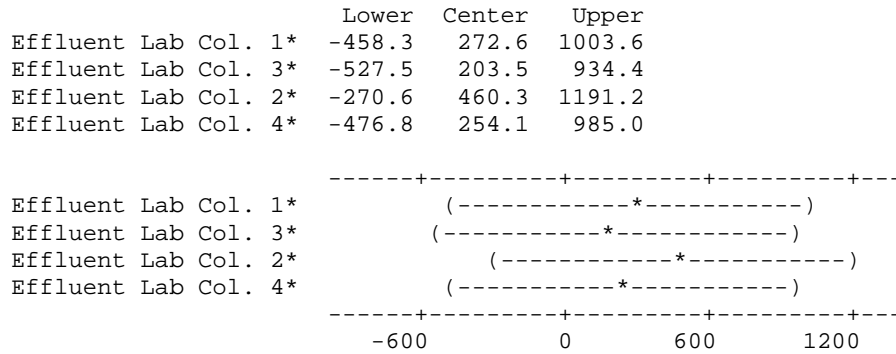
	N	Mean	Grouping
Effluent Lab Col. 2*	3	899.3	A
Effluent Lab Col. 1*	3	711.6	A
Effluent Lab Col. 4*	3	693.1	A
Effluent Lab Col. 3*	3	642.5	A
Influent-2	3	439.0	A

Means that do not share a letter are significantly different.

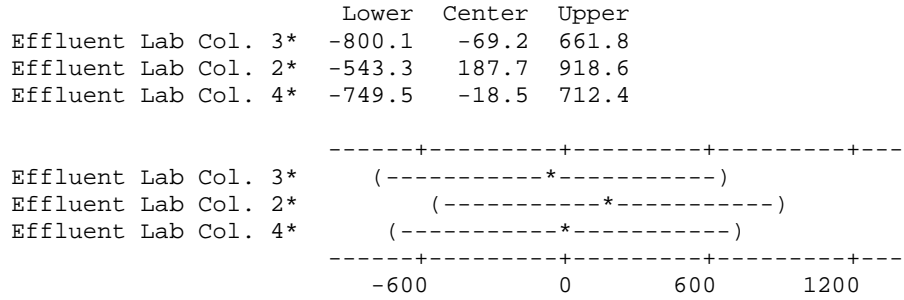
Tukey 95% Simultaneous Confidence Intervals
All Pairwise Comparisons

Individual confidence level = 99.18%

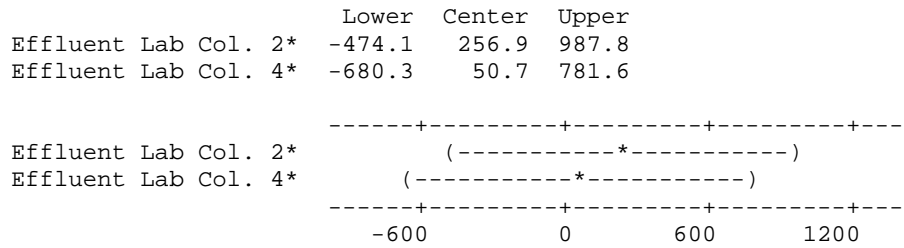
Influent-2 subtracted from:



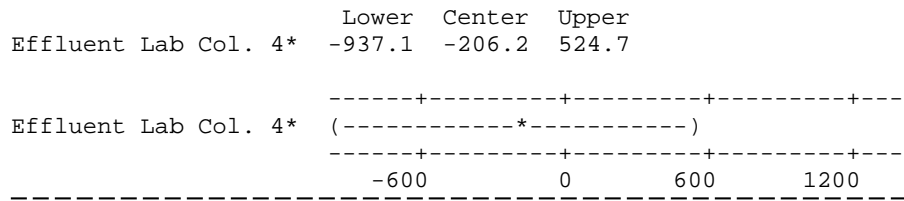
Effluent Lab Col. 1* subtracted from:



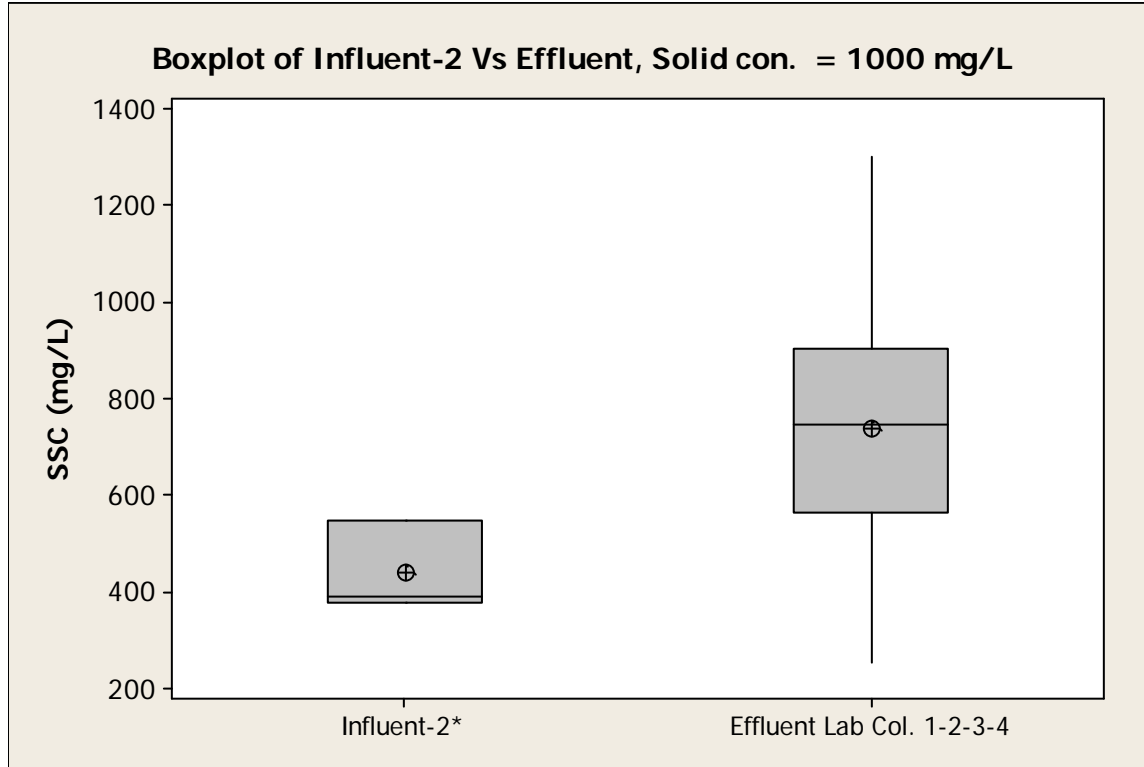
Effluent Lab Col. 3* subtracted from:



Effluent Lab Col. 2* subtracted from:



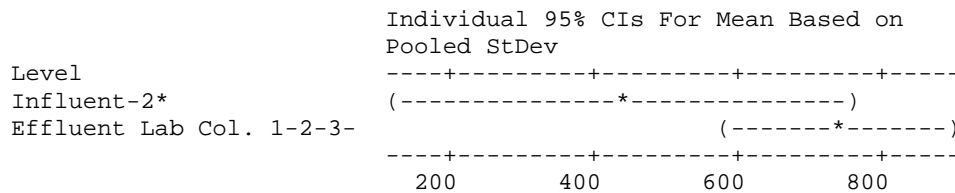
One-way ANOVA Comparison for Infiltration Rates Through Pea gravel vs Coarse Gravel, High Solid Concentration and Combined Data.



Source	DF	SS	MS	F	P
Factor	1	212594	212594	3.23	0.095
Error	13	854825	65756		
Total	14	1067419			

S = 256.4 R-Sq = 19.92% R-Sq(adj) = 13.76%

Level	N	Mean	StDev
Influent-2*	3	439.0	95.5
Effluent Lab Col. 1-2-3-	12	736.6	275.8



Pooled StDev = 256.4

Grouping Information Using Tukey Method

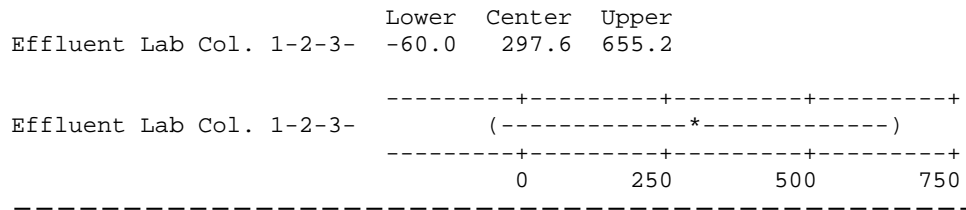
	N	Mean	Grouping
Effluent Lab Col. 1-2-3-4	12	736.6	A
Influent-2*	3	439.0	A

Means that do not share a letter are significantly different.

Tukey 95% Simultaneous Confidence Intervals
All Pairwise Comparisons

Individual confidence level = 95.00%

Influent-2* subtracted from:



APPENDIX E: SAND-PEAT COLUMN AND SMARTDRAIN™ FIELD PERFORMANCE

Appendix E.1: Full-factorial Data Analysis for Peat-Sand Media Particle Retention Experiments

Note: Full-factorial data analyses were performed after removing the outliers. These outliers are effluent SSCs from lab column consisting of 50% peat and 50% sand mixture ($D_{50} = 1.3 \text{ mm}$, $C_u = 20$, and density = 1.1 g/cm^3).

Analysis of Variance for SSC (mg/L) (coded units)

Source	DF	Seq SS	Adj SS	Adj MS	F	P
Main Effects	3	15463.6	14655.7	4885.2	9.16	0.00
T	1	8716	5934.1	5934.1	11.12	0.001
U	1	6677.2	3728.5	3728.5	6.99	0.01
C	1	70.4	34.1	34.1	0.06	0.801
2-Way Interactions	3	10542.8	10464.6	3488.2	6.54	0.001
T*U	1	9941	10134.6	10134.6	19	0.00
T*C	1	81.3	0.00	0.00	0.00	0.997
U*C	1	520.5	554.2	554.2	1.04	0.312
3-Way Interactions	1	43.2	43.2	43.2	0.08	0.777
T*U*C	1	43.2	43.2	43.2	0.08	0.777
Residual Error	60	32011.4	32011.4	533.5		
Pure Error	60	32011.4	32011.4	533.5		
Total	67	58061				

Effects and Half-Effects, and Using a Sand-peat Mixture

Case	Texture (T)	Uniformity (U)	Compaction(C)	TU	TC	UC	TUC	SSC (mg/L)
1	-	-	-	+	+	+	-	-10.66
2	+	-	-	-	-	+	+	37.97
3	-	+	-	-	+	-	+	7.75
4	+	+	-	+	-	-	-	-0.25
5	-	-	+	+	-	-	+	-1.19
6	+	-	+	-	+	-	-	44.01
7	-	+	+	-	-	+	-	1.31
8	+	+	+	+	+	+	+	-3.16
Y								
(grand)								9.4722
	T	U	C	TU	TC	UC	TUC	
Avg. Y@-1	-0.70	17.53	8.70	22.76	9.46	12.58	8.60	
Avg. Y@+1	19.64	1.41	10.24	-3.82	9.49	6.36	10.34	
Δ	20.34	-16.12	1.54	-26.58	0.03	-6.22	1.74	
Δ/2	10.17	-8.06	0.77	-13.29	0.01	-3.11	0.87	

$$\hat{y} = \bar{y} \pm \left(\frac{\Delta T}{2}\right) T \pm \left(\frac{\Delta U}{2}\right) U \pm \left(\frac{\Delta TU}{2}\right) TU \quad (1)$$

where: \hat{y} = predicted response (Y pred)

\bar{y} = grand mean (Y grand)

$\frac{\Delta}{2}$ = half-effects of each factor or interaction

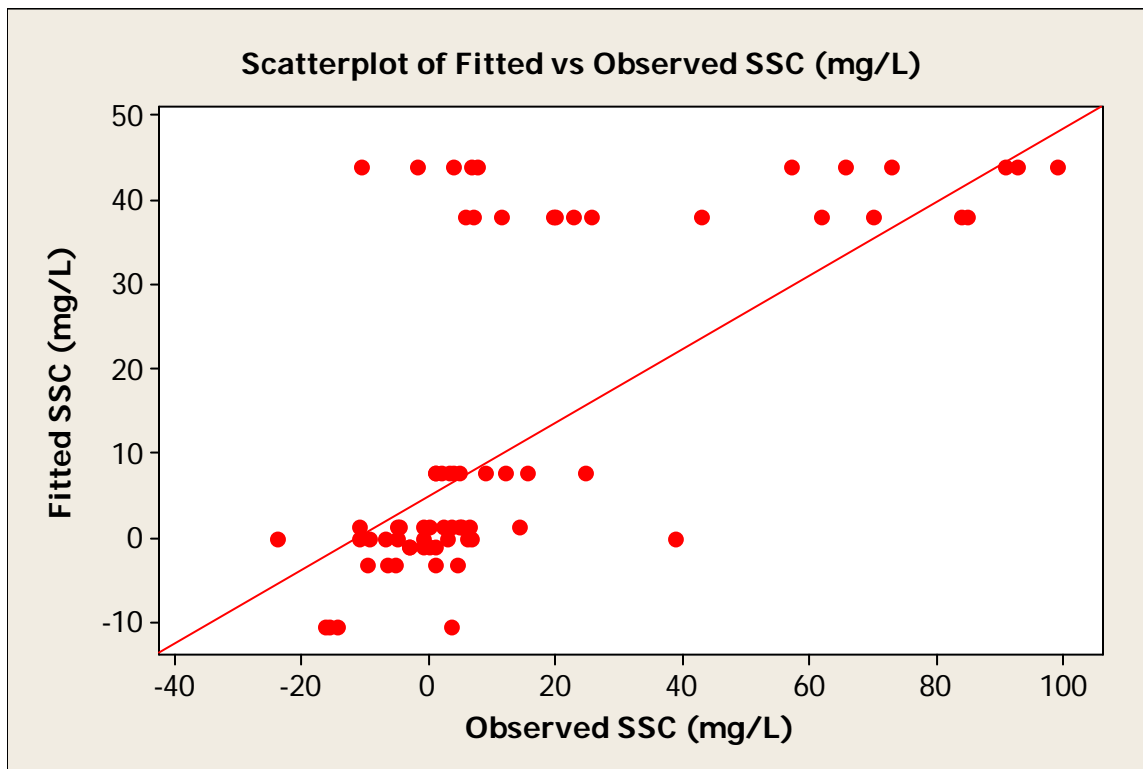
T = texture

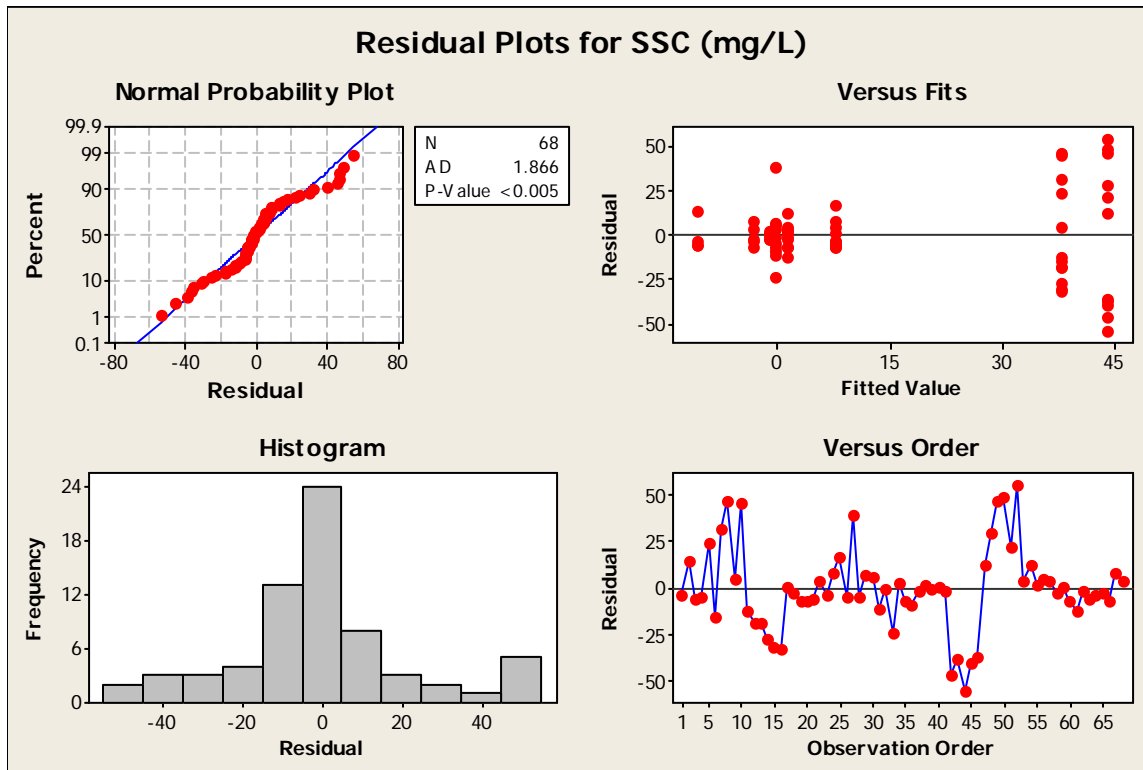
U = uniformity of the mixture

C = compaction

The final prediction equation is given as:

$$\text{Effluent SSC (mg/L)} = 9.47 + 10.2T - 8.1U - 13.3TU$$





Unusual Observations for SSC (mg/L)

Obs	StdOrder	SSC (mg/L)	Fit	SE Fit	Residual	St Resid
8	8	84.91	37.97	6.67	46.94	2.12R
10	10	83.81	37.97	6.67	45.84	2.07R
42	42	-1.90	44.01	6.96	-45.92	-2.08R
44	44	-10.53	44.01	6.96	-54.54	-2.48R
49	49	91.00	44.01	6.96	46.99	2.13R
50	50	92.63	44.01	6.96	48.62	2.21R
52	52	98.95	44.01	6.96	54.93	2.49R

R denotes an observation with a large standardized residual.

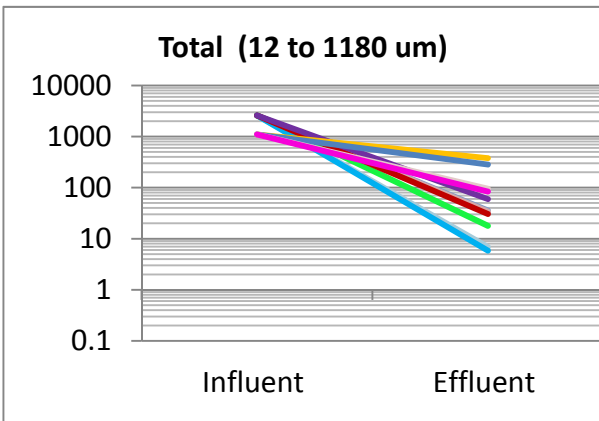
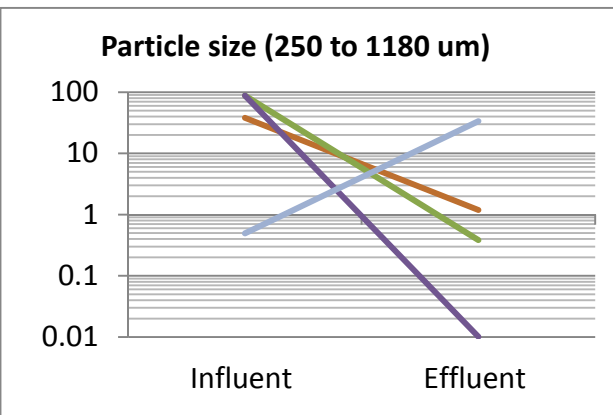
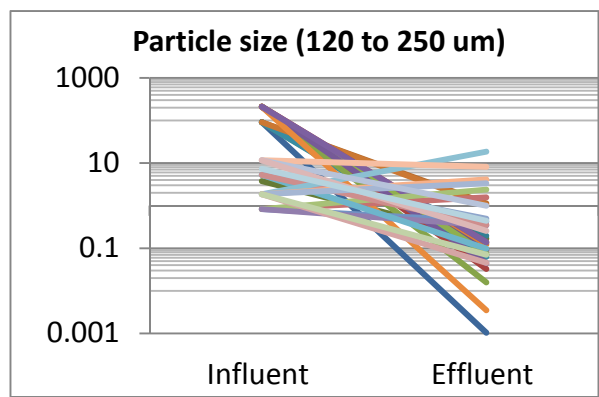
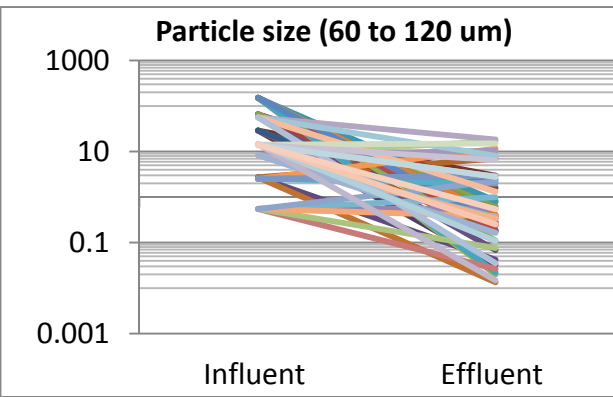
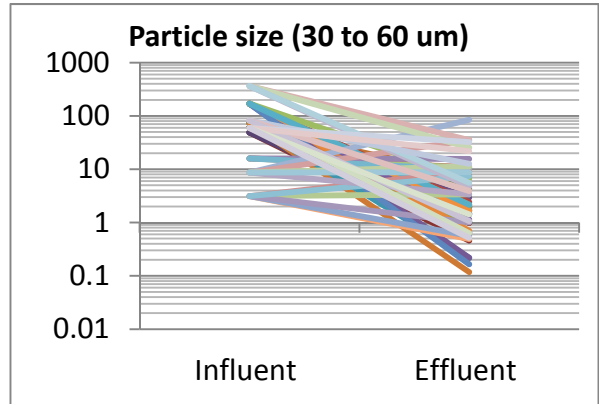
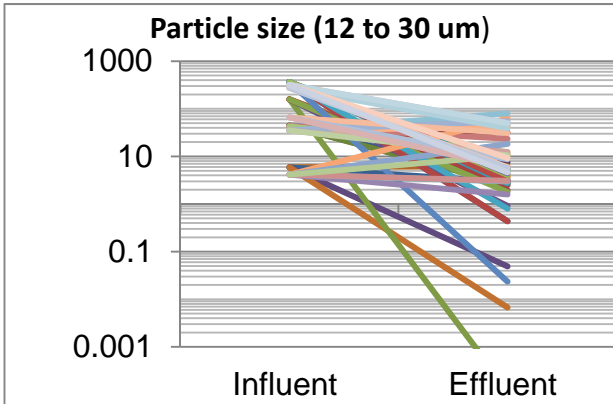
Standard Error Calculations for effluent SSC (mg/L) Tests.

Condition	1	2	3	4	13	14	15	16
SSC (mg/L)	-14.3	61.8	9.0	39.0	-3.0	-1.9	4.8	-6.7
	3.6	22.9	4.9	-5.0	1.0	6.7	14.3	-5.2
	-16.2	70.0	1.1	6.7	-1.0	-10.5	3.6	-9.5
	-15.8	84.9	1.0	6.0	0.0	4.0	6.3	4.5
		42.9	1.9	-11.0	-2.9	7.6	5.0	1.0
		83.8	12.0	-0.9		57.00	-1.00	
		25.5	4.0	-23.8		73.00	2.22	
		20.0	15.6	3.0		91.00	-5.00	
		19.6	24.8	-7.0		92.63	-11.00	
		11.4	3.3	-9.5		65.71	0.00	
		7.0				98.95	-4.76	
		5.8						
Standard Dev.	9.6	29.6	7.7	16.5	1.8	43.0	6.8	5.8
Square Root N	2.0	3.5	3.2	3.2	2.2	3.3	3.3	2.2
Standard Error	4.8	8.6	2.4	5.2	0.8	13.0	2.0	2.6
Avg. SSC (mg/L)	-10.7	38.0	7.7	-0.3	-1.2	44.0	1.3	-3.2
(n-1)*Si²	274.4	9660.1	536.1	2462.3	12.3	18472.5	460.5	133.3
(n-1)	3.0	11.0	9.0	9.0	4.0	10.0	10.0	4.0
Pooled Standard Error	23.1							

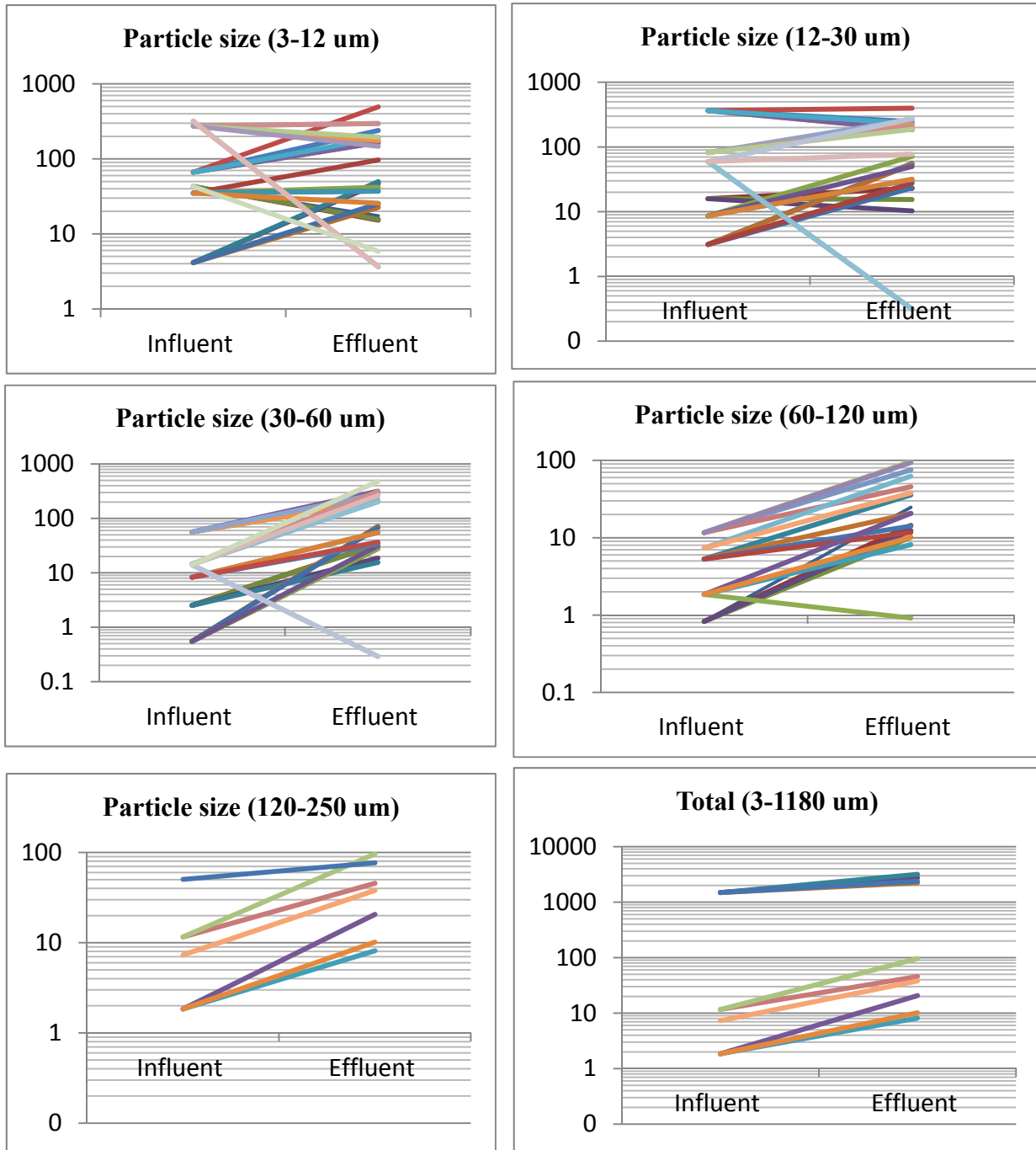
Actual SSC (mg/L) for Each Factorial Conditions

Condition	1	2	3	4	5	6	7	8
SSC (mg/L)	-14.3	61.8	9.0	39.0	-3.0	-1.9	4.8	-6.7
	3.6	22.9	4.9	-5.0	1.0	6.7	14.3	-5.2
	-16.2	70.0	1.1	6.7	-1.0	-10.5	3.6	-9.5
	-15.8	84.9	1.0	6.0	0.0	4.0	6.3	4.5
		42.9	1.9	-11.0	-2.9	7.6	5.0	1.0
		83.8	12.0	-0.9		57.00	-1.00	
		25.5	4.0	-23.8		73.00	2.22	
		20.0	15.6	3.0		91.00	-5.00	
		19.6	24.8	-7.0		92.63	-11.00	
		11.4	3.3	-9.5		65.71	0.00	
		7.0				98.95	-4.76	
		5.8						
Avg.	-10.7	38.0	7.7	-0.3	-1.2	44.0	1.3	-3.2

SC Line Performance Plots for Sand-Peat Mixture

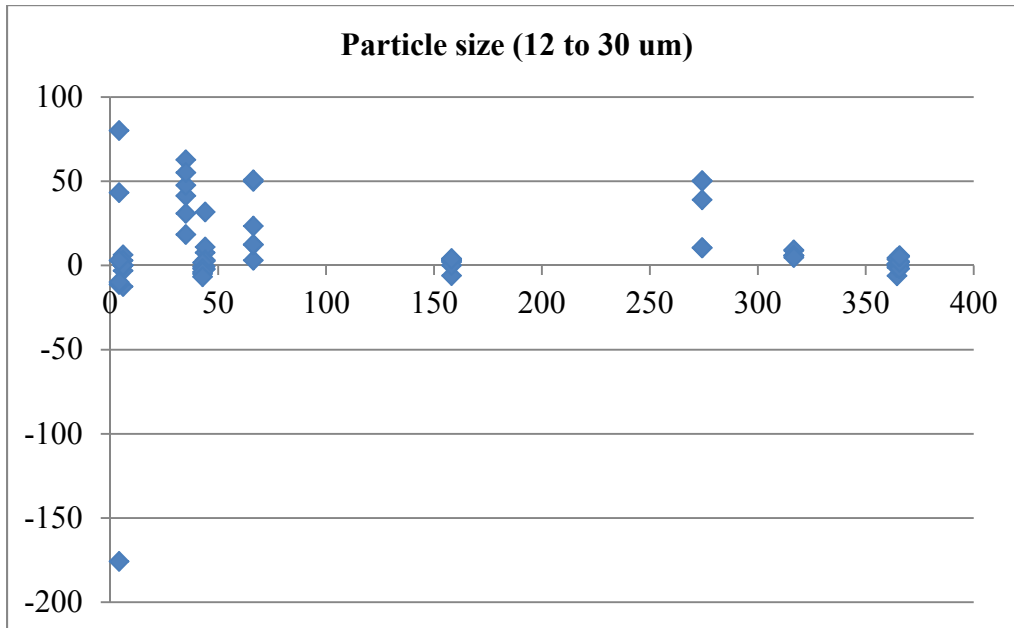


SSC Line Performance Plots for the Coarse Media



No significant reduction was observed for the coarse materials due to washing of fines with the coarse material.

Appendix E.2: SmartDrain™ Field Performance Solid 12 to 30 um Particle Size Analysis.



Effluent is a constant value (7.8 mg/L, 3.7 COV)

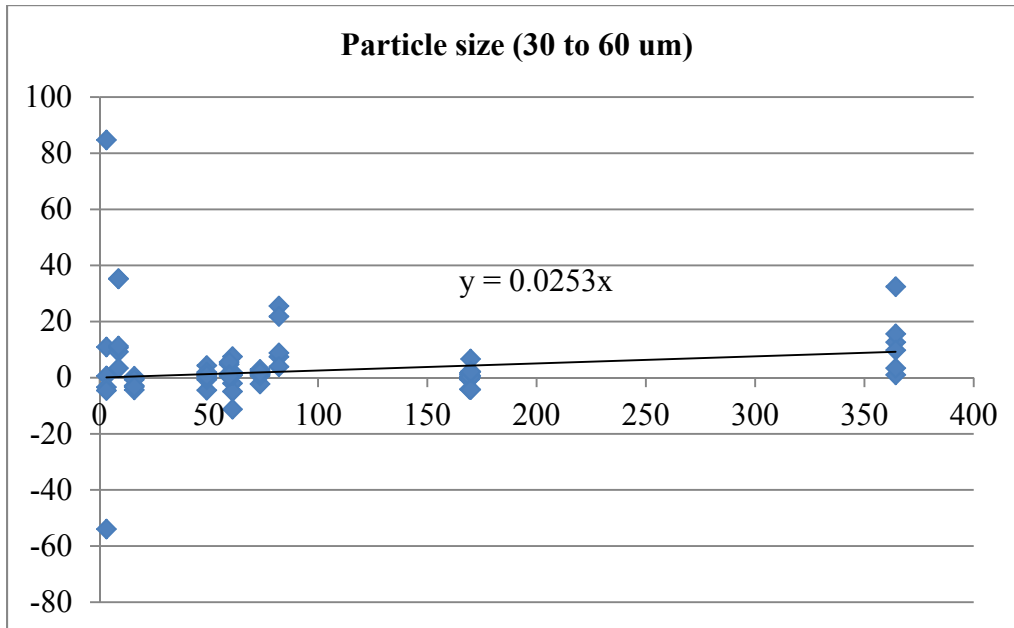
12-30 um Particle Size Summary Output

<i>Regression Statistics</i>	
Multiple R	0.181497912
R Square	0.032941492
Adjusted R Square	0.019783597
Standard Error	29.07356476
Observations	77

<i>ANOVA</i>					
	<i>df</i>	<i>SS</i>	<i>MS</i>	<i>F</i>	<i>Significance F</i>
Regression	1	2188.268837	2188.268837	2.588833421	0.11182116
Residual	76	64240.68475	845.2721677		
Total	77	66428.95358			

	<i>Coefficients</i>	<i>Standard Error</i>	<i>t Stat</i>	<i>P-value</i>	<i>Lower 95%</i>	<i>Upper 95%</i>
Intercept	0	#N/A	#N/A	#N/A	#N/A	#N/A
X Variable 1	0.025471562	0.015830824	1.608985215	0.111765974	0.006058256	0.057001381

Appendix E.3: SmartDrain™ Field Performance Solid 30 to 60um Particle Size Analysis.



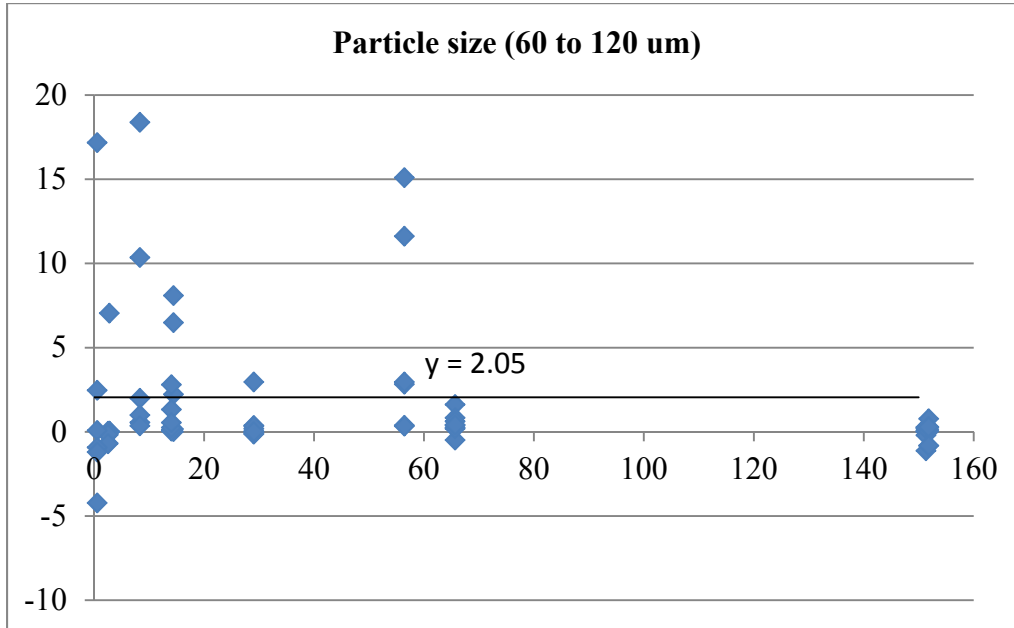
30-60 um Particle Size Summary Output

<i>Regression Statistics</i>	
Multiple R	0.234502476
R Square	0.054991411
Adjusted R Square	0.041833517
Standard Error	14.28101326
Observations	77

<i>ANOVA</i>					
	<i>df</i>	<i>SS</i>	<i>MS</i>	<i>F</i>	<i>Significance F</i>
Regression	1	901.9672049	901.9672049	4.4225495	0.038821718
Residual	76	15499.99781	203.9473396		
Total	77	16401.96502			

	<i>Coefficients</i>	<i>Standard Error</i>	<i>t Stat</i>	<i>P-value</i>	<i>Lower 95%</i>	<i>Upper 95%</i>
Intercept	0	#N/A	#N/A	#N/A	#N/A	#N/A
X Variable 1	0.02528103	0.012021493	2.102985853	0.03877718	0.001338152	0.049223909

Appendix E.4: SmartDrain™ Field Performance Solid 60 to 120um Particle Size Analysis.



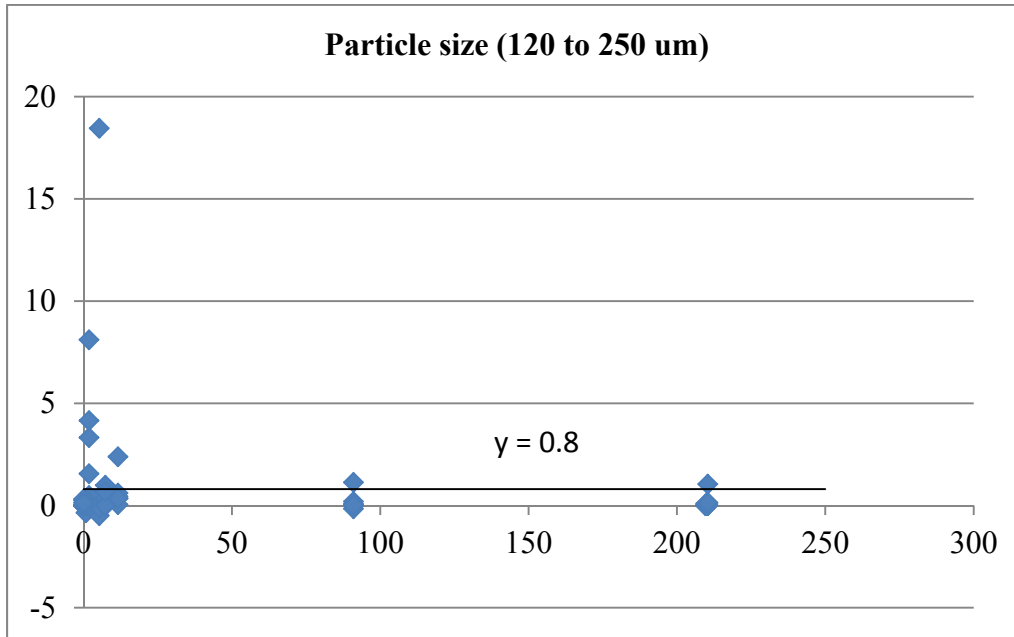
Summary Output

<i>Regression Statistics</i>	
Multiple R	0.167648888
R Square	0.02810615
Adjusted R Square	0.015147565
Standard Error	3.900570402
Observations	77

<i>ANOVA</i>					
	<i>df</i>	<i>SS</i>	<i>MS</i>	<i>F</i>	<i>Significance F</i>
Regression	1	32.99894255	32.99894255	2.168921238	0.145009388
Residual	75	1141.08371	15.21444946		
Total	76	1174.082652			

	<i>Coefficients</i>	<i>Standard Error</i>	<i>t Stat</i>	<i>P-value</i>	<i>Lower 95%</i>	<i>Upper 95%</i>
Intercept	2.047673794	0.59111651	3.464078161	0.000882902	0.870109338	3.225238249
X Variable 1	-0.011629132	0.007896332	-1.472725785	0.145009388	-0.027359432	0.004101168

Appendix E.5: SmartDrain™ Field Performance Solid 120 to 250um Particle Size Analysis.



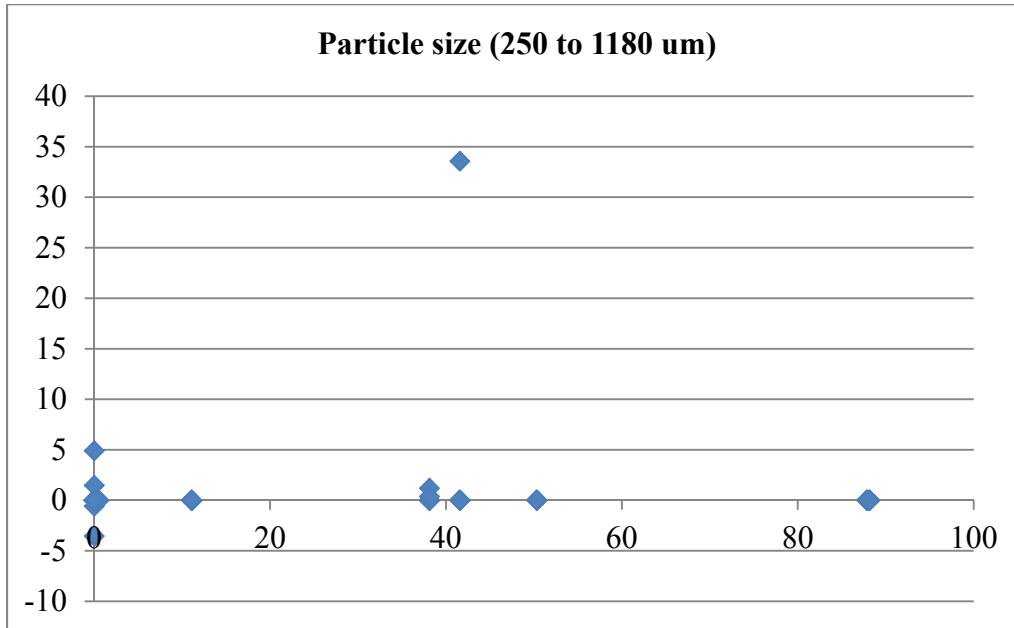
Summary Output

Regression Statistics	
Multiple R	0.125133971
R Square	0.015658511
Adjusted R Square	0.002533957
Standard Error	2.351932355
Observations	77

ANOVA					
	<i>df</i>	<i>SS</i>	<i>MS</i>	<i>F</i>	<i>Significance F</i>
Regression	1	6.599569063	6.599569063	1.193069998	0.278207449
Residual	75	414.8689353	5.531585804		
Total	76	421.4685043			

	<i>Coefficients</i>	<i>Standard Error</i>	<i>t Stat</i>	<i>P-value</i>	<i>Lower 95%</i>	<i>Upper 95%</i>
Intercept	0.790800684	0.321983531	2.456028359	0.016362705	0.149376607	1.432224761
X Variable 1	-0.003509003	0.003212556	-1.092277436	0.278207449	-0.009908743	0.002890737

Appendix E.6: SmartDrain™ Field Performance Solid 250 to 1180 um Particle Size Analysis.



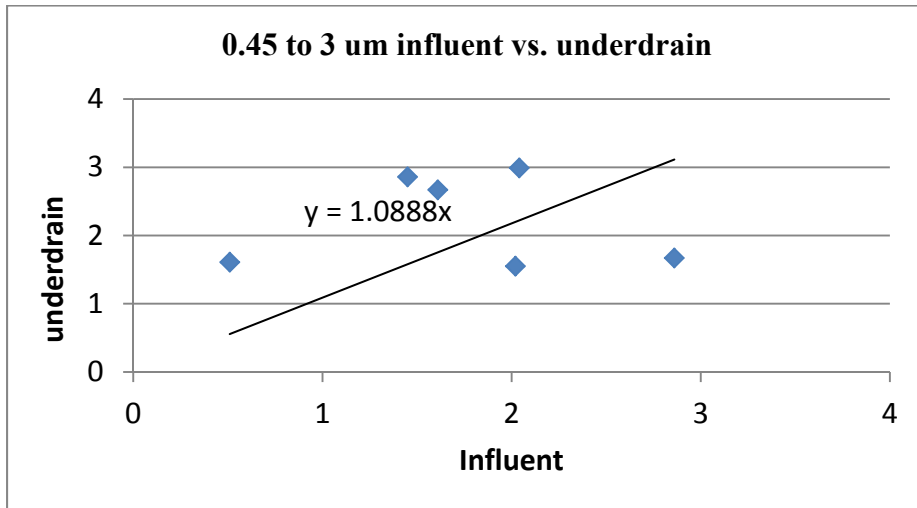
Effluent is a constant value (0.5 mg/L, 8 COV)

<i>Regression Statistics</i>	
Multiple R	0.105839209
R Square	0.011201938
Adjusted R Square	-0.001955957
Standard Error	3.896238542
Observations	77

<i>ANOVA</i>					
	<i>df</i>	<i>SS</i>	<i>MS</i>	<i>F</i>	<i>Significance F</i>
Regression	1	13.07044084	13.07044084	0.860992085	0.356437829
Residual	76	1153.731283	15.18067478		
Total	77	1166.801724			

	<i>Coefficients</i>	<i>Standard Error</i>	<i>t Stat</i>	<i>P-value</i>	<i>Lower 95%</i>	<i>Upper 95%</i>
Intercept	0	#N/A	#N/A	#N/A	#N/A	#N/A
X Variable 1	0.008974941	0.009672351	0.927896592	0.356398786	-0.010289214	0.028239096

Appendix E.7: Underdrain SmartDrain™ Field Performance Solid 0.45 to 3 um Particle Size Analysis



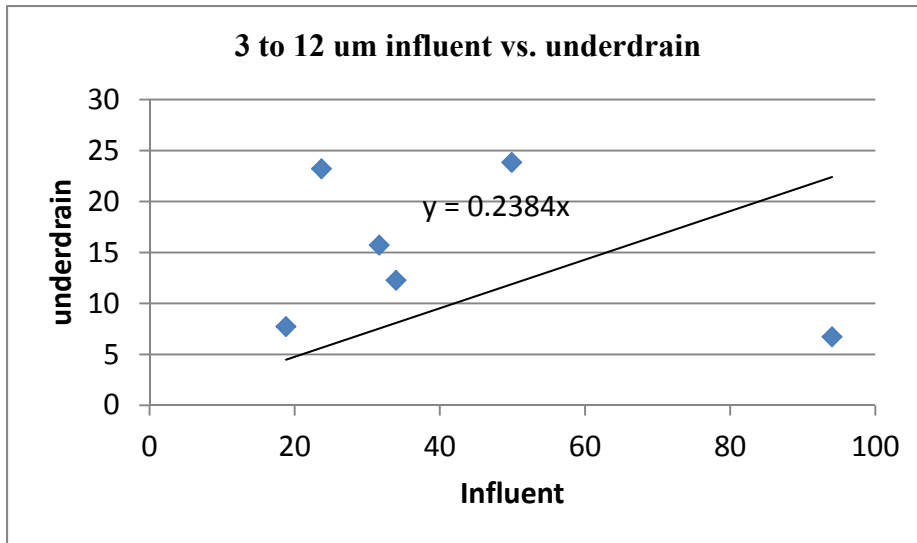
Regression Statistics	
Multiple R	0.889415292
R Square	0.791059562
Adjusted R Square	0.591059562
Standard Error	1.156961625
Observations	6

ANOVA					
	df	SS	MS	F	Significance F
Regression	1	25.3393	25.3393	18.93026	0.012149
Residual	5	6.692801	1.33856		
Total	6	32.0321			

	Coefficients	Standard Error	t Stat	P-value	Lower 95%	Upper 95%
Intercept	0	#N/A	#N/A	#N/A	#N/A	#N/A
X Variable 1	1.088757175	0.250238	4.350892	0.007353	0.445501	1.732014

0.45 to 3 um	influent	underdrain	%reduction	sign test diff	
	4/7/2013	0.51	1.61	-215.7	
	4/9/2013	2.02	1.55	23.3	
	5/2/2013	1.61	2.67	-65.8	
	5/27/2013	2.86	1.67	41.6	
	6/5/2013	1.45	2.86	-97.2	
	6/9/2013	2.04	2.99	-46.6	
min		0.51	1.55	-215.7	
max		2.86	2.99	41.6	
median		1.82	2.17	-56.2	2 of 6
average		1.75	2.23	-60.1	p > 0.5 by Sign test
stdev		0.78	0.68	92.8	
COV		0.45	0.31	-1.5	

Appendix E.8: SmartDrain™ Field Performance Solid 3 to 12 um Particle Size Analysis



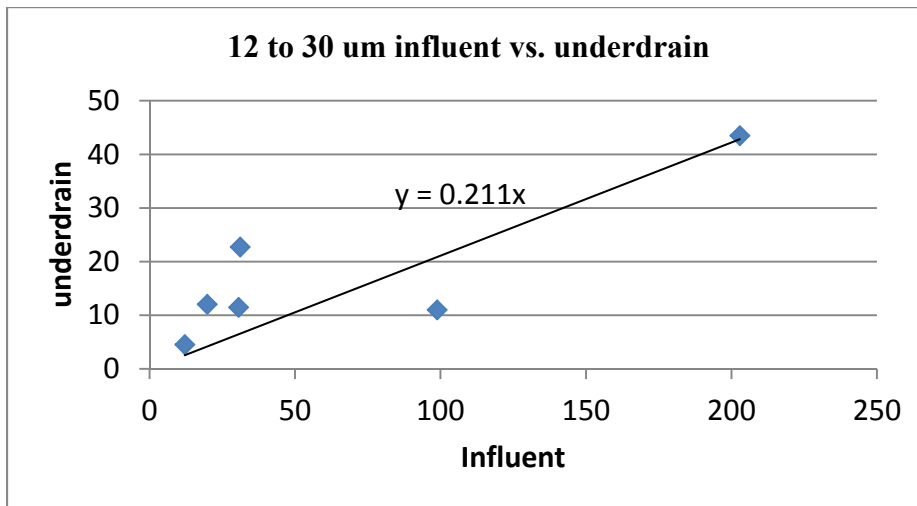
Regression Statistics	
Multiple R	0.71276036
R Square	0.50802733
Adjusted R Square	0.30802733
Standard Error	12.59005564
Observations	6

ANOVA					
	df	SS	MS	F	Significance F
Regression	1	818.4109	818.4109	5.163166	0.085514
Residual	5	792.5475	158.5095		
Total	6	1610.958			

	Coefficients	Standard Error	t Stat	P-value	Lower 95%	Upper 95%
Intercept	0	#N/A	#N/A	#N/A	#N/A	#N/A
X Variable 1	0.238367359	0.104903	2.27226	0.072234	-0.03129	0.50803

3 to 12 um	influent	underdrain	% reduction	
	31.66	15.73	50.3	
	23.69	23.21	2	
	18.8	7.74	58.8	
	94.04	6.73	92.8	
	33.96	12.28	63.8	
	49.9	23.85	52.2	
min	18.8	6.73	2	
max	94.04	23.85	92.8	
median	32.81	14.01	55.5	6 of 6
average	42.01	14.92	53.3	p = 0.031 by
stdev	27.62	7.41	29.5	Sign test
COV	0.66	0.5	0.6	

Appendix E.9: SmartDrain™ Field Performance Solid 12 to 30 um Particle Size Analysis



Regression Statistics	
Multiple R	0.917107961
R Square	0.841087011
Adjusted R Square	0.641087011
Standard Error	9.476891771
Observations	6

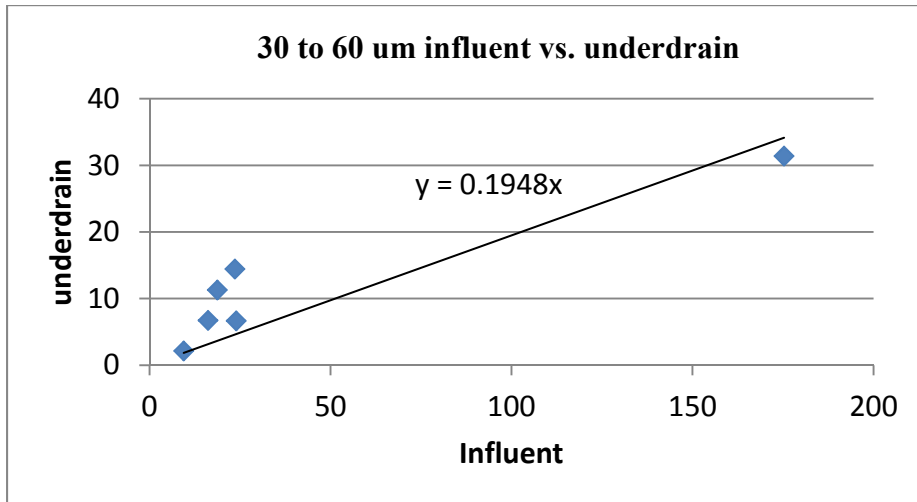
ANOVA					
	df	SS	MS	F	Significance F
Regression	1	2376.749	2376.749	26.46376	0.006771
Residual	5	449.0574	89.81148		
Total	6	2825.807			

	Coefficients	Standard Error	t Stat	P-value	Lower 95%	Upper 95%
Intercept	0	#N/A	#N/A	#N/A	#N/A	#N/A
X Variable 1	0.21101367	0.041019	5.144294	0.003632	0.105571	0.316456

12 to 30 um	influent	underdrain	% reduction		
	4/7/2013	202.88	43.48	78.6	
	4/9/2013	19.85	12.05	39.3	
	5/2/2013	12.13	4.52	62.7	
	5/27/2013	98.83	11.01	88.9	
	6/5/2013	30.61	11.48	62.5	
	6/9/2013	31.18	22.73	27.1	
min		12.13	4.52	27.1	
max		202.88	43.48	88.9	
median		30.90	11.77	62.6	
average		65.91	17.55	59.8	
stdev		73.91	13.99	23.2	
COV		1.12	0.80	0.4	

6 of 6
p = 0.031 by
sign test

Appendix E.10: SmartDrain™ Field Performance Solid 30 to 60 um Particle Size Analysis



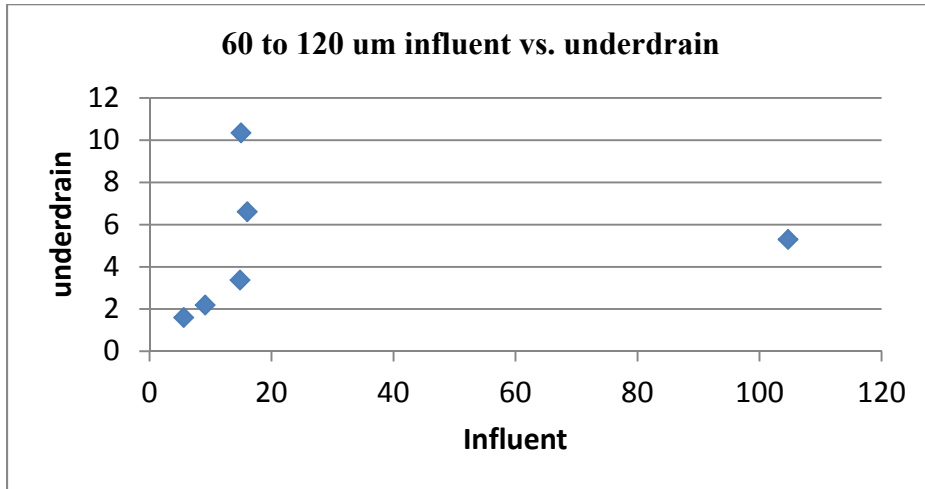
<i>Regression Statistics</i>	
Multiple R	0.93439672
R Square	0.873097231
Adjusted R Square	0.673097231
Standard Error	5.993031812
Observations	6

<i>ANOVA</i>					
	<i>df</i>	<i>SS</i>	<i>MS</i>	<i>F</i>	<i>Significance F</i>
Regression	1	1235.534	1235.534	34.40024	0.004219
Residual	5	179.5822	35.91643		
Total	6	1415.116			

	<i>Coefficients</i>	<i>Standard Error</i>	<i>t Stat</i>	<i>P-value</i>	<i>Lower 95%</i>	<i>Upper 95%</i>
Intercept	0	#N/A	#N/A	#N/A	#N/A	#N/A
X Variable 1	0.194796442	0.033212	5.865172	0.002043	0.109421	0.280172

30 to 60 um	influent	underdrain	% reduction	
4/7/2013	175.3	31.39	82.1	
4/9/2013	16.17	6.73	58.4	
5/2/2013	9.44	2.14	77.3	
5/27/2013	18.73	11.29	39.7	
6/5/2013	23.59	14.43	38.8	
6/9/2013	23.93	6.65	72.2	
min	9.44	2.14	38.8	
max	175.3	31.39	82.1	
median	21.16	9.01	65.3	6 of 6
average	44.53	12.11	61.4	p = 0.031
stdev	64.29	10.35	18.9	
COV	1.44	0.86	0.3	

Appendix E.11: SmartDrain™ Field Performance Solid 60 to 120 um Particle Size Analysis



underdrain is a constant value (4.9 mg/L, 3.3 mg/L st dev)

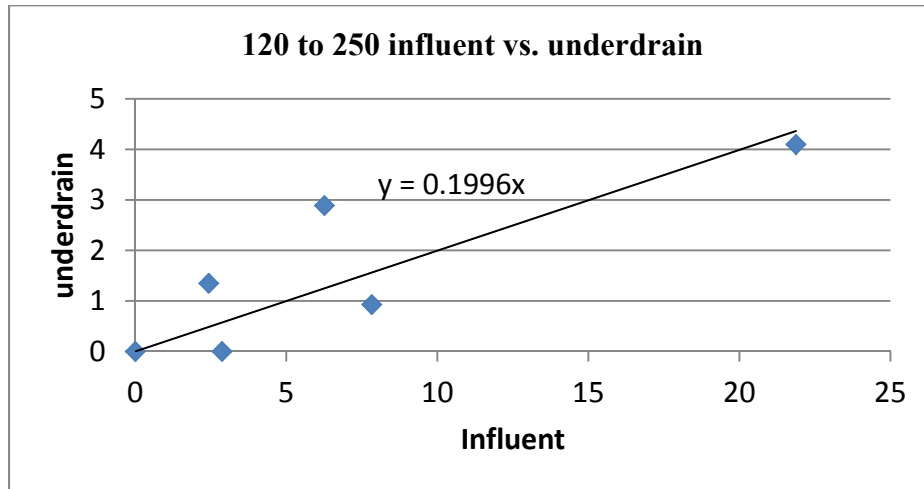
<i>Regression Statistics</i>	
Multiple R	0.586740876
R Square	0.344264856
Adjusted R Square	0.144264856
Standard Error	5.090870366
Observations	6

ANOVA					
	<i>df</i>	<i>SS</i>	<i>MS</i>	<i>F</i>	<i>Significance F</i>
Regression	1	68.03279	68.03279	2.62503	0.180506
Residual	5	129.5848	25.91696		
Total	6	197.6176			

	<i>Coefficients</i>	<i>Standard Error</i>	<i>t Stat</i>	<i>P-value</i>	<i>Lower 95%</i>	<i>Upper 95%</i>
Intercept	0	#N/A	#N/A	#N/A	#N/A	#N/A
X Variable 1	0.07601782	0.046919	1.620194	0.166116	-0.04459	0.196627

60 to 120 um	influent	underdrain	% reduction		
	4/7/2013	104.67	5.30	94.9	
	4/9/2013	9.13	2.19	76.0	
	5/2/2013	5.60	1.60	71.4	
	5/27/2013	14.85	3.37	77.3	
	6/5/2013	15.00	10.35	31.0	
	6/9/2013	16.03	6.61	58.8	
min		5.60	1.60	31.0	
max		104.67	10.35	94.9	
median		14.93	4.34	73.7	6 of 6
average		27.55	4.90	68.2	p = 0.031
stdev		38.00	3.27	21.6	
COV		1.38	0.67	0.3	

Appendix E.12: SmartDrain™ Field Performance Solid 120 to 250 um Particle Size Analysis



Regression Statistics	
Multiple R	0.920764951
R Square	0.847808095
Adjusted R Square	0.647808095
Standard Error	0.920702824
Observations	6

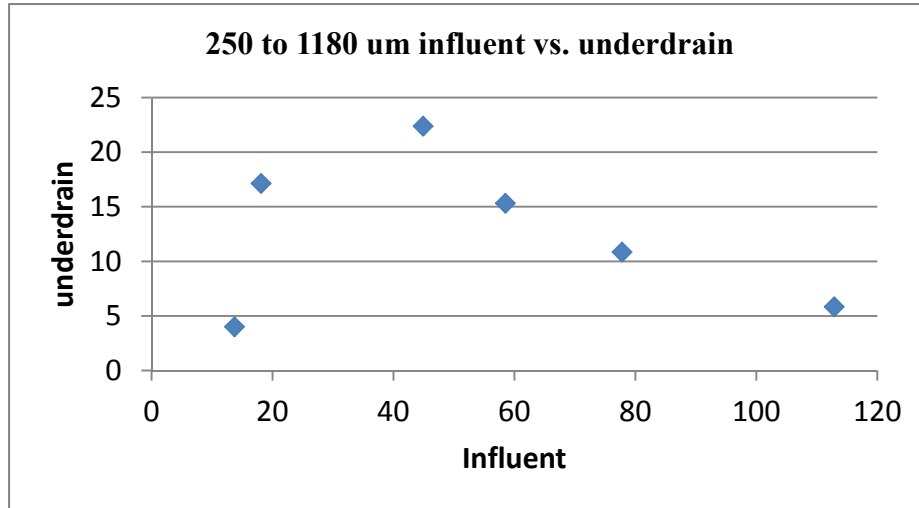
ANOVA					
	<i>df</i>	<i>SS</i>	<i>MS</i>	<i>F</i>	<i>Significance F</i>
Regression	1	23.61103	23.61103	27.85326	0.00618
Residual	5	4.238468	0.847694		
Total	6	27.8495			

	<i>Coefficients</i>	<i>Standard Error</i>	<i>t Stat</i>	<i>P-value</i>	<i>Lower 95%</i>	<i>Upper 95%</i>
Intercept	0	#N/A	#N/A	#N/A	#N/A	#N/A
X Variable 1	0.19955098	0.037811	5.277619	0.003251	0.102355	0.296747

120 to 250 um	influent	underdrain	% reduction	
	4/7/2013	21.87	4.10	81.3
	4/9/2013	2.87	0.00	100.0
	5/2/2013	0.00	0.00	n/a
	5/27/2013	7.83	0.93	88.1
	6/5/2013	6.26	2.89	53.8
	6/9/2013	2.43	1.35	44.4
min		0.00	0.00	44.4
max		21.87	4.10	100.0
median		4.57	1.14	81.3
average		6.88	1.55	73.5
stdev		7.86	1.64	23.5
COV		1.14	1.06	0.3

5 of 5
p = 0.063 by
Sign test

Appendix E.13: SmartDrain™ Field Performance Solid 250 to 1180 um Particle Size Analysis



Underdrain is a constant value (12.6 mg/L, 7.0 mg/L st dev)

Regression Statistics	
Multiple R	0.692418419
R Square	0.479443267
Adjusted R Square	0.279443267
Standard Error	11.16574719
Observations	6

ANOVA					
	<i>df</i>	<i>SS</i>	<i>MS</i>	<i>F</i>	<i>Significance F</i>
Regression	1	574.1359	574.1359	4.605101	0.098428
Residual	5	623.3696	124.6739		
Total	6	1197.506			

	<i>Coefficients</i>	<i>Standard Error</i>	<i>t Stat</i>	<i>P-value</i>	<i>Lower 95%</i>	<i>Upper 95%</i>
Intercept	0	#N/A	#N/A	#N/A	#N/A	#N/A
X Variable 1	0.15232541	0.070983	2.14595	0.084678	-0.03014	0.334792

250 to 1180 um	influent	underdrain	% reduc.	
	4/7/2013	58.52	15.32	73.8
	4/9/2013	77.78	10.85	86.1
	5/2/2013	13.71	4.00	70.8
	5/27/2013	112.86	5.83	94.8
	6/5/2013	18.12	17.14	5.4
	6/9/2013	44.90	22.39	50.1
min		13.71	4.00	5.4
max		112.86	22.39	94.8
median		51.71	13.09	72.3
average		54.32	12.59	63.5
stdev		37.53	7.02	32.3
COV		0.69	0.56	0.5

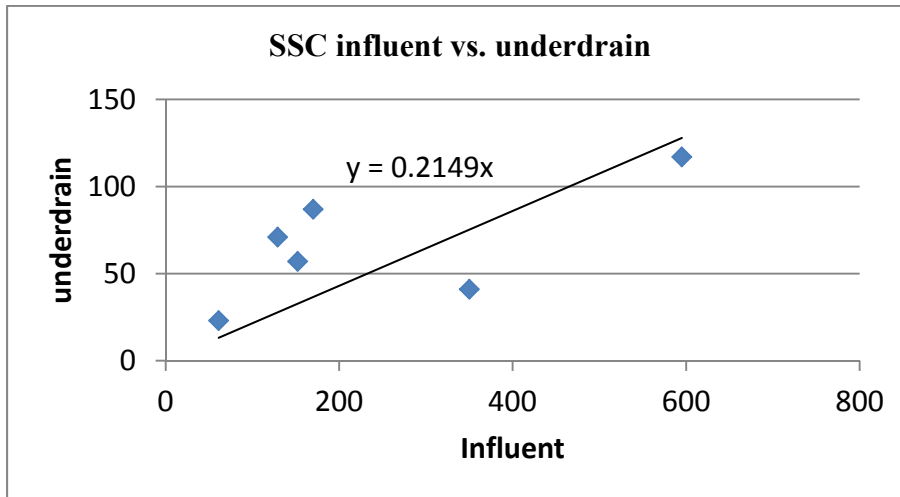
6 of 6
p = 0.031 by
Sign test

Appendix E.14: SmartDrain™ Field Performance Solid > 1180 um Particle Size Analysis

>1180	influent	underdrain	% reduc.	
4/7/2013	0	0	0	n/a
4/9/2013	0	0	0	n/a
5/2/2013	0	0	0	n/a
5/27/2013	0	0	0	n/a
6/5/2013	0	0	0	n/a
6/9/2013	0	0	0	n/a
min	0	0	0	0
max	0	0	0	0
median	0	0	0	#NUM!
average	0	0	0	#DIV/0!
stdev	0	0	0	#DIV/0!
COV	#DIV/0!	#DIV/0!	#DIV/0!	#DIV/0!

Underdrain is a constant value (0 mg/L)

Appendix E.15: SmartDrain™ Field Performance SSC Influent Vs. Underdrain



Regression Statistics	
Multiple R	0.89359853
R Square	0.798518333
Adjusted R Square	0.598518333
Standard Error	35.77332742
Observations	6

ANOVA					
	<i>df</i>	<i>SS</i>	<i>MS</i>	<i>F</i>	<i>Significance F</i>
Regression	1	25359.35	25359.35	19.81615	0.011233
Residual	5	6398.655	1279.731		
Total	6	31758			

	<i>Coefficients</i>	<i>Standard Error</i>	<i>t Stat</i>	<i>P-value</i>	<i>Lower 95%</i>	<i>Upper 95%</i>
Intercept	0	#N/A	#N/A	#N/A	#N/A	#N/A
X Variable 1	0.214944315	0.048285	4.451534	0.006693	0.090823	0.339066

total	influent	underdrain	% reduction	
	4/7/2013	595.0	117.0	80.3
	4/9/2013	152.0	57.0	62.5
	5/2/2013	61.0	23.0	62.3
	5/27/2013	350.0	41.0	88.3
	6/5/2013	129.0	71.0	45.0
	6/9/2013	170.0	87.0	48.8
min		61.0	23.0	45.0
max		595.0	117.0	88.3
median		161.0	64.0	62.4
average		242.8	66.0	64.5
stdev		197.5	33.5	17.0
COV		0.8	0.5	0.3

6 of 6
p = 0.031 by
Sign test